

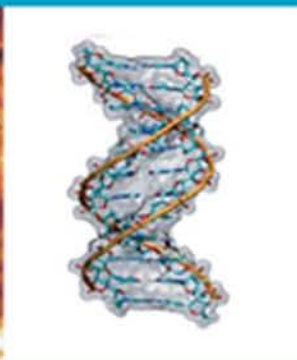
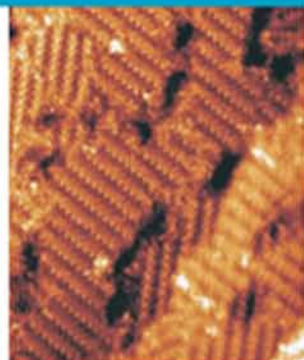
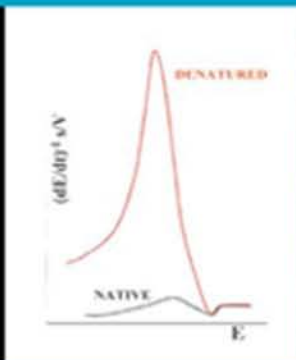
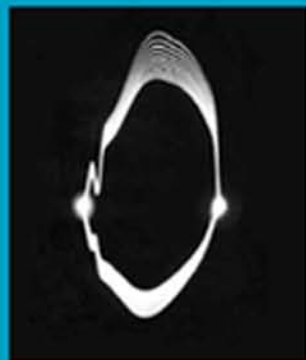


PERSPECTIVES IN BIOANALYSIS

VOLUME 1

ELECTROCHEMISTRY OF NUCLEIC ACIDS AND PROTEINS

*Towards Electrochemical Sensors for
Genomics and Proteomics*



E. PALEČEK | F. SCHELLER | J. WANG
(EDITORS)

PERSPECTIVES IN
BIOANALYSIS
VOLUME 1

This page intentionally left blank

PERSPECTIVES IN BIOANALYSIS

**ELECTROCHEMISTRY OF NUCLEIC ACIDS
AND PROTEINS – TOWARDS
ELECTROCHEMICAL SENSORS
FOR GENOMICS AND PROTEOMICS**

EDITORS

EMIL PALEČEK

INSTITUTE OF BIOPHYSICS
ACADEMY OF SCIENCES
OF THE CZECH REPUBLIC
KRALOVOPOLSKA 135
612 65 BRNO
CZECH REPUBLIC

F. SCHELLER

UNIVERSITÄT POTSDAM,
ANALYTISCHE BIOCHEMIE
KARL-LIEBKNECHT STR., 24-25
HAUS 25, B 2.13-14
14475 GOLM
GERMANY

J. WANG

CENTER FOR BIOELECTRONICS
AND BIOSENSORS
BIODESIGN INSTITUTE
DEPARTMENTS OF CHEMICAL
& MATERIALS ENGINEERING
AND CHEMISTRY
ARIZONA STATE UNIVERSITY
1001 S. MCALLISTER AVE
P.O. BOX 875801 TEMPE
AZ 85287-5801, USA

VOLUME 1



ELSEVIER

Amsterdam – Boston – Heidelberg – London – New York – Oxford
Paris – San Diego – San Francisco – Singapore – Sydney – Tokyo

ELSEVIER B.V.
Radarweg 29
P.O. Box 211, 1000 AE Amsterdam
The Netherlands

ELSEVIER Inc.
525 B Street, Suite 1900
San Diego, CA 92101-4495
USA

ELSEVIER Ltd
The Boulevard, Langford Lane
Kidlington, Oxford OX5 1GB
UK

ELSEVIER Ltd
84 Theobalds Road
London WC1X 8RR
UK

© 2005 Elsevier B.V. All rights reserved.

This work is protected under copyright by Elsevier B.V., and the following terms and conditions apply to its use:

Photocopying

Single photocopies of single chapters may be made for personal use as allowed by national copyright laws. Permission of the Publisher and payment of a fee is required for all other photocopying, including multiple or systematic copying, copying for advertising or promotional purposes, resale, and all forms of document delivery. Special rates are available for educational institutions that wish to make photocopies for non-profit educational classroom use.

Permissions may be sought directly from Elsevier's Rights Department in Oxford, UK: phone (+44) 1865 843830, fax (+44) 1865 853333, e-mail: permissions@elsevier.com. Requests may also be completed on-line via the Elsevier homepage (<http://www.elsevier.com/locate/permissions>).

In the USA, users may clear permissions and make payments through the Copyright Clearance Center, Inc., 222 Rosewood Drive, Danvers, MA 01923, USA; phone: (+1) (978) 7508400, fax: (+1) (978) 7504744, and in the UK through the Copyright Licensing Agency Rapid Clearance Service (CLARCS), 90 Tottenham Court Road, London W1P 0LP, UK; phone: (+44) 20 7631 5555; fax: (+44) 20 7631 5500. Other countries may have a local reprographic rights agency for payments.

Derivative Works

Tables of contents may be reproduced for internal circulation, but permission of the Publisher is required for external resale or distribution of such material. Permission of the Publisher is required for all other derivative works, including compilations and translations.

Electronic Storage or Usage

Permission of the Publisher is required to store or use electronically any material contained in this work, including any chapter or part of a chapter.

Except as outlined above, no part of this work may be reproduced, stored in a retrieval system or transmitted in any form or by any means, electronic, mechanical, photocopying, recording or otherwise, without prior written permission of the Publisher.

Address permissions requests to: Elsevier's Rights Department, at the fax and e-mail addresses noted above.

Notice

No responsibility is assumed by the Publisher for any injury and/or damage to persons or property as a matter of products liability, negligence or otherwise, or from any use or operation of any methods, products, instructions or ideas contained in the material herein. Because of rapid advances in the medical sciences, in particular, independent verification of diagnoses and drug dosages should be made.

First edition 2005

Library of Congress Cataloging in Publication Data

A catalog record is available from the Library of Congress.

British Library Cataloguing in Publication Data

A catalogue record is available from the British Library.

ISBN-10: 0-444-52150-X

ISBN-13: 978-0-444-52150-7

ISSN: 1871-0069

○ The paper used in this publication meets the requirements of ANSI/NISO Z39.48-1992 (Permanence of Paper). Printed in The Netherlands.

Working together to grow
libraries in developing countries

www.elsevier.com | www.bookaid.org | www.sabre.org

ELSEVIER

BOOK AID
International

Sabre Foundation

Contents

<i>Contributors</i>	xi
<i>Preface</i>	xv

Chapter 1 Polarography of DNA. Retrospective View

Emil Paleček

1. Introduction	1
2. Retrospective view	5
3. Oscillographic polarography at controlled A.C.	8
4. Electrogenerated products	9
5. Nürnberg's cyclic voltammetry with HMDE	10
6. Summary and conclusion	11
List of abbreviations	12
Acknowledgments	12
References	12

Chapter 2 Electrochemical Properties of Nucleic Acid Components

Vladimír Vetterl and Stanislav Hason

1. Introduction	18
2. Adsorption and two-dimensional condensation	18
3. Electroreduction and electrooxidation of nucleic acid components	51
4. Concluding remarks	57
List of abbreviations	58
Acknowledgments	60
References	60

Chapter 3 Electrochemistry of Nucleic Acids

Emil Paleček and František Jelen

1. Introduction	74
2. Electrochemical methods and electrodes	77
3. Adsorption of nucleic acids	80
4. Reduction and oxidation of nucleic acids at electrodes	86
5. Changes in DNA conformation at surfaces	104
6. Electrochemical principles in NA biosensors	121
7. Electrochemical DNA biosensors: Future prospects	149
8. Summary and conclusion	150
List of abbreviations	152
Acknowledgments	153
References	153

Chapter 4 Electrochemical Nucleic Acid Biosensors

Joseph Wang

1. Introduction	175
2. Electrochemical biosensing of DNA hybridization	177
3. Conclusions and outlook	189
Acknowledgment	190
References	190

Chapter 5 Amplified Electrochemical and Photoelectrochemical Analysis of DNA

Eugenii Katz, Bilha Willner and Itamar Willner

1. Introduction	195
2. Enzyme-amplified electrochemical analysis of DNA	202
3. Amplified electrochemical detection of DNA using nucleic acid-functionalized metallic or semiconductor nanoparticles	211
4. Nano- and micro-objects as carriers for the amplified electrochemical detection of DNA	219
5. Analysis of DNA by direct conductivity measurements	227
6. Amplified sensing of DNA in the presence of magnetic particles	230
7. Photoelectrochemical detection of DNA	233
8. Conclusions and perspectives	239
Acknowledgments	241
References	241

Chapter 6 Fully Electrical Microarrays

R. Hintsche, B. Elsholz, G. Piechotta, R. Woerl, C.G.J. Schabmueller, J. Albers, V. Dharuman, E. Nebling, A. Hanisch, L. Blohm, F. Hofmann, B. Holzapfl, A. Frey, C. Paulus, M. Schienle and R. Thewes

1. Introduction	247
2. Principle and instrumentation of electrical detection	248
3. Low-density electrical DNA arrays	251
4. Integrated CMOS DNA arrays	256
5. Electrical label-free detection of DNA arrays	261
6. Electrical protein microarrays	264
7. Electrical hapten microarrays	267
List of abbreviations	271
References	272

Chapter 7 Carbon Electrodes in DNA Hybridisation Research

G. Marrazza, F. Lucarelli and M. Mascini

1. DNA probe immobilisation	280
2. Hybridisation reaction	283
3. Labelling and electrochemical detection	284
4. Conclusions	293
List of abbreviations	293
References	294

Chapter 8 Conducting Polymers for DNA Sensors and DNA Chips: from Fabrication to Molecular Detection

Pascal Mailley, André Roget and Thierry Livache

1. Introduction	297
2. ECP-based genosensors: Design and fabrication	298
3. DNA hybridisation detection at ECP–DNA interfaces	310
4. Conclusions	324
List of abbreviations	325
References	325

Chapter 9 Control of Chloride Ion Exchange by DNA Hybridization at Polypyrrole Electrode

Temitope Aiyekorun, Liz Thompson, Janusz Kowalik, Mira Josowicz and Jiří Janata

1. Introduction	331
2. Principle of operation	333
3. Procedures	335
4. Overview of selectivity studies	336
5. Time versus detection limit	337
6. Summary	340
Acknowledgments	341
References	342

Chapter 10 Threading Intercalators as Redox Indicators

Shigeori Takenaka

1. Introduction	345
2. What is a threading intercalator	346
3. Ferrocenylnaphthalene diimide derivatives as a threading intercalator	347
4. Immobilization of a thiolated oligonucleotide on the gold electrode	350
5. DNA sensor based on ferrocenylnaphthalene diimide as an electrochemical hybridization indicator	352
6. SNP detection with a ferrocenylnaphthalene diimide-based DNA sensor	354
7. Mediated current in DNA detection	359
8. Electrochemical gene detection based on supramolecular complex formation	360
9. DNA chips based on ferrocenylnaphthalene diimide	362
10. Conclusion	363
List of abbreviations	364
Acknowledgments	364
References	365

Chapter 11 Nanoparticle-Based Electrochemical DNA Detection

Joseph Wang

1. Introduction	369
2. Nanoparticle-based bioelectronic detection of DNA	371

3. Conclusions	381
Acknowledgments	382
References	382

Chapter 12 Detecting DNA Damage with Electrodes

Miroslav Fojta

1. Introduction	386
2. Relations between DNA damage and the DNA electrochemical behavior	389
3. Electrochemical sensors for DNA damage	394
4. Electrochemically controlled DNA damage	405
5. Non-covalent DNA interactions with genotoxic substances	407
6. Detection of mutations in DNA sequences	411
7. Applications	413
8. Conclusions	415
List of abbreviations	416
Acknowledgments	417
References	418

Chapter 13 Sensors for Genotoxicity and Oxidized DNA

James F. Rusling

1. Introduction	433
2. Constructing ultrathin sensor films	434
3. Voltammetric sensors for screening toxicity	438
4. Sensors for oxidized DNA	444
5. Summary and outlook for the future	448
Acknowledgments	448
References	449

Chapter 14 Electrochemical Immunosensors on the Route to Proteomic Chips

Axel Warsinke, Walter Stöcklein, Eik Leupold, Edith Micheel and
Frieder W. Scheller

1. Introduction	451
2. From immunoassays to immunosensors	452
3. Electronic protein chips	471
4. Summary and conclusion	475
List of abbreviations	476
Acknowledgments	477
References	477

Chapter 15 Self-Assembly of Biomolecules on Electrode Surfaces; Oligonucleotides, Amino Acids, and Proteins toward the Single-Molecule Level

Hainer Wackerbarth, Jingdong Zhang, Mikala Grubb, Allan Glargaard Hansen, Bee Lean Ooi, Hans Erik Mølager Christensen and Jens Ulstrup

1. Introduction	485
2. Theory and experiment of scanning tunneling microscopy	487
3. From mononucleotides to oligonucleotides	492
4. Amino acids and protein monolayers	498
5. Concluding remarks	509
List of abbreviations	511
Acknowledgments	511
References	511

Chapter 16 Direct Electrochemistry of Proteins and Enzymes

Elena E. Ferapontova, Sergey Shleev, Tautgirdas Ruzgas, Leonard Stoica, Andreas Christenson, Jan Tkac, Alexander I. Yaropolov and Lo Gorton

1. Introduction	517
2. Haem enzymes	525
3. Copper redox proteins and enzymes	551
Acknowledgments	575
References	575

Chapter 17 Amperometric Enzyme Sensors based on Direct and Mediated Electron Transfer

Sabine Borgmann, Gerhard Hartwich, Albert Schulte and Wolfgang Schuhmann

1. Electron-transfer pathways between redox proteins and electrode surfaces	599
2. ET pathways in recognition of DNA hybridisation	629
3. Conclusion and outlook	636
List of abbreviations	637
References	637

Chapter 18 Catalytic Hydrogen Evolution at Mercury Electrodes from Solutions of Peptides and Proteins

Michael Heyrovský

1. Catalytic reactions in electrochemistry	657
2. Catalytic hydrogen evolution at electrodes	658
3. Catalysis by peptides and proteins	668
4. Summary and conclusions	679
List of abbreviations	680
References	680

Chapter 19 Electroactivity of Proteins: Possibilities in Biomedicine and Proteomics

Emil Paleček

1. Introduction	690
2. Electroactivity of peptides at carbon and mercury electrodes	694
3. Electroactivity of proteins	701
4. Redox states of peptides and proteins	716
5. Aggregation of proteins	718
6. Signals of thiolated oligodeoxynucleotides in cobalt-containing solutions	725
7. DNA–protein interactions	726
8. Introduction of electroactive markers to probe the protein structure	732
9. Summary and conclusion	736
List of abbreviations	739
Acknowledgments	740
References	740

Chapter 20 Polarography of Proteins: A History

Petr Zuman and Emil Paleček

1. Introduction	755
2. Electrochemistry of proteins	756
3. Summary and conclusions	765
Acknowledgments	765
References	765

Index	773
--------------	-----

Contributors

Numbers in parentheses indicate the pages where the authors' contributions can be found.

T. Aiyeorun (331), Georgia Institute of Technology, School of Chemistry and Biochemistry, Atlanta, GA, USA

J. Albers (247), Department of Biotechnical Microsystems, Fraunhofer Institute for Silicon Technology, Fraunhoferstr.1, Itzehoe, Germany

S. Billová (751), Institute of Biophysics, Academy of Sciences of the Czech Republic, Královopolská 135, 61265 Brno, Czech Republic

L. Blohm (247), eBiochip Systems GmbH, Itzehoe, Germany

S. Borgmann (599), Anal. Chem. – Elektroanalytik & Sensorik, Ruhr-Universität Bochum, Bochum, Germany

H.E.M. Christensen (485), Department of Chemistry, Technical University of Denmark, Lyngby, Denmark

A. Christenson (517), Department of Analytical Chemistry, Lund University, Lund, Sweden

V. Dharuman (247), Department of Biotechnical Microsystems, Fraunhofer Institute for Silicon Technology, Fraunhoferstr.1, Itzehoe, Germany

B. Elsholz (247), Department of Biotechnical Microsystems, Fraunhofer Institute for Silicon Technology, Fraunhoferstr.1, Itzehoe, Germany

E.E. Ferapontova (517), Department of Analytical Chemistry, Lund University, Lund, Sweden & Group of Bioinformatics, Novosibirsk IT center, Voskhod 26a, Novosibirsk 630102, Russia

M. Fojta (385), Institute of Biophysics, Academy of Sciences of the Czech Republic, Královopolská 135, 61200 Brno, Czech Republic

A. Frey (247), Infineon Technologies AG, Corporate Research, Munich, Germany

Lo Gorton (517), Department of Analytical Chemistry, Lund University, Lund, Sweden

M. Grubb (485), Department of Chemistry, Technical University of Denmark, Lyngby, Denmark

A. Hanisch (247), Department of Biotechnical Microsystems, Fraunhofer Institute for Silicon Technology, Fraunhoferstr.1, Itzehoe, Germany

A.G. Hansen (485), Walter Schottky Institut, Technische Universität München, 85748 Garching, Germany

G. Hartwich (599), Anal. Chem. – Elektroanalytik & Sensorik, Ruhr-Universität Bochum, Bochum, Germany

- S. Hason** (17), Institute of Biophysics, Academy of Sciences of the Czech Republic, Královopolská 135, 61265 Brno, Czech Republic
- M. Heyrovský** (657), J. Heyrovský Institute of Physical Chemistry, Academy of Sciences of the Czech Republic, Dolejškova, Prague, Czech Republic
- R. Hintsche** (247), CTO/CSO eBiochip Systems GmbH, Fraunhoferstr. 1, Itzehoe, Germany
- F. Hofmann** (247), Infineon Technologies AG, Corporate Research, Munich, Germany
- B. Holzapfl** (247), Infineon Technologies AG, Corporate Research, Munich, Germany
- J. Janata** (331), Georgia Institute of Technology, School of Chemistry and Biochemistry, Atlanta, GA, USA
- F. Jelen** (73), Institute of Biophysics, Academy of Sciences of the Czech Republic, Kralovopolska 135, 61265 Brno, Czech Republic
- M. Josowicz** (331), Georgia Institute of Technology, School of Chemistry and Biochemistry, Atlanta, GA, USA
- E. Katz** (195), Institute of Chemistry, The Hebrew University of Jerusalem, Jerusalem, Israel
- J. Kowalik** (331), Georgia Institute of Technology, School of Chemistry and Biochemistry, Atlanta, GA, USA
- E. Leupold** (451), Department of Analytical Biochemistry, Institute of Biochemistry and Biology, University of Potsdam, Karl-Liebknecht-Strasse, Golm, Germany
- T. Livache** (297), CEA Grenoble, 17 Avenue des Martyrs 38054, Grenoble Cedex 9, France
- F. Lucarelli** (279), Department of Chemistry, University of Florence, Italy
- P. Mailley** (297), CEA Grenoble, 17 Avenue des Martyrs 38054, Grenoble Cedex 9, France
- G. Marrazza** (279), Department of Chemistry, University of Florence, Italy
- M. Mascini** (279), Department of Chemistry, University of Florence, Italy
- E. Micheel** (451), Department of Analytical Biochemistry, Institute of Biochemistry and Biology, University of Potsdam, Karl-Liebknecht-Strasse, Golm, Germany
- E. Nebling** (247), Department of Biotechnical Microsystems, Fraunhofer Institute for Silicon Technology, Fraunhoferstr.1, Itzehoe, Germany
- B.L. Ooi** (485), Department of Chemistry, Technical University of Denmark, Lyngby, Denmark
- E. Paleček** (1, 73, 689, 755), Institute of Biophysics, Academy of Sciences of the Czech Republic, Královopolská 135, 61200 Brno, Czech Republic
- C. Paulus** (247), Infineon Technologies AG, Corporate Research, Munich, Germany
- G. Piechotta** (247), Department of Biotechnical Microsystems, Fraunhofer Institute for Silicon Technology, Fraunhoferstr.1, Itzehoe, Germany
- A. Roget** (297), CEA Grenoble, 17 Avenue des Martyrs 38054, Grenoble Cedex 9, France

- T. Ruzgas** (517), Biomedical Laboratory Science, Health and Society, Malmö University, Malmö, Sweden
- J.F. Rusling** (433), Department of Chemistry, University of Connecticut, Storrs, CT and Department of Pharmacology, University of Connecticut Health Center, Farmington, CT, USA
- C.G.J. Schabmueller** (247), Department of Biotechnical Microsystems, Fraunhofer Institute for Silicon Technology, Fraunhoferstr.1, Itzehoe, Germany
- F.W. Scheller** (451), Department of Analytical Biochemistry, Institute of Biochemistry and Biology, University of Potsdam, Karl-Liebknecht-Strasse, Golm, Germany
- M. Schienle** (247), Infineon Technologies AG, Corporate Research, Munich, Germany
- W. Schuhmann** (599), Anal. Chem. – Elektroanalytik & Sensorik, Ruhr-Universität Bochum, Bochum, Germany
- A. Schulte** (599), Anal. Chem. – Elektroanalytik & Sensorik, Ruhr-Universität Bochum, Bochum, Germany
- S. Shleev** (517), Department of Analytical Chemistry, Lund University, Lund, Sweden & Laboratory of Chemical Enzymology, A.N. Bakh Institute of Biochemistry, The Russian Academy of Sciences, Leninsky prospect 33, 119071 Moscow, Russia
- W. Stöcklein** (451), Department of Analytical Biochemistry, Institute of Biochemistry and Biology, University of Potsdam, Karl-Liebknecht-Strasse, Golm, Germany
- L. Stoica** (517), Department of Analytical Chemistry, Lund University, Lund, Sweden
- S. Takenaka** (345), Department of Materials Science, Faculty of Engineering, Kyushu Institute of Technology, Kitakyushu, Japan
- R. Thewes** (247), Infineon Technologies AG, Corporate Research, Munich, Germany
- L. Thompson** (331), Georgia Institute of Technology, School of Chemistry and Biochemistry, Atlanta, GA, USA
- J. Tkac** (517), Department of Analytical Chemistry, Lund University, Lund, Sweden
- J. Ulstrup** (485), Department of Chemistry, Technical University of Denmark, Lyngby, Denmark
- V. Vetterl** (17), Institute of Biophysics, Academy of Sciences of the Czech Republic, Královopolská 135, 61265 Brno, Czech Republic
- J. Wang** (175, 369), Department of Chemical and Materials Engineering, Arizona State University, Tempe, AZ, USA
- H. Wackerbarth** (485), Department of Chemistry, Technical University of Denmark, Lyngby, Denmark
- A. Warsinke** (451), Department of Analytical Biochemistry, Institute of Biochemistry and Biology, University of Potsdam, Karl-Liebknecht-Strasse, Golm, Germany
- B. Willner** (195), Institute of Chemistry, The Hebrew University of Jerusalem, Jerusalem, Israel

I. Willner (195), Institute of Chemistry, The Hebrew University of Jerusalem, Jerusalem, Israel

R. Woerl (247), Department of Biotechnical Microsystems, Fraunhofer Institute for Silicon Technology, Fraunhoferstr.1, Itzehoe, Germany

A.I. Yaropolov (517), Laboratory of Chemical Enzymology, A.N. Bakh Institute of Biochemistry, The Russian Academy of Sciences, Leninsky prospect 33, 119071 Moscow, Russia

J. Zhang (485), Department of Chemistry, Technical University of Denmark, Lyngby, Denmark

P. Zuman (755), Department of Chemistry, Clarkson University, Potsdam, NY, USA

Preface

The topic of this book is the electroanalytical chemistry of nucleic acids and proteins, development of electrochemical sensors and their application in biomedicine and in the new fields of genomics and proteomics. A substantial part of the book is devoted to the electrochemistry of DNA and RNA (Chapters 2 and 3) and to the development of sensors for detecting DNA damage (Chapters 12 and 13) and DNA hybridization (Chapters 3–11). After intensive coverage of several crime cases by media the popularity of DNA can be compared to that of movie stars. For many of those who know something more about the nature of DNA, it is the most interesting and most important of all molecules. It is the molecule of life. Chromosomal DNA is the largest, naturally occurring, well-defined molecule. Its relatively regular structure is closely related to the DNA functions, such as storage of genetic information, its replication and copying into RNA. Moreover, DNA (and RNA) can form excellent sensing recognition layers and many of its properties can be utilized in the development of the DNA sensors. It is the nucleotide sequence (containing the genetic information) in specific segments of the human genome, which stays in the center of attention of DNA analysis for biology, medicine, pharmacy and a number of areas of practical life. Determination of the average nucleotide sequence of the human genome (containing 3×10^9 base pairs) was a difficult and expensive task, which took several years. Now we want to have information about nucleotide sequences in specific parts of the human genome of individuals in hours or minutes. It appears that electrochemical detection can greatly contribute to such a goal.

The knowledge of nucleotide sequence in the human genome represents one of the pillars of 21st century medicine, but it does not tell us what proteins are being made where, in what amounts, under what conditions, whether and how they are postsynthetically modified, etc. Such information should be provided by proteomics. The term “proteome” (coined about 10 years ago) represents total protein complement of the genome. Among the main activities of proteomics are: (a) identification of all the proteins made in the given cell, tissue or organism; (b) determination of how the proteins interact; (c) resolving the three-dimensional structures of the proteins to find the spots where binding of drug might affect their activity. At present, 2-D gel electrophoresis, mass spectrometry and X-ray crystallography are the most important methods in proteomics (see Appendix to Chapter 19 for details).

Proteins greatly differ from DNA in their physico-chemical properties, structures and particularly in multiplicity of their functions. Their electrochemical analysis is thus more complicated, requiring multiple approaches, which take into consideration the properties of individual proteins. We may thus ask a question: Can electrochemistry extend the arsenal of methods useful in proteomics? The great potential of electrochemical analysis in proteomics,

summarized in this book, suggests that the answer to this question should be positive.

This book will tell you about recently developed highly sophisticated methods of electrochemical analysis of nucleic acids and proteins and the development of biosensors. In addition it will summarize the ways, which in the past century led to the present state of electrochemical analysis of nucleic acids and proteins.

The story began several years after the First World War in Prague (Czechoslovakia).

In 1922, Jaroslav Heyrovský invented polarography, a new electroanalytical method working with spontaneously renewed mercury dropping electrode. Shortly afterwards (1924) he constructed in collaboration with M. Shikata the first automatically recording instrument – the polarograph. The ability of proteins to catalyze hydrogen evolution at mercury electrodes, manifested by d.c. polarographic signals, was discovered only 8 years after the invention of polarography (Chapters 18 and 20). In the 1930s polarography of proteins was closely connected with the names of J. Heyrovský and R. Brdička. Polarography of proteins soon found application in medicine, particularly in oncology, and for a number of years, “Brdička’s reaction” was intensively studied as a tool in cancer diagnostics (Chapter 20). In 1959, J. Heyrovský was awarded the Nobel Prize in chemistry.

Owing to the development of new methods in protein analysis, the interest in the polarographic catalytic signals of proteins gradually weakened, and since the 1970s the attention of electrochemists turned to direct electrochemistry of a limited number of redox-active center containing proteins. This approach resulted in a very interesting branch of protein electrochemistry, the present state of which is reflected in this book (Chapters 14–17). The development of electrochemical immunosensors represents an important step toward proteomics (Chapter 14). In addition it appears that the ability of proteins to catalyze hydrogen evolution measured by modern electrochemical methods (Chapters 18 and 19) may become useful in biomedicine and proteomics (Chapter 19).

In the 1930s the nature and biological role of proteins was much better understood than those of nucleic acids. The role of DNA as a material of heredity was discovered in 1944, and its double-helical structure, closely connected to its biological functions such as storage of genetic information, replication and transcription, was discovered in 1953 by Watson and Crick. Five years later the first paper was published showing that DNA and RNA are polarographically active (Chapters 1 and 3). Further research revealed that the polarographic signals of native double-stranded DNA greatly differed from that of denatured single-stranded DNA, suggesting that bases are hidden in the interior of the native DNA molecule, while in denatured DNA they are accessible for the electrode processes. These results were in good agreement with the Watson–Crick DNA double-helical structure as well as with the concepts of DNA denaturation and renaturation, developed in the beginning of the 1960s. In contrast, these results were in contradiction to the DNA structure, proposed by L. Pauling (1953), with the sugar phosphate backbone inside the molecule and bases located on the molecule surface. Regrettably, when L. Pauling proposed his incorrect DNA model no data on polarography of DNA were yet available.

Classical d.c. polarography was poorly suitable for the analysis of chromosomal DNA, and thus from its very beginning the electrochemical analysis of DNA was carried out with the oscillopolarography at controlled alternating current (invented by J. Heyrovský in 1941), which (due to its cyclic mode) might be considered as a predecessor of cyclic voltammetry (CV) and of the present constant current chronopotentiometry. Starting from 1966 oscillographic polarography of DNA was gradually replaced by differential pulse polarography as well as by other methods, such as a.c. polarography, CV, square-wave voltammetry and constant current chronopotentiometry. These methods combined with mercury electrodes showed great sensitivity for changes in DNA conformation (Chapter 3), including minor changes resulting from damage to DNA by various chemical and physical agents (Chapters 3 and 12). In the second half of the 1970s oxidation of adenine and guanine residues in DNA and RNA at carbon electrodes was observed, marking the beginning of application of solid electrodes in nucleic acid electrochemistry (Chapters 2, 3 and 7). Introduction of electroactive markers into DNA research dates back to the beginning of the 1980s, while first DNA-modified electrodes were prepared about 5 years later.

Up to the beginning of the 1990s electrochemistry of nucleic acids was a domain of a mere handful of laboratories in Europe. Progress in genomics and particularly in the Human Genome Project in that time stimulated enormous interest in new methods capable to unravel the genetic information stored in the nucleotide sequence of DNA. Only after the construction of DNA arrays (chips) with optical detection the attempts to develop DNA chips with electrochemical detection (which is simpler and should be less expensive) have become popular among electrochemists. Since the middle of the 1990s the electrochemistry of nucleic acids and the development of DNA sensors have become a booming field involving large number of laboratories all over the world. Similar increase in the interest in electrochemistry of proteins can be expected if the electrochemical analysis meets the requirements of proteomics. This book shows that such expectations are not unrealistic.

Electrochemistry of nucleic acids and proteins should not be a domain of electrochemists alone. It requires interdisciplinary approaches and teams including physicists, chemists, biologists as well as biotechnologists, both experimentalists and theorists. The book is thus intended for a wide variety of readers unified by their interest not only in electrochemistry of nucleic acids and proteins but also in modern biotechnologies, nanotechnologies, surface chemistry, bioelectronics, etc. It is hoped that the book will spark imagination in students and young scientists to create new tools for science and medicine of the 21st century.

Helpful assistance of Dr. Zdenek Pechan and Mrs. Petra Mittnerová and other colleagues in handling all Chapters, Figures, Permissions, etc. is gratefully acknowledged.

Brno, July 2005

Emil Paleček, Joseph Wang

This page intentionally left blank

Polarography of DNA. Retrospective View

Emil Paleček

Institute of Biophysics, Academy of Sciences of the Czech Republic, 612 65 Brno, Czech Republic

Contents

1. Introduction	1
1.1. Early studies	3
2. Retrospective view	5
2.1. Conditions for polarographic analysis of native and denatured DNAs	6
2.2. Different polarographic methods and mercury electrodes	7
2.3. DNA surface denaturation	7
3. Oscillographic polarography at controlled A.C.	8
4. Electrogenerated products	9
5. Nürnberg's cyclic voltammetry with HMDE	10
6. Summary and conclusion	11
List of abbreviations	12
Acknowledgments	12
References	12

1. INTRODUCTION

Since the discovery of the structure of the DNA double helix (1953), marking the beginning of the molecular biology, the nucleic acid research has become a vast field covered by an enormous amount of literature. When considering the history of electrochemistry of nucleic acids we may ask a question: Did electrochemistry enter this field too late, too early or in time? The answer to this question is not easy and it will depend on the person who is asked. Electrochemists believed that doing electrochemical analysis of nucleic acids in the 1950s and 1960s was too early. Their standpoint was related to several factors, some of which can be understood if the situation in different parts of the Iron Curtain-divided world is considered. In his book A.M. Bond (Bond, 1980) describes the situation as follows:

“... during the 1950s and 1960s, most large analytical laboratories and teaching institutions in English-speaking countries had only one simple d.c. polarograph, with few people familiar with its operation, and thus there was a high probability that the instrument was simply gathering dust. During this period, a most conservative and generally uninspiring approach to teaching this method of analysis inhibited the advancement of polarography; a wide gap was created between capabilities reported from research-orientated electrochemical institutions using the newer methods and those attributed to polarography in analytical laboratories which still retained ideas formulated from the use of conventional d.c. polarography. The relative decline in the routine use



Fig. 1. D.c. polarograms of a, native and b, thermally denatured calf thymus DNA at concentration of 0.5 mg mL^{-1} . DNA was denatured by heating at 100°C in 7 mM NaCl with 0.7 mM sodium citrate, pH 7.0. Both curves start at 0.0 V , $100 \text{ mV}/\text{scale}$ unit, dropping mercury electrode (DME), saturated calomel electrode; background electrolyte: 0.5 M ammonium formate with 0.1 M sodium phosphate, pH 7.0. Under the same conditions native DNA produced a well developed differential (derivative) pulse polarographic peak II; more negative peak III of denatured DNA was detectable at concentrations lower by 2–3 orders of magnitude (Section 3). Reproduced from E. Paleček and V. Vetterl, *Biopolymers* (1968, 6, 917) with permission.

of polarography, compared with the upsurge in interest of other techniques, is therefore not difficult to understand. By contrast, in Eastern European and other countries where electroanalytical chemistry has traditionally enjoyed much wider acceptance the educational problem is not evident and polarographic methods have more than held their own in popularity since the inception of the technique.”

In fact d.c. polarography was perhaps the worst electrochemical technique to study long chromosomal DNA samples available at that time (Figure 1). Availability of newer polarographic methods in Eastern European countries was of limited use in DNA analysis because in these countries, and particularly in the J. Heyrovský country, Czechoslovakia, Mendel’s genetics was considered a reactionary, bourgeois teaching almost up to 1965. In fact it was G. Mendel who 100 years earlier discovered the elements of heredity (in the city of Brno in the same country), of course, without knowing that they were composed of DNA. There were also other reasons not to analyze DNA by polarography in that time. Particularly it was a poor knowledge of DNA chemistry among electrochemists¹ and little interest

¹As late as in 1971, E. Paleček was asked after his lecture at an electrochemical meeting in Sweden: “What is this DNA? Is it something like our milk which precipitates when a storm is coming?” On the

among biochemists to learn modern polarographic and voltammetric techniques, requiring usually more skill and knowledge than e.g. optical methods. In the J.N. Davidson and E. Chargaff book *The Nucleic Acids* from 1955 (Chargaff and Davidson, 1955) a palette of methods and approaches is contained, while electrochemical methods and approaches are limited to a small paragraph (p. 120) claiming that adenine is reducible polarographically in 0.1 N perchloric acid whereas guanine, cytosine and uracil are not. From this point of view it may be concluded that electrochemical analysis entered the field of nucleic acids rather late.

In contrast, when polarography entered the field of protein research in 1930 (Heyrovsky and Babicka, 1930) (Chapter 20), the situation in this field was very different. It was only in 1951 when the alpha-helix structure in proteins was introduced by L. Pauling and in 1953 the amino acid sequence of insulin was determined by F. Sanger. Only in the beginning of the 1960s the first spatial organization of the protein molecule (myoglobin) was discovered (Dickerson, 1963; Kendrew, 1963). So, after 1930 for several decades there was a great interest in polarography of proteins as in a new method of protein analysis, particularly in relation to its application in oncology. On the other, polarography of nucleic acids in the first decades of its existence found no application in medicine or in any other practical area.

Only in the 1990s it was the progress in genome sequencing and particularly the progress of the Human Genome Project, which stimulated the field of DNA electrochemical research. After the success of electrochemical glucose sensors for diabetes, it became apparent that electrochemistry might complement the optical detection in DNA arrays and chips for parallel analysis of DNA sequences and offer less expensive devices. Knowledge of details of nucleotide sequences of the individual human genomes represents important information necessary for tailored drug prescriptions and new therapeutic approaches for individuals in the 21st century. It is hoped that electrochemical detection will decrease the costs of DNA analysis and will be particularly useful in decentralized DNA analysis.

1.1. Early studies

I started my polarographic studies of DNA and RNA as a graduate student at the Institute of Biophysics in Brno, Czechoslovakia. In 1958–1961 when I published my first papers on electroactivity of nucleic acids (Figure 2) in several journals (Paleček, 1958a, 1960a, b, 1961), including *Nature*, most of the electrochemists were oriented to the d.c. polarographic studies of relatively simple molecules. My first attempt to use polarography in nucleic acid research met with adverse reactions of most of my fellow electrochemists. There were, however, some exceptions and among them Professor J. Heyrovský was very supporting, showing extraordinary understanding and interest in the studies of

(footnote continued)

other, when the same speaker gave a talk at Gordon Conference on Nucleic acids in 1963, the response was: “Finally polarography comes in.”

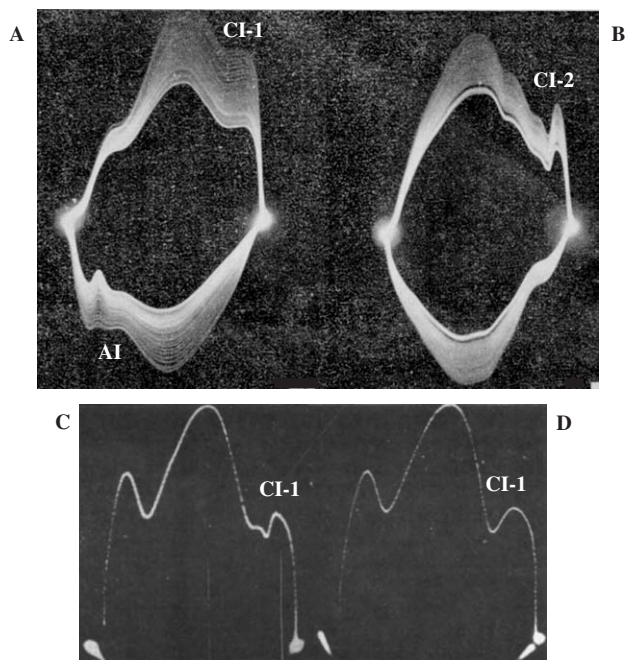


Fig. 2. (A, B) Oscillopolarograms dE/dt against (E) (A) of native calf thymus DNA at a concentration of $100 \mu\text{g mL}^{-1}$ and (B) of apurinic acid (DNA was depurinated by acid treatment). Ammonium formate (2 M) was used as background electrolyte. Note the presence of an AI due to guanine residues in the curve of native DNA and absence of this indentation in apurinic acid in which no guanine residue was present. Adapted from E. Paleček, *Nature* 1960, 188, 656 with permission. (C, D) Cathodic part of the oscillopolarogram (“first curve” method): (C) thermally denatured and (D) native calf thymus DNA at concentration of $100 \mu\text{g mL}^{-1}$. Ammonium formate (0.3 M) with 50 mM sodium phosphate (pH 7) was a background electrolyte. Note the indentation CI-2 on the curve of denatured DNA and absence of this indentation in native DNA. In (A) and (B) the dropping mercury electrode was repeatedly polarized by a sinusoidal a.c. while in the “first curve” method (C, D) only one cycle of a.c. was applied. Adapted from E. Paleček, *Biochim. Biophys. Acta* (1965, 94, 293) with permission.

DNA. Clearly he behaved as a man who knew the importance and at least some properties of DNA. Thanks to Professor R. Kalvoda few years ago I saw a photo of J. Heyrovský from the Nobel Prize ceremony and I identified two scientists standing next to Professor J. Heyrovský (Figure 3) as Severo Ochoa and Arthur Kornberg. They received their awards for their work on RNA and DNA biosynthesis. Naturally meeting these men in the great days of J. Heyrovský Nobel Prize award most probably stimulated his interest in nucleic acid electrochemistry. In 1960 he awarded E. Paleček the J. Heyrovský Prize for Young Scientists.

Since the end of 1950s research in polarography of nucleic acids developed for about a decade in East European countries (particularly in Brno, Czechoslovakia, Jena, GDR and Warsaw, Poland). Moreover, already in 1961 I.R. Miller in

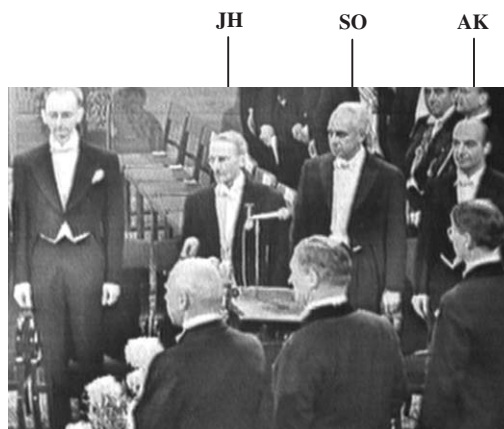


Fig. 3. Photograph from the Nobel Prize Ceremony (1959). Jaroslav Heyrovský (JH) standing next to Severo Ochoa (SO) and Arthur Kornberg (AK). SO and AK were awarded for their research into RNA and DNA. The photo was kindly provided by Dr. Michael Heyrovský.

Rehovot, Israel measured the differential capacitance of the DME double layer in solutions of DNA and RNA and described the adsorption/desorption properties of DNA, including the desorption peak, later denominated as peak 1. He mentioned the possibility of DNA unwinding at the positively charged electrode surface. Hanging mercury drop electrode (HMDE) was used by Berg's group in Jena to perform a.c. voltammetry of DNA. In the beginning of the 1970s Nürnberg's group in Jülich, BRD, applied linear sweep voltammetry (in combination with HMDE) for the study of native (ds) and denatured (ss) DNAs. Contribution of the Nürnberg's group will be briefly summarized below (Section 5). Shortly after Nürnberg, a French group of J. Reynaud in Orleans arrived with the application of phase-sensitive a.c. polarography (Reynaud, 1977, 1980). Using phase-in mode of this method they showed a new peak of native dsDNA corresponding the derivative pulse polarography (DPP) peak II (cf. Chapter 3).

2. RETROSPECTIVE VIEW

Considering the present goals of electrochemistry of nucleic acids (i.e., the development of the DNA hybridization sensors), the most important steps in the research of electrochemistry of NAs in the first 3 to 4 decades can be summarized.

- (a) Finding of conditions enabling measurements of DNA (and RNA) reduction and capacitive signals under conditions close to physiological (1958–1961) (Paleček, 1958b, 1960a, b, 1961).
- (b) Excellent resolution of ds and ssDNA on mercury electrodes and the ability to follow DNA denaturation and renaturation (Paleček, 1964, 1965, 1965a, b,

- 1966; Paleček and Janík, 1962; Paleček and Frary, 1966). Oscillographic polarography at controlled a.c., differential pulse polarography and a.c. polarography proved to be suitable for this purpose (1962–1966).
- (c) High sensitivity of DPP to DNA damage inducing minor changes in DNA structure (1967–1969) (Paleček, 1967, 1968, 1969).
 - (d) Studies of weak DNA interactions with small molecules binding preferentially to dsDNA, such as intercalators, used later as, “redox indicators.” This work started by Berg *et al.* in Jena (Berg, 1976; Berg and Eckardt, 1970; Berg *et al.*, 1981; Berg and Schütz, 1970; Berg and Bär, 1967) and later it has been continued by a number of other authors (Chapter 3).
 - (e) Discovery of the DNA surface denaturation at a negatively charged electrode surface (1974) and its dependence on pH and intactness of the DNA duplex (Paleček, 1974; Valenta and Grahmann, 1974; Valenta and Nürnberg, 1974a; Brabec and Paleček, 1976a, b; Nürnberg and Valenta, 1976) (Chapter 3).
 - (f) Application of carbon electrodes in nucleic acid research (1978). With these electrodes guanine and adenine residues in nucleic acids produced voltammetric oxidation signals (Brabec and Dryhurst, 1978; Brabec, 1981).
 - (g) Introduction of covalently bound electrochemical markers into DNA (1981–1984) (Lukasova *et al.*, 1982; Lukasova *et al.*, 1984; Paleček and Hung, 1983; Paleček and Jelen, 1984; Paleček *et al.*, 1981; Paleček *et al.*, 1984); reviewed in (Paleček, 1992).
 - (h) Conception of DNA analysis by DNA-modified electrodes (1986). This conception made it possible not only to use the immobilized DNA as a recognition layer but also to reduce the volume of DNA sample from milliliters to microliters, making thus possible to analyze samples whose large-scale preparation was laborious and/or expensive (Paleček, 1988; Paleček and Postbieglová, 1986).

Other important steps not directly related to the DNA sensors were reviewed elsewhere (Paleček, 1981, 1996, 2002). Some of the above points are discussed in Chapter 3 of this book or elsewhere in the literature (Paleček *et al.*, 2002), others will be briefly commented below.

2.1. Conditions for polarographic analysis of native and denatured DNAs

It was shown that efficient screening of the polyanionic DNA is necessary to obtain well-developed signals of ssDNA at neutral pH. Moreover, in the reduction of ssDNA at this pH, protonation of adenine and cytosine was involved. 0.3–0.6 M ammonium formate buffered to neutral pH and other ammonium salts, as well as CsCl proved well suited as background electrolytes. In these electrolytes, the large difference in the responses of native dsDNA and denatured ssDNA were observed. At acid pH values the difference between ss and dsDNA decreased probably due to protonation of dsDNA destabilizing the DNA structure and attracting dsDNA to the negatively charged surface. At low NaCl concentrations faradaic responses of ssDNA at neutral pH were very

small or absent. Probably this was one of the reasons why for some time DNA was erroneously claimed in the literature as non-reducible.

2.2. Different polarographic methods and mercury electrodes

It was the DME in combination with methods working with small voltage excursion during the drop lifetime, which produced DNA responses reflecting changes in the DNA structure in solution. DNA renaturation and hybridization was discovered by J. Marmur *et al.* at Harvard University in 1960–1963 (Marmur *et al.*, 1963). Polarography was among the first techniques capable to follow DNA renaturation (1961). DNA renaturation/hybridization is the main principle of the functioning of the DNA recognition layer in the DNA hybridization sensors. The role of DME in the DNA analysis was not well understood for a long time. Some results obtained with DME and HMDE greatly differed. These problems are discussed in Chapter 3.

2.3. DNA surface denaturation

Interestingly, DNA surface denaturation was independently demonstrated in the same year by Nürnberg *et al.* at HMDE at weakly acid pH (Valenta and Grahmann, 1974; Valenta and Nürnberg, 1974a) and by Paleček at DME at neutral pH (Paleček, 1974). Naturally, data obtained by these authors greatly differed from each other but the conclusion was the same: DNA is denatured/unwound at the electrode surface. At first sight it appears strange that such DNA denaturation was observed at DME. The reason was that a method working with large voltage excursions during the drop lifetime, i.e., the normal pulse polarography (NPP) was used. This method holds the initial potential almost through the whole drop lifetime and only at the end of the drop time a voltage pulse is applied. Using this method the dsDNA responses strongly depended on the initial potential, suggesting that DNA is denatured at the electrode surface only in a narrow potential range around -1.2 V. In this potential range dsDNA produced a peak, characteristic for denatured ssDNA. This peak was not observed in native dsDNA by differential pulse polarography and other polarographic methods working with small voltage excursions during the drop life time. Using linear sweep voltammetry with HMDE at pH 5.6 Nürnberg *et al.* did not observe the strong dependence of the dsDNA responses on the initial potential. Such dependence was however later found at pH 6.0. The DNA surface denaturation was studied by means of different techniques by Nürnberg's and Paleček's groups for several years. Their studies provided a complex picture of the DNA interfacial behavior and its dependence on pH (Chapter 3). The conclusions made by both groups were opposed by Berg who tried to explain the experimental results by the DNA conductivity and other hypothetical properties of chromosomal DNA adsorbed at the mercury surface. His speculations have never been confirmed. For several years, not very well-founded discussions on DNA structure at the mercury electrodes were the usual

parts of bioelectrochemical meetings, where only few people understood the merits of the controversy. DNA surface denaturation was recently detected also by surface plasmon resonance at negatively charged gold electrode and at other surfaces by various methods (Chapter 3).

3. OSCILLOGRAPHIC POLAROGRAPHY AT CONTROLLED A.C.

Less than 20 years after his discovery of d.c. polarography, Jaroslav Heyrovský arrived with a new polarographic method, the so-called oscillographic polarography at controlled a.c. (Heyrovský, 1941). In this method, the dropping mercury electrode was polarized by an alternating current of frequency 50 Hz and changes of the electrode potential were measured in dependence on time (Heyrovský and Forejt, 1943, 1953; Kalvoda, 1963, 1965, 2002). Usually derivative curves were recorded, such as dE/dt against t or dE/dt against E . The latter function yielding an oval-shaped curve (Figure 2) was more frequently used. The upper part of this curve showed the course of the cathodic polarization in the range from about 0 to -2 V (depending on the background electrolyte composition). The lower part displayed the anodic polarization from -2 V back to zero. Two striking bright points were observed on the oscilloscope screen: One, marking the most positive potentials (on the left, Figure 2), was due to mercury dissolution and the other one was due to discharge of the cation of the background electrolyte. Presence of an electroactive substance (depolarizer) in the solution was manifested by indentations (incisions). Potentials of these indentations corresponded to half-wave potentials in d.c. polarography. Comparison of the potentials of the indentations provided an information about reversibility of the given electrode process. The area or depth of the indentations depended on concentration of the analyte, similarly to the height of the d.c. polarographic wave. Both redox and adsorption/desorption phenomena were reflected by this method. The method was very fast and simple, possessing advantages of its cyclic mode, later appreciated in cyclic voltammetry.

Due to the division of the world by the Iron Curtain, oscillographic polarography was, with a few exceptions, a domain of Czechoslovakian and later East European scientists. The method was applied with a great enthusiasm by a group of scientists but most of the well-known Czech electrochemists were rather sceptical about the importance of this technique. Nevertheless, several international meetings at the Smolenice Castle in Slovakia at the beginning of the 1960s showed the power and versatility of the new polarographic technique.

First commercially available instrument for the oscillographic polarography, Polaroscope P 524 was produced in Czechoslovakia already in the first half of the 1950s. In contrast, instruments for cyclic voltammetry (CV) became commercially available only at the end of the 1960s. First instruments for CV were developed by Randles (1948) and Sevcik (1948). Of course, Polaroscope P 524 was based on simple technology not corresponding to the technological development in the Western countries. Its price was amazing – about 3000 Kcs, that

is less than 100US\$. In my laboratory, we constructed in 1962 a multi-functional instrument, using constant rectangular a.c., capable to display single-sweep oscillograms at different frequencies (Figure 2C, D).

I recall our excitement when we (biochemistry students D. Kalab, Z. Pechan and myself) were told in 1954 by our supervisor Professor V. Moravek to bring the newly bought Polaroscope P 524 to the laboratory for our diploma work. With Polaroscope P 524, we observed indentations of a number of biologically important compounds, such as various amino acids (Kalab, 1955, 1956; Kalab and Franek, 1955) which did not produce any signals with d.c. polarograph, which we had in our laboratory.

After finishing my university studies I joined the Institute of Biophysics of the Czechoslovak Academy of Sciences where I was asked to study effects of ionizing radiation on DNA. In poorly equipped laboratories of this institute there was a little hope that I can get some publishable results. With the experience from my university studies I soon realized that, under the given conditions, oscillographic polarography might be a right technique to analyze DNA.

The anodic indentation (AI) of DNA (Figure 2) and guanine was a typical oscillographic phenomenon requiring its cyclic mode, which could not be observed by d.c. polarography. On the other hand, the indentation CI-2 (Figure 2) had a counterpart in the d.c. polarographic wave (Figure 1) but the concentration of denatured DNA required for the d.c. polarographic analysis was too high². Naturally, d.c. polarography yielded no significant analogy to the capacitive indentation CI-1 of native and denatured DNA (Figures 1 and 2).

There is no doubt that oscillographic polarography at controlled a.c. was an indispensable part of the beginning of electrochemical research of nucleic acids. In the middle of the 1960s Barker's differential pulse polarography (DPP) gradually replaced this method. DPP was a good substitute only for the cathodic part of the oscillogram, offering no analogy to the oscillogram anodic part. Almost 10 years later, cyclic voltammetry (CV) was used in nucleic acid research (Section 5), without considering the anodic signal of guanine residues. It took another 10 years before responses of DNA guanine residues were studied by CV and square wave voltammetry (Chapter 3).

Regretfully, the potentialities of oscillographic polarography at controlled a.c. (constant a.c. chronopotentiometry, according to the present nomenclature) were not fully utilized in the 1960s. After about 40 years we are discovering the power of the constant current chronopotentiometry in nucleic acid (Chapter 3) and protein electrochemical research (Chapter 19).

4. ELECTROGENERATED PRODUCTS

Macroscale electrolysis was performed on a mercury pool electrode with denatured DNA (Brabec and Paleček, 1970a), as well as with the synthetic homopolyribonucleotides, such as poly(C) (Brabec and Paleček, 1970b) and

²High concentrations of DNA should be avoided during the denaturation to prevent DNA aggregation after removal of the denaturation conditions.

poly(A) (Brabec and Paleček, 1973). In addition, electrolysis of DNA was also carried out at the mercury drop electrode (Brabec and Paleček, 1970b). These experiments clearly showed reduction of adenine and cytosine residues in the studied nucleic acids, manifested by changes in the UV absorption spectra of the reduction products. Electrolysis of DNA and poly(C) but not of poly(A) was accompanied by the formation of an insoluble product containing, in addition to the reduced material, also a small fraction of unreduced bases.

5. NÜRNBERG'S CYCLIC VOLTAMMETRY WITH HMDE

In the beginning of the 1970s Nürnberg's laboratory in Jülich (BRD) entered the field of nucleic acid electrochemistry. In that time Hans Wolfgang Nürnberg was an experienced electrochemist with a good knowledge of modern polarographic/voltammetric methods. His collaboration with Geoffrey Cecil Barker³ gave him an insight into advanced polarographic techniques such as derivative and normal pulse polarography (invented by G.C. Barker). Surprisingly, Nürnberg did not start his research of nucleic acids with these methods but with triangular sweep voltammetry [reviewed in (Nürnberg and Valenta, 1976)] (Nürnberg and Valenta, 1977), probably because pulse polarography was already used almost for a decade in Paleček's laboratory (Paleček, 1966) [reviewed in (Paleček, 1971, 1980, 1983)] while results of CV with HMDE were missing. In addition to CV, Nürnberg *et al.* applied also phase-sensitive a.c. voltammetry and other sophisticated techniques such as his "double-step sweep technique," which they successfully applied in studies of the DNA surface denaturation. One of the closest collaborators of H.W. Nürnberg was P. Valenta from the J. Heyrovský's Institute who immigrated to Germany after the Soviet invasion to Czechoslovakia in 1968.

Nürnberg's systematic studies covered electrochemical behavior of nucleic acid components, small oligonucleotides, native and denatured chromosomal DNA and some biosynthetic polynucleotides (Valenta and Grahmann, 1974; Valenta and Nürnberg, 1974a, b; Nürnberg and Valenta, 1976, 1977; Nürnberg, 1978; Sequaris *et al.*, 1981b, 1985a, b; Czochralska *et al.*, 1985). The results of Nürnberg's group were basically in agreement with those of oscillographic polarography at controlled a.c., showing irreversible reduction of protonated denatured DNA in an adsorbed state and significant differences between the behavior of native and denatured DNA. Compared to a.c. oscillopolarography, methods used by Nürnberg were better suited for quantitative evaluation and calculation of some electrochemical parameters. Moreover, when working with HMDE, blocking of the electrode by the reduction product was much more

³G.C. Barker not only pioneered the modern polarographic methods and instrumentation, which became of great use in nucleic acid electrochemistry but he also applied square wave voltammetry and his more recently developed modulation polarography to DNA and RNA analysis (Barker and McKeown, 1976; Barker and Gardner, 1992). Already in the 1980s he draw some conclusions about the DNA conductivity from his photo-polarographic studies (Barker, 1986, 1987). His contribution to the nucleic acid electrochemistry was recently discussed (Paleček, 2002; Paleček and Heyrovský, 2002).

significant than in differential pulse polarographic experiments with DME. Perhaps the most important result of the Nürnberg's group was the discovery of the surface denaturation (deconformation) of native dsDNA at HMDE in 1974 (Brabec and Paleček, 1976a; Valenta and Nürnberg, 1974a). In the same year Paleček independently observed DNA surface denaturation at DME when using normal pulse polarography at neutral pH (Paleček, 1974) (Section 2.3., Chapter 3). To escape the necessity of using ammonium formate or other salts to follow DNA reduction at neutral pH, Nürnberg *et al.* measured at pH 5.6, where no special salts were necessary. At this pH, native DNA adsorbed at the electrode was significantly protonated and the positive charges markedly affected its surface denaturation. Nevertheless, both Nürnberg's and Paleček's data clearly showed that dsDNA is denatured at the electrode surface. The effect of interaction of DNA with the electrically charged surfaces is at present again an interesting topic closely related to the development of DNA sensors and to modeling of DNA interactions with membranes and other surfaces in cells (Chapter 3). In the first half of the 1980s Nürnberg extended his research by introducing surface-enhanced Raman spectroscopy in nucleic acid electrochemistry (Ervin *et al.*, 1980; Koglin *et al.*, 1985; Sequaris *et al.*, 1981a) and by studies of nucleic acid interactions with metals (Kaba *et al.*, 1985) and voltammetric detection of DNA damage (Sequaris *et al.*, 1982, 1985b). Sudden death of Hans Wolfgang Nürnberg on his way to the Electrochemical Society meeting in 1985 represented a great loss for the development of electrochemistry and particularly of the field of nucleic acid electrochemical research.

6. SUMMARY AND CONCLUSION

First report on polarographic reducibility of adenine dates back to 1946. Electroactivity of nucleic acids and of the rest of their monomeric constituents was briefly described by Paleček in 1958 (Paleček, 1958b) followed by more detailed studies in the next 3 years (Paleček, 1960a, b, 1961). DNA constituents were studied in detail in Elving's laboratory at the University of Michigan, Ann Arbor reviewed in (Janik and Elving, 1968). In the 1960s Paleček's laboratory at the Institute of Biophysics, Czechoslovak Academy of Sciences in Brno was oriented mainly to polarography of DNA. Using oscillographic polarography at controlled a.c. it was shown in the beginning of 1960s that denatured ssDNA is reducible at the mercury electrode and that signals of native dsDNA greatly differ from those of ssDNA [reviewed in (Paleček, 1969, 1971, 1976)]. In 1961 Miller studied DNA and RNA adsorption at the dropping electrode using the bridge method (Miller, 1961a, b). Soon it was recognized that electrochemical methods are useful tools in studies of DNA denaturation and renaturation/hybridization. These methods brought an early evidence of DNA premelting and polymorphy of the DNA double helix (Paleček, 1976).

D.c. polarography was of little use in studies of long chromosomal DNA molecules because its sensitivity was too low for the given purpose (Paleček and Vetterl, 1968). In the middle of the 1960s derivative (differential) pulse polarography complemented the oscillographic polarography and the former method

dominated the field in the following decades. Also other methods, such as a.c. polarography, normal pulse polarography (NPP), linear sweep and CV at mercury electrodes were applied.

In the first years electrochemistry of nucleic acids at mercury electrodes was studied by a handful of laboratories in East Europe (H. Berg and J. Flemming, Jena, GDR; B. Czochralska, J. Filipski and M. Wrona in Warsaw, Poland; E. Paleček, B. Janik and V. Vetterl in Brno, Czechoslovakia). Later West Germany (H.W. Nürnberg in Julich), France (J.A. Reynaud in Orleans) and England (G.C. Barker, Harwell) joined the club. In 1976 Paleček's former graduate student V. Brabec visited with G. Dryhurst at the University of Oklahoma, Oklahoma City as a postdoctoral fellow. They showed that adenine and guanine residues in DNA and RNA are oxidizable at carbon electrodes. From the middle of the 1990s we have been witnessing a growing interest in electrochemistry of nucleic acids in relation to the progress in genomic and particularly in the Human Genome Project. At present electrochemists focus their investigations on creation of electrochemical sensors for DNA hybridization and DNA damage. Their results are overviewed in Chapters 3–13 and 15 of this book.

LIST OF ABBREVIATIONS

a.c.	alternating current
CV	cyclic voltammetry
DME	dropping mercury electrode
DPP	differential pulse polarography
HMDE	hanging mercury dropping electrode
dsDNA	double stranded deoxyribonucleic acid
ssDNA	double stranded deoxyribonucleic acid

ACKNOWLEDGMENTS

The author is indebted to Professor Petr Zuman for stimulating discussions and to Dr. M. Heyrovsky for critical reading of the manuscript and valuable advice. This work was supported by a grant S 5004107 of the Academy of Sciences of the Czech Republic.

REFERENCES

- Barker, C.G. and D. McKeown, 1976, Modulation polarography of DNA and some types of RNA, *Bioelectrochem. Bioenerg.* 3, 373.
Barker, G.C., 1986, Electron exchange between mercury and denatured DNA strands, *J. Electroanal. Chem.* 214, 373.
Barker, G.C., 1987, Photocurrents due to the capture of dry and hydrated electrons by nucleic acid molecules, *J. Electroanal. Chem.* 226, 171.

- Barker, G.C. and A.W. Gardner, 1992, Forty years of square-wave polarography, *Analyst* 117, 1811.
- Berg, H., 1976, Polarographic possibilities in protein and nucleic acid research. *Topics Bioelectrochem. Bioenerg.*, Vol. 1, Ed. G. Milazzo, Wiley, London, 39.
- Berg, H. and H. Bär, 1967, Photodynamische Destabilisierung der DNS-doppelhelix, *Stud. Biophys.* 3, 133.
- Berg, H. and K. Eckardt, 1970, Zur interaktion von anthracyclinen und anthracyclinonen mit DNS, *Z. Naturforsch.* 25, 362.
- Berg, H., G. Horn, U. Luthardt and W. Ihn, 1981, Interactions of antracycline antibiotics with biopolymers. Part V. Polarographic behavior of complexes with DNA, *Bioelectrochem. Bioenerg.* 128, 537.
- Berg, H. and H. Schütz, 1970, Polarographic determination of complexes of antibiotics with deoxyribonucleic acid, 480.
- Bond, A.M., 1980, *Modern Polarographic Methods in Analytical Chemistry*, Marcel Dekker, New York.
- Brabec, V., 1981, Nucleic acid analysis by voltammetry at carbon electrodes, *Bioelectrochem. Bioenerg.* 8, 437.
- Brabec, V. and G. Dryhurst, 1978, Electrochemical behavior of natural and biosynthetic polynucleotides at the pyrolytic graphite electrode a new probe for studies of polynucleotide structure and reactions, *J. Electroanal. Chem.* 89, 161.
- Brabec, V. and E. Paleček, 1970a, The influence of salt and pH on polarographic currents produced by denatured DNA, *Biophysik* 6, 290.
- Brabec, V. and E. Paleček, 1970b, The reducibility of polynucleotides and their a.c. polarographic behaviour, *J. Electroanal. Chem.* 27, 145.
- Brabec, V. and E. Paleček, 1973, Interaction of polyadenylic acid with the mercury electrode, *Z. Naturforsch.* 28c, 685.
- Brabec, V. and E. Paleček, 1976a, Interaction of nucleic acids with electrically charged surfaces II. Conformational changes in double-helical polynucleotides, *Biophys. Chem.* 4, 79.
- Brabec, V. and E. Paleček, 1976b, Interaction of nucleic acids with electrically charged surfaces III. Surface denaturation of DNA on the mercury electrode in two potential regions, *Stud. Biophys.* 60, 105.
- Chargaff, E. and J.N. Davidson, 1955, *The Nucleic Acids – Chemistry and Biology*, Eds. E. Chargaff and J.N. Davidson, Academy Press Inc., Publishers, New York.
- Czochralska, B., E. Bojarska, P. Valenta and H.W. Nürnberg, 1985, On the participation of adenine reduction in the electrochemical reduction of the coenzyme NAD⁺, *Bioelectrochem. Bioenerg.* 14, 503.
- Dickerson, R.E., 1963, X-ray analysis and protein structure. *The Proteins*. 2nd ed., Vol. II, Ed. H. Neurath, Academic Press Inc., New York, 603.
- Ervin, K.M., E. Koglin, J.M. Sequaris, P. Valenta and H.W. Nurnberg, 1980, Surface enhanced Raman spectra of nucleic acid components adsorbed at a silver electrode, *J. Electroanal. Chem.* 114, 179.
- Heyrovský, J., 1941, Použití oscilografu v polarografii, *Chem, listy* 35, 155.
- Heyrovsky, J. and J. Babicka, 1930, Polarographic studies with the dropping mercury cathode. Part XIII. Effect of albumins, *Collect. Czech. Chem. Commun.* 2, 370.
- Heyrovský, J. and J. Forejt, 1943, Oszillographische Polarographie, *Z. Phys. Chem.* 143, 77.
- Heyrovský, J. and J. Forejt, 1953, *Oscilografická polarografie*. Státní nakladatelství technické literatury (State Publishing House of Technical Literature) Prague.
- Janik, B. and P.J. Elving, 1968, Polarographic behavior of nucleosides and nucleotides of purines, pyrimidines, pyridines, and flavins, *Chem. Rev.* 68, 295.
- Kaba, L., J.M. Sequaris, P. Valenta and H.W. Nurnberg, 1985, Voltammetric study on the interaction of the heavy-metals Cd(II) and Mn(II) with transfer-RNA, DNA and other polynucleotides, *Toxicol. Environ. Chem.* 10, 103.
- Kalab, D., 1955, Einige Möglichkeiten von oscillographischen Analysen in der organischen und biologischen Chemie, *Pharmazie* 10, 528.

- Kalab, D., 1956, Anwendung der oscillographischen Polarographie zur quantitativen Analyse einiger Aminosäuren, *Pharmazie* 11, 265.
- Kalab, D. and F. Franek, 1955, Das oscillographische Verhalten einiger Aminosäuren auf der stationären Quecksilberbedeckten Platinelektrode, *Pharmazie* 10, 31.
- Kalvoda, R., 1963, Technika oscilopolarografických měření (Techniques of oscillographic measurements) in Czech. Státní nakladatelství technické literatury Praha.
- Kalvoda, R., 1965, *Techniques of Oscillographic Polarography*, Publishers of Technical Literature, Elsevier Publishing Company, Amsterdam.
- Kalvoda, R., 2002, 60 Years of oscillographic polarography and its contribution to electroanalytical stripping analysis, *Electroanal.* 14, 469.
- Kendrew, J.C., 1963, Myoglobin and the structure of proteins, *Science* 139, 1259.
- Koglin, E., J.M. Squaris, H.W. Lewinsky, P. Valenta and H.W. Nürnberg, 1985, Surface-enhanced Raman-spectroscopy (SERS) of bio-polymers, *Fresen. Z. Anal. Chem.* 321, 638.
- Lukasova, E., F. Jelen and E. Paleček, 1982, Electrochemistry of osmium-nucleic acid complexes: A probe for single-stranded and distorted double-stranded regions in DNA, *Gen. Physiol. Biophys.* 1, 53.
- Lukasova, E., M. Vojtiskova, F. Jelen, T. Sticzay and E. Paleček, 1984, Osmium-induced alternation in DNA structure, *Gen. Physiol. Biophys.* 3, 175.
- Marmur, J., R. Rownd and C.L. Schildkraut, 1963, Denaturation and renaturation of deoxyribonucleic acid. *Progress in Nucleic Acid Research*, Vol. 1, Eds. J.N. Davidson and W.E. Cohn, Academic Press, London, 231.
- Miller, I.R., 1961a, The structure of DNA and RNA in the water-mercury interface, *J. Mol. Biol.* 3, 229.
- Miller, I.R., 1961b, Temperature dependence of the adsorption of native DNA in a polarized water-mercury interface, *J. Mol. Biol.* 3, 357.
- Nürnberg, H.W., 1978, General contours of bioelectrochemical behavior of nucleic acids at charged interfaces as revealed by model studies at the interface electrode/solution, *Bioelectrochem. Bioener.* 5, 314.
- Nürnberg, H.W. and P. Valenta, 1976, Voltametric studies of the electrochemical and interfacial behaviour of DNA at charged interfaces, *Croat. Chem. Acta* 48, 623.
- Nürnberg, H.W. and P. Valenta, 1977, Bioelectrochemical behaviour and deconformation of native DNA at charged interfaces. *Ions in Macromolecular and Biological Systems*. 29th Symp. of the Colston Res. Soc. Univ. Bristol, Eds. D.H. Everett and B. Vincent, Scientifica, Bristol, 201.
- Paleček, E., 1958a, Oscillographische polarographie der nucleinsäuren und ihrer bestandteile, *Naturwissenschaften* 45, 186.
- Paleček, E., 1958b, Oscillographische polarographie der nucleinsäuren und ihrer bestandteile, *Naturwissenschaften* 45, 186.
- Paleček, E., 1960a, Oscillographic polarography of highly polymerized deoxyribonucleic acid, *Nature* 188, 656.
- Paleček, E., 1960b, Oscillographische Polarographie der Nucleinsäurekomponenten, *Collect. Czech. Chem. Commun.* 25, 2283.
- Paleček, E., 1961, Oscillographic polarography of deoxyribonucleic acid degradation products, *Biochim. Biophys. Acta* 51, 1.
- Paleček, E., 1964, Denaturation of deoxyribonucleic acids, *Abhandlungen der Deutschen Akademie der Wissenschaften zu Berlin*, 270.
- Paleček, E., 1965, Polarographic behaviour of deoxyribonucleic acids. *International symposium on macromolecular chemistry*. Prague: Preprints of scientific communications Prague, 1. Vol. 26.
- Paleček, E., 1965a, Changes in oscillographic behaviour of deoxyribonucleic acids at temperatures below denaturation temperature, *J. Mol. Biol.* 11, 839.
- Paleček, E., 1965b, A simple oscillographic technique for recognition and estimation of denatured deoxyribonucleic acid, *Biochim. Biophys. Acta* 94, 293.
- Paleček, E., 1966, Polarographic behaviour of native and denatured deoxyribonucleic acids, *J. Mol. Biol.* 20, 263.

- Paleček, E., 1967, The polarographic behaviour of double-helical DNA containing single-strand breaks, *Biochim. Biophys. Acta* 145, 410.
- Paleček, E., 1968, Deoxyribonucleic acid conformational changes at temperatures below melting temperature, *Arch. Biochem. Biophys.* 125, 142.
- Paleček, E., 1969, Polarographic techniques in nucleic acid research. *Progress in Nucleic Acid Research and Molecular Biology*, Vol. 9, Eds. J.N. Davidson and W.E. Cohn, Academic Press, New York, 31.
- Paleček, E., 1971, Nucleic acid structure analysis by polarographic techniques. *Methods in Enzymology: Nucleic Acids*, Part D, Vol. 21, Eds. L. Grossman and K. Moldave, Academic Press, New York, 3.
- Paleček, E., 1974, Normal pulse polarography of double-helical DNA: Dependence of the wave height on starting potential, *Collect. Chem. Commun.* 39, 3449.
- Paleček, E., 1976, Premelting changes in DNA conformation, *Prog. Nucl. Res. Mol. Biol.* 18, 151.
- Paleček, E., 1980, Polarographic analysis of nucleic acids, *Proc. Electroanal. Hyg. Environ., Clin. Pharm. Chem.*, Ed. W.F. Smyth, Elsevier, Amsterdam, 79.
- Paleček, E., 1981, Polarography of biopolymers, *Bioelectrochem. Bioenerg.* 8, 469.
- Paleček, E., 1983, Modern polarographic (voltammetric) methods in biochemistry and molecular biology. Part II. Analysis of macromolecules. *Topics in Bioelectrochemistry and Bioenergetics*, Vol. 5, Ed. G. Milazzo, Wiley, London, 65.
- Paleček, E., 1988, Adsorptive transfer stripping voltammetry: Determination of nanogram quantities of DNA immobilized at the electrode surface, *Anal. Biochem.* 170, 421.
- Paleček, E., 1992, Probing of DNA structure with osmium tetroxide complexes in vitro, *Meth. Enzymol.* 212, 139.
- Paleček, E., 1996, From polarography of DNA to microanalysis with nucleic acid-modified electrodes, *Electroanal.* 8, 7.
- Paleček, E., 2002, Past, present and future of nucleic acids electrochemistry, *Talanta* 56, 809.
- Paleček, E. and B.D. Frary, 1966, A highly sensitive pulse-polarographic estimation of denatured deoxyribonucleic acid in native deoxyribonucleic acid samples, *Arch. Biochem. Biophys.* 115, 431.
- Paleček, E. and M. Heyrovský, 2002, Geoffrey Cecil Barker 1915–2000 – Obituary, *Talanta* 56, 805.
- Paleček, E. and M.A. Hung, 1983, Determination of nanogram quantities of osmium-labeled nucleic acids by stripping (inverse) voltammetry, *Anal. Biochem.* 132, 236.
- Paleček, E. and B. Janík, 1962, Polarographic behavior of cytosine, *Arch. Biochem. Biophys.* 98, 527.
- Paleček, E. and F. Jelen, 1984, Nucleotide sequence-dependent opening of the DNA double helix at electrically charged surface. Charge and Field Effects in Biosystems, Eds. M.J. Allen and P.N.R. Usherwood, Abacus Press, Tonbridge, UK, 361.
- Paleček, E. and I. Postbieglová, 1986, Adsorptive stripping voltammetry of bimacromolecules with transfer of the adsorbed layer, *J. Electroanal. Chem.* 214, 359.
- Paleček, E. and V. Vetterl, 1968, Polarographic reducibility of denatured DNA, *Biopolymers* 6, 917.
- Paleček, E., M. Fojta, F. Jelen and V. Vetterl, 2002, Electrochemical analysis of nucleic acids. *The Encyclopedia of Electrochemistry*, Eds. A. J. Bard and M. Stratmann, Vol. 9, (Ed. G. Wilson), Wiley-VCH, Weinheim, 365.
- Paleček, E., F. Jelen, M.A. Hung and J. Lasovsky, 1981, Reaction of the purine and pyrimidine derivatives with the electrode mercury, *Bioelectrochem. Bioenerg.* 8, 621.
- Paleček, E., M. Vojtiskova, F. Jelen and E. Lukasova, 1984, Introduction of an electroactive marker into the polynucleotide chain: A new probe for distorted regions in the DNA double helix, *Bioelectrochem. Bioenerg.* 12, 135.
- Reynaud, J.A., 1977, A model of DNA adsorption at the Hg/electrolyte interface, *Bioelectrochem. Bioener.* 4, 380.
- Reynaud, J.A., 1980, Polarography as a tool in the investigation of interfacial behavior of nucleic acids, *Bioelectrochem. Bioenerg.* 7, 267.

- Sequaris, J.M., H.W. Nürnberg and P. Valenta, 1985b, Voltammetric studies of damages in DNA by mutagenic and carcinogenic chemicals, *Toxicol. Environ. Chem.* 10, 83.
- Sequaris, J.M., P. Valenta and H.W. Nürnberg, 1981a, Rapid differential pulse voltammetric determination of 7-methylguanine, *J. Electroanal. Chem.* 122, 263.
- Sequaris, J.M., P. Valenta and H.W. Nürnberg, 1982, A new electrochemical approach for the in vitro investigation of damage in native DNA by small gamma-radiation doses, *Int. J. Radiat. Biol.* 42, 407.
- Sequaris, J.M., P. Valenta and H.W. Nürnberg, 1985a, Application of voltammetry in the structure elucidation of bio-polymers, *Fresenius Z. Anal. Chemie* 321, 645.
- Sequaris, J.M., E. Koglin, P. Valenta and H.W. Nürnberg, 1981b, Surface-enhanced Raman-scattering (SERS) spectroscopy of nucleic-acids, *Ber. Bunsen-Gesellschaft physik. Chemie* 85, 512.
- Valenta, P. and P. Grahmann, 1974, Electrochemical behaviour of natural and biosynthetic polynucleotides at the mercury electrode. Part. 1. The adsorption of denatured deoxyribonucleic acid at the hanging mercury drop electrode, *J. Electroanal. Chem.* 49, 41.
- Valenta, P. and H.W. Nürnberg, 1974a, The electrochemical behaviour of DNA at electrically charged interfaces, *Biophys. Struct. Mech.* 1, 17.
- Valenta, P. and H.W. Nürnberg, 1974b, Electrochemical behaviour of natural and biosynthetic polynucleotides at the mercury electrode. II. Reduction of denatured DNA at stationary and dropping mercury electrode, *J. Electroanal. Chem.* 49, 55.

Electrochemical Properties of Nucleic Acid Components

Vladimír Vetterl and Stanislav Hason

*Institute of Biophysics, Academy of Sciences of the Czech Republic, Královopolská 135, 612 65
Brno, Czech Republic*

Contents

1. Introduction	18
2. Adsorption and two-dimensional condensation	18
2.1. Mercury electrodes	18
2.2. Mercury film electrodes based on the graphite substrates	23
2.2.1. Optical roughness and surface morphology of the mercury-modified graphite surfaces	23
2.2.2. Phase transitions in adsorbed nucleic acid nucleoside layers at Hg-modified graphite electrodes: experimental aspects	26
2.2.3. Adsorption and kinetics of phase transitions of adenosine at the mercury-modified graphite surfaces	28
2.2.4. Adsorption and kinetics of phase transitions of cytidine at the mercury-modified graphite surfaces	31
2.3. Solid amalgam-alloy electrodes	33
2.3.1. Optical roughness and surface morphology of the solid amalgam-alloy surfaces	34
2.3.2. Adsorption of adenosine at the different solid amalgam-alloy electrodes	34
2.4. Solid metal electrodes	36
2.4.1. Gold electrodes	36
2.4.2. Silver electrodes	41
2.4.3. Copper electrodes	44
2.4.4. Bismuth electrodes	45
2.5. Semiconductor electrodes	46
2.5.1. Single-crystal n-CdSe	46
2.5.2. Silicon	46
2.5.3. Gallium arsenide	47
2.6. Minerals, soils and resins	48
2.7. Adsorption of base and/or nucleosides mixtures	49
2.7.1. Adsorption at Hg electrode	49
2.7.2. Adsorption at Au(111)	50
2.8. Adsorption of bases at Hg from non-aqueous solvents	51
3. Electroreduction and electrooxidation of nucleic acid components	51
3.1. Electroreduction at mercury electrode	51
3.1.1. Determination of picogram quantities of DNA by stripping transfer voltammetry	53
3.2. Electrooxidation at carbon electrodes	53
3.3. Electrooxidation at diamond electrode	56

3.4. Effect of uracil adsorption on the oxygen reduction at platinum electrode	56
3.5. Sparingly soluble compounds at the mercury electrode	57
4. Concluding remarks	57
List of abbreviations	58
Acknowledgments	60
References	60

1. INTRODUCTION

The encounter of molecules at biological interfaces like cell membranes and nuclear matrix is the initial step in the biomolecular processes and a prerequisite for the manifestation of the biological effects of biopolymers in living cells (Berezney and Coffey, 1974; Neumann, 1978; Gasser and Laemmli, 1986). It has been known that electric fields having magnitudes equivalent to those existing at a charged cell surface/biological fluid interface affect the conformation of DNA in solution (Porschke and Jung, 1985; Neumann, 1986a, b). This in turn may influence its biological function. As a rough model of a biological surface/biological fluid interface an electrolyte solution–electrode interface can be employed to study the interfacial behaviour of nucleic acids. Mercury electrodes, the charge of which can be easily changed and controlled in a relatively wide range have proved to be suitable for such experiments.

The interaction of organic molecules with metal interfaces is an interesting topic for a variety of technological and fundamental applications (Buess-Herman, 1994; Kolb, 1992; Lipkowski *et al.*, 1994; Lorenz, 1958). In recent years, self-assembled thin films have drawn attention in the electrochemical context largely due to the possible applications of these materials in areas such as molecular electronics, chemical and biosensor technologies. Varying the electrode potential at an electrode–electrolyte interface may flexibly control the growth and the structure of self-assembled thin films of organic molecules. The organic thin films can be used to create interfaces for manipulating reactions in electrochemical analysis but also in electrosynthesis and electrocatalysis (Herrero *et al.*, 2001; Magnussen, 2002).

2. ADSORPTION AND TWO-DIMENSIONAL CONDENSATION

2.1. Mercury electrodes

The bases, nucleosides and nucleotides are surface-active substances. Like a number of other neutral organic molecules (Miller, 1995), they are strongly adsorbed at the mercury electrodes in a broad region of potentials with maximum adsorption usually around the potential of electrocapillary maximum. The measurement of the impedance of the electrified interfaces started to be widely used for investigation of the interactions of nucleic acids and their components with the electrode surface since 1961, when I.R. Miller (Miller, 1961a, b) published his pioneering work on differential capacitance of the mercury electrode

double layer in the solutions of nucleic acids. Differential capacitance of the electrode double layer is a sensitive indicator of the adsorption. When nucleic acids and/or nucleic acid bases, nucleosides and nucleotides are adsorbed at the electrode surface, they remove from the surface the molecules and ions of the solvent and thus lower the value of the differential capacitance of the electrode double layer, because the solvent has usually much higher dielectric permittivity than nucleic acids. Among bases guanine is most strongly adsorbed at Hg electrodes (Vetterl, 1965, 1966a, b). The dependence of surface concentration of the adsorbed molecules on their bulk concentration was described by Frumkin and Ising adsorption isotherms (Brabec *et al.*, 1996; Jehring, 1974; Retter, 1987, 1992; Retter *et al.*, 1989; Vetterl, 1966a, b).

In 1965, we have found that nucleic acid bases possess an extraordinary high ability of self-association at the electrode surface and undergoes a two-dimensional (2-D) condensation forming a monomolecular layer (Vetterl, 1965, 1966a, b). By this high condensation ability nucleic acid bases differ from most of the other purine and pyrimidine derivatives, which currently do not occur in nucleic acids (like isocytosine, isoguanine, xanthine, etc.). The 2-D condensation was observed also with some of the halogen-, aza- and methyl derivatives of common nucleic acid bases and with most of the nucleosides and nucleotides commonly occurring in nucleic acids. This interesting physical property of nucleic acid components has probably played a significant role in the origin of life on the earth (see Chapter 2.6) (Sowerby *et al.*, 1996, 1998a, b, c; Sowerby and Heckl, 1998; Sowerby and Petersen, 1997). The driving force of 2-D condensation of nucleic acid bases are hydrogen bonds between flat oriented adsorbed molecules (de Levie and Wandlowski, 1994) and/or stacking interactions between perpendicularly adsorbed molecules (Brabec *et al.*, 1977, 1979; Retter and Lohse, 1982; Retter *et al.*, 1989), i.e. forces which are responsible for the stability of the double helical conformation of DNA. It looks like the nature has chosen as building blocks of the genetic material just such compounds which show a strong ability of self-association by hydrogen bonds or stacking forces in order to maintain the stability of the genetic material.

In the presence of the compact films of nucleic acid bases, nucleosides and/or nucleotides, which are stable only in particular ranges of applied electrode potentials, all solvent molecules are replaced from the electrode surface by the condensed nucleic acid components, the differential capacitance of the electrode double layer is depressed considerably, giving rise to characteristic “pits” on capacitance–potential ($C-E$) curves and sharp spikes on cyclic voltammograms (CVs) (Buess-Herman, 1986). Such capacitance “pits” were for the first time observed by Lorenz in 1958 with the near-saturated solutions of nonanoic acid (Lorenz, 1958) and explained by the formation of condensed film at the electrode surface. The position of the current spikes on the cyclic voltammogram (CV) and the pit edges on the $C-E$ curves depend on the direction of the potential scan (hysteresis), and the width of the condensed film decreases with increasing temperature. These characteristics are typical properties of 2-D physisorbed condensed films.

From the temperature dependence of the pit width and/or from the surface tension measurements and from the course of adsorption isotherms the

interaction energies of adsorbed molecules and the area occupied per one adsorbed molecule can be determined (Brabec *et al.*, 1996). The area occupied per one adsorbed molecule gives information about orientation of molecules at the electrode surface (adenine and uracil in the planar orientation occupy about 0.60 nm^2 , in the perpendicular orientation about 0.40 nm^2) (Brabec *et al.*, 1977; Buess-Herman, 1994; Buess-Herman *et al.*, 1992; Dražan and Vetterl, 1998; Lipkowski *et al.*, 1986; Mousty and Quarin, 1990; Retter *et al.*, 1989; Temerk *et al.*, 1986). With neutral bases, the capacitance pit is usually observed near the potential of electrocapillary maximum (potential of zero charge, pzc). Halogen ions can induce a second potential region of condensation, as it was observed with cytosine (Jursa and Vetterl, 1984) and adenine (Vetterl and de Levie, 1991). The existence of two potential regions of condensation was explained by different orientation of the adsorbed molecules in these regions. The orientation of bases and nucleosides in the compact film, the effect of ions in the solvent and substituents of bases on the film formation and the energy of the interaction between bases in the compact film were investigated (Jursa and Vetterl, 1986, 1989; Brabec *et al.*, 1989; Vetterl *et al.*, 2000). Reviews of these studies were published previously (Brabec *et al.*, 1996; Paleček, 2002).

Two-dimensional first-order phase transitions of molecules adsorbed on homogeneous surfaces often proceed via nucleation and growth processes. The kinetics of the film formation can be studied by potential jump experiments. Depending on the start and final potentials different shapes of capacitance or current transients can be detected. The transients can be analysed by Avrami equation (Buess-Herman, 1994; Donner *et al.*, 1997; Retter, 1980, 1984a; Retter and Lohse, 1982; Prado *et al.*, 2001). The capacitance transients (C-t curves) have usually an S-shape with Avrami exponent $m = 2$ (instantaneous nucleation) or $m = 3$ (progressive nucleation), see Chapter 2.2.4. Unusual time dependence—slow increase of capacitance with time—was observed with uracil and explained by fractal growth (Pospíšil and Wandlowski, 1989 a,b). Oscillations were observed on C-t curves with adenine (Vetterl and de Levie, 1991). A mathematical model was developed which takes into account the simultaneous processes of adsorption of the molecules from the bulk, surface diffusion of the adsorbed molecules and their consumption at the edge of the growing nuclei. From the numerical solutions of the model equations, several regimes of the process of nucleation and growth can be obtained depending on the ratios of the system parameters. The existence of these different growth regimes was provided experimentally in: 5-bromocytosine-mercury system (Pohlmann *et al.*, 1996; Retter, 1984a, b), quinoline derivatives-mercury system (Buess-Herman and Gierst, 1984; Buess-Herman *et al.*, 1981a, b, 1983a, b) and thymine-mercury system (de Levie, 1988; Sridharan and de Levie, 1986, 1987a, b).

The role of the potential of zero charge and of the potential of maximum adsorption during the adsorption of neutral molecules at the electrode surface is not yet well understood. One of the new methods for the determination of the potential of maximum adsorption in condensed layers is based purely on a qualitative analysis of the shape of current–time transients, which change their sign at the potential of maximum adsorption and become inverted. The method was applied to the systems of thymine and adenine, respectively, adsorbed on

mercury electrodes (Donner *et al.*, 2000; Pohlmann *et al.*, 1996). The knowledge of the potential of maximum adsorption with respect to the potential of zero charge of the pure electrolyte allows to calculate the orientation and reorientation of the organic dipoles in relation to the electrode surface. It was found that the potential of maximum adsorption is a function of the temperature, the pH value and the potential of pre-polarization (Donner *et al.*, 2000; Pohlmann *et al.*, 1996).

The influence of the cell resistance on the transient current signal after applying a potential step in condensation experiments has been investigated (Donner, 2001). The cell resistance was simulated by an external resistance in order to avoid chemical and double-layer effects. It could also be shown that the shape of current transients depend sensitively on whether potentiostatic or non-potentiostatic conditions exist on the surface during the phase transitions. Potentiostatic conditions are only fulfilled for small capacities and electrolyte concentrations higher than 0.1 M on one hand and for relatively slow adsorption kinetics on the other these conditions were fulfilled for the mercury electrode. On gold electrodes in the physisorption region the simple interface model of a pure capacitor could not be applied. Probably, additional reactions take place simultaneously with the adsorption process (Donner and Kirste, 2001).

Methylation of nucleic acid bases plays an important role in molecular genetics. The intermolecular interactions between bases in nucleic acids which are involved in the processes of molecular recognition and transfer of genetic information are of a similar nature as the interactions between bases adsorbed at the electrode surface lead to a 2-D condensation. We have therefore studied the effect of methylation on the 2-D condensation of nucleic acid bases in a more detailed.

The effect of methylation on the association of adenine at pH 4.8 was studied at 5°C (Jursa and Vetterl, 1989). 1-Methyladenine does not associate on the electrode surface not even at low temperatures if the ionic strength of the solvent is low. With increasing NaCl concentration, the compact surface film is formed at 5°C only near the potential of zero charge and not on the negatively charged electrode surface unlike with adenine at the same pH 4.8. The effect of methylation on the adsorption and association of adenine derivatives and adenosine at pH 8 and 9 was studied as well; the results are summarized in Brabec *et al.* (1996).

We have compared the adsorption and 2-D condensation of 5-methylcytosine with that of cytosine. The 2-D condensation of 5-methylcytosine molecules adsorbed at the mercury surface resulting in the formation of a compact layer and capacitance pit on $C-E$ curves starts to occur at much lower bulk concentrations of 5-methylcytosine than it was observed with cytosine and it is much faster. The capacitance pit of 5-methylcytosine was observed at two different potential regions, around -0.5 and -1.2 V, (Figure 1A, B). The dependence of the $C-E$ curves on pH has shown that the capacitance pit appears in the range between pH 4 and 5.8, i.e. at the pH values close to the pK of 5-methylcytosine ($pK = 4.6$) similarly as it was observed with cytosine (Šponer *et al.*, 1996). The existence of the two separate potential regions of 2-D condensation of cytosine and 5-methylcytosine can be explained by different orientations of adsorbed cytosine and/or 5-methylcytosine molecules in the two

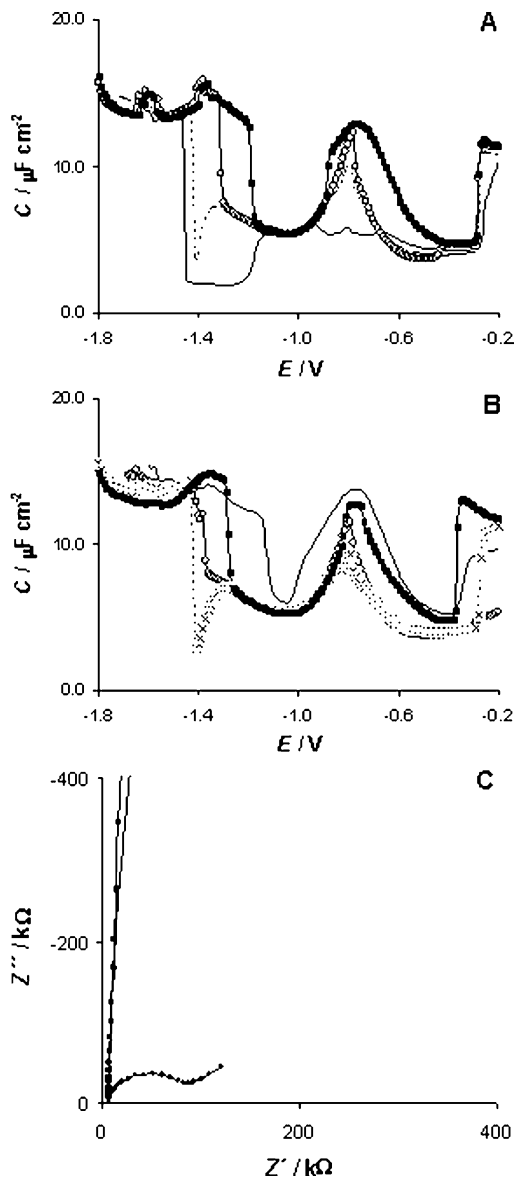


Fig. 1. (A) Temperature dependence of the capacitance–potential curves (C – E curves) of 8 mM 5-methylcytosine in 1.0 M NaCl with BR buffer at pH 5.1 on the HMDE: (—) 5°C; (...) 10°C; (○) 15°C; (■) 20°C. (B) pH dependence of the C – E curves of 5-methylcytosine at 10°C on the HMDE: (—) 4.0 pH; (○) 4.6 pH; (x) 5.1 pH; (■) 5.8 pH. Potential was scanned from positive to negative values. (C) Nyquist plot (frequency dependence of complex impedance $Z = Z' + iZ''$) of 8 mM 5-methylcytosine in 1 M NaCl with BR buffer at 10°C on the HMDE: (—) –0.8 V; (■) –1.12 V; (●) –1.5 V (Ignac and Vetterl, unpublished results).

potential regions. The peak observed around -0.8 V on the $C-E$ curves of 5-methylcytosine is obviously a tensammetric peak resulting from the reorientation of the adsorbed molecules. Electrochemical impedance spectroscopy (EIS) measurement confirms the tensammetric character of this peak (Figure 1C).

2.2. Mercury film electrodes based on the graphite substrates

More than 35 years ago it was shown that graphite substrates modified by mercury layers, which are known as mercury film electrodes (MFE), could be successfully used in electrochemical analysis and detection of traces of heavy metals in environmental or food samples in similar potential windows, to those of a mercury electrode itself (Brainina and Neyman, 1993; Brainina *et al.*, 1989; Copeland *et al.*, 1973; Florence, 1979, 1980, 1986; Frenzel, 1993; Kounaves and Deng, 1991; Kounaves *et al.*, 1986; Wikiel and Kublik, 1984; Wikiel and Osteryoung, 1989; Wu, 1994, 1996; Zakharchuk and Brainina, 1998; Zakharchuk *et al.*, 1999). The reason for this is that the Hg-modified graphite electrodes combine the advantages of graphite and mercury electrodes. It means that these electrodes have a wide interval of working potentials, adequate reproducibility of the electrode surface and are less affected by surfactants than solid metal electrodes. The use of MFEs is rather restricted due to the fact that the Hg-modified surface is stable only for a short time (from minutes to hours). The possibilities of the use of the MFEs in electrochemical analysis of different inorganic ions and organic compounds in different environmental and analytical samples have been reviewed recently (Economou and Fielden, 2003).

During the last decade the MFEs have been employed for voltammetric and/or impedance analysis of DNA, RNA and synthetic polynucleotides (Hasoň *et al.*, 2002a, b, 2005; Kostečka *et al.*, 2004; Kubičarova *et al.*, 2000a, b; Wu *et al.*, 1997).

Recently, we have shown that Hg-modified graphite electrodes can be successfully used for the study of the adsorption, 2-D condensation and formation of ordered adlayers and kinetics of the phase transition during different adlayers of nucleic acids components (Hasoň and Vetterl, 2002a, b; Hasoň *et al.*, 2003). It means that with the MFEs the effect of the surface morphology of the underlying graphite substrates on the adsorption and kinetics of the 2-D condensation of the nucleic acid components in the same potential windows as with a hanging mercury drop electrode (HMDE) can be investigated.

2.2.1. Optical roughness and surface morphology of the mercury-modified graphite surfaces

We applied a diffractive optical element (DOE)-based sensor and optical microscope (Nikon Eclipse ME600L) for the inspection of the optical roughness and visualization of the surface morphology of the bare and Hg-modified graphite surfaces, respectively. The theory of the DOE sensor and the technical

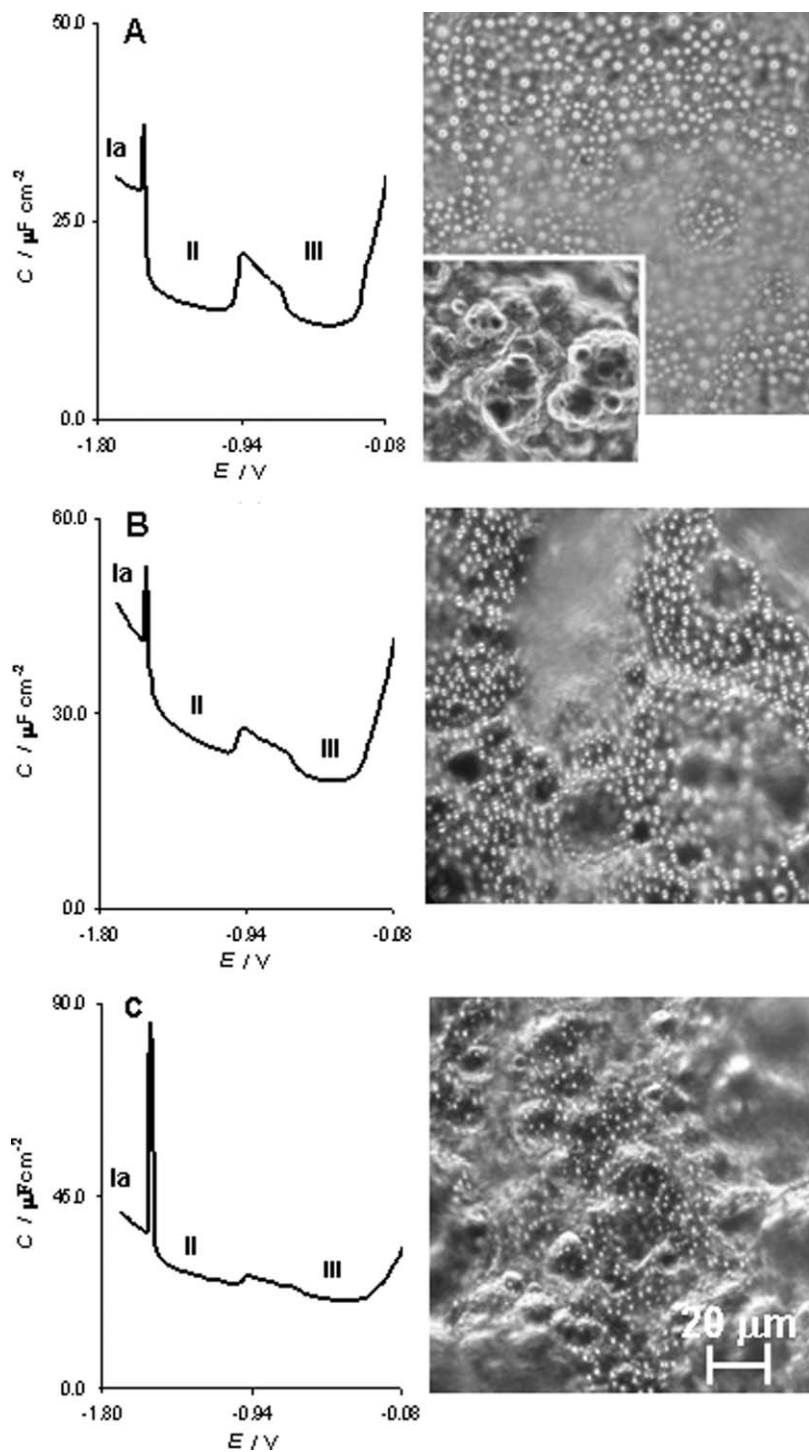
arrangement of experiments for optical surface quality measurement are described in greater detail elsewhere (Friesem and Amitai, 1996; Latta, 1971a, b; Räsänen *et al.*, 1995). In brief, the DOE sensor obeys the laws of hologram imagery since the sensing element is a computer-generated hologram. During the surface quality inspection, the reconstructed wave front from a laser (HeNe, $\lambda = 632.8$ nm) is guided via the sample surface under test to the DOE aperture (4×4 mm²). The perfectly reconstructed wave front that diffracts from the DOE used forms a 4×4 light spot matrix in its back focal plane. This means that if the electrode surface is a true rough surface, the image of the 4×4 light spot matrix in the back focal plane of the DOE will be distorted. By analysing the magnitude of the distortion in the DOE image it is thus possible to gain information about the surface quality of the electrodes studied.

The pyrolytic graphite electrode with basal orientation (PGEb) has a rough surface, corrugated with cracks (Figure 2A). The DOE images revealed that the average optical roughness R_a of the PGEb fluctuated around 0.040 μm . The glassy carbon electrode (GCE) surface is relatively smooth in comparison with the bare PGEb, with typical polishing lines running over the electrode surface (Figure 3A). The average value of R_a for GCE is about 0.034 μm .

During the Hg-electrodeposition on the PGEb surface the Hg droplets filled the small corrugations and scratches (Figure 2C, thickness about 20 nm) followed by covering also larger cavities and ruts of PGEb (Figure 2B, thickness about 100 nm). At longer deposition time the smaller mercury droplets coalesced to form a bigger one and it seems that the overall morphology of the thick Hg-modified PGEb surface becomes smoother and mercury forms a true Hg-film (Figure 2A, thickness about 500 nm). The overall magnitude of the optical roughness R_a of the 0.1 and 1 μm Hg-modified PGEb is 0.036 and 0.032 μm , respectively.

The mercury forms on the GCE surface inhomogeneously scattered droplets of different diameter (Figure 3C). The density of Hg droplets increases with the increasing thickness of the deposited Hg-layer on the GCE, but Hg-modified GCE surface still includes uncovered areas (dark spots in Figure 3A). These uncovered areas are larger on thin Hg-modified GCE (Figure 3B) than on the thick one (Figure 3A). It seems that mercury forms on the GCE droplets of different diameter gradually coalesced into bigger drops rather than a continuous film. The R_a of the 0.1 and 1 μm Hg-modified GCE surfaces were 0.052 and 0.040 μm , respectively.

Fig. 2. Capacitance–potential curves of 15 mM adenosine in 0.1 M NaCl at pH 5 on the: (A) 0.5 μm Hg-modified PGEb, (B) 0.1 μm Hg-modified PGEb and (C) 0.02 μm Hg-modified PGEb electrode. Potential was scanned from positive to negative values. The different adsorption states are labelled Ia, II and III. The temperature of measurement was 10°C. The inserts show microscope images of the: (A) unmodified and 0.5 μm Hg-modified pyrolytic graphite electrode with basal orientation (PGEb); (B) 0.1 μm Hg-modified PGEb; (C) 0.02 μm Hg-modified PGEb. Images were recorded by an optical microscope Nikon Eclipse ME600L (magnification was 1000 \times). (Part A is partially adapted from Hasoň and Vetterl, 2004, Figure 1(B), with permission from Elsevier.)



2.2.2. Phase transitions in adsorbed nucleic acid nucleoside layers at Hg-modified graphite electrodes: experimental aspects

In this chapter we have focused on the kinetics of phase transitions of the nucleoside's adlayers starting from the dilute adsorption adlayer Ia to the 2-D condensed adlayer II (Ia \rightarrow II) in acidic and/or alkaline solution at the Hg-modified graphite surfaces. The kinetics of these phase transitions were investigated by means of current transients ($j-t$ curves) using the double potential step technique (Buess-Herman, 1986).

The procedure of the double potential step was: Before the potential jump (step) we applied on the electrode the initial potential was $E_i = -1.8$ V (waiting time t at the E_i was 5 s). During this initial period, the surface of Hg-modified graphite electrode was electrochemically cleaned without any mechanical damage to the Hg-layer. After this initial period the first potential jump to the pre-treatment potential E_p follows. At E_p the dilute adsorption adlayer Ia was formed. The waiting time t at the E_p was almost 2 s. Finally, the second potential step from the pre-treatment potential E_p (dilute adlayer Ia) to different final potentials E_f in the 2-D condensed adlayer II followed. It means that during the second potential jump the phase transitions of the nucleoside's adlayers (Ia \rightarrow II) were triggered.

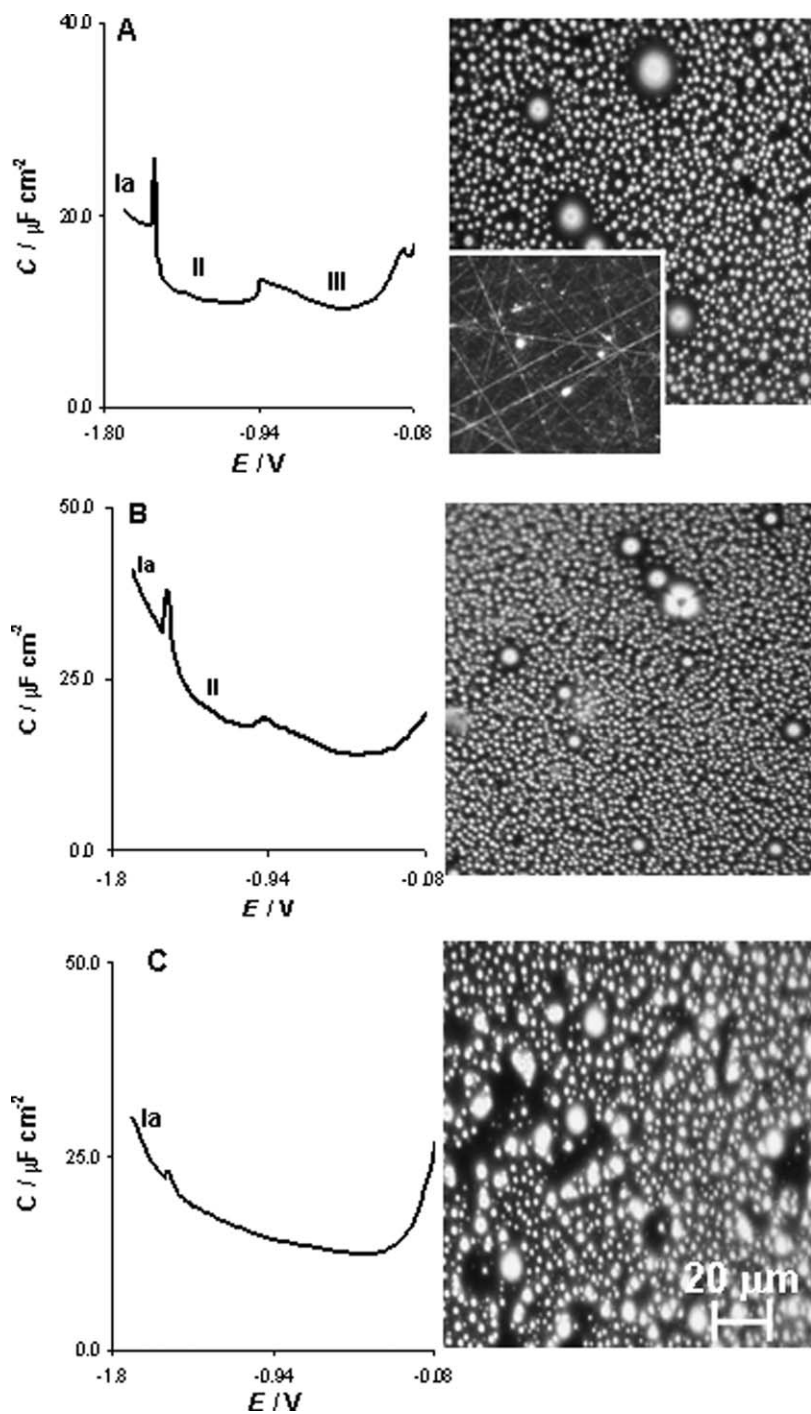
The $j-t$ curves were characterized by an exponential decay followed by a pronounced maximum and finally by a decrease of current (Figure 4A). The initial exponential decay of these $j-t$ curves can be associated with the sum of the double-layer charging due to the potential step itself and the Langmuir-type (dilute) adsorption before the nucleation starts (Kolb, 2001; Wandlowski, 2002). The current maximum is associated with a nucleation and growth process (Buess-Herman, 1992; Buess-Herman *et al.*, 1999; Fleischmann and Thirsk, 1963). The $j-t$ curves of the phase transients of Ia \rightarrow II of nucleosides were fitted (non-linear analysis) according to the equation, which is based on a generalized form of the Bewick–Fleischman–Thirsk model of 2-D polynucleation and growth (Fleischmann and Thirsk, 1963):

$$j(t) = k_1 t^{(m-1)} \exp(-k_3 t^m) + k_4 \exp(-k_5 t), \quad (1)$$

where

$$\begin{aligned} k_1 &= q_{\text{nucleation}} m k_3, \\ k_4 &= q_{\text{adsorption}} k_5, \end{aligned}$$

Fig. 3. Capacitance–potential curves of 15 mM adenosine in 0.1 M NaCl at pH 5 on the: (A) 0.5 μm Hg-modified GCE, (B) 0.1 μm Hg-modified GCE and (C) 0.02 μm Hg-modified GCE electrode. Potential was scanned from positive to negative values. The different adsorption states are labelled Ia, II and III. The temperature of measurement was 10°C. The inserts show microscope images of the: (A) unmodified and 0.5 μm Hg-modified glassy carbon electrode (GCE); (B) 0.1 μm Hg-modified GCE; (C) 0.02 μm Hg-modified GCE. Images were recorded by an optical microscope Nikon Eclipse ME600L (magnification was 1000 \times). (Part A is partially adapted from Hasoň and Vetterl, 2004, Figure 1(C), with permission from Elsevier.)



k_3 is a coefficient which combines the rates of nucleation and growth, m (Avrami exponent) reflects the dimensionality and the nature of the nucleation process, $q_{\text{nucleation}}$ corresponds to the total charge involved in the nucleation, k_5 reflects the rate coefficient of the adsorption on defects and $q_{\text{adsorption}}$ is the corresponding charge. With $m = 2$ or 3 , the first term in equation (1) reduces to the case of instantaneous ($m = 2$) or progressive ($m = 3$) nucleation, provided that we assume a constant growth rate.

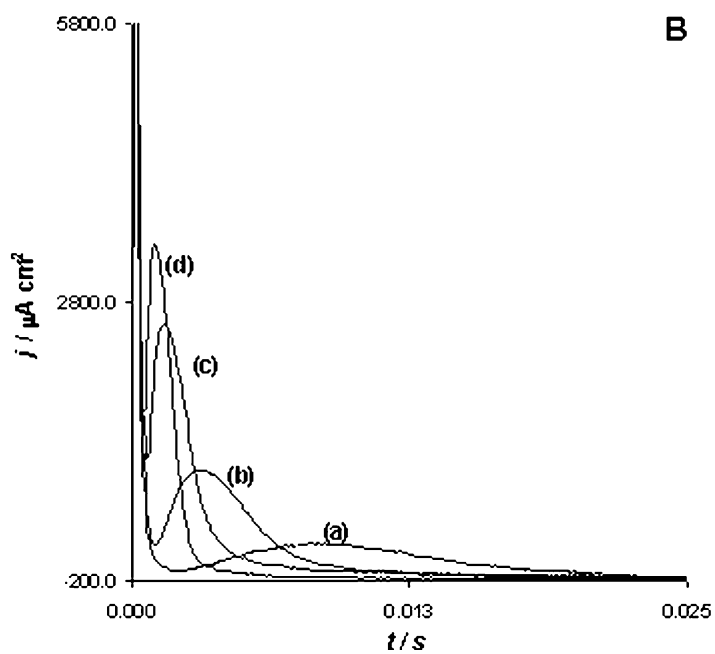
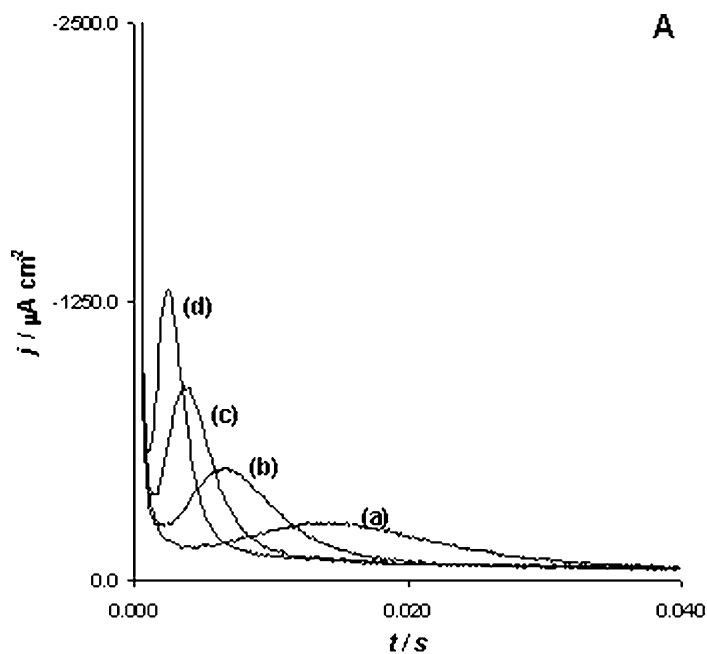
After the formation of nucleotide adlayer at the Hg-modified graphite surface the current of the current transient did not drop to zero (typical response for polynucleation and growth process detected at HMDE and/or solid metal electrodes), but crossed the zero charge lines and became negative (Figure 4B). A similar result was observed after the same potential jump with supporting electrolyte without nucleoside. It seemed that the presence of a catalytic process in the supporting electrolyte gave an additional “offset current”. Therefore, this “offset current” was subtracted from the current response.

2.2.3. Adsorption and kinetics of phase transitions of adenosine at the mercury-modified graphite surfaces

Adenosine in acid solution (pH 5) forms two different 2-D condensed films at the Hg-modified PGEb surface down to $0.02\ \mu\text{m}$ thickness, similarly to the HMDE (Figure 2A–C). The centre of the first (adlayer II) was located around $-1.2\ \text{V}$; the second 2-D film was formed at more positive potentials around $-0.5\ \text{V}$ (adlayer III). These 2-D condensed adlayers of adenosine were detected only at Hg-modified GCE surface down to $0.2\ \mu\text{m}$ thickness (Figure 3A–C).

Non-linear analysis of the phase transitions of Ia \rightarrow II of adenosine in acid solution for the time shorter than 80 ms at the $2\ \mu\text{m}$ Hg-modified PGEb can be described by a model that combines a Langmuir-type adsorption step with a nucleation according to a power law and linear growth mechanism (Avrami exponent $m = 2.44 \pm 0.02$; Figure 5A). During the Ia \rightarrow II of adenosine the offset current at the $2\ \mu\text{m}$ Hg-modified PGEb was not observed. The rate of the phase transitions Ia \rightarrow II of adenosine increases on the thinner Hg-modified PGEb, but a well-developed current maxima of Ia \rightarrow II can be observed at the thick Hg-modified PGEb (the thickness of Hg-layer is as high as $1\ \mu\text{m}$). The current maxima of the phase transitions of Ia \rightarrow II increases at the $2\ \mu\text{m}$ Hg-modified GCE in comparison with $2\ \mu\text{m}$ Hg-modified PGEb.

Fig. 4. (A–B) Experimental $j-t$ curves of 15 mM adenosine in 0.1 M NaCl at pH 5 on the $0.4\ \mu\text{m}$ platinum amalgam-alloy substrate recorded after a double potential step: (A) $E_i = -1.8\ \text{V}$, $E_p = -0.959\ \text{V}$; and (B) $E_i = -1.8\ \text{V}$, $E_p = -1.598\ \text{V}$. (A) Final potential was: (a) $-0.990\ \text{V}$; (b) $-1.005\ \text{V}$; (c) $-1.020\ \text{V}$; and (d) $-1.035\ \text{V}$. (B) Final potential was: (a) $-1.510\ \text{V}$; (b) $-1.495\ \text{V}$; (c) $-1.480\ \text{V}$; and (d) $-1.465\ \text{V}$. The waiting time at the initial (E_i) and pre-treatment (E_p) potentials was 5 s and 2 s, respectively. The temperature of measurement was 5°C . (Part B is adapted from Hasoň *et al.*, 2004, Figure 11(A), with permission from Elsevier.)



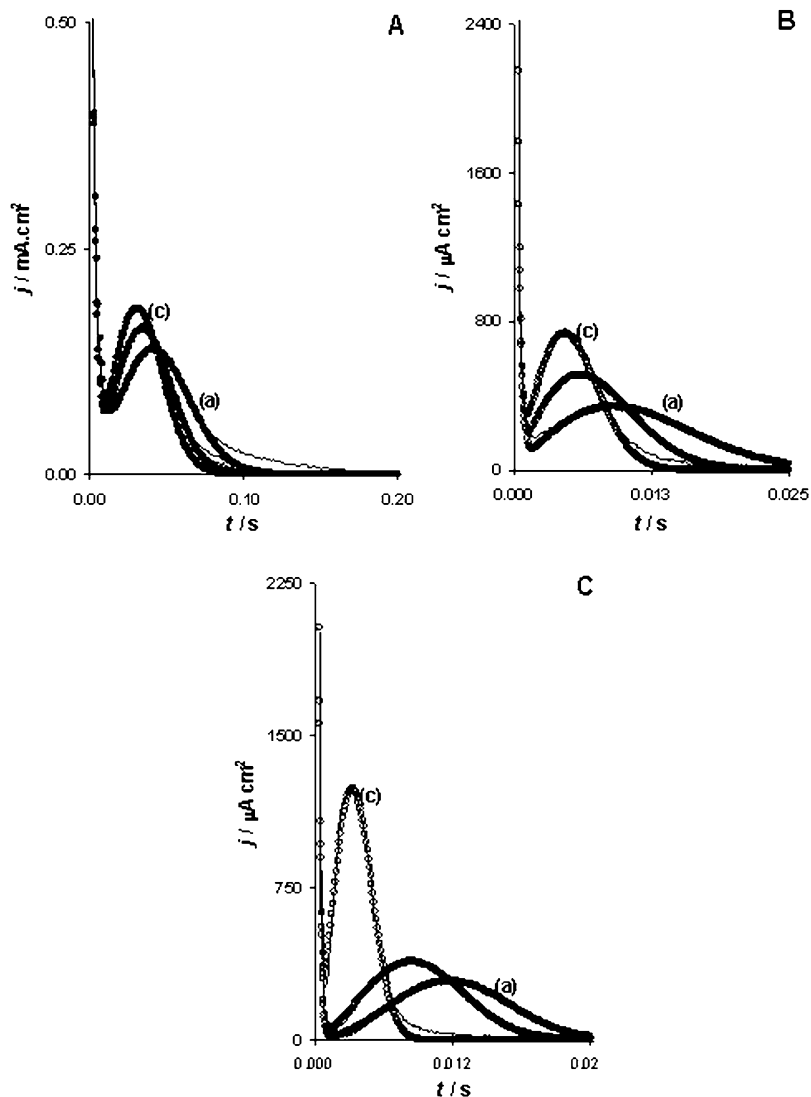


Fig. 5. (A–C) Experimental $j-t$ curves of 14 mM adenosine in 0.1 M NaCl at pH 5 on the: (A) 2 μm Hg-modified PGEb; (B) 0.04 μm copper amalgam-alloy; (C) 0.04 μm platinum amalgam-alloy substrate recorded after a double potential step from the initial potential $E_i = -1.2\text{ V}$ to the pre-treatment potential E_p , the second potential step was from E_p (region Ia) to various final potential (E_f) close to the potential of negative edge of the capacitance pit II. (A) Pre-treatment potential E_p was -1.558 V , final potential E_f was: (a) -1.470 V ; (b) -1.468 V ; (c) -1.466 V . (B) Pre-treatment potential E_p was -1.535 V , final potential E_f was: (a) -1.440 V ; (b) -1.435 V ; (c) -1.430 V . (C) Pre-treatment potential E_p was -1.598 V , final potential E_f was: (a) -1.520 V ; (b) -1.515 V ; (c) -1.505 V . In the case of the phase transition of adenosine on the amalgam-alloy substrates the “offset current” was subtracted. The open circles represent transitions calculated using equation (1). The waiting time at the initial and pre-treatment potentials was 5 and 2 s, respectively. The measurement temperature was 5°C . (Part A is adapted from Hasoň *et al.*, 2003, Figure 1(B); parts B and C are adapted from Hasoň *et al.*, 2004, Figure 7(B) and 11(B), respectively, with permission from Elsevier.)

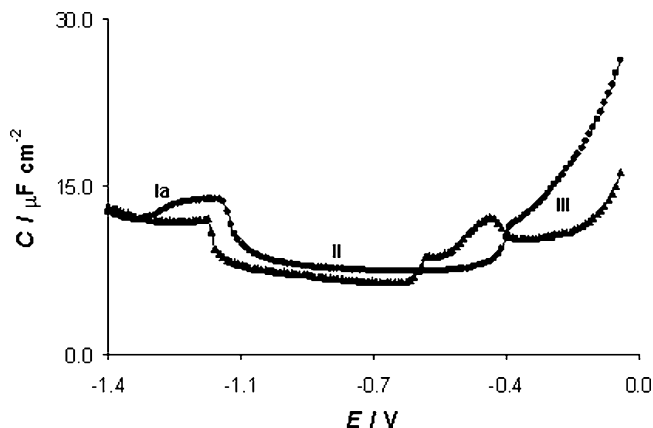


Fig. 6. Capacitance–potential curves of 30 mM cytidine in 0.5 M NaCl with BR buffer on the 2 μm Hg-modified pyrolytic graphite electrode at different pHs: (●) pH 5.0, and (▲) pH 8.3. Potential was scanned from positive to negative values. The different adsorption states are labelled Ia, II and III. The temperature of measurement was 10°C. (Adapted from Hasoň and Vetterl, 2002a, Figure 1(A), with permission from Elsevier.)

2.2.4. Adsorption and kinetics of phase transitions of cytidine at the mercury-modified graphite surfaces

Cytidine forms well-developed 2-D condensed adlayers in a broad range of pH at the 2 μm Hg-modified graphite surfaces, similarly as in the HMDE (Figure 6). In acid (pH 5) solution, only one kind of condensed layer (region II) is formed. In alkaline solution, cytidine forms two different 2-D adlayers. The centre of the first (adlayer II) is located around -0.8 V; the second 2-D film is formed at more positive potentials around -0.2 V (adlayer III). The 2-D condensed adlayers of cytidine were better developed at the 2 μm Hg-modified PGEb in comparison with 2 μm Hg-modified GCE. The 2-D adlayers of cytidine were poorly developed at the Hg-modified pyrolytic graphite electrode with edge plane oriented due to a higher resistance of the electrode surface. On the other hand, the 2-D cytidine adlayers were still well-developed at the 0.1 μm Hg-modified PGEb. It can be concluded that a higher stability of the 2-D condensed films of cytidine at the Hg-modified PGEb is due to the formation of a true Hg-film. Contrary to this, the mercury forms still droplets on the GCE rather than a continuous film and 2-D condensed adlayers are less stable.

The non-linear analysis of the phase transitions of Ia \rightarrow II of cytidine in acid and/or alkaline solution at the 2 μm Hg-modified PGEb can be described by a model which combines a Langmuir-type adsorption step with an instantaneous nucleation process and linear growth mechanism (Avrami exponent $m = 2.08 \pm 0.04$ (Figure 7A, acid solution) and $m = 2.1 \pm 0.07$ (Figure 7B, alkaline solution)). During the Ia \rightarrow II of cytidine the offset current at the Hg-modified PGEb was observed. The current transients of cytidine at thinner Hg-modified PGEb (the Hg-thickness was changed from 0.1 to 1 μm) were characterized by an experimental decay of the current without the current maximum. The $j-t$ curves of cytidine at 2 μm Hg-modified GCE did not show the exponential decay typical of rate control

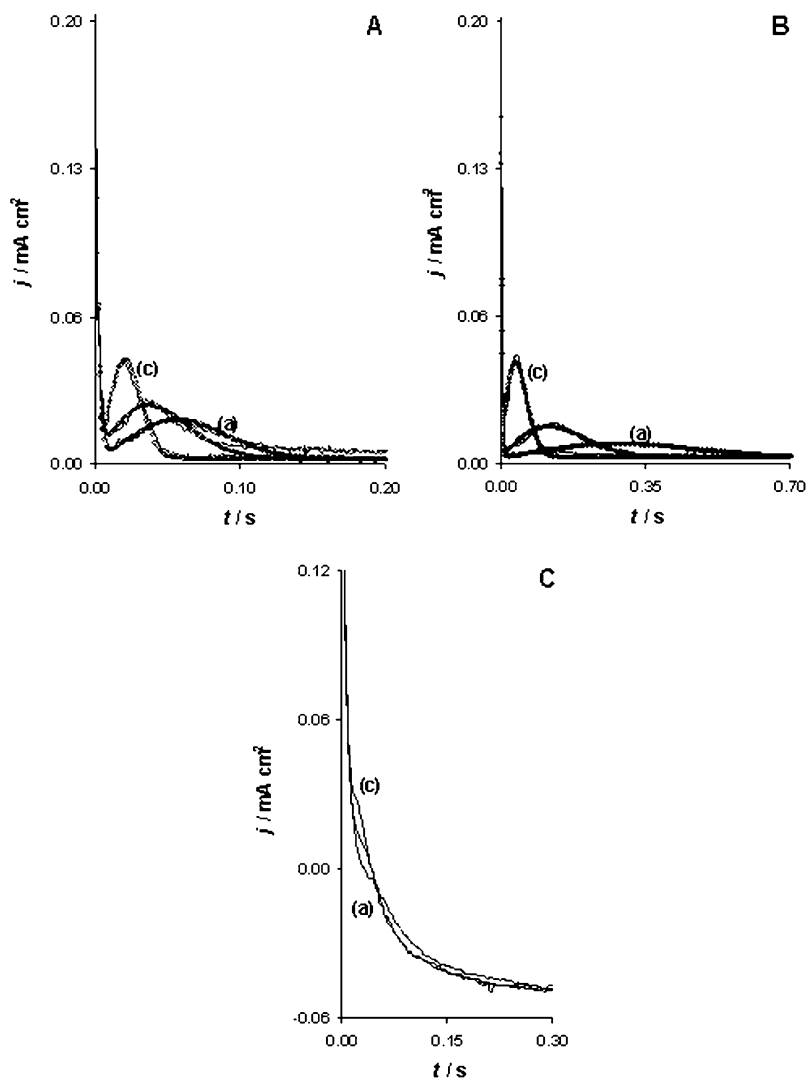


Fig. 7. (A–C) Experimental j - t curves of 30 mM cytidine in 0.5 M NaCl + BR buffer recorded after a potential step from initial potential $E_i = -1.2$ V (region Ia) to various final potentials close to the potential of negative edge of the capacitance pit II on the $2\ \mu\text{m}$ Hg-modified PGEb at: (A) pH 5 and (B) pH 8.3; and (C) $2\ \mu\text{m}$ Hg-modified GCE. (A) Final potential E_f was: (a) -0.985 V; (b) -0.980 V; (c) -0.970 V. (B) Final potential was: (a) -1.050 V; (b) -1.040 V; (c) -1.020 V. (C) Final potential was: (a) -0.960 V; (b) -0.955 V; (c) -0.950 V. In the case of the phase transition of cytidine on the Hg-modified PGEb the “offset current” was subtracted. The open circles represent transitions calculated using equation (1). The waiting time at the initial potentials was 20 s. The measurement temperature was 5°C . (Parts A and B are adapted from Hasoň and Vetterl, 2002b, Figure 6(B) and (D), respectively; part 3 is adapted from Hasoň and Vetterl, 2002b, Figure 13(A), with permission from Elsevier.)

by diffusion, random adsorption or both (Guidelli *et al.*, 1996), they exhibit rather a shoulder (Figure 7C). A pronounced current maximum during the Ia \rightarrow II was not observed and only the adsorption process took place.

The phase transitions of Ia \rightarrow II of cytidine in acid solution at the HMDE can be described by a model 2-D one-step nucleation according to an exponential law (Retter, 1984a, b). A progressive nucleation with $m = 3$ can be used for fitting of the Ia \rightarrow II transients of cytidine in alkaline solution at the HMDE (Hasoň and Vetterl, 2002c). The 2-D condensed cytidine film in alkaline solution is not stable for a long time and gets destroyed (Hasoň and Vetterl, 2002c). Such a behaviour was observed earlier by Pospíšil and Wandlowski with an ordered film of uracil (Wandlowski and Pospíšil, 1989a, b) and by Vetterl and de Levie with ordered film of adenine (Vetterl and de Levie, 1991) at Hg electrode.

2.3. Solid amalgam-alloy electrodes

Another appropriate solid substrate for electrodeposition of mercury and preparation of the Hg-modified surfaces are the noble metals, such as silver, gold, platinum, iridium and/or copper (Cizkowska *et al.*, 1994; Donten and Kublik, 1985, 1986, 1993; Golas *et al.*, 1987; Kounaves and Buffle, 1987, 1988; Kounaves and Deng, 1993; Wechter and Osteryoung, 1989). The deposited mercury at these substrates does not form a true mercury film, since these metals dissolve in mercury, but actually a metal-mercury amalgam/alloy surface layer is formed (Donten and Kublik, 1985; Kounaves and Deng, 1993). The amalgam-alloy layer has a longer lifetime (from hours to days) in comparison with Hg-film, but non-uniform composition of the amalgam layer and possible interaction of the analyte with the metal substrate can be detected sometimes. The advantage of these electrodes is minimal toxicity. Another possibility, in context of non-toxicity, is the use of a dental amalgam (Mikkelsen *et al.*, 2001).

The possibilities of the use of the solid amalgam electrodes (MeAEs) as well as the dental amalgam electrodes in electrochemical analysis of the different inorganic ions and organic compounds in different environmental and analytical samples have been reviewed (Economou and Fielden, 2003; Mikkelsen and Schröder, 2003; Yosypchuk and Novotný, 2002).

In the 1980s, the liquid indium amalgam–electrolyte interface served to the studies of 2-D condensation of organic molecules (Freyman *et al.*, 1997). However, it was shown that the liquid gallium is not suitable for studies of the formation of condensed phases at low temperatures (Buess-Herman *et al.*, 1999).

In the beginning of the 1990s, the studies of 2-D condensation of thymine at platinum amalgam-alloy surfaces by surface plasmon excitation were performed (Tadjeddine and Rahmani, 1991).

Quite recently, we described the kinetics of phase transitions of adenosine at MeAEs (Hasoň *et al.*, 2004; Hasoň and Vetterl, 2004). With MeAEs the effect of the surface morphology on kinetics of the 2-D condensation of the nucleic acid component in the same potential windows as with HMDE can be studied. With this fact the MeAEs are an alternative to very expensive single-crystal metal electrodes. In addition the amalgam-alloy has a minimal toxicity and a much longer lifetime (from hours to days) in comparison with liquid Hg-films.

2.3.1. Optical roughness and surface morphology of the solid amalgam-alloy surfaces

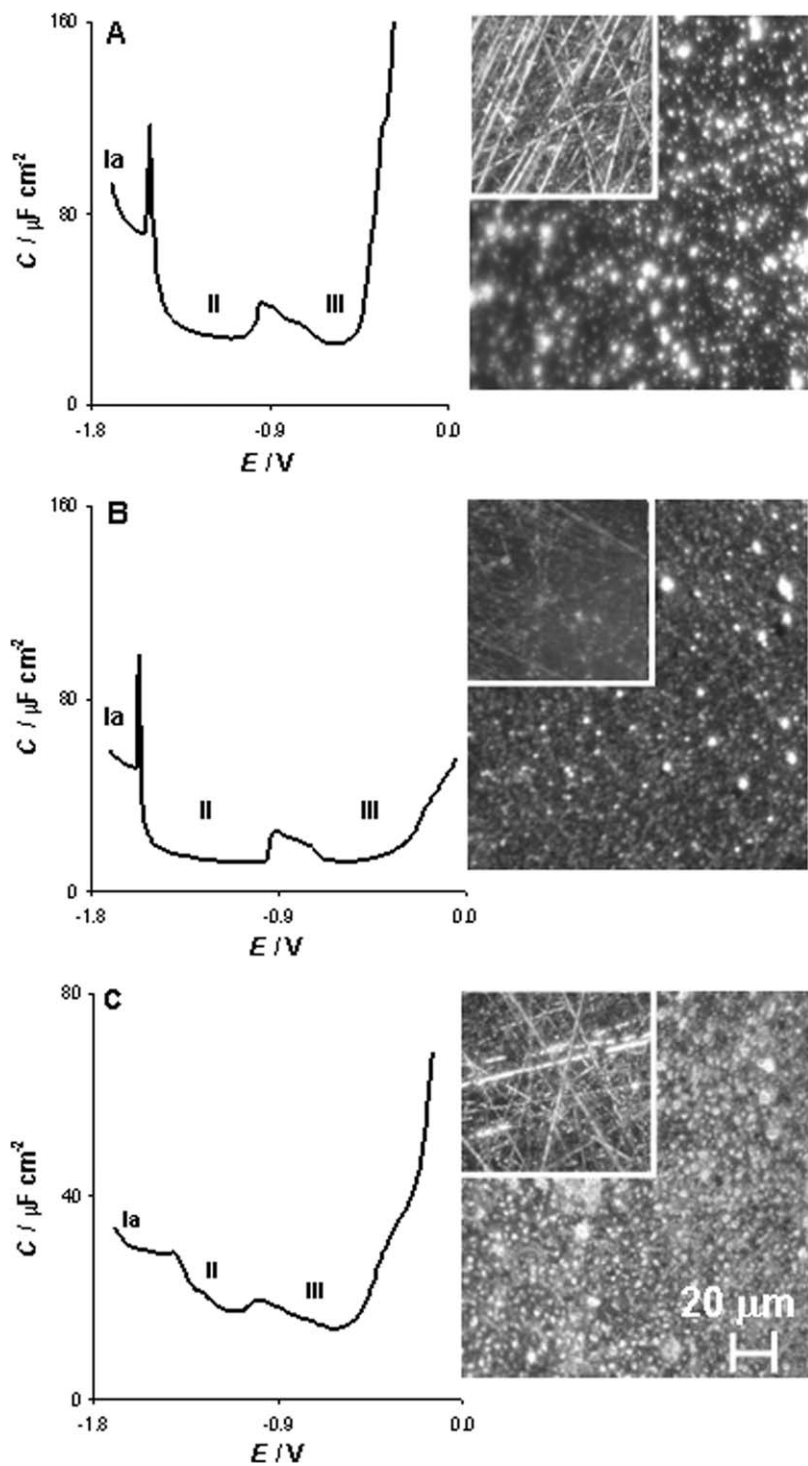
From DOE sensor measurement we observed that after the amalgamation process the surface roughness of amalgam-alloy layer (the thickness of amalgam-alloy layer was changed in the interval from 0.04 to 0.2 μm) becomes higher for each of the used metallic substrate in comparison with the unmodified mechanically treated metal electrode surfaces. The optical roughness R_a of the polycrystalline metal electrodes used increases in the order: silver (AgE, $R_a = 0.036 \mu\text{m}$) < platinum (PtE, $R_a = 0.036 \mu\text{m}$) < copper electrode (CuE, $R_a = 0.055 \mu\text{m}$). The R_a of the 0.04- μm -thick amalgam-alloy layer decreases in the order: copper amalgam-alloy (CuA, $R_a = 0.056 \mu\text{m}$, Figure 8A) > platinum amalgam-alloy (PtA, $R_a = 0.045 \mu\text{m}$, Figure 8B) > silver amalgam-alloy (AgA, $R_a = 0.043 \mu\text{m}$, Figure 8C). After longer amalgamation process the R_a is very similar for each of the 0.4 μm amalgam-alloy layers ($R_{a(\text{AgA})} = 0.055 \mu\text{m}$; $R_{a(\text{PtA})} = 0.056 \mu\text{m}$; $R_{a(\text{CuA})} = 0.054 \mu\text{m}$). It was observed that the difference between the optical roughness R_a of the modified and unmodified CuE substrate has the lowest value. It seems that the amalgam-alloy layer is more homogeneously distributed on CuE substrate than on AgE and PtE substrates.

2.3.2. Adsorption of adenosine at the different solid amalgam-alloy electrodes

Both 2-D condensed adenosine adlayers II and III are well developed at the copper amalgam-alloy (CuAE) and platinum amalgam-alloy PtAE substrates when the thickness of the amalgam-alloy layer is as low as 40 nm (Figure 8A–B). The adlayer II of adenosine is formed at temperatures up to 35°C, the adlayer III disappeared at 25°C. The condensed film II is only slightly affected by a thickness of the amalgam-alloy layer. The 2-D condensed adlayers were stable for several hours. On the other, these 2-D adlayers are poorly developed and have a very short lifetime (only several minutes) on the silver amalgam-alloy electrode (Figure 8C).

Non-linear analysis of the phase transitions of Ia \rightarrow II of adenosine at the 40 nm CuAE can be described by a model that combines a Langmuir-type adsorption step with an instantaneous nucleation and linear growth mechanism (Avrami exponent $m = 2.07 \pm 0.08$; Figure 5B). The phase transitions of Ia \rightarrow II of adenosine at the 40 nm PtAE can be described by a model, which combines a Langmuir-type adsorption step with a nucleation according to a power law and linear growth mechanism (Avrami exponent $m = 2.55 \pm 0.06$; Figure 5C). During

Fig. 8. Capacitance–potential curves of 15 mM adenosine in 0.1 M NaCl at pH 5 on the: (A) 0.04 μm copper amalgam-alloy; (B) 0.04 μm platinum amalgam-alloy; (C) 0.04 μm silver amalgam-alloy electrode. Potential was scanned from positive to negative values. The different adsorption states are labelled Ia, II and III. The temperature of measurement was 10°C. The inserts show microscope images of the unmodified polycrystalline metal and amalgam-alloy electrodes surfaces: (A) Cu; (B) Pt; (C) Ag. Images were recorded by an optical microscope Nikon Eclipse ME600L (magnification was 1000 \times). (Parts A and B are partially adapted from Hasoň and Vetterl, 2004, Figure 1(E) and (D), with permission from Elsevier.)



the Ia \rightarrow II of adenosine the offset current at both the CuAE and PtAE substrates was detected. The phase transitions were 2.5 times faster at the CuAE than at the PtAE substrate. The rate of the phase transition Ia \rightarrow II was slightly dependent on the thickness of the amalgam-alloy layer.

2.4. Solid metal electrodes

Early measurements of camphor adsorbed on zinc or tin electrodes indicated that the observation of the 2-D condensation was not restricted to the ideal defect-free surfaces of liquid metals (Batrakov *et al.*, 1974; Gorodetskii *et al.*, 1972). During the 80 years of the last century came appropriate the experimental procedures for the preparation and treatment of well-defined solid electrodes as well as their electrochemical characterisation (Hamelin, 1985). Due to this knowledge the investigations of molecular adsorption onto single-crystal electrodes rapidly gained increasing interest. The use of such substrates has opened a new field of research, which has been investigating the role played by the electrode surface on the stability of 2-D molecular assemblies. In the beginning of the 90 years of 20th century it was observed that the bases of the nucleic acids can form the 2-D condensed adlayers at the high-oriented pyrolytic graphite (HOPG) substrates, and on a basal faces of a single-crystal electrodes (Popov *et al.*, 1992a, b; Srinivasan and Gopalan, 1993; Srinivasan *et al.*, 1991, 1992; Tao *et al.*, 1993; Tao and Shi, 1994a, b). Detailed studies of the adsorption of pyridine and the nucleic acid bases and nucleosides on various gold, silver and more recently on copper (Furukawa *et al.*, 1997; Kawai *et al.*, 1997; Nakagawa *et al.*, 1997; Tanaka *et al.*, 1996, 1999) single-crystal electrodes have provided clear evidence of the importance of the nature as well as of the crystallographic orientation of the electrodes (Bare and Buess-Herman, 1998; Bare *et al.*, 1998; Buess-Herman, 1985, 1986, 1992, 1994; Buess-Herman *et al.*, 1999; Hölzle *et al.*, 1994, 1995a, b, c, 1996; Dretschkow *et al.*, 1997; Dretschkow and Wandlowski, 1998; Roelfs *et al.*, 1997; Wandlowski, 2002; Wandlowski and Hölzle, 1996a, b; Wandlowski *et al.*, 1996a, b; Wu *et al.*, 1998). In addition, with single-crystal electrodes it was possible to use another experimental technique studying the formation and/or dissolution of self-assembled monolayers at the electrode surface such as scanning tunneling microscopy (STM) (Kolb, 2000, 2001; Wandlowski, 2000, 2002), atomic force microscopy (AFM) and Raman spectroscopy (García-Ramos *et al.*, 1996; García-Ramos and Sánchez-Cortés, 1997; Sánchez-Cortés and García-Ramos, 2000, 2001).

2.4.1. Gold electrodes

2.4.1.1. Cytosine and cytidine. The adsorption of cytosine at Au electrode from 0.1 M NaClO₄ and HClO₄ aqueous solutions was studied by *in situ* surface-enhanced infrared absorption spectroscopy and cyclic voltammetry (CV) (Ataka and Osawa, 1999). From the spectral analysis, it was found that cytosine is physisorbed at negative potentials and is chemisorbed at positive

potentials. Both the physisorbed and chemisorbed molecules are oriented with the N(3), C = O and NH₂ moieties directed towards the surface. A pair of redox peaks observed in the cyclic voltammogram was ascribed to the transformation between the physisorbed and chemisorbed states (Ataka and Osawa, 1999; Wandlowski *et al.*, 1996a, b). The structure and stability of a densely packed 2-D condensed adlayer at a rather positive potential (chemisorbed state) was characterized employing *in situ* STM. This state contains highly ordered domains with a unit cell with the following dimensions: $a = 7.3 \pm 0.3$ Å, $b = 8.7 \pm 0.3$ Å and $\gamma = 50^\circ \pm 5^\circ$. The proposed packing model assumes the coordination of the N(3) ring nitrogen of cytosine with gold atoms (Tao *et al.*, 1993; Wandlowski *et al.*, 1996a, b). The kinetics of dissolution of the chemisorbed adlayer was analysed by comparison with a model based on hole nucleation and growth in combination with a parallel Langmuir-type desorption process (Wandlowski *et al.*, 1996a, b).

We showed (Hasoň and Vetterl, 2002a) that cytidine in the acid (pH 4.2) and neutral solution (pH 7.0) formed at the Au (1 1 1) the physisorbed 2-D condensed adlayer in potential window from -0.3 to $+0.07$ V (region II). At positive potential (around potential $+0.23$ V) cytidine forms ordered chemisorbed adlayer in acid and neutral solution (region IV). In contrast to region II, the extent of region IV is only slightly affected by temperature or concentration change (Figure 9).

2.4.1.2. Uracil, its methyl derivatives, and uridine. The adsorption of uracil on different crystallographic orientation of gold single-crystal electrodes by electrochemical and microscopic techniques was described. The influence of adsorption of uracil on the driving force for the $(p \times \sqrt{3}) \leftrightarrow (1 \times 1)$ transition of the Au(1 1 1) surface by *in situ* X-ray scattering was studied (Wandlowski *et al.*, 1996a, b; Wu *et al.*, 1998). The overall driving force is a combination of the driving force due to charge and the driving force due to the adsorbate. The results show that the two driving forces are of comparable magnitude and that the interpretation of the surface reconstruction phenomena given in terms of either purely charge or a purely adsorbate effect is an oversimplification (Wu *et al.*, 1998). A physisorbed uracil film of planar oriented and via hydrogen bonds connected molecules exists at negative electrode charges of Au(1 0 0). Coupled with changes in the electronic state of the adsorbed uracil this monolayer undergoes a first-order phase transition when altering the electrode potential towards more positive values. A chemisorbed adlayer was finally formed simultaneously with the substrate surface structural transition (hex) \rightarrow (1×1) . Uracil changes its orientation from planar to perpendicular, and a substrate-specific surface coordination complex was created. The physisorbed films on Au(1 1 1)- $(p \times \sqrt{3})$, Au(1 0 0)-(hex) and Au(1 0 0)- (1×1) are rather similar. They display characteristic properties of a hydrogen-bonded network of planar-oriented uracil molecules. At sufficiently positive electrode potentials, uracil deprotonates and forms highly ordered chemisorbed, perpendicularly oriented surface coordination complexes. The organic molecule occupies $(\sqrt{3} \times \sqrt{3})R30$ degrees-positions of the Au(1 1 1)- (1×1) lattice. The chemisorbed uracil film on

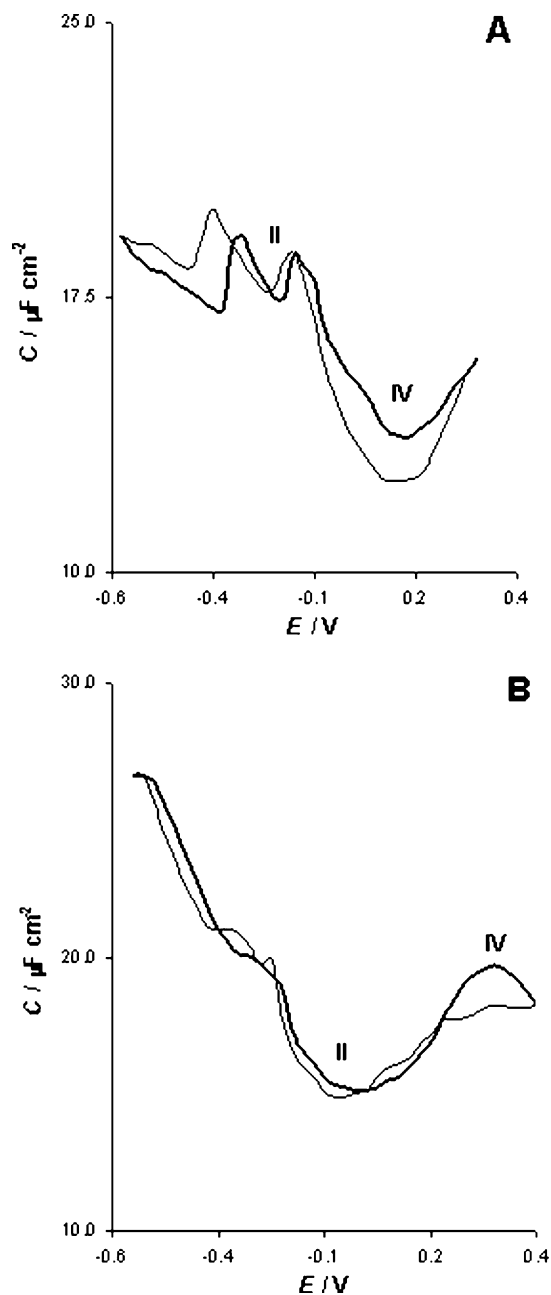


Fig. 9. Capacitance–potential curves of 50 mM cytidine in 0.1 M KClO_4 on the Au(111) at different pHs: (A) pH 7.0 and (B) pH 4.2. (—) Potential scan from -0.6 V to more positive values; (---) potential scan from $+0.4\text{ V}$ to more negative values. The different 2-D condensed adlayer are labelled II and IV. The temperature of measurement was 25°C (Hasoň and Vetterl, unpublished results).

Au(100)-(1 × 1) is of oblique symmetry and consists of interdigitated regular arrays of stacks, each containing four molecules (Dretschkow *et al.*, 1997; Dretschkow and Wandlowski, 1998). Two adsorbed states with different vibrational frequencies were observed for uracil in 0.1 M LiClO₄ solution, which have pronounced interaction with water molecules and electrolyte ions (Futamata and Dieising, 1999). The infrared spectra show that uracil and thymine adopt similar coordination forms with the surface with both exocyclic oxygen atoms and deprotonated N3 facing in towards the surface in a vertically oriented chemisorbate. Thymine exhibits smaller ordered domains, which are expanded in one direction to allow for the spatial requirements of methyl group on thymine (Li *et al.*, 1999).

The kinetics of formation of condensed physisorbed film of uracil on Au(100)-(hex), Au(111)-(p × √3) and Au(100)-(1 × 1) were investigated by double potential steps in order to reduce the effect of pre-adsorption on the immediate phase transition kinetics. These primary transients could be modelled with an exponential law of nucleation and an induction time in combination with 2-D surface diffusion-controlled growth (Wandlowski and Dretschkow, 1997).

The adsorption and phase formation of uracil on massive Au[n(111)-(110)] single-crystal and Au(111-20 nm) film electrodes was studied by attenuated total reflection surface-enhanced infrared reflection absorption spectroscopy (ATR-SEIRAS) (Pronkin and Wandlowski, 2003). At $E < 0.15$ V uracil molecules are disordered and planar oriented, co-adsorbed with weakly hydrogen-bonded interfacial water (region I). Around the potential of zero charge a 2-D condensed, physisorbed film of planar-oriented molecules, interconnected by directional hydrogen bonds is formed (region II). At more positive potentials the increase of intensity and a large negative shift of the carbonyl combination bands, characteristic to uracil coordinated to metal ions (region III) was observed. Band intensities and peak positions reach rather constant values at $E > 0.80$ V (region IV), where uracil undergoes an orientational change from planar to perpendicular accompanied by the formation of a chemisorbed adlayer composed of molecular islands. Time-resolved ATR-SEIRAS experiments demonstrate that the transformation of chemisorbed uracil into lower coverage adlayers proceeds in the following steps: (i) perpendicularly oriented uracil molecules change their orientation towards a tilted or planar arrangement depending on the final potential; (ii) desorption of strongly hydrogen-bonded second-layer water and sulphate species; (iii) adsorption of weakly hydrogen-bonded water (Pronkin and Wandlowski, 2003).

The interfacial behaviour of 1,3-dimethyluracil (1,3-DMU) on Au(111) was investigated quantitatively using chronocoulometry. The adsorption parameters such as film pressure, relative Gibbs surface excess, Gibbs energy of adsorption and electrosorption valency were determined as a function of electrode potential and charge density for concentrations of 1,3-DMU up to 50 mM. The values of the relative Gibbs surface excess and the small shift of the zero charge potential due to 1,3-DMU adsorption indicate that the organic molecules are oriented parallel to the electrode surface within the entire region of an ideal polarizable interface. The Gibbs energy at maximum adsorption is equal to -35.4 kJ mol⁻¹ and suggests weak chemisorption (Wandlowski and Hölzle, 1996a, b).

A stable condensed physisorbed film of 5,6-dimethyluracil (5,6-DMU) was formed between the limits of the hydrogen evolution (at -0.3 V) and the lifting of the surface reconstruction (at 0.4 V) in the bulk solution concentration on the Au(1 1 1). The onset of hydrogen evolution led to the formation of “bubble”-like structures which disrupted the stability of the film causing a disordering process which takes place within the whole scanned area. Stepping the potential back to the region of stability allowed the real-time observation of the film reorganization. An anisotropic evolution of the film was found (Cunha and Nart, 2001).

STM images of 5-chloride uracil and 5-bromide uracil adsorbed on Au(1 1 1) in sulphuric acid solution under potential control has shown that the change of the halogen substituents leads to dramatic changes in the molecular packing structure of the films (Cunha *et al.*, 2001). Both molecules form highly ordered films, but while 5-bromide uracil has a lying, hydrogen bond stabilised, positioning, 5-chloride uracil assumes an upstanding positioning (Cunha *et al.*, 2001).

The first and second layer adsorbates on Au thin film electrodes were elucidated with respect to deprotonation of organic monolayers or Cu-UPD (under potential deposition) on Au(1 1 1) using attenuated total reflection-infrared spectroscopy (Futamata, 2003). The $\nu(\text{Cl-O})$ band from ClO_4^- ions at the second layer, located outside the uracil monolayer, shows invariant frequency, while the ClO_4^- band at the bare Au surface increases with the potential. The Cl^- ions co-adsorb with sulphate species during the Cu-UPD process. In contrast to the XPS (X-ray photoelectron spectroscopy) data, the surface coverage of the halide ions does not change significantly at the second UPD peak (Futamata, 2003).

The kinetics of dissolution of condensed chemisorbed layer of uridine on Au(1 1 1), Au(13,13,12) and Au(554) were studied by current transients (Van Krieken and Buess-Herman, 1998). All the transients were satisfactorily described by a model that combines a desorption step with a simultaneous hole nucleation and growth process. On the basis of a model considering an exponential law of nucleation and a surface diffusion-controlled growth, it was found that an increase of the step density of the electrode surface by affecting the ordering of the organic layer enhances markedly the rate of formation of holes in the film but slows down the expansion of the holes. The influence of the temperature and of the surfactant concentration on the nucleation and growth parameters was also reported (Bare *et al.*, 1998; Scharfe *et al.*, 1995; Van Krieken and Buess-Herman, 1998). The effect of Au surface structure on the adenine adsorption was studied recently by CV and capacitance measurements (Martins *et al.*, 2005).

2.4.1.3. Oligonucleotides. Double-stranded oligonucleotides (poly(dA₃₀).poly(dT₃₀)) adsorbed at gold electrodes, were investigated by various techniques, including CV, quartz crystal microbalance (QCM), electrochemical scanning tunnelling microscopy (EC-STM) and surface-enhanced Raman scattering spectroscopy (SERS). CV and QCM results show that double-stranded poly(dA₃₀).poly(dT₃₀) forms at the gold electrode surface a saturated monolayer of

double-stranded DNA(dsDNA) lying flat on surfaces. EC-STM was used as evidence directly that dsDNA forms a highly ordered and compact monolayer film on the gold substrate, whereas single-stranded DNA(poly(dT₃₀)) adopts a coiled configuration and, therefore, cannot form an ordered structure on the gold substrate. Moreover, it was demonstrated by SERS experiments that partial denaturation of duplexes occurs arising from the different interfacial orientations of A and T bases on the gold electrode surface. The DNA-modified gold surface is stable in a wide range of potentials (Zhang *et al.*, 2002).

Organized oligonucleotide monolayers on polycrystalline Au and single-crystal Au(1 1 1) are extensively studied by Wackerbarth *et al.* (Wackerbarth *et al.*, 2004a; Wackerbarth *et al.*, 2004b) and the results are reviewed in his chapter of this book (Chapter 15).

2.4.1.4. DNA. Complementary, single strands of DNA (ssDNA), one bound to a gold electrode and the other to a gold nanoparticle were hybridized on the surface to form a self-assembled, dsDNA bridge between the two gold contacts (Nogues *et al.*, 2004). The adsorption of an ssDNA monolayer at each gold interface eliminates non-specific interactions of the dsDNA with the surface, allowing bridge formation only upon hybridization. The technique used, in addition to providing a good electrical contact, offers topographical contrast between the gold nanoparticles and the non-hybridized surface and enables accurate location of the bridge for the electrical measurements. Reproducible AFM conductivity measurements were performed and significant qualitative differences were detected between conductivity in ss- and dsDNA. The ssDNA was found to be insulating over a 4 eV range between $+/-2$ V under the studied conditions, while the dsDNA, bound to the gold nanoparticle, behaved like a wide band gap semiconductor and passes significant current outside a 3 eV gap (Nogues *et al.*, 2004).

DNA molecules were adsorbed specifically on gold surfaces (Aqua *et al.*, 2003). The specificity of the adsorption was controlled by a novel approach, in which the gold surface was first blocked with a hydrophobic layer (C-18-SH) to various extents, followed by the adsorption of thiolated DNA. The technique was applied both for short and for long strands of DNA. It was shown that the reactivity of the thiolated short DNA in a ligation reaction is enhanced by more than an order of magnitude by the presence of the alkylthiol layer. Due to the hydrophobic and insulating nature of the C-18-SH layer, this blocking method is advantageous for electronic measurements (Aqua *et al.*, 2003).

2.4.2. Silver electrodes

The formation of uracil adlayers on Ag(1 1 1) and Ag(1 0 0) in aqueous solutions was studied by CV and capacitance–potential measurements (Hölzle *et al.*, 1995a; Wandlowski, 1995). It was founded evidence for the existence of two distinctly different organized uracil layers at both crystal planes. The first was formed at medium coverages and potentials close to the potential of zero charge

of the electrolyte, and corresponds to a 2-D condensed physisorbed film. The second type of adlayer was formed at rather positive charge densities and shows extreme temperature stability. This film was assigned as chemisorbed uracil. The adsorption of 6-methyluracil, thymine and 5,6-dimethyluracil from aqueous solutions on Ag(1 1 1) was investigated by CV, capacity measurements and current transients, to elucidate the role of the electrode surface and of the intermolecular forces in the formation of ordered adlayers. From the calculated free adsorption enthalpies stability sequences for the condensed physisorbed phase were established (Hölzle *et al.*, 1996).

The short-time adsorption of uracil on Ag(1 1 1) was interpreted by a model that accounts for diffusion-controlled random adsorption of uracil molecules according to a Frumkin isotherm, followed by their progressive nucleation and by growth of the resulting clusters. The long-time behaviour was explained by a model that considers the formation of a new 2-D phase and the nucleation and growth of water holes within this new phase, up to the attainment of a steady state (Foresti *et al.*, 1995; Guidelli *et al.*, 1996). The structure of the chemisorbed uracil overlayer that is formed on Ag(1 1 1) at potentials positive to -0.70 V following a 2-D disorder–order phase transition was investigated by *in situ* STM as well. The uracil molecules were arranged in parallel rows. A packing model in which the rows consist of chains of flat, H-bonded uracil molecules was hypothesized (Cavallini *et al.*, 1998).

The adsorption of uridine on Ag(1 1 1) was investigated as well. The kinetics of the interfacial rearrangements were investigated by recording current–time curves. When single potential steps were applied starting from the chemisorbed layer, the transients are predominantly associated with the dissolution of the initial layer. Those transients were analyzed in terms of a model which combines a Langmuir-type desorption step and a dissolution which proceeds from holes growing with a time-dependent rate (Van Krieken and Buess-Herman, 1999).

The potential-induced changes in thymine coordination on polycrystalline silver electrodes were studied by SERS for potentials positive to the potential of zero charge up to the end of the double layer range (Aroca and Bujalski, 1999; Cunha *et al.*, 2003). Two distinct sets of spectra could be obtained in the range of potentials studied. Both states correspond to chemisorbed phases of thymine on silver, where a distinct heteroatom is responsible for the bond with the surface. At less positive potentials, one of the ring oxygen atoms is responsible for the chemical bond and the molecule assumes a tilted position. At more positive potentials, one of the ring nitrogen atoms, possibly deprotonated, establishes a new bond with the surface, aligning the molecule's axis closer to the surface normal (Cunha *et al.*, 2003).

The Raman and SERS spectra of uracil were measured and the vibration spectra of uracil and deprotonated uracil in the condensed phase were predicted by calculations using density functional theory (DFT) (Giese and McNaughton, 2002a). On the basis of these calculations combined with normal Raman spectroscopy, two different tautomers corresponding to N(1) and N(3)-deprotonated uracil were identified in alkaline aqueous solution, the N(1)-deprotonated species being slightly more common. In the SERS spectra of alkaline uracil solution in a silver sol, contributions from both tautomers are detected. The

ratio of the two tautomers depends on the concentration of analyte. At neutral pH uracil adsorbs to the silver colloid exclusively in its N(3) deprotonated form. The interaction between uracil and an electrochemically roughened silver electrode is similar to the interaction between uracil and the silver colloid. Spectral changes caused by varying the applied electrode potential are most likely due to the inductive effect of the metal rather than a molecular reorientation at the metal surface (Giese and McNaughton, 2002a).

The SERS spectra of adenine and three deuterated analogues adsorbed on colloids, electrochemically roughened electrodes and vacuum deposited island films of silver were also investigated (Giese and McNaughton, 2002b). Surface selection rules derived from the electromagnetic enhancement model were employed to deduce adenine orientations on the different surfaces. On the colloids, adenine adopts an almost perpendicular orientation interacting with the metal surface via N(7) and the exocyclic amino group. On the electrodes, adenine adsorbs in a more tilted orientation while on the island films the tilt is even more pronounced. Interaction with the electrodes takes place through N(7) and the amino group, while interaction with the island film may be solely through N(7).

The surface-coverage study of the SERS of cytosine and its derivatives indicated that these molecules tend to be predominantly edge-on adsorbed at lower concentrations. At high concentrations the orientation was not completely perpendicular due to the increasing contribution to the SERS spectrum from molecules placed in layers different to the first one. The SERS intensity changes observed in presence of Cl^- were governed by the electromagnetic enhancement mechanism, while the changes of the spectral profile were rather connected to the charge-transfer mechanism, due to the relative increasing importance of the first layer in the SERS spectrum. The pH-dependent intensity changes were due to a transition from a first layer to a multilayer configuration with increasing pH (Sánchez-Cortés and García-Ramos, 2001). The SERS observation showed the chemisorption of dimethylcytosine on the silver surface. Dimethylcytosin is also chemisorbed on colloidal metals, and it is observed that the growing interaction strength is in the order $\text{Ag} < \text{Au} < \text{Cu}$ (Sánchez-Cortés and García-Ramos, 2000).

SERS of hypoxanthine molecule on silver colloid showed that the molecule exists as [keto-N(9) H(9)] form in the surface adsorbed state at acidic and normal pH, but it occurs as [enol-O(6) H(1), N(9) H(9)] form at alkaline pH. It was substantiated by the appearance of an intense carbonyl-stretching mode at 1690 cm^{-1} , a medium-intense in-plane $\text{C}=\text{O}$ bending mode at 655 cm^{-1} and disappearance of the C(6)–O(6) H(1) stretching mode in SER spectra in acidic and normal pH. Hypoxanthine molecule is adsorbed on the metal surface at acidic pH (pH 2) through the N(3) atom with the molecular plane lying almost perpendicular on the silver substrate, while at alkaline pH the molecule is oriented nearly parallel to the silver surface via non-bonding electrons of N(1), N(3), N(7) and O(6) (Chowdhury *et al.*, 2000).

Self-assembled monolayers (SAM) of NAD formed at two silver surfaces with different roughness were investigated by SERS technique combined with Raman mapping. On the basis of the analysis of the recorded Raman mapping spectra together with reference to the calculation results of minimized energy

conformation of NAD, an adsorption mode of SAM of NAD at silver surface was suggested including adenine moiety of the perpendicular orientation onto the surface via N(7) and amino group as well as a flat orientation for the nicotinamide moiety. The various degree of roughness of silver surface mostly impacted on the dynamic process rather than the thermodynamics of SAM formulation of NAD (Yang *et al.*, 2004).

2.4.3. Copper electrodes

It was observed that DNA base molecules form low-dimensional superstructures on Cu(1 1 1) surfaces through hydrogen bonding among molecules and through their epitaxial nature on the surface. The formation of characteristic self-assembled structures depend not only on the coverage of the molecules but also on the deposition rate and both parameters indicate that a dynamic process at the surface plays an important role in its formation. STM images revealed that the chemical inertness of the Cu(1 1 1) substrate allows the molecules to diffuse over the surface to spontaneously self-assemble themselves into their own unique structure: adenine into one-dimensional molecular chains, thymine into 2-D islands, guanine into 2-D square lattices and cytosine into one-dimensional zigzag molecule cluster networks (Furukawa *et al.*, 1997; Kawai *et al.*, 1997; Nakagawa *et al.*, 1997; Tanaka *et al.*, 1996). It was elucidated that the most stable hydrogen-bonded dimer plays a very important role as nuclei in the self-assembly formation of the adenine molecule. It was observed that the nuclei hydrogen-bonded dimers diffuse in the substrate, and self-assemble themselves into two different characteristic superstructures, a “one-dimensional chain structure” and a “two-dimensional hexagonal structure”, through two distinct kinds of hydrogen bond pattern at low coverage and low deposition rate. It was also found that chemically modified adenine with an alkyl chain, which prevents the formation of the nucleic dimer, forms randomly aggregated small clusters (Furukawa *et al.*, 1997; Kawai *et al.*, 1997; Tanaka *et al.*, 1996). Novel superstructures of self-assembled uracil molecules were also observed at lower temperatures at Cu(1 1 1). Isolated uracil trimers are formed at low coverage, and 2-D islands with a hexagonal superstructure are built up at increased coverage. The dominant force responsible for the formation of the trimers and the islands is electrostatic interaction through anisotropic hydrogen bonds between uracil molecules (Furukawa *et al.*, 1997, 2000; Kawai *et al.*, 1997; Tanaka *et al.*, 1996).

Semi-empirical molecular orbital (MO) calculation indicated that there exists predominantly stable dimer structures for the guanine, cytosine and adenine molecules, while such phenomena was not observed among the possible thymine dimer and even trimer structures. Based on experimental and theoretical results, the authors concluded that specific hydrogen-bonded nucleus formation is a decisive process in the 2-D self-assembly formation of DNA base molecules on Cu(1 1 1) surfaces (Furukawa *et al.*, 2001).

Using the pulse injection method, ssDNA and ds plasmid DNA were deposited on Cu(1 1 1) surfaces under ultrahigh vacuum (UHV) conditions. The STM images revealed that DNA molecules are adsorbed directly onto a clean

Cu(1 1 1) surface. The ssDNA oligomers have exhibited the images of individual internal base molecules and the helix structures made of complementary base sequences. For the ds plasmid DNA, the images have shown the Watson–Crick double-helix structure (Tanaka *et al.*, 1999).

STM images of poly(dA-dT)-poly(dA-dT) and poly(dG-dC)-poly(dG-dC) adsorbed on Cu(1 1 1) substrates revealed that the two DNA molecules have different adsorbed structures and topographic heights. The observed structural differences originate from the inherent differences in the stability of the adenine–thymine (A–T) and guanine–cytosine (G–C) base pairs (Nishimura *et al.*, 2002).

The adsorption of adenine, guanine, cytosine and thymine on Cu(1 1 0) was investigated by reflection absorption infrared spectroscopy in UHV as well. Cytosine exhibited characteristic asymmetric and symmetric NH_2 stretching signal. The asymmetric stretching signal was missing in the submonolayer region, indicating that the whole molecule was standing upright, with the NH_2 group sticking out of the surface. Thymine was also proved to stand upright at the surface. Guanine exhibited weakened infrared signals, indicating that the core purine ring was tilted on the surface, with an interaction of $\text{NH}-\text{C}=\text{O}$ side of the molecule. Adenine at coverages below one monolayer gave no absorption signals, evidencing the molecules laid flat on the surface (Yamada *et al.*, 2004). From electron energy loss spectroscopy, Chen showed that the molecular plane of adenine is parallel to the substrate with a tilted $\text{C}-\text{NH}_2$ bond. *Ab initio* calculations confirm the molecular orientation and show an sp^3 hybridization on the N(amino) atom, which is directly bonded to the substrate. The origin of the chains lies in the formation of homochiral rows of molecules, linked by two types of H-bonding interactions, commensurate with the substrate (Chen *et al.*, 2002).

2.4.4. Bismuth electrodes

The electrochemical impedance method has been used for the quantitative study of uracil adsorption kinetics at the bismuth single-crystal plane in aqueous Na_2SO_4 solution. Analysis of impedance data demonstrates that the adsorption process of uracil is complicated and limited by the mixed kinetics, i.e. by the slow adsorption and diffusion steps. Analysis of the Cole-Cole and other dependences indicates that, at small frequencies and higher uracil concentrations, 2-D association of the uracil molecules is possible. Non-linear regression analysis has been used for fitting the experimental complex plane (Z'' , Z') plots. The classical Frumkin–Melik–Gaikazyan circuit in the region of higher frequencies and lower uracil concentrations (less than or equal to 2×10^{-3} M), and the modified Frumkin–Melik–Gaikazyan equivalent circuit (taking into account the inhomogeneous semi-infinite diffusion) at uracil concentrations greater than or equal to 2×10^{-3} M fit with a reasonable accuracy the experimental Z'' , Z' -plots. It was found that the values of the double layer capacitance, partial charge transfer resistance, adsorption capacitance and Warburg-like diffusion impedance depend noticeably on the electrode potential and concentration of uracil (Kasuk *et al.*, 2003).

2.5. Semiconductor electrodes

2.5.1. Single-crystal *n*-CdSe

The adsorption of adenine (A), thymine (T), guanine (G) and cytosine (C), and base pairs onto single-crystal *n*-CdSe substrates was studied in several solvents, using the band gap photoluminescence (PL) of the semiconductor as a probe (Meeker and Ellis, 2000). In methanol solution, all four bases cause similar, reversible PL quenching. The PL changes can be well fit by a dead-layer model, indicating that adsorption increases the depletion width of the semiconductor by 200–300 Å. In dimethylsulfoxide (DMSO) solution, there is no PL response to individual bases. However, the complementary A-T and G-C base pairs yield a PL response, providing evidence that the surface can promote base pair formation. The A-T and C-G responses in DMSO correspond to depletion width increase of 100 and 200 Å. In chloroform solution, the PL response of C-G base pairs can be distinguished from those of C and G individually, whereas A, T and A-T are experimentally indistinguishable (Meeker and Ellis, 2000).

2.5.2. Silicon

The STM images showed that adenine and thymine are adsorbed on Si(100)- 2×1 surfaces. The double bright molecular images are located on the neighbouring two Si dimer rows and have ellipsoidal shapes. An extended Huckel MO calculation of the adenine adsorbed on the Si cluster gives the form of the hybridized orbital in this system. This calculation explains the adsorption site and the surface local density of states corresponding to the observed STM images (Kasaya *et al.*, 1995, 1996).

Due to semi-empirical MO calculation the local surface density of states for the adsorbed molecules of adenine on the Si surface was revealed. The energy level diagrams of the MOs of the Si cluster on which the molecules are adsorbed are shown (Kasaya *et al.*, 1998).

The STM images show that uracil is able to form ordered structures on the surface of Si(100)- 2×1 on which the molecules adsorb preferentially along dimer rows. The high-resolution electron energy-loss spectroscopy (HREEL) spectra show a stronger intensity of the in-plane modes compared with the out-of-plane vibrations. This indicates that the orientation of the molecular plane is more upright. The observation of a distinctive Si–H band in the vibrational spectra of Si(100)- 2×1 exposed to uracil indicates that adsorption of the molecule occurs through cleavage of an O–H/N–H bond. The vibrational spectra show that only the enol tautomer interacts with the surface, mainly through cleavage of the OH bond and the formation of an Si–O linkage (Lopez *et al.*, 2002).

The adsorption of uracil on the Si(001) surface was investigated by DFT calculations using a plane-wave basis in conjunction with ultrasoft pseudopotentials. There exists a pronounced tendency for molecular fragmentation, leading to the dissociation of hydrogen from the molecules and possibly to oxygen insertion into Si dimers (Seino *et al.*, 2003). The results showed that

semiconductor surface electronic properties can be tuned within a very wide range by organic functionalization even with only one molecular species (Seino *et al.*, 2004).

Reflectance anisotropy spectra (RAS) for energetically favoured models of uracil covered Si(001) surfaces were calculated within the independent particle approximation (Seino and Schmidt, 2004). While for low coverage mainly an attenuation of the features typical for the clean surface is found, the calculations predicted the appearance of new peaks for higher coverage, suggesting the usage of RAS for the analysis of organic/inorganic interfaces (Seino and Schmidt, 2004).

The interface formed between cytosine and hydrogen-passivated Si(111) substrates was investigated by spectroscopic methods and density functional calculations of optimized adsorbate geometries. The cytosine was thermally evaporated by organic molecular beam deposition onto flat and vicinal H-passivated Si(111) substrates under UHV conditions. In order to take advantage of surface-enhanced Raman scattering at rough metal surfaces, silver was evaporated onto the biomolecular adsorbate. Polarization-dependent Raman measurements reveal that the cytosine molecules align along the steps on vicinal H-passivated Si(111) surfaces. The orientation of the molecular plane of the cytosine molecule deduced from the SER spectra can be well reproduced with density functional calculations of the optimized geometries of an adsorbed cytosine molecule at a step edge of H-passivated Si(111) slab. As the binding energy of cytosine at the substrate step is as large as -0.41 eV, one can conclude that the coverage with silver does not affect the preferential adsorption geometry of the cytosine molecule (Silaghi *et al.*, 2004).

DNA molecules can be selectively adsorbed onto a SiO₂ surface in SiO₂/SiH pattern, fabricated using photolithography, by adding MgCl₂ to a DNA solution (Tanaka *et al.*, 2001, 2004). Since DNA molecules can be adsorbed onto a Si substrate through Mg²⁺, the adsorption of DNA molecules in a SiO₂/SiH pattern is influenced by the concentration of MgCl₂ and the difference in chemical property between a SiO₂ surface and a SiH surface (Tanaka *et al.*, 2001, 2004). DNA molecules attach to a hydrophilic SiO₂ surface but not to a hydrophobic SiH surface. This result indicates that it is possible to fabricate micropatterning on a Si surface by using a DNA template and photolithography (Tanaka *et al.*, 2001).

2.5.3. Gallium arsenide

GaAs-based electronic devices have interesting applications in spintronics and as sensors. In the past, methods were developed to stabilize the surface of GaAs, since it is known to be highly sensitive and unstable. It turns out, however, that these particular properties can be used for controlling the electronic characteristics of the devices, by adsorbing molecules that affect the surface properties. The adsorption of molecules that can be bound to GaAs through their phosphate group was studied (Artzi *et al.*, 2003). Phosphate functional groups can be found in many biological molecules; therefore, the binding of organic phosphate

to a semiconductor surface can provide the first step towards a new line of hybrid bioorganic/inorganic electronic devices. The adsorption of tridecyl phosphate (TDP) was investigated and compared with the adsorption of dodecanoic acid (lauric acid), which contains a carboxylic binding group. The alkyl phosphate monolayer is found to bind to the GaAs surface more strongly than any other functional group known to date. The authors showed that the adsorption of a DNA nucleotide (5'-AMP) as well as ssDNA on the GaAs surface occurs through the phosphate groups (Artzi *et al.*, 2003). Hence, DNA can be bound to these surfaces with no need for chemical modifications.

2.6. Minerals, soils and resins

The adsorption of organic molecules onto the surfaces of inorganic solids has long been considered a process relevant to the origin of life. The equilibrium adsorption isotherms for the nucleic acid purine and pyrimidine bases dissolved in water on the surface of crystalline graphite was determined by Sowerby (Sowerby and Petersen, 1997; Sowerby *et al.*, 1998a, b, c, 2001a, b). The adsorption behaviour of the individual bases was significantly different and decreased in the series: guanine > adenine > hypoxanthine > thymine > cytosine > uracil. In the same sequence decreased the adsorption of nucleic acid base at the mercury electrode determined by differential capacitance measurement (Vetterl, 1966a, b). Sowerby (Sowerby *et al.*, 2001a,b) proposed that such differential properties were relevant to the prebiotic chemistry of the bases and may have influenced the composition of the primordial genetic architecture. The combinatorial arrangements of planar arranged purine and pyrimidine bases could provide the necessary complexity to act as a primitive genetic mechanism and may have relevance to the origin of life (Denton *et al.*, 2003; Sowerby *et al.*, 1996, 2000, 2001a,b, 2002; Sowerby and Heckl, 1998; Sowerby and Petersen, 2002; Hansson *et al.*, 2002).

The iron oxide hydroxide minerals goethite and akaganeite were likely constituents of the sediments present in, for instance, geothermal regions of the primitive Earth (Holm *et al.*, 1993). They may have adsorbed organics and catalysed the condensation processes which led to the origin of life. The binding to and reactions of nucleotides and oligonucleotides with these minerals was investigated. The adsorption of adenosine, 5'-AMP, 3'-AMP, 5'-UMP and 5'-CMP to these minerals was studied. Adenosine did not bind to goethite and akaganeite. The adsorption isotherms for the binding of the nucleotides revealed that they all had close to the same affinity for the mineral. Binding to goethite was about four times stronger than to akaganeite. There was little difference in the adsorption of each nucleotide suggesting the binding was between the negative charge on the phosphate group and the positive charges on the mineral surface. The absence of binding of adenosine is consistent with this explanation (Holm *et al.*, 1993).

In order to study the effects of large-surface-area solids on the formation of biomacro-molecules, copper(II)-nucleosides complexes were studied in water at high pH and after contact with the cavity walls of 13X-zeolite (Ciani *et al.*, 2003).

The results were mainly collected by electron spin resonance in continuous (cw-ESR) and pulsed (ESE) wave. Particular attention was dedicated to adenosine as a nucleoside model for the formation of compounds which were fully characterised in alkaline water solution and after adsorption on commercial 13X-zeolite. In aqueous solution, adenosine was coordinated to copper(II) through deprotonated hydroxyl groups in the 2' and 3' positions of the ribose unit. When adsorbed on zeolite, both cw-ESR and ESE showed that a fraction of the adsorbed complexes did not change their structure and showed high mobility in the zeolite faujasite cavity. The remaining fraction directly interacted with Al-27 nuclei of the zeolite framework. Other copper(II)-nucleosides behaved in the same manner (Ciani *et al.*, 2003).

Recently, SERS was used to characterise adenine adsorption on and release from specimens of two meteorites, the Zagami Martian meteorite and the Murchison meteorite (El Amri *et al.*, 2004). Powdered meteoritic material was incubated with very dilute adenine solutions. An adenine SER response of the resulting supernatant weaker than that of the initial solution indicated that adenine was bound to the meteorite. A SER signal with the pellet meant the adenine that was initially adsorbed on it was transferred to the silver colloid SER probe. Adenine adsorption on and release from the Murchison carbonaceous chondrite and the mineral Zagami meteorite depended on the composition of the meteorites. Adenine was much more strongly bound to the Murchison meteorite, which contains biorganic matter, than to the purely mineral Zagami meteorite (El Amri *et al.*, 2004).

Enantiomeric interactions between nucleic acid bases and amino acids on solid surfaces was studied as well (Chen and Richardson, 2003).

Adsorption kinetics of nucleic acid bases and nucleosides as ligands on cobalt(II)-carboxylated diaminoethyl sporopollenin (CDAE-sporopollenin) have been performed using continuous column runs (Ayar and Gurten, 2003). Adsorption rate measurements were carried out by using a UV-Vis spectrophotometer, and rate control step of the adsorption process was determined. The results show that the type of ligand has a great effect on ligand adsorption behaviour. External ligand concentrations play a significant role on adsorption rate of nucleic acid bases (Ayar and Gurten, 2003).

2.7. Adsorption of base and/or nucleosides mixtures

2.7.1. Adsorption at Hg electrode

The condensed monolayer of nucleic acid bases can be stabilized either by stacking interactions between bases oriented perpendicularly to the electrode surface (Brabec *et al.*, 1996; Jursa and Vetterl, 1984; Paleček, 2002; Retter, 1980, 1984; Retter *et al.*, 1989; Vetterl, 1976; Vetterl and de Levie, 1991; Vetterl and Pokorný, 1980) or by hydrogen bonds between planar-oriented bases (de Levie, 1988; de Levie and Wandlowski, 1994; Sridharan and de Levie, 1987). Some information about the orientation in the surface can bring the measurement of the adsorption of mixtures of complementary and non-complementary bases and/or nucleosides.

The electrosorption of mixtures of complementary and non-complementary bases (Brabec *et al.*, 1978) and nucleosides (Ueharra and Elving, 1981) was studied more than 20 years ago. It was found that mixtures of non-complementary bases when only one of which was able to form a capacitance pit exhibit an initial dilute adsorption region (Brabec *et al.*, 1978). At critically defined bulk solution concentrations of bases capable to form the pit, a surface reorientation occurs even in the presence of the base in the solution incapable to form the pit. However, mixtures of complementary bases, exhibit only a dilute adsorption region. Even at bulk solution concentrations considerably greater than those required to observe the flat-to-perpendicular reorientation for the single bases the mixed base system does not exhibit such a surface phenomenon. Thus one of the contributing factors to stabilization of the dilute (flat) adsorption layer in the mixed complementary base system is the Watson–Crick hydrogen bonding between the base pairs on the electrode surface (Brabec *et al.*, 1978). Similar results were obtained with the mixtures of nucleosides (Ueharra and Elving, 1981).

The condensation behaviour of adenine at the mercury surface with respect to a possible reorientation during the phase transition was investigated in 2001 by Kirste and Donner (2001). They found that, in contrast to thymine, randomly adsorbed adenine yields a negative dipole contribution with regard to the displaced water molecules. During the condensation, reorientation takes place in such a way that this negative dipole contribution is reinforced. Co-adsorption of the complementary DNA bases adenine and thymine leads to destabilization of both the condensed and the randomly adsorbed layers. In place of the attractive lateral forces between adenine and thymine in a pure condensed monolayer, another kind of interaction occurs between adenine and thymine in a mixed adsorbate. Hence, the phase transition disappears when a critical ratio of adenine to thymine is reached (Kirste and Donner, 2001).

A mixed monolayer constituted by chemisorbed 6-thioguanine and physisorbed guanine molecules was studied recently by Arias *et al.* (2004). The mixed monolayer was characterised by chronoamperometry, CV and phase-sensitive ac voltammetry under *in situ* conditions, and the experimental data revealed a compact packing of molecules in the film. *Ex situ* measurements in the presence of dissolved oxygen proved that the mixed monolayer is stable in solutions lacking 6TG and G (Arias *et al.*, 2004).

2.7.2. Adsorption at Au(111)

The adsorption of adenine as well as the co-adsorption of A-T and U-T on Au(111) was studied (Camargo *et al.*, 2002, 2003). It was found that adenine is chemisorbed in two different states. Mutual interaction between adenine and thymine could be detected only at negative potentials where both molecules are oriented with their plane parallel to the surface. This interaction depends on the concentration of thymine, the pH value, the temperature and the roughness of the surface. At positive potentials where T-A are oriented perpendicular to the electrode surface no hints for their interaction could be found (Camargo *et al.*, 2002, 2003). Thymine prevents the uracil adsorption and no interaction between the non-complementary bases T-U was found (Camargo *et al.*, 2002, 2003).

2.8. Adsorption of bases at Hg from non-aqueous solvents

The 2-D phase transition of adenine adsorbed at the Hg/ethylene glycol solution interface was studied (Benedetti *et al.*, 2004). Equilibrium aspects are effectively rationalized by using a model that was originally developed for the 2-D phase transition of adenine adsorbed at the Hg/aqueous solution interface. The attention was mainly focused on the validation of the model itself in the case of a solvent different from water. The results obtained in the two different solvents were compared in terms of structural (orientation of the adsorbate at the interface) and related thermodynamic (liquid like \rightarrow solid like 2-D standard entropy variation) properties. It was found that the kinetics of formation of the 2-D solid-like phase follows a nucleation and growth mechanism in close similarity with the results obtained in water (Benedetti *et al.*, 2004).

3. ELECTROREDUCTION AND ELECTROOXIDATION OF NUCLEIC ACID COMPONENTS

As early as in 1958 it was shown by Paleček that all five bases usually occurring in nucleic acids give oscillographic signals. With adenine, cytosine and guanine, the oscillographic signals were observed with their nucleosides and nucleotides as well (Paleček, 1958).

3.1. Electroreduction at mercury electrode

Adenine and cytosine in protonated forms and their nucleosides and nucleotides can be reduced at mercury electrodes in aqueous solutions.

Adenine gives a single, large, pH-dependent and diffusion-controlled polarographic wave ($E_{1/2} = -0.975$ to 0.084 ; pH between 1 and 6). The reduction wave of adenine has almost a constant height up to pH 4 or 5, when it begins to decrease with increasing pH and disappears at pH 6 or 7. The mechanism of electrode reactions was studied mostly by Elving and Janík (Janík and Elving, 1968; Webb *et al.*, 1973). The reduction of adenine involves a primary potential controlling reduction of the N(1) = C(6) double bond to give 1,6-dihydro-6-aminopurine (Figure 10). This compound is reduced in a $2e^- - 2H^+$ process to give 1,2,3,6-tetrahydro-6-aminopurine. The reduction mechanism is the same in adenine nucleosides and nucleotides.

Cytosine also exhibits a single, pH-dependent polarographic reduction wave ($E_{1/2} = -1.125$ to 0.073 ; pH between 4 and 6) (Webb *et al.*, 1973). The basic reaction pattern involves a rapid protonation at the N(3) position to form electroactive species (Figure 11). A two-electron reduction of the N(3) = C(4) double bond then occurs to form a carbanion. Protonation of the latter followed by deamination, regenerates the N(3) = C(4) bond giving 2-oxypyrimidine. Protonation and further one-electron reduction of 2-oxypyrimidine gives a free radical, which then dimerizes to 6,6'-bis(3,6)-dihydropyrimidone-2. The same mechanism of reduction is proposed for cytosine nucleosides and nucleotides.

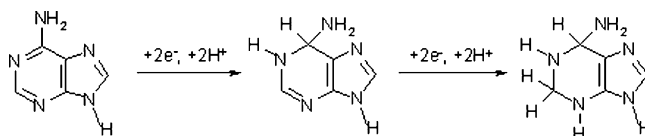


Fig. 10. Reaction scheme for polarographic reduction of adenine.

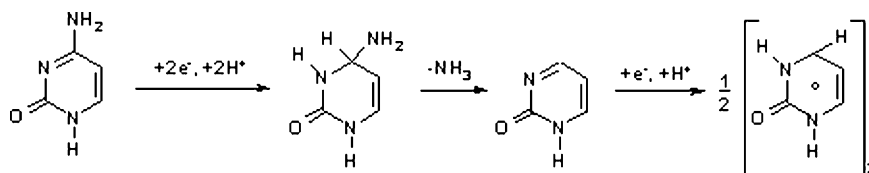


Fig. 11. Reaction scheme for polarographic reduction of cytosine.

Guanine can be reduced at the mercury electrode at highly negative potentials close to background discharge (Studničková *et al.*, 1989; Trnková *et al.*, 1980). Reduction of adenine, cytosine and inosine was studied using elimination polarography (Havran *et al.*, 1998; Trnková *et al.*, 2001).

Thymine and uracil are reduced at the mercury electrode in non-aqueous media (Cummings and Elving, 1978,1979). Cathodic stripping voltammetry (CSV) and cathodic transfer stripping voltammetry developed by Paleček (Paleček *et al.*, 1989) can be used to determine low concentrations of substances that form sparingly soluble compounds with electrode mercury (see Paragraph 3.5.) (Brainina, 1971; Brainina and Neyman, 1993).

In the middle of the 1980s, it was shown that the nucleic acids bases can be determined by CSV at the hanging mercury drop electrode (HMDE) at nanomolar levels in the presence of a small amount of copper ions as sparingly soluble compounds of Cu(I) with the purine bases (Glodowski *et al.*, 1986, 1987; Househam *et al.*, 1987). It was observed that the sparingly soluble compounds of Cu(I) with the purine bases can be accumulated at the electrode surface either by reduction of Cu(II) ions at the HMDE or by oxidation of the copper liquid amalgam. The purine base-Cu(I) complex was stripped either cathodically or anodically with detection limits of 0.3 and 20 nM, respectively (Glodowski *et al.*, 1986, 1987; Househam *et al.*, 1987). Recently, Farias *et al.* (2001, 2003) determined a very low concentration of adenine by CSV at the HMDE in the presence of copper in alkaline medium (detection limit was a 0.03 nM at 6-min accumulation time). The determination of purine bases of acid hydrolysed DNA in alkaline medium of 0.005 M NaOH on the silver or copper amalgam electrode modified by a liquid mercury meniscus (Yosypchuk *et al.*, 2002), and polished solid silver amalgam electrode (Fadrná *et al.*, 2004) in the presence of copper ions with detection limits of 4.4 and 1.75 nM (related to the monomer) was performed as well, respectively.

Elimination voltammetry with linear scan (EVLS) has been applied to the resolution of reduction signals of adenine and cytosine in short synthetic homooligodeoxynucleotides (dA(9) and dC(9)) (Trnková *et al.*, 2003). In comparison

with the common electrochemical methods (linear sweep, differential pulse and square-wave voltammetry) EVLS enables one to resolve the overlapped signals by using the function, which eliminates the charging and kinetic currents (I-c, I-k) and conserves the diffusion current (I-d). For the adsorbed electroactive substance, this elimination function gives a good readable peak-counterpeak which has successfully been utilized to the analysis of overlapped reduction signals of adenine and cytosine on HMDE. The height and potential of signals studied were affected by the $dC(9)/dA(9)$ ratio, the time of accumulation, the stirring speed during the adsorption and pH. Our results showed that EVLS in connection with the adsorption procedure is a useful tool for qualitative and quantitative studies of short oligonucleotides (Trnková *et al.*, 2003).

3.1.1. Determination of picogram quantities of DNA by stripping transfer voltammetry

Highly sensitive label-free techniques of DNA determination are particularly interesting in relation to the present development of the DNA sensors. It was shown (Jelen *et al.*, 2002, 2004) that subnanomolar concentrations (related to monomer content) of unlabelled DNA can be determined using copper amalgam electrodes modified by a liquid mercury meniscus or HMDEs in the presence of copper. In the first step, DNA is hydrolyzed for 30 min in 0.5 M perchloric acid at 75°C, and the acid-released purine bases are directly determined by the CSV. The electrochemical step involves generation of Cu(I)-purine base residue complex on a mercury electrode surface, transfer of electrode with accumulated complex into supporting electrolyte where voltammetric measurement is performed. Analysis is carried out in 14 μ L drop volume (two-electrode connection) or in 30 μ L drop (three-electrode connection) on a platinum plate, which is used as a counter electrode. Supporting electrolyte was 0.05 M borate buffer, pH 9.2 with 6.3 μ M Cu(II). This method enables to accumulate under the controlled potential and determine subnanomolar concentration of DNA corresponding to the amount of 200 pg of DNA. We recently detected the picomolar level of oligodeoxynucleotides (ODN) containing purine bases (250 pM of acid hydrolysed (A)₈₀ ODN, related to the monomer) via surface accumulation of the purine base residue-Cu(I) complex at the mercury-modified graphite electrodes (Figure 12) (Hasoň *et al.*, 2005).

3.2. Electrooxidation at carbon electrodes

Purine bases, nucleosides and nucleotides are oxidized in a wide pH range at carbon electrodes (Dryhurst and Elving, 1968; Dryhurst and Pace, 1970; Dryhurst, 1997).

The mechanism of electrooxidation of adenine at the graphite electrode (Dryhurst and Elving, 1968) involves two sequential $2e^- - 2H^+$ oxidations to give first 2-oxy- and 2,8-dioxyadenine (Figure 13). Then, a further two electron oxidation at the C(4) = C(5) double bond occurs to give a dicarbonium ion.

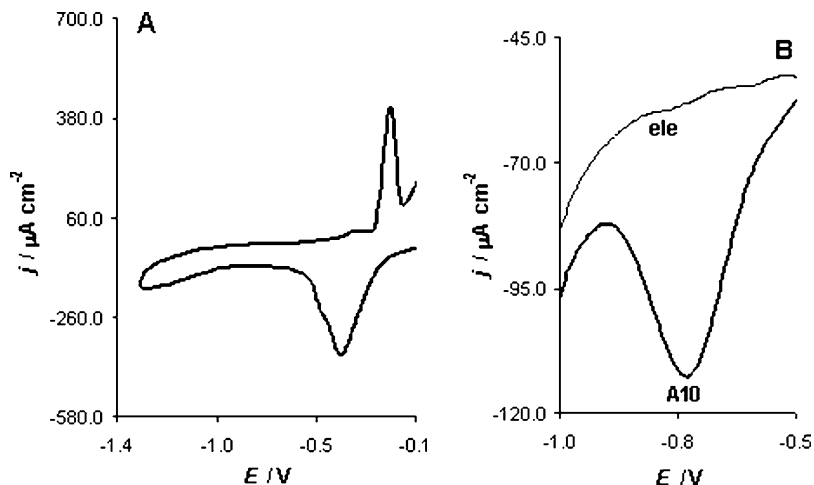


Fig. 12. (A) The steady-state cyclic voltammogram of 0.05 M sodium borate (pH 9.3) in presence of 20 μM Cu(II) ions on the 0.4 μm Hg-modified PGEb. (B) The parts of cyclic voltammograms of 0.05 M sodium borate in presence of: (ele) 20 μM Cu(II), and (A10) 50 nM (A)₁₀ + 20 μM Cu(II). Before the potential scan the accumulation of the (A)₁₀-Cu(I) complex at the 0.4 μm Hg-modified PGEb surface was performed. The accumulation conditions were: potential accumulation of $E_{\text{AC}} = -0.38$ V; accumulation time of $t_{\text{AC}} = 8$ min; rate of stirring $\omega = 3000$ min^{-1} . The scan rate of the measured CVs was $v_{\text{scan}} = 1$ V s^{-1} . The measurement was performed at room temperature. (Parts A and B are partially adapted from Hasoň *et al.*, 2005, Figures 4(B) and 5, respectively, with permission from Elsevier.)

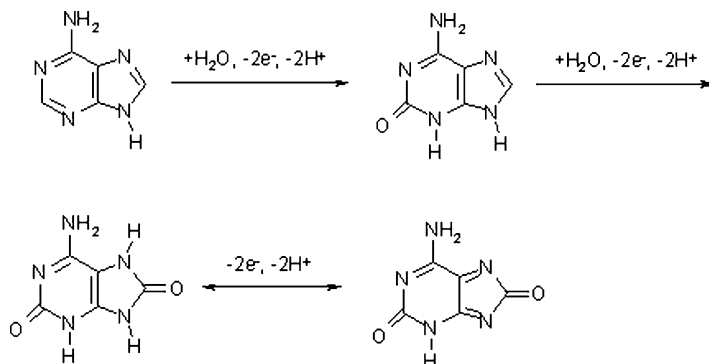


Fig. 13. Reaction scheme for electrochemical oxidation of adenine.

Guanine is oxidized by an initial $2e^- - 2H^+$ attack at the N(7) = C(8) to give 8-oxyguanine, which is immediately oxidized in a further $2e^- - 2H^+$ process to the diimine (Dryhurst and Elving, 1968; Dryhurst, 1977) (Figure 14). The latter product undergoes secondary hydration, fragmentation and oxidation to parabanic acid or secondary hydrolysis to oxalyguanidine. Close to 4.7 electrons are transferred during oxidation of guanine, which accounts for the four electrons involved in the primary electron-transfer process plus the extra electrons required

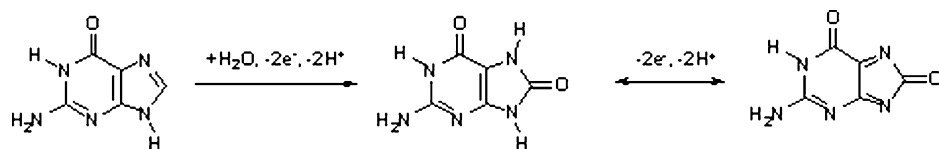


Fig. 14. Reaction scheme for electrochemical oxidation of guanine.

for the origin of parabanic acid. Oxidation of the guanine reduction product (7,8-dihydrogen guanine) can be observed using CV (Jelen *et al.*, 1997; Paleček *et al.*, 1986, 1997). The electrochemical oxidation of adenosine (Goyal and Sangal, 2002) and AMP (Goyal and Sangal, 2003) has been studied in phosphate buffers in the pH range 1.4–9.8 at a pyrolytic graphite electrode. Oxidation has been found to proceed in a single well-defined peak. The kinetic studies of the UV-absorbing intermediate generated during electrooxidation were followed spectrophotometrically and the decay occurred in a pseudo-first-order reaction. On the basis of electrochemical, spectrochemical and product analysis, a detailed redox mechanism for the formation of the oxidation products in neutral and alkaline medium have been proposed (Goyal and Sangal, 2002, 2003).

Electrochemical impedance spectroscopy was used to study the adsorption and oxidation at GCEs of guanine, its corresponding nucleoside, guanosine and adenine (Oliveira-Brett *et al.*, 2002a,b). Impedance studies at different concentrations and applied potentials show that all three bases are adsorbed on the electrode, blocking the surface. Irradiating the electrode with low-frequency (20 kHz) ultrasound whilst recording the impedance spectra increased transport of molecules to the electrode surface with cavitation cleaning the surface and removing strongly adsorbed molecules of bases. In this way, sonoelectrochemical experiments enabled the electrode processes to be studied in the absence of adsorption and the oxidation rate constants were calculated (Oliveira-Brett *et al.*, 2002a, b).

Oxidation of thymine and cytosine at carbon electrode was observed by Oliveira-Brett and Matysik (Brett and Matysik, 1997).

The voltammetric oxidation of all DNA monophosphate nucleotides was investigated over a wide pH range by differential pulse voltammetry (DPV) with a GCE (Oliveira-Brett *et al.*, 2004). Experimental conditions such as the electrode size, supporting electrolyte composition and pH were optimized to obtain the best peak potential separation and higher currents. This enabled the simultaneous voltammetric determination of all four DNA bases in equimolar mixtures and detection limits in the nanomolar range at physiological pH. It was also possible to detect the oxidation of each of the purine and pyrimidine nucleotides free in solution or as monomers in ssDNA (Oliveira-Brett *et al.*, 2004).

Graphite-epoxy composites (GEC) have an uneven surface allowing DNA, oligonucleotides and free DNA bases to be adsorbed using a simple and fast wet-adsorption procedure (Erdem *et al.*, 2004). In contrast with other transducers commonly used for electrochemical genosensing, the oxidation potentials are much lower when GEC is used. Free guanine base is oxidized at +0.35 V

while adenine oxidation occurs at +0.63 V (vs Ag|AgCl). Cytosine and inosine-free bases show no peaks within the experimental potential range. The oxidation of DNA guanine moieties occurs at a potential of +0.55 V while DNA adenine bases are oxidized at +0.85 V. A novel label-free hybridization genosensor using GEC as an electrochemical transducer for the specific detection of a sequence related with *Salmonella* spp. was developed (Erdem *et al.*, 2004). The extent of hybridization onto the GEC surface between the probe and the target has been determined by DPV using the oxidation signal of guanine coming from the target. The hybridization event has also been detected in co-existing salmon testes DNA (stDNA) as interference (Erdem *et al.*, 2004).

3.3. Electrooxidation at diamond electrode

Boron doped diamond (BDD) is a promising material for electroanalytical chemistry mainly due to its chemical stability, its high electrical conductivity and to the large amplitude of its electroactive window in aqueous media. The latter feature allowed to study the direct oxidation of the two electroactive nucleosides, guanosine and adenosine (Fortin *et al.*, 2004). The BDD electrode was first activated by applying high oxidizing potentials, allowing to increase anodically its working potential window through the oxidation of CH surface groups into hydroxyl and carbonyl terminations. Guanosine (1.2 V vs. Ag/AgCl) and adenosine (1.5 V vs. Ag/AgCl) could then be detected electrochemically with an acceptable signal to noise ratio. The electrochemical signature of each oxidizable base was assessed using DPV, in solutions containing one or both nucleosides. These experiments pointed out the existence of adsorption phenomena of the oxidized products onto the diamond surface. Scanning electrochemical microscopy (SECM) was used to investigate these adsorption effects at the microscopic scale. The usefulness of BDD electrodes for the direct electrochemical detection of synthetic oligonucleotides is also evidenced (Fortin *et al.*, 2004).

3.4. Effect of uracil adsorption on the oxygen reduction at platinum electrode

The rate of oxygen reduction in 0.5 M H₂SO₄ has been controlled by adsorbing uracil and its alkyl derivatives on a Pt electrode. Addition of an ethyl group to C(5), or methyl groups to the C(5) and C(6) positions of uracil enhances the reaction rate. 5-Ethyluracil and 5,6-dimethyluracil have such an effect, however, only when their concentrations in the electrolyte are less than or equal to 0.1 mM. Substitution of the hydrogen on N(3) with -CH₃, or exocyclic oxygens with -OCH₃ groups results in the inhibition of the reaction; 1,3-dimethyluracil and 2,4-dimethoxypyrimidine (0.1 mM) are two systems that cause inhibition. Interaction between the surface Pt atoms and the N(3) and O sites on the organic molecule, especially in the presence of -CH₃ or -C₂H₅ groups on the C(5) and/or C(6) centres, are essential for the enhancement of the reaction rate. Results of rotating disc electrode experiments suggest that at low overpotentials,

5-ethyluracil and 5,6-dimethyluracil increase the exchange current to produce higher reaction rates (Saffarian *et al.*, 2001).

3.5. Sparingly soluble compounds at the mercury electrode

All nucleic acid bases and a number of purine and pyrimidine derivatives produced sparingly soluble compounds with mercury and could be determined by the CSV at nanomolar and subnanomolar concentrations (Paleček *et al.*, 2002). Groups responsible for the formation of the mercury compounds may involve exocyclic and ring nitrogens in dependence of the nature of the base and experimental conditions (Paleček *et al.*, 1982). At alkaline pH the mercury-binding site of adenine is the 6-aminogroup. Pyrimidine nucleosides are inactive because of substitution of the pyrimidine ring by a sugar residue at N(1), involved in the mercury binding in bases. In contrast to other pyrimidine nucleosides, pseudouridine (in which the sugar moiety is bound to C(5) while N(1) is free) produces electrochemical responses typical of mercury compounds (Paleček, 1985). Purine nucleosides (the sugar residues bound to N(9)) behave similarly to their parent bases.

4. CONCLUDING REMARKS

Nucleic acid bases possess an extraordinary high ability of self-association at the electrode surface and undergoes a 2-D condensation forming a monomolecular layer. By this high condensation ability, nucleic acid bases differ from most of the other purine and pyrimidine derivatives, which currently do not occur in nucleic acids (like isocytosine, isoguanine, xanthine, etc.). Two-dimensional first-order phase transitions of molecules adsorbed on homogeneous surfaces often proceed via nucleation and growth processes. The kinetics of these phase transitions were investigated by means of current transients ($j-t$ curves) using the double potential step technique. Depending on the start and final potentials different shapes of capacitance or current transients can be detected. The $j-t$ curves were mostly characterised by an exponential decay followed by a pronounced maximum and finally by a decrease of current. The initial exponential decay of these $j-t$ curves can be associated with the sum of the double-layer charging due to the potential step itself and the Langmuir-type (dilute) adsorption before the nucleation starts. The current maximum is associated with nucleation and growth process.

We showed that Hg-modified graphite electrodes can be successfully used for the study of the adsorption, 2-D condensation and formation of ordered adlayers and kinetics of the phase transition between different adlayers of nucleic acid components. It means that with the MFEs the effect of the surface morphology of the underlying graphite substrates on the adsorption and kinetics of the 2-D condensation of the nucleic acid components in the same potential windows as with an HMDE can be investigated.

At the end of the last century the investigations of molecular adsorption onto single-crystal electrodes rapidly gained increasing interest. The use of such

substrates has opened a new field of research, which has been investigating the role played by the electrode surface on the stability of 2-D molecular assemblies. Detailed studies of the adsorption of pyridine and the nucleic acid bases and nucleosides on various gold, silver and more recently on copper single-crystal electrodes have provided clear evidence of the importance of the nature as well as of the crystallographic orientation of the electrodes.

Quite recently, we described the kinetics of phase transitions of purine nucleotides at MeAEs. It means that the MeAEs are an alternative for the study of the adsorption, 2-D condensation and formation of ordered adlayers and kinetics of the phase transition between different adlayers of nucleic acids components to very expensive single-crystal metal electrodes. In addition the amalgam-alloy has a minimal toxicity and a much longer lifetime (from hours to days) in comparison with liquid Hg-films.

Adenine and cytosine protonated forms and their nucleosides and nucleotides can be reduced at mercury electrodes in aqueous solutions. Guanine can be reduced at the mercury electrode at highly negative potentials close to background discharge. Purine bases, nucleosides and nucleotides are oxidized in a wide pH range at carbon electrodes.

The adsorption of organic molecules onto the surfaces of inorganic solids has long been considered a process relevant to the origin of life. The equilibrium adsorption isotherms for the nucleic acid purine and pyrimidine bases dissolved in water on the surface of crystalline graphite was determined by Sowerby. The adsorption behaviour of the individual bases was significantly different and decreased in the series: guanine > adenine > hypoxanthine > thymine > cytosine > uracil. In the same sequence decreased the adsorption of nucleic acid base at the mercury electrode determined by differential capacitance measurement proposed that such differential properties were relevant to the prebiotic chemistry of the bases and may have influenced the composition of the primordial genetic architecture.

LIST OF ABBREVIATIONS

AFM	atomic force microscopy
AMP	adenosine monophosphate
ATR	attenuated total reflection
Ag (100), Ag (111)	single crystal Ag
Au (100), Au (111)	single crystal Au
BDD	boron doped diamond
BR buffer	Britton-Robinson buffer
C	differential capacitance of the electrode double layer
CV	cyclic voltammogram, cyclic voltammetry
CSV	cathodic stripping voltammetry
Cu (110), Cu (111)	single crystal Cu

DFT	density functional theory
DNA, ssDNA, dsDNA, stDNA	deoxyribonucleic acid, single stranded DNA, double stranded DNA, salmon testes DNA
DMSO	dimethylsilfoxide
DOE	diffractive optical element
DPV	differential pulse polarography
E	electrode potential
EIS	electrochemical impedance spectroscopy
ESR	electron spin resonance
EVLS	elimination voltammetry with linear scan
GaAs	gallium arsenide
GCE	glassy carbon electrode
GEC	graphite-epoxy composite
HMDE	hanging mercury drop electrode
HREEL	high resolution electron energy-loss spectroscopy
HOPG	high oriented pyrolytic graphite
j	electric current density
MeAE	metal-mercury amalgam electrode
MFE	mercury film electrode
MO	molecular orbital
NAD	nicotineamide adenine dinucleotide
m	Avrami exponent
ODN	oligodeoxynucleotide
PGE _b	pyrolytic graphite electrode with basal orientation
PL	photoluminescence
pzc	potential of zero charge
QCM	quartz crystal microbalance
q	electric charge
R_a	optical roughness
RAS	reflectance anisotropy spectra
RNA	ribonucleic acid
SAM	self assembled monolayers
SECM	scanning electrochemical microscopy
SEIRAS	surface enhanced infrared reflection absorption spectroscopy
SERS	surface enhanced Raman spectroscopy
Si (001), Si (111)	single crystal Si
SPR	surface plasmon resonance
STM	scanning tunneling microscopy
TDP	tridecylphosphate
UHF	ultra high vacuum
UMP	uridine monophosphate
UPD	underpotential deposition
Z'	real part of the complex impedance
Z''	imaginary part of the complex impedance
2-D	two-dimensional

ACKNOWLEDGMENTS

This work was supported by the Grant Agency of the Academy of Sciences of the Czech Republic KJB 4004305 (S. H.), S5004107 (V. V.) and institutional grant Z 5004920. The authors are indebted for helpful discussions to Prof. E. Paleček and Dr. F. Jelen. We also appreciate the great help of Dr. L. Strašák in the manuscript preparation and arrangement of references.

REFERENCES

- Aqua, T., R. Naaman and S.S. Daube, 2003, Controlling the adsorption and reactivity of DNA on gold, *Langmuir* 19, 10573–10580.
- Arias, Z.G., J.L.M. Alvarez and J.M.L. Fonseca, 2004, Electrochemical characterization of a mixed self-assembled monolayer of 6-thioguanine and guanine on a mercury electrode, *J. Colloid Interf. Sci.* 276, 132–137.
- Aroca, R. and R. Bujalski, 1999, Surface enhanced vibrational spectra of thymine, *Vib. Spectrosc.* 19, 11–21.
- Artzi, R., S.S. Daube, H. Cohen and R. Naaman, 2003, Adsorption of organic phosphate as a means to bind biological molecules to GaAs surfaces, *Langmuir* 19, 7392–7398.
- Ataka, K. and M. Osawa, 1999, In situ infrared study of cytosine adsorption on gold electrodes, *J. Electroanal. Chem.* 460, 188–196.
- Ayar, A. and A.A. Gurten, 2003, Determination of the rate control step of purin and pyrimidine bases adsorption on cobalt(II)-CDAE-sporopollenin, *Colloid. Surf. A* 229, 149–155.
- Bare, S. and C. Buess-Herman, 1998, On the formation and dissolution kinetics of two-dimensional uracil ordered phases at the gold single crystal electrode aqueous solution interface, *Colloid. Surf. A* 134, 181–191.
- Bare, S., M. Van Krieken, C. Buess-Herman and A. Hamelin, 1998, Effect of the crystallographic orientation of gold single-crystal electrodes on the occurrence of 2D phase transitions in adsorbed organic monolayers, *J. Electroanal. Chem.* 445, 7–11.
- Batratkov, V.V., B.B. Damaskin and Y.P. Ipatov, 1974, Determination of charge and evaluation of zero charge potential of faces of zinc single crystals according to the effect of sodium fluoride concentration on the desorption potential of camphor, *Elektrokhimiya* 10, 144.
- Benedetti, L., G. Camurri, C. Fontanesi, P. Ferrarini and R. Giovanardi, 2004, On the 2D phase transition of adenine adsorbed at the mercury/ethylene glycol solution interface, *Electrochim. Acta* 49, 1655–1662.
- Berezney, R. and D.S. Coffey, 1974, Identification of a nuclear protein matrix, *Biochem. Biophys. Res. Commun.* 60, 1410–1417.
- Brabec, V., S.D. Christian and G. Dryhurst, 1977, Interfacial behavior of uracil at the mercury-solution interface. Evidence for surface reorientation processes, *J. Electroanal. Chem.* 85, 389–405.
- Brabec, V., S.D. Christian and G. Dryhurst, 1978, Adsorption of mixtures of complementary and non-complementary nucleic acid bases at the mercury-solution interface, *Bioelectrochem.* 5, 635–649.
- Brabec, V., M.H. Kim, S.D. Christian and G. Dryhurst, 1979, Interfacial behavior of adenine and its nucleosides and nucleosides, *J. Electroanal. Chem.* 100, 111–133.
- Brabec, V., V. Vetterl, V. Kleinwachter and J. Reedijk, 1989, Interfacial behaviour of trideoxyribonucleotide d(CpGpG) and its complex with the antitumour drug cisplatin at the mercury-electrolyte solution interface, *Bioelectrochem. Bioenerg.* 21, 199–204.
- Brabec, V., V. Vetterl and O. Vrana, 1996, Experimental techniques in bioelectrochemistry, *Electroanalysis of Biomacromolecules*, Vol. 3, Eds. V. Brabec, D. Walz and G. Milazzo, pp. 287–359. Birkhauser-Verlag, Basel.

- Brainina, K.Z., 1971, Film stripping voltammetry, *Talanta* 18, 513–539.
- Brainina, K.Z. and E. Neyman, 1993, *Electroanalytical Stripping Methods*, Wiley, New York.
- Brainina, K.Z., A.V. Tchernyshova, N.Y. Stozhko and L.N. Kalnyshevskaya, 1989, In-situ modified electrodes in stripping voltammetry, *Analyst* 114, 173–180.
- Brett, A.M.O. and F.M. Matysik, 1997, Voltammetric and sonovoltammetric studies on the oxidation of thymine and cytosine at a glassy carbon electrode, *J. Electroanal. Chem.* 429, 95–99.
- Buess-Herman, C., 1985, Non-faradaic phase-transitions in adsorbed organic layers. 2. Experimental aspects, *J. Electroanal. Chem.* 186, 41–50.
- Buess-Herman, C., 1986, Trends in interfacial electrochemistry and electrochemical engineering, *Phase Transitions in Adsorbed Layers*, Vol. C179, Ed. A.F. Silva, Reidel, Dordrecht, 205–253.
- Buess-Herman, C., 1992, Adsorption of organic molecules at metal electrodes, *Dynamics of Adsorption and Two-Dimensional Phase Transitions at Electrode Surfaces*, Eds. J. Lipkowski and P.N. Ross, New York, 77–118.
- Buess-Herman, C., 1994, Self-assembled monolayers at electrode metal surfaces, *Progr. Surf. Sci.* 46, 335–375.
- Buess-Herman, C., S. Bare, M. Poelman and M. Van Krieken, 1999, *Interfacial electrochemistry: theory, experiment and applications, Ordered Organic Adlayers at Electrode Surfaces*, Ed. A. Wieckowski, Marcel Dekker, New York, 427–447.
- Buess-Herman, C., C. Franck and L. Gierst, 1992, On the influence of molecular structure on the orientation and the occurrence of phase transition in organic adsorbed layers at the mercury-water interface, *J. Electroanal. Chem.* 329, 91–102.
- Buess-Herman, C. and L. Gierst, 1984, Potential step chronocoulometry of dioxygen in aqueous alkaline solutions saturated with isoquinoline, *Electrochim. Acta* 29, 303–309.
- Buess-Herman, C., L. Gierst and N. Vanlaethem-Meuree, 1981a, On the behaviour of molecules of the quinoline group at the water-mercury interface: Part I. Electrocapillary study of the O-quinoline in solutions containing only an “inert” electrolyte, *J. Electroanal. Chem.* 123, 1–19.
- Buess-Herman, C., G. Quarin and L. Gierst, 1983a, On the behaviour of molecules of the quinoline group at the water-mercury interface: Part IV B. The kinetics of two-dimensional phase transitions displayed by 3-methyl-isoquinoline, *J. Electroanal. Chem.* 148, 97–116.
- Buess-Herman, C., G. Quarin, L. Gierst and J. Lipkowski, 1983b, On the behaviour of molecules of the quinoline group at the water-mercury interface: Part IV A. Electrocapillary study of 3-methyl-isoquinoline, *J. Electroanal. Chem.* 148, 79–95.
- Buess-Herman, C., N. Vanlaethem-Meuree, G. Quarin and L. Gierst, 1981b, On the behaviour of molecules of the quinoline group at the water-mercury interface: Part II. Electrocapillary study of isoquinoline in solutions containing only an “inert” electrolyte, *J. Electroanal. Chem.* 123, 21–34.
- Camargo, A.P.M., H. Baumgartel and C. Donner, 2002, Adsorption behaviour of DNA bases at the Au(111) electrode, *Phys. Chem. Comm.* 151–157.
- Camargo, A.P.M., H. Baumgartel and C. Donner, 2003, Co-adsorption of the DNA bases thymine and adenine at the Au(111) electrode, *Phys. Chem. Chem. Phys.* 5, 1657–1664.
- Cavallini, M., G. Aloisi, M. Bracali and R. Guidelli, 1998, An in situ STM investigation of uracil on Ag(111), *J. Electroanal. Chem.* 444, 75–81.
- Chen, Q., D.J. Frankel and N.V. Richardson, 2002, Self-assembly of adenine on Cu(110) surfaces, *Langmuir* 18, 3219–3225.
- Chen, Q. and N.V. Richardson, 2003, Enantiomeric interactions between nucleic acid bases and amino acids on solid surfaces, *Nat. Mater.* 2, 324–328.
- Chowdhury, J., K.M. Mukherjee and T.N. Misra, 2000, A pH dependent surface-enhanced Raman scattering study of hypoxanthine, *J. Raman Spectrosc.* 31, 427–431.
- Ciani, L., S. Branciamore, M. Romanelli and G. Martini, 2003, Nucleoside-copper(II) system in water and on 13x-zeolite studied by continuous-wave and pulsed-wave ESR, *Appl. Magn. Reson.* 24, 55–71.

- Cizkowska, M., M. Donten and Z. Stojek, 1994, Preparation of a mercury disk microelectrode based on solid silver amalgam, *Anal. Chem.* 66, 4112–4115.
- Copeland, T.R., J.H. Christie, R.A. Osteryoung and R.K. Skogerboe, 1973, Analytical application of pulsed voltammetric stripping at thin film mercury electrodes, *Anal. Chem.* 45, 2171–2175.
- Cummings, T.E. and P.J. Elving, 1978, Electrochemical reduction of uracil in dimethyl sulfoxide, *J. Electroanal. Chem.* 94, 123–145.
- Cummings, T.E. and P.J. Elving, 1979, Electrochemical reduction of thymine in dimethyl sulfoxide autoprotonation of the radical anion and reduced free radical, *J. Electroanal. Chem.* 102, 237–248.
- Cunha, F.G.C., J.R. Garcia, F.C. Nart, P. Corio and M. Temperini, 2003, Surface-enhanced Raman spectroscopy study of the potential dependence of thymine on silver electrodes, *J. Solid. State Electr.* 7, 576–581.
- Cunha, F. and F. Nart, 2001, In situ scanning tunneling microscopy study of 5,6-dimethyl uracil on Au(111), *J. Brazil. Chem. Soc.* 12, 715–721.
- Cunha, F., E. Sa and F. Nart, 2001, In situ STM study of the adsorption of halogen derivatives of uracil on Au(111), *Surf. Sci.* 480, L383–L388.
- de Levie, R., 1988, The dynamic double layer: Two-dimensional condensation at the mercury-water interface, *Chem. Rev.* 88, 599–609.
- de Levie, R. and T. Wandlowski, 1994, Hydrogen bonding and two-dimensional condensation in uracils, *J. Electroanal. Chem.* 366, 265–270.
- Denton, M.J., P.K. Dearden and S.J. Sowerby, 2003, Physical law not natural selection as the major determinant of biological complexity in the subcellular realm: New support for the pre-darwinian conception of evolution by natural law, *Biosystems* 71, 297–303.
- Donner, C. and S. Kirste, 2001, Influence of the electrolyte resistance on the transient response in nonfaradaic phase transition experiments on mercury and Au (111), *Langmuir* 17, 1630–1636.
- Donner, C., St. Kirste, L. Pohlmann and H. Baumgärtel, 1997, The appearance of athermal nuclei of thymine at Au (111) and the shape of current-time transients, *Chem. Phys. Letters* 280, 287–295.
- Donner, C., L. Pohlmann, S. Kirste and H. Baumgartel, 2000, Two-dimensional condensation of small organic molecules at electrodes, *Chem. Anal.* 45, 175–188.
- Donten, M. and Z. Kublik, 1985, General-characteristics of the copper-based mercury film electrodes, *J. Electroanal. Chem.* 196, 275–290.
- Donten, M. and Z. Kublik, 1986, Application of a copper-based mercury film electrode in cathodic stripping voltammetry, *Anal. Chim. Acta* 185, 209–218.
- Donten, M. and Z. Kublik, 1993, Voltammetric examination of platinum-based mercury film-submicroelectrodes and mercury submicroelectrodes, *Chem. Anal.* 38, 789–803.
- Dražan, V. and V. Vetterl, 1998, Adsorption and condensation of xanthine at the mercury/solution interface, *Collect. Czech. Chem. Commun.* 63, 1977–1993.
- Dretschkow, T., A.S. Dakkouri and T. Wandlowski, 1997, In-situ scanning tunneling microscopy study of uracil on Au(111) and Au(100), *Langmuir* 13, 2843–2856.
- Dretschkow, T. and T. Wandlowski, 1998, In-situ scanning tunneling microscopy study of uracil on Au(100), *Electrochim. Acta* 43, 2991–3006.
- Dryhurst, G., 1977, *Electrochemistry of Biological Molecules*, Academic Press, New York.
- Dryhurst, G. and P.J. Elving, 1968, Electrochemical oxidation of adenine: Reaction products and mechanisms, *J. Electrochem. Soc.* 115, 1014–1022.
- Dryhurst, G. and G.F. Pace, 1970, Electrochemical oxidation of guanine at the pyrolytic graphite, *J. Electrochem. Soc.* 117, 1259–1265.
- Economou, A. and P.R. Fielden, 2003, Mercury film electrodes: Developments, trends and potentialities for electroanalysis, *Analyst* 128, 205–212.
- El Amri, C., M.H. Baron and M.C. Maurel, 2004, Adenine adsorption on and release from meteorite specimens assessed by surface-enhanced Raman spectroscopy, *J. Raman Spectrosc.* 35, 170–177.

- Erdem, A., M.I. Pividori, M. del Valle and S. Alegret, 2004, Rigid carbon composites: A new transducing material for label-free electrochemical genosensing, *J. Electroanal. Chem.* 567, 29–37.
- Fadrná, R., B. Yosypchuk, M. Fojta, T. Navrátil and L. Novotný, 2004, Voltammetric determination of adenine, guanine, and DNA using liquid mercury free polished silver solid amalgam electrode, *Anal. Lett.* 37, 399–413.
- Farias, P.A.M., A.D.R. Wagener and A.A. Castro, 2001, Ultratrace determination of adenine in the presence of copper by adsorptive stripping voltammetry, *Talanta* 55, 281–290.
- Farias, P.A.M., A.D.R. Wagener, M.B.R. Bastos, A.T. da Silva and A.A. Castro, 2003, Cathodic adsorptive stripping voltammetric behaviour of guanine in the presence of copper at the static mercury drop electrode, *Talanta* 61, 829–835.
- Fleischmann, M. and H.R. Thirsk, 1963, Advances in electrochemistry and electrochemical engineering. Metal Deposition and Electrocrystallization, Vol. 3, Eds. P. Delahay and C. Tobias, Wiley-Interscience, New York, 123–210.
- Florence, T.M., 1979, Cathodic stripping voltammetry. Part I. Determination of organic sulfur compounds, flavins and porphyrins at the sub-micromolar level, *J. Electroanal. Chem.* 97, 219–236.
- Florence, T.M., 1980, Comparison of linear scan and differential pulse anodic stripping voltammetry at a thin mercury film glassy carbon electrode, *Anal. Chim. Acta* 119, 217–223.
- Florence, T.M., 1986, Electrochemical approaches to trace element speciation in waters: A review, *Analyst* 111, 489–505.
- Foresti, M.L., G. Aloisi, M. Innocenti, H. Kobayshi and R. Guidelli, 1995, Crystal-face effects on adsorption of ionic and nonionic species on Ag electrodes: An electrochemical and STM study, *Surf. Sci.* 335, 241–251.
- Fortin, E., J. Chane-Tune, P. Mailley, S. Szunerits, B. Marcus, J.P. Petit, M. Mermoux and E. Vieil, 2004, Nucleosides and ODN electrochemical detection onto boron doped diamond electrodes, *Bioelectrochemistry* 64, 303–306.
- Frenzel, W., 1993, Mercury films on glassy carbon support: Attributes and problems, *Anal. Chim. Acta* 273, 123–137.
- Freymann, M., M. Poelman and C. Buess-Herman, 1997, Two-dimensional ordering of coumarin at the indium amalgam electrolyte interface, *Israel J. Chem.* 37, 241–246.
- Friesem, A.A. and Y. Amitai, 1996, Trends in optics, Planar Diffractive Elements for Compact Optics, Ed. A. Consortini, Academic Press, San Diego, 61–72.
- Furukawa, M., H. Tanaka and T. Kawai, 1997, Scanning tunneling microscopy observation of two-dimensional self-assembly formation of adenine molecules on Cu(111) surfaces, *Surf. Sci.* 392, L33–L39.
- Furukawa, M., H. Tanaka and T. Kawai, 2000, Formation mechanism of low-dimensional superstructure of adenine molecules and its control by chemical modification: A low-temperature scanning tunneling microscopy study, *Surf. Sci.* 445, 1–10.
- Furukawa, M., H. Tanaka and T. Kawai, 2001, The role of dimer formation in the self-assemblies of DNA base molecules on Cu(111) surfaces: A scanning tunneling microscope study, *J. Chem. Phys.* 115, 3419–3423.
- Futamata, M., 2003, Characterization of the first layer and second layer adsorbates on Au electrodes using ATR-IR spectroscopy, *J. Electroanal. Chem.* 550–551, 93–103.
- Futamata, M. and D. Diesing, 1999, Adsorbed state of pyridine, uracil and water on gold electrode surfaces, *Vibrational Spectroscopy* 19, 187–192.
- García-Ramos, J.V., J.C. Otero, J.J. Marcos and S. Sánchez-Cotés, 1996, Excitation profiles of the surface enhanced Raman spectroscopy bands of 1,5-dimethylcytosine on silver colloids, *Biospectroscopy* 2, 243–248.
- García-Ramos, J.V. and S. Sánchez-Cortés, 1997, Colloids employed in the SERS of bio-molecules: Activation when exciting in the visible and near-infrared regions, *J. Mol. Str.* 405, 13–28.
- Gasser, S.M. and U.K. Laemmli, 1986, Cohabitation of scaffold binding regions with upstream/enhancer elements of three developmentally regulated genes of *Drosophila-Melanogaster*, *Cell* 46, 521–530.

- Giese, B. and D. McNaughton, 2002a, Surface-enhanced Raman spectroscopic study of uracil. The influence of the surface substrate, surface potential, and pH, *J. Phys. Chem. B* 106, 1461–1470.
- Giese, B. and D. McNaughton, 2002b, Surface-enhanced Raman spectroscopic and density functional theory study of adenine adsorption to silver surfaces, *J. Phys. Chem. B* 106, 101–112.
- Glodowski, S., R. Bilewicz and Z. Kublik, 1986, Determination of traces of purine by cathodic stripping voltammetry at the hanging copper amalgam drop electrode, *Anal. Chim. Acta* 186, 39–47.
- Glodowski, S., R. Bilewicz and Z. Kublik, 1987, Cathodic and anodic-stripping determination of traces of adenine and adenosine based on accumulation of copper(I) compounds at mercury or amalgam electrodes, *Anal. Chim. Acta* 201, 11–22.
- Golas, J., Z. Galus and J. Osteryoung, 1987, Iridium-based small mercury electrodes, *Anal. Chem.* 59, 389–392.
- Gorodetskii, V.V., I.P. Slutskii and V.V. Losery, 1972, Cinovy amalgam, *Elek.* 8, 1401.
- Goyal, R.N. and A. Sangal, 2002, Electrochemical oxidation of adenosine at solid electrodes, *J. Electroanal. Chem.* 521, 72–80.
- Goyal, R.N. and A. Sangal, 2003, Electrochemical oxidation of adenosine monophosphate at a pyrolytic graphite electrode, *J. Electroanal. Chem.* 557, 147–155.
- Guidelli, R., M.L. Foresti and M. Innocenti, 1996, Two-dimensional phase transitions of chemisorbed uracil on Ag(111): Modeling of short- and long-time behavior, *J. Phys. Chem.* 100, 18491–18501.
- Hamelin, A., 1985, Modern aspects of electrochemistry. Double-Layer Properties at sp and sd Metal Single-Crystal Electrodes, Vol. 16, Eds. B.E. Conway, R.E. White and J.O'M. Bockris, Plenum, New York, 1–101.
- Hasoň, S., J. Dvořák, F. Jelen and V. Vetterl, 2002a, Interaction of DNA with echinomycin at the mercury electrode surface as detected by impedance and chronopotentiometric measurements, *Talanta* 56, 905–913.
- Hasoň, S., J. Dvořák, F. Jelen and V. Vetterl, 2002b, Impedance analysis of DNA and DNA-drug interactions on thin mercury film electrodes, *Crit. Rev. Anal. Chem.* 32, 167–179.
- Hasoň, S., F. Jelen, L. Fojt and V. Vetterl, 2005, Determination of picogram quantities of oligodeoxynucleotides by stripping voltammetry at mercury modified graphite electrode surfaces, *J. Electroanal. Chem.* 577, 263–272.
- Hasoň, S., S.-P. Simonaho, R. Silvennoinen and V. Vetterl, 2003, On the adsorption and kinetics of phase transients of adenosine at the different carbon electrodes modified with a mercury layer, *Electrochim. Acta* 48, 651–668.
- Hasoň, S., S.-P. Simonaho, R. Silvennoinen and V. Vetterl, 2004, Detection of phase transients in two-dimensional adlayers of adenosine at the solid amalgam electrode surfaces, *J. Electroanal. Chem.* 568, 65–77.
- Hasoň, S. and V. Vetterl, 2002a, Two-dimensional condensation of nucleic acid components at mercury film and gold electrodes, *Bioelectrochemistry* 56, 43–45.
- Hasoň, S. and V. Vetterl, 2002b, Application of carbon electrodes modified with a mercury layer of a different thickness for studies of the adsorption and kinetics of phase transients of cytidine, *J. Electroanal. Chem.* 536, 19–35.
- Hasoň, S. and V. Vetterl, 2002c, On the formation kinetics of two-dimensional cytidine films, *Bioelectrochemistry* 57, 23–32.
- Hasoň, S. and V. Vetterl, 2004, Application of thin film mercury electrodes and solid amalgam electrodes in electrochemical analysis of the nucleic acids components: Detection of the two-dimensional phase transients of adenosine, *Bioelectrochemistry* 63, 37–41.
- Hansson, T.K., C.A. Cohn, H.S. Larsson, S.J. Sowerby and N.G. Holm, 2002, Fate of prebiotic adenine, *Geochimica et cosmochimica Acta* 66(Suppl. 1), A310.
- Havran, L., L. Trnková and O. Dračka, 1998, Inosine reduction study at low pH by a combination of electrochemical methods, *J. Electroanal. Chem.* 454, 65–73.
- Herrero, E., L.J. Buller and H.D. Abruna, 2001, Underpotential deposition at single crystal surfaces of Au, Pt, Ag and other materials, *Chem. Rev.* 101, 1897–1930.

- Holm, N.G., G. Ertem and J.P. Ferris, 1993, The binding and reactions of nucleotides and polynucleotides on iron-oxide hydroxide polymorphs, *Origins Life Evol. B* 23, 195–215.
- Hölzle, M.H., D.M. Kolb, D. Krznaric and B. Cosovic, 1996, Adsorption and phase formation of uracil derivatives on gold and silver single-crystal electrodes, *Ber. Bunsenges. Phys. Chem.* 100, 1779–1790.
- Hölzle, M.H., D. Krznaric and D.M. Kolb, 1995a, Phase-transitions in thymine adlayers on silver single-crystal electrodes, *J. Electroanal. Chem.* 386, 235–239.
- Hölzle, M.H., U. Retter and D.M. Kolb, 1994, The kinetics of structural changes in Cu adlayers on Au(111), *J. Electroanal. Chem.* 371, 101–109.
- Hölzle, M.H., T. Wandlowski and D.M. Kolb, 1995b, Structural transitions in uracil adlayers on gold single-crystal electrodes, *Surf. Sci.* 335, 281–290.
- Hölzle, M.H., T. Wandlowski and D.M. Kolb, 1995c, Phase transition in uracil adlayers on electrochemically prepared island-free Au(100)-(1 × 1), *J. Electroanal. Chem.* 394, 271–275.
- Househam, B.C., C.M.G. Van Der Berg and J.P. Riley, 1987, The determination of purines in fresh and sea-water by cathodic stripping voltammetry after complexation with copper(I), *Anal. Chim. Acta* 200, 291–303.
- Janik, B. and P.J. Elving, 1968, Polarographic behavior of nucleosides and nucleotides of purines, pyrimidines, pyridines, and flavins, *Chem. Rev.* 68, 295–319.
- Jehring, H., 1974, *Elektrosorptionanalyse Mit Der Wechselstrompolarographie*, Akademie-Verlag, Berlin.
- Jelen, F., A. Kouřilová, P. Pečinka and E. Paleček, 2004, Microanalysis of DNA by stripping transfer voltammetry, *Bioelectrochemistry* 63, 249–252.
- Jelen, F., M. Tomschik and E. Paleček, 1997, Adsorptive stripping square-wave voltammetry of DNA, *J. Electroanal. Chem.* 423, 141–148.
- Jelen, F., B. Yosypchuk, A. Kouřilová, L. Novotný and E. Paleček, 2002, Label-free determination of picogram quantities of DNA by stripping voltammetry with solid copper amalgam or mercury electrodes in the presence of copper, *Anal. Chem.* 74, 4788–4793.
- Jursa, J. and V. Vetterl, 1984, Effect of Cl⁻, Br⁻ and I⁻ ions on the adsorption and association of cytosine at a mercury electrode, *Bioelectrochem. Bioenerg.* 12, 137–146.
- Jursa, J. and V. Vetterl, 1986, The effect of pH and ionic strength on the association of cytosine on the surface of a mercury electrode, *Studia Biophys.* 114, 75–82.
- Jursa, J. and V. Vetterl, 1989, Association of methyl, amino and hydroxy derivatives of adenine at a mercury electrode at various sodium chloride concentrations, *J. Electroanal. Chem.* 289, 237–244.
- Kasaya, M., H. Tabata and T. Kawai, 1995, Scanning tunneling microscopy observation and theoretical calculation of the adsorption of adenine on Si(100)2 × 1 surfaces, *Surf. Sci.* 342, 215–223.
- Kasaya, M., H. Tabata and T. Kawai, 1996, Scanning tunneling microscopy and molecular orbital calculation of thymine and adenine molecules adsorbed on the Si(100)2 × 1 surface, *Surf. Sci.* 357–358, 195–201.
- Kasaya, M., H. Tabata and T. Kawai, 1998, Scanning tunneling microscopy and molecular orbital calculation of organic molecules adsorbed on the Si(100)2 × 1 surface, *Surf. Sci.* 406, 302–311.
- Kasuk, H., G. Nurk, K. Lust and E. Lust, 2003, Adsorption kinetics of uracil on bismuth single crystal planes, *J. Electroanal. Chem.* 550, 13–31.
- Kawai, T., H. Tanaka and T. Nakagawa, 1997, Low dimensional self-organization of DNA-base molecules on Cu(111) surfaces, *Surf. Sci.* 386, 124–136.
- Kirste, S. and C. Donner, 2001, Coadsorption of the complementary base pair adenine-thymine at the mercury/electrolyte interface, *Phys. Chem. Chem. Phys.* 3, 4384–4389.
- Kolb, D.M., 1992, Structure of electrified interfaces, *Surface Reconstruction at Metal-Electrolyte Interfaces*, Eds. J. Lipkowsky and P.N. Ross, VCH, New York, 65.
- Kolb, D.M., 2000, Structure studies of metal electrodes by in-situ scanning tunneling microscopy, *Electrochim. Acta* 45, 2387–2402.
- Kolb, D.M., 2001, *Electrochemical surface science*, *Angew. Chem. Int. Ed.* 40, 1162–1181.

- Kostečka, P., L. Havran, H. Pivoňková and M. Fojta, 2004, Voltammetry of osmium-modified DNA at a mercury film electrode, application in detecting DNA hybridization, *Bioelectrochemistry* 63, 245–248.
- Kounaves, S.P. and J. Buffle, 1987, An iridium-based mercury-film electrode. 1. Selection of substrate and preparation, *J. Electroanal. Chem.* 216, 53–69.
- Kounaves, S.P. and J. Buffle, 1988, An iridium based mercury film electrode. Part II. Comparison of mercury-film electrode behaviors: Theory versus reality, *J. Electroanal. Chem.* 239, 113–123.
- Kounaves, S.P. and W. Deng, 1991, The effect of mercury film electrode morphology on square-wave voltammetric peak current response as a function of frequency, *J. Electroanal. Chem.* 306, 111–124.
- Kounaves, S.P. and W. Deng, 1993, Analytical utility of the iridium-based mercury ultramicroelectrode with square-wave anodic-stripping voltammetry, *Anal. Chem.* 65, 375–379.
- Kounaves, S.P., J.J. O'Dea, P. Chandrasekhar and J. Osteryoung, 1986, Square wave voltammetry at the mercury film electrode: Theoretical treatment, *Anal. Chem.* 58, 3199–3202.
- Kubičarova, T., M. Fojta, J. Vidic, L. Havran and E. Paleček, 2000a, Mercury film electrode as a sensor for the detection of DNA damage, *Electroanalysis* 12, 1422–1425.
- Kubičarova, T., M. Fojta, J. Vidic, D. Suznjevic, M. Tomschik and E. Paleček, 2000b, Voltammetric and chronopotentiometric measurements with nucleic acids-modified mercury film at glassy carbon electrode, *Electroanalysis* 12, 1390–1396.
- Latta, J.N., 1971a, Computer-based analysis of hologram imagery and aberrations. I. Hologram types and their nonchromatic aberrations, *Appl. Opt.* 10, 599–608.
- Latta, J.N., 1971b, Computer-based analysis of hologram imagery and aberrations. II. Aberrations induced by a wavelength shift, *Appl. Opt.* 10, 609–618.
- Li, W.H., W. Haiss, S. Floate and R.J. Nichols, 1999, In-situ infrared spectroscopic and scanning tunneling microscopy investigations of the chemisorption phases of uracil, thymine, and 3-methyl uracil on Au(111) electrodes, *Langmuir* 15, 4875–4883.
- Lipkowski, J., C. Buess-Herman, J.P. Lambert and L. Gierst, 1986, Mechanism of electron transfer through monomolecular films of neutral organics species adsorbed at an electrode surface, *J. Electroanal. Chem.* 202, 169–189.
- Lipkowski, J., L. Stolberg, D.-F. Yang, B. Pettinger, S. Mirwald, F. Henglein and D.M. Kolb, 1994, Molecular adsorption at metal electrodes, *Electrochim. Acta* 39, 1045–1056.
- Lopez, A., Q. Chen and N.V. Richardson, 2002, Combined STM, HREELS and *Ab Initio* study of the adsorption of uracil on Si(100) 2×1 , *Surf. Interf. Anal.* 33, 441–446.
- Lorenz, W., 1958, Über Die Geschwindigkeit Der Adsorption Und Der Zweidimensionalen Assoziation Höherer Fettsäuren an Der Grenzfläche Quecksilber-Elektrolytlösung, *Z. Elektrochem.* 62, 192–200.
- Magnussen, O.M., 2002, Ordered anion adlayers in metal electrode surfaces, *Chem. Rev.* 102, 679–725.
- Martins, A., A. Queirós and F. Silva, 2005, Surface-structure sensitive adsorption of adenine on gold electrodes, *ChemPhysChem* 6, 1056–1060.
- Meeker, K. and A.B. Ellis, 2000, Adsorption of DNA bases onto a semiconductor surface: Evidence for surface-mediated promotion and detection of complementary base pair formation, *J. Phys. Chem. B* 104, 2500–2505.
- Mikkelsen, Ö. and K.H. Schröder, 2003, Amalgam electrodes for electroanalysis, *Electroanalysis* 15, 679–687.
- Mikkelsen, Ö., K.H. Schroder and T.A. Aarhaug, 2001, Dental amalgam, an alternative electrode material for voltammetric analyses of pollutants, *Coll. Czech. Chem. Commun.* 66, 465–472.
- Miller, I.R., 1995, *Bioelectrochemistry: General introduction, Adsorption and Surface Reactions*, Vol. 1, Eds. S.R. Caplan, I.R. Miller and G. Milazzo, Basel Birkhäuser, Verlag, Basel, 288–362.
- Miller, I.R., 1961a, The structure of DNA and RNA in the water-mercury interface, *J. Mol. Biol.* 3, 229–240.

- Miller, I.R., 1961b, Temperature dependence of the adsorption of native DNA in a polarized water-mercury interface, *J. Mol. Biol.* 3, 357–361.
- Mousty, C. and G. Quarin, 1990, Adsorption de L'adenosine a L'electrode de Mercure-II. Etudes Thermodynamique et Cinetique de la Formation de la Phase Condensee aux Densites de Charges Fortement Negatives, *Electrochim. Acta* 35, 1291–1302.
- Nakagawa, T., H. Tanaka and T. Kawai, 1997, Two-dimensional self-assembly of uracil molecules on Cu(111) surfaces: A low-temperature STM study, *Surf. Sci.* 370, L144–L148.
- Neumann, E., 1978, Ions in Macromolecular and Biological Systems, Eds. D.H. Everett and B. Vincent, *Scientechica*, Bristol, 170–191.
- Neumann, E., 1986a, Digression on biochemical membrane reactivity in weak electromagnetic fields, *Bioelectrochem. Bioenerg.* 16, 565–567.
- Neumann, E., 1986b, Chemical electric field effects in biological macromolecules, *Progr. Biophys. Mol. Biol.* 47, 197–231.
- Nishimura, M., H. Tanaka and T. Kawai, 2002, Structure of linear double-stranded deoxyribonucleic acid adsorbed on Cu(111) surfaces: A low-temperature scanning tunneling microscopy study, *Jpn. J. Appl. Phys. Part-1 Regular Papers Short Notes & Review Papers* 41, 7510–7511.
- Nogues, C., S.R. Cohen, S.S. Daube and R. Naaman, 2004, Electrical properties of short DNA oligomers characterized by conducting atomic force microscopy, *Phys. Chem. Chem. Phys.* 6, 4459–4466.
- Oliveira-Brett, A.M., C.M.A. Brett and L.A. Silva, 2002a, An impedance study of the adsorption of nucleic acid bases at glassy carbon electrodes, *Bioelectrochemistry* 56, 33–35.
- Oliveira-Brett, A.M., L.A. da Silva and C.M.A. Brett, 2002b, Adsorption of guanine, guanosine, and adenine at electrodes studied by differential pulse voltammetry and electrochemical impedance, *Langmuir* 18, 2326–2330.
- Oliveira-Brett, A.M., J.A.P. Piedade, L.A. Silva and V.C. Diculescu, 2004, Voltammetric determination of all DNA nucleotides, *Anal. Biochem.* 332, 321–329.
- Paleček, E., 1958, Oscillographische polarographie der Nucleinsäuren und ihrer Bestandteile, *Die Naturwissenschaften* 45, 186–187.
- Paleček, E., 1985, Determination of pseudouridine at submicromolar concentrations by cathodic stripping voltammetry at a mercury electrode, *Anal. Chim. Acta* 174, 103–113.
- Paleček, E., M. Fojta, F. Jelen and V. Vetterl, 2002, The encyclopedia of electrochemistry, *Electrochemical Analysis of Nucleic Acids*, Vol. 9, (Bioelectrochemistry), Eds. A.J. Bard and M. Stratsmann, pp. 365–429, Wiley-VCH, Verlag, Weinheim.
- Paleček, E., F. Jelen and I. Posthieglová, 1989, Adsorptive transfer stripping voltammetry offers new possibilities in DNA research, *Stud. Biophys.* 130, 51–54.
- Paleček, E., F. Jelen and L. Triková, 1986, Cyclic voltammetry of DNA at a mercury electrode: An anodic peak specific for guanine, *Gen. Physiol. Biophys.* 5, 315–329.
- Paleček, E., J. Osteryoung and R.A. Osteryoung, 1982, Interactions of methylated adenine derivatives with the mercury electrode, *Anal. Chem.* 54, 1389–1394.
- Paleček, E., M. Tomschik, V. Staňková and L. Havran, 1997, Chronopotentiometric stripping of DNA at mercury electrodes, *Electroanalysis* 9, 990–997.
- Pohlmann, L., C. Donner and H. Baumgartel, 1996, First-order phase transitions on electrodes: The role of surface diffusion, *Surf. Sci.* 359, 280–290.
- Popov, A., N. Dimitrov and T. Vitanov, 1992a, Adsorption of thymine on the (111) face of a silver single crystal, *Electrochim. Acta* 37, 2373–2376.
- Popov, A., R. Naneva, N. Dimitrov, T. Vitanov, V. Bostanov and R. de Levie, 1992b, Two-dimensional condensation of thymine on a basal face of a cadmium single crystal, *Electrochim. Acta* 37, 2369–2371.
- Porschke, D. and M. Jung, 1985, The conformation of single-stranded oligonucleotides and of oligonucleotide-oligopeptide complexes from their rotation relaxation in the nanosecond time range, *J. Biomol. Struct. Dynam.* 2, 1173–1184.
- Prado, C., I. Navarro, M. Rueda, M.H. Francois and C. Buess-Herman, 2001, Kinetics of condensation of adenine at the mercury vertical bar electrolyte interface, *J. Electroanal. Chem.* 500, 356–364.

- Pronkin, S. and T. Wandlowski, 2003, Time-resolved in situ ATR-SEIRAS study of adsorption and 2D phase formation of uracil on gold electrodes, *J. Electroanal. Chem.* 550, 131–147.
- Räsänen, J., M. Savolainen, R. Silvennoinen and K.-E. Peiponen, 1995, Optical sensing of surface roughness and waviness by computer-generated hologram, *Opt. Eng.* 34, 2574–2580.
- Retter, U., 1980, On the two-dimensional nucleation in the adsorption of cytosine at the mercury/electrolyte interface, *J. Electroanalysis Chem.* 106, 371–375.
- Retter, U., 1984a, Two-dimensional one-step nucleation according to an exponential law in the formation of condensed adsorption films, *J. Electroanal. Chem.* 179, 25–29.
- Retter, U., 1984b, On the temperature dependence of the two-dimensional condensation of 5-iodocytosine at the mercury/electrolyte interface, *J. Electroanal. Chem.* 165, 221–230.
- Retter, U., 1987, On adsorption according to the lattice gas model (Ising Model), *J. Electroanal. Chem.* 236, 21–30.
- Retter, U., 1992, On the thermodynamic properties of several two-dimensional ising lattices, *J. Electroanal. Chem.* 329, 81–89.
- Retter, U. and H. Lohse, 1982, On the transition from progressive to instantaneous nucleation in the adsorption of adenosine at the mercury/electrolyte interface, *J. Electroanal. Chem.* 134, 243–250.
- Retter, U., V. Vetterl and J. Jursa, 1989, On the stability of condensed adsorption films, *J. Electroanal. Chem.* 274, 1–9.
- Roelfs, B., E. Bunge, C. Schroter, T. Solomun, H. Mayer, R.J. Nichols and H. Baumgartel, 1997, Adsorption of thymine on gold single-crystal electrodes, *J. Phys. Chem. B* 101, 754–765.
- Saffarian, H.M., R. Srinivasan, D. Chu and S. Gilman, 2001, Effect of adsorbed uracil and its derivatives on the rate of oxygen reduction on platinum in acid electrolytes, *J. Electroanal. Chem.* 504, 217–224.
- Sánchez-Cortés, S. and J.V. García-Ramos, 2000, Surface-enhanced Raman of 1,5-dimethylcytosine adsorbed on a silver electrode and different metal colloids: Effect of charge transfer mechanism, *Langmuir* 16, 764–770.
- Sánchez-Cortés, S. and J.V. García-Ramos, 2001, Influence of coverage in the surface-enhanced Raman scattering of cytosine and its methyl derivatives on metal colloids: Chloride and pH effects, *Surf. Sci.* 473, 133–142.
- Scharfe, M., A. Hamelin and C. Buess-Herman, 1995, On the occurrence of two-dimensional phase transitions of uridine at the aqueous solution-gold single crystal interface, *Electrochim. Acta* 40, 61–67.
- Seino, K. and W.G. Schmidt, 2004, Reflectance anisotropy of uracil covered Si(001) surfaces: *Ab Initio* predictions, *Surf. Sci.* 548, 183–186.
- Seino, K., W.G. Schmidt and F. Bechstedt, 2004, Organic modification of surface electronic properties: A first-principles study of uracil on Si(001), *Phys. Rev. B* 69 Art no. 245309.
- Seino, K., W.G. Schmidt, M. Preuss and F. Bechstedt, 2003, Uracil adsorbed on Si(001): Structure and energetics, *J. Phys. Chem. B* 107, 5031–5035.
- Silaghi, S.D., R. Scholz, G. Salvan, Y.J. Suzuki, M. Friedrich, T.U. Kampe and D.R.T. Zahn, 2004, Metal deposition onto biomolecular layers on silicon surfaces: A study of interface formation using Raman spectroscopy, *Appl. Surf. Sci.* 234, 113–119.
- Sowerby, S.J., C.A. Cohn and W.M. Heckl, 2001a, Differential adsorption of nucleic acid bases: Relevance to the origin of life, *Proc. Natl. Acad. Sci. USA* 98, 820–822.
- Sowerby, S.J., M. Edelwirth and W.M. Heckl, 1998a, Molecular mechanics simulation of uracil adlayers on molybdenum disulfide and graphite surfaces, *Appl. Phys. A* 66, S649–S653.
- Sowerby, S.J., M. Edelwirth and W.M. Heckl, 1998b, Self-assembly at the prebiotic solid-liquid interface: Structures of self-assembled monolayers of adenine and guanine bases formed on inorganic surfaces, *J. Phys. Chem. B* 102, 5914–5922.
- Sowerby, S.J., M. Edelwirth, M. Reiter and W.M. Heckl, 1998c, Scanning tunneling microscopy image contrast as a function of scan angle in hydrogen-bonded self-assembled monolayers, *Langmuir* 14, 5195–5202.

- Sowerby, S.J. and W.M. Heckl, 1998, The role of self-assembled monolayers of the purine and pyrimidine bases in the emergence of life, *Origins Life Evol. B.* 28, 283–310.
- Sowerby, S.J., W.M. Heckl and G.B. Petersen, 1996, Chiral symmetry breaking during the self-assembly of monolayers from achiral purine molecules, *J. Mol. Evol.* 43, 419–424.
- Sowerby, S.J., N.G. Holmand and G.B. Petersen, 2001b, Origins of life: A route to nanotechnology, *Biosystems* 61, 69–78.
- Sowerby, S.J. and G.B. Petersen, 1997, Scanning tunneling microscopy of uracil monolayers self-assembled at the solid/liquid interface, *J. Electroanal. Chem.* 433, 85.
- Sowerby, S.J. and G.B. Petersen, 2002, Life before RNA, *Astrobiology* 2, 231–239.
- Sowerby, S.J., G.B. Petersen and N.G. Holm, 2002, Primordial coding of amino acids by adsorbed purine bases, *Origins Life Evol. B.* 32, 35–46.
- Sowerby, S.J., P.A. Stockwell, W.M. Heckl and G.B. Petersen, 2000, Self-programmable, self-assembling two-dimensional genetic matter, *Origins Life Evol. B.* 25, 81–99.
- Šponer, J., J. Leszczynski, V. Vetterl and P. Hobza, 1996, Base stacking and hydrogen bonding in protonated cytosine dimer: The role of molecular ion-dipole and induction interactions, *J. Biomol. Struct. Dyn.* 13, 695–706.
- Sridharan, R. and R. de Levie, 1986, Condensed Thymine Films at the Mercury Water Interface. Part I. General Features, *J. Electroanal. Chem.* 201, 133–143.
- Sridharan, R. and R. deLevie, 1987a, Condensed thymine films at the mercury/water interface. Part IV. Scholastic measurements, *J. Electroanal. Chem.* 218, 287–296.
- Sridharan, R. and R. de Levie, 1987b, Condensed thymine films at the mercury water interface. Part V. Phase-transitions, *J. Electroanal. Chem.* 230, 241–256.
- Srinivasan, R. and P. Gopalan, 1993, Order and stability of an electrochemically condensed adenine layer on graphite, *J. Phys. Chem.* 97, 8770–8775.
- Srinivasan, R., J.C. Murphy, R. Fainchtein and N. Pattabiraman, 1991, Electrochemical STM of condensed guanine on graphite, *J. Electroanal. Chem.* 312, 293–300.
- Srinivasan, R., J.C. Murphy and N. Pattabiraman, 1992, STM observations of 2-dimensional condensed layers on solid electrodes, *Ultramicroscopy* 42, 453–459.
- Studničková, M., L. Trnková, J. Zetek and Z. Glázt, 1989, Reduction of guanosine at a mercury electrode, *Bioelectrochem. Bioenerg.* 21, 83–86.
- Tadjeddine, A. and A. Rahmani, 1991, Formation of condensed film at a mercury-electrolyte interface observed by surface plasmon excitation, *Electrochim. Acta* 36, 1855–1857.
- Tanaka, H., T. Nakagawa and T. Kawai, 1996, Two-dimensional self-assembly of DNA base molecules on Cu(111) surfaces, *Surf. Sci.* 364, L575–L579.
- Tanaka, H., Ch. Hamai, T. Kanno and T. Kawai, 1999, High-resolution scanning tunneling microscopy imaging of DNA molecules on Cu(111) surfaces, *Surf. Sci.* 432, L611–L616.
- Tanaka, S., L.T. Cai, H. Tabata and T. Kawai, 2001, Formation of two-dimensional network structure of DNA molecules on Si substrate, *Jpn. J. Appl. Phys. Part 2-Letters* 40, L407–L409.
- Tanaka, S., M. Taniguchi and T. Kawai, 2004, Selective adsorption of DNA onto SiO₂ surface in SiO₂/SiH pattern, *Jpn. J. Appl. Phys. Part 1-Regular Papers Short Notes & Review Papers* 43, 7346–7349.
- Tao, N.J., J.A. De Rose and S.M. Lindsay, 1993, Self-assembly of molecular superstructures studied by in situ scanning tunneling microscopy: DNA bases on Au(111), *J. Phys. Chem.* 97, 910–919.
- Tao, N.J. and Z. Shi, 1994a, Monolayer guanine and adenine on graphite in NaCl solution: A comparative STM and AFM study, *J. Phys. Chem.* 98, 1464–1471.
- Tao, N.J. and Z. Shi, 1994b, Kinetics of oxidation of guanine monolayers at the graphite-water interface studied by AFM/STM, *J. Phys. Chem.* 98, 7422–7426.
- Temerk, Y.M., M.M. Kamal, M.E. Ahmed and Z.A. Ahmed, 1986, The interfacial behaviour of guanosine mono-, di- and tri-phosphate in solutions of varying pH at charged interfaces, *Bioelectrochem. Bioenerg.* 16, 497–507.
- Trnková, L., J. Friml and O. Dračka, 2001, Elimination voltammetry of adenine and cytosine mixtures, *Bioelectrochemistry* 54, 131–136.

- Trnková, L., F. Jelen and I. Postbieglová, 2003, Application of elimination voltammetry to the resolution of adenine and cytosine signals in oligonucleotides. I. Homooligonucleotides dA9 and dC9, *Electroanalysis* 15, 1529–1535.
- Trnková, L., M. Studničková and E. Paleček, 1980, Electrochemical behaviour of guanine and its derivatives. I. Fast cyclic voltammetry of guanosine and calf thymus DNA, *Bioelectrochem. Bioenerg.* 7, 644–658.
- Ueharra, M. and P.J. Elving, 1981, Electrochemical examination of nucleoside interaction, adenosine-guanosine and cytidine-guanosine, *Bioelectrochem. Bioenerg.* 8, 523–535.
- Van Krieken, M. and C. Buess-Hermann, 1998, On the dissolution kinetics of two-dimensional uridine layers adsorbed on gold single-crystal electrodes, *Electrochim. Acta* 43, 2831–2841.
- Van Krieken, M. and C. Buess-Hermann, 1999, On the adsorption of uridine at the Ag(III)/aqueous solution interface, *Electrochim. Acta* 45, 675–683.
- Vetterl, V., 1965, Adsorption of DNA components on the mercury electrode, *Experientia* 21, 9–11.
- Vetterl, V., 1966a, Adsorption isotherm of some purine and pyrimidine derivatives, *Abhandlungen der DAW* 4, 493–500.
- Vetterl, V., 1966b, Differentielle Kapazität Der Elektrolytischen Doppelschicht in Anwesenheit Einiger Purin- Und Pyrimidinderivative, *Collect. Czech. Chem. Commun.* 31, 2105–2126.
- Vetterl, V., 1976, Electric field effect in the adsorption of adenosine and cytosine, *Bioelectrochem. Bioenerg.* 3, 338–345.
- Vetterl, V. and R. de Levie, 1991, The effect of halide ions on the condensation of adenine at the mercury-water interface, *J. Electroanal. Chem.* 310, 305–315.
- Vetterl, V., N. Papadopoulos, V. Dražan, L. Strašák, S. Hason and J. Dvorník, 2000, Nucleic acid sensing by impedance measurements, *Electrochim. Acta* 45, 2961–2971.
- Vetterl, V. and J. Pokorný, 1980, Reorientation of the cytosine derivatives at the electrode surface, *Bioelectrochem. Bioenerg.* 7, 517–526.
- Wackerbarth, H., M. Grubb, J.D. Zhang, A.G. Hanse and J. Ulstru, 2004b, Long-range order of organized oligonucleotide monolayers on Au(111) electrodes, *Langmuir* 20, 1647–1655.
- Wackerbarth, H., R. Marie, M. Grubb, J.D. Zhang, A.G. Hansen, I. Chorkendorff, C.B.V. Christensen, A. Boisen and J. Ulstru, 2004a, Thiol- and disulfide-modified oligonucleotide monolayer structures on polycrystalline and single-crystal Au(111), *J. Solid State Electr.* 8, 474–481.
- Wandlowski, T., 1995, Phase-transitions in uracil adlayers on Ag, Au and Hg electrodes-substrate effects, *J. Electroanal. Chem.* 395, 83–89.
- Wandlowski, T., 2000, Dynamic and structural studies at electrochemical interfaces, *Ach-Models Chem.* 137, 393–414.
- Wandlowski, T., 2002, The encyclopedia of electrochemistry, *Phase Transitions in Two-Dimensional Adlayers at Electrode Surfaces: Thermodynamics, Kinetics, and Structural Aspects*, Eds. M. Urbakh and M. Gileadi, Vol. 1, Wiley-VCH, Weinheim, 383.
- Wandlowski, T. and T. Dretschkow, 1997, Two-dimensional nucleation according to an exponential law with surface diffusion-controlled growth in the phase formation of uracil on Au(*hkl*), *J. Electroanal. Chem.* 427, 105–112.
- Wandlowski, T. and M.H. Hölzle, 1996a, Adsorption of 1,3-dimethyluracil at the Au(111)/aqueous electrolyte interface. A chronocoulometric study, *Langmuir* 12, 6597–6603.
- Wandlowski, T. and M.H. Hölzle, 1996b, Structural and thermodynamic aspects of phase transitions in uracil adlayers. A chronocoulometric study, *Langmuir* 12, 6604–6615.
- Wandlowski, T., D. Lampner and S.M. Lindsay, 1996a, Structure and stability of cytosine adlayers on Au(111): An in-situ STM study, *J. Electroanal. Chem.* 404, 215–226.
- Wandlowski, T., B.M. Ocko, O.M. Magnussen, S. Wu and J. Lipkowski, 1996b, The surface structure of Au(111) in the presence of organic adlayer: A combined electrochemical and surface X-ray scattering study, *J. Electroanal. Chem.* 409, 155–164.

- Wandlowski, T. and L. Pospisil, 1989a, The growth of compact layers at the electrode interface part II. The formation and stability of organic films, *J. Electroanal. Chem.* 258, 179–192.
- Wandlowski, T. and L. Pospisil, 1989b, The growth of compact layers at the electrode interface. Part IV. Fractal character of uracil films at the mercury-aqueous electrolyte interface, *J. Electroanal. Chem.* 270, 319–329.
- Webb, J.W., B. Janik and P.J. Elving, 1973, Cytosine nucleoside-nucleotide series electrochemical study of reduction mechanism, association, and separation, *J. Am. Chem. Soc.* 95, 991–1003.
- Wechter, C. and J. Osteryoung, 1989, Square wave and linear scan anodic stripping voltammetry at iridium-based mercury film electrodes, *Anal. Chem.* 61, 2092–2097.
- Wikiel, K. and Z. Kublik, 1984, Voltammetry at the mercury film electrodes – comparison of theoretical and experimental results obtained for indium in thiocyanate medium, *J. Electroanal. Chem.* 161, 269–281.
- Wikiel, K. and J. Osteryoung, 1989, Square wave voltammetry at a mercury film electrode: Experimental results, *Anal. Chem.* 61, 2086–2092.
- Wu, H.P., 1994, Nature and stability of mercury thin-films on glassy-carbon electrodes under fast-scan anodic-stripping voltammetry, *Anal. Chem.* 66, 3151–3157.
- Wu, H.P., 1996, Dynamics and performance of fast linear scan anodic stripping voltammetry of Cd, Pb, and Cu using in situ-generated ultrathin mercury films, *Anal. Chem.* 68, 1639–1645.
- Wu, J., Y. Huang, J. Zhou, J. Luo and Z. Lin, 1997, Electrochemical behaviors of DNA at mercury film electrode, *Bioelectrochem. Bioenerg.* 44, 151–154.
- Wu, S., J. Lipkowski, O.M. Magnussen, B.M. Oeko and T. Wandlowski, 1998, The driving force for $(p \times \sqrt{3}) \leftrightarrow (1 \times 1)$ phase transition of Au(111) in the presence of organic adsorption: A combined chronocoulometric and surface X-ray scattering study, *J. Electroanal. Chem.* 446, 67–77.
- Yamada, T., K. Shirasaka, A. Takano and M. Kawai, 2004, Adsorption of cytosine, thymine, guanine and adenine on Cu(110) studied by infrared reflection absorption spectroscopy, *Surf. Sci.* 561, 233–247.
- Yang, H.F., Y. Yang, Z. Liu, Z.R. Zhang, G.L. Shen and R.Q. Yu, 2004, Self-assembled monolayer of NAD at silver surface: A Raman mapping study, *Surf. Sci.* 551, 1–8.
- Yosypchuk, B., M. Heyrovský, E. Paleček and L. Novotný, 2002, Use of solid amalgam electrodes in nucleic acid analysis, *Electroanalysis* 14, 1488–1493.
- Yosypchuk, B. and L. Novotný, 2002, Nontoxic electrodes of solid amalgams, *Crit. Rev. Anal. Chem.* 32, 141–151.
- Zakharchuk, N.F. and K.Z. Brainina, 1998, The surface morphology of mercury plated glassy-carbon electrodes and stripping voltammetry of heavy metals, *Electroanalysis* 10, 379–386.
- Zakharchuk, N.F., S.Y. Saraeva, N.S. Borisova and K.Z. Brainina, 1999, Modified thick-film graphite electrodes: Morphology and stripping voltammetry, *Electroanalysis* 11, 614–622.
- Zhang, R.Y., D.W. Pang, Z.L. Zhang, J.W. Yan, J.L. Yao, Z.Q. Tian, B.W. Mao and S.G. Sun, 2002, Investigation of ordered ds-DNA monolayers on gold electrodes, *J. Phys. Chem. B* 106, 11233–11239.

This page intentionally left blank

Electrochemistry of Nucleic Acids

Emil Paleček and František Jelen

*Institute of Biophysics, Academy of Sciences of the Czech Republic, Kralovopolska 135, 612 65
Brno, Czech Republic*

Contents

1. Introduction	74
2. Electrochemical methods and electrodes	77
2.1. Methods	77
2.1.1. Elimination voltammetry with linear scan (EVLS)	77
2.2. Electrodes	78
2.2.1. Solid amalgam electrodes	79
3. Adsorption of nucleic acids	80
3.1. Adsorption of DNA at mercury electrodes depends on its structure	82
3.1.1. DME and HMDE may show different responses of dsDNA	83
3.2. Adsorption of oligonucleotides	84
4. Reduction and oxidation of nucleic acids at electrodes	86
4.1. Oxidation	87
4.1.1. Solid electrodes	87
4.1.2. Mercury electrodes	89
4.2. Reduction	90
4.2.1. Reduction of ss nucleic acids	91
5. Changes in DNA conformation at surfaces	104
5.1. History	104
5.2. Effects of electrochemical methods and types of mercury electrodes	104
5.2.1. Methods working with large voltage excursions during the DME drop lifetime or with stationary electrodes	105
5.3. Changes in DNA conformation at mercury surfaces as detected by conventional polarographic and voltammetric methods	106
5.3.1. Conditions not involving ionization of DNA bases	107
5.3.2. Conditions involving ionization of bases	112
5.4. Carbon electrodes	114
5.5. Changes in DNA structure at DNA-modified electrodes	114
5.5.1. Mercury electrodes	115
5.5.2. DNA-modified platinum and gold electrodes	117
5.5.3. Other methods and surfaces	120
5.6. Concluding remarks	120
6. Electrochemical principles in NA biosensors	121
6.1. DNA hybridization and detection at the same surface	122
6.1.1. Immobilization of DNA at electrode surfaces	123
6.1.2. Blocking and interfacing the electrode (transducer) surface	124
6.2. DNA hybridization and detection at two different surfaces	128
6.2.1. Length determination of long repetitive sequences	131

6.3. Electroactive markers covalently bound to DNA	132
6.3.1. Osmium labels	134
6.3.2. Ferrocene and other labels	136
6.4. Electrocatalytic oxidation of DNA	137
6.5. DNA conductivity in DNA sensors	141
6.5.1. DNA conductivity	141
6.5.2. Charge transfer in DNA sensors	142
6.6. Changes in DNA structure signaling DNA hybridization	145
7. Electrochemical DNA biosensors: Future prospects	149
8. Summary and conclusion	150
List of abbreviations	152
Acknowledgments	153
References	153

1. INTRODUCTION

First reports about the ability of nucleic acids to produce analytically useful electrochemical reduction and oxidation signals were published by the end of the 1950s and in the beginning of the 1960s (Paleček, 1958, 1960a, 1961), reviewed in Paleček (1969b) (Chapter 1). It was shown that these signals are due to residues of bases in DNA and RNA. Adenine (A) and cytosine (C) residues in DNA produced reduction signals (Figure 1), while guanine (G) residues yielded anodic signals due to oxidation of the guanine reduction product (reviewed in Janik and Elving, 1968; Paleček *et al.*, 2002b). In addition, it was shown that all nucleic bases produced sparingly soluble compounds with the electrode mercury (Paleček, 1958, 1960a, 1980b, 1985, 2005; Paleček *et al.*, 1981). At the same time the electrode processes responsible for the reduction of A, C, and G at the mercury electrodes were elucidated (reviewed in Janik and Elving, 1968) (see Chapter 2). Electrochemical analysis sensitively reflected DNA denaturation and minor changes in the DNA structure (reviewed in Paleček, 1971, 1976, 1983). Oscillographic polarography at controlled a.c. and derivative/differential pulse polarography yielded the early evidence of the DNA premelting and of the polymorphy of the DNA double-helical structure (reviewed in Paleček, 1976).

For almost four decades the research into the electrochemistry of nucleic acids was performed by a handful of laboratories located mainly in East Europe and in France. In recent years, the situation has dramatically changed. Electrochemistry of nucleic acids has become a booming field involving a number of laboratories in various countries, including USA, Europe, Japan, China, etc. Numerous reviews (Drummond *et al.*, 2003; Erdem and Ozsoz, 2002; Fojta, 2002, 2004; Gooding, 2002; Homs, 2002; Katz *et al.*, 2004; Kerman *et al.*, 2003; Labuda *et al.*, 2005; Maruyama *et al.*, 2001; Mascini *et al.*, 2001; Paleček, 2005; Paleček and Fojta, 2001, 2005; Paleček *et al.*, 2002b; Tarlov and Steel, 2003; Thorp, 1998; Tombelli *et al.*, 2001; Vercoutere and Akesson, 2002; Wang, 2000a, 2002, 2003; Wang *et al.*, 2005a), and several special issues, e.g. (*Analytica Chimica Acta*, 2003; *Biosensors and Bioelectronics*, 2004; *Talanta*, 2002) were published since 2001. This change was related to the expectation that electrochemical methods will soon complement the optical detection of DNA

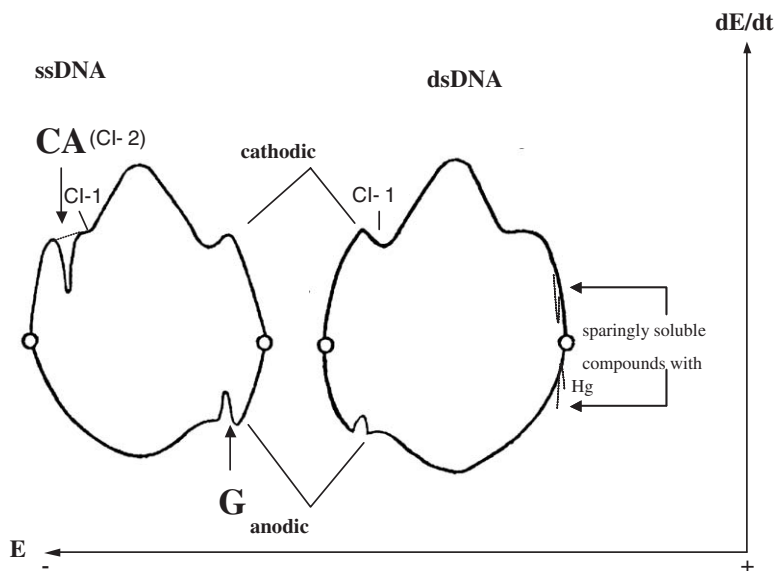


Fig. 1. Schematic representation of curves $dE/dt = f(E)$ of native double-stranded (ds) and thermally denatured single-stranded (ss) DNAs obtained by means of oscillographic polarography at controlled alternating current. Cathodic indentation CA (originally denominated as CI-2) is due to reduction of cytosine and adenine residues and corresponds to the DPP peak III (see Figure 9), or LSV peak 3 (Figure 15); Indentation CI-1 is of capacitive nature corresponding to a.c. polarographic/voltammetric peak 1 (Figure 3), LSV peak 1 or DPP peak I. Anodic indentation G (originally A I) is due to oxidation of the reduction product of guanine residues. Background electrolyte: 0.5 M ammonium formate, 50 mM sodium phosphate, pH 6.9; dropping mercury electrode. Sparingly soluble compounds with the electrode mercury are produced by all nucleic acid bases as well as by purine nucleosides and nucleotides. Adapted from Paleček (2002). Copyright 2002, with permission from Elsevier.

and RNA in the DNA hybridization sensors (Section 6 and Chapters 4–11) increasingly used in genomics and in various areas of practical life. Also other types of promising DNA sensors have been developed, including sensors for DNA damage (Chapters 12 and 13). Another reason for an increased interest in the nucleic acid electrochemistry can be seen in an easy availability of the synthetic oligodeoxyribonucleotides (ODN).

For about three decades biosynthetic polynucleotides, chromosomal and (less frequently) viral DNAs and RNAs were used in electrochemical research into nucleic acids (Paleček *et al.*, 2002b). Working with these nucleic acids required some knowledge in biochemistry and skill to handle properly the nucleic acid samples. With the exception of commercially available calf thymus and salmon sperm DNAs and some biosynthetic polynucleotides, the nucleic acid samples had to be isolated, purified and characterized in the researcher's laboratory. This was rather difficult and discouraging for most electrochemists. At present well defined, highly purified ODNs are available for affordable prices providing thus attractive objects for the electrochemical research. In addition to the

Table 1. Custom DNA-oligonucleotides synthesis^a

(Calculated for scale 200 nmol, HPLC purity)

Oligodeoxynucleotide	Price/base – EURO from 0.74 to 1.35	Mean value – EURO ~1 ~20 ^b
End modifications		
	Price/modification	
Biotin 3'/5'	from 32 to 45	~38.5
Aminolink C6 5'	from 24 to 30	~27
SH mod. 5'	from 41 to 60	~50.5
SH mod. 3'	from 41 to 150	~95.5
Phosphorylation 3'/5'	from 21 to 30	~25.5
Succinate 3'/5'	from 24 to 41	~32.5
Ferrocene 5'		~270
Base modifications		
2'-Deoxyuridine	9	
5-Methyl-dC	55	
2-Aminopurine	140	
Dye modifications		
Different fluorescent dyes or Molecular Probes' dyes (e.g. Tamra, Rox, AMCA, Texas Red, etc.) from 40 to 100		
Double-dye modifications (if available) from 80 to 100		
Custom PNA synthesis		
Price/base		~40

Data were taken from materials of European and US companies.

^aLength: Without mod.-up to 100 bases, dyes-up to 70 bases SH-up to 45 bases, PNA -up to 50 bases.^bPolyacrylamide gel electrophoresis (PAGE) purification.

conventional unmodified ODNs, also chemically modified ODNs (Table 1) as well as oligoribonucleotides (ORN) can be bought. Both ORNs and chemically modified ODNs are, however, more expensive than simple ODNs. Relatively short oligonucleotides (usually 10–20 nucleotides) represent an interesting object of the electrochemical research but it should not be forgotten that structures and some properties of longer natural DNAs may significantly differ from those of the short ODNs. Electrochemical studies should thus not be limited to short oligonucleotides but an appreciable attention should be paid also to natural nucleic acids, their fragments and segments amplified by the polymerase chain reaction (PCR).

There is no doubt that electrochemical methods offer, in addition to the development of the DNA biosensors, a number of interesting possibilities in the contemporary nucleic acid research, including studies of the DNA–protein interactions (see Chapter 19), DNA damage (see Chapters 12 and 13), highly sensitive

NA determination down to atto- and zettomole quantities, effect of surface charge on structure and properties of the nucleic acid adsorbed at the surface, highly sensitive detection of impurities in DNA and RNA samples, etc. Electrochemical research into DNA and RNA is a vast field requiring more researchers with some knowledge both in electrochemistry and biochemistry of nucleic acids.

2. ELECTROCHEMICAL METHODS AND ELECTRODES

2.1. Methods

Till 1965, mainly the so-called oscillographic polarography at controlled alternating current (invented by the Nobel laureate J. Heyrovsky in the beginning of the 1940s (Kalvoda, 1965) was used in the electrochemical analysis of nucleic acids (reviewed in Palecek, 1969b). Sensitivity of the classical direct current (d.c.) polarography was found too low to study large chromosomal DNA molecules (Palecek and Vetterl, 1968). Later other methods such as Barker's derivative (Palecek and Frary, 1966) and Osteryoung's differential pulse polarography (Palecek and Doscocil, 1974), a.c. polarography (Palecek, 1966) and linear scan and cyclic voltammetry were applied in nucleic acids research. Recently, constant current chronopotentiometry (Cai *et al.*, 1996, 1997; Fojta *et al.*, 1997a; Hason *et al.*, 2002a; Kubicarova *et al.*, 2000a; Palecek *et al.*, 1997; Tomschik *et al.*, 1998, 1999; Wang and Kawde, 2002; Wang *et al.*, 1997b, c, e, f, 1998b, c, 1999a, b, 2002a) and the so-called elimination voltammetry with linear scan (EVLS) (Dracka, 1996) proved to be useful tools in this research area. With the exception of EVLS, electrochemical methods were well described in a number of books, including recent J. Wang's *Analytical Electrochemistry* (Bard and Faulkner, 2000; Bockris *et al.*, 1999; Bond, 1980; Wang, 2000b). We shall very briefly summarize some properties of the less well-known EVLS method.

2.1.1. Elimination voltammetry with linear scan (EVLS)

EVLS enables the elimination of selected partial voltammetric currents contributing to a total current (Adams, 1969; Bard and Faulkner, 2000). The basic idea of elimination of the chosen current lies in the different dependencies of various voltammetric currents on the scan rate. The elimination can be thus achieved by a function obtained by linear combination of total voltammetric currents measured at different scan rates. One of the scan rates is taken as the reference scan rate, while the others are chosen as multiples or fractions of the reference scan rate. Best EVLS results were obtained with EVLS function eliminating kinetic and charging currents and conserving the diffusion current. Compared to usual voltammetric methods, EVLS showed some advantages: (i) the expansion of available electrode potential range, (ii) increase of current sensitivity, (iii) better peak resolution, (iv) easy identification of the current nature, and (v) the detection of minor electrode processes overlapped by a major one (Adams, 1969; Bard and Faulkner, 2000; Dracka, 1996; Trnkova and Dracka, 1996).

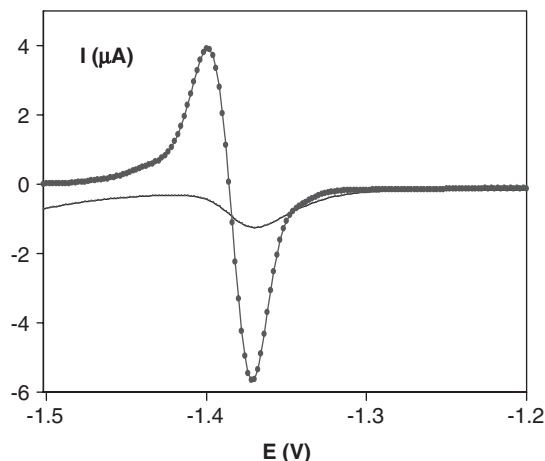


Fig. 2. LSV and EVLS reduction signals of ODN – $1.5 \mu\text{M d(A)}_9$ in 0.2 M acetate buffer (pH 5.3), reference curve ($v = 200 \text{ mV/s}$), potential step 2 mV , time of accumulation 120 s , accumulation and starting potential -0.1 V , ●●●● elimination curve. The elimination function $f(I)$ eliminates simultaneously kinetic and charging currents (I_c , I_k) and conserves the diffusion current I_d Hanging mercury drop electrode (HMDE). Potentials are given against the saturated calomel electrode (SCE). Adapted from Trnkova *et al.* (2003). Copyright 2003, with permission from Wiley-VCH Verlag GmbH&Co. KGaA, Weinheim.

For irreversible redox processes with substance in an adsorbed state, elimination of charging and kinetic currents combined with conservation of the diffusion current provided a characteristic peak–counterpeak form (Figure 2), indicating adsorption (Trnkova and Dracka, 1993; Trnkova *et al.*, 2000, 2002, 2003, 2004) and improving resolution and sensitivity of the analysis (without any baseline correction). These special EVLS signals were applied in analysis of DNA and ODNs (Trnkova, 2005; Trnkova *et al.*, 2000, 2002, 2003, 2004) (Section 3.2).

2.2. Electrodes

For more than one decade only mercury dropping electrodes (DME) were used in the electrochemical research of nucleic acids (reviewed in Paleček, 1971, 1983). In the 1970s stationary mercury electrodes and carbon electrodes were applied (reviewed in Berg, 1976; Brabec *et al.*, 1996; Paleček, 1996). Mercury and carbon electrodes were extensively used to study electroactivity and adsorption/desorption properties of DNA. Later carbon (Chapter 7) (Marrazza *et al.*, 1999a,b; Mascini *et al.*, 2001; Wang, 2003c; Wang *et al.*, 1995, 1996b, 1997d, 1998a, 2000c) (reviewed in Brabec *et al.*, 1996; Paleček, 1971, 1996; Paleček and Hung, 1983; Paleček and Fojta, 2001; Paleček *et al.*, 1993; Prado *et al.*, 2002) gold, Sections 6.1.2. and 6.5.2 and indium tin oxide (ITO), Section 6.4, copper, silver and platinum electrodes have been increasingly applied in relation to the development of DNA sensors. Gold electrodes were

predominantly applied to measure responses of DNA redox indicators, ITO electrodes were used in electrocatalytic oxidation of DNA guanine residues and copper electrodes were reported as suitable for studies of DNA sugar oxidation (Brazill *et al.*, 2000; Singhal and Kuhr, 1997a, b).

Potential window of mercury electrodes is usually between 0 and -2 V at neutral and weakly alkaline pHs.¹ In contrast, the potential windows of most of the solid electrodes are shifted by approximately 1 V to more positive values.² Solid electrodes are thus better for studying NA oxidation, while mercury electrodes suit well for investigating reduction of nucleic acids and attached redox indicators. The atomically smooth and highly reproducible surfaces of liquid mercury are ideal for a.c. impedance measurements and offer great potentialities in studies of DNA self-assembled monolayers (Section 6.1.2.2), until recently limited to gold surfaces (Section 6.1.2.1). DME and hanging mercury drop electrode (HMDE) are excellent tools in electrochemical analysis but they have been of little use in biosensors requiring sturdy, easy to handle solid electrodes. With relatively low hydrogen overvoltage these electrodes do not allow to measure reduction signals of a number of compounds, including nucleic acids. Highly sensitive signals due the catalytic hydrogen evolution produced e.g. by proteins (Chapters 1,18 and 19) and chemically modified nucleic acids (Section 6.3) appear at potentials too negative to be measured by the above solid electrodes. To overcome these difficulties, attempts have been made to apply solid mercury-containing electrodes in nucleic acid research.

2.2.1. Solid amalgam electrodes

Amalgam electrodes were used for decades to analyze various compounds, including biomolecules (Kalab, 1955, 1956; Kalab and Franek, 1955; Pechan *et al.*, 1955; Stock *et al.*, 1947). They were prepared usually by dipping a suitable metal substrate (e.g. a copper wire) in liquid mercury. These electrodes suffered from some drawbacks, such as poor stability and reproducibility of their preparation. Recently, solid amalgam electrodes (SAE, based on amalgamation of soft metal powders) (Yosypchuk and Novotny, 2002a–c) and dental amalgam electrodes (Mikkelsen and Schroder, 2003) were introduced showing excellent properties as substitutes for HMDE. SAE comprising solid amalgam of metals or metallic alloys, exhibiting high affinity to liquid mercury, represent non-toxic, well-defined and reproducible electrodes. They can be prepared as polished (p-SAE) or mercury meniscus-modified (m-SAE). m-SAE bears on its surfaces a very small amount of mercury which cannot be accidentally removed due to its strong adhesion to the solid amalgam support. M-SAEs represent the best alternative of a liquid mercury electrode with potential windows very close to that of HMDE (Table 2). Recently, SAEs have been used in analysis of nucleic acids and proteins and their components and in DNA hybridization sensors (Yosypchuk and Novotny, 2002a–c, 2003). Mercury-modified copper

¹Potentials are given against saturated calomel electrode if not stated otherwise.

²An overview of potential ranges of mercury, carbon and platinum electrodes in different media is given in Wang (2000b).

Table 2. Range of working potentials of different electrodes

Electrode (disc's diameter)	Potential range, V							
	0.1 M HClO ₄		0.2 M acetate pH 4.8		0.05 M Na ₂ B ₄ O ₇ pH 9.2		0.1 M NaOH	
HMDE	-1.19	0.44	-1.7	0.31	-1.98	0.15	-1.97	-0.07
AgE (0.40 mm)	-0.64	0.39	-0.99	0.36	-1.2	0.38	-1.41	0.19
p-AgSAE (0.70 mm)	-1.12	0.45	-1.51	0.31	-1.88	0.16	-1.96	-0.06
m-AgSAE (0.70 mm) (0.54 mm)	-1.08	0.43	-1.44	0.21	-1.92	0.16	-1.95	-0.07
m-CuSAE (0.48 mm)	-1.11	0.44	-1.39	0.3	-1.92	0.15	-1.99	-0.06
AuE (0.40 mm)	-1.17	0.06	-1.44	-0.03	-1.75	0.95	-1.85	-0.24
m-AuSAE (0.40 mm)	-0.54	1.69	-0.91	1.49	-1.39	1.15	-1.62	0.81
m-IrSAE (0.67 mm)	-1.12	0.45	-1.47	0.31	-1.9	0.16	-1.91	-0.05
	-1.01	0.43	-1.32	0.29	-1.63	0.15	-1.72	-0.06

Experimental results were obtained by linear sweep voltammetry; reference electrode SCE; scan rate 0.02 V/s; the potential limits correspond to 1 mA current level; air oxygen was removed by nitrogen. Adapted from Yosypchuk and Novotny (2002b). Copyright 2002, with permission from CRC Press LLC.

solid amalgam electrode (M-CuSAE) were particularly useful in determination of subnanomolar concentrations of A and G released from DNA by acid treatment (Jelen *et al.*, 2002b), while m-AgSAE were applied in catalytic reactions of osmium-modified DNAs (Yosypchuk *et al.*, 2005). It can be expected that non-toxic SAE and dental amalgam electrodes will extend the palette of solid electrodes indispensable in electrochemistry of nucleic acids and proteins and particularly in biosensors.

3. ADSORPTION OF NUCLEIC ACIDS

Nucleic acids are usually strongly adsorbed on electrodes. Irreversible adsorption of RNA and/or DNA was observed at mercury, carbon and other electrodes (Paleček *et al.*, 2002b). DNA-modified mercury and carbon electrodes can easily be prepared by immersing the bare electrode into the DNA solution for a short time, followed by the electrode washing. Compared to mercury and carbon electrodes adsorption of NAs at gold and ITO electrodes is much weaker and no DNA-modified gold electrodes prepared by spontaneous physical adsorption of unmodified DNA were reported. On the other hand, Au electrodes with chemisorbed end-thiolated ODNs were widely used in DNA hybridization sensors (Section 6.1.2). Reduction and oxidation of DNA and RNA at mercury and carbon electrodes proceed in an adsorbed state; NA adsorption should be thus considered also in faradaic electrode processes. It is interesting that negatively charged DNA and RNA can remain adsorbed on mercury electrodes at highly negative potentials (close to $-2V$) (Fojta *et al.*, 1997b). At these electrodes even stronger adsorption of peptide nucleic acid (PNA), which backbone is not charged, was observed (Section 3.2).

Miller (1961a) was perhaps the first who studied adsorption of DNA. Using DME he showed that adsorption of chromosomal DNA was diffusion controlled for partly covered surfaces and that the differential capacitance reached a constant value after the surface became fully covered. He calculated the area per adsorbed nucleotide around 95 \AA^2 for denatured DNA. Later about 85 \AA^2 per nucleotide for short chains of poly(U) (containing about 100 monomeric units) was obtained by Janik and Sommer (1973a); the area decreased with the increasing length of the polynucleotide chain down to about 75 \AA^2 (for polynucleotides containing about 1500 monomeric units) suggesting that the orientation of these RNA molecules on the electrode depended on the chain length.

According to theory the adsorption of a linear flexible polymer (forming a random coil) should result in a change in the polymer conformational topology. Such molecules form cooperative structures of adsorbed segment trains alternating with three-dimensional loops. Ellipsometry (Humphreys and Parsons, 1977) suggested a rather diffuse arrangement of molecules of denatured DNA in the adsorbed layer, with DNA strands extending into the bulk of solution. A.c. polarography of synthetic polyribonucleotides (Janik and Sommer, 1973a) showed that the fraction of segments in contact with the surface decreased as the m.w. of the polynucleotide increased and became constant at high m.w. (above 3×10^6). Because of their size, the loops extended beyond the outer double layer and could not thus affect significantly the differential capacitance. The ratio of loops to adsorbed segments increased with the polynucleotide length and the change in the differential capacitance, induced at a constant NA concentration (related to the monomer content), decreased with increasing chain length. It was further shown that the height of the tensammetric peak increased with the chain length, but no significant variation of the peak potential was observed. The dependencies of the intensity of the voltammetric (adsorption/desorption, tensammetric) signal on the DNA concentration reached limiting values and did not show any characteristics for multilayer adsorption (Brabec and Palecek, 1972). It was concluded that adsorption of NAs on mercury electrodes proceeded only in one layer, or that the formation of further layers did not influence intensity of the electrochemical signals.

It was found (Brabec and Palecek, 1972) that all monomeric constituents of DNA, i.e., the base, sugar and phosphoric acid residues could participate in the DNA adsorption on mercury electrodes (Palecek *et al.*, 2002b). The extent of their participation depended on pH and ionic strength of the solvent and on the electric charge of the electrode surface (Figure 3). At neutral pH and moderate ionic strengths hydrophobic bases were adsorbed most strongly on the hydrophobic mercury electrode surface. At low ionic strengths and on the positively charged electrode surface electrostatic adsorption of the negatively charged DNA and RNA was observed both on mercury and carbon electrodes. Adsorption of ssDNA and ssRNA on mercury, carbon and other electrodes was recently reviewed (Palecek *et al.*, 2002b). Further we shall limit ourselves only to basic data necessary to understand better the following sections and to some recent papers.

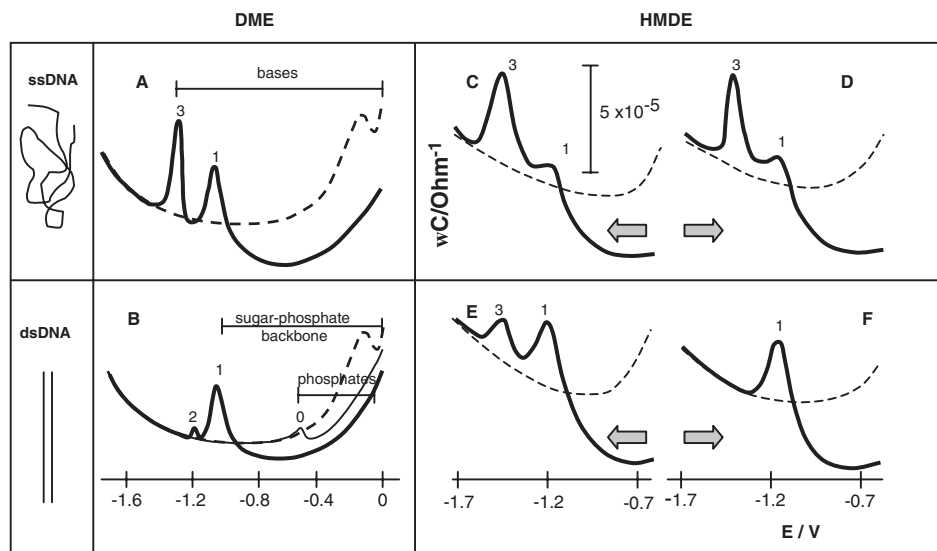


Fig. 3. A.c. polarograms and voltammogram of ss (A, C, D) and ds (B, E, F) calf thymus DNA. (A, B) Schematic representation of a.c. polarograms and the role of the DNA constituents in the DNA adsorption at DME. DNA polarograms obtained (solid curves) at moderate ionic strength (0.5 M KCl) and (light curve in B part) at low ionic strength (10 mM sodium phosphate) at pH 8; broken curve, background electrolytes. At low ionic strengths dsDNA is adsorbed mainly electrostatically (via unscreened negatively charged phosphates) at the positively charged electrode. At moderate ionic strengths dsDNA can be adsorbed via its backbone even at a negatively charged electrode. (C, D, E, F) A.c. voltammograms presented as adsorptive stripping admittance ($Y = wC$, where w is angular frequency and C is capacitance) curves of ss and dsDNA with negative- (C, E) and positive-going (D, F) scans. DNA in concentration of $40 \mu\text{g/mL}$ in 0.5 M NaCl with 0.05 M sodium phosphate, pH 7.8. The a.c. voltage amplitude was 10 mV (peak-to-peak), potential step 5 mV. If not stated otherwise, in further figures potentials are given against SCE. Adapted from Paleček (1995) and Jelen *et al.* (2000b). Copyright 1995 and 2000, with permission from Elsevier and Wiley-VCH, respectively.

3.1. Adsorption of DNA at mercury electrodes depends on its structure

It was shown that at the mercury electrodes adsorption/desorption behavior of DNA strongly depended on the structure of the DNA molecules (reviewed in Paleček, 1983, 1988a, b; Paleček *et al.*, 2002b). At moderate ionic strengths, for example in 0.3 M NaCl the phosphate charges were screened by sodium ions and intact linear dsDNA was adsorbed at DME almost as an electroneutral compound (Brabec and Paleček, 1972; Brabec *et al.*, 1983; Paleček *et al.*, 2002b) via sugar-phosphate backbone. The tensammetric (adsorption/desorption) peak appeared on C-E curves at about -1.1 V (denoted as peak 1, Figure 3B). In dsDNA containing some ss or distorted regions in which the hydrophobic bases were able to contact the electrode surface, another adsorption/desorption peak appeared on C-E curves around potential -1.3 V (peak 2).

This peak corresponded to the desorption (reorientation) of distorted regions of dsDNA which were adsorbed via bases more firmly than intact DNA double-helical segments (Figure 3B). At low ionic strengths (<0.1 M) the dsDNA was electrostatically adsorbed via charged phosphate groups at positively charged electrode surface. At negative potentials unscreened phosphate charges were repulsed from the electrode (Brabec, 1980; Brabec and Palecek, 1972) and dsDNA was only weakly adsorbed via sporadic bases if available. The corresponding reorientation peak (Brabec and Palecek, 1972; Brabec *et al.*, 1996) appeared around the potential of zero charge (p.z.c.) (Figure 3B).

In difference to dsDNA, bases in ssDNA are freely accessible for the interaction with the environment and adsorption of ssDNA on mercury electrodes is governed in a wide potential range by strong interaction of hydrophobic purine and pyrimidine bases with the hydrophobic mercury surface. At about -1.1 V peak 1, corresponding to the desorption of sugar-phosphate backbone was observed followed by peak 3 around -1.4 V, reflecting adsorption/desorption of DNA segments adsorbed via bases (Figure 3A).

3.1.1. DME and HMDE may show different responses of dsDNA

It should be stressed that (at neutral pH and moderate ionic strength) a.c. polarographic (tensammetric) curves of dsDNA obtained with DME greatly differ from those of ssDNA (Figure 3B, E, F). In intact chromosomal dsDNA only peak 1 was observed while peak 3 was always absent; peak 3 was thus specific for ssDNA. In contrast, a.c. voltammetry with HMDE displayed smaller differences between ds and ssDNAs, showing peak 3 even with intact dsDNA (Figure 3C–F). It was shown that dsDNA was unwound at HMDE in a narrow potential range due to strains resulting from the effect of the electric field on DNA firmly immobilized at the electrode surface (Section 5). Because the DNA surface denaturation took place (around neutral pH) at about -1.2 V, i.e. at potentials less negative than the potential of peak 3 (at about -1.4 V), in dsDNA the height of this peak was influenced by the history of the electrochemical experiment, if the potential was scanned in negative direction (and the HMDE was used). Problems of the DNA structure at the electrode surface will be discussed in detail in Section 5. It is interesting that similar differences between ss and ds DNAs were observed both in their adsorption/desorption and redox behavior at DME and HMDE (Sections 4 and 5).

Adsorption/desorption behavior of nucleic acids at electrodes can be studied by a number of methods (reviewed in Palecek *et al.*, 2002b). Among them particularly attractive appear measurements of frequency dependencies of the impedance of the electrode double layer by means of electrochemical impedance spectroscopy (EIS) (Brett and Brett, 1993; Fu *et al.*, 2005; Hason *et al.*, 2002a, b; MacDonald, 1987; Pospisil, 1996; Sluyters-Rehbach and Sluyters, 1982; Strasak *et al.*, 2002; Vetterl *et al.*, 2000). Using EIS adsorption kinetics and mobility of the adsorbed NA segments as well as mechanism of electrode processes were studied. Strongest frequency effects were observed at the potentials of adsorption/desorption peaks. With more flexible ss NAs the frequency effect was larger

than with the more rigid ds ones. In biopolymers the frequency effect depended upon the rate of migration of adsorbed trains from the surface phase to the loops extending to the solution and *vice versa*. Such segment migration could occur only in combination with rearrangement of the whole biopolymer molecule, EIS thus appeared capable to provide information about the structure of the adsorbed nucleic acid.

3.2. Adsorption of oligonucleotides

Early studies of oligonucleotides were limited to adsorption of short oligonucleotides (2–5-mers) on mercury electrodes by a.c. polarography (Krznaric *et al.*, 1975; Krznaric *et al.*, 1978; Valenta and Krznaric, 1977; Webb *et al.*, 1973) and surface tension measurements (Brabec and Kavunenko, 1987). With oligoriboadenylates it was found that the shorter molecules (dinucleotides and trinucleotides) were adsorbed with all A residues oriented flat at the electrode surface and with all sugar or sugar–phosphate residues close to the surface. The tetranucleotides and longer oligomers seemed to be adsorbed with a maximum of three A rings directly anchored to the electrode surface (Brabec and Kavunenko, 1987). The first study of a self-complementary ODN duplex 10-mer d(CCAGGCCTGG) showed strong adsorption of this ODN on HMDE and its ability to produce reduction and oxidation signals. By measuring the anodic peak G (resulting from guanine residues) it was possible to detect this ODN at subnanomolar concentrations by adsorptive stripping (Paleček *et al.*, 1990). A short hairpin d(GCGAAGC) was analyzed by cyclic voltammetry (CV) and elimination voltammetry (Section 2.1.1) at HMDE under similar conditions and a splitting of the guanine anodic peak was observed (Trnkova *et al.*, 2004). Such splitting might be related to the specific location of guanines in the ODN molecule. More work will be necessary to understand better this phenomenon.

Adsorption of PNA and DNA decamers (GTAGATCACT and complementary sequences) at HMDE was studied by means of a.c. impedance (Fojta *et al.*, 1997b). In Figure 4C–E the curves of PNA and DNA decamers (CATCTAGTGA) as well as of histone (obtained with biomolecule-modified electrodes) were compared. At negatively charged surface DNA produced adsorption/desorption peak. Neither PNA nor histone displayed any adsorption/desorption peak. Among the molecules tested, positively charged histone (known to bind polyanionic DNA in chromatin) showed the smallest ΔC at the positively charged surface. At highly negative potentials (more negative than -1.5 V) the DNA decamer and histone curves almost coincided with the curve of the background electrolyte while PNA showed an appreciable ΔC , suggesting that its molecules remained adsorbed at the negatively charged electrode (Figure 4). The behavior of the PNA suggested an attraction between the PNA molecules at the electrode surface at higher surface coverages. Prolonged exposure of DNA to highly negative potentials resulted in removal of almost all DNA from the surface while PNA remained adsorbed under the same conditions.

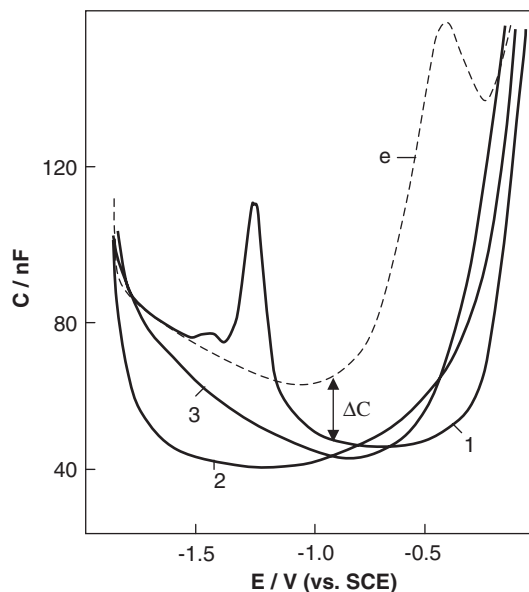


Fig. 4. Adsorptive transfer C–E curves of DNA (1), PNA (2) and histone (3). Concentrations: DNA and PNA 10 $\mu\text{g}/\text{mL}$; histone 30 $\mu\text{g}/\text{mL}$. DNA was adsorbed under conditions securing full coverage of the electrode from 0.1 M NaCl, 5 mM sodium phosphate (pH 7), and PNA and histone were adsorbed from 5 mM sodium phosphate at room temperature. e, background electrolyte (0.3 M NaCl, 50 mM sodium phosphate, pH 8.5), HMDE. Adapted from Fojta *et al.* (1997b). Copyright 1997, with permission from Biophysical Society.

In recent years a number of papers were published on electrochemistry of ODNs serving as sequence-specific probes in DNA sensors, reporting on their immobilization at surfaces (Section 6), formation and properties of self-assembled monolayers (Section 6.1.2), etc. but only few papers were published concerning their redox and adsorption/desorption properties. Because of widespread use of DNA biosensor technology, interest in the fundamentals of the ODN adsorption on the electrodes used in DNA biosensors has recently been growing. Competitive adsorption of 5-mer homo ODNs by *ex situ* Fourier transform infrared spectroscopy (FTIR) investigation showed base content dependence in the strength of binding of these small ODNs to gold surfaces (Kimura-Suda *et al.*, 2003). The question of how such DNA base interactions affect DNA-thiol attachment to the gold surface was not investigated until recently. Migration studies suggested sequence dependence in the orientation of 43- and 36-mer ODNs attached to nanoparticles (Parak *et al.*, 2003). Recently, results of the first systematic study on sequence-dependent kinetics of short ss ODN surface immobilization were published (Wolf *et al.*, 2004). By measuring film coverage for both non-thiolated and thiolated 25-mer ODNs as a function of adsorption time, the relative contribution of specific thiol-surface interactions and DNA-surface (non-specific) interactions to their overall mechanism of DNA-thiol attachment to gold was determined. It was

shown that sequence-dependent non-specific base interactions with the surface played a significant role in DNA–thiol immobilization, influencing both the kinetics and the extent of ODN adsorption. Sequences such as poly(dA), that initially formed strong contact with the surface, hindered long time thiol adsorption. In contrast, sequences such as poly(dT), that initially bound slowly and weakly to the surface, did not obstruct further thiol adsorption, resulting in higher film coverage and Langmuir immobilization kinetics. A comparison of non-thiolated with thiolated ODNs revealed that the former ODN contacted the surface in a more horizontal orientation, whereas thiolated ODNs attained a more upright orientation. The surface coverage and the time dependence of the adsorption process of thiolated ODNs depended on the ODN nucleotide composition. Similar results were obtained by voltammetric studies of thiolated and non-thiolated ODN adsorption and redox behavior at mercury electrodes (E. Paleček and V. Ostatná, unpublished, 2005). At these electrodes A, C and G residues produced their specific reduction and oxidation signals in both types of the ODNs. Thiolated ODNs yielded additional signals due to the formation of the Hg–S bond. Concentration and time dependences of these signals provided first information about the electrochemical behavior of thiolated ODNs at mercury electrodes (see also Section 6.1.2.2 and Chapter 19).

4. REDUCTION AND OXIDATION OF NUCLEIC ACIDS AT ELECTRODES

The ability of nucleic acids to accept or deliver electrons on interaction with electrodes was reported more than 40 years ago (Paleček, 1958, 1960a, 1961, reviewed in Paleček, 1969b). This finding was confirmed and studied for decades in several laboratories (reviewed in Paleček, 1983; Sequaris, 1992) but it remained unrecognized by a number of electrochemists. Until recently from time to time papers were published, which claimed that NAs are electroinactive, (e.g. Ihara *et al.*, 1996) and should be therefore labeled with electroactive compounds. Reasons for this long-lasting misunderstanding are not completely clear. Probably, the first reports on DNA electroinactivity at DME (Berg, 1957) played some role. Moreover, in the last decade, when the research of DNA hybridization sensors became popular, many researchers used gold electrodes for their electrochemical studies of DNA, finding DNA electroinactive at these electrodes. Similarly, no faradaic signals of DNA were obtained with ITO electrodes (Section 6.4). Gold electrodes are well suited for immobilization of thiolated ODNs (Section 6.1.2) but unlabeled chromosomal DNA appears poorly adsorbed at gold electrodes and the literature on electroactivity of NA on these electrodes is scarce. Already in 1981, oxidation of purine bases at the gold electrodes (where measurement of the respective anodic currents is complicated by simultaneous formation of gold oxides) was discussed by Hinnen *et al.* (1981). Electrooxidation of purine nucleotides as well as of native and denatured DNA at gold microelectrodes was reported by Pang *et al.*

(1995). Recently, Ferapontova and Domingues (2003) reported oxidation of guanine at polycrystalline gold electrode. If suitable electrochemical methods are used DNA and RNA produce (reviewed in Brabec *et al.*, 1996; Palecek, 1983, 1996; Palecek and Fojta, 2001; Palecek *et al.*, 2002b; Sequaris, 1992) well-developed reduction and oxidation signals at mercury electrodes (reviewed in Labuda *et al.*, 2005; Palecek, 1983, 1996; Palecek *et al.*, 2002b) and oxidation signals at carbon electrodes (Brabec, 1981; Brabec *et al.*, 1996; Palecek *et al.*, 2002b).

4.1. Oxidation

4.1.1. Solid electrodes

Oxidation of guanine and adenine residues in polynucleotides at carbon electrodes was reported already by the end of the 1970s (Brabec, 1981, 1983; Brabec and Dryhurst, 1978) and shortly afterwards voltammetric oxidation signals were utilized in DNA and RNA research (Brabec, 1981; Brabec *et al.*, 1996; Palecek *et al.*, 1993). DNA voltammetric peaks were, however, poorly developed and the sensitivity of the DNA and RNA analysis was substantially lower than that obtained with mercury electrodes. Only in 1995 it was shown that application of sophisticated baseline correction greatly improved the shape of the oxidation peaks and sensitivity of the NA analysis at carbon electrodes (Cai *et al.*, 1996; Tomschik *et al.*, 1999; Wang *et al.*, 1995, 1996a). Using constant current chronopotentiometric stripping analysis (CPSA) or square wave stripping voltammetry the sensitivity of the DNA and RNA determination increased by 2–3 orders of magnitude (Figure 5) becoming comparable to the sensitivities obtained with mercury electrodes (Palecek, 1996; Wang, 1999). Further improvement was recently obtained by using carbon fiber microelectrodes for the NA analysis in unstirred solution and at low ionic strength (Wang *et al.*, 1997a) and by the application of carbon nanotubes (Cai *et al.*, 2003b; Kohli *et al.*, 2004; Wang, 2005; Xu *et al.*, 2004) whose potentialities have not yet been fully exploited. Quite recently it has been shown by Brett *et al.* (Oliveira-Brett *et al.*, 2004) that in addition to guanine and adenine also pyrimidine bases such as cytosine and thymine can produce their oxidation signals at highly positive potentials on carbon electrodes. More details about nucleic electrochemistry on carbon electrodes can be found in Chapter 7 and in some recent reviews (Palecek *et al.*, 1998; Popovich and Thorp, 2002; Thorp, 2004; Wang, 2005).

Application of carbon nanotubes in nucleic acid electroanalysis and particularly in biosensors is a new promising field (Baughman *et al.*, 2002; Cai *et al.*, 2003a; Rao *et al.*, 2001; Wang and Musameh, 2005; Wang *et al.*, 2004; Zhao *et al.*, 2002), reviewed in Wang (2005). It has been shown that carbon nanotubes can enhance electrochemical reactivity of important biomacromolecules (Gooding *et al.*, 2003b; Yu *et al.*, 2003) including oxidation of guanine residues in DNA (Wang *et al.*, 2004). These nanotubes also may be useful as reservoirs of enzymes and other catalytically active compounds

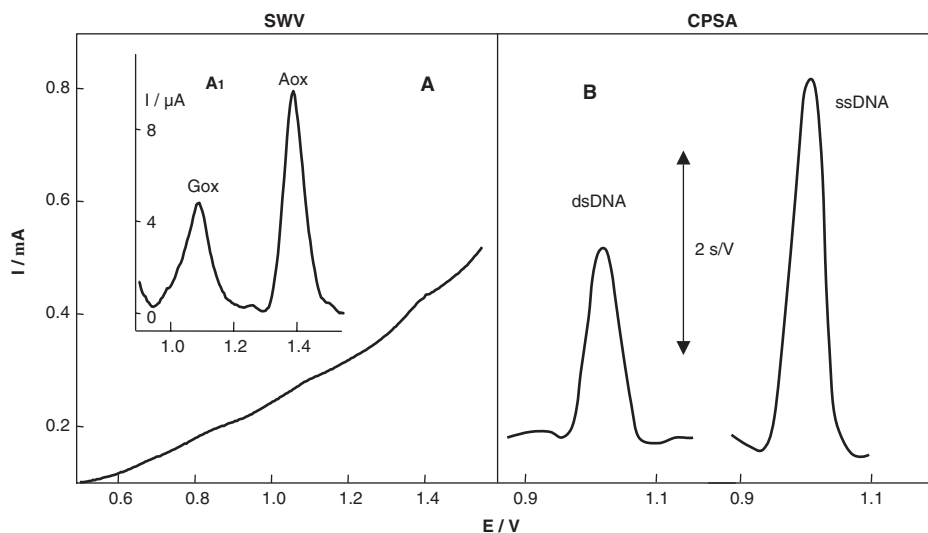


Fig. 5. Oxidation of DNA at carbon electrodes. (A) Raw square wave voltammetric curve of oligodeoxynucleotide (AAAAGGAGAG). (A1) The same curve after moving average baseline correction. Oxidation peaks of adenine (Aox) and guanine (Gox) are shown. SWV: frequency 350 Hz, amplitude 10 mV, potential step 5 mV, $t_A = 5$ min at 0.5 V, concentration of D10-pu 10 ng/mL. (B) Constant-current chronopotentiometric stripping analysis (CPSA) of ds and ssDNA. Only peak Gox is displayed. Experiment was performed with 100 $\mu\text{g/mL}$ of dsDNA and 50 $\mu\text{g/mL}$ of ssDNA. PGE, 0.2 M sodium acetate (pH 5.0) was used as a background electrolyte. Potentials are given against Ag/AgCl/3 M KCl reference electrode. Adapted from Tomschik *et al.* (1999) and Paleček and Fojta (2001). Copyright 1999 and 2001, with permission from Elsevier and American Chemical Society.

in DNA sensors, particularly in combination with the double surface technique (Section 6.2).

Among other solid electrodes applied in NA electrochemistry were silver (Brabec and Niki, 1985; Fan *et al.*, 1999; Koglin and Sequaris, 1986; Trnkova, 2002; Trnkova *et al.*, 2002) and copper electrodes. With the latter electrodes combined with sinusoidal voltammetry signals due to oxidation of the sugar moiety were observed (Singhal and Kuhr, 1997a, b). The method was applied for determination of nucleotides, ODNs and DNA. Thorp's group studied DNA oxidation responses by ITO electrodes modified with nitrocellulose or nylon membranes (Napier and Thorp, 1999) or with self-assembled dicarboxylate monolayers (Napier and Thorp, 1997). In these experiments, DNA was attached to the electrode either covalently or via adsorption forces in the modifier layer. Bare ITO electrode did not adsorb DNA. Oxidation of guanine in DNA was mediated by a redox metal chelate $[\text{Ru}(\text{bipy})_3]$ which shuttled electrons to the electrode surface from DNA in solution or attached at the modifier film (Napier and Thorp, 1997, 1999); immobilization of a redox mediator at ITO electrode modified with electropolymerized poly $[\text{Ru}(\text{bipy})_3]$ film was also used (Ontko *et al.*, 1999).

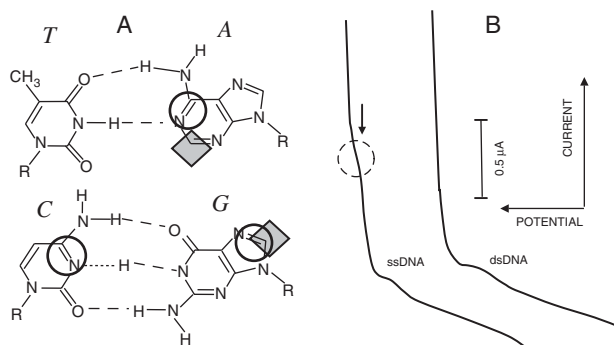


Fig. 6. (A) Representation of Watson–Crick base pairs and electroactive groups. Circles denote sites that can be reduced at mercury electrodes, R-deoxyribose residues; squares show sites oxidized at carbon electrodes. (B) d.c. polarograms of native (ds) and denatured (ss) calf thymus DNA at a concentration of 500 μg/mL showing inactivity of dsDNA and poorly developed polarographic wave of ssDNA at about -1.4 V. DNA was thermally denatured in 7 mM NaCl with 0.7 mM citrate, pH 7. Both curves start at 0.0 V. Adapted from Palecek and Fojta (2001) and Palecek and Vetterl (1968). Copyright 2001 and 1968, with permission from American Chemical Society and John Wiley & Sons.

4.1.2. Mercury electrodes

Oxidation signals of ss and dsDNA were obtained also with mercury electrodes (Janik and Palecek, 1966; Jelen and Palecek, 1986; Palecek, 1958, 1960a, b; Palecek *et al.*, 2002b; Studnickova *et al.*, 1989; Trnkova *et al.*, 1980). These signals (peak G) were due to the oxidation of the guanine reduction product. Exposition of DNA to highly negative potentials (at neutral pH between about -1.6 and -2.0 V) was necessary to obtain peak G. At these potentials reduction of G residues took place involving the 7,8 double bond of the imidazole ring in guanine as a primary reduction site (Figure 6). In the anodic process reoxidation of the G reduction product back to guanine occurred. Protonation of G residues was involved in the electrode process (Palecek *et al.*, 1986b; Studnickova *et al.*, 1989). This chemically reversible process was highly dependent on the potentials at which the guanine reduction product was formed (Jelen and Palecek, 1986; Palecek *et al.*, 1986b). Characteristic S-shaped curve (Figure 7A) showed that at switching potentials around -1.8 V CV peak G attained the highest values. On the other hand at these potentials peak G decreased with each cycle in a repeated cycle mode probably due to deeper reduction of guanine at more negative potentials. At less negative potentials the height of the peak did not change with repeated cycles (Figure 7B) showing very good chemical reversibility of the electrode process.

In measurements close to neutral pH presence of some salts in the background electrolyte, such as 0.6 M ammonium formate, 0.1 M MgCl₂ or Mg(ClO₄)₂ (Palecek *et al.*, 1986b) was required to obtain a well-developed peak (usually denominated as peak G). Similarly as in the case of the DNA reduction signals, these salts played a role in screening of the DNA negative charges and probably also in protonation of DNA at the electrode surface.

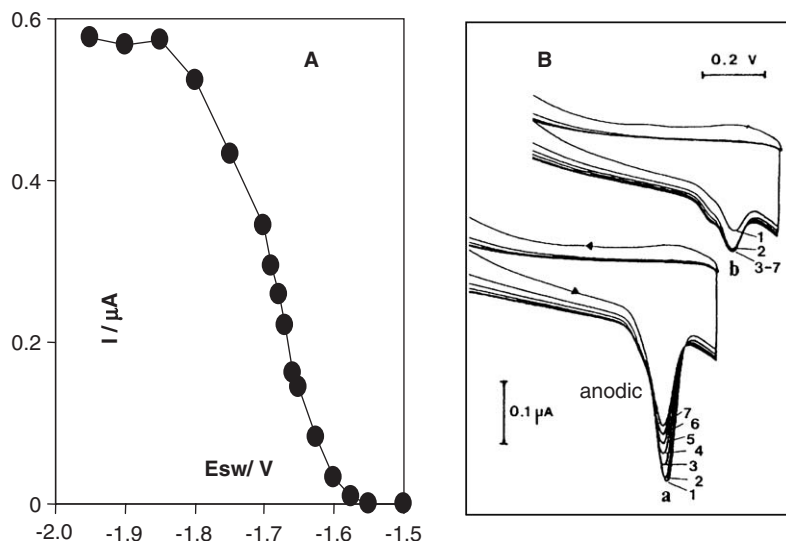


Fig. 7. (A) Dependence of the anodic voltammetric peak G of 2×10^{-4} M poly(A,U,G) on switching potential, E_{sw} . CV measurements were performed with an HMDE in 0.6 M ammonium formate, 0.1 M sodium phosphate, pH 6.8. Scan rate = 0.2 V/s, $E_a = -0.1$ V, $t_A = 140$ s, without stirring. (B) Sections of repetitive adsorptive transfer stripping (AdTS) cyclic voltammograms of linearized pAT32 DNA (56 $\mu\text{g/mL}$) showing anodic peak G. E_{sw} a, -1.85 V and b, -1.65 V. DNA in 10 mM Tris-HCl, 5 mM EDTA, pH 7.7 was adsorbed at the HMDE for t_A 2 min from a 4 μL drop of a DNA solution (at an open circuit). The electrode was then washed and transferred into an electrolytic cell containing 5 ml of deaerated 0.3 M ammonium formate and 50 mM sodium phosphate, pH 6.9. $E_a = -0.1$ V; $E_{sw} = -1.85$ V, scan rate 0.2 V/s, SCE. Adapted from (A) Jelen and Paleček (1986) and (B) Teijeiro *et al.* (1993). Copyright 1986 and 1993, with permission from Elsevier and Adenine Press, respectively.

Cyclic modes (such as CV) were used to obtain well-developed and symmetrical peak G (documenting involvement of adsorption in the electrode process). Alternatively, a short exposition of mercury electrodes (HMDE, mercury film or solid amalgam electrodes) to sufficiently negative potentials, followed by scanning to positive potentials, was used to obtain this peak (Jelen *et al.*, 1997; Tomschik *et al.*, 1999). Peak G offered a better alternative for the determination of NAs at concentrations below ppm (by stripping techniques) as compared to the asymmetrical reduction peak of adenine and cytosine residues, formed at potentials too close to the background discharge. Constant current chronopotentiometric stripping analysis (Tomschik *et al.*, 1998) and square wave voltammetric stripping (Jelen *et al.*, 1997) were used to study peak G at concentrations below 1 ppm.

4.2. Reduction

So far electroreduction of nucleic acids was observed only at mercury electrodes. It was shown that mercury electrodes are particularly sensitive to DNA

minor conformational changes such as those induced by nucleases, chemical and physical agents, including ionizing radiation. Linear native dsDNA at neutral pH and moderate ionic strengths showed no d.c. polarographic reduction signal (with DME) at room temperature (Palecek, 1966; Palecek and Vetterl, 1968) even at concentrations as high as 0.5 mg/mL (Figure 6B). Denatured DNA and other ssNAs containing adenine and/or cytosine residues were, under the same conditions, d.c. polarographically reducible (Brabec and Palecek, 1970a, b, 1973; Janik and Sommer, 1972, 1973b; Janik *et al.*, 1972; Palecek, 1966, 1969a, 1972; Palecek and Vetterl, 1968; Palecek and Duskocil, 1974; Reynaud *et al.*, 1977; Valenta and Grahmann, 1974; Valenta and Nurnberg, 1974a; Valenta *et al.*, 1974, 1975), reviewed in Palecek *et al.* (2002b). D.c. polarographic signals yielded by chromosomal denatured ssNAs were rather low due to slow transport of their molecules to the electrode. D.c. polarography thus did not appear suitable for biochemical analysis requiring more sensitive methods. Derivative pulse polarography (which was applied for DNA analysis already in the middle of 1960s) allowed, however, the ssDNA determination at μM and submicromolar concentrations (Palecek, 1971) (related to the monomer content). Electrode processes of ssNAs taking place at the mercury electrodes were intensively studied. They will be briefly reviewed in the following paragraphs.

4.2.1. Reduction of ss nucleic acids

ssNAs containing C and/or A were reducible at neutral and weakly acidic pH producing d.c. polarographic (with DME) or voltammetric (using HMDE) reduction signals at about -1.4V . Protonated forms of the NAs were subjected to an irreversible reduction in an adsorbed state (Brabec, 1974; Brabec and Palecek, 1970a, b, 1973, 1974; Palecek, 1969a, 1972; Palecek and Vetterl, 1968; Palecek and Duskocil, 1974; Valenta and Grahmann, 1974; Valenta and Nurnberg, 1974a; Valenta *et al.*, 1974, 1975). In the range of pH 6.0–8.7 (in a background electrolyte with ammonium formate) both A and C residues were reduced in denatured DNA (Brabec and Palecek, 1974).

4.2.1.1. Effect of pH and salts. Around neutral pH the electrochemical responses were dependent on the nature and concentration of salts (Brabec and Palecek, 1970a; Palecek, 1969a; Palecek and Brabec, 1972) in the background electrolyte. The dependence of the wave heights of single-stranded (ss) polynucleotides on pH was S-shaped (Figure 8). Some organic and inorganic salts and polyamines (Brabec, 1974; Brabec and Palecek, 1970a; Janik and Sommer, 1973b; Palecek, 1969a, 1983; Palecek and Brabec, 1972) shifted the S-shaped curves to higher pH values. In the descending part of the S-shaped curve the d.c. polarographic wave had a maximum-like appearance, while at lower pH values usual d.c. polarographic wave appeared (Figure 8A). The height of this wave was almost independent of the nature and concentration of salts. The ability of salts and polyamines to shift the descending part of this S-shaped curve to

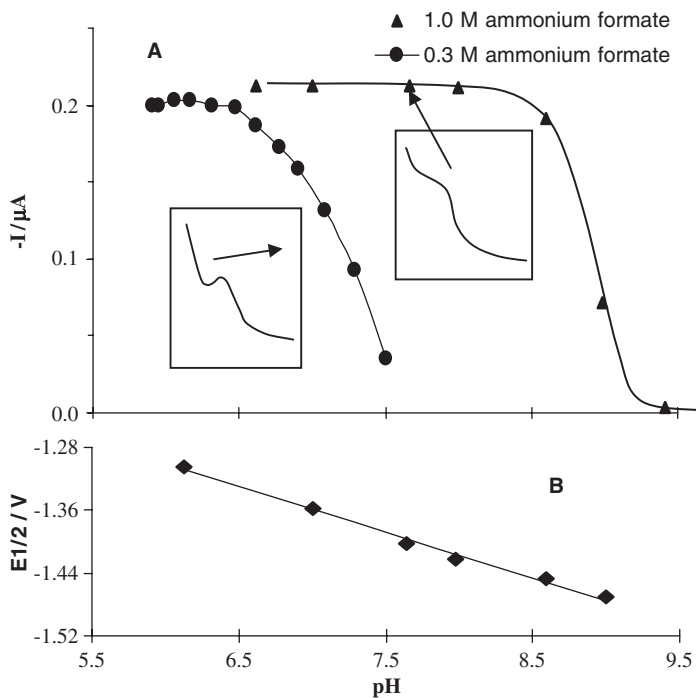


Fig. 8. Dependence of (A) the height and (B) $E_{1/2}$ of the d.c. polarographic wave of polycytidylic acid on pH. 0.1 mM poly(C) either in 0.3 or 1.0 M ammonium formate with Britton–Robinson buffer. In the descending part of the d.c. polarographic waves a maximum-like shape appeared (see insets). DME, SCE. Adapted from Paleček (1969a). Copyright 1969, with permission.

higher pH values and to influence the shape of the wave was explained by the effect of these agents on NA adsorbability and partly on NA protonation (Brabec, 1974; Brabec and Paleček, 1970a; Janik and Sommer, 1973b; Paleček, 1983). The maximum-like shape of the polarographic curve was due to a current decrease, resulting from DNA desorption at negative potentials. The relation between the height and shape of the d.c. polarographic wave on one hand and DNA adsorption/desorption properties on the other hand was reported by several authors (Brabec, 1974; Brabec and Paleček, 1970a; Janik and Sommer, 1973b; Miller, 1961a). These and other results suggested that the NA adsorption was critical in the reduction of the nucleic acids. At neutral pH, DNA as a polyanion, should be strongly repulsed from the electrode at negative potentials of the DNA reduction. Strong adsorption of ssDNA via its hydrophobic bases to the hydrophobic mercury surface prevents DNA desorption in spite of the electrostatic repulsion (which can be partially neutralized by counterions forming the DNA ionic atmosphere). The possibility that DNA protonation at the electrode could be facilitated by DNA adsorption was also considered (Paleček, 1983; Paleček and Brabec, 1972). If ssDNA was exposed at the mercury electrode to sufficiently negative potentials blocking of the

electrode surface by the NA reduction products was detected at HMDE (Jelen and Palecek, 1986; Palecek, 1969b; Valenta and Nurnberg, 1974a; Valenta *et al.*, 1974). No such effect was observed with techniques working with small voltage excursions during the drop lifetime (e.g. using d.c. polarography with DME).

In practical electrochemical experiments usually conditions corresponding to the horizontal part of the S-shaped pH dependence were chosen (Figure 8). In experiments performed close to neutral pH some ions known to efficiently screen the negatively charged DNA phosphate residues were added into the background electrolyte. Buffered 0.3–0.6 M ammonium formate or CsCl were among the salts widely used for this purpose (Brabec, 1980; Palecek, 1983; Palecek *et al.*, 2002b). D.c. polarographic currents obtained within the horizontal part of the S-shaped pH dependence showed characteristics of the adsorption currents (Brabec, 1974; Brabec and Palecek, 1970a, 1973; Filipiński *et al.*, 1971; Janik and Sommer, 1973b; Palecek, 1969a; Palecek and Brabec, 1972; Valenta and Grahmann, 1974; Valenta and Nurnberg, 1974a) provided the electrode surface was fully covered. At partial electrode coverage, characteristics typical for diffusion-controlled currents were obtained (Brabec, 1974; Brabec and Palecek, 1970a, 1973; Palecek and Vetterl, 1968).

To our knowledge, the reduction of ssDNA represented the first case of the electrochemical reduction of a giant biomacromolecule with the m.w. of the order of 10^7 and the contour length about 0.01 mm. Criteria based on theories and experience with the low-molecular weight substances for DNA electrochemistry were therefore applied with caution. Nevertheless, the agreement between the data obtained experimentally for calf thymus ssDNA (Brabec, 1974; Brabec and Palecek, 1970a), poly(A) (Brabec and Palecek, 1973) as well as for chromophoredextrins (m.w. up to 5×10^5) on one hand (Berg, 1976), and those calculated on the basis of Ilkovic (Heyrovsky and Kuta, 1965) or Koryta equations (Koryta, 1953) on the other hand, was surprisingly good.

4.2.1.2. Differential (derivative) pulse polarography (DPP). Wide use of DPP in electrochemical analysis of organic compounds (Wolff and Nurnberg, 1966) started in the second half of the 1960s; practically in the same time DPP became one of the most efficient methods in electrochemical analysis of nucleic acids (Palecek and Frary, 1966). Since that time DPP and later DP voltammetry (DPV) were for about two decades the major methods utilized in studies of nucleic acids using DME, HMDE and carbon electrodes. In the 1990s these methods were complemented by square wave voltammetry (Tomschik *et al.*, 1999) and constant current chronopotentiometry (Wang *et al.*, 1995). Recently, elimination voltammetry has been applied in studies dealing with the resolution of reduction signals of adenine and cytosine in short synthetic homo-oligodeoxynucleotides (dA₉ and dC₉) and DNA (Trnkova *et al.*, 2000, 2003).

Peak III of ssDNA. As an example of DP-polarograms of ss and dsDNAs and RNA are shown in Figure 9. At low sensitivity of the instrument denatured ssDNA produced a well-developed peak III while native dsDNA, in agreement with the results of d.c. polarography (Palecek and Vetterl, 1968), appeared

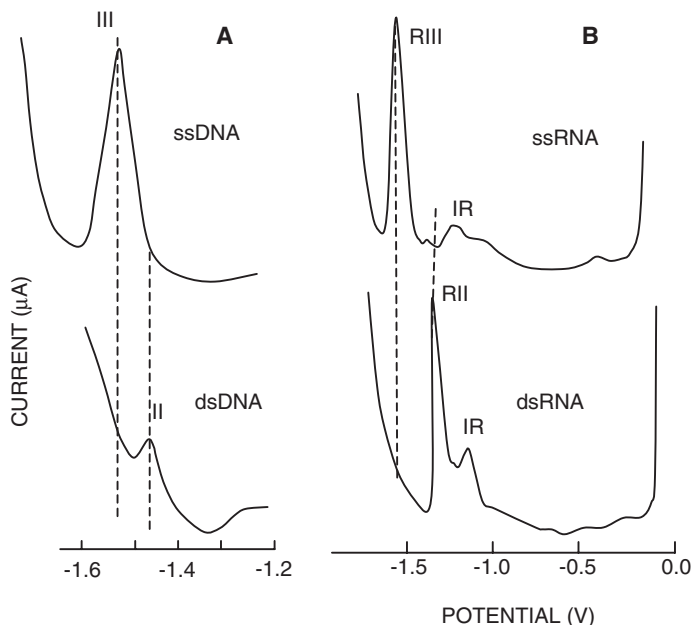


Fig. 9. DP polarograms of ds and ss DNA and RNA. (A) – DNA. dsDNA from calf thymus at a concentration of 470 $\mu\text{g}/\text{mL}$ and ssDNA at a concentration of 50 $\mu\text{g}/\text{mL}$. (B) ssRNA at a concentration of 250 $\mu\text{g}/\text{mL}$ and dsRNA at a concentration of 500 $\mu\text{g}/\text{mL}$. Measurements were performed on the A 3100 Southern–Harwell pulse polarography, Mark II, which did not display current values (see Table 3 to compare current and potential on DP polarograms). The potentials were measured against the mercury pool at the bottom of the polarographic vessel. Adapted from (A) Paleček (1971) and (B) Paleček and Dorskocil (1974). Copyright 1971 and 1974, with permission from Academic Press.

inactive. At high sensitivity of the instrument (and high DNA concentration) additional peaks were observed; both ds and ssDNAs yielded peak I. dsDNA produced also peak II, which was not observed with ssDNA. From the analytical point of view peak I was of little interest; it responded weakly to changes in DNA conformation and its height was comparable to that of peak III only at low DNA concentrations, while at higher concentrations of ssDNA peak III was substantially larger than peak I. As early as in 1966 we suggested (Paleček and Frary, 1966) that peak I was of non-faradaic (capacitive) nature. This assumption was supported by correspondence of peak I potential with that of the capacitive oscillopolarographic indentation CI-I (Figure 1) and of the tensammetric (a.c. polarographic) peak 1 (Figure 3) produced by dsDNA at potentials of its desorption. Later it was shown (Anson *et al.*, 1976; Barker and McKeown, 1976; Flanagan *et al.*, 1977; Jacobsen and Lindseth, 1976) that other surface-active substances yielded non-faradaic DPP peaks related to the desorption of the substance. Reduction and tensammetric pulse-polarographic signals of ss polynucleotides were studied in detail and diagnostic criteria for classification of small peaks of ds nucleic acids were proposed (Paleček *et al.*, 1987).

Effect of molecular weight of ss polyribonucleotides. D.c. and normal pulse polarography (NPP) (Janik and Sommer, 1972, 1976) was used to study the effect of lengths of ss poly(A) molecules on their d.c. and NPP responses. Using 16 poly(A) samples with m.w. in the range of 3×10^4 – 3×10^6 (i.e. chain lengths from about 90 to 9000 nucleotides) a correlation was found between the current magnitudes, intrinsic viscosity and sedimentation coefficients S_{20} of the samples. The log–log plots of m.w. against current intensity were linear with the slope $-1/4$. In principle, electrochemical methods could be used for fast determination of the lengths of the nucleic acids. More detailed work would be, however, necessary to establish a ready-to-use method.

Unlike peak I, peaks II and III were of great analytical significance. It was shown that all reducible ss nucleic acids studied, i.e., denatured ssRNA (obtained by thermal denaturation of viral double-stranded RNA), poly(A) (Brabec and Palecek, 1973; Palecek, 1969a, 1971, 1972; Palecek *et al.*, 1974) and poly(C) (Brabec and Palecek, 1973; Palecek, 1969a, 1971) produced well-developed peaks similar to peak III of denatured ssDNA (Figure 9). The height of the DPP peaks depended on the pulse amplitude in an unusual way (Palecek, 1972). At small pulse amplitudes (up to about 10 mV) linear dependence was observed, but the peaks obtained at the amplitude of 50 and 100 mV were much higher than could be expected for the linear dependence. This dependence was explained by accumulation of the nucleic acid on the electrode surface and the proximity of reduction and desorption potentials (Palecek, 1972; Palecek *et al.*, 1987). At high pulse amplitude ss nucleic acids were determined by DPP at concentrations down to about 100 ng/mL.

Peak II of ds nucleic acids. Almost all ds nucleic acids studied, i.e., RNA (a replicative form of phage f2 RNA), poly(rA)·poly(rU), poly(rC)·poly(rI), poly(dA)·poly(dT), poly(dA–dT)·poly(dA–dT), produced peak II (Jelen and Palecek, 1985; Palecek, 1983). The only exception was poly(rG)·poly(rC) which did not yield any DPP peak at a wide variety of pHs and ionic strengths (Jelen and Palecek, 1979). In contrast, the alternating double-stranded copolymer poly(dG–dC)·poly(dG–dC) (with the same base composition) produced a peak similar to those of other ds polynucleotides. DP peaks of dsNAs were utilized in NA structure research (Section 4.2.1.3). Peak II was always less negative and substantially smaller than peak III of the corresponding ss nucleic acid (Figure 9). The difference in the potentials of peak II and III was about 70 and 180 mV in chromosomal DNA and phage RNA, respectively (Table 3). The highest amount of data were obtained with DNA; the work with RNA was limited to biosynthetic polyribonucleotides and few natural RNAs, producing results in a reasonable agreement with those obtained with DNAs.

For all polarographic and voltammetric signals of DNA obtained with mercury and carbon electrodes adsorbed DNA was responsible. These methods thus reported about the properties of DNA at the electrode surface. It has been shown, however, that under certain conditions electrochemical methods can report on changes in DNA structure in solution, while under different conditions relatively slow changes in the DNA structure, occurring secondarily at the electrode surface can be observed.

Table 3. Heights, summit potential E_s , and half-width $W1/2$ of derivative pulse-polarographic peaks of RNA and DNA^a

Sample	Concentration ($\mu\text{g/mL}$)	Peak	Height (μA)	E_s (V)	$W1/2$ (mV)
dsRNA	400	II R	0.62	-1.3	55
Thermally denatured RNA	80	III R	0.64	-1.48	75
Native DNA	400	II	0.05	-1.48	—
Thermally denatured DNA	80	III	1.42	1.55	85

^aThe measurements were performed in 0.3 M ammonium formate with 0.1 M sodium phosphate pH 7 with the polarographic analyzer PAR 174 at pulse amplitude of 50 mV with DME, R-peak of RNA. Potentials were measured against mercury pool at the bottom of the polarographic vessel. Adapted from Paleček and Dorskocil (1974). Copyright 1974, with permission from Academic Press.

4.2.1.3. *Changes of DNA structure in solution can be detected electrochemically.* It was shown that the electrochemical signals of chromosomal denatured ssDNA obtained with mercury and carbon electrodes greatly differed from those of native dsDNA (Figures 1, 3, 5, 6B, 9). ssDNA produced a d.c. polarographic reduction wave while native dsDNA was under the same conditions d.c. polarographically inactive (Figure 6B). The d.c. polarographic inactivity of dsDNA (at neutral pH, moderate ionic strengths and room temperature) was explained by the inaccessibility of the reduction sites for the electrode process. In the B-form of dsDNA the reduction sites are hidden in the interior of the DNA molecule forming a part of the Watson–Crick hydrogen bonding system (Figure 6A). It should be noted that higher concentration of dsDNA produced DP polarographic peak II (Figure 9A, Table 3) which was almost by two orders of magnitude smaller than peak III of the thermally denatured ssDNA (if the height of peak III was extrapolated to the concentration of dsDNA at which peak II was observed). Peak II was highly sensitive to DNA damage by chemical and physical agents involving DNA strand breaks (Fojta, 2004; Paleček, 1983) (Chapter 12). Similar sensitivity was observed with peak IIR of dsRNA (Figure 9B) (Paleček and Dorskocil, 1974). Peak II was assigned to labilized regions in the DNA double helix, including DNA ends and single-strand breaks. At room temperature peak II was produced by nicked circular DNA but not by covalently closed-circular (supercoiled) DNA (see below) (Fojta, 2004; Vojtiskova *et al.*, 1981). UV irradiation (at 254 nm) of linear dsDNA, similarly to other physical and chemical agents, produced an increase of peak II (Paleček, 1983; Vorlickova and Paleček, 1974).

In contrast to the reduction sites, oxidation sites of adenine and guanine (Figure 6A) are closer to the surface of the dsDNA molecule and not involved in the hydrogen-bonding system. Consequently, the formation of the double helix does not prevent them from oxidation at the graphite electrodes. ssDNA produced larger oxidation signals than dsDNA but the differences were much smaller than those obtained with DP polarography or voltammetry with

mercury electrodes (Figure 5). It was assumed that the differences in oxidation signals of ds and ssDNA observed at carbon electrodes were related to the different flexibilities of the ss and dsDNA (Brabec *et al.*, 1996) (greater flexibility of the ss molecules allowed a better adherence of DNA to the uneven surfaces of the carbon electrodes). DNA single-strand breaks were not detectable at carbon electrodes (Cahova-Kucharikova *et al.*, 2005; Cai *et al.*, 1996; Kubicarova *et al.*, 2000b).

Polarographic techniques (including DPP with DME) were applied also to studies of protonated ds structures of polyriboadenylic and polyribocytidylic acids (Brabec and Palecek, 1972; Palecek, 1972; Palecek *et al.*, 1974). Protonated ds structures of both of these biosynthetic polynucleotides greatly differs from the Watson–Crick DNA and RNA duplexes. Reduction sites of adenine and cytosine residues are better accessible in protonated ds structures than in non-protonated DNA duplexes. It was thus not surprising that the differences between the electrochemical signals of protonated ds duplexes and their (non-protonated) ss forms were much smaller than in ss and dsDNAs. Nevertheless it was possible to obtain dependencies of electrochemical signals on pH indicating the structural transitions of these polynucleotides (Brabec and Palecek, 1972; Palecek, 1972). With longer polynucleotides larger differences in electrochemical signals between ss and protonated ds structures were observed (Palecek *et al.*, 1974), suggesting that these signals were affected by different diffusion coefficients of long ss and ds polynucleotides.

DPP peak III (Figure 9B) was used to monitor full or partial DNA denaturation, DNA renaturation (Palecek, 1976) or formation of polynucleotide complexes (Jelen and Palecek, 1985; Palecek, 1969c) and to detect traces of ssDNA in dsDNA (Palecek, 1971; Palecek and Frary, 1966). Figure 10 shows the time course of renaturation of RNA at two different ionic strengths and temperatures. Using peaks III and II renaturation of DNA and RNA could be followed in real time. The results of the electrochemical measurements were in agreement with those of optical measurements. Moreover, a negative correlation between the content of ssRNA, reflected by peak IIIIR, and antiviral and interferon-inducing activities was found (Palecek and Dorskocil, 1974). The DPP thermal denaturation curves corresponded well to optical density curves, if DNA was exposed to elevated temperatures and the measurements were performed at room temperature after quick cooling of the DNA sample (Palecek, 1969b, 1976; Palecek *et al.*, 1977). Similarly, the alkaline melting curve of chromosomal DNA obtained by means of adsorptive transfer stripping cyclic voltammetry (peak G was measured) agreed with the UV absorption (260 nm) melting curve (Palecek, 1988a).

DNA premelting. If thermal denaturation of chromosomal DNA was done in such a way that the DPP measurements were performed at elevated temperature, peak II increased with temperature in the temperature range where no changes in DNA absorbancy were detectable. These premelting changes were later detected by circular dichroism and other methods (reviewed in Palecek, 1976). In supercoiled DNA (see below) no premelting changes were observed above 40°C (Vojtiskova *et al.*, 1981). Above 40°C an inflexion appeared on DP polarogram and grew with temperature in the premelting

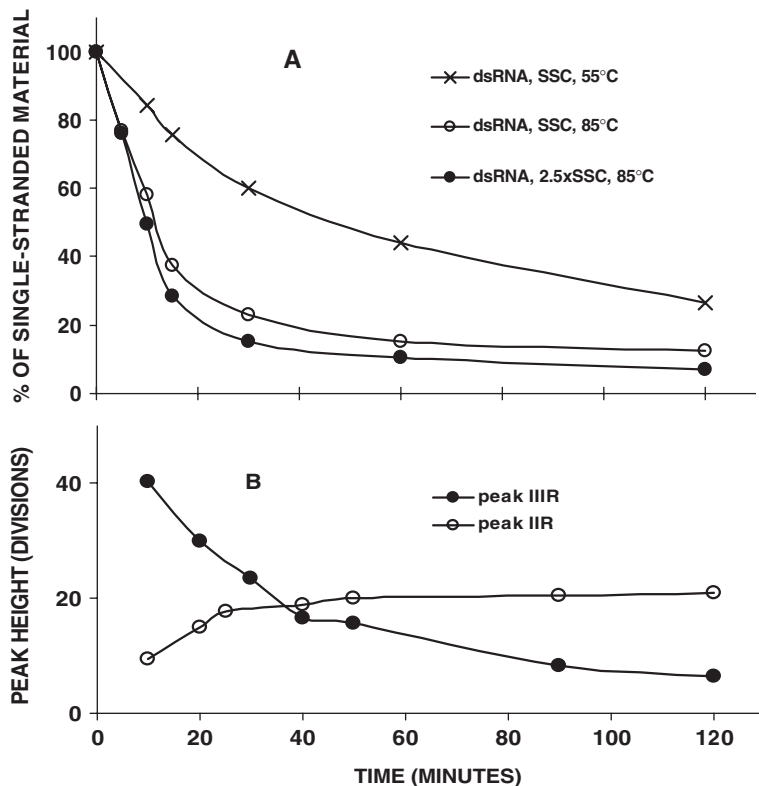


Fig. 10. Time-course of renaturation of phage f2 dsRNA. (A) Thermally denatured ssRNA was incubated (●—●) at 85°C in 2.5 × sodium saline citrate (SSC) or (o—o) at 85°C in SSC, and (x—x) at 55°C. Samples were withdrawn in time intervals given in the graph and quickly cooled. DPP measurements were performed at room temperature at a RNA concentration of 3.2 μg/mL in 0.3 M ammonium formate with 0.2 M sodium acetate, pH 5.6; PAR 174. (B) (o—o) peak IIR. (●—●) peak IIIR. ssRNA (108 μg/mL) in 0.01 × SSC was heated for 6 min at 100°C. Then it was placed into a thermostated polarographic vessel with the same volume of 0.6 M ammonium formate with 0.2 M sodium phosphate, pH 7, preheated to 58°C. The pulse polarograms were measured at 58°C in times given in the graph. Southern-Harwell A 3100, amplifier sensitivity 1/8. Adapted from Paleček and Doskocil (1974). Copyright 1974, with permission from Academic Press.

region. It should be noted that in supercoiled DNA no molecular ends are present.

Using the adsorption transfer stripping method it was shown that the temperature at which dsDNA was adsorbed at the electrode (but not the temperature at which the electroreduction took place), played a decisive role in the manifestation of the DNA premelting (Paleček, 1988b). This result is in agreement with the assumption that it was the DNA structure (affected by the temperature in the time of adsorption of the DNA molecule) which determined the electrochemical response (Paleček, 1976), while the effect of temperature on the electroreduction was of lesser importance.

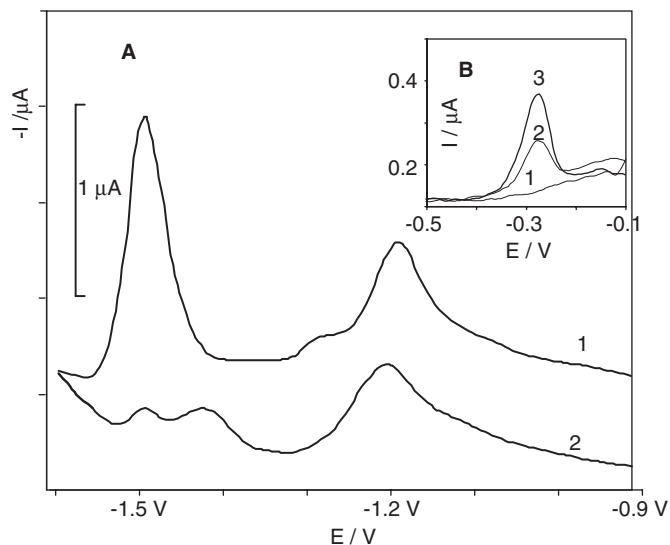


Fig. 11. Adsorptive square wave voltammograms of long ssODN and dsODNs (97-mers). (A) cathodic response, (B) anodic response (peak G). 1- $(TTC)_{24}(T)_{25}$, 2 - duplex $[(TTC)_{24}(T)_{25}] \cdot [(GAA)_{24}(A)_{25}]$. 3 - ODN $(GAA)_{24}(A)_{25}$, $0.25 \mu\text{M}$ ODN in 0.1 M NaCl , pH 7 was adsorbed from a $10 \mu\text{L}$ sample drop at 0°C for 60 s at open current circuit. Then the ODN-modified HMDE was washed, and transferred into background electrolyte (0.3 M ammonium formate, 50 mM sodium phosphate, pH 6.9) and measured at room temperature. SWV: frequency 380 Hz , step potential 5 mV , amplitude 25 mV , initial potential (A) -0.6 V or (B) -1.85 V . Potentials are given against $\text{Ag}/\text{AgCl}/3 \text{ M KCl}$ reference electrode. Hybridization: A mixture of complementary ODN aliquots in 0.1 M NaCl , pH 7 was incubated at 90°C for 30 min, and then slowly cooled to room temperature (F. Jelen and E. Palecek, unpublished).

Large differences between the signals of ss and dsNAs (obtained with mercury electrodes) (Figure 9) were observed with chromosomal, plasmid and viral nucleic acids (Palecek, 1983; Palecek *et al.*, 2002b) but not with short ODNs. For example, a ds decamer ODN compared to a ss decamer showed almost no difference in its voltammetric signals (Palecek *et al.*, 1990) (F. Jelen and E. Palecek, unpublished, 2005). This lack of differences in the electrochemical behavior of ss and dsODNs might be due to unwinding of the ends of the ODN, flatly lying at the electrode surface. In long dsDNA molecules such unwinding can be neglected, while in a ds decamer it may involve a major part of the ODN. To test this assumption we have recently measured several ss and dsODNs of different lengths and we found that the ratio ss/ds of the cathodic responses depended on the ODN lengths. Figure 11A shows a very small square wave voltammetry (SWV) cathodic response of 97-mer duplex ODN $[(TTC)_{24}(T)_{25}] \cdot [(GAA)_{24}(A)_{25}]$ as compared to high peak C (due to reduction of cytosine residues) of ss $(TTC)_{24}(T)_{25}$. In agreement with the previous measurements of the anodic peak G in long chromosomal ss and dsDNAs (Section 4.1.2) peak G of ss $(GAA)_{24}(A)_{25}$ was only about twice as high than the peak of ds $[(TTC)_{24}(T)_{25}] \cdot [(GAA)_{24}(A)_{25}]$ (Figure 11B). This was attributed to

the location of the electroactive site of guanine out of the DNA duplex interior (Figure 6). Ss(TTC)₂₄(T)₂₅ produced no peak G in accordance with absence of guanine residues in this ODN (Figure 11B).

Supercoiled DNA. About 40 years ago, Vinograd *et al.* (1965) discovered the twisted circular form of polyoma virus (Lebowitz, 1990; Paleček, 1991). Three forms of polyoma DNA were visualized in the electron microscope – open, linear and twisted (supercoiled, superhelical). Twisted appearance of this DNA was explained by the formation of superhelical turns in the circular molecule. It soon became apparent that circular DNAs that existed in many organisms, were supercoiled. Even linear DNA could supercoil in the cell if constrained into topologically different domains (see Section 5.5.1.2 for more detail). Experimental methods suitable for studies of supercoiled (sc) DNA are rather limited. No crystals of scDNA have been obtained, and the molecules are too large to be studied by NMR. Electron microscopy and cryoelectron microscopy were important in the study of the global shapes of scDNA (Adrian *et al.*, 1990; Bednar *et al.*, 1994). Raman spectroscopy, circular dichroism, dynamic light scattering and scattering time-resolved fluorescence anisotropy measurements of intercalated ethidium, were applied to studies of supercoiled DNA (reviewed in Vologodskii and Cozzarelli, 1994). In general, the conformational problem of scDNA is sufficiently complex to require a combination of different experimental approaches and theoretical analysis. scDNAs are very interesting models for studies of various DNA properties, including the DNA interfacial behavior. Electrochemical studies of these interesting DNAs have been, however, limited to very few laboratories because highly purified scDNAs are not commercially available. With commercially available kits their isolation is now rather easy but purification requires usually density gradient ultracentrifugation followed by further purification steps. Various electrochemical methods and particularly DPP, a.c. impedance and a.c. voltammetric and CV measurements with HMDE, proved useful in investigations of scDNA (Boublikova *et al.*, 1987; Fojta *et al.*, 1998; Paleček, 1988b; Paleček *et al.*, 1986a; Teijeiro *et al.*, 1993; Vojtiskova *et al.*, 1981). It was shown that breakage of single fosfodiesteric bond in the scDNA molecule can be sensitively detected by electrochemical methods (Boublikova *et al.*, 1987; Fojta and Paleček, 1997, and references therein).

Adsorptive transfer stripping voltammetry was used to investigate alkaline denaturation of supercoiled and linearized plasmid DNA (Teijeiro *et al.*, 1993). Up to pH 11.5 there were no changes in peaks G and CA (Figure 12). Both peaks increased between pH 11.5 and 11.9 only in linear DNA, while no changes were observed in these peaks of scDNA up to pH 12.5. Between pH 12.5 and 12.7 a striking increase of both peaks was observed. Physical properties and denaturation of scDNA were studied by various methods (Paleček, 1991). Using sedimentation measurements it was shown that alkaline denaturation of scDNA was entirely reversible up to pH 12.6 (at an ionic strength of about 0.25) (Rush and Warner, 1970). The voltammetric data (Figure 12) obtained under slightly different ionic conditions were thus in an agreement with the sedimentation measurements but compared to sedimentation, voltammetry produced additional information about the behavior of AT and GC pairs (Teijeiro *et al.*, 1993).

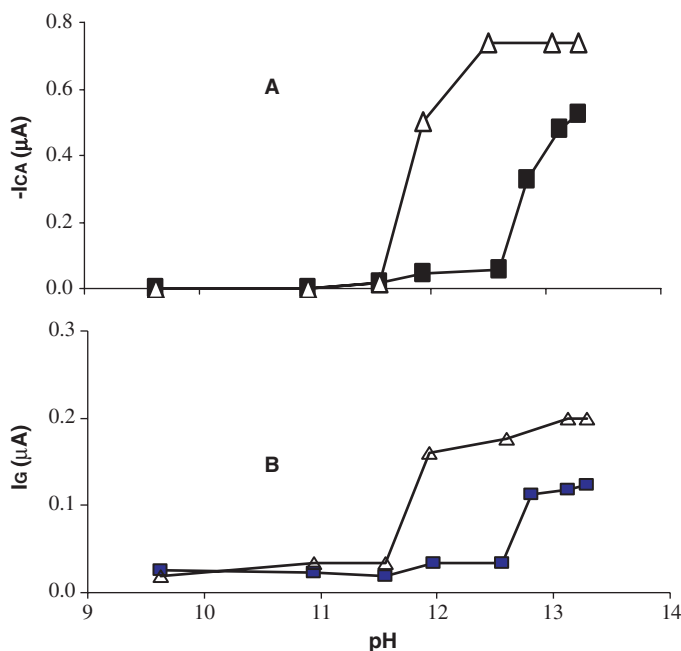


Fig. 12. Alkaline denaturation of ■, supercoiled and Δ , linearized plasmid DNA. pAT32 DNA at a concentration of $10.3 \mu\text{g/mL}$ was adsorbed at the HMDE from a Britton–Robinson buffer at pH indicated in the graph. The electrode was then washed and transferred into an electrolytic cell containing 5 mL of deaerated 0.3 M ammonium formate and 50 mM sodium phosphate, pH 6.9. CV: initial potential -0.1 V; switching potential -1.85 V, scan rate 0.2 V/s. Adapted from Teijeiro *et al.* (1993). Copyright 1993, with permission from Adenine Press.

a.c. impedance measurements represent a useful method for investigation of DNA adsorption that is not perturbed by chemical reactions that may accompany the DNA redox processes at electrodes. It was shown in Section 3.1.1 that adsorption behavior of ss and ds DNAs at the mercury electrodes greatly differed. Our further studies showed that a.c. impedance responses of sc plasmid DNA differed qualitatively from that of chromosomal DNA and open circular and linear plasmid DNAs (Fojta and Palecek, 1997). Similar to chromosomal linear ds and denatured ss DNAs (reviewed in Palecek, 1983), various forms of circular plasmid DNA adsorbed at the electrically charged mercury/water interface in a wide potential range. A detailed comparison of the C–E curves of relaxed, native and highly supercoiled DNA revealed quantitative differences in ΔC and in the height of peak 1 (Figures 13 and 14), suggesting that these DNA species may interact with the electrically charged surface and respond to the alternating voltage in different ways (Fojta *et al.*, 1998). The adsorption/desorption behavior of covalently closed-circular DNAs was influenced by the DNA negative superhelix density ($-\sigma$). Studies of topoisomer distributions showed two superhelix density-dependent structural transitions at midpoints of $-\sigma$ about 0.04 and 0.07. The first transition (explained by changes in global structure of circular DNAs) was

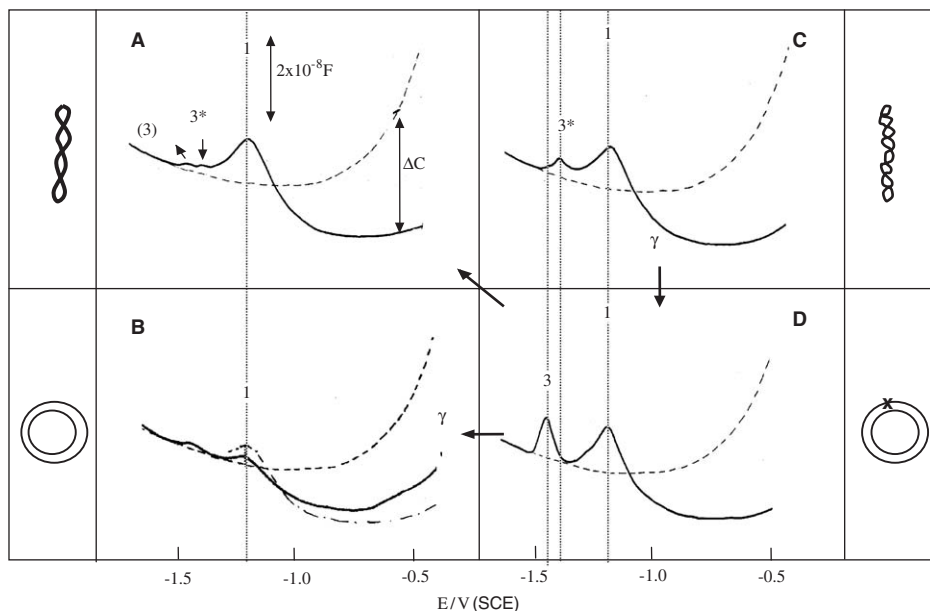


Fig. 13. Sections of C–E curves of a HMDE modified with pUC19 DNA: (A) supercoiled DNA at native superhelix density; (B) topoisomerase I-relaxed DNA (C) highly supercoiled DNA ($-\sigma \geq 0.11$); D, open circular DNA. DNA concentration was $100 \mu\text{g/mL}$, adsorption time $t_A = 120 \text{ s}$; in B, (---), $250 \mu\text{g/mL}$, $t_A = 180 \text{ s}$; (---), background electrolyte. The response of open circular DNA prepared from covalently closed circular DNA by γ -irradiation (arrows marked “ γ ”) was not influenced by the superhelix density of the original covalently closed circular DNA. In panel (A) the meaning of the capacitance decrease (ΔC) is displayed. DNA was adsorbed at the electrode from a drop ($4 \mu\text{L}$) of solution containing 0.2 M NaCl and 0.01 M Tris-HCl buffer, pH 7.4, at room temperature. DNA-modified electrodes were then washed in water and in background electrolyte solution and placed into a cell containing blank background electrolyte (0.3 M NaCl , $0.05 \text{ M sodium phosphate}$, pH 8.5). Adapted from Fojta *et al.* (1998). Copyright 1998, with permission from American Chemical Society.

indicated by changes in peak 1. The other one, occurring at more negative $-\sigma$, was manifested by peak 3^* which had not previously been observed (see below).

Figure 13 shows striking differences in presence and absence of peak 3 in different forms of circular DNA. This peak was produced by open circular DNA (Figure 13D) and linearized denatured DNA (not shown) but not by any investigated covalently closed-circular DNA (Figure 13A–C). Compared to scDNA at native negative superhelix density ($-\sigma$ about 0.05) highly supercoiled DNA ($-\sigma = 0.11$) gave rise to peak 3^* (Figure 13C), which was about 50 mV less negative than peak 3 produced by open circular and denatured DNAs. The height of peak 3^* decreased with relieving of the superhelical stress and disappeared close to the native superhelix density. Peak 3^* was assigned to disturbances of the DNA structure resulting from strong superhelical stress in DNA molecules with highly negative σ .

In addition to the *ex situ* experiments with DNA-modified HMDE, a.c. polarographic measurements with DME immersed into the DNA solution were

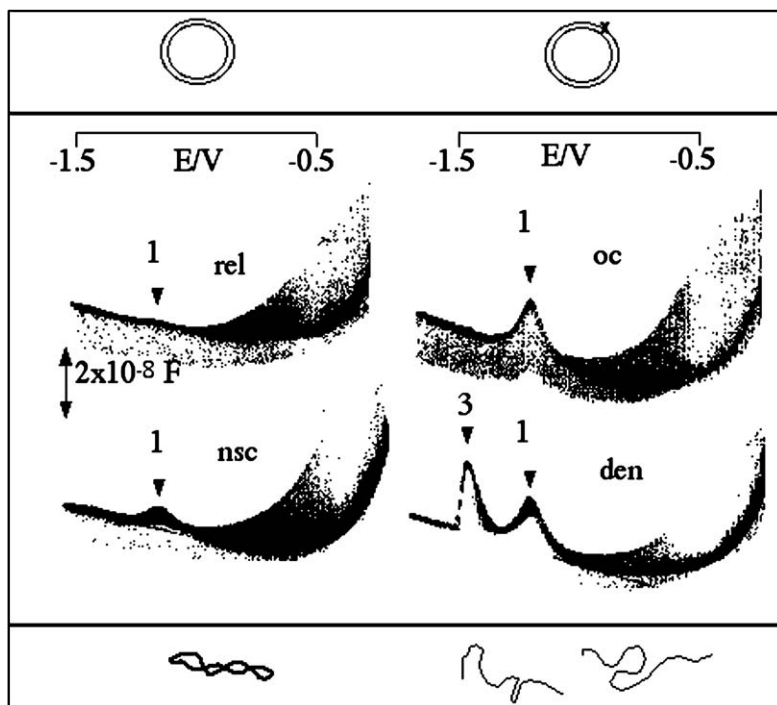


Fig. 14. A.c. polarograms (C–E curves with DME) of various forms of plasmid pUC19 DNA (indicated in the figure) measured in 0.3 M NaCl, 0.03 M NaHCO₃, pH 9.5. DNA concentration 200 μg/mL. Rel, relaxed DNA; oc, open circular DNA; nsc, supercoiled DNA at native supercoiled density; den, denatured linear DNA. Measurements were performed in 80–100 μL of solution on air. In contrast to the other a.c. impedance measurements, in this experiment the mercury electrode was immersed directly in the DNA solution during the measurements. Scan rate 1 mV/s, drop lifetime 10 s. SCE. Adapted from Fojta *et al.* (1998). Copyright 1998, with permission from American Chemical Society.

performed (Figure 14). Polarograms of scDNA at native $-\sigma$, relaxed (circular) dsDNA and linearized denatured ssDNA at DME qualitatively corresponded to the behavior of the same DNAs observed with DNA-modified HMDE (Figure 13). In contrast the behavior of open circular (oc) DNA at the DME (Figure 14B) greatly differed from that obtained with HMDE (Figure 13D). The most striking difference was the absence of peak 3 at the C–E curve obtained with DME (Figure 13B), which agreed with the earlier DPP studies (Vojtiskova *et al.*, 1981) not showing any peak III (characteristic for ssDNA) as well as with the structure of ocDNA in solution, which should be virtually free from ss regions. Presence of peak 3 on the C–E curve of ocDNA was explained by secondary opening of the dsDNA structure at the electrode surface (Section 5).

We may thus conclude that techniques working with small voltage excursions during the drop life time, such as a.c. and d.c. polarography (i.e. methods working with DME) are able to reflect changes in conformation of long DNA molecules in solution. In such a case secondary changes in the DNA structure at

the electrode can be neglected. If, however, techniques working with large voltage excursions during the drop lifetime or with a hanging mercury drop or solid electrodes are used, large changes in the DNA structure may take place at the electrode. This problem will be discussed in the next section.

5. CHANGES IN DNA CONFORMATION AT SURFACES

5.1. History

Investigations of the effect of the electric field on the conformation of DNA at the electrode surface started in the 1960s (Chapter 1). Already in 1961 the differential capacitance of ds (native) and ss (denatured) DNAs adsorbed at DME was measured in unbuffered solutions by Miller (1961a, b). He concluded that at positive potentials a partial unwinding of double-stranded DNA took place on the electrode, whereas at negative potentials DNA preserved its double-helical structure. In 1968, Flemming (1968) used a.c. voltammetry in combination with HMDE to study DNA. He did not confirm Miller's conclusion about the DNA surface unwinding and assumed that DNA preserved its double-helical structure over the whole range of potentials reached at HMDE under the given conditions. This assumption was defended for some time by Berg *et al.* (reviewed in Berg, 1976; Paleček, 1983).

It has been shown in the previous section that most of the electrochemical methods, and particularly the DPP, are well suited for studies of the DNA thermal denaturation and that this method showed good correlation with optical method reflecting the DNA structure in solution (Figures 3, 5, 9, 10, 12, 14). On the other hand, since the first attempts in 1966 (Paleček and Frary, 1966) to apply pulse polarography to the analysis of nucleic acids it was apparent that (NPP, working with DME) did not simply reflect the DNA structure in solution. The results of this technique poorly correlated with those of non-electrochemical methods and differed markedly from the results obtained by means of DPP. Only in 1974, NPP of DNA was studied in a greater detail (Paleček, 1974) and an explanation of the disagreement between the DPP and NPP results was offered (Paleček, 1974, 1983).

5.2. Effects of electrochemical methods and types of mercury electrodes

There are substantial differences in polarization of the DME in NPP and DPP (DPV). DPP works with small voltage excursions during the drop lifetime (Figure 15A). The time for which DNA was exposed to the electric field in DPP at the DME was relatively short (usually 1 s). The electrochemical signal thus reflected changes in DNA conformation, which occurred either (a) in solution or (b) at the electrode surface during the drop lifetime charged to the potentials at which the electrode process responsible for the measured signal took place. Eventual changes in DNA conformation occurring at more positive or more negative potentials did not affect the polarographic signals. Similar properties

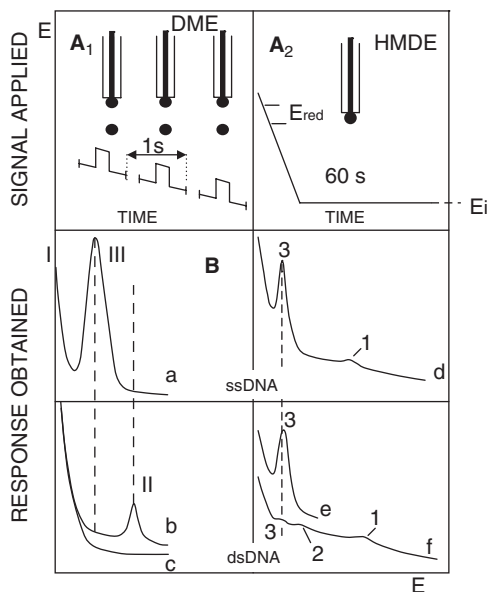


Fig. 15. A_1 , signals applied and responses obtained: in DPP with the DME (representing a technique working with small voltage excursion during the drop lifetime; A_2 , LSV with HMDE. (A_1): in DPP a single voltage pulse (usually of 10–50 mV) is applied to each drop of mercury dropping from the DME in 1 s intervals. The voltage ramp is scanned 1 mV/s. (A_2): in LSV, HMDE is kept for a certain time interval t at the initial potential E_i . During this waiting time t , DNA is adsorbed at the electrode and may undergo certain changes in its secondary structure due to its prolonged interaction with the electrode surface. After the waiting time t , the electrode potential is changed (usually 0.5–5 V/s) to more negative values (passing necessarily the region U); ssDNA is reduced at about -1.4 V (E_{red}). B, The height of the voltammetric peak 3 is proportional to the amount of ssDNA reduced at the electrode surface. If DNA is adsorbed at HMDE this peak can indicate the extent of surface denaturation of dsDNA. (a,d) ssDNA (b,c,e,f) dsDNA (in the bulk of solution); (b) dsDNA at higher concentrations (300–400 $\mu\text{g}/\text{mL}$) and a high sensitivity of the instrument; (c) dsDNA at a concentration as usual for measurements of ssDNA (20–30 $\mu\text{g}/\text{mL}$); (d, f) E_i in the region T (e.g. -0.6 V); (e) E_i in the region U (e.g. -1.2 V), for region U and T see [Figures 16c and 17](#). SCE. Reproduced from [Jelen and Palecek \(1985\)](#). Copyright 1985, with permission from the Slovak Academy of Sciences.

have also other techniques working with small potential excursions during the drop life time, such as a.c. and d.c. polarography (working with DME).

5.2.1. Methods working with large voltage excursions during the DME drop lifetime or with stationary electrodes

In contrast, NPP (which also uses DME) works with large voltage excursions during the drop lifetime ([Bond, 1980](#)), holding the electrode at the initial potential for a substantial part of the drop lifetime. With this method all changes in DNA conformation, which occurred at the initial potential and during the

potential scanning, could influence the resulting electrochemical signal (because the DNA whose conformation would be irreversibly disturbed at less negative potentials was still at the electrode surface when the reduction process took place); in other words the resulting polarogram was affected by the history of the experiment (potential scanning from the initial potential to the potential of the measured signal) even if DME was used. When working with stationary electrodes (such as HMDE) the resulting signal (regardless of the electrochemical technique) could also be affected by the history of the experiment, taking place at a single surface. In this arrangement, the scan rate and scan direction played important roles. Conformational changes occurring in DNA secondarily at the electrode surface could be, however, minimized by experimental conditions, such as high scan rates, direction of the potential scanning and choice of suitable initial potentials. On the other hand, stationary electrodes were well suited for studies of the effects of the electric field on the conformation of the nucleic acid anchored at the surface. In this respect, the DNA-modified electrodes particularly appeared useful, allowing separation of the DNA immobilization from the electrode processes, and providing data not complicated by the DNA diffusion (from the bulk of solution to the electrode) during the electrode processes.

5.3. Changes in DNA conformation at mercury surfaces as detected by conventional polarographic and voltammetric methods

The results so far obtained suggest that dsDNA can be unwound at certain potentials on the mercury and other electrode surfaces and that, in addition to the effect of potential scanning and type of the electrode, the DNA ionization and the solution conditions can play important roles (Section 5.3.2). For the first two decades studies of the changes in conformation of dsDNA were predominantly performed by means of conventional polarographic (using DME) and voltammetric methods (using HMDE), reviewed in [Berg \(1976\)](#) [Paleček \(1969b, 1971, 1976\)](#). Later solid electrodes and DNA-modified electrodes were applied. Most of the work was, however, done with conventional methods using the bare electrode immersed in the analyzed NA solution. These methods created a solid base for further studies of DNA structure and properties at the electrode surface. In this section, we shall first summarize the results obtained with conventional methods.

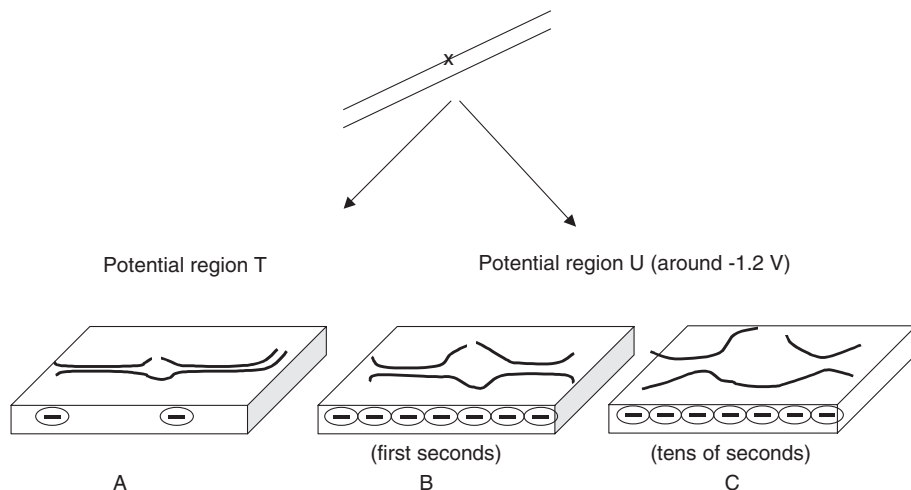
The acid–base behavior of nucleotides is one of their most important physical characteristic. It determines their charges, tautomeric structures as well as their abilities to donate or accept hydrogen bonds, which are the key features of the base recognition in DNA and RNA. In the range between pH 5 and 9 DNA is usually a polyanion carrying one negative charge per each nucleotide phosphate. Under these conditions bases and sugar residues are uncharged. At pH < 5 protonation of A, C and G residues should be considered while at pH > 9 deprotonation of G, T and U residues in DNA or RNA may take place. At substantially higher pHs ionization of deoxyribose (and ribose) may occur. Free bases have pK_{as} of 3.5 and 4.2 for N1 of adenine and N3 of cytosine, respectively, and 9.2 and 9.7 for N1 of guanine and N3 of thymine ([Moody](#)

et al., 2004; Saenger, 1984). These values shift from neutrality in a Watson–Crick base pair due to the stability conferred by base pairing (Narlikar and Herschlag, 1997). On the other hand, numerous folded state pK_{as} are perturbed toward neutrality for RNA and DNA, with values ranging from 3.8 to 6.6 (Huppler *et al.*, 2002). pK_{as} shifted toward neutrality can participate in RNA and DNA catalysis (Bevilacqua, 2003).

5.3.1. Conditions not involving ionization of DNA bases

The early data showed that the NPP and linear sweep voltammetry (LSV) signals, produced at neutral pH by native dsDNA, were strongly dependent on the initial potential (E_i) that is the potential to which the DME was charged for a certain time (about 1–2 s) before the application of the voltage rectangular pulse (in NPP) or the linear voltage sweep (in LSV) (Figure 15B). On the other hand, the signals yielded by denatured ssDNA were almost independent of E_i . With native dsDNA the highest signals were observed in a narrow potential range around -1.2 V (Unwinding region, U). In this range only peak III (NPP wave III) appeared, whose potential corresponded to the potential of the peak of ssDNA. As a result of interactions of dsDNA with the electrode charged to more positive E_i (region T), relatively small peaks II and III were observed; in the region U peak II (produced only by native dsDNA) decreased and disappeared. The changes in the electrochemical signals, resulting from the exposition of dsDNA immobilized at the electrode to the potentials of region U, were thus similar to those resulting from DNA denaturation in solution (exposed for example to elevated temperatures or strongly alkaline pHs (see Section 4.2.1.3) (Brabec and Palecek, 1976a; Palecek, 1974). The process involving dsDNA at the electrode surface charged to potentials of the region U were interpreted as due to opening of the DNA double helix at the electrode surface resulting in an increased accessibility of bases. It was assumed (Palecek, 1983, 1996 and references therein) that the opening of the dsDNA was due to a strong electrostatic repulsion of the negatively charged DNA phosphates from the electrode surface to which DNA was firmly adsorbed via hydrophobic bases. In linear dsDNA molecules, bases could be available for the interaction with electrode at the ends of the molecule, at single-strand breaks, at transiently opened DNA regions, etc. (Scheme 1).

5.3.1.1. Potential region U of DNA surface denaturation. It was shown that the potential of the region U corresponded to the potential of the tensammetric peak 1 of native dsDNA (Figure 3) suggesting the DNA surface denaturation in this region may be related to the DNA desorption (Brabec and Palecek, 1976a; Palecek, 1974). The characteristic changes in the region U (Figures 15f and 16c) were observed both under complete and incomplete surface coverage both at DME and HMDE (Brabec and Palecek, 1976a; Palecek, 1974; Palecek and Kwee, 1979). The extent of these changes depended on the salt or polyamine concentrations in solution (Brabec and Palecek, 1976a; Palecek and Kwee, 1979) and on the damage induced to DNA. To explain the DNA surface denaturation a rough



Scheme 1. Changes in DNA structure at the surface of the mercury electrode. (A) Adsorption of a dsDNA segment at the electrode surface at potentials close to the zero charge (region T) may result in limited opening of the DNA duplex in the vicinity of the end of the molecule and/or single-strand breaks (or other disturbances of the DNA structure). (B, C) At potentials around -1.2 V (region U) relatively slow opening of the DNA duplex is taking place manifested by the peak 3 (characteristic for ssDNA). Opening of chromosomal calf thymus (native) DNA at neutral pH takes about 90–120 s.

tentative scheme was put forward (Brabec and Paleček, 1976a; Paleček, 1974). It could be expected that in the vicinity of the potential of zero charge, segments of dsDNA were adsorbed via sugar–phosphate backbone (Section 3.1) as well as via sporadic bases located in the labile regions of the DNA double helix (Section 4.2.1.3). As the electrode potential was made more negative, DNA segments adsorbed mainly through the sugar–phosphate backbone could be desorbed. In contrast, the segments attached to the surface more strongly via bases remained adsorbed even at potentials of the region U. At these potentials a situation could arise where the DNA molecule was anchored on the surface by an ss segment S_{ads} (involving one end of the DNA strand), while the adjacent ds segments (not involving significant base adsorption) were strongly electrostatically repulsed from the negatively charged electrode, putting the DNA molecule under stress. Such stress might induce unwinding of the dsDNA segment. From the segment S_{ads} , the surface denaturation could proceed to further regions of the molecule. The unwound ss regions formed in the vicinity of the segment S_{ads} were readily adsorbed via bases and their adsorption stimulated the unwinding process further. Considering the length of the molecule of chromosomal DNA one would expect that the unwinding process took place mainly in the outer part of the double layer and in the bulk of solution.

DNA opening at the mercury electrode was relatively slow (in about 100 s about 90% of a chromosomal DNA was opened) and its rate increased with shifting of the potential (to which DNA was exposed at the electrode) to more negative values (Nurnberg and Valenta, 1976; Paleček, 1974). The process was

completed in a time ranging from tens of seconds to few minutes (Palecek and Kwee, 1979). The duplex opening was partially irreversible (Nurnberg and Valenta, 1976; Palecek, 1974) and depended on the DNA nucleotide sequence (Jelen and Palecek, 1985). With calf thymus DNA both AT and GC pairs were involved in the early stage of the opening process (Nurnberg and Valenta, 1976; Palecek, 1974). Irreversible opening of dsDNA in the potential region U imply that when the initial potential of HMDE is less negative than region U and the potential is scanned in negative direction (at usual scan rates) surface denaturation of dsDNA cannot be avoided. Flemming and Berg (1974) studied adsorption/desorption behavior of DNA at HMDE and observed peak 3 (Figure 3E) at a.c. voltammogram of dsDNA, if the potential was scanned in the negative direction, but they did not explain their results in terms of opening of the DNA structure (Berg, 1976; Flemming and Berg, 1974). Instead they offered a complicated mechanism (Berg, 1976), which was not confirmed (Section 5.5.1.1).

Opening of dsDNA at mercury electrodes at potentials of the region U was observed at ionic strengths between about 0.1 and 1.0. At very low ionic strengths dsDNA could be adsorbed on the negatively charged mercury electrode only very weakly (Brabec and Palecek, 1972; Nurnberg and Valenta, 1976; Palecek, 1974). Under these conditions, DNA interfacial behavior can be different because of strong repulsion between the polyanionic DNA molecule and the negatively charged mercury electrode. In 10 mM KClO_4 , where probably only electrostatic interactions were involved, no differences in the differential capacity of ss and sonicated dsDNA were observed (Hinnen *et al.*, 1981). Under conditions of moderate ionic strengths at potentials positive (region T) or negative (region W) to the region U (Figure 16C) no extensive surface changes in DNA conformation (comparable to those observed in region U) were detected (Palecek, 1983; Palecek and Kwee, 1979). The absence of DNA opening in region W was explained by inability of dsDNA to adsorb strongly at the mercury electrode charged to highly negative potentials.

The DNA opening at the electrode surface was probably not completely identical with the known DNA denaturation in solution. Considering the immobilization of the DNA molecule at the surface some special features and/or limitations of the opening process could be expected. For example, formation of partially unwound dsDNA, in which some bases were accessible for the interaction with electrode surface, or a "ladder DNA" might be compatible with the experimental data (Nurnberg and Valenta, 1977; Palecek, 1966, 1974, 1983, 1992a).

Voltammetric behavior of biosynthetic ds polydeoxynucleotides (a) with alternating nucleotide sequences, such as poly(dA-dT)·poly (dA-dT), poly(dA-dU)·poly(dA-dU), poly(dG-dC)·poly(dG-dC) and (b) homopolymer pairs poly(dA)·poly (dT), poly(rA)·poly (rU) and poly (dG)·poly (dC) (Jelen and Palecek, 1985; Palecek and Jelen, 1984) was studied using HMDE. Both types of ds duplexes showed distinguished regions U, but the interfacial behavior of these duplexes was strongly influenced by the nucleotide sequence. The behavior of polynucleotides with alternating sequences differed from that of homopolymer pairs (Figure 16A-C). Duplexes with alternating sequences displayed a very narrow half-width (<100 mV) region U and the rate of opening of the double helix strongly depended on the electrode potential within the

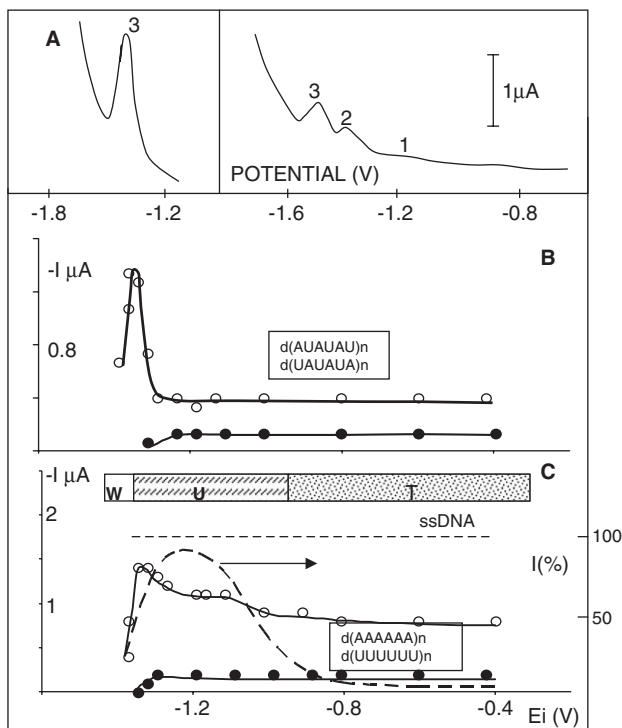


Fig. 16. Dependence of the voltammetric behavior of biosynthetic polynucleotides with different nucleotide sequences on the initial potential (E_i). (A): voltammetric peaks of poly (dA-dU) · poly (dA-dU). $E_i = -0.6$ V (left), $E_i = -1.35$ V (right); (B): ●—●, peak 2; ○—○, peak 3; (C): poly (rA) · poly (rU), ●—●, peak 2; ○—○, peak 3; ---, calf thymus DNA (data extracted from Paleček and Kwee (1979)), peak height expressed in percents of the height of peak of thermally denatured DNA. DNA at a concentration of $100 \mu\text{g/mL}$, concentration of other polynucleotides was 5×10^{-5} M (related to phosphorus content). Background electrolyte: 0.3 M ammonium formate with 0.05 M sodium phosphate (pH 6.9). HMDE, scan rate 0.5 V/s, waiting time 60 s. U is the potential region in which relatively slow opening of the DNA double helix occurs, involving an appreciable part of the molecule (provided the time of DNA interaction with the electrode is sufficiently long). T is the potential region where fast opening of the DNA double helix takes place; it is limited to several percents of the molecule in the vicinity of certain anomalies in the DNA primary structure (e.g. single-strand breaks). W is the potential region where no changes in the DNA conformation were detected. Potentials were measured against SCE. Reproduced from Jelen and Paleček (1985). Copyright 1985, with permission from the Slovak Academy of Sciences.

region U. In the homopolymer pairs, the width of region U was comparable to that of natural DNA (> 200 mV) but it was composed of two distinct phases (Figure 16C). Poly (dG) · poly (dC) produced no region U. The differences between the interfacial behavior of DNA duplexes with alternating sequences and homopolymer pairs were explained by non-equal adsorbabilities of purine and pyrimidine chains in the homopolymer pair molecule (resulting from the known different adsorbabilities of purine and pyrimidine bases) contrasting to

equal adsorbability of both chains in alternating sequence polynucleotide molecules (Figure 16B, C).

5.3.1.2. Potential region T. Interaction of dsDNA with the electrode surface charged to the potentials of the region T (Figure 16C) did not result in any sign of extensive surface denaturation (as in region U), even if the time of the DNA interaction with electrode surface was prolonged to minutes (Palecek and Kwee, 1979). A small peak 3 observed on LS voltammograms (Figure 16A) (Brabec and Palecek, 1976a) (independent of time of DNA interaction with the electrode) was indicative of a limited surface denaturation, which proceeded very quickly, affected only a small part of the adsorbed DNA molecule (probably the DNA strand ends) and stopped. Experimental results obtained with a large mercury pool electrode (Brabec and Palecek, 1978) agreed with this assumption. Peak 3 (in the region T) increased in γ -irradiated DNA containing a small number of ss breaks and other types of damage induced by ionizing radiation (Brabec and Palecek, 1976a). These results suggested that the conformational changes in DNA adsorbed at the electrode at potentials of the region T were due to increased accessibility of bases in the labilized regions of the DNA molecule, including its strand ends. Heights of peak 3 in DNA homopolymer pairs in the region T were higher than in corresponding alternating sequence duplexes. This peak produced by duplexes composed only of G \times C pairs was smaller than peak III of the A \times T and A \times U containing duplexes (Jelen and Palecek, 1985). This result suggests that the limited opening of dsDNA in the region T was affected by higher stability of the G \times C pairs in DNA.

It should be stressed that native dsDNA which did not produce any peak III on DP polarograms yielded this peak on LS voltammograms obtained either with DME or HMDE. The mechanism responsible for the peak III of dsDNA on LS voltammograms is not yet fully understood. The process might involve the initial step of the mechanism suggested for the surface denaturation in the region U. At potentials of region U the repulsion forces (which drove the DNA unwinding of the dsDNA segments next to the segment S_{ads}) between the electrode and the adsorbed DNA should be much stronger than at less negative potentials of the region T. Thus in the region T the DNA unwinding might be limited to the segment S_{ads} having no ability to continue in the neighboring segments as it is the case in the region U. Conformational changes in the region T might be due to direct effect of the electric field (Valenta *et al.*, 1974; Valenta and Nurnberg, 1974b), affecting the DNA structure of the DNA segment laying flatly on the electrode surface (Brabec *et al.*, 1983, 1996).

5.3.1.3. Effect of DNA cross-linking. Investigations of DNA adducts with platinum drugs such as monofunctional diethylenetriaminedichloroplatinum(II) (dien-Pt) and bifunctional trans- and cis-diamminedichloroplatinum(II) showed that the effects observed in region U were inhibited by interstrand crosslinks (produced by the bifunctional compounds) but not by other types of adducts formed in DNA by dien-Pt (Kasparova *et al.*, 1987; Zaludova *et al.*, 1997). This

finding was in a good agreement with the opening of dsDNA at the electrode surface. Such a DNA opening should be inhibited by formation of covalent bonds (cross-links) between the DNA strands limiting or preventing DNA unwinding (Paleček, 1991).

5.3.2. Conditions involving ionization of bases

5.3.2.1. Surface denaturation at alkaline pHs. At alkaline pHs DNA was not reducible at mercury electrodes (Section 4.2). On the other hand it produced capacitive (non-faradaic) peaks on LS voltammograms qualitatively similar to those observed at neutral pH (Figure 17B). DNA signals of a similar nature could be observed also by other methods such as a.c. and DP voltammetry (or polarography with DME) (Paleček, 1980c, 1983). The non-faradaic peaks of denatured DNA at alkaline pH were substantially lower than the faradaic ones (observed in 0.3 M ammonium formate, pH 6.9) (Figure 17). At pH 8.7 the heights of peaks 2 and 3 of native dsDNA changed in dependence on E_i (Figure 17B) in a similar way as at neutral pH (Figure 16C). Up to pH 10.8 the peak heights were practically independent on E_i in the region around the potential of the zero charge but at E_i more negative than -0.6 V they increased with increasing pH (Figure 17B). At pH 12 (where the beginning of DNA alkaline denaturation in the bulk of solution can be expected) the height of peak 3 at E_i around p.z.c. increased about 10-fold (compared to pH 9.8) and between E_i -0.2 and -0.9 V this peak was practically independent of E_i . The height of peak 3 at E_i of denatured ssDNA was independent of E_i in a wide range of potentials and pHs. The behavior of dsDNA in dependence on E_i in alkaline media was very similar to that observed at neutral pH (Figures 16C and 17B). It was therefore concluded that the mechanism responsible for the DNA surface denaturation at weakly alkaline pHs did not substantially differ from that at neutral pH. The effect of DNA protonation on surface denaturation of DNA will be discussed in the next paragraphs.

5.3.2.2. DNA surface denaturation at acid pH. Nurnberg and Valenta (1977) studied the electrochemical behavior at HMDE by means of LSV at weakly acid pH (mostly at pH 5.6). Independently but in parallel with Paleček's laboratory they detected in 1974 DNA unwinding at the electrode surface (Nurnberg and Valenta, 1976, 1977; Valenta and Grahmann, 1974; Valenta and Nurnberg, 1974a, b; Valenta *et al.*, 1974). At pH 5.6, they observed only small dependence of the LSV peak of dsDNA on E_i , without any well-distinguished regions U and T. Later it was shown (Brabec and Paleček, 1976b; Paleček and Jelen, 1980) that the presence of the distinct T and U regions were dependent on pH (Figure 17) as well as on the intactness of the dsDNA sample. With a relatively intact sample of calf thymus DNA, marked regions T and U were observed at pH 6.0 (Figure 17A). Decreasing the pH resulted in an increase of the electrochemical signal in the region T, without any significant signal change in region U. These changes were not in accord with protonation of DNA in solution suggesting

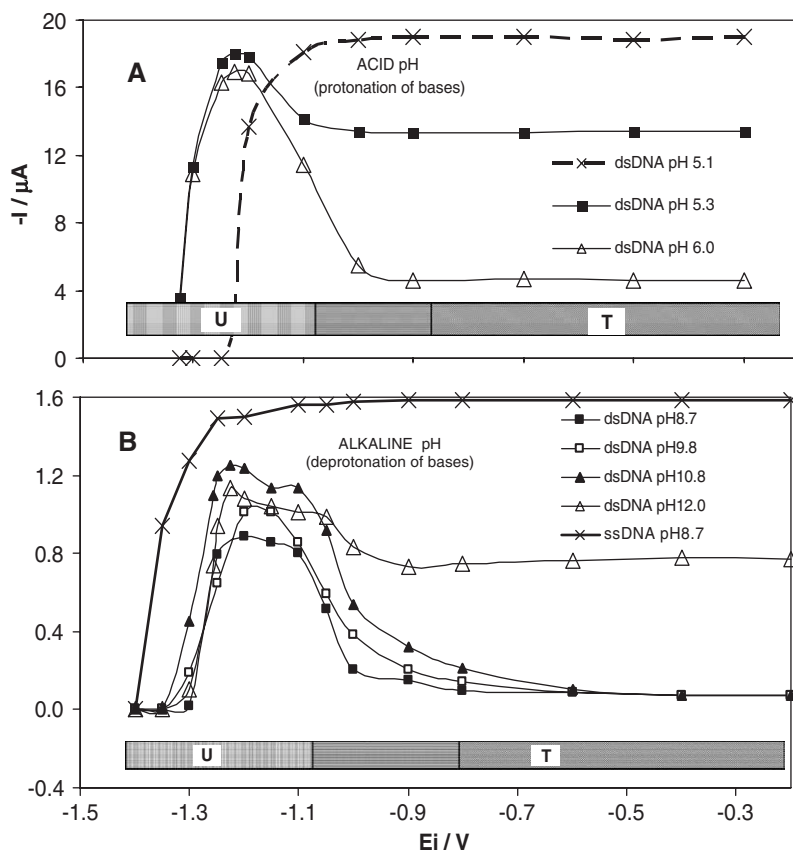


Fig. 17. Dependence of the height of the DNA voltammetric peak 3 on initial potential E_i (A) at acid pH's. dsDNA at concentration of $420\ \mu\text{g/mL}$: $\triangle-\triangle$, pH 6.0; $\blacksquare-\blacksquare$, pH 5.3; $x-x$, pH 5.1. The graphical indication of the region T and U is valid only for the curve of dsDNA at pH 6.0. (B) at alkaline pH's. dsDNA: $\blacksquare-\blacksquare$, pH 8.7; $\square-\square$, pH 9.8; $\blacktriangle-\blacktriangle$, pH 10.8; $\triangle-\triangle$, pH 12.0. ssDNA: $x-x$, pH 8.7. PAR 174, DME, LSV, scan rate 5 V/s, waiting time 60 s. Potentials were measured against SCE. Adapted from Brabec and Palecek (1976b) and Palecek (1983). Copyright 1976 and 1983, with permission from John Wiley and Sons Ltd.

that DNA protonation at the electrode surface might take place. At pH 5.1 no separate T and U regions were observed.

Based on their studies at acid pH's, Nurnberg *et al.* (Malfoy *et al.*, 1976; Valenta and Nurnberg, 1974b) concluded that the DNA unwinding was due to the effect of the electric field on the DNA adsorbed at the electrode surface and suggested a detailed mechanism of DNA surface deconformation. This mechanism (which might be efficient at pH's below pH 6) did not, however, explain the existence of the regions T and U observed at neutral and alkaline pH's (Figures 16C and 17B). We therefore preferred the tentative mechanism suggested for neutral pH (Section 5.3.1) and considered the mechanism operating at acid pH's as a special variant of the mechanism acting at neutral pH. At

pH < 5 protonation of adenine, cytosine and guanine residues in solution (Izatt *et al.*, 1971) gained importance (Section 5.3) decreasing the thermal stability of the dsDNA structure. DNA protonation could be facilitated at the electrode surface and adsorbed DNA could accept proton even at pH > 5 (Sections 4.2 and 5.3). In partially protonated DNA adsorbed on the electrode at potentials of the region T via the destabilized regions, further protonation and destabilization might take place on the surface in a close neighborhood of the adsorbed DNA segments. Such destabilization could provide further distorted DNA regions with bases available for their adsorption and electron transfer processes on the electrode. Compared to the DNA surface denaturation in the region U at neutral pH, which was relatively slow (Paleček, 1992a), changes in DNA structure at acid pHs were faster resembling the behavior of damaged DNA in the region T at neutral pH.

5.4. Carbon electrodes

It was reported that voltammetric signals of dsDNA (due to oxidation of guanine and adenine residues) at graphite electrodes were increased as a result of exposing the electrode to sufficiently negative potentials (between -0.4 and -0.8 V) prior to potential scanning (Brabec *et al.*, 1996). These signals depended on the DNA base content, showing higher signals in AT-rich DNAs. It was concluded that dsDNA was unwound at the negatively charged graphite surface. More work with carbon electrodes will be necessary to understand this phenomenon better.

5.5. Changes in DNA structure at DNA-modified electrodes

The above results were obtained by conventional polarographic (using DME) or voltammetric (using HMDE or carbon electrode) methods, i.e. with the electrode immersed into the DNA solution during the measurements. In 1986, we introduced a different arrangement in which DNA was first attached to HMDE, the DNA-modified mercury electrode was washed and immersed in an empty background electrolyte to perform the electrochemical measurements (Paleček and Postbieglova, 1986). We then used the DNA-modified electrodes to study the effect of electrode potential on the DNA structure at the electrode surface (Paleček and Fojta, 2001; Paleček *et al.*, 1993; Teijeiro *et al.*, 1993).

Earlier H. Berg and J. Flemming offered a complex model of the DNA interaction with the mercury electrodes (reviewed in Berg, 1976). This model was based on an assumption that in the region U (where the DNA molecules were supposed to be oriented perpendicularly to the electrode surface) the DNA surface concentration was higher than in the region T (where the DNA molecules were expected to lay flatly at the surface). After introducing the DNA-modified HMDE, we saw a chance to test directly the Berg's model by investigating the behavior of the immobilized DNA immersed in a blank background electrolyte.

5.5.1. Mercury electrodes

5.5.1.1. Linear DNA molecules. In experiments with the DNA-modified electrodes, dsDNA was immobilized (by physical adsorption) at the HMDE at potential $E_a -0.1$ V (i.e. in the region T, at the potential more positive than the p.z.c.). The electrode was then washed and transferred to the background electrolyte not containing any DNA, followed by exposure to potentials E_{bx} (varying from -0.1 to -1.55 V) for 100 s prior the CV measurements (Palecek, 1992a). We observed a distinct region U, showing a steep increase in peaks CA and G, similar to that obtained earlier with HMDE immersed in a DNA solution during the measurements (Section 5.3). With the DNA-modified HMDE immersed in the empty electrolyte, the amount of DNA attached to the electrode surface could not increase (because there was no DNA in the bulk of solution to diffuse to the electrode and to reoccupy the empty surface resulting from reorientation of the DNA molecules). If in this system, the flatly oriented DNA molecules orient themselves perpendicularly to the electrode (as assumed by Berg, 1976), a decrease of the DNA surface concentration should be expected because most of their parts would extend to the bulk of solution, outside the electrode double layer, without producing any electrochemical response. We may thus conclude that the results obtained with the DNA-modified electrode (Palecek, 1992a) were in agreement with conception of the DNA surface denaturation (Section 5.3) and unambiguously excluded the alternative explanation offered by Berg and Flemming (reviewed in Berg, 1976).

Experiments with the DNA-modified electrodes brought also other important information about the behavior of DNA at the electrode surface. For example, signals of dsDNA (but not of ssDNA) displayed typical premelting changes when dsDNA was attached to HMDE at different temperatures and voltammetric measurements were performed (after the medium exchange) at room temperature (Palecek, 1988b); this was surprising because DNA premelting was reversible in solution (as observed with DME) (Palecek, 1976). If dsDNA was placed in a denaturing medium (e.g. 0.2 M NaOH) and adsorbed at the mercury electrode, no sign of the DNA renaturation was observed after transfer of the DNA-modified electrode to a non-denaturing medium (Fojta, 2004; Palecek, 1988b). Also composition of the medium from which DNA was adsorbed affected the signals at neutral pH in an usual empty background electrolyte (Jelen and Palecek, 1985; Palecek, 1988a; Palecek *et al.*, 1993). A.c. voltammetry of DNA complexes with intercalators (Fojta, 2004; Fojta *et al.*, 2000; Palecek, 1980a) suggested that changes in DNA conformation (induced by the intercalator) may be conserved after the intercalator removal from the electrode surface. All these data suggested that DNA might keep its conformation (attained at the surface after its adsorption at the electrode) even after changing the experimental conditions (e.g. placing the electrode with the DNA layer into different media). Thus the observed irreversibility of the opening of dsDNA in the region U (Palecek, 1974) was in agreement with the finding that the electrode tends to fix DNA in the spatial arrangement in which the molecule was adsorbed at the electrode surface (Jelen and Palecek, 1985; Palecek, 1988a; Palecek *et al.*, 1993).

5.5.1.2. Open- and closed-circular DNAs. Among the circular DNAs (Section 4.2.1.3) sc plasmid DNAs represent the most frequently used forms of closed duplex (cd) DNA (or covalently closed-circular DNA). Plasmid DNAs of different m.w. can be obtained but usually DNAs containing about 3000 base pairs are used. cdDNAs do not contain any molecular ends and strand interruption and their extensive unwinding in solution (under the conditions inducing denaturation of linear DNA) is prevented for topological reasons (Bates and Maxwell, 1993; Fojta *et al.*, 2000). Introduction of a single break into the phosphodiesteric backbone of the cdDNA molecule results in formation of an open-circular (oc) DNA molecule.

Exposure of the scDNA to the potentials of the region U at the HMDE surface resulted in no detectable DNA opening as indicated by absence of faradaic (Teijeiro *et al.*, 1993) or capacitive (Fojta and Paleček, 1997) signals characteristic for ssDNA. This finding was in agreement with the limitations in the duplex unwinding of these DNA molecules (Bates and Maxwell, 1993; Fojta and Paleček, 1997). A.c. impedance C–E curves of scDNA as well as relaxed DNA (covalently closed DNA circle, free of supercoiling, in which unwinding in solution is also prevented) produced no a.c. impedance peak 3 (Figure 13A, B). If in scDNA, a single-strand interruption was introduced (e.g. by γ -irradiation or enzymatically, using DNase I) the resulting ocDNA molecule produced a.c. impedance peak 3 (Figure 13D), suggesting that a substantial portion of bases in the molecule were able to interact with the HMDE surface. On the other hand, if instead of HMDE the dropping mercury electrode was used, no peak 3 was produced by the same ocDNA (Figure 14) suggesting absence of an appreciable amount of bases capable to interact with the electrode. In contrast to ocDNA, the results of measurements with DME and HMDE of either scDNA or of denatured DNA did not qualitatively differ. Absence of peak 3 on the C–E curves of ocDNA obtained with DME was in agreement with solution structure of ocDNA, in which almost all bases should be included in an intact B-DNA structure and not accessible for interactions with the environment. In difference to relaxed and scDNAs unwinding of ocDNA is not topologically restrained and ocDNA can be denatured under conditions sufficient for denaturation of linear DNAs. We may thus conclude there is a good qualitative agreement between the measurements with DME and HMDE of the DNAs (a) in which bases are accessible for the interaction with the environment, such as in ssDNA or (b) bases are hidden in the interior of the DNA duplexes but unwinding is prevented by the DNA topology, such as in relaxed and scDNAs (Figures 13A, B and 14). On the other hand in the DNAs, in which bases are hidden in the interior, but DNA unwinding in solution is not prevented, large differences in their electrochemical behavior at DME and HMDE can be observed (Figures 13D and 14). These differences can be explained by unwinding of the latter DNAs at the surface of HMDE (at potentials of region U) but not at DME. At DME the DNA is adsorbed again and again at newly formed mercury drops (Figure 15A). The DNA which is adsorbed at DME charged to potentials of peak 3 cannot be denatured at the mercury drops whose potentials are within the region W and out of region U (Figure 14).

A detailed investigation by means of CV showed small but significant changes in the height of guanine anodic peak (I_G) of scDNA exposed to the potentials of region U (Figure 18B). These changes were time dependent but slower than those yielded by the linearized DNA. Under the same conditions, the cathodic peak CA (characteristic for ssDNAs) was absent in the scDNA (Figure 18A). It was concluded that little or no base pair opening occurred in scDNA as a result of its prolonged interaction with the electrode surface. On the other hand, the increase of I_G in the region U (Figure 18B) suggested that some process, differing from DNA denaturation, was taking place at the electrode. This process strikingly differed from the alkaline denaturation of scDNA and thermal denaturation of linear DNA (Section 4.2.1.3), which were accompanied by parallel changes in peaks G and CA. The observed increase in peak G not accompanied by the appearance of peak CA might be due to changes in orientation of the scDNA molecules at the surface and/or to changes in DNA conformation not involving significant base pair opening. Further work will be necessary to elucidate the behavior of scDNA at the electrode surface.

Compared to chromosomal DNA, where the signals indicating the DNA unwinding in the region U reached up to about 90% of the intensity of the signal of the denatured DNA (Figure 16C), the extent of the unwinding of linearized plasmid DNA was much smaller (Palecek and Fojta, 2001; Palecek *et al.*, 1993; Teijeiro *et al.*, 1993). This was probably due to the absence of single-strand breaks in the linearized plasmid DNA. Chromosomal DNA molecules contain usually a large number of strand breaks which are the source of bases accessible for the interaction with the electrode surface (producing reduction signals in the region T) and from which the DNA unwinding in the region U can start. In contrast to the linearized plasmid DNA and chromosomal DNAs (Figures 16C and 18A) used in earlier studies, the scDNA produced no peak CA due to its contact with the electrode charged to potentials of the region T (Figure 18A), suggesting that the DNA molecular ends are important for the appearance of this peak.

The above data suggested that HMDE and particularly the DNA-modified HMDE are useful tools in studies of the interfacial properties of DNA, including changes in DNA conformation at the electrode surface. On the other hand, mercury electrodes and especially the DME can be used also to study changes in DNA conformation in solution. For this purpose, polarographic methods working with small voltage excursions during the DME drop lifetime are suited best (Section 4.2.1.3). If HMDE is used, the surface changes in the DNA structure can be minimized by choosing proper conditions, including fast voltage scanning.

5.5.2. DNA-modified platinum and gold electrodes

It was shown by M. J. Heller's team (Sosnowski *et al.*, 1997) that electric fields can be used to regulate hybridization and denaturation of ODNs immobilized on Pt-electrodes. A streptavidin-containing agarose permeation layer was applied over the electrodes in the low-density (25 electrodes) microchip array. This layer (i) served as a matrix for attachment of biotinylated ODNs, (ii) for permitting ion flow and distancing the ODN from potentially damaging

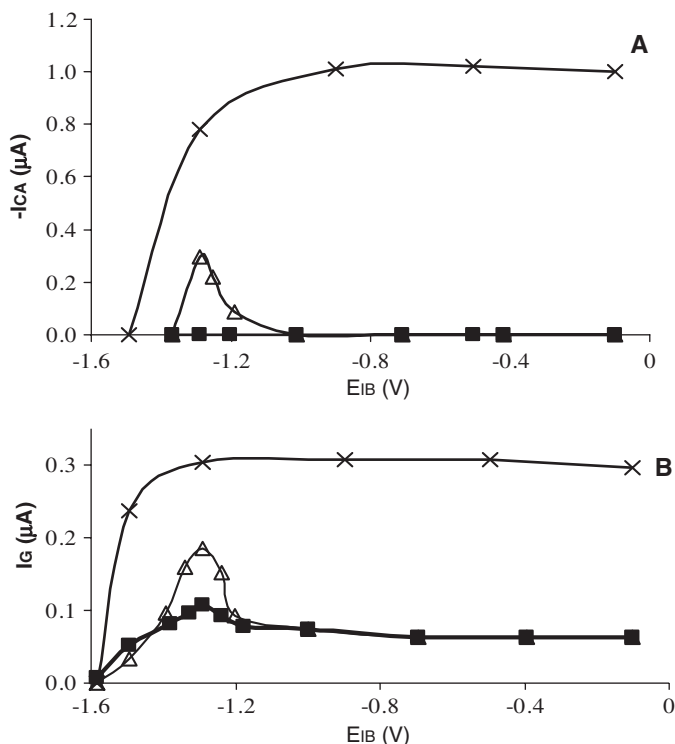


Fig. 18. Dependence of the height of the AdTS CV peaks (A), CA (I_{CA}) and (B), G (I_G) of ■, supercoiled, Δ , linearized double-stranded and x, denatured (linearized) DNA on the initial potential (E_{iB}). DNA at a concentration of $28 \mu\text{g/mL}$ in 0.3 M ammonium formate, 50 mM sodium phosphate, $\text{pH } 6.9$ was adsorbed at HMDE for t_A 4 min from a $4 \mu\text{L}$ drop of a DNA solution (at an open current circuit). The electrode was then washed and transferred into a voltammetric cell with 5 mL of the background electrolyte where it was charged to the potential E_{iB} (indicated in the graph) for the time $t_B = 100 \text{ s}$ followed by CV measurements. Potentials were measured against SCE. Adapted from Teijeiro *et al.* (1993). Copyright 1993, with permission from Adenine Press.

electrochemical reactions which may take place on the electrode. Bodipy Texas red was used as a fluorescent label of ODNs and changes in fluorescence were measured to indicate the DNA hybridization or denaturation at the electrodes. Positively biased electrodes were capable of significantly accelerating the DNA hybridization; at least 25-fold acceleration was observed as compared to neutral (open-current circuit) test sites. Application of negative potentials resulted in DNA denaturation. Using the controlled electric fields it was possible to efficiently and rapidly discriminate single-base pair mismatches. The observed acceleration of the hybridization or induction of DNA denaturation and the single-base mismatch discrimination could hardly be explained by a pure electric field effect because DNA in the permeation layer was too far from the electrode surface. Under the given conditions, the electric field strength was estimated to be too low (around 300 V/m) to cause the above observations.

Reduction of hybrid duplex stability by local pH changes combined with an electric field effect was considered as a more plausible explanation.

Optical surface plasmon resonance (SPR) spectroscopy was used by Georgiadis and coworkers (Heaton *et al.*, 2001) to monitor hybridization kinetics for monolayer DNA films on gold in the presence of an applied electrostatic field. The d.c. field denatured surface-immobilized DNA duplexes or enhanced hybridization of DNA. Discrimination between matched and mismatched hybrids was achieved by proper adjustment of the electrode potential. The monolayer films of thiolated ODNs were tethered directly to the SPR gold sensor surface through an Au–thiol attachment. The attractive d.c. field (+300 mV) was used, in a reversible manner, to increase the rate of ODN hybridization. Application of the repulsive potential (−300 mV) to two-base-mismatched hybrids resulted in rapid denaturation of most of the immobilized duplexes (about 75%) within a few minutes (Figure 19), whereas in fully complementary duplex DNA little loss of ssDNA was detected

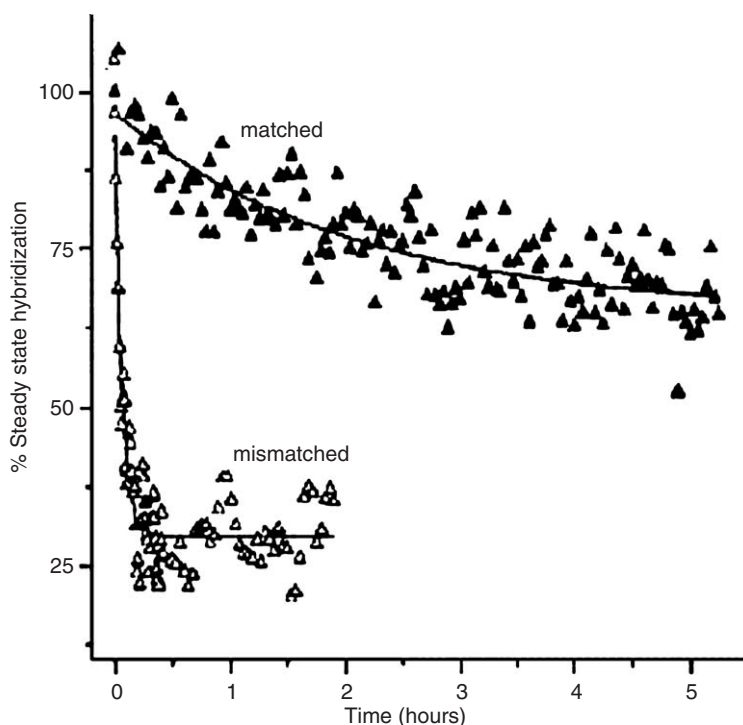


Fig. 19. Discrimination between the fully complementary hybrid (closed triangles) and 2-bp mismatched hybrid (open triangles) by electric field-induced denaturation on the same surface. After passive hybridization for 14 h, a d.c. electrochemical potential of 300 mV vs. Ag/AgCl was applied and the percent hybridization monitored as loss of ssDNA from the interface by *in situ* SPR. The same discrimination is also observed for hybrids formed by electrostatically assisted hybridization. Experimental conditions were 1 M NaCl solution containing 1 μ M ODN target. Data were obtained by using the same regenerated probe surface. Adapted from Heaton *et al.* (2001). Copyright 2001, with permission from the National Academy of Sciences.

even after many hours of exposure to the d.c. field. In contrast to the DNA denaturation reported by Heller's group (Sosnowski *et al.*, 1997), the monolayer DNA thiol films used in this work were attached directly to the gold surface. Therefore, the immobilized DNA was exposed to a field gradient at the interface of the order of 10^9 V/m close to the d.c. field strength affecting DNA adsorbed at mercury electrode surfaces.

5.5.3. Other methods and surfaces

Opening of the DNA double helix at the surface was observed also by atomic force microscopy (AFM). dsDNA molecule attached to an AFM tip and a gold surface was overstretched, and the mechanical stability of the DNA double helix was tested. Stretching experiments with single DNA molecules showed a highly cooperative transition, where the natural B-DNA was converted into a new overstretched conformation called S-DNA (Clausen-Schaumann *et al.*, 2000). The B-S transition at 65 piconewtons (pN) in λ -phage DNA was followed by a second conformational transition at 150 pN, during which the DNA duplex melted into two single strands. Upon relaxation, the two single strands recombined to the dsDNA conformation. Both the B-S and the melting transitions took place at significantly higher forces in poly(dG-dC) compared to poly(dA-dT) (Bensimon *et al.*, 1995). Belotserkovskii and Johnston reported low levels of DNA denaturation at room temperature in the presence of certain types of polypropylene tube surfaces (Belotserkovskii and Johnston, 1996, 1997). If DNA fragments contained $(GT)_n \cdot (CA)_n$ or $(GA)_n \cdot (CT)_n$ sequences, multimeric complexes were formed. This surface activity was inhibited by addition of micromolar concentrations of an ODN prior to adding dsDNA. It was unclear what might attract DNA to the polypropylene surface. Electrostatic considerations predict that DNA in water solution should be repelled from an object with a low dielectric constant such as a polypropylene tube wall. Belotserkovskii and Johnston suggested that such a repulsion could be overcome by hydrophobic interactions between the polypropylene surface and the bases of denatured ssDNA (Belotserkovskii and Johnston, 1997). The reaction was not observed in tubes made of borosilicate glass. It was shown that dsDNA adsorbed on phospholipid membranes adopted an altered conformation interpreted as DNA denaturation (Budker *et al.*, 1980).

5.6. Concluding remarks

The above results show that DNA denaturation results from the DNA interaction with some electrodes and other surfaces. It has been known for decades in many DNA laboratories that partial DNA denaturation can occur upon drying of DNA after ethanol precipitation. Almost 20 years ago, it was shown that such denaturation of DNA fragments might involve intrastrand hairpin formation producing misleading interpretations of the mobility shift assays (Svaren *et al.*, 1987). If few bases are released from the DNA duplex and adsorb at the hydrophobic surface, the adsorption may cause local dehydration and

denaturation of a short segment of dsDNA in a close neighborhood of the adsorbed bases. This denaturation may be facilitated by high AT content in the DNA segment or other factors decreasing the stability of the dsDNA structure. Such limited DNA denaturation may thus take place even in the absence of a strong electric field as reported in Refs. (Belotserkovskii and Johnston, 1997; Sosnowski *et al.*, 1997). If sufficiently strong repulsive electric field acts on dsDNA firmly anchored at the surface, the repulsive forces (eventually combined with the DNA dehydration) may distort or denature the DNA double-helical structure (Section 5.3). These intuitive conclusions are buttressed by recent theoretical studies (Vainrub and Pettitt, 2000), which show that the melting temperature of an 8-mer ODN is significantly decreased by the repulsive negatively charged surface while the positively charged surface increases the stability of the duplex. These effects depend on the distance of DNA from the surface and on the ionic strength. At low ionic strength, such as 0.01 M NaCl, electrostatic effects are stronger because of the longer Debye screening length. At low ionic strengths the attractive surface may increase the DNA melting temperature to such an extent that DNA, which would not be able to hybridize in solution, still hybridizes at the positively charged surface. Such situation can arise with DNA covalently attached (chemisorbed) to the surface. If, however, DNA is physically attached to the surface, the ionic strength may affect not only the stability of the DNA duplex but also the groups involved in the DNA adsorption and the adsorption strength.

The structure of DNA partially denatured at the surface is not fully understood. It can be expected that the DNA spatial arrangement of such DNA will differ from that of ssDNA in solution and depend on the nature and charge of the surface as well as on ionic conditions close to the surface. Combination of electrochemical and optical methods as well as scanning force microscopy and other methods will be necessary to understand better the spatial arrangement and behavior of DNA at electrically charged surfaces.

The ability of surfaces to stimulate DNA renaturation/hybridization or DNA denaturation/unwinding depending on the surface charge is important for the development of modern DNA biotechnologies, including DNA chips. In addition to this DNA ability may also be biologically relevant because in cells DNA interacts with a number of electrically charged surfaces and biomacromolecules. Interactions of DNA with cell walls and particularly DNA interaction in chromatin, which depends on histone chemical modification such as acetylation and phosphorylation (Zlatanova and Leuba, 2004) represent only some of possible examples.

6. ELECTROCHEMICAL PRINCIPLES IN NA BIOSENSORS

A biosensor usually consists of a selective biological recognition element associated with a transducer, which translates the recognition event into a physically measurable value. In DNA hybridization sensors the recognition element is usually the ssDNA with a defined nucleotide sequence, usually denoted as a probe DNA. This DNA sequence is challenged with another ssDNA

(Chapters 4 and 5) in solution, whose sequence is tested (target DNA, tDNA). If the sequence is complementary³ to the DNA probe sequence the hybrid dsDNA (double-helical, duplex DNA) is formed. Electrochemical detection of the DNA hybridization event is one of the crucial steps of the nucleotide sequence determination in the DNA hybridization sensor. Development of the electrochemical DNA hybridization sensors is a booming field covered in this book by an overview (Chapter 4) and by several other chapters concerning specific modern technologies based on nanoparticles (Chapters 5 and 11), conductive polymers (Chapters 8 and 9), etc. used in DNA sensors. Here we wish to deal with some electrochemical principles, which may be important in further research and development of the DNA sensors.

6.1. DNA hybridization and detection at the same surface

For almost one decade of the development of the electrochemical DNA hybridization sensors two important steps, that is the DNA hybridization and electrochemical detection, were performed at a single surface, the detection electrode (DE). Some methods of the detection of the DNA duplex formation at DE are shown in Figure 20. Such arrangement was simple and convenient but it had some disadvantages, which, in some cases, limited the biosensor performance. Among the tools for the detection of the DNA hybridization event (DNA duplex formation) redox indicators preferentially binding to dsDNA (Figure 20), such as intercalators and groove binders (Paleček *et al.*, 2002b) were perhaps most favored. At present, such indicators are less favored but their usefulness is still investigated (Del Pozo *et al.*, 2005; de-los-Santos-Alvarez *et al.*, 2005; Jin *et al.*, 2004; Kerman *et al.*, 2004). Among the intercalators bis-intercalators (Jelen *et al.*, 2000a, 2002a) and threading intercalators (Sato *et al.*, 2004; Takenaka *et al.*, 2000) showing the highest preference for dsDNA appear useful in DNA sensors (Section 10). In 2002 a new technique was proposed (Jelen *et al.*, 2002b; Paleček *et al.*, 2002a, d; Wang *et al.*, 2002b), in which the DNA hybridization was performed at one surface and the detection of the DNA hybridization at another surface; this technique was denominated as double-surface technique (DST). We shall deal first with the more common single-surface arrangement and return to DST in Section 6.2. Following paragraphs will focus on some steps important for recognition of the complementary DNA nucleotide sequence: (a) Immobilization of the (capture) probe DNA serving for capture and recognition of tDNA, (b) blocking and interfacing of the electrode surface, (c) efficiency of DNA hybridization at surfaces and (d) formation of the self-assembled monolayers of thiolated ODNs at metal electrodes. In these steps, an important role is played by a number of factors, including the material of the electrode, the method of DNA immobilization at the surface, the density of the probe DNA layer etc.

³The ability of DNA to reform its double-helical structure from the separated single strands, i.e. DNA renaturation and hybridization, was discovered about 40 years ago by J. Marmur and P. Doty while working at Harvard (Marmur, J. and D. Lane, 1960; Marmur, J., R. Rownd and C.L. Schildkraut, 1963). E. Paleček was a postdoc to J. Marmur in 1962–1963.

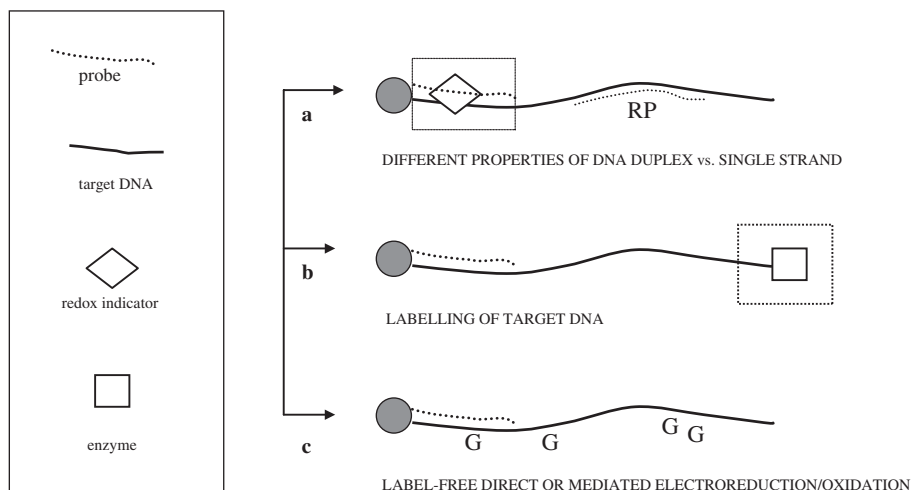


Fig. 20. Scheme of DNA hybridization and electrochemical detection at a single (electrode) surface; various ways of detection. Probe DNA (usually 15- to 20-mer ssODN) is immobilized at the electrode surface and hybridized with a target DNA in solution. On interaction of the probe with the complementary target DNA a DNA duplex is formed. (a) Formation of the duplex at the electrode surface is manifested either (i) by changes in the properties (a.c. impedance, conductivity, etc.) of the DNA duplex vs. ssDNA, or (ii) by a redox indicator binding preferentially to the DNA duplex, (iii) by a reporter probe (RP) which is end-labeled by an electroactive marker; RP should be complementary to a DNA sequence near to the duplex (located close to the electrode surface). (b,c) Presence of target DNA is detected at the electrode surface. (b) With end-labeled DNA, by the signal of an electroactive marker or (c) with unlabeled DNA, using the signal due to electroactivity of DNA (usually guanine oxidation is measured) (see Chapter 5 for other methods aimed at an amplified DNA electrochemistry, including DNA synthesis at the electrode surface. Adapted from Palecek *et al.* (2002d). Copyright 2002, with permission from Elsevier.

6.1.1. Immobilization of DNA at electrode surfaces

In DNA hybridization sensors the probe DNA (with the known nucleotide sequence) is usually immobilized at the surface to challenge the target DNA (with the unknown sequence) in solution (see also Chapter 11). In principle, an opposite arrangement, i.e. immobilization of target DNA at a surface followed by hybridization with the labeled probe DNA, is also possible. Such approach has been, however, rarely applied (Azek *et al.*, 2000; Bagel *et al.*, 2000). Its use in combination with small electrodes in single-surface technique (SST) may cause some difficulties (e.g. covalent immobilization of target DNA is difficult, with longer target DNAs the density of hybridized duplex DNA segments/mm² of the electrode area can be low). This approach may, however, be convenient in combination with the DST, in which a large surface for DNA hybridization can be used. Further we shall consider only the immobilization of the relatively short probe DNA at the electrode surfaces, commonly used in SST.

Probe DNAs (usually short 20–30-mer ODNs) were immobilized to the electrode surface using either covalent or non-covalent binding. *Adsorption* served

well for binding DNA to carbon electrodes (Mascini *et al.*, 2001; Paleček *et al.*, 1998; Popovich and Thorp, 2002; Wang *et al.*, 1997f). Electrostatic binding of DNA to the positively charged carbon electrodes via the DNA sugar–phosphate backbone (carrying the negative charge) was sufficiently strong and did not make bases inaccessible for the hybridization with target DNA. On the other hand, adsorption of unmodified ssDNA to the mercury electrode, regardless of its charge, strongly decreased or eliminated the DNA hybridization (Cai *et al.*, 1997; Tomschik *et al.*, 1999) because of strong adsorption of the hydrophobic bases on the hydrophobic mercury surface.

Covalent binding of the DNA probe via its ends was preferred because it could be well controlled and the non-specific molecules weakly bound to the surface could be easily removed. Immobilization of DNA probes to different electrodes including gold and ITO was recently reviewed (Drummond *et al.*, 2003; Popovich and Thorp, 2002; Tarlov and Steel, 2003; Thorp, 1998, 2004). Carbodiimide or silane chemistries were used for covalent binding of DNA to carbon electrodes (Mikkelsen, 1996; Schülein *et al.*, 2002). Avidin (streptavidin)–biotin binding was applied to attach DNA to various surfaces (reviewed in Drummond *et al.*, 2003; Popovich and Thorp, 2002; Tarlov and Steel, 2003). This technique was used to immobilize biotinylated probe DNA also to carbon electrodes (Masarik *et al.*, 2003). ITO electrodes could be modified via phosphonate self-assembled monolayers (Armistead and Thorp, 2001) and silane overlayers (Eckhardt *et al.*, 2001). Carbon and gold surfaces were well suited as electrode materials in DNA sensors; with the latter electrode, covalent attachment of DNA was necessary. Various aspects of DNA immobilization on different surfaces and particularly at gold electrodes were recently summarized in a review by Tarlov and Steel (Tarlov and Steel, 2003). In Section 6.1.2.1 only a brief summary on DNA immobilization at gold electrodes will be given.

6.1.2. Blocking and interfacing the electrode (transducer) surface

With real DNA samples, non-specific interactions (involving non-complementary targets, overhangs of long target DNAs, various impurities in DNA samples, etc.) at the electrode surfaces could interfere with the hybridization signals. To prevent such non-specific interactions efficient interfacing between the DNA system and the electrode surface were elaborated. Thiols and conducting polymers were found suitable for this purpose.

Conducting polymers were either synthesized chemically (e.g. polyphenylenes) or electropolymerized as thin films onto an electrode (e.g. polythiophenes and polypyrroles). Experimentally obtained conductivities of conjugated polymers were several orders of magnitude lower than those of metals. They were, however, sufficiently high to be considered as molecular wires. Reversible redox processes in these polymers controlled by potential and cyclic voltammograms were used to provide electrochemical signatures of the studied polymers. Conducting polymers such as copolymer functionalized with osmium complex, polyazines, polyanilines, polypyrroles, or polythiophenes (Cosnier, 1999; Sadik, 1999; Wang *et al.*, 2001a), reviewed in Livache *et al.* (1998), were

applied for blocking and interfacing the transducer, and also for modulation of the DNA interactions at surfaces and for generating signals monitoring such interactions. More details are in Chapters 8 and 9.

Self-assembled monolayers (SAMs) result usually from adsorption of amphifunctional molecules possessing high affinity toward the surface. Perhaps the most investigated systems involve SAMs of alkanethiols (including both RSH and RSSR) on gold (Finklea, 2000). In the last decade, alkanethiol self-assembly methods were used to fabricate DNA-probe modified gold surfaces with known probe coverages exhibiting high efficiency of the DNA hybridization (Herne and Tarlov, 1997).

6.1.2.1. Self-assembled monolayers of thiolated ODNs on gold surfaces. Among a number of methods of DNA immobilization at surfaces, the well-known thiol-gold interaction has been used most frequently for this purpose (Tarlov and Steel, 2003) (Chapter 15). Thiol or disulfide end-labeled DNA probes were directly attached to gold via its -SH group forming a self-assembled monolayer. SAMs of thiolated DNAs resembled the self-assembly of alkanethiols studied in detail in recent years (Herne and Tarlov, 1997; Huang *et al.*, 2001; Levicky *et al.*, 1998; O'Brien *et al.*, 2000; Okahata *et al.*, 1992). After the DNA self-assembly taking usually 4–16 h, a second SAM was usually created using alkanethiol molecules to limit non-specific adsorption of other compounds and particularly of the non-complementary DNA or RNA [(Gooding *et al.*, 2003a) for a recent review on SAM]. Moreover, the alkanethiol SAM prevented interactions between the probe and gold surface, leaving probes in largely up-right position accessible for DNA hybridization. Films containing a thiol-derivatized ssDNA probe and a diluent thiol, mercaptohexanol, were prepared on the gold surface (Peterlinz and Georgiadis, 1997). The thickness and dielectric constant of the film were determined by two-color surface plasmon resonance, and the DNA amount tethered to the surface was quantified. Measurements of the kinetics of hybridization and thermally induced dehybridization indicated a high efficiency of the hybridization process.

Efficiency of DNA hybridization and stability of DNA at surfaces. Various factors may influence the hybridization efficiency. The probe should be sufficiently long to secure the binding specificity in the presence of a large number of non-specific sequences. On the other hand, too long probe may be less favorable for the DNA hybridization. Steel and coworkers showed (Steel *et al.*, 2000) that the random-coil nature of DNA probes directly influenced the probe packing density. Surface packing density increased with the probe length up to 24 bases and decreased in probes containing 30 or more bases. It was assumed that the probes, whose length did not exceed 24 bases, had highly extended configuration, while in longer probes a more random-coil configuration was expected.

Presence of a spacer (linker) between the ODN probe and the surface could increase the hybridization yields up to two orders of magnitude. The length, charge and hydrophobicity of the linker played a critical role in the DNA hybridization (Chrisney *et al.*, 1996; Gray *et al.*, 1997; Maskos and Southern, 1992,

1993; Mir and Southern, 2000; Shchepinov *et al.*, 1997). Among these properties the spacer length appeared the most important in affecting the DNA hybridization (Shchepinov *et al.*, 1997). At polypropylene surfaces an optimal spacer length corresponded to 40 atoms. On the other hand with DNA probes linked to gold almost 100% hybridization was obtained with a six-methylene linker (Levicky *et al.*, 1998; Steel *et al.*, 1998). The reason for the above discrepancy was not clear; different substrates and the ODN coupling chemistry might play some role. Experimentally determined values for optimal probe coverage were in the range of 10^{12} – 10^{13} DNA probes/cm² while packing density of the *n*-alkanethiol SAMs on gold was about 5×10^{14} /cm², i.e., by almost two orders of magnitude higher than DNA probe density (Poirier, 1997). Thermal stability of thiol-attached DNA probes was limited to 75°C (Tarlov and Steel, 2003).

Temperatures of melting of the DNA duplexes (covalently bound via organosilane chemistry to fused silica optical fibers) were influenced by the surface density of the immobilized DNA. At the highest surface density (about 5×10^{12} probes/cm²) the lowest duplex stability was observed (Punno *et al.*, 1999; Tarlov and Steel, 2003; Watterson *et al.*, 2000).

Electrochemical technique for direct measurement of the melting temperature (T_m) of DNA attached to gold via an alkanethiol linker was proposed (Meunier–Prest *et al.*, 2003). In this technique a special thin layer cell was used, allowing the recording of cyclic voltammograms under controlled temperature conditions. T_m of immobilized DNA was obtained via the square-wave voltammetric response of methylene blue as a function of temperature. T_m increased linearly with the ionic strength similarly as in solution but with values by 12°C higher. In solution the intercalation of methylene blue between the bases of dsDNA destabilized DNA, in contrast to stabilization of DNA attached to the gold surface. SAMs were shown to be stable at potentials between +0.8 and –1.4 V (against SCE) (Gooding *et al.*, 2003a; Hobara *et al.*, 1998, 1999; Ma and Lennox, 2000; Mirsky, 2002; Wang *et al.*, 2000a). At higher temperature thiol SAMs of DNA should be used with care because at these temperatures DNA monolayer can desorb (Meunier–Prest *et al.*, 2003). Self-assembled monolayer containing a viologen group was formed on a gold electrode via Au–S bonds (Li *et al.*, 1997). Binding of dsDNA to this layer resulted in a positive shift of the redox potential of the viologen signals indicating hydrophobic interactions. Recently, SAMs composed of other substances were proposed (Arias *et al.*, 2004; Wang *et al.*, 2005b).

6.1.2.2. Self-assembled monolayers on mercury surfaces. SAMs at solid surfaces have many advantages, including their easy characterization not only by electrochemistry but also by different optical methods. Solid surface cannot be, however, atomically flat over a large area and the resulting SAMs thus accommodate defects such as grain boundaries and pinholes (Finklea, 2000; Muskala and Mandler, 2000). In the last decade formation of extremely low defect density alkanethiol SAMs at liquid mercury surfaces were reported (Brucknerlea *et al.*, 1993, 1995; Mandler and Turyan, 1996; Muskala and Mandler, 1999, 2000; Muskala *et al.*, 1996; Slowinski *et al.*, 1996, 1997). The term mercaptans originated from high affinity of these compounds toward mercury. Liquid mercury

offered atomically flat surfaces with good electric conductivity and high affinity toward thiols. At those surfaces highly organized, 2-D arrays of adsorbed molecules were obtained. Lattice structure of solid surface, for example Au[1 1 1], determined the organization of the layer of adsorbed molecules, while on liquid mercury surfaces, the intermolecular interactions of the adsorbed molecules were probably governed by intermolecular interactions of the adsorbed molecules (Muskal and Mandler, 2000). At mercury electrodes thiols could be adsorbed either physically or chemically depending on the electrode potential. Under open circuit current or at sufficiently positive potentials thiols are chemisorbed by a process that was similar to the self-assembly process of thiol monolayers on gold. This chemisorption was accompanied by an anodic signal corresponding to the oxidation of mercury followed by formation of a Hg–thiol adduct. This adduct was reduced at negative potentials producing a cathodic signal from which the excess of surface coverage could be calculated. With short chemisorbed thiols, multilayers were observed at positive potentials, which turned into dense self-assembled monolayers at more negative potentials (Muskal and Mandler, 2000). In the last decade thioalkane SAMs at mercury electrodes were investigated rather intensively while corresponding studies of thiolated ODNs were missing.

Oligonucleotide SAMs. Recently, we found that thiol-end-labeled ODN (HS–ODN) can form SAM at hanging mercury drop electrodes (Ostatna *et al.*, 2005) (E. Palecek and V. Ostatna, unpublished, 2005). We showed that in alkaline cobalt-containing solutions HS–ODNs produced several electrochemical signals potentially useful in DNA–protein interaction studies (Chapter 19). In addition in neutral solutions not containing cobalt we observed reduction and oxidation signals (due to bases, known in unmodified DNAs, Section 4.2) as well as the signal due to reduction of the HgS–ODN compound (typical for thiolated DNAs). We used these signals to obtain information about the properties of the adsorbed HS–ODN layers. Immobilization of HS–ODN at HMDE was conveniently traced by voltammetric reduction peak of cytosine and/or adenine close to -1.5 V. These signals provided information about contacts of the bases with the electrode surface. Reduction of the Hg–S bond produced another peak close to -1.5 V. The dependence of these signals on the ODN bulk concentration and accumulation time suggested that at low surface concentrations the molecules of HS–(CTT)₇ laid flatly at the electrode surface. With their increasing surface concentration the ODN molecules tended to change their orientation to upright position forming a SAM (Scheme 2). After DNA self-assembly a second SAM was formed using 6-mercaptohexanol that prevented interactions between DNA bases and the mercury surface, leaving DNA in a largely end-tethered configuration, accessible for the DNA hybridization. If solid amalgam electrodes (Yosypchuk and Novotny, 2002b) were used (Section 2.2.1) instead of HMDE, similar voltammetric signals were obtained (Ostatna *et al.*, 2005).

Our measurements pointed to fundamentally different adsorption modes of thiolated and thiol-free ODNs at the mercury surface. At low ODN surface concentrations flat orientation prevailed with hydrophobic bases contacting the electrode surface in both types of ODNs (Scheme 2). At higher surface concentrations, islands of HS–ODN molecules in upright position were formed but

(and accumulation) of DNA at DE, after the DNA selective capture, is beneficial for increasing sensitivity of the electrochemical detection; (3) during the DNA hybridization the DE should be blocked or interfaced to increase the selectivity of the DNA hybridization and to eliminate false-positive signals. On the other hand, blocking or interfacing of DE may decrease the sensitivity of the DNA determination; etc. Optimization of hybridization and detection at a single DE surface may thus be difficult, particularly when long tDNA molecules are analyzed. These problems prompted development of a new approach, the so-called double-surface technique. In 2004, this new approach proved particularly successful by demonstrating (a) the highest sensitivity of the DNA detection in an electrochemical biosensor (Wang *et al.*, 2004) and (b) the ability to detect the lengths of expanded DNA repetitive sequences in long DNAs (> 5000 base pairs) not detectable by single-surface techniques.

In 2002, we showed that DST can be conveniently used in DNA hybridization sensors (Palecek *et al.*, 2002a). We used for DNA hybridization commercially available superparamagnetic Dynabeads oligo(dT) (DBT), with the covalently attached DNA probe (dT)₂₅ (surface H) (Figure 21). Mercury and solid amalgam electrodes (i.e. the electrodes at which DNA hybridization was difficult) as well as carbon electrodes served as DEs. Due to minimum non-specific DNA and RNA adsorption at the hydrophilic beads (developed especially for the RNA and DNA hybridization), we achieved very high specificity of the DNA hybridization. Optimum DE was chosen only with respect to the electrochemical processes of the analyte, regardless of the DE suitability for the immobilization of the DNA probe. By means of DST, detection of relatively long tDNAs was possible (Fojta *et al.*, 2004a, b). Approximately at the same time Wang *et al.* applied the same principles using different type of magnetic beads [streptavidin-coated beads to which biotinylated probe DNA was bound (Wang, 2002; Wang *et al.*, 2002b; Willner and Katz, 2003)] (Sections 4 and 11). Application of DST to DNA chips relies on microfluidic systems (Wang *et al.*, 2000b), included into the chip to manipulate the analyte at different surfaces. A number of methods of magneto-switchable electrocatalytic and biocatalytic transformation methods were developed by Willner *et al.* (Katz *et al.*, 2002; Patolsky *et al.*, 2003; Weizmann *et al.*, 2003), reviewed in Wang *et al.* (2005a) and Willner and Katz (2003).

Magnetic beads proved very convenient for DS technique but also other materials and approaches were used. For example, in an arrangement, between the typical single- and double-surface techniques, a membrane (non-conductive but semipermeable) with immobilized DNA was used for DNA hybridization and carbon electrode placed below the membrane served as the DE (Napier and Thorp, 1999; Pividori *et al.*, 2001). Nitrocellulose (NC) and functionalized nylon membranes proved excellent carrier materials in current biochemical studies of biomacromolecules, due to hydrophilicity and high sorption ability of these membranes with respect to immobilized macromolecules (Babkina *et al.*, 1996; Kiechle, 1999; Kurien and Scofield, 2003; Tomkinson and Stillman, 2002). In spite the rapid expansion of modern microarray-based methods, immobilization of nucleic acids onto such membranes still belongs to the most frequently applied techniques in various areas of biochemistry and molecular biology. The

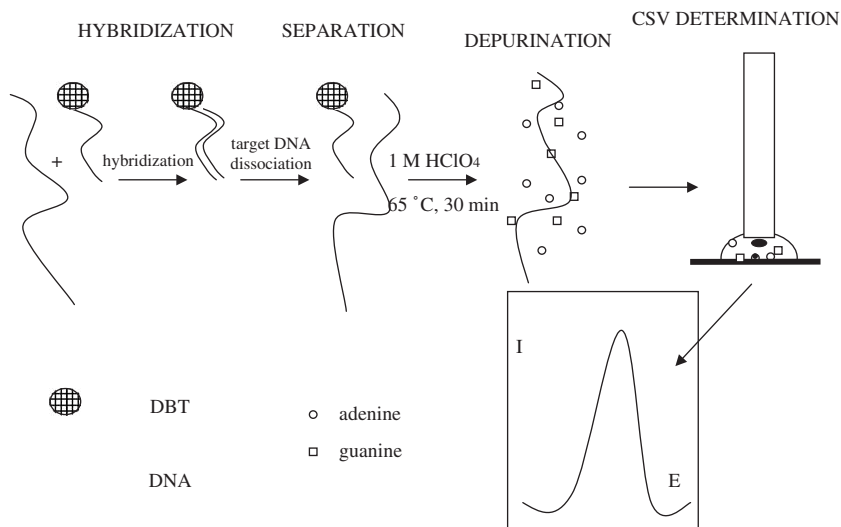


Fig. 21. Scheme the double-surface technique of DNA (or RNA) hybridization in which Dynabeads oligo(dT)25 (DBT) are used as surface H and a HMDE as DE. The detection is based on the cathodic stripping voltammetry (CSV) of adenine released from DNA by acid treatment. Adenine, producing a sparingly soluble compound with the electrode mercury, can be determined by CSV at nanomolar concentrations (Paleček, 1980b) and at subnanomolar concentrations (in the presence of copper or at copper solid amalgam electrodes). Adapted from Paleček *et al.* (2002a). Copyright 2002, with permission from Elsevier.

advantages of the NC or nylon membranes were utilized also in DNA electrochemical analysis. For example, Pividori *et al.* (2001) proposed an amperometric sensor involving nylon membrane carrying target DNA placed on a graphite composite electrode. In this sensor, a horse radish peroxidase-labeled probe was used to detect specific nucleotide sequence. Nitrocellulose or nylon membranes with immobilized DNA were also used as coatings of mercury film (Babkina and Ulakhovich, 2004; Babkina *et al.*, 2003, 2004) or ITO (Napier and Thorp, 1999) electrodes. In these experiments usual dot-blot analysis was combined with electrochemical detection, i.e. DNA was adsorbed on a membrane, followed by DNA hybridization or interaction with low molecular mass compounds and further steps necessary for the electrochemical detection. Then the membrane was mechanically attached (e.g. using an o-ring) to the electrode to perform the electroanalysis. Since direct electrical communication between the membrane-confined DNA and the electrode was precluded, such analysis involved a soluble species capable of diffusion through the membrane to the electrode surface. For example, DNA anchored at NC or nylon membrane-modified ITO electrode was detected using the electrocatalytic scheme proposed by Thorp *et al.* (Napier and Thorp, 1999 and references therein). Their technique was based on oxidation of the DNA guanine residues by a soluble ruthenium mediator. Another approach was proposed by Babkina *et al.* (1996), while determining autoantibodies to DNA. DNA and its enzyme label

(cholinesterase) were coimmobilized in nitrocellulose membrane attached to a mercury film electrode.

Recently, we have prepared NC membrane-coated glassy carbon electrodes (GCE) for the detection of DNA hybridization via a biocatalytic/electrochemical protocol (Kourilova *et al.*, 2005). Target DNA was confined to the sensor surface by direct mixing with the NC solution prior to its deposition onto the electrode membrane. Membrane-immobilized DNA hybridized with a biotinylated probe that was recognized by streptavidin–alkaline phosphatase conjugate. This enzyme transformed the electroinactive naphthyl phosphate substrate into an electroactive product (1-naphthol) that penetrated through the NC membrane to the GCE surface producing an anodic signal. In difference to the previously published papers (Babkina and Ulakhovich, 2004; Babkina *et al.*, 1996, 2000, 2003, 2004; Napier and Thorp, 1999; Pividori *et al.*, 2001), this experimental arrangement is better amenable for parallel DNA analysis on chips.

Application of DST with magnetic beads resulted in various highly sensitive assays, which would be difficult or impossible to obtain by means of SST. They included label-free DNA and RNA detection (Jelen *et al.*, 2002b), sensitive detection of osmium-modified DNA, yielding catalytic signals at mercury electrodes and SAE (Fojta *et al.*, 2002, 2003, 2004b; Havran *et al.*, 2004), differently coded reporter probes (Fojta *et al.*, 2004b; Wang *et al.*, 2003a), enzyme-linked immunoassays (Palecek *et al.*, 2002c), nanoparticle labels reviewed in Wang (2003), including electroactive beads (Wang *et al.*, 2003c) and indium microrod tags (Wang *et al.*, 2003b) enabling a very high sensitivity of the DNA detection (Chapters 4 and 11). Particularly interesting appears the use of carbon nanotubes (Chapter 11) (Cai *et al.*, 2003b; Kohli *et al.*, 2004; Wang, 2005; Wang *et al.*, 2004; Xu *et al.*, 2004), determination of point mutations by means of a MutS protein (Palecek *et al.*, 2004) and the possibility of determination of the length of the DNA repetitive sequences without using any additional non-electrochemical method. The latter determination is briefly discussed below.

6.2.1. Length determination of long repetitive sequences

Long repetitive sequences were considered for decades to be useless junk DNA. Now it becomes clear that at least some of these sequences represent biologically important DNA segments (Eddy, 2001; Mattick, 2003; Storz, 2002; Yelin *et al.*, 2003). Moreover, genomic expansions of DNA trinucleotide repeats are related to neurodegenerative diseases such as myotonic dystrophy (CTG), fragile X syndrome (CGG triplet), Friedreich ataxia (FRDA; GAA), etc. Determination of the triplet length expansion is used in molecular–biological diagnosing of these diseases (Campuzano *et al.*, 1996; Paulson and Fischbeck, 1996). Fast DNA sensors capable to detect the triplet are therefore sought. Reporter probes (RP) are well suited for this purpose, but in SST (Section 6.1) the requirement of RP binding to tDNA sequences that are close to the electrode surface limits the use of RPs. In contrast, in DST positioning of the RP binding site on tDNA does not play a significant role. To determine the length of the CGG or CTG

triplet repeats it was necessary to combine electrochemistry with DNA radioactive labeling (Yang and Thorp, 2001).

Recently, we proposed a new electrochemical double surface method to detect the length of the triplet expansion in FRDA (Fojta *et al.*, 2004a). In this method DNA fragments or PCR amplified target DNA were thermally denatured and modified by osmium tetroxide 2,2'-bipyridine (Os,bipy) (Section 6.3.1) known to react with pyrimidine but not with purine bases (Paleček, 1992b). To capture the $(GAA)_n$ triplet repeat-containing DNA strand at the magnetic beads with covalently attached oligo(dT)₂₅ (serving as surface H in the DS electrochemical technique) we utilized (dA)₁₈ stretch naturally occurring next to this repeat (Figure 22). Then the biotin-labeled reporter probe (CTT)₁₂ (RP-biot) was hybridized to the captured target DNA to obtain an electrochemical signal characterizing the length of the $(GAA)_n$ triplet repeat expansion. The number of pyrimidines in tDNA was independent of the length of the $(GAA)_n$ triplet repeat and the electrochemical signal of Os,bipy-modified pyrimidines was thus related to the number of DNA molecules captured at the beads. The length of the triplet expansion was calculated from the ratio of the electrochemical signal intensities of hybridized RP (enzyme-linked assay)/tDNA Os,bipy label. Os,bipy-modification of pyrimidines in (CTT)_n repeat of the complementary strand (Figure 22) effectively prevented reassociation of the purine and pyrimidine strands after the DNA denaturation (Paleček *et al.*, 2002d) which resulted in about 10-fold increase of the signals obtained for the RW59 amplicon or *EcoRI*-linearized plasmid pRW3821. The RP-biot was detected via an electrochemical enzyme-linked assay involving binding of streptavidin-alkaline phosphatase conjugate to the RP-biot and transformation of the electrochemically inactive substrate 1-naphthylphosphate into an electroactive 1-naphthol product which was determined at carbon electrodes using an anodic peak N (Paleček *et al.*, 2002c). Os,bipy-modified pyrimidine residues within sequences flanking the homopurine $(GAA)_n$ repeat in tDNA were determined either at carbon or at mercury electrodes. Compared to carbon electrodes mercury electrodes allow to reach more negative potentials where a catalytic signal of DNA-Os,bipy (offering higher sensitivity of the determination) can be measured (Jelen *et al.*, 1991; Kizek *et al.*, 2002; Paleček, 1992b). Principles of this assay can be utilized in determination of lengths of expansions of different neurodegenerative disease-associated triplet repeats (Campuzano *et al.*, 1996; Paulson and Fischbeck, 1996; Yang and Thorp, 2001) and can be adapted for the length determination of any repetitive sequence.

6.3. Electroactive markers covalently bound to DNA

DNA and RNA are naturally electroactive but both their oxidation and reduction are electrochemically irreversible, occurring at highly positive or highly negative potentials. Electroactive markers were introduced into DNA to obtain electrochemical signals at potentials closer to the potential of zero charge and/or to increase the sensitivity of the analysis. Most of these markers either underwent reversible electrode reactions at less extreme potentials or produced high

electron yield catalytic signals. Electroactive osmium labels were introduced into DNA already in the beginning of the 1980s (Lukasova *et al.*, 1982, 1984; Palecek and Hung, 1983; Palecek and Jelen, 1984; Palecek *et al.*, 1984). To our knowledge they were the first electroactive labels covalently bound to DNA.

6.3.1. Osmium labels

6.3.1.1. *Osmium tetroxide complexes with nitrogen ligands (Os^{VIII}, L).* Os^{VIII}, L binds to pyrimidine residues in ssDNA and RNA through the addition to the 5,6 double bond of the pyrimidine ring (Figure 23). DNA modification with Os, L is simple and fast and can be performed under conditions close to physiological (Jelen *et al.*, 1991; Lukasova *et al.*, 1982, 1984; Palecek, 1992b; Palecek and Hung, 1983; Palecek and Jelen, 1984; Palecek *et al.*, 1984). Os, L -modified DNA produced a signal at about -1.2 V at mercury and SAE (Yosypchuk, 2004). This signal was due to the catalytic hydrogen evolution, capable to detect ssDNA at subnanomolar concentrations. In addition three redox couples between 0 and at about -0.6 V were produced at mercury (Figure 24) and carbon electrodes (Figure 25) (Fojta *et al.*, 2002, 2003, 2004b; Havran *et al.*, 2004; Jelen *et al.*, 1991; Kizek *et al.*, 2002; Lukasova *et al.*, 1982).

The first experiments were done with osmium tetroxide, pyridine (Os^{VIII}, py), but osmium tetroxide, 2,2'-bipyridine ($Os^{VIII}, bipy$) soon replaced less convenient

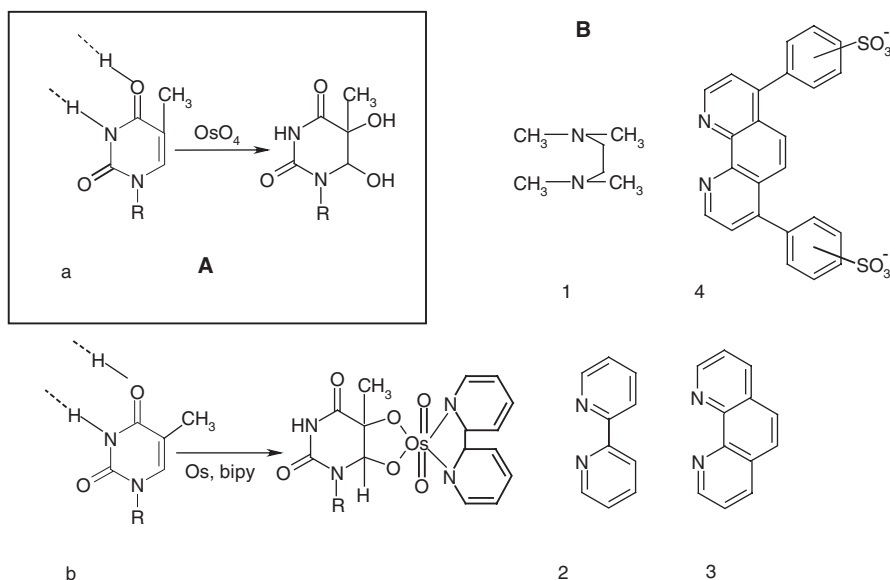


Fig. 23. (A) Reaction of osmium tetroxide (alone) with thymine. (B) Formation of the adduct between osmium tetroxide, pyridine, and thymine along with some tertiary amines which can replace pyridine in the osmium tetroxide complex; (1) tetramethylethylenediamine (TEMED); (2) 2,2'-bipyridine (bipy); (3) 1,10 phenanthroline (phe); (4) bathophenanthroline disulphonic acid (bpd); dotted bonds show hydrogen bonding in the Watson–Crick base pair. Only final reaction products are shown. Adapted from Palecek (1992b). Copyright 1992, with permission from Academic Press.

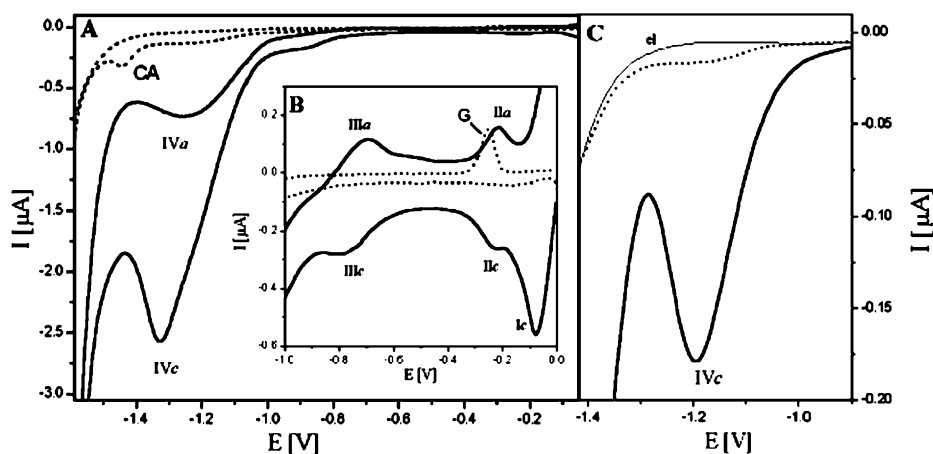


Fig. 24. (A) Adsorptive stripping cyclic voltammograms (AdSCV) of unmodified ssDNA (dashed line) and ssDNA modified with 2 mM Os,bipy (DNA-Os,bipy) (full line) at a concentration of $10 \mu\text{g/mL}$. Background electrolyte: 0.3 M ammonium formate and 0.05 M sodium phosphate (pH 7.0), t_a 1 min, scan rate 0.1 V/s, initial potential 0 V, switching potential -1.85 V . (B) Section of the DNA and DNA-Os,bipy cyclic voltammograms measured at scan rate 1 V/s, other conditions as in (A). (C) Adsorptive stripping differential pulse voltammograms of ssDNA modified with 2 mM Os,bipy (full line) and with 2 mM Os,py (dashed line) at a concentration of 800 ng/mL. Background electrolyte (thin full line): Britton–Robinson buffer pH 4.0, t_a 1 min, pulse amplitude 0.05 V, scan rate 0.01 V/s, $E_a -0.6 \text{ V}$. Potentials are given against Ag/AgCl/3 M KCl reference electrode. Peak a is characteristic for the DNA-Os,bipy adduct. Adapted from Havran *et al.* (2004). Copyright 2004, with permission from Elsevier.

(Os^{VIII},py) (Palecek, 1992b). Later Os^{VIII},bipy and other Os^{VIII},L complexes have been widely applied as probes of the DNA structure *in vitro* and *in vivo* in connection with DNA sequencing techniques and immunoassays (reviewed in Palecek, 1991, 1992b,c, 1994; Palecek *et al.*, 1992). Os^{VIII},bipy-modified tDNA and end-labeled reporter probes have been conveniently used in DNA hybridization sensors (Section 6.2). End-labeling of oligonucleotides with Os^{VIII},bipy can be performed in any biological laboratory without any organic chemistry equipment. End-labeling of homopurine recognition sequences, including the use of multiple labels is particularly easy (Fojta *et al.*, 2004a, b).

6.3.1.2. Osmium (VI) complexes (Os^{VI}, L). In difference to osmium tetroxide complexes, six-valent potassium osmate, $\text{K}_2\text{Os}_2(\text{OH})_4$, in the presence of pyridine did not react with the nucleic acid bases. Almost 30 years ago it was shown that $\text{K}_2\text{Os}_2(\text{OH})_4$, py reacted with the ribose residue of any usual ribonucleosides (Figure 26) (Daniel and Behrman, 1976a,b; Palecek, 1992b). Such an RNA-specific reaction may be of use for site-specific labeling of a *cis*-diol in unphosphorylated ribose residues at 3'-ends of the RNA molecules. In spite of the potential usefulness of this reaction no reports were published on its application to natural RNAs or longer synthetic oligoribonucleotides until now. Recently, we

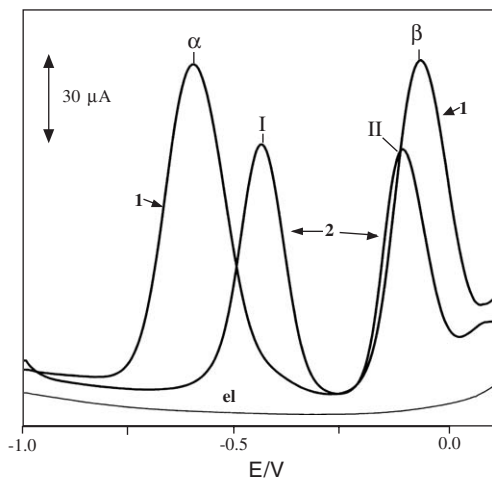


Fig. 25. Adsorptive transfer stripping (AdTS) cyclic voltammogram at a PGE of: (1) Os,bipy-modified denatured (ss)DNA (ssDNA-Os,bipy; purified by dialysis); (2) Os,bipy alone; (3) unmodified ssDNA and (el), background electrolyte. Initial potential -1.0 V, quiescent time 1 s, switching potential $+1.0$ V, scan rate 1 V/s; background electrolyte 0.2 M sodium acetate, pH 5.0 ; DNA (50 $\mu\text{g/mL}$) or Os,bipy (0.1 M) was accumulated at the electrode from a 7 μL drop of 0.25 M NaCl for $t_A = 60$ s, followed by washing the electrode with distilled water and transfer into a voltammetric cell containing blank background electrolyte. Potentials are given against Ag/AgCl/ 3 M KCl reference electrode. Peak alpha is characteristic for the DNA-Os, bipy adduct. Adapted from Fojta *et al.* (2002). Copyright 2002, with permission from Elsevier.

attempted to modify the 3'-end ribose in a 21-mer oligonucleotide and we found conditions under which the modification proceeded well. We showed that similarly to the $\text{DNA}_{\text{bases}}\text{-Os}^{\text{VIII}}$, L adducts, the $\text{RNA}_{\text{ribose}}\text{-Os}^{\text{VI}}$, L adducts can be sensitively detected at carbon and mercury (Figure 27) electrodes (M. Trefulka and E. Paleček, unpublished, 2005). In spite of these advantages of Os,L reagents, the ferrocene ODN label (which can hardly be prepared in a biological laboratory, and as a commercial product it is rather expensive) is at present perhaps the most favored ODN electroactive marker.

6.3.2. Ferrocene and other labels

Ferrocene has perhaps been the most frequently used electroactive label in DNA hybridization sensors (Anne *et al.*, 2003; Baca *et al.*, 2004; Fan *et al.*, 2003; Gibbs *et al.*, 2005; Ihara *et al.*, 1996; Immoos *et al.*, 2004b; Popovich *et al.*, 2002; Sato *et al.*, 2004; Yu *et al.*, 2000, 2001). Ferrocene-labeled ODNs were prepared by covalent linkage of a ferrocenyl group to the amino hexyl-terminated ODN (Ihara *et al.*, 1996, 1997). Using high-performances liquid chromatography (HPLC) equipped with an electrochemical detector DNA and RNA were determined at femtomole level (Ihara *et al.*, 1996). Uridine-conjugated ferrocene ODNs were synthesized and ferrocene-labeled signaling probes with different redox potentials were prepared for reliable detection of

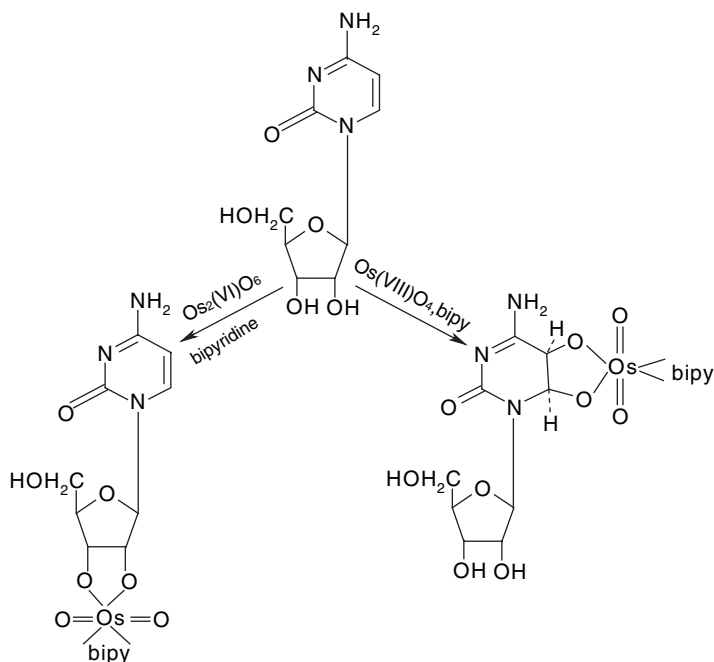


Fig. 26. Formation of oxoosmium(VI) nucleoside sugar esters (as a product of the reaction of cytidine with potassium osmate(VI) and pyridine) and of heterocyclic osmate esters (resulting from the reaction of the same nucleotide with osmium tetroxide(VIII) and pyridine). Adapted from [Palecek \(1992b\)](#). Copyright 1992, with permission from Academic Press.

point mutations in DNA ([Yu *et al.*, 2000, 2001](#)). Ferrocene labels and other labels mentioned below required solid state organic chemistry and in difference to the Os,L labels they could hardly be used for labeling of longer NAs, such as plasmid and chromosomal DNAs, viral RNAs, etc. Other compounds, such as daunomycin ([Kelley *et al.*, 1999a](#)), viologen and thionine ([Mao *et al.*, 2003](#)) were used as electroactive labels of ODNs. End-labeling of DNA with biotin and thiol groups has been widely applied (Section 6.2). Electroactive labels were introduced into DNA not only by chemical methods, but also by means of enzymes such as DNA polymerases capable to incorporate in DNA synthetic ferrocene tethered to dUTP ([Patolsky *et al.*, 2002](#)).

6.4. Electrocatalytic oxidation of DNA

Redox reactions of guanine and its residues in nucleic acids are intensively studied because of their great biological significance, particularly in aging and various diseases (Chapters 12 and 13). Among the NA bases, G is most easily oxidizable by different oxidants, including singlet oxygen, hydroxyl radicals, transition metal complexes and alkylating agents. Guanine redox reactions have been found useful in nucleic acid analysis (Section 4.1.2), including the

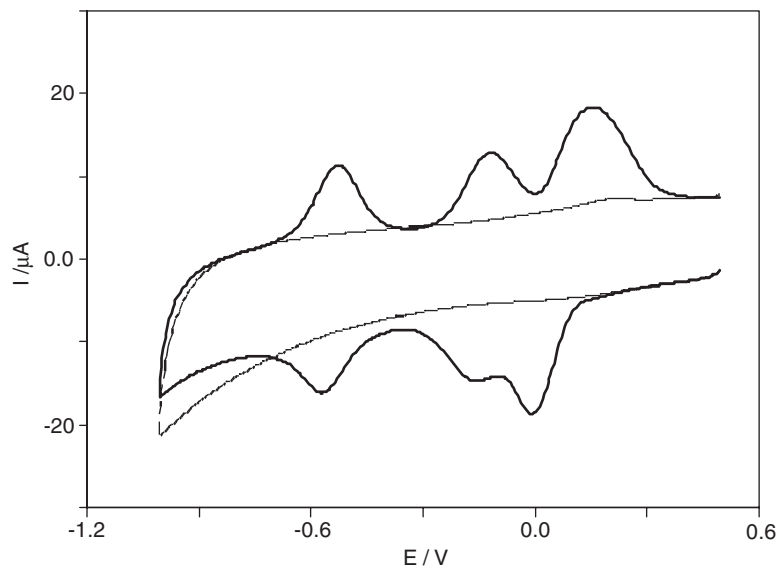


Fig. 27. Cyclic voltammogram of 40 mM adenine riboside (adenosine) (thick line) modified with Os(VI),bipy (thin line) in 0.2 M sodium acetate, pH 5.0. AUTOLAB, PGE, Ag/AgCl/3 M KCl reference electrode, scan rate 1 V/s, accumulation time 60 s (M. Trefulka and E. Paleček, unpublished).

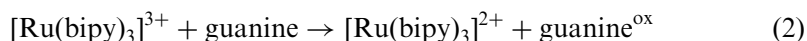
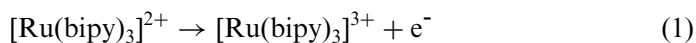
development of the DNA hybridization sensors (Thorp, 2004) and in the research into the electron transfer reactions along the DNA double helix (Giese and Wessely, 2001).

Electrocatalysis refers to catalysis of electrochemical reactions. Electrocatalyst increases the rate of the electrochemical reaction, usually calculated from the electrolytic current (Banica and Ion, 2000). Using electrocatalytic reaction either the catalyst or some substrate compounds (not amenable to direct electrochemical analysis) can be determined quantitatively. Electrocatalysis was performed at bare and modified electrodes. Catalytic layers on electrode surfaces were ingeniously engineered yielding a great variety of chemical and biochemical sensors.

Thorp and coworkers (Armistead and Thorp, 2000, 2001; Eckhardt *et al.*, 2001; Holmberg *et al.*, 2003; Johnston *et al.*, 1994, 1995; Napier and Thorp, 1997, 1999; Ontko *et al.*, 1999; Popovich and Thorp, 2002; Ropp and Thorp, 1999; Szalai and Thorp, 2000; Thorp, 1998) pioneered the use of mediators and electrocatalysis on ITO electrodes in electrochemistry of NAs. In the last decade a lot of important basic research was done which was utilized in the development of the DNA hybridization sensors (Popovich and Thorp, 2002; Tarlov and Steel, 2003). This work was reviewed in a recent comprehensive review (Thorp, 2004) (see also Section 4). We therefore limit ourselves to a short summary and some interesting aspects of this work.

To increase the sensitivity of the guanine-based electrochemical analysis Thorp *et al.* (Thorp, 2004) investigated the application of transition-metal

complexes for mediating oxidation of guanine and found that ruthenium trisbipyridyl $[\text{Ru}(\text{bipy})_3]^{2+}$ was an effective oxidation catalyst of guanine. Addition of DNA to a solution of $[\text{Ru}(\text{bipy})_3]^{2+}$ resulted in a catalytic enhancement of the $[\text{Ru}(\text{bipy})_3]^{2+}$ oxidation peak at cyclic voltammograms (Figure 28). These voltammograms were indicative of a scheme where the electrogenerated Ru(III) was reduced to Ru(II) by DNA guanine residues, setting up an electrocatalytic cycle (Johnston *et al.*, 1995):



In this reaction guanine was oxidized by a single electron to guanine^{ox} and the electrogenerated $[\text{Ru}(\text{bipy})_3]^{3+}$ underwent a thermal reaction with guanine to regenerate $[\text{Ru}(\text{bipy})_3]^{2+}$ which was then oxidized on the electrode. The additional current in the electrocatalytic signal arose thus from the reoxidation of the $[\text{Ru}(\text{bipy})_3]^{2+}$ as shown in equation (2). Such observations were originally made with $[\text{Re}(\text{O})_2(\text{py})_4]^{2+/+}$ (Johnston *et al.*, 1994) but later $[\text{Ru}(\text{bipy})_3]^{3+}$ was shown to be a more stable catalyst. The assignment of guanine as the electron donor is supported by numerous lines of evidence (Thorp, 2004), the electron transfer reaction of $[\text{Ru}(\text{bipy})_3]^{3+}$ with guanine is probably a proton-coupled reaction (Weatherly *et al.*, 2001, 2003) but the precise mechanism of the guanine oxidation is still under investigation.

Binding of the metal complex to DNA was studied in detail. At high ionic strengths binding of $[\text{Ru}(\text{bipy})_3]^{2+}$ to DNA was negligible (Johnston and Thorp, 1996). At low ionic strengths a number of effects of DNA binding on electrochemical signals $[\text{Os}(\text{bipy})_3]^{2+}$ complex were found (Welch and Thorp, 1996; Welch *et al.*, 1995), including tighter binding of the 3^+ form than for the 2^+ form due to the higher charge of the former. Thus, the redox potentials of the Os(III/II) couple were different for the DNA-bound and free forms (Welch and Thorp, 1996). Similar effects were originally found with $[\text{Co}(\text{phen})_3]^{2+}$ by Carter and Bard (1987); Carter *et al.* (1989). The diffusion coefficient of the bound form corresponded to that of DNA and with chromosomal DNA this coefficient differed from that of the free form by almost one order of magnitude (Welch and Thorp, 1996; Welch *et al.*, 1995). It was thus concluded that the majority of the electrochemistry occurred through the free $[\text{Ru}(\text{bipy})_3]^{2+}$. It could be expected that binding of the metal complex to DNA should occur in a relative proximity to the guanine residue, from which an electron should be abstracted. It was found that electrons were transferred to a $[\text{Ru}(\text{bipy})_3]^{3+}$ that was bound between 2.5 and 5 base pairs from the guanine donor (Sistare *et al.*, 1999). Sensitivity of 44 attomol/mm² (or 3×10^9 molecules) was reported for 1497 base pair PCR product (Armistead and Thorp, 2000).

A number of groups observed that in two adjacent guanines present in a DNA sequence, the 5'-guanine was preferably oxidized (Hall *et al.*, 1996; Meggers *et al.*, 1998; Saito *et al.*, 1998; Schuster, 2000; Sugiyama and Saito, 1996). The lowest reactivity was observed for a guanine with a thymine on the G 3'-side (Sugiyama and Saito, 1996). The CV of $[\text{Ru}(\text{bipy})_3]^{2+}$ was measured

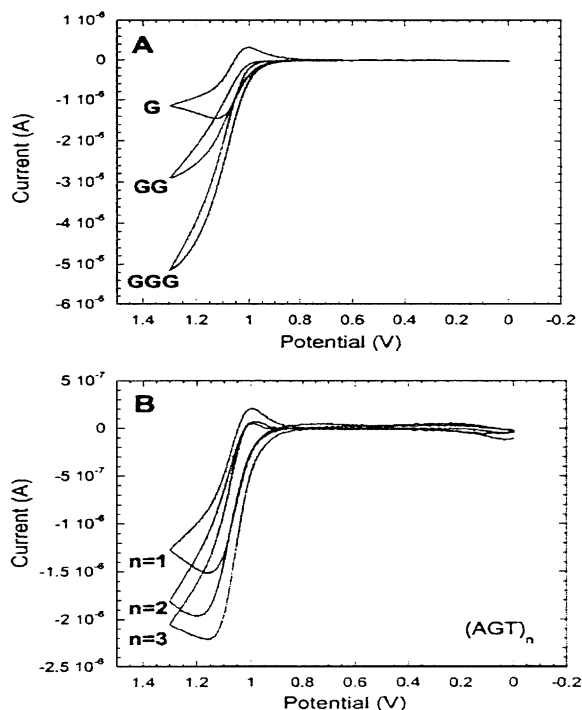


Fig. 28. Cyclic voltammograms of $\text{Ru}(\text{bipy})_3^{2+}$ in the presence of the DNA at pH 7. A, added sequences are the duplex forms of G15 (G), GG16 (containing doublet GG), and GGG17 (containing triplet GGG). B, added sequences are the duplex forms of G15 ($n = 1$), $\text{G} \times \text{G}18$ ($n = 2$), and $\text{G} \times \text{G} \times \text{G}21$ ($n = 3$) (containing isolated guanine residues). Potentials are given against Ag/AgCl/3 M KCl reference electrode. Adapted from Sistare *et al.* (2000). Copyright 2002, with permission from the American Chemical Society.

by Thorp's group in the presence of the sequence d(AAATATAGTATAA-AAA) (G15) and in the presence of the same sequences in which the single G was replaced either with GG (GG16) or with GGG (GGG17) (Sistare *et al.*, 2000). The results were indicative of very rapid electron transfer for GG16 and GGG17 (Figure 28A). It was shown that the faster oxidation rates for the guanine multiplets were not due simply to the increase of guanine concentration. The increase of electrocatalytic currents from ODNs containing two and three isolated guanines was much lower (Figure 28B) than that produced by GG16 and GGG17 (Figure 28A), suggesting that it was the guanine multiplets that enhanced the guanine reactivity. The rate constants were calculated and the ratio for the 5'-G compared to isolated guanine, $k_{\text{GG}}/k_{\text{G}}$, of 12 ± 2 (across a broad range of scan rates) and DNA concentrations was found. Later studies of similar sequences by other authors (Johnston *et al.*, 1995) were consistent with the results of Thorp's group (Sistare *et al.*, 2000) shown in Figure 28.

The work of Thorp *et al.* (Thorp, 2004) relied on special properties of ITO electrodes. These electrodes (1) are optically transparent and can be fabricated on glass (Armstrong *et al.*, 1976; Popovich *et al.*, 2002); (2) at neutral pH they

can access potentials up to 1.4 V (Popovich *et al.*, 2002); (3) they do not adsorb DNA appreciably (Grover and Thorp, 1991); (4) the direct oxidation of guanine is extremely slow even when DNA is intentionally attached to the electrode (Armistead and Thorp, 2000, 2001). In difference to carbon electrodes yielding oxidation signals of guanine and adenine (Section 4.1), no significant signals resulted from direct oxidation of guanine at ITO electrodes. These properties of ITO electrodes made them suitable for developing systems for studies of electrocatalytic oxidation of nucleic acids. Most efficient electron transfer between the mediator and ITO electrode was obtained at polycrystalline ITO films probably due to the higher density of defects.

Reactivity of guanine residues in DNA decreased in the following way: ssDNA > mismatched dsDNA > dsDNA. Detection of base mismatches using the guanine-Ru(III) reaction was, however, difficult because properly paired guanines in the DNA duplex obscured the effect of the mismatch. 8-Oxo-7, 8-dihydroxyguanine (8-oxoG) arises from oxidative DNA damage and its occurrence in DNA represents one of the important signs of the DNA damage (Chapters 12 and 13). 8-oxoG is oxidized at less positive potentials than guanine (Steenken *et al.*, 2000) and the rate of its oxidation (in a DNA duplex paired with cytosine) by Os(III) is approximately an order of magnitude higher than for guanine oxidation by Ru(III) (Thorp, 2004). If a mixture of $[\text{Ru}(\text{bipy})_3]^{2+}$ and $[\text{Os}(\text{bipy})_3]^{2+}$ was used in the presence of a single guanine-containing ODN only the $[\text{Ru}(\text{bipy})_3]^{2+}$ signal was enhanced but when guanine was replaced by 8-oxoG, enhancement of $[\text{Os}(\text{bipy})_3]^{2+}$ was observed (Ropp and Thorp, 1999). Using 8-oxoG-Os(III) reaction it was possible to detect TTT deletion (deletions of three thymines is common genetic mutation in cystic fibrosis). Adenine (8-oxoG)adenine sequence hybridized to TTT wild-type sequence gave a relatively small current enhancement while in the mutant the adenine(8-oxoG)adenine sequence formed a bulge which produced a significantly higher current enhancement.

6.5. DNA conductivity in DNA sensors

6.5.1. DNA conductivity

The idea that dsDNA may function as a conduit for fast electron transport along the axis of its base-pair stack was advanced more than 40 years ago (Porath *et al.*, 2004 and references therein). But later low-temperature experiments suggested charge migration within the frozen water layer surrounding the DNA double helix (Warman *et al.*, 1996). In the recent decade, investigations of the DNA conductivity became a hot topic because of its relevance for a number of biological processes, such as those involved in mutagenesis and cancer, and for molecular electronic. The literature on the DNA conductivity was reviewed in several articles, e.g. (Barbara and Olson, 1999; Grinstaff, 1999) and in 2004 a special volume of *Topics in Current Chemistry* (2004) was devoted to this topic. Here, only a brief summary will be presented with special attention to application of DNA charge transport in electrochemical sensors for DNA hybridization.

Solution chemistry experiments on a number of short DNA molecules indicated high charge transfer rates between a donor and acceptor, which were located at distant DNA sites (Porath *et al.*, 2004). Several mechanisms were proposed for DNA-mediated charge transport, in dependence on the structural aspects of the system under investigation, including the DNA base content and/or sequence. These advances stimulated interest in DNA for nanoelectronics and led to a set of direct electrical transport measurements. A number of ingenious experiments with single molecules, bundles and networks were performed showing that it is possible to transport charge carriers along DNA molecules. After some initial controversial reports on the conductance of DNA devices, recent results indicated that short DNA molecules were capable of transporting charge carriers, similarly to DNA bundles and DNA networks. On the other hand it was shown that transport through single DNA molecules, longer than 40 nm was blocked. This might be due to the DNA interaction with the surface which may induce defects in the DNA molecules disturbing the electronic structure of dsDNA (including the DNA surface denaturation, see Section 5) and blocking the charge transport. The question whether DNA has properties of a metal, semiconductor or an insulator was frequently asked. This terminology originates from solid-state physics. It is, however, questionable whether such terminology can describe adequately the orbital energetics and the electronic transport through one-dimensional soft polymer, such as DNA, that is formed of a large number of sequential segments. A large number of junctions and phase-coherent “islands” may influence the transport mechanism along the molecule. In some cases such junctions can constitute a rate-limiting step for the transport. In spite of the outstanding progress in controlling the self-assembly of DNA on electrodes (Section 6.1.2), unanimously accepted explanation of the mechanisms responsible for the charge mobility through the dsDNA structure is not yet available. On the other hand, charge transfer in self-assemblies of thiolated dsODNs was exploited in development of the electrochemical DNA sensors (Drummond *et al.*, 2003).

6.5.2. Charge transfer in DNA sensors

Electrochemistry at chemically modified surfaces has been applied to investigate charge transport in various media including thioalkanes and proteins (Armstrong *et al.*, 2000; Chi *et al.*, 2001; Creager *et al.*, 1999; Finklea, 1996; Immoos *et al.*, 2004c; Munge *et al.*, 2003; Nahir and Bowden, 1996; Niki *et al.*, 2003; Sachs *et al.*, 1997). Barton and coworkers reported self-assembly of 15–20 base pair dsODNs (containing different nucleotide sequences) covalently attached to gold surfaces via thiol tethers and demonstrated unique charge transfer characteristics through this assemblies (Drummond *et al.*, 2003). They developed electrochemical assays for DNA hybridization, including detection of point mutations as well as for DNA damage and DNA–protein interactions. Typically, DNA duplexes were prepared in solution and self-assembled on gold electrodes. The electrode was then treated with planar redox active molecules, such as methylene blue (MB) which was non-covalently bound (intercalated) to

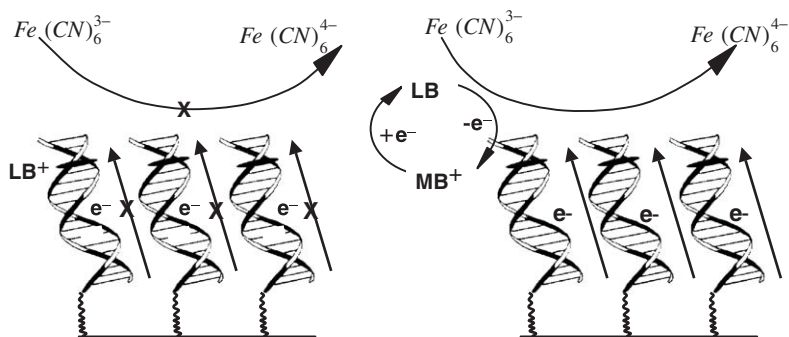


Fig. 29. Scheme of electrochemical assay for mismatches through DNA-mediated charge transport. On the right is shown an electrode modified with well-matched duplex DNA. Current flows through the well-stacked DNA to reduce methylene blue (MB^+) intercalated near the top of the film, to leucomethylene blue (LB). LB goes on to reduce ferricyanide in solution, thereby regenerating MB^+ catalytically, leading to an amplification of the hybridization signal. In the case of a DNA film containing mismatched duplexes (left), current flow through the DNA duplex is attenuated, MB^+ is not reduced, and the catalytic signal is lost. Adapted from Drummond *et al.* (2003). Copyright 2003, with permission from the author.

the densely-packed DNA-modified gold electrode. It was shown that these intercalators bound near the solution accessible interface of the densely packed DNA-modified surfaces eliminating the need for covalent binding (Boon *et al.*, 2000, 2002a, b, 2003; Kelley *et al.*, 1999b; Sam *et al.*, 2001). The reduction of the intercalator at the top of the film through a DNA mediated reaction reflected base-pair stacking within the film (Figure 29). With intact stacking MB was efficiently reduced at the DNA film but in presence of an intervening mismatch or other duplex perturbation attenuation of MB reduction was observed (Boon *et al.*, 2000, 2002a, b; Kelley *et al.*, 1999a, b). In some cases, the MB signal was amplified through an electrocatalytic cycle. MB served as a catalyst for the reduction of ferricyanide diffusing in solution outside of the DNA film (Boon *et al.*, 2000, 2002b, Kelley *et al.*, 1999a). It was shown that both the direct and catalytic reduction of MB took place via charge transfer through the DNA base stack (Boon *et al.*, 2003; Kelley *et al.*, 1997a). Thus DNA mediated charge transfer electrochemistry represented a sensitive probe of nucleic acid structure and base stacking. Even minor perturbations in stacking diminished the MB reduction signal (Boon *et al.*, 2002b; Kelley *et al.*, 1999a). Electrochemical reduction of DNA intercalators was used to study DNA-protein interactions (Boon *et al.*, 2002a) and hybridization of antisense oligonucleotides (Boon *et al.*, 2002b). Charge transfer in right-handed A- and B-form DNA double helices and in left-handed Z-DNA was investigated (Boon and Barton, 2003). The A-DNA was examined in the context of a DNA/RNA hybrid duplex and Z-DNA at high Mg^{2+} concentrations in duplexes containing methylated cytosine in $\text{d}(\text{CG})_n$ sequences. Efficient charge transfer was detected in both A- and B-DNA using MB reduction as a probe. In Z-DNA films lower level of MB reduction was observed. Less efficient but not completely attenuated charge

transfer in Z-DNA can be due to different base stacking related to different structural parameters and particularly to the alternating syn-anti-sugar conformation in Z-DNA (in difference to A- and B-DNA there is no intra-strand stacking in Z-DNA), etc.

Alternatively, the intercalating probe was site-specifically coupled to the HS-ODN before the self-assembly to control precisely the location of the intercalator (Kelley *et al.*, 1999a). This technique was used to probe the distance dependence of the charge transfer by preparing a series of DNA-modified electrodes in which the through helix distance from the intercalator (daunomycin, DM) to the gold surface spanned over 4.5 nm. It was found that the electrochemical response of the intercalated DM was not dependent on its location in the DNA helix (Kelley *et al.*, 1999a). Considering the very shallow distance dependence of the charge transfer in solution (Boon and Barton, 2002; Hall *et al.*, 1996; Kelley *et al.*, 1997b; Nunez *et al.*, 1999; Wan *et al.*, 1999; Yoo *et al.*, 2003) and striking dependence of the presence of a single-base mismatch in the duplex, the role of the length of the linker was tested (Drummond *et al.*, 2004). A homologous series of DM-labeled ODN assemblies featuring thiol-terminated linkers possessing different numbers (n) of methylene units conjugates (with n ranging from 4 to 9) were constructed. The resulting ODN-DM molecules were self-assembled on gold electrodes with excess Mg^{2+} to obtain dense monolayers (surface coverages ranged from 30 to 75 pmol/cm²). Irrespective of linker lengths a chemically reversible reduction of DM was observed at about -0.6 V (vs. Ag/AgCl 1 M KCl). On the other hand, the intensity of the electrochemical response decreased with increasing linker length. It was concluded that in the time scale of the CV experiments (scan rates ~ 1 V/s) the ODN-DM conjugates behaved as discrete redox-active entities, with electrochemical responses independent of the DM intercalation site in a good agreement with results of the scanning tunneling microscopy (STM) studies of the self-assemblies on gold (Ceres and Barton, 2003). Irrespective of the mechanism of the charge transfer through the ODN assembly, charge transfer through the σ -bonded linker followed semiclassical superexchange theory. Thus, when the linker lengths and the DM positions varied the charge transfer through the σ -bonded linker was the rate-limiting step (Drummond *et al.*, 2004).

The conclusions of Barton *et al.* (Boon and Barton, 2002; Drummond *et al.*, 2004; Kelley *et al.*, 1999a; Yoo *et al.*, 2003) based on voltammetric responses of their systems were supported by the results of investigation of thiol-modified ODN films on gold surfaces using electrochemical *in situ* scanning tunnelling microscopy (Ceres and Barton, 2003). This technique revealed effective charge transport on gold (under conditions close to physiological) depending upon ODN orientation and integrity of base-pair stacking. Base mismatches behaved as electronic perturbations exerting strong effects on the ODN conductivity in agreement with electrochemical (Boon *et al.*, 2000), photophysical (Kelley *et al.*, 1997b) and biochemical (Bhattacharya and Barton, 2001) studies. dsDNA was suggested (Ceres and Barton, 2003) as a promising candidate in molecular electronics under the conditions that the orbitals could efficiently overlap with the electronic states and the environment did not disturb the DNA double helical structure, forming non-native poorly stacked DNA conformations.

DNA-mediated charge transport through DNA self-assemblies at gold electrodes was exploited to examine the effect of the presence of base analogs and DNA damage products in ODN duplexes (Boal and Barton, 2005). General trends in how base modifications affect charge transfer efficiency were found. A decrease in the charge transfer efficiency was caused by: (a) modifications of the Watson–Crick hydrogen bonding system or addition of steric bulk; (b) base structure modification inducing conformational changes such as burying of hydrophilic groups within the DNA double helix. On contrary addition or subtraction of methyl groups, not disrupting hydrogen bonding interactions, did not show a large effect on charge transfer efficiency. No simple correlation between the charge transfer efficiency and DNA melting temperatures was found. It was suggested that the sensitive detection methodology (monitoring the electrocatalytic reduction of MB) might be useful as a possible damage detection for DNA repair enzymes and in diagnostic applications.

The results of Barton's group showed an interesting and convincing picture of charge transfer in relatively short DNA double helices (Drummond *et al.*, 2003). It has been shown in many experiments that efficient charge transfer reactions can occur in short well-stacked ODNs self-assembled at the gold surfaces (Bhattacharya and Barton, 2001; Boal and Barton, 2005; Boon and Barton, 2002, 2003; Boon *et al.*, 2000, 2002a, b, 2003; Ceres and Barton, 2003; Drummond *et al.*, 2003, 2004; Hall *et al.*, 1996; Kelley *et al.*, 1997a, b, 1999a, b, 1998; Nunez *et al.*, 1999; Sam *et al.*, 2001; Wan *et al.*, 1999; Yoo *et al.*, 2003). Recently, several papers have been published which do not show any charge transfer through similar ODN helices under different experimental conditions (Anne *et al.*, 2003; Fan *et al.*, 2003; Immoos *et al.*, 2004a, b; Mao *et al.*, 2003). These papers will be briefly summarized in the following section where we shall return to the problem of the charge transfer in DNA.

6.6. Changes in DNA structure signaling DNA hybridization

After the discovery of the right-handed B-DNA double-helical structure, other DNA structures were found such as local segments of left-handed Z-DNA, cruciform and triplex structures stabilized by DNA supercoiling (Section 5.5.1.2) (Palecek, 1991). Some of them can be formed also by ODNs and/or linear DNA fragments *in vitro* and utilized in DNA hybridization sensors. Stem-loop structure resembling half of a cruciform was the first one applied for this purpose and soon it became popular as an optical molecular beacon. In many of molecular beacons the DNA was labeled with a fluorophore and its quencher at either of its ends. In the folded hairpin-loop DNA structure the quencher was held in close proximity to the fluorophore making this beacon inactive (Figure 30). In the presence of a complementary target DNA a rigid linear DNA duplex was formed, the stem-loop structure was lost and the fluorophore was removed from the quencher proximity making thus possible a strong emission enhancement. In an attempt to create a molecular beacon, which would be potentially useful for miniaturized and parallelized array-based optical assay, its solid-state version was recently introduced (Broude, 2002). Almost in the same

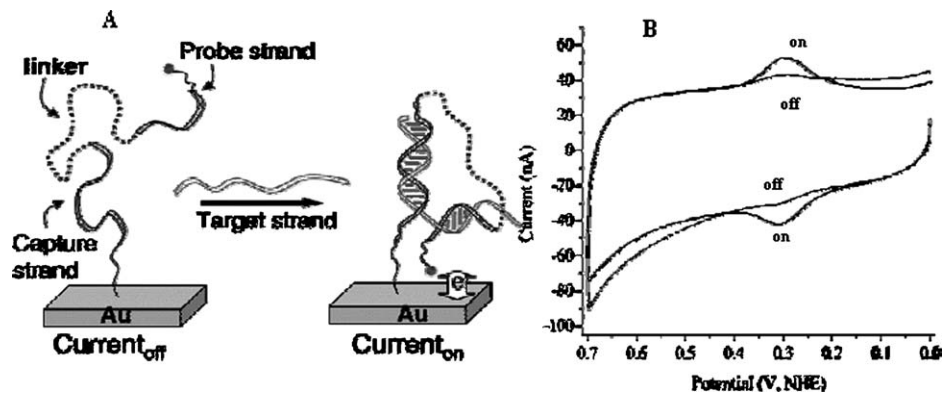


Fig. 30. (A) Electrochemical detection of target nucleic acid sequences using a DNA wrap assay as opposed to a conventional sandwich assay. (B) Cyclic voltammograms of 5'-Fc-DNA-PEG-DNA-SH-3' modified gold ball electrodes in the absence (off) and presence (on) of target DNA (200 nM, Fc-ferrocene, PEG-polyethyleneglycol). (Conditions: 100 mV/s, 25 mM phosphate buffer, 100 mM NaCl, pH 7.0). Adapted from Immoos *et al.* (2004a). Copyright 2004, with permission from the American Chemical Society.

time electrochemical variants of molecular beacon were proposed (Fan *et al.*, 2003; Paleček, 2004). In contrast to solution optical molecular beacon, its surface-attached version used instead of a chemical quencher the gold surface (to which the stem-loop structure was attached) as a solid quenching agent. In the electrochemical sensor the ss ODN was labeled by a redox marker, such as ferrocene (Fan *et al.*, 2003; Immoos *et al.*, 2004a, b) or thionine (Mao *et al.*, 2003) at one of its ends and immobilized via its -SH group at the other end to the gold electrode. In the stem-loop structure redox marker was located close to the electrode surface producing a distinguished cyclic voltammetric redox pair in absence of the complementary target DNA. The voltammetric signals were caused by electron tunnelling between redox marker and the electrode. Hybridization of tDNA with the loops of the stem-loop structures resulted in formation of a rigid rod-like duplex DNA, which moved the redox marker away from the electrode surface. The increase in the distance of the electroactive label from the electrode surface caused a decrease or elimination of the electrochemical signal, because efficiency of electron tunneling decreased exponentially with increasing distance.

After the first excitement with the stem-loop structures (Fan *et al.*, 2003; Paleček, 2004; Thorp, 2004) further papers were published showing that similar results can be obtained using ssODN probes (Anne *et al.*, 2003; Immoos *et al.*, 2004a) instead of the stem-loop structure (Fan *et al.*, 2003; Mao *et al.*, 2003). Anne *et al.* (2003) used 3'-ferrocenylated $-(dT)_{20}$ -5'-cystaminyldisulfide derivative which was chemically reduced to its 5'-ethylthiol form and immobilized to the gold electrode at low surface coverage (corresponding to about 10% of that for a monolayer). The CV responses indicated that all ferrocene markers reached the surface. After exposing the ODN-modified electrode to the complementary $(dA)_{20}$ in 0.1 M NaClO₄ for 2 h the redox response disappeared. No

experiment with non-complementary ssDNA was reported. Immoos *et al.* (2004a) exploited DNA conformational changes that occurred when a surface-attached ODN-poly(ethyleneglycol triblock molecule bound a complementary ODN strand (Figure 30). Immobilized at a gold electrode via its 3'-SH group, the 5'-terminal ferrocene label of this system was repelled from the negatively charged electrode (covered with mercaptopropionic acid) and was thus electrochemically inaccessible. Upon binding the complementary strand to the immobilized capture strand, the former strand bound also the probe segment, forcing the 5'-terminal ferrocene label to a location close to the electrode surface. Using this method a target sequence characteristic for a gene overexpressed in prostate cancer was detected. In difference to the methods based on DNA hairpins (Fan *et al.*, 2003; Immoos *et al.*, 2004a, b; Mao *et al.*, 2003; Steichen and Buess-Herman, 2005) and simple ss probe ODNs (Anne *et al.*, 2003), Immoos *et al.* (2004a) proposed a “signal-on” approach which appears more convenient than the hairpin-based signal-off devices.

In most of the above methods, formation of stem-loop structure and its transformation into a DNA duplex at the electrode surface was expected without providing any evidence that such a process really took place at the surface. Immoos *et al.* (2004b) used ellipsometry to characterize their ferrocene-labeled ODNs at Au(111). Their measurements gave thickness $29 \pm 0.4 \text{ \AA}$ for the hairpin ODN and $41.6 \pm 0.5 \text{ \AA}$ for duplex DNA after the target hybridization. These results agree well with those obtained by Kelley *et al.* (1998) showing about 28 \AA for hairpin and 42 \AA for a duplex. Recently, Steichen and Buess-Herman proposed a label-free method to detect hybridization of complementary ssDNA with the loop of the hairpin immobilized on a polycrystalline gold electrode using impedance spectroscopy in the presence of $[\text{Fe}(\text{CN})_6]^{3-/4-}$ (Steichen and Buess-Herman, 2005). Addition of the complementary ODN to the hairpin probe decreased the electron transfer rate, R_{ct} while an opposite effect was observed when ssDNA probe was used instead of a hairpin (Figure 31). These results were explained by the conformational change of the DNA hairpin probe, due to the DNA hybridization, and by smaller surface concentration of the hairpin as compared to the ssDNA probe. Addition of non-complementary ODN induced no change in the impedance spectra. The above data suggest that the conformation of the hairpin sequence ODN on the surface is different from that of ssDNA and that upon the hybridization, some conformational change is taking place which probably differs from that resulting from hybridization of ssDNA probe with ssDNA target. It can be expected that neutron reflectivity, X-ray photoelectron spectroscopy (XPS), AFM and other methods will provide more detailed picture of the DNA structure and its transitions at the electrode surfaces. Both optical and electrochemical biosensors based on binding-modulated donor-acceptor distances have been recently reviewed by Fan *et al.* (2005).

Taking together, the results in Section 6.5.1 show two strikingly different phenomena: (a) transfer through π -stacked bases in the perfectly matched DNA duplex well documented by J. Barton *et al.* (Boal and Barton, 2005; Ceres and Barton, 2003; Drummond *et al.*, 2003, 2004) and (b) extinction of the charge transfer resulting from the DNA duplex formation at the electrode surface. The reader may ask a question: are these two categories of the experimental results

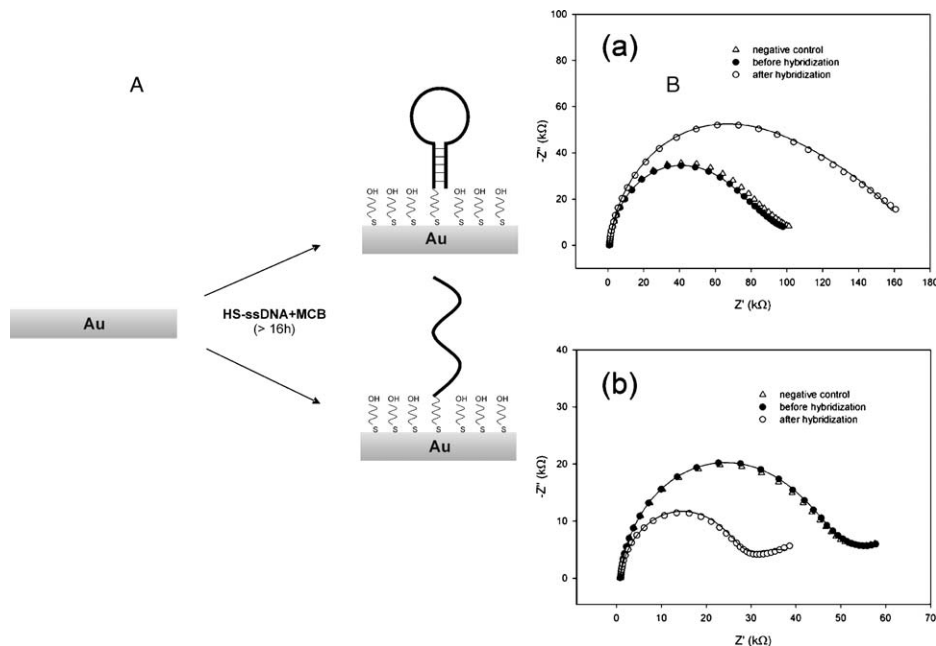


Fig. 31. (A) Representation of the formation of the mixed SAM of thiolated hairpin and linear single-stranded oligonucleotides (HS-ssDNA) and 4-mercaptobutan-1-ol (MCB) at a gold electrode. (B) Impedance spectra of: (a) Au-linear ssDNA/MCB ($x_{DNA} = 0.2$), (b) Au-hairpin ssDNA/MCB ($x_{DNA} = 0.2$) before addition of the complementary strand 1 μ M (●) and a non-complementary strand 1 μ M (Δ), which is a negative control. Measurements performed in a 0.01 M phosphate buffer (pH 7.4) in the presence of $[\text{Fe}(\text{CN})_6]^{3-/4-}$ (5×10^{-3} M, 1:1) at +0.21 V. Adapted from Steichen and Buess-Herman (2005). Copyright 2003, with permission from Elsevier.

in contradiction or can they be both correct and understandable? Before answering this question we may summarize some important differences between experiments mentioned in Sections 6.5.1. In Barton's work always a redox active marker was intercalated in DNA duplex (bound either covalently or non-covalently) and the ODN layer at the gold surface was tightly packed; ODN duplexes were prepared in solution. In experiments summarized in this section neither ferrocene nor thionine (Mao *et al.*, 2003) were intercalated, the packing of the ODN layer was either not mentioned or low density coverage was reported; duplexes were prepared by ODN hybridization at electrode surfaces. There were certainly other differences between the two groups of experiments, but even those mentioned above might be sufficient to start solving of the puzzle. The results of Barton *et al.* (Section 6.5.1) suggest that intercalation of the redox marker and proper packing of the assembly might be critical for the charge transfer through π -stacked bases in DNA duplexes. Considering that the charge transfer through the σ -bonded linker decrease with the linker length (Drummond *et al.*, 2004) we may expect that using two linkers at each ODN ends, as it is the case in experiments in this Section (one linker for $-\text{SH}$ group

and the other one for ferrocene), will substantially decrease the charge transfer. Non-intercalated redox marker, freely interacting with the solvent (compared to intercalated marker in an intimate contact with DNA duplex interior) may represent another obstacle for the charge transfer. In tightly packed self-assembled ODN, duplexes are in upright position, cannot lay flatly at the surface and are not exposed to surface interaction which may disturb the electronic structure of the DNA duplex (Sections 5 and 6).

So far the above two approaches and their experimental settings were isolated and no explanation (based on experimental testing) of the observed differences in dsDNA conductivity was offered. We believe that performing well-designed tests should be relatively easy and comparable testing of these two different approaches may help to understand better electrical properties of DNA.

7. ELECTROCHEMICAL DNA BIOSENSORS: FUTURE PROSPECTS

This book (Chapters 4–13) reflects tremendous progress in the research and development of biosensors for DNA hybridization and DNA damage reached in the last decade. At present, electrochemical detection of a specific nucleotide sequence in relatively short ODNs (about 15–30 nucleotides) can be easily performed. Also determination of single-base mismatches (Bhattacharya and Barton, 2001; Kelley *et al.*, 1999b; Palecek *et al.*, 2004; Sosnowski *et al.*, 1997) is now possible (Chapters 4, 5 and 19). The practical DNA analysis is, however, done with amplified DNA fragments, which are usually much longer than 30-mer ODNs. Most of the electrochemical experiments have been, however, carried out with model ODNs and only a smaller fraction of the experimental work was performed with PCR-amplified DNA fragments (Fojta *et al.*, 2004a; Kara *et al.*, 2003; Ozkan *et al.*, 2002; Ozsoz *et al.*, 2003; Palecek *et al.*, 2002c, d; Patolsky *et al.*, 2001, 2002; Wang *et al.*, 2001b) (Section 5). It was shown that, using the double surface technique, sequence and length of even very long repetitive nucleotide sequences (> 2000 base pairs) can be determined electrochemically (Section 6.2).

On the other hand, electrochemical detection of non-amplified DNA has not been reported. DNA in a human cell contains about 3×10^9 base pairs. Let us imagine that we wish to detect an exact 30-nucleotide sequence in human DNA. It would be necessary to find it in an excess of 10^8 base pairs. This would be perhaps more difficult than to look for a needle in a haystack. Recently, reached tremendous increase in sensitivity of the DNA detection (Chapter 11, Section 6.2) raises hopes that the sensitivity necessary for the detection of non-amplified DNA will soon be available. The solution of the problem of extremely high selectivity of the DNA determination in a very large excess of non-complementary DNA will require more work. Detection of non-amplified DNA represents thus a challenge, which can be met by using most sensitive single- and double-surface methods employing electrode miniaturization and amplification of the electrochemical signals, including electrocatalysis. Double surface techniques might be particularly successful in attempts to significantly increase both the sensitivity and selectivity of the DNA and RNA detection. In the last decade, DNA electrochemical analysis made a great progress and it is

not excluded that using the known principles, determination of nucleotide sequences in non-amplified DNA from prokaryotes will become possible. Analysis of RNA, which has obtained little attention among electrochemists, may represent another interesting challenge for future research. We believe that for the same analysis of human chromosomal DNA new principles should be sought to overcome the problem of insufficient selectivity of the present methods.

8. SUMMARY AND CONCLUSION

Electroactivity of nucleic acids was discovered about 45 years ago. It was shown that at mercury electrodes adenine and cytosine were reduced in ssDNA, while guanine produced an anodic signal due to oxidation of guanine reduction product. About 15 years later it was shown that oxidation of guanine and adenine took place at carbon electrodes. DNA signals at mercury electrodes were highly sensitive to changes in DNA structure due to DNA denaturation and renaturation as well as to minor structural changes resulting from DNA premelting and DNA damage. Changes in DNA structure were reflected not only by the DNA faradaic responses but also by non-faradaic signals due to adsorption/desorption of DNA. Also RNA signals responded to changes in RNA structure but compared to DNA much less work was done.

Methods working with small voltage excursions during the drop lifetime (of the dropping mercury electrode), such as DPP, reflected changes of DNA structure in solution. On the other hand, methods working with large voltage excursions or experiments with HMDE disclosed changes in dsDNA structure occurring secondarily at the electrode surface. At neutral pH and weakly alkaline pHs DNA surface denaturation occurred in a narrow potential range (around -1.2 V against SCE) and was relatively slow. DNA surface denaturation depended on DNA ionization showing differences in the DNA behavior at alkaline and acidic pHs. Recently, DNA unwinding was observed at other negatively charged electrodes and other surfaces.

Already in the 1960s polarographic behavior of organic compounds weakly bound to DNA was studied and in the beginning of the 1980s electroactive osmium labels were covalently bound to DNA and used as probes of the DNA structure. In the middle of the 1980s DNA-modified electrodes were introduced, which then have become increasingly popular, particularly in relation to the development of the DNA sensors.

In the 1990s, dramatic progress in biochemistry and molecular biology and particularly advances in nucleotide sequencing of genomes of different organisms (including the human genome) stimulated interest in DNA hybridization sensors. In addition to sensors with optical detection, electrochemical detection showed great promise because of a number of advantages and particularly simple design, low energy requirements and low cost. By the end of the century, a number of conceptions of electrochemical sensor were available based on carbon, gold or ITO electrodes, differing in the ways of DNA immobilization at the electrode surface and methods of DNA detection. In these methods both the

DNA hybridization (specific interaction of complementary DNA with the immobilized DNA probe resulting in formation of a DNA duplex) and detection of the DNA hybridization event were performed at the same surface. In the beginning of the 2000s a new conception was introduced in which hybridization was performed at one surface (optimized for DNA hybridization) and DNA detection at another surface. This double-surface technique has some advantages but is more complicated, requiring some microfluidic system if incorporated in DNA arrays. At present time, various electrochemical sensors for DNA hybridization are available which can be used for determination of specific nucleotide sequences, DNA point mutations and lengths of long repetitive sequences in amplified DNA fragments. Remarkable sensitivities of the electrochemical DNA determination were reached in recent years. Determination of a specific DNA sequence in a genome without amplification of DNA remains, however, a challenge, because of very high excess of non-complementary DNA in the analyzed samples requiring enormous selectivity of the analysis.

Several interesting principles have been used in the development of the DNA sensors. They include:

1. *Amplified electrochemical analysis* (Chapter 5) involving electrocatalytic and biocatalytic reactions and labeling of DNA (involved in the recognition process) by micro- and nanoparticles (Chapter 11). These approaches (some of them completely new) helped to greatly increase the sensitivity of the DNA analysis. Particularly promising appears the combination of electrochemical and biochemical principles, including the use of catalytic nucleic acids such as ribozymes and DNA enzymes.
2. *Investigation of charge transport* between a redox indicator intercalated in dsDNA and a gold electrode covered with self-assembled monolayer (SAM) of DNA. This charge transport is inhibited by disturbances in the DNA base stacking, such as single-base mismatches or certain kinds of DNA damage. It can be expected that further investigation of this charge transport will help to understand better the electrical properties of DNA.
3. *Tracing of changes in conformation of DNA* covalently bound to the electrode surface and effect of the electrode charge on the DNA conformation. Such experiments represent not only an elegant way of the detection of the DNA hybridization but they can provide biologically relevant information about the DNA structure at charged surfaces. Moreover, the rate of DNA hybridization or denaturation can be influenced by controlling the charge of the electrode to which DNA is immobilized.
4. *Application of conductive polymers* (Chapters 8 and 9) and other interesting approaches (Gibbs *et al.*, 2005; Hwang *et al.*, 2005; Park and Hahn, 2004) which may find use in further development of the DNA sensors.

There is no doubt that at present time sensors for DNA hybridization and DNA damage (Chapters 12 and 13) lead the field of the electrochemistry of nucleic acids. Generally, these trends are beneficial for this research field but the increasing interest in electrochemical DNA sensors results, in some cases, in production of papers, which are scientifically superficial or too technical. It appears probable that DNA sensors will be successfully commercialized soon. This

would require further research into nucleic acid electrochemistry to improve the first commercial devices. On the other hand, it cannot be excluded that the development of the electrochemical DNA sensors will not win the race (what I consider as a less probable case) and some other types of inexpensive DNA sensors will become commercially successful. Even in such a case, electrochemistry of nucleic acids will remain an important scientific field because of its relevance to a number of biological and biochemical problems.

LIST OF ABBREVIATIONS

A	adenine
a.c.	alternating current
AdTS	adsorptive transfer stripping
AFM	atomic force microscopy
C	cytosine
cd	closed duplex
CPSA	constant current chronopotentiometric stripping analysis
CV	cyclic voltammetry
DBT	Dynabeads oligo(T)
d.c.	direct current
DE	detection electrode
DM	daunomycin
DME	mercury dropping electrode
DPP	differential (derivative) pulse polarography
DPV	differential (derivative) pulse voltammetry
ds	double-stranded
DST	double-surface technique
EIS	electrochemical impedance spectroscopy
EVLS	elimination voltammetry with linear scan
FRDA	Friedreich ataxia
FTIR	Fourier transform infrared spectroscopy
G	guanine
GCE	glassy carbon electrode
H	hybridization surface
HMDE	hanging mercury drop electrode
HPLC	high-performance liquid chromatography
ITO	indium tin-oxide
LS	linear sweep
LSV	linear sweep voltammetry
m-AgSAE	mercury-modified silver solid amalgam electrode
MB	methylene blue
m-CuSAE	mercury-modified copper solid amalgam electrode
m-SAE	mercury meniscus-modified solid amalgam electrode
NA	nucleic acid

NC	nitrocellulose
NPP	normal pulse polarography
oc	open circular
ODN	oligodeoxyribonucleotides
ORN	oligoribonucleotides
PCR	polymerase chain reaction
PNA	peptide nucleic acid
poly(A)	polydeoxyadenylic acid
poly(rA)	polyriboadenylic acid
p-SAE	polished solid amalgam electrode
p.z.c.	potential of zero charge
RP	reporter probe
SAE	solid amalgam electrode
SAM	self-assembled monolayer
sc	supercoiled
SCE	saturated calomel electrode
SPR	surface plasmon resonance
ss	single-stranded
SST	single-surface technique
STM	scanning tunneling microscopy
SWV	square wave voltammetry
tDNA	target DNA
tm	temperature of melting
XPS	X-ray photoelectron spectroscopy
σ	density

ACKNOWLEDGMENTS

The authors are indebted to Drs. M. Fojta, L. Havran and V. Dorcak for critical reading of the manuscript and stimulating discussion. This work was supported by a grant IBS 5004355 of the Academy of Sciences of the Czech Republic.

REFERENCES

- Adams, R.N., 1969, *Electrochemistry at Solid Electrodes*, Marcel Dekker, New York.
- Adrian, M., B. ten Heggeler-Bordier, W. Wahli, A.Z. Stasiak, A. Stasiak and D. Dubochet, 1990, Direct visualization of supercoiled DNA molecules in solution, *EMBO J.* 9, 4551.
- Analytica Chimica Acta*, 2003, *Anal. Chim. Acta*, Special issue (No. 1) on emerging technologies for nucleic acid analysis 469, 1.
- Anne, A., A. Bouchardon and J. Moiroux, 2003, 3'-ferrocene-labeled oligonucleotide chains end-tethered to gold electrode surfaces: Novel model systems for exploring flexibility of short DNA using cyclic voltammetry, *J. Am. Chem. Soc.* 125, 1112.
- Anson, F.C., J.B. Flanagan, K. Takahashi and A. Yamada, 1976, Some virtues of differential pulse polarography in examining adsorbed reactants, *J. Electroanal. Chem.* 67, 253.

- Arias, Z.G., J.L.M. Alvarez and J.M.L. Fonseca, 2004, Electrochemical characterization of the self-assembled monolayer of 6-thioguanine on the mercury electrode, *Electroanalysis* 16, 1044.
- Armistead, P.M. and H.H. Thorp, 2000, Modification of indium tin oxide electrodes with nucleic acids: Detection of attomole quantities of immobilized DNA by electrocatalysis, *Anal. Chem.* 72, 3764.
- Armistead, P.M. and H.H. Thorp, 2001, Oxidation kinetics of guanine in DNA molecules adsorbed onto indium tin oxide electrodes, *Anal. Chem.* 73, 558.
- Armstrong, F. A., R. Camba, H. A. Heering, J. Hirst, L. J. C. Jeuken, A. K. Jones, C. Leger and J. P. McEvoy, 2000, Fast voltammetric studies of the kinetics and energetics of coupled electron-transfer reactions in proteins, *Faraday Discuss.* 191.
- Armstrong, N.R., A.W.C. Lin, M. Fujihira and T. Kuwana, 1976, Electrochemical and surface characteristics of tin oxide and indium oxide electrodes, *Anal. Chem.* 48, 741.
- Azek, F., C. Grossiord, M. Joannes, B. Limoges and P. Brossier, 2000, Hybridization assay at a disposable electrochemical biosensor for the attomole detection of amplified human cytomegalovirus DNA, *Anal. Biochem.* 284, 107.
- Babkina, S.S., E.P. Medyantseva, H.C. Budnikov and M.P. Tyshiek, 1996, New variants of enzyme immunoassay of antibodies to DNA, *Anal. Chem.* 68, 3827.
- Babkina, S.S. and N.A. Ulakhovich, 2004, Amperometric biosensor based on denatured DNA for the study of heavy metals complexing with DNA and their determination in biological, water and food samples, *Bioelectrochemistry* 63, 261.
- Babkina, S.S., N.A. Ulakhovich and Y.I. Zyavkina, 2000, Determination of platinum in pharmaceuticals and biological objects using an amperometric biosensor based on deoxyribonucleic acid, *Ind. Lab.* 66, 779.
- Babkina, S.S., N.A. Ulakhovich and Y.I. Zyavkina, 2004, Amperometric DNA biosensor for the determination of auto-antibodies using DNA interaction with Pt(II) complex, *Anal. Chim. Acta* 502, 23.
- Babkina, S.S., N.A. Ulakhovich, Y.I. Zyavkina and E.N. Moiseeva, 2003, Adsorption of lead(II) and cadmium(II) ions on the surface of a cellulose membrane modified with denatured deoxyribonucleic acid, *Russian J. Phys. Chem.* 77, 797.
- Baca, A.J., F.M. Zhou, J. Wang, J.B. Hu, J.H. Li, J.X. Wang and Z.S. Chikneyan, 2004, Attachment of ferrocene-capped gold nanoparticle-streptavidin conjugates onto electrode surfaces covered with biotinylated biomolecules for enhanced voltammetric analysis, *Electroanalysis* 16, 73.
- Bagel, O., C. Degrand, B. Limoges, M. Joannes, F. Azek and P. Brossier, 2000, Enzyme affinity assays involving a single-use electrochemical sensor. Applications to the enzyme immunoassay of human chorionic gonadotropin hormone and nucleic acid hybridization of human cytomegalovirus DNA, *Electroanalysis* 12, 1447.
- Banica, F.G. and A. Ion, 2000, Electrocatalysis-based kinetic determinations, *Encyclopedia of Analytical Chemistry*, Ed. R.A. Meyers, Wiley, Chichester, 11115.
- Barbara, P. F. and E. J. C. Olson, 1999, Experimental electron transfer kinetics in a DNA environment. Electron transfer from isolated molecules to biomolecules, Pt 2. Vol. 107, *Ad. Chem. Phys.* 647.
- Bard, A.J. and L.R. Faulkner, 2000, *Electrochemical Methods: Fundamentals and Applications*, Wiley, New York.
- Barker, G.C. and D. McKeown, 1976, Modulation polarography of DNA and some types of RNA, *Bioelectrochem. Bioenerg.* 3, 373.
- Bates, A.D. and A. Maxwell, 1993, *DNA Topology*, Ed. D. Male, Oxford University Press, Oxford.
- Baughman, R.H., A.A. Zakhidov and W.A. de Heer, 2002, Carbon nanotubes – the route toward applications, *Science* 297, 787.
- Bednar, J., P. Furrer, A. Stasiak, J. Dubochet, E.H. Egelman and A.D. Bates, 1994, The twist, writhe and overall shape of supercoiled DNA change during counterion-induced transition from a loosely to a tightly interwound superhelix: Possible implications for DNA structure *in vivo*, *J. Mol. Biol.* 235, 825.

- Belotserkovskii, B.P. and B.H. Johnston, 1996, Polypropylene tube surfaces may induce denaturation and multimerization of DNA, *Science* 271, 222.
- Belotserkovskii, B.P. and B.H. Johnston, 1997, Denaturation and association of DNA sequences by certain polypropylene surfaces, *Anal. Biochem.* 251, 251.
- Bensimon, D., A.J. Simon, V. Croquette and A. Bensimon, 1995, Stretching DNA with a receding meniscus – Experiments and models, *Phys. Rev. Lett.* 74, 4754.
- Berg, H., 1957, Polarographische untersuchungen an nucleinsäuren und nucleasen. I. Mitt. Polarographische nachweis von proteinen neben nucleinsäuren, *Biochem. Z.* 329, 274.
- Berg, H., 1976, Polarographic possibilities in protein and nucleic acid research, *Top. Bioelectrochem. Bioenerg.*, Vol. 1, Ed. G. Milazzo, Wiley, London, 39.
- Bevilacqua, P.C., 2003, Mechanistic considerations for general acid-base catalysis by RNA: Revisiting the mechanism of the hairpin ribozyme, *Biochemistry* 42, 2259.
- Bhattacharya, P.K. and J.K. Barton, 2001, Influence of intervening mismatches on long-range guanine oxidation in DNA duplexes, *J. Am. Chem. Soc.* 123, 8649.
- Biosensors and Bioelectronics, 2004, *Biosensors Bioelectron.* (Iss. 5), DNA biosensors, characterization and applications, 20, 917.
- Bloomfield, V.A., 1996, DNA condensation, *Curr. Opin. Struct. Biol.* 6, 334.
- Boal, A.K. and J.K. Barton, 2005, Electrochemical detection of lesions in DNA, *Bioconjugate Chem.* 16, 312.
- Bockris, J.M.O., B.E. Conway and R.E. White, Eds., 1999, *Modern Aspects of Electrochemistry*, Kluwer Academic/Plenum Press, New York.
- Bond, A.M., 1980, *Modern Polarographic Methods in Analytical Chemistry*, Marcel Dekker, New York.
- Boon, E.M. and J.K. Barton, 2002, Charge transport in DNA, *Curr. Opin. Struct. Biol.* 12, 320.
- Boon, E.M. and J.K. Barton, 2003, DNA electrochemistry as a probe of base pair stacking in A-, B-, and Z-form DNA, *Bioconjugate Chem.* 14, 1140.
- Boon, E.M., J.K. Barton, P.I. Pradeepkumar, J. Isaksson, C. Petit and J. Chattopadhyaya, 2002b, An electrochemical probe of DNA stacking in an antisense oligonucleotide containing a C3'-endo-locked sugar, *Angew. Chem. Int. Ed.* 41, 3402.
- Boon, E.M., D.M. Ceres, T.G. Drummond, M.G. Hill and J.K. Barton, 2000, Mutation detection by electrocatalysis at DNA-modified electrodes, *Nat. Biotechnol.* 18, 1096.
- Boon, E.M., N.M. Jackson, M.D. Wightman, S.O. Kelley, M.G. Hill and J.K. Barton, 2003, Intercalative stacking: A critical feature of DNA charge-transport electrochemistry, *J. Phys. Chem. B* 107, 11805.
- Boon, E.M., J.E. Salas and J.K. Barton, 2002a, An electrical probe of protein-DNA interactions on DNA-modified surfaces, *Nat. Biotechnol.* 20, 282.
- Boublikova, P., M. Vojtiskova and E. Palecek, 1987, Determination of submicrogram quantities of circular duplex DNA in plasmid samples by adsorptive stripping voltammetry, *Anal. Lett.* 20, 275.
- Brabec, V., 1974, Influence of adsorbability of denatured deoxyribonucleic acid on its polarographic reducibility, *J. Electroanal. Chem.* 50, 235.
- Brabec, V., 1980, Interaction of nucleic acids with electrically charged surfaces. VII. The effect of ionic strength of neutral medium on the conformation of DNA adsorbed on the mercury electrode, *Biophys. Chem.* 11, 1.
- Brabec, V., 1981, Nucleic acid analysis by voltammetry at carbon electrodes, *Bioelectrochem. Bioenerg.* 8, 437.
- Brabec, V., 1983, Polarographic reducibility of polyuridylic acid, *Gen. Physiol. Biophys.* 2, 193.
- Brabec, V. and G. Dryhurst, 1978, Electrochemical oxidation of polyadenylic acid at graphite electrodes, *J. Electroanal. Chem.* 91, 219.
- Brabec, V., V. Glezers and V. Kadysh, 1983, Adsorption of deoxyribonucleic acid at mercury electrodes from alkaline solutions of higher ionic strength, *Coll. Czech. Chem. Commun.* 48, 1257.
- Brabec, V. and A.P. Kavunenko, 1987, Interfacial behaviour of oligoriboadenylates at the mercury-solution interfaces, *J. Electroanal. Chem.* 237, 261.

- Brabec, V. and K. Niki, 1985, Raman scattering from nucleic acids adsorbed at a silver electrode, *Biophys. Chem.* 23, 63.
- Brabec, V. and E. Palecek, 1970a, The influence of salt and pH on polarographic currents produced by denatured DNA, *Biophysik* 6, 290.
- Brabec, V. and E. Palecek, 1970b, The reducibility of polynucleotides and their a.c. polarographic behaviour, *J. Electroanal. Chem.* 27, 145.
- Brabec, V. and E. Palecek, 1972, Adsorption of single-stranded and double-helical polynucleotides on the mercury electrode, *Biopolymers* 11, 2577.
- Brabec, V. and E. Palecek, 1973, Interaction of polyadenylic acid with the mercury electrode, *Z. Naturforsch.* 28c, 685.
- Brabec, V. and E. Palecek, 1974, Polarographic reduction of adenine and cytosine residues in denatured DNA, *Z. Naturforsch.* 29c, 323.
- Brabec, V. and E. Palecek, 1976a, Interaction of nucleic acids with electrically charged surfaces. II. Conformational changes in double-helical polynucleotides, *Biophys. Chem.* 4, 79.
- Brabec, V. and E. Palecek, 1976b, Interaction of nucleic acids with electrically charged surfaces. III. Surface denaturation of DNA on the mercury electrode in two potential regions, *Stud. Biophys.* 60, 105.
- Brabec, V. and E. Palecek, 1978, Interactions of nucleic acids with electrically charged surface. Part IV. Local changes in the structure of DNA adsorbed on mercury electrode in the vicinity of zero charge, *J. Electroanal. Chem.* 88, 373.
- Brabec, V., V. Vetterl and O. Vrana, 1996, Electroanalysis of biomacromolecules. Experimental techniques in bioelectrochemistry, *Bioelectrochemistry: Principles and Practice*, Vol. 3, Eds. V. Brabec, D. Walz and G. Milazzo, Birkhauser Verlag, Basel, Switzerland, 287.
- Brazill, S.A., P. Singhal and W.G. Kuhr, 2000, Detection of native amino acids and peptides utilizing sinusoidal voltammetry, *Anal. Chem.* 72, 5542.
- Brett, C.M.A. and A.M.O. Brett, 1993, *Electrochemistry, Principles, Methods, and Applications*, Oxford University Press, Oxford.
- Broude, N.E., 2002, Stem-loop oligonucleotides: A robust tool for molecular biology and biotechnology, *Trends Biotechnol.* 20, 249.
- Brucknerlea, C., J. Janata, J. Conroy, A. Pungor and K. Caldwell, 1993, Scanning-tunneling-microscopy on a mercury sessile drop, *Langmuir* 9, 3612.
- Brucknerlea, C., R.J. Kimmel, J. Janata, J.F.T. Conroy and K. Caldwell, 1995, Electrochemical studies of octadecanethiol and octanethiol films on variable surface-area mercury sessile drops, *Electrochim. Acta* 40, 2897.
- Budker, V.G., A.A. Godovikov, L.P. Naumova and I.A. Slepneva, 1980, Interaction of polynucleotides with natural and model membranes, *Nucleic Acids Res.* 8, 2499.
- Cahova-Kucharikova, K., M. Fojta, T. Mozga and E. Palecek, 2005, Use of DNA repair enzymes in electrochemical detection of damage to DNA bases *in vitro* and in cells, *Anal. Chem.* 77, 2920.
- Cai, H., X.N. Cao, Y. Jiang, P.G. He and Y.Z. Fang, 2003b, Carbon nanotube-enhanced electrochemical DNA biosensor for DNA hybridization detection, *Anal. Bioanal. Chem.* 375, 287.
- Cai, X., G. Rivas, P.A.M. Farias, H. Shirashi, J. Wang, M. Fojta and E. Palecek, 1996, Trace measurements of plasmid DNAs by adsorptive stripping potentiometry at carbon paste electrodes, *Bioelectrochem. Bioenerg.* 401, 41.
- Cai, X., G. Rivas, H. Shirashi, P. Farias, J. Wang, M. Tomschik, F. Jelen and E. Palecek, 1997, Electrochemical analysis of formation of polynucleotide complexes in solution and at electrode surfaces, *Anal. Chim. Acta* 344, 64.
- Cai, H., Y. Xu, P.G. He and Y.Z. Fang, 2003a, Indicator free DNA hybridization detection by impedance measurement based on the DNA-doped conducting polymer film formed on the carbon nanotube modified electrode, *Electroanalysis* 15, 1864.
- Campuzano, V., L. Montermini, M.D. Molto, L. Pianese, M. Cossee, F. Cavalcanti, E. Monros, F. Rodius, F. Duclos, A. Monticelli, F. Zara, J. Canizares, H. Koutnikova, S.I. Bidichandani, C. Gellera, A. Brice, P. Trouillas, G. DeMichele, A. Filla, R. DeFrutos,

- F. Palau, P.I. Patel, S. DiDonato, J.L. Mandel, S. Coccozza, M. Koenig and M. Pandolfo, 1996, Friedreich's ataxia: Autosomal recessive disease caused by an intronic GAA triplet repeat expansion, *Science* 271, 1423.
- Carter, M.T. and A.J. Bard, 1987, Voltammetric studies of the interaction of tris (1,10-phenanthroline) cobalt(III) with DNA, *J. Am. Chem. Soc.* 109, 7528.
- Carter, M.T., M. Rodriguez and A.J. Bard, 1989, Voltammetric studies of the interaction of metal-chelates with DNA. 2. Tris-chelated complexes of cobalt(III) and iron(II) with 1,10-phenanthroline and 2,2'-bipyridine, *J. Am. Chem. Soc.* 111, 8901.
- Ceres, D.M. and J.K. Barton, 2003, In situ scanning tunneling microscopy of DNA-modified gold surfaces: Bias and mismatch dependence, *J. Am. Chem. Soc.* 125, 14964.
- Chi, Q.J., J.D. Zhang, J.E.T. Andersen and J. Ulstrup, 2001, Ordered assembly and controlled electron transfer of the blue copper protein azurin at gold (111) single-crystal substrates, *J. Phys. Chem. B* 105, 4669.
- Chrisley, L.A., G.U. Lee and C.E. Oferrall, 1996, Covalent attachment of synthetic DNA to self-assembled monolayer films, *Nucleic Acids Res.* 24, 3031.
- Clausen-Schaumann, H., M. Rief, C. Tolksdorf and H.E. Gaub, 2000, Mechanical stability of single DNA molecules, *Biophys. J.* 78, 1997.
- Cosnier, S., 1999, Biomolecule immobilization on electrode surfaces by entrapment or attachment to electrochemically polymerized films. A review, *Biosensors and Bioelectron.* 14, 443.
- Creager, S., C.J. Yu, C. Bamdad, S. O'Connor, T. MacLean, E. Lam, Y. Chong, G.T. Olsen, J.Y. Luo, M. Gozin and J.F. Kayyem, 1999, Electron transfer at electrodes through conjugated "molecular wire" bridges, *J. Am. Chem. Soc.* 121, 1059.
- Daniel, F.B. and E.J. Behrman, 1976a, Osmium(VI) complexes of the 3',5'-dinucleoside monophosphates, ApU and UpA, *Biochemistry* 15, 565.
- Daniel, F.B. and E.J. Behrman, 1976b, Reactions of oxoosmium ligand complexes with nucleosides, *J. Am. Chem. Soc.* 97, 7352.
- de-los-Santos-Alvarez, P., M.J. Lobo-Castanon, A.J. Miranda-Ordieres and P. Tunon-Blanco, 2005, Electrocatalytic oxidation of NADH by Brilliant Cresyl Blue-DNA intercalation adduct, *Electrochim. Acta* 50, 1107.
- Del Pozo, M.V., C. Alonso, F. Pariente and E. Lorenzo, 2005, Electrochemical DNA sensing using osmium complexes as hybridization indicators, *Biosensors Bioelectron.* 20, 1549.
- Dracka, O., 1996, Theory of current elimination in linear voltammetry, *J. Electroanal. Chem.* 402, 18.
- Drummond, T.G., M.G. Hill and J.K. Barton, 2003, DNA-based electrochemical sensors, *Nat. Biotechnol.* 21, 1192.
- Drummond, T.G., M.G. Hill and J.K. Barton, 2004, Electron transfer rates in DNA films as a function of tether length, *J. Am. Chem. Soc.* 126, 15010.
- Eckhardt, E., M. Espenhanh, N. Napier, N.D. Popovich, H.H. Thorp and R. Witver, 2001, DNA Arrays: Technologies and Experimental Strategies, Ed. E.V. Grigonenko, CRC Press, Boca Raton, FL, 39.
- Eddy, S.R., 2001, Non-coding RNA genes and the modern RNA world, *Nat. Rev. Gen.* 2, 919.
- Erdem, A. and M. Ozsoz, 2002, Electrochemical DNA biosensors based on DNA-drug interactions, *Electroanalysis* 14, 965.
- Fan, C., K.W. Plaxco and A.J. Heeger, 2003, Electrochemical interrogation of conformational changes as a reagentless method for the sequence-specific detection of DNA, *Proc. Natl. Acad. Sci. USA* 100, 9134.
- Fan, C., K.W. Plaxco and A.J. Heeger, 2005, Biosensors based on binding-modulated donor-acceptor distances, *Trends Biotechnol.* 23, 186.
- Fan, C., H. Song, X. Hu, G. Li, J. Zhu, X. Xu and D. Zhu, 1999, Voltammetric response and determination of DNA with a silver electrode, *Anal. Biochem.* 271, 1.
- Ferapontova, E.E. and E. Dominguez, 2003, Direct electrochemical oxidation of DNA on polycrystalline gold electrodes, *Electroanalysis* 15, 629.
- Filipski, J., J. Chmielowski and M. Chorazy, 1971, Polarographic behaviour of deoxyribonucleic acid, *Biochim. Biophys. Acta* 232, 451.

- Finklea, H.O., 1996, Electrochemistry of organized monolayers of thiols and related molecules on electrodes, *Electroanalytical Chemistry*, Vol. 19, Eds. A.J. Bard and I. Rubinstein, Marcel Dekker, New York, 109.
- Finklea, H.O., 2000, Self-assembled monolayers on electrodes, *Encyclopedia of Analytical Chemistry*, Vol. 11, Ed. R.A. Meyers, Wiley, New York, 10090.
- Flanagan, J.B., K. Takanashi and F.C. Anson, 1977, Reactant adsorption in differential pulse polarography. Effects of adsorptive depletion of reactant, non-linear adsorption isotherms and uncompensated resistance, *J. Electroanal. Chem.* 81, 261.
- Flemming, J., 1968, Über die Adsorption von DNS in der Grenzfläche Quecksilber-Elektrolyt, *Biopolymers* 6, 1697.
- Flemming, J. and J. Berg, 1974, On the association of DNA at the mercury|electrolyte interface, *Bioelectrochem. Bioenerg.* 1, 459.
- Fojta, M., 2002, Electrochemical sensors for DNA interactions and damage, *Electroanalysis* 14, 1449.
- Fojta, M., 2004, Mercury electrodes in nucleic acid electrochemistry: Sensitive analytical tools and probes of DNA structure. A review, *Coll. Czech. Chem. Commun.* 69, 715.
- Fojta, M., R.P. Bowater, V. Stankova, L. Havran, D.M.J. Lilley and E. Palecek, 1998, Two superhelix density-dependent DNA transitions detected by changes in DNA adsorption/desorption behavior, *Biochemistry* 37, 4853.
- Fojta, M., L. Havran, S. Billova, P. Kostecka, M. Masarik and R. Kizek, 2003, Two-surface strategy in electrochemical DNA hybridization assays: Detection of osmium-labeled target DNA at carbon electrodes, *Electroanalysis* 15, 431.
- Fojta, M., L. Havran, J. Fulneckova and T. Kubicarova, 2000, Adsorptive transfer stripping AC voltammetry of DNA complexes with intercalators, *Electroanalysis* 12, 926.
- Fojta, M., L. Havran, R. Kizek and S. Billova, 2002, Voltammetric microanalysis of DNA adducts with osmium tetroxide, 2,2'-bipyridine using a pyrolytic graphite electrode, *Talanta* 56, 867.
- Fojta, M., L. Havran, R. Kizek, S. Billova and E. Palecek, 2004b, Multiply osmium-labeled reporter probes for electrochemical DNA hybridization assays: Detection of trinucleotide repeats, *Biosensors Bioelectron.* 20, 985.
- Fojta, M., L. Havran and E. Palecek, 1997a, Chronopotentiometric detection of DNA strand breaks with mercury electrodes modified with supercoiled DNA, *Electroanalysis* 9, 1033.
- Fojta, M., L. Havran, M. Vojtiskova and E. Palecek, 2004a, Electrochemical detection of DNA triplet repeat expansion, *J. Am. Chem. Soc.* 126, 6532.
- Fojta, M. and E. Palecek, 1997, Supercoiled DNA-modified mercury electrode: A highly sensitive tool for the detection of DNA damage, *Anal. Chim. Acta* 342, 1.
- Fojta, M., V. Vetterl, M. Tomschik, F. Jelen, P. Nielsen, J. Wang and E. Palecek, 1997b, Adsorption of peptide nucleic acid and DNA decamers at electrically charged surfaces, *Biophys. J.* 72, 2285.
- Fu, Y.Z., R. Yuan, L. Xu, Y.Q. Chai, Y. Liu, D.P. Tang and Y. Zhang, 2005, Electrochemical impedance behavior of DNA biosensor based on colloidal Ag and bilayer two-dimensional sol-gel as matrices, *J. Biochem. Biophys. Methods* 62, 163.
- Gibbs, J.M., S.J. Park, D.R. Anderson, K.J. Watson, C.A. Mirkin and S.T. Nguyen, 2005, Polymer-DNA hybrids as electrochemical probes for the detection of DNA, *J. Am. Chem. Soc.* 127, 1170.
- Giese, B. and S. Wessely, 2001, The significance of proton migration during hole hopping through DNA, *Chem. Commun.*, 2108.
- Gooding, J.J., 2002, Electrochemical DNA hybridization biosensors, *Electroanalysis* 14, 149.
- Gooding, J.J., F. Mearns, W.R. Yang and J.Q. Liu, 2003a, Self-assembled monolayers into the 21(st) century: Recent advances and applications, *Electroanalysis* 15, 81.
- Gooding, J.J., R. Wibowo, J.Q. Liu, W.R. Yang, D. Losic, S. Orbons, F.J. Mearns, J.G. Shapter and D.B. Hibbert, 2003b, Protein electrochemistry using aligned carbon nanotube arrays, *J. Am. Chem. Soc.* 125, 9006.
- Gray, D.E., S.C. CaseGreen, T.S. Fell, P.J. Dobson and E.M. Southern, 1997, Ellipsometric and interferometric characterization of DNA probes immobilized on a combinatorial array, *Langmuir* 13, 2833.

- Grinstaff, M.W., 1999, How do charge travel in DNA?, *Angew. Chem. Int. Ed.* 38, 3629.
- Grover, N. and H.H. Thorp, 1991, Efficient electrocatalytic and stoichiometric oxidative cleavage of DNA by oxoruthenium(IV), *J. Am. Chem. Soc.* 113, 7030.
- Hall, D.B., R.E. Holmlin and J.K. Barton, 1996, Oxidative DNA damage through long-range electron transfer, *Nature* 382, 731.
- Hason, S., J. Dvorak, F. Jelen and V. Vetterl, 2002a, Interaction of DNA with echinomycin at the mercury electrode surface as detected by impedance and chronopotentiometric measurements, *Talanta* 56, 905.
- Hason, S., J. Dvorak, F. Jelen and V. Vetterl, 2002b, Impedance analysis of DNA and DNA-drug interactions on thin mercury film electrodes, *Crit. Rev. Anal. Chem.* 32, 167.
- Havran, L., M. Fojta and E. Palecek, 2004, Voltammetric behavior of DNA modified with osmium tetroxide 2,2'-bipyridine at mercury electrodes, *Bioelectrochemistry* 63, 239.
- Heaton, R.J., A.W. Peterson and R.M. Georgiadis, 2001, Electrostatic surface plasmon resonance: Direct electric field-induced hybridization and denaturation in monolayer nucleic acid films and label-free discrimination of base mismatches, *Proc. Natl. Acad. Sci. USA* 98, 3701.
- Herne, T.M. and M.J. Tarlov, 1997, Characterization of DNA probes immobilized on gold surfaces, *J. Am. Chem. Soc.* 119, 8916.
- Heyrovsky, J. and J. Kuta, 1965, *Principles of Polarography.*, Czechoslovak Academy of Sciences, Prague.
- Hinnen, C., A. Rousseau, R. Parsons and J.A. Reynaud, 1981, Comparison between the behaviour of native and denatured DNA at mercury and gold electrodes by capacity measurements and cyclic voltammetry, *J. Electroanal. Chem.* 125, 193.
- Hobara, D., O. Miyake, S. Imabayashi, K. Niki and T. Kakiuchi, 1998, In-situ scanning tunneling microscopy imaging of the reductive desorption process of alkanethiols on Au(111), *Langmuir* 14, 3590.
- Hobara, D., T. Sasaki, S. Imabayashi and T. Kakiuchi, 1999, Surface structure of binary self-assembled monolayers formed by electrochemical selective replacement of adsorbed thiols, *Langmuir* 15, 5073.
- Holmberg, R.C., M.T. Tierney, P.A. Ropp, E.E. Berg, M.W. Grinstaff and H.H. Thorp, 2003, Intramolecular electrocatalysis of 8-oxo-guanine oxidation: Secondary structure control of electron transfer in osmium-labeled oligonucleotides, *Inorg. Chem.* 42, 6379.
- Homs, W.C.I., 2002, DNA sensors, *Anal. Lett.* 35, 1875.
- Huang, E., M. Satjapipat, S.B. Han and F.M. Zhou, 2001, Surface structure and coverage of an oligonucleotide probe tethered onto a gold substrate and its hybridization efficiency for a polynucleotide target, *Langmuir* 17, 1215.
- Humphreys, M.W. and R. Parsons, 1977, Ellipsometry of DNA adsorbed at mercury electrodes a preliminary study, *J. Electroanal. Chem.* 75, 427.
- Huppler, A., L.J. Nikstad, A.M. Allmann, D.A. Brow and S.E. Butcher, 2002, Metal binding and base ionization in the U6 RNA intramolecular stem-loop structure, *Nat. Struct. Biol.* 9, 431.
- Hwang, S., E. Kim and J. Kwak, 2005, Electrochemical detection of DNA hybridization using biometallization, *Anal. Chem.* 77, 579.
- Ihara, T., Y. Maruo, S. Takenaka and M. Takagi, 1996, Ferrocene-oligonucleotide conjugates for electrochemical probing of DNA, *Nucleic Acids Res.* 24, 4273.
- Ihara, T., M. Nakayama, M. Murata, K. Nakano and M. Maeda, 1997, Gene sensor using ferrocenyl oligonucleotide, *Chem. Commun.* 17, 1609.
- Immoos, C.E., J. Chou, M. Bayachou, E. Blair, J. Greaves and P.J. Farmer, 2004c, Electrocatalytic reductions of nitrite, nitric oxide, and nitrous oxide by thermophilic cytochrome P450CYP119 in film-modified electrodes and an analytical comparison of its catalytic activities with myoglobin, *J. Am. Chem. Soc.* 126, 4934.
- Immoos, C.E., S.J. Lee and M.W. Grinstaff, 2004a, DNA-PEG-DNA triblock macromolecules for reagentless DNA detection, *J. Am. Chem. Soc.* 126, 10814.
- Immoos, C.E., S.J. Lee and M.W. Grinstaff, 2004b, Conformationally gated electrochemical gene detection, *ChemBioChem.* 5, 1100.

- Izatt, R.M., J.J. Christensen and J.H. Rytting, 1971, Sites and thermodynamic quantities associated with proton and metal ion interaction with ribonucleic acid, deoxyribonucleic acid, and their constituent bases, nucleosides and nucleotides, *Chem. Rev.* 71, 439.
- Jacobsen, E. and H. Lindseth, 1976, Effects of surfactants in differential pulse polarography, *Anal. Chim. Acta* 86, 123.
- Janik, B. and P.J. Elving, 1968, Polarographic behavior of nucleosides and nucleotides of purines, pyrimidines, pyridines, and flavins, *Chem. Rev.* 68, 295.
- Janik, B. and E. Paleček, 1966, The nature of electrode processes of guanine and its derivatives, *Z. Naturforsch. B* 21b, 1117.
- Janik, B. and R.G. Sommer, 1972, Polarography of polynucleotides. I. Correlation of current magnitudes with molecular weight, viscosity and sedimentation characteristics of polyadenylic acid, *Biochim. Biophys. Acta* 269, 15.
- Janik, B. and R.G. Sommer, 1973a, Polarography of polynucleotides. IV. Effect of the molecular weight of poly(U) on its absorption at a charged surface, *Biopolymers* 12, 2803.
- Janik, B. and R.G. Sommer, 1973b, Polarography of polynucleotides. III. Polyadenylic acid: The electrode process and interaction with polyamines, *Biophys. J.* 13, 449.
- Janik, B. and R.G. Sommer, 1976, Structural studies of synthetic polynucleotides by polarographic techniques, *Bioelectrochem. Bioenerg.* 3, 622.
- Janik, B., R.G. Sommer and A.M. Bobst, 1972, Polarography of polynucleotides. II. Conformations of poly(adenylic acid) at acidic pH, *Biochim. Biophys. Acta* 281, 152.
- Jelen, F., A. Erdem and E. Paleček, 2000a, Cyclic voltammetry of echinomycin and its complexes with DNA, *J. Biomol. Struct. Dyn.* 17, 1176.
- Jelen, F., A. Erdem and E. Paleček, 2002a, Cyclic voltammetry of echinomycin and its interaction with double-stranded and single-stranded DNA adsorbed at the electrode, *Bioelectrochem* 55, 165.
- Jelen, F., M. Fojta and E. Paleček, 1997, Voltammetry of native double-stranded, denatured and degraded DNAs, *J. Electroanal. Chem.* 427, 49.
- Jelen, F., P. Karlovsky, P. Pecinka, E. Makaturova and E. Paleček, 1991, Osmium tetroxide reactivity of DNA bases in nucleotide sequencing and probing of DNA structure, *Gen. Physiol. Biophys.* 10, 461.
- Jelen, F. and E. Paleček, 1979, Polarography of polynucleotides. Nonreducibility of double-stranded poly(guanylic acid), poly(cytidylic acid), *J. Electroanal. Chem.* 100, 93.
- Jelen, F. and E. Paleček, 1985, Nucleotide sequence-dependent opening of double-stranded DNA at an electrically charged surface, *Gen. Physiol. Biophys.* 4, 219.
- Jelen, F. and E. Paleček, 1986, Chemically reversible electroreduction of guanine in a polynucleotide chain, *Biophys. Chem.* 24, 285.
- Jelen, F., V. Vetterl, P. Belusa and S. Hason, 2000b, Adsorptive stripping analysis of DNA with admittance detection, *Electroanalysis* 12, 987.
- Jelen, F., B. Yosypchuk, A. Kourilova, L. Novotny and E. Paleček, 2002b, Label-free determination of picogram quantities of DNA by stripping voltammetry with solid copper amalgam or mercury electrodes in presence of copper, *Anal. Chem.* 74, 4788.
- Jin, B.K., X.P. Ji and T. Nakamura, 2004, Voltammetric study of interaction of Co(phen)(3)(3+) with DNA at gold nanoparticle self-assembly electrode, *Electrochim. Acta* 50, 1049.
- Johnston, D.H., Ch.-Ch. Cheng, K.J. Campbell and H.H. Thorp, 1994, Trans-dioxorhenium(V)-mediated electrocatalytic oxidation of DNA at indium tin-oxide electrodes: Voltammetric detection of DNA cleavage in solution, *Inorg. Chem.* 33, 6388.
- Johnston, D.H., K.C. Glasgow and H.H. Thorp, 1995, Electrochemical measurement of the solvent accessibility of nucleobases using electron transfer between DNA and metal complexes, *J. Am. Chem. Soc.* 117, 8933.
- Johnston, D.H. and H.H. Thorp, 1996, Cyclic voltammetry studies of polynucleotide binding and oxidation by metal complexes: Homogeneous electron-transfer kinetics, *J. Phys. Chem.* 100, 13837.
- Kalab, D., 1955, Einige Möglichkeiten von oscillographischen Analysen in der organischen und biologischen Chemie, *Pharmazie* 10, 528.

- Kalab, D., 1956, Anwendung der oscillographischen Polarographie zur quantitativen Analyse einiger Aminosäuren, *Pharmazie* 11, 265.
- Kalab, D. and F. Franek, 1955, Das oscillographische Verhalten einiger Aminosäuren auf der stationären quecksilberbedecketen Platinelektrode, *Pharmazie* 10, 31.
- Kalvoda, R., 1965, *Techniques of Oscillographic Polarography*, Elsevier, New York.
- Kara, P., D. Ozkan, A. Erdem, K. Kerman, S. Pehlivan, F. Ozkinay, D. Unuvar, G. Itirli and M. Ozsoz, 2003, Detection of achondroplasia G380R mutation from PCR amplicons by using inosine modified carbon electrodes based on electrochemical DNA chip technology, *Clin. Chim. Acta* 336, 57.
- Kasparova, D., O. Vrana, V. Kleinwachter and V. Brabec, 1987, The effect of platinum derivatives on interfacial properties of DNA, *Biophys. Chem.* 28, 191.
- Katz, E., L. Sheeney-Haj-Ichia, A.F. Buckmann and I. Willner, 2002, Dual biosensing by magneto-controlled bioelectrocatalysis, *Angew. Chem. Inter. Ed.* 41, 1343.
- Katz, E., I. Willner and J. Wang, 2004, Electroanalytical and bioelectroanalytical systems based on metal and semiconductor nanoparticles, *Electroanalysis* 16, 19.
- Kelley, S.O., J.K. Barton, N.M. Jackson and M.G. Hill, 1997a, Electrochemistry of methylene blue bound to a DNA-modified electrode, *Bioconjugate Chem.* 8, 31.
- Kelley, S.O., J.K. Barton, N.M. Jackson, L.D. McPherson, A.B. Potter, E.M. Spain, M.J. Allen and M.G. Hill, 1998, Orienting DNA helices on gold using applied electric fields, *Langmuir* 14, 6781.
- Kelley, S.O., E.M. Boon, J.K. Barton, N.M. Jackson and M.G. Hill, 1999b, Single-base mismatch detection based on charge transduction through DNA, *Nucleic Acids Res.* 27, 4830.
- Kelley, S.O., R.E. Holmlin, E.D.A. Stemp and J.K. Barton, 1997b, Photoinduced electron transfer in ethidium-modified DNA duplexes: Dependence on distance and base stacking, *J. Am. Chem. Soc.* 119, 9861.
- Kelley, S.O., N.M. Jackson, M.G. Hill and J.K. Barton, 1999a, Long-range electron transfer through DNA films, *Angew. Chem. Int. Ed.* 38, 941.
- Kerman, K., M. Kobayashi and E. Tamiya, 2003, Recent trends in electrochemical DNA biosensor technology, *Maeas. Sci. Technol.* 15, R1.
- Kerman, K., D. Ozkan, P. Kara, H. Karadeniz, Z. Ozkan, A. Erdem, F. Jelen and M. Ozsoz, 2004, Electrochemical detection of specific DNA sequences from PCR amplicons on carbon and mercury electrodes using Meldola's Blue as an intercalator, *Turk. J. Chem.* 28, 523.
- Kiechle, F.L., 1999, DNA technology in the clinical laboratory – overview, *Arch. Pathol. Lab. Med.* 123, 1151.
- Kimura-Suda, H., D.Y. Petrovykh, M.J. Tarlov and L.J. Whitman, 2003, Base-dependent competitive adsorption of single-stranded DNA on gold, *J. Am. Chem. Soc.* 125, 9014.
- Kizek, R., L. Havran, M. Fojta and E. Palecek, 2002, Determination of nanogram quantities of osmium-labeled single stranded DNA by differential pulse stripping voltammetry, *Bioelectrochemistry* 55, 119.
- Koglin, E. and J.M. Sequaris, 1986, Surface enhanced Raman-scattering of biomolecules, *Top. Curr. Chem.* 134, 1.
- Kohli, P., M. Wirtz and C.R. Martin, 2004, Nanotube membrane based biosensors, *Electroanalysis* 16, 9.
- Koryta, J., 1953, Über den Einfluss der Farbstoffe der Eosin-Gruppe auf die reversible Oxydoreduktion an der tropfenden Quecksilberelektrode, *Coll. Czech. Chem. Commun.* 18, 206.
- Kourilova, A., S. S. Babkina, K. Cahova, L. Havran, F. Jelen, E. Palecek and M. Fojta, 2005, DNA hybridization on membrane-modified carbon electrodes, *Anal. Lett.*, in press.
- Krznaric, D., P. Valenta and H.W. Nurnberg, 1975, Electrochemical behaviour of mono- and oligonucleotides. I. Effects of charge and configuration of adenine mononucleotides on their adsorption at the mercury-solution interface, *J. Electroanal. Chem.* 65, 863.
- Krznaric, D., P. Valenta, H.W. Nurnberg and M. Branica, 1978, Electrochemical behavior of mono- and oligonucleotides. Part III. Adsorption parameters of the dilute and compact adsorption layer of adenosine and adenine mononucleotides, *J. Electroanal. Chem.* 93, 41.

- Kubicarova, T., M. Fojta, J. Vidic, L. Havran and E. Palecek, 2000b, Mercury film electrode as a sensor for the detection of DNA damage, *Electroanalysis* 12, 1422.
- Kubicarova, T., M. Fojta, J. Vidic, M. Tomschik, D. Suznjevic and E. Palecek, 2000a, Voltammetric and chronopotentiometric measurements with nucleic acid-modified mercury film on a glassy carbon electrode, *Electroanalysis* 12, 1390.
- Kurien, B.T. and R.H. Scofield, 2003, Protein blotting: A review, *J. Immunol. Methods* 274, 1.
- Labuda, J., M. Fojta, F. Jelen and E. Palecek, 2005, Electrochemical sensors with DNA recognition layer. *Encyclopedia of Sensors*, Ed. C.A. Grimes, American Scientific Publishers, Stevenson Ranch, CA, USA, in press.
- Lebowitz, J., 1990, Through looking glass: The discovery of supercoiled DNA, *Trends Biochem. Sci.* 15, 202.
- Levicky, R., T.M. Herne, M.J. Tarlov and S.K. Satija, 1998, Using self-assembly to control the structure of DNA monolayers on gold: A neutron reflectivity study, *J. Am. Chem. Soc.* 120, 9787.
- Li, J., G. Cheng and S. Dong, 1997, Electrochemical study of interactions between DNA and viologen-thiol self-assembled monolayers, *Electroanalysis* 9, 834.
- Livache, T., H. Bazin, P. Caillat and A. Roget, 1998, Electroconducting polymers for the construction of DNA or peptide arrays on silicon chips, *Biosensors Bioelectron.* 13, 629.
- Lukasova, E., F. Jelen and E. Palecek, 1982, Electrochemistry of osmium-nucleic acid complexes: A probe for single-stranded and distorted double-stranded regions in DNA, *Gen. Physiol. Biophys.* 1, 53.
- Lukasova, E., M. Vojtiskova, F. Jelen, T. Sticzay and E. Palecek, 1984, Osmium-induced alternation in DNA structure, *Gen. Physiol. Biophys.* 3, 175.
- Ma, F.Y. and R.B. Lennox, 2000, Potential-assisted deposition of alkanethiols on Au: Controlled preparation of single- and mixed-component SAMs, *Langmuir* 16, 6188.
- MacDonald, J.R., 1987, *Impedance Spectroscopy*, Wiley, New York.
- Malfoy, B., J.M. Sequaris, P. Valenta and H.W. Nurnberg, 1976, Electrochemical behaviour of natural and biosynthetic polynucleotides at the mercury electrode V. Stages of deconformation of native DNA at charged interfaces, *Bioelectrochem. Bioenerg.* 3, 440.
- Mandler, D. and I. Turyan, 1996, Applications of self-assembled monolayers in electroanalytical chemistry, *Electroanalysis* 8, 207.
- Mao, Y.D., C.X. Luo and Q. Ouyang, 2003, Studies of temperature-dependent electronic transduction on DNA hairpin loop sensor, *Nucleic Acids Res.* 31, e108.
- Marmur, J. and D. Lane, 1960, Strand separation and specific recombination in deoxyribonucleic acids: Biological studies, *Proc. Natl. Acad. Sci. USA* 46, 453.
- Marmur, J., R. Rownd and C.L. Schildkraut, 1963, Denaturation and renaturation of deoxyribonucleic acid, *Progress in Nucleic Acid Research*, Vol. 1, Eds. J.N. Davidson and W.E. Cohn, Academic Press, London, 231.
- Marrazza, G., I. Chianella and M. Mascini, 1999a, Disposable DNA electrochemical biosensors for environmental monitoring, *Anal. Chim. Acta* 387, 297.
- Marrazza, G., I. Chianella and M. Mascini, 1999b, Disposable DNA electrochemical sensor for hybridization detection, *Biosensors Bioelectron.* 14, 43.
- Maruyama, K., J. Motonaka, Y. Mishima, Y. Matsuzaki, I. Nakabayashi and Y. Nakabayashi, 2001, Detection of target DNA by electrochemical method, *Sens. Actuators B-Chem.* 76, 215.
- Masarik, M., R. Kizek, K.J. Kramer, S. Billova, M. Brazdova, J. Vacek, M. Bailey, F. Jelen and J.A. Howard, 2003, Application of avidin-biotin technology and adsorptive transfer stripping square-wave voltammetry for detection of DNA hybridization and avidin in transgenic avidin maize, *Anal. Chem.* 75, 2663.
- Mascini, M., I. Palchetti and G. Marrazza, 2001, DNA electrochemical biosensors, *Fresenius J. Anal. Chem.* 369, 15.
- Maskos, U. and E.M. Southern, 1992, Parallel analysis of oligodeoxyribonucleotide (oligonucleotide) interactions. 1. Analysis of factors influencing oligonucleotide duplex formation, *Nucleic Acids Res.* 20, 1675.

- Maskos, U. and E.M. Southern, 1993, A study of oligonucleotide reassociation using large arrays of oligonucleotides synthesized on a glass support, *Nucleic Acids Res.* 21, 4663.
- Mattick, J.S., 2003, Challenging the dogma: The hidden layer of non-protein-coding RNAs in complex organisms, *Bioessays* 25, 930.
- Meggers, E., M.E. Michel-Beyerle and B. Giese, 1998, Sequence dependent long range hole transport in DNA, *J. Am. Chem. Soc.* 120, 12950.
- Meunier-Prest, R., S. Raveau, E. Finot, G. Legay, M. Cherkaoui-Malki and N. Latruffe, 2003, Direct measurement of the melting temperature of supported DNA by electrochemical method, *Nucleic Acids Res.* 31, e150.
- Mikkelsen, S.R., 1996, Electrochemical biosensors for DNA sequence detection, *Electroanalysis* 8, 15.
- Mikkelsen, O. and K.H. Schroder, 2003, Amalgam electrodes for electroanalysis, *Electroanalysis* 15, 679.
- Miller, I.R., 1961a, The structure of DNA and RNA in the water-mercury interface, *J. Mol. Biol.* 3, 229.
- Miller, I.R., 1961b, Temperature dependence of the adsorption of native DNA in a polarized water-mercury interface, *J. Mol. Biol.* 3, 357.
- Mir, K.U. and E.M. Southern, 2000, Determining the influence of structure on hybridization using oligonucleotide arrays (vol 17, pg 788, 1999), Correction, *Nat. Biotechnol.* 18, 1209.
- Mirsky, V.M., 2002, New electroanalytical applications of self-assembled monolayers, *Trends Anal. Chem.* 21, 439.
- Moody, E.M., T.S. Brown and P.C. Bevilacqua, 2004, Simple method for determining nucleobase pK(a) values by indirect labeling and demonstration of a pK(a) of neutrality in dsDNA, *J. Am. Chem. Soc.* 126, 10200.
- Munge, B., S.K. Das, R. Ilagan, Z. Pendon, J. Yang, H.A. Frank and J.F. Rusling, 2003, Electron transfer reactions of redox cofactors in spinach Photosystem I reaction center protein in lipid films on electrodes, *J. Am. Chem. Soc.* 125, 12457.
- Muskal, N. and D. Mandler, 1999, Thiol self-assembled monolayers on mercury surfaces: The adsorption and electrochemistry of omega-mercaptopalanoic acids, *Electrochim. Acta* 45, 537.
- Muskal, N. and D. Mandler, 2000, The electrochemistry of thiol self-assembled monolayers (SAMs) on a hanging mercury drop electrode (HMDE), *Curr. Sep.* 19, 49.
- Muskal, N., I. Turyan and D. Mandler, 1996, Self-assembled monolayers on mercury surfaces, *J. Electroanal. Chem.* 409, 131.
- Nahir, T.M. and E.F. Bowden, 1996, The distribution of standard rate constants for electron transfer between thiol-modified gold electrodes and adsorbed cytochrome c, *J. Electroanal. Chem.* 410, 9.
- Napier, M.E. and H.H. Thorp, 1997, Modification of electrodes with dicarboxylate self-assembled monolayers for attachment and detection of nucleic acids, *Langmuir* 13, 6342.
- Napier, M.E. and H.H. Thorp, 1999, Electrocatalytic oxidation of nucleic acids at electrodes modified with nylon and nitrocellulose membranes, *J. Fluorescence* 9, 181.
- Narlikar, G.J. and D. Herschlag, 1997, Mechanistic aspects of enzymatic catalysis: Lessons from comparison of RNA and protein enzymes, *Annu. Rev. Biochem.* 66, 19.
- Niki, K., W.R. Hardy, M.G. Hill, H. Li, J.R. Sprinkle, E. Margolish, K. Fujita, R. Tanimura, N. Nakamura, H. Ohno, J.H. Richards and H.B. Gray, 2003, Coupling to lysine-13 promotes electron tunneling through carboxylate-terminated alkanethiol self-assembled monolayers to cytochrome c, *J. Phys. Chem. B* 107, 9947.
- Nunez, M.E., D.B. Hall and J.K. Barton, 1999, Long-range oxidative damage to DNA: Effects of distance and sequence, *Chem. Biol.* 6, 85.
- Nurnberg, H.W. and P. Valenta, 1976, Voltammetric studies of the electrochemical and interfacial behavior of DNA at charged interfaces, *Croat. Chem. Acta* 48, 623.
- Nurnberg, H. W. and P. Valenta, 1977, Bioelectrochemical behaviour and deconformation of native DNA at charged interfaces, *Ions in Macromolecular and Biological Systems*, 29th Symp. of the Colston Res. Soc. Univ. Bristol, Eds. D.H. Everett and B. Vincent, Scientifica, Bristol, 201.

- O'Brien, J.C., J.T. Stickney and M.D. Porter, 2000, Self-assembled double-stranded DNA (dsDNA) microarrays for protein: dsDNA screening using atomic force microscopy, *J. Am. Chem. Soc.* 122, 5004.
- Okahata, Y., Y. Matsunobu, K. Ijiri, M. Mukae, A. Murakami and K. Makino, 1992, Hybridization of nucleic-acids immobilized on a quartz crystal microbalance, *J. Am. Chem. Soc.* 114, 8299.
- Oliveira-Brett, A.M., J.A.P. Piedade, L.A. Silva and V.C. Diculescu, 2004, Voltammetric determination of all DNA nucleotides, *Anal. Biochem.* 332, 321.
- Ontko, A.C., P.M. Armistead, S.R. Kircus and H.H. Thorp, 1999, Electrochemical detection of single-stranded DNA using polymer-modified electrodes, *Inorg. Chem.* 38, 1842.
- Ostatna, V., F. Jelen, T. Hianik and E. Palecek, 2005, Electrochemical responses of thiolated oligodeoxynucleotides in cobalt-containing solutions, *Electroanalysis* 17, 1413.
- Ozkan, D., A. Erdem, P. Kara, K. Kerman, B. Meric, J. Hassmann and M. Ozsoz, 2002, Allele-specific genotype detection of factor V Leiden mutation from polymerase chain reaction amplicons based on label-free electrochemical genosensor, *Anal. Chem.* 74, 5931.
- Ozsoz, M., A. Erdem, K. Kerman, D. Ozkan, B. Tugrul, N. Topcuoglu, H. Ekren and M. Taylan, 2003, Electrochemical genosensor based on colloidal gold nanoparticles for the detection of factor V Leiden mutation using disposable pencil graphite electrodes, *Anal. Chem.* 75, 2181.
- Palecek, E., 1958, Oszillographische Polarographie der Nucleinsäuren und ihrer Bestandteile, *Naturwissenschaften* 45, 186.
- Palecek, E., 1960a, Oscillographic polarography of highly polymerized deoxyribonucleic acid, *Nature* 188, 656.
- Palecek, E., 1960b, Oszillographische Polarographie der Nucleinsäurekomponenten, *Coll. Czech. Chem. Commun.* 25, 2283.
- Palecek, E., 1961, Oscillographic polarography of deoxyribonucleic acid degradation products, *Biochim. Biophys. Acta* 51, 1.
- Palecek, E., 1966, Polarographic behaviour of native and denatured deoxyribonucleic acids, *J. Mol. Biol.* 20, 431.
- Palecek, E., 1969a, Polarography of single-stranded homopolynucleotides, *J. Electroanal. Chem.* 22, 347.
- Palecek, E., 1969b, Polarographic techniques in nucleic acid research, *Progress in Nucleic Acid Research and Molecular Biology*, Vol. 9, Eds. J.N. Davidson and W.E. Cohn, Academic Press, New York, 31.
- Palecek, E., 1969c, Polarographic behaviour of polycytidylic acid and its double-stranded complex with polyinosinic acid, *Experientia* 25, 13.
- Palecek, E., 1971, Nucleic acid structure analysis by polarographic techniques, *Methods in Enzymology: Nucleic Acids*, part D, Vol. 21, Eds. L. Grossman and K. Moldave, Academic Press, New York, 3.
- Palecek, E., 1972, Polarographic study of structural transition of homopolynucleotides caused by protonation, *Coll. Czech. Chem. Commun.* 37, 3198.
- Palecek, E., 1974, Normal pulse polarography of double-helical DNA: Dependence of the wave height on starting potential, *Coll. Czech. Chem. Commun.* 39, 3449.
- Palecek, E., 1976, Premelting changes in DNA conformation, *Progress in Nucleic Acid Research and Molecular Biology*, Vol. 18, Ed. W.E. Cohn, 151.
- Palecek, E., 1980a, Polarographic analysis of nucleic acids, *Proc. Electroanal. Hyg. Environ. Clin. Pharm. Chem.*, Ed. W.F. Smyth, Elsevier, Amsterdam, 79.
- Palecek, E., 1980b, Reaction of nucleic acid bases with the mercury electrode: Determination of purine derivatives at submicromolar concentrations by means of cathodic stripping voltammetry, *Anal. Biochem.* 108, 129.
- Palecek, E., 1980c, Use of modern polarographic techniques in the DNA research, *DNA-Recombination, Interaction and Repair*, Eds. S. Zadrzil and J. Sponar, Pergamon Press, Oxford, 359.
- Palecek, E., 1983, Modern polarographic (voltammetric) methods in biochemistry and molecular biology. Part II. Analysis of macromolecules, *Top. Bioelectrochem. Bioenerg.*, Vol. 5, Ed. G. Milazzo, London, 65.

- Palecek, E., 1985, Determination of pseudouridine at submicromolar concentrations by cathodic stripping voltammetry at a mercury electrode, *Anal. Chim. Acta* 174, 103.
- Palecek, E., 1988a, Adsorptive transfer stripping voltammetry: Determination of nanogram quantities of DNA immobilized at the electrode surface, *Anal. Biochem.* 170, 421.
- Palecek, E., 1988b, New trends in electrochemical analysis of nucleic acids, *Bioelectrochem. Bioenerg.* 20, 171.
- Palecek, E., 1991, Local supercoil-stabilized DNA structures, *Crit. Rev. Biochem. Mol. Biol.* 26, 151.
- Palecek, E., 1992a, Adsorptive transfer stripping voltammetry. Effect of the electrode potential on the structure of DNA adsorbed at the mercury electrode, *Bioelectrochem. Bioenerg.* 28, 71.
- Palecek, E., 1992b, Probing of DNA structure with osmium tetroxide complexes *in vitro*, *Methods in Enzymology*, Vol. 212, Eds. J.N. Abelson and M.I. Simon, Academic Press, New York, 139.
- Palecek, E., 1992c, Probing of DNA structure in cells with osmium tetroxide,2,2'-bipyridine, *Methods in Enzymology*, Vol. 212, DNA Structures, Part B, Eds. J. N. Abelson and M. I. Simon, Academic Press, New York, 305.
- Palecek, E., 1994, Probing of DNA structure with osmium tetroxide complexes *in vitro* and in cells, *Nucleic Acids and Molecular Biology*, Vol. 8, Eds. F. Eckstein and D.M.J. Lilley, Springer, Berlin, 1.
- Palecek, E., 1995, Nucleic Acids. Electrochemical and immunochemical analysis, *Encyclopedia of Analytical Science*, Ed. A. Totwshend, Academic Press, London, 3600.
- Palecek, E., 1996, From polarography of DNA to microanalysis with nucleic acid-modified electrodes, *Electroanalysis* 8, 7.
- Palecek, E., 2002, Past, present and future of nucleic acids electrochemistry, *Talanta* 56, 809.
- Palecek, E., 2004, Surface-attached molecular beacons light the way for DNA sequencing, *Trends Biotechnol.* 22, 55.
- Palecek, E., 2005, Nucleic acids. Electrochemical methods, *Encyclopedia of Analytical Science*, 2e, Ed. C.F. Poole, Elsevier, London, 399.
- Palecek, E. and V. Brabec, 1972, The relation between the polarographic behavior of DNA and its conformation in solution, *Biochem. Biophys. Acta* 262, 125.
- Palecek, E., V. Brabec, F. Jelen and Z. Pechan, 1977, Pulse-polarographic analysis of nucleic acids and proteins, *J. Electroanal. Chem.* 75, 471.
- Palecek, E., S. Billova, L. Havran, R. Kizek, A. Miculkova and F. Jelen, 2002d, DNA hybridization at microbeads with cathodic stripping voltammetric detection, *Talanta* 56, 919.
- Palecek, E., P. Boublikova and F. Jelen, 1986a, Cyclic voltammetry of nucleic acids and determination of submicrogram quantities of deoxyribonucleic acids by adsorptive stripping voltammetry, *Anal. Chim. Acta* 187, 99.
- Palecek, E. and J. Duskocil, 1974, Pulse-polarographic analysis of double-stranded RNA, *Anal. Biochem.* 60, 518.
- Palecek, E. and M. Fojta, 2001, Detecting DNA hybridization and damage, *Anal. Chem.* 73, 74A.
- Palecek, E. and M. Fojta, 2005, Electrochemical DNA sensors, *Bioelectronics*, Eds. I. Willner and E. Katz, Wiley-VCH, Weinheim, 127.
- Palecek, E., M. Fojta and F. Jelen, 2002a, New approaches in the development of DNA sensors: Hybridization and electrochemical detection of DNA and RNA at two different surfaces, *Bioelectrochemistry* 56, 85.
- Palecek, E., M. Fojta, F. Jelen and V. Vetterl, 2002b, Electrochemical analysis of nucleic acids, *The Encyclopedia of Electrochemistry, Bioelectrochemistry*, Vol. 9, Eds. A.J. Bard and M. Stratsmann, Wiley-VCH, Weinheim, 365.
- Palecek, E., M. Fojta, M. Tomschik and J. Wang, 1998, Electrochemical biosensors for DNA hybridization and DNA damage, *Biosensors Bioelectron.* 16, 621.
- Palecek, E. and B.D. Frary, 1966, A highly sensitive pulse-polarographic estimation of denatured deoxyribonucleic acid samples, *Arch. Biochem. Biophys.* 115, 431.
- Palecek, E. and M.A. Hung, 1983, Determination of nanogram quantities of osmium-labeled nucleic acids by stripping (inverse) voltammetry, *Anal. Biochem.* 132, 236.

- Paleček, E. and F. Jelen, 1980, Interaction of nucleic acids with electrically charged surfaces. VII. Dependence of changes in DNA double helical structure on pH and on potential of the mercury electrode, *Bioelectrochem. Bioenerg.* 7, 317.
- Paleček, E. and F. Jelen, 1984, Nucleotide sequence-dependent opening of the DNA double helix at electrically charged surface, *Charge and Field Effects in Biosystems*, Eds. M.J. Allen and P.N.R. Usherwood, Abacus Press, Tonbridge, UK, 361.
- Paleček, E., F. Jelen, M.A. Hung and J. Lasovsky, 1981, Reaction of the purine and pyrimidine derivatives with the electrode mercury, *Bioelectrochem. Bioenerg.* 8, 621.
- Paleček, E., F. Jelen, E. Minarova, K. Nejedly, J. Paleček, P. Pecinka, J. Rícicova, M. Vojtiskova and D. Zachova, 1992, Osmium tetroxide complexes: Single-strand selective probes of the DNA structure *in vitro* and in cells, *Structural Tools for the Analysis of Protein-Nucleic Acid Complexes*, Vol. Volume in Series Advances in Life Sciences, Eds. D. M. J. Lilley, H. Heumann and D. Suck, Birkhauser, Basel, 1.
- Paleček, E., F. Jelen, C. Teijeiro, V. Fucik and T.M. Jovin, 1993, Biopolymer-modified electrodes. Voltammetric analysis of nucleic acids and proteins at the submicrogram level, *Anal. Chim. Acta* 273, 175.
- Paleček, E., F. Jelen and L. Trnkova, 1986b, Cyclic voltammetry of DNA at a mercury electrode: An anodic peak specific for guanine, *Gen. Physiol. Biophys.* 5, 315.
- Paleček, E., F. Jelen and V. Vetterl, 1987, Reduction and tensammetric pulse-polarographic currents of polynucleotides, *Coll. Czech. Chem. Commun.* 52, 2810.
- Paleček, E., R. Kizek, L. Havran, S. Billova and M. Fojta, 2002c, Electrochemical enzyme-linked immunoassay in a DNA hybridization sensor, *Anal. Chim. Acta* 469, 73.
- Paleček, E., V. Kolar, F. Jelen and U. Heinemann, 1990, Electrochemical analysis of the self-complementary B-DNA decamer d(CCAGGCCTGG), *Bioelectrochem. Bioenerg.* 23, 285.
- Paleček, E. and S. Kwee, 1979, Absence of unwinding of double-helical DNA in the surface of mercury electrode charged to DNA reduction potentials at neutral pH, *Coll. Czech. Chem. Commun.* 44, 448.
- Paleček, E., M. Masarik, R. Kizek, D. Kuhlmeier, J. Hassmann and J. Schulein, 2004, Sensitive electrochemical determination of unlabeled MutS protein and detection of point mutations in DNA, *Anal. Chem.* 76, 5930.
- Paleček, E. and I. Postbieglova, 1986, Adsorptive stripping voltammetry of biomacromolecules with transfer of the adsorbed layer, *J. Electroanal. Chem.* 214, 359.
- Paleček, E., M. Tomschik, V. Stankova and L. Havran, 1997, Chronopotentiometric stripping of DNA at mercury electrodes, *Electroanalysis* 9, 990.
- Paleček, E. and V. Vetterl, 1968, Polarographic reducibility of denatured DNA, *Biopolymers* 6, 917.
- Paleček, E., M. Vojtiskova, F. Jelen and E. Lukasova, 1984, Introduction of an electroactive marker into the polynucleotide chain: A new probe for distorted regions in the DNA double helix, *Bioelectrochem. Bioenerg.* 12, 135.
- Paleček, E., V. Vetterl and J. Sponar, 1974, Structural transition of polyadenylic acid due to protonation: The influence of the length of single strands on the polarographic behaviour of the double-helical form, *Nucleic Acids Res.* 1, 427.
- Pang, D.-W., Y.-P. Qi, Z.-L. Wang, J.-K. Cheng and J.-W. Wang, 1995, Electrochemical oxidation of DNA at a gold microelectrode, *Electroanalysis* 7, 774.
- Parak, W.J., T. Pellegrino, C.M. Micheal, D. Gerion, S.C. Williams and A.P. Alivisatos, 2003, Conformation of oligonucleotides attached to gold nanocrystals probed by gel electrophoresis, *Nano Lett.* 3, 33.
- Park, N. and J.H. Hahn, 2004, Electrochemical sensing of DNA hybridization based on duplex-specific charge compensation, *Anal. Chem.* 76, 900.
- Patolsky, F., A. Lichtenstein and I. Willner, 2001, Detection of single-base DNA mutations by enzyme-amplified electronic transduction, *Nat. Biotechnol.* 19, 253.
- Patolsky, F., Y. Weizmann, E. Katz and I. Willner, 2003, Magnetically amplified DNA assays (MADA): Sensing of viral DNA and single-base mismatches by using nucleic acid modified magnetic particles, *Angew. Chem. Inter. Ed.* 42, 2372.

- Patolsky, F., Y. Weizmann and I. Willner, 2002, Redox-active nucleic-acid replica for the amplified bioelectrocatalytic detection of viral DNA, *J. Am. Chem. Soc.* 124, 770.
- Paulson, H.L. and K.H. Fischbeck, 1996, Trinucleotide repeats in neurogenetic disorders, *Annu. Rev. Neurosci.* 19, 79.
- Pechan, Z., D. Kalab and E. Palecek, 1955, Oscillopolarographische Detektion der Stoffe auf dem Filtrierpapier, *Pharmazie* 10, 526.
- Peterlinz, K.A. and R.M. Georgiadis, 1997, Observation of hybridization and dehybridization of thiol-tethered DNA using two-color surface plasmon resonance spectroscopy, *J. Am. Chem. Soc.* 119, 3401.
- Piunno, P.A.E., J. Watterson, C.C. Wust and U.J. Krull, 1999, Considerations for the quantitative transduction of hybridization of immobilized DNA, *Anal. Chim. Acta* 400, 73.
- Pividori, M.I., A. Merkoci and S. Alegret, 2001, Classical dot-blot format implement as an amperometric hybridization genosensor, *Biosensors Bioelectron.* 16, 1815.
- Poirier, G.E., 1997, Characterization of organosulfur molecular monolayers on Au(111) using scanning tunneling microscopy, *Chem. Rev.* 97, 1117.
- Popovich, N.D. and H.H. Thorp, 2002, New strategies for electrochemical nucleic acid detection, *Interface* 11, 30.
- Popovich, N.D., S.S. Wong, B.K.H. Yen, H.Y. Yeom and D.C. Paine, 2002, Influence of microstructure on the electrochemical performance of tin-doped indium oxide film electrodes, *Anal. Chem.* 74, 3127.
- Porath, D., G. Cuniberti and R. Di Felice, 2004, Charge transport in DNA-based device, *Top. Curr. Chem.* 237, 183.
- Pospasil, L., 1996, Electrochemical impedance and related techniques. Experimental techniques in bioelectrochemistry, Vol. 3, *Bioelectrochemistry: Principles and Practice*, Eds. V. Brabec, D. Walz and G. Milazzo, Birkhauser, Basel, Switzerland, 1.
- Prado, C., G.U. Flechsig, P. Grundler, J.S. Foord, F. Marken and R.G. Compton, 2002, Electrochemical analysis of nucleic acids at boron-doped diamond electrodes, *Analyst* 127, 329.
- Rao, C.N.R., B.C. Satishkumar, A. Govindaraj and M. Nath, 2001, Nanotubes, *Chem. Phys. Chem.* 2, 78.
- Reynaud, J.A., B. Malfoy, J.M. Sequaris and P.J. Sicard, 1977, A model of DNA at the Hg/electrolyte interface, *Bioelectrochem. Bioenerg.* 4, 380.
- Ropp, P.A. and H.H. Thorp, 1999, Site-selective electron transfer from purines to electrocatalysts: Voltammetric detection of a biologically relevant detection in hybridized DNA duplexes, *Chem. Biol.* 6, 599.
- Rush, M.G. and R.C. Warner, 1970, Alkali denaturation of covalently closed circular duplex deoxyribonucleic acid, *J. Biol. Chem.* 245, 2704.
- Sachs, S.B., S.P. Dudek, R.P. Hsung, L.R. Sita, J.F. Smalley, M.D. Newton, S.W. Feldberg and C.E.D. Chidsey, 1997, Rates of interfacial electron transfer through conjugated spacers, *J. Am. Chem. Soc.* 119, 10563.
- Sadik, O.A., 1999, Bioaffinity sensors based on conducting polymers: A short review, *Electroanalysis* 11, 839.
- Saenger, W., 1984, *Principles of Nucleic Acid Structure*, Springer, New York.
- Saito, I., T. Nakamura, K. Nakatani, Y. Yoshioka, K. Yamaguchi and H. Sugiyama, 1998, Mapping of the hot spots for DNA damage by one-electron oxidation: Efficacy of GG doublets and GGG triplets as a trap in long-range hole migration, *J. Am. Chem. Soc.* 120, 12686.
- Sam, M., E.M. Boon, J.K. Barton, M.G. Hill and E.M. Spain, 2001, Morphology of 15-mer duplexes tethered to Au(111) probed using scanning probe microscopy, *Langmuir* 17, 5727.
- Sato, S., T. Nojima and S. Takenaka, 2004, Electrochemical gene detection based on supramolecular complex formation by ferrocenyl-beta-cyclodextrin and adamantyl-naphthalene diimide bound to double stranded DNA, *J. Organometal. Chem.* 689, 4722.
- Schüle, J., B. Graßl, J. Krause, C. Schulze, C. Kugler, P. Müller, W.M. Bertling and J. Hassmann, 2002, Solid composite electrodes for DNA enrichment and detection, *Talanta* 56, 875.

- Schuster, G.B., 2000, Long-range charge transfer in DNA: Transient structural distortions control the distance dependence, *Acc. Chem. Res.* 33, 253.
- Sequaris, J. M., 1992, Analytical voltammetry of biological molecules, Wilson and Wilson's *Comprehensive Analytical Chemistry*, Vol. XXVII: Analytical Voltammetry, Eds. G. Svehla and J.G. Vos, Elsevier, Amsterdam, 115.
- Shchepinov, M.S., S.C. CaseGreen and E.M. Southern, 1997, Steric factors influencing hybridisation of nucleic acids to oligonucleotide arrays, *Nucleic Acids Res.* 25, 1155.
- Singhal, P. and W.G. Kuhr, 1997a, Direct electrochemical detection of purine- and pyrimidine based nucleotides with sinusoidal voltammetry, *Anal. Chem.* 69, 3552.
- Singhal, P. and W.G. Kuhr, 1997b, Ultrasensitive voltammetric detection of underivatized oligonucleotides and DNA, *Anal. Chem.* 69, 4828.
- Sistare, M.F., S.J. Coddin, G. Heimlich and H.H. Thorp, 2000, Effects of base stacking on guanine electron transfer: Rate constants for G and GG sequences of oligonucleotides from catalytic electrochemistry, *J. Am. Chem. Soc.* 122, 4742.
- Sistare, M.F., R.C. Holmberg and H.H. Thorp, 1999, Electrochemical studies of polynucleotide binding and oxidation by metal complexes: Effects of scan rate, concentration, and sequence, *J. Phys. Chem. B* 103, 10718.
- Slowinski, K., R.V. Chamberlain, R. Bilewicz and M. Majda, 1996, Evidence for inefficient chain-to-chain coupling in electron tunneling through liquid alkanethiol monolayer films on mercury, *J. Am. Chem. Soc.* 118, 4709.
- Slowinski, K., R.V. Chamberlain, C.J. Miller and M. Majda, 1997, Trough-bond and chain-to-chain coupling. Two pathways in electron tunneling through liquid alkanethiol monolayers on mercury electrodes, *J. Am. Chem. Soc.* 119, 11910.
- Sluyters-Rehbach, M. and J.H. Sluyters, 1982, The investigation of the adsorptive behaviour of electroactive species by means of admittance analysis. 1. Theory of the case of reversible charge-transfer, *J. Electroanal. Chem.* 136, 39.
- Sosnowski, R.G., E. Tu, W.F. Butler, J.P. O'Connell and M.J. Heller, 1997, Rapid determination of single base mismatch mutations in DNA hybrids by direct electric field control, *Proc. Natl. Acad. Sci. USA* 94, 1119.
- Steel, A.B., T.M. Herne and M.J. Tarlov, 1998, Electrochemical quantitation of DNA immobilized on gold, *Anal. Chem.* 70, 4670.
- Steel, A.B., R.L. Levicky, T.M. Herne and M.J. Tarlov, 2000, Immobilization of nucleic acids at solid surfaces: Effect of oligonucleotide length on layer assembly, *Biophys. J.* 79, 975.
- Steenken, S., S.V. Jovanovic, M. Bietti and K. Bernhard, 2000, The trap depth (in DNA) of 8-oxo-7,8-dihydro-2' deoxyguanosine as derived from electron-transfer equilibria in aqueous solution, *J. Am. Chem. Soc.* 122, 2373.
- Steichen, M. and C. Buess-Herman, 2005, Electrochemical detection of the immobilization and hybridization of unlabeled linear and harpin DNA on gold, *Electrochem. Commun.* 7, 416.
- Stock, J.T., C.J.O.R. Morris, J.E.B. Randles and L. Airey, 1947, *Polarography*, *Analyst* 72, 291.
- Storz, G., 2002, An expanding universe of noncoding RNAs, *Science* 296, 1260.
- Strasak, L., J. Dvorak, S. Hason and V. Vetterl, 2002, Electrochemical impedance spectroscopy of polynucleotide adsorption, *Bioelectrochemistry* 56, 37.
- Studnickova, M., L. Trnkova, J. Zetek and Z. Glatz, 1989, Reduction of guanosine at a mercury electrode, *Bioelectrochem. Bioenerg.* 21, 83.
- Sugiyama, H. and I. Saito, 1996, Theoretical studies of GC-specific photocleavage of DNA via electron transfer: Significant lowering of ionization potential and 5'-localization of HOMO of stacked GG bases in B-form DNA, *J. Am. Chem. Soc.* 118, 7063.
- Svaren, J., S. Inagami, E. Lovgren and R. Chalkley, 1987, DNA denatures upon drying after ethanol precipitation, *Nucleic Acids Res.* 15, 8739.
- Szalai, V.A. and H.H. Thorp, 2000, Electrocatalysis of guanine electron transfer: New insights from submillimeter carbon electrodes, *J. Phys. Chem. B* 104, 6851.

- Takenaka, S., K. Yamashita, M. Takagi, Y. Uto and H. Kondo, 2000, DNA sensing on a DNA probe-modified electrode using ferrocynaphthalene diimide as the electrochemically active ligand, *Anal. Chem.* 72, 1334.
- Talanta, 2002, Special issue on electrochemistry of nucleic acids and development of electrochemical DNA sensors, 56
- Tarlov, M.J. and A.B. Steel, 2003, DNA-Based Sensors. Biomolecular Films. Design, Function, and Applications, Ed. J.F. Rusling, Marcel Dekker, New York, 545.
- Teijeiro, C., K. Nejedly and E. Palecek, 1993, Cyclic voltammetry of submicrogram quantities of supercoiled, linear and denatured DNAs with DNA-modified mercury electrode, *J. Biomol. Struct. Dyn.* 11, 313.
- Thorp, H.H., 1998, Cutting out the middleman: DNA biosensors based on electrochemical oxidation, *Trends Biotechnol.* 16, 117.
- Thorp, H.H., 2004, Electrocatalytic DNA oxidation, Long-Range Charge Transfer in DNA II, 237, Ed. G.B. Schuster, Topics in Current Chemistry, 159.
- Tombelli, S., G. Marrazza and M. Mascini, 2001, Recent advances on DNA biosensors, *Int. J. Env. Anal. Chem.* 80, 87.
- Tomkinson, J.L. and B.A. Stillman, 2002, Nitrocellulose: A tried and true polymer finds utility as a post-genomic substrate, *Front. Biosci.* 7, C1.
- Tomschik, M., L. Havran, M. Fojta and E. Palecek, 1998, Constant current chronopotentiometric stripping analysis of bioactive peptides at mercury and carbon electrodes, *Electroanalysis* 10, 103.
- Tomschik, M., F. Jelen, L. Havran, L. Trnkova, P.E. Nielsen and E. Palecek, 1999, Reduction and oxidation of peptide nucleic acids and DNA at mercury and carbon electrodes, *J. Electroanal. Chem.* 476, 71.
- Topics in Current Chemistry, 2004, Long-Range Charge Transfer in DNA I and II, 236 and 237, *Top. Curr. Chem.*, respectively, 237.
- Trnkova, L., 2002, Electrochemical behaviour of DNA at a silver electrode studied by cyclic and elimination voltammetry, *Talanta* 56, 887.
- Trnkova, L., 2005, Identification of current nature by elimination voltammetry with linear scan, *J. Electroanal. Chem.* 582, 258.
- Trnkova, L. and O. Dracka, 1993, Application of elimination polarography to the study of electrode processes, *J. Electroanal. Chem.* 348, 265.
- Trnkova, L. and O. Dracka, 1996, Elimination voltammetry. Experimental verification and extension of theoretical results, *J. Electroanal. Chem.* 413, 123.
- Trnkova, L., F. Jelen and I. Postbieglova, 2003, Application of elimination voltammetry to the resolution of adenine and cytosine signals in oligonucleotides. I. Homooligodeoxynucleotides dA(9) and dC(9), *Electroanalysis* 15, 1529.
- Trnkova, L., R. Kizek and O. Dracka, 2000, Application of elimination voltammetry to adsorptive stripping of DNA, *Electroanalysis* 12, 905.
- Trnkova, L., R. Kizek and O. Dracka, 2002, Elimination voltammetry of nucleic acids on silver electrodes, *Bioelectrochemistry* 55, 131.
- Trnkova, L., I. Postbieglova and M. Holik, 2004, Electroanalytical determination of d(GCGAAGC) hairpin, *Bioelectrochemistry* 63, 25.
- Trnkova, L., M. Studnickova and E. Palecek, 1980, Electrochemical behaviour of guanine and its derivatives. I. Fast cyclic voltammetry of guanosine and calf thymus DNA, *Bioelectrochem. Bioenerg.* 7, 644.
- Vainrub, A. and B.M. Pettitt, 2000, Thermodynamics of association to a molecule immobilized in an electric double layer, *Chem. Phys. Lett.* 323, 160.
- Valenta, P. and P. Grahmann, 1974, Electrochemical behaviour of natural and biosynthetic polynucleotides at the mercury electrode. Part 1. The adsorption of denatured deoxyribonucleic acid at the hanging mercury drop electrode, *J. Electroanal. Chem.* 49, 41.
- Valenta, P. and D. Krznaric, 1977, Electrochemical behaviour of mono- and oligonucleotides. IV. The adsorption of adenine oligonucleotides at the mercury-solution interface, *J. Electroanal. Chem.* 75, 437.

- Valenta, P. and H.W. Nurnberg, 1974a, Electrochemical behaviour of natural and biosynthetic polynucleotides at the mercury electrode. II. Reduction of denatured DNA at stationary and dropping mercury electrode, *J. Electroanal. Chem.* 49, 55.
- Valenta, P. and H.W. Nurnberg, 1974b, The electrochemical behaviour of DNA at electrically charged interfaces, *Biophys. Struct. Mech.* 1, 17.
- Valenta, P., H.W. Nurnberg and P. Klahre, 1974, Electrochemical behaviour of natural and biosynthetic polynucleotides at the mercury electrode. III. A comparative study on the electrochemical properties of native and denatured DNA, *Bioelectrochem. Bioenerg.* 1, 487.
- Valenta, P., H.W. Nurnberg and P. Klahre, 1975, Electrochemical behaviour of natural and biosynthetic polynucleotides at the mercury electrode. IV. Reduction and adsorption of polyriboadenylic acid at the hanging mercury electrode, *Bioelectrochem. Bioenerg.* 2, 204.
- Vercoutere, W. and M. Akeson, 2002, Biosensors for DNA sequence detection, *Curr. Opin. Chem. Biol.* 6, 816.
- Vetterl, V., N. Papadopoulou, V. Drazan, L. Strasak, S. Hason and J. Dvorak, 2000, Nucleic acid sensing by impedance measurements, *Electrochim. Acta* 45, 2961.
- Vinograd, J., J. Lebowitz, R. Radloff, R. Watson and P. Laipis, 1965, The twisted circular form of polyoma viral DNA, *Proc. Natl. Acad. Sci. USA* 53, 1104.
- Vojtiskova, M., E. Lukasova, F. Jelen and E. Palecek, 1981, Polarography of circular DNAs, *Bioelectrochem. Bioenerg.* 8, 487.
- Vologodskii, A.V. and N.R. Cozzarelli, 1994, Conformational and thermodynamic properties of supercoiled DNA, *Annu. Rev. Biophys. Biomol. Struct.* 23, 609.
- Vorlickova, M. and E. Palecek, 1974, A study of changes in DNA conformation caused by ionizing and ultra-violet radiation by means of pulse polarography and circular dichroism, *Int. J. Radiat. Biol.* 26, 363.
- Wan, C.Z., T. Fiebig, S.O. Kelley, C.R. Treadway, J.K. Barton and A.H. Zewail, 1999, Femtosecond dynamics of DNA-mediated electron transfer, *Proc. Natl. Acad. Sci. USA* 96, 6014.
- Wang, J., 1999, Electroanalysis and biosensors, *Anal. Chem.* 71, 328R.
- Wang, J., 2000a, From DNA biosensors to gene chips, *Nucleic Acids Res.* 28, 3011.
- Wang, J., 2000b, *Analytical Electrochemistry*, 2nd ed, Wiley-VCH, New York.
- Wang, J., 2002, Electrochemical nucleic acid biosensors, *Anal. Chim. Acta* 469, 63.
- Wang, J., 2003, Nanoparticle-based electrochemical DNA detection, *Anal. Chim. Acta* 500, 247.
- Wang, J., 2005, Carbon-nanotube based electrochemical biosensors: A review, *Electroanalysis* 17, 7.
- Wang, J., X. Cai, J. Fernandez, D. Grant and M. Ozsoz, 1997a, Membrane-covered carbon electrodes for electrochemical measurements of oligonucleotides in presence of DNA and RNA, *Anal. Chem.* 69, 4056.
- Wang, J., X. Cai, C. Jonsson and M. Balakrishnan, 1996a, Adsorptive stripping potentiometry of DNA at electrochemically pretreated carbon paste electrodes, *Electroanalysis* 8, 20.
- Wang, J., X.H. Cai, G. Rivas, H. Shiraiishi and N. Dontha, 1997b, Nucleic-acid immobilization, recognition and detection at chronopotentiometric DNA chips, *Biosensors Bioelectron.* 12, 587.
- Wang, J., X. Cai, J.Y. Wang, C. Jonsson and E. Palecek, 1995, Trace measurement of RNA by potentiometric stripping analysis at carbon paste electrodes, *Anal. Chem.* 67, 4065.
- Wang, J., J.R. Fernandes and L.T. Kubota, 1998a, Polishable and renewable DNA hybridization biosensors, *Anal. Chem.* 70, 3699.
- Wang, J., P. Grundler, G.U. Flechsig, M. Jasinski, J.M. Lu, J.Y. Wang, Z.Q. Zhao and B.M. Tian, 1999b, Hot-wire stripping potentiometric measurements of trace mercury, *Anal. Chim. Acta* 396, 33.
- Wang, J., P. Grundler, G.U. Flechsig, M. Jasinski, G. Rivas, E. Sahlin and J.L.L. Paz, 2000c, Stripping analysis of nucleic acids at a heated carbon paste electrode, *Anal. Chem.* 72, 3752.

- Wang, J., M. Jiang and A.N. Kawde, 2001a, Flow detection of UV radiation-induced DNA damage at a polypyrrole-modified electrode, *Electroanalysis* 13, 537.
- Wang, J., M. Jiang, A.M. Kawde and R. Polsky, 2000a, Electrochemically induced deposition of thiol-based monolayers onto closely spaced microelectrodes, *Langmuir* 16, 9687.
- Wang, J., E. Katz and I. Willner, 2005a, Biomaterial-nanoparticles hybrid systems for sensing and electronic devices, *Bioelectronics*, Eds. I. Willner and E. Katz, Wiley-VCH, Weinheim, 231.
- Wang, J. and A.B. Kawde, 2002, Amplified label-free electrical detection of DNA hybridization, *Analyst* 127, 383.
- Wang, J., A.N. Kawde, A. Erdem and M. Salazar, 2001b, Magnetic bead-based label-free electrochemical detection of DNA hybridization, *Analyst* 126, 2020.
- Wang, J., A.N. Kawde, M. Musameh and G. Rivas, 2002a, Dual enzyme electrochemical coding for detecting DNA hybridization, *Analyst* 127, 1279.
- Wang, J., G.D. Liu and M.R. Jan, 2004, Ultrasensitive electrical biosensing of proteins and DNA: Carbon-nanotube derived amplification of the recognition and transduction events, *J. Am. Chem. Soc.* 126, 3010.
- Wang, J., G. Liu and A. Merkoci, 2003a, Electrochemical coding technology for simultaneous detection of multiple DNA targets, *J. Am. Chem. Soc.* 125, 3214.
- Wang, J., G.D. Liu and Q.Y. Zhu, 2003b, Indium microrod tags for electrochemical detection of DNA hybridization, *Anal. Chem.* 75, 6218.
- Wang, J. and M. Musameh, 2005, Carbon-nanotubes doped polypyrrole glucose biosensor, *Anal. Chim. Acta* 539, 209.
- Wang, J., M. Ozsoz, X.H. Cai, G. Rivas, H. Shiraishi, D.H. Grant, M. Chicharro, J. Fernandes and E. Palecek, 1998c, Interactions of antitumor drug daunomycin with DNA in solution and at the surface, *Bioelectrochem. Bioenerg.* 45, 33.
- Wang, J., E. Palecek, P.E. Nielsen, G. Rivas, X.H. Cai, H. Shiraishi, N. Dontha, D. Luo and P.A.M. Farias, 1996b, Peptide nucleic acid probes for sequence-specific DNA biosensors, *J. Am. Chem. Soc.* 118, 7667.
- Wang, J., R. Polsky, A. Merkoci and K.L. Turner, 2003c, "Electroactive beads" for ultrasensitive DNA detection, *Langmuir* 19, 989.
- Wang, J., R. Polsky, B. Tian and M.P. Chatrathi, 2000b, Voltammetry on microfluidic chip platforms, *Anal. Chem.* 72, 5285.
- Wang, J., G. Rivas, X.H. Cai, M. Chicharro, N. Dontha, D.B. Luo, E. Palecek and P.E. Nielsen, 1997d, Adsorption and detection of peptide nucleic acids at carbon paste electrodes, *Electroanalysis* 9, 120.
- Wang, J., G. Rivas, X.H. Cai, M. Chicharro, C. Parrado, N. Dontha, A. Begleiter, M. Mowat, E. Palecek and P.E. Nielsen, 1997e, Detection of point mutation in the p53 gene using a peptide nucleic acid biosensor, *Anal. Chim. Acta* 344, 111.
- Wang, J., G. Rivas, X. Cai, E. Palecek, P. Nielsen, H. Shiraishi, N. Dontha, D. Luo, C. Parrado, M. Chicharro, P.A.M. Farias, F.S. Valera, D.H. Grant, M. Ozsoz and M.N. Flair, 1997f, DNA electrochemical biosensors for environmental monitoring, A review, *Anal. Chim. Acta* 347, 1.
- Wang, J., G. Rivas, J.R. Fernandes, M. Jiang, J.L.L. Paz, R. Waymire, T.W. Nielsen and R.C. Getts, 1998b, Adsorption and detection of DNA dendrimers at carbon electrodes, *Electroanalysis* 10, 553.
- Wang, J., G. Rivas, C. Parrado, X.H. Cai and M.N. Flair, 1997c, Electrochemical biosensor for detecting DNA sequences from the pathogenic protozoan *Cryptosporidium parvum*, *Talanta* 44, 2003.
- Wang, J., E. Sahlin and J.L.L. Paz, 1999a, Small-volume electrochemical detection of trace nucleic acids using a vibrating electrode system, *Electroanalysis* 11, 380.
- Wang, S.F., W. Wang and H.C. Cai, 2005b, Recognition and detection of dsDNA at a thionalid self-assembled monolayer modified gold electrode, *Sens. Actuators B-Chem.* 104, 8.
- Wang, J., D.K. Xu, A. Erdem, R. Polsky and M.A. Salazar, 2002b, Genomagnetic electrochemical assays of DNA hybridization, *Talanta* 56, 931.

- Warman, J.M., M.P. deHaas and A. Rupprecht, 1996, DNA: A molecular wire?, *Chem. Phys. Lett.* 249, 319.
- Watterson, J.H., P.A.E. Piuino, C.C. Wust and U.J. Krull, 2000, Effects of oligonucleotide immobilization density on selectivity of quantitative transduction of hybridization of immobilized DNA, *Langmuir* 16, 4984.
- Weatherly, S.C., I.V. Yang, P.A. Armistead and H.H. Thorp, 2003, Proton-coupled electron transfer in guanine oxidation: Effects of isotope, solvent, and chemical modification, *J. Phys. Chem.* 107, 372.
- Weatherly, S.C., I.V. Yang and H.H. Thorp, 2001, Proton-coupled electron transfer in duplex DNA: Driving force dependence and isotope effects on electrocatalytic oxidation of guanine, *J. Am. Chem. Soc.* 123, 1236.
- Webb, J.W., B. Janik and P.J. Elving, 1973, Di- and oligonucleotide phosphates of adenine and cytosine. Electrochemical study of reduction, adsorption, and association, *J. Am. Chem. Soc.* 95, 8495.
- Weizmann, Y., F. Patolsky, E. Katz and I. Willner, 2003, Amplified DNA sensing and immunosensing by the rotation of functional magnetic particles, *J. Am. Chem. Soc.* 125, 3452.
- Welch, T.W., A.H. Corbett and H.H. Thorp, 1995, Electrochemical determination of nucleic acid diffusion-coefficients through noncovalent association of a redox-active probe, *J. Phys. Chem.* 99, 11757.
- Welch, T.W. and H.H. Thorp, 1996, Distribution of metal complexes bound to DNA determined by normal pulse voltammetry, *J. Phys. Chem.* 100, 13829.
- Willner, I. and E. Katz, 2003, Magnetic control of electrocatalytic and bioelectrocatalytic processes, *Angew. Chem. Int. Ed.* 42, 4576.
- Wolf, L.K., Y. Gao and R.M. Georgiadis, 2004, Sequence-dependent DNA immobilization: Specific versus nonspecific contributions, *Langmuir* 20, 3357.
- Wolff, G. and H.W. Nurnberg, 1966, Anwendungen der Pulse-Polarographie in der organischen Analyse. Teil I. Aromatische Nitroverbindungen, *Z. Anal. Chem.* 216, 169.
- Xu, Y., H. Cai, P.G. He and Y.Z. Fang, 2004, Probing DNA hybridization by impedance measurement based on CdS-oligonucleotide nanoconjugates, *Electroanalysis* 16, 150.
- Yang, I.V. and H.H. Thorp, 2001, Modification of indium tin oxide electrodes with repeat polynucleotides: Electrochemical detection of trinucleotide repeat expansion, *Anal. Chem.* 73, 5316.
- Yelin, R., D. Dahary, R. Sorek, E.Y. Levanon, O. Goldstein, A. Shoshan, A. Diber, S. Biton, Y. Tamir, R. Khosravi, S. Nemzer, E. Pinner, S. Walach, J. Bernstein, K. Savitsky and G. Rotman, 2003, Widespread occurrence of antisense transcription in the human genome, *Nature Biotechnol.* 21, 379.
- Yoo, J., S. Delaney, E.D.A. Stemp and J.K. Barton, 2003, Rapid radical formation by DNA charge transport through sequences lacking intervening guanines, *J. Am. Chem. Soc.* 125, 6640.
- Yosypchuk, B., M. Fojta, L. Havran and E. Palecek, 2005. Voltammetric behavior of osmium-labelled DNA at mercury meniscus-modified solid amalgam electrodes. Detecting DNA hybridization, *Electroanalysis*, in press.
- Yosypchuk, B. and L. Novotny, 2002a, Determination of iodates using silver solid amalgam electrodes, *Electroanalysis* 14, 1138.
- Yosypchuk, B. and L. Novotny, 2002b, Nontoxic electrodes of solid amalgams, *Crit. Rev. Anal. Chem.* 32, 141.
- Yosypchuk, B. and L. Novotny, 2002c, Cathodic stripping voltammetry of cysteine using silver and copper solid amalgam electrodes, *Talanta* 56, 971.
- Yosypchuk, B. and L. Novotny, 2003, Copper solid amalgam electrodes, *Electroanalysis* 15, 121.
- Yu, X., D. Chattopadhyay, I. Galeska, F. Papadimitrakopoulos and J.F. Rusling, 2003, Peroxidase activity of enzymes bound to the ends of single-wall carbon nanotube forest electrodes, *Electrochem. Commun.* 5, 408.

- Yu, C.J., Y.J. Wan, H. Yowanto, J. Li, C.L. Tao, M.D. James, C.L. Tan, G.F. Blackburn and T.J. Meade, 2001, Electronic detection of single-base mismatches in DNA with ferrocene-modified probes, *J. Am. Chem. Soc.* 123, 11155.
- Yu, C.J., H. Yowanto, Y.J. Wan, T.J. Meade, Y. Chong, M. Strong, L.H. Donilon, J.F. Kayyem, M. Gozin and G.F. Blackburn, 2000, Uridine-conjugated ferrocene DNA oligonucleotides: Unexpected cyclization reaction of the uridine base, *J. Am. Chem. Soc.* 122, 6767.
- Zaludova, R., A. Zakovska, J. Kasparkova, Z. Balcarova, V. Kleinwachter, O. Vrana, N. Farrell and V. Brabec, 1997, DNA interactions of bifunctional dinuclear platinum(II) antitumor agents, *Eur. J. Biochem.* 246, 508.
- Zhao, Q., Z. Gan and Q. Zhuang, 2002, Electrochemical sensors based on carbon nanotubes, *Electroanalysis* 14, 1609.
- Zlatanova, J. and S.H. Leuba, 2004, *Chromatin Structure and Dynamics: State-of-the-Art*, New Comprehensive Biochemistry, Vol. 39, Ed. G. Bernardi, Elsevier, Amsterdam.

This page intentionally left blank

Electrochemical Nucleic Acid Biosensors

Joseph Wang

*Department of Chemical and Materials Engineering, Box 876006, Arizona State University,
Tempe, AZ 85287, USA*

Contents

1. Introduction	175
2. Electrochemical biosensing of DNA hybridization	177
2.1. Surface immobilization	177
2.2. The hybridization event	179
2.3. Electrochemical transduction of DNA hybridization	180
2.3.1. Indicator-based detection	181
2.3.2. Use of enzyme labels for detecting DNA hybridization	183
2.3.3. Use of nanoparticle tracers	184
2.3.4. Label-free electrochemical biosensing of DNA hybridization	185
2.3.5. Other attractive routes and amplification schemes	188
3. Conclusions and outlook	189
Acknowledgment	190
References	190

1. INTRODUCTION

Wide-scale genetic testing requires the development of easy-to-use, fast, inexpensive, miniaturized analytical devices. Traditional methods for detecting DNA hybridization, such as gel electrophoresis or membrane blots, are too slow and labor intensive. *Biosensors* offer a promising alternative for faster, cheaper, and simpler nucleic-acid assays. Biosensors are small devices employing biochemical molecular recognition properties as the basis for a selective analysis. Such devices intimately couple a biological recognition element with a physical transducer. The major processes involved in any biosensor system are the analyte recognition, signal transduction, and readout. Common transducing elements, including optical, electrochemical, or mass-sensitive devices, generate light, current, or frequency signals, respectively. There are two types of biosensors, depending on the nature of the recognition event. Bioaffinity devices rely on the selective binding of the target analyte to a surface-confined ligand partner (e.g., antibody, oligonucleotide). In contrast, in biocatalytic devices, an immobilized enzyme is used for recognizing the target substrate. For example, single-use sensor strips with immobilized glucose oxidase have been widely used for personal monitoring of diabetes.

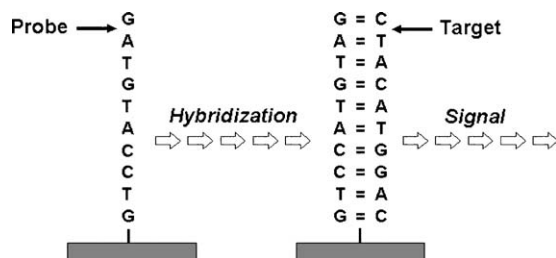


Fig. 1. Steps involved in the detection of a specific DNA sequence using an electrochemical DNA hybridization biosensor. (Reproduced from Gooding, 2002 with permission.)

DNA hybridization biosensors commonly rely on the immobilization of a single-stranded (ss) oligonucleotide probe onto a transducer surface to recognize – by hybridization – its complementary target sequence. The binding of the surface-confined probe and its complementary target strand is translated into a useful electrical signal (Figure 1). Transducing elements reported in the literature have included optical (Piunno *et al.*, 1995), electrochemical (Palecek and Fojta, 2001), and microgravimetric (Okahata *et al.*, 1992) devices. The two major requirements for a successful operation of a DNA biosensor are high specificity (including observation of a change in a single nucleotide) and high sensitivity. Even though nucleic acids are relatively simple molecules, finding the sequence that contains the desired information and distinguishing between perfect matches and mismatches are very challenging tasks.

Electrochemical transducers have received considerable recent attention in connection to the detection of DNA hybridization (Palecek and Fojta, 2001; Gooding, 2002; Mikkelsen, 1996; Drummond *et al.*, 2003). The foundation of these devices can be traced to the discovery of the electrochemical properties of nucleic acids about 40 years ago (Palecek, 1958, 1960). Modern electrical DNA hybridization biosensors and bioassays offer remarkable sensitivity, compatibility with modern microfabrication technologies, inherent miniaturization, low cost (disposability), minimal power requirements, and independence of sample turbidity or optical pathway. Such devices are thus extremely attractive for obtaining the sequence-specific information in a simpler, faster, and cheaper manner, compared to traditional hybridization assays. In addition, electrochemistry offers innovative routes for interfacing the nucleic acid recognition system with the signal-generating element and for amplifying electrical signals. Direct electrical reading of DNA interactions thus offers great promise for developing simple, rapid, and user-friendly DNA-sensing devices (in a manner analog to miniaturized blood-glucose meters). Recent efforts have led to different new strategies for electrical detection of DNA hybridization (Wang, 1999; Mikkelsen, 1996; Palecek and Fojta, 2001; Gooding, 2002; Drummond *et al.*, 2003). This activity has led to ultrasensitive detection of multiple DNA targets, and produced reusable devices that require minimal use of reagents. Such electrochemical avenues for generating the hybridization signal are the subject of the present chapter.

2. ELECTROCHEMICAL BIOSENSING OF DNA HYBRIDIZATION

Electrochemical detection of DNA hybridization usually involves monitoring of a current response, resulting from the Watson–Crick base-pair recognition event, under controlled potential conditions (Wang, 1999; Mikkelsen, 1996; Palecek and Fojta, 2001). The probe-coated electrode is commonly immersed into a solution of a target DNA whose nucleotide sequence is to be tested. When the target DNA contains a sequence which matches that of the immobilized oligonucleotide probe DNA, a hybrid duplex DNA is formed at the electrode surface (Figure 1). Such hybridization event is commonly detected via the increased current signal of an electroactive indicator (that preferentially binds to the DNA duplex), in connection to the use of enzyme or redox labels, or from other hybridization-induced changes in electrochemical parameters (e.g., capacitance or conductivity).

In the following sections, we will focus on the major steps involved in electrochemical biosensing of DNA hybridization, namely the design of the nucleic acid recognition layer, the actual hybridization event, and the transformation of this recognition event into an electrical signal (Figure 1). As will be illustrated below, the success of such devices requires a proper combination of synthetic-organic and surface chemistries, DNA recognition, and electrical detection protocols.

2.1. Surface immobilization

The probe *immobilization* step plays a major role in the overall performance of electrochemical DNA biosensors. The achievement of high sensitivity and selectivity requires maximization of the hybridization efficiency and minimization of non-specific adsorption events, respectively. The probes are typically short oligonucleotides (25–40 mer) that are capable of hybridizing with specific and unique regions of the target nucleotide sequence. Control of the *surface chemistry* and coverage is essential for assuring high reactivity, orientation/accessibility, and stability of the surface-bound probe, as well as for avoiding non-specific binding/adsorption events. For example, it was demonstrated recently that the density of immobilized ssDNA can influence the thermodynamics of hybridization, and hence the selectivity of DNA biosensors (Watterson *et al.*, 2000). Greater understanding of the relationship between the surface environment of biosensors and the resulting analytical performance is desired. This is particularly important as the physical environment of hybrids at solid/solution interface can differ greatly from that of hybrids formed in the bulk solution (Watterson *et al.*, 2000). Several useful schemes for attaching nucleic acid probes onto electrode surfaces have thus been developed. The exact immobilization protocol often depends on the electrode material used for signal transduction.

Common probe immobilization schemes include attachment of biotin-functionalized probes to *avidin*-coated surfaces (Ebersole *et al.*, 1990), self-assembly of organized monolayers of thiol functionalized probes onto gold transducers

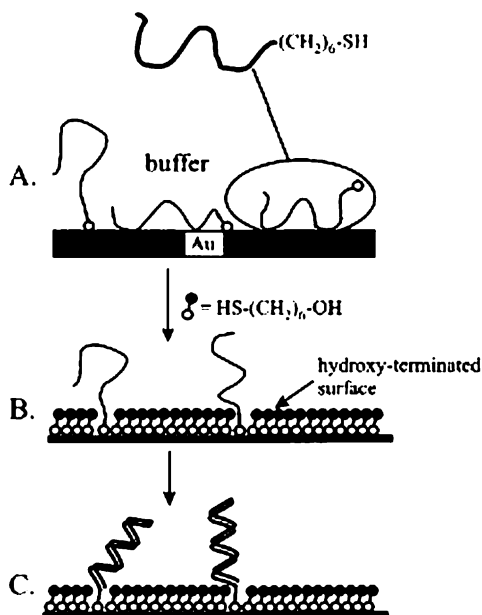


Fig. 2. Schematic preparation of the mixed thiol-derivatized single-stranded oligonucleotide/6-mercapto-1-hexanol monolayer in a solution containing the target DNA. (A) Adsorption of the ssDNA (HS-ssDNA); (B) formation of the mixed layer after the addition and adsorption of mercaptohexanol; (c) Hybridization step. (Reproduced from Levicky *et al.*, 1998 with permission.)

(Levicky *et al.*, 1998), carbodiimide covalent binding to an activated surface (Millan *et al.*, 1992), use of conducting polymers (Livache *et al.*, 1995), as well as adsorptive accumulation onto carbon-paste or thick-film carbon electrodes (Wang *et al.*, 1996a). The use of *alkanethiol self-assembly* methods has been particularly attractive for fabricating reproducible probe-modified surfaces with high hybridization activity (Levicky *et al.*, 1998). For this purpose, the DNA is commonly immobilized on gold by forming mixed monolayers of thiol-derivatized single-stranded oligonucleotide and 6-mercapto-1-hexanol (Figure 2). The thiolated probe is 'put upright' as a result of such co-assembly with a short-chain *alkanethiol*. The latter, along with a hydrophilic linker (between the thiol group and DNA), is often used for minimizing non-specific adsorption effects (of unwanted non-hybridized DNA adsorbates). Such monolayer-based structures can also provide a general route for linking to the surface relevant (enzyme or redox) labels.

The *electropolymerization* route is attractive for localizing the oligonucleotide probes on small electrode surfaces, as desired for the fabrication of high-density DNA arrays. The copolymerization of pyrrole monomers with pyrrole monomers functionalized with the oligonucleotide is particularly attractive for this task (Livache *et al.*, 1995).

Despite this considerable progress there are many fundamental questions concerning the surface orientation and accessibility, and the nature of the

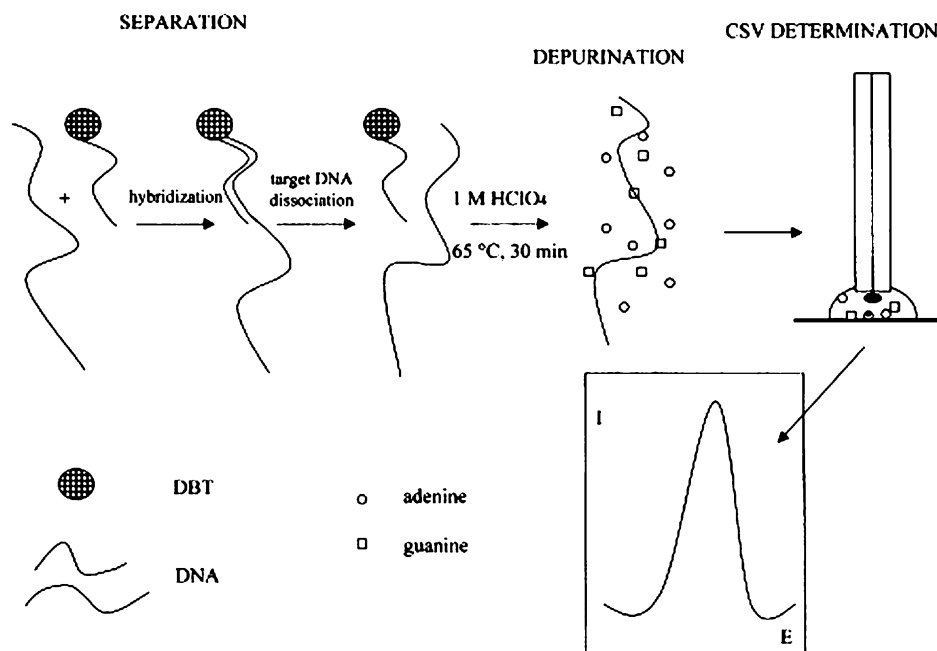


Fig. 3. The coupling of magnetic separation and electrochemical detection of DNA hybridization, illustrated here using an enzyme tracer. (a) Introduction of the oligomer-coated beads; (b) addition of the biotinylated target (T) oligomer – hybridization event; (c) addition of the streptavidin-enzyme and its conjugation with the biotinylated target (of the duplex); (d) addition and enzymatic reaction of the substrate; (e) placement of a droplet onto the thick-film electrode. (Reproduced from [Palecek *et al.*, 2002b](#) with permission.)

interfacial molecular interactions. Surface characterization techniques (e.g., XPS, reflectance IR ellipsometry) can shed useful insights into the surface coverage and organization ([Levicky *et al.*, 1998](#)).

Palecek ([Palecek *et al.*, 2002c](#)) and Wang ([Wang *et al.*, 2002a](#)) proposed a new method in which the DNA hybridization is performed at commercially available magnetic beads, while the electrochemical detection on detection electrodes (DE) (e.g., [Figure 3](#)). Such magnetic isolation of the duplex and efficient removal of unwanted (non-hybridized) constituents successfully address errors associated with *non-specific adsorption* effects and obviates the need for designing advanced surface layers. High sensitivity and specificity in the detection of relatively long DNA targets has been documented ([Palecek *et al.*, 2002b](#)).

2.2. The hybridization event

The development of electrochemical DNA biosensors (as well as other DNA biosensors) requires proper attention to experimental variables affecting the hybridization event at the transducer–solution interface. These include the salt concentration, temperature, viscosity, the presence of accelerating agents,

contacting time, base composition (%G + C), and length of probe sequence. Careful control of the hybridization event is thus required. The stability of hybrids formed between strands with mismatched bases is decreased according to the number and location of the mismatches. Many DNA biosensors are not capable of selectively detecting a point mutation, as desired in numerous practical situations. Controlling the stringency of hybridization, particularly using elevated temperatures, can thus be used for discriminating among oligonucleotide hybrids (including mismatch discrimination). Control of the hybridization time can be used for tuning the linear dynamic range, with shorter time offering an extended range at the cost of lower sensitivity (Wang *et al.*, 1997a,b). Detection limits ranging from the nanomolar to the picomolar concentration range can thus be achieved in connection to 5 and 60 min hybridization times. Even lower detection limits can be attained in connection to advanced amplification protocols (described below).

We have demonstrated that significantly enhanced selectivity can be achieved by the use of *peptide nucleic acid* (PNA) probes (Wang *et al.*, 1996b). Such DNA analog possess an uncharged pseudopeptide backbone (instead of the charged phosphate-sugar one of natural DNA). Owing to their neutral backbone, PNA probes offer greater affinity in binding to complementary DNA, and improved distinction between closely related sequences (including the detection of single-base imperfections). This is attributed to the fact that a mismatch in PNA/DNA duplexes is much more destabilizing than in DNA/DNA duplexes (with a lowering of the t_m by 15°C vs. 11°C, respectively). Such mismatch discrimination is of particular importance in the detection of disease-related mutations.

Proper attention should be given also to the reusability of the DNA biosensors, namely to the regeneration of the surface-bound single-stranded probe after each assay. Both thermal and chemical (sodium hydroxide, urea) regeneration schemes have been shown useful for ‘removing’ the bound target in connection with different DNA biosensor formats. Even more elegant is the use of controlled electric fields for facilitating the denaturation of the duplex (Cheng *et al.*, 1998). Such electronic control has been used also for differentiating among oligonucleotide hybrids. Mechanically renewed electrodes, including polishable biocomposites and graphite pencils, have also been used for regenerating a ‘fresh’ probe layer (Wang *et al.*, 1998a, 2000). Alternately, one can use “one-shot” *screen-printed electrodes*, similar to those used for self-testing of blood glucose, and hence obviate the need for regeneration (Wang *et al.*, 1996a). Such disposable DNA sensor strips also meet the needs of many decentralized genetic testing.

2.3. Electrochemical transduction of DNA hybridization

The hybridization event is usually detected via the increased current signal of a redox indicator (that associates with the newly formed surface hybrid), or from changes in electrochemical parameters (such as capacitance or conductivity), or in the redox activity of the nucleic acid resulting from the duplex formation.

2.3.1. Indicator-based detection

Earlier devices have relied primarily on the use of redox hybridization *indicators* (Mikkelsen, 1996). Such indicators are small electroactive DNA-intercalating or groove-binding substances, that possess a much higher affinity for the resulting hybrid compared to the single-stranded probe. Accordingly, the concentration of the indicator at the electrode surface increases when hybridization occurs, resulting in increased electrochemical response. Besides effective differentiation between ss- and double-stranded (ds) DNA, the indicator should possess a well-defined, low-potential, voltammetric response. Such properties of redox indicators are essential for attaining high sensitivity and selectivity. Both linear-scan or square-wave voltammetric modes (Millan and Mikkelsen, 1993) or constant-current *chronopotentiometry* (Wang *et al.*, 1996c) can be used to detect the association of the redox indicator with the surface duplex.

Mikkelsen's group, that pioneered the use of redox indicators, demonstrated its utility for detecting the cystic fibrosis $\Delta F508$ deletion sequence associated with 70% of cystic fibrosis patients (Millan *et al.*, 1994). A detection limit of 1.8 fmol was demonstrated for the 4000-base DNA fragment in connection to a $\text{Co}(\text{bpy})_3^{3+}$ marker. High selectivity toward the disease sequence – but not to the normal DNA – was achieved by performing the hybridization at an elevated temperature of 43°C. Such use of the electrochemical transduction mode requires that proper attention be given to the choice of the indicator and its detection scheme. Our laboratory demonstrated the use of the $\text{Co}(\text{phen})_3^{3+}$ indicator, in connection to a carbon-paste chronopotentiometric transducer and PNA probes, for detecting single-base imperfections in the p53 gene (Wang *et al.*, 1997a,b). Other useful redox-active indicators include bisbenzimidazole dyes such as Hoechst 33258 (Hashimoto *et al.*, 1994) or anthracycline antibiotics such as daunomycin (Marrazza *et al.*, 1999). A daunomycin-based chronopotentiometric biosensor was combined with PCR amplification of DNA extracted from whole blood for the genetic detection of apolipoprotein E polymorphism (Marrazza *et al.*, 2000).

New electroactive indicators, offering better distinction between ss- and dsDNA have been developed for attaining higher sensitivity. Very successful has been the recent use of a threading intercalator ferrocenyl naphthalene diimide (FND) (Takenaka *et al.*, 2000) that binds to the DNA duplex more tightly than usual intercalators and displays a negligible affinity to the single-stranded probe. This duplex-specific *threading indicator* resulted in a detection limit of 10 zmol in connection to differential pulse voltammetric monitoring of the hybridization event (Figure 4). The oligonucleotide probe was chemisorbed onto gold electrodes through a thiol anchor. Table 1 summarizes common redox-active indicators used in electrochemical DNA hybridization biosensors. Oligonucleotides bearing electroactive reporter molecules, such as ferrocene or anthraquinone tags, have also been considered for electrical detection of surface hybridization (Ihara *et al.*, 1997, Kertesz *et al.*, 2000). *Ferrocene tags* are being used in a new hand-held device, the CMS eSensor™ system of Motorola Inc., that can detect up to 48 different sequences in connection to elegant surface chemistry (combining self-assembly of thiolated probes and phenylacetylene “molecular wires”)

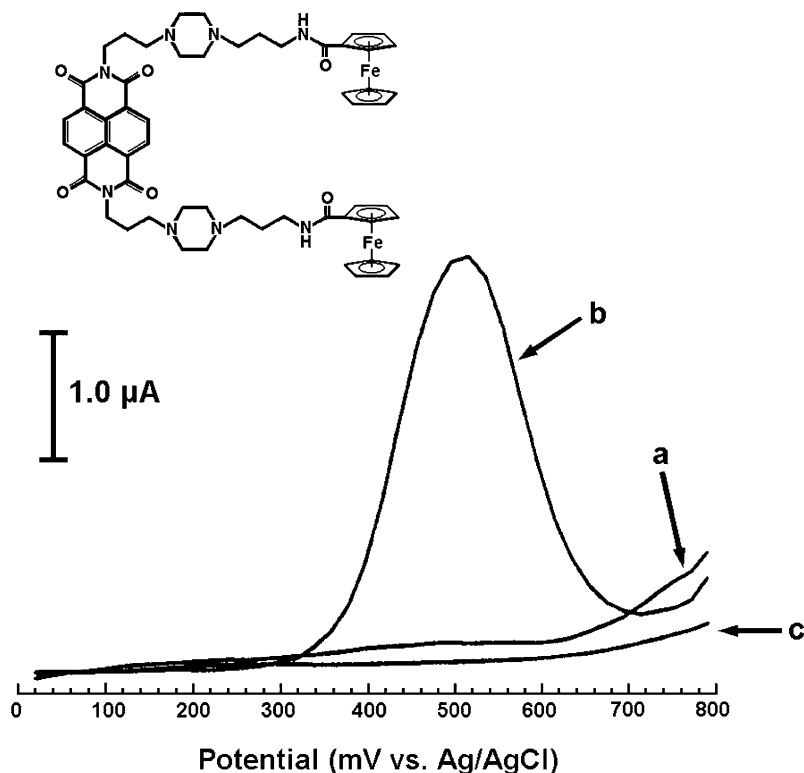


Fig. 4. Differential pulse voltammograms for the ferrocenyl naphthalene diimide indicator at the dT₂₀-modified electrode before (a) and after (b) hybridization with dA₂₀. Also shown, the chemical structure of the indicator. (Reproduced from Takenaka *et al.*, 2000 with permission.)

Table 1. Examples of redox-active indicators used for the biosensing of DNA hybridization

Indicator	Detection mode transducer	Electrode	E _{p,a} /vs. Ag/AgCl, V	References
Co(bpy) ₃ ³⁺	Cyclic voltammetry	Carbon paste	0.15	Millan and Mikkelsen, 1993
Co(phen) ₃ ³⁺	Chronopotentiometry	Carbon paste	0.15	Wang <i>et al.</i> , 1996
Hoechst 33258	Pulse voltammetry	Gold	0.58	Hashimoto <i>et al.</i> , 1994
Daunomycin	Chronopotentiometry	Screen-printed	0.45	Marrazza <i>et al.</i> , 1999
Ferrocenyl naphthalene diimide	Pulse voltammetry	Gold	0.50	Takenaka <i>et al.</i> , 2000

and a highly sensitive alternative-current voltammetric detection (Umek *et al.*, 2000). An attractive reagentless biosensor, based on a ferrocene-tagged DNA stem-loop structure, was developed recently (Fan *et al.*, 2003). Such use of *molecular-beacon* like labeled DNA leads to hybridization-induced changes in the

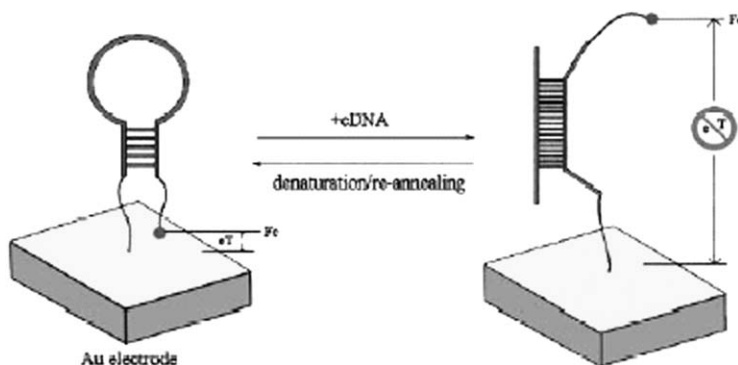


Fig. 5. Electrical detection of DNA hybridization based on surface-confined molecular beacons. The hybridization event changes the distance between the label (conjugated to the oligonucleotide probe) and the electrode surface. (Based on Fan *et al.*, 2003.)

distance between the label and the electrode surface, and hence in the electron-transfer efficiency (Figure 5). The resulting changes in the cyclic voltammetric signal offer convenient measurements of DNA targets down to the 10 pM level, and an impressive dynamic range over six orders of magnitude.

2.3.2. Use of enzyme labels for detecting DNA hybridization

Enzyme labels have been widely used in bioaffinity sensors, particularly in immunosensors. The use of enzyme tags to generate electrical signals offers also great promise for ultrasensitive electrical detection of DNA hybridization. Heller's group (de Lumley *et al.*, 1996; Zhang *et al.*, 2003) demonstrated that a direct low-potential sensitive amperometric monitoring of the hybridization event could be achieved in connection to the use of *horseradish peroxidase* (HRP) labeled target and an electron-conducting redox polymer. In this system the hybridization of enzyme-labeled oligo(dA)₂₅ target with oligo(dT)₂₅ probe, covalently attached to electron-conducting redox hydrogel, resulted in the 'wiring' of the enzyme to the transducer and in a continuous hydrogen-peroxide electroreduction current. A single-base mismatch in an 18-base oligonucleotide was thus detected using a 7- μm -diameter carbon fiber electrode. Such enzymatic amplification facilitated measurements down to the zmol (3000 copies; 0.5 fM) level using 10 μl sample droplets (Zhang *et al.*, 2003) (Figure 6). A HRP label has been combined by Willner's group (Patolsky *et al.*, 1999) with a biocatalytic precipitative accumulation of the enzyme-generating product to achieve multiple amplifications, and hence extremely low detection limits. *Chronopotentiometry* and *faradaic impedance spectroscopy* were employed for detecting the biocatalyzed deposition reaction. Applicability for the detection of mutations relevant to the Tay-Sachs genetic disorder was demonstrated. The use of *enzyme-linked immunoassay* for electrical sensing of DNA hybridization was also demonstrated (Palecek *et al.*, 2002b). Such protocol relied on modifying the DNA target with osmium tetroxide, 2,2'-bipyridine (Os,bipy). The

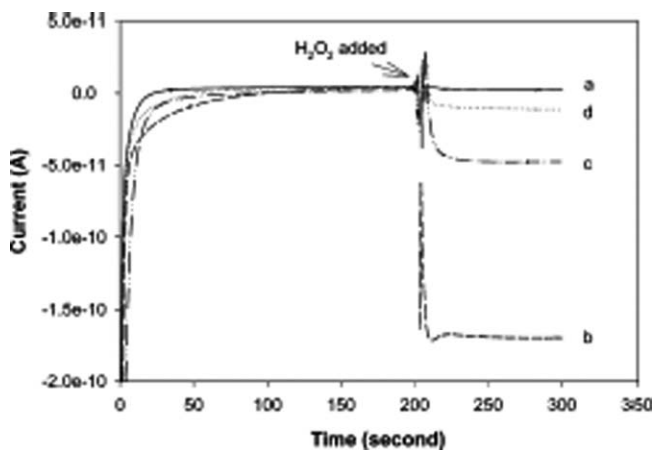


Fig. 6. Highly sensitive amperometric monitoring of DNA hybridization based on the use of HRP labeled target and an electron-conducting redox polymer. Current increments upon raising the hydrogen peroxide concentration from 0 to 1 mM. (a) Without the analyzed sequence in the droplet; (b) with 0.1 fM perfectly matched analyzed sequence; (c) as in (b), but with a mismatched base; (d) as in (b), with two mismatched bases. (Reproduced from Zhang *et al.*, 2003 with permission.)

DNA-Os,bipy adduct was determined by an enzyme immunoassay. A one-step enzymatic reaction involving glucose oxidase was recently used for the direct detection of genes in mRNA extracted from animal tissues (Xie *et al.*, 2004).

Enhanced amplification of DNA-sensing processes was also achieved by using *liposomes* labeled with multiple HRP tags in connection to faradaic impedance spectroscopic detection (Alfonta *et al.*, 2001) (e.g., Figure 7). Such use of functionalized liposomes resulted in a dramatic signal amplification (of ca. 10^5). The same enzyme label was employed for quantitative pulse amperometric monitoring of PCR amplification (Wojciechowski *et al.*, 1999) and for differential pulse measurements of sequences related to human cytomegalovirus DNA (Azek *et al.*, 2000). Another attractive enzyme for amplified electrical assay, *bilirubin oxidase*, can be used in connection ambient oxygen as the substrate, to offer the detection of ~ 1000 DNA copies (Zhang *et al.*, 2004). The coupling of enzyme-based DNA assays with an efficient magnetic removal of unwanted sample constituents has been illustrated in our laboratory (Wang *et al.*, 2002a). A dramatic amplification of alkaline phosphatase (ALP)-based electrical DNA hybridization was obtained using *carbon nanotubes* (CNT), carrying numerous enzyme tracers and accumulating the enzymatically liberated product on CNT-modified transducer (Wang *et al.*, 2004). A coverage of around 9600 enzyme molecules per CNT (i.e., binding event) allowed ultrasensitive measurements down to the 1.3 zmol level in 25 μ l samples.

2.3.3. Use of nanoparticle tracers

Recent activity has led to powerful *nanoparticle*-based electrochemical DNA hybridization assays (Wang *et al.*, 2001a; Authier *et al.*, 2001; Cai *et al.*, 2002;

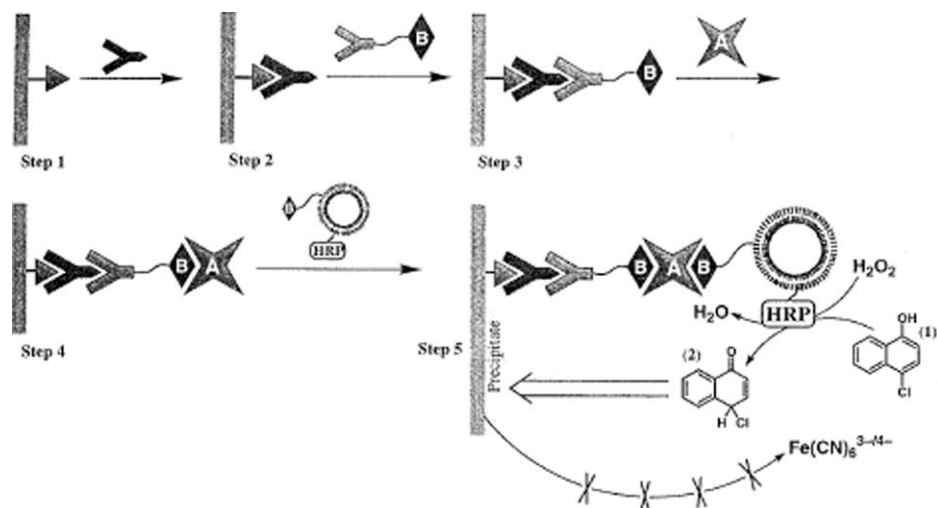


Fig. 7. Amplified electrical detection of DNA hybridization using HRP-functionalized liposomes and biocatalytic precipitation of the product of the enzymatic reaction. (Reproduced from Alfonta *et al.*, 2001 with permission.)

Ozsoz *et al.*, 2003). Such protocols have relied on binding of the *gold* (Wang *et al.*, 2001a; Authier *et al.*, 2001), *silver* (Cai *et al.*, 2002), or CdS (Wang *et al.*, 2002c) nanoparticles to the captured target, followed by dissolution and anodic-stripping electrochemical measurement of the metal tracer. This method takes advantage of the inherent signal amplification (preconcentration) of electrochemical *stripping analysis* of dissolved metal particle tags. Catalytic enlargement of the colloidal gold label has been useful for further enhancing the sensitivity of nanoparticle-based stripping DNA detection (Wang *et al.*, 2001a). Solid-state measurements of metal-nanoparticle tracers (without acid dissolution) have also been described (Wang *et al.*, 2002b).

Inorganic nanocrystals have paved the way for a multi-target electrochemical DNA detection (Wang *et al.*, 2003a). Three encoding nanoparticles (zinc sulfide, cadmium sulfide, and lead sulfide) have thus been used to differentiate the signals of three DNA targets in connection with a sandwich hybridization assay and stripping voltammetry of the corresponding metals (Figure 8). Each hybridization event thus yields a distinct voltammetric peak, whose position and size reflects the identity and level, respectively, of the corresponding target. Recent efforts have demonstrated the ability to create large particle-based libraries for electrochemical coding, based on the judicious design of encoded ‘identification’ beads or wires (Wang *et al.*, 2003b). By incorporating different levels of multiple metal-particle markers, such beads or rods lead to a large number of unique stripping voltammetric signatures (i.e., electrical barcodes).

2.3.4. Label-free electrochemical biosensing of DNA hybridization

Increased attention has been given recently to direct *label-free* electrochemical detection schemes, in which the hybridization event triggers a change in an

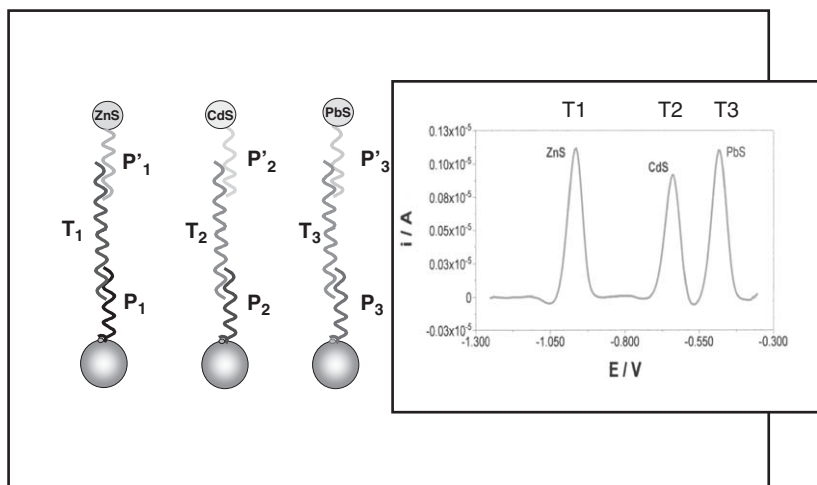
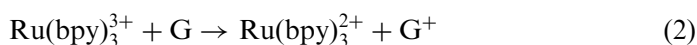
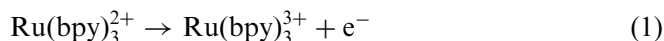


Fig. 8. Use of different quantum-dot tracers for electrical detection of multiple DNA targets. Stripping voltammograms for a solution containing dissolved ZnS, CdS, and PbS nanoparticle tracers. (Reproduced from Wang *et al.*, 2003a with permission.)

electrical signal. Such protocols greatly simplify the sensing protocol (as they eliminate the need for the indicator addition/association/detection steps) and offers an instantaneous detection of the duplex formation. Such direct, *in-situ* detection can be accomplished by monitoring changes in the intrinsic redox activity of the nucleic acid target or probe or changes in the electrochemical properties of the interface.

The electroactivity of DNA was demonstrated by Palecek over 40 years ago (Palecek, 1958, 1960). Palecek (1958) also demonstrated the ability of electroanalysis to monitor DNA renaturation processes. Among the four nucleic acids bases, the *guanine* moiety is most easily oxidized and is most suitable for such indicator-free hybridization detection (Palecek, 1996). It is possible to exploit changes in the guanine response accrued from the hybridization event for label-free detection of target DNA (Johnston *et al.*, 1995; Wang *et al.*, 1998b; Wang *et al.*, 2001b; Palecek *et al.*, 2002a). To overcome the limitations of the probe sequences (absence of G), guanines in the probe sequence were substituted by inosine residues (pairing with C's) and the hybridization was detected through the target DNA guanine signal (Wang *et al.*, 1998b). A greatly amplified guanine signal, and hence hybridization response, can be obtained by using the electrocatalytic action of a $\text{Ru}(\text{bpy})_3^{2+}$ redox mediator (Johnston *et al.*, 1995). This involves the following catalytic cycle:



The presence of a guanine-containing nucleic acid target thus creates a catalytic cycle that results in a large current output (Figure 9). The ability of this

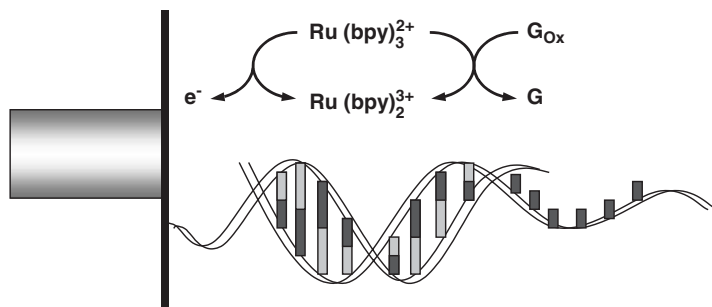


Fig. 9. Schematic representation of guanine oxidation mediated by a ruthenium complex. (Reproduced from *Li et al.*, 2003 with permission.)

approach to detect mutations or deletions involving guanine bases has been demonstrated (*Ropp and Thorp*, 1999). A single microtiter plate thus allows 672 measurements (480 tests and 192 controls). Tin-doped indium oxide (ITO) electrodes (with probes linked to a self-assembled phosphonate monolayers) have been particularly useful for such $\text{Ru}(\text{bpy})_3^{2+}$ -mediated guanine-oxidation hybridization detection protocol (*Napier et al.*, 2000; *Popovich et al.*, 2002). The coupling of the $\text{Ru}(\text{bpy})_3^{2+}$ -mediated guanine oxidation with CNT nanoelectrode array has facilitated the detection of subattmoles of DNA targets (*Koehne et al.*, 2004). Such CNT array was applied for label-free detection of DNA PCR amplicons, and offered the detection of less than 1000 target amplicons. In addition to anodic measurements of the target guanine, it is possible to use *cathodic stripping* measurements of the target adenine for sensitive detection of DNA hybridization (*Palecek et al.*, 2002c). A copper amalgam electrode was shown very useful for label-free cathodic stripping voltammetric measurements of acid-released purine bases, following the hybridization on a separate magnetic bead surface (*Jelen et al.*, 2002).

It is also possible to exploit different rates of electron transfer through ss- and dsDNA for probing hybridization (including mutation detection) via the perturbation in charge migration through DNA. Barton's group demonstrated that such *charge transport* is disrupted by the presence of a single-base mismatch (*Kelley et al.*, 1999; *Boon et al.*, 2001). Such disruption and point mutation were detected, using a gold electrode modified with thiolated DNA, by monitoring changes in the charge transport between an electroactive methylene-blue intercalator and a ferricyanide redox species. A substantially smaller electrocatalytic signal was observed in the presence of the single-base mismatch. Such detection of mismatches is not dependent on thermodynamic destabilization at the mismatch site, and hence does not require a stringent hybridization control. Prospects for designing electronic circuits based on manipulation of charge transport through DNA were discussed (*Aich et al.*, 1999).

Direct, label-free, electrical detection of DNA hybridization has also been accomplished by monitoring changes in the *conductivity* of conducting polymer molecular interfaces, e.g., using DNA-substituted or doped polypyrrole (PPy) films (*Korri-Youssoufi et al.*, 1997; *Wang et al.*, 1999). For example, Garnier's group has demonstrated that a 13-mer oligonucleotide substituted *polypyrrole*

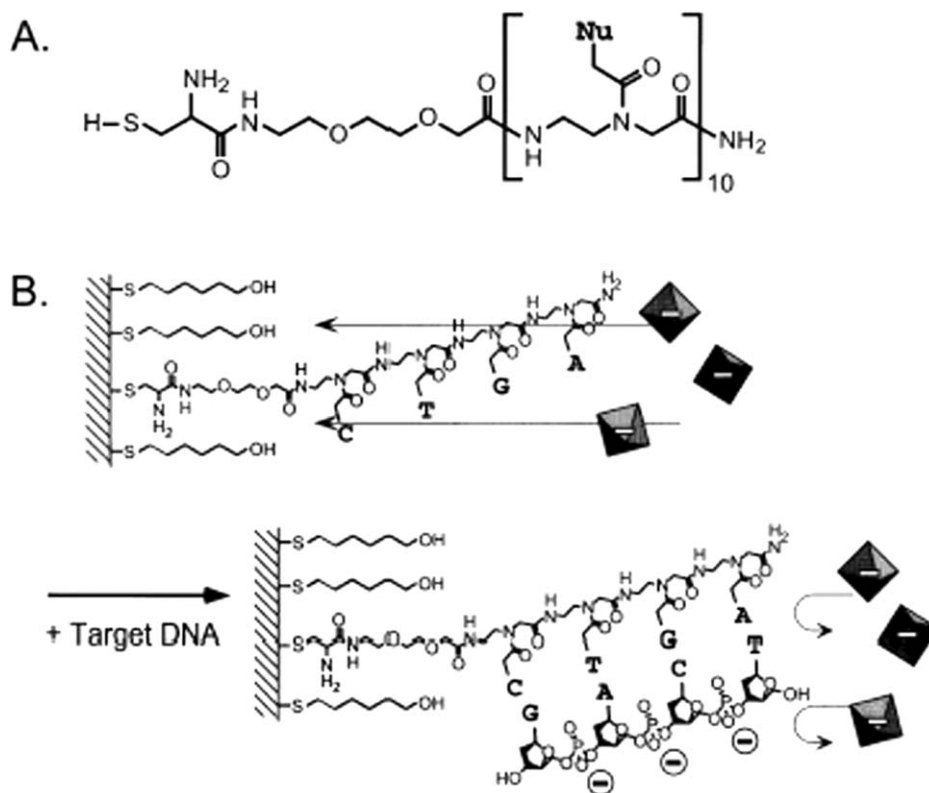


Fig. 10. An ion-channel sensor based on a PNA probe immobilized on gold electrode, and detection of the hybridization based on the electrostatic repulsion of a negatively charged redox marker (shown as an octahedron). (Reproduced from Aoki *et al.*, 2000 with permission.)

film displays a decrease current response during the duplex formation (Korri-Youssoufi *et al.*, 1997). Such change in the electronic properties of PPy has been attributed to bulky conformational changes along the polymer backbone due to its higher rigidity following the hybridization. Janata's group (Thompson *et al.*, 2003) developed a label-free cyclic-voltammetric hybridization detection protocol based on modulating the ion-exchange properties of the PPy/DNA layer (associated with changes in the charge during the hybridization event). Label-free real-time conductivity detection of DNA hybridization can also be accomplished using one-dimensional nanowires, bridging two closely spaced electrodes. This relies on the binding of negatively charged DNA target to neutral PNA probes – immobilized on p-type silicon nanowires – that leads to an increase conductance owing to an increased surface charge (Hahm and Lieber, 2004).

2.3.5. Other attractive routes and amplification schemes

New avenues for generating the hybridization signal are currently being explored in several laboratories. Siontorou *et al.* (1997) reported on the use of

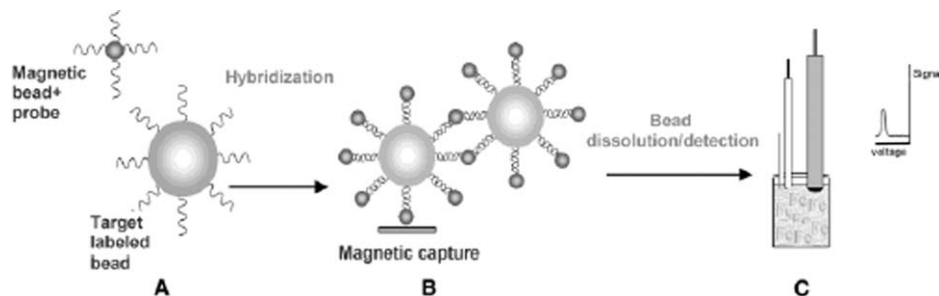


Fig. 11. Steps involved in the protocol: (A) Introduction of probe-coated magnetic beads and target-labeled 'electroactive beads'. (B) Hybridization and magnetic separation. (C) Dissolution of the spheres in acetonitrile, release of the marker and its chronopotentiometric detection at a glassy carbon electrode. Fc represents the ferrocene marker.

self-assembled bilayer *lipid membranes* (BLMs) for the direct monitoring of DNA hybridization. A decrease in the ion conductivity across the lipid membrane surface, containing the single-stranded probe, was observed during the formation of the duplex. This was attributed to alterations in the ion permeation associated with structural changes in the BLM accrued by the desorption of the dsDNA. The mechanism of interaction between oligonucleotides and BLM films was examined (Hianik *et al.*, 2000). Umezawa's group developed a novel *ion-channel* protocol for the indirect biosensing of DNA hybridization (Aoki *et al.*, 2000). The system relied on the electrostatic repulsion of the diffusing ferrocyanide redox marker, accrued from the hybridization of the negatively charged target DNA and the neutral PNA probe (Figure 10). High specificity toward mismatch oligonucleotides was demonstrated. Willner's group described a related approach for amplifying DNA hybridization signals, based on the use of negatively charged liposomes (Patolsky *et al.*, 2000). Such *liposomes* bind to the bound target to form a 'giant' negatively charged interface that repels the anionic redox probe. The resulting barrier to the interfacial electron transfer was monitored by Faradaic impedance spectroscopy. Internal encapsulation electroactive tags within polymeric carrier beads offer an attractive route for ultrasensitive electrical DNA detection (Wang *et al.*, 2003c) (Figure 11). The resulting '*electroactive beads*' are capable of carrying a huge number ($> 10^9$) of the *ferrocene* marker molecules and offer a remarkable amplification of single hybridization events (along with zmol detection limits).

Johansson's group demonstrated that changes in the *capacitance* of a thiolated-oligonucleotide modified gold electrode, provoked by hybridization to the complementary strand (and the corresponding displacement of solvent molecules from the surface), can be used for monitoring in high sensitivity and speed the hybridization event (Berggren *et al.*, 1999).

3. CONCLUSIONS AND OUTLOOK

Over the past decade we have witnessed a tremendous progress toward the development of electrochemical DNA biosensors. Such devices are of considerable

interest due to their tremendous promise for obtaining sequence-specific information in a faster, simpler, and cheaper manner compared to traditional nucleic acid assays. The instrumentation for electrochemical DNA detection is significantly cheaper and smaller than that of comparably sensitive non-electrochemical methods. In addition to excellent economic prospects, such devices offer innovative routes for interfacing (at the molecular level) the DNA-recognition and signal-transduction elements, i.e., an exciting opportunity for fundamental research. The realization of instant decentralized (medical, forensic, or environmental) DNA testing would require additional developmental work. Particular attention should be given to the major challenges associated with assays of real-world genomic samples, including the mismatch discrimination, signal amplification, non-specific adsorbates, as well as integration of various processes (including sample collection, DNA extraction and amplification, with the actual hybridization detection) on a single microchip platform containing multiple functional elements and related microfluidic network. Such integration and miniaturization should lead to significant advantages in terms of cost, speed, sample/reagent consumption, simplicity, and automation. An attractive example is the recently developed self-contained disposable DNA biochips, combining electrochemical detection with electrochemical pumping, sample preparation (cell pre-concentration and lysis), and PCR amplification, that have been successfully applied for whole blood analysis (Liu *et al.*, 2004). Electronic readouts are expected to be particularly attractive for DNA microarrays. The multiplexing of multiple biosensors into useful sensor arrays should lead to the simultaneous analysis of multiple nucleic acid sequences, and hence to the generation of characteristic hybridization patterns and acquisition of expression information. Screening of DNA-protein or DNA-drug interactions would also benefit from such DNA microarrays. Given the rapid pace of advances in this field, the development of miniaturized, easy-to-use electrochemical DNA diagnostic systems for large-scale genetic testing seems a realistic goal.

ACKNOWLEDGMENT

The author gratefully acknowledges financial support from the National Science Foundation (grant numbers CHE 0209707 and OCE-332918).

REFERENCES

- Aich, P., S. Labiuk, L. Tari, L. Delbaere, W. Roesler, K. Falk, R. Steer and J. Lee, 1999, M-DNA: A complex between divalent metal ions and DNA which behaves as a molecular wire, *J. Mol. Biol.* 294, 477.
- Alfonta, L., A.K. Singh and I. Willner, 2001, Liposomes labeled with biotin and horseradish peroxidase: A probe for the enhanced amplification of antigen-antibody or oligonucleotide-DNA sensing processes by the precipitation of an insoluble product on electrodes, *Anal. Chem.* 73, 91.
- Aoki, H., P. Buhlmann and Y. Umezawa, 2000, Electrochemical detection of a one-base mismatch in an oligonucleotide using ion-channel sensors with self-assembled PNA monolayers, *Electroanalysis* 12, 1272.

- Authier, L., C. Grossiord, P. Berssier and B. Limoges, 2001, Gold nanoparticle-based quantitative electrochemical detection of amplified human cytomegalovirus DNA using disposable microband electrodes, *Anal. Chem.* 73, 4450.
- Azek, F., C. Grossiord, M. Joannes, B. Limoges and P. Brossier, 2000, Hybridization assay at a disposable electrochemical biosensor for the attomole detection of amplified human cytomegalovirus DNA, *Anal. Biochem.* 284, 107.
- Berggren, C., P. Stalhandske, J. Brundell and G. Johansson, 1999, A feasibility study of a capacitive biosensor for direct detection of DNA hybridization, *Electroanalysis* 11, 156.
- Boon, E.M., D. Ceres, T. Drummond, M. Hill and J.K. Barton, 2001, Mutation detection by electrocatalysis at DNA-modified electrodes, *Nat. Biotechnol.* 18, 1096.
- Cai, H., Y. Xu, N. Zhu, P. He and Y. Fang, 2002, An electrochemical DNA hybridization detection assay based on a silver nanoparticle label, *Analyst* 127, 803.
- Cheng, J., E. Sheldon, L. Wu, L. Gerrue, J. Carrino, M. Heller and M. O'Connell, 1998, Preparation and hybridization analysis of DNA/RNA from *E. coli* on microfabricated bioelectronic chips, *Nat. Biotechnol.* 16, 541.
- de Lumley, T., C. Campbell and A. Heller, 1996, Direct enzyme-amplified electrical recognition of a 30-base model oligonucleotide, *J. Am. Chem. Soc.* 118, 5504.
- Drummond, T.G., M.G. Hill and J.K. Barton, 2003, Electrochemical DNA sensors, *Nat. Biotechnol.* 21, 1192.
- Ebersole, R., J. Miller, J. Moran and M. Ward, 1990, Spontaneously formed functionally active avidin monolayers on metal surfaces: A strategy for immobilizing biological reagents and design of piezoelectric biosensors, *J. Am. Chem. Soc.* 112, 3239.
- Fan, C., K. Plaxco and A.J. Heeger, 2003, Electrochemical interrogation of conformational changes as a reagentless method for the sequence-specific detection of DNA, *Proc. Natl. Acad. Sci. USA* 100, 9134.
- Gooding, J.J., 2002, Electrochemical DNA hybridization biosensors, *Electroanalysis* 14, 1149.
- Hahn, J. and C.M. Lieber, 2004, Direct ultrasensitive electrical detection of DNA and DNA sequence variations using nanowire nanosensors, *Nano Lett.* 4, 51.
- Hashimoto, K., K. Ito and Y. Ishimori, 1994, Sequence-specific gene detection with a gold electrode modified with DNA probes and an electrochemically active dye, *Anal. Chem.* 66, 3830.
- Hianik, T., M. Fajkus, B. Sivak, I. Rosenberg, P. Kois and J. Wang, 2000, The changes in dynamics of solid supported lipid films following hybridization of short sequence DNA, *Electroanalysis* 12, 495.
- Ihara, T., M. Nakayama, M. Murata, K. Nakano and M. Maeda, 1997, Gene sensor using ferrocenyl oligonucleotide, *Chem. Comm.* 1609.
- Jelen, F., B. Yosypchuk, L. Novotny and E. Palecek, 2002, Label-free determination of picogram quantities of DNA by stripping voltammetry with solid copper amalgam or mercury electrodes in the presence of copper, *Anal. Chem.* 74, 4788.
- Johnston, D.H., K. Glasgow and H.H. Thorp, 1995, Electrochemical measurement of the solvent accessibility of nucleobases using electron transfer between DNA and metal complexes, *J. Am. Chem. Soc.* 117, 8933.
- Kelley, S.O., E. Boon, J.K. Barton, M. Jackson and M. Hill, 1999, Single-base mismatch detection based on charge transduction through DNA, *Nucleic Acids Res.* 27, 4830.
- Kertez, V., N. Whittemore, G. Inamati, M. Manoharan, P. Cook, D. Baker and J.Q. Chambers, 2000, Electrochemical detection of surface hybridization of oligodeoxynucleotides bearing anthraquinone tags at gold electrodes, *Electroanalysis* 12, 889.
- Koehne, J.E., H. Chen, A.M. Cassell, Q. Yi, J. Han, M. Meyyappan and J. Li, 2004, Miniaturized multiplex label-free electronic chip for rapid nucleic acid analysis based on carbon nanotube nanoelectrode arrays, *Clin. Chem.* 50, 1886.
- Korri-Yousoufi, H., F. Garnier, P. Srivtava, P. Godillot and A. Yassar, 1997, Toward bioelectronics: Specific DNA recognition based on an oligonucleotide-functionalized polypyrrole, *J. Am. Chem. Soc.* 119, 7388.
- Levicky, R., T. Herne, M. Tarlov and S. Satija, 1998, Using self-assembly to control the structure of DNA monolayers on gold: A neutron reflectivity study, *J. Am. Chem. Soc.* 120, 9787.

- Li, J., H.T. Ng, A. Cassell, W. Fan, H. Chen, Q. Ye, J. Koehne and M. Meyyappan, 2003, Carbon nanotube nanoelectrode array for ultrasensitive DNA detection, *Nano Lett.* 3, 597.
- Liu, R., J. Yang, R. Lenigk, J. Bonanno and P. Grodzinski, 2004, Self-contained, fully integrated biochip for sample preparation, polymerase chain reaction amplification, and DNA microarray detection, *Anal. Chem.* 76, 1824.
- Livache, T., A. Roget, E. Dejean, C. Barthet, G. Bidan and R. Teoule, 1995, Biosensing effects in functionalized electroconducting-conjugated polymer layers – Addressable DNA matrix for the detection of gene mutations, *Synth. Met.* 71, 2143.
- Marrazza, G., I. Chianella and M. Mascini, 1999, Disposable DNA electrochemical biosensors for environmental monitoring, *Anal. Chim. Acta* 387, 297.
- Marrazza, G., G. Chiti, M. Mascini and M. Anichini, 2000, Detection of human apolipoprotein E genotypes by DNA electrochemical biosensor coupled with PCR, *Clin. Chem.* 46, 31.
- Mikkelsen, S.R., 1996, Electrochemical biosensors for DNA sequence detection, *Electroanalysis* 8, 15.
- Millan, K., A. Spurmanis and S.R. Mikkelsen, 1992, Covalent immobilization of DNA onto glassy carbon electrodes, *Electroanalysis* 4, 929.
- Millan, K. and S.R. Mikkelsen, 1993, Sequence-selective biosensor for DNA based on electroactive hybridization indicators, *Anal. Chem.* 65, 2317.
- Millan, K.M., A. Saraulo and S.R. Mikkelsen, 1994, Voltammetric DNA biosensor for cystic fibrosis based on a modified carbon paste electrode, *Anal. Chem.* 66, 2943.
- Napier, M.E., K. Mikulecky, K. Scaboo, A. Eckhardt, N. Baron, N. Popovich and M. Geladi, 2000, Direct electrochemical detection of nucleic acids, *Clin. Chem.* 46, A207.
- Okahata, Y., Y. Matsunobo, K. Ijio, M. Mukae, A. Murkami and K. Makino, 1992, Hybridization of nucleic acids immobilized on a quartz crystal microbalance, *J. Am. Chem. Soc.* 114, 8299.
- Ozsoz, M., A. Erdem, K. Kerman, D. Okzan, B. Tugrul, N. Topcuoglu, H. Ekren and M. Taylan, 2003, Electrochemical genosensor based on colloidal gold nanoparticles for the detection of factor V leiden mutation using disposable pencil graphite electrodes, *Anal. Chem.* 75, 2181.
- Palecek, E., 1958, Oszillographische Polarographie der Nucleinsäuren und ihrer Bestandteile, *Naturwissenschaften* 45, 186.
- Palecek, E., 1960, Oscillographic polarography of highly polymerized deoxyribonucleic acid, *Nature* 188, 656.
- Palecek, E., 1996, From polarography of DNA to microanalysis with nucleic acid modified electrodes, *Electroanalysis* 8, 7.
- Palecek, E., S. Billova, L. Havran, R. Kizek, A. Miculkova and F. Jelen, 2002a, DNA hybridization at microbeads with cathodic stripping voltammetric detection, *Talanta* 56, 919.
- Palecek, E. and M. Fojta, 2001, Detecting DNA hybridization and damage, *Anal. Chem.* 73, 75A.
- Palecek, E., M. Fojta and F. Jelen, 2002c, New approaches in the development of DNA sensors: Hybridization and electrochemical detection of DNA and RNA at two different surfaces, *Bioelectrochemistry* 56, 85.
- Palecek, E., R. Kizek, L. Havran, S. Billova and M. Fojta, 2002b, Electrochemical enzyme-linked immunoassay in a DNA hybridization sensor, *Anal. Chim. Acta* 469, 73.
- Patolsky, F., E. Katz, A. Bardea and I. Willner, 1999, Enzyme-linked amplified electrochemical sensing of oligonucleotide–DNA interactions by means of the precipitation of an insoluble product and using impedance spectroscopy, *Langmuir* 15, 3703.
- Patolsky, F., A. Lichtenstein and I. Willner, 2000, Electrochemical transduction of liposome-amplified DNA sensing, *Angew. Chem. Int. Ed.* 39, 940.
- Piunno, P., U. Krull, R. Hudson, M. Damha and H. Cohen, 1995, Fiber-optic DNA sensor for fluorometric nucleic acid determination, *Anal. Chem.* 67, 2635.
- Popovich, N.D., A.E. Eckhardt, J.C. Mikulecky, M.E. Napier and R.S. Thomas, 2002, Electrochemical sensor for detection of unmodified nucleic acids, *Talanta* 56, 821.

- Ropp, P. and H.H. Thorp, 1999, Site-selective electron transfer from purines to electrocatalysts: Voltammetric detection of a biologically relevant deletion in hybridized DNA duplexes, *Chem. Biol.* 6, 599.
- Siontorou, C., D. Nikolelis, P. Piuanno and U. Krull, 1997, Detection of DNA hybridization using self assembled BLMs, *Electroanalysis* 9, 1067.
- Takenaka, S.K., M. Yamashita, M. Takagi, Y. Uto and H. Kondo, 2000, DNA sensing on a DNA probe-modified electrode using ferrocenylnaphthalene diimide as the electrochemically active ligand, *Anal. Chem.* 72, 1334.
- Thompson, L., J. Kowalik, M. Josowicz and J. Janata, 2003, Label-free DNA hybridization probe based on a conducting polymer, *J. Am. Chem. Soc.* 125, 324.
- Umek, R.M., S.S. Lin, Y.P. Chen, B. Irvine, G. Paulluconi, V. Chan, Y. Chong, L. Cheung, J. Vielmetter and D.H. Farkas, 2000, Bioelectronic detection of point mutations using discrimination of the H63D polymorphism of the Hfe gene as a model, *Molec. Diagn.* 5, 321.
- Wang, J., 1999, Towards genoelectronics: Electrochemical biosensing of DNA hybridization, *Chem. Eur. J.* 5, 1681.
- Wang, J., X. Cai, G. Rivas and H. Shiraishi, 1996c, Stripping potentiometric transduction of DNA hybridization processes, *Anal. Chim. Acta* 326, 141.
- Wang, J., X. Cai, B. Tian and H. Shiraishi, 1996a, Microfabricated thick-film electrochemical sensor for nucleic acid determination, *Analyst* 121, 965.
- Wang, J., J. Fernandes and L. Kubota, 1998a, Polishable and renewable DNA hybridization biosensors, *Anal. Chem.* 70, 3699.
- Wang, J., M. Jiang, A. Fortes and B. Mukherjee, 1999, New label-free DNA recognition based on doping nucleic-acid probes within conducting polymer films, *Anal. Chim. Acta* 402, 7.
- Wang, J., A. Kawde and E. Sahlin, 2000, Renewable pencil electrodes for highly sensitive stripping potentiometric measurements of DNA and RNA, *Analyst* 125, 5.
- Wang, J., G. Liu and M. Jan, 2004, Ultrasensitive electrical biosensing of proteins and DNA: Carbon-nanotube derived amplification of the recognition and transduction events, *J. Am. Chem. Soc.* 126, 3010.
- Wang, J., G. Liu and A. Merkoçi, 2003a, Electrochemical coding technology for simultaneous detection of multiple DNA targets, *J. Am. Chem. Soc.* 125, 3214.
- Wang, J., G. Liu, R. Polsky and A. Merkoçi, 2002c, Electrochemical stripping detection of DNA hybridization based on cadmium sulfide nanoparticle tags, *Electrochem. Commun.* 4, 722.
- Wang, J., G. Liu and G. Rivas, 2003b, Encoded beads for electrochemical identification, *Anal. Chem.* 75, 4661.
- Wang, J., A. Nasser, A. Erdem and M. Salazar, 2001b, Magnetic bead-based label-free electrochemical detection of DNA hybridization, *Analyst* 126, 2020.
- Wang, J., E. Palecek, P. Nielsen, G. Rivas, X. Cai, H. Shiraishi, N. Dontha, D. Luo and P. Farias, 1996b, Peptide nucleic acids probes for sequence-specific DNA biosensors, *J. Am. Chem. Soc.* 118, 7667.
- Wang, J., R. Polsky, A. Merkoçi and K. Turner, 2003c, Electroactive beads for ultrasensitive DNA detection, *Langmuir* 19, 989.
- Wang, J., G. Rivas, X. Cai, M. Chicharro, C. Parrado, N. Dontha, A. Begleiter, M. Mowat, E. Palecek and P. Nielsen, 1997a, Detection of point mutation in the p53 gene using a peptide nucleic acid biosensor, *Anal. Chim. Acta* 344, 111.
- Wang, J., G. Rivas, J. Fernandes, J.L. Paz, M. Jiang and R. Waymire, 1998b, Indicator-free electrochemical DNA hybridization biosensor, *Anal. Chim. Acta* 375, 197.
- Wang, J., G. Rivas, C. Parrado, X. Cai and M. Flair, 1997b, Electrochemical biosensor for detecting DNA sequences from the pathogenic protozoan *Cryptosporidium parvum*, *Talanta* 44, 2003.
- Wang, J., D. Xu, A. Erdem, R. Polsky and M. Salazar, 2002a, Genomagnetic electrochemical assay of DNA hybridization, *Talanta* 56, 931.
- Wang, J., D. Xu, A. Kawde and R. Polsky, 2001a, Metal-nanoparticle based electrochemical stripping detection of DNA hybridization, *Anal. Chem.* 73, 5576.

- Wang, J., D. Xu and R. Polsky, 2002b, Magnetically-induced solid-state electrochemical detection of DNA hybridization, *J. Am. Chem. Soc.* 124, 4208.
- Watterson, J., P. Piunno, C. Wust and U. Krull, 2000, Effects of oligonucleotide immobilization density on selectivity of quantitative transduction of hybridization of immobilized DNA, *Langmuir* 16, 4984.
- Wojciechowski, M., R. Sundseth, M. Moreno and R. Henkens, 1999, Multichannel electrochemical detection system for quantitative monitoring of PCR amplification, *Clin. Chem.* 45, 1690.
- Xie, H., Y.H. Yu, F. Xie, Y. Lao and Z. Gao, 2004, A nucleic acid biosensor for gene expression analysis in nanograms of mRNA, *Anal. Chem.* 76, 4023.
- Zhang, Y., H. Kim and A. Heller, 2003, Enzyme-amplified amperometric detection of 3000 copies of DNA at a 0.5 fM concentration, *Anal. Chem.* 75, 3267.
- Zhang, Y., A. Pothukuchy, W. Shin, Y. Kim and A. Heller, 2004, Detection of 1000 copies of DNA by an electrochemical enzyme-amplified sandwich assay with ambient oxygen as the substrate, *Anal. Chem.* 76, 4093.

Amplified Electrochemical and Photoelectrochemical Analysis of DNA

Eugenii Katz, Bilha Willner and Itamar Willner

Institute of Chemistry, The Hebrew University of Jerusalem, Jerusalem 91904, Israel

Contents

1. Introduction	195
2. Enzyme-amplified electrochemical analysis of DNA	202
3. Amplified electrochemical detection of DNA using nucleic acid-functionalized metallic or semiconductor nanoparticles	211
4. Nano- and micro-objects as carriers for the amplified electrochemical detection of DNA	219
5. Analysis of DNA by direct conductivity measurements	227
6. Amplified sensing of DNA in the presence of magnetic particles	230
7. Photoelectrochemical detection of DNA	233
8. Conclusions and perspectives	239
Acknowledgments	241
References	241

1. INTRODUCTION

The elucidation of the human genome paved a tremendous interest in the development of rapid and selective DNA detection methods. The high-throughput analysis of DNA and DNA mutants has enormous diagnostic significance for the early detection of genetic disorders in embryos or newborns, or for the continuous detection of mutations that lead to fatal diseases such as cancer. The analysis of DNA has other important implications such as the rapid detection of pathogens for clinical diagnostics or homeland security. Other practical applications of DNA analysis include tissue matching, environmental and food quality control, forensic applications, and more.

Not surprisingly, the development of analytical procedures for the analysis of DNA attracts substantial scientific and industrial efforts. The fundamental topics that need to be addressed upon the development of DNA analysis systems include: (i) the sensitivity of the analytical procedures. (ii) the specificity of the analytical method, and its ability to detect single-base mismatches. (iii) the possibility to apply the procedure for the parallel and high-throughput analysis of many DNA targets. (iv) the complexity of the analytical procedure, and the number of analytical steps involved in the protocol. This latter aspect has important consequences on the duration of the analysis and its cost-effectiveness.

Any analytical protocol for the analysis of a target DNA involves the hybridization of the target analyte with a complementary nucleic acid and the subsequent imaging of the formation of the double-stranded hybrid by physical means. The optical detection of DNA has been a subject of intense research, and fluorescence (Epstein *et al.*, 2002), surface plasmon resonance (SPR) (Wang *et al.*, 2004; Kobori *et al.*, 2004), chemiluminescence (Miao and Bard, 2004; Xu and Bard, 1995), and other optical methods (Vodinh *et al.*, 1994) were widely applied for sensing DNA. In this context, the development of arrays of nucleic acids (DNA chips) that enable the parallel optical imaging of numerous nucleic acid strands, represents a major breakthrough that advanced gene analysis (Mockler and Ecker, 2005; Lagally and Mathies, 2004; Auroux *et al.*, 2004). The recent accomplishments in nanotechnology, and the discovery of the unique size-controlled optical properties of metal or semiconductor nanoparticles (NPs) (quantum dots) introduced new approaches for the optical detection of DNA. The metal–metal interparticle plasmon interactions (Mirkin *et al.*, 1996), the size-controlled emission properties of semiconductor NPs (Bruchez *et al.*, 1998), or the semiconductor NP-stimulated fluorescence resonance energy transfer (FRET) (Ihara *et al.*, 2002; Patolsky *et al.*, 2003a) were applied to develop analytical procedures for the analysis of DNA. Chemiluminescence provides an alternative means for the photonic detection of DNA (Patolsky *et al.*, 2002a) and recent studies have applied catalytic nucleic acids as DNAzymes for chemiluminescence generation in DNA detection schemes (Xiao *et al.*, 2004b).

An alternative approach for DNA analysis involves the electronic readout of the DNA hybridization event. Bioelectronic detection of DNA is a subject of immense research in the past two decades. The bioelectronic DNA sensing device (Palecek and Jelen, 2002; Zhai *et al.*, 1997; Mikkelsen, 1996; Fojta, 2002; Wang *et al.*, 1997; Nicolini *et al.*, 1997) (Figure 1) includes an electronic element that upon recognizing the target DNA transduces the hybridization event into an electronic signal to the macroscopic environment. The transducer is usually modified with a nucleic acid interface that is complementary to the analyte DNA. Hybridization of the analyte DNA with the sensing matrix alters the interfacial properties of the transducer, thus allowing the quantitative assay of the DNA. Electrodes (Palecek and Jelen, 2002), field-effect transistors (ISFET) (Shin *et al.*, 2004), or piezoelectric crystals (Nicolini *et al.*, 1997) were widely applied to transduce DNA hybridization events at the respective interfaces. Changes in the impedance properties of the conductive surfaces (Katz and Willner, 2003; Alfonta *et al.*, 2001; Patolsky *et al.*, 1999a) or control of the redox functions of the electrodes (Gibbs *et al.*, 2005; Immoos *et al.*, 2004a,b) were employed to transduce the hybridization events on electrode supports. Similarly, the control of the gate potential of ISFET devices, and consequently, the current flow through the devices, was controlled by the DNA hybridization (Shin *et al.*, 2004). Also, mass changes occurring upon the hybridization of DNA on functionalized piezoelectric crystals were employed to electronically transduce DNA sensing by following the crystal frequency changes (Nicolini *et al.*, 1997).

Besides the optical and electronic transduction of DNA hybridization, recent efforts are directed to the application of micro/nanoscale devices and single

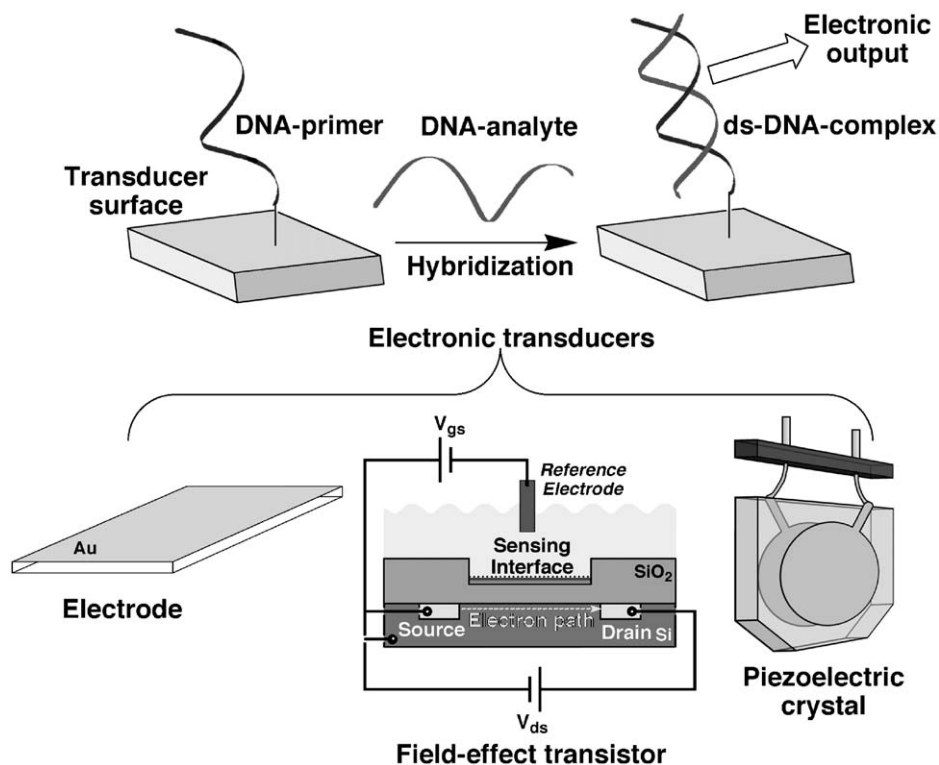


Fig. 1. Bioelectronic DNA sensors based on conductive electrodes, field-effect transistors and piezoelectric crystals.

molecule interactions to follow base-pairing. The force exerted to unzip a double-stranded DNA assembled between an AFM tip and a surface, and the effect of base mismatches on the “unzipping” force was used to sense DNA (Sattin *et al.*, 2004; Albrecht *et al.*, 2003; Krautbauer *et al.*, 2003). Also, the force interactions between a hydrophobic AFM tip and the double-strand formed between a peptide nucleic acid (PNA) and a DNA was used to probe the hybridization process (Lioubashevski *et al.*, 2001). Microscale mechanical devices were used to analyze DNA and single-base mismatches. For example, the stress developed on an AFM cantilever, and the resulting deflection of the cantilever, as a consequence of electrostatic repulsive interactions formed on the lever upon hybridization of the DNA, was employed to analyze nucleic acids and single-base mismatches (Fritz *et al.*, 2000; Wu *et al.*, 2001). Also, the magneto-mechanical deflection of cantilevers modified with nucleic acid-functionalized magnetic particles as labels was reported to monitor DNA hybridization and single-base mismatches in the double-stranded DNA (Weizmann *et al.*, 2004).

The electrochemical transduction of nucleic acids hybridization became a common practice in DNA analysis. Early examples have included the application of redox labels that bind to DNA (Jelen *et al.*, 2002; Gooding, 2002).

The enhanced binding of the redox labels to double-stranded DNA due to electrostatic attraction and intercalation to major or minor groove regions was used to probe the DNA duplex formation. Redox labels such as Co(III)-tris phenanthroline, $\text{Co}(\text{Phen})_3^{3+}$, the redox dyes, such as Hoechst dye 33258 or methylene blue, were employed in these electrochemical studies (Hashimoto *et al.*, 1994; Erdem *et al.*, 1999). Composite redox-active intercalators such as the bisferrocene-tethered naphthalene diimide (**1**) were used for the electrochemical analysis of double-stranded DNA (Figure 2(A)) with a reported detection limit of ca. 10^{-20} mol (Takenaka *et al.*, 2000). Figure 2(B), curves (b) and (c), show differential pulse voltammograms recorded in the presence, and in the absence, of the double-stranded DNA reacted with the redox-active intercalator, respectively. A different approach for the electrochemical analysis of DNA has included the application of redox-tethered beacons as sensing elements (Fan *et al.*, 2003), (Figure 3(A)) Ferrocene tethered to the beacon termini exhibited effective electrical communication with the electrode, leading to an amperometric signal (Figure 3(B)). The hybridization of the analyte DNA with

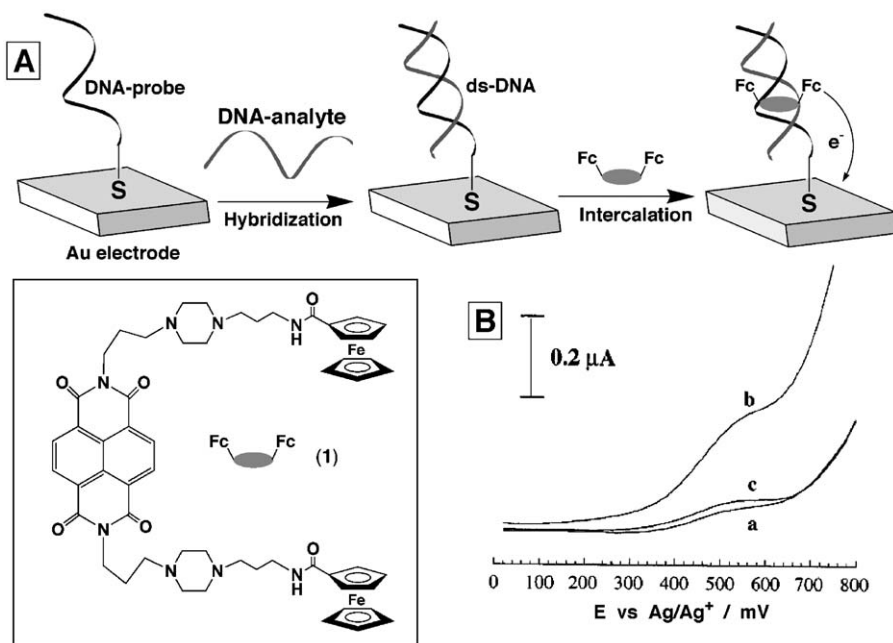


Fig. 2. (A) Electrochemical analysis of DNA using the bisferrocene-tethered naphthalene diimide (**1**) as a redox-active intercalator associated with the surface-confined ds-DNA. (B) Differential pulse voltammograms recorded in the presence of CCGCTTATCTT-CAGTTTTTCG-functionalized Au electrode: (a) before hybridization, (b) after hybridization with the plasmid DNA, which carried a part of the yeast choline transport gene with a complementary oligonucleotide sequence, and (c) after the interaction with the plasmid DNA that did not carry the complementary oligonucleotide. The data were obtained in acetate buffer, 50 mM, pH = 5.2, scan rate, 100 mV s^{-1} , pulse amplitude, 50 mV. (Part B is adapted from Takenaka *et al.*, 2000, Figure 3(A), with permission.)

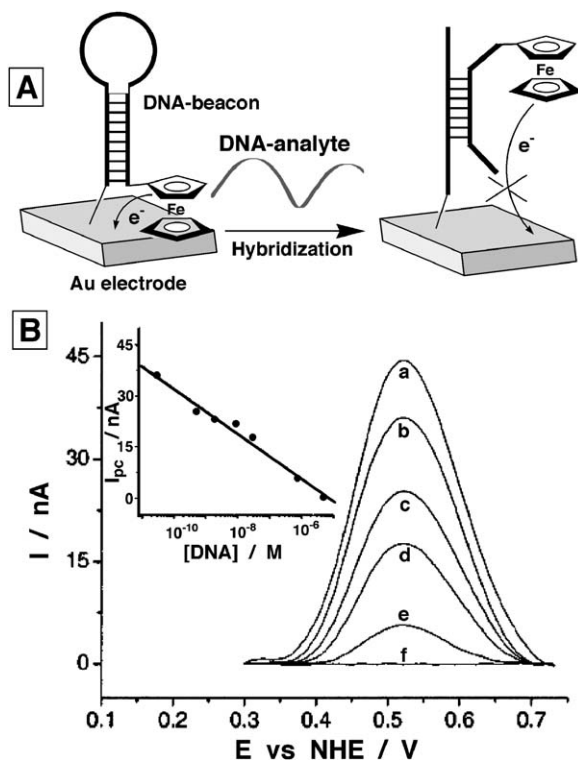


Fig. 3. (A) Electrochemical DNA sensor based on a redox-active label-functionalized DNA beacon self-assembled monolayer on a Au electrode. (B) Anodic linear sweep voltammograms of the DNA sensor in the presence of different concentrations of the complementary DNA: (a) 0 M, (b) 30 pM, (c) 500 pM, (d) 30 nM, (e) 800 nM, and (f) 5 μ M. The hybridization time interval was 30 min. Inset: the calibration curve of the anodic peak currents recorded at different concentrations of the DNA-analyte. (Part B is adapted from Fan *et al.*, 2003, Figure 2, with permission.)

the hairpin loop distorted the redox label from electrical contact with the electrode, and blocked its amperometric signal. This concept was recently extended by Holmberg *et al.* (2003) by applying electrocatalytic reactions that employ the redox functions of the relay to activate secondary biocatalytic reactions.

The use of charge transport properties of double-stranded DNA have been suggested as a method to follow DNA hybridization and mismatches in the duplexes (Kelley *et al.*, 1999) (Figure 4(A)). The redox-active intercalator methylene blue (2) is reduced to the leuco-form by electron transport through the double-stranded DNA. The latter reduced intercalator mediates the reduction of ferricyanide in the electrolyte solution, giving rise to an amperometric response, Figure 4(B). A mismatch in the double-stranded DNA was reported to perturb the electron transfer through the DNA, and to block the electrochemistry of methylene blue, and consequently, the reduction of $[\text{Fe}(\text{CN})_6]^{3-}$. A further method for the electrochemical detection of DNA was developed by Motorola Clinical Micro Sensors, and it is based on long-range electron transfer

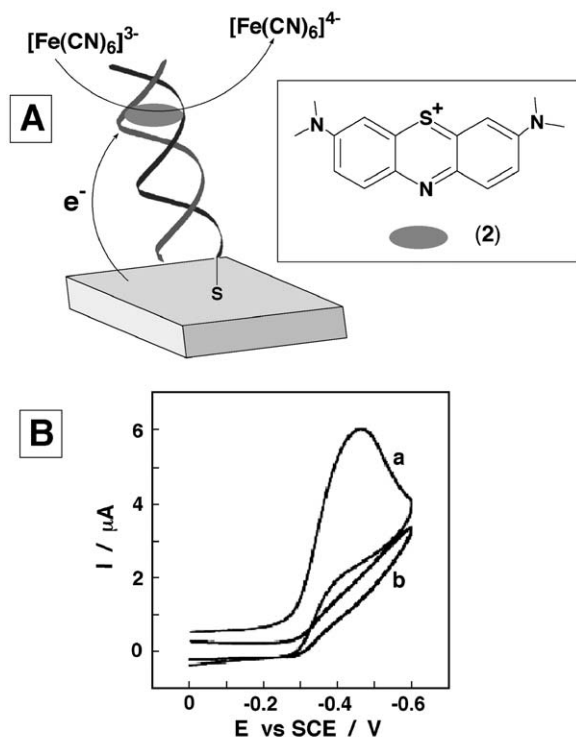


Fig. 4. (A) Electrochemical DNA analysis based on the electrocatalyzed reduction of ferricyanide by the redox-active intercalator, methylene blue (2), associated with the ds-DNA assembly. (B) Cyclic voltammograms recorded after reaction of the DNA-primer with: (a) fully complementary DNA-analyte, (b) One-base mismatch-containing DNA. The data were recorded in the presence of ferricyanide, 2 mM, and methylene blue, 2 μ M, potential scan rate, 100 mV s^{-1} . (Part B is adapted from Kelley *et al.*, 1999, Figure 7, with permission.)

using molecular wires as conductors (Umek *et al.*, 2001) (Figure 5(A)). An ordered mixed monolayer composite, consisting of a thiolated nucleic acid primer (3), an aryl-acetylene molecular wire (4) (for electrical conduction) and an oxyethylene alcohol-terminated component (5) (to prevent non-specific adsorption), was linked to an electrode. A tri-component “sandwich-type” hybridization process was then used for the electrochemical detection of the target DNA (6). The single-stranded DNA target was hybridized with the nucleic acid units (3) associated with the monolayer. A single-strand part of the target was then hybridized with a signaling-probe nucleic acid bound to ferrocene (7). The electrical contacting of the ferrocene units with the electrode through the aryl-acetylene wires provided a means to readout the hybridization of the interface with the sensing interfaces (Figure 5(B)).

The development of electrochemical DNA sensors of practical utility relies, however, on the design of systems with high sensitivities. Most of the direct electrochemical DNA detection schemes reveal limited sensitivities and require the pre-PCR (polymerase chain reaction) amplification of the target analytes.

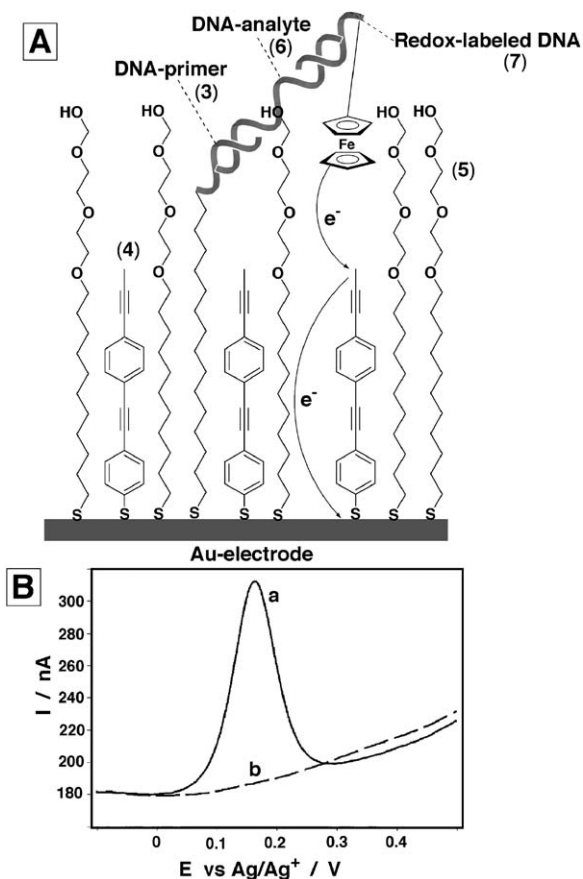


Fig. 5. (A) Electrochemical DNA sensor based on long-range electron transfer across a composite mixed monolayer. (B) Voltammograms recorded after the DNA-primer was reacted with: (a) the complementary DNA-analyte; (b) a foreign non-complementary DNA, followed by the reaction with a redox-labeled DNA (7). (Part B is adapted from Umek *et al.*, 2001, Figure 1(C), with permission.)

The intrinsic limitations in PCR amplification, and the duration associated with the PCR processes, suggest that the design of amplified electrochemical DNA sensors could be an attractive analytical method for DNA analysis. The concept of amplified electrochemical analysis is schematically depicted in Figure 6. The analyzed DNA (8) is hybridized with the sensing nucleic acid (9) that is associated with the electrode. A third, labeled nucleic acid (10), is hybridized with the single-stranded segment of the analyzed DNA. The label activates then a chemical or physical process that amplifies the primary hybridization process with the analyte. Such amplification may be catalytic or biocatalytic processes that release numerous electroactive molecules as a result of a single recognition event. Alternatively, the label associated with the hybrid complexes generated by a few recognition events may catalyze the formation of nanostructures that either alter the electrical properties of the system (e.g., conductivity), or eventually, may lead

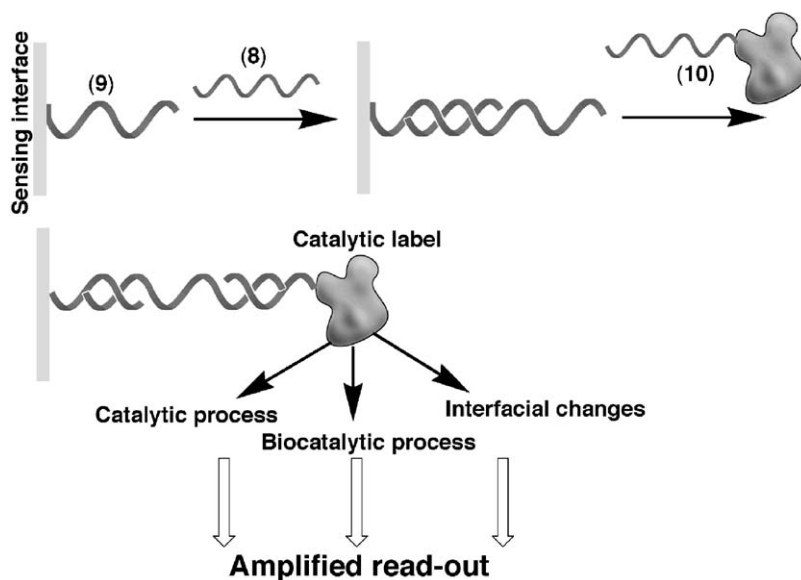


Fig. 6. Amplified DNA sensing using catalytically active labels.

to the dissolution of numerous electroactive molecular or ionic components. A different method to amplify the DNA recognition event may include the association of a label that significantly alters the interfacial properties of the electrode, to an extent that the capacitance or the electron transfer features at the electrode support are altered. The present chapter reviews different analytical schemes for the amplified electrochemical detection of DNA. The discussion addresses the sensitivities of the different methods and describes the complexity of the different analytical schemes by detailing the amplification steps.

2. ENZYME-AMPLIFIED ELECTROCHEMICAL ANALYSIS OF DNA

Figure 7 depicts the principle for the biocatalytic amplification of DNA sensing. An enzyme label linked to a nucleic acid is hybridized with the complex formed between the primer and the analyte DNA. The enzyme stimulates the bioelectrocatalytic oxidation (or reduction) of a substrate, leading to a catalytic current upon the formation of numerous product units (**Figure 7(A)**). Alternatively, the enzyme may either generate a redox-active product that is electrochemically analyzed, **Figure 7(B)**, or eventually, the biocatalyst may yield a product that controls the surface properties of the electrode (e.g., an insulating precipitate on the electrode) (**Figure 7(C)**). The enzymatic amplification of electrochemical DNA analysis has many further modifications and extensions. For example, molecular species that interact with double-stranded DNA may be electrocatalytically activated to yield the substrate for a biocatalytic process.

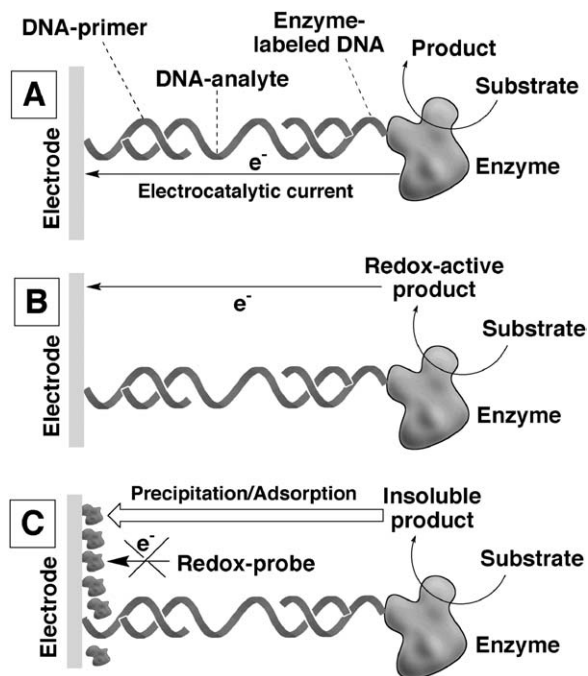


Fig. 7. Amplified electrochemical DNA sensing employing biocatalytic labels that result in: (A) a bioelectrocatalytic process, (B) generation of a redox-active product, (C) yielding interfacial changes, e.g., the precipitation of an insoluble product on the conductive support.

Heller and co-workers (De Lumley-Woodyear *et al.*, 1996) have used horseradish peroxidase (HRP) linked to a nucleic acid as bioelectrocatalytic label for the amplified amperometric detection of DNA (Figure 8). The hybridization of the DNA functionalized with a biocatalytic label (11) to a DNA probe (12), and the integration of the biocatalytic DNA duplex conjugate with a redox-active hydrogel (13), enabled the electrical contacting of the biocatalyst toward the bioelectrocatalyzed reduction of H_2O_2 . A hydrogel (13) consisting of polyacrylamide-hydrazide functionalized with $[\text{Os}(\text{dmebpy})_2\text{Cl}]^{+/2+}$ (dmebpy = 4,4'-dimethyl-2,2'-bipyridine) redox-active units was modified with a nucleic acid that probed the hybridization process. The transport of electrons from the electrode to the biocatalyst by means of the tethered osmium complexes activated the bioelectrocatalyzed reduction of H_2O_2 to H_2O and the formation of a bioelectrocatalytic current as a result of the duplex formation. A similar system was successfully applied to detect electrochemically single-base mismatches in DNA by controlling the hybridization temperature (Caruana and Heller, 1999) (Figure 9(A)). The nucleic acid probe (14) was linked to the hydrogel (13), and the fully complementary nucleic acid (15) bound to soybean peroxidase (SBP) was hybridized with the DNA probe. The nucleic acids (15a) or (15b), that include four-base mismatches or a single-base mismatch, were similarly linked to the SPB biocatalyst. Figure 9(B) shows the chronoamperometric transients observed upon hybridization of the 15-modified hydrogel with

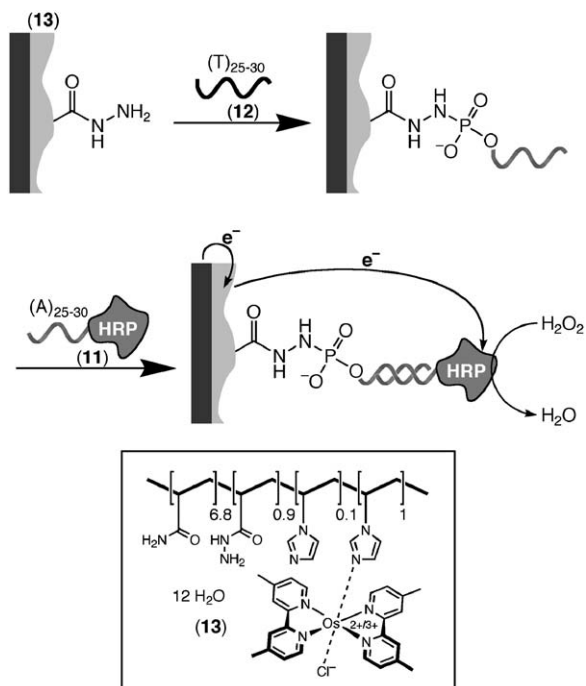


Fig. 8. Enzyme-amplified analysis of DNA in a redox-active hydrogel.

14, curve (a), and the mutants **15a** or **15b**, curves (b) and (c), respectively. The hybridization was conducted at 57°C, a temperature that is higher than the melting temperature of **14/15a** or **14/15b**, but lower than the melting temperature of **14/15**. Only the fully complementary nucleic acid-modified SBP gave an amperometric signal as a result of the bioelectrocatalyzed reduction of H₂O₂, indicating that temperature-controlled hybridization of the analyzed DNA may be used as an effective tool to induce selectivity in the sensing.

A different approach for the amplified bioelectrocatalytic detection of DNA through mediated electrical contacting of a redox enzyme with the electrode was demonstrated by the incorporation of redox mediator units into the replicated DNA hybrid complex (Patolsky *et al.*, 2002b). A thiolated nucleic acid (**16**) complementary to a sequence of the 7249-base M13mp18 DNA was assembled on a Au electrode and hybridized with the analyte DNA (Figure 10). The resulting double-stranded complex was then interacted with the nucleotide mixture (dNTPs) that included the ferrocene-tethered deoxyuridine triphosphate (dUTP) (**17**) in the presence of polymerase (Klenow fragment), and replication of the duplex structure between (**16**) and the M13mp18 DNA was activated. This process led to the incorporation of the redox-active ferrocene units into the replicated DNA. The ferrocene units bound to the double-stranded assembly associated with the electrode activated the bioelectrocatalyzed oxidation of glucose in the presence of glucose oxidase, giving rise to an electrocatalytic anodic current that provides an amplified

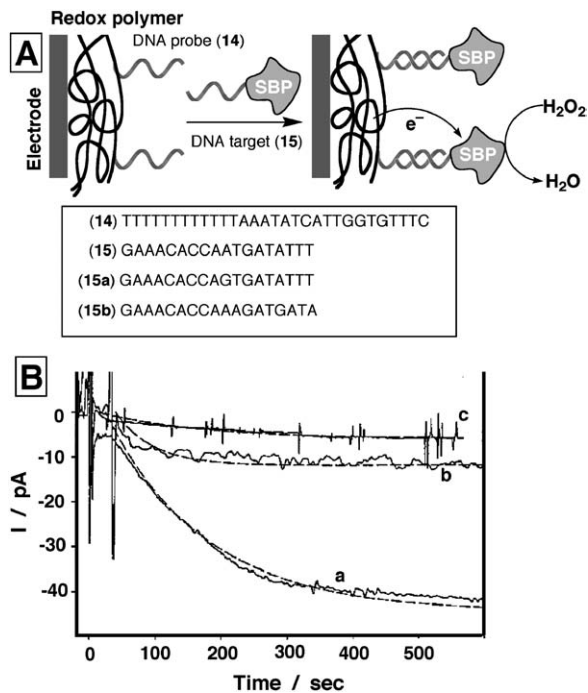


Fig. 9. (A) Amperometric transduction of the formation of a double-stranded complementary DNA complex using an SBP–DNA conjugate as a bioelectrocatalytic amplifier. (B) Increase of the electrocatalytic currents recorded at 57 °C after adding the SBP-labeled target DNA: (a) perfectly matched target; (b) target with a single mismatched base; and (c) target with four mismatched bases. The dashed lines represent the best fit of the data to the theory. (Part B is adapted from Caruana and Heller, 1999, Figure 3, with permission.)

readout signal for the primary hybridization of the M13mp18 DNA with the sensing interface. The surface coverage of the double-stranded complex on the electrode is controlled by the bulk concentration of the analyte M13mp18 DNA, and thus the surface coverage of the electrode with the ferrocene-labeled replica, and the resulting transduced currents are controlled by the concentration of the analyte. This enabled the quantitative analysis of M13mp18 DNA with a detection limit that corresponded to 1×10^{-13} M.

A different method to employ enzymes for the amplified detection of DNA involves the application of the biocatalyst label that stimulates the precipitation of an insoluble product on the electrode support. The formation of an insulating film represents an amplification path, since numerous insoluble molecules are generated by the enzyme label as a result of a single recognition event. The resulting insulating film alters the interfacial properties of the electrode, a process that can be monitored by impedance spectroscopy that follows the electron transfer resistances and capacitances at the electrode interface (Katz and Willner, 2003). Figure 11 depicts two configurations for the amplified analysis of DNA using alkaline phosphatase (AlkPhos) as the biocatalyst, and the oxidative hydrolysis of 5-bromo-4-chloro-3-indolyl phosphate (**18**) to the insoluble indigo

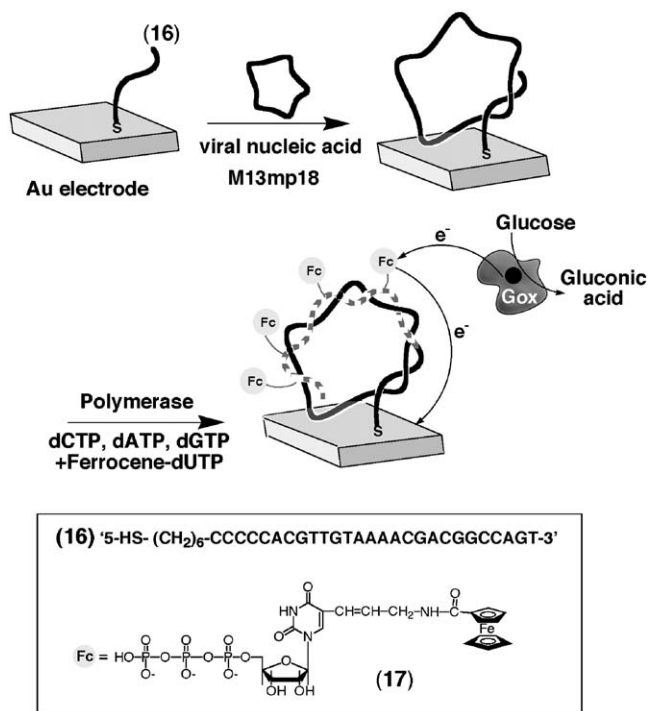


Fig. 10. Amplified electrochemical detection of the viral M13mp18 DNA by the generation of a redox-active replica and the bioelectrocatalyzed oxidation of glucose.

derivative (19) as the amplification route (Patolsky *et al.*, 2003b). In one configuration, Figure 11(A), the probe nucleic acid (20) was assembled on a Au-electrode, and this was hybridized with the analyte DNA (21). The sandwich-type hybridization of the biotin-modified nucleic acid (22), followed by the association of the avidin–alkaline phosphatase conjugate (23) led to the formation of the biocatalytic label on the electrode interface, and to the biocatalyzed precipitation of insoluble product (19) on the electrode. In the second configuration, Figure 11(B), the enzyme was functionalized with the nucleic acid (24) that resulted in the direct hybridization of the biocatalytic label with the probe–analyte complex, and to the precipitation of 19 on the electrode. The analysis of DNA by these two amplification schemes was followed electrochemically using Faradaic impedance spectroscopy (and in parallel by microgravimetric quartz crystal microbalance measurements). The electron transfer resistance at the electrode interface, in the presence of a redox indicator solubilized in the electrolyte solution, was significantly affected by the formation of the insoluble product on the surface. Figure 12(A) shows the impedance spectra (in the form of Nyquist plots) obtained upon the analysis of 21 according to the scheme outlined in Figure 11(A). The interfacial electron transfer resistance (semicircle diameter of the plots lying on the Z_{re} -axis) increased upon the build-up of the nucleic acid complexes on the electrode, and it was significantly altered upon the precipitation of 19. As the surface coverage of the hybridized analyte DNA is

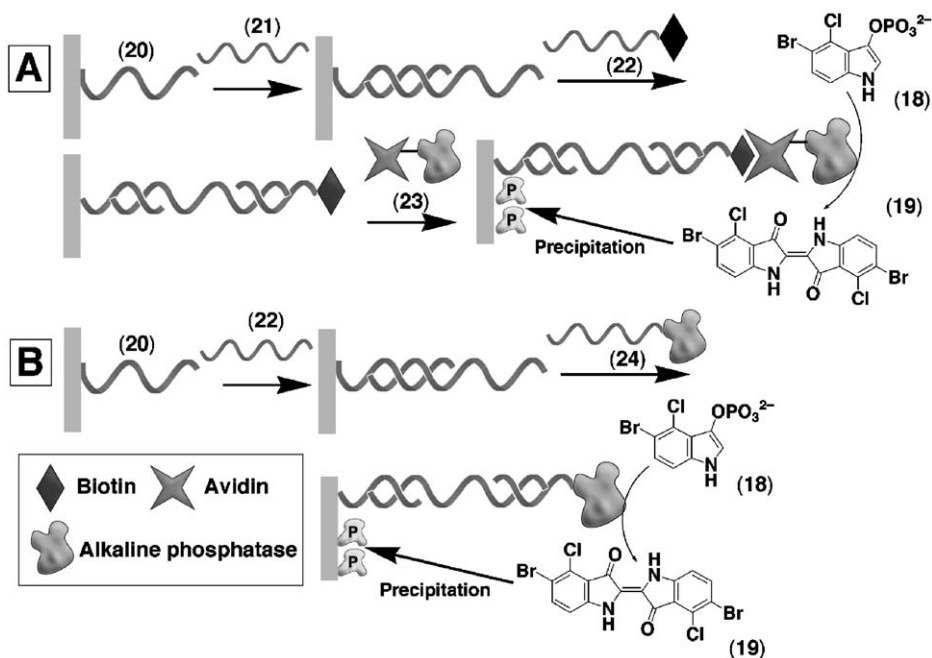


Fig. 11. Amplified detection of a target DNA by the biocatalyzed precipitation of an insoluble product (19) on the electrode support using: (A) a biotin-labeled nucleic acid and an avidin/alkaline phosphatase conjugate. (B) A nucleic acid-functionalized alkaline phosphatase conjugate.

controlled by its bulk concentration, the surface density of the biotin tags, and consequently, of the alkaline phosphatase–avidin conjugate units (23), as well as the extent of the generated precipitate, are related to the bulk concentration of the analyzed DNA. Indeed, it was found that the increase in the interfacial electron transfer resistances of the electrode was controlled by the concentration of the analyzed DNA, thus enabling the quantitative determination of the DNA concentrations. The sensitivity limit for the detection of DNA by this method was claimed to be 1×10^{-13} M. Results for the quantitative electrochemical analysis of the DNA (21) by the configuration shown in Figure 11(B) are displayed in Figure 12(B,C). The interfacial electron transfer resistance increased upon the biocatalyzed precipitation of 19 by the nucleic acid (24)-functionalized alkaline phosphatase. The increase in the interfacial electron transfer resistance at the electrode interface, due to the precipitation of 19 was controlled by the concentration of the DNA, and the quantitative analysis of 21 was demonstrated (Figure 12(C)). The latter sensing configuration was successfully applied to analyze the DNA extracted from blood samples for the existence of the mutation that leads to the Tay-Sachs genetic disorder. The biocatalyzed precipitation of an insoluble product for the amplified analysis of DNA was also accomplished by other systems such as horseradish peroxidase and 4-chloro-1-naphthol as substrate (Patolsky *et al.*, 1999a).

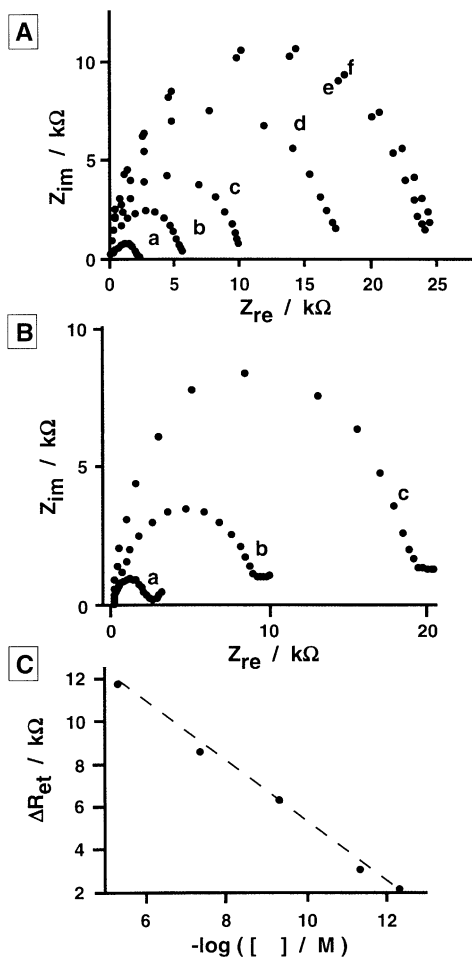


Fig. 12. (A) Faradaic impedance spectra (Nyquist plots) of: (a) the **20**-functionalized Au electrode; (b) after interaction of the sensing electrode with **21** (5×10^{-6} M), pre-treated with **22** (1×10^{-5} M) for 30 min at 37°C ; (c) upon reacting the resulting assembly with the avidin/alkaline phosphatase conjugate (**23**) (10 nmol mL^{-1}); (d) after the biocatalyzed precipitation of **19** for 20 min in the presence of **18** (2×10^{-3} M) in 0.1 M Tris-buffer at $\text{pH} = 7.4$; and (e) and (f) after the biocatalyzed precipitation of **19** for 30 and 40 min, respectively. (B) Faradaic impedance spectra (Nyquist plots) of (a) the **20**-functionalized Au electrode, (b) after the interaction of the sensing electrode with the target DNA **21** (5×10^{-6} M) pre-treated with the **24**/alkaline phosphatase conjugate (7×10^{-5} M) for a period of 60 min, (c) after the biocatalyzed precipitation of **19** for 30 min in the presence of **18** (2×10^{-3} M) in 0.1 M Tris-HCl buffer at $\text{pH} = 7.4$. (C) The changes in the electron-transfer resistance, R_{et} , upon the sensing of different concentrations of the target DNA (**21**) by the amplified biocatalyzed precipitation of **19** onto the transducer for a period of 30 min. (Adapted from Patolsky *et al.*, 2003b, Figures 3 and 6, with permission.)

The biocatalyzed precipitation of an insoluble product on a conductive support, as an amplification route for electrochemical analysis (Patolsky *et al.*, 1999b), was further applied to analyze DNA or RNA genes of viruses (Patolsky *et al.*, 2001a, 2003a,b), and to develop a method for the amplified detection of single-base mismatches in DNA (Patolsky *et al.*, 2001b). Figure 13(A) outlines the procedure for the detection of the 11161 base RNA of the vesicular stomatitis virus (VSV) (**25**) (Patolsky *et al.*, 2001a). The electrode was modified with the probe nucleic acid (**26**) that hybridized with the RNA extracted from VSV cells. The replication of the double-stranded assembly in the presence of the nucleotide mixture dNTPs, that included biotin-labeled dUTP and reverse transcriptase as replication enzyme, resulted in the biotin-labeled replica on the electrode surface. The subsequent coupling of the avidin–alkaline phosphatase conjugate (**23**) to the labeled replica, followed by the biocatalyzed precipitation of **19** on the electrode provides the route to analyze the viral RNA. The insulation of the electrode by the insoluble film was then analyzed by means of Faradaic impedance spectroscopy. This analysis method involves two consecutive biocatalytic amplification steps: in the first step numerous biotin tags are introduced into the DNA replica as a result of a single RNA-binding event. In the second step, a collection of alkaline phosphatase units are bound to the biotin tags, and these catalyze the formation of the precipitate **19**. Figure 13(B) displays the impedance spectra upon analyzing 1×10^{-12} M VSV RNA. The increase in the interfacial electron transfer resistance upon replication by reverse transcriptase, $\Delta R_{\text{et}} = 4.5 \text{ k}\Omega$, was attributed to the increase of the negative charge associated with the interface as a result of replication, that led to electrostatic repulsion of the negatively charged redox label in the electrolyte, $[\text{Fe}(\text{CN})_6]^{3-/4-}$, and to a barrier for electron transfer at the interface. The precipitation of **19** resulted in a pronounced insulation of the electrode and to a high interfacial electron transfer barrier, $\Delta R_{\text{et}} = 14.0 \text{ k}\Omega$. The extent of electrode insulation was controlled by the concentration of the viral RNA, and the procedure enabled the analysis of the RNA with a detection limit of 1×10^{-17} M. The same method was applied for the amplified analysis of M13mp18 DNA (Patolsky *et al.*, 2001a).

The application of the method in the amplified detection of single-base mismatches in DNA (Patolsky *et al.*, 2001b) is schematically outlined in Figure 14. The analysis of a 41-base oligonucleotide (**27**) that includes a single G-mutation, as compared to the normal gene (**28**), is exemplified. A probe DNA (**29**) complementary to the mutant or normal gene, up to one base before the mutation site, was immobilized on the electrode. Hybridization of the interface with either the mutant (**27**) or the normal gene (**28**) followed by the interaction of the double-stranded assemblies with biotinylated dCTP and polymerase, resulted in the incorporation of the biotin label only into the double strand that included the mutant. The subsequent association of the avidin–alkaline phosphatase conjugate to the sensing interface, followed by the biocatalyzed oxidative hydrolysis of **18** yielding insoluble indigo derivative (**19**) resulted in the isolation of the conductive electrode support that was read out by Faradaic impedance spectroscopy. Note that precipitation occurs only if the single-base mutant (**27**) is hybridized with the sensing interface. The similar sequence of the reactions

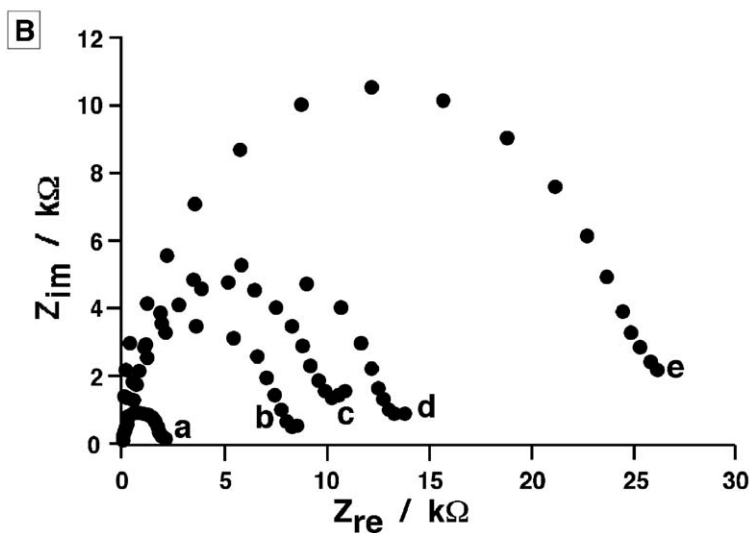
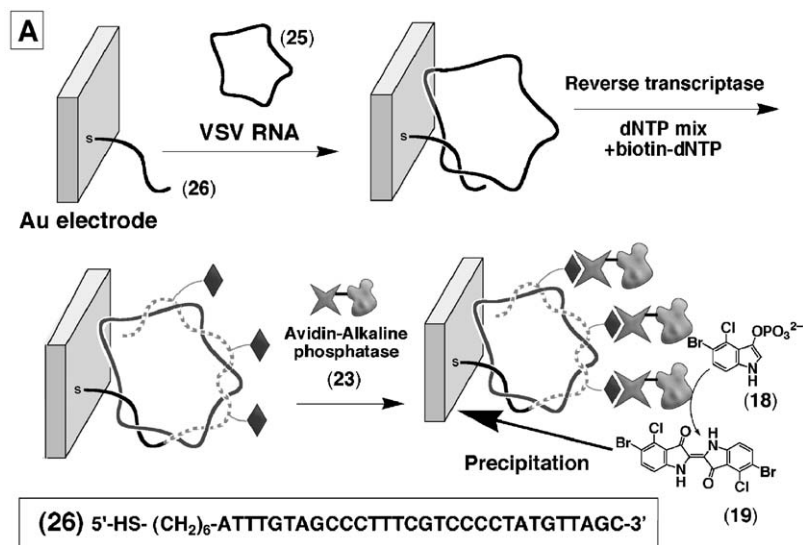


Fig. 13. (A) Amplified electronic transduction of the analysis of a viral RNA by the reverse transcriptase-induced replication of **25** while incorporating biotin labels into the replica, and the biocatalyzed precipitation of an insoluble product on the transducer. (B) Faradaic impedance spectra (Nyquist plots) upon the amplified sensing of VSV RNA: (a) the **26**-functionalized Au electrode; (b) after hybridization with the VSV RNA (**25**), 1×10^{-12} M; (c) after the reverse transcription for 45 min in the presence of dGTP, dATP, dTTP, dCTP, and biotinylated dCTP (1:1:2/3:1:1/3, each base 1 mM); (d) after the association of the avidin-alkaline phosphatase conjugate (**23**); (e) after the biocatalyzed precipitation of **19** for 20 min in the presence of **18** (2×10^{-3} M). (Part B is adapted from Patolsky *et al.*, 2001a, Figure 5(A), with permission.)

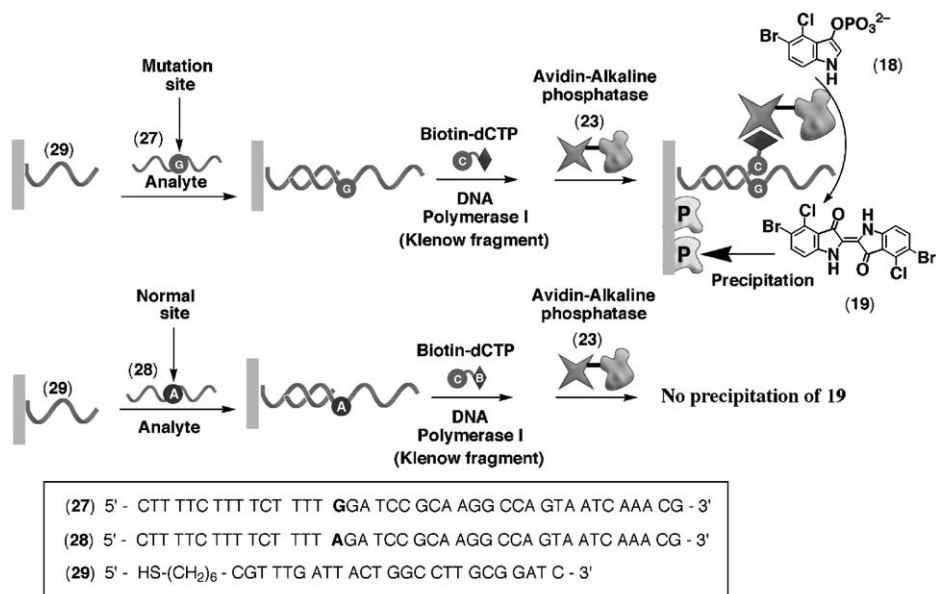


Fig. 14. Electronic transduction of the analysis of a single-base mutation in an analyte DNA using the biocatalytic precipitation of an insoluble product on the transducer as an amplification route.

performed on the sensing interface functionalized with the normal gene (28) does not result in the binding of the biocatalytic conjugate and, thus, does not result in the precipitation process. The biocatalyzed precipitation of 19 provides a means to amplify the sensing process, and the extent of precipitate formed on the transducer surface is controlled by the amount of the DNA-mutant associated with the sensing interface and the time interval employed for the biocatalyzed precipitation. This method was successfully applied for the analysis of one of the genes responsible for the Tay–Sachs genetic disorder in real blood samples with no need for PCR pre-amplification.

3. AMPLIFIED ELECTROCHEMICAL DETECTION OF DNA USING NUCLEIC ACID-FUNCTIONALIZED METALLIC OR SEMICONDUCTOR NANOPARTICLES

The unique electronic, optical, and catalytic properties of metal or semiconductor NPs have been elucidated in the past decade (Shipway *et al.*, 2000; Daniel and Astruc, 2004). By the conjugation of metal or semiconductor NPs with biomolecules, new hybrid materials of new functionalities were generated, and these enabled the development of new electrochemical, electronic, or optical biosensor systems (Katz and Willner, 2004; Katz *et al.*, 2004). For example, the reconstitution of an apo-enzyme on a Au NP allowed the electrical contacting of the biocatalyst with the electrode (Xiao *et al.*, 2003). The

electrical contacting of glucose oxidase by this method generated a bioelectrocatalytically active enzyme electrode that was applied for glucose sensing. The optical detection of DNA was extensively studied by the application of nucleic acid-functionalized Au NPs. The aggregation of the NPs resulted in interparticle plasmon interactions and the change of the color of the aggregates upon hybridization (Mirkin *et al.*, 1996). Similarly, nucleic acid-functionalized Au-NPs were applied as mass-labels for the microgravimetric quartz-crystal-microbalance (QCM) analysis of DNA (Zhou *et al.*, 2000; Patolsky *et al.*, 2000b). The catalytic enlargement of the NPs provided a means to amplify the QCM analysis path (Willner *et al.*, 2002). The optical detection of DNA was, similarly, accomplished by the application of the fluorescence properties of semiconductor NPs (Patolsky *et al.*, 2003a). The replication of double-stranded DNA complexes between a primer nucleic acid and the analyte DNA on the CdS-ZnS NPs, with the concomitant incorporation of a dye into the DNA replica, enabled the readout of the primary hybridization process by a FRET process from the semiconductor NPs to the dye units.

The use of metal or semiconductor NPs for the amplified detection of DNA involves usually two steps (Figure 15(A)). In the first step, the nucleic acid-functionalized NPs are used as labels that hybridize with analyte DNA on a surface. The surface may be an electrode, a glass support or eventually, magnetic particles. The hybridization of the NP labels with the different surfaces is aimed to facilitate the separation of the hybridized NP labels from non-hybridized particles. In the second step, the NPs are dissolved by electrochemical or chemical means. The released ions are then analyzed by stripping voltammetry. Since the number of the NPs relates directly to the concentration of the analyte on the surface, and as numerous ions are released upon the dissolution of the NPs, the stripping voltammograms provide a quantitative signal for the amplified detection of the analyzed DNA. In a further modification of this protocol, Figure 15(B), the catalytic functions of the metal NPs are utilized for the enhanced amplified detection of the analytical process. The metal NPs associated with the double-stranded DNA linked to the separation matrix are used as catalyst for the deposition of a metal on the NPs. The catalytic enlargement of the NPs may include the same metal constituting the NPs or, eventually, other metals (e.g., silver (Ag) on Au NPs). The deposition and enlargement of the NPs increases the metal mass, and thus, the content of released ions is increased and the amplified electrochemical analysis of the target DNA is enhanced.

Magnetic particles were functionalized with avidin and were employed to bind the biotin-labeled nucleic acid (30) that acted as the sensing interface (Wang *et al.*, 2001b). Hybridization of Au NPs functionalized with the complementary DNA (31) enabled the magnetic separation of the magnetic particle/double-stranded DNA/Au NP conjugates, and their purification from any free Au NPs by washing. The subsequent dissolution of the Au NPs in a HBr/Br₂ solution generated the Au(III)-ions that were analyzed in a separate electrochemical cell by the accumulation of Au on a carbon electrode and the potentiometric stripping off of the accumulated metal (Figure 16).

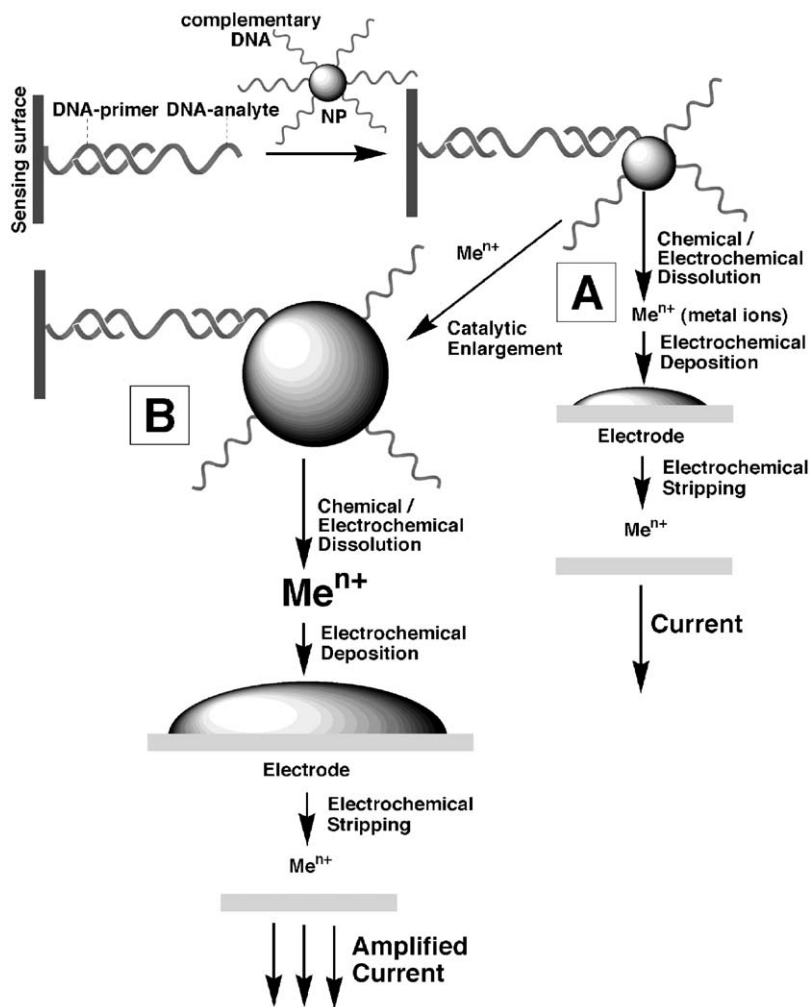


Fig. 15. (A) DNA analysis based on stripping voltammetry of metal NPs associated with the sensing interface. (B) Sequential amplification of DNA analysis by stripping analysis using the catalytic enlargement of the metal NPs associated with the sensing interface, and the dissolution of the enlarged NPs.

Similarly, Ag NPs were employed for the electrochemical detection of DNA (Cai *et al.*, 2002). The sensing nucleic acid was immobilized on a chitosan-modified glassy carbon electrode (GCE), and the complementary Ag-labeled DNA was hybridized with the interface. The oxidative dissolution of the metal NPs was followed by the electrochemical detection of the released Ag^+ by anodic stripping voltammetry at a carbon fiber ultramicroelectrode. Figure 17 shows the stripping voltammograms observed upon analyzing the complementary nucleic acid-functionalized Ag NPs, a nucleic acid that includes a single base mismatch, and a non-complementary nucleic acid, using

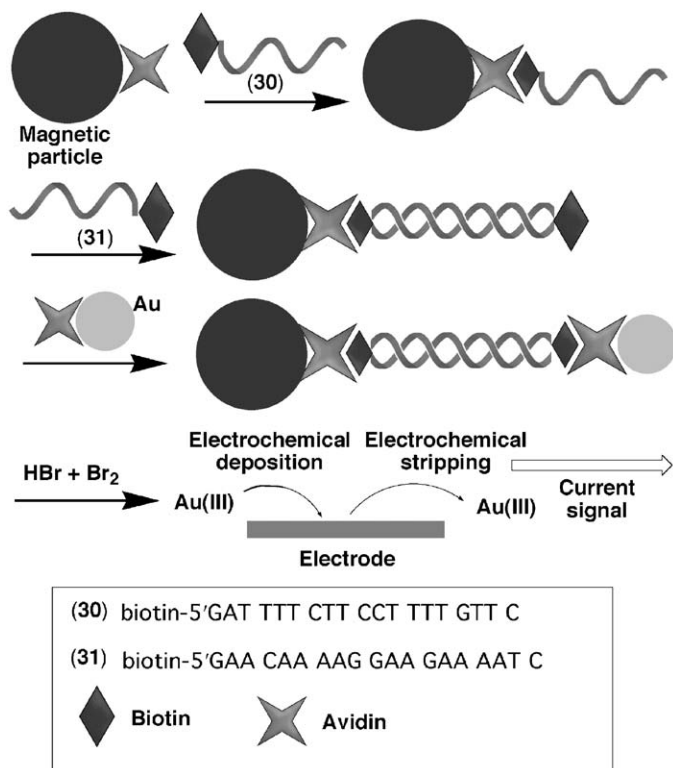


Fig. 16. Analysis of DNA by stripping voltammetry of metal NPs associated with the sensing interface linked to magnetic particles.

this procedure. The voltammetric responses were found to correlate with the concentration of the complementary Ag-labeled nucleic acid, and the sensitivity limit for analyzing the complementary DNA was estimated to be ca. 1×10^{-12} M. An interesting use of the method for the analysis of the 406-base pair human cytomegalovirus DNA (HCMV DNA) using disposable microband electrodes was reported (Authier *et al.*, 2001). The sensing nucleic acids were immobilized on a polystyrene microwell support and the target HCMV DNA was hybridized with the sensing interface. The subsequent hybridization of Au NPs functionalized with nucleic acid complementary to the HCMV resulted in the labeling of the analyzed DNA with the amplifying metal NPs. The subsequent dissolution of the Au NPs with HBr/Br₂ was followed by the quantitative determination of the released Au(III) by anodic stripping voltammetry that used screen-printed microband electrodes. The latter electrode configuration enabled the enhanced mass transfer of the Au(III) by non-linear diffusion during the electrodeposition time interval, thus allowing the sensitive detection of the ions. The method enabled the amplified analysis of the HCMV DNA with a sensitivity limit of 5×10^{-12} M.

NPs of higher complexity such as Cu/Au core-shell NPs were similarly applied in the amplified electrochemical analysis of DNA (Cai *et al.*, 2003). Pyrrole was

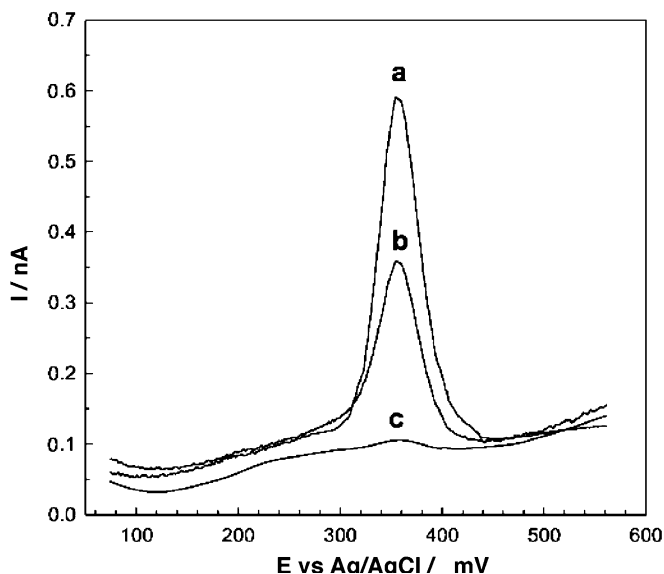


Fig. 17. Analysis of DNA using anodic stripping voltammetry of silver NPs associated with the oligonucleotide probe after its hybridization with: (a) the complementary oligonucleotide sequence; (b) the oligonucleotide sequence that contains a single-base mismatch; (c) a non-complementary oligonucleotide sequence. The data were recorded on a 5- μm diameter carbon fiber electrode. (Adapted from *Cai et al.*, 2002, Figure 4. Reproduced with permission of the Royal Society of Chemistry.)

electropolymerized on a glassy carbon electrode and a nucleic acid was electrochemically adsorbed on the polymer interface. The hybridization of the $\text{Cu}/\text{Au}_{\text{core-shell}}$ NPs functionalized with a nucleic acid complementary to the sensing oligonucleotide, followed by the acidic oxidative dissolution of the Cu-shell released Cu^{2+} that were analyzed by stripping voltammetry. Also, altering the shape of the amplifying label further enhanced the analytical procedures. This has been demonstrated by the use of indium (In) microrods tags instead of NPs as amplifying labels (*Wang et al.*, 2003c). The use of metal microrods instead of NPs increases the amount of released ions, and thus enhances the sensitivity capacity. The In microrods were prepared by the electrodeposition of the metal in membrane pores, followed by the dissolution of the membrane support, and the purification of the rods (*Martin*, 1995). Biotinylated magnetic particles were modified with a biotinylated nucleic acid (**32**) through an avidin linker. The target DNA (**33**) was hybridized with the nucleic acid associated with the magnetic particles, and the resulting double-stranded hybrid was collected by means of an external magnet. The resulting assembly was further hybridized with the In-microrods functionalized with the thiolated nucleic acid (**34**) that is complementary to another segment of the target DNA (Figure 18). The magnetic collection of the In-labeled DNA onto an electrode surface enabled then the chronopotentiometric stripping of the metal. The analysis of the DNA reached an impressive detection limit that was claimed to be lower than 250 zmol. A related approach has utilized the catalytic deposition of Ag on Ag clusters as a

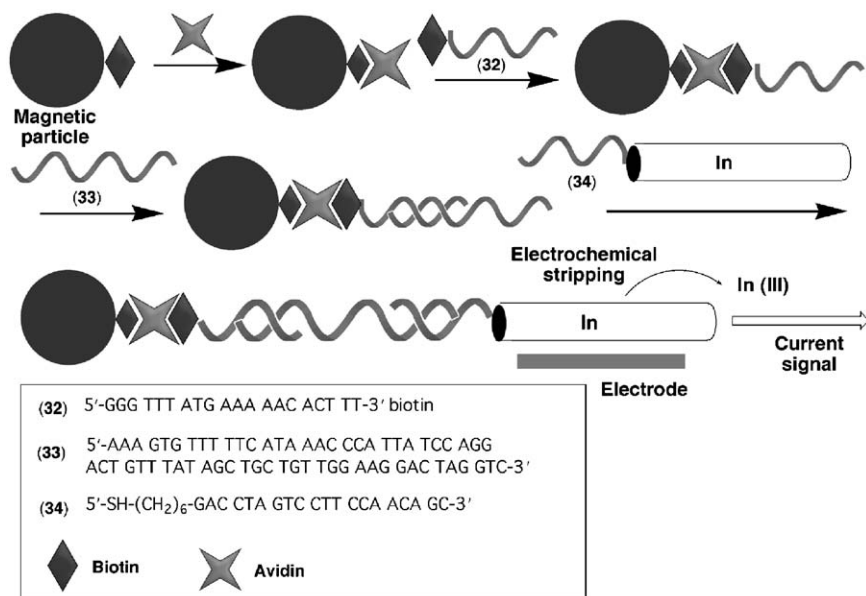


Fig. 18. Analysis of DNA using anodic stripping voltammetry of In nanorods associated with an oligonucleotide duplex assembly.

means to amplify the DNA analysis (Wang *et al.*, 2003e). The deposition of Ag on Ag clusters formed on a DNA template was used to generate Ag-nanowires on DNA templates (Braun *et al.*, 1998). Similarly, a nucleic acid primer (35) was assembled on a Au-electrode, and the complementary nucleic acid analyte (36) was hybridized with the interface (Figure 19). The binding of Ag⁺ ions to the phosphate residues was followed by the reduction of the Ag⁺ ions to Ag clusters on the DNA template. The subsequent dissolution of the Ag clusters and the chronopotentiometric stripping of the released ions enabled the quantitative analysis of the complementary DNA (Wang *et al.*, 2003e).

The catalytic properties of metal NPs, and particularly the catalyzed deposition of metals on metal NP seeds, provide a means to enlarge the NPs, and thus to enhance the amplifying capacity of the labels. For example, biotinylated magnetic particles were modified with a biotinylated nucleic acid through an avidin linker, and a Au NP functionalized with the complementary nucleic acid was hybridized with the functionalized magnetic particles, and the resulting hybrid was separated by means of an external magnet. The subsequent catalytic enlargement of the NPs by the chemical deposition of Ag on the Au NP seeds, followed by the dissolution of the Ag metal (with HNO₃) and the potentiometric stripping detection of the released ions (Figure 20) was used for the amplified electrochemical detection of the hybridized DNA (Wang *et al.*, 2001a).

NPs of other compositions may be similarly used as labels for the amplified analysis of DNA. For example, metal sulfide NPs provide versatile surfaces for the immobilization of thiolated DNA. Lead sulfide (PbS) NPs were used as labels for the amplified DNA detection (Zhu *et al.*, 2004). Polypyrrole was

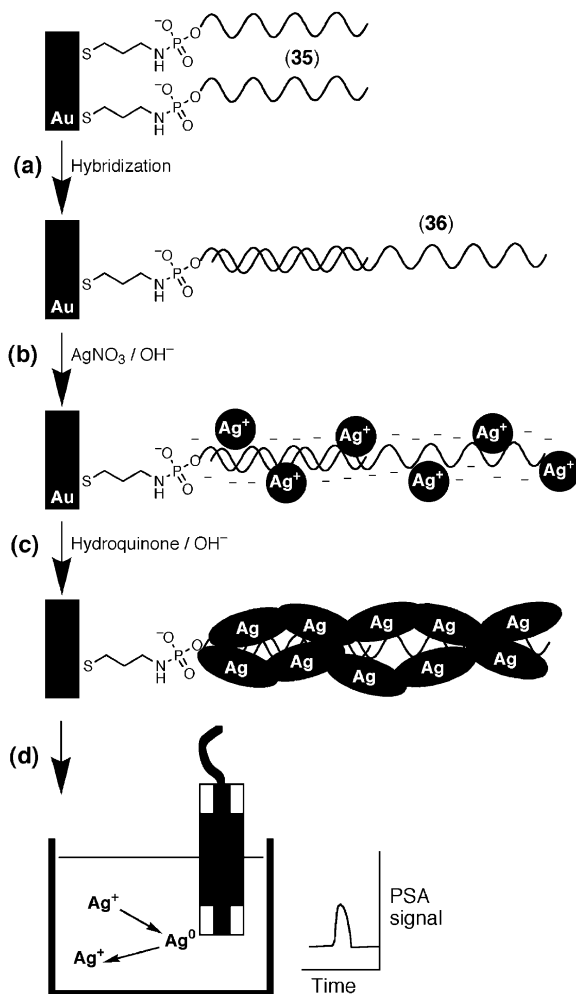


Fig. 19. Outline of the steps involved in the amplified electrochemical detection of DNA by the catalytic deposition of silver clusters on the DNA duplex: (a) hybridization of the complementary target DNA (36) with the DNA probe (35) that is covalently linked to the electrode surface through a cystamine monolayer; (b) loading of the Ag⁺ ions onto the immobilized DNA; (c) reduction of Ag⁺ ions by hydroquinone to form silver aggregates on the DNA backbone; (d) dissolution of the silver aggregates in an acidic solution, and transfer of the solution to the detection cell for stripping potentiometric measurements (PSA = potentiometric stripping analysis.)

electropolymerized on a glassy carbon electrode, and the sensing nucleic acid was immobilized on the polymer interface. The hybridization of the complementary nucleic acid-functionalized PbS NPs with the nucleic acid adsorbed on the surface was followed by the acidic dissolution of the particles. The anodic potentiometric stripping of the released Pb²⁺ ions was then used as the electrochemical signal for the primary hybridization process. A detection limit

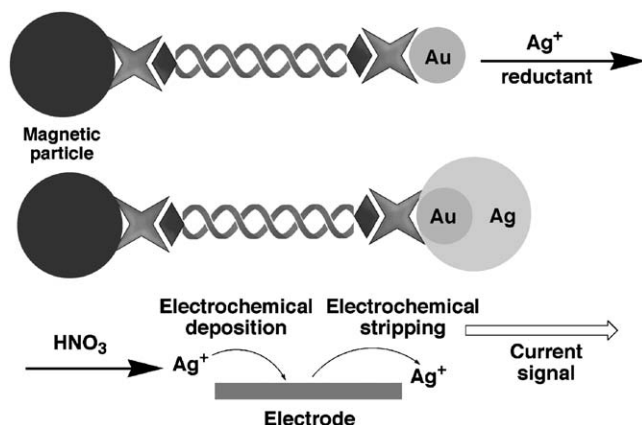


Fig. 20. Amplified analysis of DNA by anodic stripping voltammetry of NPs associated with an oligonucleotide duplex assembly that employs the catalytic enlargement of the NPs and the generation of Au/Ag core-shell NPs.

for analyzing the complementary DNA that corresponds to 3×10^{-13} M was reported, and a DNA analyte that includes three-base mismatches as compared to the fully complementary DNA was easily differentiated by the analytical process. Other metal sulfides such as CdS NP were employed as labels for the amplified detection of DNA (Wang *et al.*, 2002). The dissolution of the NPs by 1 M HNO_3 followed by the analysis of the released Cd^{2+} ions by electrochemical stripping was used for the detection of the hybridization process. This method was further developed to analyze in parallel, and simultaneously, different DNA analytes, by the use of different metal sulfide NPs (Wang *et al.*, 2003a). Magnetic particles were functionalized with three different nucleic acids (37), (38), and (39) that act as sensing oligonucleotides for three different analyte DNAs (40), (41), and (42) (Figure 21(A)). The hybridization of nucleic acids complementary to the hybridized DNAs, followed by the association of the three different metal sulfide NP labels, (43)–PbS, (44)–CdS, and (45)–ZnS, generated the encoded labels for the parallel analysis of different DNA targets. The dissolution of the NPs followed by the electrochemical stripping of the different metal ions enabled then the amplified quantitative analysis of the different DNAs. Figure 21(B) shows the stripping voltammograms observed upon the analysis of three different DNA targets, 43, 44, and 45, by means of PbS, CdS, and ZnS encoded NP labels, respectively. A detection limit of 2.7×10^{-10} M was reported for analyzing the different target DNAs.

Nucleotide-labeled Au NPs were used for the electrochemical detection of single-base polymorphism (Kerman *et al.*, 2004b). Au NPs were modified with a single-nucleotide capping, e.g., C–Au NP or T–Au NPs. The sequential hydrogen bonding of the nucleotide-functionalized NPs to a base mismatch lacking intra-DNA hydrogen bonding, e.g., to a G–A mismatched pair, followed by the electrochemical oxidation of the associated Au NPs allowed the electrochemical detection of single-base polymorphism. This method was further extended for the parallel bioelectronic detection of all eight possible one-base mismatches

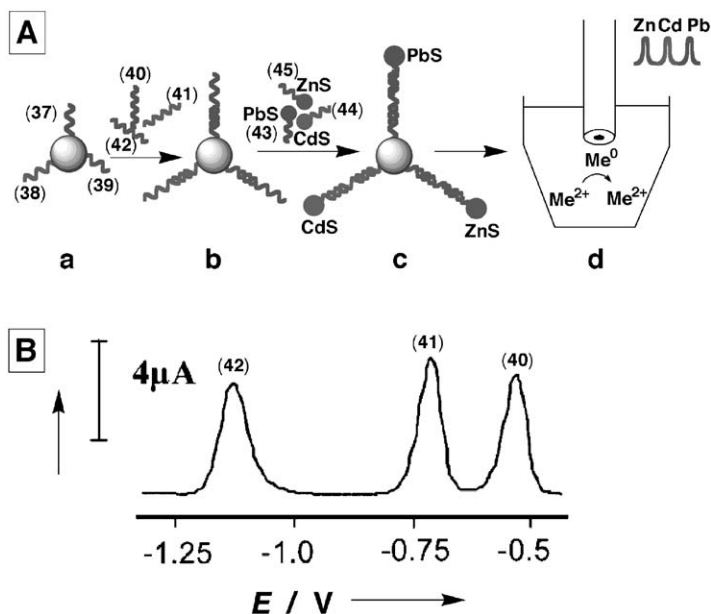


Fig. 21. (A) Multitarget electrochemical detection of DNA by different nanocrystal labels: (a) introduction of probe-modified magnetic beads; (b) hybridization with the DNA targets; (c) second hybridization with the NP-labeled oligonucleotides; (d) dissolution of the NPs and the electrochemical detection of the released ions. (B) Stripping voltammogram corresponding to the simultaneous analysis of three different 60-mer DNA targets (40–42; 54 nM each), which are related to the BRCA1 breast cancer gene. The DNA molecules are labeled with ZnS NPs, CdS NPs, and PbS NPs. (Part B is adapted from Wang *et al.*, 2003a, Figure 2, with permission.)

using four different metal sulfide NPs (ZnS, CdS, PbS, or CuS) functionalized with A, C, G, or T, that acted as specific encoded labels for analyzing the different base mismatches (Liu *et al.*, 2005) (Figure 22(A)). The specific hydrogen-bonded structures between the encoded NPs and the mismatched bases provide a fingerprint for the mismatched base configuration. The fingerprint can then be electrochemically imaged by the dissolution of the NP structures and the identification of the NP codes by electrochemical stripping voltammetry. Figure 22(B) depicts the stripping voltammograms upon analyzing three different base mismatches by the nucleotide-encoded NPs. This method was also extended to analyze several base mismatches in a single DNA duplex.

4. NANO- AND MICRO-OBJECTS AS CARRIERS FOR THE AMPLIFIED ELECTROCHEMICAL DETECTION OF DNA

The high surface area of NPs, nanotubes, microbeads, or liposomes allows the surface modification of these objects with electroactive and nucleic acid components, or the incorporation of the electroactive components into the volume of these nano/microstructures. Such functionalized nano/microstructures enable the

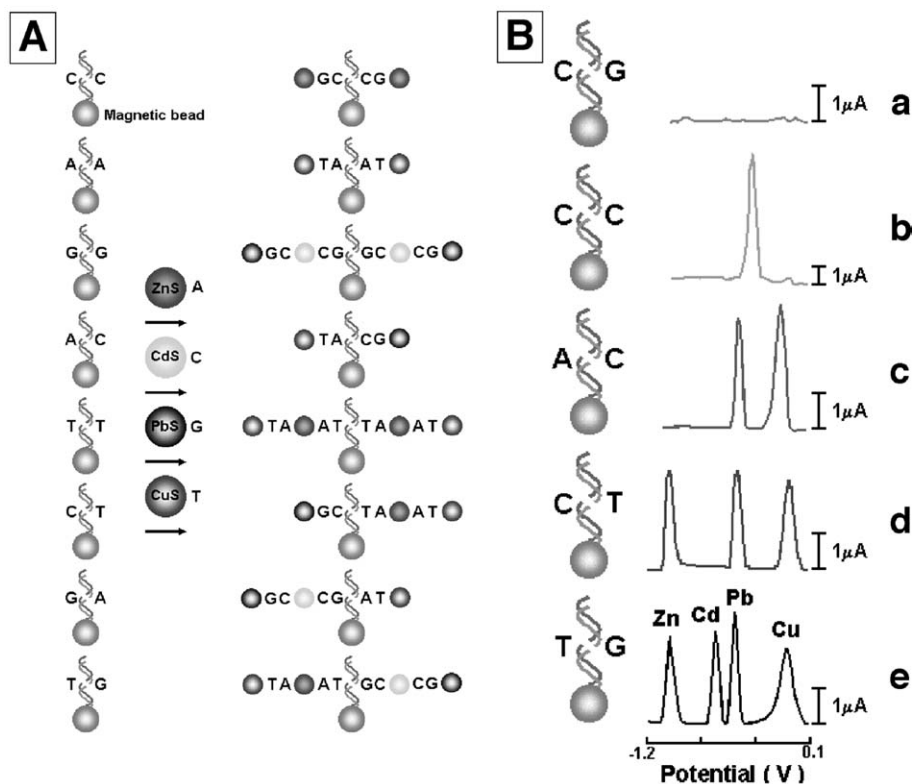


Fig. 22. (A) Electrochemical coding of all eight possible one-base mismatches in duplex DNAs using inorganic nanocrystal tracers. Use of mismatch-containing hybrids (captured on magnetic beads) followed by sequential additions of ZnS-linked adenosine-5' monophosphate, CdS-linked cytidine-5' monophosphate, PbS-linked guanosine-5' monophosphate, and CuS-linked thymidine-5' monophosphate. Also shown (right) are the corresponding assemblies of nanocrystal-linked DNA/magnetic beads. (B) Stripping voltammograms for the analysis of fully complementary DNA (a), and hybrids containing C-C (b), A-C (c), C-T (d), and T-G (e) mismatches using adenosine-5' monophosphate/ZnS, cytidine-5' monophosphate/CdS, guanosine-5' monophosphate/PbS and thymidine-5' monophosphate/CuS conjugates. The data were recorded in a 0.1 M acetate buffer (pH 4.9) containing $10 \mu\text{g mL}^{-1}$ of Hg(II). (Adapted from Liu *et al.*, 2005, Figures 1 and 2, with permission.)

increase of the contents of the electrochemically active units linked to the double-stranded DNA complexes, thus enhancing the sensitivity of the analytical procedures.

Electroactive polystyrene beads were employed for the amplified electrochemical analysis of DNA (Wang *et al.*, 2003d). The electroactive ferrocene carboxaldehyde label (46) was immobilized in polystyrene beads acting as carrier units. Magnetic particles functionalized with a nucleic acid (47) were then hybridized with the complementary nucleic acid (48)-functionalized polystyrene beads, which included the electroactive label (Figure 23(A)). The separation of the hybrid duplex structures of the polystyrene/magnetic particles, followed by

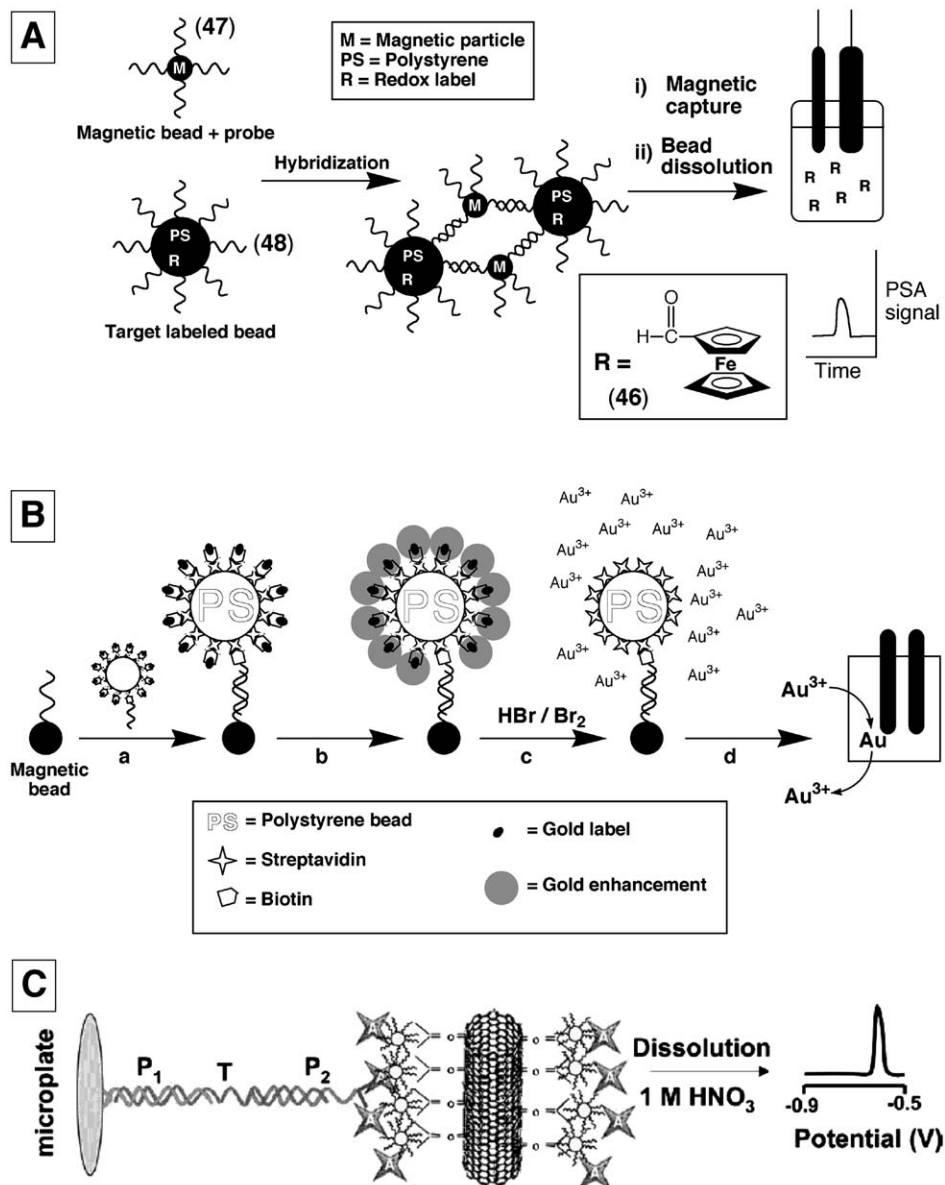


Fig. 23. (A) The amplified detection of DNA with polystyrene beads loaded with the ferrocene redox marker (46). (B) The amplified detection of DNA by using nucleic acid–Au NP-functionalized beads as labels and electroless catalytic deposition of gold on the NPs as a means of amplification: (a) hybridization of the nucleic acid–Au NP-functionalized beads with the target DNA that is associated with a magnetic bead; (b) the enhanced catalytic deposition of gold on the NPs; (c) dissolution of the gold clusters; (d) the detection of the released Au³⁺ ions by stripping voltammetry. (C) The amplified detection of DNA with carbon nanotubes, which are loaded with CdS nanoparticles as redox markers for the stripping voltammetry.

the dissolution of the beads, released numerous electroactive molecular units of ferrocene carboxaldehyde as a result of a single recognition event. The amperometric detection of the released redox compound allowed the analysis of DNA with a detection limit corresponding to 0.1 ng L^{-1} . Related processes have employed polystyrene beads modified with nucleic acid-functionalized Au NPs (Kawde and Wang, 2004) (Figure 23(B)) or carbon nanotubes modified with nucleic acid-functionalized CdS NPs (Wang *et al.*, 2003b) (Figure 23(C)) as multifunctional labels for the amplified detection of the target DNA. In these systems, the polystyrene beads or the carbon nanotubes act as carriers for the Au or CdS NPs and as a carrying element for a nucleic acid that is complementary to the target DNA. The dissolution of the Au NPs or the CdS provided numerous released ions as a result of a single recognition event. The released ions were then analyzed by stripping voltammetry as discussed in Section 3.

Liposomes were employed as nanostructures for the electrochemical amplification of DNA analyses (Patolsky *et al.*, 2000a, 2001c). The fabrication of negatively charged liposomes that act as labels for tagging DNA hybridization yields a negatively charged membrane environment at the recognition sites associated with electrodes. The changes in the interfacial properties of the electrodes due to the liposome tags were then used to readout the sensing processes. Figure 24(A) depicts one configuration for the amplified electrochemical analysis of DNA. The Au electrode was modified with a sensing nucleic acid (49) that hybridized with the analyte DNA (50). Negatively charged liposomes that included the nucleic acid (51), which is complementary to the analyte, were then hybridized to the duplex-functionalized electrode to yield a negatively charged interface. As the liposome (ca. 10 nm in diameter) yields a negatively charged micromembrane interface, the interfacial electron transfer to a negatively charged redox probe is anticipated to be perturbed. The interfacial electron transfer resistance as a result of the association of the liposome tags was monitored by Faradaic impedance spectroscopy. Figure 25(A) shows the Faradaic impedance spectra observed upon the analysis of the target DNA (50). Each of the hybridization processes is accompanied by an increase in the interfacial electron transfer resistance due to the enhanced electrostatic repulsion of the redox label $[\text{Fe}(\text{CN})_6]^{3-/4-}$ from the electrode interface. The most pronounced increase in the interfacial electron transfer resistance was observed upon the hybridization of the liposome tags, $\Delta R_{\text{ct}} = 7.5 \text{ k}\Omega$. This increase in the interfacial electron transfer resistance was attributed to the formation of a negatively charged membrane interface that introduces a barrier for electron transfer to the redox label solubilized in the electrolyte solution as a result of its electrostatic repulsion from the electrode surface. Since the surface coverage of the liposome tags associated with the electrode is controlled by the number of hybridization events, the changes in the interfacial electron transfer resistances are controlled by the concentration of the analyte DNA. Figure 25(A), inset, depicts the derived calibration curve corresponding to the changes in the interfacial electron transfer resistances, which results upon the analysis of different concentrations of 50. The sensitivity limit for the analysis of 50 was $1 \times 10^{-12} \text{ M}$. A different configuration for the analysis of DNA by tagged liposomes is shown in Figure 24(B). Biotin-labeled, negatively charged, liposomes

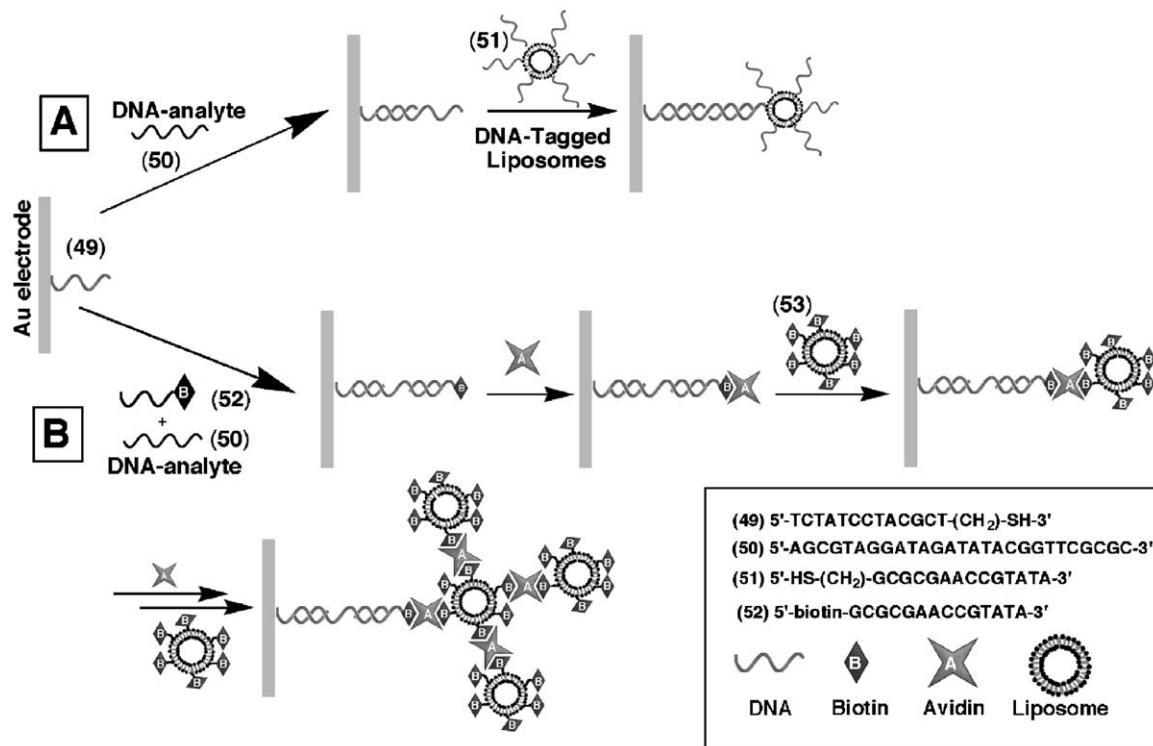


Fig. 24. Amplified analysis of a target DNA by: (A) oligonucleotide-functionalized liposomes. (B) Biotin-functionalized liposomes using avidin as a linker.

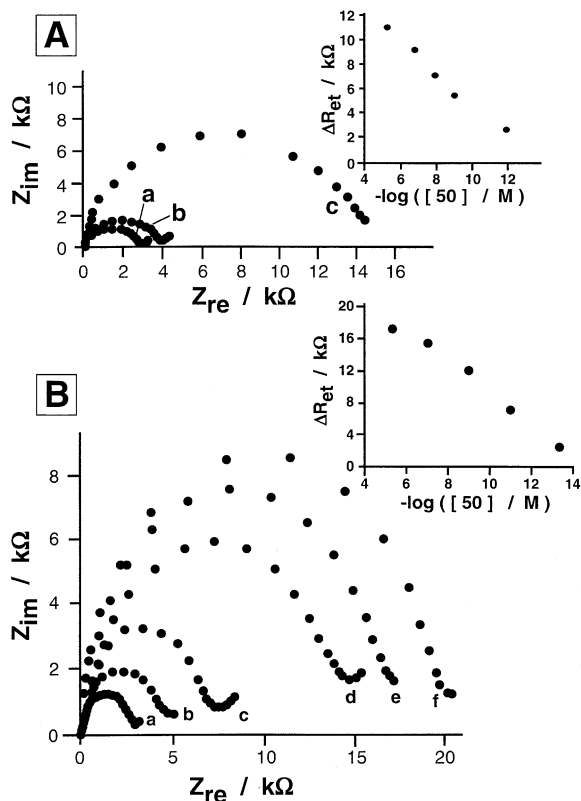


Fig. 25. (A) Faradaic impedance spectra of (a) the **49**-functionalized Au electrode, (b) after interaction of the sensing interface with **50**, 5×10^{-6} M, 15 min, and (c) after interaction with the **51**-functionalized liposomes. Inset: changes in the electron transfer resistance of the **49**-functionalized electrode upon treatment with variable concentrations of the analyte DNA (**50**), and upon the secondary amplification with the **51**-functionalized liposomes. (B) Faradaic impedance spectra of: (a) the **49**-functionalized Au electrode, (b) after interaction of the sensing electrode with **50**, 5×10^{-6} M, which was pre-treated with avidin, (c) after interaction with the biotinylated liposomes (**53**), (d) after treatment of the interface for a second time with avidin, (e) after interaction of the interface for a second time with the biotinylated liposomes. Inset: calibration plot corresponding to the changes in the electron-transfer resistance of the sensing interface upon analyzing different concentrations of DNA (**50**), and enhancement of the sensing process by a double-step avidin/biotinylated liposome amplification path. (Adapted from Patolsky *et al.*, 2001c, Figure 6, with permission.)

are used as the tags for the amplified detection of the DNA (**50**). A biotin-labeled nucleic acid (**52**) is hybridized with the duplex structure formed between the sensing nucleotide (**49**) and the analyte DNA (**50**). The biotin-labeled liposomes are then linked to the tri-component, biotin-labeled, double-stranded complex bound to the electrode by an avidin bridge. The resulting biotin-liposome tags enable further amplification of the micromembrane interface by the dendritic binding of generation of liposome tags by avidin-bridging units. Thus, the formation of a single duplex structure between the sensing interface

and **50**, may yield a negatively charged membrane microenvironment by the dendritic build-up of a controlled number of the liposome tags. Figure 25(B) shows the Faradaic impedance spectra observed upon the analysis of **50** according to the scheme outlined in Figure 24(B). The binding of the first generation of the avidin/biotin-labeled liposomes to the interface resulted in the increase of the electron transfer resistances to 7.2 and 15.5 k Ω , respectively. The association of the second generation of the liposome tags using the avidin linker increased the interfacial electron transfer resistance to 21 k Ω . The increase in the values of the interfacial electron transfer resistances was attributed to the electrostatic repulsion of the redox label $[\text{Fe}(\text{CN})_6]^{3-/4-}$ from the electrode support. The analyte **50** was analyzed with a detection limit of 1×10^{-15} M using a two-step amplification path that included the assembly of two generations of the biotin-functionalized liposome tags (Figure 25(B) inset).

The biotin-functionalized liposomes were also employed for the amplified identification of a single-base mutation in a gene (Patolsky *et al.*, 2001c) (Figure 26(A)). This is exemplified with the analysis of a gene where an A-base in the normal gene (**54**) is exchanged by a G-base to yield a mutant gene (**55**). The primer nucleotide (**56**) complementary to the normal or mutant gene up to the base prior to the mutation site was immobilized on the electrode. The hybridization of the sensing interface with the normal gene (**54**) or the mutant (**55**) was followed by the treatment of the resulting duplex with the biotinylated dCTP and polymerase. The biotin-labeled C-base was introduced via polymerization only in the mutant double-stranded assembly. The biotinylated C-base incorporated into the double strand was then identified by the association of the biotin-functionalized liposomes using avidin as linker. The binding of the liposomes to the analyzed DNA was followed by impedance spectroscopy. Figure 26(B) shows the impedance spectra observed upon the association of the avidin linker and tagged liposomes to the biotin-labeled DNA. The change in the interfacial electron transfer resistance as a result of binding of the liposomes corresponded to $\Delta R_{\text{et}} = 7.2$ k Ω . As the surface coverage of the mutant on the electrode is controlled by its bulk concentration, the surface density of the linked liposomes correlated with the concentration of the mutant, and thus, the changes in the interfacial electron transfer resistances, ΔR_{et} , were dominated by the concentration of the mutant (Figure 26(B) inset). Using this method, the mutant was analyzed with a sensitivity limit of 1×10^{-13} M.

Other nanoobjects such as carbon nanotubes (Kerman *et al.*, 2004a) or nanoparticles (Xu *et al.*, 2004) were similarly used as carriers for nucleic acid tags that alter the interfacial properties of electrodes and thus were employed for the amplified electrochemical detection of DNA. For example, the hybridization of CdS NPs functionalized with nucleic acid complementary to an oligonucleotide interface associated with an electrode yield a highly negatively charged interface that repels the negatively charged redox label $[\text{Fe}(\text{CN})_6]^{3-/4-}$ and perturbs the electron transfer at the electrode interface. The barrier for electron transfer was followed by Faradaic impedance spectroscopy.

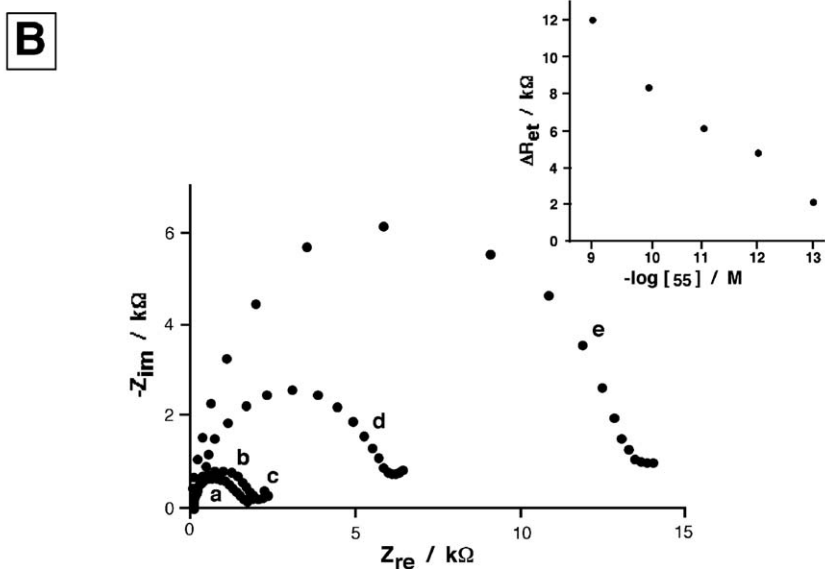
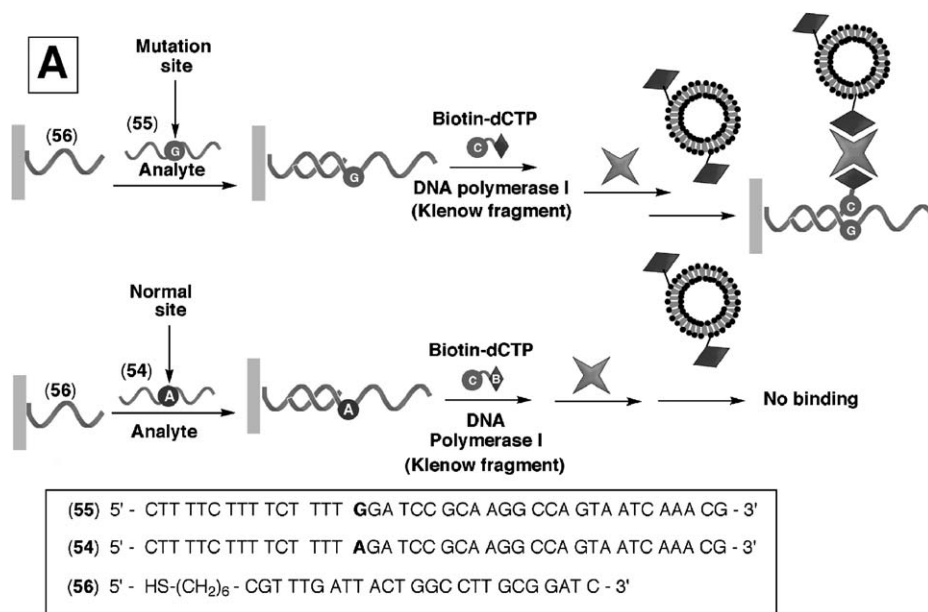


Fig. 26. (A) Electronic transduction of a single-base mutation in the target-DNA (55) using the polymerase-induced coupling of a biotinylated-base to the probe (56), and the use of biotin-labeled liposomes as an amplification route. (B) Faradaic impedance spectra (Z_{im} vs. Z_{re}) upon the analysis of the single-base mismatch in 55: (a) the 56-functionalized electrodes, (b) the 56-functionalized electrode after hybridization with 55, 1×10^{-9} M, (c) after reaction of the double-stranded interface with biotinylated-dCTP, $20 \mu\text{M}$, and polymerase Klenow fragment, 20 U mL^{-1} , (d) after the interaction of the electrode with avidin, $2.5 \mu\text{g mL}^{-1}$, and (e) after the interaction of the interface with the biotinylated liposomes (lipid concentration 0.25 mM). Inset: calibration curve corresponding to the R_{et} values observed upon the sensing of different concentrations of the mutant 55 according to the process outlined in part A. (Part B was adapted from Patolsky *et al.*, 2001c, Figure 9, with permission.)

5. ANALYSIS OF DNA BY DIRECT CONDUCTIVITY MEASUREMENTS

The catalytic properties of metal NPs that stimulate the deposition of metals on the NPs by reduction processes became a general practice in developing biosensor systems (Fritzsch and Taton, 2003). The catalytic enlargement of Au NPs by the NADH cofactor generated by the NAD^+ -dependent enzyme lactate dehydrogenase/lactate/ NAD^+ system (Xiao *et al.*, 2004a), or the catalytic reduction of AuCl_4^- and the enlargement of Au NP seeds by H_2O_2 generated by the glucose oxidase/glucose/ O_2 biocatalytic system (Zayats *et al.*, 2005), were employed to develop colorimetric assays for these biocatalytic processes. The catalytic deposition of Ag on Au NP/nucleic acid conjugates hybridized to a target DNA associated with surfaces, using a Ag^+ /hydroquinone as metal enhancement solution, was used for the optical detection of DNA using the NP absorbance as optical imaging technique (Taton *et al.*, 2000). The large scattering coefficients of metal particles were used for the optical imaging of biosensing events (Schultz, 2003). For example, the enlargement of Au NPs, nucleic acid conjugates, hybridized with a target DNA associated with an interface, using a Ag-enhancement solution was used to generate Au/Ag core-shell NP tags for the sensitive optical detection of DNA using light scattering as optical imaging method (Storhoff *et al.*, 2004). Similarly, the catalytic, chemically induced, deposition of gold on Au NP/nucleic acid conjugates hybridized with nucleic acid/DNA duplexes associated with piezoelectric crystals was used for the amplified microgravimetric quartz-crystal-microbalance analysis of DNA (Patolsky *et al.*, 2000a).

The catalytic deposition of metals on metal NPs organized in an appropriate geometrical configuration on surfaces allows the growth of the NPs to the extent that intimate contact between the NPs is achieved. The intimate physical contact between enlarged NPs between two electrodes allows then the electrical short-circuit bridging of the electrodes. The amplified electrical detection of DNA by the catalytic enlargement of metal NPs and the monitoring of the conductivity in between two microelectrodes was accomplished (Möller *et al.*, 2001; Park *et al.*, 2002). Figure 27(A) outlines the principal for analyzing the target DNA (Park *et al.*, 2002). Two Au-microelectrodes, separated by a 20- μm gap, were organized on a Si support by photolithographic means (Figure 27(C)). A sensing nucleic acid (57) was immobilized in the gap consisting of the Si support. The hybridization of the target DNA (58) with the sensing interface was then followed by the secondary hybridization of the nucleic acid (59)-Au NP conjugate that acts as probe to follow the hybridization of 58 (Figure 27(B)). The subsequent catalytic enlargement of the Au NPs by the deposition of Ag using the Ag^+ /hydroquinone developing system yielded electrically contacted particles that enhanced the conductivity (or reduced the resistance) of the gap domain separating the two electrodes. Figure 27(D), curve (a), shows the resistivity changes of the gap, upon analyzing the target (58), as a function of the Ag-deposition time. While the gap reveals a high resistance prior to the enlargement by the Ag, $R > 2 \times 10^8 \Omega$, the deposition of Ag for 25 min yielded a conductive domain, $R \approx 100 \Omega$. The method enabled also the discrimination of

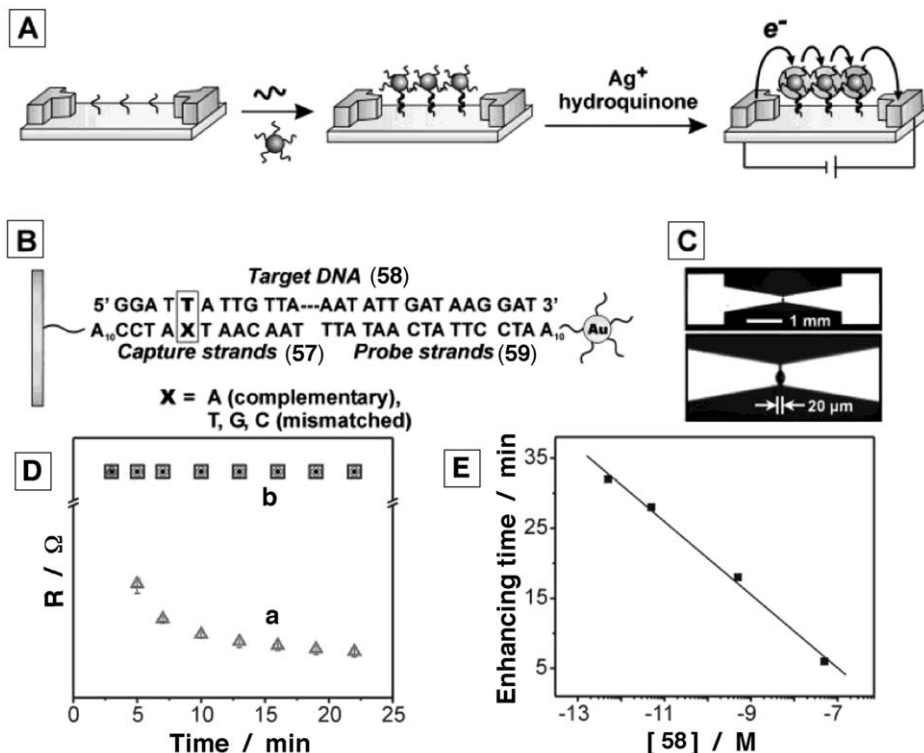


Fig. 27. (A) Analysis of DNA by the enhancement of the conductivity between electrodes by the catalytic enlargement of Au NPs associated with the DNA assembly. (B) The DNA/NPs assembly for the electrical analysis. (C) The microelectrode array used for the resistance/conductance measurements. (D) Resistance of the electrode array measured as a function of the time interval of Ag enhancing in the presence of: (a) the complementary and (b) non-complementary DNA. (E) A graph of the Ag-enhancing time required to reach a resistance value of 100 kΩ as a function of target-DNA concentration. (Adapted from Park *et al.*, 2002, Figures 1 and 2, with permission.)

single-nucleotide polymorphism. The elimination of the hybridization of the single-base mismatched nucleotide was accomplished by controlling the temperature at which hybridization was performed (the mismatched duplex exhibited a lower melting temperature) or by controlling the composition of the hybridization and rinsing buffers. For example, when the G-base replaced the complementary A-base in the analyzed DNA, no hybridization of single-base mutant to the sensing interface occurred, and consequently no Au NP labels or catalytic enhancement of the NPs occurred. As a result, analyzing the single-base mutant, resulted in an insulating domain between the electrodes (Figure 27(D) curve (b)). As the content of hybridized analyte DNA (58) is controlled by its bulk concentration, the surface coverage of the Au NP labels is controlled by the concentration of the analyte DNA (58). As a result, the time interval to

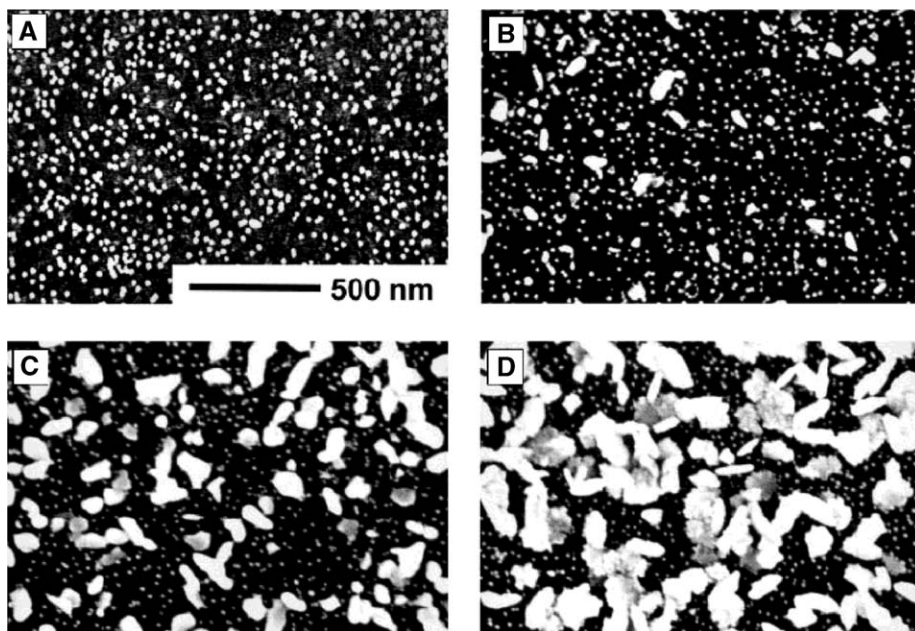


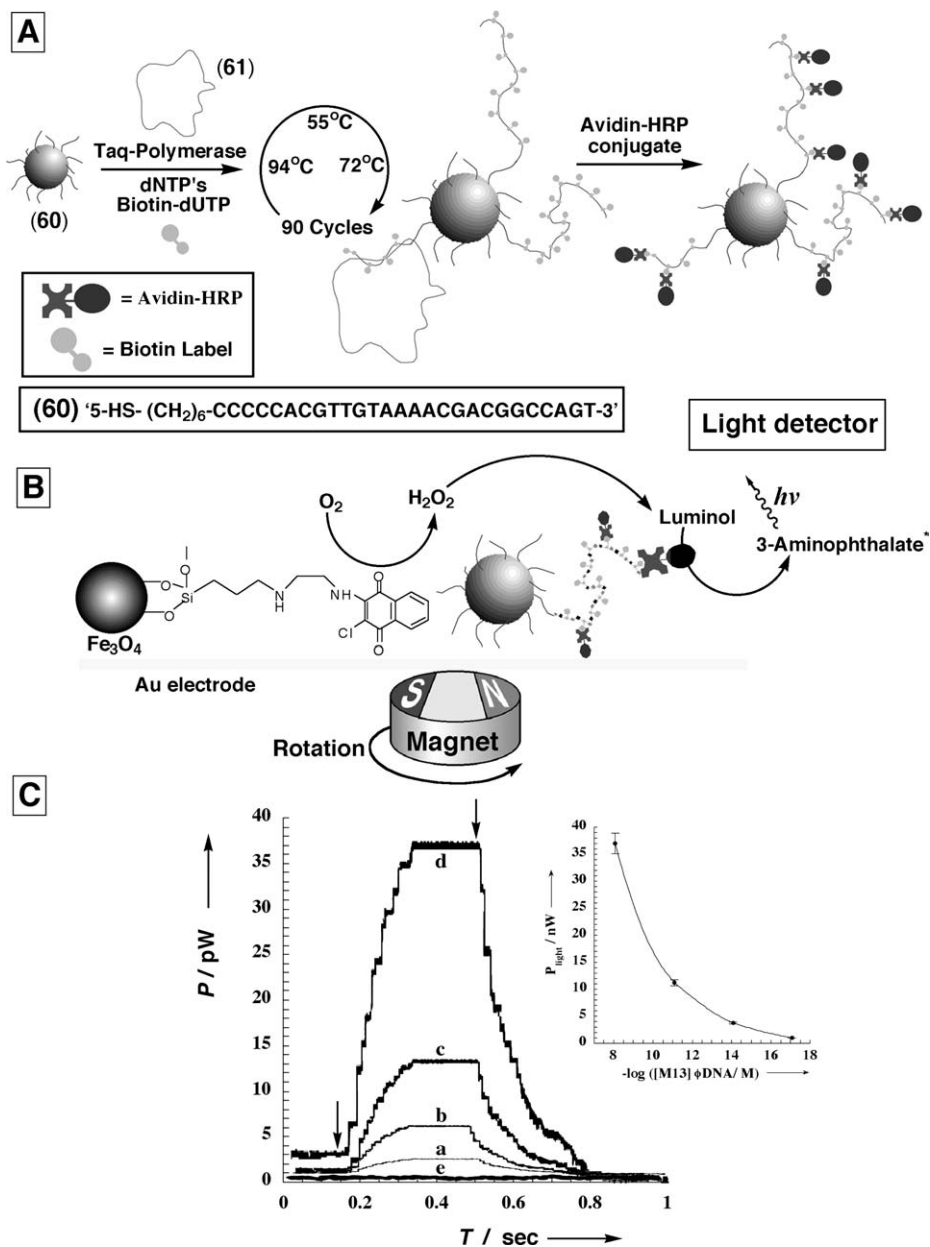
Fig. 28. SEM images of the NP probes on an ITO-coated glass surface upon the analysis of DNA based on the conductivity measurements: (A) before silver deposition, (B) after a 3-min treatment with the enhancement solution, (C) after a 6-min treatment with the enhancement solution, and (D) after a 9-min treatment with silver enhancement solution. (Adapted from Park *et al.*, 2002, Figure 3, with permission.)

generate a conductive array between the microelectrodes was found to correlate with the concentration of the analyzed DNA (Figure 27(E)). The formation of the conductive domain between the electrodes by the catalytic deposition of Ag on the Au NP labels was found to be a time-dependent process (cf. Figure 27(D) curve (a)). Scanning electron microscopy (SEM) images, Figure 28, indicated that in the resulting conductive array, the Au NP were enlarged with Ag to the extent that intimate contact between the particles was achieved and paths for transporting electrons between the electrodes were generated (Figure 28(D)). This technology was already practically implemented. DNA chips consisting with pre-designed microelectrode arrays, and handy conductivity detectors that follow the metal enhancement are available on the market (Urban *et al.*, 2003). A related approach has employed interdigitated Al electrodes on an Al₂O₃ support (Moreno-Hagelsieb *et al.*, 2004). An amino-functionalized nucleic acid acting as sensing probe was covalently linked to an aldehyde-modified siloxane interface. After hybridization of the analyte, a biotin-labeled nucleic acid complementary to a single-stranded segment of the analyte was further hybridized to the duplex linked to the support. The binding of a Au NP-labeled anti-biotin antibody to the surface, followed by the catalytic deposition of Ag on the Au NPs led to the electrical contacting of the originally separated electrodes.

6. AMPLIFIED SENSING OF DNA IN THE PRESENCE OF MAGNETIC PARTICLES

Magnetic particles are extensively used as labels for biomolecules such as antibodies or DNA and used to aid the separation of biomolecular complexes from complex analysis mixtures (Häfeli *et al.*, 1997; Uhlén *et al.*, 1994). Recently, magnetic particles were used to switch “ON” and “OFF” bioelectrocatalytic processes in the presence of an external magnet (Willner and Katz, 2003). For example, magnetite particles were functionalized with electron relay units that electrically contact redox enzymes with electrodes (Katz *et al.*, 2002b). The attraction of the functionalized magnetic particles to the electrode support by means of the external magnet, activated the bioelectrocatalytic functions of the respective enzymes, upon the application of the appropriate potential. The retraction of the functionalized magnetic particles from the electrode, by means of the external magnet, blocked the bioelectrocatalytic functions of the enzymes (Hirsch *et al.*, 2000; Katz *et al.*, 2002a,b). A major advance in the application of functionalized magnetic particles for amplified electrochemical biosensing was accomplished by the rotation of the magnetic particles by an external rotating magnet (Katz and Willner, 2002). It was found that the rotation of redox-relay functionalized magnetic particles enhance the bioelectrocatalytic reactions in the presence of enzymes, and the rate of the biocatalytic processes was found to linearly relate to $\omega^{1/2}$ (ω = rotation speed). The enhancement of the bioelectrocatalytic processes was attributed to a hydrodynamic effect, whereby the transport of the enzyme and substrate to the electrode support is controlled by hydrodynamic forces rather than by diffusion. In a detailed study that compared the bioelectrocatalytic transformations at the rotating magnetic particles, and at a rotating disc electrode, it was concluded that each of the magnetic particles behaves as a microrotating electrode that drives at its interface hydrodynamically controlled bioelectrocatalysis (Katz and Willner, 2005). The functionalized rotating magnetic particles were also applied for the enhanced electrochemically induced generation of chemiluminescence (Willner and Katz, 2003). Magnetic particles (Fe_3O_4 magnetite) functionalized with a naphthoquinone-capping interface were attracted to an electrode surface by an external magnet. Electrochemical reduction of the naphthoquinone units, under oxygen, resulted in the hydroquinone-catalyzed reduction of O_2 to H_2O_2 . The electro-generated H_2O_2 was then utilized, to stimulate the generation of chemiluminescence in the presence of HRP (Sheeney-Haj-Ichia *et al.*, 2000). The rotation of the redox-functionalized magnetic particles by means of an external rotating magnet enhanced the chemiluminescence through the hydrodynamic transport of HRP/luminol to the electrode.

This principle was used for the amplified ultrasensitive detection of DNA (Weizmann *et al.*, 2003) and for the detection of telomerase activity in cancer cells (Patolsky *et al.*, 2004). Figure 29(A) depicts the application of the method for the analysis of the 7249-base M13mp18 DNA (Patolsky *et al.*, 2003c). The 27-base DNA primer (**60**), which is complementary to a segment of the analyte DNA (**61**) was linked to the magnetic particles. The hybridization of the **60**-functionalized magnetite particles with the M13mp18 DNA was followed by a



polymerization process in the presence of the dNTPs nucleotide mixture that included biotin-labeled dUTP. The replication introduced biotin labels into the replicated nucleic acid that is associated with the magnetic particles. This replication process was followed by a sequence of thermal cycles, by which the analyzed M13mp18 DNA was dissociated from the particles, and rehybridized with another primer (**60**) linked to the particles, and further replicated to introduce the biotin labels into the replica. The resulting biotin-labeled nucleic acid-functionalized magnetic particles were reacted with the avidin–HRP, and subsequently mixed with the naphthoquinone-functionalized magnetic particle. The particle mixture was collected on the electrode support, and a potential was applied on the electrode to reduce the naphthoquinone to the hydroquinone units that catalyze the reduction of O_2 to H_2O_2 , while rotating the mixture of the magnetic particles. In the presence of luminol and the HRP coupled to the DNA replica, the system led to the generation of chemiluminescence. **Figure 29(B)** shows the electrogenerated chemiluminescence as a function of the speed of rotation of the particles, upon analyzing the M13mp18 DNA, 8×10^{-9} M. The effect of the speed of rotation of the particles on the intensity of the emitted light, and thus on the sensitivity of the analytical procedure is self-evident. **Figure 29(B)**, inset, shows the light intensities generated upon analyzing different concentrations of M13mp18 DNA, and the resulting calibration curve. The analyte DNA could be sensed by this method with a sensitivity limit that corresponded to 8×10^{-17} M.

A related method was applied to analyze single-base mismatches in DNA (*Patolsky et al.*, 2003c). According to this method, the nucleic acid complementary to the analyzed mutant up to one base prior to the mutation site was linked to the magnetic particles. After the hybridization of the mutant with the magnetic particles, the hybrid was subjected to replication in the presence of polymerase and the biotin-labeled base complementary to the mutation site. The biotin label was introduced only if the mutant existed in the double-stranded assembly. (Cf. Section 4 for the similar analysis of single-base mismatches by functionalized liposomes.) The subsequent coupling of the avidin–HRP conjugate to the biotin-labeled magnetic particles was followed by mixing the biomolecular-functionalized magnetic particles with the naphthoquinone-modified magnetic particles. The magnetic attraction of the magnetic particle mixture was then subjected to the electrocatalyzed reduction of O_2 to H_2O_2 , and the HRP-/luminol-driven generation of chemiluminescence. As before, the rotation of the magnetic particles amplified the sensing process.

This methodology was further applied for the detection of telomerase activity in cancer cells (*Patolsky et al.*, 2004). Telomers are G-rich nucleic acid segments that include constant repeat units at the ends of the chromosomes, and their function is believed to protect the chromosomal DNA from erosion (*Preston*, 1997). During the cell life cycle, the telomers are constantly shortened, and at a certain length the cell is triggered to end proliferation (*Blasco*, 2003). In certain cells, the enzyme telomerase is generated. This is a ribonucleoprotein-type biocatalyst that stimulates the elongation of the telomers by the characteristic repeat units. The telomerase-induced elongation of the telomers prevents the cellular trigger to terminate the proliferation, and the cells are transformed

into immortal malignant or cancerous cells (Preston, 1997). Indeed, in over 95% of different cancer cells elevated amounts of telomerase were detected, and the biocatalyst is considered as a versatile marker for cancer cells (Testorelli, 2003). The amplified analysis of telomerase activity by means of the rotating magnetic particles is shown in Figure 30(A) (Patolsky *et al.*, 2004). Magnetic particles were functionalized with a nucleic acid sequence (62) that is recognized by telomerase. Interaction of the magnetic particles with a HeLa cancer cell extract that included telomerase, in the presence of the nucleotide mixture dNTPs and biotin-labeled dUTP, resulted in the telomerase-induced elongation of the telomers, with the concomitant incorporation of the biotin labels into the telomers. Binding of the avidin–HRP conjugate to the resulting telomer units, followed by mixing of the functionalized magnetic particles with the naphthoquinone-functionalized magnetic particle, yielded the particle mixture for the chemiluminescence detection of telomerase activity. The attraction of the particle mixture to the electrode support, followed by their rotation on electrode surface, by means of the external magnet, enabled the amplified chemiluminescent detection of the activity of telomerase (Figure 30(B)). The electrochemical reduction of the naphthoquinone units led to the electrocatalytic reduction of O₂ to H₂O₂ and the latter product activated the generation of chemiluminescence in the presence of luminol and HPR conjugated to the telomer units. Figure 31(A) shows the intensities of the emitted chemiluminescent upon analyzing the extract of 100,000 HeLa cells at variable rotation speeds of the particles. Figure 31(B) shows the calibration curve corresponding to the light intensities generated by extracts originating from variable numbers of HeLa cells, and using a constant rotation speed of 2000 rpm. The results indicate that the method enables the detection of telomerase activity originating from 10 HeLa cancer cells (Figure 31(B), inset). This method was successfully applied to analyze cancer-containing tissues; Figure 32(A) shows the analysis of the telomerase activity originating from HeLa cells and 293-kidney cancer cells, and the results are compared to the control analysis of normal human fibrinogen (NHF) cells, or heat-treated, telomerase-deactivated, HeLa cells. Similarly, Figure 32(B) shows the light intensities observed upon analyzing telomerase activity originating from lung adenocarcinoma and lung squamous epithelial carcinomas, in comparison to the light emitted upon the analysis of healthy tissues or normal NHF cell extracts.

7. PHOTOELECTROCHEMICAL DETECTION OF DNA

Semiconductor quantum dots reveal unique electronic and optical properties (Shipway *et al.*, 2000). The intense fluorescence properties of semiconductor quantum dots are lately used to develop stable fluorescence labels for biorecognition reactions (Gerion *et al.*, 2002; Katz and Willner, 2004). Also, the fluorescence properties of quantum dots are used to stimulate FRET, and to follow biorecognition reactions, such as DNA hybridization and replication (Patolsky *et al.*, 2003a). One possible use of the photophysical properties of semiconductor

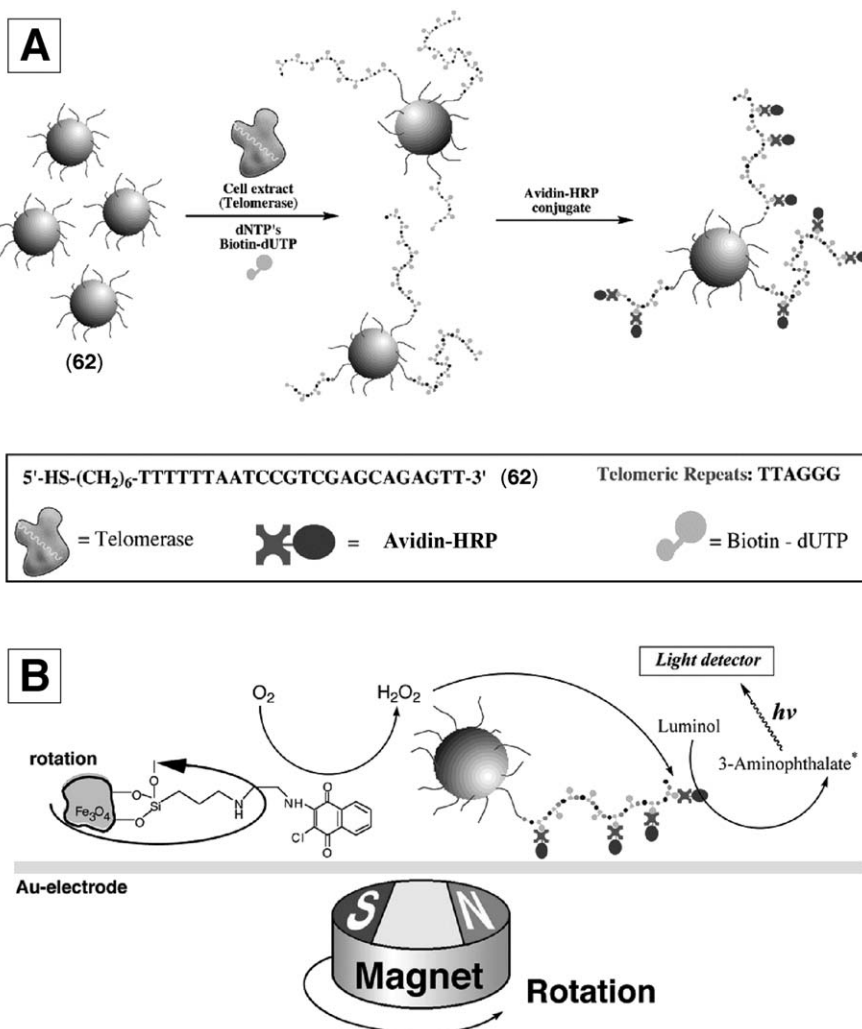


Fig. 30. Amplified detection of telomerase activity by multilabeled rotating magnetic particles: (A) labeling of telomers generated on magnetic particles with biotin by the telomerase-induced elongation of the primer units (62) and further binding of avidin–HRP conjugates. (B) Generation of chemiluminescence by the rotation of the mixture of magnetic particles that consists of the HRP-labeled telomer-functionalized magnetic particles and the naphthoquinone-functionalized magnetic particles on the electrode surface.

NPs is, however, the generation of photocurrents as a result of the photoexcitation of the semiconductor nanostructures. Semiconductor NPs such as TiO_2 or CdS are widely used as photoactive materials for the generation of photocurrents (Kamat, 2002). The photoinduced generation of an electron–hole pair in the conduction- and valence-band levels of the semiconductor can be followed by transferring the conduction band electrons to the electrode, or the filling of the valence band holes with electrons supplied by the electrode, two processes that

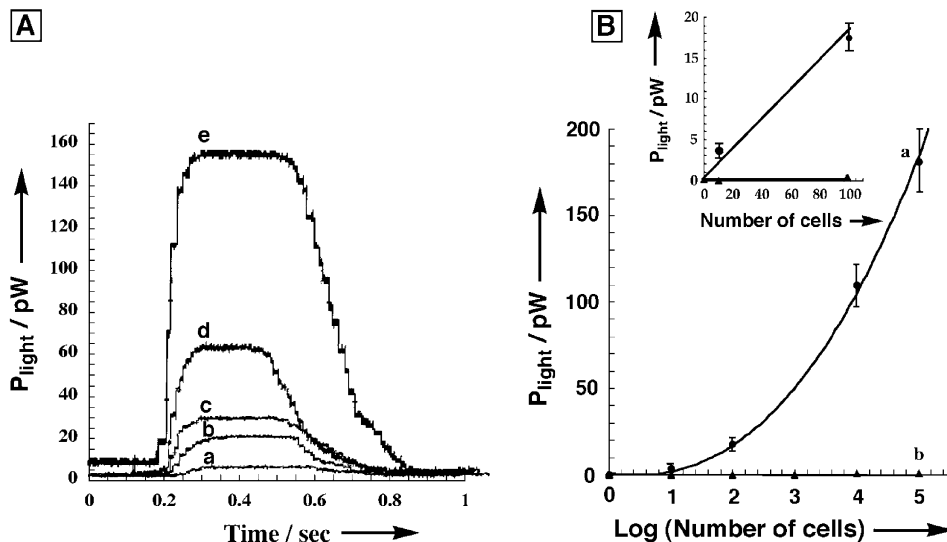


Fig. 31. Amplified detection of telomerase activity by multilabeled rotating magnetic particles according to Figure 30: (A) chemiluminescence intensities obtained with HeLa cell extracts (100,000 cells), at different rotation speeds: (a) 0 rpm, (b) 20 rpm, (c) 60 rpm, (d) 400 rpm, and (e) 2000 rpm. (B) Calibration curve corresponding to chemiluminescence intensities of extracts containing: (a) different numbers of HeLa cells at a constant rotation speed of 2000 rpm; (b) cell-free control sample. Inset: enlargement of calibration curve showing chemiluminescence signal intensities obtained from extracts containing 100 and 10 cells. (Adapted from Patolsky *et al.*, 2004, Figure 3, with permission.)

lead to the formation of photocurrents. Thus, semiconductor NPs conjugated to biomolecules may act as labels for the detection of biorecognition or biocatalytic processes by the photoelectrochemical effect. Although numerous studies employing semiconductor NPs for photoelectrochemical applications were reported (Kamat, 2002; Frank *et al.*, 2004), the use of biomolecule–semiconductor NPs hybrid systems for bioanalytical applications through photoelectrochemistry is scarce, and only recently some advances in this area were reported. For example, the biocatalyzed hydrolysis of thioacetylcholine to thiocholine in the presence of acetylcholine esterase was coupled to the photochemical excitation of CdS NPs associated with an electrode to yield photocurrents (Pardo-Yissar *et al.*, 2003). The inhibition of the enzyme retarded the photocurrent generation, and the process was used to follow the inhibition of the enzyme.

Nucleic acid-functionalized CdS NPs were used as labels for the photoelectrochemical amplified detection of DNA (Willner *et al.*, 2001). A Au surface was functionalized with the thiolated nucleic acid (63) that is complementary to 5'-end of the analyzed DNA (64). The CdS NPs (2.6 ± 0.4 nm diameter) were derivatized with the nucleic acid (65) that is complementary to the 3'-end of the analyte DNA (64) to yield the three-component double-stranded DNA on the electrode. The resulting interface was then reacted with CdS NPs functionalized with 63, which were pre-hybridized with the analyte DNA (64), to yield a second

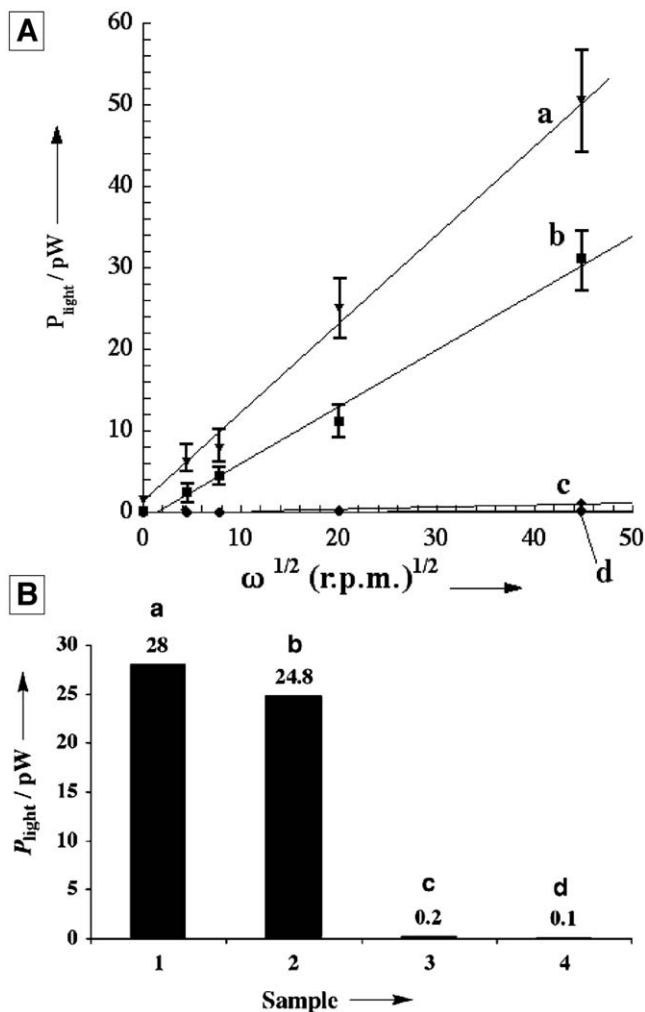


Fig. 32. (A) Electrogenenerated chemiluminescence intensities generated by extracts containing different types of cells at variable rotation speeds: (a) 1000 HeLa cells; (b) 1000 293-kidney cells; (c) 100,000 NHF cells; (d) 100,000 HeLa cells heat-treated at 95 °C for 20 min. (B) Electrogenenerated chemiluminescence intensities obtained by analyzing extracts from: (a) lung adenocarcinomas, (b) lung squamous epithelial carcinomas, (c) healthy tissues, and (d) normal NHF-cell extract. (Adapted from Patolsky *et al.*, 2004, Figures 4 and 5, with permission.)

generation of CdS NPs on the electrode support (Figure 33(A)). By the alternate reaction of the surface with **63**-functionalized CdS NPs pre-hybridized with **64**- and **65**-derivatized CdS NPs pre-hybridized with **64**, controlled numbers of CdS NPs generations were assembled on the electrode. Upon the photoexcitation of the semiconductor/DNA assemblies in the presence of the sacrificial electron donor triethanolamine, TEOA, a photocurrent was developed in the system (Figure 33(B)). The photocurrent formation was attributed to the photoexcitation of the CdS NPs that yield an electron-hole pair. The transfer of the

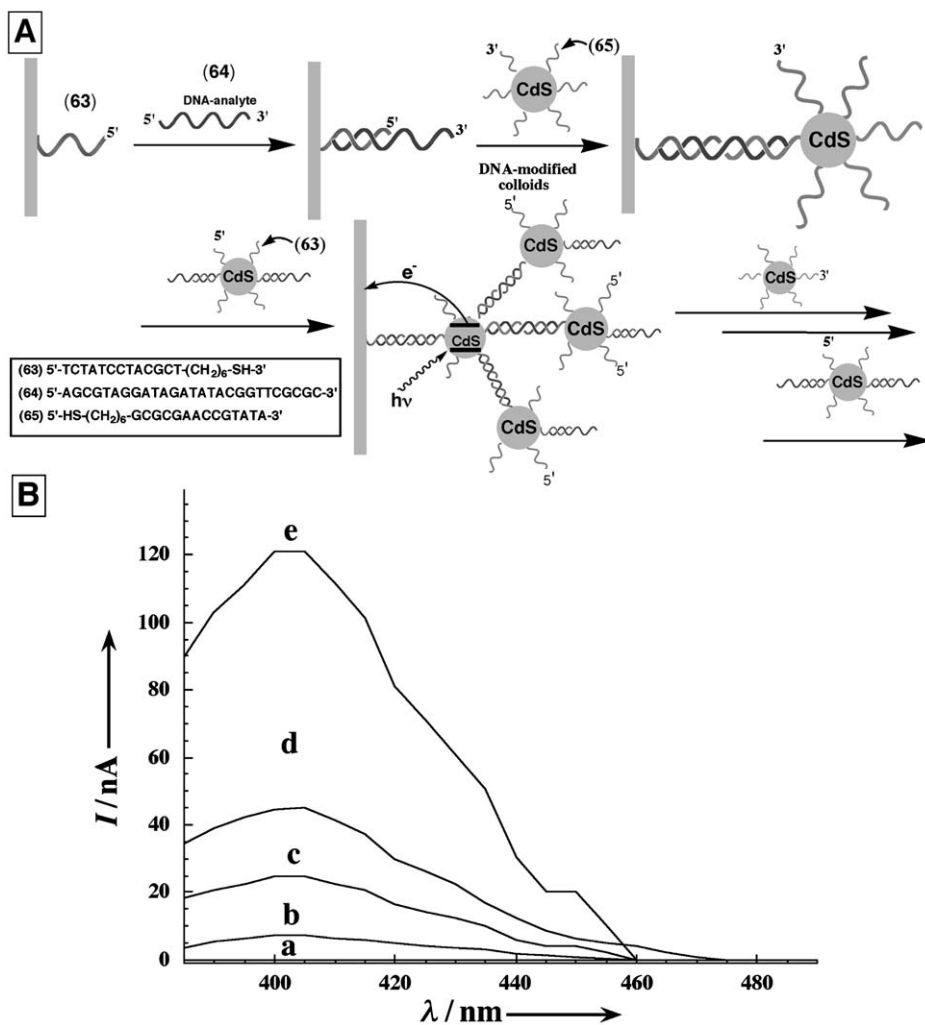


Fig. 33. (A) The assembly of an oligonucleotide/DNA-cross-linked array of CdS NPs on a Au electrode, and the photoelectrochemical response of the nanoarchitecture. (B) Photo-current action spectra of Au electrodes that include controlled numbers of oligonucleotide/DNA-cross-linked CdS NP layers: (a) prior to the deposition of CdS NPs. (b)–(e) One–four oligonucleotide/DNA-cross-linked CdS NP layers. (Part B is adapted from Willner *et al.*, 2001, Figure 3(A), with permission.)

conduction-band electrons to the electrode, and the concomitant supply of electrons to the valence band by the sacrificial electron donor yield the steady-state generation of the photocurrent. The photocurrent action spectra in this system followed the absorbance features of the CdS NPs, indicating that the photocurrent originates from the photoexcitation of the NPs. The photocurrent intensities were found to depend on the number of NP generations assembled on the electrode support. Furthermore, a non-linear increase in the

photocurrent intensities as a function of the number of CdS NPs generation was observed. The increase of the photocurrents upon the build-up of the generations of the CdS NPs on the surface was attributed to the higher content of CdS NPs for the generation of the photocurrents. The non-linear increase was attributed to a dendritic-type effect, where the hybridization of **64** is favored as the number of generations of CdS particles is higher, due to the availability of more binding sites for hybridization.

Beyond the analytical impact of the later system, which provides the amplified photoelectrochemical analysis of the DNA (**64**), the understanding of the mechanism of photocurrent generation in the system has important fundamental interest. The charge transport through DNA is a subject of extensive scientific debate (Kelley and Barton, 1999; Ratner, 1999; Asai, 2003). While several studies claimed that DNA exhibits conductivity (Fink and Schöenberger, 1999) and even superconductivity (Endres *et al.*, 2004) other studies supported the contradicting results, claiming that DNA acts as an insulating, protein-like, matrix (Storm *et al.*, 2001). To date increasing evidence exist that, indeed, double-stranded DNA behaves as a non-conductive medium, yet in the presence of special base-sequences electron or holes may migrate through the duplex DNA (Giese, 2002; O'Neill and Barton, 2004). The generation of the photocurrent in the CdS- DNA-layered aggregate (Figure 33) raised the immediate questions regarding the mechanism of transporting of the conduction-band electrons to the electrode, and the possible participation of the DNA in the photocurrent generation. It was claimed that due to the low coverage of the CdS NPs/DNA aggregates on the surface, because of the low concentration of **64**, the NP aggregates lie on the surface yielding an intimate contact with the electrode that leads to the photocurrent. This explanation implies, however, that due to the three-dimensional structure of the NP aggregates, part of the CdS NPs are not electrically contacted with the electrode, and thus do not contribute to the resulting photocurrent. This explanation was supported by the fact that Ru(III)-hexamine, $\text{Ru}(\text{NH}_3)_6^{3+}$, which binds to DNA was able to electrically contact the latter part of insulated CdS NPs, and enhance the photocurrent of the systems (Willner *et al.*, 2001). It was suggested that $\text{Ru}(\text{NH}_3)_6^{3+}$ acts as a trap for the conduction-band electrons, and it mediates the transfer of the conduction-band electrons to the electrode support.

Further insight into the charge transport properties in DNA/CdS NP duplex assemblies was recently reported by the incorporation of intercalators into the DNA duplex (Gill *et al.*, 2005). It was found that methylene blue (**66**), a typical intercalator into double-stranded DNA, facilitated the generation of the photocurrent. Application of the potential corresponding to 0 V vs. SCE maintains methylene blue (**66**) in its oxidized form, and thus the intercalator acts as an electron acceptor (Figure 34(A)). Photoexcitation of the CdS NPs in the presence of TEOA resulted in an anodic current that originated from the methylene blue-mediated transport of the conduction-band electrons, and the concomitant neutralization of valence-band holes by transferring electrons from the sacrificial electron donor in solution. Application of a potential of -0.4 V vs. SCE on the electrode that keeps the intercalator units in their reduced leuco-methylene blue state (**67**) resulted in a photocurrent in the opposite (cathodic) direction, in

the presence of O₂ (Figure 34(B)). Namely, upon the photoexcitation of the CdS NPs the conduction-band electrons were transferred to O₂ acting as an acceptor, while filling the valence-band holes with electrons from the intercalator electron donor units. This process led to the formation of a cathodic photocurrent in the system. By switching the potential on the electrode from 0 to -0.4 V and back, the photocurrents in the systems could be reversibly cycled between anodic and cathodic values, respectively, depending on the redox state of the intercalator units (Figure 34(C)). Besides the significance of these results in demonstrating that redox active intercalators mediate electron transport through DNA, that lead to the formation of photocurrents, the results may provide new directions in developing photoelectrochemically based DNA sensors. The perturbation of the intercalation, due to mismatches in the duplex DNA, is anticipated to inhibit the mediated photocurrent generation, and thus a method for the sensitive detection of single-base mismatch may be envisaged.

8. CONCLUSIONS AND PERSPECTIVES

Substantial advances were accomplished in the past decades in developing electrochemical DNA (or nucleic acids) sensors. A major challenge is, however, the sensitivity of the bioelectronic sensing devices. The polymerase chain reaction (PCR) is a versatile tool to amplify the DNA content in analytical samples, and electrochemical DNA sensors provided, for many years, just a tool to analyze the PCR products. The real challenges of DNA bioelectronics are, however, to develop ultrasensitive methods for the detection of DNA without the need to amplify the analyte by PCR, and with the target goal of detecting a single DNA molecule. Such procedures might circumvent the intrinsic disadvantages of PCR amplification and could introduce new dimensions into the area of DNA analysis. Significant advances in the amplified electrochemical analysis of DNA were accomplished in the past decade. The use of enzymes, NPs, liposomes, nanorods, or carbon nanotubes represent a few labels that altered the sensitivity regions for analyzing DNA. While a decade ago the electrochemical analysis of DNA concentrations corresponding to 10⁻⁸–10⁻⁹ M was a record, 10 years later the detection of DNA concentrations in the range of 10⁻¹⁷–10⁻¹⁹ M is feasible, through the use of amplification methods. Is it, however, possible to further develop the amplification methods and stretch them toward the detection of individual DNA molecules? The answer to this question is probably “NO”. This is not due to the lack of imagination to develop novel amplification routes, but because of the extremely slow hybridization rate of the analyte with the sensing interface at these low concentrations of the analyte, and because of the complexity of the resulting sensing systems. Thus, it seems that scientists will need to evolve new concepts to resolve these goals. In fact, recent advances in DNA chemistry indicate the existence of “seeds” for the new era of electrochemical DNA sensors. The synthesis of catalytic DNAs (DNAzymes) is now a common practice in DNA chemistry (Achenbach *et al.*, 2004). Specifically, DNAzymes that cleave other

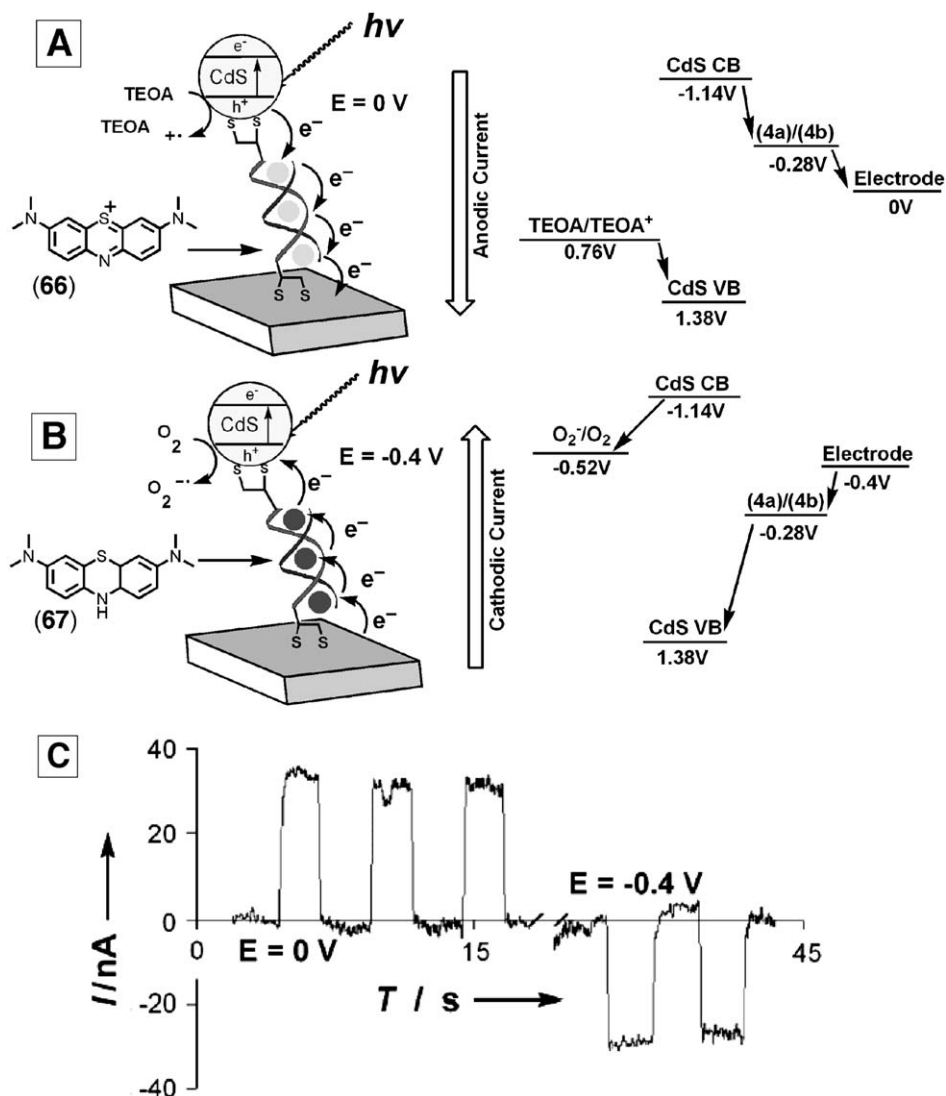


Fig. 34. Directionally electroswitchable photocurrents in the CdS NPs/ds-DNA/intercalator system. (A) enhanced cathodic photocurrent generation in the presence of the reduced methylene blue intercalator (**66**) (applied potential $E = -0.4\text{ V}$). (B) Enhanced anodic photocurrent generation in the presence of the oxidized methylene blue intercalator (**67**) (applied potential $E = 0\text{ V}$). The redox levels of the components participating in the different photocurrent-generating systems are presented on the right side of the scheme. (C) Electrochemically switched anodic and cathodic photocurrents generated in the CdS NPs/ds-DNA/**66/67** systems at 0 and -0.4 V , respectively, in the presence of TEOA, 20 mM and O_2 (under equilibrium with air). Photocurrents were generated upon irradiation of $\lambda = 420\text{ nm}$.

sequence-specific DNA segments are available. The design of DNA sequences that replicate their DNAzyme activities, as a result of an individual hybridization event with a target DNA has, thus, great promises in future DNA sensing. The integration of such DNA “replicating machines” with amplified electrochemical detection routes are then anticipated to provide the optimal sensitivities.

Another issue relating to the future applications of amplified electrochemical DNA sensing relates to the high throughput and parallel analysis of DNAs. While optical imaging of DNA hybridization on DNA arrays is already a viable technology, the parallel sensing of DNAs on electrode arrays is an emerging technology. The adaptation of the various amplification methods to these electrode arrays would definitely contribute to the successful application of bioelectronics in DNA analysis.

ACKNOWLEDGMENTS

Our research on amplified DNA biosensing was supported by the Israel Ministry of Science and The Horowitz Foundation, The Hebrew University of Jerusalem.

REFERENCES

- Achenbach, J.C., W. Chiuman, R.P.G. Cruz and Y. Li, 2004, DNAzymes: From creation *in vitro* to application *in vivo*, *Curr. Pharm. Biotechnol.* 5, 321–336.
- Albrecht, C., K. Blank, M. Lalic-Multhaler, S. Hirler, T. Mai, I. Gilbert, S. Schiffmann, T. Bayer, H. Clausen-Schaumann and H.E. Gaub, 2003, DNA: A programmable force sensor, *Science* 301, 367–370.
- Alfonta, L., A. Bardea, O. Khersonsky, E. Katz and I. Willner, 2001, Chronopotentiometry and Faradaic impedance spectroscopy as signal transduction methods for the biocatalytic precipitation of an insoluble product on electrode supports: Routes for enzyme sensors, immunosensors and DNA-sensors, *Biosens. Bioelectron.* 16, 675–687.
- Asai, Y., 2003, Theory of electric conductance of DNA molecule, *J. Phys. Chem. B* 107, 4647–4652.
- Auroux, P.A., Y. Koc, A. DeMello, A. Manz and P.J.R. Day, 2004, Miniaturised nucleic acid analysis, *Lab. Chip* 4, 534–546.
- Authier, L., C. Grossiord and P. Brossier, 2001, Gold nanoparticle-based quantitative electrochemical detection of amplified human cytomegalovirus DNA using disposable microband electrodes, *Anal. Chem.* 73, 4450–4456.
- Blasco, M.A., 2003, Mammalian telomeres and telomerase: Why they matter for cancer and aging, *Eur. J. Cell Biol.* 82, 441–446.
- Braun, E., Y. Eichen, S. Sivan and G. Ben-Yoseph, 1998, DNA-templated assembly and electrode attachment of a conducting silver wire, *Nature* 391, 775–778.
- Bruchez, M., Jr., M. Moronne, P. Gin, S. Weiss and A.P. Alivisatos, 1998, Semiconductor nanocrystals as fluorescent biological labels, *Science* 281, 2013–2015.
- Cai, H., N. Zhu, Y. Jiang, P. He and Y. Fang, 2003, Cu@Au alloy nanoparticle as oligonucleotides labels for electrochemical stripping detection of DNA hybridization, *Biosens. Bioelectron.* 18, 1311–1319.
- Cai, H., Y. Xu, N. Zhu, P. He and Y. Fang, 2002, An electrochemical DNA hybridization detection assay based on a silver nanoparticle label, *Analyst* 127, 803–809.

- Caruana, D.J. and A. Heller, 1999, Enzyme-amplified amperometric detection of hybridization and of a single base pair mutation in an 18-base oligonucleotide on a 7- μ m-diameter microelectrode, *J. Am. Chem. Soc.* 121, 769–774.
- Daniel, M.-C. and D. Astruc, 2004, Gold nanoparticles: Assembly, supramolecular chemistry, quantum-size-related properties, and applications toward biology, catalysis, and nanotechnology, *Chem. Rev.* 104, 293–346.
- De Lumley-Woodyear, T., C.N. Campbell and A. Heller, 1996, Direct enzyme-amplified electrical recognition of a 30-base model oligonucleotide, *J. Am. Chem. Soc.* 118, 5504–5505.
- Endres, R.G., D.L. Cox and R.R.P. Singh, 2004, Colloquium: The quest for high-conductance DNA, *Rev. Mod. Phys.* 76, 195–214.
- Epstein, J.R., I. Biran and D.R. Walt, 2002, Fluorescence-based nucleic acid detection and microarrays, *Anal. Chim. Acta* 469, 3–36.
- Erdem, A., K. Kerman, B. Meric, U.S. Akarca and M. Ozsoz, 1999, DNA electrochemical biosensor for the detection of short DNA sequences related to the hepatitis B virus, *Electroanalysis* 11, 586–588.
- Fan, C., K.W. Plaxco and A.J. Heeger, 2003, Electrochemical interrogation of conformational changes as a reagentless method for the sequence-specific detection of DNA, *Proc. Natl. Acad. Sci. USA* 100, 9134–9137.
- Fink, H.-W. and C. Schönberger, 1999, Electrical conduction through DNA molecules, *Nature* 398, 407–410.
- Fojta, M., 2002, Electrochemical sensors for DNA interactions and damage, *Electroanalysis* 14, 1449–1463.
- Frank, A.J., N. Kopidakis and J. van de Lagemaat, 2004, Electrons in nanostructured TiO₂ solar cells: Transport, recombination and photovoltaic properties, *Coord. Chem. Rev.* 248, 1165–1179.
- Fritz, J., M.K. Baller, H.P. Lang, H. Rothuizen, P. Vettiger, E. Meyer, H.-J. Güntherodt, C. Gerber and J.K. Gimzewski, 2000, Translating biomolecular recognition into nanomechanics, *Science* 288, 316–318.
- Fritzsche, W. and T.A. Taton, 2003, Metal nanoparticles as labels for heterogeneous, chip-based DNA detection, *Nanotechnology* 14, R63–R73.
- Gerion, D., W.J. Parak, S.C. Williams, D. Zanchet, C.M. Micheel and A.P. Alivisatos, 2002, Sorting fluorescent nanocrystals with DNA, *J. Am. Chem. Soc.* 124, 7070–7074.
- Gibbs, J.M., S.J. Park, D.R. Anderson, K.J. Watson, C.A. Mirkin and S.T. Nguyen, 2005, Polymer–DNA hybrids as electrochemical probes for the detection of DNA, *J. Am. Chem. Soc.* 127, 1170–1178.
- Giese, B., 2002, Long-distance electron transfer through DNA, *Annu. Rev. Biochem.* 71, 51–70.
- Gill, R., F. Patolsky, E. Katz and I. Willner, 2005, Electrochemical control of the photocurrent direction in intercalated DNA/CdS nanoparticle systems, *Angew. Chem. Int. Ed.* 44, 4554–4557.
- Gooding, J.J., 2002, Electrochemical DNA hybridization biosensors, *Electroanalysis* 14, 1149–1156.
- Häfeli, U., W. Schütt, J. Teller and M. Zborowski, Eds., 1997, *Scientific and Clinical Applications of Magnetic Carriers*, Plenum Press, New York.
- Hashimoto, K., K. Ito and Y. Ishimori, 1994, Sequence-specific gene detection with a gold electrode modified with DNA probes and an electrochemically active dye, *Anal. Chem.* 66, 3830–3833.
- Hirsch, R., E. Katz and I. Willner, 2000, Magneto-switchable bioelectrocatalysis, *J. Am. Chem. Soc.* 122, 12053–12054.
- Holmberg, R.C., M.T. Tierney, P.A. Ropp, E.E. Berg, M.W. Grinstaff and H.H. Thorp, 2003, Intramolecular electrocatalysis of 8-oxo-guanine oxidation: Secondary structure control of electron transfer in osmium-labeled oligonucleotides, *Inorg. Chem.* 42, 6379–6387.
- Ihara, T., Y. Chikaura, S. Tanaka and A. Jyo, 2002, Colorimetric SNP analysis using oligonucleotide-modified nanoparticles, *Chem. Commun.* 2152–2153.

- Immoos, C.E., S.J. Lee and M.W. Grinstaff, 2004a, DNA-PEG-DNA triblock macromolecules for reagentless DNA detection, *J. Am. Chem. Soc.* 126, 10814–10815.
- Immoos, C.E., S.J. Lee and M.W. Grinstaff, 2004b, Conformationally gated electrochemical gene detection, *Chem. Bio. Chem.* 5, 1100–1103.
- Jelen, F., A. Erdem and E. Palecek, 2002, Cyclic voltammetry of echinomycin and its interaction with double-stranded and single-stranded DNA adsorbed at the electrode, *Bioelectrochemistry* 55, 165–167.
- Kamat, P.V., 2002, Photoinduced transformations in semiconductor-metal nanocomposite assemblies, *Pure Appl. Chem.* 74, 1693–1706.
- Katz, E. and I. Willner, 2002, Magneto-stimulated hydrodynamic control of electrocatalytic and bioelectrocatalytic processes, *J. Am. Chem. Soc.* 124, 10290–10291.
- Katz, E. and I. Willner, 2003, Probing biomolecular interactions at conductive and semiconductive surfaces by impedance spectroscopy: Routes to impedimetric immunosensors, DNA-sensors, and enzyme biosensors, *Electroanalysis* 15, 913–947.
- Katz, E. and I. Willner, 2004, Integrated nanoparticle-biomolecule hybrid systems: Synthesis, properties and applications, *Angew. Chem. Int. Ed.* 43, 6042–6108.
- Katz, E. and I. Willner, 2005, Enhancement of bioelectrocatalytic processes by the rotation of mediator-functionalized magnetic particles on electrode surfaces: Comparison with a rotating disk electrode, *Electroanalysis* 17, 1616–1626.
- Katz, E., I. Willner and J. Wang, 2004, Electroanalytical and bioelectroanalytical systems based on metal and semiconductive nanoparticles, *Electroanalysis* 16, 19–44.
- Katz, E., L. Sheeney-Haj-Ichia, A.F. Bückmann and I. Willner, 2002a, Dual biosensing by magneto-controlled bioelectrocatalysis, *Angew. Chem. Int. Ed.* 41, 1343–1346.
- Katz, E., L. Sheeney-Haj-Ichia and I. Willner, 2002b, Magneto-switchable electrocatalytic and bioelectrocatalytic transformations, *Chem. Eur. J.* 8, 4138–4148.
- Kawde, A.-N. and J. Wang, 2004, Amplified electrical transduction of DNA hybridization based on polymeric beads loaded with multiple gold nanoparticle tags, *Electroanalysis* 16, 101–107.
- Kelley, S.O., E.M. Boon, J.K. Barton, N.M. Jackson and M.G. Hill, 1999, Single-base mismatch detection based on charge transduction through DNA, *Nucleic Acids Res.* 27, 4830–4837.
- Kelley, S.O. and J.K. Barton, 1999, Electron transfer between bases in double helical DNA, *Science* 283, 375–381.
- Kerman, K., M. Saito, Y. Morita, Y. Takamura, M. Ozsoz and E. Tamiya, 2004b, Electrochemical coding of single-nucleotide polymorphisms by monobase-modified gold nanoparticles, *Anal. Chem.* 76, 1877–1884.
- Kerman, K., Y. Morita, Y. Takamura, M. Ozsoz and E. Tamiya, 2004a, DNA-directed attachment of carbon nanotubes for enhanced label-free electrochemical detection of DNA hybridization, *Electroanalysis* 16, 1667–1672.
- Kobori, A., S. Horie, H. Suda, I. Saito and K. Nakatani, 2004, The SPR sensor detecting cytosine-cytosine mismatches, *J. Am. Chem. Soc.* 126, 557–562.
- Krautbauer, R., M. Rief and H.E. Gaub, 2003, Unzipping DNA oligomers, *Nano Lett.* 3, 493–496.
- Lagally, E.T. and R.A. Mathies, 2004, Integrated genetic analysis microsystems, *J. Phys. D* 37, R245–R261.
- Lioubashevski, O., F. Patolsky and I. Willner, 2001, Probing of DNA and single-base mismatches by chemical force microscopy using peptide nucleic acid-modified sensing tips and functionalized surfaces, *Langmuir* 17, 5134–5136.
- Liu, G., T.M.H. Lee and J. Wang, 2005, Nanocrystal-based bioelectronic coding of single nucleotide polymorphisms, *J. Am. Chem. Soc.* 127, 38–39.
- Martin, C.R., 1995, Template synthesis of electronically conductive polymer nanostructures, *Acc. Chem. Res.* 28, 61–68.
- Miao, W.J. and A.J. Bard, 2004, Electrogenerated chemiluminescence. 77. DNA hybridization detection at high amplification with $[\text{Ru}(\text{bpy})_3]^{2+}$ -containing microspheres, *Anal. Chem.* 76, 5379–5386.

- Mikkelsen, S.R., 1996, Electrochemical biosensors for DNA sequence detection, *Electroanalysis* 8, 15–19.
- Mirkin, C.A., R.L. Letsinger, R.C. Mucic and J.J. Storhoff, 1996, A DNA-based method for rationally assembling nanoparticles into macroscopic materials, *Nature* 382, 607–609.
- Mockler, T.C. and J.R. Ecker, 2005, Applications of DNA tiling arrays for whole-genome analysis, *Genomics* 85, 1–15.
- Möller, R., A. Csáki, J.M. Köhler and W. Fritsche, 2001, Electrical classification of the concentration of bioconjugated metal colloids after surface adsorption and silver enhancement, *Langmuir* 17, 5426–5430.
- Moreno-Hagelsieb, L., P.E. Lobert, R. Pampin, D. Bourgeois, J. Remacle and D. Flandre, 2004, Sensitive DNA electrical detection based on interdigitated Al/Al₂O₃ microelectrodes, *Sensors Actuators B* 98, 269–274.
- Nicolini, C., V. Erokhin, P. Facci, S. Guerzoni, A. Ross and P. Paschkevitch, 1997, Quartz balance DNA sensor, *Biosens. Bioelectron.* 12, 613–618.
- O'Neill, M.A. and J.K. Barton, 2004, DNA charge transport: Conformationally gated hopping through stacked domains, *J. Am. Chem. Soc.* 126, 11471–11483.
- Palecek, E. and F. Jelen, 2002, Electrochemistry of nucleic acids and development of DNA sensors, *Crit. Rev. Anal. Chem.* 32, 261–270.
- Pardo-Yissar, V., E. Katz, J. Wasserman and I. Willner, 2003, Acetylcholine esterase-labeled CdS nanoparticles on electrodes: Photoelectrochemical sensing of the enzyme inhibitors, *J. Am. Chem. Soc.* 125, 622–623.
- Park, S.-J., T.A. Taton and C.A. Mirkin, 2002, Array-based electrical detection of DNA with nanoparticle probes, *Science* 295, 1503–1506.
- Patolsky, F., A. Lichtenstein and I. Willner, 2000a, Amplified microgravimetric quartz-crystal-microbalance assay of DNA using oligonucleotide-functionalized liposomes or biotinylated liposomes, *J. Am. Chem. Soc.* 122, 418–419.
- Patolsky, F., K.T. Ranjit, A. Lichtenstein and I. Willner, 2000b, Dendritic amplification of DNA analysis by oligonucleotide-functionalized Au-nanoparticles, *Chem. Commun.* 1025–1026.
- Patolsky, F., A. Lichtenstein, M. Kotler and I. Willner, 2001a, Electronic transduction of polymerase or reverse transcriptase induced replication processes on surfaces: Highly sensitive and specific detection of viral genomes, *Angew. Chem. Int. Ed.* 40, 2261–2265.
- Patolsky, F., A. Lichtenstein and I. Willner, 2001b, Detection of single-base DNA mutations by enzyme-amplified electronic transduction, *Nat. Biotechnol.* 19, 253–257.
- Patolsky, F., A. Lichtenstein and I. Willner, 2001c, Electronic transduction of DNA sensing processes on surfaces: Amplification of DNA detection and analysis of single-base mismatches by tagged liposomes, *J. Am. Chem. Soc.* 123, 5194–5205.
- Patolsky, F., A. Lichtenstein and I. Willner, 2003b, Highly sensitive amplified electronic detection of DNA by biocatalyzed precipitation of an insoluble product onto electrodes, *Chem. Eur. J.* 9, 1137–1145.
- Patolsky, F., E. Katz, A. Bardea and I. Willner, 1999a, Enzyme-linked electrochemical sensing of oligonucleotide–DNA interactions by means of impedance spectroscopy, *Langmuir* 15, 3703–3706.
- Patolsky, F., E. Katz and I. Willner, 2002a, Amplified DNA detection by electrogenerated biochemiluminescence and by the catalyzed precipitation of an insoluble product on electrodes in the presence of the doxorubicin intercalator, *Angew. Chem. Int. Ed.* 41, 3398–3402.
- Patolsky, F., M. Zayats, E. Katz and I. Willner, 1999b, Precipitation of an insoluble product on enzyme-monolayer-electrodes for biosensor applications: Characterization by Faradaic impedance spectroscopy, cyclic voltammetry and microgravimetric quartz-crystal-microbalance analyses, *Anal. Chem.* 71, 3171–3180.
- Patolsky, F., R. Gill, Y. Weizmann, T. Mokari, U. Banin and I. Willner, 2003a, Lighting-up the dynamics of telomerization and DNA replication by CdSe–ZnS quantum dots, *J. Am. Chem. Soc.* 125, 13918–13919.

- Patolsky, F., Y. Weizmann, E. Katz and I. Willner, 2003c, Magnetically amplified DNA assays (MADA): Sensing of viral DNA and single base mismatches using nucleic acid-modified magnetic particles, *Angew. Chem. Int. Ed.* 42, 2372–2376.
- Patolsky, F., Y. Weizmann, E. Katz and I. Willner, 2004, Amplified telomerase analysis by using rotating magnetic particles: The rapid and sensitive detection of cancer cells, *Chem. Bio. Chem.* 5, 943–948.
- Patolsky, F., Y. Weizmann and I. Willner, 2002b, Redox-active nucleic-acid replica for the amplified bioelectrocatalytic detection of viral DNA, *J. Am. Chem. Soc.* 124, 770–772.
- Preston, R.J., 1997, Telomeres, telomerase and chromosome stability, *Radiat. Res.* 147, 529–534.
- Ratner, M., 1999, Electronic motion in DNA, *Nature* 397, 480–481.
- Sattin, B.D., A.E. Pelling and M.C. Goh, 2004, DNA base pair resolution by single molecule force spectroscopy, *Nucleic Acids Res.* 32, 4876–4883.
- Schultz, D.A., 2003, Plasmon resonant particles for biological detection, *Curr. Opin. Biotechnol.* 14, 13–22.
- Sheeney-Haj-Ichia, L., E. Katz, J. Wasserman and I. Willner, 2000, Magneto-switchable electrogenerated biochemiluminescence, *Chem. Commun.* 158–159.
- Shin, J.K., D.S. Kim, H.J. Park and G. Lim, 2004, Detection of DNA and protein molecules using an FET-type biosensor with gold as a gate metal, *Electroanalysis* 16, 1912–1918.
- Shipway, A.N., E. Katz and I. Willner, 2000, Nanoparticle arrays on surfaces for electronic, optical and sensoric applications, *Chem. Phys. Chem.* 1, 18–52.
- Storhoff, J.J., S.S. Marla, P. Bao, S. Hagenow, H. Mehta, A. Lucas, V. Garimella, T. Patno, W. Buckingham, W. Cork and U.R. Müller, 2004, Gold nanoparticle-based detection of genomic DNA targets on microarrays using a novel optical detection system, *Biosens. Bioelectron.* 19, 875–883.
- Storm, A.J., J. van Noort, S. de Vries and C. Dekker, 2001, Insulating behavior for DNA molecules between nanoelectrodes at the 100nm length scale, *Appl. Phys. Lett.* 79, 3881–3883.
- Takenaka, S., K. Yamashita, M. Takagi, Y. Uto and H. Kondo, 2000, DNA sensing on a DNA probe-modified electrode using ferrocenylnaphthalene diimide as the electrochemically active ligand, *Anal. Chem.* 72, 1334–1341.
- Taton, T.A., C.A. Mirkin and R.L. Lestinger, 2000, Scanometric DNA array detection with nanoparticle probes, *Science* 289, 1757–1760.
- Testorelli, C., 2003, Telomerase and cancer, *J. Exp. Clin. Cancer Res.* 22, 165–169.
- Uhlén, M., E. Hornes and O. Olsvik, Eds., 1994, *Advances in Biomagnetic Separation*, Eaton, Natick, 1994.
- Umek, R.M., S.W. Lin, J. Vielmetter, R.H. Terbrueggen, B. Irvine, C.J. Yu, J.F. Kayyem, H. Yowanto, G.F. Blackburn, D.H. Farkas and Y.-P. Chen, 2001, A versatile platform for molecular diagnostics, *J. Mol. Diagn.* 3, 74–84.
- Urban, M., R. Möller and W. Fritzsche, 2003, A paralleled readout system for an electrical DNA-hybridization assay based on a microstructured electrode array, *Rev. Sci. Instrum.* 74, 1077–1081.
- Vodinh, T., K. Houck and D.L. Stokes, 1994, Surface-enhanced Raman gene probes, *Anal. Chem.* 66, 3379–3383.
- Wang, J., D. Xu, A.-N. Kawde and R. Polsky, 2001b, Metal nanoparticle-based electrochemical stripping potentiometric detection of DNA hybridization, *Anal. Chem.* 73, 5576–5581.
- Wang, J., G. Liu and A. Merkoçi, 2003a, Electrochemical coding technology for simultaneous detection of multiple DNA targets, *J. Am. Chem. Soc.* 125, 3214–3215.
- Wang, J., G. Liu, M.R. Jan and Q. Zhu, 2003b, Electrochemical detection of DNA hybridization based on carbon-nanotubes loaded with CdS tags, *Electrochem. Commun.* 5, 1000–1004.
- Wang, J., G. Liu, R. Polsky and A. Merkoçi, 2002, Electrochemical stripping detection of DNA hybridization based on cadmium sulfide nanoparticle tags, *Electrochem. Commun.* 4, 722–726.

- Wang, J., G. Liu and Q. Zhu, 2003c, Indium microrod tags for electrochemical detection of DNA hybridization, *Anal. Chem.* 75, 6218–6222.
- Wang, J., R. Polsky, A. Merkoçi and K.L. Turner, 2003d, “Electroactive beads” for ultrasensitive DNA detection, *Langmuir* 19, 989–991.
- Wang, J., R. Polsky and D. Xu, 2001a, Silver-enhanced colloidal gold electrochemical stripping detection of DNA hybridization, *Langmuir* 17, 5739–5741.
- Wang, J., O. Rincón, R. Polsky and E. Dominguez, 2003e, Electrochemical detection of DNA hybridization based on DNA-templated assembly of silver cluster, *Electrochem. Commun.* 5, 83–86.
- Wang, J., G. Rivas, X. Cai, E. Palecek, P. Nielsen, H. Shiraishi, N. Dontha, D. Luo, C. Parrado, M. Chicharro, P.A.M. Farias, F.S. Valera, D.H. Grant, M. Ozsoz and M.N. Flair, 1997, DNA electrochemical biosensors for environmental monitoring, *Anal. Chim. Acta* 347, 1–8.
- Wang, R.H., S. Tombelli, M. Minunni, M.M. Spiriti and M. Mascini, 2004, Immobilisation of DNA probes for the development of SPR-based sensing, *Biosens. Bioelectron.* 20, 967–974.
- Weizmann, Y., F. Patolsky, E. Katz and I. Willner, 2003, Amplified DNA sensing and immunosensing by the rotation of functional magnetic particles, *J. Am. Chem. Soc.* 125, 3452–3454.
- Weizmann, Y., F. Patolsky, O. Lioubashevski and I. Willner, 2004, Magneto-mechanical detection of nucleic acids and telomerase activity in cancer cells, *J. Am. Chem. Soc.* 126, 1073–1080.
- Willner, I. and E. Katz, 2003, Magnetic control of electrocatalytic and bioelectrocatalytic processes, *Angew. Chem. Int. Ed.* 42, 4576–4588.
- Willner, I., F. Patolsky and J. Wasserman, 2001, Photoelectrochemistry with controlled DNA-cross-linked CdS nanoparticle arrays, *Angew. Chem. Int. Ed.* 40, 1861–1864.
- Willner, I., F. Patolsky, Y. Weizmann and B. Willner, 2002, Amplified detection of single-base mismatches in DNA using microgravimetric quartz-crystal-microbalance transduction, *Talanta* 56, 847–856.
- Wu, G., H. Ji, K. Hansen, T. Thundat, R. Datar, R. Cote, M.F. Hagan, A.K. Chakraborty and A. Majumdar, 2001, Origin of nanomechanical cantilever motion generated from biomolecular interactions, *Proc. Natl. Acad. Sci. USA* 98, 1560–1564.
- Xiao, Y., V. Pavlov, R. Gill, T. Bourenko and I. Willner, 2004b, Lighting up biochemiluminescence by the surface self-assembly of DNA-hemin complexes, *Chem. Bio. Chem.* 5, 374–379.
- Xiao, Y., V. Pavlov, S. Levine, T. Niazov, G. Markovitch and I. Willner, 2004a, Catalytic growth of Au nanoparticles by NAD(P)H cofactors: Optical sensors for NAD(P)⁺-dependent biocatalyzed transformations, *Angew. Chem. Int. Ed.* 43, 4519–4522.
- Xiao, Y., F. Patolsky, E. Katz, J.F. Hainfeld and I. Willner, 2003, ‘Plugging into enzymes’: Nanowiring of redox-enzymes by a gold nanoparticle, *Science* 299, 1877–1881.
- Xu, X.H. and A.J. Bard, 1995, Immobilization and hybridization of DNA on an aluminum(III) alkanebisphosphonate thin-film with electrogenerated chemiluminescent detection, *J. Am. Chem. Soc.* 117, 2627–2631.
- Xu, Y., H. Cai, P.-G. He and Y.-Z. Fang, 2004, Probing DNA hybridization by impedance measurement based on CdS–oligonucleotide nanoconjugates, *Electroanalysis* 16, 150–155.
- Zayats, M., R. Baron, I. Popov and I. Willner, 2005, Biocatalytic growth of Au nanoparticles: From mechanistic aspects to biosensors design, *Nano Lett.* 5, 21–25.
- Zhai, J.H., H. Cui and R.F. Yang, 1997, DNA based biosensors, *Biotechnol. Adv.* 15, 43–58.
- Zhou, X.C., S.J. O’Shea and S.F.Y. Li, 2000, Amplified microgravimetric gene sensor using Au nanoparticle modified oligonucleotides, *Chem. Commun.* 2000, 953–954.
- Zhu, N., A. Zhang, Q. Wang, P. He and Y. Fang, 2004, Lead sulfide nanoparticle as oligonucleotides labels for electrochemical stripping detection of DNA hybridization, *Electroanalysis* 16, 577–582.

Fully Electrical Microarrays

R. Hintsche^{1,2}, B. Elsholz¹, G. Piechotta¹, R. Woerl¹,
C.G.J. Schabmueller¹, J. Albers¹, V. Dharuman¹, E. Nebling¹,
A. Hanisch¹, L. Blohm², F. Hofmann³, B. Holzapfl³, A. Frey³,
C. Paulus³, M. Schienle³ and R. Thewes³

¹*Fraunhofer Institute for Silicon Technology ISIT, Biotechnical Microsystems, Itzehoe, Germany*

²*Biochip Systems GmbH, Itzehoe, Germany*

³*Infineon Technologies AG, Corporate Research, Munich, Germany*

Contents

1. Introduction	247
2. Principle and instrumentation of electrical detection	248
3. Low-density electrical DNA arrays	251
4. Integrated CMOS DNA arrays	256
4.1. Extended CMOS processing	257
4.2. Circuit design issues and system integration	260
5. Electrical label-free detection of DNA arrays	261
6. Electrical protein microarrays	264
7. Electrical hapten microarrays	267
List of abbreviations	271
References	272

1. INTRODUCTION

To further establish biochip technology in biochemistry and medical diagnosis, it will be necessary to provide accurate, practical, cost-effective systems and nevertheless portable devices for use in field applications and point of care diagnosis. The key principle of biochips is the detection and quantification of molecular complexes by affinity binding on transducers, arranged as arrays, which mainly use the evaluation of colorimetric or fluorescence signals (Sapsford *et al.*, 2004) or electrochemical methods (Palecek and Fojta, 2005). At present the acceptance of biochip technology for on-site use, e.g. diagnosis or environmental control is limited by rather expensive and complex instrumental systems. There is a need to provide reliable and cost-effective systems that can be operated with minimal training.

These criteria can be fulfilled by electrical biochip microarray systems, where semiconductor technology enables the construction of compact instruments with high integration at acceptable production costs. The advantage of fully electrical microarrays is the intrinsic high spatial resolution and direct

transduction of biochemical reactions into electrical responses without the common intermediate optical components. Here, the power of complementary metal oxide semiconductor (CMOS) technology can be used and enable the integration of electrochemical readout, data acquisition and data handling using the same common and cost-effective industrial technology. We have developed the so-called fully electronic biochip, where the CMOS electronics is in the silicon bulk of the same chip carrying a medium-density microarray with about 100–1000 positions at its surface. On the other hand a two chip solution has been realised, where the electrical microarray is designed as a disposable and the CMOS electronics is arranged in a second nondisposable application-specific integrated circuit (ASIC). This “two chip solution” is used for low-density electrical microarrays offering up to 32 positions.

The function of those fully electrical biochips is based on the readout of position-specific currents as a result of local electrochemical reactions of arrayed microelectrodes. On top of these electrodes different biomolecules are immobilised on those array positions and employed to recognise and capture their natural counterparts following the highly specific key/lock principle. At array positions with the resulting formation of so called affinity complexes an enzyme labelling, that creates electroactive species, are made and enable the electric transduction and quantification. All types of affinity complexes, such as nucleic acids, proteins and haptens, may be detected by the same type of electrical readout. Only common biochemical reactions, reagents and assay formats are used to perform this analyses.

In one case, the formation of double-stranded DNA (dsDNA) hybrids, the affinity complexing can be measured also label free using the same microarrays and applying electrical impedance spectroscopy.

In this chapter, we discuss the principles and several exemplary applications of silicon-based electrical microarrays, showing the power of this emerging technology.

2. PRINCIPLE AND INSTRUMENTATION OF ELECTRICAL DETECTION

The key feature of the fully electrical biochip technology is microarrays made in silicon technology. They carry several array positions with interdigitated electrodes (Aoki *et al.*, 1988; Niwa *et al.*, 1990) on its surface. The chips are fabricated using standard silicon manufacturing methods in industrial lines allowing a high-volume production and to minimise the cost per chip. The principles of this technical platform have been presented earlier (Wollenberger *et al.*, 1994; Paeschke *et al.*, 1996a; Hintsche *et al.*, 2000; Albers *et al.*, 2003).

An example of design and layout of such a transducer interface is presented in the scheme of a low-density chip shown in Figure 1. It depicts a microarray with 16 positions and magnified views onto a single position and onto the interdigitated electrode fingers. Each position of 0.5 mm diameter includes a large number of 800-nm-wide gold electrodes separated by 400-nm-wide gaps.

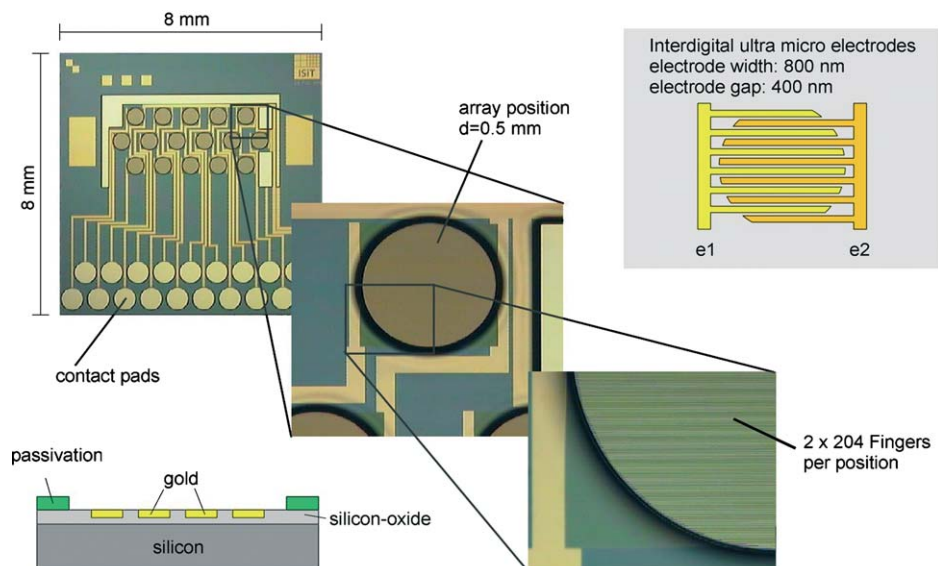


Fig. 1. Overview of the chip design and layout. Depicted diagonally are the silicon chip with magnified views of an assay position. Top right is a figure showing the dimensions and arrangement of the interdigitated gold electrodes. Bottom left shows a cross-section of the chip.

The so-called ultramicroelectrodes show an optimal hemispheric diffusion of the species to be detected towards the sensing electrode surface and thus increase the signal to noise ratio. Only electrode gaps below $1\ \mu\text{m}$ enable more than ten-fold amplification rates of the potentiometric readout as discussed below.

Using intrinsic properties of standard semiconductor materials and varied deposition and etching processes, the microarray surface is separated into hydrophilic array positions and hydrophobic interdistant areas. Such a hydrophilic array position, which is well situated to separate droplets with different reagents from the next one, is indicated as a 0.5 mm circle in the scheme below.

For loading the different affinity-binding molecules onto the microarray each of the array positions on the chip is separately topped with a droplet of capture solution using an automated piezodispensing device. Here minute amounts of liquid are shot out of a capillary by a piezo-electric crystal to form the droplets on the different positions. Image recognition is used for positioning and quality control.

The printed microarrays are mounted in disposable plastic cartridges with an internal flow cell ($6\ \mu\text{l}$ volume). This cartridge allows easy handling and integration into the portable device, which also carries reagents and waste containers.

The microarrays offer contact pads (Figure 1) for the proprietary easy electrical connection via mechanical contacts. This avoids the conventional wire bonding and hence the packaging of the microarrays is simplified.

The electrical readout is based on electrochemical detection of reversible redox molecules produced only at those microarray positions, where affinity binding was accomplished. The same transducing principles and identical biointerfaces have been applied to the medium-density fully electronic CMOS-microarrays and the low-density microarrays. The quantitative electrical detection is achieved by the sensitivity enhancing redox recycling of electrode active products of used label enzymes (e.g. β -galactosidase, alkaline phosphatase). The enzyme converts the electrochemical inactive substrate *p*-aminophenyl phosphate (*p*-APP) (Razumas *et al.*, 1980, Tang *et al.*, 1988) by hydrolysis into the electrochemical active form *p*-aminophenol (*p*-AP). The measurement is conducted at a potential of -50 and 350 mV against the reference electrode. The electric signal is enhanced by a factor of more than 10 through the recycling of the released *p*-AP between the anodic and cathodic interdigitated fingers, a process called redox recycling (Niwa *et al.*, 1990, 1993). The principle is shown in Figure 2.

The position-specific electric responses are measured as the initial slope of current generated at the respective electrode pairs of the microarray. The quantification of the targeted molecules is achieved by measuring a period of a few seconds and monitoring of the generated electrons in “stopped flow” mode.

For processing the assay formats and the multichannel electrical detection of nucleic acids, proteins and haptens, a modular fully automated measurement system has been developed. It is manufactured in industrial lines and available on the market. The main part is a microprocessor-controlled device, which includes the measurement electronics and a fluidic system. A special controller software and a user interface for noneducated operators has been developed. This configuration allows a comfortable and flexible control of processing the assay formats. The multichannel electrochemical readout as well as a powerful

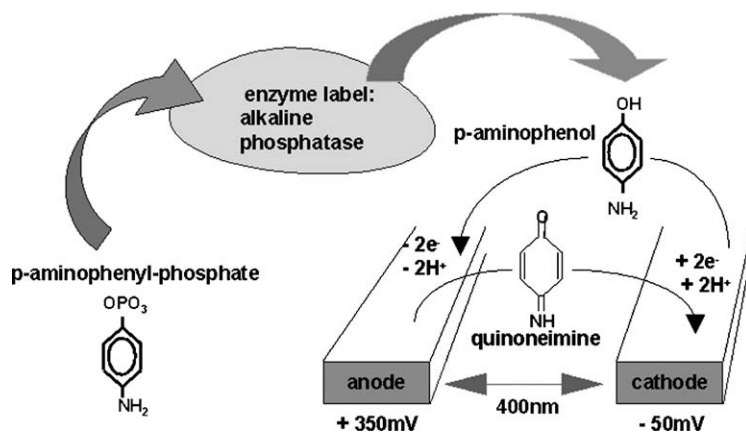


Fig. 2. Scheme of based redox recycling. The electrochemical inactive substrate *p*-APP is enzymatically hydrolysed by alkaline phosphatase into the electrochemical active *p*-AP, which is oxidised at the anode to quinoneimine. Subsequently, after diffusion to the cathode, quinoneimine can be reduced to *p*-AP again and start another cycle of the redoxreaction. Electrode dimensions and distances in the sub- μm range led to enhanced signal intensity.

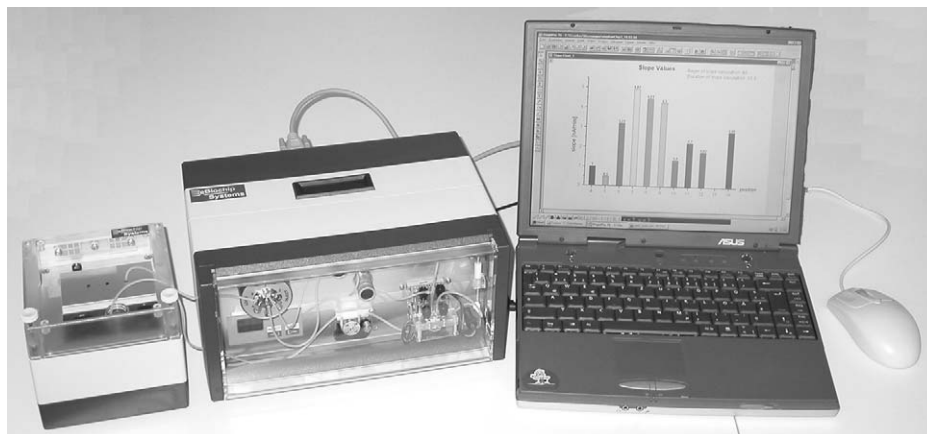


Fig. 3. Photograph of the measurement system setup. On the left, the reagent reservoir with a cooling system can be seen. The instrument in the centre includes the multipotentiostat, the fluidic system and the electrical biochip, on the right the data evaluation is visualised.

and easy to handle acquisition and evaluation of the measurement data has been combined with a comfortable data presentation at different levels of abstraction.

The portable instrument of 2.8 kg weight shown in [Figure 3](#) is able to handle up to seven different reagents. It offers free programmable steps of dosing, washing, reactions and wasting. The user may also select optimised programmes for hybridisation of nucleic acids, processing protein sandwich enzyme-linked immunosorbent assay (ELISA) or performing competitive ELISAs for haptens. In the whole run, the microarray and a separated flow chamber can be temperature controlled to realise optimal conditions and temperature profiling. The small box at the left of the figure is an optional refrigerator for sensitive reagents or sample storing.

The readout of all position-specific current responses requires approximately 10 s. The measurement data is transmitted to the graphing and data analysis software “ORIGIN”, which runs on a PC. Different types of graphs or diagrams can be chosen for visualisation and evaluation of the results.

3. LOW-DENSITY ELECTRICAL DNA ARRAYS

The idea of developing DNA microarrays originated in the late 1980s when techniques for decoding genes and later even whole genomes became more and more feasible. Sequencing by hybridisation on oligonucleotide microarrays was favoured as an alternative to establish sequencing methods. In common, DNA arrays are based on the fixation of oligonucleotides on a solid support and can be made by different techniques ([Southern *et al.*, 1992](#); [O’Donnell *et al.*, 1997](#); [Beier and Hoheisel, 1999](#); [Zammatteo *et al.*, 2000](#)). By hybridisation, the target DNA binds specifically to the corresponding capture sequence site ([Maskos and Southern, 1992](#)). Density is a key element for function and use of DNA arrays

and depending on the number of different capture sites, microarrays are therefore classified as low-density (Call *et al.*, 2001; Wang *et al.*, 2002; Lacroix *et al.*, 2002) or high-density arrays (up to 10^6 sites- cm^2) (Fodor *et al.*, 1991; Pease *et al.*, 1994; Lipshutz *et al.*, 1999). The main applications are genetic analysis by sequencing (Chee *et al.*, 1996; Wallraff *et al.*, 1997) and gene expression (Lockhart *et al.*, 1996; Wodicka *et al.*, 1997) or single nucleotide polymorphism (SNP) analysis (Gilles *et al.*, 1999; Hirschhorn *et al.*, 2000). The gained information leads to comprehensive and detailed understanding of gene functions and is of immense value in diagnostics, pharmacogenomics (Jain, 2000; Nees and Woodworth, 2002) and related fields. High-density microarrays are well commercialised (Rubenstein, 2003) today and a broadly applied tool for research in microbiology (Schena *et al.*, 1998; Graves, 1999; Blohm and Guiseppi-Elie, 2001; Ochs and Godwin, 2003). Caused by the extremely small feature size on such arrays, most methods are based on high resolution, optical detection with sophisticated, but cost-intensive instrumentation. Manufacturing of high-density arrays is linked with high technical and financial requirements, justified in the above mentioned applications with high information density or high sample throughput.

Low-density arrays are established, where lower costs and flexibility are needed and where the number of samples and their complexity is limited. Research on biosensors, combined with DNA array technology, is developing tools for Point of Care diagnostic, for health care and for agricultural and environmental monitoring (Wang, 2000). Integrated in fully automated biosensing systems (Yang *et al.*, 2002; Liu *et al.*, 2004) a fast, accurate and sensible analysis of harmful microorganisms also in the “field” gets possible with portable devices. The rapid detection and identification of biological agents in the environment is still a challenging task, but for the driving force for the development of use in the military sector and homeland security.

The first electrochemical DNA biosensor, based on hybridisation, had been developed in 1993 by Millan and Mikkelsen (Millan and Mikkelsen, 1993), and today many applications for similar gene sensors exist (Gooding, 2002; Kerman *et al.*, 2004). Some of them use electrochemical impedance spectroscopy (EIS, for details see Chapter 5), others the doublestrand-specific recognition and detection with intercalators (Takenaka *et al.*, 2000; Maruyama *et al.*, 2002; Ruba *et al.*, 2004). Electrochemical biosensors that approach have the advantage of being cost-effective, robust and particle tolerant, compared to optical systems. They allow less purification and sample preparation efforts and require simpler assay protocols. There are already a few examples where the combination of electrochemical detection and low-density microarrays for DNA analysis has been commercialised (Feng and Nerenberg, 1999).

The technical platform, described here, offers optimal features for fully electrical DNA-microarrays with up to 16 positions, freely designed for the particular application. The ultramicroelectrode gold surface, allows a coupling method with alkanethiol modified capture oligonucleotide sequences and leads to a highly specific biointerface for target recognition. Spontaneously, the thiol groups of the captures are forming polarised covalent bonds between sulfur and gold. The generated self-assembled monolayer (SAM) (Herne and Tarlov, 1997; Steel *et al.*, 2000; Gooding *et al.*, 2003a) is additionally stabilised by van der

Waals interaction of the neighbouring methylene functions. The length of capture sequences is typically in the range between 20 and 40 nucleotides. After the position-specific immobilisation from aqueous oligonucleotide solutions, single-stranded target DNAs are hybridised to the complementary array position. A biotin label on the target structure enables the later coupling of enzyme conjugates, such as ExtrAvidin[®] alkaline phosphatase. The electrical readout is performed as described in Chapter 2.

The diagnosis of pathogens (Olive and Bean, 1999; Anthony *et al.*, 2000; Westin *et al.*, 2001) is an application for low-density electrical microarrays, where low detection limits are decreed by federal regulations. To achieve these limits additional DNA amplification by polymerase chain reaction (PCR) (Mullis and Faloona, 1987; Anderson *et al.*, 2000; Liu *et al.*, 2004) is usually required. An array for the parallel identification of multiple target DNAs from Epstein–Barr virus (EBV), cytomegalovirus (CMV) and herpes simplex virus (HSV) was recently developed (Nebling *et al.*, 2004). The experiments were designed for viral DNA detection after PCR amplification with a universal primer pair, targeting gene variants, encoding for DNA polymerase in all three viruses. Although the sequence of the variants is highly conserved in the region where the PCR primer pair binds, there are still sections, that are characteristic for a certain virus type. These sections are used to design the individual capture sequence for the corresponding herpes virus.

In order to have internal standards on the microarray, a biotinylated oligonucleotide was immobilised as a positive control in one position, whereas another array position was used as a negative control with a capture DNA sequence, not binding to the targets. The activity of the surface attached enzyme conjugate was first determined to estimate the density of immobilised capture oligonucleotides and the hybridisation efficiency. For the calculation it was assumed that the “current signal slope” is proportional to the surface density of capture oligonucleotides. The accessibility of the electrode surface was tested in measurements with redox-recycling with *p*-AP. The number of capture oligonucleotides was $235,000 \mu\text{m}^{-2}$ molecules. The value is in a range well according to the maximum oligonucleotide density of $300,000 \text{ molecules } \mu\text{m}^{-2}$ (Steel *et al.*, 2000). After hybridisation the target density was determined to $132,000 \text{ molecules } \mu\text{m}^{-2}$, which is equivalent to a hybridisation efficiency of 56% (Nebling *et al.*, 2004). In a practical example for the application, viral DNA was amplified via PCR from a clinical blood sample. The 588 bp PCR product was specifically detected on the microarray only at the CMV capture positions and clearly identified as the CMV-amplicon. The scheme, how the PCR product hybridises to the capture sequence, forming a 30 bp duplex with a short and a long overhang, is shown in Figure 4.

After denaturation the hybridisation of PCR products is hindered by re-annealing with the second strand. The capture oligonucleotide is in competition for the target sequence. In addition, the sterical demand on the surface is high and the diffusion rate is low. Still, the right hybridisation conditions enable the generation of a strong current signal, corresponding to a relative hybridisation rate of 50% ($60,000 \text{ molecules } \mu\text{m}^{-2}$ for 588 nt) compared to that for short synthetic targets (30 nt). This example for the PCR-based identification of

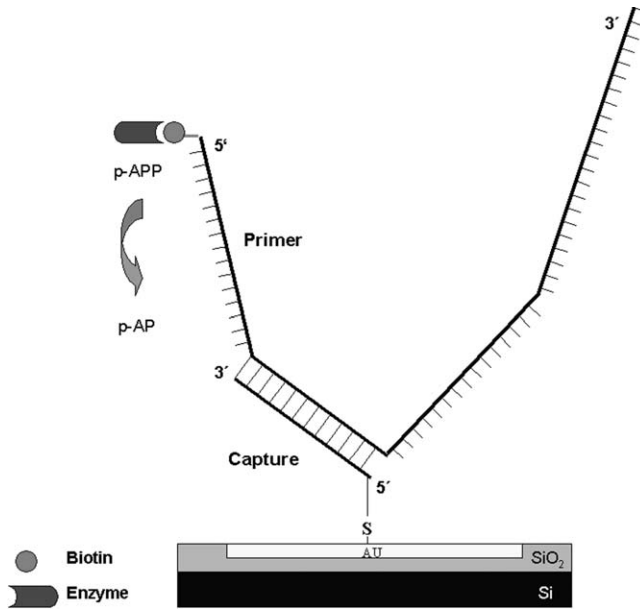


Fig. 4. Scheme of PCR product based detection. The biotin label is introduced through the PCR primer of the target strand. Usually the primer sequences in the hybridisation scheme are designed in a way that the biotin label and therefore also the enzyme conjugate is positioned in close proximity to the surface.

different virus types, thus demonstrates the required sensitivity and selectivity for broader use in DNA analysis.

Using 16S Ribosomal RNA (rRNA) as the target instead of genomic DNA is an alternative way to identify bacteria on electrical microarrays. Urinary tract infections (Warren, 1996) are a good example and of commercial interest, because bacteria tests from infected patient are the most frequent microbiological test. The infections are characterised by a high bacteria concentration of 10^4 – 10^6 cells mL⁻¹ in the patient's urine. As a model for the identification of the involved pathogens we designed a low-density microarray with electrochemical detection, targeting the 16S rRNA of typical members of the involved bacteria classes. The array enables the detection of *Escherichia coli* from the class of Enterobacteriaceae, of *Enterococcus faecalis*, representing the only Enterococcus species and of *Staphylococcus aureus* and *epidermidis*. The two *Staphylococcus* species must be differentiated, because *Staphylococcus epidermidis* is also found in healthy patients. rRNA is present in high copy numbers in cells (500–70,000 copies/cell), depending on the growth period and the respective microorganism. Together with the above-mentioned strong occurrence of bacteria in urinal tract infections, assays can be designed, avoiding time and labour-intensive amplification steps, like PCR.

The sequence information in rRNA is highly conserved throughout evolution. Still, microorganisms can be identified by the 16S rRNA on nucleic acid microarrays (Chandler *et al.*, 2003; Peplies *et al.*, 2004), if several factors are

adjusted to each other. The regions targeted by the capture sequences must show enough diversification, in order to distinguish between different species. The flanking regions should be highly conserved to allow universal helper oligonucleotides to be used. They are needed to break up secondary structures to improve duplex formation in the later hybridisation with the capture sequence (Fuchs *et al.*, 2000; Barken *et al.*, 2004). Biotinylated detector oligonucleotides as a third type, enable the conjugation with the ExtrAvidin[®] enzyme complex. The intact RNA molecule consists of roughly 1500 nt, with the above mentioned drawbacks for effective hybridisation. To increase the hybridisation efficiency it is advantageous to cleave the 16S rRNA (Small *et al.*, 2001), with our method, statistically into average fragments of approximately 150 nt. In this case, the detection oligonucleotide has to be selected to bind close to the capture region. In general the fragmented target RNA is coupled to the electrode surface by the capture sequence, followed by “sandwich hybridisation” (Wicks *et al.*, 1998; Rautio *et al.*, 2003) with the biotinylated detection oligonucleotide (Figure 5).

The observed detection limit of the method was shown to be approx. 10^4 cells mL⁻¹ with a total assay time of 1.5 h. This covers the required bacteria concentration for urinal tract infections. In a series of experiments, the identification of all four different bacteria species was accomplished. In summary, we developed a 16S rRNA microarray-based technique with electrochemical

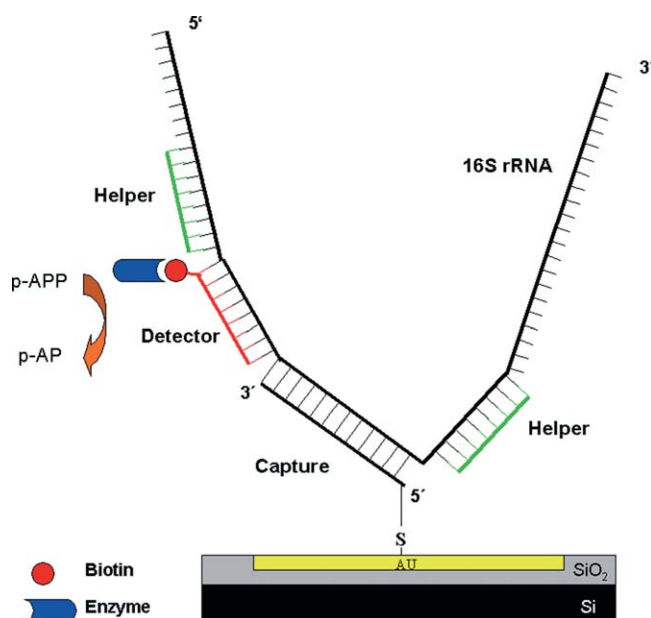


Fig. 5. Scheme of the 16S rRNA-based detection. Flanking the capture and detector region, helper oligonucleotides are used to increase the accessibility by breaking up secondary structures. The detector region is also chosen to be near the surface.

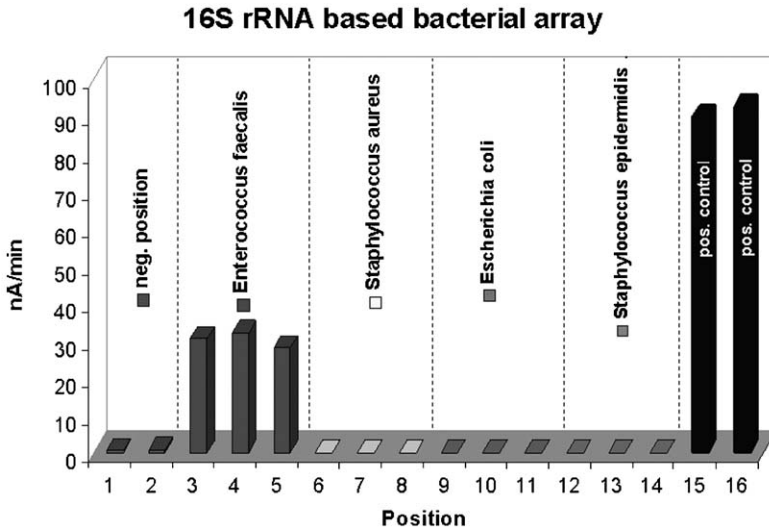


Fig. 6. 16S rRNA-based bacterial array. The sample contained *Enterococcus faecalis* RNA.

detection, that requires no amplification step and still gives enough sensitivity and selectivity for identification of different pathogen bacteria (Figure 6).

4. INTEGRATED CMOS DNA ARRAYS

The chips considered so far consist of a passivated silicon substrate material and of the sensor elements at their surface as described above in this chapter. This approach is reasonable and cost-effective as long as only a relatively low number of sites per chip is required so that the amount of interconnects to an external read-out apparatus is not too high. With increasing number of test sites per chip, however, an interconnect problem occurs. The increasing number of interconnects needed to contact all sensor sites translates into a decreasing area per contact pad on-chip and into a decreasing available area for each sensor so that the signal currents also decrease. Lowered interconnect reliability at decreasing signal strengths eventually result in a severe loss of signal integrity, reliability and yield.

Active chips, i.e., chips with active on-chip circuitry, allow to amplify and process the weak sensor signals on-chip (i.e., in a close neighbourhood to the sensor) and to operate such chips with a low number of contact pads independent of the numbers of test sites per chip. Such active chips manufactured on the basis of a specifically extended Complementary-Metal-Oxide-Semiconductor (CMOS) process are presented in the following section.

Note that application of such chips is not only driven by the fact, that in the case of a higher number of test sites per chip a technical show-stopper occurs. Although the *costs per chip* are increasing for CMOS-based chips, the *costs per data point* decrease at increasing numbers of test sites per chip. Consequently,

active CMOS-based sensor array chips represent a technically and economically attractive solution for medium- and high-density chips.

4.1. Extended CMOS processing

In Figure 7 (left), a simplified schematic cross-section of a standard CMOS process is depicted showing the most important layers and materials. Processing of extra materials, such as gold as in our case, directly within a CMOS production line is usually impossible, since such materials may cause contamination problems, which significantly lower the performance and yield of the fabricated integrated circuits.

For that reason, the concept of CMOS post-processing is preferred (Figure 7, right). This concept has been used to fabricate the CMOS chips shown in Figure 8, starting with an 8 × 4 array with fully analog sensor site circuitry and a 30 pad broad electrical interface (2001), to a customer-oriented 16 × 8 array with in-sensor site analog-to-digital conversion and 6 pad pure digital electronic interface (2004) (Sze, 1981; Hofmann *et al.*, 2002; Thewes *et al.*, 2002, 2004a, b; Schienle *et al.*, 2004).

Therefore, the basic CMOS technology used is a 5 V, 6'' *n*-well process specifically optimised for analog applications (high-ohmic poly-silicon resistors, poly-poly-capacitors) with a minimum gate length of 0.5 μm and an oxide thickness of 15 nm. After standard CMOS processing, a Ti/Pt/Au stack with layer thicknesses of 50 nm, 50 nm and 300–500 nm, respectively, is evaporated (Hofmann *et al.*, 2002). The gold electrodes are structured in a lift-off process. For the contact pads we also use the gold metallisation. Figure 9 shows a tilted scanning electron microscope (SEM) cross-section of a fully processed chip with metal oxide semiconductor (MOS) transistors, two aluminium metal layers from the CMOS process and sensor finger electrodes. Note that the nitride layer on top of the sensor electrodes is only used for preparation purposes.

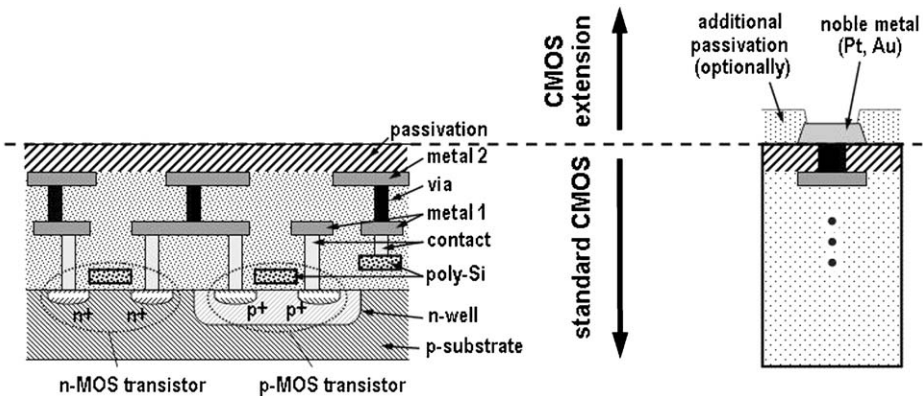


Fig. 7. Simplified schematic cross-section of a standard CMOS process (left) and required process extension to provide Au sensor electrodes (right).

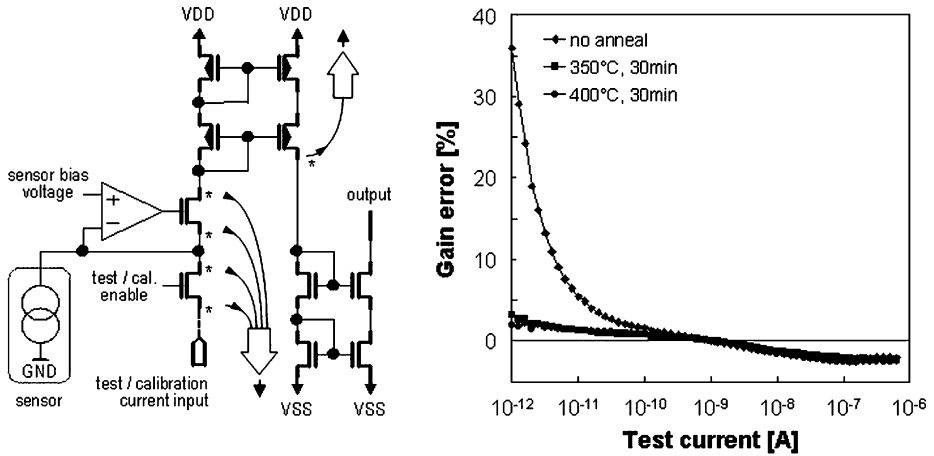


Fig. 10. Left: simplified schematic diagram of a sensor site test circuit designed to control the bias voltage of the sensor electrode and to amplify the sensor current by a factor of $10 \times 10 = 100$ (generator branch), specified range = 1 pA–100 nA. Right: current gain error of the circuit as a function of the input test current normalised to the gain at test current = 1 nA for different annealing options after gold processing.

regulation loop to control the bias voltage of the (generator) electrode. The electrode current is recorded and amplified by a factor of approximately 100 using two cascode current mirrors in series. A complementary circuit is used for the collector branch, too, but for simplicity here we consider the generator branch only. The circuit can be electrically characterised using a test/calibration input (Hofmann *et al.*, 2002; Thewes *et al.*, 2004a).

Figure 10 (right) shows the measured gain as a function of the input current (average value of all test sites from a 16×8 array test chip). Data are shown with and without additional annealing steps after the gold process module is performed. If no annealing step is applied, a severe deviation of the gain is obtained for input currents below 10 pA. This effect coincides with an increase of the transistor interface state density (Sze, 1981). Whereas reasonable densities are of the order 10^{10} cm^{-2} , here values above $2 \times 10^{11} \text{ cm}^{-2}$ are obtained, which lead to leakage currents at the circuit nodes labelled by asterisks in Figure 10 (Hofmann *et al.*, 2002; Thewes *et al.*, 2004a). Thus, a degradation of the transfer characteristics for low current occurs.

Application of forming gas annealing steps (N_2, H_2 at $400^\circ\text{C}/350^\circ\text{C}$, 30 min.) after gold processing significantly reduces the interface state density again and leads to reasonable transfer characteristics. However, in addition to the CMOS process front-end parameters considered so far in this context, the characteristics of the gold electrodes with and without annealing must be investigated. Measured resistance data of gold and aluminium lines, and of the related via connections are given in Table 1. The data without annealing step and with annealing at 350°C are similar for all parameters. At 400°C , however, a 1.2-fold increase of the gold resistance occurs. SEM photos reveal that this increase

Table 1. Square resistances of gold and aluminium 2 lines, resistance of the related via connections and transistor interface state densities without and with annealing steps at different temperatures after Au processing. Crucial values are emphasised by a light grey background

	Square resistance Au lines ($\text{m}\Omega\Box^{-1}$)	Resistance via holes (Al to Au) ($\text{m}\Omega$)	Square resistance Al 2 lines ($\text{m}\Omega\Box^{-1}$)	Interface state density (cm^{-2})
CMOS only (i.e. without Au process)	—	—	—	$\sim 10^{10}$
CMOS + Au process, no anneal	48	370	79	$\sim 2 \times 10^{11}$
CMOS + Au process, N_2/H_2 anneal with 350°C, 30 min	51	360	76	$< 10^{10}$
CMOS + Au process, N_2/H_2 anneal with 400°C, 30 min	61	340	74	$< 2 \times 10^9$

coincides with a rearrangement of grains and deformations within the gold layer, moreover, a change of the electrochemical behaviour is found. Consequently, annealing at 350°C provides us with a process window where both device and electrode properties are optimised (Hofmann *et al.*, 2002).

4.2. Circuit design issues and system integration

Besides reliable and cost-effective packaging and a user-friendly read-out apparatus including software, full system integration also requires to develop a chip with comprehensive electronic functionality on-chip and a pure digital electronic interface with a low number of interconnect pads independent of the number of test sites on the chip, to allow robust and user-friendly application. A chip with a design, which fulfils these criteria is shown in Figure 8 (left) (Thewes *et al.*, 2004a). In the periphery, the chip e.g. provides bandgap references, D/A-converters to provide the required voltages for electrochemical operation on-chip, and a serial digital, six pad electronic interface; circuitry of the array in the centre of the chip utilises analog-to-digital signal conversion realised within each sensor site (Schienle *et al.*, 2004). The related concept is briefly discussed in the following. It provides an (electronic) dynamic range > five decades (circuit operation is specified for a sensor current range from 10^{-12} A to 10^{-7} A) and allows to sample the data from all sites simultaneously.

As shown in Figure 11, the voltage of the sensor electrode is controlled by a regulation loop via an operational amplifier and a source follower transistor.

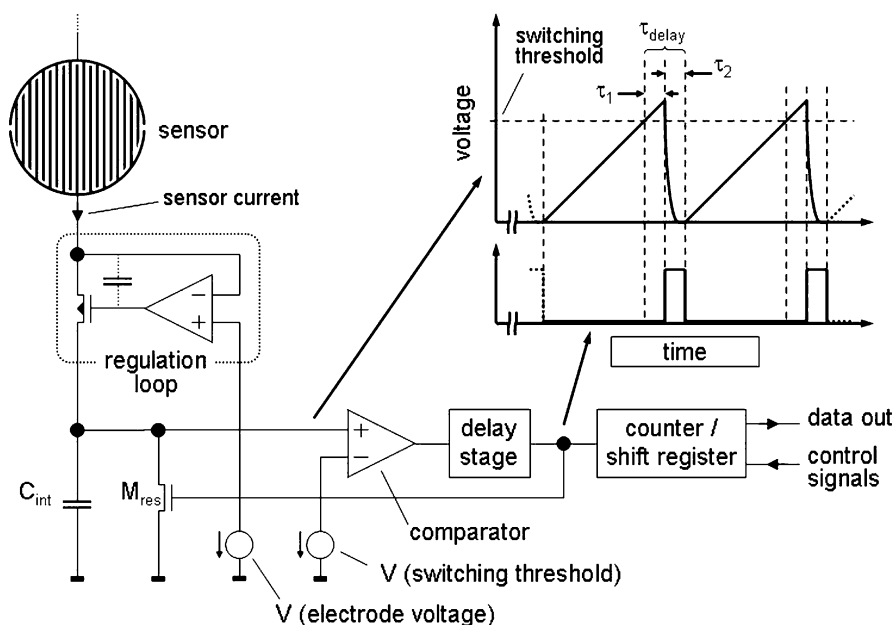


Fig. 11. Schematic circuit principle used for in-sensor site A/D-conversion based on current-to-frequency conversion.

Analog-to-digital conversion is achieved by first translating the sensor current into frequency. An integrating capacitor (C_{int}) is charged by the sensor current until a predefined switching level is reached, which is monitored by a comparator stage. When the value of that level is exceeded, the circuit generates a reset pulse and the capacitor is discharged (transistor M_{res}) again, so that a sawtooth-like voltage at the integrating capacitor generator is obtained. The delay stage at the output of the comparator is operated as a pulse shaping unit to ensure a sufficient length of the reset pulse and thus a complete discharge of the integrating capacitor in the reset phase. Finally, the number of reset pulses within a given time frame is counted with a 24-stage, in-sensor-site digital counter. During sensor site read-out operation, the counter is converted into a shift register by a control signal and the digital data are provided to the output serially. An in-depth discussion of that circuit is given elsewhere (Schienle *et al.*, 2004).

5. ELECTRICAL LABEL-FREE DETECTION OF DNA ARRAYS

The electrical DNA microarray (Nebling *et al.*, 2004) described above require enzymatic labelling. Eliminating the need for labels has the advantage of simplifying the electrical readout, of reducing the cost per analysis, of increasing the speed of the method and of allowing the design of compact, portable detection systems. In the field of DNA array sensors, label-free detection was achieved by monitoring the change in conductance or resistance and capacitance of the

transducer. Capacitive- or impedimetric-based DNA sensors have been constructed by immobilising capture DNA onto the electrode surface. Through target hybridisation a change in the capacitance or the resistance could be induced. The applications of capacitive (Berggren *et al.*, 2001) and impedance methods (Katz and Willner, 2003; Guan *et al.*, 2004) in monitoring various biomolecular interactions including DNA are reviewed.

Interdigitated electrode arrays (IDAs) have received greater attention in the field of impedimetric biosensing (Ehret *et al.*, 1997; Saum *et al.*, 1998; Van Gerwen *et al.*, 1998; Laureyn *et al.*, 2000). The first label-free impedance sensor for studying avidin–ferritin molecular interaction was described (Paeschke *et al.*, 1996b). Studies describing DNA molecular interactions (Jacobs, 1998) followed. These studies suggest that the electrical field between the IDA electrodes increases proportionally with an applied potential, when the interelectrode distance is reduced (Montelius *et al.*, 1995) and enhance the analytical sensitivity (Jacobs *et al.*, 1995; Paeschke *et al.*, 1996a). Nanoscale Pd-IDA (Van Gerwen *et al.*, 1998) and Ti-IDA (Laureyn *et al.*, 2000) electrodes in different dimensions (500 nm electrode width/500 nm spacing down to 250 nm electrode width/200 nm spacing) are fabricated on silicon and the binding of glucose oxidase (GOX) with proteins and DNA have been investigated. The complexing was generally confirmed by decreased capacitance. On Pt-IDAs fabricated on borosilicate glass substrates (Gheorghe and Elie, 2003; Hang and Elie, 2004) an 11% increase in impedance has been found due to DNA hybridisation. A conducting polypyrrole integrated IDA surface has been reported for the label-free detection of avidin or antibodies with the luteinising hormone (Lillie *et al.*, 2001) and for discriminating double-stranded DNA (dsDNA) from single-stranded DNA (ssDNA) layers (Frace *et al.*, 2002). The binding of the target was identified again by a decrease in impedance.

In our group, the direct detection of DNA hybridisation on miniaturised Au-IDA electrodes embedded in SiO₂ has been investigated since 1993 employing the two-electrode impedance technique. The same type of IDA microarrays as described in Chapter 2 have been used with the electrode dimensions of 1 μm width, 800 nm gap and a length of 1 mm.

The last series of experiments to be published (Dharuman *et al.*, 2004) used a capture DNA layer on Au electrode surfaces, which was made with a self-assembling thiol-modified 27 mer oligonucleotide. The presence of the ssDNA layer was sensitively indicated by an increase of the impedance in the low-frequency region compared to the impedance of the bare electrode, shown in the Niquist plot in Figure 12A. The increase at lower frequencies should be related to the effective overlapping of diffusion layers arising from layer defects of thiol self-assemblies (Sabatani and Rubinstein, 1987; Finklea *et al.*, 1993; Diao *et al.*, 2001) as well as microelectrode edge effects of IDA structures (Stulik *et al.*, 2000).

We have concluded from these findings, that these two effects may create higher negative fields and repulsion to charge transfer reaction. Therefore, the redox couple Fe(CN)₆^{2-/-3-} has been used in order to expand the impedance changes due to nucleic acid hybridisation in the IDAs covering layer (Figure 12A, curves a and b). This clearly demonstrates that the presence of the redox couple enhances the measuring effect.

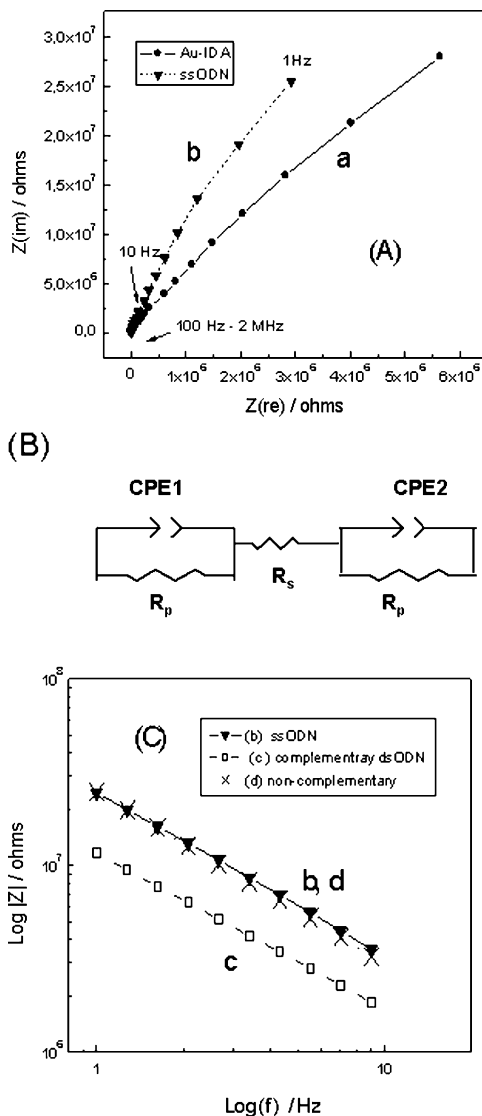


Fig. 12. (A) Nyquist impedance behaviour of a bare Au-IDA (curve a) and ssDNA capture layer (curve b) measured in presence of $10 \mu\text{M}$ $\text{K}_3\text{Fe}(\text{CN})_6$ in phosphate buffer of pH 7.4. (B) Equivalent circuit for IDA. CPE, constant phase element; R_p , polarisation resistance; R_s , solution resistance. (C) Comparative Bode impedance behaviour of ssDNA covered Au-IDA before (curve b) and after (curve c) hybridisation. Curve d represents the impedance behaviour of control after hybridisation.

The equivalent circuit that fits this experimental data is shown in [Figure 12B](#). The double layer capacitance is represented by the constant phase element. The impedance measurements before and after hybridisation revealed a decrease of approximately 50% for the formed double strand ([Figure 12C](#), curves b and c), while no difference for non-complementary target was observed ([Figure 12C](#),

curve d). The decreased impedance after hybridisation is attributed to the increase in negative charge density in the DNA layer and its consequent effect on the electrical field lines at IDA structures (Van Gerwen *et al.*, 1998) and ion-gating effect (Gooding *et al.*, 2003b).

The frequency-dependent impedance method shown above is time consuming and difficult to perform in the low-frequency region due to intervening diffusion effects. These could be overcome with transient impedance techniques such as the charge injection (Mikkelsen and Purdy, 1985). This avoids any frequency scanning and allows measuring times of microseconds. Additionally, simple and fast multiplexing may be adapted to the electrical microarrays. The method involves a rapid perturbation of the interfacial equilibrium with a quantum of charge pulse causing a potential change, equivalent to the double layer capacitance of the working electrode. The relaxation of the open circuit potential is observed as a function of time. The perturbation period is very short, typically several milliseconds, which eliminates the ohmic contribution and perturbation effects on diffusional layers.

A successful application of this technique to detect DNA hybridisation on 8 positions of the electrical microarrays described in the chapters above was recently shown. A modified microarray with eight different positions has been used. Each position with a diameter of 900 μm includes a large number of 800-nm wide gold electrodes separated by 400 nm wide gaps. Two different synthetic oligonucleotide sequences (27 mer) as a model system were immobilised on the array positions on the chip.

The potential relaxation process at the respective positions are depicted in Figures 13A and B. Again the redox mediator $\text{K}_3\text{Fe}(\text{CN})_6$ in phosphate buffer solution was used. It caused significant differences due to hybridisation of layers on IDAs as shown in Figures 13A and B. In these figures, curves a and b are representing the relaxation behaviour of DNA before and after hybridisation in presence of $\text{K}_3\text{Fe}(\text{CN})_6$.

The results of both label-free impedance methods applied to the DNA microarrays are promising and further research is now focusing on new applications. These applications require still some efforts to create well-defined homogeneous biointerfaces, for highly reproducible target binding. The technique is well suitable for integration with microfluidics and electronics in one complete, compact system.

6. ELECTRICAL PROTEIN MICROARRAYS

The transfer of classical ELISA formats on biochips offers a great potential for automation, sensitivity increase, portability, time saving and flexibility of protein detection for various applications.

Especially in the field of food analysis, medical research and diagnosis, and biological warfare detection, several approaches and development levels of protein biosensors have been realised (Askari *et al.*, 2001; Rowe Taitt *et al.*, 2002; Delehanty and Ligler, 2002; Liu *et al.*, 2003; Dupont *et al.*, 2004). Independent of the way of signal readout (optically or electrochemically), the

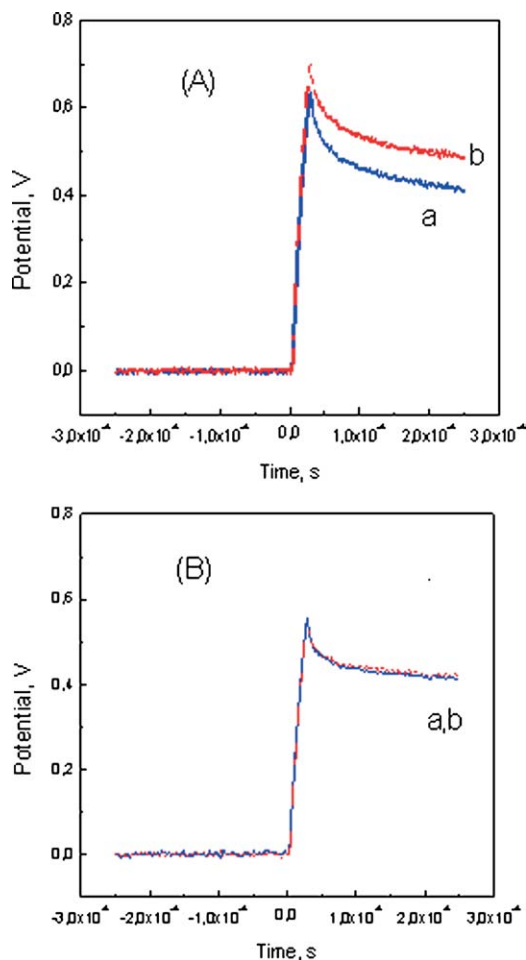


Fig. 13. (A) Relaxation curves of double-layer potential (curve a: single-stranded capture layer) (curve b: double-layer after hybridisation) in the presence of $5 \mu\text{M}$ $\text{K}_3\text{Fe}(\text{CN})_6$ in phosphate buffer (pH 7.4). (B) Relaxation of double-layer potential with time observed in non-hybridising (non-complementary) control experiments.

platform for biosensor detection is a glass or silicon substrate on which the biochemical, ELISA analogous reactions take place. In the case of proteins, these are commonly sandwich ELISA formats.

In our group an automated electrochemical protein detection device has been developed. It is based on low-density microarrays with 16 positions of $500 \mu\text{m}$ diameter (Figure 1).

The assay principle of the protein microarray is schematically depicted in Figure 14. The assay steps include:

- Immobilisation of capture antibodies on gold electrode surface;
- binding of target protein;
- binding of detection antibody;

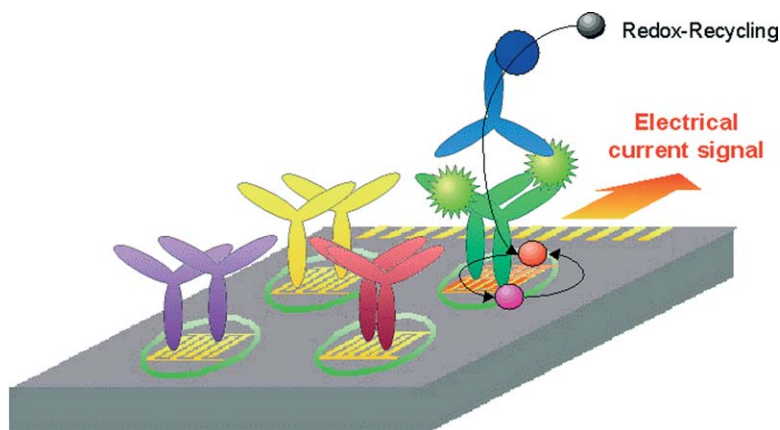


Fig. 14. Scheme of an electrical protein microarray using sandwich ELISA formats.

- enzyme labelling;
- substrate cleavage and electrical readout.

The construction and signal readout of the protein detection using the electrical microarray in regarding to the general principle is shown in Chapter 2.

Each array position is covered with the respective capture antibody or an internal standard substance via piezoelectric spotting of nanoliter drops. During an incubation phase, the capture molecules are allowed to immobilise on the electrode surfaces via self-assembling of cystein residues of amino acid side groups.

After blocking of free binding sides, the disposable carrying the protein microarray is inserted into the chip adapter with the flow cell. The sample solution is pumped over the chip surface and the position-specific affinity binding with the antibodies of the respective array positions take place. In the next step, enzyme labelled detection antibodies are incubated and bind to the affinity complexes only. Then the label enzyme substrate *p*-aminophenyl phosphate is flushed over and the electric readout of the redox recycling response is performed. This current is proportional to the bound enzyme, which means proportional to the amount of analyte in the solution.

In addition, an unspecifically coated control position for deriving the background current is measured on every chip as well as a 100% positive internal standard.

Those procedures provide, on the one hand, functional control and quality control and on the other a statistic tool for quantification and chip-to-chip equilibration. A useful application of these electrical protein microarrays is the bioweapon toxin analyser, which enters the market now. Toxins of relevance are the bacterial products Botulinus toxin of the bacterium *Clostridium botulinum* and the Staphylococcal enterotoxin B (SEB) of the bacterium *Staphylococcus aureus* as well as the plant toxin ricin from the plant *Ricinus communis*.

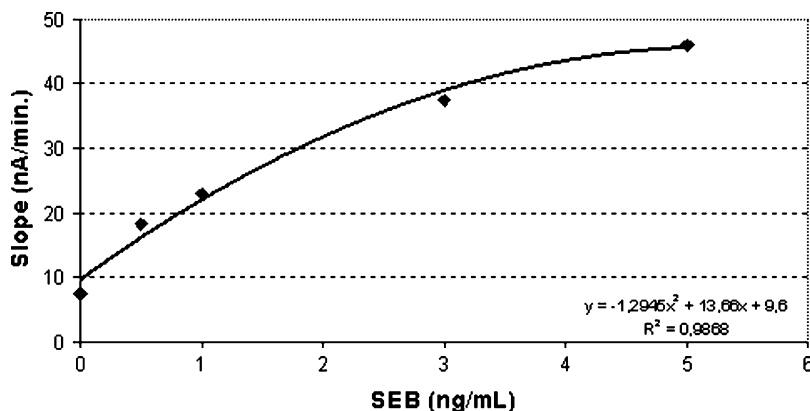


Fig. 15. Calibration curve for SEB between 0 and 5 ng mL⁻¹.

An assay for biological warfare toxins was established with polyclonal capture antibodies, biotinylated polyclonal detection antibodies and an ExtrAvidin[®] alkaline phosphatase conjugate. The measurements were carried out in collaboration with the German Armed Forces Scientific Institute for Protection Technologies in Munster, Germany.

For antibody immobilisation, array positions were spotted with ~30 nL of antibody solution, negative control and positive internal standard, respectively. For the measurements, the chip and the assay solutions were inserted into the automated detector. The programme, running with a total assay time of 29 min, included all incubation, washing and reconstitution steps.

During the on-site tests the following results have been obtained. In Figure 15, the concentration-dependent curve for the measurement of SEB is displayed.

It is obvious, that SEB can be detected in the lower ppb range. The detection limit for SEB was determined by measurement and calculation (Figure 16). The standard deviation for 0 ng mL⁻¹ SEB was multiplied by 3. The lowest measured value above is the real detection limit.

Following this procedure, the detection limit for SEB was determined to be 0.3 ng mL⁻¹. An array of SEB and ricin on the same chip using varying concentrations of each analyte in the sample resulted in independent and reproducible results. For SEB a concentration range between 0 and 15 ng mL⁻¹ was selected and for ricin between 0 and 25 ng mL⁻¹. The differences in the gradient are caused by different binding constants of the antibodies (Figure 17).

From this and other applications, it can be concluded that any protein sandwich ELISA, which is running in common microtitre plates can be transferred to this platform of electrical microarrays resulting in reduced running times and reagents.

7. ELECTRICAL HAPTEN MICROARRAYS

During the last years much effort has been spent on the development of biological detection systems for small molecules. Detection of haptens like

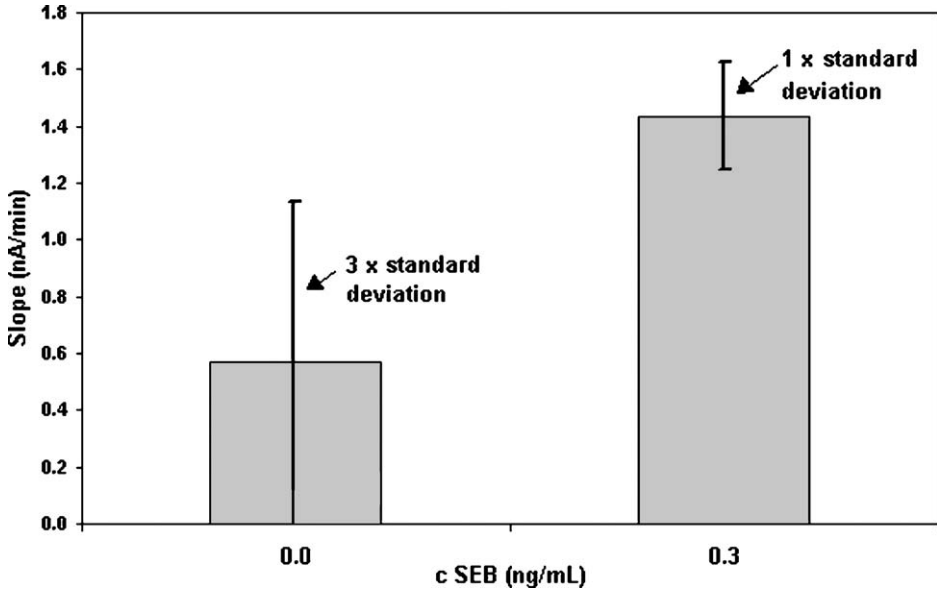


Fig. 16. Determination of the detection limit for SEB. Calculated were the threefold standard deviation of the mean value ($N = 3$) of the blank values. The signal above was defined as detection limit. It is 0.3 ng mL^{-1} for SEB.

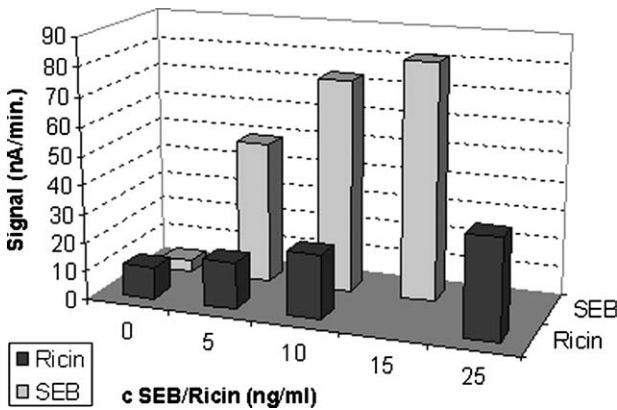


Fig. 17. Parallel detection of SEB and ricin with varying concentrations between 0 and 15 ng mL^{-1} for SEB and between 0 and 25 ng mL^{-1} for ricin.

explosives, biological toxins and antibiotics is the main goal (Pestka, 1991; Beier and Stanker, 2000; Loomans *et al.*, 2003; Wilson *et al.*, 2003; Estevez-Alberola and Marco, 2004; Lee *et al.*, 2004). To achieve high sensitivities, physical test methods like high-pressure liquid chromatography (HPLC) or gas chromatography with mass detection (GC-MS) are enabled (Sorensen *et al.*, 2003). These methods are expensive and require well-equipped analytical laboratories. The

need of small, inexpensive and fast test devices forced the development of biological tests with antibody – antigen interaction, so called immunoassays. Available methods based on enzyme immunoassays (EIAs) equipped mostly with optical detection (Suhren, 2002). Narang *et al.* (1998) detect explosives like trinitrotoluol (TNT) and cyclotrimethylenetrinitramine (RDX) with high sensitivity in a capillary immunoassay. For the detection of antibiotics in food, some tests are in the market – conventional competitive ELISAs (R-Biopharm AG, 2003) as well as automated assays like the Parallax- β -lactam system (Huth *et al.*, 2002) and the Parallel Affinity Sensor Array system (PASA) (Knecht *et al.*, 2004), for example. The Parallax- β -Lactam system is able to detect six different β -lactam-antibiotics with detection limits between 2.9 and 33.7 ng mL⁻¹ based on a capillary fluorescent immunoassay. The detection limits of the PASA system are between 0.12 and 32 ng mL⁻¹ and 10 antibiotics were detected in parallel directly in milk samples. Surface plasmon resonance (SPR) was also used for high-sensitive chloramphenicol detection in milk (Biacore, 2003). The detection limit of 0.025 ng/mL is below the given maximum residue limit (MRL) of 0.05 ng mL⁻¹ (Commission Regulation, 1990). However, this method cannot be used as a small mobile detector.

The rapid, inexpensive, on-site detection and quantification of antibiotics in food is of high commercial interest. Fast and easy to use small test systems for parallel identification of the commonly used antibiotics like penicillin G (PenG) and chloramphenicol (CAP) with high sensitivity and reproducibility are not in the market today.

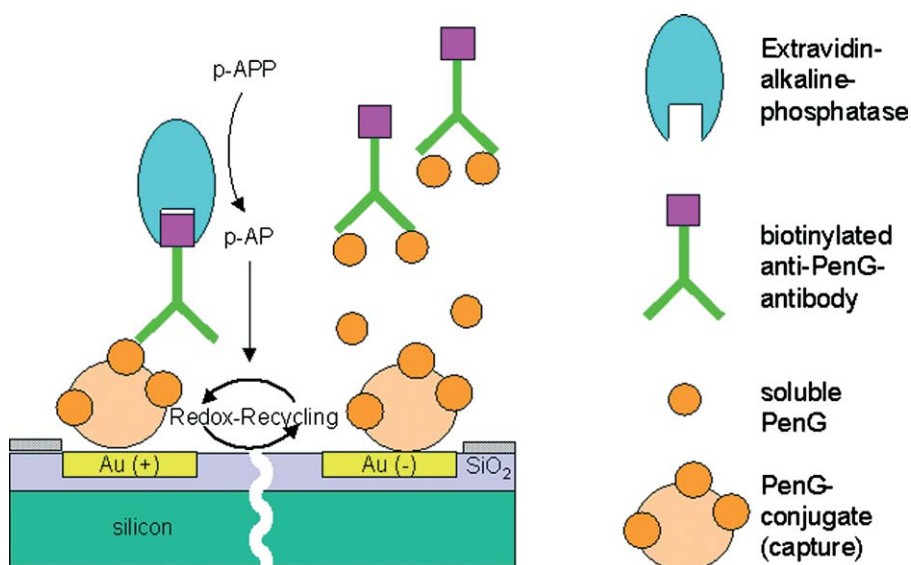


Fig. 18. Scheme of the biological interface at a PenG position. In absence of PenG a high signal results from redox recycling of the enzymatically converted substrate *p*-aminophenyl phosphate (*p*-APP) into *p*-aminophenol (*p*-AP) (left part of position). In contrast to this a PenG containing probe shows no signal (right part of position).

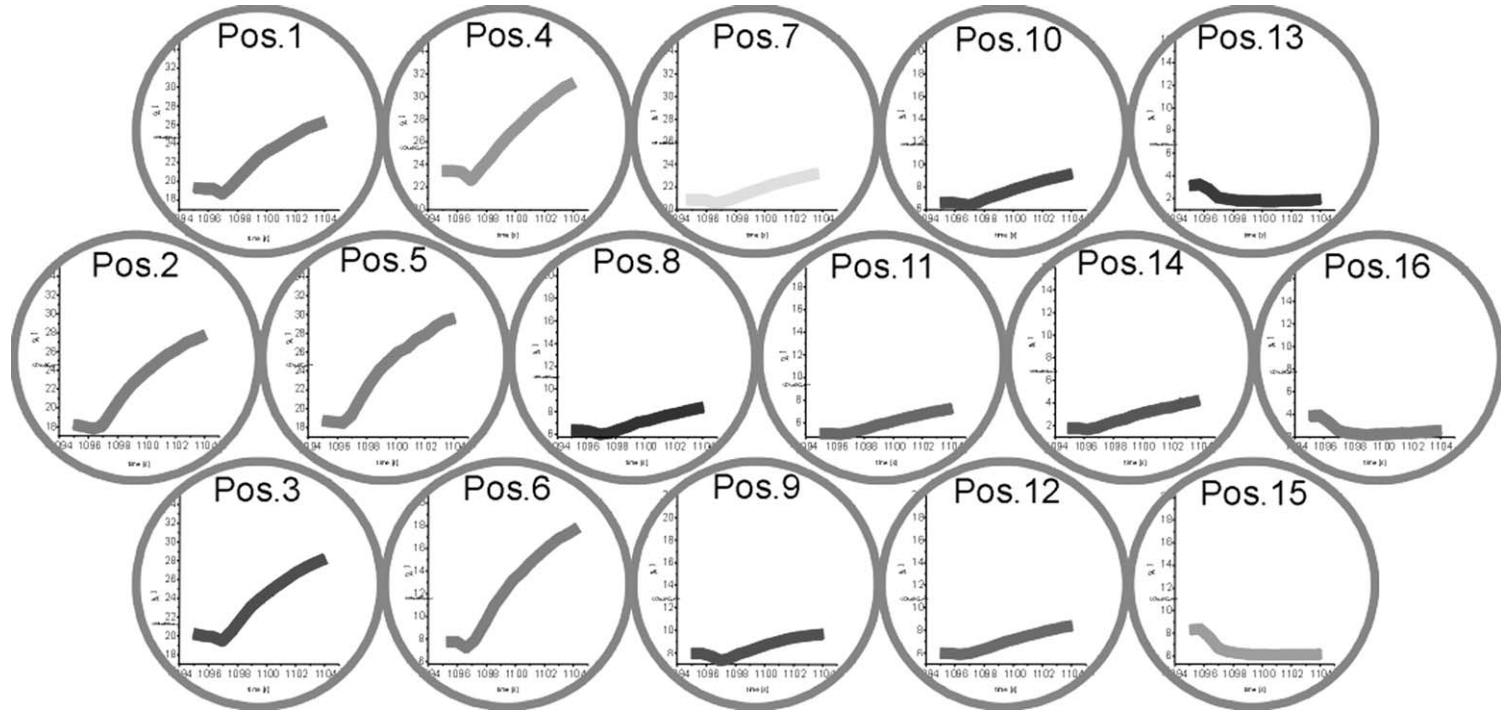


Fig. 19. Current response curves of all 16 positions. Positions 1–6 were used for positive control, positions 7–12 and 14 were used for PenG detection and positions 13, 15, 16 for negative control.

We have developed a competitive assay on microarrays for detection of PenG and CAP. As an example, the PenG assay will be described as follows.

The PenG assay is performed at the same microarrays with 16 positions as described above. The same detection procedure and a multiplexed 16 channel potentiostat (model "CIPO", eBiochip Systems GmbH) (Hintsche *et al.*, 2000) were used. The biological interface of this assay is illustrated in Figure 18.

For preparing the hapten microarrays a PenG protein conjugate was spotted by an automated piezodispensing device onto 7 chip positions. These captured molecules were immobilised via thiol links to the gold electrodes (Bain and Whitesides, 1989). Another 6 positions were covered with a biotinylated protein for simulating an internal standard of 100%. Three positions were left uncovered to derive the background current as a negative control.

Raw milk from cow and packed milk from the supermarket were used as matrices and spiked with PenG.

Performing the analytic process, spiked sample together with biotinylated anti-PenG antibody was pumped automatically over the chip surface. The competition between PenG in the solution and immobilised PenG on the seven microarray positions for binding of the anti-PenG antibody results in an amount of biotinylated complexes on the electrodes, negative proportional to the PenG concentration. Because of this competition effect the PenG positions do not reach the values of the positive control positions. After common labelling of these positions with alkaline phosphatase, the substrate *p*-APP was added and redox recycling was measured in a stopped flow modus.

The resulting current responses for each position are shown in Figure 19. The curves represent the slope of current during the first seconds after the flow stopped. The measured samples were containing 6 ng mL^{-1} PenG.

An internal calibration was made by using the positive and negative control positions. For this assay the linear fit is between 2 and 10 ng mL^{-1} PenG. The maximum residue limit (MRL) of PenG in food is 4 ng mL^{-1} (Commission Regulation, 1990). Our detection limit is 2 ng mL^{-1} at present.

This microarray platform was tested to be useful for simultaneous detection of more antibiotics in parallel.

LIST OF ABBREVIATIONS

ASIC	application-specific integrated circuit
Bp	base pairs
CAP	chloramphenicol
CMOS	complementary metal oxide semiconductor
CMV	cytomegalovirus
D/A-	digital/analog-
DsDNA	double-stranded deoxyribonucleic acid
EBV	Epstein-Barr virus
EIA	Enzyme immunosorbent assay
EIS	electrochemical impedance spectroscopy

ELISA	enzyme-linked immunosorbent assay
GC-MS	gas chromatography–mass spectrometry
GOX	glucose oxidase
HPLC	high-pressure liquid chromatography
HSV	herpes simplex virus
IDA	interdigitated electrode array
MOS	metal oxide semiconductor
MRL	maximum residue limit
Nt	nucleotides
<i>p</i> -AP	<i>p</i> -aminophenol
<i>p</i> -APP	<i>p</i> -aminophenyl phosphate
PASA	parallel affinity sensor arraysystem
PC	personal computer
PCR	polymerase chain reaction
PenG	penicillin-G
RDX	cyclotrimethylenetrinitramine
rRNA	ribosomal ribonucleic acid
SAM	self assembled monolayer
SEB	staphylococcal enterotoxin B
SEM	scanning electron microscope
SNP	single nucleotide polymorphism
SPR	surface plasmon resonance
ssDNA	single-stranded desoxyribonucleic acid
TNT	trinitrotoluene

REFERENCES

- Albers, J., T. Grunwald, E. Nebling, G. Piechotta and R. Hintsche, 2003, Electrical biochip technology – a tool for microarrays and continuous monitoring, *Anal. Bioanal. Chem.* 377, 521–527.
- Anderson, R.C., X. Su, G.J. Bogdan and J. Fenton, 2000, A miniature integrated device for automated multistep genetic assays, *Nucl. Acids Res.* 28, e60.
- Anthony, R.M., T.J. Brown and G.L. French, 2000, Rapid diagnosis of bacteremia by universal amplification of 23S ribosomal DNA followed by hybridization to an oligonucleotide array, *J. Clin. Microbiol.* 38, 781–788.
- Aoki, K., M. Morita, O. Niwa and H. Tabei, 1988, Quantitative analysis of reversible diffusion-controlled currents of redox soluble species at interdigitated array electrodes under steady-state conditions, *J. Electroanal. Chem.* 256, 269–282.
- Askari, M., J.P. Alarie, M. Moreno-Bondi and T. Vo-Dinh, 2001, Application of an antibody biochip for p53 detection and cancer diagnosis, *Biotechnol. Prog.* 17, 543–552.
- Bain, C.D. and G.M. Whitesides, 1989, Formation of monolayers by the coadsorption of thiols on gold: Variation in the length of the alkyl chain, *J. Am. Chem. Soc.* 111(18), 7164–7175.
- Barken, K.B., M. Gabig-Ciminska, A. Holmgren and S. Molin, 2004, Effect of unlabeled helper probes on detection of an RNA target by bead-based sandwich hybridization, *Biotechniques* 36, 124–132.
- Beier, M. and J.D. Hoheisel, 1999, Versatile derivatisation of solid support media for covalent bonding on DNA-microchips, *Nucl. Acids Res.* 27, 1970–1977.

- Beier, R. and L. Stanker, 2000, Application of immunoassay for detection of antibiotics in foods and feed: A review, recent research developments in agricultural and food chemistry, August 28.
- Berggren, C., B. Bjarnason and G. Johansson, 2001, Capacitive biosensors, *Electroanalysis* 13, 173–180.
- Biacore, 2003, *Q-Flex*[®]-Kit Chloramphenicol.
- Blohm, D.H. and A. Guiseppi-Elie, 2001, New developments in microarray technology, *Curr. Opin. Biotech.* 12, 41–47.
- Call, D.R., F.J. Brockman and D.J. Chandler, 2001, Detection and genotyping *Escherichia coli* O157:H7 using multiplexed PCR and nucleic acid microarray, *Int. J. Food Microbiol.* 67, 71–80.
- Chandler, D.P., G.J. Newton, J.A. Small and D.S. Daly, 2003, Sequence versus structure for the direct detection of 16S rRNA on planar oligonucleotide microarrays, *Appl. Environ. Microbiol.* 69, 2950–2958.
- Chee, M., R. Yang, E. Hubbell, A. Berno, X.C. Huang, D. Stern, J. Winkler, D.J. Lockhart, M.S. Morris and S.P.A. Fodor, 1996, Accessing genetic information with high-density DNA arrays, *Science* 274, 610–614.
- Commission Regulation (EEC) No. 2377/90, 1990, *Off. J. Eur. Commun.* L224, 1–8.
- Delehanty, J.B. and F.S. Ligler, 2002, A microarray immunosensor for simultaneous detection of proteins and bacteria, *Anal. Chem.* 74, 5681–5687.
- Dharuman, V., T. Grunwald, E. Nebling, J. Albers, L. Blohm and R. Hintsche, 2004, Label-free impedance detection of oligonucleotide hybridisation on interdigitated ultramicroelectrodes using electrochemical redox probes, *Biosensors Bioelectron.*, article in press.
- Diao, P., M. Guo and R. Tung, 2001, Characterisation of defects in the formation process of self-assembled thiol monolayers by electrochemical impedance spectroscopy, *J. Electroanal. Chem.* 495, 98–105.
- Dupont, D., O. Rolet-Repecaud and S. Muller-Renaud, 2004, Determination of the heat treatment undergone by milk by following the denaturation of alpha-lactalbumin with a biosensor, *J. Agric. Food Chem.* 52, 677–681.
- Ehret, R., W. Baumann, M. Brischwein, A. Schwinde, K. Stegbauer and B. Wolf, 1997, Monitoring of cellular behaviour by impedance measurements on interdigitated electrode structures, *Biosensors Bioelectron.* 12, 29–41.
- Estevez-Alberola, M.C. and M.P. Marco, 2004, Immunochemical determination of xenobiotics with endocrine disrupting effects, *Anal. Bioanal. Chem.* 378, 563–575.
- Feng, L. and M. Nerenberg, 1999, Electronic microarray for DNA analysis, *Gene. Ther. Mol. Biol.* 4, 183–191.
- Finklea, H., D.A. Sinder, J. Fedyk, E. Sabatani, Y. Gafni and I. Rubinstein, 1993, Characterisation of octadecanethiol coated gold electrodes as microarray electrodes by cyclic voltammetry and ac impedance spectroscopy, *Langmuir* 9, 3660–3667.
- Fodor, S.P., J.L. Read, M.C. Pirrung, L. Stryer, A.T. Lu and D. Solas, 1991, Light-directed, spatially addressable parallel chemical synthesis, *Science* 251, 767–773.
- Frace, G., G. Lillie, T. Hianik, P. Payne and P. Vadgama, 2002, Reagentless biosensing using electrochemical impedance spectroscopy, *Bioelectrochemistry* 55, 1–3.
- Fuchs, B.M., F.O. Glöckner, J. Wulf and R. Amann, 2000, Unlabeled helper oligonucleotides increase the in situ accessibility to 16S rRNA of fluorescently labeled oligonucleotide probes, *Appl. Environ. Microbiol.* 66, 3603–3607.
- Gheorghie, M. and A.G. Elie, 2003, Electrical frequency dependent characterisation of DNA hybridization, *Biosensors Bioelectron.* 19, 95–102.
- Gilles, P.N., D.J. Wu, C.B. Foster, P.J. Dillon and S.J. Chanock, 1999, Single nucleotide polymorphic discrimination by an electronic dot blot assay on semiconductor microchips, *Nat. Biotechnol.* 17, 365–370.
- Gooding, J.J., 2002, Electrochemical DNA hybridization biosensors, *Electroanalysis* 14, 1149–1156.
- Gooding, J.J., A. Chou, F.J. Mearns, E. Wong and K.L. Jericho, 2003b, The ion gating effect: Using a change in flexibility to allow label free electrochemical detection of DNA hybridization, *Chem. Commun.* 15, 1938–1939.

- Gooding, J.J., F. Mearns, W. Yang and J. Liu, 2003a, Self-assembled monolayers into the 21st century: Recent advances and applications, *Electroanalysis* 15, 81–96.
- Graves, D.J., 1999, Powerful tools for genetic analysis come of age, *TIBTECH* 17, 127–134.
- Guan, J.G., Y.Q. Miao and Q.J. Zhang, 2004, Impedimetric biosensors, *J. Biosci. Bioeng.* 97, 219–226.
- Hang, T.C. and A.G. Elie, 2004, Frequency dependent and surface characterisation of DNA immobilisation and hybridization, *Biosensors Bioelectron.* 19, 1537–1548.
- Herne, T.M. and M.J. Tarlov, 1997, Characterization of DNA probes immobilized on gold, *J. Am. Chem. Soc.* 119, 8916–8920.
- Hintsche, R., J. Albers, H. Bernt and A. Eder, 2000, Multiplexing of microelectrode arrays in voltammetric measurements, *Electroanalysis* 12, 660–665.
- Hirschhorn, J.N., P. Sklar, K. Lindblad-Toh, Y.-M. Lim, M. Ruiz-Gutierrez, S. Bolk, B. Langhorst, S. Schaffner, E. Winchester and E.S. Lander, 2000, SBE-Tags: An array-based method for efficient single-nucleotide polymorphism genotyping, *Proc. Natl. Acad. Sci. USA* 97, 12164–12619.
- Hofmann, F., A. Frey, B. Holzapfl, M. Schienle, C. Paulus, P. Schindler-Bauer, D. Kuhlmeier, J. Krause, R. Hintsche, E. Nebbling, J. Albers, W. Gumbrecht, K. Plehnert, G. Eckstein and R. Thewes, 2002, Fully electronic DNA detection on a CMOS chip: Device and process issue, *Technical Digest, International Electron Device Meeting (IEDM)*, pp. 488–491.
- Huth, S.P., P.S. Warholc, J.M. Devou, L.K. Chaney and G.H. Clark, 2002, Parallax beta-lactam: A capillary-based fluorescent immunoassay for the determination of penicillin-G, ampicillin, amoxicillin, cloxacillin, cephalixin and ceftiofur in bovine milk, *J. AOAC Int.* 85, 355–364.
- Jacobs, P., 1998. Proceedings of the second International conference on Microreaction technology, New Orleans, Louisiana, USA, March 8, 12.
- Jacobs, P., A. Varlan and W. Sansen, 1995, Design optimisation of planar electrolytic conductivity sensors, *Med. Bio. Eng. Comp.* 33, 802–810.
- Jain, K.K., 2000, Applications of biochip and microarray systems in pharmacogenomics, *Pharmacogenomics* 1, 289–307.
- Katz, E. and I. Willner, 2003, Probing biomolecular interactions at conductive and semi-conductive surfaces by impedance spectroscopy: Routes to impedimetric immunosensors, DNA-sensors, and enzyme sensors, *Electroanalysis* 15, 913–947.
- Kerman, K., M. Kobayashi and E. Tamiya, 2004, Recent trends in electrochemical DNA biosensor technology, *Meas. Sci. Technol.* 15, R1–R11.
- Knecht, B.G., A. Strasser, R. Dietrich, E. Märtlbauer, R. Niessner and M.G. Weller, 2004, Automated microarray system for the simultaneous detection of antibiotics in milk, *Anal. Chem.* 76, 646–654.
- Lacroix, M., N. Zammateo, J. Remacle and G. Leclercq, 2002, A low-density DNA microarray for analysis of markers in breast cancer, *Inter. J. Biol. Markers* 17, 5–23.
- Laureyn, W., D. Neils, P. Van Gerwen, K. Baert, L. Hermans, R. Magnee, J.-J. Pireaux and G. Maes, 2000, Nanoscaled interdigitated titanium electrodes for impedimetric biosensing, *Sens. Actuat. B* 68, 360–370.
- Lee, N.A., S. Wang, R.D. Allan and I.R. Kennedy, 2004, A rapid aflatoxin B1 ELISA: Development and validation with reduced matrix effects for peanuts, corn, pistachio, and soybeans, *J. Agric. Food Chem.* 52, 2746–2755.
- Lillie, G., P. Payne and P. Vadgama, 2001, Electrochemical impedance spectroscopy as a platform for reagentless bioaffinity sensing, *Sens. Actuat. B* 78, 249–256.
- Lipshutz, R.J., S.P. Fodor, T.R. Gingeras and D.J. Lockhart, 1999, High-density synthetic oligonucleotide arrays, *Nat. Genet. Suppl.* 21, 20–24.
- Liu, R.H., J. Yang, R. Lenigk, J. Bonanno and P. Grodzinski, 2004, Self-contained, fully integrated biochip for sample preparation, polymerase chain reaction amplification, and DNA microarray detection, *Anal. Chem.* 76, 1824–1831.
- Liu, Y., J. Ye and Y. Li, 2003, Rapid detection of *Escherichia coli* O157:H7 inoculated in ground beef, chicken carcass, and lettuce samples with an immunomagnetic chemiluminescence fiber-optic biosensor, *J. Food Prot.* 66, 512–517.

- Lockhart, D.J., D.J. Dong, H. Byrne, M.T. Follettie, M.V. Gallo, M.S. Chee, M. Mittmann, C. Wang, M. Kobayashi, H. Horton and E.L. Brown, 1996, Expression monitoring by hybridization to high-density oligonucleotide arrays, *Nat. Biotechnol.* 14, 1675–1680.
- Loomans, E.E., J. Van Wiltenburg, M. Koets and A. Van Amerongen, 2003, Neamin as an immunogen for the development of a generic ELISA detecting gentamicin, kanamycin, and neomycin in milk, *J. Agric. Food Chem.* 51, 587–593.
- Maruyama, K., Y. Mishima, K. Minagawa and J. Motonaka, 2002, DNA sensor with a dipyrrophenazine complex of osmium(II) as an electrochemical probe, *Anal. Chem.* 74, 3698–3703.
- Maskos, U.E.M. and E. Southern, 1992, Parallel analysis of oligodesoxyribonucleotide (oligonucleotide) interactions. I. Analysis of factors influencing oligonucleotide duplex formation, *Nucl. Acids Res.* 20, 1675–1678.
- Mikkelsen, S.R. and W.C. Purdy, 1985, Single pulse coulometric analysis, *Anal. Lett.* 18, 1703–1716.
- Millan, K.M. and S.R. Mikkelsen, 1993, Sequence-selective biosensor for DNA based on electroactive hybridization indicators, *Anal. Chem.* 65, 2317–2323.
- Montelius, L., J.O. Tegenfeldt and T.G. Ling, 1995, Fabrication and characterisation of a nanosensor for admittance spectroscopy of biomolecules, *J. Vac. Sci. Technol. A* 13, 1755–1760.
- Mullis, K.B. and F. Faloona, 1987, Specific synthesis of DNA in vitro via a polymerase catalyzed chain reaction, *Meth. Enzymol.* 155, 335–350.
- Narang, U., P.R. Gauger, A.W. Kusterbeck and F.S. Ligler, 1998, Multianalyte detection using a capillary-based flow immunosensor, *Anal. Biochem.* 255, 13–19.
- Nebling, E., T. Grunwald, J. Albers, P. Schäfer and R. Hintsche, 2004, Electrical detection of viral DNA using ultramicroelectrode arrays, *Anal. Chem.* 76, 689–696.
- Nees, M. and C.D. Woodworth, 2002, Microarrays: Spotlight on gene function and pharmacogenomics, *Curr. Cancer Drug Targets* 1, 155–175.
- Niwa, O., M. Morita and H. Tabei, 1990, Electrochemical behavior of reversible redox species at interdigitated array electrodes with different geometries: Consideration of redox cycling and collection efficiency, *Anal. Chim.* 62, 447–452.
- Niwa, O., Y. Xu, H.B. Halsall and W.R. Heineman, 1993, Small-volume voltammetric detection of 4-aminophenol with interdigitated array electrodes and its application to electrochemical enzyme immunoassay, *Anal. Chem.* 65, 1559–1563.
- Ochs, M.F. and A.K. Godwin, 2003, Microarrays in cancer: Research and applications, *BioTechniques* 34, 4–15.
- O'Donnell, M.J., K. Tang, H. Koster, C.L. Smith and C.R. Cantor, 1997, High-density, covalent attachment of DNA on silicon wafers for analysis by MALDI-ToF mass spectrometry, *Anal. Chem.* 69, 2438–2443.
- Olive, D.M. and P. Bean, 1999, Principles and applications of methods for DNA-based typing of microbial organisms, *J. Clin. Microbiol.* 37, 1661–1669.
- Paeschke, M., F. Dietrich, A. Uhlig and R. Hintsche, 1996a, Voltammetric multi-channel measurements using silicon fabricated microelectrode arrays, *Electroanalysis* 8, 891–898.
- Paeschke, M., L.M. Buchmann, R. Seitz and R. Hintsche, 1996b, Fabrication and investigation of nanometer sized dielectric interdigitated transducers for detection of biomolecular binding, *Microsystem Technologies'96*, Eds. H. Reichl and A. Heuberger, VDE-Verlag, Frankfurt am Main, 399.
- Palecek, E. and M. Fojta, 2005, Electrochemical DNA sensors, *Bioelectronics*, Eds. I. Willner and E. Katz, Wiley-VCH, Weinheim, 127.
- Pease, A.C., D. Solas, E.J. Sullivan, M.T. Cronin, C.P. Holmes and S.P. Fodor, 1994, Light-generated oligonucleotide arrays for rapid DNA sequence analysis, *Proc. Natl. Acad. Sci. USA* 91, 5022–5026.
- Peplies, J., S.C.K. Lau, J. Pernthaler, R. Amann and F.O. Glöckner, 2004, Application and validation of DNA microarrays for the 16S rRNA-based analysis of marine bacterioplankton, *Environ. Microbiol.* 6, 638–645.

- Pestka, J.J., 1991, High performance thin layer chromatography ELISAGRAM. Application of a multi-hapten immunoassay to analysis of the zearalenone and aflatoxin mycotoxin families, *J. Immunol. Meth.* 136, 177–183.
- Rautio, J., K.B. Barken, J. Lahdenperä, A. Breitenstein, S. Molin and P. Neubauer, 2003, Sandwich hybridisation assay for quantitative detection of yeast RNAs in crude cell lysates, *Microbial. Cell Factories* 2, 1–9.
- Razumas, V.J., J.J. Kulys and A.A. Malinauskas, 1980, Kinetic amperometric determination of hydrolase activity, *Anal. Chim. Acta* 117, 387–390.
- R-Biopharm AG: RIDASCREEN[®]-Tests, 2003, Darmstadt, Germany.
- Rowe Taitt, C., G.P. Anderson, B.M. Lingerfelt, M.J. Feldstein and F.S. Ligler, 2002, Nine-analyte detection using an array-based biosensor, *Anal. Chem.* 74, 6114–6120.
- Rüba, E., J.R. Hart and J.K. Barton, 2004, $\langle \text{Ru}(\text{bpy})_2(\text{L}) \rangle \text{Cl}_2$: Luminescent metal complexes that bind DNA base mismatches, *Inorg. Chem.* 43, 4570–4578.
- Rubenstein, K., 2003, Commercial aspects of microarray technology, *BioTechniques* 34, 52–54.
- Sabatani, E. and I. Rubinstein, 1987, Organised self-assembling monolayers on electrodes. 2. Monolayer-based ultramicroelectrodes for the study of very rapid electrode kinetics, *J. Phys. Chem.* 81, 6663–6669.
- Sapsford, K.E., Y.S. Shubin, J.B. Delehanty, J.P. Golden, C.R. Taitt, L.C. Shriver and F.S. Ligler, 2004, Fluorescence-based array biosensors for detection of biohazards, *J. Appl. Microbiol.* 96, 47–58.
- Saum, A.E.G., R.H. Cumming and F.J. Rowell, 1998, Use of substrate coated electrodes and AC impedance spectroscopy for the detection of enzyme activity, *Biosensors Bioelectron.* 13, 511–518.
- Schena, M., R.A. Heller, T.P. Theriault, K. Konrad, E. Lachenmeier and R.W. Davis, 1998, Microarrays: Biotechnology's discovery platform for functional genomics, *TIBTECH* 16, 301–306.
- Schienze, M., A. Frey, F. Hofmann, B. Holzapfl, C. Paulus, P. Schindler-Bauer and R. Thewes, 2004, A fully electronic DNA sensor with 128 positions and in-pixel A/D conversion, *J. Solid-St. Circ. (JSSC)*, December issue, in press.
- Small, J., D.R. Call, F.J. Brockman, T.M. Straub and D.P. Chandler, 2001, Direct detection of 16S rRNA in soil extracts by using oligonucleotide microarrays, *Appl. Environ. Microbiol.* 67, 4708–4716.
- Sorensen, L.K., T.H. Elbaek and H. Hansen, 2003, Determination of chloramphenicol in bovine milk by liquid chromatography/tandem mass spectrometry, *J. AOAC Int.* 86, 703–706.
- Southern, E.M., U. Maskos and J.K. Elder, 1992, Analyzing and comparing nucleic acid sequences by hybridization to arrays of oligonucleotides: Evaluation using experimental models, *Genomics* 13, 1008–1017.
- Steel, A.B., R.L. Levicky, T.M. Herne and M.J. Tarlov, 2000, Immobilization of nucleic acids at solid surfaces: Effect of oligonucleotide length on layer assembly, *Biophys. J.* 79, 975–981.
- Stulik, K., C. Amatore, K. Holub, V. Marecek and W. Kutner, 2000, Microelectrodes, definitions, characterisation and applications, *Pure Appl. Chem.* 72, 1483–1492.
- Suhren, G., 2002, *Kieler Milch. Forsch.* 54, 35–73.
- Sze, S.M., 1981, *Physics of Semiconductor Devices*, Wiley, New York.
- Takenaka, S., K. Yamashita, M. Takagi, Y. Uto and H. Kondo, 2000, DNA sensing on a DNA probe-modified electrode using ferrocenylnaphthalene diimide as the electrochemically active ligand, *Anal. Chem.* 72, 1334–1341.
- Tang, H.T., C.E. Lunte, H.B. Halsall and W.R. Heinemann, 1988, p-Aminophenyl phosphate: An improved substrate for electrochemical enzyme immunoassay, *Anal. Chim. Acta* 214, 187–195.
- Thewes, R., F. Hofmann, A. Frey, B. Holzapfl, M. Schienze, C. Paulus, P. Schindler, G. Eckstein, C. Kassel, M. Stanzel, R. Hintsche, E. Nebling, J. Albers, J. Hassman, J. Schülein, W. Goemann and W. Gumbrecht, 2002, Sensor arrays for fully electronic DNA detection on CMOS, *Technical Digest, International Solid-State Circuit Conference (ISSCC)*, pp. 350–351 and 472–473.

- Thewes, R., F. Hofmann, A. Frey, M. Schienle, C. Paulus, P. Schindler-Bauer, B. Holzapfl and R. Brederlow, 2004a. CMOS-based DNA Sensor Arrays, Enabling Technologies for MEMS and Nanodevices, Eds. H. Baltes, O. Brand, G.K. Fedder, C. Hierold, J.G. Korvink and O. Tabata, Wiley-VCH.
- Thewes, R., C. Paulus, M. Schienle, F. Hofmann, A. Frey, R. Brederlow, P. Schindler-Bauer, M. Augustyniak, M. Atzesberger, B. Holzapfl, M. Jenkner, B. Eversmann, G. Beer, M. Fritz, T. Haneder and H.-C. Hanke, 2004b, Integrated circuits for the biology-to-silicon interface, Proc. European Solid-State Device Research Conference (ESSDERC) and Proc. European Solid-State Circuits Conference (ESSCIRC), pp. 19–28.
- Van Gerwen, P.V., W. Laureyn, W. Laureys, H. Huyberechts, M. Op De Beeck, K. Baert, J. Suls, W. Sansen, P. Jacobs, L. Hermans and R. Martens, 1998, Nanoscaled interdigitated electrode arrays for biochemical sensors, *Sens. Actu. B* 49, 73–80.
- Wallraff, G., J. Labadie, P. Brock, R. DiPietro, T. Nguyen, T. Huynh, W. Hinsberg and G. McGall, 1997, DNA Sequencing on a chip, *Chemtech* 27, 22–23.
- Wang, J., 2000, From DNA biosensors to gene chips, *Nucl. Acids Res.* 28, 3011–3016.
- Wang, R.-F., M.L. Beggs, L.H. Robertson and C.E. Cerniglia, 2002, Design and evaluation of oligonucleotide-microarray method for the detection of human bacterial in fecal samples, *FEMS Microbiol. Lett.* 213, 175–182.
- Warren, J.W., 1996. Clinical presentations and epidemiology of urinary tract infections, *Am. Soc. Microbiol.*, Washington, 3–21.
- Westin, L., C. Miller, D. Vollmer, C. Canter, R. Radtkey, M. Nerenberg and J.P. O'Connell, 2001, Antimicrobial resistance and bacterial identification utilizing a microelectronic chip array, *J. Clin. Microbiol.* 39, 1097–1104.
- Wicks, B., D.B. Cook, M.R. Barer, A.G. O'Donnell and C.H. Self, 1998, A sandwich hybridization assay employing enzyme amplification for termination of specific ribosomal RNA from unpurified cell lysates, *Anal. Biochem.* 259, 258–264.
- Wilson, R., C. Clavering and A. Hutchinson, 2003, Electrochemiluminescence enzyme immunoassays for TNT and pentaerythritol tetranitrate, *Anal. Chem.* 75, 4244–4249.
- Wodicka, L., H. Dong, M. Mittmann, M.-H. Ho and D.J. Lockhart, 1997, Genome-wide expression monitoring in *Saccharomyces cerevisiae*, *Nat. Biotechnol.* 15, 1359.
- Wollenberger, U., M. Paeschke and R. Hintsche, 1994, Interdigitated array microelectrodes for the determination of enzyme, *Analyst* 119, 1245–1249.
- Yang, J.M., J. Bell, H. Ying, M. Tirado, D. Thomas, A.H. Forster, R.W. Haigis, P.D. Swanson, B. Wallace, B. Martinsons and M. Krihak, 2002, An integrated, stacked microlaboratory for biological agent detection with DNA and immunoassays, *Biosensors Bioelectron.* 17, 605–618.
- Zammatteo, N., L. Jeanmart, S. Hamels, S. Courtois, P. Louette, L. Hevesi and J. Remacle, 2000, Comparison between different strategies of covalent attachment of DNA to glass surfaces to build DNA microarrays, *Anal. Biochem.* 280, 143–150.

This page intentionally left blank

Carbon Electrodes in DNA Hybridisation Research

G. Marrazza, F. Lucarelli and M. Mascini

Chemistry Department, Florence University, via della Lastruccia 3, 50019 Florence, Italy

Contents

1. DNA probe immobilisation	280
1.1. Adsorption at fixed potential	280
1.2. Avidin–biotin system	280
1.3. Covalent immobilisation by carbodiimide	281
2. Hybridisation reaction	283
3. Labelling and electrochemical detection	284
3.1. Electroactive intercalative compounds/groove binders	284
3.2. Indicator-free approach	287
3.3. Enzyme labels for hybridisation detection	289
3.4. Biomagnetic assays	292
4. Conclusions	293
List of abbreviations	293
References	294

DNA biosensors based on carbon electrodes are under intense investigation by many research groups. Carbon electrodes are particularly attractive for sensing applications because of their low cost, wide working potential window, good electrical conductivity and relatively low background currents.

Several carbon-based surfaces have been investigated as electrochemical transducers for DNA hybridisation biosensors. Carbon paste (Wang *et al.*, 1996a), highly orientated pyrolytic graphite electrodes (Hashimoto *et al.*, 1994) can be used for the highly sensitive hybridisation detection. Other carbon electrodes such as, pencil lead (Wang *et al.*, 2000) and carbon fibre electrodes (Caruana and Heller, 1999) have been also successfully employed. Although, glassy carbon electrodes are not suitable for direct detection of DNA oxidation peaks (Cai *et al.*, 1996) their utility for direct covalent attachment of DNA probes (Millan *et al.*, 1992) or electro-polymerisation of probe-supporting redox hydrogels (de Lumley-Woodyear *et al.*, 1996) has been demonstrated.

Screen-printed carbon electrodes have also been used to detect trace levels of nucleic acids (Cai *et al.*, 1996; Marrazza *et al.*, 1999). Thick-film electrochemical transducers can be easily mass produced at low cost and thus treated as disposable. Disposable sensors overcome the problem of electrode surface fouling, which usually results in loss of sensitivity and reproducibility. The use of screen-printed electrodes appears to be one of the most promising approaches, since it meets the needs of decentralised genetic testing. For example, genosensors based on

screen-printed carbon electrodes were successfully used for the detection of specific DNA sequences in real samples (Marrazza *et al.*, 2000; Lucarelli *et al.*, 2002).

The following sections will give relevant examples of electrochemical genosensors developed using carbon transducers. Each step in the assays procedure (probe immobilisation, hybridisation reaction, labelling and electrochemical detection) will be discussed in detail.

1. DNA PROBE IMMOBILISATION

The probe immobilisation step plays the major role in determining the overall performance of an electrochemical DNA biosensor. The achievement of high sensitivity and selectivity requires maximisation of the hybridisation efficiency and minimisation of non-specific adsorption, respectively. Control of the surface chemistry and coverage is essential for assuring high reactivity, orientation, accessibility and stability of the surface-confined probe as well as for minimising non-specific adsorption events. Different strategies to immobilise the DNA probe are described in the following sections.

1.1. Adsorption at fixed potential

The ability of DNA to adsorb firmly and irreversibly at carbon electrodes was demonstrated by Palecek and co-workers more than 10 years ago (Palecek *et al.*, 1993).

Adsorption at controlled potential is actually the simplest method to immobilise DNA (or peptide nucleic acid (PNA)) probes onto pre-treated carbon-based surfaces (Palecek *et al.*, 1993; Wang *et al.*, 1996a; Marrazza *et al.*, 1999; Erdem *et al.*, 1999). This method does not require special reagents or nucleic acid modifications. An oxidative pre-treatment of carbon surfaces is necessary to enhance the adsorptive accumulation of DNA (Wang *et al.*, 1995). On the other hand, the potential applied during immobilisation (generally +0.5 V vs. Ag/AgCl) enhances the stability of the probe through the electrostatic attraction between the positively charged surface and the negatively charged sugar-phosphate backbone of DNA (Figure 1A). The inherent oxidation signals of DNA bases onto carbon surfaces can be used to monitor the immobilisation process (Figure 1B).

However, using this immobilisation procedure, the non-covalently bound probes have multiple sites of contact with the transducer surface. Most of them could be inaccessible for hybridisation, resulting in poor hybridisation efficiency.

1.2. Avidin–biotin system

The avidin–biotin interaction is one of the strongest non-covalent binding events, characterised by an affinity constant of $10^{15} \text{ L} \times \text{mol}^{-1}$ (Diamandis and Christopoulos, 1991). This interaction has some unique characteristics that make it ideal as a bridge system in many applications, such as enzyme-linked immuno- and DNA hybridisation assays.

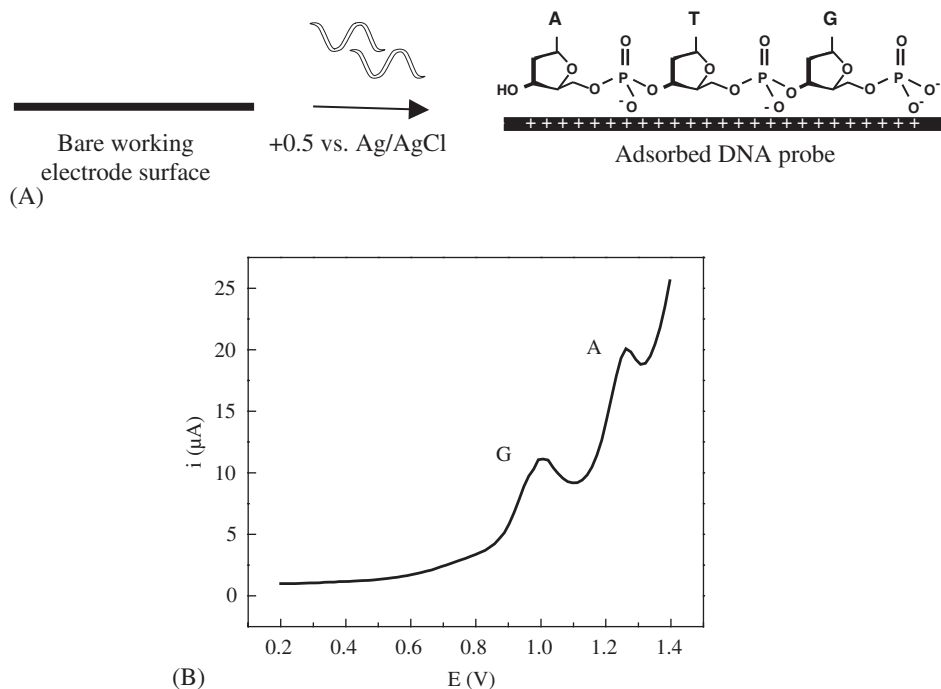


Fig. 1. (A) DNA probe immobilisation by applying a positive potential (a 3-mer is shown for clarity of presentation). (B) Oxidation signals of DNA sequences immobilised on a screen-printed carbon electrode using square wave voltammetry. Peak G: guanine ($E_p = +0.99$ V vs. Ag-SPE); peak A: adenine ($E_p = +1.26$ V vs. Ag-SPE).

Marrazza *et al.* (1999) reported the immobilisation of synthetic oligonucleotides onto disposable carbon strips using an avidin–biotin based procedure. This procedure involved the controlled formation of avidin layers (by adsorption) onto the electrode surface and the subsequent binding of a DNA probe biotinylated at its 5' end. However, the avidin layer inhibited the electrochemical oxidation of daunomycin, the indicator used to detect the hybridisation; a shorter and simpler immobilisation by adsorption at controlled potential allowed higher reproducibility and sensitivity.

Campbell *et al.* (2002) described the modification of carbon electrodes with a film of codeposited avidin and redox polymer. Incorporation of avidin into the electron-conducting hydrogel provided a platform to which biotinylated oligonucleotides could be promptly and simply attached. This immobilisation procedure resulted in higher probe hybridisation efficiency.

1.3. Covalent immobilisation by carbodiimide

Carbodiimide condensation chemistry is widely used for covalent immobilisation of, for example, amino-linked oligonucleotides onto activated surfaces (Figure 2).

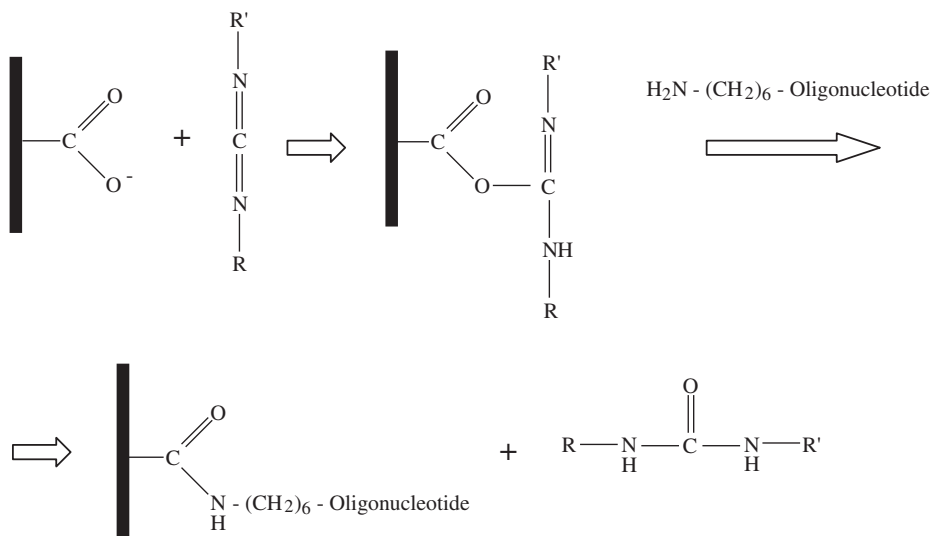


Fig. 2. Carbodiimide chemistry. The carbodiimide derivate ($\text{R}'\text{-N}=\text{C}=\text{N}\text{-R}$) reacts with oxidized groups present onto the electrode surface to form an active ester intermediate. In the presence of an amino-linked oligonucleotide an amide bond is formed with release of an isourea product.

Millan *et al.* (1992) reported the covalent immobilisation of synthetic oligonucleotides onto electrochemically oxidised glassy carbon surfaces by using a water-soluble carbodiimide. The immobilisation process was monitored by using $\text{Co}(\text{bpy})_3^{3+}$, a minor groove binder that was preconcentrated at the electrode surface because of its interaction with DNA. The immobilisation chemistry was later improved by employing *N*-hydroxysulfosuccinimide (NHS) with a water-soluble carbodiimide reagent (EDC) to activate carboxylate groups on the glassy carbon electrode surface (Millan and Mikkelsen, 1993). Single-stranded DNA was covalently bound to these groups through deoxyguanosine residues.

Carbon paste electrodes, modified by inclusion of 5% stearic acid, were also explored for covalent immobilisation of DNA (Millan *et al.*, 1994). The selected DNA probe, enzymatically elongated at the 3'-end with dG residues, was immobilised at stearic acid-modified electrodes by using the water-soluble carbodiimide and NHS to activate the carboxylate groups on the surface. Such a covalent immobilisation procedure resulted in a high hybridisation efficiency of the immobilised DNA probes; moreover, the regeneration of the probe-modified surface was achieved by simple rinsing in hot water.

The covalent immobilisation of synthetic oligonucleotides having a C6 spacer and a terminal amino group onto conductive polycarbonate/carbon fibre electrodes was explored by Schülein *et al.* (2002). The immobilisation proceeded through the formation of amide bonds between the carboxylic functionality at the electrode surface and the amino-terminal end of the oligonucleotides. The electrode coverage was estimated using fluorescein-labelled oligonucleotides.

de Lumley-Woodyear *et al.* (1996) reported the immobilisation of short oligonucleotides onto a film of a polyacrylamide-based, electron-conducting redox hydrogel, formed onto a vitreous carbon electrode. The DNA was covalently bound by carbodiimide coupling to the hydrazine functionality of the hydrogel surface. Improved results were obtained by using a 7- μm -diameter carbon fibre electrode (Caruana and Heller, 1999). In this case, the redox polymer was first electrophoretically deposited onto the microelectrode and then a carbodiimide-activated single-stranded probe was covalently attached to the redox-polymer film. The immobilisation process was monitored via the increased separation of ferrocene methanol peak potentials.

2. HYBRIDISATION REACTION

The kinetics and mechanism of the hybridisation reaction in solution has been widely studied. Hybridisation involves a two steps process: nucleation and zippering. Nucleation is the rate-limiting step. It is assumed that the nature of the hybridisation reaction at solid surfaces closely approximates that of the solution-phase reaction, but its rate is about 10–100 times slower. Efficient hybridisation of a target to surface-bound probes can be impeded by several phenomena. For example, the immobilised probe may not be accessible for hybridisation because of some steric interferences arising from neighbouring probe strands and the sensor surface itself.

The rate of hybridisation and the stability of the duplex depend on several factors, such as salt concentration, temperature, use of accelerating agents, base composition (G + C content) and length of the probe sequence.

The salt concentration markedly affects the rate of hybridisation reaction. Below 0.1 M NaCl, a two-fold increase of salt concentration increases the hybridisation rate by 5–10 fold or even more. The rate levels off when the concentration exceeds 1.2 M NaCl. However, since that high salt concentrations stabilise mismatched duplexes, the use of high ionic strength solutions is not recommended for single-base mutation analysis (Hames and Higgins, 1985).

The rate of hybridisation strongly depends on the temperature. The maximum rate is observed 20–25°C below melting temperature (T_m) of the duplex (Hames and Higgins, 1985). However, depending on salt concentration annealing may effectively occur at temperatures well below the optimum value.

The overall sensitivity of a hybridisation assay is strongly influenced by the hybridisation time. Moreover, the hybridisation process can be facilitated using appropriate reagents. The presence of guanidine-HCl in the target solution was shown to highly increase the rate of hybridisation (Wang *et al.*, 1997a,b). The stringency of hybridisation can be additionally altered using formamide. Formamide decreases the T_m of nucleic acid hybrids. Use of 30–50% formamide in the hybridisation solutions allows the incubation temperature to be reduced to 30–42°C.

The effect of sequence length on hybridisation rate is well known. The lower hybridisation yield of assays in which long probes and/or targets are used is

attributed to the higher steric hindrance and also the slower mass transport rate of the target towards the surface immobilised probe (Hames and Higgins, 1985).

3. LABELLING AND ELECTROCHEMICAL DETECTION

Several electroanalytical strategies have been investigated for transducing the hybridisation event at carbon surfaces. Hybridisation has been detected via an increase in the current signal of an electroactive indicator, in conjunction with the use of enzyme or redox labels, or from other hybridisation-induced changes in electrochemical parameters. Recent applications rely on the use of the most sophisticated, sensitive and fast techniques, including differential pulse voltammetry (DPV), square wave voltammetry (SWV) and potentiometric stripping analysis (PSA).

3.1. Electroactive intercalative compounds/groove binders

The single-stranded probe can be distinguished from the double-stranded hybrid obtained at the electrode surface using small DNA-intercalating or groove-binding compounds as electroactive indicators. The hybridisation indicator should possess a well defined voltammetric response at low potentials, in order to maximise the sensitivity of detection.

The electrochemical detection of hybridisation based on the use of an electroactive intercalator is illustrated in Figure 3. The modified electrodes are immersed in the indicator solution before and after the hybridisation reaction. After a certain period of incubation, an electrochemical method is applied to

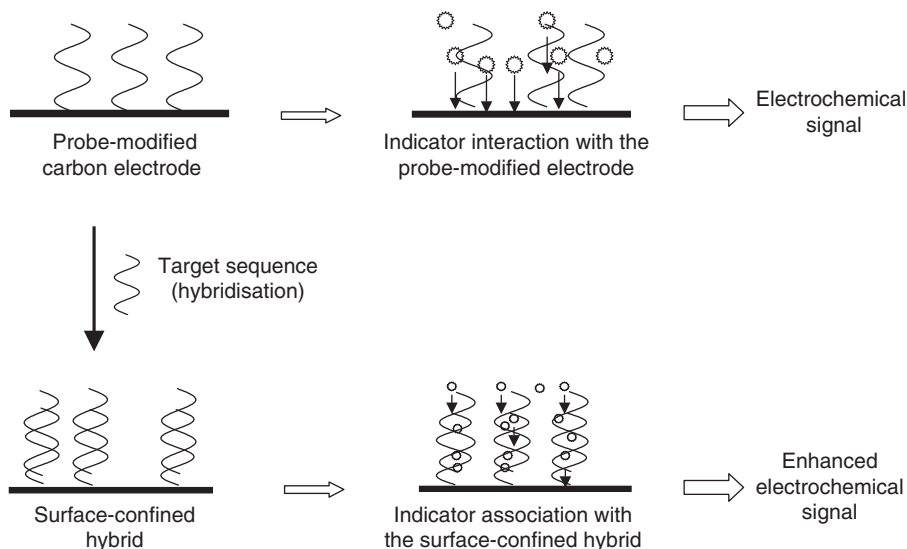


Fig. 3. Hybridisation detection based on the use of redox indicators.

quantify the indicator associated with the nucleic acids. When the redox marker has a higher affinity for the double-stranded hybrid compared to the single-stranded probe, enhanced electrochemical responses are observed at hybridised sensors. However, a few variants of this procedure have been developed.

Millan *et al.* (1994) demonstrated the utility of the $\text{Co}(\text{bpy})_3^{3+}$ minor groove binder for the detection of the cystic fibrosis ΔF508 deletion sequence. $\text{Co}(\text{bpy})_3^{3+}$ was also used by Wang's group to detect sequences related to a bacterial pathogen (Wang *et al.*, 1997a). $\text{Co}(\text{phe})_3^{3+}$ is another indicator that has been widely used to detect sequences related to bacterial (Wang *et al.*, 1997b, 1998b) and viral pathogens (Erdem *et al.*, 1999; Wang *et al.*, 1996a). Chronopotentiometric detection of the $\text{Co}(\text{phe})_3^{3+}$ or $\text{Co}(\text{bpy})_3^{3+}$ markers resulted in detection limits of $0.05 \mu\text{g}/\text{mL}$ of oligonucleotide target sequence (Wang *et al.*, 1997a).

Ozsoz's group reported the use of methylene blue (MB) as hybridisation indicator. MB strongly associated with the guanine bases of single-stranded probes and the decrease of the indicator peak which followed hybridisation, thus reflected the extent of duplex formation. The capability of MB to detect single-base mutations in short synthetic oligonucleotides (Erdem *et al.*, 2000) and sequences related to TT and Hepatitis B virus in amplified PCR samples (Meric *et al.*, 2002) was demonstrated with the use of DPV and SWV, respectively.

Another useful electroactive indicator is the intercalating anthracycline antibiotic daunomycin. A detection limit of $0.01 \mu\text{g}/\text{mL}$ of target sequence was reported for the linear sweep voltammetric measurement of this label intercalated between the base-pairs of a surface-formed hybrid (Hashimoto *et al.*, 1994). Figure 4 shows the oxidation reaction of this intercalator.

The DPV measurement of the daunomycin peak potential shift (hybrid vs. probe) was used by Marrazza *et al.* (1999) to detect the presence and the amount of complementary sequence. Nevertheless the shift was not reproducible and more than $4 \mu\text{g}/\text{mL}$ of complementary sequence were necessary to confirm the hybridisation.

In contrast, a daunomycin-based chronopotentiometric genosensor, described by the same authors, successfully detected apolipoprotein E (apoE) genotypes in DNA samples extracted from human blood and amplified by PCR (Marrazza *et al.*, 2000). The oligonucleotide probes were immobilised on the

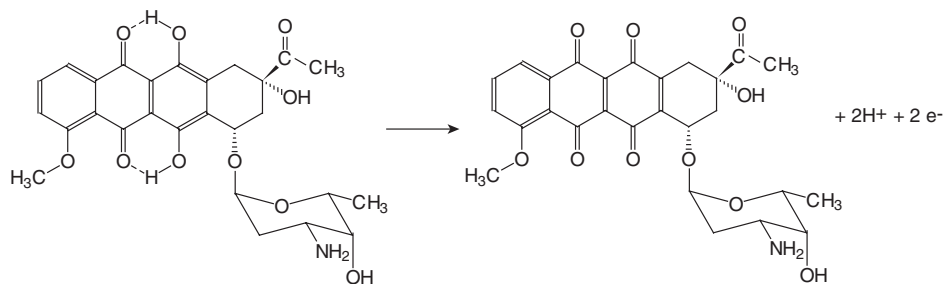


Fig. 4. Electrochemical oxidation of daunomycin.

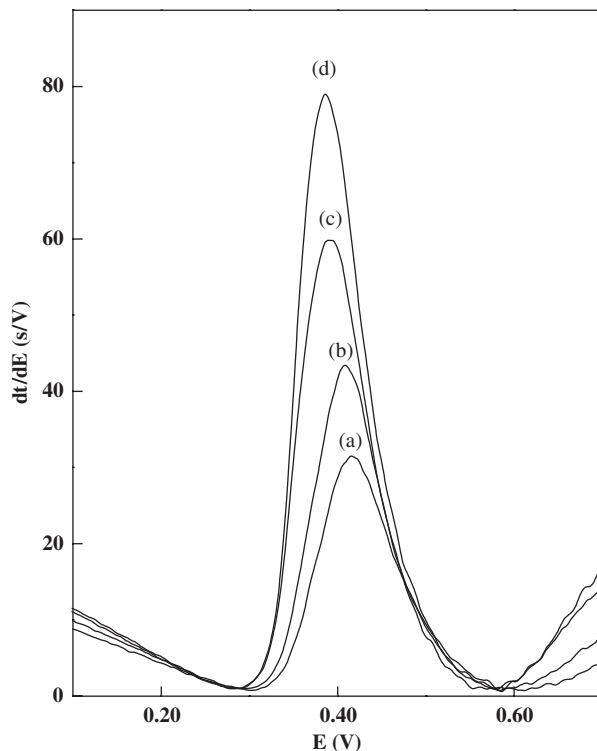


Fig. 5. Chronopotentiograms for daunomycin at probe-modified electrodes exposed to buffer a) and 1, 2 and 3 mg L^{-1} of target sequence (signals b, c and d respectively). Probe immobilisation (4 $\mu\text{g mL}^{-1}$ in a stirred $2 \times \text{SSC}$ buffer solution): 2 min at +0.5 V. Hybridisation: 10 μL of diluted and thermally denatured apoE samples or PCR blank onto the working electrode surface for 10 min. Interaction with daunomycin (50 μM): 2 min, in dark conditions. PSA transduction: stripping current +1 μA ; initial potential of +0.1 V. Each measurement was repeated at least three times.

screen-printed carbon electrodes by adsorption at controlled potential. Using two different probes, it was possible to investigate both positions in which the apoE polymorphisms take place, thus recognising different genotypes. The samples hybridised at the electrode surface were classified through the chronopotentiometric quantification of the daunomycin indicator. Figure 5 displays typical chronopotentiograms for daunomycin at probe-modified sensor exposed to buffer and increasing concentrations of the oligonucleotide target. Table 1 summarises the results for seven real samples from different genotypes analysed with both probes. Probe 1 is characteristic of allele $\epsilon 3$ and $\epsilon 2$, and the 100% complementary sequence is represented by genotypes $\epsilon 3/\epsilon 3$, $\epsilon 2/\epsilon 2$ and $\epsilon 2/\epsilon 3$. The genotypes $\epsilon 3/\epsilon 4$ and $\epsilon 2/\epsilon 4$ had 50% of each of the two sequences. Probe 2 is characteristic of allele $\epsilon 3/\epsilon 4$ and the 100% complementary sequence is represented by genotypes $\epsilon 3/\epsilon 3$ and $\epsilon 3/\epsilon 4$. The genotypes $\epsilon 2/\epsilon 2$ represented the mismatch sequence and genotypes $\epsilon 2/\epsilon 3$ had 50% of each of the two sequences. The results in Table 1 demonstrated that each sample could be assigned to a

Table 1. Electrochemical genotyping of PCR amplified samples using daunomycin as the redox indicator. Probe immobilisation (4 $\mu\text{g/mL}$ in a stirred $2 \times \text{SSC}$ buffer solution): 2 min at +0.5 V. Hybridisation: 10 μL of diluted and thermally denatured apoE samples or PCR blank onto the working electrode surface for 10 min. Interaction with daunomycin (50 μM): 2 min, in dark conditions. PSA transduction: stripping current +1 μA ; initial potential of +0.1 V. Each measurement was repeated at least three times.

Sample	Probe 1 Δ area (ms)	Probe 2 Δ area (ms)
PCR blank	-343 ± 179	-274 ± 84
$\epsilon 3/\epsilon 3$	$+875 \pm 138$	$+719 \pm 218$
$\epsilon 3/\epsilon 4$	$+270 \pm 99$	$+710 \pm 237$
$\epsilon 3/\epsilon 4$	$+110 \pm 127$	$+707 \pm 197$
$\epsilon 2/\epsilon 3$	$+658 \pm 111$	$+225 \pm 182$
$\epsilon 2/\epsilon 2$	$+629 \pm 260$	-171 ± 69
$\epsilon 2/\epsilon 2$	$+774 \pm 75$	-289 ± 185

certain genotype. Samples containing the complementary sequences gave a significant increase of daunomycin peak area compared with the signal observed with a blank solution. Samples containing 50% complementary sequences gave a much lower increase and samples containing only mismatch sequences gave a decrease in the daunomycin peak area.

More recently, new electroactive indicators have been developed for attaining higher sensitivity. Two classes of intercalators, bis- and threading intercalators, seem to be particularly interesting (Palecek and Fojta, 2001).

3.2. Indicator-free approach

Label-free electrochemical detection schemes greatly simplify the sensing protocols, as they eliminate the use of indicators. Moreover, the assay safety is improved, since the indicators are usually toxic or carcinogenic compounds.

One of the most elegant approaches relies on the intrinsic electroactivity of the nitrogenous bases of nucleic acids. The voltammetric behaviour of guanine and adenine was characterised more than 30 years ago (Dryhurst and Face, 1970; Dryhurst and Elving, 1968) and it is shown in Figures 6 and 7, respectively.

The first indicator-free scheme was introduced by Wang *et al.* (1996b). The hybridisation was detected by monitoring the decrease of the guanine peak of the immobilised probe (i.e. oligo d(G)₂₀), following the addition of the complementary oligo d(C)₂₀ target. However, this procedure was not applicable in most cases (e.g., for guanine containing targets).

Such a limitation has been overcome by developing a new approach, based on the use of inosine-modified (guanine-free) probes (Wang *et al.*, 1998a; Wang and Kawde, 2001; Lucarelli *et al.*, 2002). The inosine moiety still forms a specific base-pair with the cytosine residue (Casegreen and Southern, 1994), but its oxidation signal is well separated from that of guanine. This results in a flat

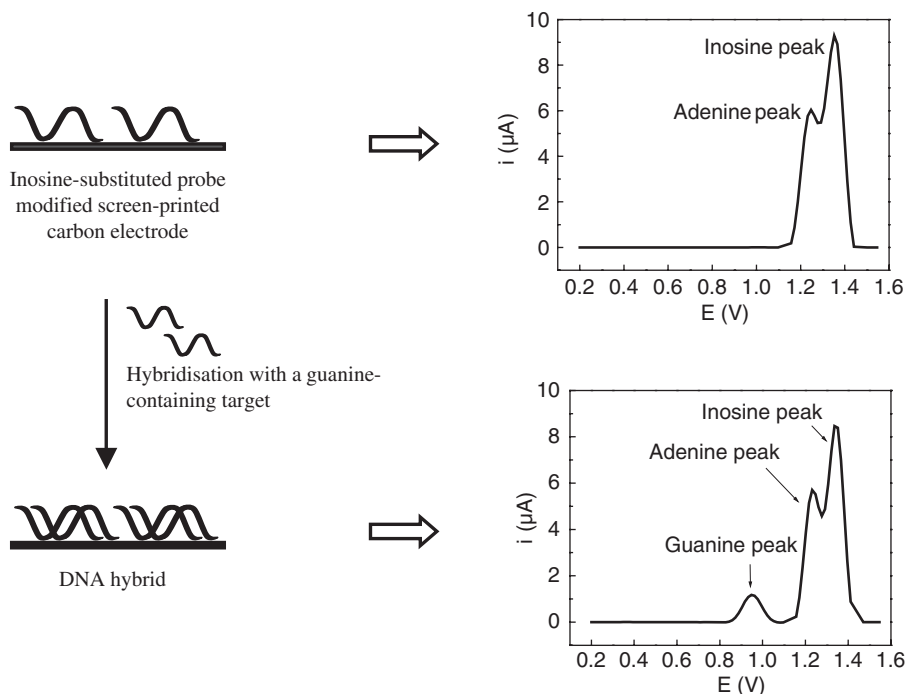


Fig. 8. Sequence-specific analysis based on the measurement of the intrinsic electrochemical signal of the guanine moiety. When using an inosine-substituted probe, duplex formation is indicated by the appearance of the oxidation signal of the guanine bases of the target sequence.

Table 2. Analysis of PCR amplified samples based on the measurement of the intrinsic electrochemical signal of the guanine moiety. Inosine-substituted probe immobilisation ($4\ \mu\text{g}/\text{mL}$ in a stirred $2 \times \text{SSC}$ buffer solution): 2 min at $+0.5\ \text{V}$. Hybridisation: $10\ \mu\text{L}$ of diluted and thermally denatured apoE or non-specific samples onto the working electrode surface for 10 min. Square-wave voltammetric detection: scan between $+0.2$ and $+1.35\ \text{V}$ in acetate buffer (frequency = $200\ \text{Hz}$; amplitude = $40\ \text{mV}$; step potential = $15\ \text{mV}$). Each measurement was repeated at least three times.

Samples	Guanine peak area ($\text{A} \times \text{V}$)
Non-complementary amplicon 1	$(2.8 \pm 0.6) \times 10^{-9}$
Non-complementary amplicon 2	$(3.1 \pm 1.6) \times 10^{-9}$
Non-complementary amplicon 3	$(3.6 \pm 2.0) \times 10^{-9}$
apoE amplicon 1	$(1.70 \pm 0.44) \times 10^{-8}$
apoE amplicon 2	$(1.93 \pm 0.08) \times 10^{-8}$
apoE amplicon 3	$(1.98 \pm 0.19) \times 10^{-8}$
apoE amplicon 4	$(2.12 \pm 0.52) \times 10^{-8}$
apoE amplicon 5	$(1.85 \pm 0.20) \times 10^{-8}$
apoE amplicon 6	$(1.77 \pm 0.27) \times 10^{-8}$
apoE amplicon 7	$(1.24 \pm 0.39) \times 10^{-8}$

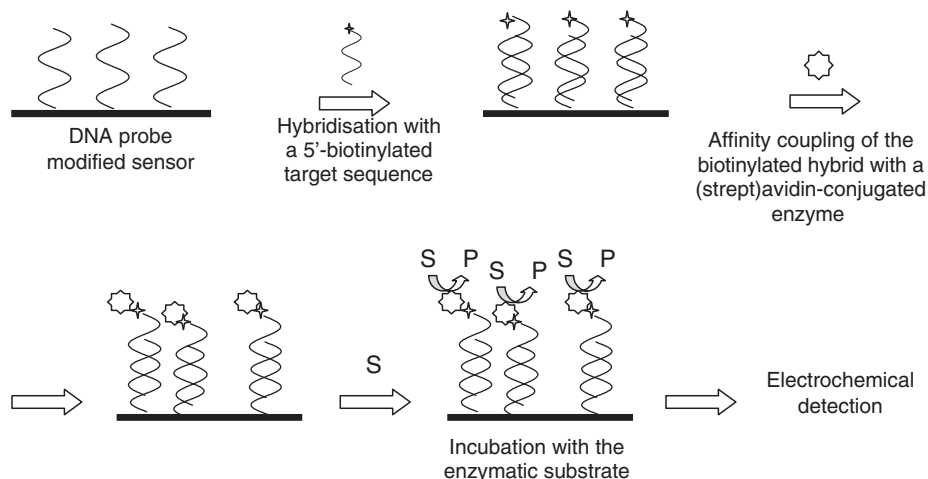


Fig. 9. Schematic presentation of an enzyme-linked DNA biosensor.

A horseradish peroxidase (HRP)-labelled DNA probe was used by Heller and co-workers in combination with the covalent immobilisation of the target sequence (de Lumley-Woodyear *et al.*, 1996). Upon hybridisation, the enzyme was electrically “wired” to the electrode surface and H_2O_2 was detected by amperometry.

The thermostable soybean peroxidase (SBP), covalently bound to target oligonucleotides, was also used by Heller’s group for the enzyme-amplified amperometric detection of DNA hybridisation (Caruana *et al.*, 1999). The accurate control of assay temperature allowed an easy discrimination between full-matching, single-base and four-base mismatching sequences. The hybridisation reaction was monitored in real time. About 34,000 copies of SBP-labelled hybrid could be detected in a 10 min assay.

Campbell *et al.* (2002) reported an enzyme-amplified amperometric sandwich test for RNA and DNA. DNA or RNA sequences were simultaneously allowed to hybridise with a HRP-labelled detection sequence and the surface-confined probe. A decrease in the H_2O_2 electroreduction current indicated the presence of the analyte DNA or RNA in solution.

An electrochemical enzyme-amplified hybridisation assay for the detection of human cytomegalovirus DNA in PCR samples was described by Azek *et al.* (2000). The biosensor format involved: (a) adsorption of denatured PCR products (target) onto the sensing area of a screen-printed carbon electrode; (b) hybridisation with a short, biotinylated, DNA probe; (c) hybrid labelling with a streptavidin-conjugated HRP and (d) differential pulse voltammetric detection of the enzyme-generated product. The electrochemical method showed a higher sensitivity compared with the agarose gel electrophoresis quantification and a microtiter plate-based spectrophotometric hybridisation assay; 3.6×10^5 copies/mL of amplified human cytomegalovirus DNA (406 bp) could be detected.

Pividori *et al.* (2001) designed an enzyme-labelled amperometric genosensor based on a concept adapted from classical dot-blot DNA analysis. The

analytical procedure consisted of five steps: (a) DNA target immobilisation by adsorption onto a nylon membrane; (b) hybridisation between the target DNA and the biotinylated probe; (c) hybrid labelling with a streptavidin-conjugated HRP; (d) integration of the modified membrane onto a graphite-polymer composite electrode transducer and (e) amperometric detection of H_2O_2 . Sensor selectivity against a three-base mismatched oligonucleotide probe was demonstrated. The ssDNA-modified membrane could be conserved for at least 3 months (at 4°C) without a significant decrease of performances.

3.4. Biomagnetic assays

The major problem encountered by several biosensing formats is the non-specific adsorption of non-hybridised oligonucleotides onto the probe-modified electrode surface. This has been overcome by conducting the hybridisation and the transduction steps at different surfaces (magnetic beads and unmodified electrodes, respectively). This novel strategy was independently announced by Wang's and Palecek's groups (Wang *et al.*, 2001; Palecek *et al.*, 2002). The efficient magnetic isolation of the duplex allowed the discrimination against non-hybridised DNA, including non-complementary sequences and an excess of mismatched oligonucleotides.

An enzyme-linked genomagnetic hybridisation assay was proposed by Wang *et al.* (2002). The protocol employed probe-modified magnetic beads able to hybridise in solution with a biotinylated DNA target. After hybrid labelling with streptavidin-conjugated alkaline phosphatase, the enzyme-generated α -naphthol was detected at bare screen-printed electrodes by using differential pulse voltammetry. The bio-analytical assay was applied for the detection of short sequences related to breast-cancer BRCA1; a detection limit of $10\ \mu\text{g/L}$ was achieved.

Palecek's group described a magnetic beads-based, enzyme-linked immunoassay for the detection of the DNA hybridisation event (Palecek *et al.*, 2002). Paramagnetic beads, with a covalently bound (dT)₂₅ probe, were used for the hybridisation with target DNA (synthetic 67-, 97-mer and PCR products) containing adenine stretches. Target DNA was previously modified with osmium tetroxide, 2,2'-bipyridine and the immunogenic Os(bipy)-DNA adducts were determined by an enzyme-linked immunoassay. The enzyme-generated α -naphthol was detected at bare carbon electrodes by using linear sweep voltammetry. Alternatively, Os(bipy)-modified targets were directly detected by measuring the osmium square wave voltammetric signal at pyrolytic graphite electrodes. A comparison between determination of the 67-mer target at carbon electrodes using: (a) the guanine oxidation signal (label-free detection of unmodified target); (b) direct determination of the Os(bipy)-DNA adduct and (c) its electrochemical immunoassay, showed immunoassay to be the most sensitive method (detection limit: $5\ \text{ng/mL}$). 226-bp amplicons were also successfully detected by immunoassay with high sensitivity and specificity.

Wang's group also described the approach for the electrical sensing of DNA with the lowest detection limit reported thus far (Wang *et al.*, 2004). This approach relied on the use of carbon nanotubes (CNT) which played a dual

amplification role: namely as carriers for numerous alkaline phosphatase tags and for accumulating the product of the enzymatic reaction. The CNT were first modified with both the enzyme labels and a DNA reporter probe by using the 1-ethyl-3-(3-dimethyl aminopropyl) carbodiimide (EDC); the probe-modified enzyme-loaded CNT were then used to detect target DNAs through a genomagnetic sandwich hybridisation assay. PSA was employed to measure the α -naphthol signal onto a glassy carbon electrode. The CNT-dual amplification route allowed dramatic improvement of the sensitivity. Moreover, further signal enhancement was demonstrated in connection with the use of a CNT-modified glassy carbon transducer. The electrochemical response was linear as a function of the logarithm of the target concentration between 0.01 and 100 pg/mL; a detection limit of 1 fg/mL (i.e., 820 copies) was achieved with 20 min hybridisation time.

4. CONCLUSIONS

This chapter has described the use of inexpensive carbon electrodes as transducers for electrochemical sensing of nucleic acids.

Over the past decade, enormous progresses have been made towards the development of electrochemical genosensors. Such devices are of considerable interest due to their promise for obtaining sequence-specific information in a faster, simpler and cheaper manner compared to traditional nucleic acid assays.

Indicator-based and label-free genosensors have some drawbacks, since they require the use of toxic/carcinogenic compounds or possess a relatively low sensitivity. In contrast, enzyme-amplified assays offered the best performance compared to the traditional electrophoresis-based analysis of PCR products.

In most cases, the electrochemical DNA biosensors described in this section are not reusable. Thermal or chemical regeneration of the surface-bound DNA probe often results in the desorption of the probe itself or in a severe decrease in the probe hybridisation efficiency (Wang *et al.*, 1998b). Sometimes, the electrochemical measurement damages the DNA probe; moreover, electrode surface fouling due to the use of electroactive indicators is often irreversible (Wang *et al.*, 1996a). To overcome the problems associated with this ineffective and time-consuming procedure, many groups have focused on the development of genosensors based on disposable transducers such as renewable pencil lead electrodes (Wang *et al.*, 2001) or “one-shot” screen-printed electrodes (Marrazza *et al.*, 2000).

Integration of multiple carbon sensors on a single microfabricated chip platform should lead to significant advantages in terms of reliability, cost, speed and simplicity of detection of specific DNA sequences.

LIST OF ABBREVIATIONS

PNA
Ag

peptide nucleic acid
silver

AgCl	silver chloride
Co(bpy) ₃ ³⁺	cobalt 2,2'-bipyridine
NHS	<i>N</i> -hydroxysulfosuccinimide
EDC	1-ethyl-3-(3-dimethyl aminopropyl)carbodiimide
dG	deoxyguanosine
G	guanine
C	cytosine
NaCl	sodium chloride
HCl	hydrogen chloride
<i>T</i> _m	melting temperature
DPV	differential pulse voltammetry
SWV	square wave voltammetry
PSA	potentiometric stripping analysis
Co(phe) ₃ ³⁺	cobalt 1,10-phenanthroline
MB	methylene blue
apoE	apolipoprotein E
PCR	polymerase chain reaction
d(G) ₂₀	deoxyguanosine 20-mer
HRP	horseradish peroxidase
H ₂ O ₂	hydrogen peroxide
SBP	soybean peroxidase
(dT) ₂₅	(deoxy)thymidine 25-mer
Os(bipy)	osmium tetroxide,2,2'-bipyridine
CNT	carbon nanotubes

REFERENCES

- Azek, F., C. Grossiord, M. Joannes, B. Limoges and P. Brossier, 2000, Hybridisation assay at a disposable electrochemical biosensor for the attomole detection of amplified human cytomegalovirus DNA, *Anal. Biochem.* 284, 107.
- Cai, X., G. Rivas, P.A.M. Farias, H. Shiraishi, J. Wang and E. Palecek, 1996, Evaluation of different carbon electrodes for adsorptive stripping analysis of nucleic acids, *Electroanalysis* 8 (8–9), 753.
- Campbell, C.N., D. Gal, N. Cristler, C. Banditrat and A. Heller, 2002, Enzyme-amplified amperometric sandwich test for RNA and DNA, *Anal. Chem.* 74, 158.
- Caruana, D.J. and A. Heller, 1999, Enzyme-amplified amperometric detection of hybridisation and of a single-base pair mutation in an 18-base oligonucleotide on a 7- μ M-diameter microelectrode, *J. Am. Chem. Soc.* 121, 769.
- Casegreen, S. and E. Southern, 1994, Studies on base pairing properties of deoxyinosine by solid phase hybridisation to oligonucleotides, *Nucleic acids Res.* 22 (2), 131.
- de Lumley-Woodyear, T., C.N. Campbell and A. Heller, 1996, Direct enzyme-amplified electrical recognition of a 30-base model oligonucleotide, *J. Am. Chem. Soc.* 118, 5504.
- Diamandis, E.P. and T.K. Christopoulos, 1991, The biotin-(strept)avidin system: Principles and applications in biotechnology, *Clin. Chem.* 37 (5), 625.
- Dryhurst, G. and P.J. Elving, 1968, Electrochemical oxidation of adenine: Reaction products and mechanisms, *J. Electrochem. Soc.* 115 (10), 1014.

- Dryhurst, G. and G.F. Face, 1970, Electrochemical oxidation of guanine at the pyrolytic graphite electrode, *J. Electrochem. Soc.* 117 (10), 1259.
- Erdem, A., K. Kerman, B. Meric, U.S. Akarca and M. Ozsoz, 1999, DNA electrochemical biosensor for the detection of short DNA sequences related to the hepatitis B virus, *Electroanalysis* 11 (8), 586.
- Erdem, A., K. Kerman, B. Meric, U.S. Akarca and M. Ozsoz, 2000, Novel hybridisation indicator methylene blue for the electrochemical detection of short DNA sequences related to the hepatitis B virus, *Anal. Chim. Acta* 422, 139.
- Hames, B.D. and S.J. Higgins, 1985, *Nucleic acid hybridization – a practical approach*, pp. 77–78. Oxford University Press, Oxford.
- Hashimoto, K., K. Ito and Y. Ishimori, 1994, Novel DNA sensor for electrochemical gene detection, *Anal. Chim. Acta* 286 (2), 219.
- Lucarelli, F., G. Marrazza, I. Palchetti, S. Cesaretti and M. Mascini, 2002, Coupling of an indicator-free electrochemical DNA biosensor with polymerase chain reaction for the detection of DNA sequences related to the apolipoprotein E, *Anal. Chim. Acta* 469, 93.
- Marrazza, G., I. Chianella and M. Mascini, 1999, Disposable DNA electrochemical DNA sensor for hybridisation detection, *Biosens. Bioelectron.* 14, 43.
- Marrazza, G., G. Chiti, M. Mascini and M. Anichini, 2000, Detection of human apolipoprotein E genotypes by DNA electrochemical biosensor coupled with PCR, *Clin. Chem.* 46 (1), 31.
- Meric, B., K. Kerman, D. Ozkan, P. Kara, S. Erensoy, U.S. Akarca, M. Mascini and M. Ozsoz, 2002, Electrochemical DNA biosensor for the detection of TT and Hepatitis B virus from PCR amplified real samples by using methylene blue, *Talanta* 56, 837.
- Millan, K.L., A. Saraullo and S.R. Mikkelsen, 1994, Voltammetric DNA biosensor for cystic fibrosis based on a modified carbon paste electrode, *Anal. Chem.* 66, 2943.
- Millan, K.M. and S.R. Mikkelsen, 1993, Sequence-selective biosensor for DNA based on electroactive hybridisation indicators, *Anal. Chem.* 65, 2317.
- Millan, K.M., A.J. Spurmanis and S.R. Mikkelsen, 1992, Covalent immobilization of DNA onto glassy carbon electrodes, *Electroanalysis* 4, 929.
- Palecek, E. and M. Fojta, 2001, Detecting DNA hybridisation and damage, *Anal. Chem.* 73, 74A.
- Palecek, E., F. Jelen, C. Teijeiro, V. Fucik and T.M. Jovin, 1993, Biopolymer-modified electrodes in the voltammetric determination of nucleic acids and proteins at the sub-microgram level, *Anal. Chim. Acta* 273, 175.
- Palecek, E., R. Kizek, L. Havran, S. Billova and M. Fojta, 2002, Electrochemical enzyme-linked immunoassay in a DNA hybridisation sensor, *Anal. Chim. Acta* 469, 73.
- Pividori, M.I., A. Merkoçi and S. Alegret, 2001, Classical dot-blot format implemented as an amperometric hybridisation genosensor, *Biosens. Bioelectron.* 16, 1133.
- Schülein, J., B. Graßl, J. Krause, C. Schulze, C. Kugler, P. Müller, W.M. Bertling and J. Hassmann, 2002, Solid composite electrodes for DNA enrichment and detection, *Talanta* 56, 875.
- Wang, J., X. Cai, G. Rivas, H. Shiraishi, P.A.M. Farias and N. Dontha, 1996a, DNA electrochemical biosensor for the detection of short DNA sequences related to the human immunodeficiency virus, *Anal. Chem.* 68, 2629.
- Wang, J., X. Cai, B. Tian and H. Shiraishi, 1996b, Microfabricated thick-film electrochemical sensor for nucleic acid determination, *Analyst* 121, 965.
- Wang, J., X. Cai, J. Wang, C. Jonsson and E. Palecek, 1995, Trace measurements of RNA by potentiometric stripping analysis at carbon paste electrodes, *Anal. Chem.* 67, 4065.
- Wang, J., J.R. Fernandes and L.T. Kubota, 1998b, Polishable and renewable DNA hybridisation biosensors, *Anal. Chem.* 70, 3699.
- Wang, J., A.-N. Kawde and E. Sahlin, 2000, Renewable pencil electrodes for highly sensitive stripping potentiometric measurements of DNA and RNA, *Analyst* 125, 5.
- Wang, J., A.-N. Kawde, A. Erdem and M. Salazar, 2001, Magnetic bead-based label-free electrochemical detection of DNA hybridization, *Analyst* 126, 2020.

- Wang, J. and A.-N. Kawde, 2001, Pencil-based renewable biosensor for label-free electrochemical detection of DNA hybridization, *Anal. Chim. Acta* 431, 219.
- Wang, J., G. Liu and M.R. Jan, 2004, Ultrasensitive electrical biosensing of proteins and DNA: Carbon-nanotube derived amplification of the recognition and transduction events, *J. Am. Chem. Soc.* 126, 3010.
- Wang, J., G. Rivas and X. Cai, 1997a, Screen-printed electrochemical hybridisation biosensor for the detection of DNA sequences from the *Escherichia Coli* pathogen, *Electroanalysis* 9 (5), 395.
- Wang, J., G. Rivas, J.R. Fernandes, J.L.L. Paz, M. Jiang and R. Waymire, 1998a, Indicator-free electrochemical DNA hybridisation biosensor, *Anal. Chim. Acta* 375, 197.
- Wang, J., G. Rivas, C. Parrado, X. Cai and M.N. Flair, 1997b, Electrochemical biosensor for detecting DNA sequences from the pathogenic protozoan *Cryptosporidium parvum*, *Talanta* 44, 2003.
- Wang, J., D. Xu, A. Erdem, R. Polsky and M.A. Salazar, 2002, Genomagnetic electrochemical assays of DNA hybridization, *Talanta* 56 (5), 931.

Conducting Polymers for DNA Sensors and DNA Chips: from Fabrication to Molecular Detection

Pascal Mailley, André Roget and Thierry Livache

*Chimie de la Reconnaissance et Etude des Assemblages Biologiques, CREAB, UMR 5819
Spram (CEA, CNRS, UJF), CEA Grenoble 17 Avenue des Martyrs 38054 Grenoble cedex 9,
France*

Contents

1. Introduction	297
2. ECP-based genosensors: Design and fabrication	298
2.1. How to interface ECPs and DNA	298
2.1.1. The polyelectrolyte approach	298
2.1.2. DNA immobilisation through chemical or biochemical complexation	301
2.1.3. Covalent coupling of DNA and ECPs	301
2.2. How to process ECPs for DNA array fabrication	304
2.2.1. ECP modification of microelectrode arrays	306
2.2.2. ECP modification of homogeneous conducting substrates	307
3. DNA hybridisation detection at ECP–DNA interfaces	310
3.1. DNA hybridisation transduction at passive ECP interfaces	310
3.1.1. Label-based detection	310
3.1.2. Label-free hybridisation detection	314
3.2. ECP-based transduction	316
3.2.1. ECP-based homogeneous phase bioassays	317
3.2.2. DNA sensors based on ECP supports	318
4. Conclusions	324
List of abbreviations	325
References	325

1. INTRODUCTION

Electronically conducting polymers (ECPs) are an attractive class of materials that was extensively studied during the last decades for applications in the fields of molecular electronic and molecular actuators, energy storage, special coatings and sensing. This interest comes from their intrinsic properties related to their molecular structure that allows electronic conduction, their spectroscopic and electrochemical activities and finally their straightforward processing and modification. Since their first application to biosensing by [Foulds and Lowe \(1986\)](#) and [Umana and Waller \(1986\)](#), these properties have been widely used in the field of biosensing in terms of biomolecule immobilisation and transduction of the biomolecular recognition ([Bartlett and Cooper, 1993](#); [Gerard, 2001](#); [Cosnier,](#)

1999, 2003; Emr and Yacynych, 1995). These works were essentially devoted to enzyme immobilisation and wiring. However, Shimidzu (1987) first exposed the possibility to immobilise DNA on ECP interfaces and underlined the possible implication of ECP's electroactivity to DNA sensing. Following this preliminary work, studies in conjunction between ECPs and DNA were published more recently (Minehan *et al.*, 1994; Livache *et al.*, 1994). Since these first applications which were more dedicated to DNA immobilisation, there was a tremendous interest in these biomaterials including transduction strategies based on ECP's physico-chemical activity, development of new routes of DNA immobilisation and transposition to microelectronic devices. These numerous approaches finally gave rise to real biological applications in the fields of genetic or infectious diseases (Lopez-Crapez *et al.*, 2001; Cuzin, 2001; Maillart, 2004).

This contribution reviews the application of ECPs to the design of DNA sensors in terms of DNA immobilisation and hybridisation transduction. In the first part, we describe the different chemical and electrochemical immobilisation strategies, and the processing approaches to design surfaces bearing ECP-supported DNA probes especially in the field of parallel applications (DNA chips). In the second part, the different ways of detection are reviewed including labelling and label-free strategies. A particular highlight is given to ECP-based transduction approaches.

2. ECP-BASED GENOSENSORS: DESIGN AND FABRICATION

Two topics are developed in this chapter. In the first part, DNA immobilisation strategies are described including physisorption, entrapment and chemical grafting. The second part highlights how to process ECP–DNA biomaterials for the generation of DNA arrays.

2.1. How to interface ECPs and DNA

The tremendous interest for electronically conducting polymers comes from their numerous intrinsic properties, including electronic conductivity or electrochemical addressability, for example, that make them materials of choice for DNA immobilisation. More precisely, whatever is the ECP's nature, different ways of immobilisation could be envisaged including polyelectrolyte interactions owing to ECP's polycationic charge in their oxidised state, physical entrapment, complexation with ligand-functionalised polymers or chemical grafting either at a monomer unit or by post-functionalisation of the polymer backbone. Thus, the following parts will describe the different strategies involved in DNA immobilisation at ECP interfaces.

2.1.1. The polyelectrolyte approach

Electroconducting polymers are generally obtained through oxidative chemical or electrochemical polymerisation of a monomer unit in an electrolytic solution.

This polymerisation gives a polymer bearing positive charges in its oxidised form. Thereby, these positive charges may be used to capture polyanions such as DNA and oligonucleotides. This can be effected either by adsorption on the synthesised polymer or by entrapment during the polymer growth. On the other hand, one can functionalise the native backbone with pendant cationic groups to activate such interactions.

2.1.1.1. DNA adsorption at ECP interfaces. The adsorption is typically carried out on previously synthesised polymer films, eventually after treatment to ensure the presence of positive charges at least at the polymer surface. The electropolymerisation of pyrrole provides an electroconducting polymer PPy (polypyrrole) bearing delocalised positive charges along the chain axis. As DNA is a polyanion bearing fixed strong negative charges on its phosphate diester, some authors (Minehan *et al.*, 1994) assumed that the positive charges on the polypyrrole, due to their mobility, could be redistributed to maximise their interaction with DNA. This interaction could also be increased by hydrogen bonding with the NH group of pyrrole units. The possibility to exchange small anions for DNA must also be noticed. The authors studied the impact of the ionic strength, the buffer nature and the pH on adsorption kinetics of single- and double-stranded DNA. They also performed stability studies of this interaction: desorption, competition and reversibility of binding. Marx *et al.* (1994) extended this work to poly(3-hexyl thiophene) and poly(3-undecyl thiophene). Pande *et al.* (1998) and Minehan *et al.* (2001) have assessed the impact of the polymer film morphology (rough or smooth surface) on the interaction as well as general characteristics of the polymer film such as storage conditions, age or redox state. The study of DNA adsorption on a chemically synthesised polypyrrole (FeCl₃ oxidation) was achieved by Saoudi *et al.* (2000) in phosphate buffer solution by dielectric experiments and XPS (X-ray photoelectron microscopy). Some immobilisations were realised at more acidic pH (acetate buffer, pH 5.2) on electrosynthesised polypyrrole by Cai *et al.* (2003) and Saoudi *et al.* (1997). Calf thymus DNA was also adsorbed (Gambhir *et al.*, 2001) on PPy films doped with polyvinyl sulfone (PVS). The authors showed that even a polyanion like PVS can be exchanged easily with DNA. Following the works dedicated to DNA adsorption on potentiostatically grown polyaniline films reported by Lei *et al.* (2000), Wu *et al.* (2005) recently described a new nanocomposite biomaterial based on polyaniline intercalated graphite oxide enveloped in carbon paste electrode in which DNA was immobilised in presence of Tris buffer medium.

Finally, DNA immobilisation based on electrostatic physisorption at ECP interfaces exhibits three main advantages: simplicity of the immobilisation process, mild conditions of immobilisation and accessibility of the immobilised DNA. However, the obtained biofilms show poor stability that may lead to DNA desorption. Moreover, the adsorption of short ODN remains difficult and unstable. A method reported by Farace *et al.* (2002) could overcome this drawback but may limit DNA accessibility. Thus, adsorption of small oligonucleotides was realised on pre-synthesised polymer films and was followed by potentiodynamic deposition of a thin PPy sub-layer that includes ODN within the polymer host.

2.1.1.2. ECP–DNA aggregation complexes. Some studies described the interaction between soluble polythiophene derivatives and DNA leading to the formation of soluble spectroscopically active aggregates. Complexation of DNA was realised with luminescent zwitterionic polythiophene derivative (POWT) as described by Nilsson *et al.* (2003) and Nilsson and Inganäs (2003) or with cationic polythiophene prepared by chemical oxidation (Ho *et al.*, 2002 and Ho and Leclerc, 2004). In these cases, the authors used ammonium-substituted polymers that favour strong DNA–polymer interactions. Other studies were realised with autodoped polythiophene or PEDOT doped with polystyrene sulfonate and even with this *p*-doped polymer Yamamoto *et al.* (2000) showed that interaction with DNA occurred. Apart from biosensing researches, different works were initiated by Nagarajan *et al.* (2000). The authors took the advantage of DNA duplex to serve the biomolecules as a template for the biochemical synthesis of well-ordered highly conductive polyaniline nanowires (Nagarajan *et al.*, 2000). Moreover, the authors showed that, owing to polyaniline doping behaviour, it becomes possible to reversibly manipulate DNA duplex conformation (Nagarajan *et al.*, 2001). In this way, Ma and co-workers designed a pH-sensitive transistor based on the polyaniline nanowires bridging two gold nanoelectrodes (Ma *et al.*, 2004). Finally, such strategy was extended for the fabrication of various super-structured polypyrrole morphologies in solution (Bae *et al.*, 2004) and for the patterning of silicon surfaces with polypyrrole-ordered chains (Pike *et al.*, 2003).

2.1.1.3. DNA entrapment within ECPs. The interaction of oligonucleotides with electrochemically synthesised PEDOT/PEG or PEDOT/PVP films of different thicknesses was studied by Piro *et al.* (1999). In these conditions, incorporation of ODN increased with film thickness suggesting that small anionic molecules like ODN are incorporated into the bulk of the polymer in the conditions used for DNA adsorption at ECP interfaces. More usually, ODN entrapment is made by the same author during polymer electrosynthesis owing to the ability of ODN to dope the growing polymer due to the phosphodiester group.

The entrapment of biomolecules within ECP host matrices was first developed for proteins (Foulds and Lowe, 1986; Umana, 1986) or even whole cells (Deshpande and Hall, 1990) immobilisation during electrosynthesis in the presence of electrolytes that ensure the polymer electroneutrality (counterion). The entrapment of oligonucleotides was described by Wang *et al.* (1999) and Wang and Jiang (2000) without added electrolyte on a glassy carbon electrode. The authors assumed that the roles of counterion and electrolyte are accomplished by the oligonucleotide's charge as characterised by Electrochemical Quartz Crystal Microbalance (EQCM) experiments (Wang and Jiang, 2000). In these conditions, they obtained highly adherent conductive purple films. DNA entrapment in polypyrrole on platinum, Indium Tin Oxide (ITO)-coated glass and even stainless steel was done by Misoska *et al.* (2001) using mainly galvanostatic methods. This approach was extended by Cai (2003) and Xu *et al.* (2004) to the functionalisation of multi-walled carbon nanotubes using cyclic voltammetry. DNA was also entrapped in PEDOT microtubules by Krishnamoorthy *et al.*

(2004): oligonucleotide probes with lengths varying between 5 and 20 bases were immobilised during the electrosynthesis in a buffer medium. DNA entrapment in polypyrrole in the presence of a buffer was also described by Ramanaviciene and Ramanavicius (2004).

2.1.2. DNA immobilisation through chemical or biochemical complexation

In order to anchor DNA probes more firmly at ECP interfaces using mild conditions, a classical route deals with the use of ligand-functionalised polymer films. These ligands could initiate classical organo–inorganic complexation links but could be also based on biological interactions. In such a way, a polythiophene bearing biotin residue was first described by Marx *et al.* (1994). This work is based on the chemical synthesis, using ferric chloride as oxidative agent, of a polythiophene film bearing hydroxyl groups. The obtained polymer film was further biotinylated using hydroxyl pendant groups as precursors in order to design a DNA biosensor.

In order to functionalise electrode surfaces with biotin groups, Torres-Rodriguez *et al.* (1998), Cosnier (1999) and Cosnier and Le Pellec (1999) have described the synthesis and the electropolymerisation of biotinylated pyrrole monomers. In further development, Dupont-Fillard *et al.* (2001) proposed the preparation of a DNA biosensor based on the copolymerisation of pyrrole and a bifunctional compound, “pyrrole-biotin”. The obtained film was then saturated with avidin and finally biotinylated ODNs were immobilised owing to the recognition properties of avidin and biotin (Figure 1). This indirect method of immobilisation represents a generic approach that may be involved for the capture and detection of Polymerase chain reaction (PCR) products.

On the other hand, ODN immobilisation may be accomplished using inorganic complexes. Thereby, the electrochemical synthesis of poly(2,5-dithienylpyrrole) film, functionalised by a phosphonic acid group anchored in position 1 of the pyrrole unit (Figure 2), was described by Thompson (2003). Oligonucleotide immobilisation was effected through binding of the ODN probe via a cationic magnesium bridge between the polymer phosphonic group and DNA phosphate as described in Figure 3.

2.1.3. Covalent coupling of DNA and ECPs

Different methods were developed in order to increase the stability of the link between DNA and ECP. The main part of these methods is declined in the indirect mode for which ODN probes were chemically grafted following the electrochemical or chemical synthesis of polymer conductive films bearing reactive linkers. On the other hand, the ODN probes may be directly grafted through copolymerisation of ODN-functionalised monomers and unsubstituted units.

2.1.3.1. ECP's post-functionalisation with synthetic oligonucleotides. Different groups have prepared functionalised polypyrrole bearing an activated ester

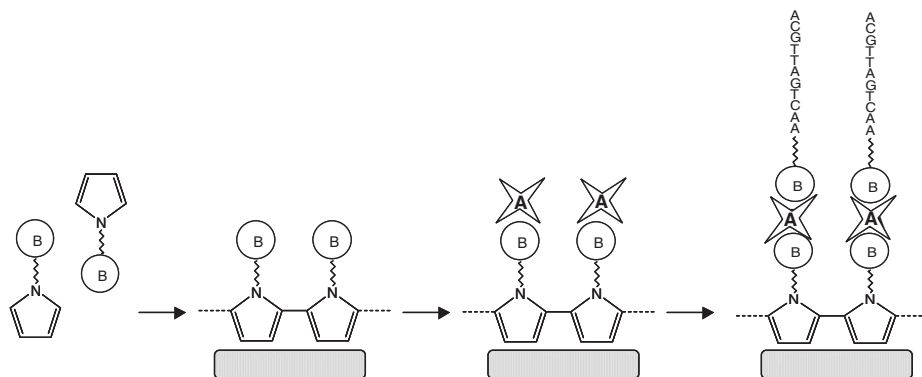


Fig. 1. Example of the use of a biotinylated ECP monomer (biotin-pyrrole) to construct a DNA sensor (Dupont-Filliard *et al.*, 2001).

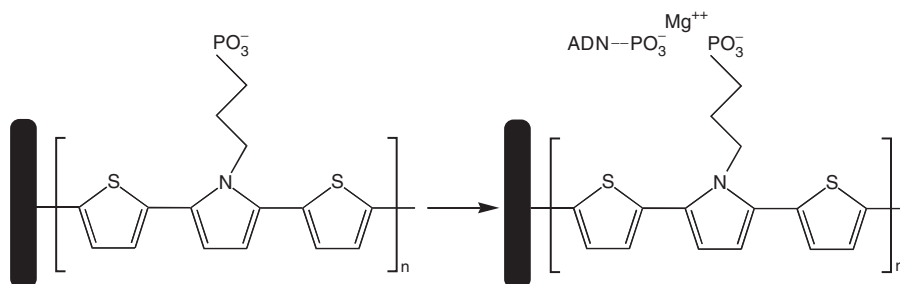


Fig. 2. DNA post-functionalisation of an ECP-modified electrode bearing complexation ligand (Thompson *et al.*, 2003).

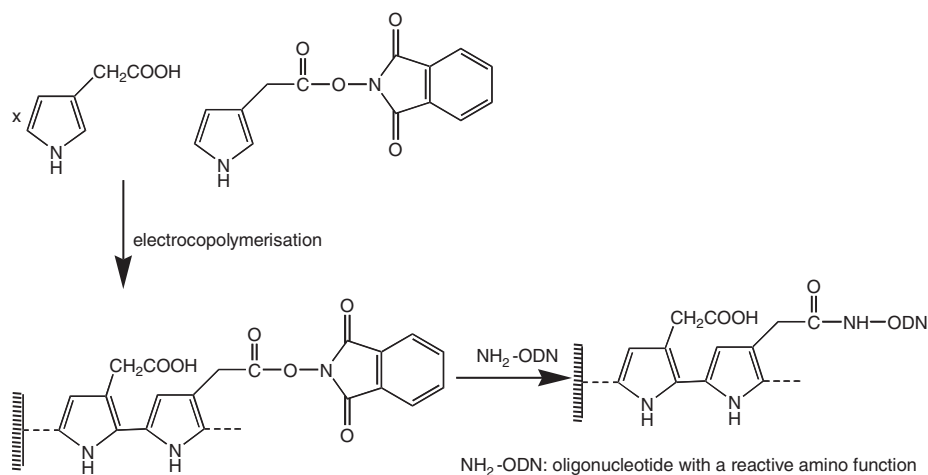


Fig. 3. DNA post-functionalisation of an ECP-modified electrode bearing NHS-activated ester allowing covalent grafting of 5'-aminated ODN (Korri-Youssoufi *et al.*, 1997).

that reacts with amine-modified ODN probes. Such works were initiated by Godillot *et al.* (1996) who studied the electrochemical polymerisation of 3-substituted pyrrole monomers. These works were first dedicated to the electrochemical surface modification with activated ester groups through electrodeposition of poly(3-NHS pyrrole) films. The authors demonstrated that the activated esters maintained their activity through chemical post-functionalisation with ferrocene bearing an amino group, the reliability of the anchoring process being revealed electrochemically. The NHS group suffering the lack of stability in aqueous medium was further replaced by *N*-hydroxyphtalimide. A copolymer of this activated ester and 3-acetic acid pyrrole was realised at 0.9 V/Saturated calomel electrode (SCE). Further reaction with a 5' amino-modified oligonucleotide led to ODN-substituted polypyrrole modified electrodes (Figure 3) (Korri-Youssoufi *et al.*, 1997). An extension of this work (Korri-Youssoufi and Makrouf, 2002) deals with the integration of a ferrocene group within the spacer arm between pyrrole and the activated ester group to design an electroactive DNA biosensor.

In the same way, poly(5-hydroxy-1,4-naphtoquinone-co-5-hydroxy-3-thioacetic acid-1,4-naphtoquinone) film was reacted with amino-modified oligonucleotides (Pham *et al.*, 2003). The use of polythiophene was also investigated via the electropolymerisation of 3-acetate *N*-hydroxyphtalimido thiophene and reaction of the resulting activated conducting film with an extra amino group of ODN (Cha *et al.*, 2003). Finally, some studies were carried out on polyaniline/polyacrylic acid composite polymer film (Gu *et al.*, 2004), amino-modified DNA being covalently linked to the carboxylic groups of polyacrylic acid.

2.1.3.2. ECP's post-functionalisation by (in situ) ODN synthesis. This is a particular method which was developed as a potential alternative to prepare biochips bearing a very high number of different oligonucleotide probes. In this case, contrary to the previously described post-functionalisation, oligonucleotides were built up on a polypyrrole film using an original chemistry derived from classical ODN synthesis (Figure 4). The latter was based on the principle described by Affymetrix (Fodor *et al.*, 1991) through an electrochemical deprotection step instead of a photochemical one to allow the elongation of the growing oligonucleotides. Thereby, this strategy involves the synthesis of phosphoramidite monomers bearing an electrolabile group in place of the acid (trityl) or photo (nitro veratryl) labile groups. As shown in Figure 4, these groups were cleaved on the support allowing the covalent coupling of the following monomer. In this way, this strategy could be implemented to polypyrrole-modified microelectrode arrays in the context of the design of high-density probe arrays.

2.1.3.3. ODN grafting by direct copolymerisation. Another method which allows the translation of electrode arrays into ODN arrays is based on the electrocopolymerisation of pyrrole with ODN covalently linked to pyrrole (Figure 5); in this case, the pyrrolylation of the ODN chain is carried out directly on the DNA synthesiser by adding a pyrrole-phosphoramidite building block (Livache *et al.*, 1994).

OLIGONUCLEOTIDE SYNTHESIS WITH ELECTROCHEMICAL DEPROTECTION

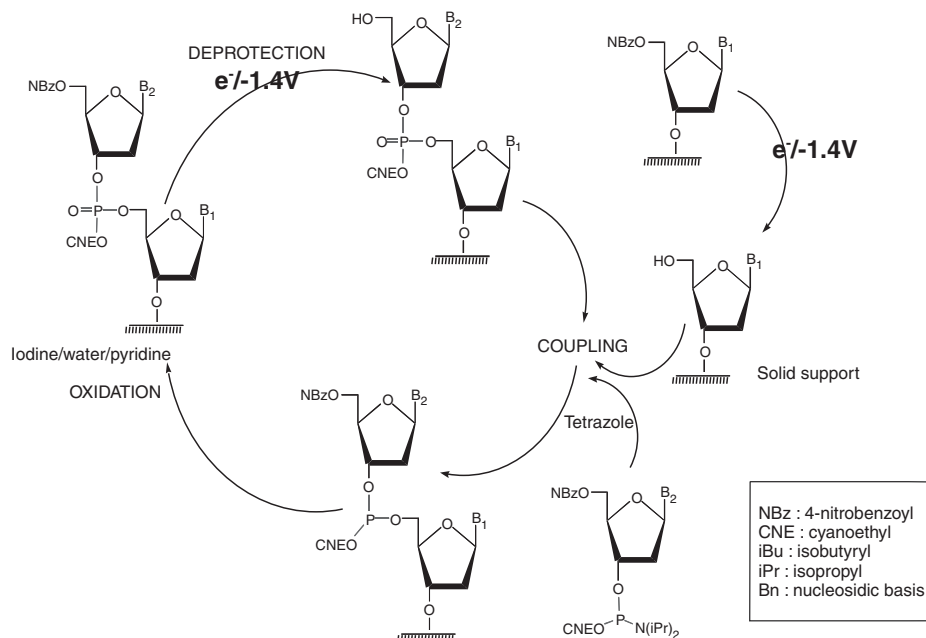


Fig. 4. In situ ODN synthesis at ECP interface directed by an electrochemical-based 5'-deprotection (Roget and Livache, 1999).

Successive copolymerisations of different oligonucleotides tethered to a pyrrole group carried out on a chip bearing an array of individually addressable microelectrodes, allow the construction of a DNA probe array (Livache *et al.*, 1998b). Due to the full control of the polymerisation conditions it becomes possible, by this way, to design highly reproducible biochips. In preliminary studies, the copolymerisation process was realised by cyclic voltamperometry (Livache *et al.*, 1994). However, further optimisation of the electrodeposition process showed that potential pulse method allows preparing reproducible coatings in terms of film thickness, ODN probes density and hybridisation detection (Guedon *et al.*, 2000). Copolymerisation of pyrrole and ODN-functionalised pyrrole appears particularly well suited for the design of low and medium complexity DNA biochips. Some interesting features, in comparison with post-functionalisation, deal with the direct and specific anchoring process of the ODN probes at electrified interfaces that brings electrode addressing or localised electrodeposition (as described in the following part), and with the perfect control of the amount of grafted oligonucleotides.

2.2. How to process ECPs for DNA array fabrication

In the field of classical biosensors, ECPs have been widely used in a “one analyte (one target), one experiment” approach. In this case, the support used is

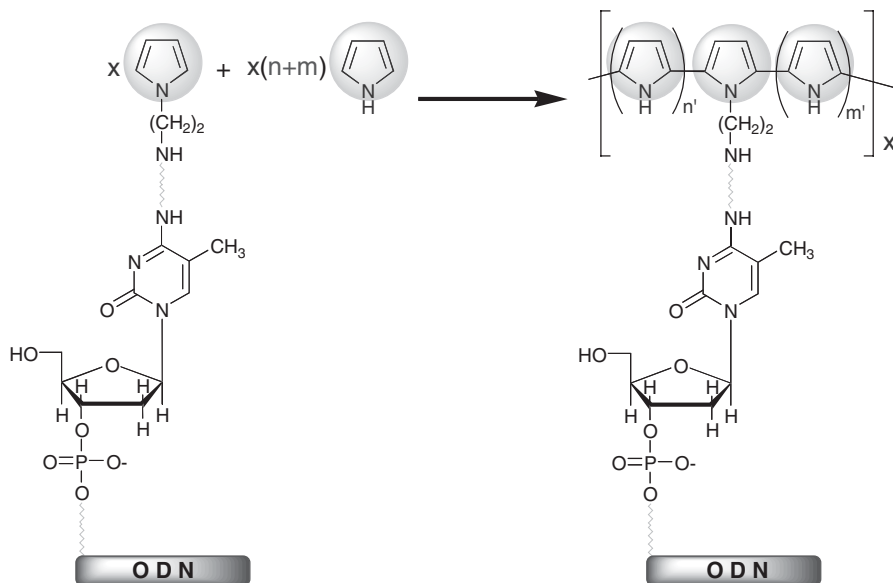


Fig. 5. Construction of ODN-grafted polypyrrole by copolymerisation of pyrrole and ODN tethered with a pyrrole moiety (Livache *et al.*, 1994).

an electrode; this electrode is dipped in an electrochemical cell and is then covered by the ECP layer using an electrochemical process (Figure 6a). The DNA can be “grafted and adsorbed” during this reaction or in a post-synthetic step. Many applications using this straightforward process have been described (Korri-Youssoufi *et al.*, 1997; Wang and Jiang, 2000). However, recent advances in microtechnologies applied to biology have prompted the development of highly parallel devices allowing a high biological analysis throughput. Among them the DNA microarrays which are a collection of systematically arranged probes grafted on a solid surface, can be used to interrogate a sample applied on the biochip leading to a “multiple analytes, one experiment” approach. In order to array DNA probes on a solid substrate to construct DNA chips, different approaches have been described (see Pirrung, 2002 for a review). Due to their specific properties, the ECPs have a special interest because (i) they can be a link between microelectronics and biology and (ii) they can be used as a transducing layer. In this way, low-complexity chips can be useful to integrate different control spots (negative, positive controls or calibration curve) into a classical biosensor analyses. The substrate for such electrochemical chips must be conductive; it involves the design of conducting surfaces that will be used as working electrodes. These surfaces can be homogeneous bearing only one electrode, or heterogeneous bearing a high number of individualised electrodes. In all cases, the major point to be solved deals with the addressing process that is to say the deposition of each probe in the specified location. This process will drive the spatial resolution and thus the complexity of the chip (number of different probes per surface unit).

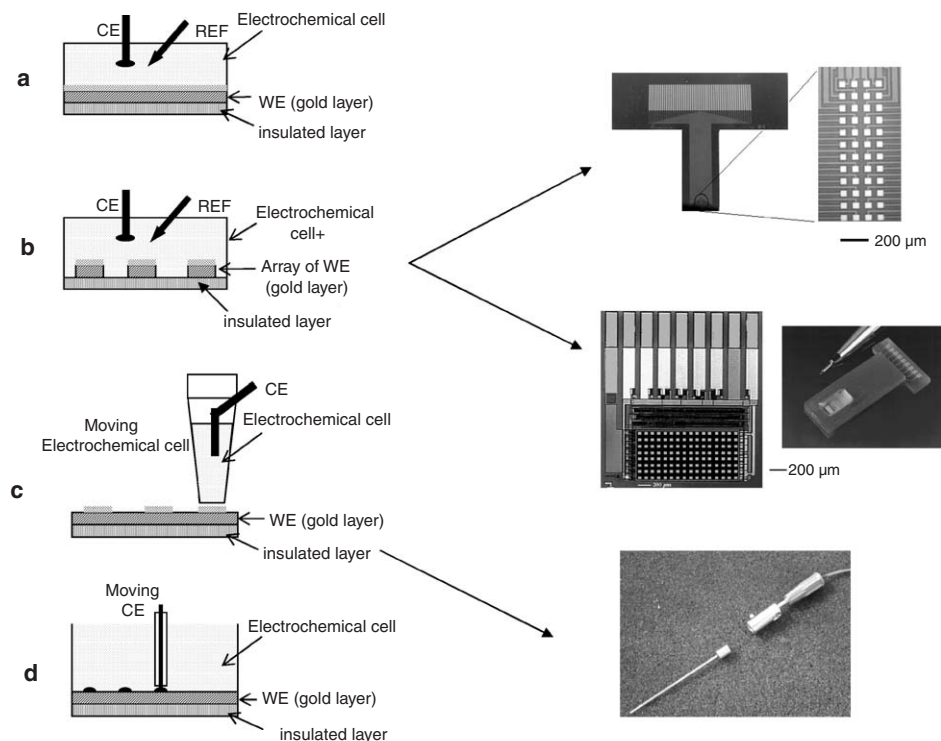


Fig. 6. Four examples of ECP processing; (a) macroelectrochemical cell and macroworking electrode, (b) macroelectrochemical cell and array of microworking electrode, (c) moving microelectrochemical cell and macroworking electrode, (d) SECM-based process using a mobile microcounterelectrode.

With this aim, different approaches have been developed; the first one is based on the use of chips bearing a microelectrode array where each microelectrode can be individually connected (Figure 6b). The second one used simpler substrate like homogeneous gold layer that implies to confine the electrical field in a precise location of the electrode.

2.2.1. ECP modification of microelectrode arrays

One of the major advantages of direct electrochemical-based DNA grafting approaches is that the growth of the polymer is limited to the electrode surface; the preparation of DNA arrays can then be done by successive polymerisation on a microelectrode array. Such an approach has been developed through the use of the copolymerisation process involving pyrrole and ODN bearing a pyrrole group. The first addressing bases were demonstrated on a four-electrode system made with four platinum wires included in a glass matrix (Livache *et al.*, 1994); the detection of DNA hybridisation was then carried out with radioactive labels.

Miniaturisation of the copolymerisation process was achieved by performing the polypyrrole syntheses on devices bearing microelectrodes. The copolymerisations were successively carried out on one addressed (connected) microelectrode; the chip was then rinsed out and another ODN grafting step was carried out on the next microelectrode. Potential step electropolymerisation rather than the classical scanning method was found to be more reproducible and faster. Two kinds of silicon chips were developed in collaboration with CEA/Leti, Grenoble-France. The first one was a 4 cm^2 passive chip bearing an array of 48 gold microelectrodes having a format of $50 \times 50\ \mu\text{m}^2$ arranged in a 4×12 matrix and including 48 gold contact pads ensuring external interconnection with the power supply (Figure 6b). The device is termed passive, that is to say one connection pad (and one track) is needed for each electrode. This silicon chip was used for the Hepatitis C virus genotyping involving a fluorescence-based detection process (Livache *et al.*, 1998b).

In order to reduce the number of external connections and the area of the chip, a multiplexed approach was chosen (Fiaccabrino *et al.*, 1994). Thereby, the second generation chip (Figure 6b) was a $3 \times 4\text{ mm}^2$ active multiplexed device bearing 128 electrodes with only nine gold Inputs/Outputs to minimise the global cost and simplify the packaging. The design of the chip has been optimised to be compatible with the electrochemical steps and the biological detection process. It means that the voltage applied during this step has to be fully withstood by the CMOS structure. Packaging of the chip (Figure 6b) is one of the key issues for this kind of CMOS chip which has to operate in a wet environment (Livache *et al.*, 1998a). These multiplexed chips have been used by Lopez-Crapez (2001) to check point mutations in the Kras gene of patients and are currently developed by Apibio-Biomerieux (France) (Cuzin, 2001). In order to decrease the cost of production, extension of this approach was proposed: it involves a parallel electrochemical DNA chip preparation directly on a $4'$ wafer, following the ODN grafting step, the chips are sawed and placed in a well of a microtiter plate (Caillat *et al.*, 2003). A simplified chip has also been recently designed by Apibio, it consists in a plastic card bearing eight working microelectrodes and integrated counter and reference electrodes ([www/apibio.fr](http://www.apibio.fr)). It can be used in conjunction with direct electrochemical detection of hybridisation events. A similar approach has been recently reported by Li *et al.* (2005), although the chemical grafting step of the DNA on the microelectrode is not well described, the authors can detect DNA hybridisation using AC-impedance spectroscopy.

2.2.2. ECP modification of homogeneous conducting substrates

The use of silicon microelectrode array as a multi-parametric device has proven to be a good interface with fluorescence or an electrochemical-based detection. However, if the device has to be used with other detection process such as optical-based technology, i.e. surface plasmon resonance (SPR) or optical wave guides, the array must be constructed on a specific substrate. In order to avoid the use of silicon chip, lithographic steps and complex connection system to deposit ECP's spots on a support, different approaches of ECP patterning have

been described. The first one deals with the nanodeposition of solubilised conducting polymer such as polypyrrole or self-doped sulfonated polyaniline via the use of “dip pen nanolithography” (Lim and Mirkin, 2002); however, no application dealing with the grafting of biomolecules was shown. The second approach deals with locally modified electrical fields allowing the addressing of electrochemical reactions. In this way, two main processes have been described involving the use of a moving microelectrochemical cell or based on the use of a scanning electrochemical microscope (SECM) to make electrochemical deposition on specified locations.

2.2.2.1. Structuration using mobile electrochemical cells. In a classical electrochemical process, the support bearing the working electrode, the counter electrode and the reference electrode are dipped in the solution contained by the electrochemical cell; that is to say that if an electrochemical polymerisation is carried out, the entire surface of the working electrode will be covered by the polymer (Figure 6a). The use of mobile miniaturised electrochemical cells that can move over the surface of the working electrode allows the limitation of the reactive area to the size of the electrochemical cell (Figure 6c). In this way, different electrochemical reactions can be carried out on a same working electrode (or working conducting surface). This process was described by Gheorghe *et al.* (2000) and Guedon *et al.* (2000). In the former paper, stainless-steel quills were used to deposit droplets of pyrrole; the polymerisation was carried out by applying a voltage between the quill and the substrate. The DNA can be integrated into the polymer by doping, however, the data about hybridisation results are not given. The latter paper (Guedon, 2000; Livache *et al.*, 2001) described the use of a micropipette tip as a moving electrochemical cell. The micropipette, including a platinum wire serving as counter electrode, was filled with the pyrrole solution (20 mM) bearing pyrrole-ODN (1–100 μM) and LiClO_4 (0.1 M). This electrochemical system was connected to a potentiostat and the micropipette tip was approached towards the working electrode using a micromanipulator. Once the solution was in contact with the interface, a stabilised potential was detected indicating the functioning of the electrochemical cell. Polymer films were formed by applying a potential pulse difference (between the substrate and the platinum wire in the microcell) of 2 V for 250–500 ms to the gold interface. Following the electrosynthesis the tip was emptied, rinsed with water and refilled. The diameter of the deposited pyrrole-ODN spot is about 600 μm and is limited by the size of the micropipette opening (verified through fluorescence imaging). When using smaller electrochemical pins, spots having a diameter in the range of 250 μm can be synthesised (Szunerits *et al.*, 2005). The *in situ* copolymerisation of each ODN probe allows further a good precision in localisation and thus a control of the probe density at the surface based on the ratio between pyrrole monomers and ODNs, plus a good precision on thickness owing to copolymerisation time control. The synthesis is also very fast since it takes only 500 ms to spot a 11-nm-thick polymer film. Thus this technology offers the possibility to design very thin films which are of the same size order than the immobilised probes; this giving rise to

a 2D-like surface structuration. The required quantities of biomolecules are furthermore very low. This together with the mild electrosynthesis conditions and the mechanical stability of the obtained films makes this immobilisation process a versatile tool for substrate modification with a range of biological probes including DNA or other biomolecules such as proteins or oligosaccharides. The “electrospot” DNA grafting process was used for the study by SPR imaging of DNA/DNA hybridisation (Guedon, 2000) or for DNA/protein interactions in the case of the study of p53 (Maillart *et al.*, 2004).

2.2.2.2. Structuration using scanning electrochemical microscopy. Another way to structure surfaces is to use the advantages of scanning electrochemical microscopy (SECM) (Szunerits *et al.*, 2004). The essence of this method is based on the generation of high concentrations of pyrrole radical cations in the gap between the gold substrate and the microelectrode (working in this case as a counter electrode) in order to deposit locally the conducting polymer. It followed the approach reported by Kranz *et al.* (1996) where local polymerisation was performed in a standard three-electrode configuration using a gold substrate as the working electrode (WE) and the microelectrode as the counter electrode (CE) in a macroelectrochemical cell (Figure 6d). In this case, it was used to construct polypyrrole towers on a conducting substrate. This approach necessitates furthermore that the microelectrode is close to the substrate (some micrometres) to concentrate the electrical field into a small area. The distance between the gold surface and the microelectrode was determined by recording the tip current at various distances from the substrate and constructing an approach curve to the surface. In order to be used for the construction of DNA arrays, once the electrode has been positioned, the cell must be filled with a mixture of pyrrole-ODN and pyrrole (Fortin *et al.*, 2005). The concentration of the pyrrole/pyrrole-ODN used had to be as high as 200 mM/10 μm to avoid the rapid consumption of the starting material in the gap which led to the demolishing of the formed polypyrrole-ODN film. The electropolymerisation was performed at 0.7 V vs. Ag^+/Ag using deposition times between 100–250 ms. To obtain homogeneous polypyrrole-ODN spots the microelectrode had to be placed at about 60 μm from the surface. Indeed, the spot size depends on the size of the microelectrode, the pyrrole concentration, the pulse time as well as on the distance z between surface and microelectrode. A compromise between the dimension of the formed spots size and the homogeneity of its surface has to be managed. A demonstration of 2D-polypyrrole structuration was carried out by monitoring the polymer synthesis in real time by SPR imaging (Szuneritz *et al.*, 2004). Another application of this SECM-based polypyrrole deposition is related to the synthesis of polypyrrole strips bearing gradient of grafted ODN (Fortin *et al.*, 2005).

All these conducting polymer processing methodologies can be chosen to be compatible with the detection process selected: a microelectrode array will be more convenient to use with an electrochemically based detection process, whereas a biological array constructed on a homogeneous conducting layer could be easier to integrate to an optical-based process.

3. DNA HYBRIDISATION DETECTION AT ECP–DNA INTERFACES

As discussed in the previous part of this contribution, ECP materials were applied to the design of genosensors owing to their ability to be chemically modified and to be electrochemically addressed at electrified interfaces. In such a way, ECPs represent a material class of choice for DNA or ODN immobilisation. However, the second topic associated with DNA biosensors and biochips deals with the end-point detection or real-time transduction of the hybridisation event. Thereby, detection or transduction methodologies could be based on DNA target labelling, including fluorophores, radioactive labels, redox markers or on label-free detection of the recognised target through DNA electrochemistry or piezoelectric and optical weighting. In the aforementioned cases, ECPs play a passive role in which it serves mainly as smart glue or eventually as electron relay. However, ECPs present their own physico-chemical activity (in terms of spectroscopic, visco-elastic or electrochemical properties, for example) that could impede the transduction process. On the other hand, one can take advantages of these physico-chemical properties. Thereby, ECPs may serve as photophysical labels in the case of DNA–ECP complexes formation in solution but also, when used as immobilisation matrices, they could be involved directly as reporting elements of the biosensitive interfaces. [Figure 7](#) summarises the involvement of ECPs in DNA hybridisation detection. The different routes of detection/transduction will be developed more completely in the following paragraphs.

3.1. DNA hybridisation transduction at passive ECP interfaces

3.1.1. Label-based detection

3.1.1.1. Non-electrochemical-based detection methods. Previously developed for molecular biology applications, radioactive or fluorescent approaches have been used in conjunction with DNA detection on conducting polymers since 1994 ([Minehan *et al.*, 1994](#) and [Livache *et al.*, 1994](#)) and since 1998 ([Livache *et al.*, 1998b](#)) for the radioactive and fluorescence approaches, respectively. The radioactive measurement was based on a ^{32}P labelling of the DNA, it allowed not only to detect the quantity of DNA hybridised but also to estimate the amount of DNA chains grafted on the support. Concerning the fluorescent detection, it has been carried out with a streptavidin–phycoerythrin conjugate to detect biotinylated PCR amplified DNA samples. This approach is fully compatible with a parallel detection and is currently applied on polypyrrole DNA chips ([Livache *et al.*, 1998a, b](#); [Lopez-Crapez *et al.*, 2001](#); [Cuzin, 2001](#)), a typical sensitivity is in the range of 10 pM of synthetic complementary target. When using these detection processes, the polypyrrole layer is used as a glue to stick locally the DNA chains on the electrodes and not as a polymer having electrical properties. In order to use the conducting properties of ECPs, an electrochemiluminescence-based DNA assay was designed by [Calvoz-Muñoz *et al.* \(2005\)](#). It involved the use of a copolymerised ODN pyrrole support; target

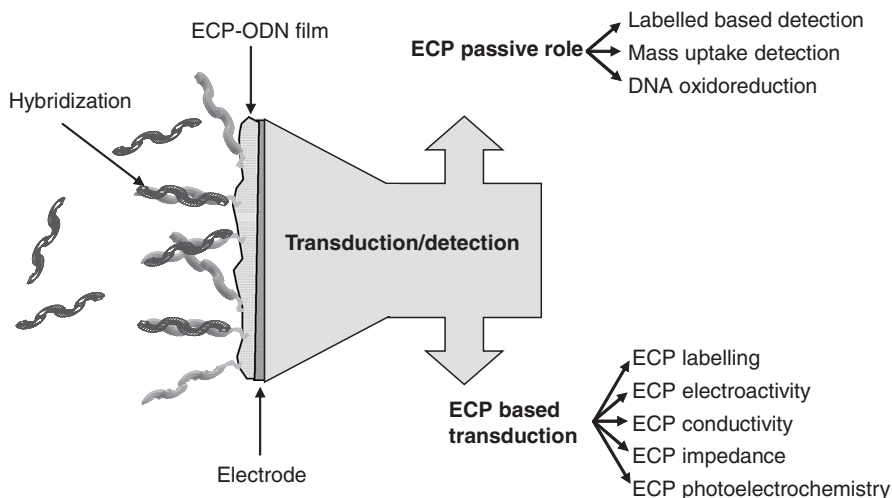


Fig. 7. Schematic of DNA-based biosensors and of the involvement of ECPs in transduction/detection methodology.

hybridisation was carried out with a biotinylated DNA and the Electrochemiluminescence (ECL) detection was performed by a biotinylated luminol derivative via a streptavidin link.

3.1.1.2. Electro-chemical based detection approaches. Electrochemistry is a simple and promising method suitable for the rapid detection of specific DNA sequence, combining high sensitivity, low cost and compatibility with micro-fabrication technology of transducers. One goal deals with obtaining an electrical signal that allows DNA detection at a reliable level competitive to fluorescence microscopy. Thereby, different electrochemical methods allowing, to a certain extent, signal amplifications have been developed in the literature. In all cases, these methods involve the association of the duplex with multiple redox markers through the use of redox intercalators, metal nanoparticles or redox enzymes. Thus, a local enhanced concentration of redox probes, at vicinity of the hybridisation event, is obtained that amplifies the electrical signal associated with biomolecular recognition. Actually, these methods were developed for DNA detection at immobilised-DNA monolayers and were extended to ECP-based DNA sensors. One has to take care of the compatibility of the electrochemical detection and the electrical/electrochemical characteristics of ECPs matrices that may be destroyed/modified by the detection process thus biasing the recognition signal.

Electrochemical labelling of the hybridisation event could be realised through the covalent grafting of a redox probe to the target DNA (Ihara *et al.*, 1997). Guisseppi-Elie *et al.* have demonstrated the feasibility of this detection method at polypyrrole-modified interfaces and for different strategies of DNA immobilisation, e.g. entrapment, ODN-modified monomers and post-functionalisation

(Lei, 2000a). During the detection step, the polypyrrole host matrix is maintained in its oxidised conductive state and then serves as an electron relay between the hybridised probes and the electrode surface. Moreover, the authors show that the hybridisation signal did not overlap with the redox process of the polymer host, thus giving rise to an acceptable signal-to-noise ratio.

Several groups have developed electrochemical genosensors using double-stranded DNA-specific binders such as redox intercalators or minor-groove binders (Takenaka, 2003). In such a way, Demeunynck *et al.* (Wang *et al.*, 2004) described a new pyridoacridone derivative bearing an amine group (Figure 8). This redox-active intercalator presents a half wave potential of -250 mV vs. Ag/AgCl (pH 7) that makes its utilisation as a redox indicator compatible with ODN-based biosensors.

Following polypyrrole technology developed by Livache *et al.* (1994), a DNA biosensor was fabricated and Figure 8 displays its voltamperometric response in DPV using this redox indicator following interaction with the polypyrrole-ODN copolymer, and after recognition with a non-complementary ODN target or with complementary strands of increasing length (10-, 20- and 40-mers). The DNA sensor response was markedly higher following hybridisation thus indicating a specific binding to the double strand. Moreover, the DPV response is amplified according to the increased number of intercalating places with the length of the duplex. This electrochemical detection was finally verified by fluorescence microscopy (Figure 8). However, signal amplification associated to intercalation is rather low since it is limited by the duplex length and so by the available intercalation positions (less than three intercalators by rotation of the duplex). Thereby, metal nanoparticles offer excellent prospects for DNA sensing owing to their optical, electrical and more particularly electrochemical properties when

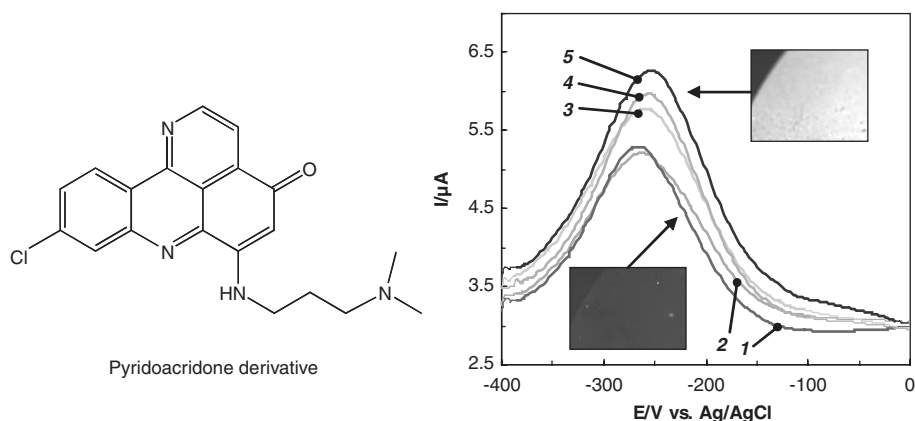


Fig. 8. Differential pulse voltammetry of pyridoacridone derivative. Electrochemical detection of DNA hybridisation using pyridoacridone derivative as redox probe on a Pt electrode modified by poly(Py-co-Py-ODN₄₀) film in the case of the pure poly(Py-co-Py-ODN₄₀) film (1), after interaction with 20nc non-complementary target (2) and after hybridisation with 10c (3), 20c (4), 40c (5) complementary ODN. Insets: Fluorescence images of the 20nc and the 40c responses following coupling with streptavidin-R-phycoerythrin.

used as redox indicator reservoir (Katz *et al.*, 2004). Cai *et al.* (2003) and Li *et al.* (2004) have demonstrated the reliability of metal nanoparticle labels, respectively, Cu/Au alloy nanoparticles and silver enhanced gold nanoparticles, for the electrochemical stripping detection of DNA hybridisation at ECP–DNA-modified interfaces.

In their work, Li *et al.* used poly(aminobenzoic acid) films in which pendant carboxylic groups were used as anchoring moieties for the ODN probes. The hybridisation detection is then based on a multi-step process that involves hybridisation of the ODN target with gold-labelled DNA targets followed by silver enhancement. The detection signal is then obtained through the direct anodic stripping of the deposited silver at a potential compatible with poly(aminobenzoic acid) matrix conductivity leading to the detection of synthetic ODN targets in the range 10 pM–10 nM. The authors applied this methodology to the detection of biotin-modified PCR amplicons using streptavidine–gold nanoparticle labels. Since the obtained signal to background ratio was low, the authors improved successfully this signal by introducing multiple biotin groups to the DNA during PCR. Contrary to Li *et al.*, Cai and co-workers proceeded to the indirect determination of Cu/Au alloy nanoparticles by measuring the amount of ionic Cu^{II} released in solution after oxidative treatment of the labels in 0.1 M HBr solution. The detection procedure (Figure 9) is then based on the hybridisation of adsorbed ODN probes at a polypyrrole interface by Cu/Au alloy nanoparticle-labelled DNA target followed by copper and gold dissolution in a microwell. The electrochemical detection is finally performed, after removing the probing electrode, on a bare glassy carbon electrode by anodic stripping voltammetry of copper. This indirect procedure allows enhancement, by a factor of 9, of the direct electrochemical stripping of the Cu/Au alloy nanoparticle leading to a limit of detection of 5 pM.

Alternatively, indirect electrochemical hybridisation detection can be accomplished using enzyme labels that generate an amplified signal via the production of electro-active compounds (Azek *et al.*, 2000), via electrode fouling (Alfonta *et al.*, 2001) or via enzyme-wiring (Caruana and Heller, 1999). Recently, Purvis *et al.* (2003) have designed ultrasensitive potentiometric immunosensors and genosensors (for more information see the commercial website of Sensor Tech Ltd., <http://www.sensortech-uts.com/>) based on coupling enzymatic activity of horseradish peroxidase labels with polypyrrole sensitivity towards local changes in ionic strength and pH. Figure 10 exemplifies the working function of such sensing methodology.

This sensor is based on potentiometric measurements and uses polypyrrole as signal relay to the recognition event (Figure 10). Thus, the biosensor detects enzyme-labelled immuno-complexes or enzyme-labelled DNA duplex formed at the surface of a polypyrrole coated screen-printed gold electrode. Detection is mediated by a secondary reaction that produces charged species. A shift in potential is measured at the sensor surface, caused by local changes in redox state, pH and/or ionic strength. The magnitude of the difference in potential is then related to the concentration of the formed receptor–target complex. In such a context, polypyrrole-supported-film morphology, thickness and quality are of primary importance. Thereby, a new electropolymerisation procedure,

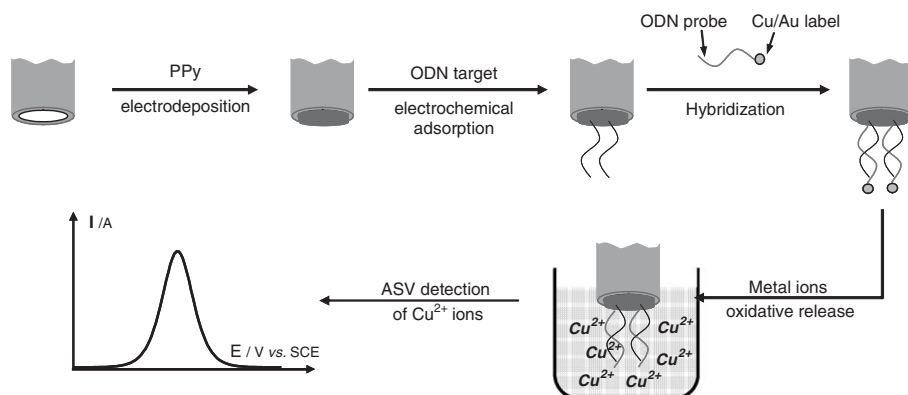


Fig. 9. Schematic representation of electrochemical procedures used by *Cai et al.* (2003) for nanoparticles-based hybridisation detection.

which warrants the sensitiveness of the ECP layer and involving Sodium dodecyl sulfate (SDS) as counterion, has been developed.

Finally, labelled detection procedures offer signal amplification compatible with trace detection. However, such methodologies involve multi-step detection that may introduce quantification errors and compromise real-time transduction of the recognition event.

In such a context, some works were focused on the direct label-free detection of DNA hybridisation using, for example, electrochemical oxidation of nucleic acids (*Jelen et al.*, 2002 and *Wang et al.*, 1997), microgravimetry (*Okahata et al.*, 1998; *Furtado and Thompson*, 1998) or optical detection such as SPR (*Lofas et al.*, 1991).

3.1.2. Label-free hybridisation detection

3.1.2.1. Mass or optical sensing on ECPs. Although the detection approaches described previously are quite sensitive, all of them need to label the DNA and/or are not very compatible with real-time monitoring of DNA interactions. For this purpose, three approaches have been developed and are based on mass sensing (Quartz crystal microbalance, QCM), on optical sensing (SPR) or on electrochemical sensing. Concerning the use of QCM, *Galasso et al.* (1998) and *Lassalle et al.* (2001a) described DNA hybridisation monitoring on a support bearing ODN covalently linked to polypyrrole by a copolymerisation process (Figure 11a). The sensitivity was in the range of 250 nM of the complementary ODN. A similar approach to detect DNA hybridisation was described by *Dupont-Filliard et al.* (Dupont-Filliard, 2001) using a regenerable surface based on a biotin–streptavidin recognition. However, if the DNA hybridisation monitoring by QCM is easy to carry out, the sensitivity remains lower than that found with other label-free methods; miniaturisation of the sensors is difficult and parallel detection possibilities are limited (*Livache et al.*, 2003). DNA polypyrrole matrices made by pyrrole copolymerisation have also been used

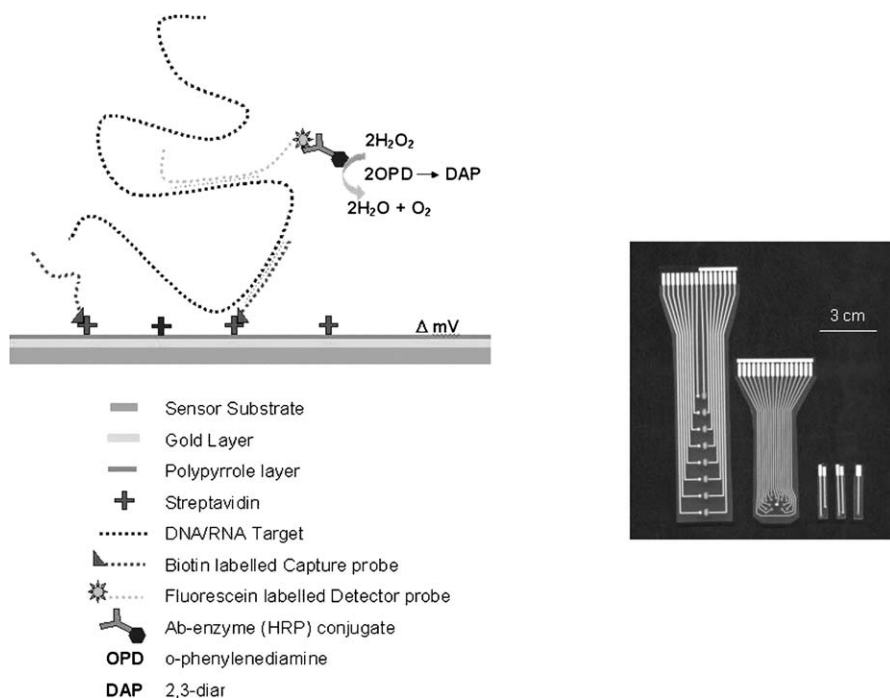


Fig. 10. Electrodes and detection procedure used by Purvis *et al.* (Sensor Tech Ltd., <http://www.sensortech-uts.com/>) for potentiometric ECP-based genosensors.

with surface plasmon resonance imaging; using this process, real-time, label-free, parallel detection can be carried out on DNA polypyrrole arrays (Guedon *et al.*, 2000). In an SPR imaging experiment, local changes in the reflectivity from a thin metal layer are recorded with a CCD camera and are exploited to monitor many different biological reactions occurring onto the molecules linked to the polypyrrole matrix. The use of conducting polymers to graft biomolecules on a gold layer for SPR imaging analysis is of special interest due to the possibility to control the thickness of the polymer during its synthesis (Livache *et al.*, 2001). The analytical sensitivity is in the range of 10 nM for a short synthetic complementary sequence. This approach can also be used to monitor the construction of double-stranded DNA chips that can be used to detect 25 DNA–protein (p53) interactions in parallel (Maillart *et al.*, 2004). Although this approach is very powerful, it cannot be fully integrated and, in this case, the polypyrrole grafting technology is just used as glue and as a convenient way to array biomolecules. Total integration of the detection process can be reached through the use of the conducting properties of the ECPs (Figure 11b).

3.1.2.2. Electrochemical sensing on ECPs. Electrochemical oxidation of electrochemically active nucleic bases, namely adenine and guanine, are studied since a long time (Dryhurst and Pace, 1970; Dryhurst, 1972; Brabec, 1981). The oxidation

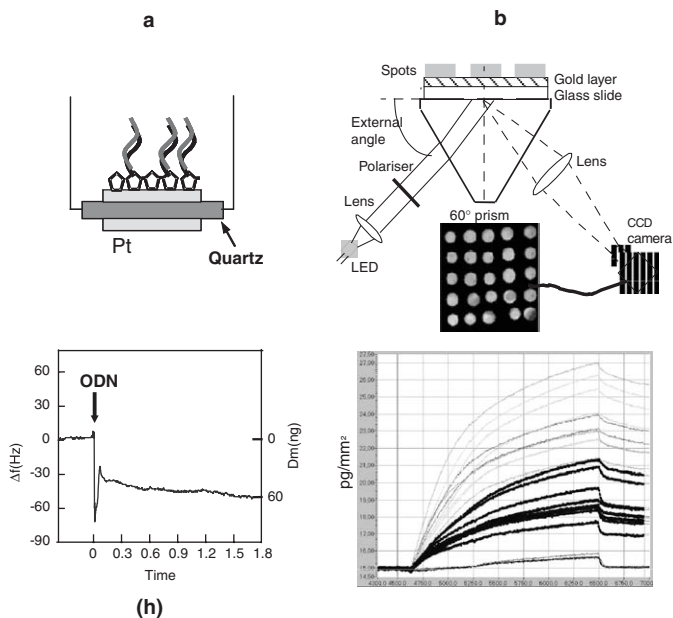


Fig. 11. Label-free detection processes associated with ECP chemistry: Examples of a quartz microbalance detection of a DNA hybridisation (**a** from Lassalle, 2001b) and a surface plasmon resonance imaging for the detection of DNA/p53 interactions (**b** from Maillart *et al.*, 2004).

process of guanine, due to its low oxidation potential (e.g. 0.66 V vs. SCE at pH 7.0) (Dryhurst and Pace, 1970) was used in DNA sensing through either direct oxidation at carbon (Wang *et al.*, 1997) electrodes or electrocatalytic oxidation using diffusing ruthenium complexes (Armistead and Thorp, 2000). Recently, Gu *et al.*, (2004) have described ssDNA probe's immobilisation at diamond electrodes coated with polyaniline/polyacrylic acid polymer films, the carboxylic acid residues of the polymer acting as binding sites for DNA attachment. Using cyclic voltammetry, the authors showed direct oxidation of both adenine and guanine in double-helix DNA at the modified diamond electrode. The recorded oxidation potentials were markedly lower than those typically reported for carbon and diamond electrodes and the authors ascribed this oxidation potential lowering to ECP matrix properties. In the same way, using adsorbed DNA probes at polyaniline intercalated graphite oxide nanocomposite, Wu *et al.* (2005) showed strong interaction between the nanocomposite electrode material and ssDNA or dsDNA that enables electrochemical DNA detection at low anodic and cathodic potentials.

3.2. ECP-based transduction

Away from the utilisation of ECPs as smart materials for biomolecule immobilisation, these molecular architectures present their own physico-chemical

behaviour which could be involved as integrated transducer. Then, ECPs have been involved in the design of biosensors and bioassays based on the modulation of the electrochemical or spectroscopic signals associated to the ECPs electroactivity or photoactivity by the recognition event. This sensing strategy was first reported in the pioneering works of Shimidzu (1987) and Emge and Bäuerle (1997) who have reported electrochemical signal modification respectively for the recognition of an ODN target by an immobilised probe or the detection of a nucleobase by its covalently anchored complementary base. The following paragraph reviews the different strategies involved in DNA hybridisation detection using ECPs as molecular transducer.

3.2.1. ECP-based homogeneous phase bioassays

Hybridisation detection has been performed on the basis of bioassays using ECP–DNA aggregates in solution. Indeed, the delocalised electronic structure of conjugated polymers is responsible for a strong absorption (and often emission) in the UV–visible range. Moreover, conjugated polymers may be sensitive to minor perturbations in their microenvironment, due to amplification by a collective system response thus opening a new field of transduction methods. Leclerc and collaborators have first proposed the use of polythiophene spectroscopic activity to detect biological interactions using avidin–biotin interactions as biological model (Faïd and Leclerc, 1996). Thus, the coupling of avidin to the biotinylated regioregular polythiophene backbone alters the geometry of the conjugated backbone inducing a red shift in the polymeric structure absorption spectra. This strategy has been extended to hybridisation detection by Leclerc and co-workers (Ho *et al.*, 2002) using water-soluble cationic polythiophenes as polymeric stains. Figure 12 displays biochromic detection of DNA hybridisation using DNA aggregation with these conjugated polyelectrolytes. The polymer *P1* shown in Figure 12 is soluble in aqueous media providing yellow colour mixtures. Such colour corresponds to a maximum of absorption at a shorter wavelength (397 nm) which is related to a random coiled conformation of the polymer backbone (Figure 12Ba and Ca). Upon the addition of oligonucleotide, the cationic polythiophene polyelectrolyte interacts strongly with the negatively charged biomolecules thus giving rise to P1–ODN complexes, the so-called duplex (Figure 12A), which absorbs light at higher wavelength (527 nm, Figure 12Bb and Cb). This red shift was attributed to an extended conjugation length of the polymer backbone that is spatially ordered upon interaction with ssDNA. This absorption spectra remain stable in presence of a non-complementary target (Figure 12Bd and Cd) thus highlighting that ODN probes conserve their specificity in DNA–ECP aggregates. Upon interaction with a perfectly matched ODN target, this spatial ordering is partially destroyed leading to a blue shift in the absorbance (Figure 12Bc and Cc). Moreover, this method enables discrimination between perfectly matched targets and single-mismatched targets, as exemplified in Figures 12Be and Ce, for which the absorption spectra displayed a mix of the two aforementioned spectra corresponding to ordered (non-hybridised) and disordered (hybridised) structures. The authors showed a detection limit at the micromolar level. Following the same

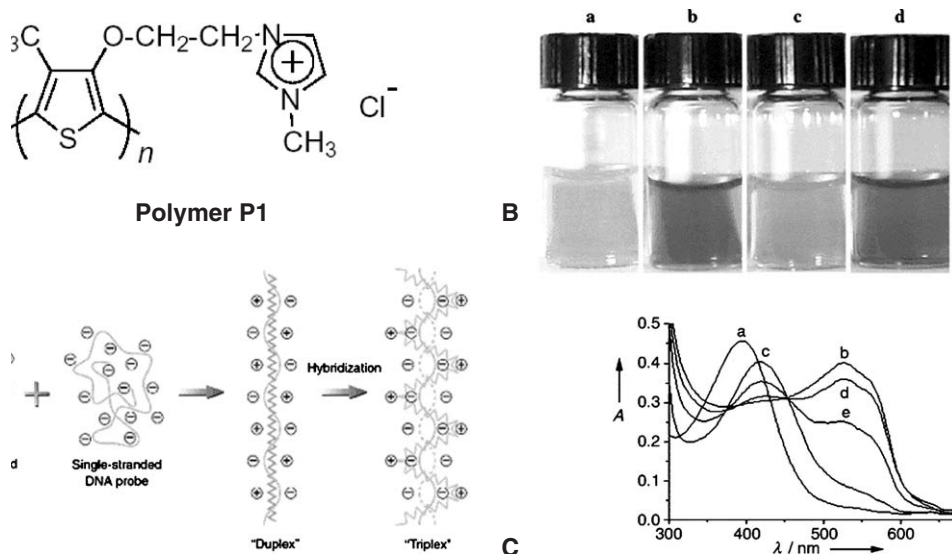


Fig. 12. Chemical structure of water-soluble cationic polythiophene **P1** used by Leclerc *et al.* (Ho and Leclerc, 2002) **A.** Synoptic of P1 aggregation with ss- and dsDNA. **B.** Photography and **C.** UV-visible spectra of P1 in solutions free of DNA (a), in presence of the 20-mer-long single-strand ODN probe (b), and after hybridisation with perfect (c), two-mismatch (d) and one-mismatch (e) complementary ODN targets at a temperature of 55°C.

methodology, but through the recording of polythiophene fluorescence, this detection limit could be decreased to a value of $2 \cdot 10^{-14}$ M of ODN target. In further developments, Leclerc *et al.* have shown the extension of this transduction tool to the use of aptamers for the selective detection of potassium ions and human α -thrombin at the femtomolar level (Ho and Leclerc, 2004).

On the same basis, a luminescent zwitterionic-polythiophene derivative (Figure 13A) has been synthesised by Nilsson *et al.* (2003) for chip and solution detection of DNA hybridisation. In the absence of ssDNA, polythiophene macromolecules form helical structures that emit light at a wavelength of 550 nm. Upon addition of ssDNA, the polyelectrolyte behaviour of the polythiophene derivative promotes backbone planarisation under interaction with ODN polyanions thus leading to a red shift in the fluorescence wavelength (i.e. 595 nm), the ratio in fluorescence intensities (540/595 nm) being directly related to the ssDNA concentration in solution. Then, the addition of complementary ODN targets to the ssDNA/polymer complex causes a blue shift of the maximum wavelength (285 nm) coupled to a huge increase in the fluorescence intensity. The authors have applied such a fluorescence enhancement to on-chip detection of DNA hybridisation using microfluidic as shown in Figure 13B.

3.2.2. DNA sensors based on ECP supports

DNA–ECP-based biosensors involve the immobilisation of DNA probes within or at the surface of ECP coatings deposited onto electrode surfaces. Thereby,

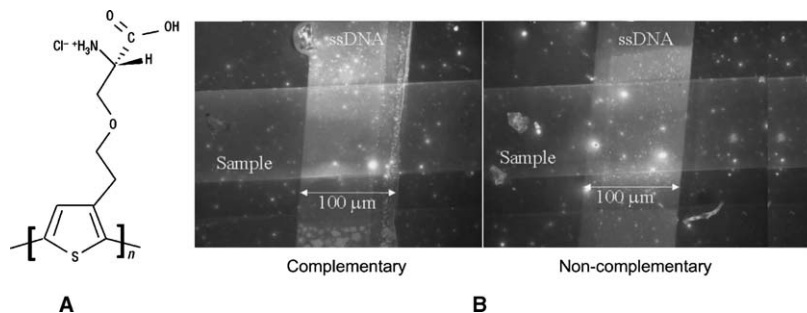


Fig. 13. Structure of water-soluble zwitterionic polythiophene used by Nilsson *et al.* (2003) (A). On-chip fluorescence detection of DNA hybridisation (B).

these ECP coatings may be electrically addressed and their electrochemical response may serve as hybridisation reporter. Three major routes can be exploited for ECP-based DNA hybridisation electrochemical detection. The first involves assessing changes in ionic exchange and/or redox properties of the ECP host using amperometry, voltamperometry or impedance microscopy. The second involves the intrinsic electrical conductivity of the polymer backbone and the latest relies on the photoelectrochemical properties of ECP semi-conductive polymers.

Following the pioneering works of Shimidzu (1987) and Emge and Bäuerle (1997), Garnier *et al.* (Korri-Youssoufi *et al.*, 1997) have first proposed the use of polypyrrole electroactivity as a transduction vector. The main problem concerns the design of polypyrrole films being, in the same time, functionalised with ODN probes and, also, exhibiting high and reproducible electrochemical activity in aqueous media. To answer this dual compartment, Garnier *et al.* synthesised 3-substituted polypyrrole films that allows ODN post-functionalisation of both bulk and surface of the host matrix. As shown in Figure 14A, the obtained ODN-functionalised film presents a remarkable electrochemical activity (curve a) at a potential of -200 mV/SCE . Upon addition of non-complementary target ODN in solution, the polymer signal is not affected (curve b) whereas after addition of increasing amounts of complementary target, the authors observed a depletion of the current response accompanied by a marked anodic shift of redox potential (curves c, d and e). More recently, Peng *et al.* (2005) described the same approach to detect DNA hybridisation using cyclic voltammetry and AC-impedance spectroscopy on a modified polypyrrole support. In an effort to obtain a more reliable signal and to decrease limits of detection, Korri-Youssoufi and Makrouf (2002) have further modified macromolecular materials used previously, and thus optimised signal sensitivity, through the integration of a ferrocene moiety within the linker arm between the polypyrrole backbone and the oligonucleotide target. Hybridisation response was then recorded through the voltamperometric signal of the ferrocene moiety at a potential of 300 mV/SCE . As previously observed by Garnier *et al.*, the voltamperometric signal of the host matrix was modulated by the hybridisation event thus giving rise to decay in the measured current and to an anodic shift of

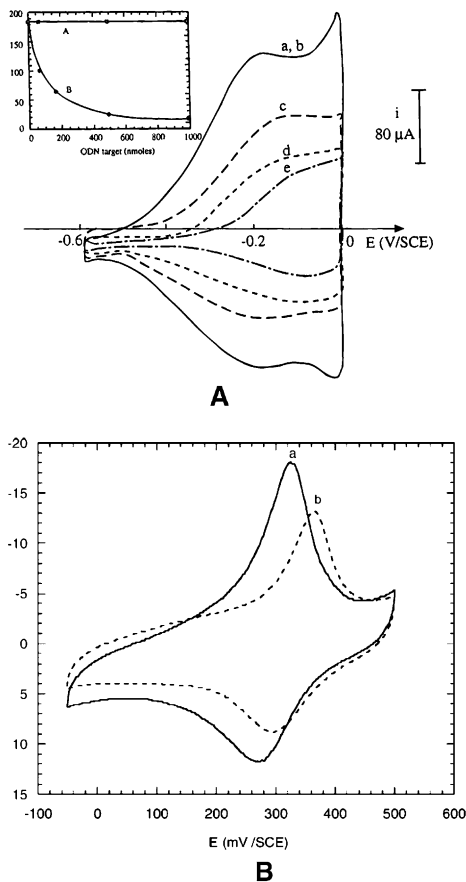


Fig. 14. (A) Voltamperometric response of DNA post-functionalised polypyrrole film in absence of DNA (a) in presence of a non-complementary target (b), and after incubation with increasing quantities (from 66 to 500 nmol) of complementary ODN targets (c, d and e). (B) Voltamperometric response of the same biomaterial functionalised with a ferrocene group after incubation in a solution containing 5 nmol of non-complementary target (a), and of complementary target (b).

the ferrocene redox potential (Figure 14B). Indeed, these changes in the electrochemical response of the polymer host may be attributed to two main contributions. First of all, these molecular materials are modified in their volume by large quantities of oligonucleotides (this quantity was estimated to 200 nmol for a thickness of 200 nm by Garnier *et al.*). Thereby, hybridisation could cause a large decrease in the permeability of the host matrix to doping anions. On the other hand, such modulation of the polypyrrole host signal may be attributed to conformational modification along the polymer backbone during its oxidation process. Indeed, such a conformational change is associated with the doping process of substituted polypyrroles which leads to a quinoid structure requiring the conjugated chains to become planar. Thus, any increase in the polymer host bulkiness and stiffness of ODN pendant groups following hybridisation may

induce a higher energetic constraint for the planarisation of the polyheterocycle backbone and hence, concomitantly, a lower electron transfer in the polypyrrole matrix after hybridisation and an increase of the oxidation potential value (McQuade *et al.*, 2000). The latter hypothesis is supported by the impact of the recognition length of the ODN target since it was accompanied by a larger shift in potential (Garnier *et al.*, 1999).

Using polythiophene backbone and same post-functionalisation strategy (Cha *et al.*, 2003) or phosphonic acid modified poly(2,5-dithienylpyrrole) post-functionalised with ODN probes through calcium dication complexation (Thompson *et al.*, 2003), similar behaviour in terms of current depletion was observed. Kumar and co-workers (Krishnamoorthy *et al.*, 2004) designed ECP-based DNA sensors through the direct entrapment of ODN probes as counter anions within the polymer matrix during the electropolymerisation process. Thus, DNA sensors were fabricated on micro-porous gold-coated polycarbonate membranes through the electropolymerisation of PEDOT containing DNA microtubes. These microtubes were grown within the membrane porosity until bridging of both gold-coated sides of the membrane. As already described by Garnier *et al.*, the authors observed a large decrease in the voltamperometric response of the polymer host after hybridisation. Moreover, owing to the geometry of the designed sensors, the conductivity of PEDOT microtubes can be assessed in respect of the hybridisation state. Thus, the polymer backbone conductivity decreased markedly with the complementary target concentration and remained stable upon the addition of a non-complementary ODN strand as proposed by Garnier *et al.* However, the aforementioned works involve bulk modification of the host matrix with ODN probes and, after surface functionalisation only, the ECP materials may respond differently to hybridisation. Thereby, Pham *et al.* have described post-functionalisation of poly(-hydroxy-1,4-naphthoquinone-co-5-hydroxy-3-thioacetic acid-1,4-naphthoquinone) (2003). The aforementioned polymer was obtained by electrocopolymerisation and exhibits a strong, but rather complex, redox signal at a potential of -0.5 V/SCE related to entrapped quinonic groups. Following functionalisation of the polymer coating with ODN probes, the authors recorded a marked decrease of the polymer voltamperometric response. The biosensor response remains stable following interaction with non-complementary targets but increased markedly upon interaction with complementary targets to tend to the native signal associated to the unmodified matrix. Such compartment was mechanistically described by the authors (Piro *et al.*, 2005) and was attributed to the transition from probes Flory coils, which occupied nearly 60% of the polymer surface and thus hindered counterion exchange along polymer redox process, to organised duplex structures that leads to a decrease in surface coverage, from a factor of 4.5, more favourable for counterion diffusion. A similar behaviour was observed by Lee and Shim (2003) for a post-functionalised poly (3'-carboxyl-5, 2', 5', 2''-terthiophene) through recording of the hybridisation event using AC-impedance microscopy. The authors have then recorded a decrease in the polymer-electrolyte interface impedance (that was maximum at an excitation frequency of 100 Hz) after hybridisation and have also shown the possible discrimination of single-point mutations. More recently, Xu and co-workers (2004)

have implemented AC-impedance spectroscopy to DNA hybridisation detection using ODN probes entrapped within a polypyrrole host matrix electrochemically grown onto carboxylic group-functionalised multi-walled carbon nanotubes modified electrode. The authors showed a sensitive decrease in the bio-interface complex impedance as already mentioned. This impedance decay, that is essentially due to a decrease in its real component, is easily readable over a large range of frequencies (Figure 15a and b) but can be markedly optimised by a factor of 3 (Figure 15c) via dsDNA metallisation through Zn^{2+} doping into the dsDNA (Figure 15c) thus allowing the discrimination of one mismatched base. The authors attributed the aforementioned larger decrease in real impedance to the higher conductivity of metallated dsDNA that allows an increase in DNA's electronic transfer rate.

Another strategy to detect DNA hybridisation deals with recording the transient amperometric response of DNA-ECP assemblies to ODN targets in solution. Wang *et al.* (1999) have first proposed this detection route for DNA biosensors based on direct entrapment of poly(dG)₂₀ or poly(dA)₂₀ ODN probes (used here as counterion) during polypyrrole growth. The authors have shown that, in its oxidised state, the ECP biocomposite material is highly sensitive to the adjunct of ODN targets in the solution and, moreover, that the obtained transient response is clearly dependent upon the target sequence (Figure 16a). So, both sensors display upward peaks upon spiking the non-complementary target and opposite peaks upon addition of the complementary strands whereas no reliable signal was obtained for DNA free polypyrrole film. The obtained sensor presents then a unique yes or no response which is moreover amplitude dependent on target ODN concentration (Figure 16b). However, the signal quantification remains difficult since it depends clearly on the nature of the immobilised sequence as exemplified by the difference in transient amperometric response between poly(dG)₂₀ or poly(dA)₂₀ ODN probes (Figure 16b). Finally, the authors have further developed this biosensor concept to the detection of short ODN targets in presence of chromosomal DNA (Wang and Mukherjee, 2001).

More recently, Ramanavicius *et al.* (Ramanaviciene and Ramanavicius, 2004) proposed the use of pulse amperometric detection to detect DNA hybridisation at entrapped-DNA polypyrrole-modified platinum electrodes. The applied signal consists here in a series of 10 potential step cycles including a first step at 600 mV vs. Ag/AgCl followed by a second pulse at 0 V vs. Ag/AgCl. The authors recorded a significant decrease in the pulse amperometric signal following hybridisation. These results were correlated to interface impedance changes passing from single-stranded probe to duplex as already described by Farace *et al.* (2002) and patented by Motorola Inc. (Gaskin *et al.*, 2001).

Electrochemical DNA biosensors based on ECP reporting generally involved the electrochemical or impedance behaviour of ECP-DNA films. However, in its reduced state, polypyrrole is a p-type semi-conductor that generates photocurrent upon light excitation. This polypyrrole photoelectrochemical response is strongly dependent on its redox state and, more interestingly, on its physico-chemical environment. This property was therefore investigated for the detection of DNA hybridisation events of ODN probes covalently linked to

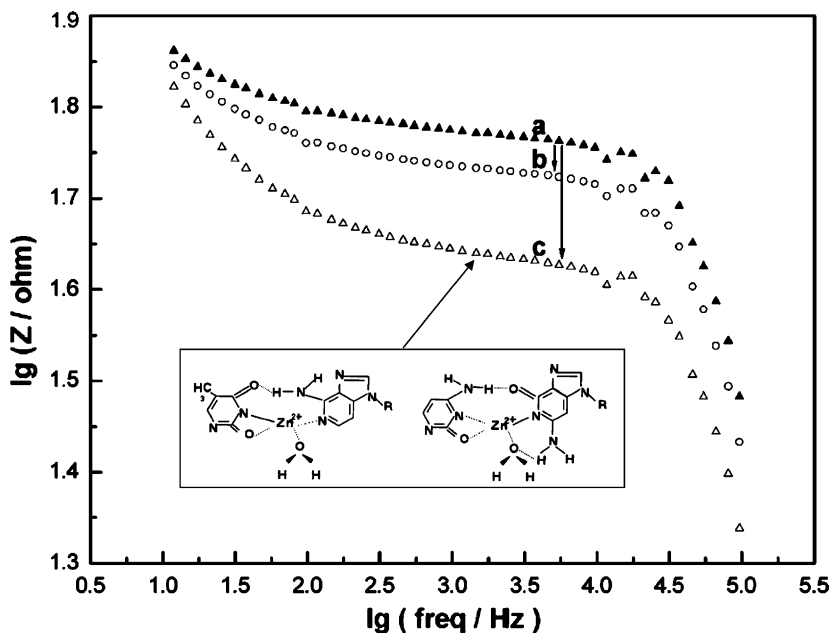


Fig. 15. AC impedance response of polypyrrole-DNA functionalised carbon-nanotube modified electrode for (a), ssDNA polypyrrole film, (b), dsDNA polypyrrole film and (c), metallated dsDNA polypyrrole film (Xu *et al.*, 2004).

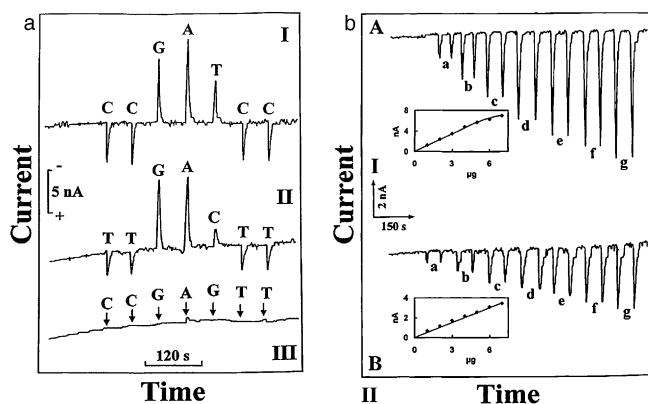


Fig. 16. Amperometric response (a) and calibration (b) of polypyrrole-DNA biosensor after addition of poly(dG)₂₀, poly(dA)₂₀, poly(dC)₂₀ and poly(dT)₂₀ ODN targets in the case of PPy-poly(dG)₂₀ (I), PPy-poly(dA)₂₀ (II) and PPy films (III) (Wang *et al.*, 1999).

polypyrrole copolymer films by Lassalle and co-workers (Lassalle *et al.*, 2001c). The spectral photocurrent response of a polypyrrole-ODN film before (Figure 17A, curve 1) and after interaction with complementary (Figure 17A, curve 2) and non-complementary (Figure 17A, curve 3) ODN targets is presented in Figure 17A. Whereas, polypyrrole-ODN film shows rather similar behaviour in

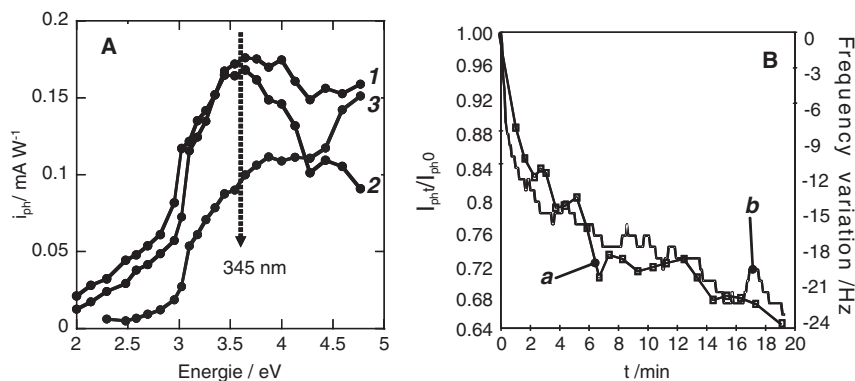


Fig. 17. (A) Normalised photocurrent spectra of polypyrrole-ODN films in a PBS solution free of ODN target (*I*), and after interaction with non-complementary ODN target (2) and complementary sequence (3) (Lassalle *et al.*, 2001a). (B) Real-time monitoring of DNA hybridisation followed by photocurrent spectroscopy ($\lambda = 340$ nm, *a*) and by quartz crystal microbalance (*b*) (Lassalle *et al.*, 2001c). Time 0 data correspond to the injection of the complementary target within the solution of analysis, target concentration = 100 nM, no imposed voltage, PBS buffer.

a solution free of ODN and after interaction with non-complementary strand, the recorded photocurrent, especially at a wavelength of 340 nm, is much lower following hybridisation. The spectral responses of the three configurations were analysed using Gärtner's model. Since the three configurations give similar band gap energy, the authors assume that the physico-chemical phenomenon responsible of photocurrent lowering after hybridisation is related to the modulation of minority carrier mobility. Moreover, by applying a fixed wavelength of 340 nm, it becomes possible to perform the real-time transduction of the hybridisation event (Figure 17B). Thus, following injection in the solution of the complementary target, a decrease of the photocurrent was recorded (black curve), that fits perfectly QCM microgravimetric real-time recording of DNA hybridisation (Lassalle *et al.*, 2001a, d).

4. CONCLUSIONS

Interfacing ECPs and DNA offer several advantages in the field of sensor design; the first one is the possibility to modify the polymer during or after its synthesis process in order to construct specific electrodes or support bearing many different DNA sequences. The processing step allows also tuning the ECP properties to fit in them with the needs of the detection approach chosen: very thin 2D film can be obtained for a SPR-based detection process or highly conducting film can be constructed if redox organics is used. Moreover, the limitation of the electrochemical reaction to the surface of an electrode allows the possibility to locally address an electro-grafting reaction on microelectrode arrays resulting in the translation of a microelectrode array into a biological array. In terms of detection

of biorecognition, these polymers are compatible either with “classical” approaches including radioactivity, fluorescence and enzymatic detection process or with more specific approaches involving electrical parameters (redox, changes of electrical properties). In this way, the electrochemical approach can be used both to write and to read the information. This latter property allows these sensors to be easily integrated in a device bearing microfluidic channels to lead to integrated analysis tool such as lab-on-a-chip. In a more general point of view, due to the possibility of addressing biomolecules or DNA on very small electrodes, new applications of DNA/ECP systems will probably occur in the near future in the field of nanoscience where the ability to address nanomaterial such as nanotubes or nanoparticles on precise locations remains one of the key points to be solved. In this way, the conjunction of DNA biological interfaces and ECP chemistry can be helpful towards the organization of such nanocompounds.

LIST OF ABBREVIATIONS

ASV	Anodic stripping voltammetry
DPV	Differential pulse voltammetry
dsDNA	double-stranded DNA
ECL	Electrochemiluminescence
ECP	Electroconducting polymer
ITO	Indium tin oxide
NHS	<i>N</i> -hydroxy succinimide
ODN	Oligodeoxynucleotides
PCR	Polymerase chain reaction
PEDOT	Poly(ethylenedioxythiophen)
QCM	Quartz crystal microbalance
SCE	Saturated calomel electrode
SDS	Sodium dodecyl sulfate
SECM	Scanning electrochemical microscopy
SPR	Surface plasmon resonance
ssDNA	single-stranded DNA
XPS	X-ray photoelectron microscopy

REFERENCES

- Alfonta, L., A.K. Singh and I. Willner, 2001, Liposomes labeled with biotin and horseradish peroxidase: A probe for the enhanced amplification of antigen–antibody or oligonucleotide-DNA sensing processes by the precipitation of an insoluble product on electrodes, *Anal. Chem.* 73, 91–102.
- Armistead, P.M. and H.H. Thorp, 2000, Modification of indium tin oxide electrodes with nucleic acids: Detection of attomole quantities of immobilized DNA by electrocatalysis, *Anal. Chem.* 72, 3764–3770.

- Azek, A., C. Grossiord, M. Joannes, B. Limoges and P. Brossier, 2000, Hybridization assay at a disposable electrochemical biosensor for the attomole detection of amplified human cytomegalovirus DNA, *Anal. Biochem.* 284, 107–113.
- Bae, A.H., T. Hatano, M. Numata, M. Takeuchi and S. Shinkai, 2004, Higher-order conformations of DNA are useful templates to create various superstructural poly(pyrrole) morphologies, *Chem. Lett.* 33, 436–437.
- Bartlett, P.N. and J.M. Cooper, 1993, A review of the immobilization of enzymes in electropolymerized films, *J. Electroanal. Chem.* 362, 1–12.
- Brabec, V., 1981, Nucleic acid analysis by voltammetry at carbon electrodes, *Bioelectrochem. Bioenerg.* 8, 437–449.
- Cai, H., Y. Xu, P.-G. He and Y.-Z. Fang, 2003, Indicator free DNA hybridization detection by impedance measurement based on the DNA-doped conducting polymer film formed on the carbon nanotube modified electrode, *Electroanalysis* 15, 1864–1870.
- Cai, H., N. Zhu, Y. Jiang, P. He and Y. Fang, 2003, Cu@Au alloy nanoparticle as oligonucleotide labels for electrochemical stripping detection of DNA hybridization, *Biosens. Bioelectron.* 18, 1311–1319.
- Caillat, P., Cuzin, M., and Hofmeister, A., 2003. Wafer scale biomolecule grafting: The first step for low cost, high throughput active biochip manufacturing, *Electron Devices Meeting, 2003. IEDM 03 Technical Digest, IEEE Int.* 8–10(Dec.), 31.4.1–31.4.4
- Calvoz-Muñoz, M.-L., A. Dupont Filliard, M. Billon, S. Guillerez, G. Bidan, C. Marquette and L. Blum, 2005, Detection of DNA hybridization by ABEI electrochemiluminescence in DNA-chip compatible assembly, *Bioelectrochemistry* 66, 139–143.
- Caruana, D.J. and A. Heller, 1999, Enzyme amplified amperometric detection of hybridization and of a single base pair mutation in a 18-base oligonucleotides on a 7- μ m-diameter microelectrode, *J. Am. Chem. Soc.* 121, 769–774.
- Cha, J., J.I. Han, Y. Choi, D.S. Yoon, K.W. Oh and G. Lim, 2003, DNA hybridization electrochemical sensor using conductive polymer, *Biosens. Bioelectron.* 18, 1241–1247.
- Cosnier, S., 1999, Biomolecule immobilization on electrode surfaces by entrapment or attachment to electrochemically polymerized films. A review, *Biosens. Bioelectron.* 14, 443–456.
- Cosnier, S., 2003, Biosensors based on electropolymerised films: New trends, *Anal. Bioanal. Chem.* 377, 507–520.
- Cosnier, S. and A. Le Pellec, 1999, Poly(pyrrole-biotin): A new polymer for biomolecule grafting on electrode surfaces, *Electrochim. Acta* 44, 1833–1836.
- Cuzin, M., 2001, DNA chips: A new tool for genetic analysis and diagnostics, *Transfus. Clin. Biol.* 8, 291–296.
- Deshpande, M.V. and E.A.H. Hall, 1990, An electrochemically grown polymer as an immobilization matrix for whole cells: Application in an amperometric dopamine sensor, *Biosens. Bioelectron.* 5, 431–448.
- Dryhurst, G., 1972, Electrochemical determination of adenine and adenosine: Adsorption of adenine and adenosine at the pyrolytic graphite electrode, *Talanta* 18, 769–787.
- Dryhurst, G. and G.F. Pace, 1970, Electrochemical oxidation of guanine at the pyrolytic graphite electrode, *J. Electrochem. Soc.* 117, 1259–1264.
- Dupont-Filliard, A., A. Roget, T. Livache and M. Billon, 2001, Reversible oligonucleotide immobilization based on biotinylated polypyrrole film, *Anal. Chim. Acta* 449, 45–50.
- Emge, A. and P. Bäuerle, 1997, Synthesis and molecular recognition properties of DNA- and RNA-base-functionalized oligo- and polythiophenes, *Synth. Met.* 84, 213–214.
- Emr, S.A. and A.M. Yacynych, 1995, Use of polymer films in amperometric biosensors, *Electroanalysis* 7, 913–923.
- Faïd, K. and M. Leclerc, 1996, Functionalized regioregular polythiophenes: Towards the development of biochromic sensors, *Chem. Commun.* 1761–1762.
- Farace, G., G. Lillie, T. Hianik, P. Payne and P. Vadgama, 2002, Reagentless biosensing using electrochemical impedance spectroscopy, *Bioelectrochemistry* 55, 1–3.
- Fiaccabrino, G.C., M. Koudelka-Hep, M. Jeannret, A. Van den Berg and N.F. de Rooij, 1994, Array of individually addressable microelectrodes, *Sens. Actuat. B* 18–19, 675–677.

- Fodor, S.P.A., J.L. Read, M.C. Pirrung, L. Stryer, A.T. Lu and D. Solas, 1991, Light-directed, spatially addressable parallel chemical synthesis, *Science* 251, 767–773.
- Fortin, E., Y. Defontaine, P. Mailley, T. Livache and S. Szunerits, 2005, Micro-imprinting of oligonucleotides and oligonucleotide gradients on gold surface: A new approach based on the combination of Scanning Electrochemical Microscopy and Surface Plasmon Resonance imaging (SECM/SPR-i), *Electroanalysis* 17, 495–503.
- Foulds, N.C. and C.R. Lowe, 1986, Enzyme entrapment in electrically conducting polymers, *J. Chem. Soc. Faraday Trans. 1*(82), 1259–1264.
- Furtado, L.M. and M. Thompson, 1998, Hybridization of complementary strands and single-base mutated oligonucleotides detected with an on-line acoustic wave sensor, *Analyst* 123, 1937–1945.
- Galasso, K., T. Livache, A. Roget and E. Vieil, 1998, Electrogravimetric detection of DNA hybridization on polypyrrole copolymer, *J. Chim. Phys.* 95, 1514–1517.
- Gambhir, A., M. Gerard, K.S. Jain and B.D. Malhotra, 2001, Characterization of DNA immobilized on electrochemically prepared conducting polypyrrole-polyvinyl sulfonate films, *Appl. Biochem. Biotech.* 96, 303–309.
- Garnier, F.P., H. Korri-Youssoufi, P. Srivastava, B. Mandrand and T. Delair, 1999, Toward intelligent polymers: DNA sensors based on oligonucleotide-functionalized polypyrroles, *Synth. Met.* 100, 89–94.
- Gaskin, M., V.-E. Choong, S. Gallagher, C. Li, G. Maracas and S. Si, 2001, Worldwide Patent WO014258, Motorola Inc.
- Gerard, M., A. Chaubey and B.D. Malhotra, 2001, Application of conducting polymers to biosensors, *Biosens. Bioelectron.* 17, 345–359.
- Gheorghe, M., C. Lei and A. Guiseppi-Elie, 2000, Low-density arrays of DNA-doped polypyrrole, *Polym. Mat. Sci. Eng.* 83, 551–552.
- Godillot, P., H. Korri-Youssoufi, P. Srivastava, A. El Kassmi and F. Garnier, 1996, Direct chemical functionalization of as-grown electroactive polypyrrole film containing leaving groups, *Synth Met.* 83, 117–123.
- Gu, H., G. Su and K.P. Loh, 2004, Conductive polymer-modified boron doped diamond for DNA hybridization analysis, *Chem. Phys. Lett.* 388, 483–487.
- Guedon, P., T. Livache, A. Roget, F. Martin, F. Lesbre, G. Bidan and Y. Levy, 2000, Characterization and optimization of a real time, parallel, label free, polypyrrole-based DNA sensor by surface plasmon resonance imaging, *Anal. Chem.* 72(24), 6003–6006.
- Ho, H.-A., M. Boissinot, M.B. Bergeron, G. Corbeil, K. Doré, D. Boudreau and M. Leclerc, 2002, Colorimetric and fluorimetric detection of nucleic acids using cationic polythiophene derivatives, *Angew. Chem. Int. Ed.* 41, 1548–1551.
- Ho, H.-A. and M. Leclerc, 2004, Optical sensors based on hybrid aptamer/conjugated polymer complexes, *J. Am. Chem. Soc.* 126, 1384–1387.
- Ihara, T., M. Nakayama, M. Murata, K. Nakano, and M. Maeda, 1997, Gene sensor using ferrocenyl oligonucleotides, *Chem. Commun.* 1609–1610.
- Jelen, F., B. Yosypchuk, A. Kourilova, L. Novotny and E. Palecek, 2002, Label-free determination of picogram quantities of DNA by stripping voltammetry with solid copper amalgam or mercury electrodes in the presence of copper, *Anal. Chem.* 74, 4788–4793.
- Katz, E., I. Willner and J. Wang, 2004, Electroanalytical and bioelectroanalytical systems based on metal and semiconductor nanoparticles, *Electroanalysis* 16, 19–44.
- Korri-Youssoufi, H., F. Garnier, P. Srivastava, P. Godillot and A. Yassar, 1997, Toward bioelectronics: Specific DNA recognition based on an oligonucleotide-functionalized polypyrrole, *J. Am. Chem. Soc.* 119, 7388–7389.
- Korri-Youssoufi, H. and B. Makrouf, 2002, Electrochemical biosensing of DNA hybridization by ferrocenyl groups functionalized polypyrrole, *Anal. Chim. Acta* 469, 85–92.
- Kranz, C., H.E. Gaub and W. Schuhmann, 1996, Polypyrrole towers grown with the scanning electrochemical microscope, *Adv. Mater.* 8, 634–637.
- Krishnamoorthy, K., R.S. Gokhale, A.Q. Contractor and A. Kumar, 2004, Novel label-free DNA sensors based on poly(3,4-ethylenedioxythiophene), *Chem. Commun.* 820–821.
- Lassalle, N., P. Mailley, E. Vieil, T. Livache, A. Roget, J.P. Correia and L.M. Abrantes, 2001a, Electronically conductive polymer grafted with oligonucleotides as electrosensors

- of DNA – Preliminary study of real time monitoring by in situ techniques, *J. Electroanal. Chem.* 509, 48–57.
- Lassalle, N., A. Roget, T. Livache, P. Mailley and E. Vieil, 2001b, Electropolymerisable pyrrole–oligonucleotide: Synthesis and analysis of ODN hybridization by fluorescence and QCM, *Talanta* 55, 993–1004.
- Lassalle, N., E.A. Vieil, J.P. Correia and L.M. Abrantes, 2001c, Study of DNA hybridization on polypyrrole grafted with oligonucleotides by photocurrent spectroscopy, *Biosens. Bioelectron.* 16, 295–303.
- Lassalle, N., E. Vieil, J.P. Correia and L.M. Abrantes, 2001d, Study of DNA hybridization by photocurrent spectroscopy, *Synth. Met.* 119, 407–408.
- Lee, T.-Y. and Y.-B. Shim, 2003, Direct hybridization detection based on oligonucleotides-functionalized conductive polymer, *Anal. Chem.* 73, 5629–5632.
- Lei, C., M. Gheorghe and A. Guiseppi-Elie, 2000, DNA immobilization and bioelectronic detection based on conducting polymers, *Polym. Mat. Sci. Eng.* 83, 552–553.
- Li, L.-L., H. Cai, T.M.-H. Lee, J. Barford and I.-M. Hsing, 2004, Electrochemical detection of PCR amplicons using electroconductive polymer modified electrode and multiple nanoparticles labels, *Electroanalysis* 16, 81–87.
- Li, C.M., C.Q. Sun, S. Song, V.E. Choong, G. Maracas and X.J. Zhang, 2005, Impedance labelless detection-based polypyrrole DNA biosensor, *Front. Biosci.* 10, 180–186.
- Lim, J.-H. and C.A. Mirkin, 2002, Electrostatically driven dip-pen nanolithography of conducting polymers, *Adv. Mater.* 14, 1474–1477.
- Livache, T., H. Bazin, P. Caillat and A. Roget, 1998a, Electroconducting polymers for the construction of DNA or peptide arrays on silicon chip, *Biosens. Bioelectron.* 13, 629–634.
- Livache, T., B. Fouque, A. Roget, J. Marchand, G. Bidan, R. Teoule and G. Mathis, 1998b, Polypyrrole DNA chip on silicon device; example of Hepatitis C virus genotyping, *Anal. Biochem.* 255, 188–194.
- Livache, T., P. Guedon, C. Brakha, A. Roget, Y. Levy and G. Bidan, 2001, Polypyrrole electrospotting for the construction of oligonucleotide arrays compatible with a surface plasmon resonance hybridization detection, *Synth. Met.* 121, 1443–1444.
- Livache, T., E. Maillart, N. Lassalle, P. Mailley, B. Corso, P. Guedon, A. Roget and Y. Levy, 2003, Polypyrrole based DNA hybridization assays: Study of label free detection processes versus fluorescence on microchips, *J. Pharm. Biomed. Anal.* 32, 687–696.
- Livache, T., A. Roget, E. Dejean, C. Barthet, G. Bidan and R. Teoule, 1994, Preparation of a DNA matrix via an electrochemically directed copolymerization of pyrrole and oligonucleotides bearing a pyrrole group, *Nucleic Acids Res.* 22, 2915–2921.
- Lofas, S.M., M. Malmqvist, I. Roennberg, E. Stenberg, B. Liedberg and I. Lundstrom, 1991, Bioanalysis with surface plasmon resonance, *Sens. Actuat. B* 5, 79–84.
- Lopez-Crapez, E., T. Livache, J. Marchand and J. Grenier, 2001, K-ras mutation detection by hybridization to a polypyrrole DNA chip, *Clin. Chem.* 47(2), 186–194.
- Ma, Y., J. Zhang, G. Zhang and H. He, 2004, Polyaniline nanowires on Si surfaces fabricated with DNA templates, *J. Am. Chem. Soc.* 126, 7097–7101.
- Maillart, E., K. Brengel-Pesce, D. Capela, A. Roget, T. Livache, M. Canva, Y. Levy and T. Soussi, 2004, Versatile analysis of multiple macromolecular interactions by SPR imaging: Application to p53 and DNA interaction, *Oncogene* 23(32), 5543–5550.
- Marx, K.A., J.O. Lim, D.S. Minehan, R. Pande, M. Kamath, S. Tripathy and D.L. Kaplan, 1994, Intelligent biomaterials properties of DNA and strategies for its incorporation into electroactive polymeric thin film systems, *J. Intel. Mater. Syst. Struct.* 5, 447–454.
- McQuade, D.T., A.E. Pullen and T.M. Swager, 2000, Conjugated polymer-based chemical sensors, *Chem. Rev.* 100, 2537–2574.
- Minehan, D.S., K.A. Marx and S. Tripathy, 1994, Kinetics of DNA binding to electrically conducting polypyrrole films, *Macromolecules* 27, 777–783.
- Minehan, D.S., K.A. Marx and S. Tripathy, 2001, DNA binding to electropolymerized polypyrrole: The dependence on film characteristics, *J. Macromol. Sci. Pure Appl. Chem.* A 38, 1245–1258.

- Misoska, V., W.E. Price, S.F. Ralph, G.G. Wallace and N. Ogata, 2001, Synthesis, characterization and ion transport studies on polypyrrole/deoxyribonucleic acid conducting polymer membranes, *Synth. Met.* 123, 279–286.
- Nagarajan, R., W. Liu, J. Kumar, S.K. Tripathy, F.F. Bruno and L.A. Samuelson, 2000, DNA conformation switching using a templated conducting polymer, *Polym. Mat. Sci. Eng.* 83, 546–547.
- Nagarajan, R., S.K. Tripathy, J. Kumar, F.F. Bruno and L.A. Samuelson, 2001, Manipulating DNA conformation using intertwined conducting polymer chains, *Macromolecules* 34, 3921–3927.
- Nilsson, K.P.R. and O. Inganäs, 2003, Chip and solution detection of DNA hybridization using a luminescent zwitterionic polythiophene derivative, *Nat. Mater.* 2, 419–421.
- Nilsson, K.P.R., J. Rydberg, L. Baltzer and O. Inganäs, 2003, Self-assembly of synthetic peptides control conformation and optical properties of a zwitterionic polythiophene derivative, *Proc. Natl. Acad. Sci. USA* 100, 10171–10174.
- Okahata, Y., M. Kawase, K. Niikura, F. Ohtake, H. Furusawa and Y. Ebara, 1998, Kinetic measurements of DNA hybridization on an oligonucleotide-immobilized 27-MHz quartz crystal microbalance, *Anal. Chem.* 70, 1288–1296.
- Pande, R., G.C. Ruben, J.O. Lim, S. Tripathy and K.A. Marx, 1998, DNA bound to polypyrrole films: High-resolution imaging, DNA binding kinetics and internal migration, *Biomaterials* 19, 1657–1667.
- Peng, H., Soeller, C. Vigar, N. Kilmartin, P.A. Cannell, M.B., Bowmaker, G.A., Cooney, R.P., Travas-Sejdic, J., 2005. Label-free electrochemical DNA sensor based on functionalised conducting copolymer, 20, 1821–1828.
- Pham, M.-C., Piro, Tran L.D., B., Ledoan, T. Dao, L.H., 2003. Direct electrochemical detection of oligonucleotides hybridization on poly (5-hydroxy-1,4- naphthoquinone-co-5-hydroxy-3-thioacetic acid-1,4- naphthoquinone) film, *Anal. Chem.* 75, 6748–6752.
- Pike, A.R., S.N. Patole, N.C. Murray, T. Ilyas, B.A. Connolly, B.R. Horrocks and A. Houlton, 2003, Covalent and non covalent attachment and patterning of polypyrrole at silicon surfaces, *Adv. Mater.* 15, 254–257.
- Piro, B., J. Haccoun, L.D. Tran, A. Rubin, H. Perrot and C. Gabrielli, 2005, Characterization of a quinine-containing electroactive polymer film used as DNA sensor. Study of the hybridization mechanism by cyclic voltammetry and electrochemical impedance spectroscopy, *J. Electroanal. Chem.* 577, 155–165.
- Piro, B., M.-C. Pham and T. Ledoan, 1999, Electrochemical method for entrapment of oligonucleotides in polymer-coated electrodes, *J. Biomed. Mater. Res.* 46, 566–572.
- Pirrung, M.C., 2002, How to make a DNA chip, *Angew. Chem. Int. Ed.* 41, 1276–1289.
- Purvis, D., O. Leonardova, D. Farmakovskiy and V. Cherkasov, 2003, An ultrasensitive and stable potentiometric immunosensor, *Biosens. Bioelectron.* 18, 1385–1390.
- Ramanaviciene, A. and A. Ramanavicius, 2004, Pulsed amperometric detection of DNA with an ssDNA/polypyrrole-modified electrode, *Anal. Bioanal. Chem.* 379, 287–293.
- Roget, A. and T. Livache, 1999, In situ synthesis and copolymerization of oligonucleotides on conducting polymers, *Mikrochim. Acta* 131, 3–8.
- Saoudi, B., C. Despas, M.M. Chehimi, N. Jammul, M. Delamar, J. Bessiere and A. Walcarius, 2000, Study of DNA adsorption on polypyrrole: Interest of dielectric monitoring, *Sens. Actuat. B* 62, 35–42.
- Saoudi, B., N. Jammul, M.-L. Abel, M.M. Chehimi and G. Dodin, 1997, DNA adsorption onto conducting polypyrrole, *Synth. Met.* 87, 97–103.
- Shimidzu, T., 1987, Functionalized conducting polymers for development of new polymeric reagents, *React. Polym.* 6, 221–227.
- Szunerits, S., L. Bouffier, B. Corso, K. Brakha, Y. Defontaine, M. Demeunynck, E. Descamps, J.-B. Fiche, E. Fortin, N. Lassalle, T. Livache, P. Mailley, A. Roget, E. Vieil, and B. Wang, 2005, Review on different strategies on DNA chip fabrication as well as DNA-sensing: Optical and electrochemical approaches, Submitted paper.
- Szunerits, S., N. Knorr, R. Calemczuk and T. Livache, 2004, New approach to writing and simultaneous reading of micropatterns: Combining surface plasmon resonance imaging with scanning electrochemical microscopy (SECM), *Langmuir* 20(21), 9236–9241.

- Takenaka, S., 2003, Electrochemical detection of DNA with small molecules, 'DNA and RNA Binders: From Small Molecules to Drugs', Eds. M. Demeunynck, C. Bailly and W.D. Wilson, Wiley-VCH, Weinheim, pp. 224–246.
- Thompson, L.A., J. Kowalik, M. Josowicz and J. Janata, 2003, Label-free DNA hybridization probe based on a conducting polymer, *J. Am. Chem. Soc.* 125, 324–325.
- Torres-Rodriguez, L.M., Roget, A. Billon, M. Livache T. and Bidan G. 1998, Synthesis of a biotin functionalized pyrrole and its electropolymerization: Toward a versatile avidin biosensor, *Chem. Commun.* 1993–1994.
- Umana, M. and J. Waller, 1986, Protein-modified electrodes. The glucose oxidase/polypyrrole system, *Anal. Chem.* 58, 2979–2983.
- Wang, B., L. Bouffier, M. Demeunynck, P. Mailley, A. Roget, T. Livache and P. Dumy, 2004, New acridone derivatives for the electrochemical DNA-hybridization labelling, *Bioelectrochemistry* 63, 233–237.
- Wang, J., X. Cai, G. Rivas, H. Shiraiishi and N. Dontha, 1997, Nucleic-acid immobilization, recognition and detection at chronopotentiometric DNA chips, *Biosens. Bioelectron.* 12, 587–599.
- Wang, J. and M. Jiang, 2000, Toward genelectronics: Nucleic acid doped conducting polymers, *Langmuir* 16, 2269–2274.
- Wang, J., M. Jiang, A. Fortes and B. Mukherjee, 1999, New label-free DNA recognition based on doping nucleic-acid probes within conducting polymer films, *Anal. Chim. Acta* 402, 7–12.
- Wang, J. and B. Mukherjee, 2001, Recognition and detection of oligonucleotides in the presence of chromosomal DNA based on entrapment within conducting polymer network, *J. Electroanal. Chem.* 500, 584–589.
- Wu, J., Y. Zou, H. Liu, G. Shen and R. Yu, 2005, A biosensor monitoring DNA hybridization based on polyaniline intercalated graphite oxide nanocomposite, *Sens. Actuat. B* 104, 43–49.
- Xu, Y., Y. Jiang, H. Cai, P.-G. He and Y.-Z. Fang, 2004, Electrochemical impedance detection of DNA hybridization based on the formation of M-DNA on polypyrrole/carbon nanotube modified electrode, *Anal. Chim. Acta* 516, 19–27.
- Yamamoto, T., T. Shimizu and E. Kurokawa, 2000, Doping behaviour of water-soluble π -conjugated polythiophenes depending on pH and interaction of the polymer with DNA, *React. Funct. Polym.* 43, 79–84.

Control of Chloride Ion Exchange by DNA Hybridization at Polypyrrole Electrode

Temitope Aiyejorun, Liz Thompson, Janusz Kowalik, Mira Josowicz and Jiří Janata

Georgia Institute of Technology, School of Chemistry and Biochemistry, Atlanta, GA 30332, USA

Contents

1. Introduction	331
2. Principle of operation	333
3. Procedures	335
3.1. Preparation of the generic probe	335
3.2. Probe characterization	335
3.3. Hybridization detection	336
4. Overview of selectivity studies	336
5. Time versus detection limit	337
6. Summary	340
Acknowledgments	341
References	342

1. INTRODUCTION

The conventional electrochemical DNA hybridization detection methods rely on the immobilization of ssDNA (probe) at the proper electrode followed by the recognition of the hybridization event through base pairing of the complementary ssDNA (target) present in the sample solution (Palecek *et al.*, 2002b; Palecek and Jelen, 2002c; Kerman *et al.*, 2004). The attachment of the oligonucleotide (probe) and its distribution, packing density and orientation affect not only the recognition of the target but also influence the sensing performance of the probe (Ye and Ju, 2003). Electrochemical approaches are based on the following options: (a) covalent attachment of the probe to a functionalized surface (Jung *et al.*, 2004; Masarik *et al.*, 2003; Fojta, 2002; Pividori *et al.*, 2000; Palecek *et al.*, 1998; Krider and Meade, 1998), (b) adsorption of the probe to the surface (Del Pozo *et al.*, 2005; Petrovykh *et al.*, 2003; Palecek *et al.*, 2002a; Steel *et al.*, 2000; Wang *et al.*, 1997), (c) embedding of the probe in a sol-gel (Phinney *et al.*, 2004) or polymeric matrix (Livache *et al.*, 1998; Emge and Baenerte, 1998), (d) affinity immobilization (Gajovic-Eichelmann *et al.*, 2003), or self-assembly (Sakao *et al.*, 2005; Di Giusto *et al.*, 2004; Kagan *et al.*, 2002; Sun *et al.*, 1998). In order to minimize the damage

of the DNA probe during the immobilization process, exposure to harsh chemicals such as acids, strong oxidants, radiation, ultrasonication, etc., should be avoided.

Our detection scheme for recognition of DNA hybridization event is based on modulation of the electrostatic barrier that requires only a minimal manipulation on the DNA as it is attached to the electrode surface. This approach relies on the fact that DNA is a negatively charged polyelectrolyte owing to ionization of the phosphate group at physiological pH (Cowan, 1996). In solution, the charge neutralization of nucleic acid is achieved through the interactions of the phosphate groups, sugar hydroxyls, and endocyclic nitrogen atoms of the nucleobases with positively charged metal ions (Cowan, 2004). Many metal ions such as Ca^{2+} , Mg^{2+} , Zn^{2+} , Cu^2 , Ba^{2+} , Co^{2+} , etc., form complexes that play different and important role in the structure and function of nucleic acids (Gao *et al.*, 1993; Cowan, 1995). These complexes may be held together by electrostatic or weaker van der Waals forces, including hydrophobic bonding (Barton, 1994). The metal ion/DNA interaction can be significantly influenced by the ligands bound to the metal ion, by the proportion of adenine and thymine bases in the ssDNA and/or by the chirality at the metal center itself. For example, it has been found that magnesium ions interact with various sites of ODN, including the phosphate oxygen and N7 of guanine (Robinson *et al.*, 2000; Tereshko *et al.*, 1999). The factors that control metal ion/DNA interactions are currently the area of great interest in cancer research.

Electrostatic binding of Mg^{2+} to the phosphate groups provides significant stabilization of the double helical structure (Cowan, 2004). The interactions may be either through direct metal ion coordination or mediated through water molecules of the hydration shell around the metal ion (Gao *et al.*, 1999). Ions such as cobalt (II), copper (II) bind exclusively by coordinating to the N7 position of guanine or purine (Cowan, 2004; Masoud *et al.*, 2004). Zinc binds to proteins which contain repeating sequences of cysteine and hystidine residues that enable specific recognition of DNA sequences that are essential to the DNA transcription factors known as “zinc finger” (Pabo *et al.*, 2001; Isalan *et al.*, 1998).

In order to employ electrostatic attraction between the phosphate anions and the magnesium cations, phosphate groups must be first introduced to the surface. The easiest way to do this is by electropolymerization of a phosphonate-bearing monomer. For this purpose we have selected 2,5-bis(2-thienyl)-*N*-(3-phosphorylpropyl)pyrrole, TPTC3PO₃H₂, as the precursor monomer. Its polymerization does not require any other reagents besides the solvent since the phosphonate group serves as a counter anion. The phosphonate group is linked to the nitrogen of the pyrrole through alkyl chain (Figure 1).

This polymer is grafted at the top of another intrinsically conducting polymer, such as polypyrrole, that acts as the electrochemically active element of the probe. It has a well-defined electrochemistry and combines good thermal and mechanical stability. It maintains its conductivity for several months (Kathirgamanathan, 1991; Bornier *et al.*, 1999). Polypyrrole has been widely used in different types of biosensors and in biotechnological applications (Cosnier, 2000) such as bioreactors (Amounas *et al.*, 2003) and drug release systems (Mak *et al.*, 2003; Brahim *et al.*, 2002).

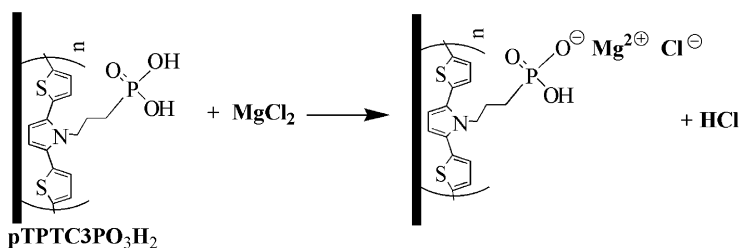


Fig. 1. Diagram of the attachment of magnesium (2^+) to pTPTC3PO₃H₂.

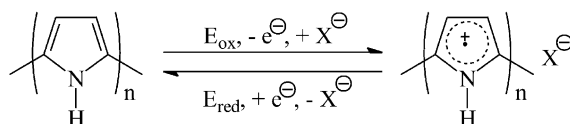


Fig. 2. Doping of polypyrrole layer.

2. PRINCIPLE OF OPERATION

Our approach is based on the reversible transport of counter ions into or out of the polypyrrole, PPy, layer when it is electrochemically oxidized or reduced (Burgmayer and Murray, 1984; Iyoda *et al.*, 1987; Shimidzu *et al.*, 1987). The movement of ions is governed by doping and undoping of the polymer, satisfying the rule of charge neutrality at all redox states of the polymer (Figure 2). The doping and undoping process can also be seen as an electrically controlled anion-exchange process (Vorotyntsev *et al.*, 1996).

The oxidation reaction introduces positive charges into the polymer chain and therefore is called “doping.” The removal of charges from the polymer during reduction is called undoping.

The PPy layer with the grafted pTPTC3PO₃H₂ allows the Mg²⁺ cation to form a bidentate complex between the phosphonate group of TPTC3PO₃H₂ and the phosphate group of the probe DNA (Figure 3).

Since the spacing of the phosphonate groups on the grafted pTPTC3PO₃H₂ does not match the spacing between the phosphate groups on the target DNA, the “attachment points” are randomly distributed. The propyl chain of the TPTC3PO₃H₂ molecule affords certain mobility to the phosphonate group, which is important for the immobilization of the bulky oligonucleotides. Thus, the pTPTC3PO₃H₂ layer only introduces the phosphonate groups to the surface of the modified electrode. On the other hand, the PPy layer, which is always much thicker, controls the exchange of chloride ion, which results in the change of voltammetric response. The direct electrical contact between the pTPTC3PO₃H₂ and PPy layer does not significantly alter the anion exchange. The key step in the operation of our probe is the formation of a duplex with target DNA, as shown in Figure 4.

First of all it is necessary to clarify some terminologies. Since no reporter molecules or labels are used in our procedure it is truly “label free” hybridization

3. PROCEDURES

In the following paragraphs we describe preparation, characterization, and testing of our probe. Most of the proof-of-principle, development and optimization work was done with a 27-mer oligonucleotide called “probe DNA” of the sequence: 5' CGA AAA TGA ATA AAC TAG TAA GGA AGT 3', its fully complementary “target DNA,” 3' GCT TTT ACT TAT TTG ATC ATT CCT TCA 5' and a fully non-complementary DNA, 3' ACT TCC TTA CTA GTT TAT TCA TTT TCG 5'. A few test experiments were done also with a 39-mer DNA, which are in full agreement with the 27-mer results.

3.1. Preparation of the generic probe

The polypyrrole is deposited from acetonitrile (ACN) solution containing 0.1 M pyrrole and 0.1 M tetraethylammonium perchlorate (TEAP) solution at a constant potential of 0.7 V versus the Ag/0.1 M AgNO₃ in ACN // 0.1 M TEAP in ACN. The deposition is carried out on a platinum disc electrode (diameter of 1.5 mm, $A = 0.018 \text{ cm}^2$), until the charge density reaches approximately 280 mC/cm². That charge density represents an optimum thickness of the polymer with sufficient ion-exchange capacity. After the polymerization, the electrode is thoroughly washed with ACN, in order to remove the monomer and soluble oligomers from the polymer film. The pTPTC3PO₃H₂ polymer is deposited over the PPy also from ACN solution containing only the monomer TPTC3PO₃H₂, in 0.1 M concentration (Hartung *et al.*, 2005). The *i-t* curves recorded during the polymerization of the PPy layer and the pTPTC3PO₃H₂ layer differ significantly. The current density is decreasing during the TPTC3PO₃H₂ polymerization indicating that the process is self-terminating, at the charge density of approximately 100 mC/cm². The primary purpose of this layer is to functionalize the PPy surface with the phosphonate groups. It does not participate in the ion-exchange process. The magnesium ion is then complexed with the surface phosphonates by dipping the modified electrode into 5 mM MgCl₂ solution. It has been found beneficial to apply a potential step of +1.2 V for 2 min while stirring, in order to achieve a long-term electrochemical stability of the modified electrode. This step apparently removes any unreacted pyrrole oligomers. The excess of Mg²⁺ is washed away with 0.1 M Tris-HCl buffer (Hartung *et al.*, 2005). After this step the electrode is allowed to relax in 5 mM MgCl₂ solution for at least 1 h before use. The electrode is now ready for the attachment of the probe DNA. In this state it can be stored for a long time, if necessary.

3.2. Probe characterization

The grafting of thin pTPTC3PO₃H₂ layer on the PPy has been confirmed by FTIR and by X-ray photoelectron spectroscopy, XPS (Thompson *et al.*, 2003;

Hartung *et al.*, 2005). From the XPS results before and after the attachment of the magnesium (II) the S2p to P2p ratio was found to be close to 2:1 (5.85 to 2.30) for the pTPTC3PO₃H₂ film. The identity of the P2p peak in the XPS spectrum correlates with the presence of phosphonate group on the pTPTC3PO₃H₂.

3.3. Hybridization detection

Probing of the hybridization event is a two-step process. First, the probe DNA molecule is attached to the Mg²⁺-modified bilayer as shown in Figure 3. This is done by immersion of the electrode in solution of probe DNA of chosen base sequence and concentration for 10 min. We used the probe DNA in a wide concentration range, from 0.5 to 100 μM, and gave it 10 min for immobilization to the electrode surface. After rinsing of the excess, unattached probe DNA molecules cyclic voltammograms are recorded. Typically, it takes less than three cycles to reach the steady-state voltammogram.

In the second step, dipping the electrode with the already attached probe DNA to the complementary target DNA solution achieves the hybridization. The concentration is chosen between 1 nM and 100 μM. The hybridization process is concentration and time dependent. For example, at 5 μM dipping for 30 min is sufficient. After the exposure to the target DNA the electrode is again rinsed with the buffer solution and steady-state cyclic voltammograms are recorded in pH 7.3 Tris buffer.

The hybridization event is evaluated by determining changes in the CV (shape and magnitude) recorded before and after the hybridization. The raw cyclic voltammograms are shown in Figure 5a. The changes in the CV due to the initial complexation of the target DNA with the magnesium ion terminated surface are very small and overlap indicating that the transport of chloride ions across the polymer/electrolyte interface is not hindered. However, when the electrode with immobilized probe DNA is exposed to the solution of the complementary target DNA a significant decrease of current is observed, which indicates the change of the height of the electrostatic barrier for the transfer of chloride ions across the polymer/solution interface. In order to amplify the hybridization effect it is best to subtract the CV signal of the target DNA from that of the probe DNA (Figure 5b).

The difference voltammogram obtained from the subtraction of the probe DNA from that of the Mg(2⁺) modified surface does not show any significant change in the barrier height and can be clearly distinguished.

4. OVERVIEW OF SELECTIVITY STUDIES

The selectivity of the response of the probe DNA modified electrode was tested against non-complementary DNA target. The results are summarized in Figure 6. In the first set, the probe is first exposed to the fully complementary target followed by the addition of the fully non-complementary target. The results are

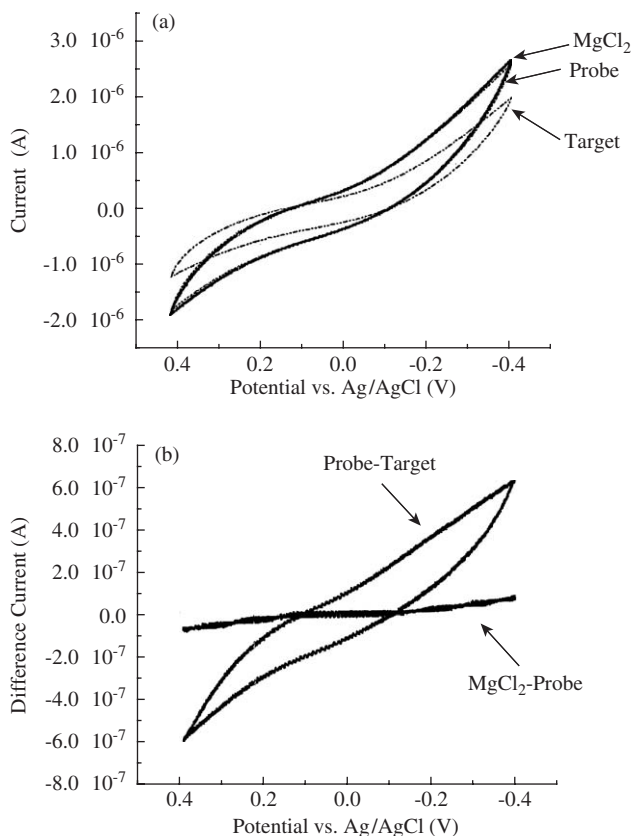


Fig. 5. Cyclic voltammograms (a) recorded before and after the hybridization step and differ CV (b). All CVs were recorded in 0.1 M Tris/HCl buffer, pH = 7.3 with 50 mV/s. The concentration of the probe DNA and of the complementary target DNA was 0.5 μ M. The immobilization time for the probe DNA was 10 min and for the hybridization 30 min.

presented as difference CV in Figure 6a. In the next set (Figure 6b), the sequence in which the electrode was exposed has been reversed. That is, the probe is first exposed to the non-complementary target followed by the exposure to the complementary target.

The result clearly indicates that there is virtually no interference by the non-complementary DNA. This is confirmed in the third set (see Figure 6c) in which the probe has been exposed to the equimolar mixture of complementary and non-complementary target. That situation more closely resembles a realistic assay in which the target and one or more non-complementary DNA molecules are present.

5. TIME VERSUS DETECTION LIMIT

The detection limit is a figure of merit and is of primary importance in any analytical technique. In the mechanism where strong binding results in the

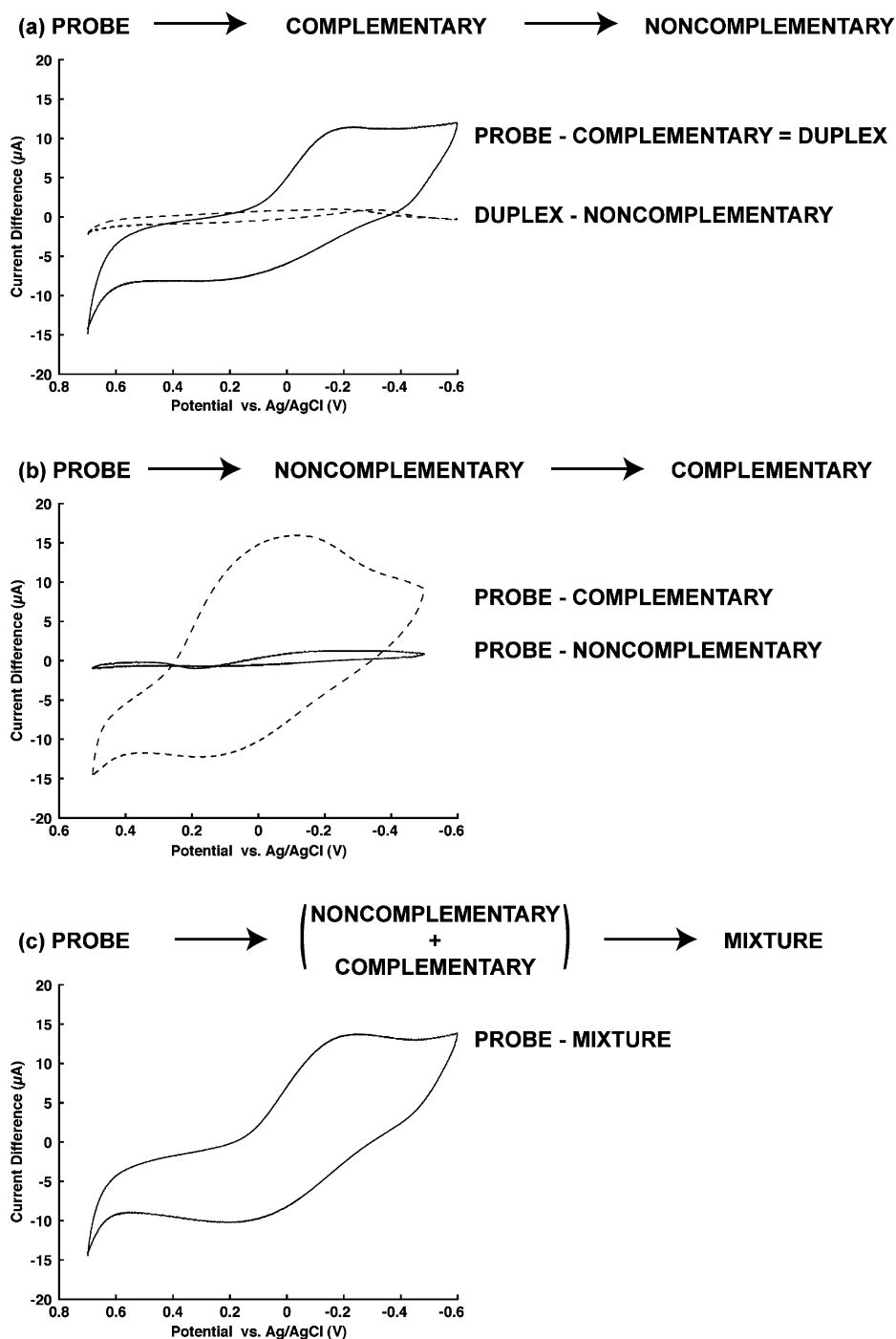


Fig. 6. Comparison between difference of the CV responses following sequential exposures (a)–(c) as indicated. Concentrations of the ssDNA probe, and of the complementary target was $2.3\ \mu\text{M}$ and of the non-complementary DNA was $3.4\ \mu\text{M}$. The soaking in target DNA was 10 min.

surface saturation, such as in this study, the detection limit trades off against the analysis time. In order to prove this point we have performed the following experiment, in which the probe has been exposed to a low concentration (1 nM) of the target DNA and the changes in the CVs were monitored continuously over 22 h. In that case the charge due to the exchange of Cl^- was obtained as the area below the cathodic branch of the CV and plotted as the function of time (Figure 7). During this experiment the solution was gently stirred even during the recording of the CV. It is quite obvious that the binding of the target DNA to the probe and the modification of the barrier are kinetically controlled.

A different modification of this experiment has been performed, in which the probe DNA was exposed briefly to a higher (0.5 μM) concentration of the complementary target DNA, washed and then measured in pH 7.3 Tris buffer over a period of several hours (Figure 8). The result is again presented as the charge passed during the cathodic half-cycle of the CV. A gradual increase of the barrier is again observed, however, the kinetics of this change is clearly different than that described in Figure 7.

These results indicate that the time evolution of the response involves multiple kinetic steps. At low concentration, a fraction of the target DNA may interact with the electrode surface reversibly and non-specifically, while some target DNA molecules may undergo specific multiple point attachment resulting in the hybridization and slow, but irreversible growth of the barrier height (Figure 7).

On the other hand, in the experiment in which the (0.5 μM) concentration is used for a relatively brief exposure, the surface may become non-specifically saturated with a randomly attached probe and target molecules that then undergo a slow, specific reorganization driven by the hybridization. In both cases,

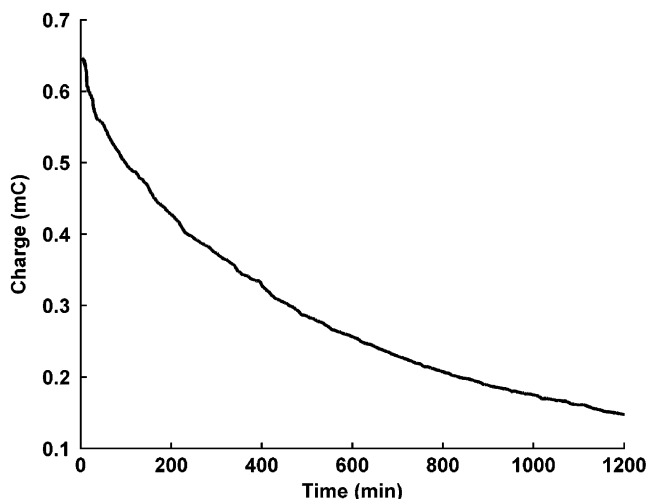


Fig. 7. Observed changes in blockage of ion-exchange current as a function of the hybridization time. The changes in the CV have been evaluated as the charge under the cathodic region of the CVs. The concentration of the complementary target DNA was 1 nM.

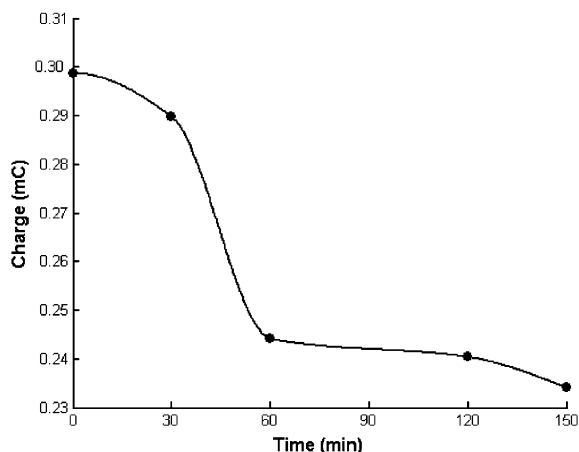


Fig. 8. Decrease of chloride ion-exchange current (charge) due to progressive blockage of the polymer/solution interface, presumably by rearrangement of the surface-bound DNA molecules. The concentration of the probe DNA and target DNA was $0.5\ \mu\text{M}$.

the result is an increase of the barrier height but the time dependence of these two processes is different, as shown in Figures 7 and 8, respectively.

6. SUMMARY

The electrochemical signal of the Pt/PPy/pTPTC3- PO_3H_2 - MgCl_2 modified electrode is due to the reversible exchange of chloride ions between the bulk of the PPy and the buffer, as the electrode is cycled between the positive and negative potential limits. The role of the chloride ion is to maintain charge neutrality in the bulk of the PPy layer during cycling. Therefore, as PPy undergoes oxidation/reduction it acts as an “electrochemically controlled ion-exchanger” for the chloride ion. The CV of the electrostatically controlled sorption to only one type of binding site, in the absence of lateral interactions between the anions, i.e. the Langmuir adsorption, is well defined. At a smooth electrode it shows as a pair of adsorption/desorption peaks (Bard and Faulkner, 2001). It is known that every preparation of PPy layer is different in terms of its morphology, pore distribution, and polymer density, resulting in a variety of available binding sites for the anion interaction. Not surprisingly, the CV has a common shape corresponding to the Cl^- exchange, but is broad, exhibiting poorly defined features. The electrostatic barrier, which is present at the solution/polymer interface affects the rate of Cl^- exchange differently for each preparation. The height of this barrier has a probabilistic meaning. It affects the average rate of the Cl^- exchange, i.e. the magnitude of the current at any potential within the CV window, but it does not result in complete “shutting down” of the ion-exchange process. The resulting variability of the shape of the CV is not a problem in the present detection scheme because the information is obtained from the difference of the CV before and after the hybridization event.

Thus, the hybridization is best discernible in the difference CVs. The height of the electrostatic barrier is directly proportional to the charge density at the interface. That, in turn, depends on the length of the oligomer and on the ionic strength. The latter can be kept constant within the experiment. Since the electrode area is constant between experiments, the only possible variability is the surface charge density due to the hybridization.

Detection limit (sometimes incorrectly referred to as “sensitivity”) is an important figure of merit in any analytical method. The detection limit is given by the number of the probe molecules immobilized at the surface, as long as there is an excess of the target molecules in the solution. We assume that every collision of the DNA target (solution) molecule with the immobilized DNA probe at the electrode surface results in irreversible binding. Thus, for the m immobilized probe molecules of DNA the detection limit in units of concentration is $m/(\text{sample volume})$. The size and shape of the electrode affects the shape of the CV (Bard and Faulkner, 2001), but not the actual recognition event. This means that the present scheme can be translated into a microelectrode format with possible lowering of the overall detection limit. Such evolution would be particularly desirable in construction of label free DNA hybridization recognition arrays. However, the experiments at low concentration of the target DNA have shown that the response and the detection limit may be affected by the slow surface reorganization of the initially randomly adsorbed DNA molecules.

It is important to note that this hybridization assay can be accomplished in a “batch” mode and that the activated electrodes can be stored for a long time. A simple dipping in a solution of the probe DNA then accomplishes the activation of the electrode. Likewise, the testing of the complementarity is done by dipping. The simplicity of these two final steps should make this approach potentially attractive for fabrication of multiprobe electrochemical hybridization arrays.

Work reported in this chapter has started as an attempt to design a simple, “label-free” DNA hybridization assay. The experiments have confirmed that the concept of modification of the barrier height by the selective DNA hybridization step is sound. However, the feasibility of a practical DNA assay based on this concept is less certain. It is possible that the hybridization detection approach presented here may not have a significant commercial application. However, it proved to be an excellent tool for teaching undergraduate chemistry. It introduces students to electrochemistry, biosensing, and to data evaluation (Aiyekorun *et al.*, 2005). In the course of the student laboratory exercises similar results have been obtained in experiments with hybridization of 39 mer of ssDNA probe and other sequences. Obviously, the number and location of mismatches will play an important role. These effects have not yet been sufficiently explored.

ACKNOWLEDGMENTS

We thank Emil Palecek and Gary Schuster for their helpful comments, and the National Science Foundation (CHE-0137391) and the Department of Energy (DE-FG05-85ER45194) for the financial support.

REFERENCES

- Aiyejorun, T., J. Kowalik, J. Janata and M. Josowicz, 2005, Label-free detection of DNA hybridization by cyclic voltammetry, *J. Chem. Educ.* (in print).
- Amounas, M., Ch. Innocent, S. Cosnier and P. Seta, 2003, Dismutation of hydrogen peroxide from water medium by catalytic reactive membrane immobilizing peroxidase and catalase by molecular recognition process, *Sep. Sci. Technol.* 38, 1291–1306.
- Bard, A. and L.R. Faulkner, Eds., 2001, *Electrochemical Methods: Fundamentals and Applications*, 2nd ed., Wiley, New York.
- Barton, J.K., 1994, *Bioinorganic Chemistry*, Eds. I.B. Bertini, H.B. Gray, S.J. Lippard and J.S. Valentine, Metal-nucleic acid interactions, University Science Books, Mill Valley, CA, 455.
- Bornier, P., S. Lefrant and G. Bidan, Eds., 1999, *Advances in Synthetic Metals Twenty Years of Progress in Science and Technology*, Elsevier, Amsterdam, The Netherlands.
- Brahim, S., D. Narinesingh and A. Guiseppi-Elie, 2002, Bioactive composite hydrogels for clinical biosensors and controlled drug release, *Polym. Prepr. (Am. Chem. Soc., Div. Polym. Chem.)* 43, 625–626.
- Burgmayer, P. and R.W. Murray, 1984, Ion gate electrodes. Polypyrrole as a switchable ion conductor membrane, *J. Phys. Chem.* 88, 2515.
- Cosnier, S., 2000, Biosensors based on immobilization of biomolecules by electrogenerated polymer films—new perspectives, *Appl. Biochem. Biotechnol.* 89, 127–138.
- Cowan, J.A., 1995, *The Biological Chemistry of Magnesium*, VCH, New York.
- Cowan, J.A., 1996, *Inorganic Biochemistry*, 2nd ed., VCH, Weinheim, Germany.
- Cowan, J., 2004, Role of metal ions in promoting DNA binding and cleavage by restriction endonucleases, *Nucleic Acids Mol. Biol.* 14, 339–360.
- Del Pozo, M.V., C. Alonso, F. Pariente and E. Lorenzo, 2005, Electrochemical DNA sensing using osmium complexes as hybridization indicators, *Biosens. Bioelectron.* 20, 1549–1558.
- Di Giusto, D.A., W.A. Wlassoff, S. Giesebrecht, J.J. Gooding and G.C. King, 2004, Multipotential electrochemical detection of primer extension reactions on DNA self-assembled monolayers, *J. Am. Chem. Soc.* 126, 4120–4121.
- Emge, A. and P. Baeuerle, 1998, Specific recognition of nucleobase-functionalized polythiophenes, *Adv. Mat.* 10, 324–330.
- Fojta, M., 2002, Electrochemical sensors for DNA interactions and damage, *Electroanalysis* 14, 1449–1463.
- Gajovic-Eichelmann, N., E. Ehrentreich-Forster and F.F. Bier, 2003, Directed immobilization of nucleic acids at ultramicroelectrodes using a novel electro-deposited polymer, *Biosens. Bioelectron.* 19, 417–422.
- Gao, Y.G., H. Robinson, R. Sanishvili, A. Joachimiak and A.H. Wang, 1999, Structure and recognition of sheared tandem G × A base pairs associated with human centromere DNA sequence at atomic resolution, *Biochemistry* 38, 16452–16460.
- Gao, Y.G., M. Sriram and A.H. Wang, 1993, Crystallographic studies of metal ion-DNA interactions: Different binding modes of cobalt(II), copper(II) and barium(II) to N7 of guanines in Z-DNA and a drug-DNA complex, *Nucleic Acids Res.* 21, 4093–4101.
- Hartung, J., J. Kowalik, J. Janata and M. Josowicz, 2005, Electropolymerization of bilayer with phosphoric acid tethers for immobilization of biomolecules, *J. Electrochem.* (in print).
- Isalan, M., A. Klug and Y. Choo, 1998, Comprehensive DNA-recognition through concerted interactions from adjacent zinc fingers, *Biochemistry* 37, 12026–12033.
- Iyoda, T., A. Ohtani, T. Shimidzu and K. Honda, 1987, Charge-controllable polypyrrole-polyelectrolyte composite membrane, *Synth. Met.* 18, 747–751.
- Jung, D.-H., B.H. Kim, Y.K. Ko, M.S. Jung, S. Jung, S.Y. Lee and H.-T. Jung, 2004, Covalent attachment and hybridization of DNA oligonucleotides on patterned single-walled carbon nanotube films, *Langmuir* 20, 8886–8891.
- Kagan, K., O. Dilsat, K. Pinar, M. Burcu, G.J. Justin and O. Mehmet, 2002, Voltammetric determination of DNA hybridization using methylene blue and self-assembled alkanethiol monolayer on gold electrodes, *Anal. Chim. Acta* 462, 39–47.

- Kathirgamanathan, P., 1991, Some applications of conducting polymers, *High Value Polymers*, Vol. 87, Ed. A.H. Fawcett, Royal Society of Chemistry, Cambridge, pp. 174–205.
- Kerman, K., M. Kobayashi and E. Tamiya, 2004, Recent trends in electrochemical DNA biosensor technology, *Meas. Sci. Technol.* 15, R1–R11.
- Krider, E.S. and T.J. Meade, 1998, Electron transfer in DNA: Covalent attachment of spectroscopically unique donor and acceptor complexes, *J. Biol. Inorg. Chem.* 3, 222–225.
- Livache, T., B. Fouque, A. Roget, J. Marchand, G. Bidan, R. Téoule and G. Mathis, 1998, Polypyrrole DNA chip on a silicon device: Example of Hepatitis C virus genotyping, *Anal. Biochem.* 255, 188–194.
- Mak, W.Ch., Ch. Chan, J. Barford, R. Mak, W. Cheung, Ch. Chiyui, J. Barford and R. Renneberg, 2003, Biosensor for rapid phosphate monitoring in a sequencing batch reactor (SBR) system, *Biosens. Bioelectron.* 19, 233–237.
- Masarik, M., R. Kizek, K.J. Kramer, S. Billova, M. Brazdova, J. Vacek, M. Bailey, F. Jelen and J.A. Howard, 2003, Application of avidin–biotin technology and adsorptive transfer stripping square-wave voltammetry for detection of DNA hybridization and avidin in transgenic avidin maize, *Anal. Chem.* 75, 2663–2669.
- Masoud, M.S., A. Soayed and A.E. Ali, 2004, Complexing properties of nucleic-acid constituents adenine and guanine complexes, *Spectrochim. Acta Part A* 60A, 1907–1915.
- Pabo, C.O., E. Peisach and R.A. Grant, 2001, Design and selection of novel Cys2His2 zinc finger proteins, *Annu. Rev. Biochem.* 70, 313–340.
- Palecek, E., M. Fojta and F. Jelen, 2002a, New approaches in the development of DNA sensors: hybridization and electrochemical detection of DNA and RNA at two different surfaces, *Bioelectrochemistry* 56, 85–90.
- Palecek E., M. Fojta, F. Jelen and V. Vetterl, 2002b, Electrochemical analysis of nucleic acids, *Encyclopedia of Electrochemistry*, Vol. 9, Eds. A.J. Bard and M. Stratmann, pp. 365–367, 369–429, Wiley-VCH GmbH & Co. KGaA, Weinheim, Germany.
- Palecek, E., M. Fojta, M. Tomschik and J. Wang, 1998, Electrochemical biosensors for DNA hybridization and DNA damage, *Biosens. Bioelectron.* 13, 621–628.
- Palecek, E. and F. Jelen, 2002c, Electrochemistry of nucleic acids and development of DNA sensors, *Crit. Rev. Anal. Chem.* 32, 261–270.
- Petrovykh, D.Y., S.H. Kimura, L.J. Whitman and M.J. Tarlov, 2003, Quantitative analysis and characterization of DNA immobilized on gold, *J. Am. Chem. Soc.* 125, 5219–5226.
- Phinney, J.R., J.F. Conroy, B. Hosticka, M.E. Power, J.P. Ferrance, J.P. Landers and P.M. Norris, 2004, The design and testing of a silica sol–gel-based hybridization array, *J. Non-Cryst. Solids* 350, 39–45.
- Pivodori, M.I., A. Merkoci and S. Alegret, 2000, Electrochemical genosensor design: Immobilization of oligonucleotides onto transducer surfaces and detection methods, *Biosens. Bioelectron.* 15, 291–303.
- Robinson, H., Y.-G. Gao, R. Sanishvili, A. Joachimiak and A.H.-J. Wang, 2000, Hexahydrated magnesium ion bind in the deep major groove and the outer mouth of A-form nuclei acid duplexes, *Nucleic Acids Res.* 28, 1760–1766.
- Sakao, Y., F. Nakamura, N. Ueno and M. Hara, 2005, Hybridization of oligonucleotide by using DNA self-assembled monolayer, *Colloids Surf. B* 40, 149–152.
- Shimidzu, T., A. Ohtani, T. Iyoda and K. Honda, 1987, Charge-controllable polypyrrole/polyelectrolyte composite membranes: Part II. Effect of incorporated anion size on the electrochemical oxidation–reduction process, *J. Electroanal. Chem.* 224, 123–135.
- Steel, A.B., R.L. Levicky, T.M. Herne and M.J. Tarlov, 2000, Immobilization of nucleic acids at solid surfaces: Effect of oligonucleotide length on layer assembly, *Biophys. J.* 79, 975–981.
- Sun, X., P. He, S. Liu, J. Ye and Y. Fang, 1998, Immobilization of single-stranded deoxyribonucleic acid on gold electrode with self-assembled aminoethanethiol monolayer for DNA electrochemical sensor applications, *Talanta* 47, 487–495.
- Tereshko, V., G. Minasov and M. Egly, 1999, A ‘hydrated-Ion’ spine in a B-DNA minor groove, *J. Am. Chem. Soc.*, 121, 3590, 6970.
- Thompson, L.A., J. Kowalik, M. Josowicz and J. Janata, 2003, Label-free DNA hybridization probe based on a conducting polymer, *J. Am. Chem. Soc.* 125, 324–325.

- Vorotyntsev, M.A., E. Viel and J. Heinze, 1996, Ionic exchange of the polypyrrole film with the PC lithium perchlorate solution during the charging process, *Electrochim. Acta* 41, 1761–1771.
- Wang, J., X. Cai, G. Rivas, H. Shiraishi and D. Narasaiah, 1997, Nucleic acid immobilization, recognition and detection at chronopotentiometric DNA chips, *Biosens. Bioelectron.* 12, 587–599.
- Ye, Y. and H. Ju, 2003, DNA electrochemical behaviors, recognition and sensing by combining with PCR technique, *Sensors* 3, 128–145.

Threading Intercalators as Redox Indicators

Shigeori Takenaka

*Department of Materials Science, Faculty of Engineering, Kyushu Institute of Technology,
Kitakyushu 804-8550, Japan*

Contents

1. Introduction	345
2. What is a threading intercalator	346
3. Ferrocenylnaphthalene diimide derivatives as a threading intercalator	347
4. Immobilization of a thiolated oligonucleotide on the gold electrode	350
5. DNA sensor based on ferrocenylnaphthalene diimide as an electrochemical hybridization indicator	352
6. SNP detection with a ferrocenylnaphthalene diimide-based DNA sensor	354
7. Mediated current in DNA detection	359
8. Electrochemical gene detection based on supramolecular complex formation	360
9. DNA chips based on ferrocenylnaphthalene diimide	362
10. Conclusion	363
List of abbreviations	364
Acknowledgments	364
References	365

1. INTRODUCTION

With the completion of the human genome sequencing project, the focus is shifting to how genetic information is applied to medicine and human welfare at large. The DNA chip technology is attracting attention as a valuable means of high-throughput analysis of genes in sample DNA and it may be one of the most useful tools in the post-genome project. The DNA chip is a material which integrates thousands of different DNA fragments in a small space on its surface. Several years have passed since research related to DNA chips first became popular all over the world. As more and more genetic information related to many diseases accumulates rapidly, future methods of gene diagnosis should be required to deal with several hundred genes across many samples, all in a single day. DNA chips of the next generation are expected to meet this requirement and the research concerning electrochemical DNA chips is important in this context. Such chips will enable quick and simple gene diagnosis electrochemically. An electrochemical DNA chip can be realized by the integration of electrochemical DNA sensors and therefore it is important to develop a high performance electrochemical DNA sensor (Palecek and Fojta, 2001; Takenaka, 2001a; Willner, 2002; Drummond *et al.*, 2003). Electrochemical DNA sensing has been achieved by three types of

approaches, including the use of a DNA probe having an electrochemical signal part, use of an electrochemical DNA ligand, and the monitoring of the change in electrochemical characteristics of the surface associated with hybridization. The sensing method using an electrochemical ligand is especially interesting in the simplicity of a whole system, where DNA detection is achieved by only a single ligand coupled with a DNA probe-immobilized electrode. This approach was first reported for a DNA-binding metal complex (Millan and Mikkelsen, 1993). Many DNA ligands showing an electrochemical activity have been applied in this sensing system to obtain higher preference for dsDNA formed from target and probe DNAs. DNA-binding metal complexes and intercalating ligands have been reported by many researchers. Hashimoto *et al.* (1994) applied Hoechst 33,258 known as a DNA groove binder in this system. Although these DNA ligands showed some preference for DNA sequence, they could not show so large discriminating ability for dsDNA. Desired ligands are those showing high preference for dsDNA with high affinity and without any sequence selectivity. Under these circumstances, the author has been studying an electrochemical gene-detecting method based on ferrocenylnaphthalene diimide as the electrochemical hybridization indicator coupled with a DNA probe-immobilized electrode (Takenaka, 2001a, 2004). The performance of ferrocenylnaphthalene diimide is based on its binding mode for double-stranded DNA (dsDNA) in the threading intercalation. In this chapter, the author describes first what the threading intercalator is and the electrochemical DNA sensor based on ferrocenylnaphthalene diimide is discussed with the electrochemical DNA chip approach.

2. WHAT IS A THREADING INTERCALATOR

A threading intercalator is one of the intercalators carrying its substituents located in the major and minor grooves of dsDNA when its intercalating plane inserts between adjacent nucleic base pairs. To form such a complex, one of the substituents has to pass through the space created between adjacent base pairs of dsDNA. "Threading" of the threading intercalator derives from this mode of interaction. Anthracycline antibiotic nogalamycin is a well-known threading intercalator. Firstly we overview the binding chemistry of nagalamycin with dsDNA to understand what the threading intercalator is. Arora (1983) reported X-ray crystallographic analysis of nogalamycin, featuring a dumbbell-like structure where nogalose and amino sugar parts are attached to the opposite sides of the rectangular anthraquinone chromophore plane along its long axis and the molecular sizes are represented by their effective diameters, 12 and 6 Å (Figure 1A). Adjacent base pairs of dsDNA can create a cavity of 3.4 Å in thickness for the classical intercalation, while a minimum cavity size of 10 Å is required for threading intercalation (Comer *et al.*, 1984). Such information suggested that the hydrogen bonding of dsDNA base pairs has to cleave before dsDNA can form an intercalated complex with nogalamycin. The fact that a threaded complex is readily formed with nogalamycin suggests that the structure of DNA duplex is dynamic in nature, where the hydrogen bonds in base pairs are rapidly broken and reformed at ambient temperature, providing temporary cavities great enough for the bulky substituents

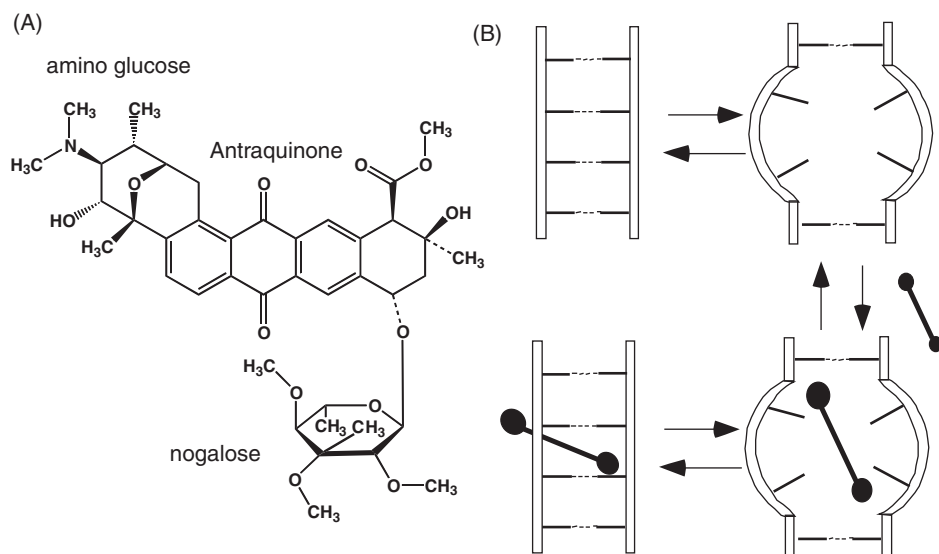


Fig. 1. (A) Structure of nogalamycin and (B) a schematic model for the threading interaction of nogalamycin to dsDNA.

of nogalamycin to penetrate (Niedle *et al.*, 1987; Wilson, 1996; Takenaka and Takagi, 1999). A regeneration of the base pairs then completes the threading intercalation. The expected process of threading intercalation is depicted in Figure 1B. The complex thus obtained can be kinetically stabilized due to the two projecting bulky substituents, which can act as anchors. The complexation of nogalamycin with dsDNA is characterized by a very small dissociation rate constant ($k_d = 0.001 \text{ s}^{-1}$, 0.5 M NaCl) (Fox *et al.*, 1985), which was in sharp contrast to classic intercalators such as ethidium bromide assuming a rate constant $k_d = 13 \text{ s}^{-1}$ under the same conditions (Wilson *et al.*, 1985). Such a small dissociation rate constant of nogalamycin from dsDNA is considered to be associated with its biological activity. Many X-ray crystallographic analyses of nogalamycin–DNA complexes have been reported for self-complementary hexanucleotides carrying different DNA sequences. For example, in the complexes with $d(\text{CGT}(\text{pS})\text{ACG})_2$ (Liaw *et al.*, 1989), where pS is an internucleotidic phosphorothioate linkage in the R configuration, nogalamycin molecules intercalate at the CG steps and its amino sugar is located in the major groove and its nogalose moiety in the minor groove of the hexamer duplex. 2D NMR study of the $d(\text{GCATGC})_2$ complex also gave a similar conclusion (Zhang and Patel, 1990). These results demonstrate that DNA can accommodate such bulky substituents for intercalation by the threading mode.

3. FERROCENYLNAPHTHALENE DIIMIDE DERIVATIVES AS A THREADING INTERCALATOR

Naphthalene bis(dicarboximide) (thereafter referred to as naphthalene diimide) derivative **1** (Figure 2) was studied as a threading intercalator by Gabbay *et al.*

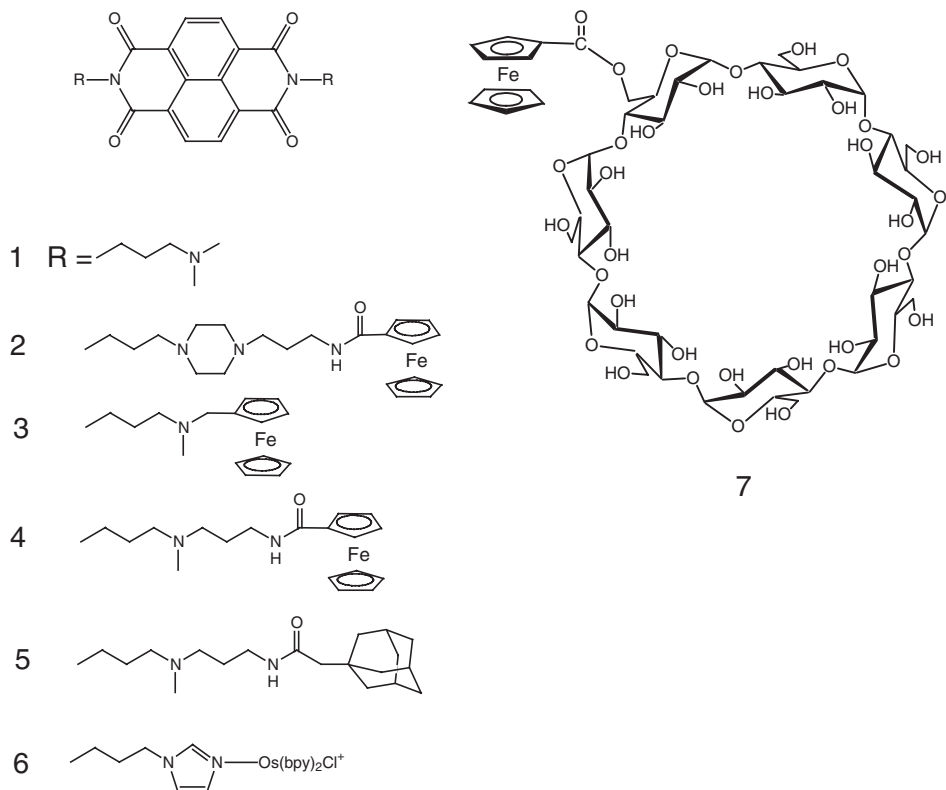


Fig. 2. Chemically synthesized naphthalene diimide **1**, ferrocenyl naphthalene diimide derivatives, **2–4**, and adamantyl naphthalene diimide **5**, imidazole-substituted naphthalene diimide complexed with $\text{Os}(\text{bpy})_2\text{Cl}_2$ (bpy: 2, 2'-bipyridinyl) **6**, and ferrocenyl- β -cyclodextrin **7**.

(1973) and Yen *et al.* (1982) extensively. Threading intercalation of naphthalene diimide has not yet been proven by direct evidence such as X-ray crystallography, but plenty of indirect evidence is available which supports threading intercalation (Tanious *et al.*, 1991). The absorption spectra of the naphthalene diimide part in **1** show a strong hypochromic effect upon binding to dsDNA and a negative Cotton effect is observed in this wavelength region in circular dichroism (CD) spectra. The DNA duplex becomes unwound when **1** binds to dsDNA and this is a typical behavior of intercalation. The salt effect on the association rate constant (k_a) for naphthalene diimide with dsDNA is somewhat different from that of the classic intercalators, where the slope of a plot of $\log k_a$ against $-\log [\text{Na}^+]$ is one for dicationic **1** in the neutral pH range, whereas classical dicationic intercalators such as quinacrine give a slope of two. This suggests that only one of the two cationic substituents in the threading intercalator is important in the association process (Jones and Wilson, 1981). The two positive charges of the conventional intercalator are placed exclusively in one of the grooves (minor groove), while that of **1** is placed evenly in the two grooves. Association kinetics of **1** with dsDNA is strongly dependent on its substituent size, implying that the association

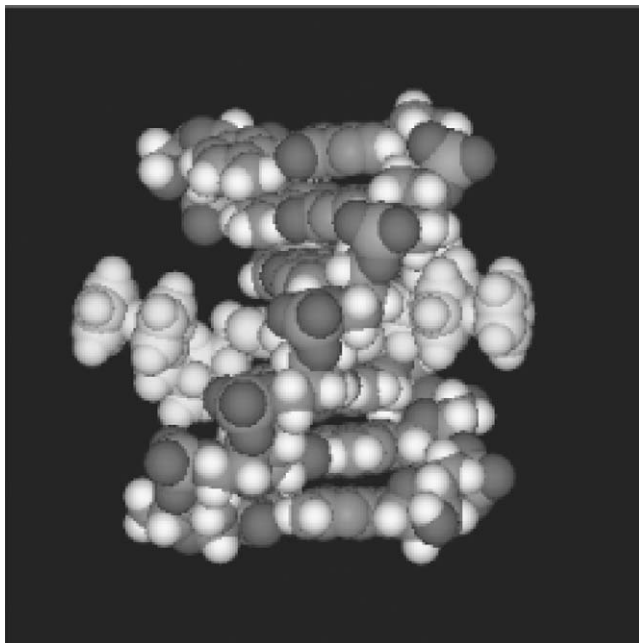


Fig. 3. An insight II molecular modeling of a complex of **3** with $d(\text{AAATTT})_2$ as dsDNA.

rate constant of **1** with dsDNA is dependent on the base pair opening process in dsDNA. Threading intercalators are expected to dissociate only very slowly from the dsDNA because of this peculiar binding mode. On the other hand, they will exert little, if any, stabilizing effect on the complex with single-stranded DNA (ssDNA). Therefore, threading intercalators should be able to discriminate dsDNA from ssDNA maximally.

With this consideration in mind, we designed and synthesized several ferrocenylnaphthalene diimide derivatives, as electrochemically active threading intercalator (**2–4** in Figure 2) (Takenaka *et al.*, 1998a, 2000; Sato *et al.*, 2000, 2001a, b). A computational modeling of a complex of **2** with dsDNA is shown in Figure 3. The two ferrocenyl moieties can be located over the major and minor grooves of dsDNA, when the naphthalene diimide part is intercalated into adjacent base pairs of dsDNA. Ferrocenylnaphthalene diimide derivatives (**2–4**) have various linker chains connecting the naphthalene diimide skeleton with ferrocene. There are different connecting patterns toward the end of the ferrocene with different redox potentials and different binding affinity for dsDNA depending upon the linker chain. As expected, ferrocenylnaphthalene diimide derivatives could form a stable complex with dsDNA, and owing to the redox activities of the ferrocene moieties, its interaction with dsDNA could be monitored electrochemically. This observation prompted us to study the electrochemical quantification of complementary DNA by using an ssDNA probe immobilized on an electrode. Before applying these derivatives to electrochemical DNA sensing, however, we studied the binding behavior of **2** with dsDNA (Takenaka *et al.*, 2000).

Ferrocenylnaphthalene diimide derivative **2** has an absorption maximum at 383 nm in buffered solution and this absorption band underwent hypochromic and bathochromic shifts, a characteristic behavior of naphthalene diimide-type threading intercalators. Spectrophotometric titration was carried out for **2** with calf thymus DNA as dsDNA in 10 mM 2-(*N*-morpholino)ethanesulfonic acid (MES) buffer and 1 mM ethylene diamine tetraacetic acid (EDTA) at pH 6.24 and 25°C. The data obtained were analyzed by Scatchard plots and fitting with the theoretical curves generated by the binding equation with a binding constant of $1.3 \times 10^5 \text{ M}^{-1}$, the maximum number of **2** bound per base pair, site size of 2, and cooperative parameter of 0.4. Scatchard analysis was not successful in the case of heat-denatured calf thymus DNA as a model of ssDNA because of the difficulty to prepare complete ssDNA: in our case, heat-denatured calf thymus DNA contained ca. 70% of dsDNA in the adopted buffered condition as estimated from its absorption spectra. Nevertheless, we were able to estimate roughly the binding constant of 10^4 M^{-1} which was four times smaller than that with intact dsDNA. The binding constants for **2** with [poly(dA-dT)]₂ and [poly(dG-dC)]₂ were similar, suggesting that **2** has no DNA sequence preference in the dsDNA binding. The dissociation rate constant of **2** from intact or heat-denatured calf thymus DNA was studied under conditions similar to that of Scatchard analysis. Stopped-flow kinetic analysis yielded a dissociation rate constant, $k_d = 0.056$ and 4.2 s^{-1} for **2** from intact and heat-denatured calf thymus DNA, respectively, in 10 mM MES buffer and 1 mM EDTA (pH 6.24) at 25°C. Although there is some ambiguity concerning heterogeneity of heat-denatured calf thymus DNA, the stability of the complex of **2** with dsDNA was over 100-times larger than that with ssDNA.

The electrochemical behavior of **3** was studied with ssDNA- or dsDNA-immobilized electrodes (Takenaka *et al.*, unpublished data). Thiolated oligonucleotide dT₂₀ was immobilized on a gold electrode through a thiol-gold linkage to form an ssDNA-immobilized electrode and the resulting electrode was allowed to hybridize with complementary dA₂₀ to form a dsDNA-immobilized electrode. After dipping in a solution containing **3**, the electrode was transferred to an electrolyte without **3** and cyclic voltammogram (CV) was measured (Figure 4). A one-step redox reaction of **3** ($E_{1/2} = 440 \text{ mV}$, $\Delta E_p = 70 \text{ mV}$) was observed only for dsDNA of the dA₂₀dT₂₀-immobilized electrode, whereas the signal intensity was barely above background for the ssDNA-immobilized electrode. This discrimination of dsDNA from ssDNA could be attributed to the formation of a stable complex of **3** with dsDNA through threading intercalation. The anodic peak of the CV curve in the case of dsDNA was greater than the cathodic one as shown in Figure 4 and this may suggest that the oxidized form of **3** has larger binding affinity for dsDNA than the reduced form and the former is hard to reduce in the polyanionic dsDNA.

4. IMMOBILIZATION OF A THIOLATED OLIGONUCLEOTIDE ON THE GOLD ELECTRODE

Until now, several methods have been reported concerning the DNA immobilization on the electrode (Lucarelli *et al.*, 2004). Since the method based on a

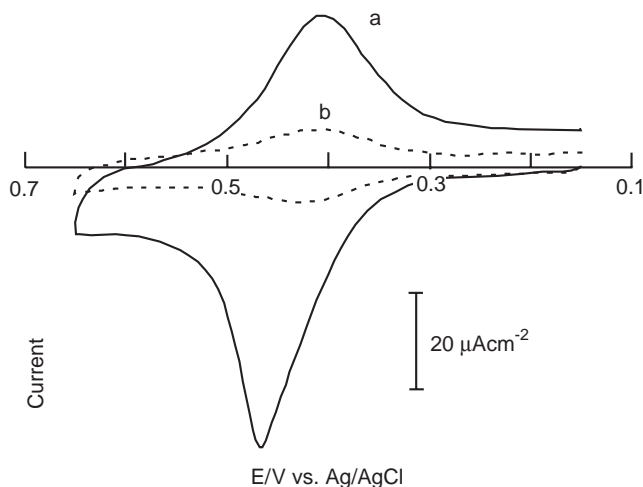


Fig. 4. Cyclic voltammograms of dT₂₀- (b) or dT₂₀dA₂₀- (a) immobilized gold electrodes in an electrolyte. The latter electrode was prepared by the hybridization of the former electrode with complementary dA₂₀. Before CV measurement, these electrodes were immersed in a solution containing **3**. It was estimated from the oxidation peak area of the CV that about 2.2 pmol mm⁻² of **3** was concentrated on the dsDNA-immobilized electrode. Assuming that 0.2 pmol mm⁻² of dsDNA were immobilized on the electrode, about 10 molecules of **3** were bound to single dsDNA molecule, a value in agreement with the quartz crystal microbalance (QCM) result.

sulfur–gold linkage is convenient and is easy to control the amount of DNA immobilized on the electrode, we adopted this method in our DNA sensing system. Three papers discussed this immobilization method in detail (Miyahara *et al.*, 2002; Yamashita *et al.*, 2002a; Takenaka, 2001b). The immobilization of an oligonucleotide on the electrode through a sulfur–gold linkage was achieved by the chemisorption of its thiol moiety on the gold surface of the electrode by the following procedure. A gold electrode having 2.0 mm² in area was polished with 6 μm, 1 μm of diamond slurry, and 0.5 μm of an alumina slurry in this order and washed with MilliQ water. This electrode was soaked in boiling 2 M NaOH for 1 h and then washed with MilliQ water. This electrode was then soaked in concentrated nitric acid, washed with MilliQ water, and dried. One μL of a 0.25 M NaCl solution containing 1 pmol of thiolated oligonucleotide was placed at the gold electrode held upside down and kept in a closed container under high humidity for 2 h at room temperature. After the electrode was washed with MilliQ water, 1 μL of 1 mM 6-mercaptohexanol was placed on the electrode for 1 h at 45°C. The electrode was kept in MilliQ water for 30 min at room temperature. The dsDNA-immobilized electrode was prepared by the hybridization of the ssDNA-immobilized electrode with a complementary oligonucleotide as follows. One microliter of 2 × SSC (0.03 M sodium citrate buffer containing 0.3 M NaCl at pH 7.0) containing 5 pmol of the complementary DNA of the same length was placed on the electrode for 1 h at 37°C to allow hybridization to proceed.

The extent of surface coverage of an electrode with dA₂₀dT₂₀ as dsDNA was evaluated by the cyclic voltammogram of a dsDNA-immobilized electrode as shown in Figure 4. The amount of **3** concentrated on the dsDNA was estimated to be 6 pmol from the area of the oxidation current in the cyclic voltammogram (Figure 4). Since about 8 molecules of **3** bind to one dsDNA (to be discussed under the quartz crystal microbalance, QCM, measurements), 0.7–0.8 pmol of dsDNA were found to have been immobilized on this electrode with 2 mm² in area (the effective surface area was assumed to be 1.2–1.5 times larger) or 0.2–0.3 pmol mm⁻² in terms of coverage density. The theoretical value is reported to be 0.4 pmol mm⁻² for similar dsDNA immobilization (Kelley *et al.*, 1997) and hence nearly 50% of the surface is covered by dsDNA, to which **3** is supposed to be accessible freely. When thiolated dT₂₀ was immobilized on the gold electrode, its amount fixed on the electrode was greater than the theoretical value (Takenaka *et al.*, 2000). The exact reason for this phenomenon is not clear now, but the fact that oligothymine tends to be adsorbed on the gold surface specifically may be responsible (Levicky *et al.*, 1998).

5. DNA SENSOR BASED ON FERROCENYLNAPHTHALENE DIIMIDE AS AN ELECTROCHEMICAL HYBRIDIZATION INDICATOR

The event of the dsDNA formation on the ssDNA-immobilized electrode can be electrochemically monitored with electrochemically active ligands carrying high preference for dsDNA. Such ligands are called “electrochemical hybridization indicators” (Takenaka, 2001a). The electrochemical DNA sensing based on these ligands is summarized in Figure 5. In brief, ssDNA as a DNA probe (oligonucleotide fragment with a sequence complementary to that of the target gene) is immobilized first on the electrode as described above. This electrode is dipped in a sample DNA solution to allow hybridization to proceed. When a target DNA fragment is present in it, dsDNA is formed with the DNA probe on the electrode. The electrochemical measurement of the electrode is made in an electrolyte containing the electrochemical hybridization indicator. The amount

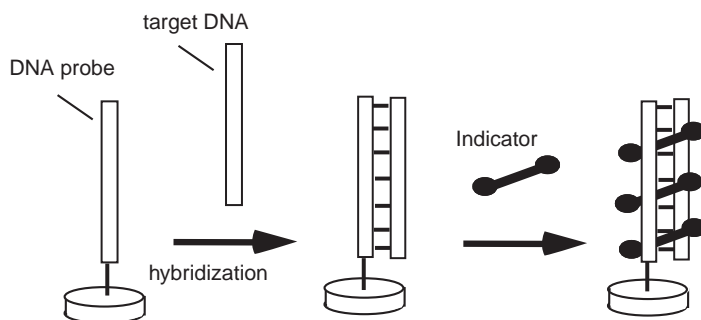


Fig. 5. Principle of the electrochemical gene detection based on an electrochemical hybridization indicator such as ferrocenylnaphthalene diimide.

of the indicator concentrated on the electrode increases with an increase in the amount of dsDNA formed on the electrode and therefore the amount of target DNA can be quantitated from this electrochemical response. As shown in Figure 5, the indicator should have the characteristics of high affinity for dsDNA without any sequence specificity. The ferrocenylnaphthalene diimide derivatives we developed meet such requirements.

Figure 6 shows a typical example of differential pulse voltammograms (DPVs) of a 20-meric oligonucleotide-immobilized electrode in an electrolyte containing 0.05 mM **2** before and after hybridization with its complementary DNA, where 5'-TTCACCAGAGGGTCCCCTGG-3' and its complementary DNA were used as the DNA probe and target DNA, respectively (Miyahara *et al.*, 2001). The DPV of 6-mercaptohexanol-immobilized electrode in the same electrolyte is also shown in Figure 6. A peak was observed at 0.4 mV in all of the DPV measurements and a peak current was ca. 0.9 μ A in the case of ssDNA. Since the peak current of the electrode masked with 6-mercaptohexanol, arising from diffusion of **2** from the bulk solution, was 0.6 μ A, the intrinsic current of **2** concentrated on ssDNA may be 0.3 μ A. The current based on the diffusion of **2** in the bulk solution to the electrode can be estimated from a method similar to that described previously (Miyahara *et al.*, 2002; Yamashita *et al.*, 2002a). Oligonucleotides (10 pmol each) of various lengths (15–50 mer) were immobilized on the electrode and the DPV current measured on the electrode in the presence of 0.05 mM **2**. The current obtained increased linearly with the length

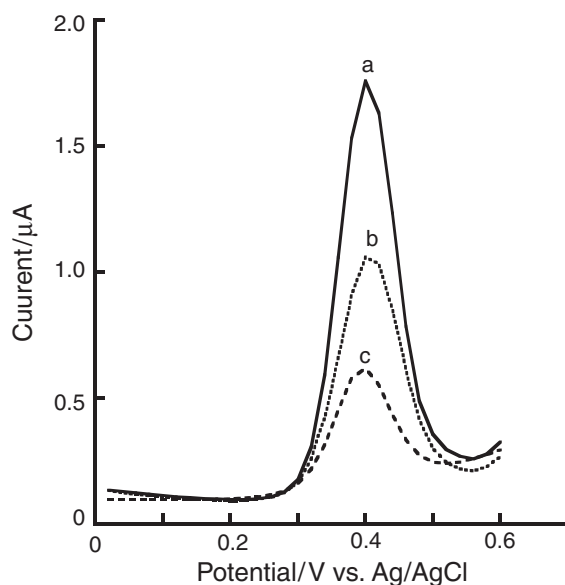


Fig. 6. Differential pulse voltammograms for 5'-TTCACCAGAGGGTCCCCTGG-3'-immobilized electrodes before (b) and after (a) hybridization with complementary oligonucleotide in 0.1 M AcOH-AcOK buffer containing 0.1 M KCl at pH 5.6 in the presence of 0.05 mM **2** at 25°C. DPV for a 6-mercaptohexanol-immobilized electrode is also shown in curve (c).

of oligonucleotide. The extrapolation of this line gave ca. $0.6\ \mu\text{A}$ and this value was regarded as the current due to diffusion. This value was independent of the DNA sequence and the base composition, as long as the DNA length is kept constant.

The dsDNA was prepared by the hybridization of $1\ \mu\text{L}$ of complementary ssDNA ($1\ \text{pmol}$) with the ssDNA-immobilized electrode in $2 \times \text{SSC}$ for 1 h at 37°C . The peak current of this electrode carrying 20-meric dsDNA was $1.5\ \mu\text{A}$ in the DPV measurement. Although the covered area on the gold electrode increased somewhat upon duplex formation, the current based on the diffusion of **2** was assumed to be constant and therefore, the current increased 3 times by the dsDNA formation (The current due to the ssDNA and dsDNA was 0.3 and $0.9\ \mu\text{A}$, respectively). The discrimination ability between ssDNA and dsDNA is not as high as that expected in the experiment in homogeneous solution (compared with Figure 4), presumably because of a difference of the homogeneous solution and heterogeneous surface on the electrode. Assuming that the current due to the diffusion is constant in each electrode, the current shift $\Delta i = (i - i_0)/i_0$ was introduced to correct for the amount of the ssDNA immobilized on the individual electrodes, where i_0 and i refer to the current before and after hybridization, respectively. Although i_0 and i values contain the background current based on the diffusion of **3**, this value is proportional to the amount of the hybridized dsDNA per DNA probe and the amount of the DNA probe immobilized on the individual electrodes can be standardized. In fact, when this index is used, the amount of dsDNA formed per DNA probe immobilized on individual electrodes could be evaluated.

6. SNP DETECTION WITH A FERROCENYLNAPHTHALENE DIIMIDE-BASED DNA SENSOR

SNP stands for single nucleotide polymorphism which exists every 500–1000 base pairs (bp) in three billion bp of human chromosomal DNA. SNP are common DNA sequence variations and strongly correlated with the individuals and hence can be used as a high-density marker of the gene. Many SNP data are already collected and some of the SNPs are correlated with some diseases or a side effect of a given drug (Brookes, 1999). Therefore, the development of rapid and highly accurate SNP detection becomes a foothold of tailor-made medications. Commonly, SNP detection is achieved by the DNA hybridization method whose principle is shown in Figure 7.

Let us consider two SNP types of allele 1 and allele 2, for example, that differ in one base as shown in Figure 7. A DNA probe fragment representing a sequence complementary to that of allele 1 is immobilized on the electrode as a DNA probe. A DNA sample containing allele 1 or allele 2 is allowed to hybridize with the DNA probe immobilized on the electrode. A fully matched or one base mismatched DNA duplex is formed from allele 1 or allele 2, respectively. In the case of Figure 7, A/C mismatched DNA duplexes are formed from allele 2 that differ from the A/T fully matched DNA duplexes in their thermal

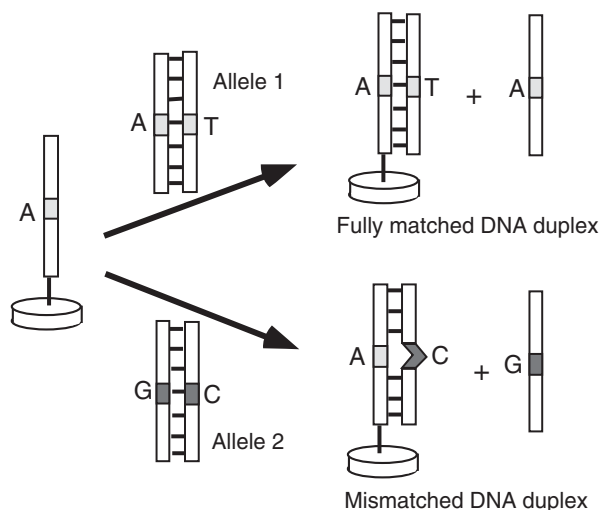


Fig. 7. Principle of SNP analysis based on the DNA hybridization method.

stability. In other words, the DNA duplex containing mismatched bases is thermally less stable because of the presence of the mismatch and tends to dissociate from the DNA probe more easily. Experimentally, the discrimination of these two duplexes can be achieved by adjusting the hybridization temperature or the washing conditions such as different buffers and salt conditions at different temperature after hybridization. This method is called allele specific hybridization (ASH) and has been used for the detection of various types of gene mutation (Beaudet *et al.*, 2001). As the size of a matched DNA region of probe DNA carrying a mismatch increases, the discrimination becomes more difficult. Therefore, 20-meric synthetic oligonucleotides are generally used as a DNA probe. However, the types of mismatched base pairs and neighboring base sequences also affect the magnitude of the difference and the ease of discrimination between the fully matched and mismatched DNA duplexes. From this viewpoint, SNP analysis coupled with enzymatic reaction such as Invader assay has been developed (Lyamichev *et al.*, 1999).

Another difficulty of SNP analysis in heterozygotes lies in the fact that there are two different alleles at a 1:1 ratio on the autosome of the human chromosome. As a gene type, there are a homozygote which has the same SNP type on both the chromosomes and a heterozygote which has two SNP types on each of the two chromosomes. Thus, detection of a 1:1 mixture of matched and mismatched DNA duplexes is necessary to analyze a heterozygous SNP sample.

Firstly, we tried electrochemical SNP detection of a homozygote by using **2** (Yamashita *et al.*, 2000, 2002a). A 20-meric oligonucleotide was immobilized on the gold electrode as a DNA probe and 20-meric complementary oligonucleotides carrying partially different base(s) were allowed to hybridize separately at 20°C where a DNA duplex can be formed with either of the combinations. This procedure gave mismatched DNA duplexes carrying mismatched base(s) at different sites on the duplex. The DPV of the resulting electrodes for the fully

matched and mismatched DNA duplexes was measured in an electrolyte containing **2** to show that the Δi value for this mismatched DNA duplex was smaller than that for the fully matched one due to the difference in the amount of bound **2** per DNA duplex.

The amount of **2** bound to the DNA duplex was evaluated by QCM experiments (Yamashita *et al.*, 2000, 2002a). A 20-meric oligonucleotide (5'-AT-TGACCGTAATGGGATAGG-3') was immobilized on the gold-covered QCM plate and dipped in buffer solution. A matched (5'-CCTATCCCATTACGGT-CAAT-3') or mismatched 20-meric oligonucleotide (5'-CCTATCCCGT-TACGGTCAAT-3', underlined is the mismatch) was added to this solution and a change in the frequency of the QCM plate was observed for both of them. A frequency decrease was observed for the fully matched and mismatched oligonucleotides under the conditions adopted (Figure 8), suggesting formation of a DNA duplex. When **2** was added to this system, the frequency of QCM decreased in proportion to the amount of **2** bound to the DNA duplex and this amount on the QCM plate was estimated from the frequency decrease in each case. It was found that 8 molecules of **2** could bind to the fully matched 20-meric oligonucleotide duplex on average, whereas 6 molecules of **2** could bind to the mismatched one. Since 8 or 6 molecules of **2** were bound to one of the fully matched or one base mismatched 20-meric oligonucleotide duplex, respectively, the current obtained here was due to bound **2** per one DNA duplex. This is reasonable in light of the nearest exclusion model and the terminal effect of the intercalation into a short DNA fragment. On the other hand, the existence of

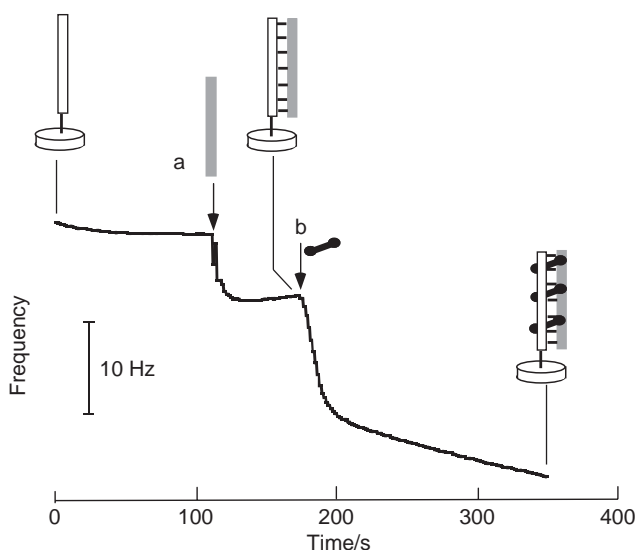


Fig. 8. Frequency change for a thiolated oligonucleotide-immobilized QCM chip upon addition of the complementary oligonucleotide (addition point a) to form dsDNA and **2** (addition point b). The final frequency changes were 7.98 ± 0.1 Hz (1.81 ± 0.02 pmol) and 11.4 ± 0.85 (15.1 ± 1.13 pmol) after addition of complementary oligonucleotide and **2**, respectively.

one base mismatch on the 20-meric oligonucleotide duplex gave 6 molecules of bound **2** on average, demonstrating that **2** could not bind to mismatched base pairs nor the base pairs neighboring the mismatched one. This should give rise to a decrease in the Δi values. In fact, (as expected) the Δi values obtained for the fully matched and mismatched DNA duplexes were $102 \pm 16.7\%$ and $78 \pm 8.1\%$, respectively. Therefore, the occurrence of an SNP in sample DNA may be detected from a decrease in Δi value from that of the fully matched DNA duplex. This discrimination is not dependent on the thermal stability of matched and mismatched DNA duplexes, and, therefore, this discrimination method is especially effective when used as a DNA chip where many DNA probes carrying different sequences with different duplex stability are integrated in a small area of the substrate surface. However, this method is limited to a DNA sample of the same size as that of the DNA probe. Furthermore, the discrimination ability would decrease with an increase in their length as described above.

To circumvent these disadvantages, a difference in the thermal stability of the fully matched or mismatched DNA duplexes was also taken into account in the mismatch discrimination. When **2** is bound to a DNA duplex region, this region is stabilized as a result of the threading intercalation. Therefore, the fully matched and mismatched DNA duplexes should be discriminated by taking advantage of a difference in their thermal stabilities after binding of **2** even where they have similar thermal stabilities in the absence of **2**.

The effective one base mismatch discrimination was realized for SNP in the cancer suppressor gene p53 by optimizing the measurement temperature. It is known that there are sites called hot spots on this gene that are prone to undergo mutation and the mutation results in impairment of the malignancy-suppressing ability of the p53 gene product. Electrochemical SNP analysis with a 20-meric oligonucleotide carrying an SNP site coupled with **2** was performed for the transition to A from G in the codon for the amino acid at position 175, 248, or 273 and the transversion to C from G in the codon for the amino acid at position 72 (Miyahara *et al.*, 2002; Takenaka *et al.*, 2001b). The optimal measuring temperature was surveyed where fully matched and mismatched 20-meric target oligonucleotides can be discriminated maximally. This turned out to be 35°C as shown in Figure 9. The magnitudes of the peak current with these DNA probe-immobilized electrodes were about 2 μ A. After hybridization at 35°C, the Δi for the fully matched and mismatched DNA duplexes were 50% and 20%, showing that mismatched DNA detection can be achieved in this system. Moreover, SNP analysis for the PCR product (275 bp of dsDNA) of exon 4 of the p53 gene was attempted by this method. In this case, the detection of a heterozygote was achieved with two DNA probes corresponding to two alleles (G or C type) in the codon for the amino acid at position 72. Since the heterozygote has two types of alleles, a significant increase in the Δi values could be observed with the two DNA probes. Individual PCR products from 22 unknown samples were tested and 68% were judged correctly or consistent with the sequencing result. This rate of hit is obviously lower than that for the model oligonucleotides due presumably to the fact that the Δi value is not enough to correct for the variability of individual electrodes with respect to the extent of

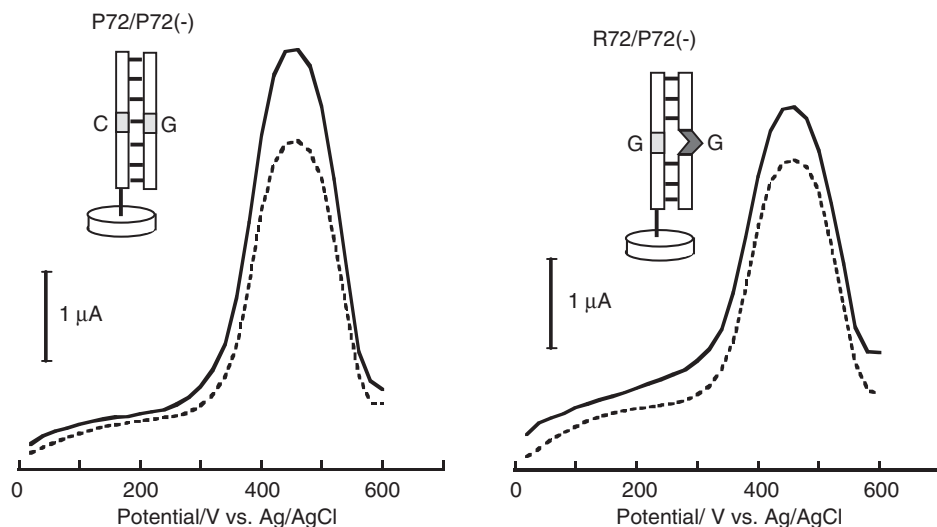


Fig. 9. DPV for P72 or R72 immobilized on the electrode before (broken line) and after hybridization (solid line) with P72(-) in the presence of 0.05 mM **2** at 35°C.

probe immobilization. In addition, the size of the sample DNA is much larger than that in the oligonucleotide system (278 bp vs. 20-mer) and the hybridization efficiency of the PCR product was lower than that of the probe DNA.

A detection system with higher reproducibility was also developed by improving the immobilization method of DNA probe on the electrode. The PCR products (350 bp) containing a mutated G818 → A transition and G916 deletion of the human lipoprotein lipase (LPL) gene were tested by this improved electrochemical DNA detection based on **2** (Yamashita *et al.*, 2002b). After optimization of the detection condition, this system was assessed with 10 unknown samples (0.2 pmol each of a PCR product) of the two types of LPL mutation, and the genotype was correctly identified in every case. Figure 10 shows an example of the detection of a heterozygote of the LPL gene. In the method described here, two different DNA probe-immobilized electrodes were necessary to detect the heterozygote.

We next devised a method of detecting heterozygous SNP with one electrode (Nojima *et al.*, 2003). Since the rate of DNA duplex formation is the same with the fully matched and mismatched DNA duplexes, a heterozygote sample containing two different alleles gives matched and mismatched duplexes at a 1:1 ratio even with a DNA probe representing one of the alleles. Since only the mismatched DNA duplex on the electrode tends to dissociate from the electrode in the measurement step, half of the hybrid DNA of a heterozygote dissociate, whereas no hybrid DNA dissociates in a homozygote carrying the same SNP type as that of the DNA probe. In the case of the homozygote carrying an SNP type different from that of the DNA probe, all hybrids dissociate from the electrode. Here, C- or G-type SNP is called W (wild) or M (mutant), respectively. The electrochemical measurement after this treatment should give a ratio of 2:1:0 for WT/WT, WT/MT and MT/MT for a homozygote carrying the same

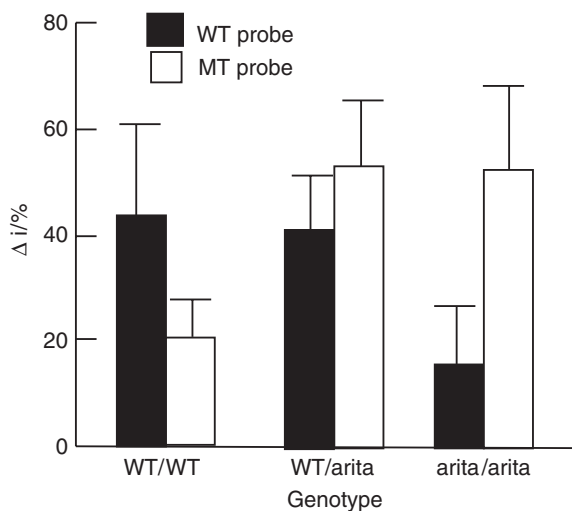


Fig. 10. Electrochemical detection of the heterozygous LPL gene. The heterozygote gave rise to a significant electrochemical signal from both electrodes for the wild and mutant-type DNA probes.

SNP type as that of the DNA probe and a heterozygote carrying an SNP type different from that of the DNA probe.

A mutated C to G transition in the codon for Ser-447 of the human LPL gene was tested by the above method. Only a DNA sample of M-type could dissociate from the electrode with a 13-meric DNA probe in 0.1 M potassium acetate buffer (pH 5.6) and 0.1 M KCl, and 0.05 mM **2** at 45°C. Under these conditions, the PCR products (231 bp) of W/W, W/M, and M/M gave Δi values 122.7 ± 16.5 , 42.7 ± 14.1 , and 17.8 ± 2.8 with a W-type DNA probe-immobilized electrode. The ratio of these values was regarded as reasonably close to the theoretical ratio of 2:1:0. Whereas, the Δi values 116.9 ± 20.0 , 53.7 ± 18.0 , and 8.0 ± 12.5 were obtained in the case of an M-type DNA probe-immobilized electrode, the ratio again reasonably close to the theoretical 0:1:2. This SNP detection for homozygotes and heterozygotes was achieved directly with chromosomal DNA treated with RNase A. Thus, ferrocenylnaphthalene diimide-based electrochemical DNA detection was successfully achieved not only with PCR products, but also with genomic samples.

7. MEDIATED CURRENT IN DNA DETECTION

Ferrocenylnaphthalene diimide bound to dsDNA is expected to act as a DNA wire because of its multiple binding on dsDNA. In the meantime, it is known that ferrocene can mediate electron transfer to the electrode from reduced glucose oxidase (Voet *et al.*, 1981). Therefore, ferrocenylnaphthalene diimide bound to dsDNA on the electrode may mediate electron transfer reaction. The reduced glucose oxidase was generated by its treatment with glucose. Figure 11 shows a

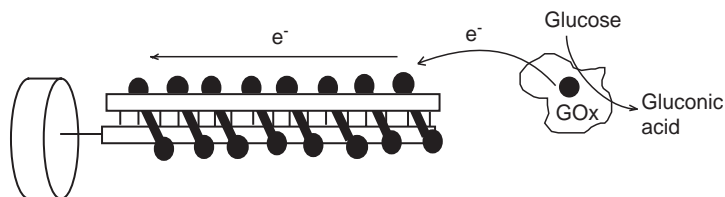


Fig. 11. Drawing of the expected electron transfer mechanism between reduced glucose oxidase and the electrode through dsDNA covered with ferrocenylnaphthalene diimide bound to the DNA duplex.

drawing of the expected electron transfer mechanism between reduced glucose oxidase and the electrode through the DNA duplex covered with many **2** molecules.

To prove the occurrence of electron transfer, **2** bound to dsDNA on the electrode was dipped in a solution containing reduced glucose oxidase and its CV curve was measured (Takenaka *et al.*, 1998b). Control experiments were performed with ferrocenecarboxylic acid and trimethylaminomethylferrocene in place of **2**. In the case of ferrocenecarboxylic acid, no mediated current was observed due presumably to the electrostatic repulsion between ferrocenecarboxylic acid and DNA polyanions on the electrode. On the other hand, a mediated current was observed in the case of **2** and trimethylaminomethylferrocene and the mediated current of **2** was nearly twice as large as that of the latter. Since cyclic voltammographic peak areas for **2** and trimethylaminomethylferrocene were identical, their amounts concentrated on the electrode were the same. It is conceivable that the larger mediated current observed for **2** derived from the ferrocene-coated DNA, as the amount of ferrocene concentrated on both electrodes is identical. However, the effect of polyferrocene was much smaller than expected, presumably because **2** and reduced glucose oxidase was segregated: the former as a mediator was concentrated on the dsDNA-immobilized electrode and the latter existed in the bulk solution. Therefore, the mediate reaction could occur only when the reduced glucose oxidase diffused to the electrode. By contrast, since some fraction of trimethylaminomethylferrocene was concentrated on the dsDNA-immobilized electrode by the electrostatic interaction and also could participate in the mediate reaction occurring in the solution, the effective mediation reaction could occur with this ferrocene.

Naphthalene diimide derivative **7** having an osmium complex as an electrocatalytic site was reported by Gao and co-workers (Tansil *et al.*, 2005). The catalytic current was obtained for the complex of **7** bound to the dsDNA region on the electrode in the presence of ascorbic acid. They succeeded in detecting 50-meric target DNA in the range of 1.0–300 pM with a detection limit of 1.5 amol.

8. ELECTROCHEMICAL GENE DETECTION BASED ON SUPRAMOLECULAR COMPLEX FORMATION

To extend the electrochemical detection based on the naphthalene diimide derivative as a threading intercalator, we designed and synthesized

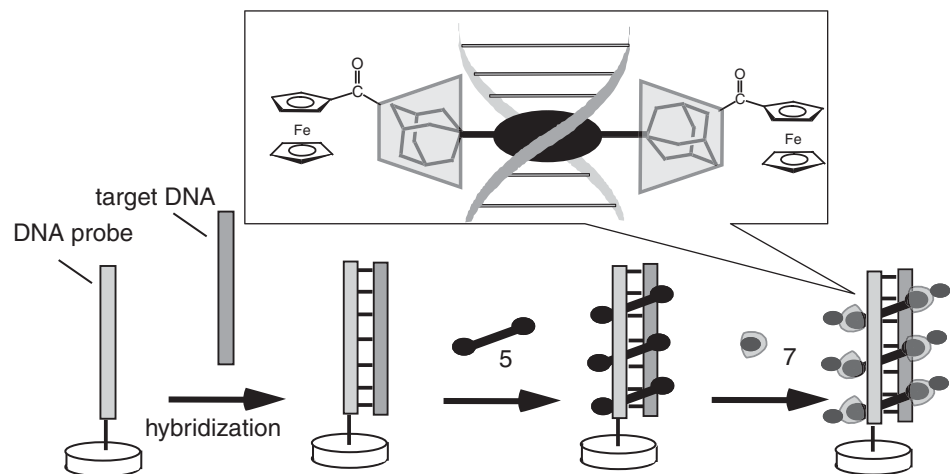


Fig. 12. Stratagem of the new DNA detection system based on **7** and **5**. A DNA probe-immobilized electrode is allowed to hybridize with sample DNA. A duplex is formed on the electrode as long as the sample DNA contains a sequence complementary to that of the probe. After immersing **7** and **5** and washing with water, the supramolecular complex remains on the electrode with dsDNA on it and one can detect the target DNA from the electrochemical signal of **7**. The putative structure of a supramolecular complex of **5**, **7**, and dsDNA is also shown in the figure. The ferrocene moiety of **7** is incorporated into the cavity of the β -cyclodextrin part in an aqueous solution.

adamantyl naphthalene diimide **5** coupled with ferrocenyl- β -cyclodextrin **7**. The chemical structures of **5** and **7** are shown in Figure 2. Compound **5** is expected to bind to dsDNA by threading intercalation where the two adamantyl moieties are located in the major and minor grooves of dsDNA. Since it is known that the ferrocene of **7** is incorporated into its cavity (Ueno *et al.*, 1982) and adamantane can be incorporated into **7** to drive the ferrocene part out (Ryabov *et al.*, 1990), **7** can bind to **5** bound to dsDNA by capping of the two adamantyl moieties projecting out in the major and minor grooves of DNA (see enlarged model structure in Figure 12). They can act as an additional anchor to prevent dissociation of the complex of **5**. Therefore, the supramolecular complex consisting of **7** and **5** bound to dsDNA is expected to be stabilized further by capping of the adamantyl moieties of **5** by **7**, thereby resulting in the improved discrimination ability for dsDNA. Furthermore, the ferrocene moieties are concentrated on the complex of **5** with dsDNA, which may facilitate electrochemical detection. From this viewpoint, we designed a new DNA detecting system based on **5** and **7** as shown in Figure 1. Target DNA can be trapped on the DNA probe-immobilized electrode by the specific interaction during the hybridization process. When this electrode is treated with a solution containing **5** and **7**, a supramolecular complex is formed on the electrode. Since this complex on the electrode is stable to washing with water, one can detect the target DNA from the electrochemical response of **7** concentrated on the electrode.

This supramolecular complex will never form with the electrode treated with non-target DNA.

This idea was tested with a 23-meric DNA fragment representing part of the UDP-glucuronosyl transferase gene as a model, which is useful for predicting severe toxicity by irinotecan. Only a perfectly matched combination of target DNA gave a current peak at 0.58 V in DPV, whereas no DPV signal was observed for the DNA probe alone or non-complementary DNA. This electrochemical gene detection based on the supramolecular complex formation was the first example and will stimulate further studies on the new application of a supramolecular complex (Sato *et al.*, 2004).

9. DNA CHIPS BASED ON FERROCENYLNAPHTHALENE DIIMIDE

A DNA chip is now an indispensable tool for gene research where many different kinds of DNA probes are integrated in a small area and generally fluorescently labeled DNA sample is allowed to hybridize on it. After washing the DNA chip with buffer solution, many kinds of genes could be analyzed simultaneously by the fluorescence signal on the surface of the DNA chip (Skena, 1999).

For the first time we succeeded in electrochemical visualization of DNA chips by scanning electrochemical microscopy (SECM) (Yamashita *et al.*, 2001). The DNA chip was prepared by spotting a DNA solution on an aminopropylsilane-coated glass substrate with a DNA microarrayer of 100 μm in diameter. Sample DNA is allowed to hybridize on the DNA chip under proper conditions and measured in an electrolyte containing **2** by SECM. Intercalator **2** was concentrated on dsDNA formed between target DNA and probe DNA on the DNA chip, enabling electrochemical visualization by SECM. A one-base mutation of the p53 gene was successfully detected for the PCR product by this method. This method is potentially applicable as a conventional DNA microarray system without any special chips such as multi-electrode array. However, there are some difficulties to be overcome for keeping the DNA chip horizontally to scan the probe electrode.

On the other hand, the studies on multi-array electrodes have been carried out as an electrochemical DNA chip. This electrochemical DNA chip system is expected to constitute a more compact instrument with good cost performance. Many researchers of companies have been developing electrochemical DNA chips and their readers coupled with new electrochemical DNA detecting technologies (Umek *et al.*, 2001; Brazill *et al.*, 2003; Patolsky *et al.*, 2002; Fan *et al.*, 2003). All of these devices have a potential to offer a relatively inexpensive, easy-to use, and portable tool for DNA analysis and present platforms for high-throughput gene diagnosis. Recently, TUM-gene Inc. developed a simultaneous multiple mutation detection (SMMD) method coupled with an electrochemical array (ECA) chip (Wakai *et al.*, 2004). Figure 13 shows the principle of this method. A DNA probe carrying an SNP site at the 3'-end was immobilized on the electrode. A sample was amplified by PCR and designed to form a hairpin structure downstream of the SNP site. This sample was allowed to hybridize on the electrode, followed by a ligation reaction, which occurred only for the matched SNP type. After

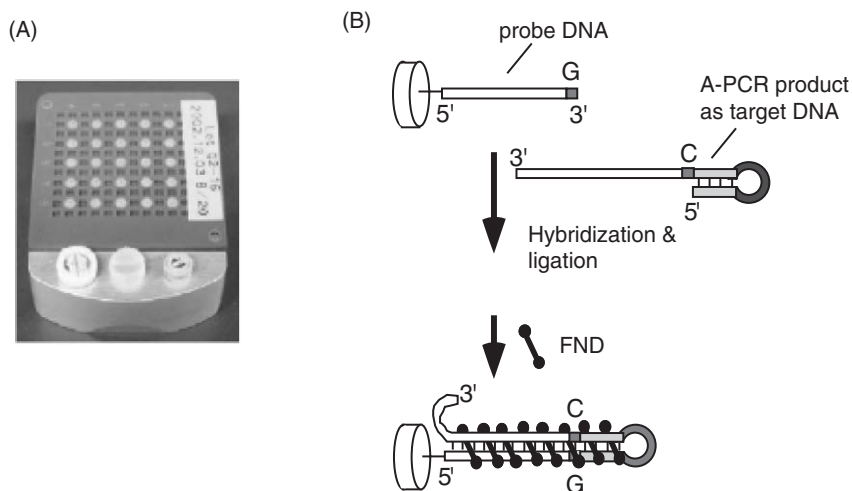


Fig. 13. (A) An electrochemical (ECA) chip having 25 gold electrodes on a ceramic substrate. The left electrode in the front is the reference electrode, and the one to the right is the counter electrode. (B) Principle of the SMMD method. Sample DNA is amplified by PCR, followed by asymmetric PCR (A-PCR) with the specially designed primers. Following hybridization with a DNA probe-immobilized electrode corresponding to the proper SNP, a ligation reaction is allowed to proceed. An electrochemical signal is obtained in the electrochemical measurement in an electrolyte containing **2** only when the target SNP was present in the sample DNA.

heat-denaturation, DPV was determined and the increased current signal was obtained in the case of the matched SNP type. In other words, the relevant SNP was (or may be) judged correctly by this procedure. As an example of this method using an ECA chip, seven different mutations of the LPL gene could be successfully achieved for 50 patients in a blind test (Wakai *et al.*, 2004). This method can be extended to other mutation types such as insertion, deletion, translocation, and short tandem repeat on a single chip by designing appropriate PCR primers, eventually realizing a diagnostic chip.

10. CONCLUSION

The rapid and simple DNA detecting technology is becoming more and more important, as so many disease-related or drug-concerning genes are being unveiled. The electrochemical DNA detecting technique is a good candidate to achieve this goal and the device thus obtained will be useful as a valuable means for a point of care. Many researchers are trying to develop several kinds of an electrochemical DNA-detecting method to meet this demand. This chapter focused on the method based on an electrochemically active ligand as an electrochemical hybridization indicator because of its ease and quickness. Especially, we summarized the electrochemical gene detection based on ferrocenylnaphthalene diimide or threading intercalator derivatives. This ligand showed a high preference for dsDNA with special stabilization of its complex by threading-type

intercalation. Ferrocenylnaphthalene diimide can be used for electrochemical gene detection and furthermore this method can be applied as the new SNP detection by taking advantage of a decrease in the amount of the ligand bound to a mismatched DNA duplex region. This can be extended to error-free diagnostic chips coupled with the SMMD-ECA chip method. Electrochemical gene detection based on the electrochemical hybridization indicator is more suited for a practical gene-detecting chip than that based on an electrochemical DNA probe because of its large and stable current response. However, the background current based on the diffusion from bulk solution and non-specific absorption has not been completely eliminated up to this day. When this weakness is overcome, the DNA chip based on ferrocenylnaphthalene diimide or other electrochemical hybridization indicators may be promising in rapid, real-time testing of genes.

LIST OF ABBREVIATIONS

DNA	deoxyribonucleic acid
dsDNA or ssDNA	double-stranded or single-stranded DNA
A	adenine
C	cytosine
G	guanine
CD	circular dichroism
k_a or k_d	association or dissociation rate constant
QCM	quartz crystal microbalance
CV	cyclic voltammetry
DPV	differential pulse voltammetry
SNP	single-nucleotide polymorphism
ASH	allele-specific hybridization
PCR	polymerase chain reaction
A-PCR	asymmetric PCR
LPL	lipoprotein lipase
W or M	wild or mutant
SECM	scanning electrochemical microscopy
SMMD	simultaneous multiple mutation detection
ECA	electrochemical array
MES	2-(<i>N</i> -morpholino)ethanesulfonic acid

ACKNOWLEDGMENTS

The author is grateful to all of his co-workers whose names appear in the papers cited in references for their enthusiasm for research. Special thanks are due to Prof. Hiroki Kondo of Kyushu Institute of Technology for advice and helpful discussions.

REFERENCES

- Arora, S.K., 1983, Molecular structure, absolute stereochemistry, and interactions of nogalamycin, a DNA-binding anthracycline antitumor antibiotic, *J. Am. Chem. Soc.* 105, 1328.
- Beaudet, L., J. Bedard, B. Breton, R.J. Mercuri and M.L. Budarf, 2001, Homogeneous assays for single-nucleotide polymorphism typing using alphascreen, *Genome Res.* 11, 600.
- Brazill, S., N.E. Hebert and W.G. Kuhr, 2003, Use of an electrochemically labeled nucleotide terminator for known point mutation analysis, *Electrophoresis.* 24, 2749.
- Brookes, J., 1999, The essence of SNPs, *Gene.* 234, 177.
- Comer, D.A., S. Neidle and J.R. Brown, 1984, Molecular models for the interaction of the anti-tumour drug nogalamycin with DNA, *Biochem. Pharmacol.* 33, 2877.
- Drummond, T.G., M.G. Hill and J.K. Barton, 2003, Electrochemical DNA sensors, *Nat. Biotechnol.* 21, 1192.
- Fan, C., K.W. Plaxco and A.J. Heeger, 2003, Electrochemical interrogation of conformational changes as a reagentless method for the sequence-specific detection of DNA, *Proc. Natl. Acad. Sci. USA* 100, 9134.
- Fox, K.R., C. Brassett and M.J. Waring, 1985, Kinetics of dissociation of nogalamycin from DNA: Comparison with other anthracycline antibiotics, *Biochem. Biophys. Acta.* 840, 383.
- Gabbay, E.J., R. DeStefano and C.S. Baxter, 1973, Topography of nucleic acid helices in solutions. XXVIII. Evidence for a dynamic structure of DNA in solution, *Biochem. Biophys. Res. Commun.* 51, 1083.
- Hashimoto, K., K. Ito and Y. Ishimori, 1994, Sequence-specific gene detection with a gold electrode modified with DNA probes and an electrochemically active dye, *Anal. Chem.* 66, 3830.
- Jones, R.L. and W.D. Wilson, 1981, Effect of ionic strength on the pKa of ligands bound to DNA, *Biopolymers.* 20, 141.
- Kelley, S.O., J.K. Barton, N.M. Jackson and M.G. Hill, 1997, Electrochemistry of methylene blue bound to a DNA-modified electrode, *Bioconjugate Chem.* 8, 31.
- Levicky, R., T.M. Herne, M.J. Tarlov and S.K. Satija, 1998, Using self-assembly to control the structure of DNA monolayers on gold: A neutron reflectivity study, *J. Am. Chem. Soc.* 120, 9787.
- Liaw, Y.-C., Y.-G. Gao, H. Robinson, G.A. van der Marel, J.H. van Boom and A.H.-J. Wang, 1989, Antitumor drug nogalamycin binds DNA in both grooves simultaneously: molecular structure of nogalamycin-DNA complex, *Biochemistry* 28, 9913.
- Lucarelli, F., G. Marrazza, A.P.F. Turner and M. Mascini, 2004, Carbon and gold electrodes as electrochemical transducers for DNA hybridisation sensors, *Biosens. Bioelectron.* 19, 515.
- Lyamichev, V., A.L. Mast, J.G. Hall, J.R. Prudent, M.W. Kaiser, T. Takova, R.W. Kwiatkowski, T.J. Sander, M. de Arruda, D.A. Acro, B.P. Neri and M.A.D. Brow, 1999, Polymorphism identification and quantitative detection of genomic DNA by invasive cleavage of oligonucleotide probes, *Nature Biotechnol.* 17, 292.
- Millan, K.M. and S.R. Mikkelsen, 1993, Sequence-selective biosensor for DNA based on electroactive hybridization indicators, *Anal. Chem.* 65, 2317.
- Miyahara, H., K. Yamashita, M. Takagi, H. Kondo and S. Takenaka, 2001, Electrochemical array (ECA) as an integrated multi-electrode DNA sensor, *Trans. IEE Japan* 121-E, 187.
- Miyahara, H., K. Yamashita, M. Kanai, K. Uchida, M. Takagi, H. Kondo and S. Takenaka, 2002, Electrochemical analysis of single nucleotide polymorphisms of p53 gene, *Talanta* 56, 829.
- Niedle, S., L.H. Pearl and J.V. Skelly, 1987, DNA structure and perturbation by drug binding, *Biochem. J.* 243, 1-13.
- Nojima, T., K. Yamashita, M. Takagi, A. Takagi, Y. Ikeda, H. Kondo and S. Takenaka, 2003, Direct detection of single nucleotide polymorphism (SNP) with genomic DNA by

- the ferrocenylnaphthalene diimide-based electrochemical hybridization assay (FND-EHA), *Anal. Sci.* 19, 79.
- Palecek, E. and M. Fojta, 2001, Detecting DNA hybridization and damage, *Anal. Chem.* 73, 75A.
- Patolsky, F., Y. Weizmann and I. Willner, 2002, Redox-active nucleic-acid replica for the amplified bioelectrocatalytic detection of viral DNA, *J. Am. Chem. Soc.* 124, 770.
- Ryabov, A.D., E.M. Tyapochkin, S.D. Varfolomeev and A.A. Karyakin, 1990, Ferrocenes inside cyclodextrin cavities do not mediate the electron transport between glucose oxidase and an electrode, *Bioelectrochem. Bioenerg.* 24, 257.
- Sato, S., K. Yamashita, M. Takagi and S. Takenaka, 2000, Ferrocenyl naphthalene diimide as a new electrochemical ligand for DNA sensing, *Nucl. Acids Symp. Series* 44, 171.
- Sato, S., S. Fujii, K. Yamashita, M. Takagi, H. Kondo and S. Takenaka, 2001a, Ferrocenyl naphthalene diimide can bind to DNA RNA hetero duplex: potential use in an electrochemical detection of mRNA expression, *J. Organomet. Chem.* 637–639, 476.
- Sato, S., H. Takamiya, K. Yamashita, M. Takagi, H. Kondo and S. Takenaka, 2001b, Linker chain effect of ferrocenyl naphthalene diimide on a double stranded DNA preference, *Nucl. Acids Res. Suppl.* 1, 269.
- Sato, S., T. Nojima and S. Takenaka, 2004, Electrochemical gene detection based on supramolecular complex formation by ferrocenyl- β -cyclodextrin and adamantylnaphthalene diimide bound to double stranded DNA, *J. Organomet. Chem.* 689, 4722.
- Schena, M.Ed., 1999, *DNA Microarray, A Practical Approach*, Oxford University Press, New York.
- Takenaka, S., Y. Uto, H. Saita, M. Yokoyama, H. Kondo and W.D. Wilson, 1998a, Electrochemically active threading intercalator with high double stranded DNA selectivity, *J. Chem. Soc. Chem. Commun.* 1111.
- Takenaka, S., Y. Uto, M. Takagi and H. Kondo, 1998b, Enhanced electron transfer from glucose oxidase to DNA-immobilized electrode aided by ferrocenyl naphthalene diimide, a threading intercalator, *Chem. Lett.* 989.
- Takenaka, S. and M. Takagi, 1999, Threading intercalators as a new DNA structural probe, *Bull. Chem. Soc. Jpn.* 72, 327.
- Takenaka, S., K. Yamashita, M. Takagi, Y. Uto and H. Kondo, 2000, DNA sensing on a DNA probe-modified electrode using ferrocenylnaphthalene diimide as the electrochemically active ligand, *Anal. Chem.* 72, 1334.
- Takenaka, S., 2001a, Threading intercalators as a new DNA structural probe, *Bull. Chem. Soc. Jpn.* 74, 217.
- Takenaka, S., H. Miyahara, K. Yamashita, M. Takagi and H. Kondo, 2001b, Base mutation analysis by a ferrocenyl naphthalene diimide derivative, *Nucleos. Nucleot. Nucl.* 20, 1429.
- Takenaka, S., 2004, Pseudo-polyferrocene coating of double stranded DNA with ferrocenylnaphthalene diimide and its application for electrochemical gene detection, *Polymer J.* 36, 503.
- Tanious, F.A., S.-F. Yen and W.D. Wilson, 1991, Kinetic and equilibrium analysis of a threading intercalation mode: DNA sequence and ion effects, *Biochemistry* 30, 1813.
- Tansil, N.C., H. Xie, F. Xie and Z. Gao, 2005, Direct detection of DNA with an electrocatalytic threading intercalator, *Anal. Chem.* 77, 126.
- Ueno, A., O. Chen, I. Suzuki and T. Osa, 1982, Detection of organic compounds by guest-responsive circular dichroism variations of ferrocene-appended cyclodextrins, *Anal. Chem.* 64, 1650.
- Umek, R.M., S.W. Lin, J. Vielmetter, R.H. Terbrueggen, B. Irvine, C.J. Yu, J.F. Kayyem, H. Yowanto, G.F. Blackburn, D.H. Farkas and Y.-P. Chen, 2001, Electronic detection of nucleic acids: A versatile platform for molecular diagnostics, *J. Mol. Diag.* 3, 74.
- Voet, J.G., J. Coe, J. Epstein, V. Matossian and T. Shipley, 1981, Electrostatic control of enzyme reactions: Effect of ionic strength on the pKa of an essential acidic group on glucose oxidase, *Biochemistry* 20, 7182.
- Wakai, J., A. Takagi, M. Nakayama, T. Miya, T. Miyahara, T. Iwanaga, S. Takenaka, Y. Ikeda and M. Amano, 2004, A novel method of identifying genetic mutations using an electrochemical DNA array, *Nucl. Acids Res.* 32, e141.

- Willner, I., 2002, Biomaterials for sensors, fuel cells, and circuitry, *Science* 298, 2407.
- Wilson, W.D., C.R. Krishnamoorthy, Y.-H. Wang and J.C. Smith, 1985, Mechanism of intercalation: Ion effects on the equilibrium and kinetic constants on the equilibrium and kinetic constants for the interaction of propidium and ethidium with DNA, *Biopolymers* 24, 1941.
- Wilson, W.D., 1996, Reversible interactions of nucleic acids with small molecules, *Nucleic Acid in Chemistry and Biology*, 2nd Ed., Eds. G.M. Blackburn and M.J. Gait, Oxford University Press, New York, 329.
- Yamashita, K., M. Takagi, H. Kondo and S. Takenaka, 2000, Electrochemical detection of base pair mutation, *Chem. Lett.* 1038.
- Yamashita, K., M. Takagi, K. Uchida, H. Kondo and S. Takenaka, 2001, Visualization of DNA microarrays by scanning electrochemical microscopy (SECM), *Analyst* 126, 1210.
- Yamashita, K., M. Takagai, H. Kondo and S. Takenaka, 2002a, Electrochemical detection of nucleic base mismatches with ferrocenyl naphthalene diimide, *Anal. Biochem.* 306, 188.
- Yamashita, K., A. Takagi, M. Takagi, H. Kondo, Y. Ikeda and S. Takenaka, 2002b, Ferrocenylnaphthalene diimide-based electrochemical hybridization assay for heterozygote deficiency of the lipoprotein lipase gene, *Bioconjugate Chem.* 13, 1193.
- Yen, S.-F., J. Gabbay and W.D. Wilson, 1982, Interaction of aromatic imides with deoxyribonucleic acid. Spectrophotometric and viscometric studies, *Biochemistry* 21, 2070.
- Zhang, X. and D.J. Patel, 1990, Solution structure of the nogalamycin–DNA complex, *Biochemistry* 29, 9451.

This page intentionally left blank

Nanoparticle-Based Electrochemical DNA Detection

Joseph Wang

*Department of Chemical and Materials Engineering, Box 876006, Arizona State University,
Tempe, AZ 85287, USA*

Contents

1. Introduction	369
1.1. Particle-based assays	369
1.2. Nanoparticle-based optical DNA assays	370
2. Nanoparticle-based bioelectronic detection of DNA	371
2.1. Why electrical detection?	371
2.2. Nanoparticle-based electrochemical hybridization assays	371
2.3. Gold and silver metal tags for electrical DNA detection	372
2.4. Use of magnetic beads	375
2.5. Inorganic colloids tracers: Toward electrical coding	376
2.6. Ultrasensitive particle-based assays based multiple amplification avenues	379
3. Conclusions	381
Acknowledgments	382
References	382

1. INTRODUCTION

The emergence of nanotechnology is opening new horizons for the application of nanomaterials in bioelectroanalytical chemistry (Niemeyer, 2001; Alivisatos, 2004). Nanotechnology is defined as the creation of functional materials, devices and systems through control of matter at the 1–100 nm scale. The use of nanomaterials in bioanalysis has taken off rapidly and will surely continue to expand. The unique properties of *nanoparticles*, nanotubes and nanowires offer excellent prospects for developing novel nanomaterial-based electrical DNA detection strategies. This chapter describes new signal amplification and coding strategies for electrical DNA detection based on the use of nanomaterial tags.

1.1. Particle-based assays

The emergence of *nanotechnology* is opening new horizons for the application of nanoparticles in analytical chemistry. In particular, nanoparticles are of considerable interest in the world of nanoscience owing to their unique physical and

chemical properties. Such properties offer excellent prospects for chemical and biological sensing (Carusu, 2001; Willner and Willner, 2002; Storhoff and Mirkin, 1999). Particularly attractive for numerous bioanalytical applications are colloidal gold and semiconductor quantum-dot nanoparticles. The power and scope of such nanomaterials can be greatly enhanced by combining them with biological recognition reactions and electrical processes (i.e., nanobioelectronics). Such coupling can dramatically enhance biological assays. There has been a substantial recent interest in utilizing biomolecules for constructing nanostructured architectures (Storhoff and Mirkin, 1999; Niemeyer, 2001) and in the tailoring and functionalizing the surfaces of nanoparticles (Carusu, 2001; Niemeyer, 2001). Nanoparticle–biopolymer conjugates offer great potential for DNA diagnostics and can have a profound impact upon bioanalytical chemistry.

1.2. Nanoparticle-based optical DNA assays

Despite their great potential, nanoparticle-based genetic testings are still in their infancy. Optical detection methods relying on nanoparticle materials functionalized with oligonucleotides have shown enhanced sensitivity and selectivity compared to conventional assays based on molecular probes. For example, Mirkin and coworkers have developed novel DNA assays utilizing distance-dependent optical properties of gold-particle modified oligonucleotides (Storhoff *et al.*, 1998). The hybridization-induced cross-linking of colloidal particles triggered a red-to-purple color change in solution (due a red shift in the surface plasmon resonance of the gold nanoparticles). Such particle-based optical assays have been combined with simultaneous multiple-target detection capability (Taton *et al.*, 2001). A scanometric DNA array, based on silver amplification of a hybridization event, represents another important contribution from Mirkin's laboratory (Taton *et al.*, 2000). Labeling the DNA target with a nanoparticle offered greater mismatch discrimination and higher sensitivity (compared to the common use of fluorophore tags). The same group reported on a highly sensitive Raman spectroscopic method for detecting DNA and RNA based on gold-nanoparticle probes labeled with oligonucleotides and Raman-active dyes (Cao *et al.*, 2002). The gold nanoparticles facilitated the formation of silver coating that acted as a surface-enhanced Raman scattering promoter, to yield femtomolar detection limits. Spectral coding opens new opportunities in gene expression studies, high throughput screening, and medical diagnostics (Han *et al.*, 2001; Nicewarner-Pena *et al.*, 2001). Nie's team described a multicolor optical coding based on embedding different sized quantum dots into polymeric microbeads at precisely controlled ratios (Han *et al.*, 2001). 'Bar-coded' metallic microrods (with segments of up to five different metals), synthesized by plating into the pores of a host membrane, were shown extremely useful for effective optical identification (Nicewarner-Pena *et al.*, 2001).

2. NANOPARTICLE-BASED BIOELECTRONIC DETECTION OF DNA

2.1. Why electrical detection?

A critical component of DNA biosensors or arrays is the method of detection. Most early devices have relied on optical transduction of the hybridization event. Typically, the hybridization event (or patterns across the chip) is being detected by a confocal scanning laser system in connection to the use of fluorescent tagging agents (Piunno *et al.*, 1995). While fluorescent detection is broadly and successfully used, it is hampered by the need for bulky and costly control instrumentation. Mass-sensitive devices, generating frequency signals in response to the increased mass (associated with the hybridization reaction), offer label-free sensitive detection, but are not suitable for routine diagnostic applications (Caruso *et al.*, 1997).

Electrochemical devices have received considerable recent attention in the development of sequence-specific DNA hybridization biosensors (Mikkelsen, 1996; Palecek and Fojta, 2001). Electrical DNA biosensors rely on the conversion of the Watson–Crick base-pair biorecognition event into a useful electrical signal. Such devices offer elegant routes for interfacing – at the molecular level – the DNA-recognition and signal-transduction elements, and are uniquely qualified for meeting the size, cost, low-volume, and power requirements of decentralized genetic diagnostics (Palecek and Fojta, 2001; Wang, 2002). While the use of electrochemical DNA biosensors or chips is at an early stage, easy-to-use hand-held electrical DNA analyzers are already approaching the marketplace (Umek *et al.*, 2000; Napier *et al.*, 2000), and are expected to have a considerable impact on future DNA diagnostics (Wilson, 1998). Electrochemical transduction of DNA hybridization events has commonly been achieved in connection to enzyme tags or electroactive indicators/intercalators. The use of nanoparticle tracers is relatively new in electrical detection, and offers unique opportunities for electrochemical transduction of DNA-sensing events.

2.2. Nanoparticle-based electrochemical hybridization assays

Inspired by the novel use of nanoparticles in optical bioassays, recent studies have focused at developing analogous particle-based electrical routes for gene detection. Such new protocols are based on the use of a wide range of nanomaterials including colloidal gold tracers, semiconductor quantum dot tags, nanowires, polymeric carrier (amplification) spheres, or magnetic (separation) beads. These nanoparticle materials offer elegant ways for interfacing DNA recognition events with electrochemical signal transduction, for dramatically amplifying the resulting electrical response, and for designing novel coding strategies.

Most of these schemes have commonly relied on a highly sensitive electrochemical stripping transduction/measurement of the metal tracer. Stripping

voltammetry is a powerful electroanalytical technique for trace metal measurements (Wang, 1985). Its remarkable sensitivity is attributed to the 'built-in' accumulation step, during which the target metals are preconcentrated (deposited) onto the working electrode. The detection limits are thus lowered by 3–4 orders of magnitude, compared to pulse-voltammetric techniques, used earlier for monitoring DNA hybridization. Such ultrasensitive electrical detection of metal tags has been accomplished in connection to a variety of new and novel DNA-linked particle nanostructure networks.

2.3. Gold and silver metal tags for electrical DNA detection

Several groups, including ours, have developed powerful nanoparticle-based electrochemical DNA hybridization assays (Authier *et al.*, 2001; Wang *et al.*, 2001a; Cai *et al.*, 2002a). Such protocols have relied on capturing the gold (Authier *et al.*, 2001; Wang *et al.*, 2001a) or silver (Cai *et al.*, 2002a) nanoparticles to the hybridized target, followed by acid dissolution and anodic-stripping electrochemical measurement of the metal tracer. The probe or target immobilization has been accomplished in connection to streptavidin-coated magnetic beads (Wang *et al.*, 2001a), through the use of chitosan or polypyrrole surface layers (Cai *et al.*, 2002a), or via adsorption onto the walls of polystyrene microwells (Authier *et al.*, 2001). Picomolar and sub-nanomolar levels of the DNA target have thus been detected. Further sensitivity enhancement can be achieved by catalytic enlargement of the gold tag in connection to nanoparticle-promoted precipitation of gold (Wang *et al.*, 2001a) or silver (Wang *et al.*, 2001b; Lee *et al.*, 2003a; Cai *et al.*, 2002b). Combining such enlargement of the metal-particle tracers, with the effective 'built-in' amplification of electrochemical stripping analysis paved the way to sub-picomolar detection limits (Wang *et al.*, 2001b). The silver enhancement relies on the chemical reduction of silver ions by hydroquinone to silver metal on the surface of the gold nanoparticles. The silver reduction time must be controlled as a trade-off between larger enhancement and contribution of nonspecific background. A significant reduction of the silver staining background signals was obtained by using an indium-tin oxide (ITO) electrode possessing low silver-enhancing properties or by modifying the gold transducer with a polyelectrolyte multilayer (Lee *et al.*, 2003a). The *silver-enhancement* electrical route has been applied recently for detection in 'Lab-on-Chip' systems in connection to on-chip PCR amplification (Lee *et al.*, 2003b). An 8 μL reaction chamber was employed in connection to gold or ITO electrodes. Prospects for developing a truly portable integrated DNA analysis system were discussed. A simplified gold-nanoparticle-based protocol was reported (Ozsoz *et al.*, 2003), relying on the pulse-voltammetric monitoring of the gold-oxide wave at $\sim 1.20\text{ V}$ at disposable pencil graphite electrode. A detection limit of 0.78 fmol was reported for PCR amplicons bound to the pencil electrode in connection hybridization to oligonucleotide–nanoparticle conjugates.

The hybridization of probe-coated magnetic beads with the gold-tagged targets results in three-dimensional network structures of 'large' (μm) magnetic beads, crossed-linked together through the DNA and gold nanoparticles. Such

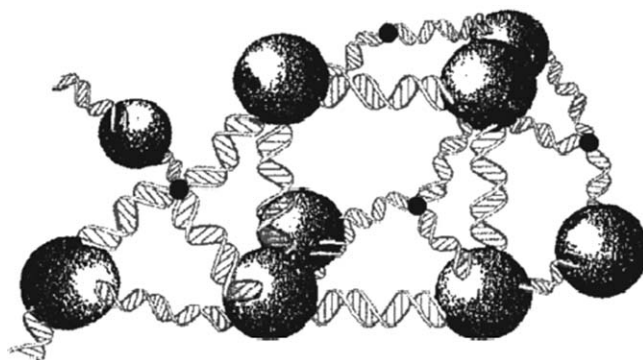


Fig. 1. DNA-linked particle nanostructure assembly associated with the hybridization of probe-coated magnetic-bead and gold-nanoparticle conjugated target.

DNA-linked nanoparticle aggregate structure is shown in [Figure 1](#). In these aggregates the DNA duplex ‘bridges’ the magnetic beads with the metal nanoparticles. No such aggregation was observed in the presence of noncomplementary or mismatched oligonucleotides. Similar DNA-induced aggregation has been exploited by Mirkin for detecting the hybridization in connection to distance-dependent color changes ([Storhoff *et al.*, 1998](#)).

Recently, we described an electrochemical protocol for detecting DNA hybridization based on preparing the metal marker along the DNA backbone (instead of capturing it at the end of the duplex) ([Wang *et al.*, 2003a](#)). Such protocol relies on DNA-template-induced generation of conducting *nanowires* as a mode of capturing the metal tag. The use of DNA as a *metallization* template has evoked substantial research activity directed to the generation of conductive nanowires and the construction of functional circuits ([Braun *et al.*, 1998](#); [Richter *et al.*, 2000](#); [Mertig *et al.*, 2002](#)). This approach was applied to grow silver ([Braun *et al.*, 1998](#)), palladium ([Richter *et al.*, 2000](#)) or platinum ([Mertig *et al.*, 2002](#)) clusters on DNA templates. Yet, the DNA-templated assembly of metal wires has not been exploited for detecting DNA hybridization. The new detection scheme ([Figure 2](#)) consists of the vectorial electrostatic ‘collection’ of silver ions along the captured DNA target, followed by hydroquinone-induced reductive formation of silver aggregates along the DNA skeleton, along with dissolution and stripping detection of the nanoscale silver cluster.

Nanoparticle-induced changes in the *conductivity* across a microelectrode gap can also be exploited for highly sensitive and selective detection of DNA hybridization. Mirkin’s group developed an array-based electrical detection utilizing oligonucleotide-functionalized gold nanoparticles and closely spaced interdigitated microelectrodes ([Park *et al.*, 2002](#)). The oligonucleotide probe was immobilized in the gap between the two microelectrodes. The hybridization event thus localizes *gold nanoparticles* in the electrode gap, and along with subsequent *silver* deposition leads to measurable conductivity signals. Such hybridization-induced *conductivity* signals, associated with resistance changes across the electrode gap, offer high sensitivity with a 0.5 pM detection limit.

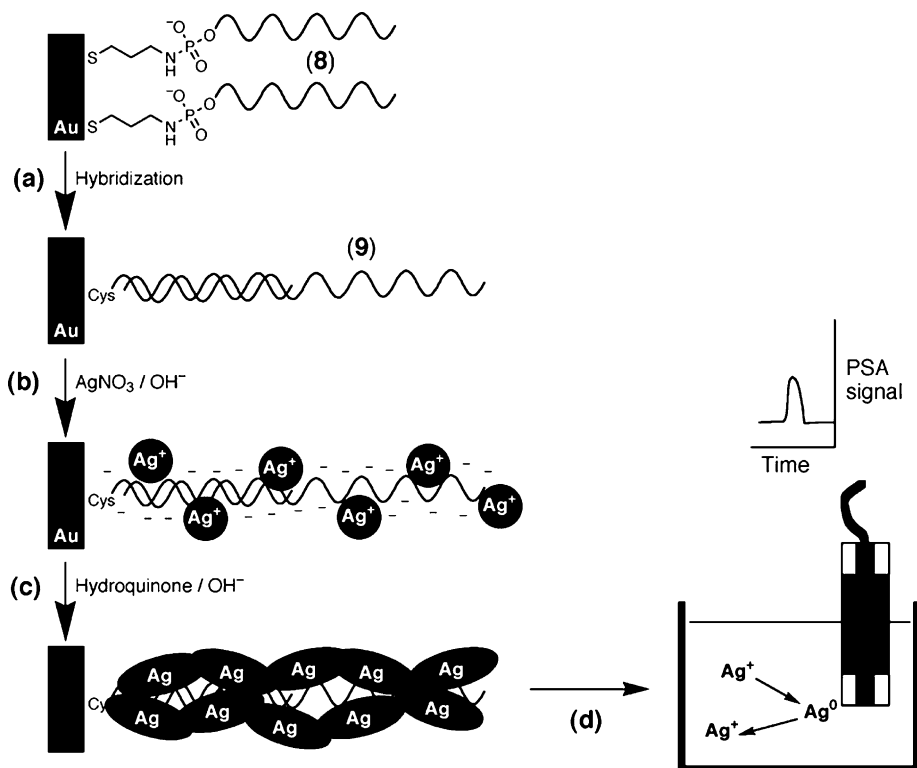


Fig. 2. Schematic representation of the protocol used for electrical detection of silver clusters produced along the DNA backbone. From top: Formation of a self-assembled cystamine monolayer; Immobilization of ssDNA 'probe' through the 5'-phosphate groups of ssDNA by the formation of phosphoramidate bond with the amino groups of the electrode surface; hybridization of the complementary target; 'loading' of the silver ion onto the DNA; hydroquinone-catalyzed reduction of silver ions to form silver aggregates on the DNA backbone; dissolution of the silver aggregates in an acid solution and transfer to detection cell; stripping potentiometric detection. From Wang *et al.* (2003a).

Control of the salt concentration allowed high point-mutation selectivity (with a factor of 100,000:1) without thermal stringency. Changes in the resistance across a microelectrode gap, resulted from the hybridization of nanoparticle-labeled DNA, have been exploited also for a paralleled *array* readout system (Urban *et al.*, 2003). A self-contained microanalyzer, allowing such parallel readout of the entire array, indicates great promise for point-of-care applications. A similar approach for enhancing the sensitivity and obtaining an excellent mismatch discrimination was described based on the assembly of several layers of nanoparticles (Li *et al.*, 2003).

Colloidal gold was employed also for improving the immobilization of DNA on electrode surfaces and hence for increasing the hybridization capacity of the surface (Cai *et al.*, 2001). Such use of nanoparticle supporting films relied on the self-assembly on 16 nm diameter colloidal gold onto a cystamine-modified gold electrode and resulted in surface densities of oligonucleotides as high as 4×10^{14}

molecules/cm². The detection of the ferrocenecarboxaldehyde tag (conjugated to the target DNA) resulted in a detection limit of 500 pM.

2.4. Use of magnetic beads

Several of the protocols described above (Wang *et al.*, 2001a, b; Palecek *et al.*, 2002) have combined the inherent signal amplification of stripping analysis with an effective discrimination against nonhybridized DNA. In addition to efficient isolation of the duplex, magnetic spheres can open the door for elegant ways for triggering and controlling electrical DNA detection (Wang *et al.*, 2002a; Hirsch *et al.*, 2000; Wang and Kawde, 2002c).

For example, an attractive magnetic triggering of the electrical DNA detection has been realized through a 'magnetic' collection of the magnetic-bead/DNA-hybrid/metal-tracer assembly onto a thick-film electrode transducer that allowed direct electrical contact of the silver precipitate (Wang *et al.*, 2002a). Such bioassay involved the hybridization of a target oligonucleotide to probe-coated magnetic beads, followed by binding of the streptavidin-coated gold nanoparticles to the captured target, catalytic silver precipitation on the gold-particle tags, a magnetic 'collection' of the DNA-linked particle assembly and solid-state stripping detection (Figure 3). The magnetic 'collection' route greatly simplifies the electrical detection of metal tracers as it eliminates the acid dissolution step.

Magnetic spheres have also been used for triggering the electron-transfer reactions of DNA (Wang and Kawde, 2002c). Changing the position of the magnet (below planar printed electrodes) was thus used for 'on/off' switching of the DNA oxidation (through attraction and removal of DNA functionalized-magnetic particles). The process was reversed and repeated upon switching the

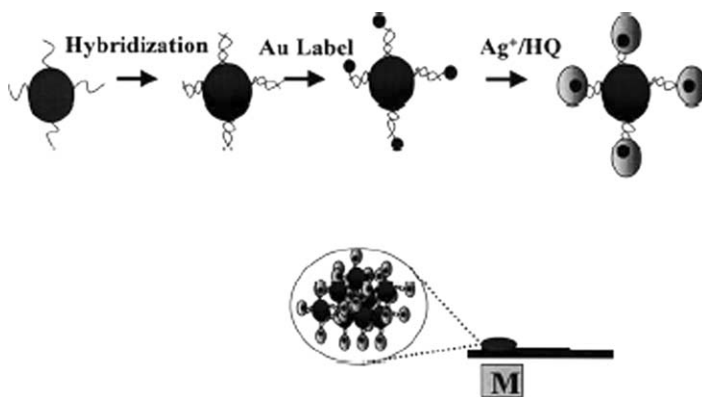


Fig. 3. Schematic of the magnetically induced solid-state electrochemical detection of DNA hybridization. The assay involves introduction of the probe-coated magnetic beads, the hybridization event (with the biotinylated target), capture of the streptavidin-gold particles, catalytic silver deposition on the gold nanoparticle tags, and positioning of an external magnet (M) under the electrode to attract the particle-DNA assembly and solid-state chronopotentiometric detection. From Wang *et al.* (2002a).

position of the magnet, with and without oxidation signals in the presence and absence of the magnetic field, respectively. Such magnetic triggering of the DNA oxidation holds great promise for DNA arrays (based on closely spaced electrodes and guanine-free inosine-substituted probes). Willner and coworkers described an amplified detection of viral DNA and of single-base mismatches using oligonucleotide-functionalized magnetic beads and an electrochemiluminescence (ECL) detection (Patolsky *et al.*, 2003). The magnetic attraction of the labeled magnetic particles and their rotation on the electrode surface was used to amplify the ECL signal. The ability of external magnetic fields to control other bioelectrochemical processes, such as biocatalytic transformations of redox enzymes was also documented by Willner's group (Hirsch *et al.*, 2000).

It is possible also to use magnetic beads as reporters (tags) for DNA hybridization detection in connection to stripping voltammetric measurements of their iron content (Wang *et al.*, 2003b). A related protocol, developed in the same study, involved probes labeled with gold-coated iron *core-shell nanoparticles*. In both cases, the captured iron-containing particles were dissolved following the hybridization, and the released iron was quantified by cathodic stripping voltammetry in the presence of the 1-nitroso-2-naphthol ligand and a bromate catalyst. Core-shell copper-gold nanoparticle tags were also shown useful by combining the favorable electrochemical behavior of the *copper* core with the attractive surface modification properties of gold shell (Cai *et al.*, 2003).

2.5. Inorganic colloids tracers: Toward electrical coding

Owing to their unique (tunable-electronic) properties, semiconductor (*quantum dots*) nanocrystals have generated considerable interest for optical DNA detection (Han *et al.*, 2001). Recent activity has demonstrated the utility of such inorganic crystals for enhanced electrical DNA detection (Willner *et al.*, 2001; Wang *et al.*, 2002b, 2003c). Willner's reported on a *photoelectrochemical* transduction of DNA sensing events in connection to DNA-cross-linked CdS nanoparticle arrays (Willner *et al.*, 2001). The electrostatic binding of the $\text{Ru}(\text{NH}_3)_6^{+3}$ electron acceptor to the ds-DNA units provided a tunneling route for the electron-band electrons and thus led to increased photocurrents (Figure 4).

We reported on the detection of DNA hybridization in connection to *cadmium-sulfide* nanoparticle tags and electrochemical stripping measurements of the cadmium (Wang *et al.*, 2002b). A nanoparticle-promoted cadmium precipitation was used to enlarge the nanoparticle tag and amplify the stripping DNA hybridization signal. In addition to measurements of the dissolved cadmium ion we demonstrated solid-state measurements following a '*magnetic*' collection of the magnetic-bead/DNA-hybrid/CdS-tracer assembly onto a thick-film electrode transducer. Such protocol combines the *amplification* features of nanoparticle/polynucleotides assemblies and highly sensitive potentiometric stripping detection of cadmium, with an effective magnetic isolation of the duplex. The low detection limit (100 fmol) was coupled to good reproducibility

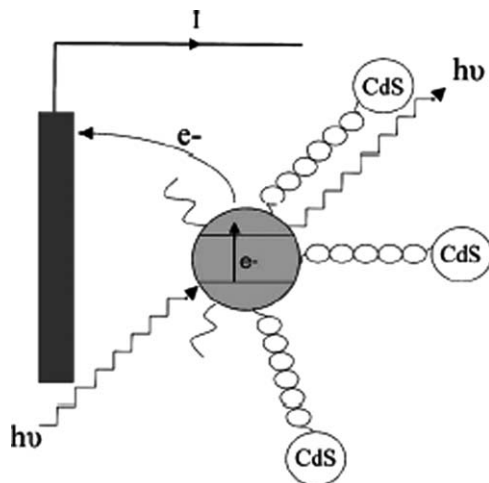


Fig. 4. Photoelectrochemical detection of nucleic acid by means of a DNA-cross-linked CdS nanoparticle array. From Willner *et al.* (2001).

(RSD = 6%). A dramatic signal enhancement was obtained by encapsulating multiple CdS nanoparticles into the host bead or by loading onto carbon-nanotube carriers (Wang *et al.*, 2003c).

Such protocol was recently extended to other inorganic colloids (e.g., ZnS or PbS) that can be similarly synthesized in reversed micelles. Such extension has paved the way to an electrochemical *coding* technology for the simultaneous detection of multiple DNA targets based on *nanocrystal* tags with diverse redox potentials (Wang *et al.*, 2003d). For example, Figure 5 displays the well-resolved stripping response of a solution obtained by dissolving simultaneously ZnS, CdS and PbS nanocrystals. These nanoparticle tracers yield well-defined and resolved stripping peaks at -1.12 V (Zn), -0.68 V (Cd) and -0.53 V (Pb) at the mercury-coated glassy-carbon electrode (vs. Ag/AgCl reference). Functionalizing the *nanocrystal* tags with thiolated oligonucleotide probes thus offered a voltammetric signature with distinct electrical hybridization signals for the corresponding DNA targets (Figure 6). The position and size of the resulting stripping peaks provided the desired identification and quantitative information, respectively, on a given target DNA. The multi-target DNA detection capability was coupled to the amplification feature of *stripping voltammetry* (to yield fmol detection limits) and with an efficient magnetic removal of nonhybridized nucleic acids to offer high sensitivity and selectivity. Up to 5–6 targets can thus be measured simultaneously in a single run in connection to ZnS, PbS, CdS, InAs and GaAs nanocrystal particles. Conducting massively parallel assays (in microwells of microtiter plates or using multi-channel microchips, with each microwell or channel carrying out multiple measurements) could thus lead to a high-throughput operation.

Recent efforts in our laboratory have aimed at developing large particle-based libraries for electrical *coding*, based on the judicious design of encoded ‘*identification*’ beads (Wang *et al.*, 2003e) or striped metal rods (Wang *et al.*,

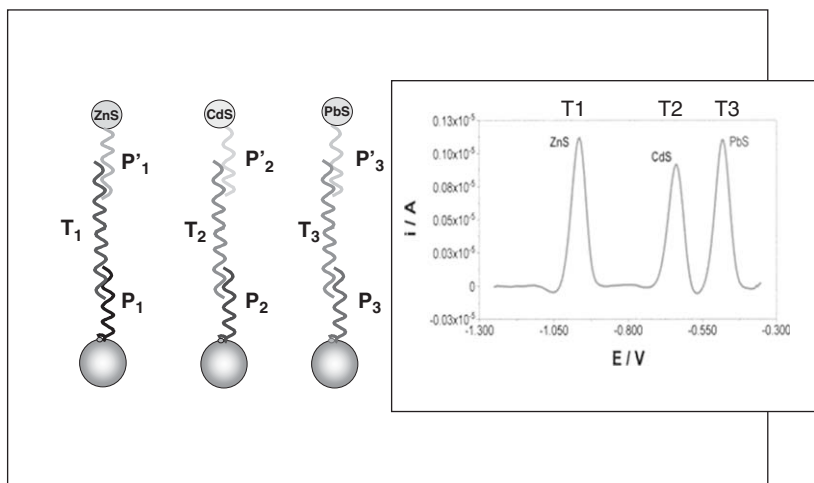


Fig. 5. Use of different quantum-dot tracers for electrical detection of multiple DNA targets. Stripping voltammograms for a solution containing dissolved ZnS, CdS, and PbS nanoparticle tracers. Conditions: 2 min accumulation at -1.4 V; square-wave voltammetric scan with a potential step, 50 mV; amplitude, 20 mV; frequency, 25 Hz. Based on Wang *et al.* (2003d).

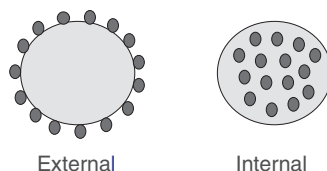


Fig. 6. Polymeric beads amplifying units based on loading numerous redox tags externally (on their outer surface) or internally (via encapsulation).

2003f). By incorporating different predetermined levels (or lengths) of multiple metal markers, such beads or rods can lead to a large number of recognizable stripping-voltammetric signatures, and hence to a reliable identification of a large number of DNA targets. For example, multi-metal cylindrical particles can be prepared by the template-directed electrochemical synthesis, by plating zinc, indium, bismuth and copper onto an alumina or polycarbonate template (porous) membrane. Capping the rod with a gold end facilitates its functionalization with a thiolated oligonucleotide probe. Each microrod thus yield a characteristic multi-peak stripping voltammogram, whose peak potentials and current intensities reflect the identity of the corresponding DNA target. The encoding patterns correlate well with the resulting voltammetric signatures. Hundreds of usable codes could be generated in connection to 4–5 different potentials and 3–4 different current intensities. In addition to powerful bioassays, such “identification beads” hold great promise for the identification of counterfeit products and related authenticity testing. The template-directed electrochemical route can also be used for preparing micrometer-long metal tags

for ultrasensitive detection (Wang *et al.*, 2003f). The linear relationship between the charge passed during the preparation and the size of the resulting microrod allows tailoring of the sensitivity of the electrical DNA assay. For example, plating of indium into the pores of a host membrane offered a greatly lower detection limit (250 zmol) compared to common bioassays spherical nanoparticle tags. Indium offers a very attractive electrochemical stripping behavior and is not normally present in biological samples or reagents. Solid-state derivative-chronopotentiometric measurements of the indium tracer have been realized through a ‘magnetic’ collection of the DNA-linked particle assembly onto a thick-film electrode transducer.

Metal nanoparticles have also shown useful for electrical coding of single nucleotide polymorphisms (SNP) (Kerman *et al.*, 2004). Such protocol relies on the hybridization of monobase-modified gold nanoparticles with the mismatched bases. The binding event leads to changes in the gold oxide peak and offers great promise for coding all mutational changes. Analogous SNP coding protocols based on different inorganic nanocrystals are currently being examined in our laboratory (Wang *et al.*, 2005). This protocol involves the addition of ZnS, CdS, PbS and CuS crystals linked to adenosine, cytidine, guanosine and thymidine mononucleotides, respectively. Each mutation captures via base pairing different nanocrystal–mononucleotide conjugates, to yield a distinct electronic fingerprint.

2.6. Ultrasensitive particle-based assays based multiple amplification avenues

We already discussed several *amplification* processes such as catalytic enlargement of the metal tracer and its electrolytic accumulation onto the electrode surface. Such protocols have been based on the use of one reporter per one hybridization event. It is possible to further enhance the sensitivity by employing multiple tags per binding event. This can be accomplished in connection to *polymeric microbeads* carrying multiple redox tracers externally (on their surface) or internally (via encapsulation; Figure 6). Combined with additional amplification units and processes, such bead-based multi-amplification protocols meet the high sensitivity demands of electrochemical DNA biosensors.

We have demonstrated a triple-*amplification* bioassay, coupling the carrier-sphere amplifying units (loaded with numerous gold nanoparticles tags) with the ‘built-in’ preconcentration of the electrochemical stripping detection and catalytic enlargement of the multiple gold-particle tags (Kawde and Wang, 2004; Figure 7). The gold-tagged beads were prepared by binding biotinylated metal nanoparticles to streptavidin-coated polystyrene spheres. SEM imaging indicated a coverage of around 80 gold particles per polystyrene bead. Such triple-amplification route offered a dramatic enhancement of the sensitivity. Willner also combined multiple amplification pathways, based on enzyme-functionalized *liposomes* and the accumulation of the biocatalytic-reaction product, for ultrasensitive DNA assays (Alfonta *et al.*, 2001). Such bioassay relied on the large surface area of liposomes for carrying a large number of

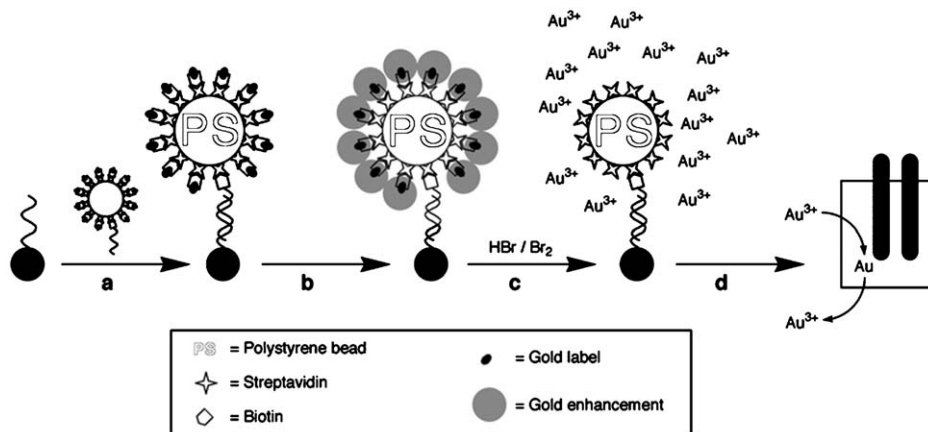


Fig. 7. Use of carrier-sphere amplifying units loaded with numerous gold nanoparticle tags: (a) hybridization effect; (b) gold enhancement effect; (c) dissolution of the tag; (d) stripping detection.

enzyme molecules. Sensing of the accumulated product was accomplished by means of chronopotentiometry.

It is also possible to use gold nanoparticle as carriers of redox markers for amplified DNA detection (Wang *et al.*, 2003g). Gold nanoparticles covered with 6-ferrocenylhexaethylthiol were used for this purpose in connection to a sandwich hybridization assay. Due to the elasticity of the DNA strands, the ferrocene/Au-nanoparticle conjugates were positioned in closed proximity to the underlying electrode to allow facile electron-transfer reaction (Figure 8). A detection limit of 10 amol was observed, along with linearity up to 150 nM. Applicability to PCR products related to the hepatitis B virus was reported.

Internal encapsulation electroactive tags within carrier beads offers an attractive alternative to their external loading. For example, ultrasensitive electrical DNA detection was reported recently based on polystyrene beads impregnated with a redox marker (Wang *et al.*, 2003h). The resulting 'electroactive beads' are capable of carrying a huge number of the ferrocenecarboxaldehyde marker molecules and hence offer a remarkable amplification of single hybridization events. This allowed chronopotentiometric detection of target DNA down to the 5.1×10^{-21} mol level ($\sim 31,000$ molecules) in connection to 20 min hybridization and 'release' of the marker in an organic medium. The dramatic signal amplification advantage is combined with a remarkable discrimination against a huge excess (10^7) of non-complementary nucleic acids. Figure 9 displays the DNA-linked particle assembly that resulted from the hybridization event. This image indicates that the $10 \mu\text{m}$ electroactive beads are cross-linked to the smaller ($\sim 0.8 \mu\text{m}$) magnetic spheres through the DNA hybrid. Current efforts are aimed at encapsulating different ferrocene markers within the polystyrene host beads in connection to multi-target DNA detection. Other marker encapsulation routes hold great promise for electrical DNA detection. Particularly attractive are the recently developed nanoencapsulated microcrystalline particles, prepared by the layer-by-layer technique, that

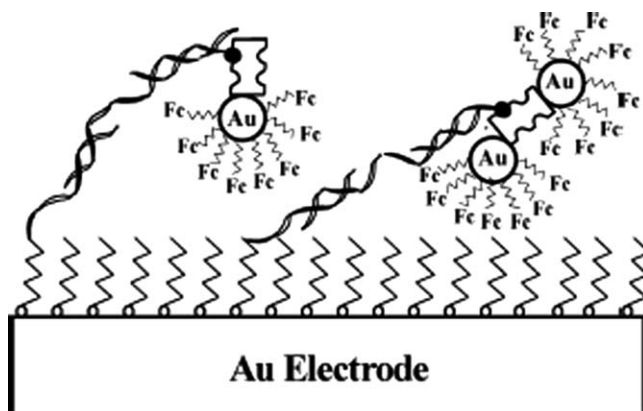


Fig. 8. Schematic representation of the amplified electrochemical detection of DNA hybridization via oxidation of the ferrocene caps on the gold-nanoparticle/streptavidin conjugates. From Wang *et al.* (2003g).

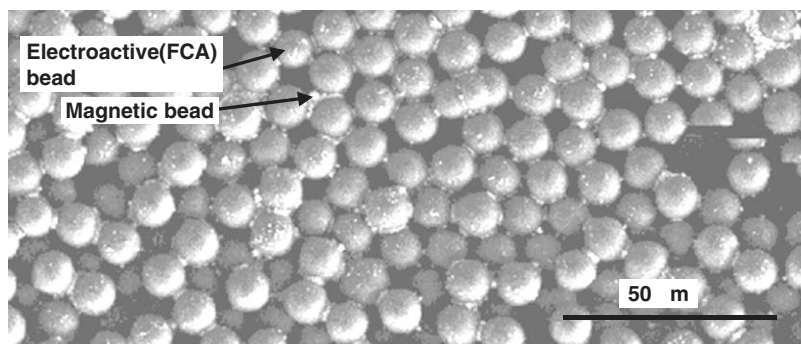


Fig. 9. Use of 'electroactive' particles for ultrasensitive DNA detection, based on polystyrene beads impregnated with a redox marker. SEM image of the resulting DNA-linked particle assembly. From Wang *et al.* (2003h).

offer large marker/biomolecule ratios and superamplified bioassays (Trau *et al.*, 2002).

3. CONCLUSIONS

The use of nanomaterials in electrical DNA detection has taken off rapidly and will surely continue to expand. Metal and semiconductor nanoparticles and nanowires have rapidly become attractive labels for electrochemical DNA assays, offering unique signal amplification and coding capabilities. A critical requirement for the successful realization of nanoparticle-based bioelectronic assays is the ability to minimize non-specific binding of DNA (or biomolecules in general). Proper attention to the surface chemistry is thus essential to ensure a low background signal. The combination of high sensitivity, specificity, and

multi-target detection capabilities permits nanoparticle-based electronic DNA assays to rival the most advanced optical protocols. Such nanomaterials-based DNA assays and devices are expected to have a major impact upon clinical diagnostics, environmental monitoring, security surveillance, or for ensuring our food safety. The high sensitivity of these nanoparticle-based electrical systems points toward the prospect of detecting DNA targets without the need for PCR amplification. It is expected that future innovative research will lead to new particle-based electrical detection strategies, that coupled with other major technological advances will result in effective, easy-to-use hand-held portable devices for DNA diagnostics. The new electrochemical detection protocols could also be adapted to planar chip-based *array* formats and could be expanded to other biological assays, particularly immunoassays. Although the present chapter has focused on DNA detection methods, such studies have broad implications on the ability to assemble DNA nanostructures on surfaces.

ACKNOWLEDGMENTS

Financial support from the National Science Foundation (grant number CHE 0506529) and NIH (R01A 1056047-01) is gratefully acknowledged.

REFERENCES

- Alfonta, L., A. Singh and I. Willner, 2001, Liposomes labeled with biotin and horseradish peroxidase: A probe for the enhanced amplification of antigen-antibody or oligonucleotide-DNA sensing processes by the precipitation of an insoluble product on electrodes, *Anal. Chem.* 73, 91.
- Alivisatos, P., 2004, The use of nanocrystals in biological detection, *Nature Biotechnol.* 22, 47.
- Authier, L., C. Grossiord, P. Berssier and B. Limoges, 2001, Gold nanoparticle-based quantitative electrochemical detection of amplified human cytomegalovirus DNA using disposable microband electrodes, *Anal. Chem.* 73, 4450.
- Braun, E., Y. Eichen, U. Sivan and G. Ben-Yoseph, 1998, DNA-templated assembly and electrode attachment of a conducting silver wire, *Nature* 391, 777.
- Cai, H., C. Xu, P. He and Y. Fang, 2001, Colloid Au-enhanced DNA immobilization for the electrochemical detection of sequence-specific DNA, *J. Electroanal. Chem.* 510, 78.
- Cai, H., Y. Xu, N. Zhu, P. He and Y. Fang, 2002a, An electrochemical DNA hybridization detection assay based on a silver nanoparticle label, *Analyst* 127, 803.
- Cai, H., Y. Wang, P. He and Y. Fang, 2002b, Electrochemical detection of DNA hybridization based on silver-enhanced gold nanoparticle label, *Anal. Chim. Acta* 469, 165.
- Cai, H., N. Zhu, Y. Ping, P. He and Y. Fang, 2003, Cu@Au alloy nanoparticle as oligonucleotides labels for electrochemical stripping detection of DNA hybridization, *Biosens. Bioelectron.* 18, 1311.
- Cao, Y.C., R. Jin and C.A. Mirkin, 2002, Nanoparticles with Raman Spectroscopic Fingerprints for DNA and RNA detection, *Science* 297, 1536.
- Caruso, F., E. Rodda, D. Furlong, K. Niikura and Y. Okahata, 1997, Quartz crystal microbalance study of DNA immobilization and hybridization for nucleic acid sensor development, *Anal. Chem.* 69, 2043.

- Carusu, F., 2001, Nanoengineering of particle surfaces, *Adv. Mat.* 13, 11.
- Han, M., X. Gao, J. Su and S. Nie, 2001, Quantum-dot-tagged microbeads for multiplexed optical coding of biomolecules, *Nat. Biotechnol.* 19, 631.
- Hirsch, R., E. Katz and I. Willner, 2000, Magneto-switchable bioelectrocatalysis, *J. Am. Chem. Soc.* 122, 12053.
- Kawde, A. and J. Wang, 2004, Amplified electrical transduction of DNA hybridization based on polymeric beads loaded with multiple gold nanoparticles tags, *Electroanal.* 16, 101.
- Kerman, K., M. Saito, Y. Morita, Y. Takamura, M. Ozsoz and E. Tamiya, 2004, Electrochemical coding of single-nucleotide polymorphisms by monobase-modified gold nanoparticles, *Anal. Chem.* 76, 1877.
- Lee, T.M.H., L.L. Li and I.M. Hsing, 2003a, Enhanced electrochemical detection of DNA hybridization based on electrode-surface modification, *Langmuir* 19, 4338.
- Lee, T.M.H., M. Carles and I.M. Hsing, 2003b, Microfabricated PCR-electrochemical device for simultaneous DNA amplification and detection, *Lab. Chip.* 3, 100.
- Li, J., M. Xue, H. Wang, L. Cheng, L. Gao, Z. Lu and M. Chan, 2003, Amplifying the electrical hybridization signals of DNA array by multilayer assembly of Au nanoparticle probes, *Analyst* 128, 917.
- Mertig, M., L.C. Ciacchi, R. Siedel, W. Pompe and A. de Vita, 2002, DNA as a selective metallization template, *Nano Lett.* 2, 841.
- Mikkelsen, S.R., 1996, Electrochemical biosensors for DNA sequence detection, *Electroanal.* 8, 15.
- Napier, M.E., K. Mikulecky, K. Scaboo, A. Eckhardt, N. Baron, N. Popovich and M. Geladi, 2000, Direct electrochemical detection of nucleic acids, *Clin. Chem.* 46, A207.
- Nicewarner-Pena, R., R. Freeman, B. Reiss, L. He, D. Pena, I. Walton, R. Cromer, C.D. Keating and M.J. Natan, 2001, Submicrometer metallic barcodes, *Science* 293, 137.
- Niemeyer, C.M., 2001, Nanoparticles, proteins, and nucleic acids: Biotechnology meets materials science, *Angew. Chem. Int. Ed.* 40, 4128.
- Ozsoz, M., A. Erdem, K. Kerman, D. Okzan, B. Tugrul, N. Topcuoglu, H. Ekren and M. Taylan, 2003, Electrochemical genosensor based on colloidal gold nanoparticles for the detection of factor V leiden mutation using disposable pencil graphite electrodes, *Anal. Chem.* 75, 2181.
- Palecek, E. and M. Fojta, 2001, Detecting DNA hybridization and damage, *Anal. Chem.* 73, 75A.
- Palecek, E., M. Fojta and F. Jelen, 2002, New approaches in the developments of DNA sensors: Hybridization and electrochemical detection of DNA and RNA at two different surfaces, *Bioelectrochemistry* 56, 85.
- Park, S., T.A. Taton and C.A. Mirkin, 2002, Array-based electrical detection of DNA with nanoparticle probes, *Science* 295, 1503.
- Patolsky, F., Y. Weizmann, E. Katz and I. Willner, 2003, Magnetically amplified DNA assays (MADA): Sensing of viral DNA and single-base mismatches by using nucleic acid modified magnetic particles, *Angew. Chem. Int. Ed.* 42, 2372.
- Piunno, P., U. Krull, R. Hudson, M. Dahma and H. Cohen, 1995, Fiber-optic DNA sensor for fluorometric nucleic acid determination, *Anal. Chem.* 67, 2635.
- Richter, J., R. Seidel, R. Kirsch, M. Mertig, W. Pompe, J. Plashke and H. Schackert, 2000, Nanoscale palladium metallization of DNA, *Adv. Mater.* 12, 507.
- Storhoff, J.J., R. Elghanian, R.C. Mucic, C.A. Mirkin and R.L. Letsinger, 1998, One-pot colorimetric differentiation of polynucleotides with single base imperfections using gold nanoparticle probes, *J. Am. Chem. Soc.* 120, 1959.
- Storhoff, J.J. and C.A. Mirkin, 1999, Programmed materials synthesis with DNA, *Chem. Rev.* 99, 1849.
- Taton, T.A., C.A. Mirkin and R.L. Letsinger, 2000, Scanometric DNA array detection with nanoparticle probes, *Science* 289, 1757.
- Taton, T.A., G. Lu and C.A. Mirkin, 2001, Two-color labeling of oligonucleotide arrays via size-selective scattering of nanoparticles probes, *J. Am. Chem. Soc.* 123, 5164.
- Trau, D., W. Yang, M. Seydack, F. Carusu and R. Renneberg, 2002, Nanoencapsulated microcrystalline particles for superamplified biochemical assays, *Anal. Chem.* 74, 5480.

- Umek, R.M., S.S. Lin, Y.P. Chen, B. Irvine, G. Paulluconi, V. Chan, Y.C. Chong, L. Cheung, J. Vielmetter and D.H. Farkas, 2000, Bioelectronic detection of point mutations using discrimination of the H63D polymorphism of the Hfe gene as a model, *Molec. Diagn.* 5, 321.
- Urban, M., R. Moller and W. Fritzsche, 2003, A paralleled readout system for an electrical DNA-hybridization assay based on a microstructured electrode array, *Rev. Sci. Instr.* 74, 1077.
- Wang, J., 1985, *Stripping Analysis*, VCH, New York.
- Wang, J., D. Xu, A. Kawde and R. Polsky, 2001a, Metal nanoparticle-based electrochemical stripping potentiometric detection of DNA hybridization, *Anal. Chem.* 73, 5576.
- Wang, J., R. Polsky and X. Danke, 2001b, Silver-enhanced colloidal gold electrical detection of DNA hybridization, *Langmuir* 17, 5739.
- Wang, J., 2002, Electrochemical nucleic acid biosensors, *Anal. Chim. Acta* 469, 63.
- Wang, J., D. Xu and R. Polsky, 2002a, Magnetically-induced solid-state electrochemical detection of DNA hybridization, *J. Am. Chem. Soc.* 124, 4208.
- Wang, J., G. Liu and R. Polsky, 2002b, Electrochemical stripping detection of DNA hybridization based on CdS nanoparticle tags, *Electrochem. Commun.* 4, 819.
- Wang, J. and A. Kawde, 2002c, Magnetic-field stimulated DNA oxidation, *Electrochem. Commun.* 4, 349.
- Wang, J., O. Rincon, R. Polsky and E. Dominguez, 2003a, Electrochemical detection of DNA hybridization based on DNA-templated assembly of silver cluster, *Electrochem. Commun.* 5, 83.
- Wang, J., G.D. Liu and A. Merkoci, 2003b, Particle-based detection of DNA hybridization using electrochemical stripping measurements of an iron tracer, *Anal. Chim. Acta* 482, 149.
- Wang, J., G. Liu, R. Jan and Q. Zhu, 2003c, Electrochemical detection of DNA hybridization based on carbon-nanotubes loaded with CdS tags, *Electrochem. Commun.* 5, 1000.
- Wang, J., G. Liu and A. Merkoçi, 2003d, Electrochemical coding technology for simultaneous detection of multiple DNA targets, *J. Am. Chem. Soc.* 125, 3214.
- Wang, J., G. Liu and G. Rivas, 2003e, Encoded beads for electrochemical identification, *Anal. Chem.* 75, 4661.
- Wang, J., G. Liu and J. Zhou, 2003f, Indium microrod tags for electrical detection of DNA hybridization, *Anal. Chem.* 75, 6218.
- Wang, J., J. Li, A. Baca, J. Hu, F. Zhou, W. Yan and D.W. Pang, 2003g, Amplified voltammetric detection of DNA hybridization via oxidation of ferrocene caps on gold nanoparticle/streptavidin conjugates, *Anal. Chem.* 75, 3941.
- Wang, J., R. Polsky, A. Merkoci and K. Turner, 2003h, Electroactive beads for ultrasensitive DNA detection, *Langmuir* 19, 989.
- Wang, J., T. Lee and G. Liu, 2005, Nanocrystal-based bioelectronics coding of SNP, *J. Am. Chem. Soc.* 127, 38.
- Willner, I., P. Patolsky and J. Wasserman, 2001, Photoelectrochemistry with controlled DNA-cross-linked CdS nanoparticle arrays, *Angew. Chem. Int. Ed.* 40, 1861.
- Willner, I. and B. Willner, 2002, Functional nanoparticle architectures for sensoric, optoelectronic, and bioelectronic applications, *Pure Appl. Chem.* 74, 1773.
- Wilson, E.K., 1998, Instant DNA detection, *Chem. Eng. News* May 25, 47.

Detecting DNA Damage with Electrodes

Miroslav Fojta

*Institute of Biophysics, Academy of Sciences of the Czech Republic, Královopolská 135, 612 65
Brno, Czech Republic*

Contents

1. Introduction	386
1.1. DNA damage and repair	386
1.2. Current methods in DNA damage analysis	387
2. Relations between DNA damage and the DNA electrochemical behavior	389
2.1. Polarographic and voltammetric techniques in studies of DNA damage	391
3. Electrochemical sensors for DNA damage	394
3.1. DNA-modified electrodes	394
3.2. Detection of DNA strand breaks	395
3.2.1. Mercury and solid amalgam electrodes	396
3.2.2. Other electrodes	399
3.3. Detection of damage to DNA bases	400
3.3.1. Guanine redox signals	401
3.3.2. Specific signals of modified DNA bases and base adducts	403
3.3.3. DNA conformation changes due to base modifications	404
3.3.4. Use of DNA repair enzymes in electrochemical detection of damage to DNA bases	405
4. Electrochemically controlled DNA damage	405
4.1. <i>In situ</i> electrochemical analysis of DNA damage at electrodes	406
5. Non-covalent DNA interactions with genotoxic substances	407
5.1. Studies of DNA–binder interactions in solution	407
5.2. DNA-modified electrodes as sensors for non-covalently binding substances	409
5.3. Changes of DNA interfacial behavior upon interactions with non-covalent binders	410
6. Detection of mutations in DNA sequences	411
6.1. Utilization of reduced stability of mismatched DNA duplexes	411
6.2. Techniques based on specific structural features of the base mismatches	411
6.3. Primer extension-based techniques	412
6.4. Trinucleotide repeat expansions	412
7. Applications	413
7.1. DNA–drug interactions	413
7.2. Toxicity and antioxidant capacity testing	414
7.3. Environmental analysis	415
8. Conclusions	415
List of Abbreviations	416
Acknowledgments	417
References	418

1. INTRODUCTION

1.1. DNA damage and repair

Genetic material (DNA) in the cells is permanently exposed to various physical or chemical agents that may cause chemical alterations in the DNA molecules. It has been estimated that 10^4 – 10^6 DNA damage events occur in a cell per day (reviewed in Friedberg, 2000, 2003; Rajska *et al.*, 2000; Scharer, 2003). Typical products of DNA damage are shown in Figure 1.

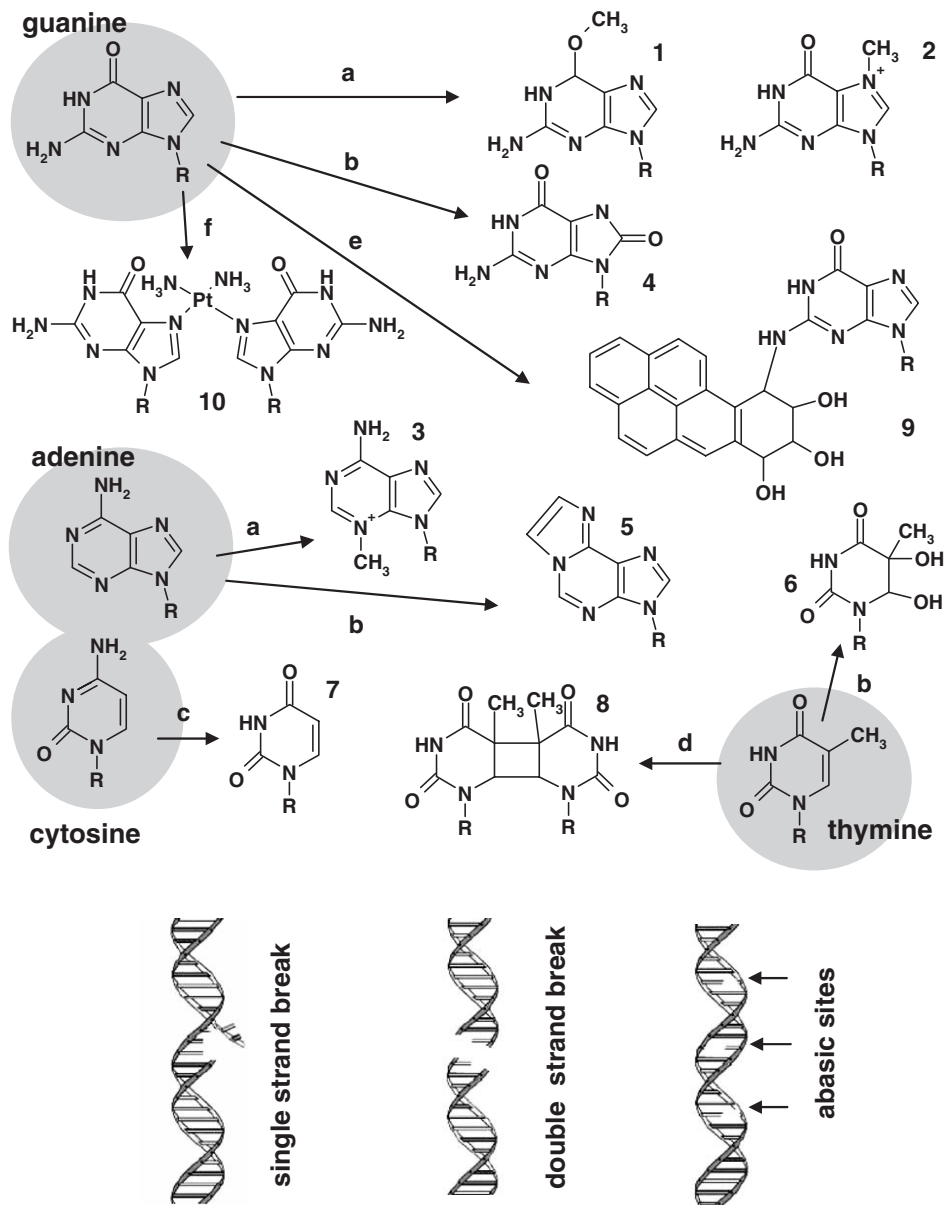
Among them, the most common lesions are apurinic sites (due to hydrolysis of the purine N-glycosidic bonds linking the base residue to deoxyribose), strand breaks (sb; i.e., interruptions of the DNA sugar-phosphate backbone), 8-oxoguanine (8-OG), and thymine glycol arising from oxidative DNA damage, or base deamination products (e.g., uracil or hypoxanthine) induced by some known mutagens (such as nitrous acid or bisulfite). Some of these lesions may be caused by intermediates or byproducts of cellular metabolism while others are induced by genotoxic agents occurring in the environment. For example, pyrimidine dimers arise from ultraviolet (UV) irradiation of DNA induced by sunlight. Different bulky adducts may be formed due to DNA interactions with metabolically activated carcinogens such as aromatic amines or polycyclic aromatic hydrocarbons. Persisting DNA damage may result in changes of the genetic information (base substitutions, mutations) or hamper vital processes such as DNA replication or transcription, which may subsequently have severe impacts on the cellular functions and life of the organisms. To maintain integrity of their genomes, cells possess enzymatic machineries capable of instant recognizing and repairing the DNA lesions (Friedberg, 2000, 2003; Rajska *et al.*, 2000; Scharer, 2003). Different products of DNA damage are repaired via different pathways. Chemically altered bases or base mismatches are excised by action of N-glycosylases and/or nucleases (through base excision repair, nucleotide excision repair or mismatch repair). Double-strand breaks (dsb), which belong to highly cytotoxic lesions, are repaired through a mechanism involving DNA recombination. Defects in either of the DNA repair pathways make the

Fig. 1. Scheme of most frequent products of DNA damage. A number of genotoxic agents attack nucleobase residues (upper panel). (a) Alkylating agents cause a variety of base lesions such as O⁶- and 7-alkyl guanine (1 and 2, respectively) or 3-alkyl adenine (3). (b) Oxidative DNA damage involves formation of 8-OG (4), 1,N⁶-ethenoadenine (5) (product of adenine reaction with acrolein generated through polyunsaturated fatty acids oxidation) or thymine glycol (6). (c) Some mutagens such as nitrous acid or bisulfite cause base deamination thus converting e.g., cytosine into uracil (7). (d) UV light yield several products among which cyclobutane pyrimidine dimers (8) belong to the most abundant ones. (e) Metabolically activated carcinogens, including polycyclic aromatic hydrocarbons form bulky DNA adducts, usually with guanine residues (9). (f) Many anticancer drugs act via inducing specific DNA damage; for example, covalent cross-link between two adjacent guanine residues (10) is typical lesion induced by cisplatin. Bottom panel shows lesions originating from interruption of phosphodiester bonds in the DNA sugar-phosphate backbone (single- or double-strand breaks) or from hydrolysis of the N-glycosidic bonds linking nucleobases with deoxyribose residues (abasic sites).

cell extremely prone to malignant transformation. Extensive, hardly repairable DNA damage often induces programmed cell death (apoptosis).

1.2. Current methods in DNA damage analysis

Analysis of DNA damage induced by various genotoxic substances, as well as detection of environmental mutagens and carcinogens, industrial pollutants and



their metabolically activated products themselves, is of great importance for human health protection. Moreover, studies of DNA damage by chemotherapeutics acting via formation of specific lesions in genomic DNA, and of repair of these damages, are important steps in development of novel anticancer drugs (Brabec and Kasparkova, 2002; Marchini *et al.*, 2001; Saijo *et al.*, 2003). Some DNA adducts are monitored as specific biomarkers of exposure of organisms to different genotoxic agents such as reactive oxygen species (ROS) (8-OG) (Gedik *et al.*, 2002; Halliwell, 1998), alkylating agents (8-hydroxyethyl guanine, 6-*O*-methylguanine) (Nakao *et al.*, 2002; Vasquez *et al.*, 2001), and so forth.

Up to now, different analytical techniques have been employed to analyze damaged DNA and to identify specific products of DNA interactions with the genotoxic species. Two basic approaches can be distinguished. In the first, the analyzed DNA is entirely hydrolyzed (into the DNA monomeric components) and the lesions are identified and quantified by chromatographic, electrophoretic and/or mass-spectrometric techniques (Collins *et al.*, 2003; Collins, 2005; England *et al.*, 1998; Guetens *et al.*, 2002; Helbock *et al.*, 1998; Inagaki *et al.*, 2001; Jenner *et al.*, 1998; Kasai, 2003; Swaminathan and Hatcher, 2002; Wang *et al.*, 1999b, c; Weimann *et al.*, 2002). For instance, products of oxidative DNA damage have been analyzed in DNA hydrolyzates using HPLC (Collins *et al.*, 2003; Collins, 2005; England *et al.*, 1998; Guetens *et al.*, 2002; Helbock *et al.*, 1998; Kasai, 2003; Weimann *et al.*, 2002), gas chromatography (Jenner *et al.*, 1998) or capillary electrophoresis (Inagaki *et al.*, 2001). These methods exhibit high sensitivities, making possible detection of one damaged base per 10^7 normal ones (Helbock *et al.*, 1998). On the other hand, they are rather laborious and may suffer from false-positive results due to accidental DNA oxidation during preparation of the samples (Cadet *et al.*, 1998; Collins *et al.*, 2004; England *et al.*, 1998; Helbock *et al.*, 1998; Jenner *et al.*, 1998). A variety of DNA adducts have been analyzed by means of so-called postlabeling techniques (Koskinen *et al.*, 2001; Stiborova *et al.*, 2002, 2004; Swaminathan and Hatcher, 2002). These approaches involve enzymatic DNA hydrolysis followed by introduction of fluorescent or radioactive (^{32}P , ^3H) tags to the hydrolysis products and their chromatographic separation and detection. The ability of some nucleases (such as nuclease P1, Falcone and Box, 1997; Li *et al.*, 2003; Stiborova *et al.*, 2004) to differentiate between intact and chemically modified DNA may be utilized for a better resolution of the damaged entities. Identification of DNA adducts has been achieved also using mass spectrometry (Cadet *et al.*, 1998; England *et al.*, 1998; Guetens *et al.*, 2002; Jenner *et al.*, 1998; Mazerska *et al.*, 2003; Swaminathan and Hatcher, 2002; Wang *et al.*, 1999c; Weimann *et al.*, 2002).

In the other group of techniques, changes in the features of whole DNA molecules (i.e., without complete hydrolysis) upon their damage are monitored. Most of these approaches involve electrophoretic determination of DNA sb. Using agarose gel electrophoresis, single strand breaks (ssb) or dsb can be determined with a relatively high sensitivity via relaxation or linearization of supercoiled (sc) plasmid DNA molecules (Boublikova *et al.*, 1987; Fojta *et al.*, 1999; Fojta and Palecek, 1997 and references therein). To detect multiple DNA strand breaking in individual cells, "comet" or alkaline elution assays are

frequently used (Cadet *et al.*, 1998; Collins *et al.*, 2003; Collins, 2004, 2005; Faust *et al.*, 2004; Marczynski *et al.*, 2002; Olive *et al.*, 2000; Pouget *et al.*, 2000; Taban *et al.*, 2004). In these techniques, number of the sb is estimated from mean length of double- (ds) or single-stranded (ss) DNA fragments, respectively. Combination of the electrophoretic methods with DNA cleavage by specific DNA repair endonucleases has been employed to detect certain DNA base lesions (Collins *et al.*, 2003; Collins, 2004, 2005; Gedik *et al.*, 2002). Number of ends (i.e., the sb) of DNA molecules in cell nuclei can be estimated by the “TUNEL” test (Loo, 2002; Migheli, 2002), a technique based on labeling of free 3'-OH polynucleotide termini through a reaction catalyzed by a terminal nucleotide transferase. Some DNA adducts have been analyzed by means of immunochemical methods utilizing their antigenic features (Buzek *et al.*, 1999; Cadet *et al.*, 1998; Cooke *et al.*, 2003; Guetens *et al.*, 2002; Kuderova-Krejcová *et al.*, 1991; Palecek *et al.*, 1989; Peccia and Hernandez, 2002; Wang *et al.*, 2003a).

2. RELATIONS BETWEEN DNA DAMAGE AND THE DNA ELECTROCHEMICAL BEHAVIOR

It has been known for more than four decades that DNA is electrochemically active and surface-active substance exhibiting distinct behavior at different electrodes (reviewed in Brabec *et al.*, 1996; Fojta, 2002, 2004; Palecek, 1969, 1971, 1976, 1980, 1983, 1996, 2002; Palecek and Fojta, 2001, 2005; Palecek *et al.*, 2002; Palecek and Jelen, 2002; Sequaris *et al.*, 1978). Depending on the electrode material and other conditions, DNA can undergo charge transfer (i.e., reduction and oxidation) and adsorption/desorption processes. DNA bases adenine, cytosine, and guanine yield redox signals at mercury (ME) and silver solid amalgam (AgSAE) electrodes while both purine bases are oxidizable at carbon and some other solid electrodes. At the ME and AgSAE, individual components of the DNA chains produce specific tensammetric signals. Studies of long-chain DNA molecules revealed that their electrochemical signals can be significantly affected by their ordered higher structures (reviewed in Brabec *et al.*, 1996; Fojta, 2004; Palecek, 1996; Palecek *et al.*, 2002; Palecek and Jelen, 2002; Sequaris *et al.*, 1978). Changes in the dsDNA structure, including those arising from covalent or non-covalent DNA interactions with genotoxic substances, may be reflected in changes of its electrochemical response. It has been recently proposed (Boon *et al.*, 2003; Rajska *et al.*, 2000) that besides the phenomena observed at the electrodes, electrochemical, and electronic features of DNA may play roles *in vivo* in processes related to DNA damage, recognition of DNA lesions, and DNA repair. The DNA double helix may function as a “molecular wire” mediating charge transfer over long distances (Boon and Barton, 2002, 2003; Hartwich *et al.*, 1999; Kelley *et al.*, 1997, 1999a, b; Odom and Barton, 2001). Moreover, sites of anomalous redox potential (such as GG doublets) occur in DNA which can easily be oxidatively attacked. Other redox potential anomalies, including base lesions (pyrimidine dimers or 8-OG) can be

recognized by the DNA repair machinery. The long-range charge transfer may allow recognition of these sites by specific proteins from remote positions (Odom and Barton, 2001; Rajska *et al.*, 2000). The charge transfer efficacy is dramatically affected by perturbations in the base stacking network in the DNA double helix [such as single base mismatches, insertion/deletion lesions or abasic sites (Boon and Barton, 2002; Rajska *et al.*, 2000)]. Some proteins involved in recognition of DNA lesions (e.g., MutY) contain redox-active prosthetic groups which have been proposed to take part in DNA-mediated redox reactions (Boon and Barton, 2002; Boon *et al.*, 2002; Rajska *et al.*, 2000).

Above and beyond the academic interest in changes of the DNA electrochemical properties upon its damage and their proposed biological consequences, the altered behavior of the damaged DNA at electrodes can be exploited analytically. Electrochemical detectors have been used as components of chromatographic (Collins *et al.*, 2003; Guetens *et al.*, 2002; Helbock *et al.*, 1998; Masuda *et al.*, 2002; Weimann *et al.*, 2002), mass spectrometric (England *et al.*, 1998; Jenner *et al.*, 1998) or capillary electrophoretic (Guetens *et al.*, 2002; Inagaki *et al.*, 2001) analyzers used in the DNA hydrolysis-based methods (see above). On the other, it has been shown that electrochemical analysis can provide information about the properties of non-hydrolyzed, highly polymeric DNA molecules (reviewed in Brabec *et al.*, 1996; Erdem and Ozsoz, 2002; Fojta, 2002, 2004; Palecek, 1969, 1971, 1976, 1980, 1983, 1996, 2002; Palecek and Fojta, 2001, 2005; Palecek *et al.*, 2002; Palecek and Jelen, 2002; Popovich and Thorp, 2002; Sequaris *et al.*, 1978; Wang, 2000, 2002). Relatively small changes in DNA structure may significantly affect behavior of the DNA at electrodes. Damage to DNA may lead to local changes of DNA conformation with concomitant alterations in the exposure of its electroactive sites to the environment and changes in the measured electrochemical signals (Mugweru and Rusling, 2002; Rusling *et al.*, 2002; Vorlickova and Palecek, 1974; Zhou *et al.*, 2003). Interruptions of the sugar–phosphate backbone of dsDNA confer increased accessibility of base moieties next to the strand ends and promote potential-dependent unwinding of the DNA at the ME surface (Section 3.2.1) (Fojta, 2002, 2004; Fojta *et al.*, 1997, 1998b; Palecek, 1983, 1992a). Damage to electroactive base residues may lead to diminution of the intrinsic oxidation or reduction DNA responses (Jelen *et al.*, 1997b; Karadeniz *et al.*, 2003; Lucarelli *et al.*, 2002a, b, 2003; Marin *et al.*, 1997, 1998; Mascini *et al.*, 2001; Perez *et al.*, 1999; Teijeiro *et al.*, 1995; Wang *et al.*, 1996a, 1997a, c) (Section 3.3.1). Some chemically modified bases [such as 8-OG (Brett *et al.*, 2000; Holmberg *et al.*, 2003; Langmaier *et al.*, 2003; Oliveira-Brett *et al.*, 2002; Piedade *et al.*, 2002; Rebelo *et al.*, 2004; Ropp and Thorp, 1999) or bulky DNA adducts with electrochemically active compounds (Fojta *et al.*, 2002a, 2004a; Havran *et al.*, 2004b; Jelen *et al.*, 1991; Kizek *et al.*, 2002; Kostecka *et al.*, 2004; Marin *et al.*, 1998; Palecek, 1992b; Palecek and Hung, 1983; Perez *et al.*, 1999; Teijeiro *et al.*, 1995)] produce new, specific electrochemical signals not yielded by the unmodified DNA (Section 3.3.3). Besides covalent DNA damage, non-covalent DNA interactions with small molecules (including potentially genotoxic agents) can be monitored via electrochemical measurements too. Formation of the non-covalent DNA-binder complexes may lead to changes of electrochemical signals

of either DNA (Fojta *et al.*, 2000a; Gherghi *et al.*, 2003b, c; Wang *et al.*, 1998b) or the binders (e.g. Carter and Bard, 1987; Carter *et al.*, 1989; Labuda *et al.*, 1999; Maruyama *et al.*, 2001; Rodriguez and Bard, 1990; Rodriguez *et al.*, 1990; Sufen *et al.*, 2002; Wang *et al.*, 1996c, 1997a, 1998b; Xu and Bard, 1995) (Section 5). Both non-covalent (Buckova *et al.*, 2002; Korbust *et al.*, 2001, 2003; Labuda *et al.*, 2002, 2003) and covalent (Fojta *et al.*, 1998a, 2004a; Palecek, 1992b) electroactive DNA binders can be utilized in redox marker-based techniques of electrochemical DNA structural probing.

2.1. Polarographic and voltammetric techniques in studies of DNA damage

The seminal work on DNA electrochemistry was connected with the dropping mercury electrode (DME) and polarographic techniques (see Chapters 1 and 3). Using oscillographic polarography at controlled AC and later differential pulse polarography (DPP), striking differences between the signals of native (ds) and denatured (ss) DNA at the DME were established (Palecek, 1964, 1966, 1967, 1969, 1971, 1976, 1980, 1983) (Chapter 3). In addition, it has been shown that structural alterations much more subtle than DNA denaturation can be monitored via measurements of the so-called peak II yielded by dsDNA at the DME in the DPP mode (Fojta, 2004; Palecek, 1976, 1983, 1996; Palecek *et al.*, 2002). Intensity of this signal responded sensitively to premelting changes of the DNA double helix (Palecek, 1976) as well as perturbations related to DNA damage. Height of the peak II increased with the number of ssb and/or dsb induced by deoxyribonuclease I, ionizing radiation or ultrasound (Palecek, 1967; Puranen and Forss, 1983). Covalently closed circular (ccc) DNA's (in which no strand ends occur) did not yield any peak II under the same conditions (Fojta, 2004; Vojtiskova *et al.*, 1981). Conformational distortions of the DNA double helix accompanying some kinds of covalent base damage (without breakage of the sugar–phosphate backbone) led to increase of the peak II height as well. Such phenomena were observed with dsDNA's irradiated with UV light (Vorlickova and Palecek, 1974) or DNA modified by some chemical agents (such as certain platinum (Brabec *et al.*, 1990, 1996; Marini *et al.*, 2002) or osmium tetroxide (Lukasova *et al.*, 1984) complexes). In addition, specific structural features of DNA lesions were reflected in the polarographic responses of damaged DNA. For example, presence of unpaired bases in denaturation lesions induced by transplatin or some other platinum complexes (Brabec *et al.*, 1990, 1996; Marini *et al.*, 2002) was indicated by the ssDNA-specific DPP peak III. Non-denaturation lesions involving distortions of the DNA double helix without disruption of the Watson-Crick base pairs were connected with increasing intensity of the peak II (Brabec *et al.*, 1990, 1996).

Analogous information about DNA damage can be obtained through measurements of adsorption/desorption (tensammetric) DNA responses in weakly alkaline background electrolytes (reviewed in Brabec *et al.*, 1996; Fojta, 2004; Palecek, 1983, 1996; Palecek *et al.*, 2002; Sequaris *et al.*, 1978). A specific AC polarographic signal (peak 2) has been attributed to distorted segments of

dsDNA, in contrast to a more negative peak 3 which is specific for ssDNA with freely accessible bases (Brabec *et al.*, 1996; Fojta, 2004; Palecek, 1983, 1996; Palecek *et al.*, 2002). The peak 2 responded to DNA damage by ionizing radiation, ultrasound, and so forth. Another tensammetric signal denoted as peak 3* (appearing in AC polarography or voltammetry at intermediate potential between peak 2 and peak 3) was observed with negatively scDNA's undergoing local helix opening transitions (connected with occurrence of unpaired bases within covalently closed DNA chains) (Fojta *et al.*, 1998a).

Polarographic techniques working with the DME are very powerful tools in studies of DNA structure in solution (reviewed in Palecek, 1976, 1983; Palecek *et al.*, 2002). On the other hand, these techniques require rather large amounts of DNA to be probed and, in addition, they are not compatible with construction of DNA biosensors. First steps toward development of such sensors, usually involving DNA immobilization at surfaces of stationary electrodes (Figure 2), were attained through introduction of hanging mercury drop electrode (HMDE) and various kinds of solid electrodes in nucleic acids electrochemical analysis. Due to a firm adsorption of nucleic acids (and also peptides or proteins Havran *et al.*, 2004a; Kizek *et al.*, 2002; Masarik *et al.*, 2004; Palecek and Fojta, 2005; Palecek *et al.*, 1993; Tomschik *et al.*, 1998, see Chapter 19) at the electrode

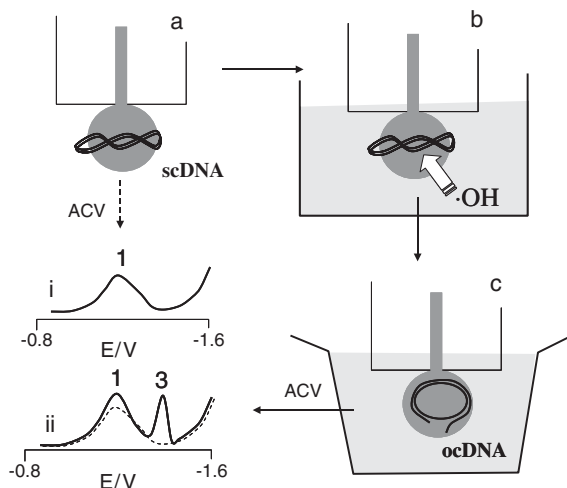


Fig. 2. Scheme of electrochemical sensor for DNA sb (or agents cleaving the DNA sugar-phosphate backbone). (a) The sensor consists of ccc (sc) DNA adsorbed at surface of HMDE (Fojta and Palecek, 1997). Instead of HMDE, MFE (Kubicarova *et al.*, 2000a) or AgSAE (Fadrna *et al.*, 2005; Kucharikova *et al.*, 2004) can be used. (b) The scDNA-modified electrode is immersed into solution containing DNA damaging agents (e.g., hydroxyl radicals) inducing the sb. (c) Then, the electrode is washed and transferred into background electrolyte and AC voltammogram is recorded. DNA containing free-strand ends (such as ocDNA involving ssb, or linDNA formed after inducing dsb) is partially unwound at the electrode surface during slow voltage scan from positive to negative potentials and yields peak 3 (curve ii) specific for ssDNA. No such signal is produced by the scDNA (curve i) whose unwinding is topologically restricted.

surfaces, these species can be efficiently pre-accumulated from diluted solutions, resulting in significant improvement of sensitivity of the nucleic acid (NA) electrochemical detection. Adsorptive stripping of DNA in connection with a variety of electrochemical techniques, including voltammetry, impedance spectroscopy or constant current chronopotentiometry (reviewed in Fojta, 2002, 2004; Palecek, 1996, 2002; Palecek *et al.*, 2002; Palecek and Jelen, 2002), was applied in various fields of DNA studies, including analysis of damaged DNA. Linear sweep (Sequaris *et al.*, 1978, 1982) and AC voltammetric (Fojta *et al.*, 1998b, 2000b, 2002b; Fojta and Palecek, 1997; Krznaric *et al.*, 1990) measurements of DNA tensammetric peaks at the HMDE were employed in investigations of electrochemical behavior of DNA exposed to γ -rays, ultrasound, enzymes, chemical nucleases, and so on (Sections 3.2 and 5). Changes in intensity of redox signals yielded by guanine residues on either HMDE or carbon electrodes (CE) have been utilized to monitor DNA damage caused by a number of genotoxic substances including alkylating agents (Jelen *et al.*, 1997b), hydrazine derivatives (Wang *et al.*, 1996a), anticancer drugs (Brabec, 2000; Marin *et al.*, 1997, 1998; Perez *et al.*, 1999; Teijeiro *et al.*, 1995), environmental pollutants (Chiti *et al.*, 2001; Lucarelli *et al.*, 2002a, b, 2003; Mascini *et al.*, 2001; Wang *et al.*, 1997a), UV light (Wang *et al.*, 1997c), and so forth (see Section 3.3.1). Voltammetric signals of some electroactive base adducts [such as 8-OG (Brett *et al.*, 2000; Langmaier *et al.*, 2003; Oliveira-Brett *et al.*, 2002), adenine ethenoderivatives (Palecek, 1986), DNA modified with mitomycin C (MC) (Marin *et al.*, 1998; Perez *et al.*, 1999; Teijeiro *et al.*, 1995) or osmium tetroxide complexes (Fojta *et al.*, 2002a, 2004a; Jelen *et al.*, 1991; Kizek *et al.*, 2002; Kostecka *et al.*, 2004; Lukasova *et al.*, 1982; Palecek, 1992b; Palecek and Hung, 1983; Yosypchuk *et al.*, 2005)] have been detected at ME, solid amalgam (MeSAE) or CE's (see Section 3.3.2). To increase the performance of electrode processes involving DNA bases, redox mediators featured by ruthenium, osmium or rhenium complexes [soluble (Johnston *et al.*, 1994, 1995; Napier and Thorp, 1997, 1999; Ropp and Thorp, 1999; Thorp, 1998) or confined in polymeric films at the electrode surface (Holmberg *et al.*, 2003; Maruyama *et al.*, 2001; Mbindyo *et al.*, 2000; Mugweru and Rusling, 2001, 2002; Ontko *et al.*, 1999; Rusling, 2004; Rusling *et al.*, 2002; Wang and Rusling, 2003; Yang and Rusling, 2002; Yang *et al.*, 2002; Zhou *et al.*, 2003)] have been employed. Electrocatalytic guanine or 8-OG oxidation by these species enhanced the electron yields and made it possible to probe accessibility of the guanine or (8-OG) moieties in mismatched (Johnston *et al.*, 1995; Ropp and Thorp, 1999) or chemically damaged (Mbindyo *et al.*, 2000; Mugweru and Rusling, 2001, 2002; Rusling, 2004; Rusling *et al.*, 2002; Wang and Rusling, 2003; Yang and Rusling, 2002; Yang *et al.*, 2002; Zhou *et al.*, 2003) DNA molecules (see Sections 3.3.3, 6, 7.2 and Chapters 3 and 13). Voltammetric and constant current chronopotentiometric (CPSA) measurements have been frequently used to detect non-covalent DNA interactions with potentially DNA-damaging small molecules (reviewed in Erdem and Ozsoz, 2002; Fojta, 2002; Palecek and Fojta, 2001, 2005; Palecek *et al.*, 1998, 2002) including toxic metal ions and their complexes, natural and man-made carcinogens, drugs, and so forth (see Section 5). These techniques involve measurements of changes of intrinsic DNA electrochemical signals

and/or of those yielded by the binders. In other approaches, redox indicators of DNA damage or non-covalent DNA interactions have been utilized. A metal-lointercalator $[\text{Co}(\text{phen})_3]^{3+}$ binding efficiently to intact dsDNA but not to degraded DNA responded to DNA damage by decrease of its voltammetric signal (Buckova *et al.*, 2002; Korbust *et al.*, 2001, 2003; Labuda *et al.*, 1999, 2002, 2003). Analogous approach was used to probe DNA interactions with non-covalently binding species in a competitive mode (Labuda *et al.*, 2000). Another indicator-based method for studies of DNA-drug binding was based on a restricted reduction/oxidation of an anionic depolarizer ferro/ferricyanide on a dsDNA-coated gold electrode due to electrostatic repulsion (Maeda *et al.*, 1992). In the presence of cationic DNA-binding drugs, signals of the indicator increased.

3. ELECTROCHEMICAL SENSORS FOR DNA DAMAGE

3.1. DNA-modified electrodes

Strong adsorption of nucleic acids at surfaces of ME's or CE's has been utilized in introduction of adsorptive transfer stripping (AdTS) techniques in NA electrochemical analysis (Palecek, 1988; Palecek *et al.*, 1993; Palecek and Postbieglova, 1986). These techniques are based on immobilization NA's onto the electrode surface followed by medium exchange and signal measurements in a blank background electrolyte (Figure 2). Application of the AdTS voltammetry in DNA or RNA (Fojta *et al.*, 1994, 1996; Palecek and Fojta, 1994) microanalysis was the first step toward wide utilization of NA-modified electrodes in development of electrochemical DNA biosensors (reviewed in Erdem and Ozsoz, 2002; Fojta, 2002, 2004; Palecek, 1996; Palecek and Fojta, 2001, 2005; Palecek *et al.*, 1998, 2002; Palecek and Jelen, 2002; Popovich and Thorp, 2002; Wang, 2000, 2002). Voltammetric or CPSA responses obtained with the DNA-modified electrodes in the blank supporting electrolyte do not differ significantly from the curves measured in the conventional adsorptive stripping technique that is, with working electrodes dipped in the analyte solution. Strikingly, upon exposure of the sensor (featured by the DNA-modified electrode) to various chemical or physical agents (including species causing DNA damage or otherwise interacting with the DNA molecules), alterations in the anchored DNA recognition layer may take place which can subsequently be detected via changes in the DNA electrochemical responses (Figure 2).

Various techniques have been applied to immobilize DNA at electrodes (see also Chapters 3, 4, and 8). Perhaps the simplest is adsorptive accumulation of the biopolymer at the surface that is well applicable for ME, AgSAE or CE's. Structure of adsorbed dsDNA at the HMDE has been shown to be stable within a relatively wide potential window, different salt concentrations and pH's (reviewed in Brabec *et al.*, 1996; Fojta, 2002, 2004; Palecek, 1983, 1996; Palecek *et al.*, 2002). Results obtained with the MeSAE's suggest that the same applies for various variants of the AgSAE (Fadrna *et al.*, 2005; Kucharikova *et al.*, 2004) (see Section 3.2.1). The DNA-modified HMDE or AgSAE can be

therefore used as a sensor for DNA damage under broad range of conditions (Section 3.2). Similarly as at the ME, adsorption of DNA at CE's can be achieved at open current circuit but moreover, it may be facilitated by the application of positive potentials conferring electrostatic attraction between the surface and negatively charged DNA (Cai *et al.*, 1996; Lucarelli *et al.*, 2002b; Mascini *et al.*, 2001; Wang *et al.*, 1996a, c, 1998b). In connection with carbon paste electrodes (CPE), "bulk modification" of the pastes with DNA (i.e., addition of DNA to the carbon powder prior to mixing with the oil component) (Vanickova *et al.*, 2000; Wang *et al.*, 1998a) has been utilized. Modification of glassy carbon electrodes (GCE) with acid-hydrolyzed DNA has been used by some authors to create a DNA sensor (Brett *et al.*, 1996, 1997a, b, c, 1998) while others have utilized "thick DNA layers" prepared via deposition of concentrated DNA solutions onto solid electrode surfaces and subsequent drying of the DNA gels (films) (Brett *et al.*, 2003; Mbindyo *et al.*, 2000; Oliveira-Brett and Diculescu, 2004a, b; Oliveira-Brett *et al.*, 2002; Pang *et al.*, 1996). Some of these protocols may yield rather poorly defined DNA layers which may also suffer from inherent instability (e.g., due to release of water-soluble DNA from the bulk-modified carbon paste or from the thick DNA layers). Nevertheless, these procedures have been successfully applied for various purposes after empirical optimization. A more sophisticated technique has been developed by Rusling and coworkers who have prepared ultrathin DNA films on CE's coated with a redox polymer (Mbindyo *et al.*, 2000; Mugweru and Rusling, 2001, 2002; Rusling, 2004; Rusling *et al.*, 2002; Wang and Rusling, 2003; Yang and Rusling, 2002; Yang *et al.*, 2002, Zhou *et al.*, 2003) (for more detail see Chapter 13). To create a biosensor for toxicity testing, the DNA films have been assembled layer-by-layer with hemoproteins that possess catalytic activity mimicking metabolic carcinogen activation (Zhou *et al.*, 2003) (see Section 7.2). Application of other electrode materials such as indium-tin oxide (ITO) (Johnston *et al.*, 1994, 1995; Napier and Thorp, 1997; Thorp, 1998; Yang *et al.*, 2002), gold (Boon *et al.*, 2000, 2002; Kelley *et al.*, 1997, 1999a, b; Maeda *et al.*, 1992; Maruyama *et al.*, 2001; Pang *et al.*, 1999, 2000; Wang *et al.*, 1999a) or various carbon materials (Napier and Thorp, 1997; Schülein *et al.*, 2002; Wang *et al.*, 2001) usually involve covalent coupling of derivatized oligodeoxyribonucleotides (ODN's) to the surface. Utilization of such techniques mainly for construction of sensors for DNA hybridization (see Section 6 and Chapters 3–11), including blocking of the electrode surface to prevent non-specific interactions, its interfacing with conductive polymers, and so on, have been recently reviewed by Tarlov and Steel (2003). Biotin-labeled ODN's have been immobilized onto bulk-phase avidin-modified CPE (Masarik *et al.*, 2003).

3.2. Detection of DNA strand breaks

Strand breaks (Figure 1) which belong to the most abundant DNA lesions (Friedberg, 2000, 2003; Scharer, 2003) are formed due to attacking the sugar moiety by ROS, as a result of some kinds of DNA base damage, and/or upon

action of endonucleases. The sb are currently detected mostly by electrophoretic techniques (Boublikova *et al.*, 1987; Fojta and Palecek, 1997; Olive *et al.*, 2000; Pouget *et al.*, 2000) and methods based on determination of the ends of DNA strands [such as the TUNEL test (Loo, 2002; Migheli, 2002)]. Electrochemical techniques applied for the detection of the DNA sb include highly sensitive determination of the sb using the HMDE, mercury film electrodes (MFE) or AgSAE (Fadrna *et al.*, 2005; Fojta, 2002; Fojta *et al.*, 1997, 1998b, 2000b, 2002b; Fojta and Palecek, 1997; Kubicarova *et al.*, 2000a; Kucharikova *et al.*, 2004) (Section 3.2.1). Other techniques, employing primarily CE's, are suitable for monitoring deeper DNA degradation (Korbut *et al.*, 2001, 2003; Labuda *et al.*, 1999, 2002, 2003) (Section 3.2.2).

3.2.1. Mercury and solid amalgam electrodes

Early polarographic studies as well as more recent measurements with DNA-modified electrodes revealed that behavior of DNA at the mercury surface is strongly dependent on accessibility of the DNA base residues. In ssDNA, the base moieties can freely communicate with the electrode surface and yield well-developed reduction (peak CA, peak III) or tensammetric (peak 3) signals (reviewed in Fojta, 2002, 2004; Palecek, 1983, 1996; Palecek and Fojta, 2005; Palecek *et al.*, 2002; Palecek and Jelen, 2002). In intact dsDNA, the nucleobases are hidden in the double helix interior and, regarding the signals of the nucleobases, the native DNA behaves as relatively inactive species. On the other hand, electrochemical behavior of the dsDNA at ME depends remarkably on its conformation and/or occurrence of local perturbations in its double-helical structure. Such defects, including ssb or ends of linear (lin) DNA molecules facilitate contacts of the DNA base residues with the electrode surface, resulting in the formation and/or enhancement of specific signals (reviewed in Fojta, 2002, 2004; Palecek, 1976, 1983, 1996; Palecek *et al.*, 2002). Transient DNA double helix opening around the ssb is detectable polarographically using the DPP peak II (see Section 2 and Chapter 3). In addition, DNA molecules lacking free chain ends (such as ccc, sc plasmid DNA) and molecules involving interruptions of the sugar–phosphate backbone [e.g., open circular (oc, containing one or more ssb per molecule) or linear (lin) DNA molecules] can be distinguished through their diverse susceptibilities to irreversible denaturation. A technique based on differential thermal DNA denaturation in solution followed by AdTS voltammetric microanalysis was used (Boublikova *et al.*, 1987; Fadrna *et al.*, 2005; Fojta and Palecek, 1997) for determination of ocDNA in samples of scDNA and for detection of ssb formed due to irradiation of the scDNA by γ -rays. Nicked (oc) or linDNA's but not the scDNA were irreversibly denatured due to heating of the samples to 85°C (Boublikova *et al.*, 1987). Only the DNA's containing free ends (i.e., the products of DNA damage) contributed to the observed changes in the intensity of cyclic voltammetry (CV) (Boublikova *et al.*, 1987) or AC voltammetric (Fadrna *et al.*, 2005; Fojta and Palecek, 1997) DNA signals. In addition to the thermal pretreatment of the DNA samples, the lin or ocDNA can be denatured also at the ME through applying certain electrical

potentials (Brabec and Palecek, 1976; Fojta, 2002, 2004; Fojta *et al.*, 2000a; Fojta and Palecek, 1997; Jelen and Palecek, 1985; Palecek, 1983, 1992a, 1996; Palecek *et al.*, 2002).

3.2.1.1. Unwinding of dsDNA at electrically charged mercury surface. When alternating current voltammetric (ACV) responses of lin dsDNA are measured at the HMDE and the potential is slowly scanned from positive to negative values, the ssDNA-specific peak 3 appears in addition to the peak 1 and peak 2 which are yielded by the dsDNA at the DME (Flemming and Berg, 1974; Fojta and Palecek, 1997; Jelen *et al.*, 1999; Palecek, 1996; Palecek *et al.*, 2002). The faradaic peak CA (corresponding to the ssDNA-specific DPP peak III) is also detected with the dsDNA at the HMDE. On the contrary, when the potential is scanned from the negative to the positive values, no ACV peak 3 is observed and the voltammogram is qualitatively identical to the dsDNA ACV curve (Flemming and Berg, 1974; Jelen *et al.*, 1999; Palecek *et al.*, 2002). At the DME, analogous phenomena could be observed only upon large potential excursions during the drop lifetime [in normal pulse polarography (Palecek, 1983)]. Although there were attempts to explain such behavior by other phenomena (Flemming and Berg, 1974) (for more details see Chapter 3), potential-induced unwinding of the DNA double helix at the electrode surface (or “surface denaturation” of DNA) is the most probable source of these effects (Fojta, 2004; Fojta and Palecek, 1997; Jelen and Palecek, 1985; Palecek, 1983, 1992a). Intensities of the ssDNA-specific peaks (i.e., peak 3 or peak CA) slowly increase due to prolonged exposure of the dsDNA at the HMDE surface to potentials around -1.2 V (potential “region U”, see Chapter 3). The same treatment does not influence the signals of ssDNA (thermally denatured in solution prior to adsorption at the electrode). A mechanism of the potential-induced surface denaturation of DNA has been proposed (Palecek, 1983, 1992a; Palecek *et al.*, 2002 and references therein) involving repulsion of the DNA phosphate groups from the negatively charged electrode surface while randomly unpaired hydrophobic bases (at the molecule ends or around ssb) remain adsorbed at the surface. The repulsive forces cause strains in the DNA molecules and, consequently, the DNA unwinding. When the electrode potential is slowly scanned from the positive to the negative values, the region U is passed through before reaching potentials at which the ssDNA-specific peaks occur. Behavior of dsDNA’s whose unwinding is restricted (such as dsDNA involving covalent interstrand cross-links or cccDNA’s) strongly supports this model. DNA cross-linked with bifunctional platinum complexes resists the double helix unwinding within the region U (Kasparova *et al.*, 1987). The cccDNA’s do not possess any strand ends and their denaturation is restricted topologically (Bates and Maxwell, 1993; Palecek, 1991; Vinograd *et al.*, 1968). Accordingly, the cccDNA’s yield no signal at potentials corresponding to the ssDNA peak 3 regardless of the scan direction (Fojta *et al.*, 1998a; Fojta and Palecek, 1997). Linear or ocDNA (formed due to introduction of ssb or dsb into the scDNA molecule, respectively) can undergo the surface denaturation within the region U, which allows detection of the sb in a single voltammetric scan (from positive

to negative potentials) without any preconditioning. Both oc and linDNA's – unlike the scDNA – yield well developed tensammetric peak 3 (Figure 2) (usually measured by ACV in alkaline media Fojta *et al.*, 1998a; Fojta and Palecek, 1997) and cathodic peak CA (e.g., using CPSA in neutral ammonium formate Fojta *et al.*, 1997).

Based on the qualitative differences between the behavior of scDNA and that of ocDNA (or linDNA) at the HMDE, damage to DNA induced by various agents cleaving the DNA sugar–phosphate backbone (including nucleases, transition metals and/or ROS) can be detected (Fojta, 2002; Fojta *et al.*, 1997, 1998b, 1999, 2000a, b, 2002b; Fojta and Palecek, 1997). In connection with ACV, this technique provides a high sensitivity allowing detection of one sb among more than 2×10^5 nucleotides (i.e., one break in about 1% of 3-kb long plasmid scDNA) (Fojta and Palecek, 1997). Considering the DNA amount used for one measurement, the lesions can be detected at the femtomole level (Cahova-Kucharikova *et al.*, 2005), making it well competitive with most of the currently used DNA damage assays [such as ^{32}P postlabeling (Bykov *et al.*, 1995), ELISA (Cooke *et al.*, 2003) or mass spectrometry (Podmore *et al.*, 1996)]. Moreover, the scDNA can easily be immobilized at the HMDE surface and the scDNA-modified electrode can serve as a simple biosensor for DNA sb or DNA-cleaving species (Fojta, 2002; Fojta *et al.*, 1997, 1998b, 1999, 2000a, b, 2002b; Fojta and Palecek, 1997) (Figure 2). This type of biosensor has been applied in experiments involving laboratory-prepared model samples as well as in various “real” specimens [natural and industrial waters or food (Fojta *et al.*, 1998b)]. The scDNA-modified electrode was also utilized as a tool for *in situ* monitoring of DNA cleavage by electrochemically generated ROS (Fojta *et al.*, 2000b, 2002b) or intermediates of reduction of chromium compounds (T. Mozga and M. Fojta, unpublished) (see Section 4). Principle of the technique was employed in a new method for the detection of DNA base damage involving DNA cleavage by DNA repair endonucleases (Cahova-Kucharikova *et al.*, 2005; Palecek and Fojta, 2001) (Section 3.3.4).

3.2.1.2. Mercury film and solid amalgam electrodes. In addition to the “classical” HMDE, other electrode types have recently been tested as tools for the DNA sb detection. These attempts have been focused on finding alternatives to the HMDE which would retain the unique features of the liquid mercury electrodes [high hydrogen overvoltage allowing measurements at highly negative potentials (Fojta, 2004; Yosypchuk and Novotny, 2002a, b) and, specifically, the sensitivity of DNA voltammetric responses to small changes in its structure (Fojta, 2004; Palecek, 1996; Palecek *et al.*, 2002)] with some useful properties of the solid electrodes (mechanical resistance, applicability as simple, and cheap sensor devices, etc.). Unlabeled as well as chemically modified NA's and their components have recently been analyzed at the MFE (Hason and Vetterl, 2002a, b; Kostecka *et al.*, 2004; Kubiarova *et al.*, 2000a, b; Wu *et al.*, 1997) or AgSAE (Fadrna *et al.*, 2004, 2005; Yosypchuk *et al.*, 2002, 2005). It has been shown that these electrodes, in which the toxic mercury content is minimized, provide similar DNA responses as the HMDE. Both redox and tensammetric signals of

ss and dsDNA, RNA, and synthetic polynucleotides could be detected with a mercury-coated GCE (MF/GCE) (Kubicarova *et al.*, 2000a, b). The MF/GCE modified with scDNA was successfully applied as a sensor for the ssb formation (Kubicarova *et al.*, 2000a). More recently, the MeSAE's were introduced in the DNA electrochemical analysis (Fadrna *et al.*, 2004, 2005; Jelen *et al.*, 2004; Kucharikova *et al.*, 2004; Yosypchuk *et al.*, 2002, 2005). Purine bases can be detected at AgSAE or CuSAE by means of the stripping voltammetric techniques (involving sparingly soluble Hg or Cu complexes) with sensitivities similar to that attained with the HMDE (Fadrna *et al.*, 2004; Jelen *et al.*, 2004; Yosypchuk *et al.*, 2002). This detection principle was utilized in techniques of DNA (as well as synthetic polynucleotide or ODN) microanalysis involving release of the purines in acidic media (Fadrna *et al.*, 2004; Jelen *et al.*, 2004; Yosypchuk *et al.*, 2002). The AgSAE was applied in various variants, including AgSAE coated with a mercury meniscus (m-AgSAE) (Kucharikova *et al.*, 2004; Yosypchuk *et al.*, 2005) or a mercury film (MF-AgSAE) (Fadrna *et al.*, 2005) as well as a liquid mercury-free mechanically polished electrode (p-AgSAE) (Fadrna *et al.*, 2005), in analysis of polymeric (non-hydrolyzed) DNA's. Responses of sc, lin, and ssDNA at the m-AgSAE or MF-AgSAE exhibited analogous differences as observed with the HMDE (see above), and both electrodes could be used for sensitive detection of the sb (Fadrna *et al.*, 2005; Kucharikova *et al.*, 2004). The p-AgSAE did not offer well developed signals of dsDNA's but allowed detection of ss (denatured) DNA (Fadrna *et al.*, 2005). DNA damage could be detected at the p-AgSAE through application of the above described thermal DNA denaturation procedure.

3.2.2. Other electrodes

At CE's, signal due to oxidation of guanine residues (peak G^{ox}) is usually used in electrochemical analysis of DNA. However, this signal exhibit no significant differences between scDNA and dsDNA molecules possessing free ends (oc or linDNA) (Cai *et al.*, 1996; Kubicarova *et al.*, 2000a). Such behavior arises partly from a relatively easy accessibility of the guanine oxidation sites via major groove of the DNA double helix (resulting in a remarkable electroactivity of dsDNA, see Chapter 3), and partly from absence of extensive DNA surface denaturation at the carbon surfaces under conditions used for the peak G^{ox} measurements (reviewed in Fojta, 2002; Palecek, 1996; Palecek *et al.*, 2002). Intensity of the peak G^{ox} therefore does not respond to formation of individual ssb or dsb and measurements of this signal at CE's can be only used to detect deeper DNA degradation [involving major changes of the DNA molecular mass, disruption of its double-helical structure and/or release of the DNA monomeric components (Brett *et al.*, 1994; Jelen *et al.*, 1997a; Labuda *et al.*, 1999)]. Another, a redox indicator-based technique for the detection of DNA damage at CE's, was developed by Labuda and coworkers (Figure 3) (Buckova *et al.*, 2002; Korbut *et al.*, 2001, 2003; Labuda *et al.*, 1999, 2000, 2002, 2003). Binding of a metallointercalator $[Co(phen)_3]^{3+}$ to dsDNA at a CE surface results in enhancement of its voltammetric signals (relatively to the same signal

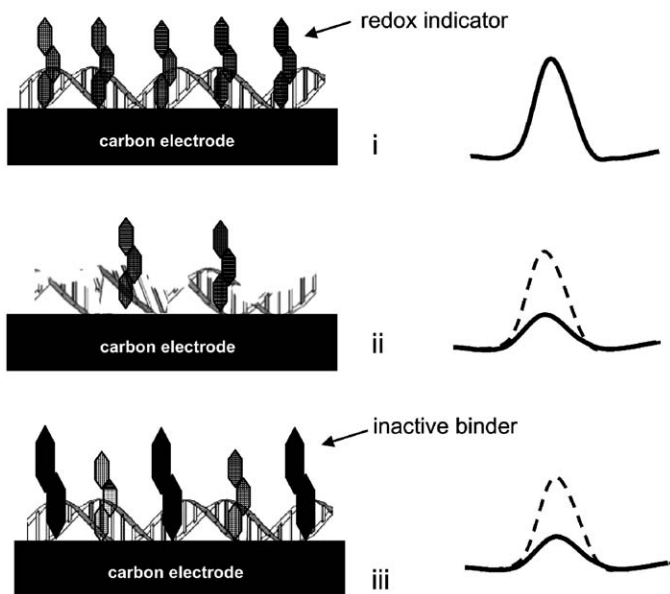


Fig. 3. Scheme of redox indicator-based sensor for DNA damage developed by Labuda *et al.* (Buckova *et al.*, 2002; Korbut *et al.*, 2001; Labuda *et al.*, 2002). (i) A metallointercalator ($[\text{Co}(\text{phen})_3]^{3+}$) binds to dsDNA immobilized at a carbon electrode surface, yielding a specific redox signal. (ii) Due to incubation with DNA damaging species, the immobilized DNA is degraded and its double-helical structure is disrupted. This results in lowered affinity of the redox indicator to the DNA layer and decrease of its signal. (iii) An analogous technique can be used also in a competitive mode to detect DNA interactions with other substances, including electroinactive ones (Labuda *et al.*, 2000).

measured at a bare electrode). Affinity of the redox indicator to degraded DNA (having lost its double-helical structure) is much lower than to the intact dsDNA, and diminution of its voltammetric peak represents the response to the DNA damage. This technique was utilized, for instance, in studies of DNA damage by chemical nucleases such as copper, 1,10-phenanthroline complex (Labuda *et al.*, 1999) or of antioxidative properties of various natural substances (Buckova *et al.*, 2002; Ferancova *et al.*, 2004; Labuda *et al.*, 2002, 2003) (see Section 7.2). To investigate temperature effects on the surface-confined DNA damage, electrically heated CPE were used in connection with the indicator-based system (Korbut *et al.*, 2001, 2003).

3.3. Detection of damage to DNA bases

In the DNA base residues, there is a number of chemically reactive moieties (see Figure 1 for examples) (Friedberg, 2000, 2003; Scharer, 2003) whose modification may alter the DNA electrochemical properties (Figure 4). Disruption of the electroactive sites in some bases (such as guanine) may lead to a loss of their intrinsic electroactivity (Jelen *et al.*, 1997b; Lucarelli *et al.*, 2002a, b, 2003;

Marin *et al.*, 1997, 1998; Perez *et al.*, 1999; Wang *et al.*, 1996a, 1997c). Other lesions (e.g., 8-OG Brett *et al.*, 2000; Langmaier *et al.*, 2003; Oliveira-Brett *et al.*, 2002, (Figure 4A) or some bulky adducts involving introduced electroactive moieties Fojta *et al.*, 2002a, 2004a; Jelen *et al.*, 1991; Lukasova *et al.*, 1982; Marin *et al.*, 1998; Palecek, 1992b; Palecek and Hung, 1983; Perez *et al.*, 1999; Teijeiro *et al.*, 1995) yield new, adduct-specific electrochemical signals. In addition, the formation of some lesions may induce changes in the dsDNA (local distortions, “unraveling”) connected with exposure of some adjacent base residues to the environment and facilitating their interactions with electrodes (Fojta *et al.*, 2000a; Gherghi *et al.*, 2003b; Mbindyo *et al.*, 2000; Mugweru and Rusling, 2002; Vorlickova and Palecek, 1974; Wang and Rusling, 2003; Zhou *et al.*, 2003) (Figure 4A).

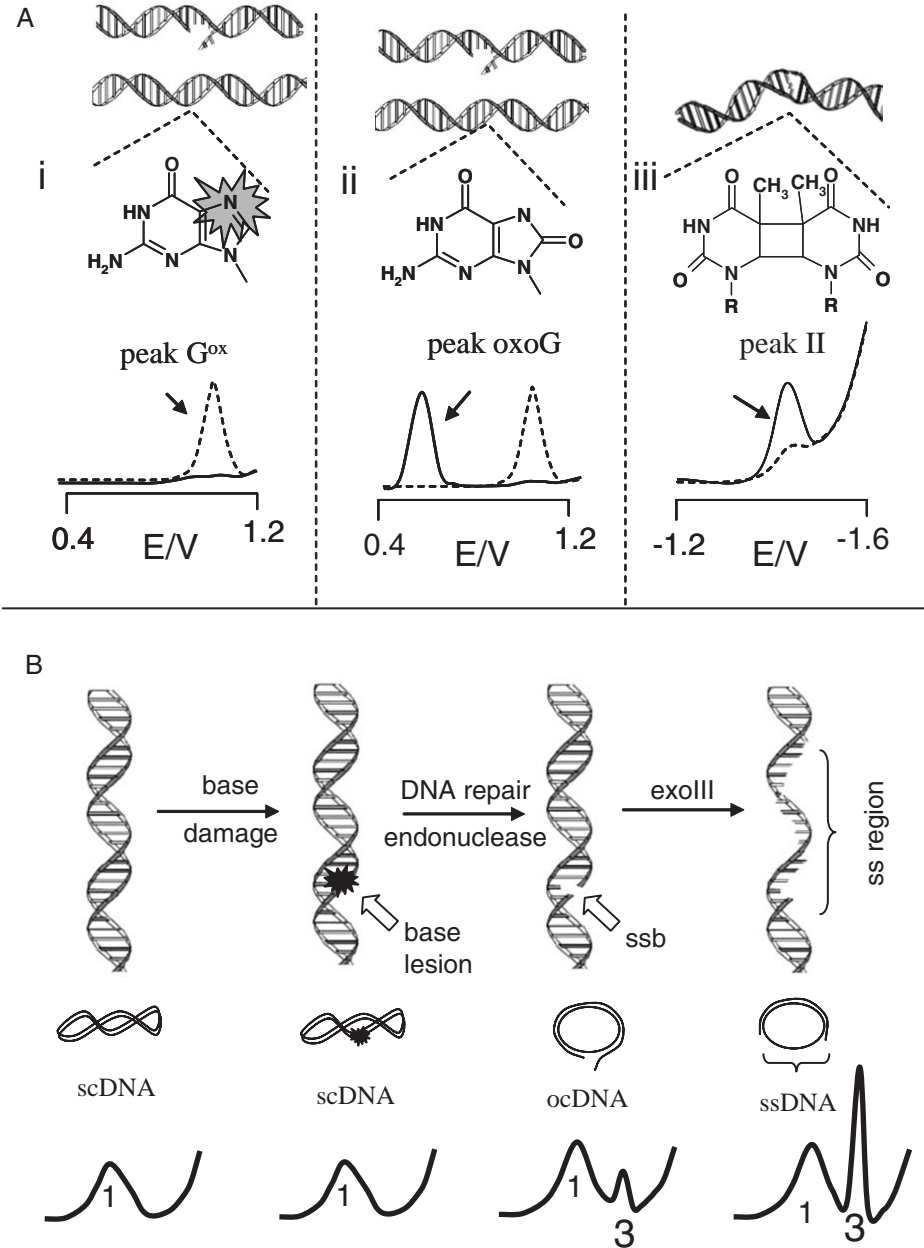
3.3.1. Guanine redox signals

Techniques based on measurements of intrinsic signals due to guanine belong to the most frequently applied techniques in DNA analysis. Guanine yields well developed redox signals at carbon as well as mercury electrodes (reviewed in Fojta, 2002, 2004; Palecek, 1996; Palecek and Fojta, 2005; Palecek *et al.*, 2002; for more details see Chapter 3). Above and beyond its favorable electrochemical properties, guanine is the most frequent target for a broad range of genotoxic agents among the DNA bases (Blackburn and Gait, 1990; Friedberg, 2000, 2003; Scharer, 2003) making it in general the most important DNA component to be analyzed in damaged DNA. Due to chemically or photochemically induced changes in the guanine moiety, its electrochemical features may be altered and signals corresponding to the parent base lost (Jelen *et al.*, 1997b; Lucarelli *et al.*, 2002a, b, 2003; Marin *et al.*, 1997, 1998; Perez *et al.*, 1999; Wang *et al.*, 1996a, 1997c). Since natural DNA's contain many guanine residues, partial decrease of the guanine peaks is usually observed, depending on the extent of the DNA damage. Decrease of the guanine redox peaks of DNA may be caused also by release of the base from the polynucleotide chains, an event often following modifications within the guanine imidazole ring.

Alkylation at the N7 position within the guanine residue results in a decrease of DNA peak G measured by cyclic or square-wave voltammetry at the HMDE. Using this signal, DNA modification by dimethyl sulfate (DMS) (facilitating also release of the modified base) was studied both in solution or using DNA-modified HMDE as an electrochemical biosensor (Jelen *et al.*, 1997b). DNA modification by MC (Marin *et al.*, 1998; Perez *et al.*, 1999; Teijeiro *et al.*, 1995) or thiotepa (Marin *et al.*, 1997), anticancer drugs known to attack primarily guanine, was monitored using the same signal. Intensity of peak G^{ox} yielded by DNA at CE's responded to the guanine damage in a similar way. DNA-modified GCE, CPE, pyrolytic graphite or screen-printed electrodes (SPE), in connection with voltammetric or chronopotentiometric detection, were applied as electrochemical biosensors for a variety of genotoxic agents including antitumor platinum complexes (Brabec, 2000), hydrazine derivatives (Wang *et al.*, 1996a), polychlorinated biphenyls, aflatoxins, anthracenes, acridines, phenol

compounds (Chiti *et al.*, 2001; Labuda *et al.*, 2000; Laschi *et al.*, 2003; Lucarelli *et al.*, 2002a, b, 2003; Mascini, 2001; Mascini *et al.*, 2001), UV light (Wang *et al.*, 1997c), arsenic oxide (Ozsoz *et al.*, 2003), and so on.

Although these types of DNA sensors are simple, inexpensive, do not require ME's and can work with poorly defined, commercially available DNA's, they



inherently suffer from a relatively low sensitivity. The reason lies in the principle of detection: when a decrease of initially large signal should be evaluated, change of the peak height has to (at least) exceed standard deviation of the measurement. Depending on the electrode material, surface pretreatment and DNA immobilization procedure, a realistic value of the experimental error of these techniques ranges between 5 and 10%. This implies that a relatively large portion of the guanine residues (one among 10–20 intact guanines in the analyzed DNA or in the sensor DNA recognition layer) has to be damaged to gain a reliable response. Another disadvantage of this “signal-off” approach is that the peak diminution may be caused by non-specific destruction of the DNA recognition layer (e.g., in the presence of surfactants) which may result in false-positives hardly recognizable from specific responses of the sensor.

3.3.2. Specific signals of modified DNA bases and base adducts

Better sensitivity (and also specificity) of DNA damage detection can be obtained when an analyzed DNA lesion yields a new signal, not produced by the undamaged DNA. 8-OG, one of the most abundant products of DNA oxidative damage, is electrochemically oxidized at CE's and some other solid electrodes (gold, ITO, and platinum), yielding a signal at significantly less positive potential than the parent guanine base (Brett *et al.*, 2000; Holmberg *et al.*, 2003; Langmaier *et al.*, 2003; Oliveira-Brett *et al.*, 2002; Rebelo *et al.*, 2004; Ropp and Thorp, 1999). Both bases can thus be easily distinguished and determined in a mixture. A signal attributed to 8-OG appeared upon oxidative damage to DNA (deposited at the GCE) mediated by adriamycin (Brett *et al.*, 2000; Oliveira-Brett *et al.*, 2002) or by a copper complex of a flavonoid quercetin (Oliveira-Brett and Diculescu, 2004a, b). Redox mediator-based techniques of differential detection of guanine and 8-OG at ITO electrodes have been proposed (Holmberg *et al.*,

Fig. 4. Principles of electrochemical detection of covalent damage to DNA base residues. (A) Changes in the DNA electroactivity due to modification of the nucleobases. (i) Intrinsic electroactivity of the guanine residues at carbon, mercury or solid amalgam electrodes may be lost due to disruption of electroactive sites in the guanine moiety (e.g. Wang *et al.*, 1996a, 1997c). (ii) Some products of base damage such as 8-OG (Brett *et al.*, 2000) yield specific electrochemical responses differing from the parent base signals. (iii) Base lesions may cause distortions of the DNA double helix. These damages (in spite of electroactivity of the modified base or resulting adduct) may be detected via increased accessibility of adjacent electroactive base moieties. For example, UV light- (Vorlickova and Palecek, 1974) or cisplatin- induced DNA (Brabec *et al.*, 1990) damage can be detected by measurements of DNA DPP peak II. (B) Utilization of DNA repair enzymes in electrochemical detection of the base damage. Some base lesions are recognized by specific endonucleases introducing ssb at the damaged sites. Formation of small number of base lesions in scDNA molecule (without interruption of the sugar-phosphate backbone) does not significantly change its voltammetric behavior at any electrodes. On the other hand, the ssb can be detected with a high sensitivity at ME or AgSAE using the principle shown in Figure 2. The signal (peak 3) may be further amplified using *E. coli* exonuclease III (exoIII) generating ss regions in oc or linDNA (but not in intact scDNA) (Cahova-Kucharikova *et al.*, 2005).

2003; Ropp and Thorp, 1999). $[\text{Os}(\text{bipy})_3]^{3+}$ complex is capable of electrocatalytic oxidation of 8-OG. On the other hand, the redox potential of the osmium mediator is insufficient to oxidize guanine which can be oxidized by, for example, ruthenium chelates (Johnston *et al.*, 1995; Ontko *et al.*, 1999; Popovich and Thorp, 2002; Thorp, 1998) (see also Chapters 3 and 13). Similarly, 1,*N*⁶-etheno-adenine [a reaction product of adenine with a chemical DNA probe chloroacetaldehyde (Palecek, 1991), but also one of lesions occurring in cells under oxidative stress (Scharer, 2003)] yielded a cathodic peak at HMDE at a potential remarkably less negative, compared to the signal of unmodified polyadenylic acid (Palecek, 1986).

In addition to simple chemical alterations in the base residues, the modified DNA may acquire specific electrochemical features from substances forming bulky DNA adducts. For example, a clinically used antitumor agent MC involving an electroactive quinine moiety covalently binds primarily to guanine residues, forming interstrand and/or intrastrand cross-links (Marin *et al.*, 1998; Perez *et al.*, 1999; Teijeiro *et al.*, 1995 and references therein). The MC-DNA adducts retain the drug electroactivity. Interactions of acid- or reductively activated MC with DNA were investigated by means of CV at HMDE (Marin *et al.*, 1998; Perez *et al.*, 1999; Teijeiro *et al.*, 1995), including studies of electrochemical MC activation (Perez *et al.*, 1999; Teijeiro *et al.*, 1995). Another class of substances forming electrochemically active covalent DNA adducts involves complexes of osmium tetroxide with nitrogenous ligands (Fojta *et al.*, 1998a, 2002a, 2003, 2004a; Havran *et al.*, 2004b; Jelen *et al.*, 1991; Kizek *et al.*, 2002; Kostecka *et al.*, 2004; Lukasova *et al.*, 1982, 1984; Palecek, 1992b; Palecek and Hung, 1983). These substances, attacking primarily thymine residues (Fojta *et al.*, 2002a; Jelen *et al.*, 1991; Palecek, 1992b), belong neither to natural genotoxic agents nor to cytostatics. Nevertheless, their interactions with DNA and physico-chemical properties of the adducts have been studied in detail due to their wide practical usability in DNA probing (Buzek *et al.*, 1999; Fojta *et al.*, 2003, 2004a; Lukasova *et al.*, 1982; Palecek, 1992b; Palecek *et al.*, 1989) (see Chapter 3).

3.3.3. DNA conformation changes due to base modifications

Damage to the DNA base residues may cause local perturbations in the dsDNA structure. These defects may involve untwisting or bending of the DNA double helix as well as rupture of the Watson–Crick pairing of the stricken and/or adjacent bases, and so forth (Blackburn and Gait, 1990; Friedberg, 2000, 2003; Scharer, 2003). These events may influence accessibility of neighboring nucleobases and, consequently, behavior of the damaged DNA at electrodes. For example, dsDNA exposed to UV light (bringing about formation of a number of base photoproducts including pyrimidine dimers, Blackburn and Gait, 1990; Bykov *et al.*, 1995; Cooke *et al.*, 2003; Friedberg, 2000, 2003; Podmore *et al.*, 1996; Scharer, 2003) exhibits increased reducibility at the DME (Figure 4A) (Vorlickova and Palecek, 1974), (see Section 2.1). Intensity of amperometric signals arising from DNA interaction with polypyrrole-modified electrodes in a

flow-through device was also remarkably affected upon exposure of the DNA to UV light, presumably due to conformational changes (Wang *et al.*, 2001). Unraveling of dsDNA after its modification with carcinogenic chemicals such as styrene oxide facilitates electrocatalytic oxidation of adjacent guanines by ruthenium mediators (Mbindyo *et al.*, 2000; Mugweru and Rusling, 2001, 2002; Wang and Rusling, 2003; Yang *et al.*, 2002, Zhou *et al.*, 2003). This phenomenon has been analytically exploited in a device proposed for toxicity screening (see Section 7.2 and Chapter 13).

3.3.4. Use of DNA repair enzymes in electrochemical detection of damage to DNA bases

The current DNA damage assays utilize endonucleases involved in DNA repair for probing certain kinds of DNA base lesions. These enzymes specifically recognize damaged bases and cleave the DNA sugar phosphate at adjacent position. The resulting sb can be detected by, for instance, electrophoretic techniques (Collins *et al.*, 2003; Gedik *et al.*, 2002) (see Section 1.2). Analogous principle (Figure 4B) have been used also in connection with the highly sensitive electrochemical detection of the sb at ME or AgSAE (see Section 3.2.1). For example, pyrimidine dimers in UV-irradiated DNA can be converted into the sb by T4 endonuclease V (Schrock and Lloyd, 1993) and subsequently determined by ACV at the HMDE or m-AgSAE (Cahova-Kucharikova *et al.*, 2005). Similarly, apurinic sites spontaneously formed in DMS-treated DNA were detected in the same way after the DNA enzymatic digestion by *E. coli* exonuclease III (exoIII) (Cahova-Kucharikova *et al.*, 2005; Palecek and Fojta, 2001). This enzyme endonucleolytically attacks the DNA next to the abasic lesions, followed by exonucleolytic degradation of one strand of the DNA from the sb (Rogers and Weiss, 1980) (Figure 4B). Formation of the ssDNA region within the dsDNA results in further enhancement of the measured signal. DNA digestion with the exoIII can be used also in combination with other lesion-specific endonucleases (Cahova-Kucharikova *et al.*, 2005). These approaches have offered electrochemical detection of small extents of base modifications, not detectable without the enzymatic treatment. In addition, the novel technique was successfully applied for probing base lesions induced by DMS or UV light in living bacterial cells (Cahova-Kucharikova *et al.*, 2005).

4. ELECTROCHEMICALLY CONTROLLED DNA DAMAGE

Electrodes and electrochemical processes can be used not only to detect, but also to induce and control DNA damage. A number of DNA damaging species can be generated electrochemically. For example, low-valency states of some transition metal ions (such as iron, copper or manganese) or their complexes undergo Fenton type reactions yielding hydroxyl radicals that are vigorous DNA-damaging agents (Fojta *et al.*, 2000b, 2002b and references therein). The reduced form of the metal can be restored electrochemically. Electrochemical

reduction of Mn^{3+} or Fe^{3+} porphine complexes in the presence of oxygen resulted in relaxation of scDNA due to the formation of ssb (Rodriguez *et al.*, 1990). Both ssb and piperidine-labile sites (due one-electron oxidation of guanine) were detected upon electrolysis of DNA solution in the presence of *trans*- $[\text{Re}(\text{O})_2(4\text{-OMe-py})_4]^+$ (Johnston *et al.*, 1994). Cleavage of DNA in solution due to electrolysis in the presence of copper–bipyridine complex was detected by HPLC (Yang *et al.*, 2004). Reactive species forming covalent adduct with guanosine were generated through electrolysis of an imidazoacridinone antitumor drug C-1311 at a platinum electrode, mimicking processes of metabolic activation of the drug (Mazerska *et al.*, 2003). Similarly tirapazamine, a cytotoxin of hypoxic cells, underwent one-electron electrochemical reduction, yielding a radical anion whose lifetime was remarkably decreased in the presence of DNA, suggesting a direct interaction between the two species (Tocher, 2001).

4.1. *In situ* electrochemical analysis of DNA damage at electrodes

Immobilization of DNA at electrodes offer a unique possibility of electrochemical control processes leading to damage to the anchored DNA and subsequent *in situ* electrochemical detection. Distinctly potential-dependent cleavage of scDNA at the surface of HMDE in the presence of iron or copper complexes and hydrogen peroxide (or oxygen which was electrochemically reduced to the H_2O_2) was detected by ACV (using the principle described in Section 3.2.1) (Fojta *et al.*, 2000b, 2002b). In the presence of iron/EDTA complex, the cleavage reaction took place at potentials sufficiently negative for reduction of Fe^{3+} ion within the chelate to Fe^{2+} yielding the Fenton reaction (Fojta *et al.*, 2000b). In the case of copper, DNA damage was observed only in a narrow potential region around the copper reduction peak. Formation of ROS probably involved stabilization of Cu^+ due to coordination interactions with DNA bases and its redox cycling $\text{Cu}^{2+}/\text{Cu}^+$ (Fojta *et al.*, 2002b). In the presence of 1,10-phenanthroline, a Cu^+ -stabilizing ligand, the DNA damage was potentiated and maximum of the effect was shifted to more negative potentials. Chromate (but not chromic salts) caused strong oxygen-independent DNA cleavage at the HMDE upon its electrochemical reduction (T. Mozga and M. Fojta, unpublished), suggesting roles of highly reactive Cr(V) or Cr(IV) intermediates (Stearns *et al.*, 1995; Stearns and Wetterhahn, 1997). A considerable extent of cleavage of the HMDE-confined scDNA was observed after applying potentials ≤ -0.1 V in aerobic media even in absence of the metal complexes. This effect was attributed to radical intermediates of electrochemical reduction of oxygen (Fojta *et al.*, 2000b, 2002b; Rodriguez *et al.*, 1990). Electrochemically induced DNA damage in the presence of an antineoplastic drug adriamycin was studied using a thick DNA layer-modified GCE. Oxidative degradation of the DNA (including formation of 8-OG) was observed upon applying negative electrode potentials bringing about one-electron reduction of the intercalated drug (Oliveira-Brett *et al.*, 2002). Electroreduced thiophene-S-oxide also induced *in situ* DNA damage in an analogous system (Brett *et al.*, 2003). Electrochemical activation of

another anticancer drug, MC, and its interactions with DNA were studied by CV at the HMDE (Perez *et al.*, 1999; Teijeiro *et al.*, 1995).

5. NON-COVALENT DNA INTERACTIONS WITH GENOTOXIC SUBSTANCES

A broad range of biologically, toxicologically and/or pharmaceutically important substances bind DNA non-covalently (reversibly; Figure 5) (Blackburn and Gait, 1990). In general, cationic species can interact with DNA at the outer surface of the double helix, being attracted by the negatively charged phosphate groups. Planar condensed aromatic ring systems intercalate into the double helix between adjacent base pairs. This interaction type involves primarily stacking (π - π) interactions. Another group of molecules exhibit so-called groove binding that involves direct contacts of the binders with inner surfaces of major or minor grooves of DNA double helix, including edges of base pairs. Depending on nature of the interacting species, hydrogen bonding, electrostatic and/or van der Waals contacts may take part in this mode of binding. Many carcinogens, cytostatics, environmental pollutants, and so on, interact with DNA reversibly prior to inducing covalent DNA damage. Intercalative or groove DNA binding of these substances leads to their accumulation at the DNA molecules, thus facilitating subsequent covalent attacks to the DNA via the binder reactive groups [such as epoxide (Mbindyo *et al.*, 2000; Mugweru and Rusling, 2001; Zhou *et al.*, 2003) or aziridine (Marin *et al.*, 1998; Perez *et al.*, 1999; Teijeiro *et al.*, 1995)]. Other substances (e.g., copper chelates) reversibly bound to DNA may mediate formation of other DNA damaging species, such as ROS, in a close vicinity of the genetic material (Fojta *et al.*, 2002b; Oliveira-Brett *et al.*, 2002; Sigman, 1990 and references therein).

5.1. Studies of DNA–binder interactions in solution

Interactions of DNA with small molecules may affect electrochemical signals of the binders (Figure 5B) as well as of the DNA (Figure 5C). Upon association with the DNA macromolecules, apparent diffusion coefficients of the binders remarkably decrease which is reflected in lowering of their diffusion-controlled signals (Carter and Bard, 1987; Carter *et al.*, 1989; Pandey and Weetall, 1994; Rodriguez and Bard, 1990; Sufen *et al.*, 2002; Wang *et al.*, 2003c, d). Electrochemical studies have been employed to determine association/dissociation constants of the binder–DNA complexes. In addition to changes in the signal intensity, peak potentials of the DNA binders may also be significantly shifted due to the complex formation (Carter *et al.*, 1989; Rodriguez and Bard, 1990; Wang *et al.*, 1998b). Complexes and associates of toxic heavy metals [lead, cadmium (Sequaris and Esteban, 1990; Sequaris and Swiatek, 1991), copper (Correia dos Santos *et al.*, 1996, 1998; Farias *et al.*, 2001; Jelen *et al.*, 2004), mercury (Johnston *et al.*, 1999), nickel (Alvarez *et al.*, 1998)] and/or their

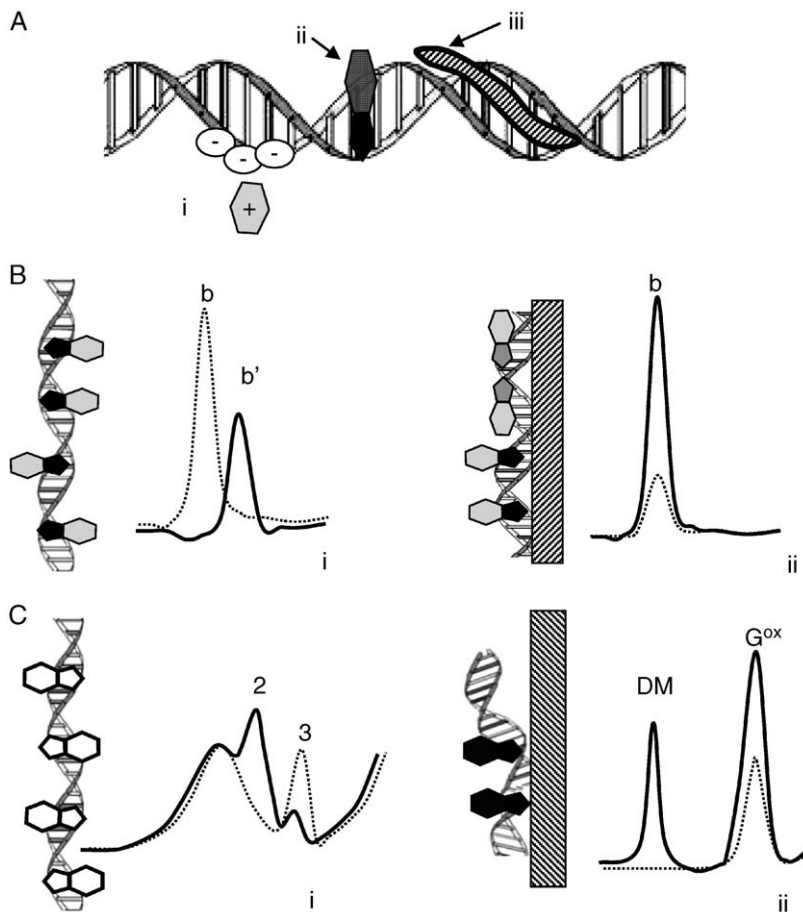


Fig. 5. Electrochemical detection of non-covalent DNA interactions with small molecules. (A) Scheme of basic modes of interactions of small molecules with dsDNA: electrostatic binding to outer surface of the double helix (i); intercalation (ii); and groove binding (iii). (B) Possible effects of the interactions on signals of an electroactive binder (b). (i) Association of the binder with large DNA molecules may result in decrease of its signal due to reduced mass transport. In addition, diminution or potential shift of the signal may be observed when an electroactive moiety of the binder is hidden upon the complex formation (e.g., in intercalation complexes; b'). (ii) On the other hand, accumulation of electroactive binders in DNA recognition layer at the electrode may result in enhancement of the binder signals. (C) Due to the complex formation, changes in the intrinsic DNA electrochemical signals may take place. (i) Adsorption/desorption behavior of dsDNA at mercury electrodes is remarkably changed in the presence of intercalators. These changes involve formation of ACV peak 2 and decrease of the peak 3 height (Fojta *et al.*, 2000a). (ii) Untwisting and bending of dsDNA adsorbed at a carbon electrode surface due to binding of an intercalator (daunomycin Wang *et al.*, 1998b) results in enhancement of the peak G^{ox} intensity (together with appearance of the DM signal).

complexes [hexaamminecobalt (Fojta *et al.*, 1996), dimeric rhodium complexes (Gil *et al.*, 2002)] with DNA, nucleobases and nucleosides have been studied electrochemically at mercury as well as solid electrodes. Ruthenium, iron or osmium organic chelates (with nitrogenous bidentate ligands such as 2,2'-bipyridine or 1,10-phenanthroline) were used in fundamental electrochemical studies (Carter and Bard, 1987; Carter *et al.*, 1989; Rodriguez and Bard, 1990; Xu and Bard, 1995) of DNA interactions with electroactive small molecules. The metal chelates, yielding well-defined electrochemical signals due to the redox active central metal ions, may undergo either electrostatic, minor groove or intercalative binding to dsDNA. The interaction mode depends on the valence (charge) of the metal and/or on the heterocyclic ligand type. Different binding modes of these chelates were reflected in the direction of the peak potential shifts. While positive shifts were observed with intercalative chelates, signals of complexes exhibiting primarily electrostatic binding were shifted to more negative potentials (Carter and Bard, 1987; Carter *et al.*, 1989; Rodriguez and Bard, 1990; Xu and Bard, 1995). Studies of interactions of zinc, copper, lead or nickel metalloporphyrins (MP) using CV at the HMDE (Qu and Li, 1997) revealed that mode of interaction of these substances with DNA were influenced by the presence of axial ligands. With MP's lacking these ligands, a strong decrease of their voltammetric signals was observed in the presence of dsDNA, suggesting that the electroactive MP moieties were deeply intercalated within the DNA double helix. On the other hand, MP's with the axial ligands exhibited only weak signal decrease upon DNA binding. Intercalative transition metal complexes have been utilized in studies of DNA-mediated charge transfer reactions (Boon and Barton, 2002, 2003; Boon *et al.*, 2000, 2002, 2003; Kelley *et al.*, 1997, 1999a, b; Odom and Barton, 2001; Rajski *et al.*, 2000) (see Chapter 3).

5.2. DNA-modified electrodes as sensors for non-covalently binding substances

Electrodes modified with dsDNA have been widely used in studies of non-covalent DNA interactions and/or as electrochemical biosensors for the reversibly binding substances. Selective accumulation of intercalators or cationic groove binders in the dsDNA recognition layer results in enhancement of the binder electrochemical signals, compared to signals obtained at bare (or ssDNA-modified) electrodes (Figure 5B). Redox indicator-based sensors for DNA hybridization (Cai *et al.*, 1997; Hashimoto *et al.*, 1994; Miyahara *et al.*, 2002; Wang *et al.*, 1996b, 1997b; reviewed in Drummond *et al.*, 2003; Gooding, 2002; Mascini *et al.*, 2001; Palecek and Fojta, 2001, 2005; Palecek *et al.*, 1998, 2002; Palecek and Jelen, 2002; Popovich and Thorp, 2002; Tarlov and Steel, 2003; Wang, 2000, 2002, see also Chapters 3–11) or damage (Korbut *et al.*, 2003; Labuda *et al.*, 1999, 2000, 2002, 2003) (Section 3.2.2) are based on the same principle. DNA-modified CPE was proposed for detection of electrochemically active aromatic amines which are important environmental pollutants (Chiti *et al.*, 2001; Mascini, 2001; Mascini *et al.*, 2001; Wang *et al.*,

1996c). Due to accumulation of these species in the DNA recognition layer via intercalation, remarkable enhancement of their CPSA signals was observed. Some of the aromatic amine derivatives affected also the DNA peak G^{ox} intensity in a concentration-dependent manner (Chiti *et al.*, 2001). Similar studies have been focused on studies of interactions of DNA with a dye ethidium bromide (Gherghi *et al.*, 2004) and with an anticancer drug daunomycin (Wang *et al.*, 1998b). Electrochemical oxidation of the daunomycin anthraquinone group intercalated into dsDNA at the CPE surface was less feasible than in the free drug, resulting in positive potential shift of the peak potential. Submicromolar concentrations of the drug-induced conformational changes in the surface-confined DNA resulting in enhancement of the DNA peak G^{ox} (Wang *et al.*, 1998b). A similar compound, adriamycin (doxorubicin) mediated electrochemically induced oxidative DNA damage in thick dsDNA layer at the GCE (Oliveira-Brett *et al.*, 2002; Piedade *et al.*, 2002) (see Section 4). Echinomycin, a natural antibiotics binding to DNA as a bisintercalator, exhibited well-defined reversible electrochemistry at HMDE (Jelen *et al.*, 2002) or MFE (Hason *et al.*, 2002) in the presence of ds but not ssDNA. A competitive variant of the redox indicator-based technique proposed by Labuda and coworkers (see Section 3.2.2) was used for the detection of non-covalent DNA binders (Labuda *et al.*, 2000; Vanickova *et al.*, 2000) (Figure 3). Signal of the $[Co(phen)_3]^{3+}$ indicator measured at DNA-modified SPE or CPE decreased with increasing concentrations of quinazoline (Labuda *et al.*, 2000), acridine or catechin (Vanickova *et al.*, 2000) competing with the cobalt complex for binding sites in the surface-confined DNA. Application of this technique is not restricted to electroactive DNA binders but can be used also to monitor DNA interactions with inactive species.

5.3. Changes of DNA interfacial behavior upon interactions with non-covalent binders

Besides the observation by Wang *et al.* (1998b) showing that daunomycin induces alterations in the structure of dsDNA adsorbed at CPE (see above), changes of the dsDNA conformation in the presence of various reversibly interacting substances (such as chloroquine, $[Co(phen)_3]^{3+}$, doxorubicin, 9-amino acridine, acridine orange or ethidium) were studied by AdTS ACV at the HMDE (Fojta *et al.*, 2000a; Gherghi *et al.*, 2003a,b). Due to intercalation, untwisting of the DNA double helix takes place, resulting in increased accessibility of the base pairs to the environment. These phenomena remarkably influence adsorption/desorption behavior of the dsDNA at the mercury surface, involving changes of the intensity of the tensammetric DNA peak 2 (enhancement) and peak 3 (diminution; see Figure 5C) (Fojta *et al.*, 2000a). It has been proposed that DNA adsorbed in the presence of the intercalators adopted a specific structure at the HMDE surface after the intercalator removal. This structure involves untwisted regions relatively firmly adsorbed at the surface (yielding the DNA peak 2) and scDNA loops protruding to the solution. Such

dsDNA structure was relatively resistant to the potential-induced surface denaturation (Section 3.2.1, Chapter 3) (causing reduced intensity of the peak 3, compared to the same dsDNA adsorbed in the absence of intercalators) unless sb were introduced into it (Fojta *et al.*, 2000a).

6. DETECTION OF MUTATIONS IN DNA SEQUENCES

Persisting (unrepaired) DNA damage in cells and/or DNA replication errors may result in changes of the genetic information, including base substitutions, insertions/deletions of single nucleotides or of longer regions of the genome. Accumulation of the mutations may cause serious disorders such as cancer or other inherited diseases. For screening these mutations, different methods have been employed, including single-strand DNA conformational polymorphism (Fleckenstein *et al.*, 2002) and various techniques of DNA hybridization (in recent years connected mainly with DNA microarrays, Heller, 2002). The progress in application of electrochemical detection in the DNA hybridization assays has recently been reviewed in numerous papers (Drummond *et al.*, 2003; Gooding, 2002; Mascini *et al.*, 2001; Palecek and Fojta, 2001, 2005; Palecek *et al.*, 1998, 2002; Palecek and Jelen, 2002; Popovich and Thorp, 2002; Tarlov and Steel, 2003; Wang, 2000, 2002), including Chapters 3–11 of this book. Here, only several examples of techniques used for the detection of DNA mutations by means of electrochemical sensors are mentioned.

6.1. Utilization of reduced stability of mismatched DNA duplexes

One group of the approaches used for the detection of point mutations (single-base substitutions or insertion/deletions) is based on different stability of mismatched DNA duplex (formed e.g., between the wild-type probe captured at an electrode surface subjected to mutant target DNA) and that of the homoduplex (formed between perfectly complementary probe and target strands). This can be reached, for example, by performing the DNA hybridization at elevated temperatures (Caruana and Heller, 1999), decreased ionic strength (Park *et al.*, 2002), or via applying peptide nucleic acid probe instead of DNA (Caruana and Heller, 1999; Wang *et al.*, 1996b, 1997b).

6.2. Techniques based on specific structural features of the base mismatches

In another group of techniques, less stringent conditions are chosen to facilitate formation of mismatched DNA hybrids at the electrode surface, and specific structural, electrical and electrochemical features of these duplexes are used to probe the point mutations (Boon *et al.*, 2000; Johnston *et al.*, 1995; Kelley *et al.*, 1997, 1999a; Ropp and Thorp, 1999). For example, accessibilities of guanine (or 8-OH) residues for oxidation by a redox mediator depends on their location in

ssDNA, mismatched or perfectly matched duplex (Johnston *et al.*, 1995; Ropp and Thorp, 1999). Electrocatalytic oxidation of the guanine by $[\text{Ru}(\text{bipy})_3]^{3+}$ followed the trend $\text{G}(\text{ss}) > \text{GA} > \text{GG} > \text{GT} > \text{GC}$. An interesting technique based on the perturbations of electronic structure of the double-helical DNA containing the single base mismatches was developed by Barton and coworkers (Boon *et al.*, 2000, Drummond *et al.*, 2003; Kelley *et al.*, 1997, 1999a). The mismatches cause disruption of the π -stacks within the mismatched DNA double helix and diminution of the DNA-mediated charge transfer. Techniques based on this principle, involving ODN's immobilized at gold electrode surface and electroactive intercalators bound at the opposite end of the anchored DNA molecules have been proposed. A considerable current flow was observed through perfectly matched duplexes but not in the presence of single base mismatches (Kelley *et al.*, 1999a).

6.3. Primer extension-based techniques

Another approach to probing point mutations (or single nucleotide polymorphisms) was proposed by Willner and coworkers who used the principle of DNA primer-extension "microsequencing", based on incorporation of biotinylated nucleotide by DNA polymerase into a primer hybridized to a target DNA at the electrode surface (Patolsky *et al.*, 2001). The labeled base was inserted only when a complementary nucleotide was present in the target strand at position next to the primer. The labeled nucleotide was subsequently detected via impedance or microgravimetric measurement of an insoluble product generated at the surface in a reaction catalyzed by alkaline phosphatase coupled to avidin bound to the biotin label.

6.4. Trinucleotide repeat expansions

Expansions of trinucleotide repeats represent a specific class of genomic mutations. These events are related to development of serious inherited diseases such as fragile X syndrome, myotonic dystrophy or Friedreich ataxia (Campuzano *et al.*, 1996; Paulson and Fischbeck, 1996). Electrochemical determination of the length of the $(\text{CGG})_n$ or $(\text{CTG})_n$ triplet repeats using the mediator-based guanine electrocatalytic oxidation technique (see Section 2.1, Chapter 13) was recently reported (Yang and Thorp, 2001). A novel double-surface electrochemical technique for the detection of the $(\text{GAA})_n$ triplet expansion was based on multiple hybridization of a labeled reporter probe (RP; see also Chapter 3) with the trinucleotide repeat captured at magnetic beads (Fojta *et al.*, 2004a, b). Either a biotinylated $(\text{TTC})_{12}$ RP detected via an electrochemical enzyme-linked assay, or a $(\text{GAA})_7\text{T}_n$ RP in which the oligoT tail was labeled with electrochemically active osmium tetroxide, 2,2'-bipyridine [yielding voltammetric signals at carbon (Fojta *et al.*, 2002a, 2003, 2004), mercury (Fojta *et al.*, 2004a; Havran *et al.*, 2004b;

Kizek *et al.*, 2002) or amalgam electrodes (Yosypchuk *et al.*, 2005)], were used in these assays.

7. APPLICATIONS

Electrochemical methods belong to the most widely used techniques of analytical chemistry applied to a broad-spectrum analytes, including biologically active compounds, drugs, carcinogens, pesticides, heavy metals, and so on, in different matrices such as water, soil, food or biological specimens (reviewed in Brainina *et al.*, 2000; Kalvoda, 2000; Locatelli, 1997). Similarly as with other detection principles (e.g., optical), the electrochemical analyses are usually based on measurements of specific physico-chemical properties of the substances of interest and primarily do not provide information about biological consequences of interactions the given substance with components of living matter [although there have been attempts to infer carcinogenic potentials of various species from their electrochemical properties (Cojocel *et al.*, 2003; Lin and Hollenberg, 2001; Novotny *et al.*, 1999; Romanova *et al.*, 2001)]. On the contrary, responses of the DNA sensors depend on specific interactions of different species with the genetic material. These interactions are usually closely related to toxicological, carcinogenic, and/or pharmacological activity of the assayed substances. The sensors for DNA damage may provide responses which are inherently non-specific concerning chemical nature of the analyte. On the other hand, these devices offer information about its effects on the genetic material. Such information may be valuable, for example, as prompt alert to dangerous harmful substances, or as important clues in targeted development of novel chemotherapeutics.

7.1. DNA–drug interactions

Many drugs and anticancer agents in particular, act through specific interactions with DNA. To study these interactions, which may involve reversible non-covalent binding and/or covalent modification of the DNA molecules, have been studied by different methods of electroanalysis, including electrochemical DNA biosensors (reviewed in Erdem and Ozsoz, 2002; Fojta, 2002). The DNA–drug interactions detected by these devices are usually the same as those related to pharmacological activities of the therapeutics. Nevertheless, the DNA component of the sensor may serve also as a non-specific anionic binding substrate for positively charged molecules of the analyte, regardless of the biological (pharmacological) relevance of the observed drug–DNA interaction (Nikolelis *et al.*, 2002; Vanickova *et al.*, 2000; Vanickova *et al.*, 2003). Some of these DNA–drug binding investigations have been reviewed in Sections 3 and 5 [including those dealing with daunomycin (Chu *et al.*, 1998; Wang *et al.*, 1998b), doxorubicin (Oliveira-Brett *et al.*, 2002; Piedade *et al.*, 2002; Yau *et al.*, 2003; Zhang and Li, 2000), echinomycin (Hason *et al.*, 2002; Jelen *et al.*, 2002),

cisplatin (Brabec, 2000), MC (Marin *et al.*, 1998; Perez *et al.*, 1999; Teijeiro *et al.*, 1995), or thiotepa (Marin *et al.*, 1997)]. Voltammetric techniques, usually in connection with CE's, were applied in studies of DNA interaction with other chemotherapeutics such as epirubicin (Erdem and Ozsoz, 2001a), mitoxantrone (Erdem and Ozsoz, 2001b; Shi *et al.*, 2003; Wang *et al.*, 2003b), actinomycin D (Gherghi *et al.*, 2003c; Wang *et al.*, 2003d) and lycorine (Karadeniz *et al.*, 2003), metronidazole (Brett *et al.*, 1997a) or benzimidazole (La-Scala *et al.*, 2002). Besides the most frequently analyzed antineoplastic agents, representatives of other classes of medicinal drugs have been also analyzed by the DNA sensors. CPE modified with DNA at its surface or in the bulk phase was applied to detect antidepressive drug phenothiazine or azepine derivatives used as local anesthetics (Vanickova *et al.*, 2000, 2003). ITO electrodes coated with DNA-modified gold nanoparticles selectively responded to mifepristone, a hormonal contraceptive agent (Xu *et al.*, 2001). Differential pulse voltammetry at HMDE was applied to monitor release of an antibacterial drug lumazine from inclusion cyclodextrin complexes in the presence of DNA to which the drug displays a high affinity (Ibrahim *et al.*, 2002). Binding of another antibacterial agent levofloxacin to dsDNA was investigated by CV at the GCE (Radi *et al.*, 2003). A redox indicator-based sensor for DNA–drug interactions, involving oriented immobilization of thiol-derivatized ds ODN's at a gold electrode surface has been proposed (Maeda *et al.*, 1992; Nakano *et al.*, 1998). The DNA layer strongly suppressed voltammetric signals of the ferro/ferricyanide redox pair due to repulsion between the negatively charged ODN's and the anionic depolarizer. Binding of a cationic drug such as quinacrine to the DNA decreased its negative charge density which facilitated the ferro/ferricyanide oxidation/reduction. Lipid bilayer membranes at the electrode surface with incorporated ssDNA were applied (Siontorou *et al.*, 1996) in analysis of a beta₁-blocker atenolol used in treatment of hypertension and myocardial infarctions.

7.2. Toxicity and antioxidant capacity testing

Electrochemical DNA sensors offer the possibility of rapid screening of toxicity or carcinogenic potential of a broad range of substances (such as novel products of chemical industry), and/or testing protective capacity of other species like antioxidants. DNA-modified CE's were proposed as simple electrochemical sensors for a variety of toxic substances, including polychlorinated biphenyls, aflatoxins, anthracene, and acridine derivatives, phenol compounds or surfactants (Chiti *et al.*, 2001; Laschi *et al.*, 2003; Lucarelli *et al.*, 2002a, b). Comparison of responses of these sensors with a currently used commercially available bioluminescence toxicity test Toxalert[®] 100 (Lucarelli *et al.*, 2002a, b) led to a conclusion that the faster and cheaper electrochemical approach may be used for preliminary screening. The redox indicator-based system responding to oxidative DNA degradation (Section 3.2.2; Figure 3) was applied to assess protective capacity of various natural antioxidants such as yeast polysaccharides (Buckova *et al.*, 2002), flavonoids (Korbut *et al.*, 2003; Labuda *et al.*, 2003)

or plant extracts (Ferancova *et al.*, 2004; Labuda *et al.*, 2002). A device for toxicity screening based on layer-by-layer assemblies of DNA and heme proteins on GCE surfaces modified with redox-active cationic polymer films was developed by Rusling and coworkers (Dennany *et al.*, 2003; Mbindyo *et al.*, 2000; Mugweru and Rusling, 2001, 2002; Mugweru *et al.*, 2004; Rusling, 2004; Rusling *et al.*, 2002; Wang and Rusling, 2003; Yang and Rusling, 2002; Yang *et al.*, 2002; Zhou *et al.*, 2003). Layers of enzymatically active hemoproteins mimicked metabolic carcinogen activation processes. For example, styrene was enzymatically converted into styrene oxide subsequently attacking guanine in the DNA layer. This DNA damage caused “unraveling” of the DNA double helix and facilitated electrocatalytic oxidation of other guanine residues which was mediated by an immobilized ruthenium complex (for more details, see Chapter 13 which is devoted specifically to sensors for genotoxicity and oxidized DNA).

7.3. Environmental analysis

Many genotoxic species occur in the environment as pollutants coming from industrial or agricultural activities of the mankind. These species can be monitored by electrochemical DNA sensors via their non-covalent interactions and/or covalent attacks of the DNA recognition element (usually resulting in damage to guanine residues or formation of sb). ME's modified with scDNA (Section 3.2.1) have been successfully applied for the detection of DNA cleaving agents in “real” samples of food, natural or waste waters (Fojta *et al.*, 1998b). A number of proposed DNA sensors based on CE's have been applied to detect different toxic and carcinogenic pollutants in natural waters, including aromatic amines (Chiti *et al.*, 2001; Mascini, 2001; Mascini *et al.*, 2001; Wang *et al.*, 1996c), hydrazine derivatives (Wang *et al.*, 1996a), polychlorinated biphenyls, aflatoxins, anthracene and acridine derivatives, phenol compounds or surfactants (Chiti *et al.*, 2001; Lucarelli *et al.*, 2002a, b). These types of DNA sensors yielded linear responses for strongly carcinogenic polycyclic aromatic hydrocarbons detected in bile of fish exposed to these substances (Lucarelli *et al.*, 2003). GCE-based DNA biosensors were utilized to detect *s*-triazine herbicides (Oliveira-Brett and da Silva, 2002) and a molluscicide niclosamide (Abreu *et al.*, 2002).

8. CONCLUSIONS

Electrochemical techniques offer different possibilities of monitoring DNA damage, its interactions with various genotoxic agents (including carcinogens, mutagens, drugs, etc.) as well as detection of mutations in DNA sequences (often arising from DNA damage in cells). A unique feature of the DNA sensors is that their responses arise from specific interactions of the substances of interest with the genetic material, forming recognition component of the sensor.

The same interactions are closely related to biological, toxicological or pharmacological activities of the analytes. Detection principles and individual types of biosensors reviewed in this chapter differ in their specificity, sensitivity and consequently, in applicability in practical analysis. All of them can be used in basic studies of DNA interactions with the damaging agents as well as in testing of toxicity or DNA protective effects of various substances. These applications usually do not require extremely high sensitivities of detection because the effects of interest can easily be followed at relatively high analyte concentrations in a dose-dependent manner. On the contrary, much higher sensitivities should be attained when a DNA sensor is applied in trace assays, for example, in environmental monitoring, detection of drugs or their metabolites in biological matrices, and so forth. In this type of assays, the “signal-off” approaches such as measurements of intrinsic redox guanine signals may be insufficiently sensitive (their sensitivity can hardly exceed detection of one lesion per several tens of intact guanine residues, see Section 3.3.1). Using sufficiently long exposure times, sensors working on this principle may yield appreciable responses to, for example, relatively massive environmental pollution. However, recognition of one lesion per 10–100 nucleotides is far below the requirements for techniques used to measure levels of DNA damage usually occurring in the cells (one lesion per 10^4 – 10^6 nucleotides). To attain such sensitivities of detection, application of the “signal-on” methods, including detection of the DNA sb with ME or AgSAE (Section 3.2.1) and measurements of specific signals of DNA adduct or complexes (basically with all electrode types) (Sections 3.3.2 and 3.3.3), seem to be more realistic. For example, voltammetric detection of DNA sb with the mercury-based electrodes offers recognition of one lesion per about 2×10^5 nucleotides corresponding to femtomole levels of the damaged entities (Cahova-Kucharikova *et al.*, 2005; Fojta and Palecek, 1997) which comply with the above-mentioned requirements. Such sensitivity is well comparable with other currently applied DNA damage assays [e.g., ELISA (Cooke *et al.*, 2003) or mass spectrometry (Podmore *et al.*, 1996)]. Recent progress in development of electrochemical DNA sensors suggest that further improvement of the existing techniques and devices may be attained via, for example, employment of DNA repair endonucleases (Section 3.3.4), application of microelectrodes, and/or arrangement of the electrochemical devices into array formats.

LIST OF ABBREVIATIONS

A	adenine
G	guanine
C	cytosine
T	thymine
8-OG	8-oxo guanine
NA	nucleic acid
ODN	oligodeoxyribonucleotide
ss	single-stranded
ds	double-stranded

sc	supercoiled
oc	open circular
ccc	covalently closed circular
lin	linear
sb	strand break
ssb	single-strand break
dsb	double-strand break
RP	reporter probe
ROS	reactive oxygen species
DMS	dimethyl sulfate
MC	mitomycin C
MP	metalloporphyrin
UV	ultraviolet
region U	region of potentials in which DNA adsorbed at the mercury electrode is slowly unwound (denatured)
AC	alternating current
ACV	alternating current voltammetry
CV	cyclic voltammetry
DPP	differential pulse polarography
CPSA	constant current chronopotentiometric stripping analysis
AdTS	adsorptive transfer stripping
ME	mercury electrode
DME	dropping mercury electrode
HMDE	hanging mercury drop electrode
MFE	mercury film electrode
MF/GCE	mercury film-coated glassy carbon electrode
MeSAE	solid amalgam electrode (where Me means metal forming the amalgam)
AgSAE	silver solid amalgam electrode
p-AgSAE	polished silver solid amalgam electrode
m-AgSAE	silver solid amalgam electrode modified with mercury meniscus
MF-AgSAE	silver solid amalgam electrode modified with mercury film
CE	carbon electrode
CPE	carbon paste electrode
GCE	glassy carbon electrode
SPE	screen-printed electrode
ITO	indium-tin oxide
HPLC	high-performance liquid chromatography
ELISA	enzyme-linked immunosorbent assay
TUNEL	terminal deoxynucleotidyl transferase-mediated deoxyuridyl triphosphate nick end-labeling

ACKNOWLEDGMENTS

This work was supported by grants 203/04/1325 from the Grant Agency of the Czech Republic and A4004402 from the Grant Agency of the Academy of

Sciences of the Czech Republic, by a purpose-endowment from the Ministry of Industry and Trade of the Czech Republic (project 1H-PK/42) and a grant No. AVOZ50040507. The author thank Dr. Ludek Havran for critical reading of the manuscript.

REFERENCES

- Abreu, F.C., M.O.F. Goulart and A.M.O. Brett, 2002, Detection of the damage caused to DNA by niclosamide using an electrochemical DNA-biosensor, *Biosens. Bioelectron.* 17, 913–919.
- Alvarez, J.L.M., J.A.G. Calzon and J.M.L. Fonseca, 1998, Electrocatalytic effects of deoxyribonucleic acids, adenine and guanine on the reduction of Ni(II) at a mercury electrode, *J. Electroanal. Chem.* 457, 53–59.
- Bates, A.D. and A. Maxwell, 1993, *DNA Topology*, IRL Press, Oxford.
- Blackburn, M.G. and M.J. Gait, 1990, *Nucleic Acids in Chemistry and Biology*, IRL Press, New York.
- Boon, E.M. and J.K. Barton, 2002, Charge transport in DNA, *Curr. Opin. Struct. Biol.* 12, 320–329.
- Boon, E.M. and J.K. Barton, 2003, Reduction of ferricyanide by methylene blue at a DNA-modified rotating-disk electrode, *Langmuir* 19, 9255–9259.
- Boon, E.M., D.M. Ceres, T.G. Drummond, M.G. Hill and J.K. Barton, 2000, Mutation detection by electrocatalysis at DNA-modified electrodes, *Nat. Biotechnol.* 18, 1096–1100.
- Boon, E.M., A.L. Livingston, N.H. Chmiel, S.S. David and J.K. Barton, 2003, DNA-mediated charge transport for DNA repair, *Proc. Natl. Acad. Sci. USA* 100, 12543–12547.
- Boon, E.M., J.E. Salas and J.K. Barton, 2002, An electrical probe of protein–DNA interactions on DNA-modified surfaces, *Nat. Biotechnol.* 20, 282–286.
- Boublikova, P., M. Vojtiskova and E. Palecek, 1987, Determination of submicrogram quantities of circular duplex DNA in plasmid samples by adsorptive stripping voltammetry, *Anal. Lett.* 20, 275–291.
- Brabec, V., 2000, DNA sensor for the determination of antitumor platinum compounds, *Electrochim. Acta* 45, 2929–2932.
- Brabec, V. and J. Kasparkova, 2002, Molecular aspects of resistance to antitumor platinum drugs, *Drug Resist. Update.* 5, 147–161.
- Brabec, V., V. Kleinwachter, J.L. Butour and N.P. Johnson, 1990, Biophysical studies of the modification of DNA by antitumor platinum coordination-complexes, *Biophys. Chem.* 35, 129–141.
- Brabec, V. and E. Palecek, 1976, Interaction of nucleic acids with electrically charged surfaces III. Surface denaturation of DNA on the mercury electrode in two potential regions, *Stud. Biophys.* 60, 105–110.
- Brabec, V., V. Vetterl and O. Vrana, 1996, *Electroanalysis of Biomacromolecules. Experimental Techniques in Bioelectrochemistry. Vol. 3, Bioelectrochemistry: Principles and Practice*, Eds. V. Brabec, D. Walz and G. Milazzo, Birkhauser Verlag, Basel, Switzerland, pp. 287–359.
- Brainina, K.Z., N.A. Malakhova and N.Y. Stojko, 2000, Stripping voltammetry in environmental and food analysis, *Fresenius J. Anal. Chem.* 368, 307–325.
- Brett, A.M.O., L.A. da Silva, H. Fujii, S. Mataka and T. Thiemann, 2003, Detection of the damage caused to DNA by a thiophene-S-oxide using an electrochemical DNA-biosensor, *J. Electroanal. Chem.* 549, 91–99.
- Brett, A.M.O., T.R.A. Macedo, D. Raimundo, M.H. Marques and S.H.P. Serrano, 1998, Voltammetric behaviour of mitoxantrone at a DNA-biosensor, *Biosens. Bioelectron.* 13, 861–867.
- Brett, A.M.O., J.A.P. Piedade and S.H.P. Serrano, 2000, Electrochemical oxidation of 8-oxoguanine, *Electroanalysis* 12, 969–973.

- Brett, A.M.O., S.H.P. Serrano, I. Gutz and M.A. LaScalea, 1997a, Electrochemical reduction of metronidazole at a DNA-modified glassy carbon electrode, *Bioelectrochem. Bioenerg.* 42, 175–178.
- Brett, A.M.O., S.H.P. Serrano, I. Gutz, M.A. La-Scalea and M.L. Cruz, 1997b, Voltammetric behaviour of nitroimidazoles at a DNA-biosensor, *Electroanalysis* 9, 1132–1137.
- Brett, A.M.O., S.H.P. Serrano and I.G.R. Gutz, 1997c, Comparison of the voltammetric behaviour of metronidazole at a DNA-modified glassy carbon electrode, a mercury thin film electrode and a glassy carbon electrode, *Electroanalysis* 9, 110–114.
- Brett, A.M.O., S.H.P. Serrano, T.R.A. Macedo, D. Raimundo, M.H. Marques and M.A. Lascalea, 1996, Electrochemical determination of carboplatin in serum using a DNA-modified glassy carbon electrode, *Electroanalysis* 8, 992–995.
- Brett, C.M.A., A.M.O. Brett and S.H.P. Serrano, 1994, On the adsorption and electrochemical oxidation of DNA at glassy carbon electrodes, *J. Electroanal. Chem.* 366, 225–231.
- Buckova, M., J. Labuda, J. Sandula, L. Krizkova, I. Stepanek and Z. Durackova, 2002, Detection of damage to DNA and antioxidative activity of yeast polysaccharides at the DNA-modified screen-printed electrode, *Talanta* 56, 939–947.
- Buzek, J., A. Kuderova, T. Pexa, V. Stankova, L. Lauerova and E. Palecek, 1999, Monoclonal antibody against DNA adducts with osmium structural probes, *J. Biomol. Struct. Dyn.* 17, 41–50.
- Bykov, V.J., R. Kumar, A. Forsti and K. Hemminki, 1995, Analysis of UV-induced DNA photoproducts by ³²P-postlabelling, *Carcinogenesis* 16, 113–118.
- Cadet, J., C. D'Ham, T. Douki, J.P. Pouget, J.L. Ravanat and S. Sauvaigo, 1998, Facts and artifacts in the measurement of oxidative base damage to DNA, *Free Radical Res.* 29, 541–550.
- Cahova-Kucharikova, K., M. Fojta, T. Mozga and E. Palecek, 2005, Use of DNA repair enzymes in electrochemical detection of damage to DNA bases, *Anal. Chem.* 77, 2920–2927.
- Cai, X., G. Rivas, P.A.M. Farias, H. Shirashi, J. Wang, M. Fojta and E. Palecek, 1996, Trace measurements of plasmid DNAs by adsorptive stripping potentiometry at carbon paste electrodes, *Bioelectrochem. Bioenerg.* 401, 41–47.
- Cai, X., G. Rivas, H. Shirashi, P. Farias, J. Wang, M. Tomschik, F. Jelen and E. Palecek, 1997, Electrochemical analysis of formation of polynucleotide complexes in solution and at electrode surfaces, *Anal. Chim. Acta* 344, 64–76.
- Campuzano, V., L. Montermini, M.D. Molto, L. Pianese, M. Cossee, F. Cavalcanti, E. Monros, F. Rodius, F. Duclous, A. Monticelli, F. Zara, J. Canizares, H. Koutnikova, S.I. Bidichandani, C. Gellera, A. Brice, P. Trouillas, G. De Michele, A. Filla, R. De Frutos, F. Palau, P.I. Patel, S. Di Donato, J.-L. Mandel, S. Cocozza, M. Koenig and M. Pandolfo, 1996, Friedreich's ataxia: Autosomal recessive disease caused by an intronic GAA triplet repeat expansion, *Science* 271, 1423–1427.
- Carter, M.T. and A.J. Bard, 1987, Voltammetric studies of the interaction of tris(1,10-phenanthroline)cobalt(III) with DNA, *J. Am. Chem. Soc.* 109, 7528–7530.
- Carter, M.T., M. Rodriguez and A.J. Bard, 1989, Voltammetric studies of the interaction of metal chelates with DNA. 2. Tris-chelated complexes of cobalt(III) and iron(II) with 1,10-phenanthroline and 2,2-bipyridine, *J. Am. Chem. Soc.* 111, 8901–8911.
- Caruana, D.J. and A. Heller, 1999, Enzyme-amplified amperometric detection of hybridization and of a single base pair mutation in an 18-base oligonucleotide on a 7- μ m diameter microelectrode, *J. Am. Chem. Soc.* 121, 769–774.
- Chiti, G., G. Marrazza and M. Mascini, 2001, Electrochemical DNA biosensor for environmental monitoring, *Anal. Chim. Acta* 427, 155–164.
- Chu, X., G.L. Shen, J.H. Jiang, T.F. Kang, B. Xiong and R.Q. Yu, 1998, Voltammetric studies of the interaction of daunomycin anticancer drug with DNA and analytical applications, *Anal. Chim. Acta* 373, 29–38.
- Cojocel, C., L. Novotny, A. Vachalkova and B. Knauf, 2003, Comparison of the carcinogenic potential of streptozotocin by polarography and alkaline elution, *Neoplasma* 50, 110–116.

- Collins, A., C. Gedik, N. Vaughan, S. Wood, A. White, J. Dubois, J.F. Rees, S. Loft, P. Moller, J. Cadet, T. Douki, J.L. Ravanat, S. Sauvaigo, H. Faure, I. Morel, M. Morin, B. Epe, N. Phoa, A. Hartwig, T. Schwerdtle, P. Dolaro, L. Giovannelli, M. Lodovici, R. Olinski, K. Bialkowski, M. Foksinski, D. Gackowski, Z. Durackova, L. Hlincikova, P. Korytar, M. Sivonova, M. Dusinska, C. Mislanova, J. Vina, L. Moller, T. Hofer, J. Nygren, E. Gremaud, K. Herbert, J. Lunec, C. Wild, L. Hardie, J. Olliver and E. Smith, 2003, Measurement of DNA oxidation in human cells by chromatographic and enzymic methods, *Free Radical Biol. Med.* 34, 1089–1099.
- Collins, A.R., 2004, The comet assay for DNA damage and repair – principles, applications, and limitations, *Mol. Biotechnol.* 26, 249–261.
- Collins, A.R., 2005, Assays for oxidative stress and antioxidant status: Applications to research into the biological effectiveness of polyphenols, *Am. J. Clin. Nutr.* 81, 261S–267S.
- Collins, A.R., J. Cadet, L. Moller, H.E. Poulsen and J. Vina, 2004, Are we sure we know how to measure 8-oxo-7,8-dihydroguanine in DNA from human cells?, *Arch. Biochem. Biophys.* 423, 57–65.
- Cooke, M.S., I.D. Podmore, N. Mistry, M.D. Evans, K.E. Herbert, H.R. Griffiths and J. Lunec, 2003, Immunochemical detection of UV-induced DNA damage and repair, *J. Immunol. Methods* 280, 125–133.
- Correia dos Santos, M.M., C.M.L.F. Lopes and M.L. Simoes-Goncalves, 1996, Voltammetric studies of purine bases and purine nucleosides with copper, *Bioelectrochem. Bioenerg.* 39, 55–60.
- Correia dos Santos, M.M., P.M.P. Sousa, A.M.M. Modesto and M.L. Simoes Goncalves, 1998, Voltammetric behaviour of copper complexes with cytosine and its nucleoside, *Bioelectrochem. Bioenerg.* 45, 267–273.
- Dennany, L., R.J. Forster and J.F. Rusling, 2003, Simultaneous direct electrochemiluminescence and catalytic voltammetry detection of DNA in ultrathin films, *J. Am. Chem. Soc.* 125, 5213–5218.
- Drummond, T.G., M.G. Hill and J.K. Barton, 2003, Electrochemical DNA sensors, *Nat. Biotechnol.* 21, 1192–1199.
- England, T.G., A. Jenner, O.I. Aruoma and B. Halliwell, 1998, Determination of oxidative DNA base damage by gas chromatography mass spectrometry. Effect of derivatization conditions on artifactual formation of certain base oxidation products, *Free Radical Res.* 29, 321–330.
- Erdem, A. and M. Ozsoz, 2001a, Interaction of the anticancer drug epirubicin with DNA, *Anal. Chim. Acta* 437, 107–114.
- Erdem, A. and M. Ozsoz, 2001b, Voltammetry of the anticancer drug mitoxantrone and DNA, *Turkish J. Chem.* 25, 469–475.
- Erdem, A. and M. Ozsoz, 2002, Electrochemical DNA biosensors based on DNA–drug interactions, *Electroanalysis* 14, 965–974.
- Fadrna, R., K. Kucharikova-Cahova, L. Havran, B. Yosypchuk and M. Fojta, 2005, Use of polished and mercury film-modified silver solid amalgam electrodes in electrochemical analysis of DNA, *Electroanalysis* 17, 452–459.
- Fadrna, R., B. Yosypchuk, M. Fojta, T. Navrátil and L. Novotny, 2004, Voltammetric determination of adenine, guanine and DNA using liquid mercury free polished silver solid amalgam electrode, *Anal. Lett.* 37, 399–413.
- Falcone, J.M. and H.C. Box, 1997, Selective hydrolysis of damaged DNA by nuclease P1, *Biochim. Biophys. Acta* 1337, 267–275.
- Farias, P.A.M., A.D. Wagener and A.A. Castro, 2001, Ultratrace determination of adenine in the presence of copper by adsorptive stripping voltammetry, *Talanta* 55, 281–290.
- Faust, F., F. Kassie, S. Knasmuller, R.H. Boedecker, M. Mann and V. Mersch-Sundermann, 2004, The use of the alkaline comet assay with lymphocytes in human biomonitoring studies, *Mutat. Res. Rev. Mutat.* 566, 209–229.
- Ferancova, A., L. Heilerova, E. Korgova, S. Silhar, I. Stepanek and J. Labuda, 2004, Anti/pro-oxidative properties of selected standard chemicals and tea extracts investigated by DNA-based electrochemical biosensor, *Eur. Food Res. Technol.* 219, 416–420.

- Fleckenstein, D.S., C.C. Uphoff, H.G. Drexler and H. Quentmeier, 2002, Detection of p53 gene mutations by single strand conformational polymorphism (SSCP) in human acute myeloid leukemia-derived cell lines, *Leuk. Res.* 26, 207–214.
- Flemming, J. and H. Berg, 1974, On the association of DNA at the mercury/electrolyte interface, *Bioelectrochem. Bioenerg.* 1, 459–465.
- Fojta, M., 2002, Electrochemical sensors for DNA interactions and damage, *Electroanalysis* 14, 1449–1463.
- Fojta, M., 2004, Mercury electrodes in nucleic acid electrochemistry: Sensitive analytical tools and probes of DNA structure, *Collect. Czech. Chem. Commun.* 69, 715–747.
- Fojta, M., R.P. Bowater, V. Stankova, L. Havran, D.M.J. Lilley and E. Palecek, 1998a, Two superhelix density-dependent DNA transitions detected by changes in DNA adsorption/desorption behavior, *Biochemistry* 37, 4853–4862.
- Fojta, M., R. Doffkova and E. Palecek, 1996, Determination of traces of RNA in submicrogram amounts of single- or double stranded DNAs by means of nucleic acid-modified electrodes, *Electroanalysis* 8, 420–426.
- Fojta, M., L. Havran, S. Billova, P. Kostecka, M. Masarik and R. Kizek, 2003, Two-surface strategy in electrochemical DNA hybridization assays: Detection of osmium-labeled target DNA at carbon electrodes, *Electroanalysis* 15, 431–440.
- Fojta, M., L. Havran, J. Fulneckova and T. Kubicarova, 2000a, Adsorptive transfer stripping AC voltammetry of DNA complexes with intercalators, *Electroanalysis* 12, 926–934.
- Fojta, M., L. Havran, R. Kizek and S. Billova, 2002a, Voltammetric microanalysis of DNA adducts with osmium tetroxide, 2,2'-bipyridine using a pyrolytic graphite electrode, *Talanta* 56, 867–874.
- Fojta, M., L. Havran, R. Kizek, S. Billova and E. Palecek, 2004a, Multiply osmium-labeled reporter probes for electrochemical DNA hybridization assays. Detection of trinucleotide repeats, *Biosens. Bioelectron.* 20, 985–994.
- Fojta, M., L. Havran, T. Kubicarova and E. Palecek, 2002b, Electrode potential-controlled DNA damage in the presence of copper ions and their complexes, *Bioelectrochemistry* 55, 25–27.
- Fojta, M., L. Havran and E. Palecek, 1997, Chronopotentiometric detection of DNA strand breaks with mercury electrodes modified supercoiled DNA, *Electroanalysis* 9, 1033–1034.
- Fojta, M., L. Havran, M. Vojtiskova and E. Palecek, 2004b, Electrochemical detection of DNA triplet repeat expansion, *J. Am. Chem. Soc.* 126, 6532–6533.
- Fojta, M., T. Kubicarova and E. Palecek, 1999, Cleavage of supercoiled DNA by deoxyribonuclease I in solution and at the electrode surface, *Electroanalysis* 11, 1005–1012.
- Fojta, M., T. Kubicarova and E. Palecek, 2000, Electrode potential-modulated cleavage of surface-confined DNA by reactive oxygen species detected by an electrochemical biosensor, *Biosens. Bioelectron.* 15, 107–115.
- Fojta, M. and E. Palecek, 1997, Supercoiled DNA modified mercury electrode: A highly sensitive tool for the detection of DNA damage, *Anal. Chim. Acta* 342, 1–12.
- Fojta, M., V. Stankova, E. Palecek, J. Mitas and P. Koscielniak, 1998b, A supercoiled DNA-modified mercury electrode-based biosensor for the detection of DNA strand cleaving agents, *Talanta* 46, 155–161.
- Fojta, M., C. Teijeiro and E. Palecek, 1994, Cyclic voltammetry with RNA-modified mercury electrode, *Bioelectrochem. Bioenerg.* 34, 69–76.
- Friedberg, E.C., 2000, Biological responses to DNA damage: A perspective in the new millennium, *Cold Spring Harbor Symp. Quant. Biol.* 65, 593–602.
- Friedberg, E.C., 2003, DNA damage and repair, *Nature* 421, 436–440.
- Gedik, C.M., S.P. Boyle, S.G. Wood, N.J. Vaughan and A.R. Collins, 2002, Oxidative stress in humans: Validation of biomarkers of DNA damage, *Carcinogenesis* 23, 1441–1446.
- Gherghi, I.C., S.T. Girousi, A.A. Pantazaki, A.N. Voulgaropoulos and R. Tzimou-Tsitouridou, 2003a, Electrochemical DNA biosensors applicable to the study of interactions between DNA and DNA intercalators, *Int. J. Environ. Anal. Chem.* 83, 693–700.
- Gherghi, I.C., S.T. Girousi, A.N. Voulgaropoulos and R. Tzimou-Tsitouridou, 2003b, Study of interactions between DNA-ethidium bromide (EB) and DNA-acridine orange (AO), in solution, using hanging mercury drop electrode (HMDE), *Talanta* 61, 103–112.

- Gherghi, I.C., S.T. Girousi, A.N. Voulgaropoulos and R. Tzimou-Tsitouridou, 2003c, Study of interactions between actinomycin D and DNA on carbon paste electrode (CPE) and on the hanging mercury drop (HMDE) surface, *J. Pharm. Biomed. Anal.* 31, 1065–1078.
- Gherghi, I.C., S.T. Girousi, A.N. Voulgaropoulos and R. Tzimou-Tsitouridou, 2004, Interaction of the mutagen ethidium bromide with DNA, using a carbon paste electrode and a hanging mercury drop electrode, *Anal. Chim. Acta* 505, 135–144.
- Gil, E.D., S.H.P. Serrano, E.I. Ferreira and L.T. Kubota, 2002, Electrochemical evaluation of rhodium dimer–DNA interactions, *J. Pharm. Biomed. Anal.* 29, 579–584.
- Gooding, J.J., 2002, Electrochemical DNA hybridization biosensors, *Electroanalysis* 14, 1149–1156.
- Guetsens, G., G. De Boeck, M. Highley, A.T. van Oosterom and E.A. de Bruijn, 2002, Oxidative DNA damage: Biological significance and methods of analysis, *Crit. Rev. Clin. Lab. Sci.* 39, 331–457.
- Halliwell, B., 1998, Can oxidative DNA damage be used as a biomarker of cancer risk in humans? Problems, resolutions and preliminary results from nutritional supplementation studies, *Free Radical Res.* 29, 469–486.
- Hartwich, G., D.J. Caruana, T. deLumley-Woodyear, Y.B. Wu, C.N. Campbell and A. Heller, 1999, Electrochemical study of electron transport through thin DNA films, *J. Am. Chem. Soc.* 121, 10803–10812.
- Hashimoto, K., K. Ito and Y. Ishimori, 1994, Sequence-specific gene detection with a gold electrode modified with DNA probes and an electrochemically active dye, *Anal. Chem.* 66, 3830–3833.
- Hason, S., J. Dvorak, F. Jelen and V. Vetterl, 2002, Interaction of DNA with echinomycin at the mercury electrode surface as detected by impedance and chronopotentiometric measurements, *Talanta* 56, 905–913.
- Hason, S. and V. Vetterl, 2002a, On the formation kinetics of two-dimensional cytidine films, *Bioelectrochemistry* 57, 23–32.
- Hason, S. and V. Vetterl, 2002b, Two-dimensional condensation of nucleic acid components at mercury film and gold electrodes, *Bioelectrochemistry* 56, 43–45.
- Havran, L., S. Billova and E. Palecek, 2004a, Electroactivity of avidin and streptavidin. Avidin signals at mercury and carbon electrodes respond to biotin binding, *Electroanalysis* 16, 1139–1148.
- Havran, L., M. Fojta and E. Palecek, 2004b, Voltammetric behavior of DNA modified with osmium tetroxide 2,2'-bipyridine at mercury electrodes, *Bioelectrochemistry* 63, 239–243.
- Helbock, H.J., K.B. Beckman, M.K. Shigenaga, P.B. Walter, A.A. Woodall, H.C. Yeo and B.N. Ames, 1998, DNA oxidation matters: The HPLC-electrochemical detection assay of 8-oxo-deoxyguanosine and 8-oxo-guanine, *Proc. Natl. Acad. Sci. USA* 95, 288–293.
- Heller, M.J., 2002, DNA microarray technology: Devices, systems, and applications, *Annu. Rev. Biomed. Eng.* 4, 129–153.
- Holmberg, R.C., M.T. Tierney, P.A. Ropp, E.E. Berg, M.W. Grinstaff and H.H. Thorp, 2003, Intramolecular electrocatalysis of 8-oxo-guanine oxidation: Secondary structure control of electron transfer in osmium-labeled oligonucleotides, *Inorg. Chem.* 42, 6379–6387.
- Ibrahim, M.S., I.S. Shehatta and A.A. Al-Nayeli, 2002, Voltammetric studies of the interaction of lumazine with cyclodextrins and DNA, *J. Pharm. Biomed. Anal.* 28, 217–225.
- Inagaki, S., Y. Esaka, M. Sako and M. Goto, 2001, Analysis of DNA adducts bases by capillary electrophoresis with amperometric detection, *Electrophoresis* 22, 3408–3412.
- Jelen, F., A. Erdem and E. Palecek, 2002, Cyclic voltammetry of echinomycin and its interaction with double-stranded and single-stranded DNA adsorbed at the electrode, *Bioelectrochemistry* 55, 165–167.
- Jelen, F., M. Fojta and E. Palecek, 1997a, Voltammetry of native double-stranded, denatured and degraded DNAs, *J. Electroanal. Chem.* 427, 49–56.
- Jelen, F., P. Karlovsky, P. Pecinka, E. Makaturova and E. Palecek, 1991, Osmium tetroxide reactivity of DNA bases in nucleotide sequencing and probing of DNA structure, *Gen. Physiol. Biophys.* 10, 461–473.

- Jelen, F., A. Kourilova, P. Pecinka and E. Palecek, 2004, Microanalysis of DNA by stripping transfer voltammetry, *Bioelectrochemistry* 63, 249–252.
- Jelen, F. and E. Palecek, 1985, Nucleotide sequence-dependent opening of double-stranded DNA at an electrically charged surface, *Gen. Physiol. Biophys.* 4, 219–237.
- Jelen, F., M. Tomschik and E. Palecek, 1997b, Adsorptive stripping square-wave voltammetry of DNA, *J. Electroanal. Chem.* 423, 141–148.
- Jelen, F., V. Vetterl, P. Belusa and S. Hason, 1999, Adsorptive stripping analysis of DNA with admittance detection, *Electroanalysis* 12, 987–992.
- Jenner, A., T.G. England, O.I. Aruoma and B. Halliwell, 1998, Measurement of oxidative DNA damage by gas chromatography mass spectrometry: Ethanethiol prevents artifactual generation of oxidized DNA bases, *Biochem. J.* 331, 365–369.
- Johnston, D.H., Ch.-Ch. Cheng, K.J. Campbell and H.H. Thorp, 1994, Trans-dioxorhenium(V)-mediated electrocatalytic oxidation of DNA at indium tin-oxide electrodes: Voltammetric detection of DNA cleavage in solution, *Inorg. Chem.* 33, 6388–6390.
- Johnston, D.H., K.C. Glasgow and H.H. Thorp, 1995, Electrochemical measurement of the solvent accessibility of nucleobases using electron transfer between DNA and metal complexes, *J. Am. Chem. Soc.* 117, 8933–8938.
- Johnston, R.F., D.M. Lewis and J.Q. Chambers, 1999, Accumulation of Hg(II) by adsorbed polyuridylic acid: Differentiation of coordinated Hg(II) and covalently mercurated species, *J. Electroanal. Chem.* 466, 2–7.
- Kalvoda, R., 2000, Environmental electroanalytical chemistry contemporary trends and prospects, *Crit. Rev. Anal. Chem.* 30, 31–35.
- Karadeniz, H., B. Gulmez, F. Sahinci, A. Erdem, G.I. Kaya, N. Unver, B. Kivcak and M. Ozsoz, 2003, Disposable electrochemical biosensor for the detection of the interaction between DNA and lycorine based on guanine and adenine signals, *J. Pharm. Biomed. Anal.* 33, 295–302.
- Kasai, H., 2003, A new automated method to analyze urinary 8-hydroxydeoxyguanosine by a high-performance liquid chromatography-electrochemical detector system, *J. Radic. Res.* 44, 185–189.
- Kasparova, D., O. Vrana, V. Kleinwachter and V. Brabec, 1987, The effect of platinum derivatives on interfacial properties of DNA, *Biophys. Chem.* 28, 191–197.
- Kelley, S.O., J.K. Barton, N.M. Jackson and M.G. Hill, 1997, Electrochemistry of methylene blue bound to a DNA-modified electrode, *Bioconjugate Chem.* 8, 31–37.
- Kelley, S.O., E.M. Boon, J.K. Barton, N.M. Jackson and M.G. Hill, 1999a, Single-base mismatch detection based on charge transduction through DNA, *Nucleic Acids Res.* 27, 4830–4837.
- Kelley, S.O., N.M. Jackson, M.G. Hill and J.K. Barton, 1999b, Long-range electron transfer through DNA films, *Angew. Chem. Int. Ed.* 38, 941–945.
- Kizek, R., L. Havran, M. Fojta and E. Palecek, 2002, Determination of nanogram quantities of osmium-labeled single stranded DNA by differential pulse stripping voltammetry, *Bioelectrochemistry* 55, 119–121.
- Korbut, O., M. Buckova, J. Labuda and P. Grundler, 2003, Voltammetric detection of antioxidative properties of flavonoids using electrically heated DNA modified carbon paste electrode, *Sensors* 3, 1–10.
- Korbut, O., M. Buckova, P. Tarapcik, J. Labuda and P. Grundler, 2001, Damage to DNA indicated by an electrically heated DNA-modified carbon paste electrode, *J. Electroanal. Chem.* 506, 143–148.
- Koskinen, M., P. Vodicka, L. Vodickova and K. Hemminki, 2001, P-32-postlabelling/HPLC analysis of various styrene-induced DNA adducts in mice, *Biomarkers* 6, 175–189.
- Kostecka, P., L. Havran, H. Pivonkova and M. Fojta, 2004, Voltammetry of osmium-modified DNA at a mercury film electrode. Application in detecting DNA hybridization, *Bioelectrochemistry* 63, 245–248.
- Krznicaric, D., B. Cosovic, J. Stuber and R.K. Zahn, 1990, Alternating current voltammetric determination of DNA damage, *Chem. Biol. Interact.* 76, 111–128.
- Kubicarova, T., M. Fojta, J. Vidic, L. Havran and E. Palecek, 2000a, Mercury film electrode as a sensor for the detection of DNA damage, *Electroanalysis* 12, 1422–1425.

- Kubicarova, T., M. Fojta, J. Vidic, D. Suznjevic, M. Tomschik and E. Palecek, 2000b, Voltammetric and chronopotentiometric measurements with nucleic acids-modified mercury film at glassy carbon electrode, *Electroanalysis* 12, 1390–1396.
- Kuderova-Krejcová, A., A.M. Poverenny and E. Palecek, 1991, Probing of DNA structure with osmium tetroxide, 2,2'-bipyridine. Adduct-specific antibodies, *Nucleic Acids Res.* 19, 6811–6817.
- Kucharikova, K., L. Novotny, B. Yosypchuk and M. Fojta, 2004, Detecting DNA damage with a silver solid amalgam electrode, *Electroanalysis* 16, 410–414.
- Labuda, J., M. Buckova, L. Heilerova, A. Caniova-Ziakova, E. Brandsteterova, J. Mattusch and R. Wennrich, 2002, Detection of antioxidative activity of plant extracts at the DNA-modified screen-printed electrode, *Sensors* 2, 1–10.
- Labuda, J., M. Buckova, L. Heilerova, S. Silhar and I. Stepanek, 2003, Evaluation of the redox properties and anti/pro-oxidant effects of selected flavonoids by means of a DNA-based electrochemical biosensor, *Anal. Bioanal. Chem.* 376, 168–173.
- Labuda, J., M. Buckova, S. Jantova, I. Stepanek, I. Surugiu, B. Danielsson and M. Mascini, 2000, Modified screen-printed electrodes for the investigation of the interaction of non-electroactive quinazoline derivatives with DNA, *Fresenius J. Anal. Chem.* 367, 364–368.
- Labuda, J., M. Buckova, M. Vanickova, J. Mattusch and R. Wennrich, 1999, Voltammetric detection of the DNA interaction with copper complex compounds and damage to DNA, *Electroanalysis* 11, 101–107.
- Langmaier, J., Z. Samec and E. Samcova, 2003, Electrochemical oxidation of 8-oxo-2'-deoxyguanosine on glassy carbon, gold, platinum and tin(IV) oxide electrodes, *Electroanalysis* 15, 1555–1560.
- La-Scalea, M.A., S.H.P. Serrano, E.I. Ferreira and A.M.O. Brett, 2002, Voltammetric behavior of benzimidazole at a DNA-electrochemical biosensor, *J. Pharm. Biomed. Anal.* 29, 561–568.
- Laschi, S., I. Palchetti, G. Marrazza and M. Mascini, 2003, Disposable electrochemical sensors and biosensors for environmental and food analysis, *Indian J. Chem. A* 42, 2968–2973.
- Li, G.D., O. Shimelis, X.J. Zhou and R.W. Giese, 2003, Scaled-down nuclease P1 for scaled-up DNA digestion, *Biotechniques* 34, 908–909.
- Lin, H.L. and P.F. Hollenberg, 2001, *N*-nitrosodimethylamine-mediated formation of oxidized and methylated DNA bases in a cytochrome P450 2E1 expressing cell line, *Chem. Res. Toxicol.* 14, 562–566.
- Locatelli, C., 1997, Anodic and cathodic stripping voltammetry in the simultaneous determination of toxic metals in environmental samples, *Electroanalysis* 9, 1014–1017.
- Loo, D.T., 2002, TUNEL assay. An overview of techniques, *Methods Mol. Biol.* 203, 21–30.
- Lucarelli, F., L. Authier, G. Bagni, G. Marrazza, T. Baussant, E. Aas and M. Mascini, 2003, DNA biosensor investigations in fish bile for use as a biomonitoring tool, *Anal. Lett.* 36, 1887–1901.
- Lucarelli, F., A. Kicela, I. Palchetti, G. Marrazza and M. Mascini, 2002a, Electrochemical DNA biosensor for analysis of wastewater samples, *Bioelectrochemistry* 58, 113–118.
- Lucarelli, F., I. Palchetti, G. Marrazza and M. Mascini, 2002b, Electrochemical DNA biosensor as a screening tool for the detection of toxicants in water and wastewater samples, *Talanta* 56, 949–957.
- Lukasova, E., F. Jelen and E. Palecek, 1982, Electrochemistry of osmium-nucleic acid complexes: A probe for single-stranded and distorted double-stranded regions in DNA, *Gen. Physiol. Biophys.* 1, 53–70.
- Lukasova, E., M. Vojtiskova, F. Jelen, T. Sticzay and E. Palecek, 1984, Osmium-induced alternation in DNA structure, *Gen. Physiol. Biophys.* 3, 175–191.
- Maeda, M., Y. Mitsuhashi, K. Nakano and M. Takagi, 1992, DNA-immobilized gold electrode for DNA-binding drug sensor, *Anal. Sci.* 8, 83–84.
- Marczynski, B., H.P. Rihs, B. Rossbach, J. Holzer, J. Angerer, M. Scherenberg, G. Hoffmann, T. Bruning and M. Wilhelm, 2002, Analysis of 8-oxo-7,8-dihydro-2'-deoxyguanosine and DNA strand breaks in white blood cells of occupationally exposed workers: Comparison

- with ambient monitoring, urinary metabolites and enzyme polymorphisms, *Carcinogenesis* 23, 273–281.
- Marchini, S., M. Broggin, C. Sessa and M. D'Incalci, 2001, Development of distamycin-related DNA binding anticancer drugs, *Expert Opin. Inv. Drug.* 10, 1703–1714.
- Marin, D., P. Perez, C. Teijeiro and E. Palecek, 1998, Interactions of surface-confined DNA with acid-activated mitomycin C, *Biophys. Chem.* 75, 87–95.
- Marin, D., R. Valera, E. de la Red and C. Teijeiro, 1997, Electrochemical study of antineoplastic drug thiotepa hydrolysis to thiol form and thiotepa–DNA interactions, *Bioelectrochem. Bioenerg.* 44, 51–56.
- Marini, V., J. Kasparkova, O. Novakova, L. Monsu Scolaro, R. Romeo and V. Brabec, 2002, Biophysical analysis of natural, double-helical DNA modified by a dinuclear platinum(II) organometallic compound in a cell-free medium, *J. Biol. Inorg. Chem.* 7, 725–734.
- Maruyama, K., Y. Mishima, K. Minagawa and J. Motonaka, 2001, Electrochemical and DNA-binding properties of dipyridophenazine complexes of osmium(II), *J. Electroanal. Chem.* 510, 96–102.
- Masarik, M., R. Kizek, K.J. Kramer, S. Billova, M. Brazdova, J. Vacek, M. Bailey, F. Jelen and J.A. Howard, 2003, Application of avidin–biotin technology and adsorptive transfer stripping square-wave voltammetry for detection of DNA hybridization and avidin in transgenic avidin maize, *Anal. Chem.* 75, 2663–2669.
- Masarik, M., A. Stobiecka, R. Kizek, F. Jelen, Z. Pechan, W. Hoyer, T.M. Jovin, V. Subramaniam and E. Palecek, 2004, Sensitive electrochemical detection of native and aggregated α -synuclein protein involved in Parkinson's disease, *Electroanalysis* 16, 1172–1181.
- Mascini, M., 2001, Affinity electrochemical biosensors for pollution control, *Pure Appl. Chem.* 73, 23–30.
- Mascini, M., I. Palchetti and G. Marrazza, 2001, DNA electrochemical biosensors, *Fresenius J. Anal. Chem.* 369, 15–22.
- Masuda, M., H. Nishino and H. Ohshima, 2002, Formation of 8-nitroguanosine in cellular RNA as a biomarker of exposure to reactive nitrogen species, *Chem. Biol. Interact.* 139, 187–197.
- Mazerska, Z., A. Zon and Z. Stojek, 2003, Electrochemical formation of the adduct between antitumor agent C-1311 and DNA nucleoside dG, *Electrochem. Commun.* 5, 770–775.
- Mbindyo, J., L. Zhou, Z. Zhang, J.D. Stuart and J.F. Rusling, 2000, Detection of chemically induced DNA damage by derivative square wave voltammetry, *Anal. Chem.* 72, 2059–2065.
- Migheli, A., 2002, Electron microscopic detection of DNA damage labeled by TUNEL, *Methods Mol. Biol.* 203, 31–39.
- Miyahara, H., K. Yamashita, M. Kanai, K. Uchida, M. Takagi, H. Kondo and S. Takenaka, 2002, Electrochemical analysis of single nucleotide polymorphisms of p53 gene, *Talanta* 56, 829–835.
- Mugweru, A. and J.F. Rusling, 2001, Catalytic square-wave voltammetric detection of DNA with reversible metallopolymer-coated electrodes, *Electrochem. Commun.* 3, 406–409.
- Mugweru, A. and J.F. Rusling, 2002, Square wave voltammetric detection of chemical DNA damage with catalytic poly(4-vinylpyridine)-Ru(bpy)₂(2+)(2+) films, *Anal. Chem.* 74, 4044–4049.
- Mugweru, A., B.Q. Wang and J. Rusling, 2004, Voltammetric sensor for oxidized DNA using ultrathin films of osmium and ruthenium metallopolymer, *Anal. Chem.* 76, 5557–5563.
- Nakano, K., S. Uchida, Y. Mitsuhashi, Y. Fujita, H. Taira and M. Maeda, 1998, DNA-modified electrodes: Molecular recognition and electrochemical response, polymer in sensors, *Theory and Practise*, Eds. N. Akmal and A.M. Usmani, ACS Symposium Series, No. 690, Amer. Chem. Soc., Washington, DC, pp., 34–45.
- Nakao, L.S., E. Fonseca and O. Augusto, 2002, Detection of C8(1-hydroxyethyl)guanine in liver RNA and DNA from control and ethanol-treated rats, *Chem. Res. Toxicol.* 15, 1248–1253.

- Napier, M.E. and H.H. Thorp, 1997, Modification of electrodes with dicarboxylate self-assembled monolayers for attachment and detection of nucleic acids, *Langmuir* 13, 6342–6344.
- Napier, M.E. and H.H. Thorp, 1999, Electrocatalytic oxidation of nucleic acids at electrodes modified with nylon and nitrocellulose membranes, *J. Fluores.* 9, 181–186.
- Nikolelis, D.P., S.S.E. Petropoulou and M.V. Mitrokotsa, 2002, A minisensor for the rapid screening of atenolol in pharmaceutical preparations based on surface-stabilized bilayer lipid membranes with incorporated DNA, *Bioelectrochemistry* 58, 107–112.
- Novotny, L., A. Vachalkova, T. Al-Nakib, N. Mohanna, D. Vesela and V. Suchy, 1999, Separation of structurally related flavonoids by GC/MS technique and determination of their polarographic parameters and potential carcinogenicity, *Neoplasma* 46, 231–236.
- Odom, D.T. and J.K. Barton, 2001, Long-range oxidative damage in DNA/RNA duplexes, *Biochemistry* 40, 8727–8737.
- Olive, P.L., R.E. Durand, J.A. Raleigh, C. Luo and C. Aquino-Parsons, 2000, Comparison between the comet assay and pimonidazole binding for measuring tumour hypoxia, *Br. J. Cancer* 83, 1525–1531.
- Oliveira-Brett, A.M. and L.A. da Silva, 2002, A DNA-electrochemical biosensor for screening environmental damage caused by *s*-triazine derivatives, *Anal. Bioanal. Chem.* 373, 717–723.
- Oliveira-Brett, A.M. and V.C. Diculescu, 2004a, Electrochemical study of quercetin–DNA interactions – Part II. *In situ* sensing with DNA biosensors, *Bioelectrochemistry* 64, 143–150.
- Oliveira-Brett, A.M. and V.C. Diculescu, 2004b, Electrochemical study of quercetin–DNA interactions: Part I. Analysis in incubated solutions, *Bioelectrochemistry* 64, 133–141.
- Oliveira-Brett, A.M., M. Vivan, I.R. Fernandes and J.A.P. Piedade, 2002, Electrochemical detection of *in situ* adriamycin oxidative damage to DNA, *Talanta* 56, 959–970.
- Ontko, A.C., P.M. Armistead, S.R. Kircus and H.H. Thorp, 1999, Electrochemical detection of single-stranded DNA using polymer-modified electrodes, *Inorg. Chem.* 38, 1842–1846.
- Ozsoz, M., A. Erdem, P. Kara, K. Kerman and D. Ozkan, 2003, Electrochemical biosensor for the detection of interaction between arsenic trioxide and DNA based on guanine signal, *Electroanalysis* 15, 613–619.
- Palecek, E., 1964, Denaturation of deoxyribonucleic acids, *Abhandlungen der DAW Berlin* 4, 270–274.
- Palecek, E., 1966, Polarographic behaviour of native and denatured deoxyribonucleic acids, *J. Mol. Biol.* 20, 263–281.
- Palecek, E., 1967, The polarographic behaviour of double-helical DNA containing single-strand breaks, *Biochim. Biophys. Acta* 145, 410–417.
- Palecek, E., 1969, Polarographic techniques in nucleic acid research, *Progress in Nucleic Acid Research and Molecular Biology*, Vol. 9, Eds. J.N. Davidson and W.E. Cohn, Academic Press, New York, pp. 31–73.
- Palecek, E., 1971, Nucleic acid structure analysis by polarographic techniques, *Methods in Enzymology: Nucleic Acids*, Part D, Vol. 21, Eds. L. Grossman and K. Moldave, Academic Press, New York, pp. 3–24.
- Palecek, E., 1976, Premelting changes in DNA conformation, *Progress in Nucleic Acid Research and Molecular Biology*, Vol. 18, Ed. W.E. Cohn, Academic Press, Inc., New York, pp. 151–213.
- Palecek, E., 1980, Polarographic analysis of nucleic acids, *Proceedings of Electroanalysis in Hygiene, Environmental, Clinical and Pharmacological Chemistry*, Ed. W.F. Smyth, Elsevier, Amsterdam, pp. 79–99.
- Palecek, E., 1983, Modern polarographic (voltammetric) methods in biochemistry and molecular biology Part II, Analysis of macromolecules, *Topics in Bioelectrochemistry and Bioenergetics*, Vol. 5, Ed. G. Milazzo, Wiley, Chichester, pp. 65–155.
- Palecek, E., 1986, Electrochemical behaviour of biological macromolecules, *Bioelectrochem. Bioenerg.* 15, 275–295.
- Palecek, E., 1988, Adsorptive transfer stripping voltammetry: Determination of nanogram quantities of DNA immobilized at the electrode surface, *Anal. Biochem.* 170, 421–431.

- Palecek, E., 1991, Local supercoil-stabilized DNA structures, *Crit. Rev. Biochem. Mol. Biol.* 26, 151–226.
- Palecek, E., 1992a, Adsorptive transfer stripping voltammetry. Effect of the electrode potential on the structure of DNA adsorbed at the mercury surface, *Bioelectrochem. Bioenerg.* 28, 71–83.
- Palecek, E., 1992b, Probing of DNA structure with osmium tetroxide complexes *in vitro*, *Methods in Enzymology*, Vol. 212, Eds. J.N. Abelson and M.I. Simon, Academic Press, New York, pp. 139–155.
- Palecek, E., 1996, From polarography of DNA to microanalysis with nucleic acid-modified electrodes, *Electroanalysis* 8, 7–14.
- Palecek, E., 2002, Past, presence and future of nucleic acids electrochemistry, *Talanta* 56, 809–819.
- Palecek, E. and M. Fojta, 1994, Differential pulse voltammetric determination of RNA at picomole level in the presence of DNA and nucleic acid components, *Anal. Chem.* 66, 1566–1571.
- Palecek, E. and M. Fojta, 2001, Detecting DNA hybridization and damage, *Anal. Chem.* 73, 74A–83A.
- Palecek, E. and M. Fojta, 2005, Electrochemical DNA sensors, *Bioelectronics*, Eds. I. Wilner and E. Katz, Wiley-VCH, Weinheim, pp. 127–192.
- Palecek, E., M. Fojta, F. Jelen and V. Vetterl, 2002, Electrochemical analysis of nucleic acids, *The Encyclopedia of Electrochemistry, Bioelectrochemistry*, Vol. 9, Eds. A.J. Bard and M. Stratsmann, Wiley-VCH, Weinheim, pp. 365–429.
- Palecek, E., M. Fojta, M. Tomschik and J. Wang, 1998, Electrochemical biosensors for DNA hybridization and DNA damage, *Biosens. Bioelectron.* 16, 621–628.
- Palecek, E. and M.A. Hung, 1983, Determination of nanogram quantities of osmium-labeled nucleic acids by stripping (inverse) voltammetry, *Anal. Biochem.* 132, 236–242.
- Palecek, E. and F. Jelen, 2002, Electrochemistry of nucleic acids and development of DNA sensors, *Crit. Rev. Anal. Chem.* 32, 73–83.
- Palecek, E., F. Jelen, C. Teijeiro, V. Fucik and T.M. Jovin, 1993, Biopolymer-modified electrodes Voltammetric analysis of nucleic acids and proteins at the submicrogram level, *Anal. Chim. Acta* 273, 175–186.
- Palecek, E., A. Krejcová, M. Vojtisková, V. Podgorodnichenko, T. Ilyina and A. Poverennyi, 1989, Antibodies to DNAs chemically modified with osmium structural probes, *Gen. Physiol. Biophys.* 8, 491–504.
- Palecek, E. and I. Postbieglova, 1986, Adsorptive stripping voltammetry of bimacromolecules with transfer of the adsorbed layer, *J. Electroanal. Chem.* 214, 359–371.
- Pandey, P.C. and H.H. Weetall, 1994, Application of photochemical reaction in electrochemical detection of DNA intercalation, *Anal. Chem.* 66, 1236–1241.
- Pang, D.W., Q. Lu, Y.D. Zhao and M. Zhang, 2000, DNA-modified electrodes VIII. Electrochemical behavior of $\text{Co}^{3+}/2^{+}$ at single-stranded DNA modified gold electrodes in the presence of 1,10-phenanthroline and the detection of trace cobalt, *Acta Chim. Sin.* 58, 524–528.
- Pang, D.W., M. Zhang, Z.L. Wang, Y.P. Qi, J.K. Cheng and Z.Y. Liu, 1996, Modification of glassy carbon and gold electrodes with DNA, *J. Electroanal. Chem.* 403, 183–188.
- Pang, D.W., Y.D. Zhao, M. Zhang, Y.P. Qi, Z.L. Wang and J.K. Cheng, 1999, DNA-Modified electrodes. Part 5. Electrochemical behavior of Co^{2+} at DNA-modified gold electrodes in the presence of 2,2'-bipyridyl, *Anal. Sci.* 15, 471–475.
- Park, S., T.A. Taton and C.A. Mirkin, 2002, Array-based electrical detection of DNA with nanoparticle probes, *Science* 295, 1503–1506.
- Patolsky, F., A. Lichtenstein and I. Willner, 2001, Detection of single-base DNA mutations by enzyme-amplified electronic transduction, *Nat. Biotechnol.* 19, 253–257.
- Paulson, H.L. and K.H. Fischbeck, 1996, Trinucleotide repeats in neurogenetic disorders, *Annu. Rev. Neurosci.* 19, 79–107.
- Peccia, J. and M. Hernandez, 2002, Rapid immunoassays for detection of UV-induced cyclobutane pyrimidine dimers in whole bacterial cells, *Appl. Environ. Microb.* 68, 2542–2549.

- Perez, P., C. Teijeiro and D. Marin, 1999, Interactions of surface-confined DNA with electroreduced mitomycin C comparison with acid-activated mitomycin C, *Chem. Biol. Interact.* 117, 65–81.
- Piedade, J.A.P., I.R. Fernandes and A.M. Oliveira-Brett, 2002, Electrochemical sensing of DNA–adriamycin interactions, *Bioelectrochemistry* 56, 81–83.
- Podmore, I.D., M.S. Cooke, K.E. Herbert and J. Lunec, 1996, Quantitative determination of cyclobutane thymine dimers in DNA by stable isotope-dilution mass spectrometry, *Photochem. Photobiol.* 64, 310–315.
- Popovich, N.D. and H.H. Thorp, 2002, New strategies for electrochemical nucleic acid detection, *Interface* 11, 30–34.
- Pouget, J.P., T. Douki, M.J. Richard and J. Cadet, 2000, DNA damage induced in cells by gamma and UVA radiation as measured by HPLC/GC-MS and HPLC-EC and comet assay, *Chem. Res. Toxicol.* 13, 541–549.
- Puranen, J. and M. Forss, 1983, Polarographically detected effect of ultrasound and irradiation on DNA solution, *Strahlentherapie* 159, 505–507.
- Qu, F. and N.-Q. Li, 1997, Comparison of metalloporphyrins interacting with DNA, *Electroanalysis* 9, 1348–1352.
- Radi, A., M.A. El Ries and S. Kandil, 2003, Electrochemical study of the interaction of levofloxacin with DNA, *Anal. Chim. Acta* 495, 61–67.
- Rajski, S.R., B.A. Jackson and J.K. Barton, 2000, DNA repair: Models for damage and mismatch recognition, *Mut. Res.* 447, 49–72.
- Rebelo, I., J.A.P. Piedade and A.M.O. Brett, 2004, Electrochemical determination of 8-oxoguanine in the presence of uric acid, *Bioelectrochemistry* 63, 267–270.
- Rodriguez, M. and A.J. Bard, 1990, Electrochemical studies of the interaction of metal chelates with DNA. 4. Voltammetric and electrogenerated chemiluminescent studies of the interaction of tris(2,2-bipyridine)osmium(II) with DNA, *Anal. Chem.* 62, 2658–2662.
- Rodriguez, M., T. Kodadek, M. Torres and A.J. Bard, 1990, Cleavage of DNA by electrochemically activated MnIII and FeIII complexes of meso-tetrakis (*N*-methyl-4-pyridiniumyl)porphine, *Bioconjugate Chem* 1, 123–131.
- Rogers, S.G. and B. Weiss, 1980, Exonuclease III of *Escherichia coli* K-12, an AP endonuclease, *Methods in Enzymology*, Vol. 65, Eds. L. Grossmann and K. Moldave, Academic Press, New York, pp. 201–211.
- Romanova, D., A. Vachalkova, K. Horvathova and A. Krutosikova, 2001, DC polarographic and UV spectrometric studies of substituted furo 3,2-b- and furo 2,3-b pyrroles, *Collect. Czech. Chem. Commun.* 66, 1615–1622.
- Ropp, P.A. and H.H. Thorp, 1999, Site-selective electron transfer from purines to electrocatalysts: Voltammetric detection of a biologically relevant detection in hybridized DNA duplexes, *Chem. Biol.* 6, 599–605.
- Rusling, J.F., 2004, Sensors for toxicity of chemicals and oxidative stress based on electrochemical catalytic DNA oxidation, *Biosens. Bioelectron.* 20, 1022–1028.
- Rusling, J.F., L.P. Zhou, J. Yang and A. Mugweru, 2002, Electrochemical toxicity sensors using layered polyanion-DNA films, *Abstr. Pap. Am. Chem. Soc.* 223, U389–U389.
- Saijo, N., T. Tamura and K. Nishio, 2003, Strategy for the development of novel anticancer drugs, *Cancer Chemoth. Pharm.* 52, S97–S101.
- Sequaris, J.-M. and M. Esteban, 1990, Cyclic voltammetry of metal/polyelectrolyte complexes: Complexes of cadmium and lead with deoxyribonucleic acid, *Electroanalysis* 2, 35–41.
- Sequaris, J.-M. and J. Swiatek, 1991, Interaction of DNA with Pb²⁺. Voltammetric and spectroscopic studies, *Bioelectrochem. Bioenerg.* 26, 15–28.
- Sequaris, J.M., P. Valenta and H.W. Nurnberg, 1982, A new electrochemical approach for the *in vitro* investigation of damage in native DNA by small gamma-radiation doses, *Int. J. Rad. Biol. Relat. Stud. Phys. Chem. Med.* 42, 407–415.
- Sequaris, J.-M., P. Valenta, H.W. Nurnberg and B. Malfoy, 1978, Voltammetric studies of the electrochemical and interfacial behavior of DNA at charged interfaces, *Bioelectrochem. Bioenerg.* 5, 483–503.

- Shi, Q.C., T.Z. Peng and S.F. Wang, 2003, Interaction of an irreversible electroactive drug-mitoxantrone and deoxyribonucleic acid, *Chinese J. Anal. Chem.* 31, 1212–1216.
- Scharer, O.D., 2003, Chemistry and biology of DNA repair, *Angew. Chem. Int. Ed.* 42, 2946–2974.
- Schrock, R.D., 3rd and R.S. Lloyd, 1993, Site-directed mutagenesis of the NH₂ terminus of T4 endonuclease. V. The position of the alpha NH₂ moiety affects catalytic activity, *J. Biol. Chem.* 268, 880–886.
- Schülein, J., B. Graßl, J. Krause, C. Schulze, C. Kugler, P. Müller, W.M. Bertling and J. Hassmann, 2002, Solid composite electrodes for DNA enrichment and detection, *Talanta* 56, 875–885.
- Sigman, D.S., 1990, Chemical nucleases, *Biochemistry* 29, 9097–9105.
- Siontorou, C.G., A.M.O. Brett and D.P. Nikolelis, 1996, Evaluation of a glassy carbon electrode modified by a bilayer lipid membrane with incorporated DNA, *Talanta* 43, 1137–1144.
- Stearns, D.M., L.J. Kennedy, K.D. Courtney, P.H. Giangrande, L.S. Phieffer and K.E. Wetterhahn, 1995, Reduction of chromium(VI) by ascorbate leads to chromium–DNA binding and DNA strand breaks *in vitro*, *Biochemistry* 34, 910–919.
- Stearns, D.M. and K.E. Wetterhahn, 1997, Intermediates produced in the reaction of chromium(VI) with dehydroascorbate cause single-strand breaks in plasmid DNA, *Chem. Res. Toxicol.* 10, 271–278.
- Stiborova, M., M. Rupertova, P. Hodek, E. Frei and H.H. Schmeiser, 2004, Monitoring of DNA adducts in humans and P-32-postlabelling methods. A review, *Collect. Czech. Chem. Commun.* 69, 476–498.
- Stiborova, M., V. Simanek, E. Frei, P. Hobza and J. Ulrichova, 2002, DNA adduct formation from quaternary benzo c phenanthridine alkaloids sanguinarine and chelerythrine as revealed by the P-32-postlabeling technique, *Chem. Biol. Interact.* 140, 231–242.
- Sufen, W., P. Tuzhi and C.F. Yang, 2002, Electrochemical studies for the interaction of DNA with an irreversible redox compound – Hoechst 33258, *Electroanalysis* 14, 1648–1653.
- Swaminathan, S. and J.F. Hatcher, 2002, Identification of new DNA adducts in human bladder epithelia exposed to the proximate metabolite of 4-aminobiphenyl using P-32-postlabeling method, *Chem. Biol. Interact.* 139, 199–213.
- Taban, I.C., R.K. Bechmann, S. Torgriksen, T. Baussant and S. Sanni, 2004, Detection of DNA damage in mussels and sea urchins exposed to crude oil using comet assay, *Mar. Environ. Res.* 58, 701–705.
- Tarlov, M.J. and A.B. Steel, 2003, DNA-based sensors. Biomolecular films, Design, Function, and Applications, Ed. J.F. Rusling, Marcel Dekker, New York, pp. 545–608.
- Teijeiro, C., P. Perez, D. Marin and E. Palecek, 1995, Cyclic voltammetry of mitomycin C and DNA, *Bioelectrochem. Bioenerg.* 38, 77–83.
- Thorp, H.H., 1998, Cutting out the middleman: DNA biosensors based on electrochemical oxidation, *Tibtech* 16, 117–121.
- Tocher, J.H., 2001, Selective interaction of tirapazamine with DNA bases and DNA – A comparison of cyclic voltammetry and electrolysis techniques, *Free Radical Res.* 35, 159–166.
- Tomschik, M., L. Havran, M. Fojta and E. Palecek, 1998, Constant current chronopotentiometric stripping analysis of bioactive peptides at mercury and carbon electrodes, *Electroanalysis* 10, 403–409.
- Vanickova, M., M. Buckova and J. Labuda, 2000, Voltammetric determination of azepine and phenothiazine drugs at DNA biosensors, *Chem. Anal.* 45, 125–133.
- Vanickova, M., J. Labuda, J. Lehotay and J. Cizmarik, 2003, Interaction of some esters of 2-, 3-, 4-alkoxyphenylcarbamic acids with surface-bound DNA at a dsDNA modified electrode – Study of local anaesthetics: Part 164, *Pharmazie* 58, 570–572.
- Vasquez, H., W. Seifert and H. Strobel, 2001, High-performance liquid chromatographic method with electrochemical detection for the analysis of *O*-6-methylguanine, *J. Chromatogr. B* 759, 185–190.

- Vinograd, J., J. Lebowitz and R. Watson, 1968, Early and late helix-coil transitions in closed circular DNA. The number of superhelical turns in polyoma DNA, *J. Mol. Biol.* 33, 173–197.
- Vojtiskova, M., E. Lukasova, F. Jelen and E. Palecek, 1981, Polarography of circular DNAs, *Bioelectrochem. Bioenerg.* 8, 487–496.
- Vorlickova, M. and E. Palecek, 1974, A study of changes in DNA conformation caused by ionizing and ultra-violet radiation by means of pulse polarography and circular dichroism, *Int. J. Radiat. Biol.* 26, 363–372.
- Wang, B.Q. and J.F. Rusling, 2003, Voltammetric sensor for chemical toxicity using Ru(bpy)₃(2)poly(4-vinylpyridine)(10)Cl (+) as catalyst in ultrathin films. DNA damage from methylating agents and an enzyme-generated epoxide, *Anal. Chem.* 75, 4229–4235.
- Wang, H.L., M.L. Lu, N. Mei, J. Lee, M. Weinfeld and X.C. Le, 2003a, Immunoassays using capillary electrophoresis laser induced fluorescence detection for DNA adducts, *Anal. Chim. Acta* 500, 13–20.
- Wang, J., 2000, From DNA biosensors to gene chips, *Nucleic Acids Res.* 28, 3011–3016.
- Wang, J., 2002, Electrochemical nucleic acid biosensors, *Anal. Chim. Acta* 469, 63–71.
- Wang, J., M. Chicharro, G. Rivas, X.H. Cai, N. Dontha, P.A.M. Farias and H. Shiraishi, 1996a, DNA biosensor for the detection of hydrazines, *Anal. Chem.* 68, 2251–2254.
- Wang, J., J.R. Fernandes and L.T. Kubota, 1998a, Polishable and renewable DNA hybridization biosensors, *Anal. Chem.* 70, 3699–3702.
- Wang, J., M. Jiang and A.N. Kawde, 2001, Flow detection of UV radiation-induced DNA damage at a polypyrrole-modified electrode, *Electroanalysis* 13, 537–540.
- Wang, J., M. Jiang and E. Palecek, 1999a, Real-time monitoring of enzymatic cleavage of nucleic acids using a quartz crystal microbalance, *Bioelectrochem. Bioenerg.* 48, 477–480.
- Wang, J., M. Ozsoz, X.H. Cai, G. Rivas, H. Shiraishi, D.H. Grant, M. Chicharro, J. Fernandes and E. Palecek, 1998b, Interactions of antitumor drug daunomycin with DNA in solution and at the surface, *Bioelectrochem. Bioenerg.* 45, 33–40.
- Wang, J., E. Palecek, P.E. Nielsen, G. Rivas, X.H. Cai, H. Shiraishi, N. Dontha, D. Luo and P.A.M. Farias, 1996b, Peptide nucleic acid probes for sequence-specific DNA biosensors, *J. Am. Chem. Soc.* 118, 7667–7670.
- Wang, J., G. Rivas, X. Cai, E. Palecek, P. Nielsen, H. Shiraishi, N. Dontha, D. Luo, C. Parrado, M. Chicharro, P.A.M. Farias, F.S. Valera, D.H. Grant, M. Ozsoz and M.N. Flair, 1997a, DNA electrochemical biosensors for environmental monitoring. A review, *Anal. Chim. Acta* 347, 1–8.
- Wang, J., G. Rivas, X.H. Cai, M. Chicharro, C. Parrado, N. Dontha, A. Begleiter, M. Mowat, E. Palecek and P.E. Nielsen, 1997b, Detection of point mutation in the p53 gene using a peptide nucleic acid biosensor, *Anal. Chim. Acta* 344, 111–118.
- Wang, J., G. Rivas, D.B. Luo, X.H. Cai, F.S. Valera and N. Dontha, 1996c, DNA-modified electrode for the detection of aromatic amines, *Anal. Chem.* 68, 4365–4369.
- Wang, J., G. Rivas, M. Ozsoz, D.H. Grant, X.H. Cai and C. Parrado, 1997c, Microfabricated electrochemical sensor for the detection of radiation-induced DNA damage, *Anal. Chem.* 69, 1457–1460.
- Wang, J., B. Tian and E. Sahlin, 1999b, Integrated electrophoresis chips/amperometric detection with sputtered gold working electrodes, *Anal. Chem.* 71, 3901–3904.
- Wang, S., T. Peng and C.F. Yang, 2003c, Investigation on the interaction of DNA and electroactive ligands using a rapid electrochemical method, *J. Biochem. Biophys. Met.* 55, 191–204.
- Wang, S., T.Z. Peng and C.F. Yang, 2003d, Investigation of the interaction of DNA and actinomycin D by cyclic voltammetry, *J. Electroanal. Chem.* 544, 87–92.
- Wang, S.F., T.Z. Peng and C.F. Yang, 2003b, Electrochemical determination of interaction parameters for DNA and mitoxantrone in an irreversible redox process, *Biophys. Chem.* 104, 239–248.
- Wang, Y.S., J.S. Taylor and M.L. Gross, 1999c, Nuclease P1 digestion combined with tandem mass spectrometry for the structure determination of DNA photoproducts, *Chem. Res. Toxicol.* 12, 1077–1082.

- Weimann, A., D. Belling and H.E. Poulsen, 2002, Quantification of 8-oxo-guanine and guanine as the nucleobase, nucleoside and deoxynucleoside forms in human urine by high-performance liquid chromatography-electrospray tandem mass spectrometry, *Nucleic Acids Res.* 30.
- Wu, J., Y. Huang, J. Zhou, J. Luo and Z. Lin, 1997, Electrochemical behaviors of DNA at mercury film electrode, *Bioelectrochem. Bioenerg.* 44, 151–154.
- Xu, J.H., J.J. Zhu, Y.L. Zhu, K. Gu and H.Y. Chen, 2001, A novel biosensor of DNA immobilization on nano-gold modified ITO for the determination of mifepristone, *Anal. Lett.* 34, 503–512.
- Xu, X.H. and A.J. Bard, 1995, Immobilization and hybridization of DNA on an aluminum(III) alkanebisphosphonate thin film with electrogenerated chemiluminescent detection, *J. Am. Chem. Soc.* 117, 2627–2631.
- Yang, I.V. and H.H. Thorp, 2001, Modification of indium tin oxide electrodes with repeat polynucleotides: Electrochemical detection of trinucleotide repeat expansion, *Anal. Chem.* 73, 5316–5322.
- Yang, J. and J.F. Rusling, 2002, Detection of DNA damage from enzyme-generated toxic metabolites using ultra-thin films and voltammetry, *Chem. Res. Toxicol.* 15, 1659–1660.
- Yang, J., Z. Zhang and J.F. Rusling, 2002, Detection of chemically induced damage in layered DNA films with Co(bpy)(3)(3+) by square-wave voltammetry, *Electroanalysis* 14, 1494–1500.
- Yang, Z.S., Y.L. Wang and Y.Z. Zhang, 2004, Electrochemically induced DNA cleavage by copper-bipyridyl complex, *Electrochem. Commun.* 6, 158–163.
- Yau, H.C.M., H.L. Chan and M.S. Yang, 2003, Electrochemical properties of DNA-intercalating doxorubicin and methylene blue on *n*-hexadecyl mercaptan-doped 5'-thiol-labeled DNA-modified gold electrodes, *Biosens. Bioelectron.* 18, 873–879.
- Yosypchuk, B., M. Fojta, L. Havran, M. Heyrovsky and E. Palecek, 2005, Voltammetric behavior of osmium-labeled DNA at silver solid amalgam electrode. Detecting DNA hybridization, *Electroanalysis* (submitted) in press.
- Yosypchuk, B., M. Heyrovsky, E. Palecek and L. Novotny, 2002, Use of solid amalgam electrodes in nucleic acid analysis, *Electroanalysis* 14, 1488–1493.
- Yosypchuk, B. and L. Novotny, 2002a, Electrodes of nontoxic solid amalgams for electrochemical measurements, *Electroanalysis* 14, 1733–1738.
- Yosypchuk, B. and L. Novotny, 2002b, Nontoxic electrodes of solid amalgams, *Crit. Rev. Anal. Chem.* 32, 141–151.
- Zhang, H.M. and N.Q. Li, 2000, Electrochemical studies of the interaction of adriamycin to DNA, *J. Pharm. Biomed. Anal.* 22, 67–73.
- Zhou, L.P., J. Yang, C. Estavillo, J.D. Stuart, J.B. Schenkman and J.F. Rusling, 2003, Toxicity screening by electrochemical detection of DNA damage by metabolites generated *in situ* in ultrathin DNA-enzyme films, *J. Am. Chem. Soc.* 125, 1431–1436.

This page intentionally left blank

Sensors for Genotoxicity and Oxidized DNA

James F. Rusling

Department of Chemistry, University of Connecticut, Storrs, CT 06269-3060 and Department of Pharmacology, University of Connecticut Health Center, Farmington, CT 06032, USA

Contents

1. Introduction	433
2. Constructing ultrathin sensor films	434
3. Voltammetric sensors for screening toxicity	438
3.1. Sensors without enzymes	438
3.2. Sensors providing bioactivation	441
3.3. Electrochemiluminescence (ECL) detection	443
4. Sensors for oxidized DNA	444
4.1. Voltammetric sensors	444
4.2. ECL sensors	446
5. Summary and outlook for the future	448
Acknowledgments	448
References	449

1. INTRODUCTION

The preceding chapter in this book provides an excellent overview and review of electrochemical methods to detect DNA damage (Fojta, 2005). It also contains short summaries of DNA damage and repair processes, and mentions alternative methods of detecting DNA damage. The present shorter chapter focuses on the development of sensors based on ultrathin films of DNA and other functional polymeric materials on carbon electrodes designed to detect DNA damage or oxidation as a basis for screening chemicals for toxicity or for clinical screening of oxidative stress.

Genotoxicity refers to a major toxicity mechanism involving reactions of molecules or their enzyme-generated metabolites with DNA, often producing covalently bound nucleobase adducts (Singer and Grunberger, 1983; Friedberg, 2003; Scharer, 2003). DNA adducts can initiate complex processes leading to carcinogenesis. *Oxidative stress* involves oxidation of biomolecules by reactive oxygen species, a sort of “oxygen biochemistry gone wrong” scenario that is often indicative of certain disease states. Genotoxicity and oxidative stress have DNA damage in common (Lindahl, 1993). Toxic chemicals and their metabolites generated by cytochrome P450 (cyt P450) enzymes in the liver can form covalent adducts with DNA in a major pathway of chemical toxicity (Jacoby, 1980). Examples of this genotoxicity pathway are presented by styrene,

benzo[a]pyrene, naphthylamines, and many others (Bond, 1989; Pauwels *et al.*, 1996; Cavalieri *et al.*, 1990), in which the metabolites are oxidized forms of their parents that react mainly with guanine and adenine moieties in DNA. Adducts of these toxic metabolites with DNA bases are biomarkers for human cancer risk (Phillips *et al.*, 2000; Warren and Shields, 1997).

Oxidative stress is strongly linked with the oxidation of DNA bases. Oxidation generates lesions that may contribute to aging and mutagenesis (Shigenaga and Ames, 1991). Guanine is the most easily oxidized DNA base, and its oxidation product 8-oxoguanine (8-oxoG) is a major biomarker of oxidative stress. DNA oxidation occurs from ionizing radiation resulting in water radiolysis and attack by the resulting hydroxyl radicals as well as attack by reactive oxygen species (Halliwell and Gutteridge, 1984; Cadet *et al.*, 1999) including singlet oxygen, superoxide and hydroxyl radicals.

DNA adducts and oxidation products can be determined accurately by separation-detection schemes involving LC-MS, LC-EC, and CE-MS (LC = liquid chromatography; MS = mass spectrometry; EC = electrochemical detection; CE = capillary electrophoresis). However, as discussed in the preceding chapter (Fojta, 2005), these methods require time-consuming hydrolysis, and workup of the DNA, and the instrumentation is expensive. Thus, simple, inexpensive sensors for DNA damage and oxidation that can be applied for screening the toxicity of new chemicals and monitoring oxidative stress would be valuable diagnostic tools. This chapter discusses recent progress toward developing such sensors in our laboratory based on detecting chemical changes in DNA by catalytic voltammetry using sensors consisting of electrodes coated with ultrathin films designed for the required task.

First, assembly of the ultrathin sensor films by layer-by-layer alternate electrostatic assembly is discussed. Next, recent applications to the electrochemical and electrochemiluminescent detection of toxic molecules and their metabolites is summarized. Finally, the specific detection of oxidized DNA by electrochemical and electrochemiluminescent sensors is discussed.

2. CONSTRUCTING ULTRATHIN SENSOR FILMS

The present chapter discusses sensors for screening the toxicity of new chemicals and for oxidative stress based on films containing the required enzyme and/or catalytic activity. Versatile, stable, films suitable for these purposes were made by using layer-by-layer alternate polyion assembly (Decher, 1997; Lvov, 2001). In this approach, films of nanometer-scale thickness were assembled by electrostatic adsorption of alternately charged layers of DNA and polyelectrolytes including redox polymers, enzymes, proteins, or synthetic polyions. These films have excellent stability, and their architecture is designed and controlled on the nanometer scale. The control of film thickness to a range <40 nm in electroanalytical sensors can minimize limitations from reactant and product mass transport to provide optimized performance.

Film construction features a series of simple adsorption steps in which the oppositely charged macromolecules (e.g. DNA, enzymes, and polyions) are

layered alternately onto an electrode from aqueous solutions. Our electrodes typically are pyrolytic graphite (PG), used for its excellent adhesive properties. PG has a negative surface charge by virtue of oxygenic surface groups. It can also be oxidized chemically or electrochemically to increase the negative surface charge density (Zhou *et al.*, 2003). However, this is not always necessary since many positive or negative polyions will adsorb onto its roughened, unoxidized surface (Ma *et al.*, 2000; Rusling and Zhang, 2003).

As an example of film construction, a mechanically roughened PG electrode is dipped into an aqueous $1\text{--}3\text{ mg mL}^{-1}$ polycation solution, and steady-state adsorption is achieved in 15–20 min that is typical for almost any polyion at this concentration range (Lvov, 2001). The surface is washed with water, and is now positively charged because of excess charge at the surface of the adsorbed polycation layer (Figure 1). This new electrode is then dipped into a solution of polyanion, which may be an enzyme or DNA, and a new layer is adsorbed that will have a negative surface charge. After washing, the DNA and enzyme adsorption steps are repeated several times until the required number of DNA/enzyme bilayers are achieved. For enzymes and DNA samples that are expensive or in short supply, adsorption steps can be done from a single 10–30 μL drop placed on the electrode surface. Other types of polyions can be used to achieve the desired film architecture. Very stable films are obtained because the strongest interactions between layers are selected at each adsorption step, and

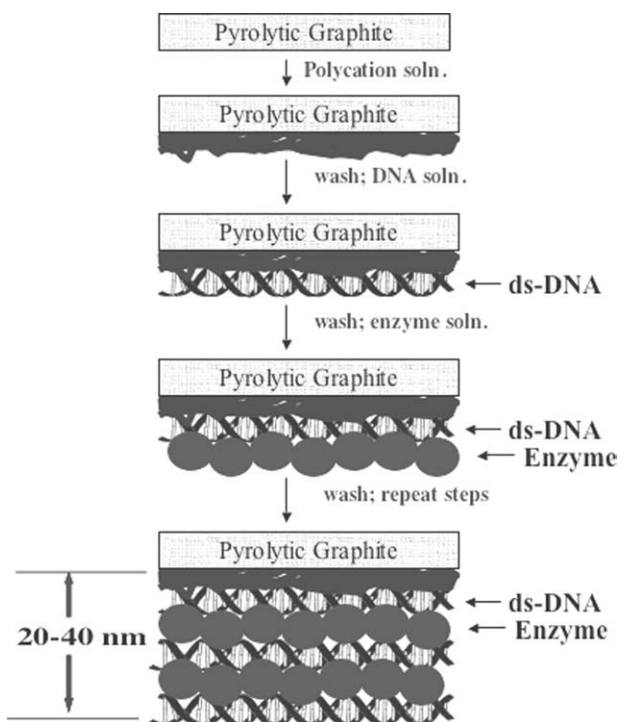


Fig. 1. Conceptual depiction of film construction for a toxicity screening sensor. The initial polycation layer could be inert or a redox catalytic polyion.

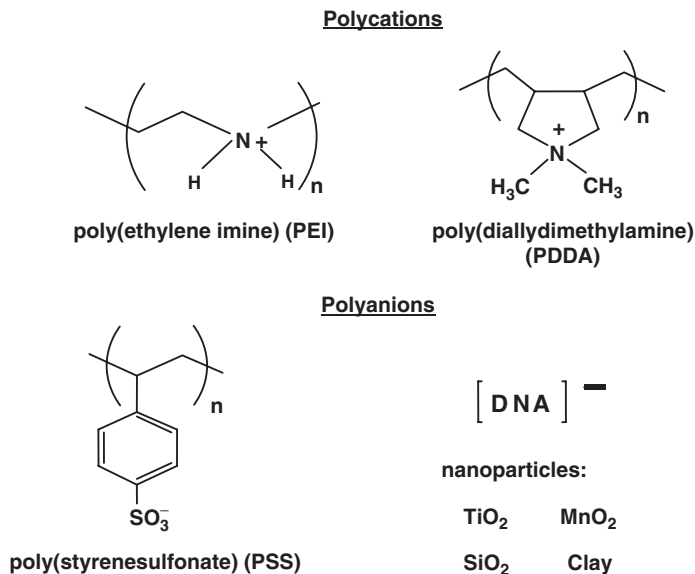


Chart 1. Some ionic polymers used for film formation.

weakly adsorbed molecules are removed in the washing steps. The technique can be automated, and has been used to make ultrathin films of a wide variety of proteins and oppositely charged polyions including DNA (Lvov, 2001). Some polyions that have been used in such films are shown in Chart 1.

It is important to address quality control of film assembly by monitoring layer growth during or after each adsorption step, especially for films being designed for the first time. This analysis can be done by quartz crystal microbalance (QCM) weighing, surface plasmon resonance, spectroscopy, voltammetry, or other appropriate methods. The use of QCM for assembly monitoring is illustrated in Figure 2 for DNA-polyion and DNA-myoglobin films grown on gold-coated quartz resonators. The frequency of the resonator decreases in direct proportion to the mass per unit area (M/A) of the gold coating, provided the viscoelasticity of the interface is constant (Buttry and Ward, 1992). Drying the film after each assembly step minimizes interfacial viscoelasticity changes and removes water. For 9 MHz quartz resonators, M/A (g cm^{-2}) is proportional to the QCM frequency shift ΔF (Hz) according to:

$$M/A = -\Delta F(1.83 \times 10^8), \quad (1)$$

where the area (A) is that of the gold disk on the resonator in cm^2 . A relation between nominal film thickness (d) and ΔF from QCM was validated by comparison of estimates based on measured mass and component density with high-resolution scanning electron microscope measurements of cross-sectional thickness for films of a variety of polyions, proteins, and nanoparticles (Lvov, 2001):

$$d(\text{nm}) \approx -(0.016 \pm 0.002)\Delta F(\text{Hz}). \quad (2)$$

Ordinary basal plane PG surfaces have a significant fraction of oxygenation, especially when mechanically roughened. In QCM experiments, the oxygen-rich PG electrode surface can be approximated by chemisorbing a mixed monolayer of 30/70 mercaptopropionic acid/mercaptopropanol onto the gold QCM resonator surface (Zhou and Rusling, 2001). After attaching such a monolayer, the surface exposed to the first polyion adsorption step is partly negative by virtue of dissociated carboxylic acid residues, similar to PG. This layer of chemisorbed organothiols corresponds to the first points in Figure 2, i.e. to layer 1. The film compositions in Figure 2 in the order of adsorption of the layers in an acronymic notation are: PDDA/PSS/CIRu-PVP/CT-ds-DNA/(Mb/CT-ds-DNA)₂ and PDDA/PSS/CIRu-PVP/CT-ds-DNA/PDDA/CT-ds-DNA. CIRu-PVP represents [Ru(bpy)₂poly(4-vinylpyridine)₁₀Cl]⁺, a metallopolycation catalyst for DNA oxidation, Mb is the model enzyme myoglobin, and the other acronyms are given in Chart 1. Equations (1) and (2) can be used with the QCM data to obtain nominal film thicknesses and component weights. The film represented in Figure 2 without Mb is ~15 nm thick and contains 0.2 μg DNA in the sensor film. The sensor films made with Mb are ~25 nm thick and contain 0.25 μg DNA. Films thickness depends critically on enzyme size so that equivalent films made with the larger cyt P450 enzymes rather than Mb are ~40 nm thick (Zhou *et al.*, 2003).

Although components in the films are adsorbed one at a time, individual layers are intimately mixed as confirmed by neutron reflectivity studies on protein films made with deuterium-labeled polyions that confirmed extensive mixing among neighboring layers (Lvov, 2001). The layers must be more

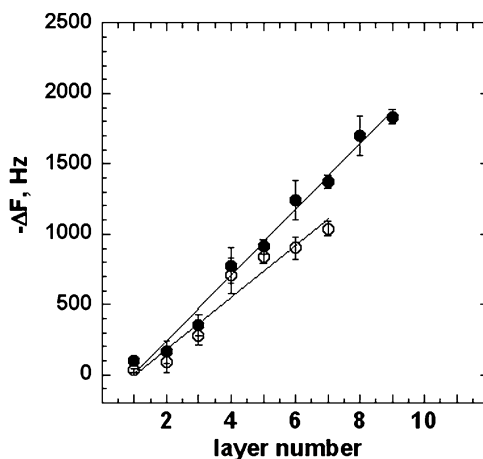


Fig. 2. QCM frequency shifts for cycles of alternate Mb/CT-ds-DNA and PDDA/CT-ds-DNA adsorption on gold resonators coated with mixed monolayers of mercaptopropionic acid/mercaptopropanol (first point) as first layer and PDDA/PSS as second and third layers. Final films are PDDA/PSS/CIRu-PVP/CT-ds-DNA/(Mb/CT-ds-DNA)₂ (●) and PDDA/PSS/CIRu-PVP/CT-ds-DNA/PDDA/CT-ds-DNA (○) (Average values for five replicate films). Reproduced with permission from Wang B. and J. F. Rusling, 2003, *Anal. Chem.* 75, 4229–4235. Copyright American Chemical Society.

extensively mixed than depicted by the bottom diagram of [Figure 1](#), or sensing schemes involving redox polymer catalyst as the initially deposited layer would not work very well since the outer DNA layer would be too far away from the catalyst sites for efficient reactions.

3. VOLTAMMETRIC SENSORS FOR SCREENING TOXICITY

3.1. Sensors without enzymes

The use of potential new drugs, agricultural pesticides, and other chemicals would lead to human exposure to these substances. Thus, to insure public safety, these materials must be tested for toxicity before full commercialization. Usual protocols involve microbiological testing followed later by extensive animal tests. While advances in speed and automation, as well as alternative approaches are on the horizon for toxicity testing, the traditional approaches remain expensive and time consuming. Consequently, most product development scenarios delay toxicity testing until reasonable indications of efficacy have been found. Thus, a considerable financial outlay may have been made before any toxicity testing has been done. Toxicity issues are thought to defeat 30–40% of all new drug candidates.

Rapid, inexpensive screening tests that could be used at very early stages of the commercial development of a chemical product would be extremely useful. Inexpensive screening might eliminate seriously toxic chemicals from further development, thus decreasing the cost of bringing new drugs and agricultural chemicals to the marketplace. Our sensors have been designed to combine enzyme bioactivation of the chemicals in the presence of DNA with measurement of DNA damage from the resulting metabolites. Certainly, all commercially viable candidates would still need to undergo microbiological and animal testing before final marketing approval, but effective screening could decrease cost by greatly decreasing the number of candidates that make it to the biological toxicity testing stage.

The principle of DNA detection in most of our toxicity sensors involves electrochemical oxidation of DNA. Guanine has an oxidation potential of 1.06 V vs. SCE at pH 7 ([Steenken and Jovanovic, 1997](#)) and is the most easily oxidized DNA base. Single-stranded (ss) DNA is more easily oxidized at guanine or adenine sites than double-stranded (ds) DNA ([Palecek, 1996](#); [Palecek and Fojta, 2001](#)) because of better accessibility of the bases to electrodes or oxidation catalysts. When the bases are internal in the helical ds-DNA structure, access to oxidizing agents is limited. As the double helix unwinds, closer access to the nucleobases is facilitated, leading to faster reaction rates and larger electrochemical signals, especially in catalytic voltammetry. Chemical DNA damage unwinds the double helix partly, and thus, also provides better access to the bases.

Sensitive DNA detection can be achieved by oxidation with soluble ([Johnston *et al.*, 1995](#); [Thorpe, 1998](#)) or polymeric ([Mugweru and Rusling, 2000](#)) ruthenium



Scheme 1.

complexes. For example, $\text{Ru}(\text{bpy})_3^{2+}$ (bpy = 2,2'-bipyridine) oxidizes only guanine bases in DNA by electrochemical catalysis (Johnston *et al.*, 1995). The reaction follows the pathway in Scheme 1.

$\text{Ru}(\text{bpy})_3^{2+}$ is oxidized by the electrode to give $\text{Ru}(\text{bpy})_3^{3+}$ (equation (3)), which reacts with DNA to give guanine radical $\text{DNA}(\text{guanine}_{\text{ox}})$ (Weatherly *et al.*, 2001) in a fast proton-coupled chemical step (equation (4)). This reaction recycles $\text{Ru}(\text{bpy})_3^{2+}$ to equation (3), providing greatly enhanced voltammetric current over that of $\text{Ru}(\text{bpy})_3^{2+}$ or DNA alone. Peak current in voltammetry increases as the rate of the chemical step in equation (4) increases. Guanine in ss-DNA reacts much more rapidly than in ds-DNA because of better accessibility, and the reaction rate at a given guanine site depends on the sequence of neighboring bases.

In the early stages of sensor development, we evaluated a number of approaches for voltammetric DNA detection. Films for this purpose were assembled with DNA but no enzymes, using the polycation PDDA as “glue” to bind the negative DNA layers together. These films were incubated with known DNA damage agents such as styrene oxide (Zhou and Rusling, 2001) and methylating agents (Wang and Rusling, 2003), and the resulting response optimized. In this way, we could develop methods to detect DNA damage without the complication of enzyme-catalyzed metabolite generation. Successful approaches based on square wave voltammetry (SWV) included catalytic DNA oxidation with soluble $\text{Ru}(\text{bpy})_3^{2+}$ (cf. Scheme 1) (Zhou and Rusling, 2001), use of a catalytic polymer such as CIRu-PVP (see below) in the film (Wang and Rusling, 2003), and the use of electroactive probe ion $\text{Co}(\text{bpy})_3^{3+}$ (Yang *et al.*, 2002), which binds more strongly to intact ds-DNA than to damaged DNA. The best sensitivity was found with ds-DNA as the outer layer of the films at low salt concentration (e.g. 50 mM NaCl).

Figure 3 shows experiments in which sensors featuring $(\text{PDDA}/\text{ds-DNA})_2$ films were incubated in various solutions, washed, and then analyzed by SWV in buffer containing $50 \mu\text{M}$ $\text{Ru}(\text{bpy})_3^{2+}$. The catalytic oxidation peak increased with time of incubation with the DNA damage agent styrene oxide (Zhou and Rusling, 2001). Controls in which the sensor was incubated with unreactive toluene or buffer showed no significant differences from sensors that had not been incubated.

Typically, in these sorts of experiments, SWV peaks increased nearly linearly over ~ 10 min of reaction with the several epoxides and methylating agents tested thus far (Zhou and Rusling, 2001; Wang and Rusling, 2003, 2005). Incubation of styrene oxide with DNA and various polynucleotides indicated that the most likely sources of the catalytic peaks are oxidations of guanine and chemically damaged adenine in partly unraveled, damaged DNA (Zhou and Rusling, 2001).

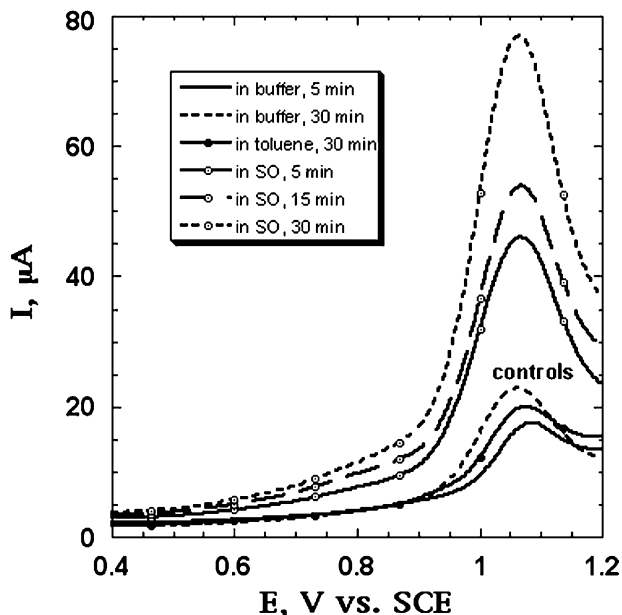


Fig. 3. SWV of $(\text{PDDA}/\text{ds-DNA})_2$ films on oxidized PG in pH 5.5 acetate buffer containing 50 mM NaCl with $50 \mu\text{M Ru}(\text{bpy})_3^{2+}$ in buffer, and after incubations at 37°C with styrene oxide (SO) or toluene. Reproduced with permission from Zhou, L. and J. F. Rusling, 2001, *Anal. Chem.* 73, 4780–4786. Copyright American Chemical Society.

To confirm that response was indeed caused by DNA adduct formation, sensor films that had been incubated with DNA damage agents were also analyzed by LC–MS to specifically detect damaged nucleobases. Neutral hydrolysis was used to remove N-7 adducts of guanine and N-3 adducts of adenine by heating of the DNA-polyion films, and the damaged nucleobase mixtures were analyzed by LC–MS (Tarun and Rusling, 2005). Results showed in general that concentrations of N-7-guanine adducts with methyl methane sulfonate (Figure 4) and styrene oxide increased with incubation time with remarkably similar trends as found for sensor response. This study also showed that PG electrodes give much better responses than carbon cloth for the sensors. Sensor data for epoxides and methylating agents correlated well with the amounts of damaged guanine, and with a measure of mutagenesis and carcinogenicity in rodents (Tarun and Rusling, 2005). Results showed that the genotoxicity sensors can be used to estimate relative DNA damage rates for chemical toxicity screening.

Incorporation of a catalytic polymer layer into the sensor films provides a “reagentless” sensor that avoids addition of a catalyst to the solution in the analysis step. Two polyions containing $\text{Ru}(\text{bpy})_2^{2+}$ were used to catalytically oxidize guanines in DNA (cf. Scheme 1). The polymer shown below in Scheme 2, denoted Ru-PVP, has six Ru–N bonds and gives reversible oxidation in films on PG electrodes at $\sim 1.15 \text{ V vs. SCE}$. This catalyst is capable of electrochemiluminescence (ECL) in thin films with DNA (Dennany *et al.*, 2003), as will be discussed later in this chapter.

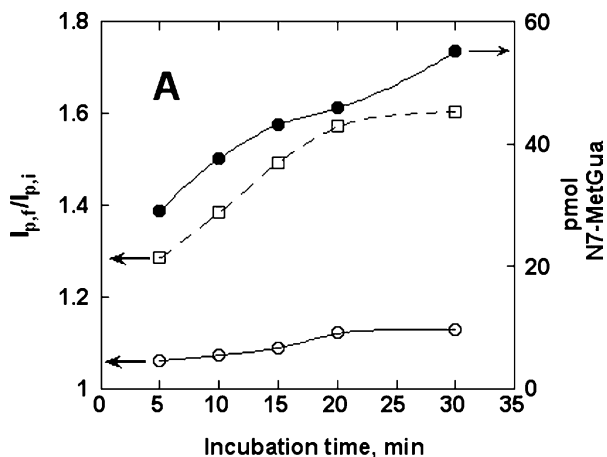
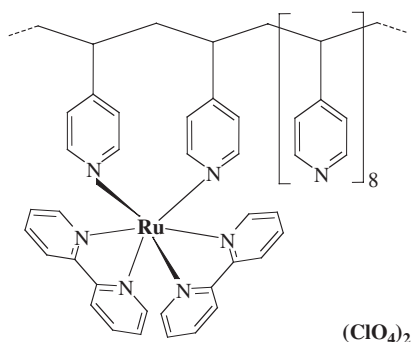


Fig. 4. Comparison of electrochemical toxicity sensor and LC-MS results. Peak current ratio $I_{p,f}/I_{p,i}$ (final/initial) for sensors made from $(\text{PDDA}/\text{ds-DNA})_2$ films on carbon cloth (○) and PG (□), and pmols of nucleobase adducts found by LC-MS (●) after incubation of sensors with 2 mM methyl methane sulfonate. LC-MS analysis was done after neutral thermal hydrolysis of the sensor films to release damaged nucleobases. Reproduced with permission from Tarun, M. and J. F. Rusling, 2005, *Anal. Chem.* 77, 2056–2062. Copyright American Chemical Society.



Scheme 2. Structure of catalytic metallopolymer $[\text{Ru}(\text{bpy})_2(\text{PVP})_{10}](\text{ClO}_4)_2$.

A similar polymer (cf. Figure 2) denoted RuCl-PVP has five Ru–N bonds and chloride as the sixth ligand, and does not provide ECL. It is reversibly oxidized at 0.75 V vs. SCE (Mugweru and Rusling, 2001, 2002), and provides more well-defined peaks on a flatter background at this lower voltage without sacrificing much sensitivity.

3.2. Sensors providing bioactivation

Many DNA-base adducts are formed from reactions with metabolites rather than the parent chemicals. Liver enzymes such as cyt P450s bioactivate

lipophilic chemicals to active metabolites that can covalently bind to DNA bases (Jacoby, 1980). For example, styrene is converted to styrene oxide, which forms nine or more adducts with guanine and adenine nucleobases in DNA (Bond, 1989; Pauwels *et al.*, 1996). Our toxicity sensors mimic these events in the liver by combining enzyme bioactivation with detection of the resulting DNA damage. To make these types of sensors, ultrathin films (20–40 nm thick) containing Mb or cyt P450_{cam} and DNA were grown layer by layer on electrodes (cf. Figure 1). Enzymes in the films were activated by hydrogen peroxide to produce metabolites that can react with ds-DNA as they diffuse out of the film. In the first demonstration of this approach, DNA damage was detected by SWV by using catalytic oxidation with dissolved Ru(bpy)₃²⁺ or via binding of Co(bpy)₃³⁺ to the outer DNA layer in the film (Zhou *et al.*, 2003). Later, enzyme-catalyzed bioactivation was detected by using an inner catalytic RuCl-PVP polymer layer in the sensor (Wang and Rusling, 2003).

Sensors using RuCl-PVP showed catalytic SWV peaks at 0.75 V vs. SCE that increased with time of the enzyme reaction (Figure 5). Here, myoglobin is used as an “enzyme model” to epoxidize styrene. The results suggest that ds-DNA in the film is damaged by styrene oxide. Control electrodes incubated with hydrogen peroxide and unreactive toluene showed catalytic oxidation peaks of similar heights to freshly prepared films. The low concentrations of hydrogen peroxide used to activate the enzymes had no influence on ds-DNA. Only peaks for films that had been activated by hydrogen peroxide and styrene together increased with reaction time.

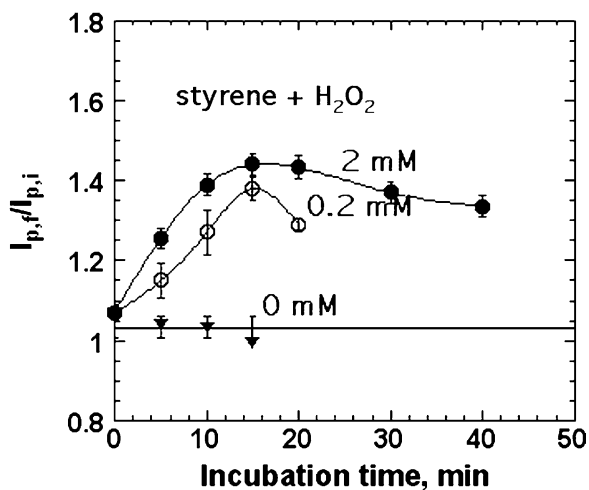


Fig. 5. Influence of incubation time on the catalytic peak ratio $I_{p,t}/I_{p,i}$ (final/initial) of PDDA/PSS/CIRu-PVP/CT-ds-DNA/(Mb/CT-ds-DNA)₂ films treated at pH 5.5 with 2 mM H₂O₂ and saturated styrene (●), 2 mM H₂O₂ and saturated toluene (▼), and 0.2 mM H₂O₂ and saturated styrene (○). Error bars show standard deviations for three trials. Reproduced with permission from Wang B. and J. F. Rusling, 2003, *Anal. Chem.* 75, 4229–4235. Copyright American Chemical Society.

Similar results were obtained using the bacterial enzyme *cyt P450_{cam}*. Sensors featuring DNA/*(cyt P450_{cam}/ST-ds-DNA)₂* films incubated with styrene and hydrogen peroxide showed a rapid increase in SWV peak current in the first 5 min of the enzyme reaction (Zhou *et al.*, 2003). No significant increases in peak current with enzyme reaction time were found for films incubated with toluene and hydrogen peroxide, styrene alone, benzaldehyde, or hydrogen peroxide alone for up to 30 min. These results are consistent with an increase in sensor response related to DNA damage.

An alternative method employing $\text{Co}(\text{bpy})_3^{3+}$ as an electroactive probe was used with the same types of enzyme/DNA films (Zhou *et al.*, 2003). $\text{Co}(\text{bpy})_3^{3+}$ reduction peaks at 0.04 V decreased as DNA was damaged by enzyme-generated styrene oxide since this complex binds better to intact than to damaged DNA (Yang *et al.*, 2002). Control incubations with unreactive controls or hydrogen peroxide showed little change in SWV peaks.

Catalytic SWV detection provided multiple measurements over 5 min of enzyme-catalyzed styrene epoxidation and was more sensitive than the $\text{Co}(\text{bpy})_3^{3+}$ binding assay. Nevertheless, the $\text{Co}(\text{bpy})_3^{3+}$ binding assay may be useful to avoid potential interferences in certain situations because of its low-measurement voltage where few electroactive species will interfere.

Polymorphism and induction of enzymes from chemical exposure lead to interindividual differences in levels and distributions of different *cyt P450s* in humans. These differences could predispose certain individuals to a higher risk of drug toxicity (Guengerich, 1989, 1993; Gonzalez, 1992). Thus it is important to identify, which human *cyt P450s* generate genotoxic metabolites. To address this issue, arrays with individually addressable electrodes coated with DNA/enzyme films as above can be used to estimate relative rates of genotoxic bioactivation. This approach was demonstrated for benzo[a]pyrene using different enzymes simultaneously. Specifically, *cyt P450_{cam}*, *cyt P450 1A2*, and Mb in an array were activated with H_2O_2 to metabolize benzo[a]pyrene. As above, DNA damage by the metabolites was detected by increases in SWV peak ratios using soluble $\text{Ru}(\text{bpy})_3^{2+}$ as catalyst (Figure 6) (Wang *et al.*, 2005). While the slopes of peak ratio vs. incubation time were similar for the three enzymes, measurements of protein concentration showed that there was much more Mb than *cyt P450s* in the respective films. When slopes of peak ratio vs. incubation time were divided by amount of enzyme, relative turnover rates in $(\text{nmol enzyme})^{-1} \text{min}^{-1}$ were 3.0 for *Cyt P450_{cam}*, 3.5 for *cyt P450 1A2*, and 0.9 for Mb. Thus, *cyt P450_{cam}* and *cyt P450 1A2* showed three-fold higher activity for genotoxic bioactivation of benzo[a]pyrene than Mb. The ability of the arrays to generate and detect metabolite-based DNA damage simultaneously for several enzymes represents a promising approach to identify and characterize enzymes involved in genotoxicity of drugs and pollutants.

3.3. Electrochemiluminescence (ECL) detection

Reaction of the Ru-PVP catalyst in Scheme 2 in thin films with DNA was shown to generate direct ECL (Dennany *et al.*, 2003). This provides another alternative

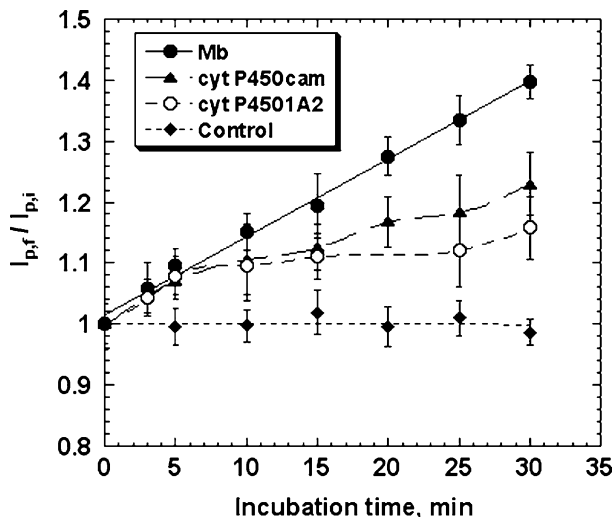


Fig. 6. Influence of incubation time with 50 μM benzo[a]pyrene and 1 mM H_2O_2 on the peak current ratios from SWV of PDDA/DNA/(enzyme/DNA)₂ films in an 8-electrode array. Control is PDDA/DNA/(Mb/DNA)₂ film in 50 μM benzo[a]pyrene alone (four replicates for Mb films, three each for cyt P450 films). Amounts of proteins in the films in nmol cm^{-2} were 0.26 for Mb, 0.060 for cyt P450_{cam}, and 0.054 for cyt P4501A2. Adapted with permission from Wang, B., I. Jansson, J. B. Schenkman and J. F. Rusling, 2005, *Anal. Chem.* 77, 1361–1367. Copyright American Chemical Society.

for detection of DNA hybridization and damage. In 10 nm thick films of cationic polymer $[\text{Ru}(\text{bpy})_2(\text{PVP})_{10}]^{2+}$ assembled layer by layer with DNA, a square wave voltammetric waveform was used to oxidize Ru^{II} sites in the metallopolymer to Ru^{III} , which oxidizes DNA. ECL was measured simultaneously with catalytic voltammetric peaks at ~ 1.15 V (Figure 7) in a simple apparatus utilizing an optical fiber positioned under the electrode outside the cell, and connected to a monochromator and photomultiplier tube. ECL was observed only when guanine bases were present in oligonucleotides in the films. This result suggested that guanine radicals initially formed by catalytic oxidation of guanines in DNA by Ru^{III} react with the metallopolymer to produce electronically excited $\text{Ru}^{\text{II}*}$ sites in the film. Simultaneous linear growth of ECL and SWV peaks occurred after incubation with known DNA damage agent styrene oxide over 20 min. The estimated detection limit was one damaged DNA base in one thousand. Control incubations of metallopolymer/ds-DNA films in buffer containing unreactive toluene resulted in no significant changes of the ECL or SWV peaks.

4. SENSORS FOR OXIDIZED DNA

4.1. Voltammetric sensors

When DNA is oxidized, a major initial product is 8-oxoG, which is an important biomarker for oxidative stress (Shigenaga and Ames, 1991).

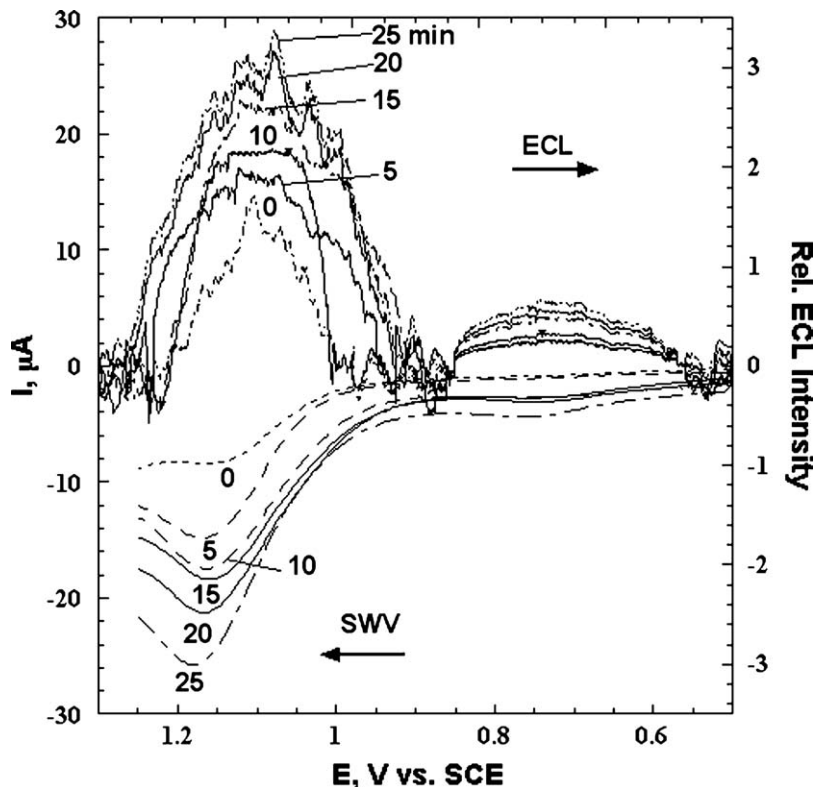


Fig. 7. SWV and ECL responses for $(\text{Ru-PVP/ds-CT DNA})_2$ films on PG electrodes in pH 5.5 buffer + 50 mM NaCl after incubations 37°C with saturated styrene oxide. Numerical labels are incubation times in minutes. Adapted with permission from Dennany, L., R. J. Forster, J. F. Rusling, 2003, *J. Am. Chem. Soc.* 125, 5213–5218. Copyright American Chemical Society.

Electrochemical catalysis using $\text{Os}(\text{bpy})_3^{2+}$ selectively oxidizes 8-oxoG, but does not oxidize guanine or other DNA nucleobases (Ropp and Thorp, 1999). To make sensors to detect oxidized DNA, films of the metallopolymer $[\text{Os}(\text{bpy})_2(\text{PVP})_{10}\text{Cl}]^+$ (ClOs-PVP) and ClRu-PVP were used to monitor oxidized DNA in solution. Sensor films were prepared as $(\text{ClRu-PVP/PSS/ClOs-PVP})_2/\text{PSS}$ on PG electrodes. ClOs-PVP is an analogous metallopolymer to ClRu-PVP, but employs the osmium complex and has a much lower formal potential. The outer layer of polyanion PSS in the film serves to inhibit adsorption of negatively charged DNA from solution, so that the sensors are reusable.

SWV peaks for the $\text{Os}^{\text{II}}/\text{Os}^{\text{III}}$ redox couple were found at about 0.33 V vs. SCE and for the $\text{Ru}^{\text{II}}/\text{Ru}^{\text{III}}$ redox couple at 0.78 V (Figure 8A). Similar peaks were found when the sensor was placed into buffer containing DNA (Curve 8A.b). The Os^{II} SWV peak was nearly unchanged, but the Ru^{II} peak increased due to oxidation of guanines in the DNA according to Scheme 1. Fenton's reagent was used to generate hydroxyl radicals to oxidize DNA. When the sensor was placed into DNA solutions that had been oxidized by Fenton's

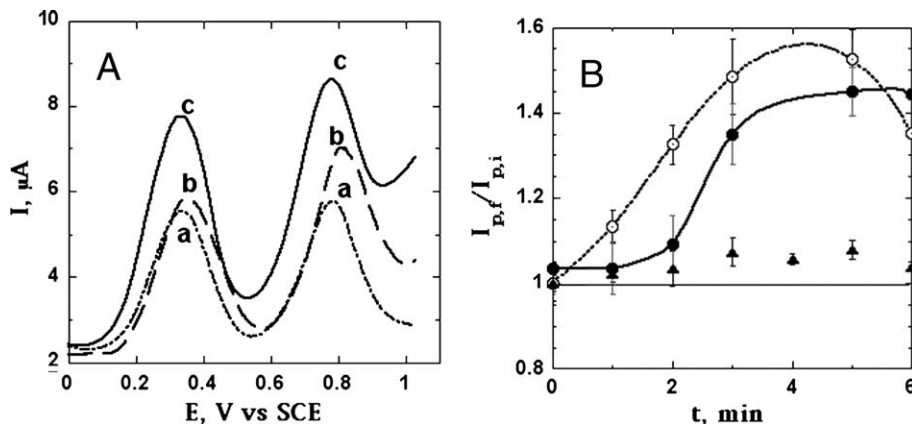


Fig. 8. Results for DNA oxidation sensors: (A) SWV at 15 Hz and 25 mV pulse height for (ClRu-PVP/PSS/ClOs-PVP)₂/PSS film (a) in pH 7.0 buffer, (b) in buffer + 0.2 mg mL⁻¹ CT ds-DNA (c) in buffer + 0.2 mg mL⁻¹ CT ds-DNA that had been incubated in Fenton reagent (0.15 mM FeSO₄ + 50 mM H₂O₂ at 37°C) for 5 min. (B) Ratio of final to initial SWV peak currents of a (Ru-PVP/PSS/Os-PVP)₂/PSS film in solution of CT DNA after incubated with Fenton reagent at different times: Os peaks (○), Ru peaks (●), Os control incubated with 50 mM H₂O₂ without FeSO₄ (▲). Adapted with permission from Mugweru, A., B. Wang, J. F. Rusling, 2004, *Anal. Chem.* 76, 5557–5563. Copyright American Chemical Society.

reagent for 5 min, both the Os^{II} and Ru^{II} peaks increased (Curve 8A.c). The major cause for the increase of the Os^{II} peak was identified as the catalytic oxidation of 8-oxoG by the Os^{II}/Os^{III} redox sites in the film by studies with homogeneous polynucleotides of each of the four bases (Mugweru *et al.*, 2004). Only poly[G] gave large increases of the Os^{II} peak. The increase in the more positive Ru^{II} peak may result from the catalytic oxidation of other oxidized bases as well as DNA helix unwinding or strand cleavage.

The SWV peak ratio for Os^{II} increased linearly over the first 3 min of oxidation with Fenton's reagent at the Fe^{II} and hydrogen peroxide concentrations used (Figure 8B). Similar increases for Fenton-oxidized DNA in solution were observed on this timescale in a specific LC–EC determination of 8-oxoG after hydrolysis of the DNA (White *et al.*, 2003). These data showed that increases in the Os^{II} peak correlate well with the amounts of 8-oxoG in the oxidized DNA. Comparisons of LC–EC and sensor results suggested that the sensor can detect about one oxidized guanine per 6000 intact guanines in DNA. The increase in the Ru^{II} peak does not begin until after 2 min of reaction with hydroxyl radical under the given conditions (Figure 8B), suggesting observation of slower oxidation processes.

4.2. ECL sensors

Direct ECL from oxidized DNA was generated in ultrathin films of cationic polymer [Os(bpy)₂(PVP)₁₀]²⁺ [PVP = poly(vinyl pyridine)] assembled layer by layer with DNA or oligonucleotides. Electrochemically oxidized Os^{II} sites

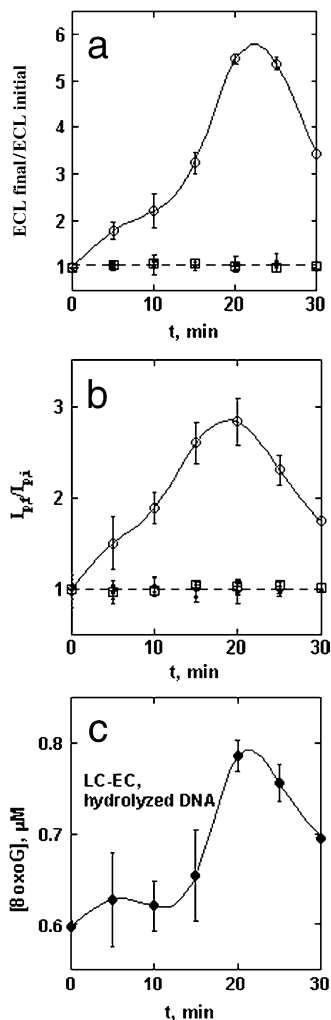


Fig. 9. Detection of DNA oxidation from reaction at 37°C with Fenton reagent (0.15 mM FeSO₄ and 5 mM H₂O₂) by three different methods. The top two graphs depict influence of incubation of (OsRu-PVP/ds-ST DNA)₂ sensors with Fenton reagent (○), with FeSO₄ alone (▲), H₂O₂ alone (□), and only pH 5.5 buffer (+) on (a) average ECL signals and (b) average SWV catalytic peak currents for the Os^{II}/Os^{III} redox couple ($n = 3$) (c) LC-EC determination of [8-oxoG] during oxidation of 1.2 mg mL⁻¹ ds-DNA in pH 5.5 by Fenton reagent under same conditions as for incubation of DNA electrodes ($n = 3$; DNA hydrolyzed before analysis). Adapted with permission from Dennany, L., R. J. Forster, B. White, M. Smyth and J. F. Rusling, 2004, *J. Am. Chem. Soc.* 126, 8835–8841. Copyright American Chemical Society.

generated ECL from films containing oxo-guanines on DNA formed by chemical oxidation using Fenton reagent (Dennany *et al.*, 2004). Peak ratios of both ECL and SWV had relatively similar shapes with incubation time with hydroxyl radicals (Figure 9a, b). Here, the concentration of hydrogen peroxide was smaller than in Figure 8 because the Os-PVP ECL polymer was more sensitive

to damage by Fenton's reagent than ClOs-PVP. Using these less-reactive conditions, the shapes of the ECL and SWV peak ratios at the Os potential were remarkably similar to each other and to the profile of 8-oxoG concentration vs. reaction time found after hydrolysis of the DNA and analysis by LC-EC (Figure 9c). These results suggest that the ECL sensor is measuring mainly 8-oxoG at the Os potential. Studies with oligonucleotides showed that films combining DNA, Ru-PVP, and Os-PVP had Os^{II} sites that produced ECL signals predominantly for 8-oxoG while Ru^{II} sites gave ECL from reaction with oxo-adenines, chemically damaged DNA, and possibly from cleaved DNA strands.

5. SUMMARY AND OUTLOOK FOR THE FUTURE

This chapter describes how sensors based on nanometer scale films of DNA, enzymes, polyions, and catalytic redox polyions can be designed for screening the toxicity of chemicals and their metabolites, and for oxidative stress. The unifying features of the approach include layer-by-layer sensor film assembly, and the electrochemical detection of DNA damage. Films containing DNA and enzymes enable detection of structural damage to DNA by SWV or ECL as a basis for toxicity screening. Sensors containing the appropriate enzymes can bioactivate chemicals to their metabolites that then may react with DNA. DNA damage can currently be detected at levels of about 0.5–1% by methods including catalytic SWV, ECL, or DNA binding probes. More importantly, sensor response vs. incubation time is a good relative estimate of the rate of nucleobase adduct formation.

Films of the osmium polymer ClOs-PVP can be used to selectively monitor DNA oxidation mainly at guanines, and Os-PVP/DNA films can be used to detect DNA oxidation by ECL. These methods may be adaptable to monitoring oxidized DNA as a clinical biomarker for oxidative stress.

An active and productive future is expected for applications of toxicity biosensors and sensors for oxidative stress. Sensor film construction is achievable by room temperature solution processing and is amenable to automation, perhaps by using robotic solutions spotters. Inexpensive sensor arrays could be developed to provide many toxicity screens simultaneously. As shown in one prototype example, future sensor arrays could be configured to detect toxicity of metabolites generated by a range of human cyt P450s.

ACKNOWLEDGMENTS

The research described herein was supported by US PHS grant No. ES03154 from the National Institute of Environmental Health Sciences (NIEHS), NIH, USA. The author is grateful for the excellent contributions of students and collaborators named in joint publications, without whom the research described would not have been possible.

REFERENCES

- Bond, J.A., 1989, Review of the toxicology of styrene, *Crit. Rev. Toxicol.* 19, 227–249.
- Buttry, D.A. and M.D. Ward, 1992, Measurement of interfacial processes at electrode surfaces with the electrochemical quartz crystal microbalance, *Chem. Rev.* 92, 1355–1379.
- Cadet, J., T. Delatour, T. Douki, D. Gasparutto, J.-P. Pouget, J.-L. Ravanat and S. Sauvaigo, 1999, Hydroxyl radicals and DNA base damage, *Mutat. Res.* 424, 9–21.
- Cavaliere, E.L., E.G. Rogan, P.D. Devaneshan, P. Cremonesi, R.L. Cerny, M.L. Gross and W.J. Bodell, 1990, Binding of benzo[*a*]pyrene to DNA by cytochrome p450 catalyzed one-electron oxidation in rat liver microsomes and nuclei, *Biochemistry* 29, 4820–4827.
- Decher, G., 1997, Fuzzy nanoassemblies, *Science* 277, 1231–1237.
- Dennany, L., R.J. Forster and J.F. Rusling, 2003, Simultaneous direct electrochemiluminescence and catalytic voltammetry detection of DNA in ultrathin films, *J. Am. Chem. Soc.* 125, 5213–5218.
- Dennany, L., R.J. Forster, B. White, M. Smyth and J.F. Rusling, 2004, Direct electrochemiluminescence detection of oxidized DNA in ultrathin films containing [Os(bpy)₂(PVP)₁₀]²⁺, *J. Am. Chem. Soc.* 126, 8835–8841.
- Fojta, M., 2005, Detecting DNA damage with electrodes *Electrochemistry of Nucleic Acids and Proteins*. In: Palecek, E., Scheller, F., Wang, J. (Eds.), Elsevier, Amsterdam, (this volume).
- Friedberg, E.C., 2003, DNA damage and repair, *Nature* 421, 436–440.
- Gonzalez, F.J., 1992, Human cytochromes P450: Problems and prospects, *Trends Pharm. Sci.* 13, 346–352.
- Guengerich, F.P., 1989, Polymorphism of cytochrome P450 in humans, *Trends Pharma. Sci.* 10, 107–109.
- Guengerich, F.P., 1993, Cytochromes P450 enzymes, *Am. Sci.* 81, 440–447.
- Halliwell, B. and M.C. Gutteridge, 1984, Oxygen toxicity, oxygen radicals, transition metals and disease, *Biochem. J.* 219, 1–14.
- Jacoby, W. B., Ed., 1980. *Enzymatic Basis of Detoxification*, Vols. I and II, Academic Press, New York.
- Johnston, D.H., K.C. Glasgow and H.H. Thorp, 1995, Electrochemical measurement of the solvent accessibility of nucleobases using electron transfer between DNA and metal complexes, *J. Am. Chem. Soc.* 117, 8933–8938.
- Lindahl, T., 1993, Instability and decay of the primary structure of DNA, *Nature* 362, 709–716.
- Lvov, Y., 2001, Thin-film nanofabrication by alternate adsorption of polyions, nanoparticles, and proteins, *Handbook of Surfaces and Interfaces of Materials*, Vol. 3. Nanostructured Materials, Micelles and Colloids, Ed. R.W. Nalwa, Academic Press, San Diego, pp. 170–189.
- Ma, H., N. Hu and J.F. Rusling, 2000, Electroactive myoglobin films grown layer-by-layer with poly(styrenesulfonate) on pyrolytic graphite electrodes, *Langmuir* 16, 4969–4975.
- Mugweru, A. and J.F. Rusling, 2001, Catalytic square-wave voltammetric detection of DNA with reversible metallopolymer-coated electrodes, *Electrochem. Commun.* 3, 406–409.
- Mugweru, A. and J.F. Rusling, 2002, Square wave voltammetric detection of chemical DNA damage with catalytic poly(4-vinylpyridine)-Ru(bpy)₂²⁺ films, *Anal. Chem.* 74, 4044–4049.
- Mugweru, A., B. Wang and J.F. Rusling, 2004, Detection of oxidized DNA by voltammetry using ultrathin films of [Os(bpy)₂(PVP)₁₀Cl]⁺ and [Ru(bpy)₂(PVP)₁₀Cl]⁺, *Anal. Chem.* 76, 5557–5563.
- Palecek, E., 1996, From polarography of DNA to microanalysis with nucleic acid-modified electrodes, *Electroanalysis* 8, 7–14.
- Palecek, E. and M. Fojta, 2001, Detecting DNA hybridization and damage, *Anal. Chem.* 73, 74A–83A.
- Pauwels, W., P. Vodicka, M. Servi, K. Plna, H. Veulemans and K. Hemminki, 1996, Adduct formation on DNA and hemoglobin in mice intraperitoneally administered with styrene, *Carcinogenesis* 17, 2673–2680.

- Phillips, D.H., P.B. Farmer, F.A. Beland, R.G. Nath, M.C. Poirier, M.V. Reddy and K.W. Turtletaub, 2000, Methods of DNA adduct determination and their application to testing compounds for genotoxicity, *Environ. Molec. Mutagen.* 35, 222–233.
- Ropp, P.A. and H.H. Thorp, 1999, Site-selective electron transfer from prunes to electrocatalysts: Voltammetric detection of a biologically relevant deletion in hybridized DNA duplexes, *Chem. Biol.* 6, 599–605.
- Rusling, J.F. and Z. Zhang, 2003, Designing functional biomolecular films on electrodes, *Biomolecular Films*, Ed. J.F. Rusling, Marcel Dekker, New York, pp. 1–64.
- Scharer, O.D., 2003, Chemistry and biology of DNA repair, *Angew. Chem. Int. Ed.* 42, 2946–2974.
- Shigenaga, M.K. and B.N. Ames, 1991, Assays for 8-Hydroxy-2'-deoxyguanosine: A biomarker of *in-vivo* oxidative DNA damage, *Free Radic. Biol. Med.* 10, 211–216.
- Singer, B. and D. Grunberger, 1983, *Molecular Biology of Mutagens and Carcinogens*, Plenum Press, New York.
- Steenken, S. and S.V. Jovanovic, 1997, How easily oxidizable is DNA: One-electron oxidation potentials of adenosine and guanosine radicals in aqueous solution, *J. Am. Chem. Soc.* 119, 617–618.
- Tarun, M. and J.F. Rusling, 2005, Quantitative measurement of DNA adducts using neutral hydrolysis and LC–MS. Validation of genotoxicity sensors, *Anal. Chem.* 77, 2056–2062.
- Thorp, H.H., 1998, Cutting out the middleman: DNA biosensors based on electrochemical oxidation, *Trends Biotechnol.* 16, 117–121.
- Wang, B., I. Jansson, J.B. Schenkman and J.F. Rusling, 2005, Evaluating enzymes that generate genotoxic benzo[a]pyrene metabolites using sensor arrays, *Anal. Chem.* 77, 1361–1367.
- Wang, B. and J.F. Rusling, 2003, Catalytic voltammetric sensor for DNA damage using $[\text{Ru}(\text{bpy})_2\text{poly}(4\text{-vinylpyridine})_{10}\text{Cl}]^+$ in layered DNA films. Damage from methylating agents and an enzyme-generated epoxide, *Anal. Chem.* 75, 4229–4235.
- Warren, A.J. and P.G. Shields, 1997, Molecular epidemiology: Carcinogen-DNA adducts and genetic susceptibility, *Proc. Soc. Exp. Biol. Med.* 216, 172–180.
- Weatherly, S.C., I.V. Yang and H.H. Thorp, 2001, Proton-coupled electron transfer in duplex DNA, *J. Am. Chem. Soc.* 123, 1236–1237.
- White, B., M.R. Smyth, J.D. Stuart and J.F. Rusling, 2003, Oscillating formation of 8-oxoguanine during DNA oxidation, *J. Am. Chem. Soc.* 125, 6604–6605.
- Yang, J., Z. Zhang and J.F. Rusling, 2002, Detection of chemically induced damage in layered DNA films with $\text{Co}(\text{bpy})_3^{3+}$ by square wave voltammetry, *Electroanalysis* 14, 1494–1500.
- Zhou, L. and J.F. Rusling, 2001, Detection of chemically induced DNA damage in layered films by catalytic square wave voltammetry using $\text{Ru}(\text{bpy})_3^{2+}$, *Anal. Chem.* 73, 4780–4786.
- Zhou, L., J. Yang, C. Estavillo, J.D. Stuart, J.B. Schenkman and J.F. Rusling, 2003, Toxicity screening by electrochemical detection of DNA damage by metabolites generated *in-situ* in ultrathin DNA-enzyme films, *J. Am. Chem. Soc.* 125, 1431–1436.

Electrochemical Immunosensors on the Route to Proteomic Chips

Axel Warsinke, Walter Stöcklein, Eik Leupold, Edith Micheel and Frieder W. Scheller

Department of Analytical Biochemistry, Institute of Biochemistry and Biology, University of Potsdam, Karl-Liebknecht-Strasse 24-25, D 14476 Golm, Germany

Contents

1. Introduction	451
2. From immunoassays to immunosensors	452
2.1. Coupling of binding assays with electrochemical indication	452
2.1.1. Antibodies : The recognition elements of immunoassays	452
2.1.2. Electrochemical indication	454
2.2. Electrochemical immunoassays	455
2.2.1. Enzyme-labeled electrochemical immunoassays	455
2.2.2. Redox-labeled immunoassays	458
2.3. Electrochemical immunosensors	463
2.3.1. Enzyme immunosensors	464
2.3.2. Redox-labeled immunosensors	467
2.3.3. Label-free immunosensors	469
3. Electronic protein chips	471
4. Summary and conclusion	475
List of abbreviations	476
Acknowledgments	477
References	477

1. INTRODUCTION

The successful elucidation of the human genome in 2000 has stimulated a new paradigm in life sciences. In the past, a sequential view from a given gene via a defined RNA to the protein was the typical object of investigations. At present a systemic approach – systems biology – has been created considering all genes, the total expressed RNA and the totality of proteins in a given system. This concept depends on a highly parallel analytical methodology, on the level of nucleic acids and proteins, and even metabolites and mediators (Figure 1).

For nucleic acids the development of biochips meets these requirements. In the near future the total genome of a species can be resequenced (or all expressed RNAs [the transcriptome] will be measured) by only applying one chip possessing several million spots.

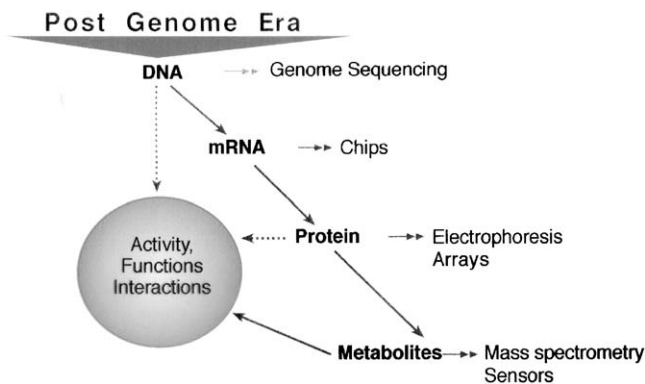


Fig. 1. Scheme of the used analytical methods for systems biology.

Systemic analysis on the protein level is considerably more complex due to the following features:

- (i) The number of different protein species is a multiple of the number of genes.
- (ii) The physico-chemical diversity of proteins, e.g. the isoelectric point, is more complex than that of nucleic acids consisting of 4(5) unique building blocks.
- (iii) Up to now no comparable methods to PCR for “protein amplification” have been found.
- (iv) Interactions between proteins cannot be reduced to a general code of “complementary” amino acids – like it works for nucleic acids – due to the highly complex three-dimensional structures. Therefore, specific binders, typically antibodies and, more recently, aptamers, must be prepared for each protein species of interest.

The aim of this chapter is to demonstrate how highly parallel protein analysis can be achieved by combining immunoassays and electrochemical biochip technology.

2. FROM IMMUNOASSAYS TO IMMUNOSENSORS

2.1. Coupling of binding assays with electrochemical indication

2.1.1. *Antibodies : The recognition elements of immunoassays*

Antibodies are considered to be well-suited recognition elements for bioassays and sensors. The high specificity and affinity of an antibody for its antigen allows a selective binding of the analyte (antigen) which occurs in the nano- to picomolar range in the presence of hundreds of other substances, even if they exceed the analyte concentration by 2–3 orders of magnitude.

An impressive example for the high specificity of an antiserum was already given by [Landsteiner and van der Scheer \(1928\)](#), when they demonstrated that an immunological method can select correctly between the optical isomers of phenyl- (*p*-aminobenzoylamino) acetate.

Thus, immunochemical analysis can handle samples without any analyte enrichment, purification or pretreatment, which is normally necessary for standard methods such as high-performance liquid chromatography (HPLC), mass spectrometry or gas chromatography. Especially for clinical diagnostics, where complex samples such as whole blood, serum or urine containing many different substances, such as proteins, amino acids, sugars, hormones etc., have to be analyzed, immunoassays have considerable advantages over standard methods with respect to time and sensitivity.

Moreover, recombinant antibody technology has now been developed to a level, which allows the expression of Fab or single-chain fragments (scFv) in *E. coli* in large quantities at an acceptable cost. In mammalian cell culture, the yield is about 0.5–1 g/L with costs of 300 £/g whereas in bacteria the yield can be as high as 3 g/L with costs of 1 £/g (Harris, 1999). However, in contrast to other bioanalytical methods such as enzymatic assays, where the enzymatic activity can often be followed directly via indication of the enzymatic product, the binding of an antigen to the appropriate antibody is accompanied by only small physico-chemical changes. In most of the existing immunoassays the binding event is visualized via an auxiliary reaction, in which one immunoreactant is labeled with a substance, which can easily be indicated by mostly spectrophotometric methods. The use of labels began when Yalow and Berson (1959) developed the first radioimmunoassay (RIA) with a radioactive compound as label. To date a huge number of different labels, including enzymes, fluorophors, redox compounds, cofactors, fluorescence quenchers, chemiluminescence metals, latex particles and liposomes have been applied in immunoassays (Blake and Gould, 1984).

In principle, immunoassays with labeled compounds are carried out in two different ways: (i) In competitive assays the labeled analyte competes with the analyte for the antigen binding sites of the antibody. The key feature of a competitive assay is that maximum assay sensitivity is attained using an amount of antibody tending to zero. The sensitivity of a competitive immunoassay is determined by the affinity of the antibody for its antigen. Since the affinity of an antibody can be in the range of 10^5 – 10^{12} M⁻¹ (Harlow and Lane, 1988) competitive immunoassays using antibodies with a $K_d = 10^{-12}$ M reach their highest sensitivity in the picomolar range. However, the lower detection limit can be decreased even further when appropriate assay conditions are chosen. (ii) In non-competitive assays (e.g. sandwich or sequential saturation assays) a significant excess of antibodies over the antigen is used. Here, diffusion processes are much more important than the affinity of the antibody used. While the lowest analyte concentration detectable using competitive design is in the order of 10^7 molecules/mL, a non-competitive method is potentially capable of measuring concentrations lower by several orders of magnitude (Ekins, 1989). In addition, due to the excess of one immunoreactant, non-competitive assays are normally much faster than their competitive counterpart.

Immunoassays have been adapted to highly sophisticated automated analyzers facilitating the analysis of a very large number of samples within a short time. Such analyzers can handle homogeneous or heterogeneous test formats, which are performed in plastic tubes or in wells of 96-, 384- or 1536-microtiter wells. To reduce costs and enhance throughput, nowadays with the help of

piezoelectrical pipetting systems and chip production technology, nanotiter plates that have an area of 2×2 cm and 625 wells with volumes of 50–100 nL have become popular.

While the goal of this technology is a high throughput of samples, the microspot assay or nanochip technology (Ekins and Chu, 1997) which is at present a fast developing technology, is focused on the detection of thousands of analytes in one sample.

In contrast to DNA analysis where different specificities can easily be predetermined by simple chemical synthesis of the nucleotide sequence, the generation of antibodies for each analyte needs much more efforts. However, in clinical diagnostics the need for the determination of such a large number of different analytes in any one patient is to date less obvious (Price, 1998). Since one immunoreactive spot on a chip usually has an area of $< 10 \mu\text{m}^2$ the benefit of this technology for immunochemical methods could be seen more in (i) a dramatic reduction of reagent consumption, (ii) in its use with cross-reactive antibodies for pattern recognition or (iii) in providing more exact results by highly multiple determinations. In Weller *et al.* (1999), described an optical immunoassay with 1600 spots per 1.8 cm^2 which can be used in environmental control for parallel determination of different pesticides. With a volume of 2 nL per spot of an antibody solution of $10 \mu\text{g/mL}$ and 1000 spots per chip the total amount of antibody per chip was calculated to be only 20 ng.

2.1.2. Electrochemical indication

Capacitive and potentiometric transducers can be used for real-time and label-free measurement of the antigen–antibody reaction. They are based on the principle that the electrode capacitance depends on the thickness and dielectric behavior of a dielectric layer on the surface of a metal plate. However, most of the electrochemical immunoassays and sensors use amperometric indication.

Since antibodies and antigens are usually not electrochemically active within the desired potential range redox-active compounds (redox label) or enzymes generating electrode-active species have to be applied as labels for amperometric indication. Thus amperometric immunoassays depend on auxiliary reactions. This has the advantage that unspecific binding of molecules other than the labeled immunoreactant will not contribute to the measuring signal.

The redox label for an amperometric immunoassay should have the following properties:

- (i) It should be electroactive in a potential range of -200 – 0 mV (Marko-Varga *et al.*, 1995).
- (ii) It should not cause electrode fouling.
- (iii) There should be no side reactions with the matrix.
- (iv) It should be stable in buffer.
- (v) Chemical groups for coupling should be available.

For an electrochemical enzyme immunoassay the labeling enzyme should fulfill the following requirements:

- (i) high catalytic activity k_{cat} ,
- (ii) generation of electrochemically active products with properties described above for the redox label,
- (iii) enzyme substrates and enzymes must be stable in buffer, and
- (iv) minimal, side reaction of the enzyme products.

In electrochemical binding assays similar principles (competitive, non-competitive) can be used as in conventional formats. Since the indication finally takes place at an interface of the transducer additional features can be used for designing separation-free assays.

2.2. Electrochemical immunoassays

2.2.1. Enzyme-labeled electrochemical immunoassays

In conventional immunoassays the application of enzymes has found widespread use. They produce products which can easily be determined spectrophotometrically or fluorometrically. In addition, due to the high catalytic power of enzymes they amplify the signal allowing detection limits down to the attomolar range (Bates, 1987). The catalytic power is clearly exemplified on alkaline phosphatase, an often used enzyme label. It is able to hydrolyze 500 molecules of *p*-nitrophenylphosphate to colored *p*-nitrophenol per second and enzyme molecule. Other effective enzyme labels are horseradish peroxidase (HRP), β -galactosidase, cholinesterase and glucose oxidase.

The enzyme-linked immunosorbent assay (ELISA), which has become the most successful standard enzyme immunoassay (EIA) is usually performed in a 96-well microtiter plate with immobilized antibodies or antigen, allowing the determination of a number of samples at once, which reduces the time per sample. After sequential incubations of sample, antibody– or antigen–enzyme conjugate and enzyme substrate reagents with washing steps in between the readout is performed by measuring the absorbance or fluorescence of each well with a standard microtiter plate reader. For heterogeneous EIAs, multiple incubation and washing steps are necessary which make automation and miniaturization difficult. Homogeneous EIAs, which can be carried out without any washing procedures are usually based on the modulation of enzymatic activity. Therefore, one immunoreactant is coupled with an enzyme (EMIT), substrate (SLFIA), inhibitor (EMMIA) or cofactor (ARIS), or immunoreactants are coupled with two cooperating enzymes (Channeling-EIA).

The most important homogeneous EIA is the enzyme multiplied immunoassay (EMIT) which was developed by Rubenstein *et al.* (1972) and has found practical application for the measurement of hormones. The principle is that if an antibody binds to an antigen–enzyme conjugate the conformation of the enzyme or the steric accessibility of the active site is changed, which is accompanied by a decrease in enzymatic activity. Usually, these assays are performed as competitive assays, resulting in a direct relationship of analyte concentration to the signal.

The easiest way to apply electrochemical methods to enzyme immunoassays is to work under standard ELISA or EMIT conditions but use an enzymatic reaction where the products can be monitored by potentiometric or amperometric transducers. The electrochemical transducer substitutes the microtiter plate reader which should reduce costs and allow measurements under field conditions. The electrodes can be integrated within the wells of microtiter plates or the enzymatic reaction products are transferred to an electrochemical measuring cell.

A number of publications describe highly sensitive amperometric determinations of the product of the reaction catalyzed by the enzyme label. Catalase is known to be one of the most active enzymes. Its catalytic reaction rate constant is approximately 10^5 s^{-1} . This enzyme was used as a marker for immunoanalysis in order to improve the sensitivity of labeled immunoagent determination (Ikariyama and Aizawa, 1988; Mirhabibollahi *et al.*, 1990b). An oxygen electrode was used for the detection of oxygen formed as a result of the enzymatic decomposition of hydrogen peroxide.

Alkaline phosphatase (aP) is one of the popular enzyme makers for immunoanalysis. This enzyme catalyzes a dephosphorylation reaction of different organic phosphates. Some of the products formed as a result of the reaction can be detected amperometrically in significantly low concentrations. This approach was introduced by Kulys *et al.* (1980). Successful development of the electrochemical immunoassay based on aP determination was achieved by W. R. Heineman and his co-workers (Tang *et al.*, 1988; Buckley *et al.*, 1989; Niwa *et al.*, 1993; Kaneki *et al.*, 1994). Instead of *p*-nitrophenylphosphate which is routinely used as the substrate in optical ELISA techniques *p*-aminophenylphosphate (*p*-APP) is applied for the electrochemical determination of aP. The alkaline phosphatase produces *p*-aminophenol (*p*-AP) which can be measured very sensitively at a glassy carbon electrode. Such an approach allows nanomolar concentrations of *p*-AP (Niwa *et al.*, 1993; Frew *et al.*, 1989; Meusel *et al.*, 1995) and phenol (Mirhabibollahi *et al.*, 1990a) to be detected amperometrically.

Phenylphosphate is much more stable than *p*-APP. The K_m of alkaline phosphatase was determined with $35 \mu\text{M}$ phenylphosphate. The turnover number k_{cat} is about $47,500 \text{ min}^{-1}$. Although the phenol produced can be measured amperometrically using an electrode potential of $+870 \text{ mV}$ (Wehmeyer *et al.*, 1986), more sensitive assays are possible using amplification by a tyrosinase/PQQ-dependent glucose dehydrogenase electrode. The lower detection limit ($> 3 \text{ SD}$) for phenol was 10 nM . The electrode response was linear between 20 and 1000 nM phenol (Scheller *et al.*, 2002).

Substrate cycling is a means well suited to achieve high sensitivity for the detection of marker enzymes. Here the product of the enzyme label is not only measured once but is reconverted to be measured again. There are analyte recycling systems known with electrochemical as well as optical detection. The sensitive measurement is not only dependent on a high amplification but also on stability and purity of the reagents.

The formation of NAD^+ from NADP^+ (Athey and McNeil, 1994), pyruvate from phosphoenolpyruvate (Makower *et al.*, 1994), phenol from phenyl phosphate (Bauer *et al.*, 1996) and aminophenol from aminophenylphosphate by the

aP label (Ghindilis *et al.*, 1995a; Bier *et al.*, 1996b) have been followed using enzymatic substrate recycling and electrodes. Besides, β -galactosidase can also be employed; here an aminophenylated galactoside is hydrolyzed.

Determination of goat IgG and human thyroid stimulating hormone (hTSH) has been performed in a sandwich-type immunoassay using an oligosaccharide dehydrogenase/laccase electrode (Bier *et al.*, 1996b). In a first investigation, aP has been used for the model compound IgG, and the liberation of *p*-aminophenol from *p*-aminophenyl phosphate was followed. This reaction, however, is known to suffer from drawbacks related to the limited stability of both *p*-aminophenyl phosphate and *p*-aminophenol in alkaline solution (Tang *et al.*, 1988). Therefore, a large blank signal, which in some cases exceeds the dynamic measuring range of the electrode, is obtained and the incubation time is limited. Furthermore, the use of aP requires a change of the pH between the immunoassay and the electrode reaction. Therefore, β -galactosidase label was used. Since the optimum pH of β -galactosidase is close to that of the bi-enzyme sensor (pH 6.5) the whole assay could be performed under the same conditions. The sensitivity of the total assay was comparable to that of the photometric test. For the determination of hTSH the sandwich-type assay has been performed using biotinylated tracer antibody and streptavidin- β -galactosidase conjugate. The measuring range extends from 0.0005 to 20 ng/mL with a detection limit of 0.3 pg/mL.

Bauer *et al.* (1996) used a tyrosinase and quinoprotein glucose dehydrogenase covered oxygen electrode as fast readout of a competitive immunoassay for the herbicide 2,4-D involving an aP label where phenyl phosphate is used as substrate for aP and the liberated phenol is indicated. The competitive immunoassay uses an immobilized antibody against 2,4-D in a microtiter plate. After competition between 2,4-D-aP conjugates and 2,4-D for 1 h and an intermediate washing step, substrate buffer has been added and transferred to a biosensor equipped with FIA after 2 min. This means a reduction of time if compared to overnight incubation, which is the time required for the standard optical method with *p*-nitrophenyl phosphate. The working range is about 0.1–10 μ g/L. The results are in good agreement with the optical reference method.

A fast and sensitive screening method for the repetitive analysis of cocaine was developed. This method, the amplified flow immunoassay (AFIA, Bauer *et al.*, 1998), consisted of three steps: first, the immuno-recognition, where cocaine binds to the aP-labeled antibody (*p*Ab-aP). Second, excess *p*Ab-aP is removed by a cocaine-modified affinity column. Third, the cocaine-*p*Ab-aP complex is detected in the column effluent.

Cocaine could be quantified between 0.38 and 3.2 nM. The lower detection limit 0.38 nM was calculated from the non-linear fit. The response time was 75 s after the injection of cocaine.

The performance of AFIA can be compared to a manually operated cocaine-immunoassay with off-line detection based on the same reagents (Eremenko *et al.*, 1998). A preincubated mixture of cocaine and *p*Ab-aP was injected there. The response time to cocaine of 1 h was decreased to 75 s for AFIA. This 50-fold acceleration was achieved avoiding dilution by on-line detection and integrating the multi-step manual protocol into one automated procedure with reduced times for immuno-recognition and label detection.

AFIA could perform more than 200 consecutive cocaine assays without regeneration of the affinity column. AFIA is 40 times more sensitive than the displacement flow immunosensor for cocaine (Ogert *et al.*, 1992). Both methods detect cocaine in similar times. But the lifetime of the displacement column is limited to 32 h or 5–15 cocaine injections. AFIA is the most sensitive and one of the fastest immunoassays for cocaine.

In commercially available amplified ELISA (AmpliQ from Dako, NovoClone AELIA from Novo BioLabs), INT-violet is used as the diaphorase substrate (Self, 1981; Johansson *et al.*, 1986). For the electrochemical approach ferricyanide was used. The ferrocyanide produced was indicated amperometrically. In similar configurations, ADH was replaced by formiate dehydrogenase, glucose dehydrogenase, carnithine dehydrogenase (Bergel *et al.*, 1989) or glycerol dehydrogenase (Tang and Johansson, 1995).

A special application of electrode supported EIA with potentiometric electrode is the commercially available Threshold Immuno-Ligand Assay System (Molecular Devices, USA). Here urease is used as the labeling enzyme. After incubation of the analyte-containing sample with urease- and avidin-labeled immunoreactants, the incubation mixture is passed through a filtration membrane with immobilized biotin. After washing, the membrane-bound urease is indicated by a light addressable potentiometric sensor (Olson *et al.*, 1990). Separation-free immunoassays are very attractive since no washing procedures are necessary. Athey *et al.* (1993) have adapted a commercially available EMIT (from Syva) –based on the modulation of the enzyme activity – for the competitive determination of theophylline in whole blood with theophylline-glucose-6-phosphate dehydrogenase conjugate. The produced NADH was determined by an amperometric detector at a potential of +150 mV *vs.* Ag/AgCl (Figure 2). Table 1 shows further examples of enzymes in electrochemical immunoassays.

2.2.2. Redox-labeled immunoassays

In non-amplified redox-labeled electrochemical immunoassays the indication of one antigen or antibody molecule will generate one signal equivalent. Since the sensitivity of an amperometric sensor for the redox label is in the lower micromolar range, this kind of assay only makes sense if the concentration of the analyte to be determined is also in that range. This is the case for instance for the determination of creatinine. In the so-called size exclusion redox-labeled immunoassay (SERI) creatinine from the sample competes with redox-labeled creatinine for the antigen binding sites of the antibody. Unbound conjugate passes through a membrane and is indicated at the electrode whereas antibody-bound conjugate is size excluded (Figure 3). This principle allows a homogeneous and therefore convenient determination of creatinine within the submicromolar to submillimolar range (Benkert *et al.*, 2000a). However, one drawback of SERI for creatinine is that the applied antibody concentration must be in the micromolar range which makes this kind of test very expensive especially if non-miniaturized measuring cells are used.

For more sensitive immunoassays, analyte accumulation or signal amplification principles are necessary. Bordes *et al.* (1997, 1999) used in a multi-analyte

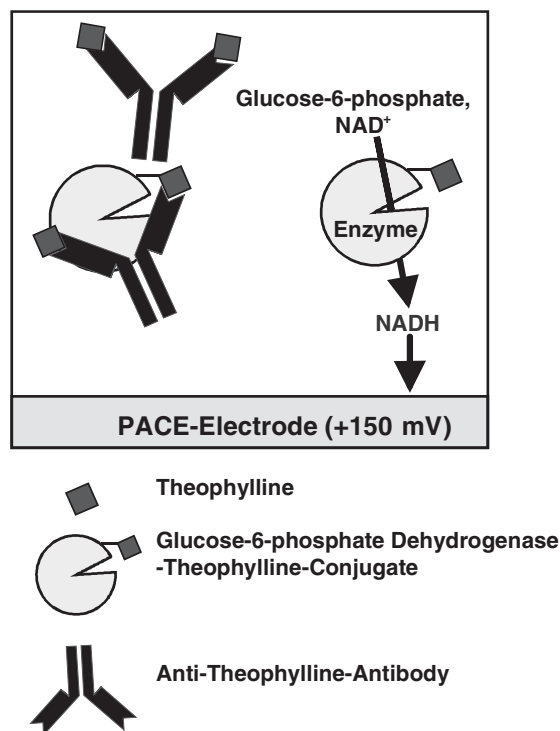


Fig. 2. Separation-free electrochemical immunoassay based on a conventional EMIT.

immunoassay, a 5-min preconcentration step of the cationic labels used (ferrocene ammonium salt with $E_p = +260$ mV, cobaltocenium salt with $E_p = -1.05$ V) at a negatively charged nafion-loaded carbon paste electrode resulting in a linear response down to 75 nM. However, to regenerate the sensor, the nafion-loaded carbon paste surface has to be renewed after each measurement.

Higher sensitivities are achieved when redox recycling is applied. Thereby the redox compound is oxidized and reduced in a cyclic manner so that the indication of one labeled antigen or antibody molecule will generate multiple signal equivalents. Redox recycling can be done in mainly three different ways by using electrode–electrode, electrode–enzyme or enzyme–enzyme couples.

Electrode–electrode coupling was used by Niwa *et al.* (1991), Wollenberger *et al.* (1994) and Hintsche *et al.* (1997) to enhance the sensitivity by one order of magnitude and to achieve thereby detection limits in the lower nanomolar range. Therefore, interdigitated array electrodes (IDA) with an electrode width of 1.5 mm and an interelectrode space of 0.8 mm were used. As the authors described, redox recycling with IDA can be used for the design of an electrode-supported ELISA (Figure 4) or for a separation-free displacement assay. Anti-hapten antibodies which have been coupled to small polymeric beads are saturated with hapten–ferrocene or hapten–peptide–ferrocene conjugates. The analyte (free hapten) displaces the conjugates which are then detected by the

Table 1. Representative examples of enzymes used in electrochemical immunoassays

Enzymes	Substrates	Products	Transducer	Reference
Glucose-6-phosphate-dehydrogenase	Glucose-6-phosphate + NAD ⁺	Gluconate-6-phosphate + <u>NADH</u>	Platinized carbon (+150 mV)	Athey <i>et al.</i> (1993)
Catalase	H ₂ O ₂	<u>O₂</u>	Clark electrode (−600 mV)	Aizawa <i>et al.</i> (1980)
Peroxidase	H ₂ O ₂ + iodide	<u>Iodine</u>	Highly dispersed carbon electrode (+127 mV)	Abdel-Hamid <i>et al.</i> (1999)
	H ₂ O ₂ + 5-aminosalicylic acid	<u>5-Aminosalicylic acid quinoneimine</u>	Graphite (0 mV)	Rishpon and Ivnitcki (1997)
	H ₂ O ₂ + hydroquinone	<u>Benzoquinone</u>	Graphite (−20 mV)	Ivnitski <i>et al.</i> (1998)
	H ₂ O ₂ + tetrathiafulvalene (TTF)	<u>TTF</u> ⁺	Screen-printed platinum (−600 mV)	Romero <i>et al.</i> (1998)
Microperoxidase	H ₂ O ₂ + electrode	2 e [−]	Graphite methacrylate (−100 mV)	Santadreu <i>et al.</i> (1999)
Alkaline phosphatase	Glucose-6-phosphate	<u>Glucose</u> + phosphate	Glassy carbon (+20 mV)	Wendzinski <i>et al.</i> (1997)
	Phenylphosphate	<u>Phenol</u> + phosphate	Gold electrode	Padeste <i>et al.</i> (1998)
	<i>p</i> -Aminophenylphosphate	<u>p</u> -Aminophenol + phosphate	Glucose oxidase-enzyme sensor (+600 mV)	Renneberg <i>et al.</i> (1983)
Glucose oxidase	Glucose + ferrocene (Oxid.)	Gluconolactone <u>ferrocene (Red.)</u>	(+870 mV)	Wehmeyer <i>et al.</i> (1986)
β -Galactosidase	<i>p</i> -Aminophenyl- β -galactoside	<u>p</u> -Aminophenol + galactose	Gold (+190 mV)	Jenkins <i>et al.</i> (1988)
Urease	Urea	<u>NH₄⁺</u> + CO ₂	Glassy carbon (+250 mV)	Ducey <i>et al.</i> (1997)
β -Lactamase	Benzyl penicilin	<u>H⁺</u>	Laccase/ODH enzyme sensor (−600 mV)	Robinson <i>et al.</i> (1987/88)
			Ammonia gas electrode (In gold)	Bier <i>et al.</i> (1996a)
			PH-FET	Campanella <i>et al.</i> (1999)
				Sergeyeva <i>et al.</i> (1999)

Indicated substances are underlined.

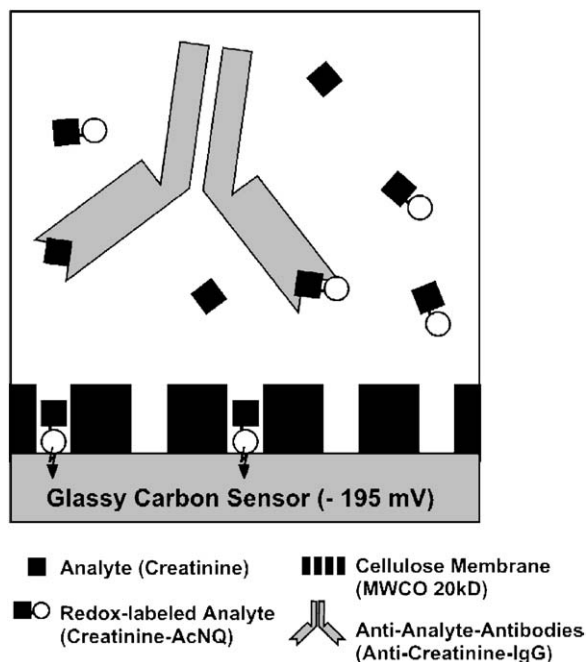


Fig. 3. Principle of size exclusion redox-labeled immunoassay (SERI) for determination of low-molecular weight analytes (e.g. creatinine).

IDA. The advantage of this kind of redox recycling is that a sensitive amperometric determination is reached without any transducer-immobilized biomolecule which makes the device more stable. However, high-quality IDA and a bipotentiostat are needed. Furthermore, the reliability of measurements in serum or whole blood has not been shown until now.

The concept of redox recycling by using *electrode–enzyme coupling* was introduced by Di Gleria *et al.* (1986). They used a lidocaine–ferrocene conjugate in combination with glucose oxidase (GOD). Since ferrocene was used as a mediator for glucose determination within GOD enzyme electrodes it was interesting to use it as the labeling compound for a homogeneous competitive immunoassay. The general principle is shown in Figure 5. The ferrocene label was oxidized at a potential of +380 mV at a gold working electrode and reduced back in the presence of glucose by the glucose oxidase reaction. A standard calibration curve for lidocaine in seven-fold diluted plasma over the concentration range 5–50 mM gave a linear relationship between catalytic current and lidocaine concentration and correlated well with the standard EMIT immunoassay.

An alternative type of redox recycling uses *enzyme–enzyme* coupling. The product of the first enzyme reaction acts as the substrate for the second, and the product of the second acts as the substrate for the first. The consumption of a co-substrate, e.g. oxygen, or the development of a co-product, e.g. hydrogen peroxide, can be measured electrochemically. Because the conversion of the label is

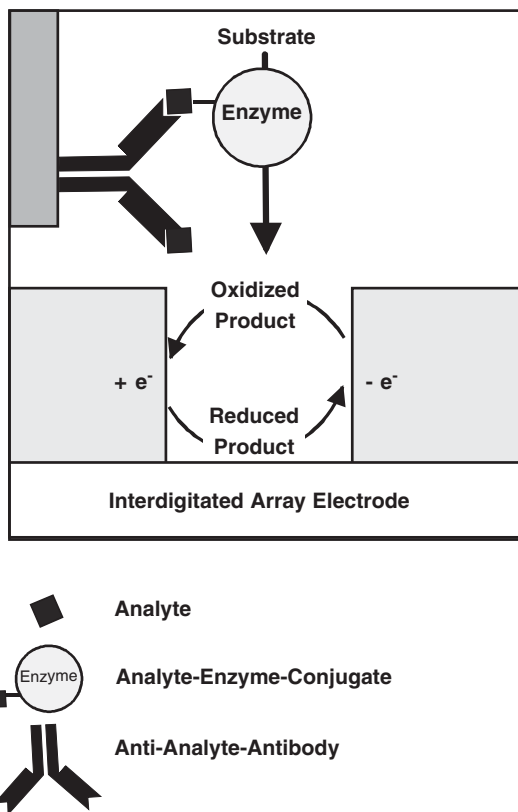


Fig. 4. Combination of an enzyme immunoassay with an interdigitated array electrode (IDA).

not performed with the electrode, this principle is also applicable to other electrochemical transducers, e.g. ion selective electrodes. For amperometric multi-enzyme electrodes amplification factors of 3–48,000 have been described for the appropriate substrates (Wollenberger *et al.*, 1993; Raba and Motolla, 1994; Bauer *et al.*, 1996, 1998). However, in redox-labeled immunoassays not the natural enzyme substrate is applied, but a hapten-coupled derivative of the substrate which is usually converted less effectively than the natural substrate. The result is that the amplification is lower than for the natural substrate.

Ghindilis *et al.* (1995b) have described a couple of PQQ dependent glucose dehydrogenase and laccase for the determination of ferrocene derivatives. Both enzymes were immobilized and sandwiched between a dialysis and a polyethylene membrane. The enzyme membrane was fixed on the top of a Clark electrode. The laccase reaction is accompanied by oxygen consumption which is indicated. Lower detection limits for a ferrocene derivative (ferrocene benzoylisothiocyanate, FBITC) which acts as hapten-coupled substrate of 0.2 or 10,000 nM were reached with or without addition of glucose, respectively, which corresponds to an amplification factor of 50,000. An anti-FBITC antibody was able to block the electrode response, thus allowing a competitive binding assay.

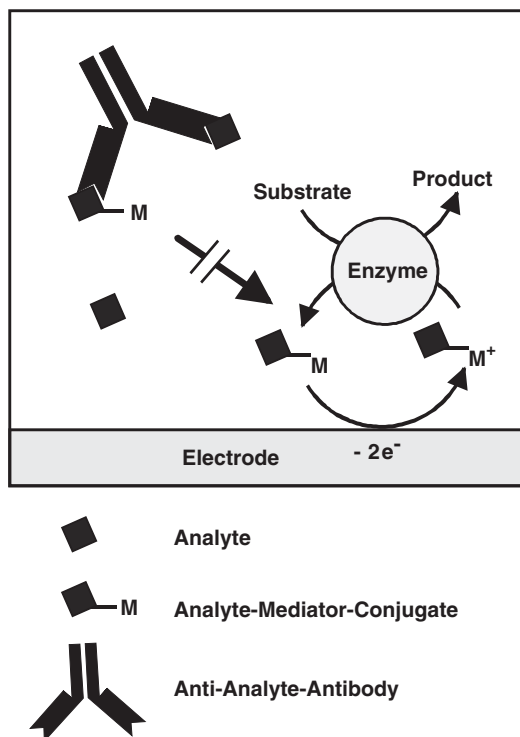


Fig. 5. Redox-recycling by an electrode and an enzyme as basis for a sensitive separation-free immunoassay.

2.3. Electrochemical immunosensors

Following the IUPAC proposal of definition for electrochemical biosensors (Thévenot *et al.*, 2001), an immunosensor is an integrated device consisting of an immunochemical recognition element in *direct* spatial contact with a transducer element. Electrochemical immunosensors employ either antibodies or their complementary binding partners, i.e. antigens or haptens as biological recognition elements in combination with electrodes or field-effect transistors.

The additional criteria of the IUPAC definition that

- sensors should be self-contained
- should perform continuous monitoring and
- should be reversible

are relaxed in this article since most of the published immunosensors are not able to fulfill those criteria. Furthermore, a subdivision in true immunosensors, immunoprobes and immunochemical systems is not used. For the differentiation between immunoassays and immunosensors the criteria of direct immobilization of the antibody or its complementary binding partner on the transducer are used.

For 30 years immunosensors have been under the process development and since 15 years they have reached the market. Commercially available immunosensor systems such as BIAcore (Biosensor, Uppsala, Sweden) and IA Sys (Affinity Sensors, Cambridge, UK) are expensive and technically demanding optical bench-sized devices, which have found their market in research laboratories for the kinetic evaluation of affinity reactions.

2.3.1. Enzyme immunosensors

Enzymes are the most prominent labels in electrochemical immunosensor development. In principle, all types of enzyme immunoassays described in Section 2.2.1 have been realized with the recognition element immobilized at the transducer surface. Alkaline phosphatase was used for the immunochemical determination of fatty acid binding protein (FABP) which is an early diagnostic marker for acute myocardial infarction (AMI). One immunoreactant is directly immobilized on the transducer. Disposable electrodes were constructed using graphite working electrodes which were coated with anti-FABP-IgG as capture antibody. A sandwich principle was applied using anti-FABP-alkaline phosphatase conjugate. A multicenter evaluation of this sensor was described in 1999 (Key *et al.*, 1999). A problem arises from the fact that *p*-APP is unstable in solution. This can cause a problem if very sensitive measurements are needed.

A few years ago, our group developed an amperometric antibody-based sensor for creatinine (Benkert *et al.*, 2000b). Therefore, we have developed monoclonal antibodies to creatinine. These antibodies were used for the construction of a creatinine sensor with GOD as label. The advantages of using glucose oxidase are the high stability of the enzyme and substrate in solution, the moderate price and above all the easy and reliable indication (without electrode fouling) at a conventional platinum electrode, which can be done *via* the consumed oxygen at -600 mV or *via* the produced hydrogen peroxide at $+600$ mV *vs.* Ag/AgCl. The first publication describing GOD as label for the development of immunosensors dates back to, when Mathiasson and Nilsson (1977) developed an albumin immunosensor based on immobilized anti-insulin antibodies. GOD was indicated by oxygen consumption measurements.

The GOD label of the described creatinine sensor was indicated via the hydrogen peroxide produced, which allows the determination of a signal increase instead of a background decrease when oxygen consumption is measured and an almost oxygen independent measurement.

For the creatinine sensor, an indirect competitive principle with an immobilized creatinine derivative was used. The creatinine derivative was coupled to a thin semi-permeable cellulose membrane covering a platinum working electrode. This membrane ensures that no high-molecular-weight compounds, e.g. GOD-labeled antibodies or redox active proteins can reach the electrode, which could adsorb to the electrode and cause unwanted reactions.

The immunoassay is performed as follows: Creatinine to be measured competes with the membrane immobilized creatinine for the antigen binding sites of the anti-creatinine antibodies (Figure 6). After a washing step the membrane-bound anti-creatinine antibodies are indicated via the additional GOD-labeled

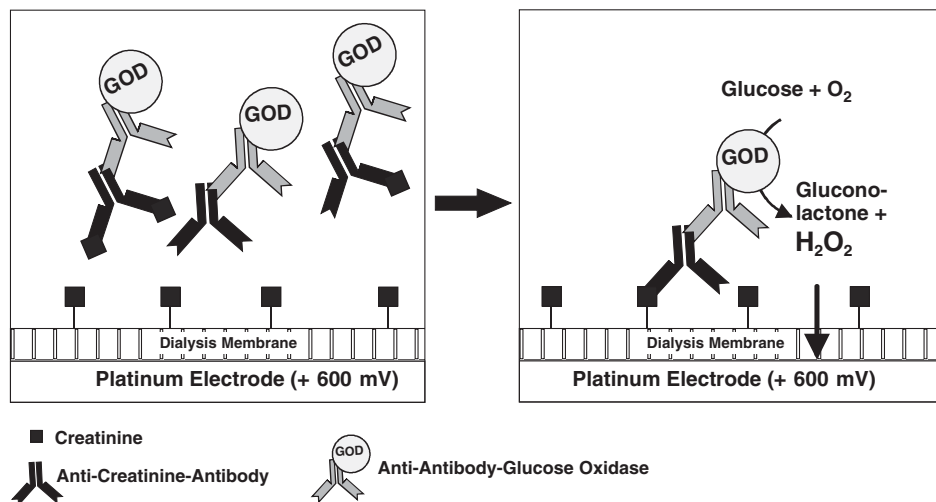


Fig. 6. Principle of an indirect competitive amperometric immunosensor for the determination of creatinine.

anti-mouse antibodies by addition of glucose and measurement of the hydrogen peroxide produced. As expected for competitive assays, there is an indirect dependence of the signal on the antigen concentration. The measuring range is between 0.01 and 10 $\mu\text{g}/\text{mL}$, which corresponds to 0.09–90 μM . The highest sensitivity for creatinine is achieved at 330 ng/mL (3 μM), the lower detection limit at 4.5 ng/mL (40 nM).

The sensor can be regenerated with HCl in about 3 min. One hundred regenerations of the sensor were performed without any loss in binding activity of the creatinine sensor. The reason is that the creatinine-modified membrane is chemically very stable. To estimate the maximum number of regeneration cycles the sensor was tested by prolonged incubation in HCl with evaluation of the binding activity in-between. No decrease was observed even after 10 h storage in HCl. Therefore, it is assumed that many more than 100 regenerations can be carried out. All in all, one measuring cycle still takes 30 min to reach the described sensitivity. If the performance will be further optimized, the developed sensor should have the potential to be applicable for creatinine measurements in a doctor's office.

Separation-free electrochemical enzyme immunosensors use different types of proximity effects:

- (i) direct electron transfer from the enzyme label to the electrode,
- (ii) "electrically wired" enzyme labels,
- (iii) substrate channeling, and
- (iv) restricted mass transfer

(i) For a number of redox enzymes the ability to catalyze electrode reactions by a mediatorless mechanism was established (Tarasewich, 1985). In such cases the electrons are transferred directly from the electrode to the substrate molecule

via the active site of the enzyme. Therefore, electrons act as the second substrate for an enzymatic reaction and the potential is shifted in the presence of the corresponding substrate. This phenomenon results in catalytic elimination of the overvoltage.

The electrocatalytic properties of several redox enzymes permit their application as labels for separation-free potentiometric or amperometric immunosensors. Binding of the electrocatalytic active enzyme label to the electrode surface initiates an electrocatalytic reaction resulting in a potential shift or a catalytic current. In the assay procedure the antigen immobilized on the electrode surface interacts with the enzyme-labeled antibody resulting in fixation of the enzyme to the electrode surface. Therefore, the formation of antigen-labeled antibody complex on the electrode surface is accompanied by a potential shift or the generation of a catalytic current. The presence of free antigen in the solution leads to a competition for labeled antibodies. The competition results in a decrease of the electrode signal, e.g. the decrease in the rate of the potential shift in this case is proportional to free antigen concentration in solution.

Laccase is known to catalyze the reaction of oxygen electroreduction via a direct mechanism (Berezin *et al.*, 1978). This property of the enzyme allows the detection of the biospecific interaction of laccase-labeled antibodies with an antigen-modified electrode. Formation of a complex between the laccase-labeled antibody and antigen on the electrode surface results in a considerable shift in electrode potential. Immunosensors based on the laccase-labeled immunogens and direct potentiometric detection of antigen-antibody interaction have been developed by Ghindilis *et al.* (1991, 1992, 1996) (Milligan and Ghindilis, 2002). The laccase near the electrode surface which catalyzes the oxygen electroreduction leads to an increase in the electrode potential due to the catalytic removal of the reaction overvoltage. Since only oxygen is needed as a laccase substrate, the sensor works substrate-free. The analysis can be performed in a competitive or in a sandwich scheme. A single measurement requires 20 min. Insulin and mouse immunoglobulin were used in a model assay. For insulin a concentration range of 10–1000 ng/mL was covered.

Peroxidase is known to catalyze direct (mediatorless) electroreduction of hydrogen peroxide (Tarasewich, 1985). The electrocatalytic properties of peroxidase permit its application as a label for immunosensors. Attachment of peroxidase to the electrode surface in the presence of H₂O₂ initiates an electrocatalytic reaction resulting in a potential shift or a catalytic current. The direct electron transfer of a peroxidase label was applied by McNeil *et al.* (1995) to the development of amperometric immunosensors using amperometric detection of hydrogen peroxide electroreduction. Based on the same principle Grennan *et al.* (2003) described a regeneration-free atrazine immunosensor by using immobilized single-chain antibody fragments on a conducting polymer-modified carbon paste screen-printed electrode. Atrazine and an atrazine-peroxidase conjugate compete for the binding to the immunosensor surface. The rate of current response was concentration-dependent, under mass transport limitation conditions. The detection limit was given to be 0.1 µg/L. Due to the nature of the printing process, no two screen-printed electrode surfaces can be considered identical, even if printed in the same batch. Therefore, calibration by using several electrodes from one batch

cannot be applied. However, the authors showed that repeated measurements can be performed on a single electrode surface. Thus the problem of calibration was solved by using self-calibration of each electrode.

(ii) If an antibody is immobilized on a mediator-modified electrode the antigen–enzyme conjugate can only be determined if it is in direct contact with the mediator (Figure 7). The so-called “electrically wired” amperometric immunosensors normally use peroxidase as label and osmium redox polymers (Lu *et al.*, 1997a,b) or tetrathiafulvalene (Wendzinski *et al.*, 1997) as mediators (for a review of peroxidase-modified electrodes, see (Ruzgas *et al.*, 1996)).

(iii) Channeling EIAs were combined with electrochemical techniques in different ways: Keay and McNeil (1998) used an electrode with co-immobilized antibodies and peroxidase. If the GOD-labeled antigen binds to the antibody H_2O_2 “channels” to the peroxidase if glucose is added (Figure 8A). The H_2O_2 which is produced in the bulk is destroyed by catalase and cannot reach the electrode. Since the peroxidase activity is measured at the electrode (+ 50 mV) the bound GOD-labeled antigen can be quantified. This principle should be applicable for competitive and sandwich formats. A similar principle but with electrode-immobilized GOD and peroxidase as label is used by the group of Rishpon (Rishpon and Ivnitcki, 1997; Ivnitcki *et al.*, 1998) (Figure 8). Here, the H_2O_2 is produced at the electrode interface and not in homogeneous solution. This has the advantage that no catalase for H_2O_2 destruction has to be used. The indication takes place by amperometric measurement of the peroxidase reaction products. It was shown that similar real-time sensorgrams can be monitored as known from BIAcore (surface plasmon resonance technique) measurements. However, the main problem is that these sensors with immobilized enzymes are difficult to regenerate and are thus one-way sensors. In the examples described above, the site-directed increase in substrate concentration for the labeling enzyme was carried out by immobilized enzymes. Another method was published by Ducey *et al.* (1997) in which they let diffuse the substrate (*p*-APP) for the label enzyme (aP) through the back of the micro-porous gold electrode so that the substrate concentration near the electrode was high. Since no immobilized enzymes are used these sensors can be regenerated.

2.3.2. Redox-labeled immunosensors

In redox-labeled immunosensors, the binding reaction is visualized *via* an electroactive labeling compound. The captured antibody is fixed to the electrode, and the redox-labeled antigen from solution competes with free antigen. The indication takes place at an unmodified electrode, which dips into the incubation solution or which is an integrated part of an electrochemical flowthrough cell. These types of electrochemical immunoassays can be applied to test tubes, 96-well microtiter plates or flow systems with reactor-immobilized antibodies. Tiefenauer *et al.* (1997) used a nanostructured gold electrode with an interelectrode space of about 30 nm. The hapten was immobilized in that space on SiO_2 . It was demonstrated that in combination with ferrocene- or heme-modified

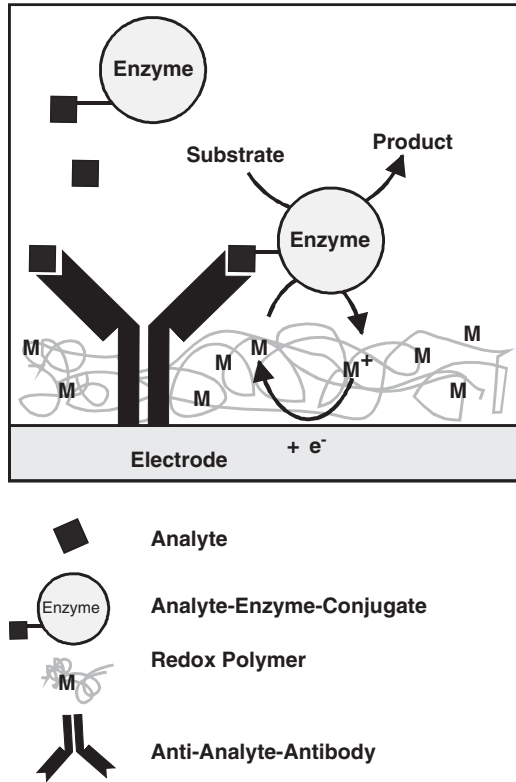


Fig. 7. Principle of “electrically wired” immunosensors.

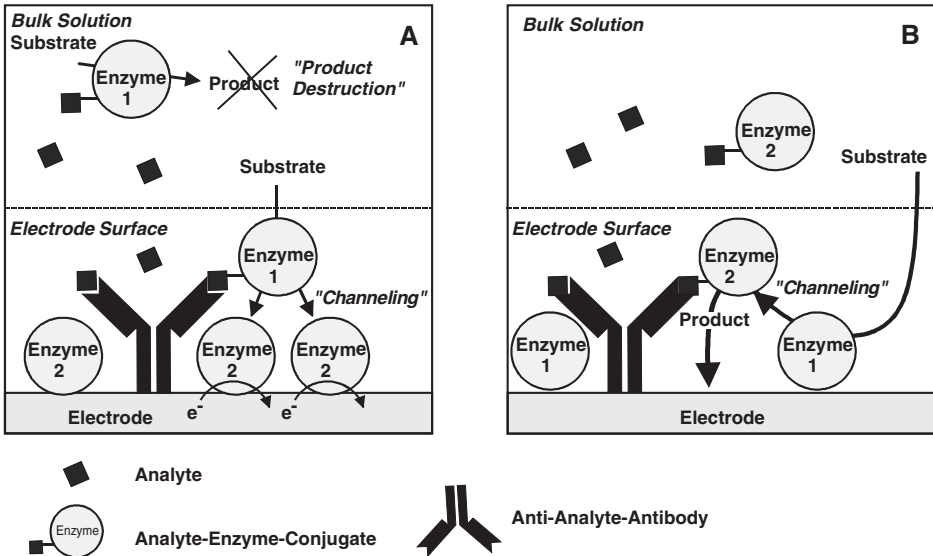


Fig. 8. Two different types of electrochemical “channeling” immunosensors.

antibodies this concept can be used to increase the efficiency of redox-labeled immunoassays.

For the determination of the herbicide 2,4-dichlorophenoxyacetic acid (2,4D) anti-2,4D-antibodies were immobilized within the enzyme layer of the indicator electrode. The sensor immobilized antibodies were loaded with a 2,4D-tyrosine conjugate (2,4D-Tyr), and after washing the sensor was ready for 2,4D measurement. 2,4D from the sample diffuses into the enzyme/antibody layer and displaces the 2,4D-Tyr conjugate. The displaced conjugate is then recycled in the presence of glucose by the co-immobilized NADH-independent oligosaccharide dehydrogenase and tyrosinase and thereby indicated via oxygen consumption. The detection limit for 2,4D was calculated to be 25 nM. The advantage of the described principle is that as long as enough 2,4D-Tyr can be displaced from the antibody complexes a regeneration step is not needed (Bier *et al.*, 1996a, b).

Dai *et al.* (2003) described an immunosensor for carcinoma antigen-125 (CA 125) with horseradish peroxidase (HRP) as the redox label. Since the direct electrochemistry of HRP was used for signal generation this sensor works substrateless and mediatorless. For the construction of the sensor, the antigen was immobilized with titanium sol-gel on a glassy carbon electrode by vapor deposition. By using a competition principle with anti-CA 125-HRP conjugate and differential pulse voltammetric (DPV) determination a peak current decrease was observed in the presence of CA 125. The detection limit for CA 125 was 1.29 U/mL. However, a washing step after conjugate incubation and oxygen exclusion during DPV measurements are necessary.

2.3.3. Label-free immunosensors

The direct electrochemical immunosensors use changes in charge densities or conductivities for transduction and do not need any auxiliary reaction. To work label free is very attractive, especially for the development of *in vivo* immunosensors since it allows real-time measurement without any additional hazardous reagents.

Thirty years ago, Janata observed in an affinity sensor a potential change when he incubated mannan with a potentiometric electrode covered with PVC membrane-immobilized ConA (Janata, 1975). Thereby, it was possible to follow the binding process directly in real time without any labeling.

In 1984, Keating and Rechnitz used a potassium sensitive electrode with a dioxin-ionophore conjugate within a PVC membrane for the determination of anti-dioxin antibodies. Although many more publications (Gothoh *et al.*, 1987; Pfeifer and Baumann, 1992; Engel and Baumann, 1994) have been published describing similar effects, it is yet not completely clear whether the potential change is a result of disturbed ion transport or of charge changes at the protein surface during binding (for a critical review see Bergveld, 1991).

Amperometric techniques have been used to monitor antigen-antibody binding in real time without using a labeled compound. A polymer-modified antibody electrode has been used in combination with pulsed amperometric detection (PAD) (Sadik and Van Emon, 1997). An antibody or antigen that binds the analyte of interest is immobilized on the surface of a membrane

electrode. The analytical signal was generated by applying a pulsed waveform between +0.6 and -0.6 V with a pulse duration of 120 and 480 ms. When the current is sampled at the end of the pulse, the component due to charging is significantly reduced or close to zero, and the level of current due to charging and discharging induced by pulsing can be treated as a constant. Under these circumstances, it has been postulated, that the change in the response level reflects only the binding of the analyte to the antibody and that the pulse amperometric technique can be used to repulse the antigen from the immobilized antibody and thereby regenerate the sensor. Recently, Grant *et al.* (2003) have used PAD for the determination of bovine serum albumin (BSA). They described that the actual source of the signal is as yet unclear but that the currents observed were due in some way to the antibody-antigen interaction. However, they described also that they and other workers had problems to reproduce the results of Sadik and van Emon. Further investigations and controls are necessary to resolve the background of the signal generation.

A further label-free amperometric immunosensor was described by Hu *et al.* (2003). They used the electrochemical activity of the antigen directly for signal generation. Therefore, gold nanoparticles modified with anti-paraoxon antibodies were immobilized on a glassy carbon electrode by using Nafion. After incubation with paraoxon and a washing step the electrochemical detection of paraoxon was done by applying cyclic voltammetric measurements between 1.0 and -0.7 V. The oxidation peak potential at -8.0 mV was used as the operating potential. The detection limit was 12 µg/L.

Since electrochemical transducers detect only species that reach the electrode surface it is possible to differentiate between molecules which are near the transducer and molecules which are within the bulk. One principle is to hinder the diffusion of a redox active substance, e.g. potassium hexacyanoferrate(II) (Susmel *et al.*, 2003) or ferrocene-labeled GOD (Blonder *et al.*, 1996) to the electrode surface by using an electrode immobilized immunoreactant. Analogous to this principle, the diffusion of an enzyme to a mediator-modified electrode can be hindered. However, this principle is especially applicable for analytes with high molecular weights (e.g. proteins or bacteria). Since the principle is sensitive to defects within the layer, high-quality monolayers with a high reproducibility have to be built up on the electrode surface.

The first capacity immunosensor was developed by Newman *et al.* (1986), who used interdigitated copper electrodes onto a glass surface isolated by a silicium oxide coated parylene layer. With silicium oxide immobilized antigen they could determine the antibodies via capacity decrease. Gebbert *et al.* (1992, 1994) described a tantalum strip onto which tantalum oxide was grown electrochemically and used for immobilization of mouse IgG. It was possible to determine anti-mouse-IgG with a measuring range of 0.2–20 ng/mL which corresponds to 1.3×10^{-12} – 1.3×10^{-10} M. As indicated in the publication (Gebbert *et al.*, 1994), the principle is limited to the determination of relatively large molecules and problems were discussed with respect to non-specific binding and noises related to the fluid or its movement.

Riepl *et al.* (1999) have used a similar principle. Instead of a tantalum oxide layer which was silanized and used to immobilize the antibody via carbodiimide,

a gold electrode was incubated with 16-mercaptohexadecanoic acid and used for the immobilization of an anti-HSA-antibody via carbodiimide. The stable gold-sulphur binding with this long-chain thiol resulted in low drifting. However, the sensitivity for antigen (HSA) determination was lower than for the previously described sensor. In 1997, further work with a gold electrode was published by Berggren and Johansson (1997). They used thioctic acid as linker for the immobilization of anti-human chorionic gonadotropin hormone (HCG) antibodies. The detection limit for HCG was calculated to be 15×10^{-15} M (0.5 pg/mL), which is extraordinarily sensitive for a direct immunosensor. Recently, Navratilova and Skladal (2004) compared three different gold sensor types (screen-printed strip sensor, screen printed finger-like structure, interdigitated array) for the construction of an immunosensor for 2,4-dichlorophenoxyacetic acid (2,4D) based on capacitance changes. The immobilization of the antibody was done by using a thiol spacer. The best performance was obtained with the strip sensor. A concentration range of 0.045–450 μ M of 2,4D was covered. After measurement it was possible to regenerate the sensor with 0.1 M formic acid.

For the detection of *E. coli*, Yang *et al.* (2004) used an array microelectrode-based electrochemical impedance immunosensor. Immobilization of the antibody and binding of *E. coli* cells increased the electron transfer resistance, which was directly measured with electrochemical impedance spectroscopy in the presence of $[\text{Fe}(\text{CN})_6]^{3-/4-}$ as a redox probe.

3. ELECTRONIC PROTEIN CHIPS

High parallelity, i.e. a large number of different recognition spots, is the key feature of chip-based analysis in protein research. High parallel analysis procedure is not possible using individual dispensing of reagents to each spot – as it is realized for the microliter and even nanoliter plates – and this causes the two following demands:

- (i) The binding partners should possess very high specificity for the target molecule in order to prevent cross-over to the compounds immobilized at the other spots. Unspecific interactions with the “carrier” material should be avoided. In order to prevent the cross talk between neighboring spots the signal generation must be restricted to the immediate vicinity of each spot.
- (ii) All electrodes or ISFETs of the chip should be readable individually.

Two different principles are feasible to avoid cross talk. Micromechanical generation of a “wall” between the spots effectively prevents the migration of products which are generated by an enzyme label. This principle was applied to create a low-density electrochemical DNA chip with 28 or 128 individual positions (Nebling *et al.*, 2004; Frey *et al.*, 2002). Therefore, polymeric ring structures of 10 μ m height, 15 μ m width and 10 μ m distance were built up around each array position by photolithography (Figure 9B).

The second method to avoid cross talk between the spots is to use assay techniques, which indicate the binding partner only at the point where the

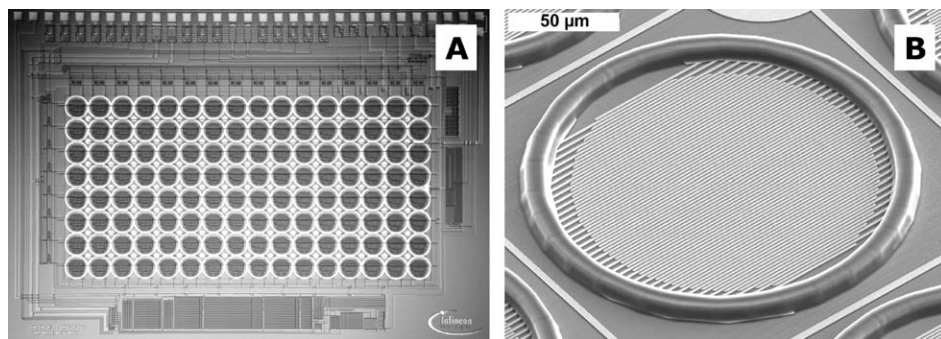


Fig. 9. (A) Fully processed electrochemical DNA sensor chip (6.4×4.5 mm) with 16×8 features. (B) Scanning electron micrograph of an interdigitated gold array feature with polymeric ring structure.

immunochemical complexation takes place. With this principle any additional mechanical barriers are not necessary. Substrate channeling assays or formats using the direct electron transfer between the marker enzyme or redox label and the electrode or label-free immunosensor principles should fulfill these demands (see Sections 2.3.1–2.3.3).

Due to a multiplicity of unsolved problems protein chips are at the very beginning of development. On the other hand, different technologies of DNA chip production may be transferred to the development of protein chips.

(i) The problem of how to get the huge number of the required antibodies immobilized on a chip with spatial resolution could be solved by the principle of “refunctionalization” of a DNA array (Niemeyer *et al.*, 1994; Bier *et al.*, 1999). Therefore, the array is incubated with proteins which are conjugated with the respective complementary oligonucleotide sequence. Due to the high specificity of hybridization the protein-DNA conjugates will be guided and immobilized on the spots due to their DNA sequences.

(ii) Electronic DNA chips allow for the integration of the signal generation using individually addressable microelectrodes or field-effect transistors by highly parallel amperometric or potentiometric measurements. Recently, a fully processed 16×8 CMOS sensor array (Figure 9A) was described with interdigitated gold electrodes arranged within a circular polymeric ring structure (Nebling *et al.*, 2004; Frey *et al.*, 2002). The interdigitated gold structures with $1 \mu\text{m}$ wide fingers, gaps of $0.8 \mu\text{m}$ and $17.000 \mu\text{m}^2$ were generated by the lift-off technique from a deposited 120-nm-thick gold electrode (Figure 9B). By using a micro spotter, single stranded DNA molecules were immobilized on the gold sensor surfaces. The biotinylated target from the sample and an alkaline phosphatase-avidin conjugate was bound subsequently. After adding *p*-aminophenylphosphate the released *p*-aminophenol was detected by electrode–electrode recycling as described in Section 2.2.2. The amplification factor was eight. The crossover of the enzymatically released *p*-aminophenol from one to the other sensor positions has been avoided due the polymeric ring structure around the electrode and the time-dependent measurement. This approach

should principally be applicable for the construction of an electric protein chip. Therefore, alkaline phosphatase-labeled antibodies could be used.

Furthermore, electrophoresis may be integrated to actively transport the sample molecule to the immobilized target (Nanogen Inc., USA). Electrophoretic accumulation of charged biomolecules by an array of focusing electrodes within a planar microchamber has been successfully demonstrated. Accumulation ratios for DNA and streptavidin as high as 200 have been achieved. However, care has to be taken with respect to gas bubbles generation and chemical stabilities of the targets (Stelzle *et al.*, 2001). The authors claimed that preconditioning steps could be integrated into lab-on-a-chip devices and would be useful to enhance sensitivity and selectivity of biochemical analysis. In a paper from Nanogen, a 500-fold increase in concentration from 5 nM to 2.5 μ M in the volume 2 μ m above an array electrode within seconds was described by applying an electrical field without any special focusing electrodes. As few as 10^6 molecules of labeled, synthetic targets have been detected (Kassegne *et al.*, 2003). Thus, for the detection of targets from PCR and SDA which are usually very high in concentration focusing electrodes are unnecessary. However, under conditions of extremely low target concentrations the authors argued that such electrodes could have some benefits. For protein chips, the accumulation by using an electrical field would also concentrate unwanted proteins and thereby also increase unspecific binding. Therefore, it is questionable if such an approach could be used to detect very low amount of proteins in cell lysates or body fluids. However, the application of electrical fields for protein chip technology will have some benefits for solving transportation and diffusion problems of the sample or labeled compounds.

(iii) Although protein microarrays with antibodies have been developed (Dove, 1999; Wingren *et al.*, 2003), alternative binders have already been explored which could overcome certain limitations of antibodies.

It is well known that DNAs and RNAs bind *in vivo* not only complementary nucleic acids but also small molecules or proteins. By using the SELEX method (Systematic Evolution of Ligands by Exponential Enrichment) (Tuerk and Gold, 1990; Ellington and Szostak, 1990), binders for proteins (Table 2), peptides, amino acids, nucleotides, drugs, vitamins and other organic and inorganic compounds have been generated. The preparation of these aptamers takes advantage of the well-established nucleic acid chemistry, polymeric chain reaction and modern separation techniques. Aptamers are selected from mainly random pools of RNA or DNA by column chromatography, or other selection techniques suitable for the enrichment of a desired property. The complexity of a typical combinatorial oligonucleotide library obtained from 1 μ mol scale solid-phase DNA synthesis is limited to 10^{14} – 10^{15} individual sequences. The enriched sequences can be amplified and mutated and can be used as a new pool for another selection step. After 8–15 cycles, aptamers can be obtained which show affinities and specificities as good as antibodies. Including cloning and sequencing, a typical SELEX experiment may take 2–3 months. Full-length aptamers are generally 70–80 nucleotides long but can be truncated to eliminate nucleotide sequences which are not necessary for target binding. Thereby, functional aptamers with less than 40 nucleotides have been obtained.

Table 2. Representative examples of proteins against which aptamers have been developed

Target Protein	K _D	Aptamer Type	References
PSMA prostate-specific antigen		RNA	Lupold <i>et al.</i> (2002)
HIV-1 gp120	> 100 nM	RNA	Sayer <i>et al.</i> (2002)
HIV-1 rev peptide		RNA	Convery <i>et al.</i> (1998)
NS3 protease domain of Hepatitis C virus	10 nM	RNA	Fukuda <i>et al.</i> (2000)
Yeast RNA polymerase II	app. 20 nM	RNA	Thomas <i>et al.</i> (1997)
Prion protein		RNA	Weiss <i>et al.</i> (1997) Proske <i>et al.</i> (2002)
Bacteriophage MS2 coat protein		RNA	Convery <i>et al.</i> (1998)
NFAT	10–100 nM	RNA	Cho <i>et al.</i> (2004)
Colicin E3	2–14 nM	RNA	Hirao <i>et al.</i> (2004)
Human-activated protein C	83 nM	RNA	Gal <i>et al.</i> (1998)
SelB	60 nM	RNA	Klug <i>et al.</i> (1999)
<i>E. coli</i> Met J repressor protein	300 nM	RNA	Mc Gregor (1999)
Subtilisin	2, 5 μM	RNA	Takeo <i>et al.</i> (1999)
Ricin A-chain	7, 3 nM	RNA	Hesselberth <i>et al.</i> (2000)
Pepocin (ribosome inactiv. protein)	20–30 nM	RNA	Hirao <i>et al.</i> (2000)
HIV-1 RT	25 pM	RNA	Kensch <i>et al.</i> (2000)
Human Oncostatin M	7 nM	RNA	Rhodes <i>et al.</i> (2000)
HIV-1 Tat protein		RNA	Yamamoto <i>et al.</i> (2000)
Tenascin-C	5 nM		Hicke <i>et al.</i> (2001)
Streptavidin	70 nM	RNA	Srisawat and Engelke (2001)
HIV-1 integrase		DNA	Jing <i>et al.</i> (1997)
Thrombin	0.5 nM	DNA	Tasset <i>et al.</i> (1997)
Neutrophil elastase		DNA	Bless <i>et al.</i> (1997)
Cytochrome <i>c</i>	400 nM	DNA	Chinnapan and Sen (2002)
NS5B (RNA-Pol of Hepatitis C virus)	nM range	DNA	Bellecave <i>et al.</i> (2003)
Platelet-derived growth factor (PDGF)-AB	0.1 nM	DNA	Green <i>et al.</i> (1996)
IgE	10 nM	DNA	Wiegand <i>et al.</i> (1996)
	35 nM	RNA	
Human RNase H1	10 nM	DNA	Pileur <i>et al.</i> (2003)
Influenza A virus hemagglutinin		DNA	Jeon <i>et al.</i> (2004)

On the therapeutic front, aptamers have made tremendous progress and are already in clinical trials only 8 years after establishment of the technology. The application of aptamers for *in vivo* diagnostics has already been explored. In comparison to antibodies, aptamers have also some features which make them very attractive for protein chips.

In contrast to antibodies, aptamers can easily be produced by chemical synthesis. Thereby reporter molecules as biotin or functional group for further conjugation can be attached at precise locations for labeling or immobilization. Aptamers containing 5-halo-uracil analogs could be used to lock the bound proteins irreversibly. This has the advantage that the cross-over to other spots can be avoided even under rigorous washing conditions. One of the obvious limitations of immunosensors is their poor capacity to regenerate the antibody surface. Therefore, one of the most attractive features of aptamers is their ability to be regenerable. Nucleic acids can withstand repeated cycles of denaturation and renaturation. Several methods can be used for regeneration: heat, salt, pH and chelating agents.

Although optical sensors (Kleijnung *et al.*, 1998; Potyrailo *et al.*, 1998; Lee and Walt, 2000), an optical sensor array (McCauley *et al.*, 2003) and an electronic tongue sensor array (Kirby *et al.*, 2004) with aptamers have already been described the development of aptamer sensors with electrochemical detection is still an unexplored field. In addition to being an alternative recognition element their ability of charge transfer within the DNA helix (Kelly and Barton, 1999) will allow new principles of signal transduction.

4. SUMMARY AND CONCLUSION

Analytical systems, which are based on electrochemical sensors have the potential for decentralized applications. Many principles for electrochemical immunosensors for the specific and sensitive determination of proteins have been developed during the last 20 years. Most of them are based on competitive or sandwich assay configurations in combination with enzyme-labeled or redox-labeled immunocomponents. Detection limits are usually within the nanomolar range. If recycling is applied, e.g. by using electrode–electrode, enzyme–electrode or enzyme–enzyme coupling, a very sensitive indication of the enzyme label or redox compound is possible. As a consequence, detection limits are shifted into the picomolar range. In addition, direct electrochemical signal transduction principles for immunosensors have been developed which avoid the use of any labeled compound.

Most electrochemical immunosensors are developed for the determination of single analytes. However, in the context of proteomics thousands of proteins have to be analyzed in parallel. This could be reached by using a large number of different recognition spots on a chip surface. Methods originally developed for DNA chips could be the basis for the immobilization of antibodies.

Two major problems must be overcome especially in the development of electrochemical protein chips: (i) The cross talk between the recognition spots during indication must be avoided, and (ii) the microelectrodes on the chip

should be read out simultaneously. Possible ways of how to do this have recently been shown with electrochemical DNA chips and should in future also be applicable to protein chips.

LIST OF ABBREVIATIONS

ADH	alcohol dehydrogenase
AELIA	amplified enzyme-linked immunoassay
AFIA	amplified flow immunoassay
AMI	acute myocardial infarction
AP	alkaline phosphatase
ARIS	apoenzyme reactivation immunoassay system
CMOS	complementary metal oxide silicon
DNA	deoxyribonucleic acid
DPV	differential pulse voltammetry
ELISA	enzyme-linked immunosorbent assay
EIA	enzyme immunoassay
EMIT	enzyme-multiplied immunoassay technique
EMMIA	enzyme modulator mediated immunoassay
FABP	fatty acid binding protein
FBITC	ferrocene benzoylisothiocyanate
FIA	flow injection analysis
GOD	glucose oxidase
HCG	human choriogonadotropin
HPLC	high-performance liquid chromatography
HRP	horseradish peroxidase
HAS	human serum albumin
HTSH	human thyroid stimulating hormone
IDA	interdigitated array
IgG	immunoglobulin G
INT	iodonitrotetrazolium
ISFET	ion-sensitive field-effect transistor
IUPAC	International Union of Pure and Applied Chemistry
NAD	nicotineamide-adenine dinucleotide
NADP	nicotineamide-adenine dinucleotide phosphate
<i>p</i> -AP	<i>p</i> -aminophenol
<i>p</i> -APP	<i>p</i> -aminophenylphosphate
PAD	pulsed amperometric detection
PCR	polymerase chain reaction
PQQ	pyrroloquinoline quinone
PVC	polyvinyl chloride
RIA	radioimmunoassay
RNA	ribonucleic acid
SD	standard deviation

SDA	strand displacement amplification
SELEX	systematic evolution of ligands by exponential enrichment
SERI	size-exclusion redox-labeled immunoassay
SLFIA	substrate-labeled fluoroimmunoassay

ACKNOWLEDGMENTS

We would like to thank Alexander Frey (Infineon Technologies, Germany) for the DNA chip photos and the Fond der Chemischen Industrie (Project No.0400137) for financial support.

REFERENCES

- Abdel-Hamid, I., A.L. Ghindilis, P. Atanasov and E. Wilkins, 1999, Flow-through immunoassay system for determination of staphylococcal protein a, *Anal. Lett.* 32, 1081.
- Aizawa, M., A. Morioka and S. Suzuki, 1980, An enzyme immunosensor for the electrochemical determination of the tumor antigen alpha-fetoprotein, *Anal. Chim. Acta* 115, 61.
- Athey, D. and C.J. McNeil, 1994, Amplified electrochemical immunoassay for thyrotropin using thermophilic β -NADH oxidase, *J. Immunol. Meth.* 176, 153.
- Athey, D., C.J. McNeil, W.R. Bailey, H.J. Hager, W.H. Mullen and L.J. Russell, 1993, Homogeneous amperometric immunoassay for theophylline in whole blood, *Biosens. Bioelectron.* 8, 415.
- Bates, D.L., 1987, Enzyme amplification in diagnostics, *Trends Biotechnol.* 5, 204.
- Bauer, C.G., A.V. Eremenko, E. Ehrentreich-Förster, F.F. Bier, A. Makower, H.B. Halsall, W.R. Heineman and F.W. Scheller, 1996, Zeptomole-detecting biosensor for alkaline phosphatase in an electrochemical immunoassay for 2,4-dichlorophenoxyacetic acid, *Anal. Chem.* 68, 2453.
- Bauer, C.G., A.V. Eremenko, A. Kühn, K. Kürzinger, A. Makower and F.W. Scheller, 1998, Automated amplified flow immunoassay for cocaine, *Anal. Chem.* 70, 4624.
- Bellecave, P., M.L. Andreola, M. Ventura, L. Tarrago-Litvak, S. Litvak and T. Astier-Gin, 2003, Selection of DNA aptamers that bind the RNA-dependent RNA polymerase of Hepatitis C virus and inhibit viral RNA synthesis *in vitro*, *Oligonucleotides* 13, 455.
- Benkert, A., F.W. Scheller, W. Schoessler, B. Micheel and A. Warsinke, 2000a, Size exclusion redox-labeled immunoassay (SERI) – A new format for homogeneous amperometric creatinine determinations, *Electroanalysis* 12, 1318.
- Benkert, A., F.W. Scheller, W. Schössler, Ch. Hentschel, B. Micheel, O. Behrsing, G. Scharte, W. Stöcklein and A. Warsinke, 2000b, Development of a creatinine ELISA and an amperometric antibody-based creatinine sensor with a detection limit in the nanomolar range, *Anal. Chem.* 72, 916.
- Berezin, I.V., V.A. Bogdanovskaya, M.R. Tarasevich, S.D. Varfolomeev and A.I. Yaropolov, 1978, Bioelectrocatalysis, Equilibrium oxygen potential in the presence of Laccase, *Doklady Akademii Nauk SSSR* 240, 615.
- Bergel, A., J. Soupe and M. Comtant, 1989, Enzymatic amplification for spectrophotometric and electrochemical assays of NAD^+ and NADH, *Anal. Biochem.* 179, 382.
- Berggren, C. and G. Johansson, 1997, Capacitance measurements of antibody-antigen interactions in a flow system, *Anal. Chem.* 69, 3651.
- Bergveld, P., 1991, A critical evaluation of direct electrical protein detection methods, *Biosens. Bioelectron.* 6, 55.

- Bier, F.F., E. Ehrentreich-Förster, Ch. Bauer and F.W. Scheller, 1996a, High sensitive Competitive immunodetection of 2,4-dichlorophenoxyacetic acid using enzymatic amplification with electrochemical detection, *Fresen. J. Anal. Chem.* 354, 861.
- Bier, F.F., E. Förster, A. Makower and F.W. Scheller, 1996b, An enzymatic amplification cycle for highly sensitive immunoassay, *Anal. Chim. Acta*, 328, 27.
- Bier, F.F., F. Kleinjung, E. Ehrentreich-Förster and F.W. Scheller, 1999, Changing functionality of surfaces by directed self-assembly using oligonucleotides – The oligo tag, *BioTechniques* 27, 752.
- Blake, C. and B.J. Gould, 1984, Use of enzymes in immunoassay techniques – A review, *Analyst* 109, 533.
- Bless, N.M., D. Smith, J. Charlton, B.J. Czermak, H. Schmal, H.P. Friedl and P.A. Ward, 1997, Protective effects of an aptamer inhibitor of neutrophil elastase in lung inflammatory injury, *Curr. Biol.* 7, 877.
- Blonder, R., E. Katz, Y. Cohen, N. Itzhak, A. Riklin and I. Willner, 1996, Application of redox enzymes for probing the antigen–antibody association at monolayer interfaces: development of amperometric immunosensor electrodes, *Anal. Chem.* 68, 3151.
- Bordes, A.L., B. Limoges, P. Brossier and C. Degrand, 1997, Simultaneous homogeneous immunoassay of phenytoin and phenobarbital using a nafion-loaded carbon paste electrode and two redox cationic labels, *Anal. Chim. Acta* 356, 195.
- Bordes, A.L., B. Schöllhorn, B. Limoges and C. Degrand, 1999, Simultaneous detection of three drugs labeled by cationic metal complexes at a nafion-loaded carbon paste electrode, *Talanta* 48, 201.
- Buckley, E., M.R. Smyth, W.R. Heineman and H.B. Halsall, 1989, Some recent developments in electrochemical immunoassays, *Anal. Proceed.* 26, 5.
- Campanella, L., R. Attioli, C. Colapicchioni and M. Tomassetti, 1999, New amperometric and potentiometric immunosensors for anti-human immunoglobulin G determinations, *Sens. Actuat. B* 55, 23.
- Chinnapen, D.J. and D. Sen, 2002, Hemin-stimulated docking of cytochrome c to a hemin-DNA aptamer complex, *Biochemistry* 41, 5202.
- Cho, J.S., Y.J. Lee, K.S. Shin, S. Jeong, J. Park and S.W. Lee, 2004, In vitro selection of specific RNA aptamers for the NFAT DNA binding domain, *Mol. Cells*, 18, 17.
- Convery, M.A., S. Rowsell, N.J. Stonehouse, A.D. Ellington, I. Hirao, J.B. Murray, D.S. Peabody, S.E. Phillips and P.G. Stockley, 1998, Crystal structure of an RNA aptamer-protein complex at 2.8 Å resolution, *Nat. Struct. Biol.* 5, 133.
- Dai, Z., F. Yan, J. Chen and H. Ju, 2003, Reagentless amperometric immunosensors based on direct electrochemistry of horseradish peroxidase for determination of carcinoma antigen-125, *Anal. Chem.* 75, 5429.
- Di Gleria, K., H.A.O. Hill, C.J. McNeil and M.J. Green, 1986, Homogeneous ferrocene-mediated amperometric immunoassay, *Anal. Chem.* 58, 1203.
- Dove, A., 1999, Proteomics: Translating genomics into products?, *Nat. Biotechnol.* 17, 233.
- Ducey, M.W., A.M. Smith, X. Guo and M.E. Meyerhoff, 1997, Competitive nonseparation electrochemical enzyme binding immunoassay (NEEIA) for small molecule detection, *Anal. Chim. Acta* 357, 5.
- Ekins, R., 1989, A shadow over immunoassay, *Nature* 340, 256.
- Ekins, R. and F. Chu., 1997, Microspot, array-based, multianalyte binding assays: The ultimate microanalytical Technology?, *Principles and Practice of Immunoassay*, Eds. C.P. Price and D.J. Newman, Macmillan Reference Ltd, London, pp. 625–646.
- Ellington, A.D. and J. Szostak, 1990, In vitro selection of RNA molecules that bind specific ligands, *Nature* 346, 818.
- Engel, L. and W. Baumann, 1994, Direct potentiometric immunoelectrodes. 4. An immunoelectrode for the trace-level determination of atrazine by separated incubation and potential measurement steps, *Fresen. J. Anal. Chem.* 349, 447.
- Eremenko, A.V., C.G. Bauer, A. Makower, B. Kanne, H. Baumgarten and F.W. Scheller, 1998, The development of a non-competitive immunoenzymometric assay of cocaine, *Anal. Chim. Acta*, 358, 5.

- Frew, J.E., N.C. Foulds, J.M. Wilshere, N.J. Forrow and M.J. Green, 1989, Measurement of alkaline phosphatase activity by electrochemical detection of phosphate esters, *Electroanal. Chem.* 266, 309.
- Frey, A., F. Hofmann, R. Peters, B. Holzapfl, M. Schienle, C. Paulus, P. Schindler-Bauer, D. Kuhlmeier, J. Krause, G. Eckstein and R. Thewes, 2002, Yielded Evaluation of gold sensor electrodes used for fully electronic DNA detection arrays on CMOS, *Microelectron. Reliab.* 42, 1801.
- Fukuda, K., D. Vishnuvardhan, S. Sekiya, J. Hwang, N. Kakiuchi, K. Taira, K. Shimotohno, P.K. Kumar and S. Nishikawa, 2000, Isolation and characterization of RNA aptamers specific for the Hepatitis C virus nonstructural protein 3 protease, *Eur. J. Biochem.* 267, 3685.
- Gal, S.W., S. Amontov, P.T. Urvil, D. Vishnuvardhan, F. Nishikawa, P.K. Kumar and S. Nishikawa, 1998, Selection of a RNA aptamer that binds to human activated protein C and inhibits its protease function, *Eur. J. Biochem.* 252, 553.
- Gebbert, A., M. Alvarez-Icasa, W. Stöcklein and R.D. Schmid, 1992, Real-time monitoring of immunochemical interactions with a tantalum capacitance flow-through cell, *Anal. Chem.* 64, 997.
- Gebbert, A., M. Alvarez-Icasa, H. Peters, V. Jäger, U. Bilitewski and R.D. Schmid, 1994, Online monitoring of monoclonal-antibody production with regenerable flow-injection immuno systems, *J. Biotech.* 32, 213.
- Ghindilis, A.L., P. Atanasov and E. Wilkins, 1996, Potentiometric immunoelectrode for fast assay based on direct electron transfer catalyzed by peroxidase, *Sensors Actuators B* 34, 528.
- Ghindilis, A.L., A. Makower, C.G. Bauer, F.F. Bier and F.W. Scheller, 1995a, Picomolar determination of *p*-aminophenol and catecholamines based on recycling enzyme amplification, *Anal. Chim. Acta* 304, 25–31.
- Ghindilis, A.L., A. Makower and F.W. Scheller, 1995b, Nanomolar determination of the ferrocene derivatives using a recycling enzyme electrode development of a redox label immunoassay, *Anal. Lett.* 28, 1.
- Ghindilis, A.L., O.V. Skorobogat'ko, V.P. Gavrilova and A.I. Yaropolov, 1992, A new approach to the construction of potentiometric immunosensors, *Biosens. Bioelectron.* 7, 301.
- Ghindilis, A.L., O.V. Skorobogat'ko and A.I. Yaropolov, 1991, Immunopotentiometric electrodes based on bioelectrocatalysis in the absence of mediators, *Biomed. Sci.* 2, 520.
- Gothoh, M., E. Tamiya, M. Momoi, Y. Kagawa and I. Karube, 1987, Acetylcholine sensor based on ion sensitive field-effect transistor and acetylcholine receptor, *Anal. Lett.* 20, 857.
- Grant, S., F. Davis, J.A. Pritchard, K.A. Law, S.P.J. Higson and T.D. Gibson, 2003, Labelless and reversible immunosensor assay based upon an electrochemical current-transient protocol, *Anal. Chim. Acta* 495, 21.
- Green, L.S., D. Jellinek, R. Jenison, A. Ostman, C.-H. Heldin and N. Janjic, 1996, Inhibitory DNA ligands to platelet-derived growth factor B-chain, *Biochemistry* 35, 14413.
- Grennan, K., G. Strachan, A.J. Porter, A.J. Killard and M.R. Smyth, 2003, Atrazine analysis using an amperometric immunosensor based on single-chain antibody fragments and regeneration-free multi-calibrant measurement, *Anal. Chim. Acta* 500, 287.
- Harlow, E. and D. Lane, 1988, *Antibodies: A laboratory manual*, Cold Spring Harbor Laboratory, Cold Spring Harbor, USA.
- Harris, B., 1999, Exploiting antibody-based technologies to manage environmental pollution, *Trends Biotechnol.* 17, 290.
- Hesselberth, J.R., D. Miller, J. Robertus and A.D. Ellington, 2000, In vitro selection of RNA molecules that inhibit the activity of ricin A-chain, *J. Biol. Chem.* 275, 4937.
- Hicke, B.J., C. Marion, Y.F. Chang, T. Gould, C.K. Lynott, D. Parma, P.G. Schmidt and S. Warren, 2001, Tenascin-C aptamers are generated using tumor cells and purified protein, *J. Biol. Chem.* 276, 48644.

- Hintsche, R., M. Paeschke, A. Uhlig and R. Seitz, 1997, Microbiosensors using electrodes made in *S_i*-technology, *Frontiers in Biosensorics I*, Eds. F.W. Scheller, F. Schubert and J. Fedrowitz, Birkhäuser, Basel, pp. 267–283.
- Hirao, I., Y. Harada, T. Nojima, Y. Osawa, H. Masaki and S. Yokoyama, 2004, In vitro selection of RNA aptamers that bind colicin E3 and structurally resemble the decoding site of 16S ribosomal RNA, *Biochemistry* 43, 3214.
- Hirao, I., K. Madin, Y. Endo, S. Yokoyama and A.D. Ellington, 2000, RNA aptamers that bind to and inhibit the ribosome-inactivating protein, pepocin, *J. Biol. Chem.* 275, 4943.
- Hu, S.Q., J.W. Xie, Q.H. Xu, K.T. Rong, G.L. Shen and R.Q. Yu, 2003, A label-free electrochemical immunosensor based on gold nanoparticles for detection of paraoxon, *Talanta* 61, 769.
- Ikariyama, Y. and M. Aizawa, 1988, Bioaffinity sensors, *Methods in Enzymology*, Ed. K. Mosbach, Academic Press Inc., New York, 137, 111–124.
- Ivnitski, D., T. Wolf, B. Solomon, G. Fleminger and J. Rishpon, 1998, An amperometric biosensor for real-time analysis of molecular recognition, *Bioelectrochem. Bioenerg.* 45, 27.
- Janata, J., 1975, Immuno-electrode, *J. Am. Chem. Soc.* 97, 2914.
- Jenkins, S.H., W.R. Heineman and H.B. Halsall, 1988, Extending the detection limit of solid-phase electrochemical enzyme-immunoassay to the attomole level, *Anal. Biochem.* 168, 292.
- Jeon, S.H., B. Kayhan, T. Ben-Yedidia and R. Arnon, 2004, A DNA aptamer prevents influenza infection by blocking the receptor binding region of the viral haemagglutinin, *J. Biol. Chem.* 279, 48410.
- Jing, N., R.F. Rando, Y. Pommier and M.E. Hogan, 1997, Ion selective folding of loop domains in a potent anti-HIV oligonucleotide, *Biochemistry* 36, 12498.
- Johansson, A., D.H. Ellis, D.L. Bates, A.M. Plumb and C.J. Stanley, 1986, Enzyme amplification for immunoassays – Detection limit of 100th of an attomole, *J. Immunol. Meth.* 87, 7.
- Kaneki, N., Y. Xu, A. Kumari, H.B. Halsall, W.R. Heineman and P.T. Kissinger, 1994, Electrochemical enzyme immunoassay using sequential saturation technique in a 20- μ l capillary: Digoxin as a model analyte, *Anal. Chim. Acta* 287, 253.
- Kassegne, S.K., H. Reese, D. Hodko, J.M. Yang, K. Sarkar, D. Smolko, P. Swanson, D.E. Raymond, M.J. Heller and M.J. Madou, 2003, Numerical modeling of transport and accumulation of DNA on electronically active biochips, *Sensors and Actuators B* 94(1), 81.
- Keating, M.Y. and G.A. Rechnitz, 1984, Potentiometric digoxin antibody measurements with antigen ionophore based membrane electrodes, *Anal. Chem.* 56, 801.
- Keay, R.W. and C.J. McNeil, 1998, Separation-free electrochemical immunosensor for rapid determination of atrazine, *Biosens. Bioelectron.* 13, 963.
- Kelly, S.O. and J.K. Barton, 1999, Electron transfer between bases in double helical DNA, *Science* 283, 375.
- Kensch, O., B.A. Connolly, H.J. Steinhoff, A. McGregor, R.S. Goody and T. Restle, 2000, HIV-1 reverse transcriptase-pseudoknot RNA aptamer interaction has a binding affinity in the low picomolar range coupled with high specificity, *J. Biol. Chem.* 275, 18271.
- Key, G., A. Schreiber, R. Feldbrügge, C.J. McNeil, P. Joergensen, M.M.A.L. Pelsers, J.F.C. Glatz and F. Spener, 1999, Multicenter evaluation of an amperometric immunosensor for plasma fatty acid-binding protein: An early marker for acute myocardial infarction, *Clin. Biochem.* 32, 229.
- Kirby, R., E.J. Cho, B. Gehrke, T. Bayer, Y.S. Park, D.P. Neikirk, J.T. McDevitt and A.D. Ellington, 2004, Aptamer-based sensor arrays for the detection and quantitation of proteins, *Anal. Chem.* 76, 4066.
- Kleinjung, F., S. Klussmann, V.A. Erdmann, F.W. Scheller, J.P. Fuerste and F.F. Bier, 1998, High-affinity RNA as a recognition element in a biosensor, *Anal. Chem.* 70, 328.
- Klug, S.J., A. Huttenhofer and M. Famulok, 1999, In vitro selection of RNA aptamers that bind special elongation factor SelB, a protein with multiple RNA-binding sites, reveals one major interaction domain at the carboxyl terminus, *RNA* 5, 1180.
- Kulys, J., V. Razumas and A. Malinauskas, 1980, Electrochemical oxidation of catechol and *p*-aminophenol esters in the presence of hydrolases, *Bioelectrochem. Bioenerg.* 7, 11.

- Landsteiner, K. and J. van der Scheer, 1928, Serological differentiation of steric isomers, *J. Exp. Med.* 48, 315.
- Lee, M. and D.R. Walt, 2000, A fibre-optic microarray biosensor using aptamers as receptors, *Anal. Biochem.* 282, 142.
- Lu, B., E.I. Iwuoha, M.R. Smyth and R. O'Kennedy, 1997a, Development of an "electrically wired" amperometric immunosensor for the determination of biotin based on a non-diffusional redox osmium polymer film containing an antibody to the enzyme label horseradish peroxidase, *Anal. Chim. Acta* 345, 59.
- Lu, B., E.I. Iwuoha, M.R. Smyth and R. O'Kennedy, 1997b, Development of an amperometric immunosensor for horseradish peroxidase (HRP) involving a non-diffusional osmium redox polymer co-immobilised with anti-HRP antibody, *Anal. Comm.* 34, 21.
- Lupold, S.E., B.J. Hicke, Y. Lin and D.S. Coffey, 2002, Identification and characterization of nuclease-stabilized RNA molecules that bind human prostate cancer cells via the prostate-specific membrane antigen, *Cancer Res.* 62, 4029.
- Makower, A., C.G. Bauer, A. Ghindilis and F.W. Scheller, 1994, Sensitive detection of cocaine by combining conjugate displacement and an enzyme substrate recycling sensor, *Biosensors 94*, Proceedings of the 3rd World Congress on Biosensors, Ed. T. Turner, Elsevier Advanced Technology, Oxford, Poster 3.27.
- Marko-Varga, G., J. Emneus, L. Gorton and T. Ruzgas, 1995, Development of enzyme-based amperometric sensors for the determination of phenolic compounds, *Trends Anal. Chem.* 14, 319.
- Matthiasson, B. and H. Nilsson, 1977, Enzyme immunoelectrode – assay of human serum albumin and insulin, *FEBS Lett.* 78, 251.
- McCauley, T.G., N. Hamaguchi and M. Stanton, 2003, Aptamer-based biosensor arrays for detection and quantification of biological macromolecules, *Anal. Biochem.* 319(2), 244.
- McGregor, A., J.B. Murray, C.J. Adams, P.G. Stockley and B.A. Connolly, 1999, Secondary structure mapping of an RNA ligand that has high affinity for the MetJ repressor protein and interference modification analysis of the protein-RNA complex, *J. Biol. Chem.* 274, 2255.
- McNeil, C.J., D. Athey and W.O. Ho, 1995, Direct electron transfer bioelectronic interfaces: Application to clinical analysis, *Biosens. Bioelectron.* 10, 75.
- Meusel, M., R. Renneberg, F. Spener and G. Schmitz, 1995, Development of heterogeneous amperometric immunosensor for the determination of apolipoprotein E in serum, *Biosens. Bioelectron.* 10, 577.
- Milligan, C. and A. Ghindilis, 2002, Laccase based sandwich scheme immunosensor employing mediatorless electrocatalysis, *Electroanalysis* 14, 415.
- Mirhabibollahi, B., J.L. Brooks and R.G. Kroll, 1990a, An improved amperometric immunosensor for the detection and enumeration of protein A-bearing *Staphylococcus aureus*, *Lett. Appl. Microbiol.* 11, 119.
- Mirhabibollahi, B., J.L. Brooks and R.G. Kroll, 1990b, Development and performance of an enzyme-linked amperometric immunosensor for the detection of *staphylococcus aureus* in foods, *J. Appl. Bacteriol.* 68, 577.
- Navratilova, I. and P. Skladal, 2004, The immunosensors for measurement of 2,4-D based on electrochemical impedance spectroscopy, *Bioelectrochemistry* 62, 11.
- Nebling, E., T. Grunwald, J. Albers, P. Schäfer and R. Hintsche, 2004, Electrical detection of viral DNA using ultramicroelectrode arrays, *Anal. Chem.* 76, 689.
- Newman, A.L., K.W. Hunter and W.D. Stanbro, 1986, Proceedings of the 2nd International Meeting on Chemical Sensors, Bordeaux, 596.
- Niemeyer, C.M., T. Sano, C.L. Smith and C.R. Cator, 1994, Oligonucleotide-directed self-assembly of proteins: Semisynthetic DNA-streptavidin hybrid molecules as connectors for the generation of macroscopic arrays and the construction of supramolecular bioconjugates, *Nucleic Acid Res* 22, 5530.
- Niwa, O., M. Morita and H. Tabei, 1991, Highly sensitive and selective voltammetric detection of dopamine with vertically separated interdigitated array electrodes, *Electroanalysis* 3, 163.

- Niwa, O., Y. Xy, B.H. Halsall and W.R. Heineman, 1993, Small-volume voltammetric detection of 4-aminophenol with integrated array electrodes and its application to electrochemical enzyme immunoassay, *Anal. Chem.* 65, 1559.
- Ogert, R.A., A.W. Kusterbeck, A. Gregory, R.B. Wemhoff, R. Burke and F.S. Ligler, 1992, Detection of cocaine using the flow immunosensor, *Anal. Lett.* 25, 1999.
- Olson, J.D., P.R. Panfili, R. Armenta, M.B. Fremmel, H. Merrick, J. Gumperz, M. Goltz and R.F. Zuk, 1990, A silicon sensor – based filtration immunoassay using biotin-mediated capture, *J. Immunol. Meth.* 134, 71.
- Padeste, C., A. Grubelnik and L. Tiefenauer, 1998, Amperometric immunosensing using microperoxidase MP-11 antibody conjugates, *Anal. Chim. Acta*, 374, 167.
- Pfeifer, U. and W. Baumann, 1992, Direct potentiometric immunoelectrodes. 1. Immobilization of proteins on titanium wire electrodes, *Fresen. J. Anal. Chem.* 343, 541.
- Pileur, F., M.L. Andreola, E. Dausse, J. Michel, S. Moreau, H. Yamada, S.A. Gaidamakov, R.J. Crouch, J.J. Toulme and C. Cazenave, 2003, Selective inhibitory DNA aptamers of the human RNase H1, *Nucleic Acid Res.* 31, 5776.
- Potyrailo, R.A., R.C. Conrad, A.D. Ellington and G.M. Hieftje, 1998, Adapting selected nucleic acid ligands (aptamers) to biosensors, *Anal. Chem.* 70, 3419.
- Price, C.P., 1998, Progress in immunoassay technology, *Clin. Chem. Lab. Med.* 36, 341.
- Proske, D., M. Hofliger, R.M. Soll, A.G. Beck-Sickinger and M. Famulok, 2002, A Y2 receptor mimetic aptamer directed against neuropeptide Y, *J. Biol. Chem.* 277, 11416.
- Raba, J. and H.A. Motolla, 1994, Online enzymatic amplification by substrate cycling in a dual bioreactor with rotation and amperometric detection, *Anal. Biochem.* 220, 297.
- Renneberg, R., W. Schoessler and F. Scheller, 1983, Amperometric enzyme sensor-based enzyme immunoassay for factor VIII-related antigen, *Anal. Lett.* 16, 1279.
- Riepl, M., V.M. Mirsky, I. Novotny, V. Tvarozek, V. Rehacek and O.S. Wolfbeis, 1999, Optimization of capacitive affinity sensors: Drift suppression and signal amplification, *Anal. Chim. Acta* 392, 77.
- Rishpon, J. and D. Ivnitiski, 1997, An amperometric enzyme-channeling immunosensor, *Biosens. Bioelectron.* 12, 195.
- Rhodes, A., A. Deakin, J. Spaul, B. Coomber, A. Aitken, P. Life and S. Rees, 2000, The generation and characterization of antagonist RNA aptamers to human oncostatin M, *J. Biol. Chem.* 275, 28555.
- Robinson, G.A., V.M. Cole and G.C. Forrest, 1987/1988, A homogeneous electrode-based bioelectrochemical immunoassay for human chorionic gonadotrophin, *Biosensors* 3, 147.
- Romero, F.J.M., M. Stiene, R. Kast, M.D. Luque de Castro and U. Bilitewski, 1998, Application of screen-printed electrodes as transducers in affinity flow-through sensor systems, *Biosens. Bioelectron.* 13, 1107.
- Rubenstein, K.E., R.S. Schneider and E.F. Ullman, 1972, Homogeneous enzyme immunoassay – New immunochemical technique, *Biochem. Biophys. Res. Commun.* 47, 846.
- Ruzgas, T., A. Csöregi, J. Emneus, L. Gorton and G. Marko-Varga, 1996, Peroxidase-modified electrodes: Fundamentals and application, *Anal. Chim. Acta* 330, 123.
- Sadik, O.A., Van Emon, J.M., 1997. Designing immunosensors for environmental monitoring, *Chem. Tech.* 38–46.
- Santadreu, M., A. Alegret and E. Fabregas, 1999, Determination of beta-HCG using amperometric immunosensors based on a conducting immunocomposite, *Anal. Chim. Acta* 396, 181.
- Sayer, N., J. Ibrahim, K. Turner, A. Tahiri-Alaoui and W. James, 2002, Structural characterization of a 2'F-RNA aptamer that binds a HIV-1 SU glycoprotein, gp 120, *Biochem. Biophys. Res. Commun.* 293, 924.
- Scheller, F.W., C.G. Bauer, A. Makower, U. Wollenberger, A. Warsinke and F.F. Bier, 2002, Immunoassays using enzymatic amplification electrodes, *Biomolecular Sensors*, Eds. E. Gizeli and C.R. Lowe, Taylor and Francis, London, pp. 207–238.
- Self, C.H., 1981, European Patent Appl. 80303478.4 (15.04.1981).
- Sergeyeva, T.A., A.P. Soldatkin, A.E. Rachkov, M.I. Tereschenko, S.A. Piletsky and A.V. El'skaya, 1999, Beta-lactamase label-based potentiometric biosensor for alpha-2 interferon detection, *Anal. Chim. Acta* 390, 73.

- Srisawat, C. and D.R. Engelke, 2001, Streptavidin aptamers: Affinity tags for the study of RNAs and ribonucleoproteins, *RNA* 7, 632.
- Stelzle, M., M. Durr and W. Nisch, 2001, On-chip electrophoresis accumulation of DNA-oligomers and streptavidin, *Fresen. J. Anal. Chem.* 371, 112.
- Susmel, S., G.G. Guilbault and C.K. O'Sullivan, 2003, Demonstration of label-less detection of food pathogens using electrochemical redox probe and screen printed gold electrodes, *Biosens. Bioelectron.* 18, 881.
- Takeo, H., S. Yamamoto, T. Tanaka, Y. Sakano and Y. Kikuchi, 1999, Selection of an RNA molecule that specifically inhibits the protease activity of subtilisin, *J. Biochem. (Tokyo)* 125, 1115.
- Tang, H.T., C.F. Lunte, H.B. Halsall and W.R. Heineman, 1988, -Aminophenyl phosphate – An improved substrate for electrochemical enzyme immunoassay, *Anal. Chim. Acta* 214, 187.
- Tang, X. and G. Johansson, 1995, Enzyme electrode for amplification of NAD^+/NADH using glycerol dehydrogenase and diaphorase with amperometric detection, *Anal. Lett.* 28, 2595.
- Tarasewich, M.R., 1985, Chapter 4: Bioelectrocatalysis. *Comprehensive Treatise of Electrochemistry*, 10th Bioelectrochemistry, Eds. S. Srinivasan, Y.A. Chizmadzhev, J.O'M. Bockris, B.E. Conway and E. Yeager, Plenum Press, New York, 275.
- Tasset, D.M., M.F. Kubik and W. Steiner, 1997, Oligonucleotide inhibitors of human thrombin that bind distinct epitopes, *J. Mol. Biol.* 272, 688.
- Thévenot, D.R., K. Toth, R.A. Durst and G.S. Wilson, 2001, Electrochemical biosensors: Recommended definitions and classification, *Biosens. Bioelectron.* 16, 121.
- Thomas, M., S. Chedin, C. Carles, M. Riva, M. Famulok and A. Sentenac, 1997, Selective targeting and inhibition of yeast RNA polymerase II by RNA aptamers, *J. Biol. Chem.* 272, 27980.
- Tiefenauer, L.X., S. Kossek, C. Padeste and P. Thiébaud, 1997, Towards amperometric immunosensor devices, *Biosens. Bioelectron.* 12, 213.
- Tuerk, C. and L. Gold, 1990, Systematic evolution of ligands by exponential enrichment: RNA ligands to bacteriophage T4 DNA polymerase, *Science* 249, 505.
- Wehmeyer, K.R., H.B. Halsall, W.R. Heineman, C.D. Volle and I.W. Chen, 1986, Competitive heterogeneous enzyme immunoassay for digoxin with electrochemical detection, *Anal. Chem.* 58, 135.
- Weiss, S., D. Proske, M. Neumann, M.H. Groschup, H.A. Kretzschmar, M. Famulok and E.L. Winnacker, 1997, RNA aptamers specifically interact with the prion protein PrP, *J. Virol.* 71, 8790.
- Weller, M.G., A.J. Schuetz, M. Winklmair and R. Niessner, 1999, Highly parallel affinity sensor for the detection of environmental contaminants in water, *Anal. Chim. Acta* 393, 29.
- Wendzinski, F., B. Gründig, R. Renneberg and F. Spener, 1997, Highly sensitive determination of hydrogen peroxide and peroxidase with tetraethialvalene-based electrodes and the application in immunosensing, *Biosens. Bioelectron.* 12, 43.
- Wiegand, T.W., P.B. Williams, S.C. Dreskin, M.H. Jouvin, J.P. Kinet and D. Tasset, 1996, High-affinity oligonucleotide ligands to human IgE inhibit binding to Fc epsilon receptor I, *J. Immunol.* 157, 221.
- Wingren, C., J. Ingvarsson, M. Lindstedt and C.A.K. Borrebaeck, 2003, Recombinant antibody microarrays – a viable option?, *Nat. Biotechnol.* 21, 223.
- Wollenberger, U., M. Paeschke and R. Hintsche, 1994, Interdigitated array microelectrodes for the determination of enzyme activities, *Analyst* 119, 1245.
- Wollenberger, U., F. Schubert, D. Pfeiffer and F.W. Scheller, 1993, Enhancing biosensor performance using multi-enzyme systems, *Trends Biotechnol.* 11, 255.
- Yalow, R.S. and S.A. Berson, 1959, Assay of plasma insulin in human subjects by immunological methods, *Nature* 184, 1648.
- Yamamoto, R., T. Baba and P.K. Kumar, 2000, Molecular beacon aptamer fluoresces in the presence of Tat protein of HIV-1, *Genes Cells* 5, 389.
- Yang, L., Y. Li and G.F. Erf, 2004, Interdigitated array microelectrode-based electrochemical impedance immunosensor for detection of *E.coli* O157:H7, *Anal. Chem.* 76, 1107–1113.

This page intentionally left blank

Self-Assembly of Biomolecules on Electrode Surfaces; Oligonucleotides, Amino Acids, and Proteins toward the Single-Molecule Level

Hainer Wackerbarth¹, Jingdong Zhang¹, Mikala Grubb¹, Allan Glargaard Hansen², Bee Lean Ooi¹, Hans Erik Mølager Christensen¹ and Jens Ulstrup¹

¹*Department of Chemistry, Technical University of Denmark, Building 207, 2800 Lyngby, Denmark*

²*Walter Schottky Institut, Technische Universität München, 85748 Garching, Germany*

Contents

1. Introduction	485
2. Theory and experiment of scanning tunneling microscopy	487
2.1. Molecular conductivity and mechanisms of the <i>in situ</i> STM process	487
2.2. Properties of the Au(111) surface	490
3. From mononucleotides to oligonucleotides	492
3.1. Self-assembly on Au(111)	492
4. Amino acids and protein monolayers	498
4.1. Network-like clusters in cysteine adlayers on Au(111)	498
4.2. Assembling of the iron-sulfur protein <i>pyrococcus furiosus</i> ferredoxin on thiolate-modified Au(111) surfaces	503
4.3. An alternative strategy for intelligent materials – artificial proteins	507
5. Concluding remarks	509
List of abbreviations	511
Acknowledgments	511
References	511

1. INTRODUCTION

Two-dimensional films of biomolecules at metallic surfaces in contact with aqueous solution are broadly important. Fundamental aspects are adsorption patterns (Horbett and Brash, 1995; Tirrell *et al.*, 2002; Kasemo, 2002), two-dimensional molecular interactions including phase transitions (Castner and Ratner, 2002), electron transfer (ET) mechanisms of DNA-based molecules (Giese, 2000; Jortner *et al.*, 2000; Bixon and Jortner, 2000, 2002) and of immobilized redox proteins (Tarlov and Bowden, 1991; Chi *et al.*, 2001; Davis *et al.*, 2002; Zhang *et al.*, 2002; Wackerbarth and Hildebrandt, 2003), and mechanisms of coupled chemical and biocatalytic processes (Shipway and Willner, 2001; Gilardi and Fantuzzi, 2001; Jeuken *et al.*, 2002). A crucial issue

for approaches to DNA hybridization, ET of metalloproteins, and enzyme catalysis is to retain functionality of the biomolecules in the adsorbed state. In this context, surface modifications are often indispensable. However, the interactions between the bare or modified surface and the adsorbed biomolecules are far from being fully understood at the molecular level. Other high-technology perspectives are based on the electronic conductivity of oligonucleotides, and the vision of surface-immobilized DNA-based structures as self-assembling components of nanoscale functional devices (Kinneret and Braun, 2004; Berlin *et al.*, 2000).

Visualization of nanoscopic structures has become possible with the introduction of the scanning probe microscopies, particularly scanning tunneling (STM) (Binnig *et al.*, 1982) and atomic force (AFM) microscopy (Magonov and Whangbo, 1996). STM can also operate outside ultra-high vacuum (UHV), particularly in aqueous environment (Sommerfeld and Hansma, 1986). By introduction of electrochemical control, STM has been developed to image surface processes *in situ* (Wiechers *et al.*, 1988; Itaya and Tomita, 1988). The *in situ* STM mode offers structural and dynamic characterization also of biomolecular monolayers directly in their natural aqueous medium, and are hence, able to illuminate biomolecule–surface interactions. The electronic properties can, further be probed at the single-molecule level in biological environment. Apart from visualization of molecular structures, *in situ* STM offers new possibilities as a component in molecular electronics, also in respect to new ET phenomena (Zhang *et al.*, 2002; Albrecht *et al.*, 2005a), in the particular *in situ* STM configuration. Fundamental microscopic mechanisms and scenarios for electron tunneling through (redox) molecules within the electrode-tip gap are thus important elements in STM data interpretation and part of the discussion in the present report.

Single-crystal, atomically planar electrode surfaces are novel in bioelectrochemistry of biological macromolecules and developed as a powerful high-resolution tool in redox metalloprotein (Zhang *et al.*, 2002) and oligonucleotide (Wackerbarth *et al.*, 2004a) electrochemistry. In particular, the high sensitivity of single-crystal electrodes allows detection of subtle non-Faradaic processes such as molecular reorientation on the surface (Roelfs *et al.*, 1997). The orientation resulting in the accessibility of the biomolecules on the surface is crucial for their functionality.

Some recent experimental and theoretical studies in our group are overviewed in this chapter, in a “bottom-up” fashion. The approach is from building blocks to higher organized systems, i.e., from mononucleotides to DNA fragments, and from amino acids to proteins, organized on single-crystal surfaces. In Section 2.1, we provide a brief overview of molecular tunneling mechanisms in STM and *in situ* STM. In Section 2.2, we describe the features of the central substrate electrode systems mostly used, the single-crystal Au(111) surface. Section 3 overviews data for mono- and oligonucleotide monolayers and offers some views on electronic conduction mechanisms across adlayers of DNA-based molecules. This is followed in Section 4.1 by an overview of electrochemical and *in situ* STM studies of amino acids and Section 4.2 is on redox metalloproteins. In Section 4.3, studies of artificial proteins on Au(111) are presented and Section 5 offers some concluding observations.

2. THEORY AND EXPERIMENT OF SCANNING TUNNELING MICROSCOPY

2.1. Molecular conductivity and mechanisms of the *in situ* STM process

In situ STM has been established as a high-resolution technique for topography, dynamics, and functionality of the electrochemical interface (Gewirth and Siegenthaler, 1995; Danilov, 1995; Lorenz and Plieth, 1998; Kolb, 2001). In contrast to *ex situ* STM, *in situ* STM rests on independent control of the substrate and tip potential. An external parameter additional to the bias voltage is hence the potential difference between the substrate and solution. A second major difference is rooted in the tunneling *phenomenon* and in static and fluctuational effects of an assembly of water molecules in the tunnel gap on the tunneling current. Static effects arise from electronic interactions with the solvent polarization and pseudopotential forces (Nitzan, 2001). The overall effects are to enhance electron tunneling compared to vacuum (Gurevich and Kuznetsov, 1975; Schmickler, 1999).

The electronic conduction properties of the molecules enclosed between the substrate and tip electrodes are determined by the intrinsic energetics and spatial features of the highest occupied (HOMO) and lowest unoccupied (LUMO) adsorbate molecular orbitals relative to the substrate and tip Fermi levels. The HOMO and LUMO properties are strongly affected by the molecular adsorbate conformation. Packing constraints in the soft adlayers can, for example, impose molecular conformations with poor electronic conductivity unfavorable for *in situ* STM. Reliable high-resolution imaging frequently requires that quasi-liquid crystalline monolayers are formed.

Tunneling through off-resonance LUMOs and HOMOs, Figure 1 bears a close relation to simple patterns of the tunneling current, i_{tunn} or conductivity, $g(V_{\text{bias}})$, where V_{bias} is the bias voltage, say (Joachim and Ratner, 2004)

$$g(V_{\text{bias}}) = \frac{di_{\text{tunn}}}{dV_{\text{bias}}} \approx g_0 \exp[-\beta(V_{\text{bias}})z], \quad (1)$$

where g_0 is a constant, z the distance between the tip and the negatively biased electrode, and $\beta(V_{\text{bias}})$ the (bias voltage dependent) decay parameter. $\beta(V_{\text{bias}})$ can be related approximately to the average energy gap, Δ , between the Fermi level of the negatively biased electrode, $\varepsilon_{\text{Fneg}}$ and the nearest bridge group orbital (LUMO), or the energy gap between the Fermi level of the positively biased electrode, $\varepsilon_{\text{Fpos}}$ and the bridge group orbital closest to this electrode (HOMO) as well as to the average nearest neighbour LUMO or HOMO exchange interactions, v_{exch} , (Kuznetsov and Ulstrup, 1999)

$$\beta(V_{\text{bias}}) \approx \frac{2}{a} \ln \left[\frac{\Delta(V_{\text{bias}})}{v_{\text{exch}}} \right], \quad (2)$$

where a is the average spatial extension of the electron transmitting orbitals. The decay is thus faster, the larger the energy gap and the weaker the exchange interactions.

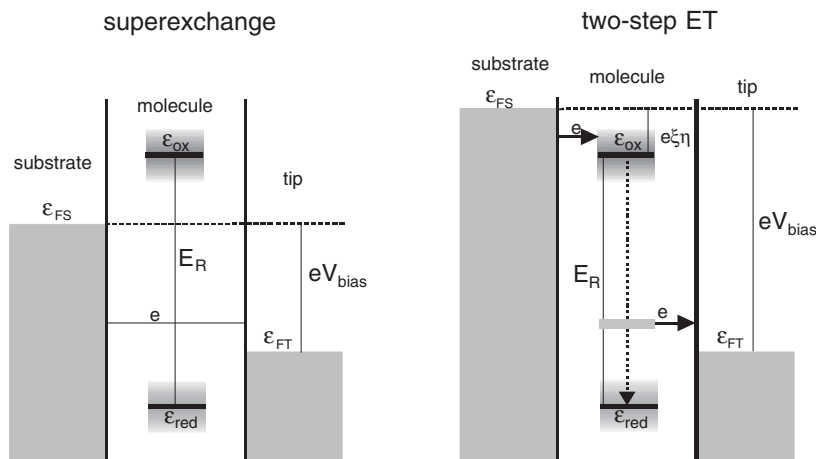


Fig. 1. Schematic representation of ET scenarios in the *in situ* STM configuration of a redox molecule. The substrate and tip are represented by two continuous electronic energy level distributions populated up to the Fermi levels, ϵ_{FS} and ϵ_{FT} , respectively. ϵ_{FS} and ϵ_{FT} are vertically displaced by the bias voltage energy, eV_{bias} . Positive V_{bias} implies, that $\epsilon_{FT} < \epsilon_{FS}$. The redox level exists in an empty (oxidized) and an occupied (reduced) state. At equilibrium, ϵ_{ox} is much higher than ϵ_{red} the energy difference being given by twice the environmental reorganization (free) energy, E_R . The quantity is large ($E_R > e/V_{bias}$) so that ϵ_{ox} is located above the Fermi energy of the negatively biased and ϵ_{red} below the Fermi energy of the positively biased electrode. The figure to the left illustrates tunneling ET from the substrate to the positively biased electrode via the vacant redox level. This level remains above both Fermi levels and assists tunneling by purely electronic coupling in a superexchange mode. The figure to the right illustrates the *in situ* STM mechanism when the combined action of the overpotential and environmental nuclear configurational fluctuations, takes ϵ_{ox} close to ϵ_{FS} so that sequential ET from substrate to molecule and from molecule to tip now occurs. Subsequent to the first ET step the reduced molecular energy level relaxes to a position below ϵ_{FT} , followed by renewed thermal activation in the second ET step. A multitude of electrons are transferred during the relaxation process between ϵ_{FS} and ϵ_{FT} if the electronic molecule–electrode couplings are strong enough.

Even the simple forms in equations (1) and (2) often constitute satisfactory frames for observed far off-resonance STM current–distance relations, i.e., $\Delta/v_{exch} \gg 1$ (Joachim and Ratner, 2004). Complex patterns, however, arise when the bridge group orbital energies approach ϵ_{Fneg} or ϵ_{Fpos} , $\Delta/v_{exch} \rightarrow 1$, (Figure 1) (Kuznetsov and Ulstrup, 1999). Different coherent and incoherent electronic-vibrational transmission patterns involving physical electronic *population* of the bridge group orbitals then arise. Environmental configurational fluctuations further affect strongly both the energetics and electronic orbital properties, endowing these with electronic transmission properties quite different from macroscopic properties such as those determined by oxidation and reduction potentials (Voityuk *et al.*, 2004). Such scenarios may apply when biomolecular monolayers are addressed electronically at the single-molecule level. Presently, we consider first briefly tunneling through a single-redox level,

which cycles through temporary electronic population and depopulation in the molecular *in situ* STM process (Figure 1).

The intermediate bridge group orbitals are not physically populated in the tunneling mechanism represented by Figure 1 to the left commonly denoted as “superexchange”, or merely “tunneling”. More detail on tunneling current/bias voltage or/overpotential relations is disclosed when low-lying redox levels in the target molecules can be addressed. These correlations display, for example, “spectroscopic features” and “negative differential resistance” in bias voltage or overpotential ranges, where the redox levels are brought to cross the Fermi level(s) (Kuznetsov and Ulstrup, 2000a; Zhang *et al.*, 2003). This class of mechanisms, in which the bridge group population is temporarily changed has been denoted as “hopping”. Mechanisms and ET scenarios of adsorbed redox molecules in the *in situ* STM tunnel gap in this limit have evolved from electrochemical ET theory (Kuznetsov and Ulstrup, 2000a,b). However, the presence of *two* electrodes, i.e., substrate and tip, causes important differences from single-electrode electrochemistry, even to the extent of new interfacial ET *phenomena*. A molecule with a discrete fluctuating electronic level is here located between the substrate and the tip, both represented by a continuous distribution of electronic levels, Figure 1 to the right. These are populated up to the Fermi levels ε_{FS} (substrate electrode) and ε_{FT} (tip), mutually shifted by the bias voltage V_{bias} . The redox molecule exists in an oxidized and reduced valence state with the equilibrium free energy level ε_{ox} and ε_{red} , respectively. ε_{ox} is significantly higher than ε_{red} as long as the ionization energy of the molecule exceeds the solvation free energy. As the localized electronic states are strongly coupled to the molecular and solvent environment, fluctuations in the latter induce corresponding fluctuations in the electronic levels. The equilibrium free energy difference between the redox levels is twice the reorganization free energy i.e., $2E_R$.

Schemes such as those displayed in Figure 1 represent different tunneling channels. In broad terms:

- In the first case (Figure 1 to the left), the oxidized electronic level remains above ε_{FS} . Neither the overpotential nor nuclear configurational fluctuation effects are sufficient to lower the level close enough to the Fermi level so that the vacant oxidized level becomes occupied. ET between substrate and tip is then mediated by superexchange via the lowered, and fluctuating, off-resonance redox level. This is equivalent to “indentations” in the tunneling barriers, cf. equation (2).
- In the second case (Figure 1 to the right), the substrate Fermi level ε_{FS} is raised close enough to the electronic redox level that the overpotential η representing the driving force $e\xi\eta$ for temporary population of the initially vacant electronic level. e is the electronic charge and ξ the fraction of the electrode-solution potential drop at the site of the redox group. Subsequent to occupation the level initiates vibrational relaxation toward the electronic level ε_{red} located below ε_{FT} . Renewed thermal activation transmits the electron to the positively biased electrode in different patterns of an overall two-step process.

- If the interactions between the redox level and both the substrate and tip are weak, the redox level relaxes fully in the intermediate state, and the process becomes a sequence of two equilibrated single-ET steps. A new tunneling phenomenon arises if the adsorbate interacts strongly with both the substrate and tip (Kuznetsov and Ulstrup, 2000a). Vibrational relaxation is again initiated after the first ET step, but a multitude of electrons flow on the way between the substrate and tip Fermi levels. This can be called vibrationally coherent two-step ET. The electron flow stops when the reduced level has crossed the Fermi level of the tip. Many electrons are hence transferred in a single *in situ* STM event. This could hold a clue to the high current density per molecule often observed in STM. The following simple analytical equation frames this pattern (Zhang *et al.*, 2002)

$$i_{\text{tunn}} = \frac{1}{2} e \kappa \rho (e V_{\text{bias}}) \frac{\omega_{\text{eff}}}{2\pi} \exp\left(-\frac{E_{\text{r}} + e V_{\text{bias}}}{4k_{\text{B}} T}\right) \cosh^{-1} \left[\frac{(\frac{1}{2} - \gamma) e V_{\text{bias}} - e \zeta \eta}{2k_{\text{B}} T} \right], \quad (3)$$

where κ_{el} is the electronic transmission coefficient for molecule–electrode ET and ρ the electronic energy density, both taken as the same for substrate and tip. ω_{eff} is the effective vibrational frequency (10^{11} – 10^{13} s⁻¹) and γ the fraction of the bias voltage drop at the site of the redox level. k_{B} is Boltzmann’s constant and T the temperature.

- In a third case (not illustrated) the vacant ε_{ox} , the occupied level, ε_{red} , or both are trapped between the Fermi levels. This happens when the bias voltage energy exceeds the reorganization free energy, $\gamma |e V_{\text{bias}}| > E_{\text{R}} - e \zeta \eta$. Activationless high tunneling currents, independent of both η and V_{bias} then emerge.

Theoretical notions in electrochemical interfacial ET have been brought to accord with these mechanisms (Zhang *et al.*, 2002) and expanded to novel molecular rectifier (Kuznetsov and Ulstrup, 2002) and transistor (Kuznetsov and Ulstrup, 2004) configurations. Chemical and physical properties as well as environmental conditions are different in these systems, but the notion of interfacial ET between the target molecules and the enclosing metal electrodes has offered a very useful common conceptual and formal frame. Experimental support is also accumulating (Tao, 1996; Albrecht *et al.*, 2005a, b).

2.2. Properties of the Au(1 1 1) surface

Hamelin and Clavilier were pioneers in the introduction of single-crystal electrode surfaces into electrochemistry. In the 1980s they developed flame-annealing and cleaning techniques for preparation of clean single-crystal metal surfaces, especially for gold and platinum. These methods are now accepted worldwide (Clavilier *et al.*, 1980; Hamelin, 1996). Electronic properties of single-crystal gold surfaces in electrochemistry are mainly based on redox processes. Electronic features of different crystallographic orientations of surfaces are reflected

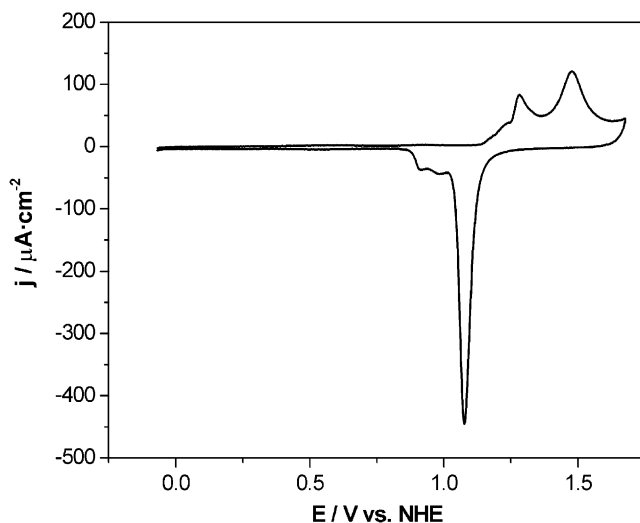


Fig. 2. Cyclic voltammogram of Au(111) in 0.1 M HClO₄ solution. Scan rate 50 mV s⁻¹.

by characteristic voltammetric peaks with well-defined peak potentials and current densities determined by the surface energy as well as by interactions with the solvent, supporting electrolyte, and temperature. Figure 2 shows a voltammogram of an Au(111) electrode in 0.1 M HClO₄ solution. The perchlorate anion adsorbs insignificantly. The Au(111) surface is oxidized at potentials positive of 1 V with two sharp anodic peaks at 1.3 and 1.5 V vs. normal hydrogen electrode (NHE) according to equation (4). This process is pH dependent. Oxide reduction gives a further needle-like sharp peak at 1 V (equation 5).



There are two other, smaller fingerprint cathodic peaks at 0.88 and 0.95 V. Hydrogen evolution occurs at potentials negative of -0.15 V. The most useful potential range is thus the double layer region in which no redox process occurs neither from gold nor solvent. The current in this range is capacitive and arises from solvent orientation (e.g., water molecules), giving a 1.0 V double-layer region with a capacitance of ca. 31 μF cm⁻². Such correspondingly low-background currents are essential to achieve high signal to noise ratio and high sensitivity for systems with weak signals, such as biomolecules (e.g. metalloproteins).

Surface structure and dynamics of bare and adsorbate-covered Au(111) in aqueous solution have been investigated extensively by *in situ* STM (Itaya, 1998; Kolb, 2001). The electronic structure from STM images reflects the topography of the surfaces. The Au(111) surface is easily reconstructed into (√3 × 22) R30° with a herringbone-like pattern in aqueous solution under potential

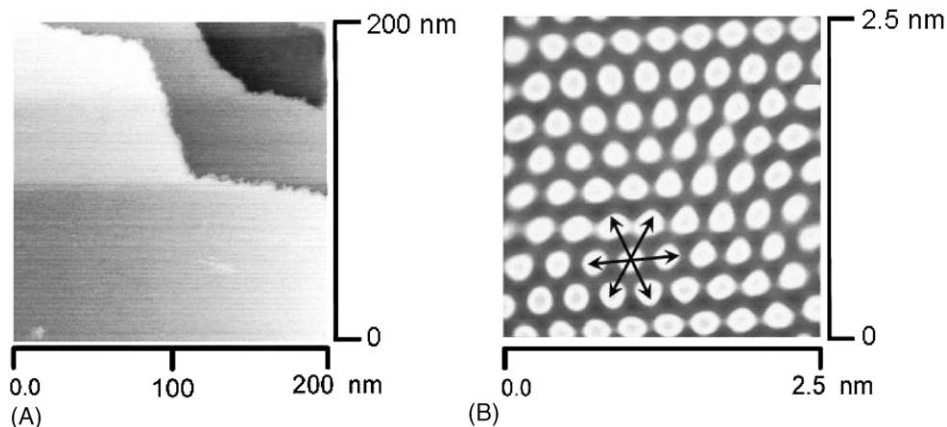


Fig. 3. *In situ* STM images of Au(111) in 0.1 M HClO₄ solution. Tunneling current $I_t = 1.0$ nA, sample potential $E_w = 0.20$ V vs. NHE, bias voltage $V_{\text{bias}} = 0.20$ V. (A) 200×200 nm² and (B) 2.5×2.5 nm².

control (Kolb, 2001), due to mobility of the gold atoms in the top surface layer. The reconstruction and de-reconstruction processes depend on the potentials and on the supporting electrolyte. Au(111) reconstruction is induced at negative potentials and lifted at positive potentials. Figure 3A shows a smooth Au(111) surface with atomically planar terraces. The step on the top terrace is higher than the nearest terrace by a single atomic layer. Atomic resolution can be obtained by zooming in on the terrace (Figure 3B). The round spots in the hexagonal pattern represent individual gold atoms. The distance between two nearest-neighbor atoms is 2.89 Å, corresponding to the diameter of gold atoms. The angles between the atomic rows as indicated by arrows in Figure 3B are 60° or multiples of 60°. This reflects the nature of (111) packing from the face-centered cubic (fcc) metal structure. The atomically resolved images are always used as substrate directions for further analysis of adsorbate layers.

3. FROM MONONUCLEOTIDES TO OLIGONUCLEOTIDES

3.1. Self-assembly on Au(111)

The intriguing properties of DNA-based molecules in two-dimensional configurations organized on solid surfaces have received intense attention over the last decade, prompted by interest both in biological DNA-“chips” (Uslu *et al.*, 2004; Service, 1998; Marie *et al.*, 2002; Southern *et al.*, 1999; Fritz *et al.*, 2000) and in the properties of the molecules in contexts of molecular electronics (Tanaka *et al.*, 2003). The molecular orientation and the accessibility of the oligonucleotides play key roles in DNA hybridization biosensors (Herne and Tarlov, 1997). Gentle control of the probe-nucleotide immobilization is required. This can be provided by electric fields, caused by an electrochemical electrode. We have exploited the high sensitivity of single-crystal electrochemistry and the high

resolution of *in situ* STM to address in novel ways chemically modified and non-modified mono- and oligonucleotides. The interfacial properties of single-nucleotide bases on Au(1 1 1) surfaces (Tao *et al.*, 1993), particularly of thymine have been mapped in great detail (Haiss *et al.*, 1998). Following the bottom-up concept, we have first focused on a thiol-modified mononucleotide with a single adenines (HS-monoA) followed by oligonucleotides with 10 adenine (HS-10A). The hexamethylene-thiol linker is covalently connected to the 5'-end of the mono- and oligonucleotide strands. For comparison, oligonucleotides containing 10 thymines (10-T) or 10 adenines (10-A) without thiol linkers were studied. This has been further extended to sequences with 13 and 25 single- and double-strand oligonucleotides with variable-base composition. The oligonucleotide strands are short enough that detailed information about their interfacial structural and dynamic behavior can be obtained compared with the complex macromolecular structure of longer oligonucleotides, but long enough to offer insight into collective properties and novel structural features, compared with single-nucleotide molecules.

Oligonucleotides were brought to adsorb at open-circuit potential by immersing the electrodes into the appropriate solution. No Faradaic processes are known for non-modified adenine and thymine oligonucleotides, in the potential range between 0.84 and -0.66 V (Palecek and Fojta, 2001). Figure 4A shows a cyclic voltammogram of linker-free 10-T adsorbed on Au(1 1 1). The broad cathodic peak at 0.23 V reflects a transition from a chemisorbed to a condensed physisorbed layer such as that found for a thymine film on Au(1 1 1) (Roelfs *et al.*, 1997). In the physisorbed layer thymine molecules lie flat on the surface in protonated and hence uncharged form. Formation of the chemisorbed layer is related to deprotonation and reorientation to a perpendicular thymine orientation on the surface. A sharp cathodic peak appears at -0.16 V at the rising of a much broader cathodic peak with a maximum at -0.19 V. The first peak can be associated with a disorder–order phase transition at -0.09 V such as for a thymine film on Au(1 1 1). The broader peak at -0.19 V is caused by desorption, where the peak widths reflect the disorder of the thymine oligonucleotide adlayer. A peak around this position was also observed in the interfacial capacitance, supporting this view. The peak charges are in the range of several hundred nC cm^{-2} , demonstrating the sensitivity of these non-Faradaic processes to the surface state of adsorbed thymine oligonucleotide.

The thiol-modified adenine mono- and oligonucleotides show a dominant peak at -0.53 V in the cyclic voltammogram in Figure 4B. The peak has disappeared in the second and third voltammetric scans. The pattern is indicative of reductive desorption of the gold-thiol bond, followed by liberation of the oligonucleotides from the surface. The presence of a gold-thiol bond was confirmed by X-ray photoelectron spectroscopy (XPS). Reductive desorption of alkylthiols is usually recorded under alkaline conditions, and described as



We have extended this to different species of thiol-modified biomolecules at neutral pH (Brask *et al.*, 2002b; Wackerbarth *et al.*, 2004c). The broadness

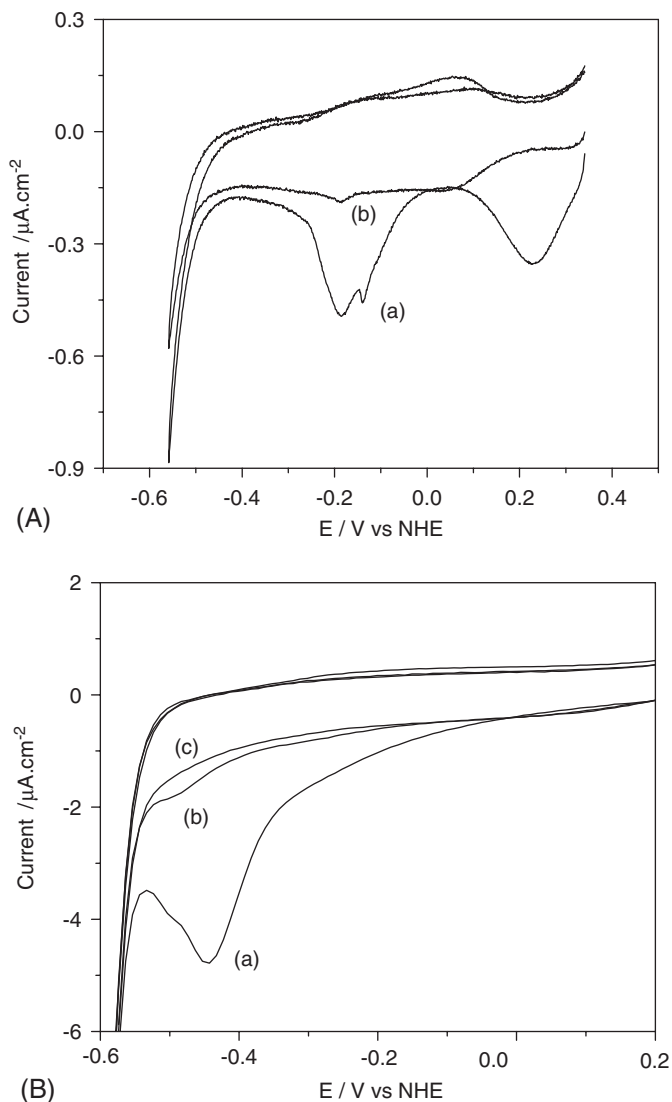


Fig. 4. Cyclic voltammograms of single-strand oligonucleotides adsorbed on Au(111) in 100 mM phosphate buffer, pH 6.9. Scan rate 10 mV s^{-1} . (A) Two successive cyclic voltammograms of 10-T; (a) first scan and (b) second scan. Two broad non-Faradaic peaks are visible, reflecting reorientation, desorption, and deprotonation. (B) Three consecutive scans of HS-10A; (a) first scan, (b) second scan, and (c) third scan. The position of the cathodic peak and its decrease indicate reductive desorption of the thiol-bound oligonucleotides. Wackerbarth *et al.* (2004c) with permission from the American Chemical Society.

reflects probably the coexistence of several adsorption modes. These could be ordered adsorbate domains separated by regions of disorder such as those suggested by *in situ* STM cf. below. The coverage of the thiol-linked oligonucleotide can be determined from the peak charge to give 27 ± 5 and $28 \pm 4\ \mu\text{C cm}^{-2}$

for HS-10A and HS-monoA, respectively (Wackerbarth *et al.*, 2004a). The reductive current peaks contain a capacitive contribution caused by the formation of the aqueous double layer on the uncoated gold surface after thiol desorption. This contribution has been estimated to $1.9 \mu\text{C cm}^{-2}$ by interfacial capacitance data. The small value is understandable as the difference in interfacial capacitance between the thiol-modified oligonucleotide layer and the bare Au(111) in 0.1 M phosphate is small compared to the difference before and after the desorption of similar long alkylthiol monolayers in alkaline aqueous solution. Hence, the resulting coverage can be determined to $260 \pm 60 \text{ pmol cm}^{-2}$. This coverage is high and suggests that the adsorbate molecules are in an upright orientation on the Au(111) surface. Similar high coverages were observed for both the thiol-modified mononucleotide and the thiol-modified single-strand oligonucleotide with 25 bases (Wackerbarth *et al.*, 2004b). This is indicative of similar adsorption modes for variable-length mono- and oligonucleotides and support adsorption in an upright position almost independent on the oligonucleotide length.

In situ STM images the electronic structure and electronic conductivity of the adsorbates. Open-circuit potential adsorptions show extensive adsorption on the Au(111) surface but little or no long-range order for linker-free oligonucleotides. Conversely, HS-monoA and HS-10A show clearly ordered domains, but first when the sample potential is lowered *in situ* to -0.47 V . Highly organized two-dimensional superstructures were also obtained by directly adsorbing the thiol-modified oligonucleotides at -0.47 V . The character of the imaged domains is unchanged in the potential range from -0.47 to 0.03 V but better quality images are achieved at 0.03 V (Figure 5). The domains disappear slowly by increasing the potentials to positive values, leaving the adlayer in a disordered state but with the same high overall coverage as in the ordered domains. Resetting the potential to -0.47 V reconstitutes an ordered structure, demonstrating the reversibility of potential induced domain formation. The domains are oriented with an angle of about 60° to each other and follow the triangular Au(111) structure. The bright spots are organized in rows with lower contrast in between. The distance between the spots along a row is about 5 \AA and the spacing between the spots in parallel rows is 11 \AA . This is also reflected by the height profiles (Figure 5). The rows form a $(\sqrt{3} \times 4) \text{ R}30^\circ$ surface lattice, with a total coverage of 288 pmol cm^{-2} , which is close to the coverage of $260 \pm 60 \text{ pmol cm}^{-2}$ determined by cyclic voltammetry. A highly ordered surface lattice was not observed for thiol-free 10-A adsorption under electrochemical potential control. This emphasizes the fundamentally different adsorption modes for thiolated and thiol-free oligonucleotide forms and extends to short oligonucleotides of rather arbitrary sequence (Petrovykh *et al.*, 2003; Wolf *et al.*, 2004).

The high coverage of the thiol-modified oligonucleotides found in both cyclic voltammetry and *in situ* STM points to an upright adsorption mode. The coverage is almost independent of the length and number of bases of the mono- and oligonucleotides. The *in situ* STM surface lattice $(\sqrt{3} \times 4) \text{ R}30^\circ$ is, moreover, the same for HS-monoA and HS-10A. The bright spots can be interpreted tentatively as the Au-thiolate bonds of the modified mono- and oligonucleotides

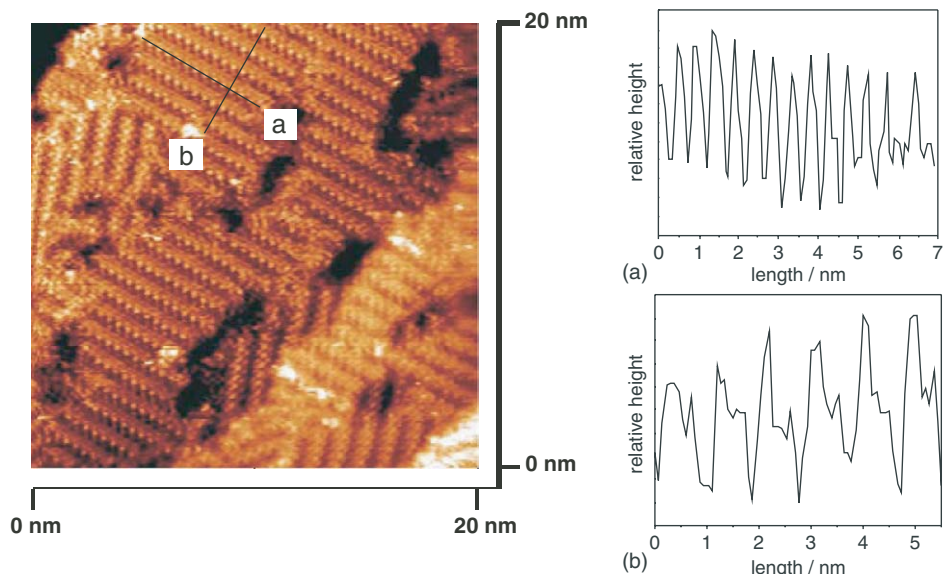


Fig. 5. *In situ* STM image of HS-10A in 10 mM phosphate buffer (pH 7.1), obtained in constant current mode. $I_t = 0.8$ nA, $E_w = 0.03$ V vs. NHE, $V_{\text{bias}} = -0.15$ V. The bright spots represent single-oligonucleotide molecule units. Relative height profiles along the lines “a” and perpendicular to the lines “b” indicated. Wackerbarth *et al.* (2004a) with permission from Wiley-VCM.

adsorbed on three-fold hollow sites, i.e., in the “hole” between three adjacent surface Au atoms. An upright orientation for thiol-modified oligonucleotides on electrostatically charged gold surface in given negative electrochemical potential range was observed by AFM (Kelley *et al.*, 1998), fluorescence intensity (Rant *et al.*, 2004), and surface plasmon resonance spectroscopy (Peterlinz *et al.*, 1997). Still under debate is the saturation coverage, ranging in the literature from 20 to 260 pmol cm⁻², depending presumably on the precise experimental and surface conditions (Steel *et al.*, 1998; Kelley *et al.*, 1999; Wackerbarth *et al.*, 2004c).

The high surface coverage of the Au(111) surface on thiol-modified single-strand mono- and oligonucleotides, and weak *in situ* STM contrast dependence on oligonucleotide chain length are at first sight surprising. Single-strand oligonucleotides are, however, structurally more flexible and their lateral extensions are much smaller than double-strand oligonucleotides. A highly negatively biased electrode surface therefore causes the soft backbone to stretch toward the solution. The lateral extensions of stretched single-strand oligonucleotides are, in fact, compatible with the $\approx 5 \times 11$ Å distances observed in the *in situ* STM images of the ordered adlayers. Close lateral packing, moreover, leaves space for counterions (not visible in STM) to compensate the strong repulsive lateral interactions. Formation of an ordered adlayer at negative electrode potential (Figure 6) can be explained by a cooperative effect of enhanced diffusion of the oligonucleotides on the Au(111) surface and sophisticated hydrophobic and electrostatic interactions between the adjacent

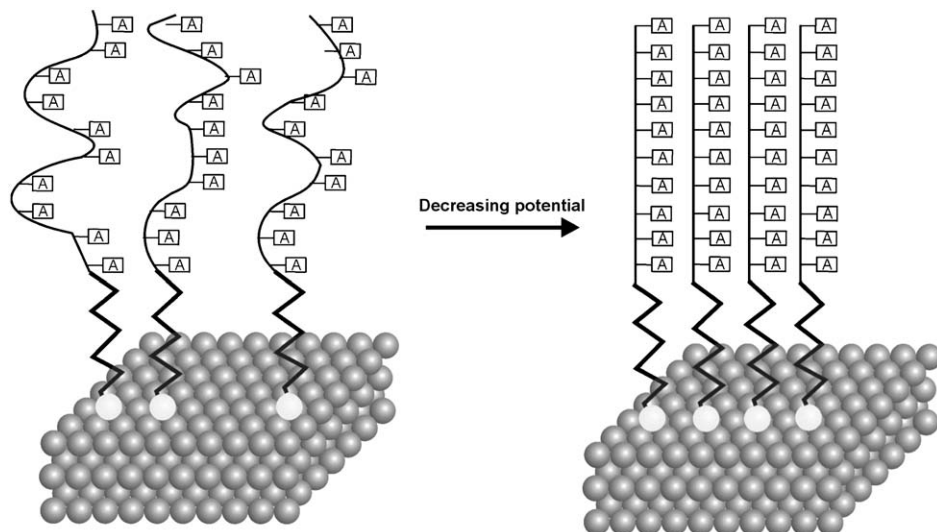


Fig. 6. Orientation of HS-10A oligonucleotide adsorbed in ordered domains on the Au(111) electrode. The gray spheres indicate the hexagonal packing of the gold crystal. The sulfur atoms (yellow spheres) are grafted to the three-fold hollow sites. The thick black lines represent the hexamethylene linker. The thin black lines including the A's represent the oligonucleotides. Repulsion between the phosphate backbone and the highly negatively polarized surface forces the oligonucleotide into a stretched configuration. Hydrophobic interactions and lateral hydrogen bonding between neighboring units stabilize the adsorption mode of the upright HS-10A.

mono- and oligonucleotides in the electric field. The latter effect may be responsible for the faster formation of the ordered lattice structure of the oligonucleotides compared to the mononucleotide. Another topic, where single-molecule resolution could be auspicious is two-dimensional or columnar DNA-based molecular aggregation induced by transition metal complexes, such as presently in intense focus (Cherstvy *et al.*, 2004).

In addition to the single-strand oligonucleotide high-density packing, the insensitivity of the tunneling current to the oligonucleotide chain length (HS-monoA vs. HS-10A) and base composition (HS-10A vs. HS-13mix) is notable, and presently perhaps more of a puzzle. Weak distance dependence of electron transport in DNA-based molecules in solution has now been observed often (Schuster, 2004) and is broadly understood. Key notions are guanine hole injection followed by one-dimensional random walk of the injected hole (Jortner *et al.*, 2000). Observed weak distance dependent electrochemical ET between a metal electrode and redox probes bound to surface-immobilized oligonucleotides (Kelley *et al.*, 1999) cannot, however, straightforwardly be referred to these frames as the electrochemical potentials of the redox probes are far from base oxidation and reduction potentials. The same applies to the *in situ* STM data, although the imaging potentials are closer to that associated with Au-S reductive desorption. The dilemma remains if superexchange is invoked, as variable-base compositions would still have widely different tunneling gaps,

equations (1) and (2). This is in line with results of Xu *et al.* (2004), who observed base-dependent ET rates for single-molecule double-strand oligonucleotides but weak distance dependence for guanine/cytosine oligonucleotides. Approaches to this important issue could rest on a particular electron or hole mediation via the Au–S bond, possibly involving surface states (Gregory *et al.*, 2001), and on the huge effect of configurational fluctuations on the electronic energetics (Voityuk *et al.*, 2004) as the single-molecule level is approached.

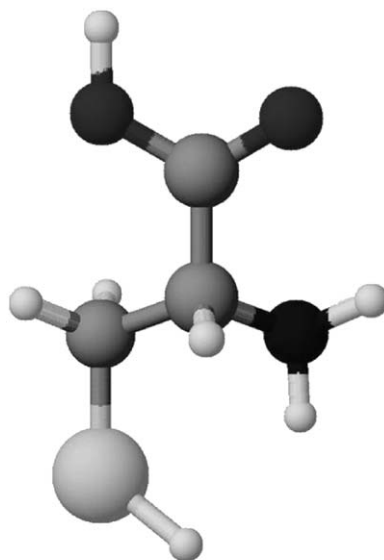
4. AMINO ACIDS AND PROTEIN MONOLAYERS

4.1. Network-like clusters in cysteine adlayers on Au(111)

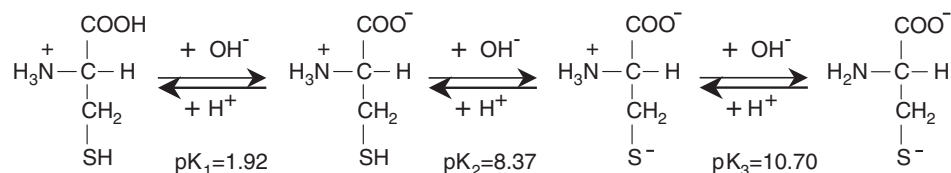
L-cysteine is an amino acid naturally present in many proteins and serves as an important precursor for the synthesis of the proteins glutathione, taurine, enzyme A, and inorganic sulfate in nature. L-cysteine plays roles not only in biochemical function, but also in nutrition and pharmacology. L-cysteine contributes to central cardiovascular control and is a suppressor of liver fibrosis. It is the only amino acid, which contains a mercapto group, which can adsorb with high affinity on gold surfaces. It is therefore important to study L-cysteine adsorption and monolayer structure on atomically planar Au(111) surfaces in solution to achieve molecular level information on the molecular packing. Sulfur-containing carboxylic acids are, further, important templates for adsorption of proteins and constitute here the immediate microscopic environment for functional proteins in the adsorbed state.

The structure of L-cysteine is shown in Figure 7, with $-\text{COOH}$, $-\text{NH}_2$, and $-\text{SH}$ groups. Both the amine and the carboxylic acid group can be protonated or deprotonated depending on pH, cysteine becoming correspondingly a cation, anion, or a zwitterion (Figure 8). Cysteine monolayers have been investigated in UHV as well as in 0.1 M HClO_4 solutions by XPS, electrochemistry, and STM on Hg, polycrystalline gold, and on single-crystal surfaces such as Au(110) and Au(111) (Ralph *et al.*, 1994; Kühnle *et al.*, 2002; Dakkouri *et al.*, 1996; Xu *et al.*, 2001; Zhang *et al.*, 2000). The cysteine molecular structure is chemically different at low and neutral pH. We focus here on L-cysteine monolayers on Au(111) addressed by comprehensive investigations of interfacial capacitance, voltammetry, and *in situ* STM in ammonium acetate (NH_4Ac) solution at pH 4.6. The reason for this supporting electrolyte is that this buffer is close to the biological media, in which cysteine operates.

Figure 9A shows a voltammogram of an L-cysteine monolayer covering Au(111) (solid line) in 50 mM NH_4Ac solution. The corresponding capacitance curves are shown in Figure 9B. Clean Au(111) surfaces reconstruct at negative potentials while the reconstruction is lifted at positive potentials. This process depends on pH and the potential. A sharp anodic peak at 0.48 V in the voltammetric and capacitance curves (dotted lines in Figure 9) is due to these effects. Acetate anions adsorb on bare Au(111) surfaces and give doublet anodic peaks (0.72 and 0.80 V) and one small cathodic peak at 0.70 V (dotted line



Molecular structure of L-cystiene

Fig. 7. Molecular structure of L-cysteine.**Fig. 8.** Ionization of L-cysteine in aqueous solution at different pH.

in **Figure 9A**). In the presence of a cysteine monolayer, the reconstruction peak at 0.50 V has totally vanished and the acetate adsorption peaks are strongly attenuated (solid line in **Figure 9A**). A similar effect is observed as a featureless curve in the capacitance measurement, as shown by the solid line in **Figure 9B**. The reason for such effects is that chemical adsorption of electrostatically bound cysteine with S–Au bonds is so strong that cysteine replaces adsorption of acetate and forms stable monolayers on the Au(111) substrate. Compared with bare Au(111), there are two additional features: an apparent increase of the double-layer current and a large cathodic peak at -0.2 V. The first feature is due to the formation of cysteine zwitterions at pH 4.6, which introduces a capacitive current in the double-layer region. The cathodic peak is due to hydrogen evolution and reductive desorption of Au–S bonds.

The formation and microscopic structure of L-cysteine monolayers on Au(111) have been explored by *in situ* STM. Random cysteine molecules initially adsorb on elbows of the reconstruction lines (i.e., the herringbone-like structures), which is a characteristic feature for Au(111). The reconstruction lines are gradually lifted and some small cysteine domains appear with either

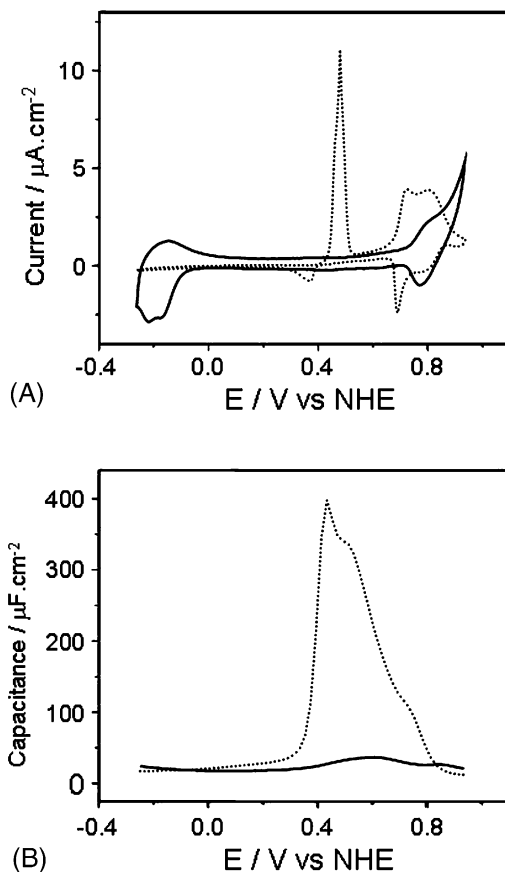


Fig. 9. Cyclic voltammetric (A) and capacitance (B) curves of bare Au(1 1 1) (dotted line) and L-cysteine (solid line) on Au(1 1 1) in 50 mM NH_4Ac (pH 4.6). Scan rate 50 mV s^{-1} .

increasing adsorption time or concentration of cysteine. The adsorption process is also potential dependent, being accelerated at positive potentials and slowing down at negative potentials. The small domains expand, become larger, and eventually cover the whole Au(1 1 1) surface at equilibrium.

Figure 10A shows representative *in situ* STM images of cysteine monolayers on Au(1 1 1). Highly ordered domains in the range of 40–80 nm are found to align with 60° or multiples 60° , reflecting the three-fold (1 1 1) symmetry feature (Figure 10A). Arrows indicate atomic row directions of Au(1 1 1). Small black holes (defects) are observed around the domain boundaries and sometimes inside the domains. Figure 10B depicts an interesting cluster-like lattice with a rectangular pattern. The periodic distance between nearest neighbor clusters along an atomic row, such as the $[\bar{1} 1 0]$ direction is $17.0 \pm 0.5 \text{ \AA}$, corresponding to six times the gold atomic diameter. The periodic distance along the perpendicular direction, i.e., $[\bar{1} \bar{1} 2]$ is $15.1 \pm 0.5 \text{ \AA}$, corresponding to three times the $\sqrt{3}$ gold atomic distance. The unit cell in cysteine monolayers is described as $(3\sqrt{3} \times 6) \text{ R}30^\circ$ indicated by the box in Figure 10B and C. The area of each unit

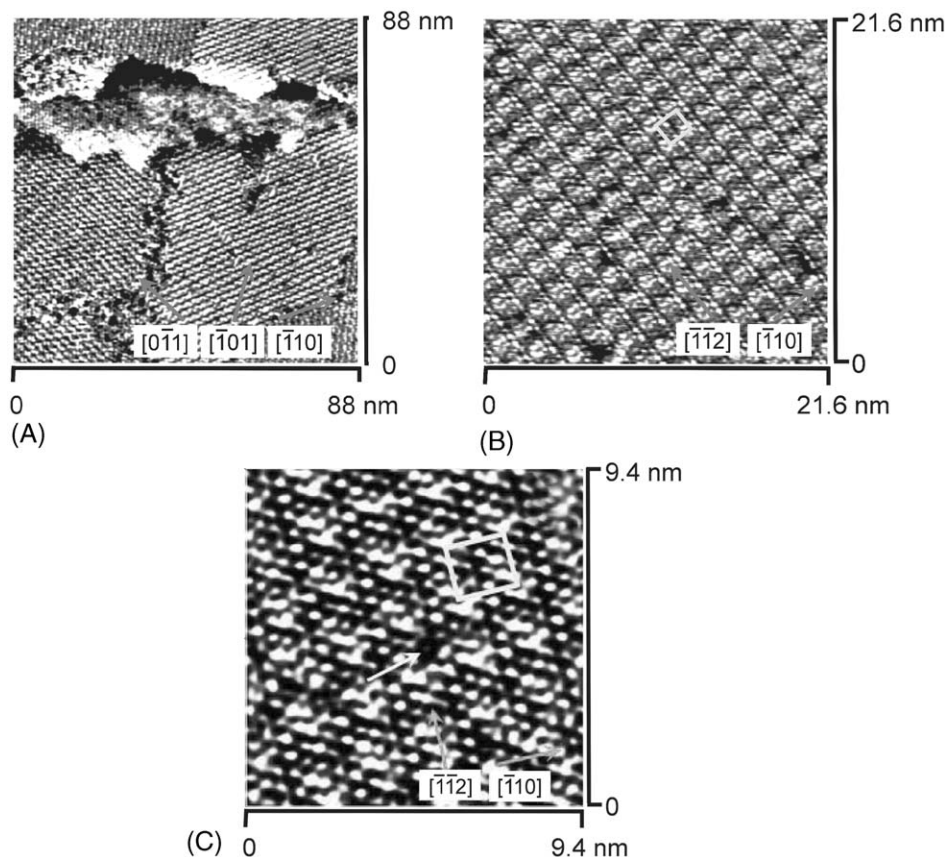


Fig. 10. *In situ* STM images of cysteine monolayer on Au(111) in 50 mM NH_4Ac (pH 4.6). $I_t = 0.80$ nA, $V_{\text{bias}} = 0.2$ V, $E_w = 0.34$ V vs. NHE.

cell is 258 \AA^2 . This value is larger than the geometric size of a single L-cysteine molecule. High-resolution *in situ* STM images further show that a number of small white spots contribute to a network-like structure in each cluster (Figure 10C) implying that each cluster may contain several cysteine molecules. Direct evidence from coverage data supports this hypothesis. The coverage of the $(3\sqrt{3} \times 6) \text{ R}30^\circ$ surface lattice is calculated as $6.4 \times 10^{-11} \text{ mol cm}^{-2}$ on Au(111). The coverage of L-cysteine monolayers on Au(111) was measured by linear voltammetry in basic solution to avoid interference from hydrogen evolution. A needle-like sharp peak emerges at -0.45 V vs. NHE corresponding to quantitative reductive dissociation of the Au–S bonds in the cysteine monolayers (equation (6)). The peak charge gives the coverage value of S–Au bonds, i.e., the cysteine monolayer coverage is $(4.0 \pm 0.4) \times 10^{-10} \text{ mol cm}^{-2}$, compared with the coverage value of $6.4 \times 10^{-11} \text{ mol cm}^{-2}$ from the surface lattice. This means that each cluster contains six cysteine molecules. This is supported by the size of the defects in the STM images. Defects appearing as black holes in STM images are caused by missing molecules in the adlayers. They could be regarded

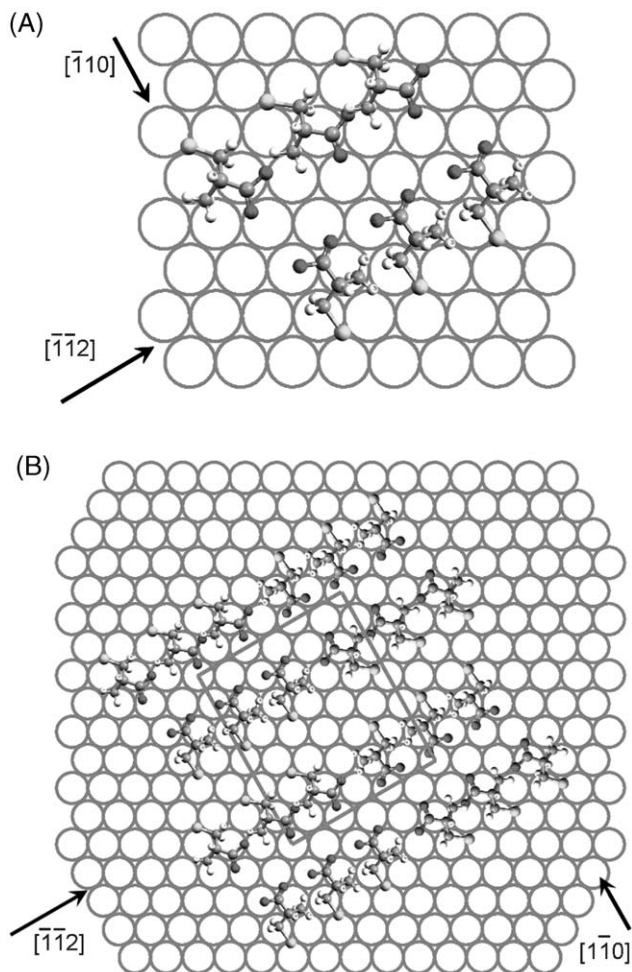


Fig. 11. Possible superstructure model of six cysteine molecules based on a hydrogen bond network. (A) single cluster and (B) clusters in a $(3\sqrt{3} \times 6)$ R30° surface lattice.

as mirrors and reflect sizes and packing of molecules on surfaces. The smallest defect area, indicated by a white arrow found in the high-resolution *in situ* STM image in Figure 10C is $41 \pm 4 \text{ \AA}^2$. This is close to the value estimated from the crystallographic structure of L-cysteine, suggesting that each cluster is indeed occupied by six cysteine molecules. The origin of cluster formation is due to hydrogen bonds.

A simple model for the L-cysteine lattice based on hydrogen bond formation is proposed in Figure 11. Figure 11A shows the superstructure of a single cluster. Six L-cysteine molecules are arranged in two rows facing each other. Sulfur atoms of cysteine molecules in each row are put on three-fold hollow sites on Au(111) along the $[\bar{1}\bar{1}2]$ direction with a periodic distance of 5.0 \AA . The sulfur rows are about 12.9 \AA apart from each other with a zigzag mode.

Carboxyl and amine groups are tilted to a certain degree vs. the $[\bar{1}\bar{1}2]$ directions, so that an amino group can be close to a carboxyl group from a neighbor cysteine molecule to match the hydrogen bonds. Both carboxyl and amine groups are saturated by hydrogen bonds not only from the same but also from the opposite row. Six cysteine molecules thus form a stable cluster by intramolecular hydrogen bond interaction. The clusters are located in lines along the $[\bar{1}10]$ direction with a periodic distance of 17.3 Å. The 180° rotated cluster of cysteine on their neighboring rows along the $[\bar{1}10]$ direction fit the STM images better (Figure 11B). This means that the configuration in every second row is similar.

L-cystine, the dimer of L-cysteine forms exactly the same surface structure on Au(111) in the same medium. *In situ* STM, electrochemistry, and XPS results are all indistinguishable from those of L-cysteine (Chi *et al.*, 1999; Zhang *et al.*, 2000). This is most likely due to cleavage of the disulfur bridge on adsorption to form Au–S bonds. On the basis of the strong affinity between cysteine and the Au surface, the blue copper protein *Pseudomonas aeruginosa* azurin molecules, for example, form monolayers on Au(111) with biological ET function retained (Chi *et al.*, 2000).

4.2. Assembling of the iron-sulfur protein *pyrococcus furiosus* ferredoxin on thiolate-modified Au(111) surfaces

In a bottom-up approach to functional biomolecules on single-crystal electrode surfaces, we now proceed from amino acids to proteins, a number of which have been studied comprehensively in our group. Ordered monolayers of small functionalized molecules such as L-cysteine, 3-mercaptopropionic acid (MPA), alkanethiols, and mercaptoamines offer a broad range of templates for adsorption of proteins and even large biological structures in functional states in well-characterized microscopic environments. There are two general methods to immobilize proteins in controlled orientation. One is that protein molecules directly adsorb on the metal surface via certain bonds such as Au–S between functional groups on the protein surface and the substrate. This is the case for yeast cytochrome *c* (Bonanni *et al.*, 2003; Hansen *et al.*, 2003; Heering *et al.*, 2004), azurin (Chi *et al.*, 2000; Facci *et al.*, 2001), and mutant azurin (Davis *et al.*, 2002). The advantage of this method is that it is straightforward, the disadvantage is that the natural protein may not contain such functional surface groups. The other method is to modify the metal surface by linker molecules with functional groups, through which specific protein surface sites interact, cf. above. Examples are azurin immobilized on alkanethiol-modified Au(111) surfaces by hydrophobic interaction between the terminal methyl group and a hydrophobic area around the Cu-center (Chi *et al.*, 2001), and nitrite reductase immobilized on cysteamine-modified Au(111) with catalytic function retained (Zhang *et al.*, 2003). This method seems general and has been used for the three major classes of ET proteins, the cytochromes, particularly cytochrome *c* (Avila *et al.*, 2000; Song *et al.*, 1993), the blue copper proteins (Chi *et al.*, 2001; Zhang

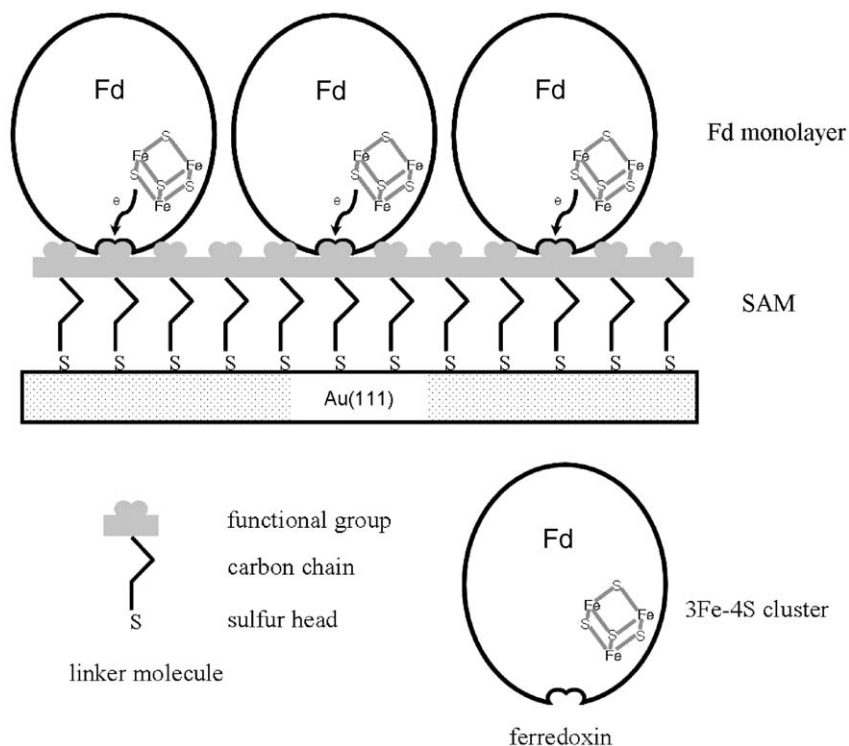


Fig. 12. A model of the *PfFd* monolayer on Au(1 1 1) modified by MPA.

et al., 2003; Davis *et al.*, 2002) and recently an iron–sulfur protein (Zhang *et al.*, 2004), *Pyrococcus furiosus* ferredoxin (*PfFd*). In the context of single-crystal electrochemistry and *in situ* STM, azurin has been studied most comprehensively. These studies have been reviewed but noval studies are in progress. The most recent single-crystal electrochemical and *in situ* STM redox metalloprotein study, focused on *PfFd*, is discussed in the following.

Ferredoxins belong to the oldest protein families on earth. Iron–sulfur cubic clusters with Fe and S at alternative corners serve as redox centers and carry the ET function. *PfFd* is a small protein with ca. 7.5 kDa molecular mass and contains a single [3Fe–4S] redox center (Figure 12). Purification and properties of this protein have been reported (Kim *et al.*, 2001). *PfFd* is stable in anaerobic environment and retains biological activity even at high temperature, up to 80°C. The X-ray crystallographic structure has been resolved recently at 1.5 Å resolution (Nielsen *et al.*, 2004). The whole protein surface is negatively charged at neutral pH. Interfacial ET of *PfFd* is not straightforward without promoters in homogeneous solution, but small organic molecules such as neomycin can promote ET of *PfFd*, corresponding to [3Fe–4S]^{+ / 0}. The presence of an additional promoter with a carboxyl group such as alanine, propionic acid, or cysteine induces a second ET to [3Fe–4S]^{0 / -}. Combination of adducts is essential and has been confirmed by voltammetry and mass spectrometry (Zhang *et al.*, 2004). Based on these investigations, we can construct *PfFd* monolayers

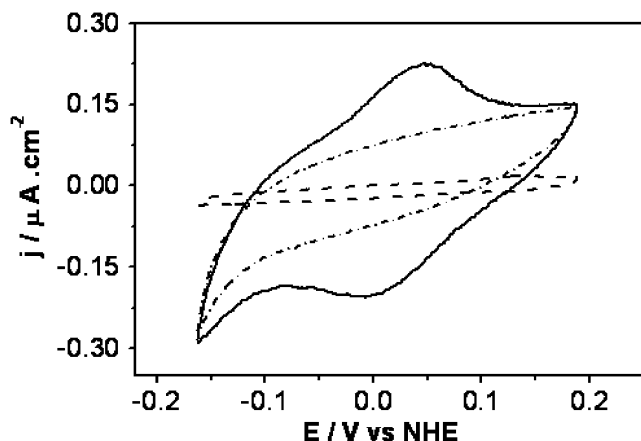


Fig. 13. Cyclic voltammograms of *PfFd*-MPA/Au(111) (solid line), MPA/Au(111) (half-dotted line), and Au(111) (dotted line) in 5 mM phosphate buffer (pH 7.9). Scan rate 50 mV s^{-1} .

on self assembled monolayers(SAMs) with the carboxyl function group on Au(111) (Figure 12). The simplest thiol containing carboxyl group is MPA.

MPA/Au(111) and bare Au(111) do not give any voltammetric redox peaks in the potential range -0.15 – 0.20 V , dotted lines in Figure 13. *PfFd*-MPA/Au(111) causes a voltammetric peak at 0.04 V vs. NHE in the same potential window and corresponding to the *PfFd* $[3\text{Fe-4S}]^{+/0}$ couple, Figure 13 solid line. The coverage of *PfFd* is $(12 \pm 3) \times 10^{-11} \text{ mol cm}^{-2}$ from the peak charge. The corresponding capacitance curves are shown in Figure 14. MPA/Au(111) increases the capacitance to 14 – $18 \mu\text{F cm}^{-2}$ (diamonds in Figure 14) in the potential range -0.15 – 0.20 V by introducing the hydrophilic group $-\text{COOH}$ on the gold surface, the presence of *PfFd* drastically lowers the capacitance to $10 \mu\text{F cm}^{-2}$, suggesting that carboxyl groups have been covered by a *PfFd* adlayer. In addition, there is a clear peak at 0.045 V from *PfFd*-MPA/Au(111) (Figure 14 circles) corresponding to the formal potential of the $[3\text{Fe-4S}]^{+/0}$ couple. These results indicate that the *PfFd* adlayer on MPA/Au(111) retains ET function.

Microstructures of MPA/Au(111) and *PfFd*-MPA/Au(111) have been further mapped by *in situ* STM in aqueous solution. A dense monolayer with numerous small 3 – 7 nm diameter pits uniformly scattered over the Au(111) surface is seen in the images. The density and size of the pits vary with the experimental conditions, the coverage being 3.7 – 4.5% over the whole area. Such pits are nearly always seen in SAMs containing thiol groups on gold surfaces. The origin of the pits is most likely due to shrinking of the gold atom from 2.88 to 2.68 \AA with Au–S bond formation. Highly ordered network-like structures are clearly observed in large domains (Figure 15A). High-resolution *in situ* STM images show ordered clusters in a $(2\sqrt{3} \times 5) \text{ R}30^\circ$ lattice (Zhang *et al.*, 2004). Each cluster contains six MPA molecules, like the cysteine monolayer. Such structures provide a suitable environment for immobilization of *PfFd* in an ET functional state.

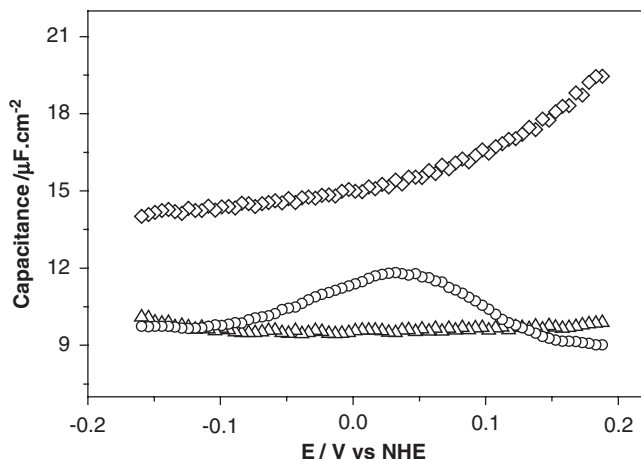


Fig. 14. Capacitance curves of *PfFd*-MPA/Au(111) (circles), MPA/Au(111) (diamonds), and Au(111) (triangles) in 5 mM phosphate buffer (pH 7.9). 100 Hz frequency, 5 mV amplitude, and 20 mV step.

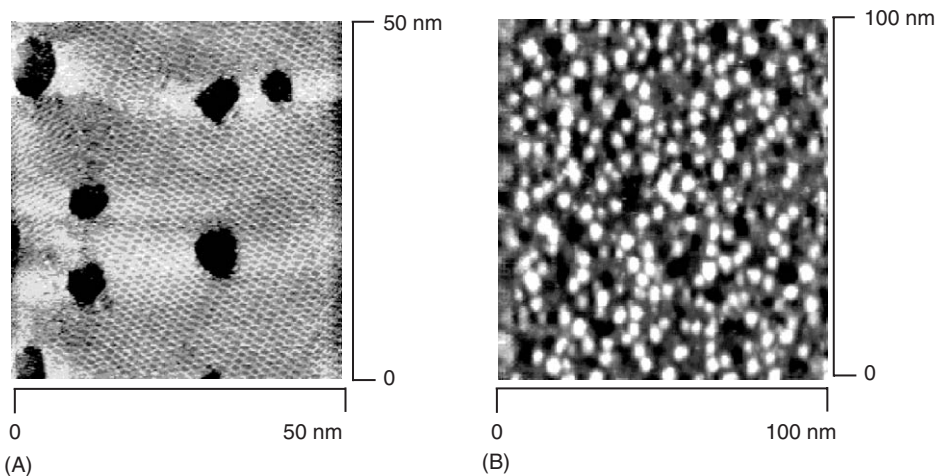


Fig. 15. *In situ* STM images of (A) MPA/Au(111) and (B) *PfFd*-MPA/Au(111) in 5 mM phosphate buffer (pH 7.9) recorded under argon protection. (A) $I_t = 0.25$ nA, $V_{\text{bias}} = -0.10$ V, $E_w = 0.10$ V vs. NHE and (B) $I_t = 0.10$ nA, $V_{\text{bias}} = -0.30$ V, $E_w = 0.14$ V vs. NHE.

Figure 15B shows a representative *in situ* STM image of a *PfFd* adlayer on top of the MPA monolayer. Protein molecules cover uniformly the whole surface. Both black hole (pits) from the MPA monolayers and white spots (*PfFd*) are clearly seen on the same image. The lateral diameter of most of the white spots is 3.0–3.5 nm, which is close to the crystallographic dimensions. There is a small portion (ca. 15%) of larger spots (4.5–5.0 nm). As known from the X-ray study, *PfFd* easily forms dimers even in crystals (Nielsen *et al.*, 2004) and

the large spots observed in the *in situ* STM images might be dimers on the surface. The coverage of *PfFd* calculated from the STM images is $(7 \pm 1) \times 10^{-11} \text{ mol cm}^{-2}$, which is comparable to the value from voltammetry. *PfFd* gives strong STM contrast compared with other proteins (Chi *et al.*, 2000; Hansen *et al.*, 2003), probably due to strong electronic contributions from the iron-sulfur cluster. Overall single-crystal electrochemistry and *in situ* STM have successfully illustrated that *PfFd* monolayers immobilized on Au(1 1 1) by the MPA-linker layer retain biological ET function at the molecular level.

4.3. An alternative strategy for intelligent materials – artificial proteins

Natural protein synthesis is performed in the cells of living organisms. Peptides can also be artificially synthesized by connecting amino acids to each other step by step, called *de novo* design. *De novo* design of proteins allows construction of isolated structural elements or whole new artificial structures. This is of interest for the development of new intelligent materials, inasmuch as novel technological relevant functions can be added to the evolutionary optimized systems. Their secondary and tertiary structural elements can be varied systematically, enabling new levels of detail in molecular structure–function relations. *De novo* proteins can also be used as probes for recognition in biosensors, drug delivery, and nanotechnology (Willner and Katz, 2000; Gilardi and Fantuzzi, 2001). *De novo* designed proteins hold, further promise for illuminating the protein folding process. We have combined the *de novo* design strategy with *in situ* STM and single-crystal electrochemistry with focus on 4- α -helix bundle (4-HB) carbo-proteins and its thiol linker attached to the Au(111)-surface. 4-HB carboproteins are intermediate-size simplified structures compared with natural proteins. Several groups have developed synthetic 4-HB proteins using different strategies (DeGrado *et al.*, 1999; Choma *et al.*, 1994; Robertson *et al.*, 1994; Rau *et al.*, 2000; Mutter and Vuilleumier, 1989). Here, we present briefly an approach using a monosaccharide template for the *de novo* design of 4-HB carboproteins (Jensen and Barany, 2000; Brask and Jensen, 2000, 2001) (Figure 16). To form the helical motif a standard peptide sequence is used containing 16 amino acids with the sequence: Ac-Tyr-Glu-Glu-Leu-Leu-Lys-Lys-Leu-Glu-Glu-Leu-Leu-Lys-Lys-Ala-Gly-H.

Interfacial capacitance measurements reflect the adsorption of the carboprotein on the Au(1 1 1) surface. Cyclic and differential pulse voltammetry of the 4-HB protein equipped with a thiol linker shows a peak around -0.51 V , indicative of reductive desorption (Brask *et al.*, 2002a). The coverage is estimated from the peak charge resulting in densely packed monolayers. However, the same 4-HB protein without linker shows also a peak, albeit smaller around this position. We therefore applied XPS, which clearly indicated the presence of a covalent gold-thiol bond. XPS data point, moreover, to extensive carboprotein coverage considering the Au(4f) intensity compared with a bare Au(1 1 1) surface. The relation between the measured intensity of the C, N, and O element signals accords with the stoichiometry of the carboprotein, indicating that the

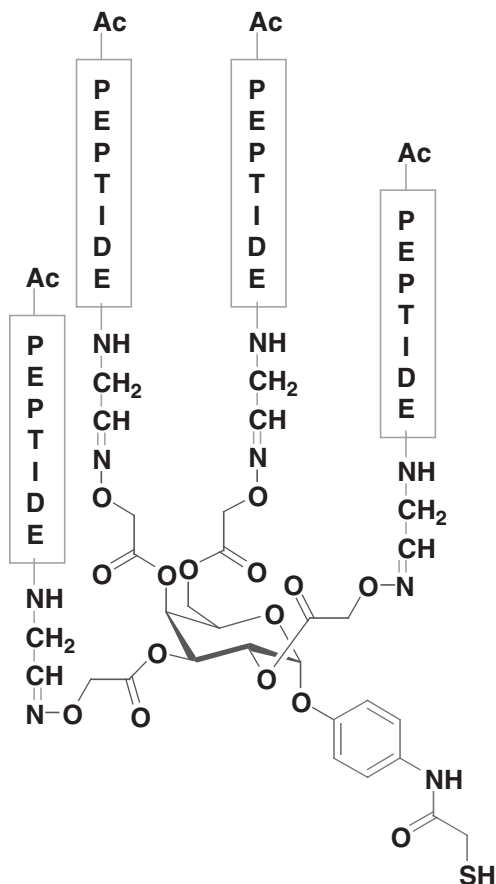


Fig. 16. Structure of 4-HB carboprotein. Peptides contain 16 amino acids with the following sequence: Ac-Tyr-Glu-Glu-Leu-Leu-Lys-Lys-Leu-Glu-Glu-Leu-Leu-Lys-Lys-Ala-Gly-H. Template is the monosaccharid, D-galactopyranose attached to the thiol linker, N-Phenylmercaptoacetamide.

protein has not degraded chemically on the Au(111) surface in UHV (Brask *et al.*, 2002a).

The voltammetric, interfacial capacitance, and XPS data point coherently toward extensive monolayer coverage of the Au(111)-electrode surface of the 4-HB-carboprotein with the thiol linker. This was confirmed by *in situ* STM under electrochemical potential control. Figure 17 shows two *in situ* STM images of the Au(111) surface covered by 4-HB-carboprotein at two different substrate potentials. The image in Figure 17A is recorded at a potential on the far positive side of the reductive desorption potential. The Au(111) surface appears fully covered, with pits scattered over the surface. Figure 17B is recorded close to the reductive desorption potential. The adsorption pattern here is quite different. White spots, indicating higher tunneling currents, with the size of individual carboprotein molecules are now observable. As the Au

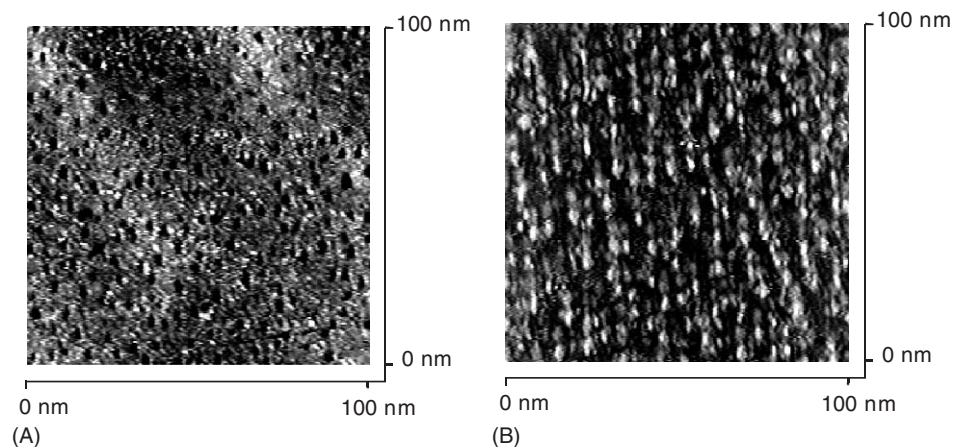


Fig. 17. *In situ* STM images of the 4-HB carboprotein adsorbed on Au(111) in 10 mM phosphate, pH 6.8. Constant-current mode, $I_t = 0.3$ nA. (A) $V_{\text{bias}} = -0.55$ V, $E_w = 0.10$ V vs. NHE and (B) $V_{\text{bias}} = 0.35$ V, $E_w = -0.57$ V vs. NHE. The sample potential induces an irreversible electron transfer process, causing a high current density, represented by the white spots.

(111)-substrate potentials approach the reductive desorption potential, the Fermi level (Figure 1 to the right) of the Au(111) electrode is brought close to the LUMO of the gold-thiol bond. An electronic gate then opens and electrons flow from the electrode to the STM tip for positive bias voltage. The electrons tunnel through the whole carboprotein, so that the higher contrast reflects the dimension of a single 4-HB-carboprotein molecule. The reduced state goes along with the dissociation of the gold-thiol bond followed by desorption. The process is, thus, *irreversible*.

This investigation suggests that the combination of totally synthetic proteins with state-of-the-art physical electrochemistry may hold promise for addressing biomolecular structure and function at the single-molecule and supramolecular levels in new ways.

5. CONCLUDING REMARKS

Characterization and mapping of surface structures of biological molecules and macromolecules such as oligonucleotides and redox metalloproteins, approach increasingly high levels of resolution and are now getting close to the nanoscale and single-molecule levels. We have overviewed some recent progress in these areas with focus on work in our group. State-of-the-art physical electrochemistry, particularly based on single-crystal, atomically planar electrode surfaces, and *in situ* STM, directly in the aqueous biological media, has been an overarching frame, supported by theoretical frames for the interfacial ET systems in novel mesoscopic configurations such as *in situ* STM.

Crucial biological function, such as ET and catalytic function of biomacromolecules, at levels of resolution, which approach the single-molecule level, is illustrated by the fragile and highly anaerobic metalloprotein *PfFd*. Such level of mapping extends both to the other two major classes of redox metalloproteins, the blue copper proteins and the heme proteins, and recently to redox-enzyme catalysis, by the blue copper enzyme copper nitrite reductase. Immobilization of functional DNA-based molecules on solid surfaces is another major area of research, rooted in the quest for DNA-based screening of biological liquids and mapping of electronic conductivity of DNA-based molecules in possible device frames. As a step toward such objectives, conditions for controlled formation of highly ordered monolayers of short single-strand short oligonucleotides, and structural mapping to single-molecule resolution, have been achieved.

In a sense our approaches can be viewed as a “single-molecule bottom-up” approach. Mapping of the fundamental biological building blocks, nucleobases, and amino acids goes in parallel with the composite biological “real” functional molecules, the oligonucleotides and (metallo)proteins. The building blocks, however, also provide physical bridging between immobilized functional macromolecules and the external electrical circuits. The highly ordered self-assembled monolayers of the building block molecules are thus templates for immobilization of the much larger, often fragile biological macromolecules, and constitute the biomimetic microscopic environment for the biological function.

Structural and functional characterization of immobilized intermediate-sized and large molecules toward the single-molecule levels have been noted to hold novel perspectives for ultra-small device-like electronic function (e.g. Joachim and Gimzewski, 1998; Kuznetsov and Ulstrup, 2004; Metzger, 2003). The existence of such devices is now beyond doubt, but approaches to the single-molecule level resolution also disclose novel interfacial ET phenomena. At the same time these hold even further perspectives for device function but also limitations. Among the former is that redox molecules in the *in situ* STM gap can be brought to display three-electrode transistor and amplifier function and to effect strongly amplified conductivity function in a single *in situ* STM electron transport event (Kuznetsov and Ulstrup, 2004; Albrecht *et al.*, 2005a, b). Among the latter stochastic “noise” (He *et al.*, 2001) and huge configurational fluctuational modulation of single-molecule conductivity (Voityuk *et al.*, 2004) are limitations for real device function.

The approaches discussed offer ways of circumventing the “noise” problems by mapping precisely conditions where structural “coherence” (i.e. highly order monolayers) can be expected to apply, with concomitant minimization of fluctuational effects on chemical and electronic function (DNA hybridization, single-molecule catalysis, ET function). With such perspectives single-molecule DNA-screening, enzyme sensing, and even combination with nanoscale metallic and semiconductor structures and arrays into multi-functional sensing devices (next-generation “labs-on-a-chip”) may be within reach. This could also become a forthcoming phase toward molecular electronics and “bioelectronics”.

LIST OF ABBREVIATIONS

4-HB	4- α -helix bundle
10-A	oligonucleotide with 10 adenines
10-T	oligonucleotide with 10 thymines
AFM	atomic force microscopy
ET	electron transfer
HOMO	highest occupied molecular orbital
HS-monoA	thiol-modified mononucleotide with single adenine
HS-10A	thiol-modified oligonucleotide with 10 adenines
HS-13mix	thiol-modified oligonucleotide with 13 bases
LUMO	lowest unoccupied molecular orbital
MPA	3-mercaptopropionic acid
NHE	Normal hydrogen electrode
<i>PfFd</i>	<i>Pyrococcus furiosus</i> ferredoxin
SAM	Self-assembled monolayer
STM	scanning tunneling microscopy
UHV	ultra-high vacuum
XPS	X-ray photoelectron spectroscopy

ACKNOWLEDGMENTS

Financial support from the Danish Technical Science Research Council, the EU Programme CIDNA, and Nanoscience Center, University of Copenhagen is acknowledged.

REFERENCES

- Albrecht, T., A. Guckian, J. Ulstrup and J.G. Vos, 2005a, Transistor-like behavior of transition metal complexes, *Nano Lett.* 5, 1451.
- Albrecht, T., A. Guckian, J. Ulstrup and J.G. Vos, 2005b, Transition metal complexes as a novel class of room temperature single-molecule transistors, *Trans. IEEE* 4, 430.
- Avila, A., B.W. Gregory, K. Niki and T.M. Cotton, 2000, An electrochemical approach to investigate gated electron transfer using a physiological model system: Cytochrome *c* immobilized on carboxylic acid-terminated alkanethiol self-assembled monolayers on gold electrodes, *J. Phys. Chem. B* 104, 2759.
- Berlin, Y.A., A.L. Burin and M.A. Ratner, 2000, DNA as a molecular wire, *Superlattices Microstruct.* 28, 241.
- Binnig, G., H. Rohrer, Ch. Gerber and E. Weibel, 1982, Surface studies by scanning tunneling microscopy, *Phys. Rev. Lett.* 49, 57.
- Bixon, M. and J. Jortner, 2000, Energetic control and kinetics of hole migration in DNA, *J. Phys. Chem. B* 104, 3906.

- Bixon, M. and J. Jortner, 2002, Long-range and very long-range charge transport in DNA, *Chem. Phys.* 281, 393.
- Bonanni, B., D. Alliata, A.R. Bizzarri and S. Cannistraro, 2003, Topological and electron-transfer properties of yeast cytochrome *c* adsorbed on bare gold electrodes, *Chem. Phys. Chem.* 4, 1183.
- Brask, J. and K.J. Jensen, 2000, Chemosselective ligation of peptide aldehydes to an aminoxy-functionalized D-galactose template, *J. Peptide Sci.* 6, 290.
- Brask, J. and K.J. Jensen, 2001, A 4- α -helix bundle protein model assembled on a D-galactopyranoside template, *Bioorg. Med. Chem. Lett.* 11, 697.
- Brask, J., H. Wackerbarth, K.J. Jensen, J. Zhang, I. Chorkendorff and J. Ulstrup, 2002a, Monolayer assemblies of a *de novo* designed 4- α -helix bundle carboprotein and its sulfur anchor fragment on Au(111) addressed by voltammetry and *in situ* scanning tunneling microscopy, *J. Am. Chem. Soc.* 125, 94.
- Brask, J., H. Wackerbarth, K.J. Jensen, J. Zhang, J.U. Nielsen, J.E.T. Andersen and J. Ulstrup, 2002b, Monolayers of a *de novo* designed 4- α -helix bundle carboprotein and partial structures on Au(111)-surfaces, *Bioelectrochemistry* 56, 27.
- Castner, D.G. and B.D. Ratner, 2002a, Biomedical surface science: Foundations to frontiers, *Surf. Sci.* 500, 28.
- Cherstvy, A.G., A.A. Kornyshev and S. Leikin, 2004, Torsional deformation of double helix in interaction and aggregation of DNA, *J. Phys. Chem. B* 108, 6508.
- Chi, Q., J. Zhang, J.E.T. Andersen and J. Ulstrup, 2001, Ordered assembly and controlled electron transfer of the blue copper protein azurin at gold (111) single-crystal substrates, *J. Phys. Chem. B* 105, 4669.
- Chi, Q., J. Zhang, E.P. Friis, J.E.T. Andersen and J. Ulstrup, 1999, Electrochemistry of self-assembled monolayers of the blue copper protein *Pseudomonas aeruginosa* azurin on Au(111), *Electrochem. Commun.* 1, 91.
- Chi, Q., J. Zhang, J.U. Nielsen, E.P. Friis, I. Chorkendorff, G.W. Canters, J.E.T. Andersen and J. Ulstrup, 2000, Molecular monolayers and interfacial electron transfer of *Pseudomonas aeruginosa* azurin on Au(111), *J. Am. Chem. Soc.* 122, 4047.
- Choma, C.T., J.D. Lear, M.J. Nelson, P.L. Dutton, D.E. Robertson and W.F. DeGrado, 1994, Design of a heme-binding four-helix bundle, *J. Am. Chem. Soc.* 116, 856.
- Clavilier, J., R. Faure, G. Guinet and R. Durand, 1980, Preparation of monocrystalline Pt microelectrodes and electrochemical study of the plane surfaces cut in the direction of the (111) and (110) planes, *J. Electroanal. Chem.* 107, 205.
- Dakkouri, A.S., D.M. Kolb, R. Edelstein-Shima and D. Mandler, 1996, Scanning tunneling microscopy study of L-cysteine on Au(111), *Langmuir* 12, 2849.
- Danilov, A.I., 1995, Scanning tunneling and atomic force microscopy in the electrochemistry of surfaces, *Russ. Chem. Rev.* 64, 767.
- Davis, J.J. and H.A.O. Hill, 2002, The scanning probe microscopy of metalloproteins and metalloenzymes, *Chem. Comm.* 2, 393.
- Davis, W.B., S. Hess, I. Naydenova, R. Haselsberger, A. Ogrodnik, M.D. Newton and M.E. Michel-Beyerle, 2002, Distance-dependent activation energies for hole injection from protonated 9-amino-6-chloro-2-methoxyacridine into duplex DNA, *J. Am. Chem. Soc.* 124, 2422.
- DeGrado, W.F., C.M. Summa, V. Pavone, F. Nastri and A. Lombardi, 1999, *De novo* design and structural characterization of proteins and metalloproteins, *Ann. Rev. Biochem.* 68, 779.
- Facci, P., D. Alliata and S. Cannistraro, 2001, Potential-induced resonant tunneling through a redox metalloprotein investigated by electrochemical scanning probe microscopy, *Ultramicroscopy* 89, 291.
- Fritz, J., M.K. Baller, H.P. Lang, H. Rothuizen, P. Vettiger, E. Meyer, H.-J. Güntherodt, C. Gerber and J.K. Gimzewski, 2000, Translating biomolecular recognition into nanomechanics, *Science* 288, 316.
- Gewirth, A.A and H. Siegenthaler, Eds., 1995, Nanoscale probes of the solid/liquid interface, Kluwer, Dordrecht, The Netherlands.

- Giese, B., 2000, Long-distance charge transport in DNA: The hopping mechanism, *Acc. Chem. Res.* 33, 631.
- Gilardi, G. and A. Fantuzzi, 2001, Manipulating redox systems: Application to nanotechnology, *Trends Biotechnol.* 19, 468.
- Gregory, B.W., B.K. Clark, J.M. Standard and A. Avila, 2001, Localization of image state electrons in the sulfur headgroup region of alkanethiol self-assembled films, *J. Phys. Chem. B* 105, 4684.
- Gurevich, Yu.Ya. and A.M. Kuznetsov, 1975, Amplification of the tunnel current by fluctuations of the potential, *Sov. Phys. Solid State* 17, 2076.
- Haiss, W., B. Roelfs, S.N. Port, E. Bunge, H. Baumgärtel and R.J. Nichols, 1998, *In situ* infrared spectroscopic studies of thymine adsorption on Au(111) electrode, *J. Electroanal. Chem.* 454, 107.
- Hamelin, A., 1996, Cyclic voltammetry at gold single-crystal surfaces. Part 1. Behaviour at low-index faces, *J. Electroanal. Chem.* 407, 1.
- Hansen, A.G., A. Boisen, J.U. Nielsen, H. Wackerbarth, I. Chorkendorff, J.E.T. Andersen, J. Zhang and J. Ulstrup, 2003, Adsorption and interfacial electron transfer of *Saccharomyces cerevisiae* yeast cytochrome *c* monolayers on Au(111) electrodes, *Langmuir* 19, 3419.
- He, H.X., J.S. Zhu, N. Tao, L. Nagahara, T. Amlani and R. Tsui, 2001, A conducting polymer nanojunction switch, *J. Am. Chem. Soc.* 123, 7730.
- Heering, H.A., F.G.M. Wiertz, C. Dekker and S. de Vries, 2004, Direct immobilization of native yeast iso-1 cytochrome *c* on bare gold: Fast electron relay to redox enzymes and zeptomole protein-film voltammetry, *J. Am. Chem. Soc.* 126, 11103.
- Herne, T.M. and M.J. Tarlov, 1997, Characterization of DNA probes immobilized on gold surfaces, *J. Am. Chem. Soc.* 119, 8916.
- Horbett, T.A. and Brash, J.L., 1995, Proteins at Interfaces II. Fundamentals and Applications, ACS Symp. Ser. 602, American Chemical Society, Washington, DC.
- Itaya, K., 1998, *In situ* scanning tunneling microscopy in electrolyte solutions, *Prog. Surf. Sci.* 58, 121.
- Itaya, K. and E. Tomita, 1988, Scanning tunneling microscopy for electrochemistry – A new concept for the *in situ* scanning tunneling microscope in electrolyte solution, *Surf. Sci.* 201, L507.
- Jensen, K.J. and G. Barany, 2000, Carbohydrates as potential templates for *de novo* design of protein models, *J. Peptide Res.* 56, 3.
- Jeuken, L.J.C., A.K. Jones, S.K. Chapman, G. Cecchini and F.A. Armstrong, 2002, Electron-transfer mechanisms through biological redox chains in multicenter enzymes, *J. Am. Chem. Soc.* 124, 5702.
- Joachim, C. and J.K. Gimzewski, 1998, A nanoscale single-molecule amplifier and its consequences, *Proc. IEEE* 86, 184.
- Joachim, C. and M.A. Ratner, 2004, Molecular wires: Guiding the superexchange interactions between two electrodes, *Nanotechnology* 15, 1065.
- Jortner, J., M. Bixon, T. Langenbacher and M.E. Michel-Beyerle, 2000, Charge transfer and transport in DNA, *Proc. Natl. Acad. Sci. USA* 95, 12759.
- Kasemo, B., 2002, Biological surface science, *Surf. Sci.* 500, 656.
- Kelley, S.O., J.K. Barton, N.M. Jackson, L.D. McPherson, A.B. Potter, E.M. Spain, M.J. Allen and M.G. Hill, 1998, Orienting DNA helices on gold using applied electric fields, *Langmuir* 14, 6781–6784.
- Kelley, S.O., N.M. Jackson, M.G. Hill and J.K. Barton, 1999, Long-range electron transfer through DNA films, *Angew. Chem. Int. Ed.* 38, 941–945.
- Kim, C., P.S. Brereton, M.F.J.M. Verhagen, and M.W.W. Adams, 2001, *Meth. Enzymol.* 334, 30.
- Kinneret, K. and E. Braun, 2004, Sequence-specific molecular lithography towards DNA-templated electronics, *Chem. Eng. Technol.* 27, 447.
- Kolb, D.M., 2001, Electrochemical surface science, *Angew. Chem. Int. Ed.* 40, 1162.
- Kühnle, A., T.R. Linderoth, B. Hammer and F. Besenbacher, 2002, Chiral recognition in dimerization of adsorbed cysteine observed by scanning tunneling microscopy, *Nature* 415, 891.

- Kuznetsov, A.M. and J. Ulstrup, 1999, *Electron Transfer in Chemistry and Biology. An Introduction to the Theory*, Wiley, Chichester, UK.
- Kuznetsov, A.M. and J. Ulstrup, 2000a, Theory of electron transfer at electrified interfaces, *Electrochim. Acta.* 45, 2339.
- Kuznetsov, A.M. and J. Ulstrup, 2000b, Mechanisms of *in situ* scanning tunneling microscopy of organized redox molecular assemblies, *J. Phys. Chem. A* 104, 11531 Errata, 2001, *J. Phys. Chem. A* 105, 7494.
- Kuznetsov, A.M. and J. Ulstrup, 2002, Mechanisms of molecular electronic rectification through electronic levels with strong vibrational coupling, *J. Chem. Phys.* 116, 2149.
- Kuznetsov, A.M. and J. Ulstrup, 2004, Single-molecule electron tunneling through multiple redox levels with environmental relaxation, *J. Electroanal. Chem.* 564, 209.
- Lorenz, W.J. and Plieth, W. Eds., 1998, *Electrochemical Nanotechnology*, Wiley-VCH, Weinheim, Germany.
- Magonov, S.M. and M.-H. Whangbo, 1996, *Surface Analysis with STM and AFM*, Verlag Chemie, Weinheim, Germany.
- Marie, R., H. Jensenius, J. Thaysen, C.B. Christensen and A. Boisen, 2002, Adsorption kinetics and mechanical properties of thiol-modified DNA-oligos on gold investigated by microcantilever sensors, *Ultramicroscopy* 91, 29.
- Metzger, R.M., 2003, Unimolecular electrical rectifiers, *Chem. Rev.* 103, 3803.
- Mutter, M. and S. Vuilleumier, 1989, Chemical approach to protein design – Template-assembled synthetic proteins (TASP), *Angew. Chem. Int. Ed.* 28, 535.
- Nielsen, M.S., P. Harris, B.L. Ooi and H.E.M. Christensen, 2004, The 1.5 Ångstrom resolution crystal structure of [Fe3S4]-ferredoxin from the hyperthermophilic archaeon *Pyrococcus furiosus*, *Biochemistry* 43, 5188.
- Nitzan, A., 2001, Electronic transmission through molecules and molecular interfaces, *Ann. Rev. Phys. Chem.* 52, 681.
- Palecek, E. and M. Fojta, 2001, Detecting DNA hybridization and damage, *Anal. Chem.* 73, 74A.
- Peterlinz, K.A., R.M. Georgiadis, T.M. Herne and M.J. Tarlov, 1997, Observation of hybridization and dehybridization of thiol-thetered DNA using two-color surface plasmon resonance spectroscopy, *J. Am. Chem. Soc.* 119, 3401.
- Petrovykh, S.Y., H. Kimura-Suda, L.J. Whitman and M.J. Tarlov, 2003, Quantitative analysis and characterization of DNA immobilized on gold, *J. Am. Chem. Soc.* 125, 5219.
- Ralph, T.R., M.L. Hitchman, J.P. Millington and F.C. Walsh, 1994, The electrochemistry of L-cystine and L-cysteine. Part I: Thermodynamic and kinetic studies, *J. Electroanal. Chem.* 375, 1.
- Rant, U., K. Arinaga, S. Fujita, N. Yokoyama, G. Abstreiter and M. Tornow, 2004, Structural properties of oligonucleotide monolayers on gold surfaces probed by fluorescence investigations, *Langmuir* 20, 10086.
- Rau, H.K., N. DeJonge and W. Haehnel, 2000, Combinatorial synthesis of four-helix bundle hemoproteins for tuning of cofactor properties, *Angew. Chem. Int. Ed.* 39, 250.
- Robertson, D.E., R.S. Farid, C.C. Moser, J.L. Urbauer, S.E. Mulholland, R. Pidikiti, J.D. Lear, A.J. Wand, W.F. DeGrado and P.L. Dutton, 1994, Design and synthesis of multi-haeme proteins, *Nature* 368, 425.
- Roelfs, B., S.N. Port, E. Bunge, C. Schröter, T. Solomun, H. Meyer, R.J. Nichols and H. Baumgärtel, 1997, Adsorption of thymine on gold single-crystal electrodes, *J. Phys. Chem. B* 101, 754.
- Schmickler, W., 1999, Theoretical aspects of the scanning tunneling microscope operating in an electrolyte solution, *Imaging of Surfaces and Interfaces*, J. Lipkowski and P.N. Ross, Eds. Wiley-VCH, New York, USA.
- Schuster, G.B. Ed., 2004, Long-Range Charge Transfer in DNA II, vol. 237, *Topics in Current Chemistry*, Springer, Berlin, Germany.
- Service, R.F., 1998, Microchip arrays put DNA on the spot, *Science* 282, 396.
- Shipway, A.N. and I. Willner, 2001, Electronically transduced molecular mechanical and information functions on surfaces, *Acc. Chem. Res.* 34, 421.

- Sommerfeld, R. and P.K. Hansma, 1986, Atomic-resolution microscopy in water, *Science* 3, 211.
- Song, S., R.A. Clark, E.F. Bowden and M.J. Tarlov, 1993, Characterization of cytochrome *c* alkanethiolate structures prepared by self-assembly on gold, *J. Phys. Chem.* 97, 6564.
- Southern, E., K. Mir and M. Shchepinov, 1999, Molecular interactions on microarrays, *Nat. Genet.* 21, 5.
- Steel, A.B., T.M. Herne and M.J. Tarlov, 1998, Electrochemical quantitation of DNA immobilized on gold, *Langmuir* 70, 4670.
- Tanaka, K., A. Tengeji, T. Kato, N. Toyama and M. Shionoya, 2003, A discrete self-assembled metal array in artificial DNA, *Science* 299, 1212.
- Tao, N.J., 1996, Probing potential-tuned resonant tunneling through redox molecules with scanning tunneling microscopy, *Phys. Rev. Lett.* 76, 4066.
- Tao, N.J., J.A. DeRose and S.M. Lindsay, 1993, Self-assembly of molecular superstructures studied by *in situ* scanning tunneling microscopy: DNA bases on Au(111), *J. Phys. Chem.* 97, 910.
- Tarlov, M.J. and E.F. Bowden, 1991, Electron-transfer reaction of cytochrome-*c* adsorbed on carboxylic-acid terminated alkanethiol monolayer electrodes, *J. Am. Chem. Soc.* 113, 1847.
- Tirrell, M., E. Kokkoli and M. Biesalski, 2002, The role of surface science in bioengineered materials, *Surf. Sci.* 500, 61.
- Uslu, F., S. Ingebrandt, D. Mayer, S. Böcker-Meffert, M. Odenthal and A. Offenhäuser, 2004, Label free fully electronic nucleic acid detection system based on a field-effect transistor, *Biosensors Bioelectron.* 19, 1723.
- Voityuk, A.A., K. Siritwong and N. Rösch, 2004, Environmental fluctuations facilitate electron-hole transfer from guanine to adenine in DNA pi stacks, *Angew. Chem. Int. Ed.* 43, 624.
- Wackerbarth, H., M. Grubb, J. Zhang, A.G. Hansen and J. Ulstrup, 2004a, Dynamics of ordered-domain formation of DNA fragments on Au(111) with molecular resolution, *Angew. Chem. Int. Ed.* 43, 198.
- Wackerbarth, H. and P. Hildebrandt, 2003, Redox and conformational equilibria and dynamics of cytochrome *c* at high electric fields, *Chem. Phys. Chem.* 4, 714.
- Wackerbarth, H., M. Grubb, J. Zhang, A.G. Hansen and J. Ulstrup, 2004c, Long-range order of organized oligonucleotide monolayer on Au(111) electrodes, *Langmuir* 20, 1647.
- Wackerbarth, H., R. Marie, M. Grubb, J. Zhang, A.G. Hansen, I. Chorkendorff, C.B.V. Christensen, A. Boisen and J. Ulstrup, 2004b, Thiol- and disulfide-modified oligonucleotide monolayer structures on polycrystalline and single-crystal Au(111) surfaces, *J. Solid State Electrochem.* 8, 474.
- Wiechers, J., T. Twomey, D.M. Kolb and R.J. Behm, 1988, An *in situ* scanning tunneling microscopy study of Au(111) with atomic scale resolution, *J. Electroanal. Chem.* 248, 451.
- Willner, I. and E. Katz, 2000, Integration of layered redox proteins and conductive supports for bioelectronic applications, *Angew. Chem. Int. Ed.* 39, 1180.
- Wolf, L.K., Y. Gao and R.M. Georgiadis, 2004, Sequence-dependent DNA immobilization: Specific versus nonspecific contributions, *Langmuir* 20, 3357.
- Xu, B., P. Zhang, X. Li and N.J. Tao, 2004, Direct conductance measurement of single DNA molecules in aqueous solution, *Nano Lett.* 4, 1105.
- Xu, Q., L. Wan, C. Wang, C. Bai, Z. Wang and T. Nozawa, 2001, New structure of L-cysteine self-assembled monolayer on Au(111): Studies by *in situ* scanning tunneling microscopy, *Langmuir* 17, 6203.
- Zhang, J., Q. Chi, A.M. Kuznetsov, A.G. Hansen, H. Wackerbarth, H.E.M. Christensen, J.E.T. Andersen and J. Ulstrup, 2002, Electronic properties of functional biomolecules at metal/aqueous solution interfaces, *J. Phys. Chem. B* 106, 1131.
- Zhang, J., Q. Chi, J.U. Nielsen, E.P. Friis, J.E.T. Andersen and J. Ulstrup, 2000, Two-dimensional cysteine and cystine cluster networks on Au(111) disclosed by voltammetry and *in situ* scanning tunneling microscopy, *Langmuir* 16, 7229.

- Zhang, J., H.E.M. Christensen, B.L. Ooi and J. Ulstrup, 2004, STM imaging and direct electrochemistry of *Pyrococcus furious ferredoxin* assembled on thiolate-modified Au(111) surfaces, *Langmuir* 20, 10200.
- Zhang, J., A.C. Welinder, A.G. Hansen, H.E.M. Christensen and J. Ulstrup, 2003, Catalytic monolayer voltammetry and *in situ* scanning tunneling microscopy of copper nitrite reductase on cysteamine-modified Au(111) electrodes, *J. Phys. Chem. B* 107, 12480.

Direct Electrochemistry of Proteins and Enzymes

Elena E. Ferapontova^{1,2}, Sergey Shleev^{1,3}, Tautgirdas Ruzgas⁴,
Leonard Stoica¹, Andreas Christenson¹, Jan Tkac¹, Alexander
I. Yaropolov³ and Lo Gorton¹

¹*Department of Analytical Chemistry, Lund University, P.O. Box 124, SE-221 00 Lund, Sweden*

²*Group of Bioinformatics, Novosibirsk IT Center, Voskhod 26a, Novosibirsk 630102, Russia*

³*Laboratory of Chemical Enzymology, A.N. Bakh Institute of Biochemistry, The Russian Academy of Sciences, Leninsky prospect 33, 119071 Moscow, Russia*

⁴*Biomedical Laboratory Science, Health and Society, Malmö University, SE-20506 Malmö, Sweden*

Contents

1. Introduction	517
2. Haem enzymes	525
2.1. Monocofactor-containing proteins	527
2.1.1. Microperoxidase	527
2.1.2. Cytochrome <i>c</i>	528
2.1.3. Peroxidase and catalase	530
2.2. Multi-cofactor-containing enzymes	539
2.2.1. Cellobiose dehydrogenase	543
2.2.2. Sulphite oxidase	546
2.2.3. Fructose dehydrogenase	548
2.2.4. Theophylline oxidase	549
3. Copper redox proteins and enzymes	551
3.1. T1 copper redox protein – azurin	554
3.2. T2 copper enzyme – galactose oxidase	556
3.3. T3 copper enzyme – tyrosinase	558
3.4. “Blue” multi-copper oxidases	562
3.4.1. Ascorbate oxidase	562
3.4.2. Bilirubin oxidase	564
3.4.3. Ceruloplasmin	566
3.4.4. Laccase	568
3.4.5. Additional enzymes	574
Acknowledgments	575
References	575

1. INTRODUCTION

The first reports on direct electron transfer (DET) between the redox protein cytochrome *c* and tin-doped indium oxide electrodes (Yeh and Kuwana, 1977)

or gold electrodes modified with 4,4'-bipyridyl (Eddowes and Hill, 1977) were published as far as 30 years ago. These findings were reported some 10–15 years after the first papers were published on combining redox enzymes and electrodes (enzyme-based amperometric biosensors or “enzyme electrodes” (Clark and Lyons, 1962; Updike and Hicks, 1967)). However, soon after that direct bioelectrocatalysis was reported for two redox enzymes, viz. laccase (Lc) and horseradish peroxidase (HRP), adsorbed on carbon electrodes (Berezin *et al.*, 1978; Yaropolov *et al.*, 1979) and then DET reactions have been demonstrated for a variety of redox proteins and enzymes, both on bare and modified electrodes, e.g. for peroxidases (Armstrong and Lannon, 1987; Jönsson and Gorton, 1989; Paddock and Bowden, 1989; Lindgren *et al.*, 2001b) and Lcs (Tarasevich *et al.*, 1979; Yaropolov *et al.*, 1996), as well as for complex, multi-cofactor-containing enzymes (Ikeda, 1992; Kinnear and Monbouquette, 1993; Ikeda, 1997; Ghindilis *et al.*, 1997; Gorton *et al.*, 1999; Armstrong and Wilson, 2000; Heffron *et al.*, 2001; Lindgren *et al.*, 2001a; Jeuken *et al.*, 2002; Leger *et al.*, 2003; Jeuken, 2003; Angove *et al.*, 2002; Sucheta *et al.*, 1992, 1993; Aguey-Zinsou *et al.*, 2003; Hoke *et al.*, 2004; Christenson *et al.*, 2004a; Ferapontova *et al.*, 2003, 2004; Elliott *et al.*, 2004; Correia dos Santos *et al.*, 2004; Christenson *et al.*, 2004b) (Table 1) and even whole bacterial cells (Bond and Lovley, 2003; Chaudhuri and Lovley, 2003).

DET reactions between redox enzymes and electrodes have been shown both indirectly, by detecting a catalytic response current in the presence of the enzyme substrate, and directly, by observing independent electrochemical activity of the redox cofactor comprising the active site in the absence of a substrate. Many of the studied complex enzymes are intracellular ones located in membranes, where they participate in biological electron transfer pathways. They contain metal components, e.g., haems, iron–sulphur clusters and copper ions, and non-metal groups, e.g., flavin, Mo-pterin (MoCo, a molybdopterin-binding domain and a Mo ion) and pyrroloquinoline quinone (PQQ) cofactors, in their active sites. The complex and highly organised multi-cofactor redox enzymes are often structured to contain domains specialised for a variety of functions, such as catalysis of electron and proton transfers, docking to redox partners and substrate binding, or anchoring to membrane structures. This requires complementary docking sites on each redox partner that often minimise the electron transfer resistance-distance between the two redox active metal or organic cofactor centres. Electrochemical studies of the bioelectrocatalytic function of these complex enzymes, revealed the importance of the “electrode environment” crucially affecting DET between the enzymes and electrodes. In many cases DET was not attained or was accompanied by a loss of enzymatic activity due to enzyme denaturation at the electrode, weak and unstable binding to the electrode, random surface orientation or by impeded internal ET between the multiple redox sites present in the enzyme, in addition to the heterogeneous electrode-enzyme ET. However, when the electrode surface was designed to resemble the surface characteristics of the partner redox protein (e.g., the surface charge distribution or hydrophilic/hydrophobic properties) then the enzyme efficiently interacted and bound to such surfaces, without dramatic conformational changes. The prerequisites for DET can be derived from the

Table 1. Redox enzymes for which DET reactions with electrodes have been shown (Adapted and updated after Gorton *et al.* (1999))

Enzyme	Cofactor	Substrate	Redox reaction	Reference
Laccases	4 Cu	O ₂	Reduction	
<i>Polyporus versicolor</i>	4 Cu (T1, T2, T3)	O ₂	Reduction	Tarasevich <i>et al.</i> (1979)
<i>Rhus vernicifera</i>	4 Cu (T1, T2, T3)	O ₂	Reduction	Yaropolov <i>et al.</i> (1996)
<i>Coriolus hirsutus/Trametes hirsuta</i>	4 Cu (T1, T2, T3)	O ₂	Reduction	Yaropolov <i>et al.</i> (1996); Shlev <i>et al.</i> (2003); Shleev <i>et al.</i> (2005a, b, c)
<i>Trametes ochracea</i>	4 Cu (T1, T2, T3)	O ₂	Reduction	Shlev <i>et al.</i> (2003); Shleev <i>et al.</i> (2005b)
<i>Coriolopsis fulvocinerea</i>	4 Cu (T1, T2, T3)	O ₂	Reduction	Shleev <i>et al.</i> (2005b)
<i>Cerrena maxima</i>	4 Cu (T1, T2, T3)	O ₂	Reduction	Shlev <i>et al.</i> (2003); Shleev <i>et al.</i> (2005b)
<i>Cerrena unicolor</i>	4 Cu (T1, T2, T3)	O ₂	Reduction	Shleev <i>et al.</i> (2005b)
Bilirubin oxidase	4 Cu (T1, T2, T3)	O ₂	Reduction	Shleev <i>et al.</i> (2004a); Tsujimura <i>et al.</i> (2004)
Ascorbate oxidase	4 Cu (T1, T2, T3)	O ₂	Reduction	Sakurai (1996); Santucci <i>et al.</i> (1998)
Galactose oxidase	1 Cu (T1)	Galactose, lactose, dihydroxyacetone		Tkac <i>et al.</i> (2002); Shleev <i>et al.</i> (2005c)
Superoxide dismutase	Cu–Zn	O ₂ ^{•-}		Borsari and Azab (1992); Wu <i>et al.</i> (1999); Ohsaka <i>et al.</i> (1996, 2002); Ge <i>et al.</i> (2003); Tian <i>et al.</i> (2004)
	Fe	O ₂ ^{•-}		Ge <i>et al.</i> (2003); Tian <i>et al.</i> (2004)
	Mn	O ₂ ^{•-}		Tian <i>et al.</i> (2004)
Peroxidases	Haem	H ₂ O ₂	Reduction	Ruzgas <i>et al.</i> (1996)
Horseradish peroxidase	Haem			Yaropolov <i>et al.</i> (1979); Jönsson and Gorton (1989); Zimmermann <i>et al.</i> (2000); Presnova <i>et al.</i> (2000)

Table 1 (*continued*)

Enzyme	Cofactor	Substrate	Redox reaction	Reference
Soybean peroxidase	Haem			Lindgren <i>et al.</i> (1997, 2000b)
Tobacco peroxidase	Haem			Lindgren <i>et al.</i> (1997, 2000b); Munteanu <i>et al.</i> (1998, 2000)
Sweet potato peroxidase	Haem			Lindgren <i>et al.</i> (2000b)
Peanut peroxidase	Haem			Munteanu <i>et al.</i> (1998)
Lignin peroxidase	Haem			Ferapontova <i>et al.</i> (2002b); Christenson <i>et al.</i> (2004a)
Manganese peroxidase	Haem			Ferapontova <i>et al.</i> (2002b)
Fungal peroxidase	Haem			Kulys and Schmid (1990); Wollenberger <i>et al.</i> (1991)
Cytochrome <i>c</i> peroxidase	Haem			Armstrong and Lannon (1987); Paddock and Bowden (1989); Scott <i>et al.</i> (1992); Scott and Bowden (1994); Mondal <i>et al.</i> (1996)
Chloroperoxidase	Haem			Ruzgas <i>et al.</i> (1995a)
Cytochrome <i>c</i> peroxidase <i>Paracoccus denitrificans</i>	2 haems			Lopes <i>et al.</i> (1998)
Bovine lactoperoxidase	Haem			Gorton <i>et al.</i> (1991a); Csöregi <i>et al.</i> (1993b)
Microperoxidase	Haem			Razumas <i>et al.</i> (1992); Tatsuma and Watanabe (1991)
Catalase	Haem			Lai and Bergel (2000, 2002); Chen <i>et al.</i> (2001); Yu and Caruso (2003); Lu <i>et al.</i> (2003); Wang <i>et al.</i> (2004); Härtl <i>et al.</i> (2004)
Cytochrome P450	Haem			
Cytochrome P450cam	Haem			Bistolos <i>et al.</i> (2004)

Cytochrome P450 2E1	Haem			Fantuzzi <i>et al.</i> (2004)
Cytochrome P450 2B4	Haem			Shumyantseva <i>et al.</i> (2004)
Hydrogenase	Fe–S cluster	H ₂ H ⁺	Oxidation Reduction	Yaropolov <i>et al.</i> (1984)
Methylamine dehydrogenase	Methoxatin-like quinone	Methylamine	Oxidation	Burrows <i>et al.</i> (1991)
Diaphorase	FAD	NADH	Oxidation	Ikeda (1992); Kobayashi <i>et al.</i> (1992); Larsson <i>et al.</i> (2001)
<i>Bacillus stearothermophilus</i>				
Bi-functional enzymes	Flavo–haem			
Cytochrome <i>b</i> ₂	FMN–haem	Lactate	Oxidation	Kulys and Svirnickas (1979); Staskeviciene <i>et al.</i> (1991)
Lactate dehydrogenase				
<i>p</i> -Cresolmethylhydrolase	FAD–haem	<i>p</i> -cresol	Oxidation	Guo <i>et al.</i> (1989)
Flavocytochrome <i>c</i> ₅₅₂	FAD–2 haem	Sulphide	Oxidation	Guo <i>et al.</i> (1990)
Cellobiose dehydrogenase		Cellobiose	Oxidation	Larsson <i>et al.</i> (1996); Lindgren <i>et al.</i> (2000a, 2001a); Christenson <i>et al.</i> (2004a); Stoica <i>et al.</i> (2005)
<i>Phanerochaete chrysosporium</i>	FAD–haem	Lactose		
<i>Sclerotium rolfii</i>	FAD–haem	Cellodextrins		
<i>Humicola insolens</i>	FAD–haem			
<i>Trametes villosa</i>	FAD–haem			
<i>Phanerochaete sordida</i>	FAD–haem			
<i>Myriococcum thermophilum</i>	FAD–haem			
Bi-functional enzymes	PQQ–haem			
D-fructose dehydrogenase	PQQ–haem	Fructose	Oxidation	Ikeda <i>et al.</i> (1991); Aizawa (1991); Khan <i>et al.</i> (1991); Gorton <i>et al.</i> (1992); Ferapontova and Gorton (2005)

Table 1 (*continued*)

Enzyme	Cofactor	Substrate	Redox reaction	Reference
Alcohol dehydrogenase		Ethanol	Oxidation	Ikeda (1992); Ikeda <i>et al.</i> (1993a); Torimura <i>et al.</i> (1997); Yanai <i>et al.</i> (1994); Ramanavicius <i>et al.</i> (1999)
<i>Gluconobacter suboxydans</i>	PQQ-4 haems			
<i>Acetobacter aceti</i>	PQQ-4 haems			
<i>Gluconobacter oxydans</i>	PQQ-4 haems			
Bi-functional enzymes	CTQ-haem			
Amine dehydrogenase	CTQ-2 haem <i>c</i>	Alkylamines	Oxidation	Fujieda <i>et al.</i> (2002)
Bi-functional enzymes	FAD-Fe-S cluster			
Succinate dehydrogenase	FAD-Fe-S cluster	Succinate	Oxidation	Sucheta <i>et al.</i> (1992); Hirst <i>et al.</i> (1996)
		Fumarate	Reduction	
Fumarate reductase	FAD-Fe-S cluster	Fumarate	Reduction	Sucheta <i>et al.</i> (1993)
Theophylline oxidase	Possibly FAD, haem	Theophylline	Oxidation	Christenson <i>et al.</i> (2004b); Ferapontova and Gorton (2005)
Bi-functional enzymes	Molibdopterin (MoCo)-haem			
Chicken liver sulphite oxidase	MoCo, haem	Sulphite	Oxidation	Elliott <i>et al.</i> (2002); Ferapontova <i>et al.</i> (2003)
Sulphite dehydrogenase	MoCo, haem	Sulphite	Oxidation	Aguey-Zinsou <i>et al.</i> (2003)
Dimethyl sulphoxide reductase	MoCo, Fe-S cluster	DMSO	Reduction	Heffron <i>et al.</i> (2001)
Trifunctional enzymes				
Aldehyde oxidoreductase	MoCo-Fe-S clusters	Aldehyde	Reduction	Correia dos Santos <i>et al.</i> (2004)

<i>Desulfovibrio gigas</i> Arsenite oxidase	MoCo–Fe–S- clusters	Arsenite	Oxidation	Hoke <i>et al.</i> (2004)
<i>Alcaligenes faecalis</i> Nitrate reductase	MoCo–Fe–S clusters-haem <i>b</i>	Nitrate	Reduction	Elliott <i>et al.</i> (2004)
D-gluconate dehydrogenase	FAD–haem–Fe–S cluster	D-gluconate	Oxidation	Ikeda (1992); Ikeda <i>et al.</i> (1988, 1993b)
Nitrite reductase	Cu (T1, T2)–multi- haem	Nitrite	Reduction	Kohzuma <i>et al.</i> (1994)

Marcus Theory (Marcus and Sutin, 1985; Marcus, 1993). The highly specific and directional protein-mediated electron transfer in biological systems is governed by factors such as distance and the bonds between the redox centres, the thermodynamic driving force for ET (i.e., the redox potential difference) between the donor and acceptor, an appropriate association of the redox couple and protein structure dynamics coupled with ET (Marcus and Sutin, 1985; Bond, 1994; Jeuken, 2003). The Marcus Theory can also be applied for heterogeneous ET reactions at electrode surfaces (Jeuken, 2003). Either direct immobilisation of the enzymes on bare electrodes or immobilisation on the electrodes modified with promoters, self-assembled monolayers (SAMs) of alkanethiols, polyelectrolytes, and surfactants were used for the construction of enzyme electrodes, where the enzyme is directly re-reduced/re-oxidised at the electrode, in the absence of a second substrate or a mediator. The use of promoters and SAMs based on thiols with appropriate head groups enabled to orient protein molecules at the electrode surface in a fashion favourable for direct electronic communication. If the orientation of the enzyme at the electrode provides a suitable ET distance between the redox centre of the enzyme and the electrode, then direct electrochemistry is expected to be observed (Guo and Hill, 1991). As an alternative way of providing an anisotropic orientation of the enzyme to facilitate direct-ET, reconstitution of the apo-enzyme on the electrode surface modified with surface-bound and electrochemically active prosthetic groups¹ was shown to be an effective way to achieve direct electrochemistry and bioelectrocatalysis of glucose dehydrogenase on PQQ-modified surfaces (Katz *et al.*, 1994), glucose oxidase on FAD-terminated SAMs (Riklin *et al.*, 1995; Willner *et al.*, 1996), and peroxidase, on a hemin-terminated SAM (Zimmermann *et al.*, 2000). Direct bioelectrocatalytic activity of some redox enzymes enabled detection of a variety of biologically important compounds, from sugars to drugs (Table 1). In most of these cases DET was proven in the presence of the enzyme substrate as a catalytic current (Figure 1A), in still fewer cases independent electrochemical proofs of DET have been shown in the absence of substrate (Figure 1B).

Furthermore, enzyme immunoassays based on DET of the commonly used HRP and Lc (used as enzyme-label) and electrodes are of great potential for application in clinical analysis (McNeil *et al.*, 1995; Ghindilis *et al.*, 1997; Ghindilis, 2000; Kuznetsov *et al.*, 2001). Up until today efficient DET reactions have been reported for some 40 redox enzymes, see Table 1, thus enabling their use for practical applications, e.g., for the development of biosensors based on DET, i.e., third-generation biosensors expected to be virtually interference free (Varfolomeev *et al.*, 1996; Ghindilis *et al.*, 1997; Gorton *et al.*, 1999; Freire *et al.*, 2003; Zhang and Li, 2004; Wollenberger, 2005), effective biofuel cells (Barton *et al.*, 2004) and selective bioorganic synthesis. The absence of mediators is the

¹In biology, the term prosthetic group or cofactor is in this context only used for tightly bound, specific non-polypeptide units required for the biological activities of the proteins. In bioelectrochemistry, the term 'cofactor' is often used synonymously with the term 'prosthetic group' or 'coenzyme'. In this chapter, the term 'cofactor' was used exclusively for redox-active non-polypeptide substructures in an enzyme, which are tightly, however, not necessarily covalently bound within the protein.

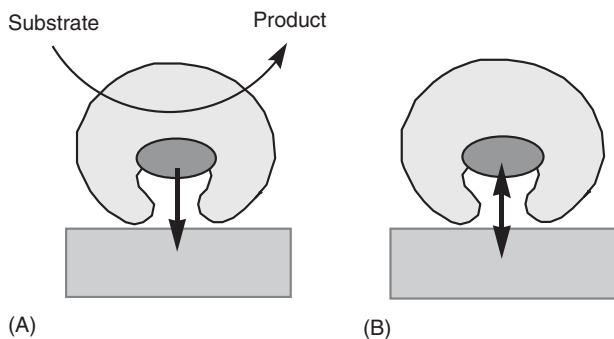


Fig. 1. Schematic representation of the electron transfer pathway in direct electron transfer between a redox enzyme and an electrode, (A) in the presence of the enzyme substrate, (B) in the absence of the enzyme substrate.

main advantage providing superior selectivity of the third-generation biosensors, both because they should operate in a potential window closer to the redox potential of the enzyme itself and therefore less prone to interfering reactions (Gorton, 1995; Gorton *et al.*, 1999; Schuhmann, 2002; Wollenberger, 2005) and also because of the elimination of a yet another reagent in the reaction sequence. Another attractive feature of systems based on DET is the possibility of modulating the desired properties of an analytical device using protein modification with genetic or chemical engineering techniques on one hand (Degani and Heller, 1987; Heller and Degani, 1988; Willner *et al.*, 1997), and novel interfacial technologies on the other hand (Whitesides *et al.*, 1991; Finklea, 1996; Baeumner, 2005; Andreescu *et al.*, 2005). The intention of this contribution is to summarise the achievements on DET between redox enzymes and electrodes with a special focus on haem and copper-containing redox enzymes, i.e., in the area where our group has been most intensively working.

2. HAEM ENZYMES

Haem enzymes involve peroxidases, catalases, cytochromes of the P450 group, and a variety of multi-cofactor complex enzymes, which contain haem(s) along with other cofactors such as flavin(s), copper, iron–sulphur cluster(s), MoCo or PQQ (Table 1). There are also haem-containing proteins such as globins and cytochromes, which under biological conditions have oxygen-carrier/oxygen-storage function (haemoglobin, Hb, and myoglobin, Mb) or comprise a component of ET chains as ET mediators (e.g., cytochrome *b*₅ and cytochrome *c*). All haem enzymes and proteins contain the *haem prosthetic group*, which consists of Fe³⁺ coordinated to a porphyrin group (Figure 2). The porphyrin nitrogens occupy four coordination positions of the haem iron, the left two unoccupied positions on either side of the haem plane are available for ligands, which strongly influence the redox potential, reactivity, and biological function of the haem protein (Dryhurst *et al.*, 1982). Not shielded by a polypeptide chain

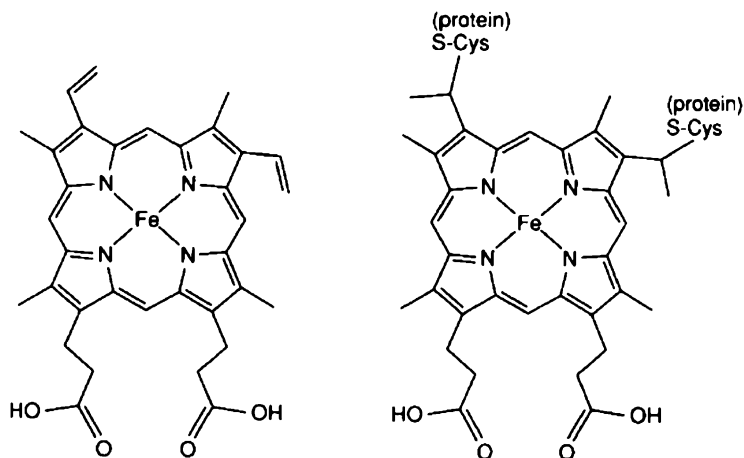


Fig. 2. Schematic representation of haem *b* and haem *c* structures.

“naked” haem exhibits heterogeneous electron transfer (ET) rates higher than 4000 s^{-1} ($\text{Fe}^{3+/2+}$ redox conversion), when adsorbed on basal pyrolytic graphite or glassy carbon (Brown and Anson, 1978; Feng *et al.*, 1995). Similarly high heterogeneous ET rates can be observed for haem adsorbed on gold electrodes modified with short thiols, e.g., ethanethiol, cystamine, and mercaptoethanol, with an apparent heterogeneous ET rate constant above 3600 s^{-1} (Gorton *et al.*, 1999). However, the electrochemical and catalytic properties of haem drastically change when it is incorporated into a proteinaceous environment, e.g., the formal potential (E^0) of the redox conversion of the haem between the $\text{Fe}^{2+}/\text{Fe}^{3+}$ states can vary over a wide potential range due to the protein environment, from -0.27 V^2 for HRP (Harbury, 1957) to 0.26 V for cytochrome *c* (Rodkey and Ball, 1950; Cusanovich and Tollin, 1996). The electrochemical response from haem-enzymes and proteins are not so pronounced as those from “naked” haem, as a result of the polypeptide environment of the haem domain active site, which makes the ET distance longer and diminishes surface concentrations of the haem as a result of increased mass of the proteins (Lötzbeyer *et al.*, 1997). However, the unique electrochemical and catalytic properties of the haem active site promote various bioelectrochemical applications of the haem-proteins and haem-enzymes, e.g., in biosensors based on DET. In the last case, establishing efficient DET communication between the haem enzymes and the electrodes is crucial for the development of third generation biosensors (Gorton *et al.*, 1999; Schuhmann, 2002; Freire *et al.*, 2003; Wollenberger, 2005). In general, there may be a variety of electron-tunnelling pathways within the enzyme molecule between the redox active centre and the protein surface (Gray and Winkler, 2003). Two groups of redox enzymes are presently distinguished, specifically, as discussed by Hill and co-workers, the intrinsic and extrinsic ones (Guo and Hill, 1991; Hill and Hunt, 1993; Hill *et al.*, 1996). With the intrinsic redox enzymes, “the catalytic reaction between an enzyme and its

²All potentials in this chapter are cited versus SHE unless stated otherwise.

substrates takes place within a highly localised assembly of redox active sites” and “there need be no electron transfer pathways from these sites to the surface of the enzyme, where, it is presumed, it would interact with the electrode” (Guo and Hill, 1991). In other words, the intrinsic enzymes do not have a redox protein as their natural partner for ET exchange and therefore electron-tunnelling pathways within the enzyme molecule do not exist. For these enzymes efficient DET reactions at the electrodes are less probable and require (1) the sites of the catalytic reaction to be close to the protein surface, (2) the possibility for enzyme deformation without losing the activity, (3) the electrode surface projecting into the enzyme, or (4) ET pathways to be introduced by enzyme modification (Guo and Hill, 1991). Only recently were attempts shown successful to project an ultramicroelectrode into the active site of an intrinsic enzyme, glucose oxidase (Xiao *et al.*, 2003).

In contrast the extrinsic enzymes do have natural redox protein partners involved in transporting electrons and therefore should have electron-tunnelling pathways between the active sites and the enzyme surface where the partner protein binds for efficient ET between the enzyme and its partner protein to occur. Thus, to realise efficient DET between redox enzymes and electrodes, a proper orientation of the redox enzyme onto the electrode through the site of the electron-tunnelling pathways where the partner protein commonly binds (for extrinsic enzymes) or through the domain of the active site exposed to the protein surface becomes important.

2.1. Monocofactor-containing proteins

2.1.1. Microperoxidase

The electrochemistry of *microperoxidases* (MP) is the best example of the “orientation” approach. Microperoxidase is produced via proteolytic digestion of cytochrome *c* and presents a haem-bound peptide of 6, 8, 9, or 11 amino acids and has a relatively simple structure exhibiting peroxidase activity (Scott and Mauk, 1996). The scarce peptide environment of MPs enables both maximum exposure of the haem to the protein surface and aqueous solubility of MPs, which have a weaker tendency of aggregation, and availability of a number of chemical functionalities for covalent coupling and modification. DET reactions of MPs at electrodes are expected to be highly efficient approaching the characteristics of the haem alone due to enhanced DET contact between an electrode and the exposed haem. However, commonly the reported ET rates e.g., for microperoxidase-11 (MP-11) on cystamine-modified gold electrodes were only between 12 s^{-1} (Lötzbeier *et al.*, 1994) and 20 s^{-1} (Narvaez *et al.*, 1997), whereas hemin adsorbed on glassy carbon or basal plane pyrolytic graphite electrodes exhibited constants higher than 4000 s^{-1} (Brown and Anson, 1978; Feng *et al.*, 1995). Special protocols developed for immobilisation of MP-11 using different immobilisation chemistries enabled to achieve high ET rates over the range of $1700\text{--}3600\text{ s}^{-1}$ with MP-11 physically adsorbed on hydrophobic alkanethiol-modified gold electrodes and MP-11 linked through its

amino-functionalities on gold electrodes using Lomant's reagent (Ruzgas *et al.*, 1999). The commonly used carbodiimide coupling to cystamine-modified electrodes resulted in a coverage of 3–4 layers of the electrode and low values of the rate constant, 13–112 s⁻¹, reflecting the interlayer ET but not the heterogeneous electrode/MP-11 electron exchange rate (Ruzgas *et al.*, 1999).

2.1.2. Cytochrome *c*

Another remarkable example of the electrode-protein “orientation” studies is the electrochemistry of cytochrome *c* at bare and differently modified electrodes. Cytochrome *c* (or ferrocyanochrome *c*) is a haem-containing redox protein active in electron transfer pathways, e.g., in the respiratory chain in the mitochondria (Scott and Mauk, 1996). Cytochrome *c* contains the *c*-type haem as a prosthetic group, which belongs to one of the two most widely spread and studied haem types (Figure 2). Another one is haem of the *b*-type, which is very similar to haem *c* except for that the haem *c* group is coordinated to cysteine residues in proteins, whereas haem *b* is not (Figure 2). Under physiological conditions cytochrome *c* does not react with molecular oxygen but is readily oxidised by its natural redox partners, cytochrome *c* oxidase, cytochrome *c* peroxidase, and a series of other complex enzymes, e.g., involved in the respiratory chain function. In cytochrome *c* the haem is partially exposed to the solution/electrode surface, and its oxidation/reduction gives a strong signal in electrochemical and spectroscopic measurements (Scott and Mauk, 1996). Horse heart cytochrome *c* has eight lysine residues localised on its surface adjacent to where the haem is most closely exposed to the protein surface. The very first reports on DET between electrodes and redox active proteins referred to cytochrome *c*, which exhibited a quasi-reversible direct electrochemistry on 4,4'-bipyridyl modified gold (Eddowes and Hill, 1977) and on tin-doped indium oxide electrodes (Yeh and Kuwana, 1977). These reports were followed by intensive studies of cytochrome *c* at unmodified and promoter-modified gold, silver, platinum, carbon, and metal oxide electrodes with different interface electrode/modifier/protein/solution (Yeh and Kuwana, 1977; Eddowes and Hill, 1977; Eddowes *et al.*, 1979, 1980; Albery *et al.*, 1981; Armstrong *et al.*, 1988; Armstrong, 1990; Song *et al.*, 1993; Bond, 1994; Hill *et al.*, 1996; Jin *et al.*, 1996; Feng *et al.*, 1997; El Kasmi *et al.*, 1998). Electrochemical studies on a variety of electrode materials revealed the importance of orientation of cytochrome *c* on the electrode surface to achieve facile electrochemistry of the protein (Armstrong, 1990). In the presence of negatively charged functionalities on the electrode surface, strong electrostatic interactions between cytochrome *c* and the electrode surface are obtained resulting in the shortest distance between the haem and the electrode surface largely facilitating ET. Initially various bipyridyl and viologen derivatives were used as promoters of the ET reactions of cytochrome *c* at the promoter-modified electrodes (Eddowes and Hill, 1977; Armstrong *et al.*, 1988). The word promoter was used to denote that these redox active compounds did not act as electron transfer mediators but only helped (promoted) ET through establishing a correct orientation of the redox protein

on the electrode (Guo and Hill, 1991; Hill and Hunt, 1993; Hill *et al.*, 1996). The promoter should have one terminal functional group for surface adsorption or binding (e.g., -N, -P, or -S functionalities, e.g., thiols for binding to Au, Pt, or Ag), groups, which minimise structural changes of the protein (hydrophilic groups) and another terminal group (e.g., negatively charged groups) for attractive interactions with the positively charged lysine residues of cytochrome *c* to provide an appropriate ET orientation of the protein at the electrode. Among the promoters, which facilitate a reversible fast electrode reaction of cytochrome *c*, were 4,4'-bipyridyl, cysteine, mercaptopropionic acid, mercaptoundecanoic acid, oligonucleotides, etc. (Eddowes *et al.*, 1979, 1980; Albery *et al.*, 1981; Song *et al.*, 1993; Feng *et al.*, 1997). Today, self-assembled monolayers (SAMs) formed by thiol derivatives on gold and silver electrodes are the most studied and the most common (and efficient) electrode modifications enabling to easily orient cytochrome *c* onto electrodes (Finklea, 1996; Taniguchi *et al.*, 2003; Schlereth, 2005; Wollenberger, 2005). SAMs of thiols bearing carboxylic head group or mixed (COOH)-(OH)-SAMs were shown to be the most suitable for DET of cytochrome *c* (Arnold *et al.*, 1997; El Kasmi *et al.*, 1998; Ge and Lisdat, 2002). Experimentally determined ET rates vary between 400 and 2000 s⁻¹; and 70 s⁻¹ was found for cytochrome *c* covalently coupled to the long-chained alkanethiol-modified gold electrode (Ge and Lisdat, 2002). When the thiol modifier is long (longer than nine carbons) then the rate of the interfacial ET drops exponentially with the thiol length, designating the rate-limiting electron tunnelling through the layer of the thiol modifier (Song *et al.*, 1993; Feng *et al.*, 1997). The rate of the ET process between cytochrome *c* and gold, however, is not dependent on the length of the thiol modifier when shorter alkanethiols (C < 6) are used to form the SAM. The differences in rate constants of surface-confined cytochrome *c* at *N*-acetyl-L-cysteine-modified gold surface were likely due to the different techniques employed (cyclic voltammetry at high sweep rates, electrochemical impedance and electroreflectance), however, the measured values can still be regarded as good estimates (Ruzgas *et al.*, 1998). As a support for that is the fact that rate constants in this case are close to the rate (800 s⁻¹) observed for interprotein ET between cytochrome *c* and its natural partner cytochrome *c* peroxidase (Pappa *et al.*, 1996b). These investigations clearly reveal that electrochemical investigations give results fully in agreement with other independent techniques.

From an electroanalytical point of view cytochrome *c*-modified electrodes are of particular interest for two principally different purposes. On the one hand, they can be used for electrochemical detection of short-lived oxygen and nitrogen radical species (Cooper *et al.*, 1993; Scheller *et al.*, 2002; Ge and Lisdat, 2002; Shipovskov *et al.*, 2004; Wollenberger, 2005). On the other hand, cytochrome *c*-electrodes can be used for electronic coupling with other redox enzymes revealing no or sluggish direct electron transfer with electrodes (Amine *et al.*, 1994; Jin *et al.*, 1996; Fridman *et al.*, 2000; Pardo-Yissar *et al.*, 2000; Rhoten *et al.*, 2000; Haas *et al.*, 2001; Scheller *et al.*, 2002; Rhoten *et al.*, 2002a,b; Ferapontova *et al.*, 2003; Katz and Willner, 2003; Katz *et al.*, 2004; Ferapontova and Gorton, 2005). For both purposes it is essential that the ET between the electrode and cytochrome *c* is as rapid as possible not limiting the

overall ET between the analyte and the electrode. This strongly motivates further efforts in measuring heterogeneous ET rates of cytochrome *c* and tethering surfaces to establish (e.g., by correct orientation) high interfacial ET of this protein. Other types of cytochromes are also intensively studied at various bare and modified electrodes to find a way to modulate DET of the proteins through their proper orientation at the electrodes, among them being microperoxidase-11 (obtained from the proteolytic digestion of cytochrome *c*) (Narvaez *et al.*, 1997; Ruzgas *et al.*, 1999), monohemic cytochromes c_{522} , c_{533} , and c_{550} (Correia dos Santos *et al.*, 2003; Yamamoto *et al.*, 2001) and tetrahaem cytochrome c_3 (Zhang *et al.*, 1994; Lojou and Bianco, 2000).

2.1.3. Peroxidase and catalase

Peroxidases are virtually the most intensively used haem-enzymes for the development of DET-based biosensors (Ruzgas *et al.*, 1996; Gorton *et al.*, 1999; Lindgren *et al.*, 2001b). Peroxidases catalyse the oxidation of a variety of organic and inorganic compounds by hydrogen peroxide or related compounds (Dunford, 1999) and thus are of special interest for detection of peroxides in the fields of healthcare, food and cosmetic analysis, and environmental protection. Mainly HRP, but also peroxidase from other sources have been used for construction of peroxidase electrodes for unmediated detection of hydrogen peroxide and other hydroperoxides (Ruzgas *et al.*, 1996; Gorton *et al.*, 1999; Lindgren *et al.*, 2000b; Gaspar *et al.*, 2001; Ferapontova *et al.*, 2002b; Lindgren *et al.*, 2001b; Christenson *et al.*, 2004a). Peroxidases have also been used in conjunction with H_2O_2 -producing oxidases for the measurement of the concentration of the oxidase substrate, such as glucose and other sugars, and a variety of amino acids, by co-immobilisation of the peroxidase with the corresponding oxidase (Ruzgas *et al.*, 1996; Ghindilis *et al.*, 1997; Gorton *et al.*, 1999) and further in affinity-based assays (Ho *et al.*, 1993; McNeil *et al.*, 1997; Zeravik *et al.*, 2003).

The majority of haem peroxidases contains a haem *b* (Figure 2) as the prosthetic redox active group (Dunford, 1999) and the catalytic activity of peroxidases is closely related to its redox states. The peroxidase catalytic cycle involves the oxidation of the native form of, e.g., HRP by H_2O_2 to compound I (E1, represents an oxidised form of HRP and consists of oxyferryl iron ($Fe^{4+} = O$) and a porphyrin π cation radical), and further a $2e^-/2H^+$ direct reduction of E1 to the initial HRP state, ferriperoxidase (Figure 3). In the case when an electrode donates electrons to E1, a direct electroreduction of E1 by the electrode may occur. This DET is characterised by a heterogeneous ET rate constant, k_s (Ruzgas *et al.*, 1995b, 2002; Gorton *et al.*, 1999). Mediated bioelectrocatalysis has more similarities with the corresponding homogeneous one (Figure 3), when the oxidised enzyme is reduced by some electron donor S, which is subsequently re-reduced at the electrode (Ruzgas *et al.*, 1995b, 2002; Gorton *et al.*, 1999). Mediated ET is usually more efficient compared to DET (Ruzgas *et al.*, 1995b, 1996, 2002; Gorton *et al.*, 1999; Lindgren *et al.*, 2001b). The reduction of E1 to ferriperoxidase is expected to occur via formation of an

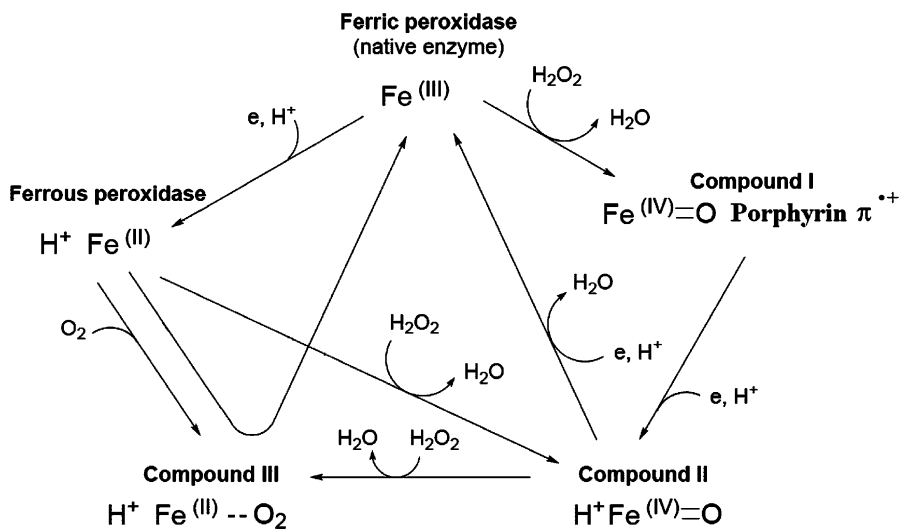


Fig. 3. Schematic representation of redox transformations of peroxidase during its biocatalytic cycles.

intermediate compound II (E2 containing an additional proton compared to the native form and E1) and then stepwise to the initial ferriperoxidase state, as in the case of homogeneous peroxidase catalysis (Dunford, 1999). The peroxidase cycle also involves the consumption and release of protons during the peroxidase redox transformations. The reduction potentials for the E1/E2 and E2/HRP(Fe³⁺) redox couples are pH-dependent and shift from 0.9 and 0.88 V at pH 7.0, respectively (Farhangrazi *et al.*, 1995; He *et al.*, 1996) to more positive values with decreasing pH, corresponding to 0.99 and 0.97 V at pH 6.0 (Hayashi and Yamazaki, 1979). Native HRP can also be directly reduced at the electrode surface to its ferrous state, at potentials of -267 mV at pH 7.0 and -217 mV at pH 6.0, respectively (Harbury, 1957). Similar to other plant peroxidases, the values of the $E^{0'}$ for the couple (Fe^{3+/2+}) of HRP are pH dependent (Dunford, 1999) since the redox process is accompanied by protonation of the ferrous form. Ferrous HRP is capable of binding O₂, which results in the formation of compound III (E3, Figure 3), which is a catalytically inactive form of the enzyme but can be reduced by the reaction with ferrous HRP. Thus, depending on experimental conditions and due to the diversity of the oxidative states of the haem, peroxidases can utilise either peroxides or molecular oxygen as oxidising substrates.

When immobilised at the electrode, HRP may exhibit a remarkable bioelectrocatalytic activity due to DET between the electrode and the haem of HRP (Yaropolov *et al.*, 1979; Jönsson and Gorton, 1989; Wollenberger *et al.*, 1990, 1991; Csöregi *et al.*, 1993b; Bogdanovskaya *et al.*, 1994; Ruzgas *et al.*, 1995b; Tatsuma *et al.*, 1998; Presnova *et al.*, 2000; Ferapontova and Gorton, 2001; Ferapontova and Puganova, 2002; Ferapontova, 2004), thus, shifting the potential of H₂O₂ electroreduction up to 0.9 V compared to bare electrodes, where the electroreduction of H₂O₂ starts below 0 V. Peroxidases from different

sources, e.g., plant, yeast, and fungal peroxidases, were demonstrated to exhibit similar direct bioelectrocatalytic activity in the reduction reaction of H_2O_2 (Armstrong and Lannon, 1987; Paddock and Bowden, 1989; Kulyš and Schmid, 1990; Lindgren *et al.*, 2000b; Gaspar *et al.*, 2001; Ferapontova *et al.*, 2002b). Therewith the electrochemistry and the bioelectrocatalytic activity of peroxidases significantly depend on the electrode materials and on the electrode modifications used. It is not surprising since the haem moiety is buried inside the protein structure (Gajhede *et al.*, 1997; Bonagura *et al.*, 2003; Sundaramoorthy *et al.*, 1995, 1997; Pappa *et al.*, 1996a; Schuller *et al.*, 1996; Poulos *et al.*, 1995), and in this case, to achieve efficient DET, the enzyme adsorption/orientation at the electrodes becomes a crucial problem. To study and explain the nature of DET in the case of peroxidases both different electrode materials, modifying layers and a variety of native and genetically engineered peroxidases have been used (Ferapontova, 2004).

Carbonaceous electrodes appeared to be most widely used for studies of peroxidase bioelectrocatalysis since 1979, when DET between carbon black and peroxidase was first demonstrated (Yaropolov *et al.*, 1979). After that, direct bioelectrocatalytic reduction of H_2O_2 was studied with HRP on spectroscopic and pyrolytic graphite, carbon black and glassy carbon (Jönsson and Gorton, 1989; Wollenberger *et al.*, 1990; Csöregi *et al.*, 1993b; Fridman *et al.*, 1994; Bogdanovskaya *et al.*, 1994; Ruzgas *et al.*, 1995b; Lindgren *et al.*, 1998, 1999; Tarasevich *et al.*, 2001a; Ferapontova and Puganova, 2002), graphite coating (Tatsuma *et al.*, 1998), and carbon fibres (Csöregi *et al.*, 1993a, 1994a, b), screen-printed graphite electrodes (Schumacher *et al.*, 2001) and boron-doped diamond electrodes (Tatsuma *et al.*, 2000) as well as with HRP incorporated into carbon paste (Wollenberger *et al.*, 1991, Gorton *et al.*, 1991b). HRP readily adsorbs on carbon surfaces and reduces H_2O_2 in the course of a DET reaction between its haem active site and the electrodes, in the absence of any mediators. The surface coverage of HRP varied for different types of electrodes and surface pretreatment, thus providing different efficiencies of direct bioelectrocatalysis (Csöregi *et al.*, 1993a; Fridman *et al.*, 1994; Ruzgas *et al.*, 1995b; Tatsuma *et al.*, 1998, 2000; Tarasevich *et al.*, 2001a). Additionally, not all adsorbed HRP molecules are active in the DET reaction with electrodes, but a portion of them, which is properly oriented at the electrode surface (Ruzgas *et al.*, 1995b; Lindgren *et al.*, 1998; Gorton *et al.*, 1999). For wild-type HRP (wHRP), around 50% of the total amount of catalytically active HRP molecules adsorbed on graphite was shown to be active in DET (Ruzgas *et al.*, 1995b; Lindgren *et al.*, 1998). Moreover, the rate of DET was restricted to 2 s^{-1} at pH 7.0 (Ruzgas *et al.*, 1995b; Lindgren *et al.*, 1998). The observed efficiency of peroxidase bioelectrocatalysis correlated with variations in the solution pH as well: with increasing $[\text{H}_3\text{O}^+]$ the efficiency of the bioelectrocatalytic reduction of H_2O_2 increased (Ferapontova and Gorton, 2001, 2002; Ferapontova and Puganova, 2002). The apparent rate constant of the heterogeneous ET between wHRP and graphite, k_s , was then found to be pH-dependent and changed from 0.54 s^{-1} , at pH 7.9, to 11 s^{-1} , at pH 6.0 (Ferapontova and Gorton, 2002) (Figure 4a, Table 2), thus offering an easy way for increasing the efficiency of DET. In fact, the DET rate is largely affected by the presence of any proton donors such as

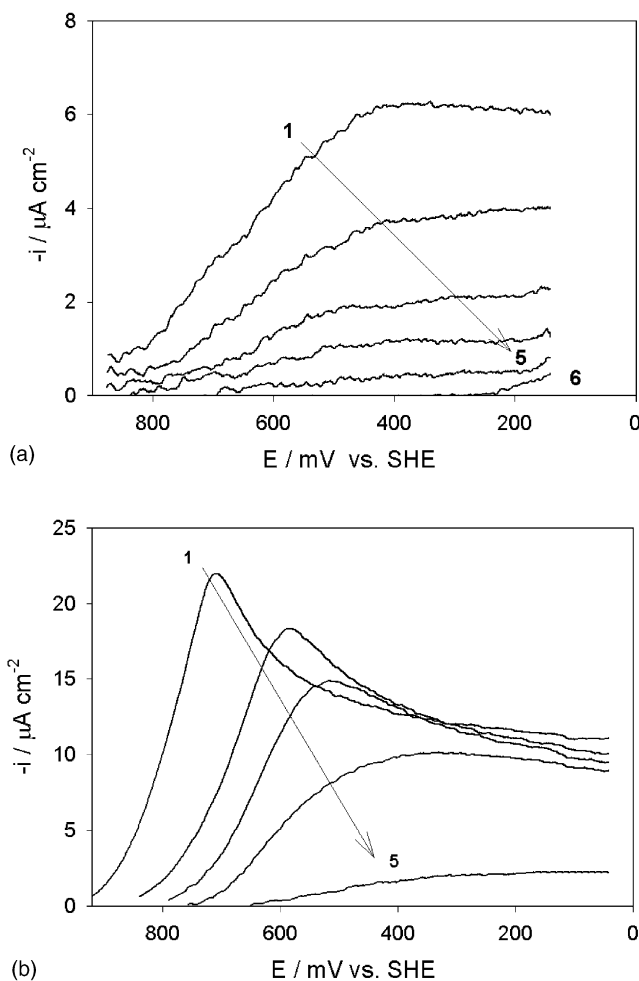


Fig. 4. Current densities for bioelectrocatalytic reduction of 10^{-4} M H_2O_2 at gold electrodes modified with (a) wHRP and (b) $\text{C}_{\text{Hisr}}\text{HRP}$ plotted as a function of the electrode potential. The solution pH was (1) 6, (2) 6.5, (3) 7.0, (4) 7.5, and (5) 8.0; (6) H_2O_2 reduction at a bare gold surface. Sweep rate 5 mV s^{-1} , background subtracted.

H_3O^+ , the ammonium cation (NH_4^+) and multi-charged cations ($[\text{La}(\text{H}_2\text{O})]^{3+}$, $[\text{Y}(\text{H}_2\text{O})]^{3+}$, and $[\text{Lu}(\text{H}_2\text{O})]^{3+}$), known for their proton donor ability (Ferapontova and Fedorovich, 1999; Ferapontova and Gorton, 2001): the k_s between wHRP and gold increased from 2.9 to 6.6 s^{-1} when changing from phosphate buffer solutions (PBS) containing 0.15 M NaCl to PBS containing $0.15 \text{ M NH}_4\text{Cl}$, at pH 7.4, and from 1.1 to 4.8 s^{-1} at pH 8.0 (Ferapontova and Gorton, 2001). However, in general, statistically random adsorption and orientation of HRP molecules at carbonaceous surfaces somehow restrict the possibilities for improvement of the bioelectrocatalytic performance of the enzyme.

One of the approaches to improve direct peroxidase bioelectrocatalysis is to use different forms of peroxidases to achieve higher DET rates and higher

Table 2. Enzymatic and bioelectrocatalytic activity of wHRP and rHRPs with different surface Cys- and His-mutations, immobilised on gold

Peroxidase	Activity (ABTS) U mg ⁻¹	% in direct ET	k_s , s ⁻¹ , pH 7.4	k_s , s ⁻¹ , pH 6.0	k_1 , 10 ⁻⁶ M ⁻¹ s ⁻¹ pH 6.0/7	k_3 , 10 ⁻⁴ M ⁻¹ s ⁻¹ with catechol
wHRP	1260	73	2.5	11.6	0.13	1.4
rHRP	565	75	29	260	0.51	10.3
C _{His} rHRP	690	86	38	426	0.53	10.5
C _{His} rHRP57Cys	575	80	31	128	0.34	1.7
C _{His} rHRP189Cys	1710	71	20	87	0.55	2.9
C _{Strep} rHRP	438	88	19	115	0.65	7.9
C _{Strep} rHRP309Cys	601	64	29	452	0.58	7.2

Note: Amperometry at 150 mV, in a wall-jet flow-through system (Ferapontova and Gorton, 2001, 2002; Ferapontova *et al.*, 2001a, 2002a; Ferapontova, 2004).

percentage of the enzyme molecules active in DET reaction with the electrode. In the search for a possible alternative to HRP in applications based on DET, a number of alternative plant peroxidases has been investigated and kinetically characterised on graphite. Some results are presented in Table 3 for fungal (lignin and manganese peroxidases, LiP and MnP, respectively), peanut (PNP), tobacco anionic peroxidase (TOP), and sweet potato plant peroxidase (SPP). As can be seen, the percentage in DET varies substantially between the peroxidases (Lindgren *et al.*, 2000b; Ferapontova *et al.*, 2002b; Christenson *et al.*, 2004a). Especially noticeable are the values obtained for SPP, revealing a high percentage in DET as well as a high rate of DET. However, DET rates were found to be in the same order of magnitude and correspond to a kinetically limiting step of DET. Another interesting effect was shown for TOP (Gazaryan *et al.*, 1996). Due to the presence of the negatively charged Glu-141 at the entrance to the active centre, TOP is believed to undergo a reversible blockade of the active site by binding an extra Ca^{2+} ion (Gazarian *et al.*, 1996). Ca^{2+} ions decrease the amount of enzyme active in DET by 17%, however, it is still higher than that for wHRP. Thus, the blockade of the active site with Ca^{2+} does not knock out DET. Ca^{2+} ions also cause a decrease in k_1 by 11%, in k_s by 38%, in k_3 by 26% (*p*-cresol) and 58% (catechol) (Munteanu *et al.*, 2000). The observation that both soluble and immobilised TOPs are subject to conformational changes in the presence of Ca^{2+} indicates that the immobilised enzyme retains the conformational flexibility on the graphite surface. Remarkable data were also obtained with fungal LiP and MnP, which in solution exhibited virtually negligible catalytic activity towards H_2O_2 reduction in the absence of their specific substrates, i.e., veratryl alcohol and Mn^{2+} , but demonstrated DET-based bioelectrocatalytic behaviour for H_2O_2 reduction similar to that observed previously for wHRP and other plant peroxidases (Ferapontova *et al.*, 2002b; Christenson *et al.*, 2004a).

Since the ability of peroxidase to participate in DET was established to be an intrinsic property of the protein, oriented binding techniques for HRP have been intensively studied as alternative approaches for improving DET communication between the peroxidase haem and the electrodes. One of the approaches involves anisotropic orientation of the enzyme through reconstitution of the holoenzyme on the electrode surface using haem-containing mixed SAM-modified gold electrodes and the HRP apoenzyme (Zimmermann *et al.*, 2000). Another possibility is to introduce into the molecular surface of recombinant HRP (rHRP) sites recognisable by metal electrodes (e.g., gold or silver), such as a polyhistidine tag or cysteine residues introduced in different surface positions of the rHRP molecule (Presnova *et al.*, 2000; Ferapontova and Gorton, 2002; Ferapontova, 2004; Gorton *et al.*, 1999; Lindgren *et al.*, 2001b; Ruzgas *et al.*, 2002; Ferapontova *et al.*, 2001a,b, 2002a). Recombinant forms of HRP with either a His-tag or a Strep-tag at the C- and N-termini (C_{His} rHRP and N_{His} rHRP, respectively), which additionally had Cys at positions 57, 189, or 309 (C-terminus) of the polypeptide chain, were produced by genetic engineering of rHRP using an *E. coli* expression system (Grigorenko *et al.*, 1999) and studied electrochemically (Presnova *et al.*, 2000; Ferapontova *et al.*, 2001a,b, 2002a). When exchanging wHRP for the non-glycosylated recombinant forms, a dramatic increase was observed in the response currents of the bioelectro-

Table 3. Biochemical properties and electrochemically determined rate constants for native plant peroxidases adsorbed on graphite electrodes in 0.1 M PBS, pH 7.0, using a rotating disc electrode (RDE)

POD	pI	MW (kDa)	Glycosylation (%)	Activity (ABTS) (U mg ⁻¹)	% in DET	Rate constants			
						k_s, s^{-1}	$k_1, M^{-1} s^{-1} 10^{-5}$	$k_3, M^{-1} s^{-1} 10^{-4}$	
								<i>p</i> -Cresol	Catechol
HRP (Ferapontova <i>et al.</i> , 2002b)	8.8	42	18	1400	48	2.3	2.0	3.8	1.4
PNP (Lindgren <i>et al.</i> , 2000b)	7.9	40	15	73	44	1.3	1.3	5.0	—
SPP (Lindgren <i>et al.</i> , 2000b)	3.5	38	16–17	1600	91	4.8	2.8	35	—
TOP (Lindgren <i>et al.</i> , 2000b)	3.5	37	11	1680	68	2.6	0.53	1.9	0.56
LiP ^a (Ferapontova <i>et al.</i> , 2002b)	3.5–4	37–42	6–13	8	10	1.6	0.25	—	0.16
LiP ^b (Christenson <i>et al.</i> , 2004a)					31	1.15	0.09		0.11
MnP (Ferapontova <i>et al.</i> , 2002b)	4.1	46	17	0.023	27	1.7	3.5	—	0.14

Note: Amperometry at 150 mV. 60 μM catechol or *p*-cresol were used for determination of k_3 .

^aLiP – from *Phanerochaete chrysosporium*.

^bLiP – from *Trametes versicolor*.

catalytic reduction of H_2O_2 due to the enhanced DET (Figure 4). Linear sweep voltammograms show sigmoid-shaped waves resulting from kinetic restrictions in the wHRP|gold system, which, however, transform for the rHRP|gold system and at high proton concentrations (for pH values below 7.0) to a peak-shaped wave reflecting favourable bioelectrocatalytic conditions. More than 75% of the HRP molecules were found to be active in DET ($90 \pm 10\%$ for $\text{C}_{\text{His}}\text{rHRP}$ and $75 \pm 20\%$ for wHRP) (Ferapontova *et al.*, 2001a, b, 2002a; Ferapontova and Gorton, 2001, 2002). k_s drastically increased when exchanging wHRP for recombinant HRPs and from pH 8.0 to pH 6.0 (Table 2, Figure 3). For recombinant HRPs, k_s exceeded 400 s^{-1} for the system $\text{C}_{\text{His}}\text{rHRP}$ |gold at pH 6.0 (Ferapontova *et al.*, 2001a, 2002a) and thus approached the data obtained with cytochrome *c* peroxidase on edge plain pyrolytic graphite (Scott and Bowden, 1994; Mondal *et al.*, 1996, 1998). However, the enhancement of the rate of DET with increasing proton concentration was not the same for different recombinant HRP forms, thus implying that there are different electron and proton transfer pathways in the peroxidase molecule. The His and Cys groups introduced into different surface positions of the rHRP molecule with high affinity for gold allowed adsorption of the rHRP molecules in different but specific orientations onto the gold surface through these attachment points resulting in different electron and proton transfer pathways from the electrode within the structure of rHRP. For different molecular orientations interfacial ET rates between gold and HRP changed from 20 to 38 s^{-1} , at pH 7.4, and from 87 to 450 s^{-1} , at pH 6.0 (Table 2) (Ferapontova *et al.*, 2001a, 2002a). Lowering pH from 7.4 to 6.0 resulted in different enhancements of the ET efficiency as well: k_s increased by 2 to 16 fold, depending on the orientation of the HRP molecule at the electrode surface defined by the position of the mutations. Comparative analysis of the k_s at pH 7.4 and 6.0 demonstrated that oriented immobilisation of rHRP through the His-tag or Cys introduced in the C-terminal area of the enzyme resulted in an enhanced DET as a consequence of a more favourable coupled electron and proton transfer pathway, compared to other cysteine mutations (Table 2) (Ferapontova and Gorton, 2001; Ferapontova *et al.*, 2001a, 2002a; Ferapontova, 2004). To summarise: (1) both deglycosylation of HRP and a specific orientation of HRP onto gold through the C- and N-termini of the enzyme enhance the efficiency of DET-based bioelectrocatalytic reduction of H_2O_2 (Ferapontova *et al.*, 2001a, b, 2002a; Ferapontova, 2004); (2) $[\text{H}_3\text{O}^+]$ strongly affects the heterogeneous ET rate, the k_s - $[\text{H}_3\text{O}^+]$ dependence being close to linear under conditions when H_3O^+ can be regarded as a proton donor, and the kinetics of the ET in the system HRP|gold electrode is determined by the ET reaction coupled to the PT reaction (Ferapontova and Gorton, 2001, 2002; Ferapontova and Puganova, 2002; Ferapontova *et al.*, 2002a; Ferapontova, 2004); (3) the oligosaccharide overcoat present in wHRP not only makes DET less efficient but also hinders PT to the active site of the enzyme, since the increase in ET rate with decreasing pH is not the same for different forms of HRP (compare the values of k_s vs. $[\text{H}_3\text{O}^+]$ in Table 2) (Ferapontova and Gorton, 2001, 2002; Ferapontova *et al.*, 2002a). Thus, the efficiency of direct peroxidase bioelectrocatalysis can be crucially enhanced both by the directed

oriented adsorption of rHRPs onto the pre-treated gold surfaces and by the introduction of proton donors in the reaction zone (e.g., by controlling pH).

Modification of electrodes with promoters (Razumas *et al.*, 1983, 1986; Li *et al.*, 1997) or incorporation of HRP in different types of modifying layers on pyrolytic graphite and glassy carbon electrodes, enabled facile DET of HRP seen through the redox chemistry of the $\text{Fe}^{3+/2+}$ couple. Incorporation of HRP in clays (Zhou *et al.*, 2002), polymers (Yu *et al.*, 2003b), and surfactant films (Zhang *et al.*, 2002b), on carbonaceous electrodes resulted in direct reversible $\text{Fe}^{3+/2+}$ electrochemistry of HRP at potentials close to -90 and to $+40$ mV at pH 7.0 and at pH 6.0, respectively. These potentials differ from the value of -180 mV, at pH 6.0, known for the redox chemistry of $\text{Fe}^{3+/2+}$ of the haem of HRP in solution, and even more negative potential values reported for higher pHs (Harbury, 1957). It is worth mentioning that the values of the $E^{0'}$ of the $\text{Fe}^{3+/2+}$ redox couple obtained for HRP in the modifying films (Zhou *et al.*, 2002; Yu *et al.*, 2003b; Zhang *et al.*, 2002b) seem to be closer to the redox potentials of the free haem, specifically, -70 mV (Kassner, 1972), and to the reported $E^{0'}$ of hemin on gold (Lötzbeier *et al.*, 1995; Zimmermann *et al.*, 2000). In most cases of the entrapment of HRP into the modifying layers of polymers and surfactants, the catalysis of molecular oxygen and H_2O_2 reduction was reported at potentials more negative than those of the $\text{Fe}^{3+/2+}$ redox process. Similar transformations at -10 mV, pH 6.0, were displayed by HRP covalently attached onto the ends of vertically oriented single-wall carbon nanotubes (Yu *et al.*, 2003a). Considering the potentials involved, the reported bioelectrocatalysis is evidently based on the $\text{Fe}^{3+/2+}$ peroxidase transformation upon interaction with molecular O_2 accompanied by the formation of E3, but not with the basic catalytic cycle of peroxidases through formation of E1 (Figure 3). Similar $\text{Fe}^{3+/2+}$ haem redox transformations and bioelectrocatalysis of peroxide and di-oxygen reduction were observed with haem-containing catalases and oxygen-binding proteins, myoglobin and haemoglobin entrapped in films of modifiers at electrodes, therewith exhibiting pseudo-enzymatic activity towards O_2 , H_2O_2 , and nitrite reductions (Rusling, 1998).

Catalases (EC 1.11.1.6) constitute haem-containing redox enzymes that act on peroxides drastically increasing the rate of disproportionation of H_2O_2 into H_2O and O_2 . DET between catalase and electrodes have been reported for glassy carbon (Lai and Bergel, 2000, 2002), on didodecyldimethylammonium bromide crystal-modified pyrolytic graphite (Chen *et al.*, 2001), polyelectrolyte encapsulated catalase on gold electrodes (Yu and Caruso, 2003), polyacrylamide hydrogel-modified pyrolytic graphite (Lu *et al.*, 2003), on single-wall carbon nanotube-modified gold electrodes (Wang *et al.*, 2004) and on nano-crystalline diamond film electrodes (Härtl *et al.*, 2004).

Cytochromes P450 are members of a large superfamily of haem-containing enzymes, which catalyse the NAD(P)H-dependent metabolism including epoxidation, hydroxylation, and heteroatom oxidation of a wide range of organic compounds. These enzymes are responsible for bioactivation and are involved in the metabolism of many xenobiotics including pharmaceuticals. The active site contains haem with an axial thiolate of a cysteine residue as fifth ligand to iron. In its resting state the enzyme is in the hexa-coordinate low-spin ferric

form. The general reaction mechanism of these enzymes (Lewis, 1996; Bistolos *et al.*, 2005) includes several steps. After substrate binding, $1e^-$ is transferred from a redox partner to the ferric haem iron, which is reduced to the ferrous state. The reduced haem binds molecular oxygen. The next steps include transfer of a second electron and proton to the ferrous-dioxygen species forming an iron-hydroperoxy intermediate. The peroxy bond is then cleaved to release water and a highly active iron-oxo ferryl intermediate, which finally leads to a single oxygen insertion into the bound substrate, release of products, and regeneration of the ferric form. The two reducing equivalents are naturally donated by NAD(P)H via flavoproteins or ferredoxin-like redox proteins. The coupling of cytochrome P450s to electrodes has been an area of intensive research (see e.g., Fantuzzi *et al.*, 2004; Shumyantseva *et al.*, 2004) and was very recently reviewed (Bistolos, 2005; Wollenberger, 2005).

2.2. Multi-cofactor-containing enzymes

Most of the complex multi-cofactor-containing enzymes are embedded in biological membranes and play important roles in metabolism and respiration of living cells (Nicholls and Ferguson, 2002). The electron-carrying groups in these enzymes are flavins, iron-sulphur clusters, MoCo (João Romão *et al.*, 1997; Kisker *et al.*, 1997b; Enemark *et al.*, 2004), pyrroloquinoline quinone (PQQ) or related structures (Duine, 1991, 2001; Davidson, 2004), haem groups, and copper ions; and many of them contain haem as one of their multiple redox centres. Usually the primary substrate reacts at a redox site different from the haem (e.g., flavin, MoCo, or PQQ) and the electrons are then transferred through an intramolecular electron transfer (IET) to the haem site of the enzyme. One example is cytochrome *c* peroxidase from *Paracoccus denitrificans*, which contains two haems for which it was electrochemically demonstrated that only one of its haems is catalytically active, whereas the other one has only ET properties (Lopes *et al.*, 1998). A similar mechanism was shown for some other complex haem-enzymes described below. The biological ET partners of such enzymes, e.g., cytochrome *c*, react with their haem domain in very rapid ET reactions (Samejima and Eriksson, 1992; Amine *et al.*, 1994; Duine, 1995). The accessibility of the haem domain for interactions with its redox partners can therefore be used to couple this class of enzymes to an appropriately treated/modified electrode, thus providing the basis for construction of DET-based enzyme electrodes (Ikeda, 1997; Gorton *et al.*, 1999; Scheller *et al.*, 2002). In these systems the haem serves as a universal “built in” mediator of IET from the specific catalytic domain to the electrode.

Only in a few cases was efficient direct bioelectrocatalysis with complex enzymes observed at bare, predominantly carbonaceous, electrodes (Ikeda *et al.*, 1988, 1989, 1991, 1992, 1993a, b; Khan *et al.*, 1991; Aizawa, 1991; Ikeda, 1992; Sucheta *et al.*, 1992, 1993; Larsson *et al.*, 1996; Hirst *et al.*, 1996; Ikeda, 1997; Gorton *et al.*, 1999; Larsson *et al.*, 2000; Elliott *et al.*, 2002; Lindgren *et al.*, 2001a; Fujieda *et al.*, 2002; Christenson *et al.*, 2004b). Reagentless non-

mediated amperometric sensors for gluconate, alcohol, and fructose were constructed through the use of their corresponding dehydrogenases immobilised on carbon paste electrodes behind a membrane (Ikeda *et al.*, 1988, 1989, 1991, 1992, 1993a, b; Ikeda, 1992, 1997). Gluconate dehydrogenase (GIDH) from *Pseudomonas fluorescens*, a trifunctional membrane-bound enzyme that catalyses the oxidation of D-gluconate seems to be unique among other multi-cofactor enzymes with respect to DET-properties. GIDH has three different cofactors, a flavin, an iron–sulphur cluster, and haem and its natural electron acceptor is ubiquinone. The substrate conversion was proposed to occur at the flavin site, with the electrons further transferred via the Fe–S cluster to the haem and then further to the electrode. Direct heterogeneous and IET reactions providing bioelectrocatalytic oxidation of D-gluconate were obtained using a variety of electrode materials, e.g., with GIDH-modified glassy carbon and pyrolytic graphite electrodes and with GIDH at gold, silver, platinum, and platinised gold (Ikeda *et al.*, 1988, 1992, 1993b; Ikeda, 1992, 1997). Bioelectrocatalytic oxidations of cellobiose and lactose were achieved with flavo- and haem-containing cellobiose dehydrogenase (Lindgren *et al.*, 2001a; Larsson *et al.*, 1996, 2000; Stoica *et al.*, 2005) and of theophylline with complex-cofactor- and haem-containing theophylline oxidase (Christenson *et al.*, 2004b), correspondingly, adsorbed onto graphite electrodes. These enzymes readily oxidise their substrates in the absence of any mediators, i.e., due to DET between the enzyme and the electrode working as a one-electron acceptor. These cases clearly demonstrate that multi-cofactor enzymes can electronically communicate with the electrodes through their haem domain, which works as a “built in mediator”, transferring electrons from the catalytic domain of the enzymes to an electrode (Aizawa, 1991; Ikeda *et al.*, 1991, 1993a; Ikeda, 1992, 1997).

However, in most cases, electrochemical studies of complex-cofactor-containing – and as a rule of thumb membrane-bound enzymes are impeded at electrodes. Under conditions when the electrode replaces a redox partner of the enzyme, e.g., cytochrome *c*, a very specific molecular interaction between the electrode and the enzyme is then necessary for the enzyme to approach the electrode to achieve efficient ET reactions from the electrode to and through the enzyme. In the absence of surfactants and stabilisers, these enzymes may also dissociate at the electrode surface into separate subunits, which are electrochemically, but not catalytically active, thus obligatorily requiring a hydrophobic reaction environment for their catalytic activities and stabilities. To achieve the required efficient DET function of these complex enzymes for both fundamental studies and possible biotechnological applications, an oriented immobilisation approach at the electrode is used, e.g., by using SAMs of promoters or alkanethiols additionally stabilised by phospholipid- or polyelectrolyte-membrane-like films. To achieve direct bioelectrocatalytic activity towards sulphite oxidation of bacterial MoCo- and haem-containing sulphite dehydrogenase (SDH), the enzyme was co-adsorbed either within a cationic didodecyldimethylammonium bromide surfactant film onto edge-plane pyrolytic graphite (EPPG) electrodes or on positively charged polylysine-modified electrodes (Aguey–Zinsou *et al.*, 2003). Both electrode modifications provided optimal surface media for an SDH function and stabilised this enzyme at

the electrode surface. Flavocytochrome c_3 (fumarate reductase), a flavohaem-enzyme, was bioelectrocatalytically active upon fumarate addition when the enzyme was co-adsorbed with polymyxin at EPPG electrodes (Turner *et al.*, 1999). Similar methodology for enzyme stabilisation and activation with polymyxin at EPPG electrodes was shown to be effective with MoCo- and haem-containing nitrate reductase (Elliott *et al.*, 2004) and MoCo- and Fe-S-cluster-containing membrane-bound *E. coli* dimethyl sulphoxide reductase (Heffron *et al.*, 2001). Bacterial quinohaem methylamine dehydrogenases (MADH) were bioelectrocatalytically active in the presence of cationic promoters such as spermidine or hexa-ammonium salts, on pyrolytic graphite or modified gold electrodes (Burrows *et al.*, 1991). FAD- and haem-containing *p*-cresolmethylhydroxylase from *Pseudomonas putida* has been shown to display (bio)electrocatalytic properties at EPPG electrodes in the presence of aminoglycoside promoters (Guo *et al.*, 1989). The reaction did also proceed at gold electrodes using a negative modifier when a redox-inactive cation acts as the bridging molecule between the negatively charged surface and the negatively charged binding sites of the haem subunit. Recently, DET reactions and direct bioelectrocatalytic activity of the MoCo and Fe-S-cluster-containing aldehyde oxidoreductase from *Desulfovibrio gigas* was shown on carbon (pyrolytic graphite and glassy carbon) and gold electrodes, the last electrode system obligatorily required the presence of a positively charged aminoglycoside (neomycin) acting as a promoter for the ET reaction (Correia dos Santos *et al.*, 2004). The group of Armstrong demonstrated a prominent example of direct electrochemistry and bioelectrocatalytic function of FAD- and Fe-S-cluster-containing succinate dehydrogenase (SDH) (Sucheta *et al.*, 1992; Hirst *et al.*, 1996; Pershad *et al.*, 1999; Armstrong, 2002) and the closely related fumarate reductase (Frd) from *Escherichia coli* (Heering *et al.*, 1997; Sucheta *et al.*, 1993; Leger *et al.*, 2001) at EPPG electrodes in the presence of polymyxin. Protein film voltammetry revealed several intramolecular electron relays operating in the multi-centred Frd. Deconvolution of CVs enabled to assign the resolved non-turnover signals to one two-electron FAD centre and three one-electron [2Fe-2S]-, [4Fe-4S]-, and [3Fe-4S]-relay centres (centres 1, 2 and 3, respectively, Figure 5). Upon addition of their substrates, in the absence of any mediators, both SDH and Frd catalysed interconversion of succinate and fumarate, depending on the applied electrochemical potential.

Modification of the electrodes by terminally functionalised alkanethiols is another approach, which may provide properties of the electrode surface mimicking the surface structure of cytochrome *c* or another biological ET partner of the complex enzymes (Finklea, 1996; Scott and Mauk, 1996; Arnold *et al.*, 1997; El Kasmi *et al.*, 1998; Schlereth, 2005). The design of the alkanethiol head groups with functional groups of different charge and polarity enables oriented immobilisation of the enzymes through non-covalent coupling between the SAMs and the haem domains of the enzymes via electrostatic, hydrophobic, and hydrophilic interactions. Macromolecular interactions between the corresponding domains of the complex enzymes and the modified electrode surface then provide an orientation of the enzyme favourable both for its DET reactions and efficient bioelectrocatalytic function (Elliott *et al.*, 2002; Kinnear

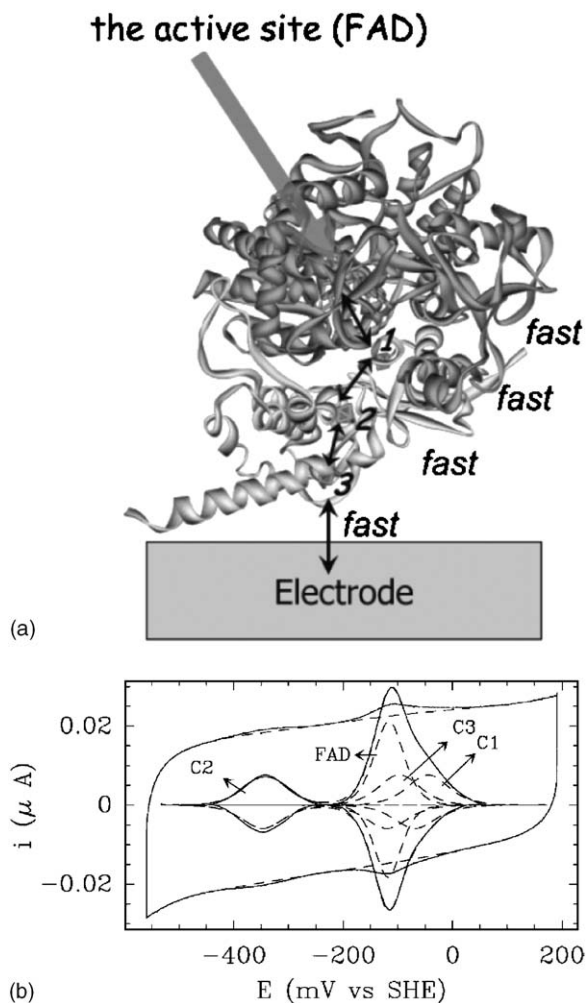


Fig. 5. (a) Schematic representation of the iron-sulphur cluster electron relays between the FAD-catalytic centre and the electrode in multi-centred fumarate reductase from *E. coli* and (b) all these electron centres detected in the non-turnover voltammogram, scan rate 20 mV s^{-1} , pH 8, the surface coverage is 6 pmol cm^{-2} . Reproduced from Leger *et al.* (2003) with permission from the American Chemical Society.

and Monbouquette, 1993; Schuhmann *et al.*, 2000; Ferapontova *et al.*, 2003, 2004; Ferapontova and Gorton, 2005; Larsson *et al.*, 2001; Lindgren *et al.*, 2001a; Christenson *et al.*, 2004a). These complex enzyme systems studied until today demonstrated the necessity for a thorough design of the electrode surface for interactions with complex redox enzymes and enzyme complexes, so that the electrochemically active domain of the enzymes will be properly oriented at the electrode surface for facile DET and at the same time provide the other domains to productively interact among each other for the inter-domain

ET to proceed efficiently as well as allowing the substrate to freely reach and interact with the catalytic domain (Ferapontova *et al.*, 2003; Stoica *et al.*, 2005).

2.2.1. Cellobiose dehydrogenase

One interesting example of an “orientated” DET-reaction approach is that between alkanethiol-modified electrodes and cellobiose dehydrogenase (CDH) (Gorton *et al.*, 1999; Lindgren *et al.*, 2000a, 2001a; Larsson *et al.*, 2001; Christenson *et al.*, 2004a; Stoica *et al.*, 2005). CDH is the only extracellular flavo-hemo enzyme known today and comprises two prosthetic groups, a flavin (FAD) and a haem (cytochrome *b* type) located in two separate domains, connected by a flexible linker region, which can be cleaved by proteases (Hallberg *et al.*, 2000; Hällberg, 2002; Zamocky *et al.*, 2004). CDH is produced by a variety of fungi, preferably by white rot fungi and is believed to be active for the initiation, support and participation in degradation of both cellulose and lignin, however, its true function remains unknown. The most well-studied CDH is the enzyme from *Phanerochaete chrysosporium*, for which the amino acid sequence as well as the structures of the individual flavo- and haem domains are known (Wood and Wood, 1992; Hällberg *et al.*, 2000; Hällberg, 2002). There is a 24-amino acid-linker region with a distance of less than 15 Å connecting the two domains in *P. chrysosporium* CDH, which allows fast intramolecular ET to occur. CDH catalyses the oxidation of cellobiose (the preferred substrate) (Henriksson *et al.*, 1998; Baminger *et al.*, 2001) and related oligosaccharides (Kremer and Wood, 1992) by a variety of electron acceptors such as quinones, metal-ion complexes, redox dyes, and organic radical species, cytochrome *c*, and to a lesser extent oxygen (Ayers *et al.*, 1978; Ander, 1994; Roy *et al.*, 1996; Henriksson *et al.*, 1998; Igarashi *et al.*, 1999). It was shown that sugar oxidation and the subsequent reduction of two-electron proton acceptors, such as benzoquinones, occur at the FAD domain, whereas one-electron (not proton) acceptors, such as cytochrome *c* or ferricyanide, are believed to need the haem domain to mediate ET from FAD. However, the role of the haem domain and how electrons are transferred from the reduced enzyme is debated (Cameron and Aust, 2000, 2001; Henriksson *et al.*, 2000; Mason *et al.*, 2002, 2003).

Our group has initiated bioelectrochemical studies of CDH and currently performs studies of electrode reactions of CDHs from different origins (Gorton *et al.*, 1999; Fridman *et al.*, 2000; Larsson *et al.*, 1996, 2000, 2001; Lindgren *et al.*, 2000a, 2001a; Christenson *et al.*, 2004a; Stoica *et al.*, 2005). As mentioned above, when CDH is adsorbed on graphite electrodes it readily oxidises cellobiose (or lactose) in the absence of any mediators (Larsson *et al.*, 1996, 2000; Lindgren *et al.*, 2001a; Stoica *et al.*, 2005). The direct electrochemistry of CDH, i.e., in the absence of a substrate, demonstrated redox activity of the haem domain between 140 and 180 mV depending on the pH (Larsson *et al.*, 2000). There was no response to cellobiose when the isolated FAD domain (obtained from papain cleavage of the linker region of CDH) was adsorbed onto graphite (Larsson *et al.*, 1996). However, the presence of a one-electron no-proton acceptor working as a mediator recovered a catalytic response to

cellobiose thus providing the full catalytic activity of the isolated FAD-domain of CDH (Larsson *et al.*, 1996). Additionally, this means that also one-electron acceptors can efficiently pick up the charge from the reduced FAD-domain of CDH. Thus, for intact native CDH the electrode communicated with the haem domain and after substrate oxidation (in the absence of any external mediators) electrons flow from the catalytic FAD-domain to the haem through internal ET and further to the electrode. The rate of the internal electron transfer is much dependent on pH and above pH 5–6 the catalytic was inhibited as a result of impeded intramolecular ET (Lindgren *et al.*, 2000a; Stoica *et al.*, 2004, 2005). Furthermore, CDH suffers from substrate (cellobiose) inhibition and this effect by cellobiose becomes more important as the pH is increased from 4.5 to 6.5 (Igarashi *et al.*, 2002; Stoica *et al.*, 2004). Spectroelectrochemistry of CDH in an aldrithiol-modified gold capillary electrode (Larsson *et al.*, 2001) and electrochemistry of CDH on alkanethiol-modified gold electrodes confirmed the role of the haem domain of intact CDH as the primary site of the electronic contact with the modified gold electrodes (Lindgren *et al.*, 2000a; Larsson *et al.*, 2001; Gorton *et al.*, 1999; Christenson *et al.*, 2004a; Stoica *et al.*, 2005). Direct electrochemistry of the haem domain of CDH was achieved when CDH was entrapped between the alkanethiol-modified gold electrode surface and a permselective dialysis membrane (Haladjian *et al.*, 1994) in the absence of any substrate (Gorton *et al.*, 1999; Lindgren *et al.*, 2000a, 2001a, Christenson *et al.*, 2004a, Stoica *et al.*, 2005) (Figure 6). Gold electrodes modified with SAMs of either positively or negatively charged alkanethiols enabled orientation of CDH minimising the distance between the electrode and the haem domain of CDH thus providing pronounced direct electrochemistry of the haem domain active site. Upon addition of cellobiose a pH-dependent catalytic current was observed (Lindgren *et al.*, 2000a; Stoica *et al.*, 2005). At high pH catalysis was inhibited as a result of that the internal ET of CDH turned off at high pH (Samejima and Eriksson, 1992; Hyde and Wood, 1996). Both the positively charged cystamine SAMs and negatively charged 3-mercaptopropionic acid SAMs at moderate pH values enabled DET between the modified electrodes and CDH (Lindgren *et al.*, 2000a). The presence of both primarily negatively and positively charged amino acid residues on the surface of the haem domain (Hallberg *et al.*, 2000) provided this “dual” affinity of the haem domain for the two oppositely charged modifiers, however, with a higher affinity for the positively charged SAM. CDHs of soft-rot origin also demonstrated DET activity on graphite and alkanethiol-modified gold electrodes (Christenson *et al.*, 2004a; Lindgren *et al.*, 2001a). Different pH optima for CDHs from *Humicola insolens*, *Sclerotium rolfsii* pre-conditioned different pH-optima for direct bioelectrocatalytic activity of these enzymes on graphite electrodes, at pH 3.5 for *Sclerotium rolfsii* CDH and at pH 7 for *Humicola insolens* CDH (Christenson *et al.*, 2004a; Lindgren *et al.*, 2001a). On gold electrodes, direct electrochemistry of the haem (but not direct bioelectrocatalysis) was achieved only with *Humicola insolens* CDH on gold modified with SAMs of 11-mercaptoundecanoic acid, but not with short-length alkanethiols.

Two recently isolated and characterised new CDHs from white-rot fungi, viz. *Trametes villosa* and *Phanerochaete sordida* (Ludwig *et al.*, 2004) were elect-

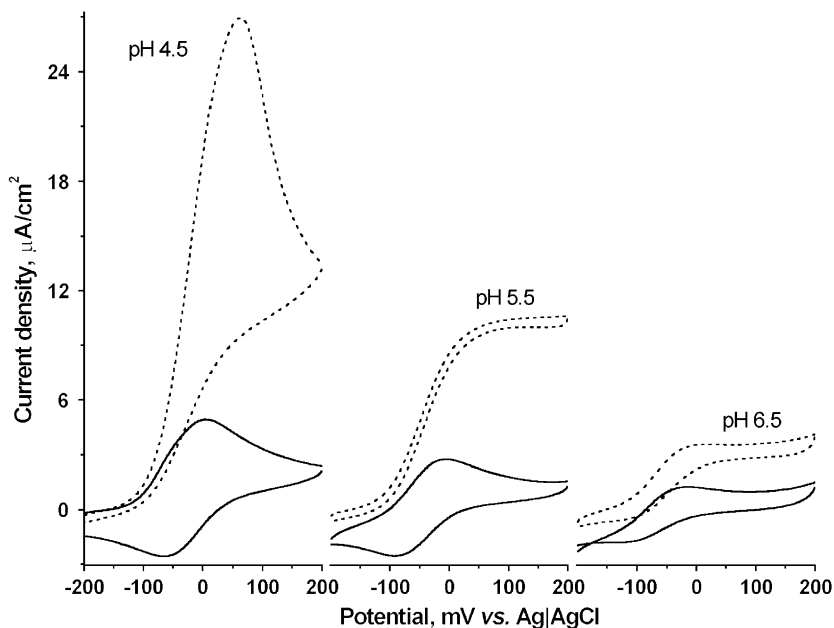


Fig. 6. Cyclic voltammetry of *Phanerochaete sordida*-CDH in the presence (dashed line) and in the absence (solid line) of 1 mM cellobiose, registered at a monothioglycerol SAM-modified permselective membrane Au electrode. Experimental conditions: scan rate 10 mV s^{-1} , $20 \text{ mM Na}_2\text{PO}_4\text{-citrate}$, pH 4.5.

rochemically investigated on SAM-modified Au electrodes using ten different types of thiols. The effect of the length of the alkyl chain, of a positive/negative charge or of hydrophobic/hydrophilic properties of the head functional group was recently investigated (Stoica *et al.*, 2005). Both CDHs showed remarkable and efficient DET characteristics between the haem domain of the CDH and the modified Au electrode, both in presence and in absence of cellobiose (Figure 6). It was proven that thiols with alcohol end-groups (hydrophilic/non-charged functional groups) orient the molecule of these enzymes in an optimum position in order to obtain the most favourable electronic communication with the electrode. For mercaptoundecanol-modified Au electrode, *Trametes villosa*-CDH showed a preserved full functional stability over an extended pH range (4.0–6.5). It is expected that the catalytic current should have a maximum between pH 4.0 and 5.0 if the enzyme, when interacting with the SAM-Au electrode surface, would retain its solution properties (Ludwig *et al.*, 2004). In the case of electrodes modified with MUD-OH there might be substantial interactions between both two domains of the enzyme with the SAM-Au electrode. The mechanism of IET is not really known (Henriksson *et al.*, 2000), but its pH dependence could be affected by a variation of the electrostatic interactions between the two domains with pH, and as a result, changing of the inter-domains distance. Implicitly, it would result in the decrease of the inter-domains ET rate. The preserved bioelectrocatalytic properties over an extended

pH range could be explained by a fixed distance the two domains that are hooked on the electrode surface and are not able to change the position with regard to each other despite a change in pH, and thus allowing a constant efficiency of the IET.

2.2.2. Sulphite oxidase

The electrochemistry of MoCo- and haem-containing sulphite oxidase (SOx) (Hille, 1996) is another example demonstrating the role of the electrode micro-environment both for DET and a direct bioelectrocatalytic function of the enzyme. SOx catalyses a $2e^-$ oxidation of sulphite to sulphate, the terminal reaction in the metabolism of the sulphur-containing amino acids cysteine and methionine, with cytochrome *c* as its physiological electron acceptor. Somehow similar to CDH, in SOx a molybdenum complex cofactor (MoCo) is connected to a haem-containing domain (a cytochrome b_5 type, cyt b_5) by a flexible polypeptide chain region (Kisker *et al.*, 1997a). Oxidation of sulphite to sulphate occurs at the Mo centre with concomitant reduction of Mo(VI) to Mo(IV). The reducing equivalents are then passed on from the Mo domain to the cyt b_5 domain of SOx and from there to cytochrome *c*. The SOx catalytic cycle and the intramolecular ET are largely affected by the composition, ionic strength, viscosity, and pH of the contacting solution (Pacheco *et al.*, 1999; Sullivan *et al.*, 1993). Additionally, the long ET distance between the Mo and the haem Fe, 32 Å, and the orientation of the molybdopterin ring system away from the second cofactor imply that the cyt b_5 domain should adopt a proper conformation for ET to occur, with a reduced metal-to-metal distance providing an efficient ET pathway (Kisker *et al.*, 1997a; Pacheco *et al.*, 1999; Feng *et al.*, 2002). The direct electrochemistry of SOx at pyrolytic graphite resulted in a bioelectrocatalytic activity of SOx more than 25 times lower than that in homogeneous catalysis with cytochrome *c* (Elliott *et al.*, 2002). Compatibility between the electrode and the enzyme surfaces was improved by using SAMs of (-OH)- and mixed (-OH/-NH₂)-terminated alkanethiols of neutral to slightly positive charge to mimic a cytochrome *c* surface (Ferapontova *et al.*, 2003). A biomembrane-like microenvironment provided by the SAM surface appeared to be suitable for immobilisation of SOx retaining its natural functions, including selective sensing of specific substrates. SOx interacted with (-OH)- and mixed (-OH/-NH₂)-terminated alkanethiol-modified gold electrodes through its haem domain, exhibiting quasi-reversible CVs with a midpoint potential of 80 mV, at pH 7.4, and with a heterogeneous ET constant of 15 s^{-1} . The efficiency of the bioelectrocatalytic $2e^-$ oxidation of sulphite catalysed by SOx in DET exchange with the electrode depended on the nature of the alkanethiol layer; i.e., the chain length and the effective charge/hydrophilicity of the SAM. Adsorption of SOx on an 11-mercapto-1-undecanol (MuD-OH) SAM, i.e., terminally functionalised with (-OH)-groups, provided efficient catalytic oxidation of sulphite, contrary to non-functionalised alkanethiols, e.g., 1-decanethiol, or (-NH₂)-terminated alkanethiol layers. Comparative studies with short-chain alkanethiols, e.g., cysteamine and 2-mercaptoethanol, revealed an evidently

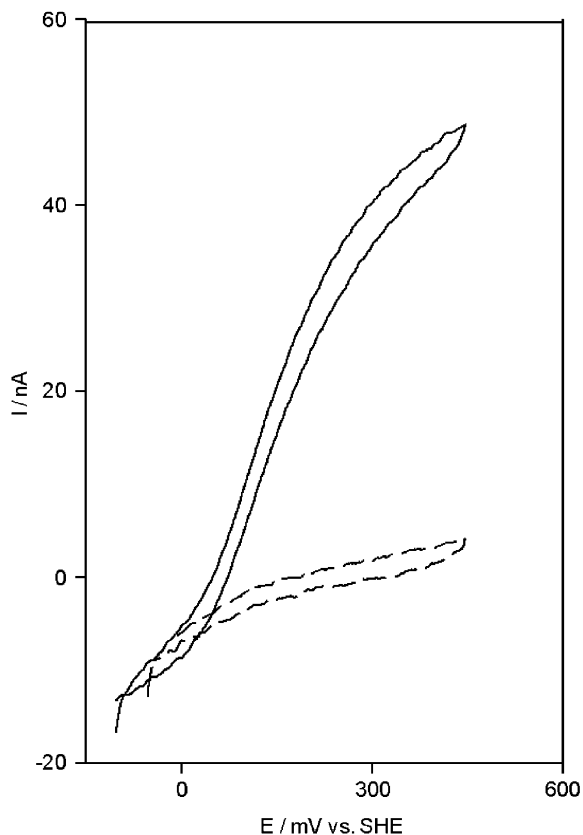


Fig. 7. Non-catalytic (dotted) and catalytic (solid line) cyclic voltammograms of SO_x adsorbed at a mixed (11-mercapto-1-undecanol/11-mercapto-1-undecanamine) SAM-modified Au electrode in 0.1 M Tris-HCl, pH 7.4; scan rate 2 mV s⁻¹. Catalysis was observed in the presence of 3.3 mM Na₂SO₃.

different mode of interaction of SO_x on these layers, onto which SO_x was not catalytically active due to conformationally impeded internal ET. Co-adsorption of MuD-OH and 11-mercapto-1-undecanamine to form a mixed SAM improved the surface properties of the SAM resulting in a higher surface coverage with bioelectrocatalytically active SO_x, but not in an increased apparent catalytic rate constant, k_{cat} , ranging in the order of 18–24 s⁻¹ at pH 7.4 (Figure 7). The achieved efficiency of DET-based SO_x bioelectrocatalysis between the enzyme and the modified electrode approached the rates characteristic for the catalysis mediated by cytochrome *c*, the natural redox partner of SO_x, revealing full retained biological function of SO_x when interacting with the SAM-modified electrode.

2.2.3. Fructose dehydrogenase

A similar rational approach of electrode modification with functionalised alkanethiols, for DET-orientation of enzymes, was shown to be efficient also with other complex membrane enzymes, such as PQQ- and haem-containing alcohol (Toyama *et al.*, 2004) and fructose dehydrogenase (Schuhmann *et al.*, 2000; Ferapontova and Gorton, 2005) and complex-cofactor-haem theophylline oxidase (Christenson *et al.*, 2004b; Ferapontova and Gorton, 2005). Pyrroloquinoline quinone (PQQ) containing enzymes belong to the group of quinoproteins discovered relatively recently (Davidson and Jones, 1991; Davidson, 1993, 2004; Duine, 1991; Duine *et al.*, 1987). Most of them are referred to as dehydrogenases; some of them have an additional cofactor located in a different subunit of the protein, in a number of cases it is a haem. Direct bioelectrocatalytic oxidation of their substrates was shown for quinohaem enzymes such as D-fructose dehydrogenase and alcohol dehydrogenase on different carbon electrodes (Ikeda *et al.*, 1989, 1991, 1992, 1993a; Ikeda, 1992, 1997; Gorton *et al.*, 1992; Parellada *et al.*, 1996), and also on bare and modified gold, silver, and platinum electrodes (Khan *et al.*, 1991; Ikeda, 1997; Yabuki and Mizutani, 1997; Schuhmann *et al.*, 2000; Ferapontova and Gorton, 2005). The membrane-bound quinohaem-alcohol dehydrogenase (ADH) comprises a PQQ catalytic domain and several *c*-type haems, one of which relays electrons from the PQQ cofactor, where a two-electron oxidation of ethanol (or some other alcohols) occurs, to the others located in the vicinity of the outer protein shell (Toyama *et al.*, 2004). Direct bioelectrocatalytic oxidation of ethanol by ADH was shown on a variety of electrode materials, e.g., carbon and carbon paste, pyrolytic graphite and glassy carbon, gold, silver, and platinum (Ikeda *et al.*, 1993a; Ikeda, 1997; Ramanavicius *et al.*, 1999; Schuhmann *et al.*, 2000; Schuhmann, 2002; Razumiene *et al.*, 2002). This indicates that ADH adsorbs preferentially through its haem domain on the electrodes (Ikeda *et al.*, 1993a; Schuhmann *et al.*, 2000), with a most pronounced direct electrochemistry and bioelectrocatalytic activity on a naked gold surface and on a negatively charged 3,3'-carboxypropionic disulphide SAM on gold, providing enzyme orientation with its haem exposed to the electrode. Bioelectrocatalytic activity of ADH at the electrodes needed co-adsorption of ADH with surfactants (1% Tween) to stabilise the enzyme by providing a membrane-mimicking environment and an enzyme orientation with the more hydrophobic side directed towards the hydrophobic electrode surface (Schuhmann *et al.*, 2000). A similar condition was necessary to provide DET between another membrane PQQ-enzyme, fructose dehydrogenase (FDH) and gold electrodes (Ferapontova and Gorton, 2005). FDH is able to selectively oxidise D-fructose to 5-keto-D-fructose, which is accompanied by the reduction of its PQQ-cofactor to PQQH₂ (Yamada, 1967; Ameyama *et al.*, 1981), which in turn can deliver its charge to the single haem through one-electron-transfer steps. The natural electron acceptors of FDH are believed to be membrane-bound ubiquinones (Anthony, 1988). FDH communicates directly with bare carbon, gold, and platinum electrodes (Ikeda *et al.*, 1991; Khan *et al.*, 1991; Ikeda, 1997). The unmediated bioelectrocatalysis of fructose oxidation by FDH on carbon paste electrodes enabled fructose deter-

mination in fruit juices within a concentration range of 0.2–20 mM, however, no direct electrochemistry of the haem or the PQQ domain of FDH could be followed in the absence of the substrate (Ikeda, 1997). DET reactions of FDH adsorbed under potentiostatic control (0.5 V) on bare Pt and Au were correlated with the redox activity of its PQQ-cofactor (the reported E^0 values of FDH were 280 mV at pH 4.5) (Khan *et al.*, 1991). Electrostatic binding of the enzyme to positively charged cysteamine SAM-modified gold electrodes exhibited direct electrochemistry of the haem centre of FDH at 68 and 110 mV, at pH 5 and 4, respectively, and upon addition of fructose direct bioelectrocatalytic oxidation of fructose (Ferapontova and Gorton, 2005). From the observations that bioelectrocatalysis was shown both through DET as well as through mediation by cytochrome *c*, a possibility of both a catalytic activity of the PQQ domain independent of haem and a catalytic function of the two active centres working “in concert” provided by the internal ET reaction can be implied. (Ferapontova and Gorton, 2005).

2.2.4. Theophylline oxidase

Theophylline oxidase (ThOx) is another complex redox metalloenzyme, which demonstrated pronounced direct electrochemistry on properly chosen alkanethiol SAMs (Christenson *et al.*, 2004b; Ferapontova and Gorton, 2005). ThOx is involved in the metabolic transformation of theophylline, one of the most commonly used drugs for treatment of the symptoms of chronic asthma (Rowe *et al.*, 1988). The catalytic mechanism of ThOx involves oxidation of theophylline acting as an electron-donating substrate, by ThOx to form 1,3-dimethyluric acid. The reduced enzyme can then in turn be re-oxidised by its natural redox partner cytochrome *c* or with other electron acceptors, such as ferricyanide, completing the biocatalytic cycle (Gupta *et al.*, 1988; de Castro *et al.*, 1989). There are still no data available on the exact number and nature of domains present in ThOx, except that the absorption features of haem dominate in the UV/vis spectrum of ThOx (de Castro *et al.*, 1989; Christenson *et al.*, 2004b; Ferapontova and Gorton, 2005). Direct electrochemical titration of microbial ThOx in an aldrithiol-modified gold capillary electrode enabled determination of the haem domain as being in DET contact with the modified gold electrode (Christenson *et al.*, 2004b). DET-based bioelectrocatalytic activity of ThOx on graphite enabled direct determination of theophylline within the millimolar concentration range, however independent evidence for DET communication between the haem domain of ThOx and graphite (in the absence of theophylline) was not obtained (Christenson *et al.*, 2004b). Direct electrochemistry of ThOx achieved on various alkanethiol-modified gold electrodes (Ferapontova and Gorton, 2005) strongly depended on the nature of the alkanethiol head groups, being pronounced only on mixed mercaptoethanol/cysteamine (and of a longer alkane chain) SAMs at 99 mV at pH 7.0 (Figure 8), but not on those electrodes modified with only mercaptoethanol or cysteamine. On both (-OH)- and mixed (-OH)/(-NH₂)-substituted SAMs, upon addition of theophylline, ThOx was bioelectrocatalytically active catalysing the oxidation of theophylline through a DET reaction with the electrode. A slightly polar/pos-

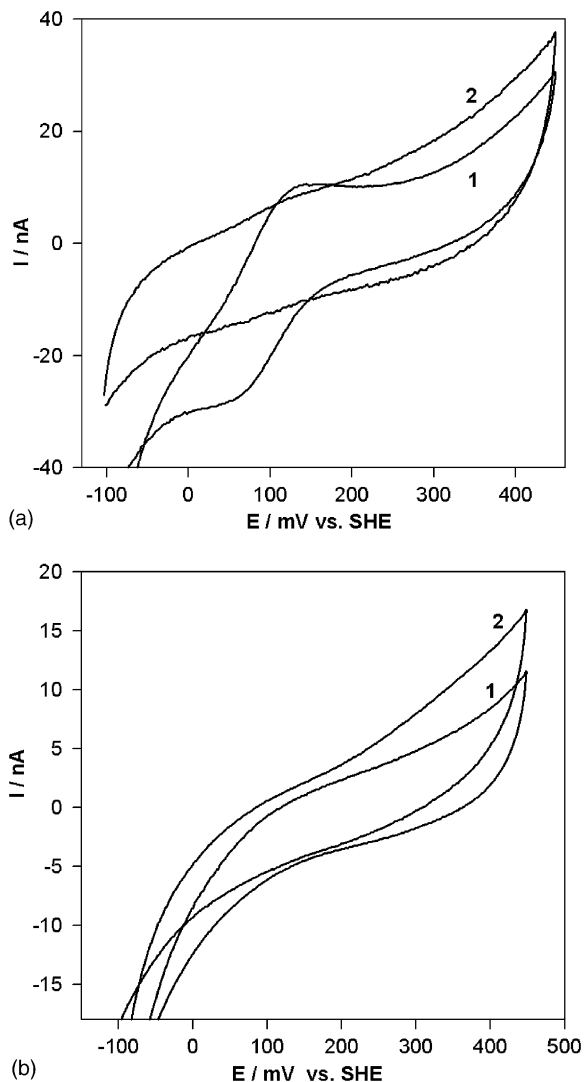


Fig. 8. Cyclic voltammograms of ThOx adsorbed at a gold electrode modified with mixed alkanethiol SAMs of (a) (2-mercaptoethanol/cysteamine) and (b) (6-mercapto-1-hexanol/6-amino-1-hexanethiol), alkanethiol molar ratio 3:1, (1) in the absence and (2) in the presence of 3 mM theophylline, scan rate v is 10 mV s^{-1} .

itive character of the electrode surface, obtained by using (-OH)- or mixed (-OH)/(-NH₂)-terminated alkanethiols, supposedly mimicked the surface of its docking site with cytochrome *c*, thus providing adsorption/orientation of ThOx through the haem domain. This orientation was favourable for DET between ThOx and the modified gold electrodes, similar to the results obtained previously with another haem-containing complex enzyme, SOx (Ferapontova *et al.*, 2003).

3. COPPER REDOX PROTEINS AND ENZYMES

Copper is an essential trace element in living systems, present in the parts per million-concentration range. It is a key cofactor in a diverse array of biological oxidation–reduction reactions and oxygen transport (Lewis and Tolman, 2004). A very notable feature of the copper proteins is that they function almost exclusively in the metabolism of O₂ or NO_x compounds and are frequently associated with oxidising organic/inorganic radicals including amino acid side-chain radicals. Cu³⁺ is not a biologically relevant oxidation state, because the formal redox potential (E^0) for the Cu³⁺/Cu²⁺ redox couple is generally very high. Cu²⁺ centres tend to adopt a six-coordinate tetragonal (distorted octahedral) geometry or five-coordinate (square pyramidal or trigonal bipyrimidal) geometry (Rorabacher, 2004), whereas for Cu⁺ centres trigonal coordination is typical (Mirica *et al.*, 2004). The relatively open trigonal coordination of Cu⁺ no doubt contributes to the exceptional O₂ reactivity of the reduced copper ion involving fast inner-sphere reduction of oxygen. The E^0 of the Cu²⁺/Cu⁺ redox couple can be modulated by ligand type and coordination geometry (up to 500 mV) and by the extended amino acid environment (up to 500 mV) compared to the E^0 -value of the Cu²⁺/Cu⁺ redox couple in water (150 mV) (Solomon *et al.*, 2004).

The copper sites in the redox proteins have historically been divided into three classes based on their spectroscopic features, which reflect the geometric and electronic structure of the active site: type 1 (T1) or blue copper, type 2 (T2) or normal copper, and type 3 (T3) or coupled binuclear copper centres (Malkin and Malmström, 1970; Reinhammar, 1984; Solomon *et al.*, 1992; Kaim and Rall, 1996) (Table 4). Over the last 20 years, this list has expanded to include the trinuclear copper clusters (composed of one type 2 and one type 3 centre) (Table 4) (Allendorf *et al.*, 1985; Messerschmidt *et al.*, 1992), the mixed-valent binuclear Cu_A centre of cytochrome *c* oxidase (COx) and nitrous oxide reductase (N₂OR) (Iwata *et al.*, 1995; Agostinelli *et al.*, 1995; Tsukihara *et al.*, 1995; Messerschmidt *et al.*, 2001), the Cu_B centre of cytochrome *c* oxidase (COx and ubiquinone oxidase) (Malmström, 1990; Kaim and Rall, 1996), and the binuclear Cu_Z centre of N₂OR (Farrar *et al.*, 1991; Oganessian *et al.*, 2004).

The type 1 or blue copper centres exhibit an extremely intense absorption band, with a molecular absorption coefficient, ϵ , of between 3500 and 6000 M⁻¹ cm⁻¹ at ~600 nm, which is responsible for the deep blue colour. This band is assigned as a cysteine sulphur to copper ligand-to-metal charge transfer (LMCT) transition (e.g., see Solomon *et al.*, 1996). Type 1 centres also exhibit a very small Cu parallel hyperfine splitting in their EPR spectra due to the high covalency at the copper site (the unpaired electron is strongly delocalised onto the cysteine ligand, thus decreasing its interaction with the nuclear spin on the copper). These sites are found in mononuclear copper proteins involved in intermolecular electron transfer pathways (azurins, plastocyanins, stellacyanins, amicyanin, and rusticyanin) (Kaim and Rall, 1996; Messerschmidt *et al.*, 2001), and the multi-copper enzymes (ascorbate

Table 4. Important properties of copper centres in various proteins

	Type 1	Type 2	Type 3	T2/T3 cluster
Aggregation state Specificity, function	Mononuclear Electron transfer	Mononuclear Catalysis and redox reactivity	Binuclear O ₂ activation for transport and oxygenation	Trinuclear O ₂ activation for oxidase function
Examples	Small “blue” copper proteins plus multi- copper oxidases	Amine oxidases, cytochrome <i>c</i> oxidase, galactose oxidase, superoxide dismutase	haemocyanin, tyrosinase	Multi-copper oxidases (AO, BOD, Cp, Lc)
Typical coordination number	Cu ²⁺ : 3 (trigonal- planar)	Cu ²⁺ : 4 or 5 (square- planar or pyramidal)	Cu ⁺ : 3 (trigonal- planar)	Cu ⁺ : 3 (trigonal)
Coordinated atoms	S (Cys), 2 N (His), S (Met) or (Leu, Phe) ^a	3 N (His) ^a	2 × 3 N (His); Cu ²⁺ : μ - η^2 : η^2 -O ₂ ²⁻	Cu ²⁺ : 4 N (His); partly (O)OH ⁻
EPR	Small ⁶³ Cu/ ⁶⁵ Cu hyperfine splitting (A _{II}), low g _{II} factor,	“Normal” Cu ²⁺ EPR parameters,	No signal (strong anti- parallel spin–spin coupling),	“Normal” Cu ²⁺ EPR parameters,
Light absorption	Intense absorption in the visible, LMCT (Cys → Cu ²⁺)	Not intense absorption, only “forbidden” ligand field interactions	Intense absorption; LMCT (O ₂ ²⁻ → Cu ²⁺)	Intense absorption; LMCT (O ₂ ²⁻ → Cu ²⁺)

^aFree coordination site, special ligand (organic radical) or other metal centres. (According to [Kaim and Rall \(1996\)](#) with some changes and additions.)

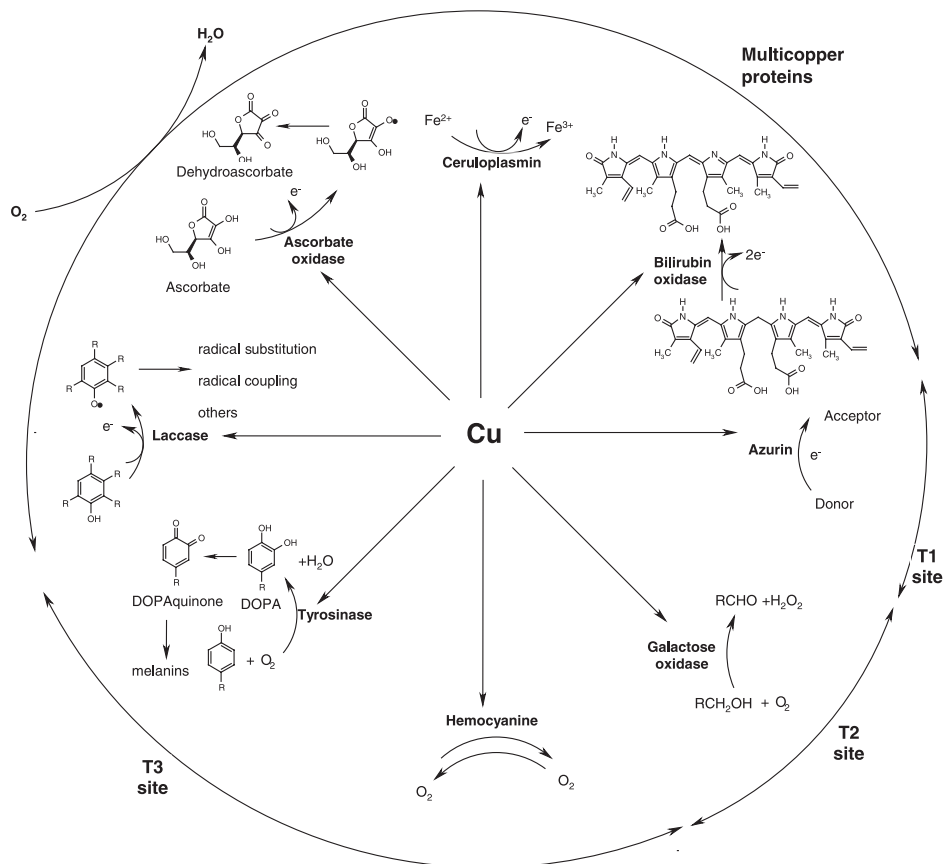


Fig. 9. Essential metabolic functions of copper-containing proteins (mostly enzymes). (According to Kaim and Rall (1996) with some additions and changes.) Reproduced from Shleev *et al.* (2005c) with permission from Elsevier.

oxidase (AO), bilirubin oxidase (BOD), Laccase (Lc), ceruloplasmin (Cp), and nitrite reductase), where they function in intra-molecular electron transfer (Solomon *et al.*, 1996; Kaim and Rall, 1996; Messerschmidt *et al.*, 2001) (Table 4).

The type 2 or normal copper centres in proteins exhibit EPR signals similar to those of tetragonal Cu(II) complexes and are often characterised by relatively weak absorption spectra, associated with ligand field transitions (Solomon *et al.*, 1996; Kaim and Rall, 1996; Messerschmidt *et al.*, 2001). Type 2 sites are present in all “blue” multi-copper oxidases, such as AO, BOD, Lc, and Cp, as well as in galactose oxidase (GalOD), prokaryotic and eukaryotic copper amine oxidases, copper-containing superoxide dismutase, and nitrite reductase (Messerschmidt *et al.*, 2001) (Table 4).

The T3 copper centre contains two ligand-bridged copper ions and is called the binuclear site. T3 sites are diamagnetic and display a distinctive absorption

band near 330 nm and a characteristic fluorescence spectrum (Wynn *et al.*, 1983; Shin and Lee, 2000; Shleev *et al.*, 2004b; Solomon *et al.*, 1996). This site is present in all blue multi-copper oxidases as well as in catechol oxidase (tyrosinase, Tyr) and hemocyanins (Hc). Together with the T2 site the T3 site forms the trinuclear copper cluster (the T2/T3 cluster) (Table 4).

All copper-containing proteins described in the chapter are divided into four groups according to the structure of their active sites, viz. type-1 copper proteins, type-2 copper enzymes, type-3 copper proteins, and “blue” multi-copper oxidases (Figure 9).

3.1. T1 copper redox protein – azurin

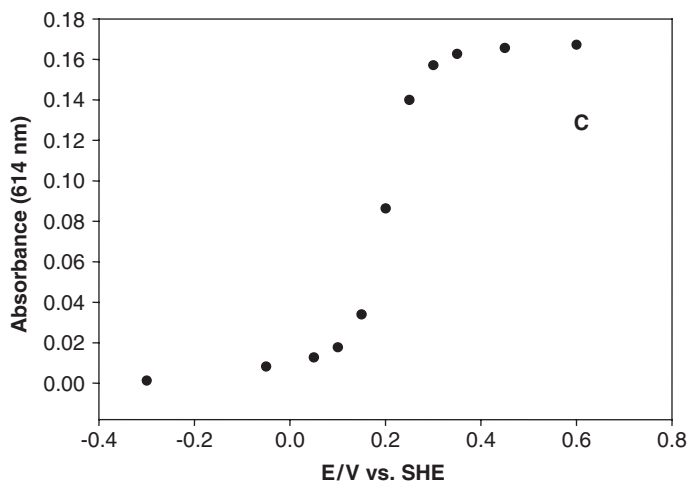
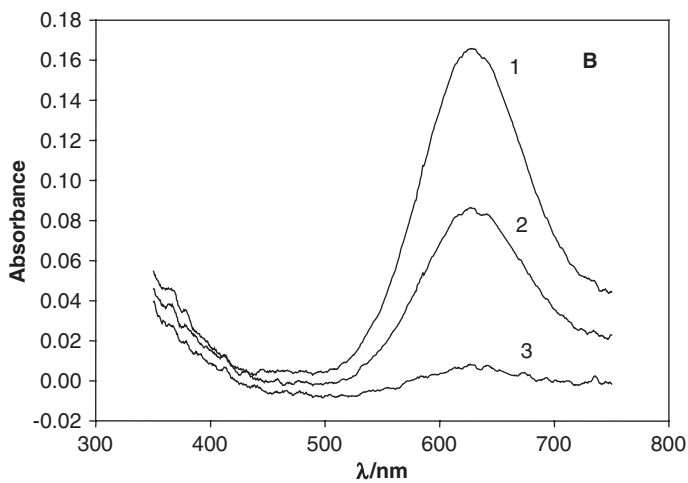
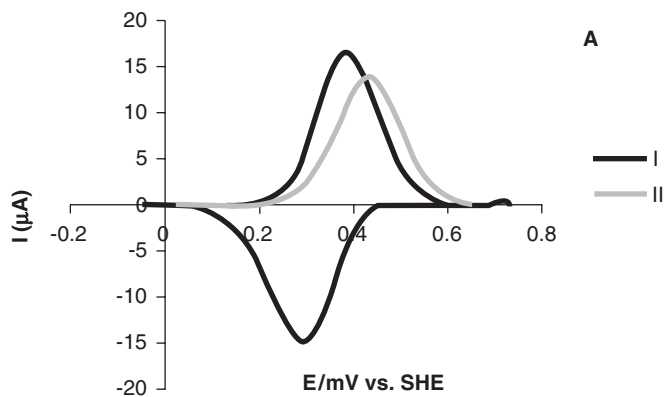
Azurin is a small bacterial protein (9–14 kDa) and is one of the simplest redox proteins that contains a mononuclear copper of the T1 type (Solomon *et al.*, 1992; Jeuken *et al.*, 2000). The copper is coordinated by cysteine, two histidines, and an axial methionine (Nar *et al.*, 1991; Adman *et al.*, 1978; Baker, 1988) (Table 4). The redox potentials of azurins from different sources were estimated and found to be in the range from 270 to 420 mV (Solomon *et al.*, 1992; Zhang *et al.*, 2002a; Pinho *et al.*, 2004). Azurin is relatively stable and it can be expressed in high yield in a heterologous system (*E. coli*) making it an ideal candidate for protein engineering studies and biosensor development (Gilardi *et al.*, 1994). This protein has a role as a natural electron transfer carrier in the bacterial anaerobic respiratory chain and is able to transfer electrons from cytochrome *c*551 to nitrate reductase.

A number of publications describing DET of azurin on different electrodes have been published (e.g., Armstrong *et al.*, 1984, 2004; Sakurai *et al.*, 1996; Jeuken *et al.*, 2002; Zhang *et al.*, 2002a; Lisdat and Karube, 2002; Zhang *et al.*, 2005). Well-resolved CVs and SWVs (Figure 10A) were obtained with the mid-point potential (E_m , taken as the average of the anodic and cathodic peak potentials) of the CVs and the peak potentials of the SWVs close to the redox potential of the T1 site of the protein (determined through potentiometric titration). This allows even a facile determination of the redox potential of azurin ($E^{0'}$ values are close to 300 mV), as well as other small “blue” redox proteins,

Fig. 10. (A) Cyclic voltammograms of *Pseudomonas aeruginosa* azurin adsorbed at gold-SAM electrodes prepared using two different procedures – I and II (scan rate: 100 mV s⁻¹; 0.02 M NaOAc, 0.1 M Na₂SO₄; pH 4.0) (See explanation in detail in Armstrong *et al.*, 2004.) Reproduced from Armstrong *et al.* (2004) with permission from The Royal Society of Chemistry.

(B) Spectroelectrochemical redox titration of *Pseudomonas aeruginosa* azurin in a capillary gold electrode (0.1 M phosphate buffer, pH 7.0). The spectra reflect (1) fully oxidised protein, (2) partly reduced azurin, and (3) fully reduced azurin. Reproduced from Shleev *et al.* (2005c) with permission from Elsevier.

(C) Spectroelectrochemical titration curves reflecting the dependence of the absorbance of the azurin solution at 614 nm vs. the applied potential. Reproduced from Shleev *et al.* (2005c) with permission from Elsevier.



such as pseudoazurin, umecyanin, plantacyanin, and plastocyanin (e.g., [Jeuken *et al.*, 2002](#); [Sakurai *et al.*, 1996](#)).

A spectroelectrochemical redox titration was performed on azurin in solution, where *Pseudomonas aeruginosa* azurin was used as a model T1 site containing redox protein ([Shleev *et al.*, 2005a](#)). A typical oxidised T1 site spectrum of azurin is shown in [Figure 10B](#), curve 1, illustrating the pronounced broad peak at 600 nm. When direct electronic communication is established between the aldrithiol-modified gold electrode and the dissolved azurin, it is possible to control the redox state of the azurin solution by the applied potential on the electrode. Direct mediatorless electron transfer has been achieved in these experiments, as demonstrated by the absorbance vs. the applied potential plot ([Figure 10C](#)). The resulting sigmoidal curve shows the expected Nernst behaviour correlated with the single T1 copper redox centre. From the data obtained in this experiment it is possible to extract the $E^{0'}$ value of the site and the number of electrons (n) involved in the redox process, which were found to be 400 mV and 0.8, respectively. This $E^{0'}$ value of *Pseudomonas aeruginosa* azurin is in good agreement with the values found from CVs of the protein on mercaptosuccinic acid-modified gold electrodes or chemisorbed protein on the gold surface ([Lisdat and Karube, 2002](#); [Andolfi *et al.*, 2004](#)). In principle, the high stability and reversible electrochemistry allow the immobilisation of azurin on an electrode surface for the construction of a second-generation biosensor that uses azurin as mediator for electron transport at the electrode surface between the enzymic system present in solution and the electrode ([Gilardi *et al.*, 1994](#)).

3.2. T2 copper enzyme – galactose oxidase

GalOD (D-galactose:oxygen 6-oxidoreductase, EC 1.1.3.9) is an extraordinary protein with many unusual and fascinating properties. The protein consists of a single polypeptide with a molecular mass of 68 kDa (639 amino acids) and dimensions of $98.0 \times 89.4 \times 86.7 \text{ \AA}$ arranged into three domains having mainly β -structure with the active site located on the solvent-accessible surface of domain II. The discovery that the enzyme contains a protein-based redox site in addition to the copper ion ([Whittaker and Whittaker, 1988](#)) was a breakthrough in research on GalOD. The enzyme exists in three distinct redox states – oxidised/active (Cu^{2+} and C-Y \cdot), semioxidised/inactive (Cu^{2+} and C-Y) and reduced (Cu^+ and C-Y). While the $E^{0'}$ of the C-Y \cdot /C-Y couple (410 mV, pH 7.0) has been known for many years, the $E^{0'}$ of the $\text{Cu}^{2+}/\text{Cu}^+$ redox couple (159 mV, pH 7.0) was resolved relatively recently ([Wright and Sykes, 2001](#)). Each of the three enzyme forms has a distinct spectroscopic signature, allowing them to be readily identified. The oxidised form of GalOD has an unusual UV–vis spectrum ([Figure 11A](#), black solid line) with strong absorption bands near 450 and 800 nm, associated with the metalloradical complex. In contrast, the semi-reduced form exhibits relatively weak absorption, and the fully reduced form is colourless. GalOD catalyses the oxidation of galactose, a large number

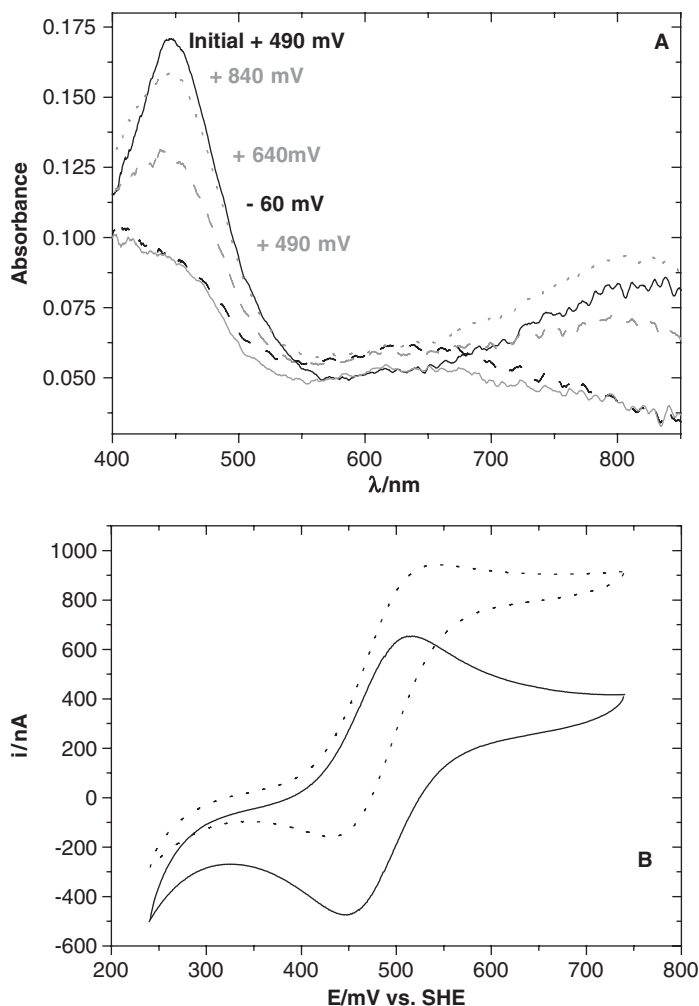


Fig. 11. (A) Spectroelectrochemical redox titration of GalOD (1.6 mg ml^{-1}) in a capillary gold electrode. Chronology of the experiment: initial +490 mV (black solid line); -60 mV (black dashed line); +490 mV (grey solid line); +640 mV (grey dashed line); +840 mV (grey dotted line) with waiting time of 15–20 min. Working potential referred vs. NHE. Reproduced from *Shleev et al. (2005c)* with permission from Elsevier.

(B) Cyclic voltammograms of GalOD (4 mg ml^{-1}) on an aldrithiol-modified gold electrode. The voltammograms were obtained before (solid line) and after addition of galactose with a final concentration of 43 mM (dotted line). Measurement performed in 100 mM phosphate buffer pH 7.3 containing 2 mM hydroxymethylferrocene as mediator with a sweep rate of 20 mV s^{-1} . Reproduced from *Shleev et al. (2005c)* with permission from Elsevier.

of primary alcohols, galactose-containing oligo/polysaccharides, glycolipids, and glycoproteins with production of an aldehyde molecule and hydrogen peroxide. Although a broad range of substrates are utilised by the enzyme, the oxidation is strictly regioselective (*Rogers and Dooley, 2001*).

Extensive spectroscopic and structural analyses led to the development of a catalytic mechanism of the enzyme. The enzyme follows a ping-pong mechanism for oxidation of the substrate, when the substrate binds to the copper, replacing a solvent molecule. Y-495 functions as a base for abstracting a proton from the substrate followed by hydrogen atom abstraction by the cofactor radical. A short-lived radical anion is formed as an intermediate and at the end the aldehyde is released. Oxygen is reduced to hydrogen peroxide with superoxide radical as a possible intermediate.

The interaction of the enzyme with mediators was studied in detail using carbon electrodes. For efficient regeneration of GalOD ferrocene derivatives, osmium complexes, tetracyanoquinodimethane (TCNQ), and hydride acceptors have been used (Hale and Skotheim, 1989; Miyata *et al.*, 1995; Yamaguchi *et al.*, 1995; Stigter *et al.*, 1996; Petersen and Steckhan, 1999). The activity of GalOD could be influenced by the applied potential when adsorbed on a graphite electrode (Tkac *et al.*, 2002). In contrast no mediated bioelectrocatalysis of GalOD in the presence of substrate and mediator has been observed for GalOD adsorbed on any modified gold surface. Mediated bioelectrochemistry has been only shown for GalOD in solution using a PME (Haladjian *et al.*, 1994) with a gold working electrode and hydroxymethyl-ferrocene as mediator (Figure 11B).

In spite of the surface exposure of the active site and efficient reaction of GalOD with other redox proteins, direct evidence to prove DET between GalOD and an electrode has been established very recently (Shleev *et al.*, 2005c; Tkac *et al.*, 2005). The reduction of GalOD in a capillary gold electrode and subsequent re-oxidation has been demonstrated, but the process is electrochemically irreversible and requires a long time (30–60 min) to achieve equilibrium after switching the working potential. An overvoltage of 350 mV is needed for re-oxidation to achieve the initial absorbance of oxidised GalOD (Figure 11A). This behaviour can be ascribed to the strong interaction of GalOD with bare gold.

To take into account the fact that DET for GalOD has been shown very recently, only first- and second-generation biosensors based on GalOD have been designed so far. For instance, different types of amperometric biosensors based on a Clark-type oxygen electrode as well as various working electrodes with adsorbed enzyme were constructed to measure galactose in different media, such as blood, serum, and foodstuffs (Vrbova *et al.*, 1992; Jia *et al.*, 2003; Sharma *et al.*, 2004a, b).

3.3. T3 copper enzyme – tyrosinase

Tyrosinase (Tyr, monophenol, dihydroxyphenylalanine (DOPA):dioxygen oxidoreductase, EC 1.14.18.1) contains a coupled binuclear copper active site (the T3 site) (Solomon *et al.*, 1996). This enzyme catalyses both the *ortho*-hydroxylation of monophenols (cresolase activity, Figure 9), and the two-electron oxidation of *o*-diphenols to *o*-quinones (catecholase activity, Figure 9).

Tyrosinase is widely distributed among eukaryota, and has also been identified in eubacteria of the *Streptomyces* genus. In fungi and vertebrates, Tyr catalyses the initial step in the formation of the pigment melanin from tyrosine. The physiological role of Tyr in plants is to oxidise phenols and protect the plant from pathogens or insects (Deverall, 1961). In insects, Tyr is thought to be involved in wound healing and possibly sclerotisation of the cuticle (Solomon *et al.*, 1996).

E^0 values of the active sites of Tyr from different sources were determined and they varied from 120 to 600 mV (e.g., Reiss and Vellinger, 1929; Ramos *et al.*, 2003; Makino *et al.*, 1974). The crystal structure of sweet potato Tyr is available (Klabunde *et al.*, 1998), which will facilitate the understanding of the function of this abundant enzyme. The two electrons required to reduce the second oxygen atom to H₂O are supplied by the substrate; thus, Tyr functions as an internal monooxygenase (Figure 9) (Rodriguez-López *et al.*, 1992), and the reaction of oxygenation of the substrate to DOPA (Figure 9), is considered to be the rate-determining step, followed by a rapid two-electron oxidation of DOPA to the quinone. The DOPA quinone product then undergoes a series of non-enzymatic polymerisation reactions to form the pigment melanin.

One of the first sensors based on immobilised Tyr on a pH electrode was constructed as early as in 1989 for the detection of DOPA, tyrosine, isoproterenol, α -methyl-DOPA, dopamine, adrenaline, and noradrenaline based on the cresolase and catecholase activities of the enzyme (Berenguer *et al.*, 1989). Since Tyr has been intensively studied due to the great interest in determining various phenols and related compounds in both environmental and biological samples, a great number of the papers describing first- and second-generation biosensors based on Tyr deposited on the different supports (carbon and metal electrodes, glass-plate support) have been published (Kotte *et al.*, 1995; Hedenmo *et al.*, 1997; Rajesh *et al.*, 2004). Different kinds of monomeric redox mediators as well as redox polymers were used in these sensors, such as osmium complexes, tetrathiafulvalene, several quinoid redox-dye derivatives, hexacyanoferrate(II)-ion doped conducting polypyrrole, to speed up the electron transfer between the electrode and the product formed as result of the oxidation of the enzyme substrate. Tyr was used either as a single sensing element or in combination with other enzymes (most often Lc and peroxidase) for monitoring phenolic compounds, lignin, catecholamines in clinical, pharmaceutical, and environmental analysis (industrial wastes, pulp and paper, pharmaceutical antibacterial products, etc.) as well as for control of food quality (wine, tea, juice, and oil) (Cosnier and Innocent, 1993; Wang and Lin, 1993; Ortega *et al.*, 1993, 1994; Yaropolov *et al.*, 1995; Marko-Varga *et al.*, 1995, 1996; Puig *et al.*, 1996; McArdle and Persaud, 1993; Burestedt *et al.*, 1996; Lindgren *et al.*, 1996; Lutz *et al.*, 1995; Nistor *et al.*, 1999; Önnerrfjord *et al.*, 1995; Campanella *et al.*, 2001; Streffer *et al.*, 2001). The enzyme electrode is based on the use of immobilised Tyr and the amperometric detection of the enzymatic product at approximately 200 mV. For the detection various equipments were used which could be roughly divided into the two types, namely batch mode and flow injection systems.

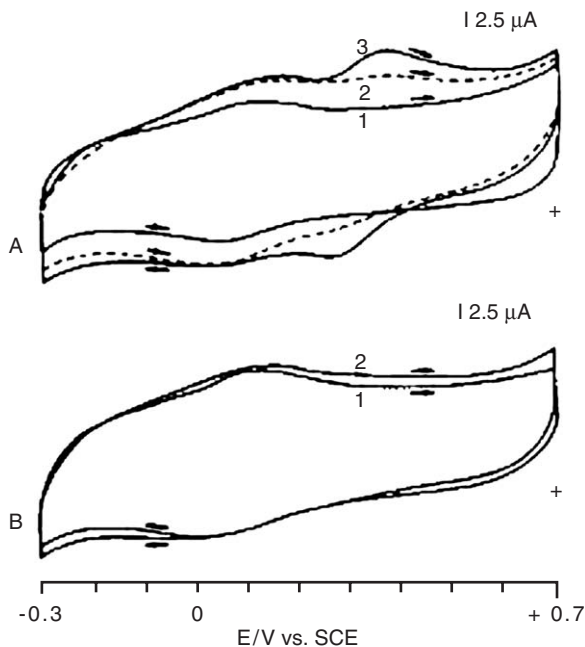


Fig. 12. Cyclic voltammograms obtained on polished graphite electrodes. (A) CV 1, bare electrode; CV 2, electrode coated with Tyr and in the presence of 10 mM benzoic acid; CV 3, electrode coated with native Tyr. (B) CV 1, bare electrode; CV 2, electrode coated with apoTyr. $E_{\text{SCE}} = +242$ mV vs. SHE. Reproduced from Yaropolov *et al.* (1996) with permission from Elsevier.

Due to all the difficulties encountered with Tyr-based electrochemical sensors, such as electrode fouling, lack of both operational and storage stability, etc. a DET connection between an electrode and immobilised Tyr is anticipated to largely promote a better use of this enzyme in conjunction with biosensors. The first publication on DET between Tyr and graphite electrode appeared in 1996 (Yaropolov *et al.*, 1996). The authors described the electrochemistry of the native, holo-, and apoenzyme-modified graphite electrodes using CV. The voltammograms exhibited peaks with a mid-point redox potential (E_m) of about 550 mV (Figure 12A). That was very close to the $E^{0'}$ value of Tyr, determined through redox titration to be about 600 mV (Makino *et al.*, 1974). In contrast, no current peaks were observed in the CVs recorded for electrodes with adsorbed apoTyr, which had negligible activity for catechol (Figure 12B). Thus, it could be concluded that the electrochemical reaction occurs with the copper ions of the holoenzyme and not with the protein component. Moreover, after incubation of the enzyme-modified electrodes with benzoic acid, the current peaks of the voltammograms disappeared (Figure 12A). No other redox transformations of Tyr were observed as the electrode potential was cycled between +950 and -50 mV (Yaropolov *et al.*, 1996). In the potential range where no redox transformations were observed, adsorption of the protein caused a reduction of the capacitive current (Figure 12A), seen as a lower background

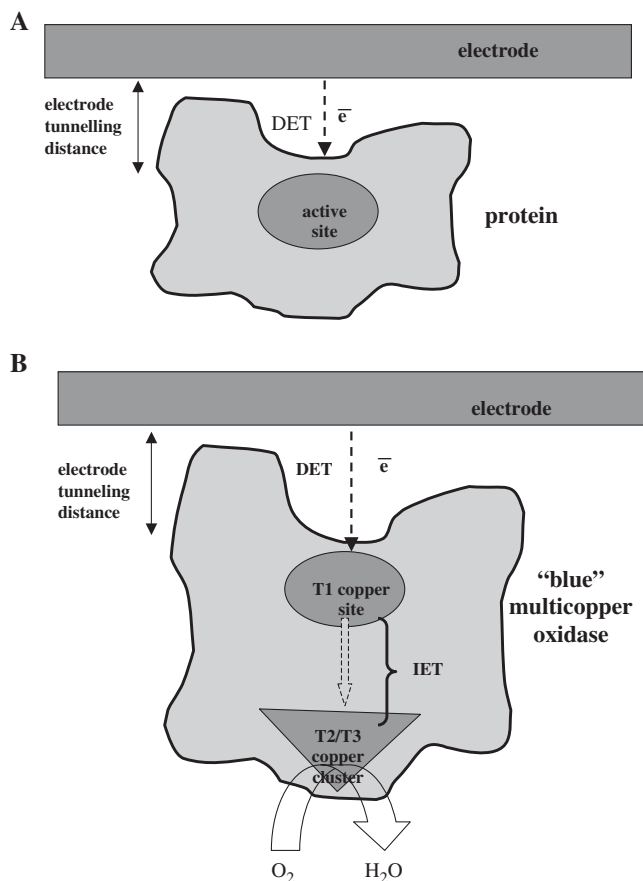


Fig. 13. (A) Proposed scheme for electrocatalytic activity of the T1, T2, and T3 copper proteins and electrode (see additional explanation in the text). Active site – T1, T2, or T3 sites of the proteins. (B) Proposed scheme for electroreduction of oxygen at carbon electrodes with adsorbed multi-copper oxidase.

current. At potentials more negative than 450 mV, oxygen-containing surface groups at the graphite electrode took part in redox transformations (Figure 12). These gave rise to a significant background current depending on the sweep rate, and interfered with those of the redox transformation caused by Tyr (Yaropolov *et al.*, 1996). Later, a paper describing DET reactions of Tyr adsorbed at a silver electrode had been published (Ye and Zhou, 1997). It was found that Tyr adsorbed on silver showed a quasi-reversible electrochemical reaction, for which some kinetic parameters, such as heterogeneous ET rate constant (k_s) were calculated.

In summary, a mechanistic scheme of the DET reactions between Tyr as well as between other proteins described above and electrodes is presented in Figure 13A. The electrons are transferred from the electrode to the active site of the adsorbed protein (either the T1 site of azurin, the T2 site of GalOD, or the

T3 site of Tyr) with an electron-tunnelling distance in the range from 5 to 10 Å according to their structures.

3.4. “Blue” multi-copper oxidases

3.4.1. Ascorbate oxidase

Ascorbate oxidase (L-ascorbate:dioxygen oxidoreductase, EC 1.10.3.3) has been obtained from different sources, such as plants, fungi, and eubacteria (White and Krupka, 1965; Itoh *et al.*, 1995; Mondovi *et al.*, 1984; Solomon *et al.*, 1996). The plant AOs are homodimers and the bacterial AO is a monomer with a significantly greater degree of glycosylation (11.2%) (Avigliano *et al.*, 1983; Itoh *et al.*, 1995). Each subunit of the enzyme contains one T1 copper and one T2/T3 trinuclear cluster. AO is one of two multi-copper oxidases, which have been crystallographically characterised (Messerschmidt *et al.*, 1992). The 1.9 Å X-ray structure of AO from *Cucurbita pepomedullosa* shows that each subunit is composed of three domains showing similar β -barrel folding, distantly related to the small blue single-Cu proteins plastocyanin and azurin (Messerschmidt *et al.*, 1989, 1992). Type 1 Cu is bound inside domain 3 by one cysteine thiolate, one methionine sulphur, and two histidine residues, as in plastocyanin. The type 2 Cu and type 3 Cu form a trinuclear cluster at the interface between domain 1 and 3, each contributing four histidine Cu ligands. The two type 3 Cu ions and the type 1 Cu are connected through a His–Cys–His stretch, which has been suggested to provide a possible direct through-bond pathway for intramolecular ET (Messerschmidt *et al.*, 1989; Solomon *et al.*, 1996).

AO is known to catalyse the oxidation of ascorbate to dehydroascorbate via disproportionation of the semidehydroascorbate radical (Figure 9) (Solomon *et al.*, 1996). However, the physiological role of this process is unclear. Most of the AO molecules present in the cells are associated with the cell wall (Reid, 1941; Newcomb, 1951), and AO activity has been shown to be strongly correlated with the rate of plant growth via cell elongation (Reid, 1941; Newcomb, 1951; Lin and Varner, 1991; Esaka *et al.*, 1992).

To the best of our knowledge the first publication describing DET reactions of AO appeared in 1996 (Sakurai, 1996). CVs of cucumber AO at a gold electrode modified with bis(4-pyridyl) disulphide, cationic bis(2-aminoethyl) disulphide, anionic 3,3'-dithiodipropionic acid, and hydrophobic diphenyl disulphide revealed $E^{0'}$ values of 369, 356, 345, and 323 mV, respectively, being very close to the $E^{0'}$ value of the T1 site (350 mV) determined with potentiometric titration (Kroneck *et al.*, 1982; Kawahara *et al.*, 1984). No direct evidence was presented in the paper concerning the nature of the electroactive group of the enzyme. In spite of the fact that other types of coppers (from the T2 and the T3 sites) were supposed to have similar $E^{0'}$ -values, it was suggested that the redox waves on the CVs came from the T1 site of the enzyme. The authors concluded that the T2/T3 cluster is more deeply buried inside the protein molecule as compared to the T1 copper according to the crystal structure of AO (Messerschmidt *et al.*, 1992).

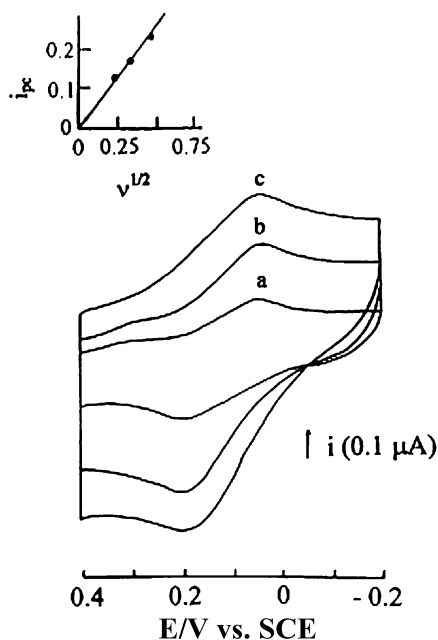


Fig. 14. Cyclic voltammograms of AO embedded within a TBMPC membrane at a gold electrode (50 mM phosphate buffer, pH 7.0, at 25 °C). Scan rates were: 50 mV s^{-1} (CV a), 100 mV s^{-1} (CV b) and 200 mV s^{-1} (CV c). Scans were typically recorded on the fifth cycle. Inset: i_p plotted against the square root of the scan rate. $E_{\text{SCE}} = +242 \text{ mV}$ vs. SHE. Reproduced from Santucci *et al.* (1998) with permission from Portland Press on behalf of the Biochemical Society.

In the same year the absence of any electrochemical activity of AO was shown at graphite between pH 5.0 and 7.2 (Yaropolov *et al.*, 1996). However, in 1998, Santucci and co-workers confirmed the possibility of DET between a gold electrode and AO and extended previous data using CV and DPV (Santucci *et al.*, 1998). Under anaerobic conditions, the CVs of membrane-trapped AO on a gold electrode in 50 mM phosphate buffer, pH 7.0 (Figure 14), showed well-defined electrochemistry for scan rates between 50 and 200 mV s^{-1} . The anodic and cathodic peak currents were almost identical, with an intensity ratio ($i_{\text{pa}}/i_{\text{pc}}$) close to unity. The linear dependence of the voltammetric peak current on the square root of the scan rate (Figure 14, inset) indicates that the redox process was diffusion controlled. The estimated E_m value, 360 mV, was close to the value measured potentiometrically under similar solvent conditions (Kroneck *et al.*, 1982; Kawahara *et al.*, 1984). The k_s was calculated to be $1.2 \times 10^{-4} \text{ cm s}^{-1}$ at 25 °C, by assuming the number of electrons involved in the ET process, n , to be equal to 1 and the diffusion coefficient, D , to be $3.0 \times 10^{-8} \text{ cm}^2 \text{ s}^{-1}$.

The electrochemical behaviour of tributylmethyl phosphonium chloride (TBMPC)-embedded T2-depleted (T2D) AO (Santucci *et al.*, 1998) at a gold electrode was similar to that of the holoprotein. The CVs had the same shape

and intensity as those illustrated in Figure 14. The $E^{0'}$ values were also identical with those of the holoprotein. Apparently, the removal of the T2 copper did not influence the electrochemical behaviour. The TBMPC-embedded apo-AO, in contrast, caused no electrochemical signals.

In spite of the well-pronounced DET reactions between AO and different electrodes first- and second-generation biosensors based on AO are prevalent. Several types of electrochemical sensors based on the pure enzyme or even tissue homogenate were developed for the determination of ascorbic acid in medicals, blood, and food (Matsumoto *et al.*, 1981; Macholan and Chmelikova, 1986; Jin *et al.*, 1992; Campanella *et al.*, 2004). Moreover, amperometric inhibitor biosensors for determination of reduced glutathione as well as for monitoring of organophosphorous pesticide were also designed (Rekha *et al.*, 2000; Sezgintürk and Dinckaya, 2004).

3.4.2. Bilirubin oxidase

Bilirubin oxidase (bilirubin:oxygen oxidoreductase, EC 1.3.3.5) is a multi-copper oxidase catalysing the oxidation of bilirubin to biliverdin with the concomitant reduction of dioxygen to water (Figure 9). The catalytic site of BOD also consists of four copper ions per molecule, which can also be classified into three types, one type 1 (T1), one type 2 (T2) and two type 3 (T3) copper ions (Solomon *et al.*, 1996; Shimizu *et al.*, 1999). It has been shown that the T1 site is the primary centre, at which electrons are accepted from reducing substrates (Solomon *et al.*, 1996; Xu *et al.*, 1996). Unfortunately, no crystallographic data of BOD have been published so far. However, the biochemical, spectral, and kinetic properties of the enzyme have been studied in detail (Guo *et al.*, 1991; Shimizu *et al.*, 1999; Xu *et al.*, 1996; Solomon *et al.*, 1996). The ligands of the T2 and T3 coppers of the active site of BOD are the same as for AO, viz. six histidines for the T2/T3 cluster. However, the ligands of the T1 copper depend on the enzyme origin, e.g., histidines, cysteine, and methionine for *Myrothecium verrucaria* BOD (Shimizu *et al.*, 1999; Sakurai *et al.*, 2003), and histidines, cysteine, and phenylalanine for BOD from *Trachyderma tsunodae* (Hirose *et al.*, 1998). $E^{0'}$ -values of the T1 site of the enzyme were determined and found to be in the range from 490 to 700 mV (Xu *et al.*, 1996; Tsujimura *et al.*, 2004). This broad range of the $E^{0'}$ -values can be probably explained by different axial ligands (Met or Phe) as well as structures of the T1 sites of the enzyme from different origins. Thus it is suggested here that BOD from different sources can belong to the groups of low and high redox potential multi-copper oxidases in compliance with a new classification of blue multi-copper oxidase proposed very recently (*vide infra*) (Shleev *et al.*, 2005c).

Investigations of DET between electrodes and BOD is a very important task due to several reasons. First of all BOD has also important biochemical properties for biotechnological application, such as high activity, stability, and low extent of glycosylation (Guo *et al.*, 1991; Xu *et al.*, 1996; Shimizu *et al.*, 1999). BOD has the ability of producing mediated bioelectrocatalytic currents for the reduction of O₂ to water near neutral pH (Tsujimura *et al.*, 2003). A biofuel cell

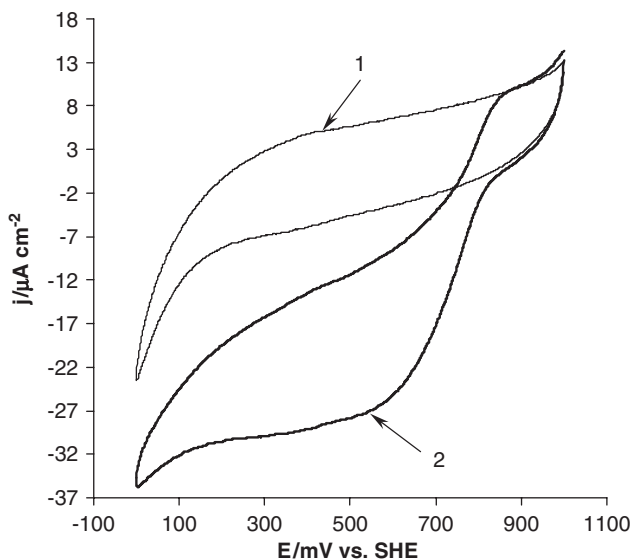


Fig. 15. Electroreduction of molecular oxygen on SPGE with adsorbed *Myrothecium verrucaria* BOD (0.1 M citrate-phosphate buffer pH 4.0; scan rate 10 mV s^{-1} ; start potential -1000 mV ; second scan; aerobic condition (0.26 mM dioxygen)). 1 – without BOD; 2 – with BOD. Reproduced from Shleev *et al.* (2004a) with permission from Elsevier.

utilising BOD for the four-electron reduction of O_2 can operate at neutral pH (Tsujimura *et al.*, 2003; Barton *et al.*, 2001, 2002). BOD has accordingly been utilised for the construction of a dioxygen biocathode operating near neutral pH in a H_2/O_2 biofuel cell (Mano *et al.*, 2002; Heller, 2004; Tsujimura *et al.*, 2001a), in glucose/ O_2 biofuel cells (Mano and Heller, 2003; Mano *et al.*, 2003b; Heller, 2004), and in a photosynthetic bioelectrochemical cell (Tsujimura *et al.*, 2001b). Moreover, several electrochemical biosensors were designed responding amperometrically to bilirubin based on BOD with and without exploiting any mediators (Wang and Ozsoz, 1990; Shoham *et al.*, 1995; Zhang *et al.*, 2004).

A number of publications on mediated electrochemistry of the enzyme have been published using different kinds of monomeric mediators as well as redox polymers (Tsujimura *et al.*, 2001a, b; Nakagawa *et al.*, 2003; Mano and Heller, 2003; Mano *et al.*, 2003a). It was shown that the potential at which the bioelectrocatalytic current for oxygen reduction starts to appear exclusively depends on the E^0 of the mediator employed. The magnitude of the bioelectrocatalytic current systematically decreased with a decrease in the potential difference between E^0 ($\text{O}_2/\text{H}_2\text{O}$) and E^0 of the mediator (Tsujimura *et al.*, 2001a, b; Nakagawa *et al.*, 2003; Mano and Heller, 2003; Mano *et al.*, 2003a).

The possibility of DET between *Myrothecium verrucaria* BOD and carbon electrodes under anaerobic and aerobic conditions has been reported very recently (Tsujimura *et al.*, 2004; Shleev *et al.*, 2004a). In the presence of the

enzyme substrate (molecular oxygen) a reduction current was recorded at BOD-modified carbon electrodes (glassy carbon electrode (GCE), spectroscopic graphite electrode (SPGE), highly oriented pyrolytic graphite electrode (HOP-GE), and plastic formed carbon electrode (PFCE)) as a result of DET between the electrode and the adsorbed enzyme (Tsujimura *et al.*, 2004; Shleev *et al.*, 2004a). Some electrochemical parameters for the electroreduction of oxygen, such as $E^{0'}$, the standard surface ET rate constant at $E^{0'}$, and the transfer coefficient, were estimated (Tsujimura *et al.*, 2004). CVs of a bare and a BOD-modified SPGE under aerobic conditions at pH 4.0 are shown in Figure 15. When adsorbed on SPGE, BOD largely decreased the overvoltage needed for the electroreduction of molecular oxygen. As can be seen from the CV (Figure 15), the electrocatalytic current at the electrode modified with BOD starts at a potential of about +800 mV with a half-wave potential for oxygen electroreduction of about +700 mV (pH 4.0), which is quite close to the redox potential of the T1 site of the enzyme.

3.4.3. *Ceruloplasmin*

Ceruloplasmin (ferroxidase, iron(II):dioxygen oxidoreductase, EC 1.16.3.1) is the most complex multi-copper oxidase in all respects (structure, function, and catalytic reactions). One of the physiologically relevant reactions catalysed by Cp is its ferroxidase activity, presented in Figure 9. Besides Fe^{2+} , Cp is able to oxidise an extensive group of organic compounds e.g., *p*-phenylenediamines, amino-phenols, catechols, and 5-hydroxyindoles (Frieden and Hsieh, 1976). Relatively recently, it has been found that human Cp exhibits an alkyl hydroperoxide peroxidase activity, which is independent of its oxidase activity (Cha and Kim, 1999). Within the scope of this chapter it is not possible to discuss and cover all properties and roles of such a complicated enzyme and the reader is advised to read recent reviews and theses (e.g., Machonkin, 2000; Bielli and Calabrese, 2002). However, some important aspects for a further electrochemical description are considered below.

Cp is a monomer with a significant amount of glycosylation (9–14%) (Solomon *et al.*, 1996). Human Cp was crystallographically characterised at a resolution of 3 Å (Zaitsev *et al.*, 1996). The structure of human Cp is far more complex compared with other three-domain structures of other “blue” multi-copper oxidases, such as AO or Lc. The molecule is composed of six compact domains, with large loop insertions, and it contains six tightly bound copper atoms. The three copper ions of the trinuclear cluster lie at the interface between the first and last domains, 1 and 6, respectively, possessing ligands from each domain, an arrangement also seen in the structures of AO and Lc (Messerschmidt *et al.*, 1992; Ducros *et al.*, 1998; Piontek *et al.*, 2002). The remaining three copper atoms are mononuclear centres held by intra-domain sites; those located on domains 4 and 6 have a typical T1 copper environment with a set of four ligands, two histidines, one methionine, and one cysteine (T1A and T1B copper sites), whereas the one (T1PR site) located in domain 2 has a different structure in that it lacks the methionine, which is replaced in the amino acid sequence by a

leucine residue, Leu 329 (Takahashi *et al.*, 1984; Ortel *et al.*, 1984; Messerschmidt and Huber, 1990), analogous to the T1 site of some fungal Lcs (*vide infra*). This residue is unable to coordinate metals, the centre is therefore a tricoordinate T1 site. Another difference is that this site is not endowed with structural elements able to bind substrates that have been found close to the other two sites (Lindley *et al.*, 1997). In the structures examined so far, the T1A centre and the trinuclear cluster are held at a distance of 13 Å, prevented from coming in contact by the protein moiety; however, the cysteine ligand of the T1 site is flanked by two histidines, each bound to a copper atom of the trinuclear cluster. This structural motif, His–Cys–His, was first noticed in the structure of AO (Messerschmidt *et al.*, 1989), than found in the crystal structure of Lc (Ducros *et al.*, 1998; Piontek *et al.*, 2002), and also bacterial multi-copper oxidases (Grass and Rensing, 2001; Enguita *et al.*, 2003). The other two T1 sites (T1B and T1PR) are located far from the T2/T3 cluster.

It was found that the T1A and T2B sites have different EPR parameters (Gunnarsson *et al.*, 1973), re-oxidation rates (Carrico *et al.*, 1971; De Ley and Osaki, 1975), and $E^{0'}$ -values (Deinum and Vänngård, 1973). The $E^{0'}$ -values of two “normal” oxidase T1 copper sites were measured by anaerobic titration procedures exploiting mediators as early as in 1973 and found to be 490 and 580 mV (Deinum and Vänngård, 1973). However, it is still unknown which value belongs to the T1A or the T1B site. As for the T1PR site, the value of its $E^{0'}$ was estimated relatively recently and found to be very high, approximately 1000 mV (Machonkin, 2000). This extremely high value of the $E^{0'}$ was found to be the reason for the inability to oxidise this copper site.

The first report of DET processes involving Cp appeared in 1996 (Yaropolov *et al.*, 1996). Figure 15A shows CVs recorded for a bare spectroscopic graphite electrode (curve 1) and for the same electrode modified with adsorbed human Cp (curve 2). Small cathodic and anodic faradaic currents corresponding to a reversible process can be seen with E_m -values of approximately 340 and 410 mV. Besides, a small reduction peak in the CV of the Cp-modified electrode can also be seen with an E_p of 600 mV (Figure 16A). These redox potentials are more negative than those of the redox potentials of the T1 copper sites of the enzyme (490, 580, and ~1000 mV) (Deinum and Vänngård, 1973; Machonkin, 2000). This difference was explained by a conformational transformation in the vicinity of the copper ions during adsorption of the enzyme or an overvoltage of the electrochemical redox reaction of the copper ions in the protein structure on the graphite electrode (Yaropolov *et al.*, 1996). However, the main evidence for DET reaction was obtained using spectroelectrochemistry (Yaropolov *et al.*, 1996). The reduction of the prosthetic groups (copper sites) of Cp was performed simultaneously as the absorbance spectrum was monitored in the region 450–700 nm in order to confirm the redox transition of Cp (Figure 16B). It was found that the T1 coppers of Cp were reduced on a platinum electrode under anaerobic conditions. The process was reversible and Cp could be re-oxidised by saturating the system with oxygen (Figure 16B).

To the best of our knowledge there is no single publication describing any successful work in the making of an electrochemical biosensor based on Cp, possibly due to the complex structure of the enzyme and the broad variety of

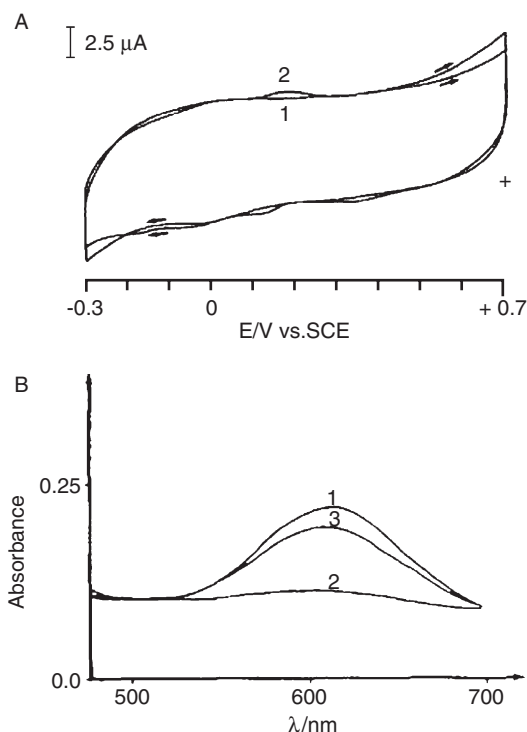


Fig. 16. (A) Cyclic voltammograms of (1) a polished naked spectroscopic graphite electrode and (2) a Cp-modified spectroscopic graphite electrode (saturated with the enzyme). Anaerobic conditions; 0.1 M phosphate buffer, pH 7.2; scan rate, 100 mV s^{-1} ; “+” indicates the start potential; $E_{\text{SCE}} = +242 \text{ mV vs. NHE}$.

(B) Changes of the absorbance spectrum during electrolysis of Cp from placental blood. (1) initial curve, (2) after electrolysis for 15 min, (3) after reoxidation with oxygen. Anaerobic conditions; 0.1 M phosphate buffer, pH 7.2; 0.1 M NaCl; $2.3 \times 10^{-5} \text{ M}$ ceruloplasmin; applied potential, 250 mV. Reproduced from Yaropolov *et al.* (1996) with permission from Elsevier.

reactions catalysed by Cp. However, several attempts have been made in order to create mediated reagentless enzyme inhibition electrodes based on the enzyme, and a few publications can be found in literature claiming the usefulness of Cp for sensing metal ions (Daigle *et al.*, 1998; Amiot *et al.*, 2001).

3.4.4. Laccase

Laccase (benzenediol: oxygen oxidoreductases, EC 1.10.3.2) catalyses the oxidation of *ortho*- and *para*-diphenols, amino-phenols, polyphenols, polyamines, lignins, and aryl diamines as well as some inorganic ions coupled to the reduction of molecular dioxygen to water (Yaropolov *et al.*, 1994; Solomon *et al.*,

1996). The physiologically relevant reaction catalysed by Lc is presented in Figure 9.

The enzyme exhibits a broad substrate specificity, which can be enhanced by the addition of redox mediators. The efficiencies of these mediators have been demonstrated in work presented in a number of publications (Yaropolov *et al.*, 1994; Call and Mucke, 1997). Due to the broad variety of reactions catalysed by Lc, this enzyme holds great promise for many potential applications, such as bioremediation (Mayer and Staples, 2002), green biodegradation of xenobiotics including pulp bleaching (Call and Mucke, 1997; Balakshin *et al.*, 2001), labelling in immunoassays (Zherdev *et al.*, 1999; Kuznetsov *et al.*, 2001), green organic synthesis (Karamyshev *et al.*, 2003), and even design of fungicidal and bactericidal Lc preparations (Johansen, 1996). Based on the electrochemical activity of Lcs from different sources on various types of electrodes, other possible applications of the enzyme have been studied, e.g., development of oxygen cathodes in biofuel cells (Tarasevich *et al.*, 1979, 2002; Palmore and Kim, 1999; Soukharev *et al.*, 2004; Barton *et al.*, 2002, 2004), and design of different types of biosensors (Yaropolov *et al.*, 1994, 1995; Marko-Varga *et al.*, 1995; Peter and Wollenberger, 1997; Smith *et al.*, 1997; Szeponik *et al.*, 1997; Daigle *et al.*, 1998; Minussi *et al.*, 2002; Duran *et al.*, 2002; Freire *et al.*, 2001; Haghghi *et al.*, 2003; Gupta *et al.*, 2004; McArdle and Persaud, 1993; Jarosz-Wilkolazka *et al.*, 2004a, b). Lcs are classified into two groups in accordance with their source, i.e., plant and fungal. However, diphenol oxidases (Lcs) have also been identified in bacteria (Givaudan *et al.*, 1993; Martins *et al.*, 2002) and insects (Barrett, 1987).

The X-ray structures of Lcs isolated from several organisms have been determined for e.g., *Coprinus cinereus* (Ducros *et al.*, 1998), *Trametes versicolor* (Piontek *et al.*, 2002; Antorini *et al.*, 2002), *Pycnoporus cinnabarinus* (Antorini *et al.*, 2002), *Melanocarpus albomyces* (Hakulinen *et al.*, 2002), and bacterial Lc from the endospore coat of *Bacillus subtilis* (Enguita *et al.*, 2003). The fungal Lc is a monomer, organised in three sequentially arranged domains and has dimensions of about $65 \times 55 \times 45$ Å (Piontek *et al.*, 2002). Each of the three domains has a similar β -barrel type architecture, related to the small blue copper proteins such as azurin or plastocyanin. Although local structural differences are apparent (e.g., in the loops organising and forming the substrate-binding pocket), all of the Lc structures show a significant degree of overall structural homology.

From the crystal structure of an enzyme/substrate complex, it is known that the electron donor substrate binds in a small negatively charged cavity near the copper T1 site (Piontek *et al.*, 2002), which lies embedded in domain 3, about 7 Å below the surface of the enzyme. The T1 copper is the primary electron acceptor site and it is connected to the trinuclear cluster by a His–Cys–His tripeptide, which is highly conserved among “blue” multi-copper oxidases, such as AO and Cp (Messerschmidt *et al.*, 1989; Zaitsev *et al.*, 1996). Moreover, for all “blue” multi-copper oxidases the distance between the T1 site and T2/T3 cluster was found to be in the range from 12 to 14 Å (Messerschmidt *et al.*, 1992; Zaitsev *et al.*, 1996; Ducros *et al.*, 1998; Piontek *et al.*, 2002). It is not astonishing because it was previously discovered that the single characteristic that has

obviously been selected in the evolution of the physiological electron tunnelling in these oxidoreductases is the simple position of redox centres within 13–14 Å of each other (Page *et al.*, 1999), a value that could be compared with that of e.g., sulphite oxidase for which a distance of more than 30 Å between the redox sites has been determined (Kisker *et al.*, 1997a; Feng *et al.*, 2003).

Oxidation of simple organic substrates occurs via a ping-pong-type mechanism (Petersen and Degn, 1978; Yaropolov *et al.*, 1986, 1994; Solomon *et al.*, 1996). Substrates are oxidised near the T1 site, and the electrons are transferred to the T2/T3 cluster, where molecular oxygen is reduced. Neither the mechanism of internal electron transfer nor the mechanism of dioxygen reduction to water is fully understood for this enzyme. However, a number of mechanistic schemes have been proposed, which are consistent with the kinetic and structural data currently available (Solomon *et al.*, 1996; Lee *et al.*, 2002).

The key characteristic of Lc is the standard redox potentials of its redox centres; the T1, T2, and T3 sites. The value of the redox potential of the T1 Cu-site has been determined using potentiometric titrations with redox mediators for a great number of different Lcs and varies between 430 (*Rhus vercinifera*) and 780 mV (Call and Mucke, 1997; Xu *et al.*, 1996, 1999; Reinhammar, 1972; Schneider *et al.*, 1999; Koroleva *et al.*, 2001; Shleev *et al.*, 2004b). It has been shown for some Lcs that T1 is the primary centre, at which electrons are accepted from reducing substrates (Yaropolov *et al.*, 1994; Solomon *et al.*, 1996; Xu *et al.*, 1996). Moreover, the catalytic efficiency ($k_{\text{cat}}/K_{\text{M}}$) for some reducing substrates depends on the redox potential of the T1 copper (Xu *et al.*, 1996, 2000). This is the reason why Lcs with a high redox potential of the T1 site are of special interest in biotechnology, e.g., for different bleaching (Paice *et al.*, 2002; Surma-Slusarska and Leks-Stepien, 2001; Balakshin *et al.*, 2001), bioremediation processes (Wong and Yu, 1999; Mayer and Staples, 2002) and in biofuel cells (Heller, 2004; Barton *et al.*, 2004). This dependence of the catalytic efficiency on the redox potential of the T1 site suggests that the rate-limiting step (or at least partially limiting step) for some reducing substrates in the catalytic cycle is the one-electron transfer from the substrate to the protein, specifically the T1 site of the Lc (Xu *et al.*, 2000). The catalytic cycle of Lc “starting” from the “native intermediate”, the substrates are oxidised near the T1 site, which then transfers the electron to the T2/T3 cluster, where molecular oxygen is reduced. However, a slow decay of the “native intermediate” leads to the “resting fully oxidised” form. In this form, the T1 site can still be reduced by a substrate, but the electron transfer to the trinuclear cluster is too slow to be catalytically relevant (for a full explanation see Solomon *et al.*, 1996; Lee *et al.*, 2002).

It has been proposed (Shleev *et al.*, 2005c) that all “blue” multi-copper oxidases can be divided into three groups depending on the $E^{0'}$ -value of the T1 site: low, middle, and high potential enzymes. From an electrochemical point of view based on the primary structures of the enzymes, it is possible to conclude that the low redox potential enzymes (340–490 mV) have methionine as an axial ligand of the T1 site. The middle redox potential enzymes (470–710 mV) have leucine and high potential “blue” oxidases (730–780 mV) have phenylalanine as an axial ligand for the T1 sites. Currently, the big differences between the $E^{0'}$ -

values of the T1 site of “blue” multi-copper oxidases are not fully understood from a biological point of view calling for further investigations (Solomon *et al.*, 2004). We would like to emphasise that the proposed classification of the “blue” multi-copper oxidases is based on their primary structures and the $E^{0'}$ -value of the T1 sites. The axial ligands cannot, however, affect so strongly the $E^{0'}$ of the enzyme, as was previously shown using site-directed mutagenesis (Kojima *et al.*, 1990; Xu *et al.*, 1998, 1999; Palmer *et al.*, 2003). The difference found in this case should not exceed 150 mV. However, even with this knowledge, it is anticipated that the new classification is valid only as a formal one and it might help for further investigations of the “blue” T1 site containing redox proteins.

In contrast to the many studies on determining the $E^{0'}$ of the T1 site, the redox potentials of the T3 sites of “blue” multi-copper oxidases were published only in the 1970s by Reinhammar (Reinhammar, 1972; Reinhammar and Vännegård, 1971). The redox potential of the T3 site was measured for two different Lcs, viz. the low potential enzyme from *Rhus vernicifera* (450 mV) and the high potential enzyme from *T. versicolor* (785 mV) (Reinhammar and Vännegård, 1971). Moreover, only two publications give values on the redox potential of the T2 site of Lcs, viz. for low and high redox potential Lcs from *R. vernicifera* and *Trametes hirsuta*, respectively (Reinhammar, 1972; Shleev *et al.*, 2005a). Based on these data it was suggested that the $E^{0'}$ -value of the T2 site for both enzymes is close to 400 mV (Shleev *et al.*, 2005a, c). One should also take into account that T2 and T3 coppers in multi-copper oxidases form integrated clusters and the given redox potentials may correspond to several redox states of the T2/T3 cluster. Moreover, the $E^{0'}$ -values were estimated under anaerobic conditions, whereas that O₂ binding to the T2/T3 cluster can change the redox state of the copper ions in the course of the catalytic cycle of these enzymes.

The first publications on DET for any large redox protein with enzymatic activity were concerned with a high potential Lc from the basidiomycetes *T. versicolor* (Berezin *et al.*, 1978; Tarasevich *et al.*, 1979). The authors of these papers showed that in the presence of molecular oxygen a reduction current was recorded at the Lc-modified carbon electrode due to DET between the electrode and the adsorbed enzyme (similar CVs, as presented in Figure 15 for BOD). A number of publications describing DET reaction between Lcs from various sources and different types of electrodes have then been published (Yaropolov *et al.*, 1996; Thuesen *et al.*, 1998; Santucci *et al.*, 1998; Gelo-Pujic *et al.*, 1999; Johnson *et al.*, 2003; Gupta *et al.*, 2004; Christenson *et al.*, 2004a). Direct and indirect evidences for DET (Christenson *et al.*, 2004a; Shleev *et al.*, 2005c) as well as kinetic parameters of the electroreduction for molecular oxygen at carbonaceous electrode materials with adsorbed Lc have been reported (Tarasevich, 1979; Lee *et al.*, 1984; Bogdanovskaya *et al.*, 1986).

The characteristics of the electroreduction of oxygen at Lc-modified graphite/carbon electrodes depend on the origin and also on the amount of enzyme on the electrode surface (Yaropolov *et al.*, 1996; Tarasevich *et al.*, 2001b; Shlev *et al.*, 2003; Shleev *et al.*, 2005b). Laccases from different sources (from *R. vernicifera* and *T. hirsuta*) catalyse the heterogeneous electroreduction of oxygen in very different potential regions. The pH dependence of the heterogeneous

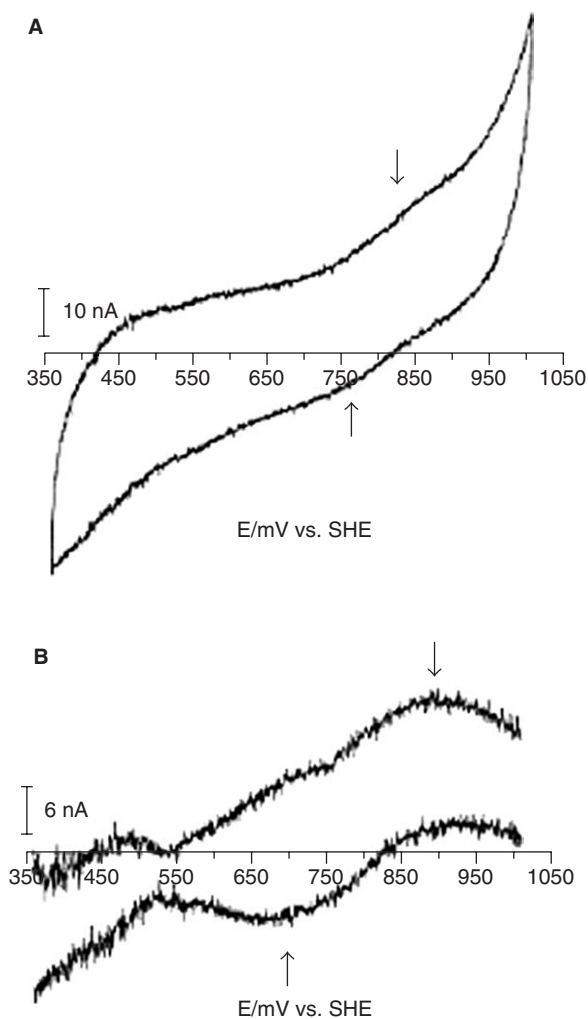


Fig. 17. (A) Cyclic voltammogram (second scan) of 2.5 pmol *P. versicolor* (*T. versicolor*) Lc adsorbed onto a pyrolytic graphite electrode (30 mM citrate, pH 3.31; ionic strength 0.1 M (NaClO₄); scan rate: 1 mV s⁻¹). (B) The background-corrected signal. Reproduced from Thuesen *et al.* (1998) with permission from Acta Chemica Scandinavica.

electrocatalytic currents for both enzymes adsorbed on electrodes was found to be very similar to that obtained for the corresponding enzyme reactions in homogeneous media (Yaropolov *et al.*, 1996). The difference in the redox potential of the T1 site of the two Lcs is most likely the major determinant of this behaviour with a similar mechanism operating for both homogeneous catalysis in solution and heterogeneous electrocatalysis at the electrode surface. A DET process has been reported on the basis of small cyclic voltammetric peaks observed for the high potential Lc from *T. versicolor* under anaerobic conditions, see Figure 17 (Thuesen *et al.*, 1998). The process was quasi-reversible with

the E_m close to the redox potential of the T1 site of this Lc (ca. 780 mV). Under aerobic conditions a clear catalytic wave was shown commencing close to the potential of the T1 site. A mechanism for the bioelectrocatalytic reduction of oxygen by Lc adsorbed on carbon electrode materials has been proposed by Tarasevich *et al.* (Tarasevich *et al.*, 2001b). At potentials close to the steady-state potential, the rate-determining step is proposed to be a concerted transfer of two electrons to the oxygen molecule. In the region of polarisation, where the current is essentially potential independent, the process is limited by the formation of a “peroxide” intermediate.

Deeper studies of the mechanism of DET between low (*R. vernicifera*) (Johnson *et al.*, 2003) and high potential Lcs from different basidiomycetes (*Trametes hirsuta*, *T. ochracea*, *Cerrena maxima*, *C. unicolor*, and *Corioliopsis fulvocinerea*) and electrodes have been carried and some results have been published (Shlev *et al.*, 2003; Shlev *et al.*, 2005a, b, c; Christenson *et al.*, 2004a). CVs using graphite electrodes modified with adsorbed Lcs were recorded in order to provide unambiguous experimental evidence for direct heterogeneous ET of these Lcs under anaerobic conditions. Osteryoung square wave voltammograms (SWV) recorded using edge-plane highly ordered pyrolytic graphite (HOPG) with and without Lcs entrapped between the electrode and a dialysis membrane in 0.1 M phosphate buffer solution at pH 6.5 show a single wave only in the presence of the enzymes, centred around +800 mV. The recorded faradaic process is very close to the potential of the T1 site and probably only the relatively high background noise of carbon electrodes (high capacitive currents) most likely prevents the observation of the same process by more conventional CV measurements. These results are in good agreement with previous data concerning DET between BOD and spectroscopic graphite electrode (Tsujiyama *et al.*, 2004; Shlev *et al.*, 2004a).

It was also found that the half-wave potentials ($E_{1/2}$) of the bioelectroreduction of oxygen as well as the steady-state potentials of the Lc-modified electrodes were very close to the redox potentials of the T1 site of Lcs (Shlev *et al.*, 2005b). Moreover, the $E_{1/2}$ of the bioelectroreduction of oxygen changed with about 15 mV/pH (Shlev *et al.*, 2005b). A similar dependence was demonstrated by Nakamura for the pH dependence of the potential of the T1 site for the low redox potential Lc from *R. vernicifera* (Nakamura, 1958) and approximately estimated by Reinhammar for the high redox potential Lc from *Polyporus versicolor* (Reinhammar, 1972). Besides, the results obtained for BOD (see above) showed that the $E_{1/2}$ of the wave for catalytic oxygen electroreduction changed with about 30 mV/pH, whereas the $E^{0'}$ (O_2/H_2O) has a 60 mV/pH dependence.

All the experiments with carbon electrodes modified with Lcs confirm that the T1 site is the primary electron acceptor from carbon electrodes during heterogeneous reduction under both aerobic and anaerobic conditions. The mechanistic scheme of this process is presented in Figure 13B. The electrons are transferred from the electrode to the T1 site of the adsorbed enzyme and then through an IET mechanism to the T2/T3 cluster, where molecular oxygen is reduced to water. Thus, to take into account the presented data for other “blue” multi-copper oxidases, for which an electrocatalytic current of reduction of

oxygen with the redox potential close to the value of the T1 site was observed. The mechanism of electroreduction of oxygen presented in Figure 13B was extended to all “blue” multi-copper oxidases adsorbed on carbonaceous electrodes.

In conclusion, the mechanism of DET between electrodes and “blue” multi-copper oxidases associated with the reduction of molecular oxygen and oxidation of substrates is not fully understood. The question is especially relevant for electrochemical investigations of “blue” multi-copper enzymes on metal electrodes, since in many cases the DET processes recorded with CV or other voltammetric techniques do not coincide with the $E^{0'}$ values evaluated with other techniques for the different copper sites identified crystallographically in the protein structures. However, it is tempting and possibly too speculative, as has been done in this contribution, based on summarising the current knowledge to propose the mechanisms outlined in Figure 13 for the electrochemical interaction between different electrode materials and copper-containing proteins from different origins causing DET reactions between the electrode and the protein.

3.4.5. Additional enzymes

Superoxide dismutase (SOD) is an enzyme protecting living organisms from oxidative stress through scavenging superoxide anions (Fridovich, 1978). SOD comprises a family of metalloproteins primarily classified into four groups: copper/zinc-containing SOD (Cu/Zn-SOD), manganese-containing SOD (Mn-SOD), iron-containing SOD (Fe-SOD), and nickel-containing SOD (Ni-SOD). The Cu/Zn-SOD is invariably a dimer, and the Mn-SOD and Fe-SOD have been isolated as either dimers or tetramers. In general, each subunit bears a functional metal ion and there has been no evidence for a strong interaction between individual functional metal centres. Due to both fundamental and applied aspects of the bioelectrochemistry of SOD a considerable attention has been paid to obtaining DET between SODs and electrodes. Fe-SOD and Cu/Zn-SOD showed quasi-reversible CVs at mercaptopropionic acid SAM-modified gold electrodes with $E^{0'}$ -values of about 90 and 290 mV and k_s -values of 35 and 65 s⁻¹, respectively (Ge *et al.*, 2003). The electrochemistry of Cu/Zn-SOD adsorbed onto cysteine SAM-modified gold electrodes exhibited an $E^{0'}$ value of 257 mV (pH 7.4) (Tian *et al.*, 2002a, b) and recently the electrochemistry of Cu/Zn-SOD, Fe-SOD, Mn-SOD was investigated on mercaptopropionic acid SAM-modified electrodes revealing quasi-reversible CVs for all three SODs with $E^{0'}$ -values of 479, 332, and 422 mV (pH 7) and k_s -values of 1.1, 3.9, and 1.9 s⁻¹, respectively (Tian *et al.*, 2004).

Mammalian cytochrome *c* oxidase, the terminal enzyme of the oxidative phosphorylation is located in the inner mitochondrial membrane, where it pumps protons against a concentration gradient from the matrix to the cytosol to support the production of ATP. Beef heart cytochrome *c* oxidase has 13 subunits ($M_W \approx 204$ kDa) and contains four redox active sites, one binuclear Cu site (Cu_a), haem *a*, and a haem *a*₃-Cu_b binuclear site, where oxygen is reduced to

water. Its natural electron donor is cyt *c* and in a number of publications cytochrome *c* oxidase has been coupled with electrodes through the use of cyt *c* acting as a mediator between the complex and the big cytochrome *c* oxidase and the electrode (see e.g., Rhoten *et al.*, 2000, 2002a, b; Katz *et al.*, 2004; Katz and Willner, 2003). DET between cytochrome *c* oxidase and an electrode was, however, also demonstrated when introduced into a lipid bilayer put on top of an octadecyl mercaptan-modified silver electrode deposited on gold electrodes (Burgess *et al.*, 1998).

ACKNOWLEDGMENTS

The authors thank the following organisations for financial support: The Swedish Research Council (Vetenskapsrådet), The European Commission (INCO project, Contract no. ICA2-CT-2000-10050) and Marie Curie Individual Fellowship, Contract no. QLK6-CT-2002-51580), The Wenner-Gren Foundations, The Swedish Institute, The Russian Foundation for Basic Research (Project no. 03-04-48937) and Novo Nordisk.

REFERENCES

- Adman, E.T., R.E. Stenkamp, L.C. Sieker and L.H. Jensen, 1978, A crystallographic model for azurin at 3Å resolution, *J. Mol. Biol.* 123, 35–47.
- Agostinelli, E., L. Cervoni, A. Giartosio and L. Morpurgo, 1995, Stability of Japanese-lacquer-tree (*Rhus vernicifera*) laccase to thermal and chemical denaturation: Comparison with ascorbate oxidase, *Biochem. J.* 306, 697–702.
- Aguey-Zinsou, K.-F., P.V. Bernhardt, U. Kappler and A.G. McEwan, 2003, Direct electrochemistry of a bacterial sulfite dehydrogenase, *J. Am. Chem. Soc.* 125, 530–535.
- Aizawa, M., 1991, Principles and applications of electrochemical and optical biosensors, *Anal. Chim. Acta* 250, 249–256.
- Albery, W.J., M.J. Eddowes, H.A.O. Hill and A.R. Hillman, 1981, Mechanism of the reduction and oxidation reaction of cytochrome *c* at a modified gold electrode, *J. Am. Chem. Soc.* 103, 3904–3910.
- Allendorf, M.D., D.J. Spira and E.I. Solomon, 1985, Low-temperature magnetic circular dichroism studies of native laccase: Spectroscopic evidence for exogenous ligand bridging at a trinuclear copper active site, *Proc. Natl. Acad. Sci. USA* 82, 3063–3067.
- Ameyama, M., E. Shinagawa, K. Matsushita and O. Adachi, 1981, D-Fructose dehydrogenase of *Gluconobacter industrius*: Purification, characterization, and application to enzymic microdetermination of D-fructose, *J. Bacteriol.* 145, 814–823.
- Amine, A., J. Deni and J.-M. Kauffmann, 1994, Amperometric biosensor based on carbon paste mixed with enzyme, lipid and cytochrome *c*, *Bioelectrochem. Bioenerg.* 34, 123–128.
- Amiot, P.L.O., S. Howell, P.D. Lee and H. Rieley, 2001, Apparatus and method for sensing metal ions, UK, WO 2001006235.
- Ander, P., 1994, The cellobiose-oxidizing enzymes CBQ and CbO as related to lignin and cellulose degradation – a review, *FEMS Microbiol. Rev.* 13, 297–312.
- Andolfi, L., D. Bruce, S. Cannistraro, G.W. Canters, J.J. Davis, H.A.O. Hill, J. Crozier, M.P. Verbeet, C.L. Wrathmell and Y. Astier, 2004, The electrochemical characteristics of blue copper protein monolayers on gold, *J. Electroanal. Chem.* 565, 21–28.
- Andreescu, D., S. Andreescu and O.A. Sadik, 2005, New materials for biosensors, biochips and molecular bioelectronics. Biosensors and Modern Biospecific Analytical Techniques, Vol. XLIV, Ed. L. Gorton, Elsevier, Amsterdam, pp. 285–327.

- Angove, H.C., J.A. Cole, D.J. Richardson and J.N. Butt, 2002, Protein film voltammetry reveals distinctive fingerprints of nitrite and hydroxylamine reduction by a cytochrome *c* nitrite reductase, *J. Biol. Chem.* 277, 23374–23381.
- Anthony, C., 1988, *Bacterial Energy Transduction*, Academic Press, San Diego.
- Antorini, M., I. Herpoel-Gimbert, T. Choinowski, J.-G. Sigoillot, M. Asther, K. Winterhalter and K. Piontek, 2002, Purification, crystallisation and X-ray diffraction study of fully functional laccases from two ligninolytic fungi, *Biochim. Biophys. Acta* 1594, 109–114.
- Armstrong, F.A., 1990, Probing metalloproteins by voltammetry, *Struct. Bond.* 72, 137–221.
- Armstrong, F.A., 2002, Protein film voltammetry: Revealing the mechanisms of biological oxidation and reduction, *Russ. J. Electrochem.* 38, 49–62.
- Armstrong, F.A., N.L. Barlow, P.L. Burn, K.R. Hoke, L.J.C. Jeuken, C. Shenton and G. R. Webster, 2004, Fast, long-range electron-transfer reactions of a “blue” copper protein coupled non-covalently to an electrode through a stilbenyl thiolate monolayer, *Chem. Commun. (UK)*, 316–317.
- Armstrong, F.A., H.A.O. Hill, B.N. Oliver and N.J. Walton, 1984, Direct electrochemistry of redox proteins at pyrolytic graphite electrodes, *J. Am. Chem. Soc.* 106, 921–923.
- Armstrong, F.A., H.A.O. Hill and N.J. Walton, 1988, Direct electrochemistry of redox proteins, *Acc. Chem. Res.* 21, 407–413.
- Armstrong, F.A. and A.M. Lannon, 1987, Fast interfacial electron transfer between cytochrome *c* peroxidase and graphite electrodes promoted by amyloglycosides: Novel electrocatalytic reduction of H₂O₂, *J. Am. Chem. Soc.* 109, 7211–7212.
- Arnold, S., Z.Q. Feng, T. Kakiuchi, W. Knoll and K. Niki, 1997, Investigation of the electrode reaction of cytochrome *c* through mixed self-assembled monolayers of alkanethiols on gold (111) surfaces, *J. Electroanal. Chem.* 438, 91–97.
- Avigliano, L., P. Vecchini, P. Sirianni, G. Marozzi, A. Marchesini and B. Mondovi, 1983, A reinvestigation on the quaternary structure of ascorbate oxidase from *Cucurbita pepo medullosa*, *Mol. Cell. Biochem.* 56, 107–112.
- Ayers, A.R., S.B. Ayers and K.-E. Eriksson, 1978, Cellobiose oxidase, purification and partial characterization of a hemoprotein from *Sporotrichum pulverulentum*, *Eur. J. Biochem.* 90, 171–181.
- Baeumner, A., 2005, *Bioanalytical microsystems: Technology and applications. Biosensors and Modern Biospecific Analytical Techniques*, Vol. XLIV, Ed. L. Gorton, Elsevier, Amsterdam, pp. 251–284.
- Baker, E.N., 1988, Structure of azurin from *Alcaligenes denitrificans*. Refinement at 1.8 Å resolution and comparison of the two crystallographically independent molecules, *J. Mol. Biol.* 203, 1071–1095.
- Balakshin, M., C.-L. Chen, J.S. Gratzl, A.G. Kirkman and H. Jakob, 2001, Biobleaching of pulp with dioxygen in laccase-mediator system – Effect of variables on the reaction kinetics, *J. Mol. Catal. B: Enz.* 16, 205–215.
- Baminger, U., S.S. Subramaniam, V. Renganathan and D. Haltrich, 2001, Purification and characterization of cellobiose dehydrogenase from the plant pathogen *Sclerotium (Athelia) rolfsii*, *Appl. Environ. Microbiol.* 67, 1766–1774.
- Barrett, F.M., 1987, Phenoloxidases from larval cuticle of the sheep blowfly, *Lucilia cuprina*: Characterization, developmental changes, and inhibition by antiphenoloxidase antibodies, *Arch. Insect Biochem. Physiol.* 5, 99–118.
- Barton, S.C., J. Gallaway and P. Atanassov, 2004, Enzymatic biofuel cells for implantable and microscale devices, *Chem. Rev.* 104, 4867–4886.
- Barton, S.C., H.-H. Kim, G. Binyamin, Y. Zhang and A. Heller, 2001, The “wired” laccase cathode: High current density electroreduction of O₂ to water at +0.7V (NHE) at pH 5, *J. Am. Chem. Soc.* 123, 5802–5803.
- Barton, S.C., M. Pickard, R. Vazquez-Duhalt and A. Heller, 2002, Electroreduction of O₂ to water at 0.6V (SHE) at pH 7 on the ‘wired’ *Pleurotus ostreatus* laccase cathode, *Biosens. Bioelectron.* 17, 1071–1074.

- Berenguer, J.J., A. Manjon and J.L. Iborra, 1989, A pH-tyrosinase biosensor for amino acids, catecholamines, and adrenergic drugs determination, *Biotechnol. Technol.* 3, 211–216.
- Berezin, I.V., V.A. Bogdanovskaya, S.D. Varfolomeev, M.R. Tarasevich and A.I. Yaroplov, 1978, Bioelectrocatalysis. Equilibrium oxygen potential in the presence of laccase, *Dokl. Akad. Nauk. SSSR* 240, 615–618.
- Bielli, P. and L. Calabrese, 2002, Structure to function relationships in ceruloplasmin: A “moonlighting” protein, *Cell. Mol. Life Sci.* 59, 1413–1427.
- Bistolas, N., A. Christenson, T. Ruzgas, C. Jung, F.W. Scheller and U. Wollenberger, 2004, Spectroelectrochemistry of cytochrome P450cam, *Biochem. Biophys. Res. Commun.* 314, 810–816.
- Bistolas, N., U. Wollenberger, C. Jung and F.W. Scheller, 2005, Cytochrome P450 biosensors — a review, *Biosens. Bioelectron.* 20, 2408–2423.
- Bogdanovskaya, V.A., V.A. Fridman, M.R. Tarasevich and F. Scheller, 1994, Bioelectrocatalysis by immobilized peroxidase: The reaction mechanism and the possibility of electroanalytical detection of both inhibitors and activators of enzyme, *Anal. Lett.* 27, 2823–2847.
- Bogdanovskaya, V.A., E.F. Gavriloza and M.R. Tarasevich, 1986, Influence of the state of carbon sorbents on the activity of immobilized phenol oxidases, *Elektrokhimiya* 22, 742–746.
- Bonagura, C.A., B. Bhaskar, H. Shimizu, H. Li, M. Sundaramoorthy, D.E. McRee, D.B. Goodin and T.L. Poulos, 2003, High-resolution crystal structures and spectroscopy of native and compound I cytochrome *c* peroxidase, *Biochemistry* 42, 5600–5608.
- Bond, A.M., 1994, Chemical and electrochemical approaches to the investigations of redox reactions of simple electron transfer metalloproteins, *Inorg. Chim. Acta* 226, 293–340.
- Bond, D.R. and D.R. Lovley, 2003, Electricity production by *Geobacter sulfurreducens* attached to electrodes, *Appl. Environ. Microbiol.* 69, 1548–1555.
- Borsari, M. and H.A. Azab, 1992, Voltammetric behavior of bovine erythrocyte superoxide dismutase, *Bioelectrochem. Bioenerg.* 27, 229–233.
- Brown, A.P. and F.C. Anson, 1978, Electron transfer with both reactant and product attached to the electrode surface, *J. Electroanal. Chem.* 92, 133–145.
- Burestedt, E., A. Navarez, T. Ruzgas, L. Gorton, J. Emnéus and G. Marko-Varga, 1996, Rate limiting steps of tyrosinase-modified electrodes for the detection of catechol., *Anal. Chem.* 68, 1605–1611.
- Burgess, J.D., M.C. Rhoten and F.M. Hawkrige, 1998, Observation of the resting and pulsed states of cytochrome *c* oxidase in electrode-supported lipid bilayer membranes, *J. Am. Chem. Soc.* 120, 4488–4491.
- Burrows, A.L., H.A.O. Hill, T.A. Leese, W.S. McIntire, H. Nakayama and G.S. Sanghera, 1991, Direct electrochemistry of the enzyme, methylamine dehydrogenase, from bacterium W3A1, *Eur. J. Biochem.* 199, 73–78.
- Call, H.P. and I. Mucke, 1997, History, overview and applications of mediated lignolytic systems, especially laccase-mediator-systems (Lignozym[®]-process), *J. Biotechnol.* 53, 163–202.
- Cameron, M.D. and S.D. Aust, 2000, Kinetics and reactivity of the flavin and heme cofactors of cellobiose dehydrogenase from *Phanerochaete chrysosporium*, *Biochemistry* 39, 13595–13601.
- Cameron, M.D. and S.D. Aust, 2001, Cellobiose dehydrogenase – An extracellular fungal flavocytochrome, *Enzyme Microb. Technol.* 28, 129–138.
- Campanella, L., A. Bonanni, E. Finotti and M. Tomassetti, 2004, Biosensors for determination of total and natural antioxidant capacity of red and white wines: Comparison with other spectrophotometric and fluorimetric methods, *Biosens. Bioelectron.* 19, 641–651.
- Campanella, L., G. Favero, L. Persi, M.P. Sammartino, M. Tomassetti and G. Visco, 2001, Organic phase enzyme electrodes: Applications and theoretical studies, *Anal. Chim. Acta* 426, 235–247.

- Carrico, R.J., B.G. Malmström and T. Vänngård, 1971, Reduction and oxidation of human ceruloplasmin. Evidence that a diamagnetic chromophore in the enzyme participates in the oxidase mechanism, *Eur. J. Biochem.* 22, 127–133.
- Cha, M.-K. and I.-H. Kim, 1999, Ceruloplasmin has a distinct active site for the catalyzing glutathione-dependent reduction of alkyl hydroperoxide, *Biochemistry* 38, 12104–12110.
- Chaudhuri, S.K. and D.R. Lovley, 2003, Electricity generation by direct oxidation of glucose in mediatorless microbial fuel cells, *Nat. Biotechnol.* 21, 1229–1232.
- Chen, X., H. Xie, J. Kong and J. Deng, 2001, Characterization for didodecyltrimethylammonium bromide crystal film entrapping catalase with enhanced direct electron transfer rate, *Biosens. Bioelectron.* 16, 115–120.
- Christenson, A., N. Dimcheva, E.E. Ferapontova, L. Gorton, T. Ruzgas, L. Stoica, S. Shleev, A.I. Yaropolov, D. Haltrich, R.N.F. Thorneley and S.D. Aust, 2004a, Direct electron transfer between ligninolytic redox enzymes and electrodes, *Electroanalysis* 16, 1074–1092.
- Christenson, A., E. Dock, L. Gorton and T. Ruzgas, 2004b, Direct heterogeneous electron transfer of theophylline oxidase, *Biosens. Bioelectron.* 20, 176–183.
- Clark, J.L.C. and C. Lyons, 1962, Electrode systems for continuous monitoring in cardiovascular surgery, *Ann. NY Acad. Sci.* 102, 29–45.
- Cooper, J.M., K.R. Greenough and C.J. McNeil, 1993, Direct electron transfer between immobilized cytochrome *c* and modified gold electrodes, *J. Electroanal. Chem.* 347, 267–275.
- Correia dos Santos, M.M., P.M. Paes de Sousa, M.L. Simoes Goncalves, L. Krippahl, J.J.G. Moura, E. Lojou and P. Bianco, 2003, Electrochemical studies on small electron transfer proteins using membrane electrodes, *J. Electroanal. Chem.* 541, 153–162.
- Correia dos Santos, M.M., P.M.P. Sousa, M.L.S. Goncalves, M.J. Romao, I. Moura and J.J.G. Moura, 2004, Direct electrochemistry of the *Desulfovibrio gigas* aldehyde oxidoreductase, *Eur. J. Biochem.* 271, 1329–1338.
- Cosnier, S. and C. Innocent, 1993, A new strategy for the construction of a tyrosinase-based amperometric phenol and *o*-diphenol sensor, *Bioelectrochem. Bioenerg.* 31, 147–160.
- Csőregi, E., L. Gorton and G. Marko-Varga, 1993a, Carbon fibre as electrode materials for the construction of peroxidase modified amperometric biosensors, *Anal. Chim. Acta* 273, 59–70.
- Csőregi, E., G. Jönsson-Pettersson and L. Gorton, 1993b, Mediatorless electrocatalytic reduction of hydrogen peroxide at graphite electrodes chemically modified with peroxidases, *J. Biotechnol.* 30, 315–337.
- Csőregi, E., L. Gorton and G. Marko-Varga, 1994a, Amperometric microbiosensors for detection of hydrogen peroxide and glucose based on peroxidase modified carbon fibres, *Electroanalysis* 6, 925–933.
- Csőregi, E., L. Gorton, G. Marko-Varga, A. Tüdös and T.W. Kok, 1994b, Peroxidase modified carbon fiber microelectrodes in flow system for detection of hydrogen peroxide and organic peroxides, *Anal. Chem.* 66, 3604–3610.
- Cusanovich, M.A. and G. Tollin, 1996, Kinetics of electron transfer of *c*-type cytochromes with small reagents, *Cytochrome c: A Multidisciplinary Approach*, Eds. R.A. Scott and A.G. Mauk, University Science Books, Sausalito, pp. 489–513.
- Daigle, F., F. Trudeau, G. Robinson, M.R. Smyth and D. Leech, 1998, Mediated reagentless enzyme inhibition electrodes, *Biosens. Bioelectron.* 13, 417–425.
- Davidson, V.L., Ed., 1993, *Principles and Applications of Quinoproteins*, Marcel Dekker, New York.
- Davidson, V.L., 2004, Electron transfer in quinoproteins, *Arch. Biochem. Biophys.* 428, 32–40.
- Davidson, V.L. and L.H. Jones, 1991, Intermolecular electron transfer from quinoproteins and its relevance to biosensor technology, *Anal. Chim. Acta* 249, 235–240.
- de Castro, A.F., S.K. Gupta and A.K. Agarwal, 1989, Enzymic determination of theophylline, *WO 8907653 A1 19890824*.
- De Ley, M. and S. Osaki, 1975, Intramolecular electron transport in human ferroxidase (ceruloplasmin), *Biochem. J.* 151, 561–566.

- Degani, Y. and A. Heller, 1987, Direct electrical communication between chemically modified enzymes and metal electrodes. I. Electron transfer from glucose oxidase to metal electrodes via electron relays, bound covalently to the enzyme, *J. Phys. Chem.* 91, 1285–1289.
- Deinum, J. and T. Vänngård, 1973, The stoichiometry of the paramagnetic copper and the oxidation–reduction potentials of type I copper in human ceruloplasmin, *Biochim. Biophys. Acta* 310, 321–330.
- Deverall, B.J., 1961, Phenolase and pectic enzyme activity in chocolate spot disease of beans, *Nature* 189, 311.
- Dryhurst, G., K.M. Kadish, F. Scheller and R. Renneberg, Eds., 1982, *Biological Electrochemistry*, Academic Press, New York.
- Ducros, V., A.M. Brzozowski, K.S. Wilson, S.H. Brown, P. Østergaard, P. Schneider, D.S. Yaver, A.H. Pedersen and G.J. Davies, 1998, Crystal structure of the type-2 Cu depleted laccase from *Coprinus cinereus* at 2.2Å resolution, *Nat. Struct. Biol.* 5, 310–316.
- Duine, J.A., 1991, Quinoproteins: Enzymes containing the quinoid cofactor pyrroloquinoline quinone, topaquinone or tryptophan–tryptophan quinone, *Eur. J. Biochem.* 200, 271–284.
- Duine, J.A., 1995, The importance of natural diversity in redox proteins for achieving cofactor-directed electron transfer, *Biosens. Bioelectron.* 10, 17–23.
- Duine, J.A., 2001, Cofactor diversity in biological oxidations: Implications and applications, *Chem. Record* 1, 74–83.
- Duine, J.A., J. Frank and J.A. Jongjan, 1987, Enzymology of quinoproteins, *Adv. Enzymol. Relat. Areas Mol. Biol.* 59, 165–212.
- Dunford, H.B., 1999, *Heme Peroxidases*, Wiley, New York.
- Duran, N., M.A. Rosa, A. D’Annibale and L. Gianfreda, 2002, Applications of laccases and tyrosinases (phenoloxidases) immobilized on different supports: A review, *Enz. Microb. Technol.* 31, 907–931.
- Eddowes, M.J. and H.A.O. Hill, 1977, Novel method for the investigation of the electrochemistry of metalloproteins: cytochrome *c*, *J. Chem. Soc., Chem. Commun.* 771–772.
- Eddowes, M.J., H.A.O. Hill and K. Uosaki, 1979, Electrochemistry of cytochrome *c*, Comparison of the electron-transfer at a surface-modified gold electrode with that to cytochrome-oxidase. *J. Am. Chem. Soc.* 101, 7113–7114.
- Eddowes, M.J., H.A.O. Hill and K. Uosaki, 1980, The electrochemistry of cytochrome *c*. Investigation of the mechanism of the 4,4'-bipyridyl surface modified gold electrode, *Bioelectrochem. Bioenerg.* 7, 527–537.
- El Kasmi, A., J.M. Wallace, E.F. Bowden, S.M. Binet and R.J. Linderman, 1998, Controlling interfacial electron-transfer kinetics of cytochrome *c* with mixed self-assembled monolayers, *J. Am. Chem. Soc.* 120, 225–226.
- Elliott, S.J., K.R. Hoke, K. Heffron, M. Palak, R.A. Rothery, J.H. Weiner and F.A. Armstrong, 2004, Voltammetric studies of the catalytic mechanism of the respiratory nitrate reductase from *Escherichia coli*: How nitrate reduction and inhibition depend on the oxidation state of the active site, *Biochemistry* 43, 799–807.
- Elliott, S.J., A.E. McElhaney, C. Feng, J.H. Enemark and F.A. Armstrong, 2002, A voltammetric study of interdomain electron transfer within sulfite oxidase, *J. Am. Chem. Soc.* 124, 11612–11613.
- Enemark, J.H., J.J.A. Cooney, J.-J. Wang and R.H. Holm, 2004, Synthetic analogues and reaction systems relevant to the molybdenum and tungsten oxotransferases, *Chem. Rev.* 104, 1175–1200.
- Enguita, F.J., L.O. Martins, A.O. Henriques and M.A. Carrondo, 2003, Crystal structure of a bacterial endospore coat component: A laccase with enhanced thermostability properties, *J. Biol. Chem.* 278, 19416–19425.
- Esaka, M., K. Fujisawa, M. Goto and Y. Kisu, 1992, Regulation of ascorbate oxidase expression in pumpkin by auxin and copper, *Plant Physiol.* 100, 231–237.
- Fantuzzi, A., M. Fairhead and G. Gilardi, 2004, Direct electrochemistry of immobilized human cytochrome P450 2E1, *J. Am. Chem. Soc.* 126, 5040–5041.
- Farhangrazi, Z.S., M.E. Fossett, L.S. Powers and W.R. Ellis, Jr., 1995, Variable-temperature spectroelectrochemical study of horseradish peroxidase, *Biochemistry* 34, 2866–2871.

- Farrar, J.A., A.J. Thomson, M.R. Cheesman, D.M. Dooley and W.G. Zumft, 1991, A model of the copper centers of nitrous oxide reductase (*Pseudomonas stutzeri*). Evidence from optical, EPR and MCD spectroscopy, *FEBS Lett.* 294, 11–15.
- Feng, C., R.V. Kedia, J.T. Hazzard, J.K. Hurley, G. Tollin and J.H. Enemark, 2002, Effect of solution viscosity on intramolecular electron transfer in sulfite oxidase, *Biochemistry* 41, 5816–5821.
- Feng, C.J., H.L. Wilson, J.K. Hurley, J.T. Hazzard, G. Tollin, K.V. Rajagopalan and J.H. Enemark, 2003, Essential role of conserved arginine 160 in intramolecular electron transfer in human sulfite oxidase, *Biochemistry* 42, 12235–12242.
- Feng, Z.Q., S. Imabayashi, T. Kakiuchi and K. Niki, 1997, Long-range electron-transfer reaction rates to cytochrome *c* across long- and short-chain alkanethiol self-assembled monolayers: Electroreflectance studies, *J. Chem. Soc., Farad. Trans.* 93, 1367–1370.
- Feng, Z.Q., T. Sagara and K. Niki, 1995, Application of potential-modulated UV–visible reflectance spectroscopy to electron transfer rate measurements for adsorbed species on electrode surfaces, *Anal. Chem.* 67, 3564–3570.
- Ferapontova, E.E., 2004, Direct peroxidase bioelectrocatalysis on a variety of electrode materials, *Electroanalysis* 16, 1101–1112.
- Ferapontova, E.E., A. Christenson, A. Hellmark and T. Ruzgas, 2004, Spectroelectrochemical study of heme- and molybdopterin cofactor-containing chicken liver sulphite oxidase, *Bioelectrochemistry* 63, 49–53.
- Ferapontova, E.E. and N.V. Fedorovich, 1999, Effect of cation adsorption on the kinetics of anion electroreduction Part I. Effect of the adsorption of inorganic cations in small concentrations on the kinetics of anion electroreduction with different elementary steps of discharge, *J. Electroanal. Chem.* 476, 26–36.
- Ferapontova, E.E. and L. Gorton, 2001, Effect of proton donors on direct electron transfer in the system gold electrode-horseradish peroxidase, *Electrochem. Commun.* 3, 767–774.
- Ferapontova, E. and L. Gorton, 2002, Effect of pH on direct electron transfer in the system gold electrode-recombinant horseradish peroxidase, *Bioelectrochemistry* 55, 83–87.
- Ferapontova, E.E. and L. Gorton, 2005, Direct electrochemistry of heme multifactor-containing enzymes on alkanethiol-modified gold electrodes, *Bioelectrochemistry* 66, 55–63.
- Ferapontova, E.E., V.G. Grigorenko, A.M. Egorov, T. Borchers, T. Ruzgas and L. Gorton, 2001a, Direct electron transfer in the system gold electrode-recombinant horseradish peroxidases, *J. Electroanal. Chem.* 509, 19–26.
- Ferapontova, E.E., V.G. Grigorenko, A.M. Egorov, T. Borchers, T. Ruzgas and L. Gorton, 2001b, Mediatorless biosensor for H₂O₂ based on recombinant forms of horseradish peroxidase directly adsorbed on polycrystalline gold, *Biosens. Bioelectron.* 16, 147–157.
- Ferapontova, E. and E. Pukanova, 2002, Effect of pH on direct electron transfer between graphite and horseradish peroxidase, *J. Electroanal. Chem.* 518, 20–26.
- Ferapontova, E., K. Schmengler, T. Borchers, T. Ruzgas and L. Gorton, 2002a, Effect of cysteine mutations on direct electron transfer of horseradish peroxidase on gold, *Biosens. Bioelectron.* 17, 953–963.
- Ferapontova, E.E., N.S. Reading, S.D. Aust, T. Ruzgas and L. Gorton, 2002b, Direct electron transfer between graphite electrodes and ligninolytic peroxidases from *Phanerochaete chrysosporium*, *Electroanalysis* 14, 1411–1418.
- Ferapontova, E.E., T. Ruzgas and L. Gorton, 2003, Direct electron transfer of heme- and molybdopterin cofactor-containing chicken liver sulfite oxidase on alkanethiol-modified gold electrodes, *Anal. Chem.* 75, 4841–4850.
- Finklea, H.O., 1996, Electrochemistry of organized monolayers of thiols and related molecules on electrodes. *Electroanalytical Chemistry*, Vol. 19, Ed. A.J. Bard, Marcel Dekker, New York, pp. 114–335.
- Freire, R.S., N. Duran and L.T. Kubota, 2001, Effects of fungal laccase immobilization procedures for the development of a biosensor for phenol compounds, *Talanta* 54, 681–686.

- Freire, R.S., C.A. Pessoa, L.D. Mello and L.T. Kubota, 2003, Direct electron transfer: An approach for electrochemical biosensors with higher selectivity and sensitivity, *J. Braz. Chem. Soc.* 14, 230–243.
- Fridman, V.A., V.A. Bogdanovskaya and M.R. Tarasevich, 1994, Kinetics and mechanism of peroxidase redox transformations on a carbon material, *Elektrokhimiya* 30, 807–811.
- Fridman, V., U. Wollenberger, V. Bogdanovskaya, F. Lisdat, T. Ruzgas, A. Lindgren, L. Gorton and F.W. Scheller, 2000, Electrochemical investigation of cellobiose oxidation by cellobiose dehydrogenase in the presence of cytochrome *c* as mediator, *Biochem. Soc. Trans.* 28, 63–70.
- Fridovich, I., 1978, The biology of oxygen radicals, *Science* 201, 875–880.
- Frieden, E. and H.S. Hsieh, 1976, Ceruloplasmin: The copper transport protein with essential oxidase activity, *Adv. Enzymol. Relat. Areas Mol. Biol.* 44, 187–236.
- Fujieda, N., M. Mori, K. Kano and T. Ikeda, 2002, Spectroelectrochemical evaluation of redox potentials of cysteine tryptophylquinone and two hemes *c* in quinohemoprotein amine dehydrogenase from *Paracoccus denitrificans*, *Biochemistry* 41, 13736–13743.
- Gajhede, M., D.J. Schuller, A. Henriksen, A.T. Smith and T.L. Poulos, 1997, Crystal structure of horseradish peroxidase C at 2.5Å resolution, *Nat. Struct. Biol.* 4, 1032–1038.
- Gaspar, S., H. Zimmermann, I. Gazaryan, E. Csöregi and W. Schuhmann, 2001, Hydrogen peroxide biosensors based on direct electron transfer from plant peroxidases immobilized on self-assembled thiol-monolayer modified gold electrodes, *Electroanalysis* 13, 284–288.
- Gazarian, I.G., L.M. Lagrimini, S.J. George and R.N.F. Thorneley, 1996, Anionic tobacco peroxidase is active at extremely low pH: Veratryl alcohol oxidation with a pH optimum of 1.8, *Biochem. J.* 320, 369–372.
- Gazaryan, I.G., L.M. Lagrimini, G.A. Ashby and R.N.F. Thorneley, 1996, Mechanism of indole-3-acetic acid oxidation by plant peroxidases: Anaerobic stopped-flow spectrophotometric studies on horseradish and tobacco peroxidases, *Biochem. J.* 313, 841–847.
- Ge, B. and F. Lisdat, 2002, Superoxide sensor based on cytochrome *c* immobilized on mixed-thiol SAM with a new calibration method, *Anal. Chim. Acta* 454, 53–64.
- Ge, B., F.W. Scheller and F. Lisdat, 2003, Electrochemistry of immobilized CuZnSOD and FeSOD and their interaction with superoxide radicals, *Biosens. Bioelectron.* 18, 295–302.
- Gelo-Pujic, M., H.H. Kim, N.G. Butlin and G.T. Palmore, 1999, Electrochemical studies of a truncated laccase produced in *Pichia pastoris*, *Appl. Environ. Microbiol.* 65, 5515–5521.
- Ghindilis, A., 2000, Direct electron transfer catalyzed by enzymes: Application for biosensor development, *Biochem. Soc. Trans.* 28, 84–89.
- Ghindilis, A.L., P. Atanasov and E. Wilkins, 1997, Enzyme-catalyzed direct electron transfer: Fundamentals and analytical applications, *Electroanalysis* 9, 661–674.
- Gilardi, G., T. den Blaauwen and G.W. Canters, 1994, Molecular recognition – design of a biosensor with genetically engineered azurin as redox mediator, *J. Control. Release* 29, 231–238.
- Givaudan, A., A. Effosse, D. Faure, P. Potier, M.L. Bouillant and R. Bally, 1993, Polyphenol oxidase in *Azospirillum lipoferum* isolated from rice rhizosphere: Evidence for laccase activity in nonmotile strains of *Azospirillum lipoferum*, *FEMS Microbiol. Lett.* 108, 205–210.
- Gorton, L., 1995, Carbon paste electrodes chemically modified with enzymes, tissues and cells. A review, *Electroanalysis* 7, 23–45.
- Gorton, L., G. Bremle, E. Csöregi, G. Jönsson-Pettersson and B. Persson, 1991a, Amperometric glucose sensors based on immobilised glucose oxidising enzymes and chemically modified electrodes, *Anal. Chim. Acta* 249, 43–54.
- Gorton, L., E. Csöregi, E. Domínguez, J. Emnéus, G. Jönsson-Pettersson, G. Marko-Varga and B. Persson, 1991b, Selective detection in flow analysis based on the combination of immobilised enzymes and chemically modified electrodes, *Anal. Chim. Acta* 250, 203–248.
- Gorton, L., E. Domínguez, G. Marko-Varga, B. Persson, G. Jönsson-Pettersson, E. Csöregi, K. Johansson, D. Narasiah, S. Ghobadi, V. Kacaniklic, T. Skotheim, P. Hale, Y. Okamoto and H.-L. Lan, 1992, Amperometric biosensors based on immobilized redox-enzymes in carbon paste electrodes, *Bioelectroanalysis*, Ed. E. Pungor, Akadémiai Kiadó, Budapest, Hungary, pp. 33–52.

- Gorton, L., A. Lindgren, T. Larsson, F.D. Munteanu, T. Ruzgas and I. Gazaryan, 1999, Direct electron transfer between heme-containing enzymes and electrodes as basis for third generation biosensors, *Anal. Chim. Acta* 400, 91–108.
- Grass, G. and C. Rensing, 2001, CueO is a multi-copper oxidase that confers copper tolerance in *Escherichia coli*, *Biochem. Biophys. Res. Commun.* 286, 902–908.
- Gray, H.B. and J.R. Winkler, 2003, Electron tunneling through proteins, *Quart. Rev. Biophys.* 36, 341–372.
- Grigorenko, V., T. Chubar, Y. Kapeliuch, T. Borchers, F. Spener and A. Egorov, 1999, New approaches for functional expression of recombinant horseradish peroxidase C in *Escherichia coli*, *Biocatal. Biotransform.* 17, 359–379.
- Gunnarsson, P.O., U. Nylén and G. Pettersson, 1973, Kinetics of the interaction between ceruloplasmin and reducing substrates, *Eur. J. Biochem.* 37, 41–46.
- Guo, L.-H. and H.A.O. Hill, 1991, Direct electrochemistry of proteins and enzymes, *Adv. Inorg. Chem.* 36, 341–375.
- Guo, L.H., H.A.O. Hill, D.J. Hopper, G.A. Lawrance and G.S. Sanghera, 1990, Direct voltammetry of the *Chromatium vinosum* enzyme, sulfide-cytochrome-*c* oxidoreductase (flavocytochrome-*c*₅₅₂), *J. Biol. Chem.* 265, 1958–1963.
- Guo, L.H., H.A.O. Hill, G.A. Lawrance, G.S. Sanghera and D.J. Hopper, 1989, Direct unmediated electrochemistry of the enzyme *p*-cresolmethylhydroxylase, *J. Electroanal. Chem.* 266, 379–396.
- Guo, J., X.X. Liang, P.S. Mo and G.X. Li, 1991, Purification and properties of bilirubin oxidase from *Myrothecium verrucaria*, *Appl. Biochem. Biotechnol.* 31, 135–143.
- Gupta, S.K., A.K. Agarwal and A.F. deCastro, 1988, A novel enzymatic approach for serum theophylline measurement, *Clin. Chem.* 34, 1267.
- Gupta, G., V. Rajendran and P. Atanassov, 2004, Bioelectrocatalysis of oxygen reduction reaction by laccase on gold electrode, *Electroanalysis* 16, 1182–1185.
- Haas, A.S., D.L. Pilloud, K.S. Reddy, G.T. Babcock, C.C. Moser, J.K. Blasié and P.L. Dutton, 2001, Cytochrome *c* and cytochrome *c* oxidase: Monolayer assemblies and catalysis, *J. Phys. Chem. B* 105, 11351–11362.
- Haghighi, B., L. Gorton, T. Ruzgas and L.J. Jönsson, 2003, Characterization of graphite electrodes modified with laccase from *Trametes versicolor* and their use for bioelectrochemical monitoring of phenolic compounds in flow injection analysis, *Anal. Chim. Acta* 487, 3–14.
- Hakulinen, N., L.-L. Kiiskinen, K. Kruus, M. Saloheimo, A. Paananen, A. Koivula and J. Rouvinen, 2002, Crystal structure of a laccase from *Melanocarpus albomyces* with an intact trinuclear copper site, *Nat. Struct. Biol.* 9, 601–605.
- Haladjian, J., P. Bianco, F. Nunzi and M. Bruschi, 1994, A permselective-membrane electrode for the electrochemical study of redox proteins. Application to cytochrome *c*₅₅₂ from *Thiobacillus ferrooxidans*, *Anal. Chim. Acta* 289, 15–20.
- Hale, P.D. and T.A. Skotheim, 1989, Cyclic voltammetry at TCNQ and TTF-TCNQ modified platinum electrodes: A study of the glucose oxidase/glucose and galactose oxidase/galactose system, *Synth. Met.* 28, C853–C858.
- Hällberg, B.M., 2002. Structural studies on the extracellular flavocytochrome cellobiose dehydrogenase from *Phanerochaete chrysosporium*, Doctoral thesis, Uppsala University, Uppsala, Sweden.
- Hällberg, B.M., T. Bergfors, K. Backbro, G. Pettersson, G. Henriksson and C. Divne, 2000, A new scaffold for binding heme in the cytochrome domain of the extracellular flavocytochrome cellobiose dehydrogenase, *Structure* 8, 79–88.
- Harbury, H.A., 1957, Oxidation–reduction potentials of horseradish peroxidase, *J. Biol. Chem.* 225, 1009–1024.
- Hayashi, Y. and I. Yamazaki, 1979, The oxidation–reduction potentials of compound I/compound II and compound II/ferric couples of horseradish peroxidases A2 and C, *J. Biol. Chem.* 254, 9101–9106.
- He, B., R. Sinclair, B.R. Copeland, R. Makino, L.S. Powers and I. Yamazaki, 1996, The structure–function relationship and reduction potentials of high oxidation states of myoglobin and peroxidase, *Biochemistry* 35, 2413–2420.

- Hedenmo, M., A. Narváez, E. Domínguez and I. Katakis, 1997, Improved mediated tyrosinase amperometric enzyme electrodes, *J. Electroanal. Chem.* 425, 1–11.
- Heering, H.A., J.H. Weiner and F.A. Armstrong, 1997, Direct detection and measurement of electron relays in a multicentered enzyme: Voltammetry of electrode-surface films of *E. coli* fumarate reductase, an iron-sulfur flavoprotein, *J. Am. Chem. Soc.* 119, 11628–11638.
- Heffron, K., C. Leger, R.A. Rothery, J.H. Weiner and F.A. Armstrong, 2001, Determination of an optimal potential window for catalysis by *E. coli* dimethyl sulfoxide reductase and hypothesis on the role of Mo(V) in the reaction pathway, *Biochemistry* 40, 3117–3126.
- Heller, A., 2004, Miniature biofuel cells, *Phys. Chem. Chem. Phys.* 6, 209–216.
- Heller, A. and Y. Degani, 1988, Direct electrical communication between chemically modified enzymes and metal electrodes. 2. Methods for bonding electron-transfer relays to glucose oxidase and D-amino-acid oxidase, *J. Am. Chem. Soc.* 110, 2615–2620.
- Henriksson, G., G. Johansson and G. Pettersson, 2000, A critical review of cellobiose dehydrogenase, *J. Biotechnol.* 78, 93–113.
- Henriksson, G., V. Sild, I. Szabo, G. Pettersson and G. Johansson, 1998, Substrate specificity of cellobiose dehydrogenase from *Phanerochaete chrysosporium*, *Biochim. Biophys. Acta* 1383, 48–54.
- Hill, H.A.O., L.H. Guo and G. McLendon, 1996, Direct electrochemistry of cytochrome *c*, *Cytochrome c: A Multidisciplinary Approach*, Eds. R.A. Scott and A.G. Mauk, University Science Books, Sausalito, pp. 317–333.
- Hill, H.A.O. and N.I. Hunt, 1993, Direct and indirect electrochemical investigations of metalloenzymes. *Methods in Enzymology*, Vol. 227, Eds. J.F. Riordan, B.L. Vallee, Academic Press, San Diego, pp. 501–522.
- Hille, R., 1996, The mononuclear molybdenum enzymes, *Chem. Rev.* 96, 2757–2816.
- Hirose, J., K. Inoue, H. Sakuragi, M. Kikkawa, M. Minakami, T. Morikawa, H. Iwamoto and K. Hiromi, 1998, Anions binding to bilirubin oxidase from *Trachyderma tsunoda* K-2593, *Inorg. Chim. Acta* 273, 204–212.
- Hirst, J., A. Sucheta, B.A.C. Ackrell and F.A. Armstrong, 1996, Electrocatalytic voltammetry of succinate dehydrogenase: Direct quantification of the catalytic properties of a complex electron-transport enzyme, *J. Am. Chem. Soc.* 118, 5031–5038.
- Ho, W.O., D. Athey, C.J. McNeil, H.J. Hager, G.P. Evans and W.H. Mullen, 1993, Mediatorless horseradish peroxidase enzyme electrodes based on activated carbon: Potential application to specific binding assay, *J. Electroanal. Chem.* 351, 185–197.
- Hoke, K.R., N. Cobb, F.A. Armstrong and R. Hille, 2004, Electrochemical studies of arsenite oxidase: An unusual example of a highly cooperative two-electron molybdenum center, *Biochemistry* 43, 1667–1674.
- Hyde, S.M. and P.M. Wood, 1996, Kinetic and antigenic similarities for cellobiose dehydrogenase from brown rot fungus *Coniophora puteana* and the white rot fungus *Phanerochaete chrysosporium*, *FEMS Microbiol. Lett.* 145, 439–444.
- Härtl, A., E. Schmich, J.A. Garrido, J. Hernando, S.C.R. Catharino, S. Walter, P. Feulner, A. Kromka, D. Steinmüller and M. Stutzmann, 2004, Protein-modified nanocrystalline diamond thin films for biosensor applications, *Nat. Mater.* 3, 736–742.
- Igarashi, K., I. Momohara, T. Nishino and M. Samejima, 2002, Kinetics of inter-domain electron transfer in flavocytochrome cellobiose dehydrogenase from the white-rot fungus *Phanerochaete chrysosporium*, *Biochem. J.* 365, 521–526.
- Igarashi, K., M.F.J.M. Verhagen, M. Samejima, M. Schülein, K.-E. Eriksson and T. Nishino, 1999, Cellobiose dehydrogenase from the fungi *Phanerochaete chrysosporium* and *Humicola insolens*, *J. Biol. Chem.* 274, 3338–3344.
- Ikeda, T., 1992, Electrochemical biosensors based on biocatalyst electrodes, *Bull. Electrochem.* 8, 145–159.
- Ikeda, T., 1997, Direct redox communication between enzymes and electrodes, *Frontiers in Biosensorics*, Vol. 1, Eds. F.W. Scheller, F. Schubert and J. Fedrowitz, Birkhäuser, Basel, pp. 243–266.
- Ikeda, T., F. Fushimi, K. Miki and M. Senda, 1988, Direct bioelectrocatalysis at electrodes modified with D-gluconate dehydrogenase, *Agric. Biol. Chem.* 52, 2655–2658.

- Ikeda, T., F. Fushimi, K. Miki and M. Senda, 1989, Amperometric biosensors based on quinoprotein-flavoprotein-dehydrogenases: Methods of steady-state current measurements and voltammetric measurements at higher sensitivity, *Bunseki Kagaku* 38, 583–588.
- Ikeda, T., D. Kobayashi, F. Matsushita, T. Sagara and K. Niki, 1993a, Bioelectrocatalysis at electrodes coated with alcohol dehydrogenase, a quinoxaline protein with heme *c* serving as a built-in mediator, *J. Electroanal. Chem.* 361, 221–228.
- Ikeda, T., S. Miyaoka and K. Miki, 1993b, Enzyme-catalyzed electrochemical oxidation of D-gluconate at electrodes coated with D-gluconate dehydrogenase, a membrane-bound flavohemoprotein, *J. Electroanal. Chem.* 352, 267–278.
- Ikeda, T., F. Matsushita and M. Senda, 1991, Amperometric fructose sensor based on direct bioelectrocatalysis, *Biosens. Bioelectron.* 6, 299–304.
- Ikeda, T., S. Miyaoka, F. Matsushita, D. Kobayashi and M. Senda, 1992, Direct bioelectrocatalysis at metal and carbon electrodes modified with adsorbed D-gluconate dehydrogenase or adsorbed alcohol dehydrogenase from bacterial membranes, *Chem. Lett.* 847–850.
- Itoh, H., A. Hirota, K. Hirayama, T. Shin and S. Murao, 1995, Properties of ascorbate oxidase produced by *Acremonium* sp. HI-25, *Biosci. Biotechnol. Biochem.* 59, 1052–1056.
- Iwata, S., C. Ostermeier, B. Ludwig and H. Michel, 1995, Structure at 2.8 Å resolution of cytochrome *c* oxidase from *Paracoccus denitrificans*, *Nature* 376, 660–669.
- Jarosz-Wilkolazka, A., G. Janusz, T. Ruzgas, L. Gorton, E. Malarczyc and A. Leonowicz, 2004a, Development of a laccase modified electrode for amperometric detection of mono- and diphenols: I. Influence of the enzyme storage method, *Anal. Lett.* 37, 1497–1513.
- Jarosz-Wilkolazka, A., T. Ruzgas and L. Gorton, 2004b, Use of laccase-modified electrode for amperometric detection of plant flavonoids, *Enzyme Microb. Technol.* 35, 238–241.
- Jeuken, L.J.C., 2003, Conformational reorganisation in interfacial protein electron transfer, *Biochim. Biophys. Acta* 1604, 67–76.
- Jeuken, L.J.C., J.P. McEvoy and F.A. Armstrong, 2002, Insights into gated electron-transfer kinetics at the electrode-protein interface: A square wave voltammetry study of the blue copper protein azurin, *J. Phys. Chem. B* 106, 2304–2313.
- Jeuken, L.J.C., P. van Vliet, M.P. Verbeet, R. Camba, J.P. McEvoy, F.A. Armstrong and G.W. Canters, 2000, Role of the surface-exposed and copper-coordinating histidine in blue copper proteins: The electron-transfer and redox-coupled ligand binding properties of His117Gly azurin, *J. Am. Chem. Soc.* 122, 12186–12194.
- Jia, N.Q., Z.R. Zhang, J.Z. Zhu and G.X. Zhang, 2003, A galactose biosensor based on the microfabricated thin film electrode, *Anal. Lett.* 36, 2095–2106.
- Jin, L., H. Liu and Y. Fang, 1992, Ascorbic acid oxidase biosensor based on the glassy carbon electrode modified with Nafion and methyl viologen, *Fenxi Huaxue* 20, 515–519.
- Jin, W., U. Wollenberger, F.F. Bier, A. Makower and F.W. Scheller, 1996, Electron transfer between cytochrome *c* and copper enzymes, *Bioelectrochem. Bioenerg.* 39, 221–225.
- João Romão, M., J. Knäblein, R. Huber and J.J.G. Moura, 1997, Structure and function of molybdopterin containing enzymes, *Prog. Biophys. Molec. Biol.* 68, 121–144.
- Johansen, C., 1996, A basic protein composition for killing or inhibiting microbial cells, *Wo, Wo* 9606532 A1 19960307.
- Johnson, D.L., J.L. Thompson, S.M. Brinkmann, K.A. Schuller and L.L. Martin, 2003, Electrochemical characterization of purified *Rhus vernicifera* laccase: Voltammetric evidence for a sequential four-electron transfer, *Biochemistry* 42, 10229–10237.
- Jönsson, G. and L. Gorton, 1989, An electrochemical sensor for hydrogen peroxide based on peroxidase adsorbed on a spectrographic graphite electrode, *Electroanalysis* 1, 465–468.
- Kaim, W. and J. Rall, 1996, Copper – A “modern” bioelement, *Angew. Chem. Int. Ed. Engl.* 35, 43–60.
- Karamyshev, A.V., S.V. Shleev, O.V. Koroleva, A.I. Yaropolov and I.Y. Sakharov, 2003, Laccase-catalyzed synthesis of conducting polyaniline, *Enz. Microb. Technol.* 33, 556–564.
- Kassner, R.J., 1972, Effects of nonpolar environments on the redox potentials of heme complexes, *Proc. Nat. Acad. Sci. USA* 69, 2263–2267.

- Katz, E., O. Lioubashevski and I. Willner, 2004, Magnetic field effects on cytochrome *c*-mediated bioelectrocatalytic transformations, *J. Am Chem. Soc.* 126, 11088–11092.
- Katz, E., D.D. Schlereth, H.-L. Schmidt and A.J.J. Olsthoorn, 1994, Reconstitution of the quinoprotein glucose dehydrogenase from its apoenzyme on a gold electrode surface modified with a monolayer of pyrroloquinoline quinone, *J. Electroanal. Chem.* 368, 165–171.
- Katz, E. and I. Willner, 2003, A biofuel cell with electrochemically switchable and tunable power output, *J. Am Chem. Soc.* 125, 6803–6813.
- Kawahara, K., S. Suzuki, T. Sakurai and A. Nakahara, 1984, Characterization of cucumber ascorbate oxidase and its reaction with hexacyanoferrate (II), *Arch. Biochem. Biophys.* 241, 179–186.
- Khan, G.F., H. Shinohara, Y. Ikariyama and M. Aizawa, 1991, Electrochemical behavior of monolayer quinoprotein adsorbed on the electrode surface, *J. Electroanal. Chem.* 315, 263–273.
- Kinnear, K.T. and H.G. Monbouquette, 1993, Direct electron transfer to *Escherichia coli* fumarate reductase in self-assembled alkanethiol monolayers on gold electrodes, *Langmuir* 9, 2255–2257.
- Kisker, C., H. Schindelin, A. Pacheco, W.A. Wehbi, R.M. Garret, K.V. Rajagopalan, J.H. Enemark and D.C. Rees, 1997a, Molecular basis of sulfite oxidase deficiency from the structure of sulfite oxidase, *Cell* 91, 973–983.
- Kisker, C., H. Schindelin and D.C. Rees, 1997b, Molybdenum-cofactor-containing enzymes: Structure and mechanism, *Ann. Rev. Biochem.* 66, 233–267.
- Klabunde, T., C. Eicken, J.C. Sacchettini and B. Krebs, 1998, Crystal structure of a plant catechol oxidase containing a dicopper center, *Nat. Struct. Biol.* 5, 1084–1090.
- Kobayashi, D., S. Qzawa, T. Mihara and T. Ikeda, 1992, Flavoenzyme-catalyzed electrochemical oxidation of NADH and NADPH in the absence of external mediators, *Denki Kagaku* 60, 1056–1062.
- Kohzuma, T., S. Shidara and S. Suzuki, 1994, Direct electrochemistry of nitrite reductase from *Achromobacter cycloclastes* IAM 1013, *Bull. Chem. Soc. Japan* 67, 138–143.
- Kojima, Y., Y. Tsukuda, Y. Kawai, A. Tsukamoto, J. Sugiura, M. Sakaino and Y. Kita, 1990, Cloning, sequence analysis, and expression of ligninolytic phenoloxidase genes of the white-rot basidiomycete *Coriolus hirsutus*, *J. Biol. Chem.* 265, 15224–15230.
- Koroleva, O.V., I.S. Yavmetdinov, S.V. Shleev, E.V. Stepanova and V.P. Gavrilova, 2001, Isolation and study of some properties of laccase from the basidiomycetes *Cerrena maxima*, *Biochemistry (Moscow)* 66, 618–622.
- Kotte, H., B. Gründig, K.D. Vorlop, B. Strehlitz and U. Stottmeister, 1995, Methylphenazonium-modified enzyme sensor based on polymer thick-films for subnanomolar detection of phenols, *Anal. Chem.* 67, 65–70.
- Kremer, S.M. and P.M. Wood, 1992, Continuous monitoring of cellulose oxidation by cellobiose oxidase from *Phanerochaete-chrysosporium*, *FEMS Microbiol. Lett.* 92, 187–192.
- Kroneck, P.M.H., F.A. Armstrong, H. Merkle and A. Marchesini, 1982, Ascorbate oxidase: Molecular properties and catalytic activity, *Adv. Chem. Ser.* 200, 223–248.
- Kulys, J. and R.D. Schmid, 1990, Mediatorless peroxidase electrode and preparation of bienzyme sensors, *Bioelectrochem. Bioenerg.* 24, 305–311.
- Kulys, J.J. and G.J.S. Svirnickas, 1979, Biochemical cell for the determination of lactate, *Anal. Chim. Acta* 109, 55–60.
- Kuznetsov, B.A., G.P. Shumakovich, O.V. Koroleva and A.I. Yaropolov, 2001, On applicability of laccase as label in the mediated and mediatorless electroimmunoassay: Effect of distance on the direct electron transfer between laccase and electrode, *Biosens. Bioelectron.* 16, 73–84.
- Lai, M.E. and A. Bergel, 2000, Electrochemical reduction of oxygen on glassy carbon: Catalysis by catalase, *J. Electroanal. Chem.* 494, 30–40.
- Lai, M.E. and A. Bergel, 2002, Direct electrochemistry of catalase on glassy carbon, *Bioelectrochemistry* 55, 157–160.

- Larsson, T., A. Lindgren and T. Ruzgas, 2001, Spectroelectrochemical study of cellobiose dehydrogenase and diaphorase in a thiol-modified gold capillary in the absence of mediators, *Bioelectrochemistry* 53, 243–249.
- Larsson, T., A. Lindgren, T. Ruzgas, S.E. Lindquist and L. Gorton, 2000, Bioelectrochemical characterisation of cellobiose dehydrogenase modified graphite electrodes: Ionic strength and pH dependences, *J. Electroanal. Chem.* 482, 1–10.
- Larsson, T., S.-E. Lindquist, M. Elmgren, M. Tessema, L. Gorton and G. Henriksson, 1996, Electron transfer between cellobiose dehydrogenase and graphite electrodes, *Anal. Chim. Acta* 331, 207–215.
- Lee, S.-K., G.S. DeBeer, W.E. Antholine, B. Hedman, K.O. Hodgson and E.I. Solomon, 2002, Nature of the intermediate formed in the reduction of O₂ to H₂O at the trinuclear copper cluster active site in native laccase, *J. Am. Chem. Soc.* 124, 6180–6193.
- Lee, C.W., H.B. Gray, F.C. Anson and B.G. Malmström, 1984, Catalysis of the reduction of dioxygen at graphite electrodes coated with fungal laccase A, *J. Electroanal. Chem.* 172, 289–300.
- Leger, C., S.J. Elliott, K.R. Hoke, L.J.C. Jeuken, A.K. Jones and F.A. Armstrong, 2003, Enzyme electrokinetics: Using protein film voltammetry to investigate redox enzymes and their mechanisms, *Biochemistry* 42, 8653–8662.
- Leger, C., K. Heffron, H.R. Pershad, E. Maklashina, C. Luna-Chavez, G. Cecchini, B.A.C. Ackrell and F.A. Armstrong, 2001, Enzyme electrokinetics: Energetics of succinate oxidation by fumarate reductase and succinate dehydrogenase, *Biochemistry* 40, 11234–11245.
- Lewis, D.F.V., 1996, *Cytochrome P450: Structure, function and mechanism*, Taylor and Francis, London.
- Lewis, E.A. and W.B. Tolman, 2004, Reactivity of dioxygen-copper systems, *Chem. Rev.* 104, 1047–1076.
- Li, J., J. Yan, Q. Deng, G. Cheng and S. Dong, 1997, Viologen-thiol self-assembled monolayers for immobilized horseradish peroxidase at gold electrode surface, *Electrochim. Acta* 42, 961–967.
- Lin, L.S. and J.E. Varner, 1991, Expression of ascorbic acid oxidase in zucchini squash (*Cucurbita pepo* L.), *Plant Physiol.* 96, 159–165.
- Lindgren, A., J. Emnéus, T. Ruzgas, L. Gorton and G. Marko-Varga, 1997, Amperometric detection of phenols using peroxidase-modified graphite electrodes, *Anal. Chim. Acta* 347, 51–62.
- Lindgren, A., L. Gorton, T. Ruzgas, U. Baminger, D. Haltrich and M. Schülein, 2001a, Direct electron transfer of cellobiose dehydrogenase from various biological origins at gold and graphite electrodes, *J. Electroanal. Chem.* 496, 76–81.
- Lindgren, A., T. Ruzgas and L. Gorton, 2001b, Direct electron transfer of native and modified peroxidases, research trends, *Current Topics in Analytical Chemistry*, Vol. 2, Ed. R. Richard, Poojapura, Trivandrum, pp. 71–94.
- Lindgren, A., T. Larsson, T. Ruzgas and L. Gorton, 2000a, Direct electron transfer between the heme of cellobiose dehydrogenase and thiol modified gold electrodes, *J. Electroanal. Chem.* 494, 105–113.
- Lindgren, A., T. Ruzgas, L. Gorton, E. Csöregi, G. Bautista Ardila, I.Y. Sakharov and I.G. Gazaryan, 2000b, Biosensors based on novel peroxidases with improved properties in direct and mediated electron transfer, *Biosens. Bioelectron.* 15, 491–497.
- Lindgren, A., F.-D. Munteanu, I.G. Gazaryan, T. Ruzgas and L. Gorton, 1998, Comparison of rotating disk and wall-jet electrode systems for studying the kinetics of direct and mediated electron transfer for horseradish peroxidase on a graphite electrode, *J. Electroanal. Chem.* 458, 113–120.
- Lindgren, A., T. Ruzgas, J. Emnéus, E. Csöregi, L. Gorton and G. Marko-Varga, 1996, Flow injection analysis of phenolic compounds with carbon paste electrodes modified with tyrosinase purchased from different companies, *Anal. Lett.* 29, 1055–1068.
- Lindgren, A., M. Tanaka, T. Ruzgas, L. Gorton, I. Gazaryan, K. Ishimori and I. Morishima, 1999, Direct electron transfer catalysed by recombinant forms of horseradish peroxidase: Insight into the mechanism, *Electrochem. Commun.* 1, 171–175.

- Lindley, P.F., G. Card, I. Zaitseva, V. Zaitsev, B. Reinhammar, E. Selin-Lindgren and K. Yoshida, 1997, An X-ray structural study of human ceruloplasmin in relation to ferroxidase activity, *J. Biol. Inorg. Chem.* 2, 454–463.
- Lisdat, F. and I. Karube, 2002, Copper proteins immobilised on gold electrodes for (bio)analytical studies, *Biosens. Bioelectron.* 17, 1051–1057.
- Lojou, E. and P. Bianco, 2000, Membrane electrodes can modulate the electrochemical response of redox proteins – direct electrochemistry of cytochrome *c*, *J. Electroanal. Chem.* 485, 71–80.
- Lopes, H., G.W. Pettigrew, I. Moura and J.J.G. Moura, 1998, Electrochemical study on cytochrome *c* peroxidase from *Paracoccus denitrificans*: A shifting pattern of structural and thermodynamic properties as the enzyme is activated, *J. Biol. Inorg. Chem.* 3, 632–642.
- Lötzbeyer, T., W. Schuhmann, E. Katz, J. Falter and H.-L. Schmidt, 1994, Direct electron transfer between the covalently immobilized enzyme microperoxidase MP-11 and a cystamine-modified gold electrode, *J. Electroanal. Chem.* 377, 291–294.
- Lötzbeyer, T., W. Schuhmann and H.-L. Schmidt, 1995, Direct electrocatalytic H₂O₂ reduction with hemin covalently immobilized at a monolayer-modified gold electrode, *J. Electroanal. Chem.* 395, 339–343.
- Lötzbeyer, T., W. Schuhmann and H.-L. Schmidt, 1997, Minizymes: A new strategy for the development of reagentless amperometric biosensors based on direct electron-transfer processes, *Bioelectrochem. Bioenerg.* 42, 1–6.
- Lu, H., Z. Li and N. Hu, 2003, Direct voltammetry and electrocatalytic properties of catalase incorporated in polyacrylamide hydrogel films, *Biophys. Chem.* 104, 623–632.
- Ludwig, R., A. Salamon, J. Varga, M. Zamocky, C.K. Peterbauer, K.D. Kulbe and D. Haltrich, 2004, Characterisation of cellobiose dehydrogenases from the white-rot fungi *Trametes pubescens* and *Trametes villosa*, *Appl. Microbiol. Biotechnol.* 64, 213–222.
- Lutz, M., H. Irth, H. Jarskog, E. Burestedt, S. Ghobadi, J. Emnéus, L. Gorton and G. Marko-Varga, 1995, Effect of different additives on activity of tyrosinase mixed into carbon paste electrodes, *Anal. Chim. Acta* 305, 8–17.
- Macholan, L. and B. Chmelikova, 1986, Plant tissue-based membrane biosensor for L-ascorbic acid, *Anal. Chim. Acta* 185, 187–193.
- Machonkin, T.E., 2000, Spectroscopic and biochemical studies of multicopper oxidases involved in iron metabolism, Doctoral thesis, Stanford University, Stanford, CA, USA.
- Makino, N., P. McMahill and H.S. Mason, 1974, The oxidation state of copper in resting tyrosinase, *J. Biol. Chem.* 249, 6062–6066.
- Malkin, R. and B.G. Malmström, 1970, State and function of copper in biological systems, *Adv. Enzymol. Ramb.* 33, 177–244.
- Malmström, B.G., 1990, Cytochrome oxidase: Some unsolved problems and controversial issues, *Arch. Biochem. Biophys.* 280, 233–241.
- Mano, N. and A. Heller, 2003, A miniature membraneless biofuel cell operating at 0.36V under physiological conditions, *J. Electrochem. Soc.* 150, A1136–A1138.
- Mano, N., J.L. Fernandez, Y. Kim, W. Shin, A.J. Bard and A. Heller, 2003a, Oxygen is electroreduced to water on a “wired” enzyme electrode at a lesser overpotential than on platinum, *J. Am. Chem. Soc.* 125, 15290–15291.
- Mano, N., F. Mao and A. Heller, 2003b, Characteristics of a miniature compartment-less glucose-O₂ biofuel cell and its operation in a living plant, *J. Am. Chem. Soc.* 125, 6588–6594.
- Mano, N., H.-H. Kim and A. Heller, 2002, On the relationship between the characteristics of bilirubin oxidases and O₂ cathodes based on their “wiring”, *J. Phys. Chem. B.* 106, 8842–8848.
- Marcus, R.A., 1993, Electron-transfer reactions in chemistry – Theory and experiment (Nobel lecture), *Angew. Chem. Int. Ed. Engl.* 32, 1111–1121.
- Marcus, R.A. and N. Sutin, 1985, Electron transfer in chemistry and biology, *Biochim. Biophys. Acta* 811, 265–322.

- Marko-Varga, G., E. Burestedt, C.J. Svensson, J. Emnéus, L. Gorton, T. Ruzgas, M. Lutz and K.K. Unger, 1996, Effect of HY-zeolites on the performance of tyrosinase-modified carbon paste electrodes, *Electroanalysis* 8, 1121–1126.
- Marko-Varga, G., J. Emnéus, T. Ruzgas and L. Gorton, 1995, Development of enzyme-based amperometric sensors for the determination of phenolic compounds, *Trends Anal. Chem.* 14, 319–328.
- Martins, L.O., C.M. Soares, M.M. Pereira, M. Teixeira, T. Costa, G.H. Jones and A.O. Henriques, 2002, Molecular and biochemical characterization of a highly stable bacterial laccase that occurs as a structural component of the *Bacillus subtilis* endospore coat, *J. Biol. Chem.* 277, 18849–18859.
- Mason, M.G., P. Nicholls, C. Divne, B.M. Hallberg, G. Henriksson and M.T. Wilson, 2003, The heme domain of cellobiose oxidoreductase: A one-electron reducing system, *Biochim. Biophys. Acta* 1604, 47–54.
- Mason, M.G., M.T. Wilson, A. Ball and P. Nicholls, 2002, Oxygen reduction by cellobiose oxidoreductase: The role of the haem group, *FEBS Lett.* 518, 29–32.
- Matsumoto, K., R. Yamada and K. Osajima, 1981, Ascorbate electrode for determination of L-ascorbic acid in food, *Anal. Chem.* 53, 1974–1979.
- Mayer, A.M. and R.C. Staples, 2002, Laccase: New functions for an old enzyme, *Phytochemistry* 60, 551–565.
- McArdle, F.A. and K.C. Persaud, 1993, Development of an enzyme-based biosensor for atrazine detection, *Analyst* 118, 419–423.
- McNeil, C.J., D. Athey and W.O. Ho, 1995, Direct electron transfer bioelectronic interfaces: Application to clinical analysis, *Biosens. Bioelectron.* 10, 75–83.
- McNeil, C.J., D. Athey and R. Renneberg, 1997, Immunosensors for clinical diagnostics, *Frontiers in Biosensorics*, Vol. 2, Eds. F.W. Scheller, F. Schubert and J. Fedrowitz, Birkhäuser, Basel, pp. 17–25.
- Messerschmidt, A. and R. Huber, 1990, The blue oxidases, ascorbate oxidase, laccase and ceruloplasmin. Modeling and structural relationships, *Eur. J. Biochem.* 187, 341–352.
- Messerschmidt, A., R. Huber, T. Poulos and K. Wieghardt, Eds., 2001, *Handbook of Metalloproteins*, Wiley, Chichester.
- Messerschmidt, A., R. Ladenstein, R. Huber, M. Bolognesi, L. Avigliano, R. Petruzzelli, A. Rossi and A. Finazzi-Agro, 1992, Refined crystal structure of ascorbate oxidase at 1.9Å resolution, *J. Mol. Biol.* 224, 179–205.
- Messerschmidt, A., A. Rossi, R. Ladenstein, R. Huber, M. Bolognesi, G. Gatti, A. Marchesini, R. Petruzzelli and A. Finazzi-Agro, 1989, X-ray crystal structure of the blue oxidase ascorbate oxidase from zucchini. Analysis of the polypeptide fold and a model of the copper sites and ligands, *J. Mol. Biol.* 206, 513–529.
- Minussi, R.C., G.M. Pastore and N. Duran, 2002, Potential applications of laccase in the food industry, *Trends Food Sci. Technol.* 13, 205–216.
- Mirica, L.M., X. Ottenwaelder and T.D.P. Stack, 2004, Structure and spectroscopy of copper-dioxygen complexes, *Chem. Rev.* 104, 1013–1045.
- Miyata, K., M. Fujiwara, J. Motonaka, T. Moriga and I. Nakabayashi, 1995, Micro enzyme-sensor with an osmium complex and porous carbon for measuring galactose, *Bull. Chem. Soc. Jpn.* 68, 1921–1927.
- Mondal, M.S., H.A. Fuller and F.A. Armstrong, 1996, Direct measurement of the reduction potential of catalytically active cytochrome *c* peroxidase compound I: Voltammetric detection of a reversible, cooperative two-electron transfer reaction, *J. Am. Chem. Soc.* 118, 263–264.
- Mondal, M.S., D.B. Goodin and F.A. Armstrong, 1998, Simultaneous voltammetric comparisons of reduction potentials, reactivities, and stabilities of the high-potential catalytic states of wild-type and distal-pocket mutant (W51F) yeast cytochrome *c* peroxidase, *J. Am. Chem. Soc.* 120, 6270–6276.
- Mondovi, B., O. Befani and S. Sabatini, 1984, Recent results on the active site of amine oxidases, *Agents Actions* 14, 356–357.
- Munteanu, F.-D., L. Gorton, A. Lindgren, T. Ruzgas, J. Emnéus, E. Csöregi, I.G. Gazaryan, I.V. Ouporov, E.A. Mareeva and L.M. Lagrimini, 2000, Direct and mediated electron

- transfer catalyzed by anionic tobacco peroxidase: Effect of calcium ions, *Appl. Biochem. Biotechnol.* 88, 321–333.
- Munteanu, F.-D., A. Lindgren, J. Ennéus, L. Gorton, T. Ruzgas, E. Csöregi, A. Ciucu, R.B. van Huystee, I.G. Gazaryan and L.M. Lagrimini, 1998, Bioelectrochemical monitoring of phenols and aromatic amines in flow injection using novel plant peroxidases, *Anal. Chem.* 70, 2596–2600.
- Nakagawa, T., S. Tsujimura, K. Kano and T. Ikeda, 2003, Bilirubin oxidase and $[\text{Fe}(\text{CN})_6]^{3-/4-}$ modified electrode allowing diffusion-controlled reduction of O_2 to water at pH 7.0, *Chem. Lett.* 32, 54–55.
- Nakamura, T., 1958, Purification and physicochemical properties of laccase, *Biochim. Biophys. Acta* 30, 44–52.
- Nar, H., A. Messerschmidt, R. Huber, M. van de Kamp and G.W. Canters, 1991, X-ray crystal structure of the two site-specific mutants His35Gln and His35Leu of azurin from *Pseudomonas aeruginosa*, *J. Mol. Biol.* 218, 427–447.
- Narvaez, A., E. Dominguez, I. Katakis, E. Katz, K.T. Ranjit, I. Ben-Dov and I. Willner, 1997, Microperoxidase-11-mediated reduction of hemoproteins: Electrochemical reduction of cytochrome *c*, myoglobin and hemoglobin and electrocatalytic reduction of nitrate in the presence of cytochrome-dependent nitrate reductase, *J. Electroanal. Chem.* 430, 227–233.
- Newcomb, E.H., 1951, Effect of auxin on ascorbic acid oxidase activity in tobacco pith cells, *P. Soc. Exp. Biol. Med.* 76, 504–509.
- Nicholls, D.G. and S.J. Ferguson, 2002, *Bioenergetics 3*, Academic Press, Elsevier, Amsterdam.
- Nistor, C., J. Ennéus, L. Gorton and A. Ciucu, 1999, Improved stability and altered selectivity of tyrosinase-based graphite electrodes for detection of phenolic compounds, *Anal. Chim. Acta* 387, 309–326.
- Oganesyan, V.S., T. Rasmussen, S. Fairhurst and A.J. Thomson, 2004, Characterization of $[\text{Cu}_4\text{S}]$, the catalytic site in nitrous oxide reductase, by EPR spectroscopy, *Dalton Trans.* 996–1002.
- Ohsaka, T., M. Shioda, F. Matsumoto, T. Okajima, F. Kitamura, and K. Tokuda, 1996, Electrode reaction of superoxide dismutase at cysteine-modified gold electrodes, *Electron Transfer in Proteins and Supramolecular Assemblies at Interfaces*, March 17–20, Yokohama National University, Kanagawa, P-33.
- Ohsaka, T., Y. Tian, M. Shioda, S. Kasahara and T. Okajima, 2002, A superoxide dismutase-modified electrode that detects superoxide ion, *Chem. Commun.* 990–991.
- Önnerfjord, P., J. Ennéus, G. Marko-Varga, L. Gorton, F. Ortega and E. Domínguez, 1995, Tyrosinase graphite-epoxy-based composite electrodes for detection of phenols, *Biosens. Bioelectron.* 10, 607–619.
- Ortega, F., E. Domínguez, E. Johansson, J. Ennéus, L. Gorton and G. Marko-Varga, 1994, Phenol oxidase based biosensors as selective detection units in column liquid chromatography for the determination of phenolic compounds, *J. Chromatogr.* 675, 65–78.
- Ortega, F., E. Domínguez, G. Jönsson-Pettersson and L. Gorton, 1993, An amperometric determination of phenolic compounds using a tyrosinase graphite electrode in a FIA system, *J. Biotechnol.* 31, 289–300.
- Ortel, T.L., N. Takahashi and F.W. Putnam, 1984, Structural model of human ceruloplasmin based on internal triplication, hydrophilic/hydrophobic character, and secondary structure of domains, *Proc. Natl. Acad. Sci. USA* 81, 4761–4765.
- Pacheco, A., J.T. Hazzard, G. Tollin and J.H. Enemark, 1999, The pH effect of intramolecular electron transfer rates in sulfite oxidase at high and low anion concentrations, *J. Biol. Inorg. Chem.* 4, 390–401.
- Paddock, R.M. and E.F. Bowden, 1989, Electrocatalytic reduction of hydrogen peroxide via direct electron transfer from pyrolytic graphite electrodes to irreversibly adsorbed cytochrome *c* peroxidase, *J. Electroanal. Chem.* 260, 487–494.
- Page, C.C., C.C. Moser, X. Chen and P.L. Dutton, 1999, Natural engineering principles of electron tunneling in biological oxidation–reduction, *Nature* 402, 47–52.

- Paice, M., R. Bourbonnais, S. Renaud, S. Labonte, G. Sacciadis, R. Berry, M. Amann, A. Candussio and R. Mueller, 2002, Pilot plant bleaching trials with laccase and mediator, *Prog. Biotechnol.* 21, 203–211.
- Palmer, A.E., R.K. Szilagyi, J.R. Cherry, A. Jones, F. Xu and E.I. Solomon, 2003, Spectroscopic characterization of the Leu513His variant of fungal laccase: Effect of increased axial ligand interaction on the geometric and electronic structure of the type 1 Cu site, *Inorg. Chem.* 42, 4006–4017.
- Palmore, G.T.R. and H.-H. Kim, 1999, Electro-enzymic reduction of dioxygen to water in the cathode compartment of a biofuel cell, *J. Electroanal. Chem.* 464, 110–117.
- Pappa, H., H. Li, M. Sundaramoorthy, D. Arciero, A. Hooper and T.L. Poulos, 1996a, Crystallization and preliminary crystallographic analysis of cytochrome c553 peroxidase from *Nitrosomonas europaea*, *J. Struct. Biol.* 116, 429–431.
- Pappa, H., S. Tajbaksh, A. Saunders, G. Pielak and T. Poulos, 1996b, Probing the cytochrome *c* peroxidase – cytochrome *c* electron transfer reaction using site specific cross-linking, *Biochemistry* 35, 4837–4845.
- Pardo-Yissar, V., E. Katz, I. Willner, A.B. Kotlyar, C. Sanders and H. Lill, 2000, Biomaterial engineered electrodes for bioelectronics, *Faraday Discuss* 116, 119–134.
- Parellada, J., E. Domínguez and V.M. Fernández, 1996, Amperometric flow injection determination of fructose in honey with a carbon paste sensor based on fructose dehydrogenase, *Anal. Chim. Acta* 330, 71–77.
- Pershad, H.R., J. Hirst, B. Cochran, B.A.C. Ackrell and F.A. Armstrong, 1999, Voltammetric studies of bidirectional catalytic electron transport in *Escherichia coli* succinate dehydrogenase: Comparison with the enzyme from beef heart mitochondria, *Biochim. Biophys. Acta* 1412, 262–272.
- Peter, M.G. and U. Wollenberger, 1997, Phenol-oxidizing enzymes: Mechanisms and applications in biosensors. *Frontiers in Biosensorics*, Vol. 1, Eds. F.W. Scheller, F. Schubert and J. Fedrowitz, Birkhäuser, Basel, pp. 63–82.
- Petersen, A. and E. Steckhan, 1999, Continuous indirect electrochemical regeneration of galactose oxidase, *Bioorgan. Med. Chem.* 7, 2203–2208.
- Petersen, L.C. and H. Degn, 1978, Steady-state kinetics of laccase from *Rhus vernicifera*, *Biochim. Biophys. Acta* 526, 85–92.
- Pinho, D., S. Besson, C.D. Brondino, E. Pereira, B. de Castro and I. Moura, 2004, Two azurins with unusual redox and spectroscopic properties isolated from the *Pseudomonas chlororaphis* strains DSM 50083T and DSM 50135, *J. Inorg. Biochem.* 98, 276–286.
- Piontek, K., M. Antorini and T. Chojnowski, 2002, Crystal structure of a laccase from the fungus *Trametes versicolor* at 1.90Å resolution containing a full complement of coppers, *J. Biol. Chem.* 277, 37663–37669.
- Poulos, T.L., W.R. Patterson and M. Sundaramoorthy, 1995, The crystal structure of ascorbate and manganese peroxidases: The role of non-heme metal in the catalytic mechanism, *Biochem. Soc. Trans.* 23, 228–232.
- Presnova, G., V. Grigorenko, A. Egorov, T. Ruzgas, A. Lindgren, L. Gorton and T. Börchers, 2000, Direct heterogeneous electron transfer of recombinant horseradish peroxidases on gold, *Farad. Discuss.* 116, 281–289.
- Puig, D., T. Ruzgas, J. Emnéus, L. Gorton, G. Marko-Varga and D. Barceló, 1996, Characterization of tyrosinase-Teflon/graphite composite electrodes for determination of catechol in environmental matrix, *Electroanalysis* 8, 885–890.
- Rajesh, Takashima, W. and K. Kaneto, 2004, Amperometric phenol biosensor based on covalent immobilization of tyrosinase onto an electrochemically prepared novel copolymer poly (N-3-aminopropyl pyrrole-co-pyrrole) film, *Sens. Actuat. B: Chem.* 102, 271–277.
- Ramanavicius, A., K. Habermüller, E. Csöregi, V. Laurinavicius and W. Schuhmann, 1999, Polypyrrole-entrapped quinoxinoprotein alcohol dehydrogenase. Evidence for direct electron transfer via conducting-polymer chains, *Anal. Chem.* 71, 3581–3586.
- Ramos, E., Johnson, T., Martin, M., Gannon, A. and Dorman, S., 2003, Formal reduction potentials of oxygen-binding proteins, 55th Southeast Regional Meeting of the American Chemical Society, Atlanta, GA, USA, 988.

- Razumas, V., A. Gudavicius and J. Kulys, 1983, Redox conversion of peroxidase on surface-modified gold electrode, *J. Electroanal. Chem.* 151, 311–315.
- Razumas, V., A. Gudavicius and J. Kulys, 1986, Kinetics of peroxidase redox conversion of viologen-modified gold electrodes, *J. Electroanal. Chem.* 198, 81–87.
- Razumas, V., J. Kazlauskaitė, T. Ruzgas and J. Kulys, 1992, Bioelectrochemistry of microperoxidases, *Bioelectrochem. Bioenerg.* 28, 159–176.
- Razumiene, J., M. Niculescu, A. Ramanavicius, V. Laurinavicius and E. Csöregi, 2002, Direct bioelectrocatalysis at carbon electrodes modified with quinohemoprotein alcohol dehydrogenase from *Gluconobacter* sp. 33, *Electroanalysis* 14, 43–49.
- Reid, M.E., 1941, Relation of vitamin C to cell size in the growing region of the primary root of cowpea seedlings, *Am. J. Bot.* 28, 410–415.
- Reinhammar, B., 1984, Laccase. *Copper Proteins Copper Enzymes*, Vol. 3, Ed. R. Lonti, CRC, Boca Raton, pp. 1–35.
- Reinhammar, B. and T.I. Vänngård, 1971, Electron-accepting sites in *Rhus vernicifera* laccase as studied by anaerobic oxidation–reduction titrations, *Eur. J. Biochem.* 18, 463–468.
- Reinhammar, B.R.M., 1972, Oxidation–reduction potentials of the electron acceptors in laccases and stellacyanin, *Biochim. Biophys. Acta* 275, 245–259.
- Reiss, P. and E. Vellinger, 1929, The potential of the arrest of multiplication of the sea urchin egg, *Arch. Phys. Biol.* 7, 80–101.
- Rekha, K., M.D. Gouda, M.S. Thakur and N.G. Karanth, 2000, Ascorbate oxidase-based amperometric biosensor for organophosphorous pesticide monitoring, *Biosens. Bioelectron.* 15, 499–502.
- Rhoten, M.C., J.D. Burgess and F.M. Hawkrige, 2000, Temperature and pH effects on cytochrome *c* oxidase immobilized in an electrode-supported lipid bilayer membrane, *Electrochim. Acta* 45, 2855–2860.
- Rhoten, M.C., J.D. Burgess and F.M. Hawkrige, 2002a, The reaction of cytochrome *c* from different species with cytochrome *c* oxidase immobilized in an electrode supported lipid bilayer membrane, *J. Electroanal. Chem.* 534, 143–150.
- Rhoten, M.C., F.M. Hawkrige and J. Wilczek, 2002b, The reaction of cytochrome *c* with bovine and *Bacillus stearothermophilus* cytochrome *c* oxidase immobilized in electrode-supported lipid bilayer membranes, *J. Electroanal. Chem.* 535, 97–106.
- Riklin, A., E. Katz, I. Willner, A. Stocker and A. Bückmann, 1995, Improving enzyme-electrode contacting by redox modification of cofactors, *Nature* 376, 672–675.
- Rodkey, F.L. and E.G. Ball, 1950, Oxidation–reduction potentials of the cytochrome *c* system, *J. Biol. Chem.* 182, 17–28.
- Rodríguez-López, J.N., J. Tudela, R. Varón, F. García-Carmona and F. García-Cánovas, 1992, Analysis of a kinetic model for melanin biosynthesis pathway, *J. Biol. Chem.* 267, 3801–3810.
- Rogers, M.S. and D.M. Dooley, 2001, Post-translationally modified tyrosines from galactose oxidase and cytochrome *c* oxidase, *Adv. Protein Chem.* 58, 387–436.
- Rorabacher, D.B., 2004, Electron transfer by copper centers, *Chem. Rev.* 104, 651–697.
- Rowe, D.J.F., I.D. Watson, J. Williams and D.J. Berry, 1988, The clinical use and measurement of theophylline, *Ann. Clin. Biochem.* 25, 4–26.
- Roy, B.P., T. Dumonceaux, A.A. Koukoulas and F.S. Archibald, 1996, Purification and characterization of cellobiose dehydrogenases from the white rot fungus *Trametes versicolor*, *Appl. Environ. Microbiol.* 62, 4417–4427.
- Rusling, J.F., 1998, Enzyme bioelectrochemistry in cast biomembrane-like films, *Acc. Chem. Res.* 31, 363–369.
- Ruzgas, T., E. Csöregi, J. Emnéus, L. Gorton and G. Marko-Varga, 1996, Peroxidase-modified electrodes: Fundamentals and application, *Anal. Chim. Acta* 330, 123–138.
- Ruzgas, T., A. Gaigalas and L. Gorton, 1999, Diffusionless electron transfer of microperoxidase-11 on gold electrodes, *J. Electroanal. Chem.* 469, 123–131.
- Ruzgas, T., L. Gorton, J. Emnéus, E. Csörgi and G. Marko-Varga, 1995a, Direct bioelectrocatalytic reduction of hydrogen peroxide at chloroperoxidase-modified graphite electrode, *Anal. Proc.* 32, 207–208.

- Ruzgas, T., L. Gorton, J. Emnéus and G. Marko-Varga, 1995b, Kinetic models of horseradish peroxidase action on a graphite electrode, *J. Electroanal. Chem.* 391, 41–49.
- Ruzgas, T., A. Lindgren, L. Gorton, H.-J. Hecht, J. Reichelt and U. Bilitewski, 2002, Electrochemistry of peroxidases, *Electroanalytical Methods for Biological Materials*, Eds. A. Brajter-Toth and J.Q. Chambers, Marcel Dekker, New York, pp. 233–254.
- Ruzgas, T., L. Wong, A.K. Gaigalas and V.L. Vilker, 1998, Electron transfer between surface-confined cytochrome *c* and an *N*-acetylcysteine-modified gold electrode, *Langmuir* 14, 7298–7305.
- Sakurai, T., 1996, Cyclic voltammetry of cucumber ascorbate oxidase, *Chem. Lett.* 481–482.
- Sakurai, T., F. Nose, T. Fujiki and S. Suzuki, 1996, Reduction and oxidation processes of blue copper proteins, azurin, pseudoazurin, umecyanin, stellacyanin, plantacyanin, and plastocyanin approached by cyclic and potential step voltammetries, *Bull. Chem. Soc. Jpn.* 69, 2855–2862.
- Sakurai, T., L. Zhan, T. Fujita, K. Kataoka, A. Shimizu, T. Samejima and S. Yamaguchi, 2003, Authentic and recombinant bilirubin oxidases are in different resting forms, *Biosci. Biotechnol. Biochem.* 67, 1157–1159.
- Samejima, M. and K.-E. Eriksson, 1992, A comparison of the catalytic properties of cellobiose:quinone oxidoreductase and cellobiose oxidase from *Phanerochaete chrysosporium*, *Eur. J. Biochem.* 207, 103–107.
- Santucci, R., T. Ferri, L. Morpurgo, I. Savini and L. Avigliano, 1998, Unmediated heterogeneous electron transfer reaction of ascorbate oxidase and laccase at a gold electrode, *Biochem. J.* 332, 611–615.
- Scheller, F.W., U. Wollenberger, C. Lei, W. Jin, B. Ge, C. Lehmann, F. Lisdat and V. Fridman, 2002, Bioelectrocatalysis by redox enzymes at modified electrodes, *Rev. Mol. Biotechnol.* 82, 411–424.
- Schlereth, D.D., 2005, Biosensors based on self-assembled monolayers, *Biosensors and Modern Biospecific Analytical Techniques*, Vol. XLIV, Ed. L. Gorton, Elsevier, Amsterdam, pp. 1–63.
- Schneider, P., M.B. Caspersen, K. Mondorf, T. Halkier, L.K. Skov, P.R. Østergaard, K.M. Brown, S.H. Brown and F. Xu, 1999, Characterization of a *Coprinus cinereus* laccase, *Enzyme Microb. Technol.* 25, 502–508.
- Schuhmann, W., 2002, Amperometric enzyme biosensors based on optimized electron-transfer pathways and non-manual immobilization procedures, *Rev. Mol. Biotechnol.* 82, 425–441.
- Schuhmann, W., H. Zimmermann, K. Habermüller and V. Laurinavicius, 2000, Electron-transfer pathways between redox enzymes and electrodes surfaces: Reagentless biosensors based on thiol-monolayer-bound and polypyrrole-entrapped enzymes, *Farad. Discuss.* 116, 245–255.
- Schuller, D.J., N. Ban, R.B. van Huystee, A. McPherson and T.L. Poulos, 1996, The crystal structure of peanut peroxidase, *Structure* 4, 311–321.
- Schumacher, J.T., H.-J. Hecht, U. Dengler, J. Reichelt and U. Bilitewski, 2001, Direct electron transfer observed for peroxidase to screen-printed graphite electrodes, *Electroanalysis* 13, 779–785.
- Scott, D.L. and E.F. Bowden, 1994, Enzyme-substrate kinetics of adsorbed cytochrome *c* peroxidase on pyrolytic graphite electrodes, *Anal. Chem.* 66, 1217–1223.
- Scott, D.L., R.M. Paddock and E.F. Bowden, 1992, The electrocatalytic enzyme function of adsorbed cytochrome *c* peroxidase on pyrolytic graphite, *J. Electroanal. Chem.* 341, 307–321.
- Scott, R.A. and A.G. Mauk, Eds., 1996, *Cytochrome c: A Multidisciplinary Approach*, University Science Books, Sausalito.
- Sezgintürk, M.K. and E. Dinckaya, 2004, An amperometric inhibitor biosensor for the determination of reduced glutathione (GSH) without any derivatization in some plants, *Biosens. Bioelectron.* 19, 835–841.
- Sharma, S.K., R. Singhal, B.D. Malhotra, N. Sehgal and A. Kumar, 2004a, Lactose biosensor based on Langmuir–Blodgett films of poly(3-hexyl thiophene), *Biosens. Bioelectron.* 20, 651–657.

- Sharma, S.K., R. Singhal, B.D. Malhotra, N. Sehgal and A. Kumar, 2004b, Langmuir–Blodgett film-based biosensor for estimation of galactose in milk, *Electrochim. Acta* 48, 2479–2485.
- Shimizu, A., J.H. Kwon, T. Sasaki, T. Satoh, N. Sakurai, T. Sakurai, S. Yamaguchi and T. Samejima, 1999, *Myrothecium verrucaria* bilirubin oxidase and its mutants for potential copper ligands, *Biochemistry* 38, 3034–3042.
- Shin, K.-S. and Y.-J. Lee, 2000, Purification and characterization of a new member of the laccase family from the white-rot basidiomycete *Coriolus hirsutus*, *Arch. Biochem. Biophys.* 384, 109–115.
- Shipovskov, S., E.E. Ferapontova, I.G. Gazaryan and T. Ruzgas, 2004, Recombinant horseradish peroxidase- and cytochrome *c*-based two-electrode system for detection of superoxide radicals, *Bioelectrochemistry* 63, 277–280.
- Shleev, S., A. Christenson, V. Serezhenkov, D. Burbaev, A. Yaropolov, L. Gorton and T. Ruzgas, 2005a, Electrochemically controlled redox transformations of T1 and T2 copper sites in native *Trametes hirsuta* laccase at bare gold electrode, *Biochem. J.* 385, 745–754.
- Shleev, S., A. Jarosz-Wilkolazka, A. Khalunina, O. Morozova, A. Yaropolov, T. Ruzgas and L. Gorton, 2005b, Direct heterogeneous electron transfer reactions of laccases from different origins on carbon electrodes, *Bioelectrochemistry* 67, 115–124.
- Shleev, S., J. Tkac, A. Christenson, T. Ruzgas, A.I. Yaropolov, J. Whittaker and L. Gorton, 2005c, Direct electron transfer between copper containing proteins and electrodes, *Biosens. Bioelectron.* 20, 2517–2554.
- Shleev, S., A. El Kasmi, T. Ruzgas and L. Gorton, 2004a, Direct heterogeneous electron transfer reactions of bilirubin oxidase at a spectrographic graphite electrode, *Electrochem. Commun.* 6, 934–939.
- Shleev, S.V., O.V. Morozova, O.V. Nikitina, E.S. Gorshina, T.V. Rusinova, V.A. Serezhenkov, D.S. Burbaev, I.G. Gazaryan and A.I. Yaropolov, 2004b, Comparison of physico-chemical characteristics of four laccases from different basidiomycetes, *Biochimie* 86, 693–703.
- Shlev, S.V., E.A. Zaitseva, E.S. Gorshina, O.V. Morozova, V.A. Serezhenkov, D.S. Burbaev, B.A. Kuznetsov and A.I. Yaropolov, 2003, Spectral and electrochemical study of laccases from basidiomycetes, *Moscow University Chem. Bull.* 44, 35–39.
- Shoham, B., Y. Migron, A. Riklin, I. Willner and B. Tartakovsky, 1995, A bilirubin biosensor based on a multilayer network enzyme electrode, *Biosens. Bioelectron.* 10, 341–352.
- Shumyantseva, V.V., Y.D. Ivanov, N. Bistolos, F.W. Scheller, A.I. Archakov and U. Wollenberger, 2004, Direct electron transfer of cytochrome P450 2B4 at electrodes modified with nonionic detergent and colloidal clay nanoparticles, *Anal. Chem.* 76, 6046–6052.
- Smith, M., C.F. Thurston and D.A. Wood, 1997, Fungal laccases: role in delignification and possible industrial applications, *Multi-Copper Oxidases*, Ed. A. Messerschmidt, World Scientific, Singapore, pp. 201–224.
- Solomon, E.I., R.K. Szilagyi, S.D. George and L. Basumallick, 2004, Electronic structures of metal sites in proteins and models: contributions to function in blue copper proteins, *Chem. Rev.* 104, 419–458.
- Solomon, E.I., M.J. Baldwin and M.D. Lowery, 1992, Electronic structures of active sites in copper proteins: Contributions to reactivity, *Chem. Rev.* 92, 521–542.
- Solomon, E.I., U.M. Sundaram and T.E. Machonkin, 1996, Multicopper oxidases and oxygenases, *Chem. Rev.* 96, 2563–2605.
- Song, S., R. Clark, E. Bowden and M. Tarlov, 1993, Characterisation of cytochrome *c*/alkanethiolate structures prepared by self-assembly on gold, *J. Phys. Chem.* 97, 6564–6572.
- Soukharev, V., N. Mano and A. Heller, 2004, A four-electron O₂-electroreduction biocatalyst superior to platinum and a biofuel cell operating at 0.88V, *J. Am. Chem. Soc.* 126, 8368–8369.
- Staskeviciene, S.L., N.K. Cenas and J.J. Kulys, 1991, Reagentless lactate electrodes based on electrocatalytic oxidation of flavocytochrome *b*₂, *Anal. Chim. Acta* 243, 167–171.

- Stigter, E.C.A., A.M. Carnicero, J.P. van der Lugt and W.A.C. Somers, 1996, Electron transfer between galactose oxidase and an electrode via a redox polymer network, *Biotechnol. Techniq.* 10, 469–474.
- Stoica, L., N. Dimcheva, D. Haltrich, T. Ruzgas and L. Gorton, 2005, Electrochemical investigation of direct electron transfer between cellobiose dehydrogenase from new fungal sources on Au electrodes modified with different alkanethiols, *Biosens. Bioelectron.* 20, 2010–2018.
- Stoica, L., A. Lindgren-Sjölin, T. Ruzgas and L. Gorton, 2004, Ultrasensitive biosensor based on cellobiose dehydrogenase (CDH) for detection of catecholamines, *Anal. Chem.* 76, 4690–4696.
- Streffer, K., E. Vijgenboom, A.W.J.W. Tepper, A. Makower, F.W. Scheller, G.W. Canters and U. Wollenberger, 2001, Determination of phenolic compounds using recombinant tyrosinase from *Streptomyces antibioticus*, *Anal. Chim. Acta* 427, 201–210.
- Sucheta, A., B.A.C. Ackrell, B. Cochran and F.A. Armstrong, 1992, Diode-like behavior of a mitochondrial electron-transport enzyme, *Nature* 356, 361–362.
- Sucheta, A., R. Cammack, J. Weiner and F.A. Armstrong, 1993, Reversible electrochemistry of fumarate reductase immobilized on an electrode surface: Direct voltammetric observations of redox centers and their participation in rapid catalytic electron transport, *Biochemistry* 32, 5455–5465.
- Sullivan, E.P., J.T. Huzzard, G. Tollin and J.H. Enemark, 1993, Electron-transfer in sulfite oxidase – effects of pH and anions on transient kinetics, *Biochemistry* 32, 12465–12470.
- Sundaramoorthy, M., K. Kishi, M.H. Gold and T.L. Poulos, 1997, Crystal structures of substrate-binding site mutants of manganese peroxidase, *J. Biol. Chem.* 272, 17574–17580.
- Sundaramoorthy, M., J. Terner and T.L. Poulos, 1995, The crystal structure of chloroperoxidase: A heme peroxidase-cytochrome P450 functional hybrid, *Structure* 3, 1367–1377.
- Surma-Slusarska, B. and J. Leks-Stepien, 2001, TCF bleaching of kraft pulps with laccase and xylanase, *J. Wood Chem. Technol.* 21, 361–370.
- Szeponik, J., B. Möller, D. Pfeiffer, F. Lisdat, U. Wollenberger, A. Makower and F.W. Scheller, 1997, Ultrasensitive bienzyme sensor for adrenaline, *Biosens. Bioelectron.* 12, 947–952.
- Takahashi, N., T.L. Ortel and F.W. Putnam, 1984, Single-chain structure of human ceruloplasmin: The complete amino acid sequence of the whole molecule, *Proc. Natl. Acad. Sci. USA* 81, 390–394.
- Taniguchi, I., H. Ishimoto, K. Miyagawa, M. Iwai, H. Nagai, H. Hanazono, K. Taira, A. Kubo, A. Nishikawa, K. Nishiyama, Z. Dursun, G.P.J. Hareau and M. Tazaki, 2003, Surface functions of 2-mercaptopyridine, 2-mercaptopyrazine and 2-mercaptoquinoxaline modified Au (111) electrodes for direct rapid electron transfer of cytochrome *c*, *Electrochem. Commun.* 5, 857–861.
- Tarasevich, M.R., 1979, Ways of using enzymes for acceleration of electrochemical reactions, *Bioelectrochem. Bioenerg.* 6, 587–591.
- Tarasevich, M.R., V.A. Bogdanovskaya, V.A. Fridman and L.N. Kuznetsova, 2001a, Kinetics and mechanism of the H₂O₂ electroreduction on the peroxidase-promoted electrodes, *Russ. J. Electrochem.* 37, 7–14.
- Tarasevich, M.R., V.A. Bogdanovskaya and L.N. Kuznetsova, 2001b, Bioelectrocatalytic reduction of oxygen in the presence of laccase adsorbed on carbon electrodes, *Russ. J. Electrochem.* 37, 833–837.
- Tarasevich, M.R., V.A. Bogdanovskaya, N.M. Zagudaeva and A.V. Kapustin, 2002, Composite materials for direct bioelectrocatalysis of the hydrogen and oxygen reactions in biofuel cells, *Russ. J. Electrochem.* 38, 335.
- Tarasevich, M.R., A.I. Yeroplov, V.A. Bogdanovskaya and S.D. Varfolomeev, 1979, Electrocatalysis of a cathodic oxygen reduction by laccase, *Bioelectrochem. Bioenerg.* 6, 393–403.
- Tatsuma, T., K. Ariyama and N. Oyama, 1998, Kinetic analysis of electron transfer from a graphite coating to horseradish peroxidase, *J. Electroanal. Chem.* 446, 205–209.

- Tatsuma, T., H. Mori and A. Fujishima, 2000, Electron transfer from diamond electrodes to heme peptide and peroxidase, *Anal. Chem.* 72, 2919–2924.
- Tatsuma, T. and T. Watanabe, 1991, Peroxidase model electrodes – heme peptide-modified electrodes as reagentless sensors for hydrogen peroxide, *Anal. Chem.* 63, 1580–1585.
- Thuesen, M.H., O. Farver, B. Reinhammar and J. Ulstrup, 1998, Cyclic voltammetry and electrocatalysis of the blue copper oxidase *Polyporus versicolor* laccase, *Acta Chem. Scand.* 52, 555–562.
- Tian, Y., L. Mao, T. Okajima and T. Ohsaka, 2002a, Superoxide dismutase-based third-generation biosensor for superoxide anion, *Anal. Chem.* 74, 2428–2434.
- Tian, Y., M. Shioda, S. Kasahara, T. Okajima, L. Mao, T. Hisaboli and T. Ohsaka, 2002b, A facilitated electron transfer of copper–zinc superoxide dismutase (SOD) based on cysteine-bridged SOD electrode, *Biochim. Biophys. Acta* 1569, 151–158.
- Tian, Y., L. Mao, T. Okajima and T. Ohsaka, 2004, Electrochemistry and electrocatalytic activities of superoxide dismutases at gold electrodes modified with a self-assembled monolayer, *Anal. Chem.* 76, 4162–4168.
- Tkac, J., T. Ruzgas and J. W. Whittaker, 2005, Direct electrode transfer reactions of galactose oxidase on modified gold electrodes, in manuscript.
- Tkac, J., I. Vostiar, P. Gemeiner and E. Sturdik, 2002, Indirect evidence of direct electron communication between the active site of galactose oxidase and a graphite electrode, *Bioelectrochemistry* 56, 23–25.
- Torimura, M., K. Kano, T. Ikeda and T. Ueda, 1997, Spectroelectrochemical characterization of quinoxinoprotein alcohol dehydrogenase from *Gluconobacter suboxydans*, *Chem. Lett.* 525–526.
- Toyama, H., F.S. Mathews, O. Adachi and K. Matsushita, 2004, Quinoxinoprotein alcohol dehydrogenases: Structure, function, and physiology, *Arch. Biochem. Biophys.* 428, 10–21.
- Tsujimura, S., M. Fujita, H. Tatsumi, K. Kano and T. Ikeda, 2001a, Bioelectrocatalysis-based dihydrogen/dioxygen fuel cell operating at physiological pH, *Phys. Chem. Chem. Phys.* 3, 1331–1335.
- Tsujimura, S., A. Wadano, K. Kano and T. Ikeda, 2001b, Photosynthetic bioelectrochemical cell utilizing cyanobacteria and water-generating oxidase, *Enz. Microb. Technol.* 29, 225–231.
- Tsujimura, S., M. Kawaharada, T. Nakagawa, K. Kano and T. Ikeda, 2003, Mediated bioelectrocatalytic O₂ reduction to water at highly positive electrode potentials near neutral pH, *Electrochem. Commun.* 5, 138–141.
- Tsujimura, S., T. Nakagawa, K. Kano and T. Ikeda, 2004, Kinetic study of direct bioelectrocatalysis of dioxygen reduction with bilirubin oxidase at carbon electrodes, *Electrochemistry* 72, 437–439.
- Tsukihara, T., H. Aoyama, E. Yamashita, T. Tomizaki, H. Yamaguchi, K. Shinzawa-Itoh, R. Nakashima, R. Yaono and S. Yoshikawa, 1995, Structures of metal sites of oxidized bovine heart cytochrome *c* oxidase at 2.8Å, *Science* 269, 1069–1074.
- Turner, K.L., M.K. Doherty, H.A. Heering, F.A. Armstrong, G.A. Reid and S.K. Chapman, 1999, Redox properties of flavocytochrome *c*₃ from *Shewanella frigidimarina* NCIMB400, *Biochemistry* 38, 3302–3309.
- Updike, S.J. and G.P. Hicks, 1967, The enzyme electrode, *Nature* 214, 986–988.
- Varfolomeev, S.D., I.N. Kurochkin and A.I. Yaropolov, 1996, Direct electron transfer effect biosensors, *Bioelectron.* 11, 863–871.
- Vrbova, E., J. Peckova and M. Marek, 1992, Preparation and utilization of a biosensor based on galactose oxidase, *Coll. Czech. Chem. Commun.* 57, 2287–2294.
- Wang, J. and Y. Lin, 1993, On-line organic-phase enzyme detector, *Anal. Chim. Acta* 271, 53–58.
- Wang, J. and M. Ozsoz, 1990, A polishable amperometric biosensor for bilirubin, *Electroanalysis* 2, 647–650.
- Wang, L., J. Wang and F. Zhou, 2004, Direct electrochemistry of catalase at a gold electrode modified with single-wall carbon nanotubes, *Electroanalysis* 16, 627–632.

- White, G.A. and R.M. Krupka, 1965, Ascorbic acid oxidase and ascorbic acid oxygenase of *Myrothecium verrucaria*, Arch. Biochem. Biophys. 110, 448–461.
- Whitesides, G.M., J.P. Mathias and C.T. Seto, 1991, Molecular self-assembly and nanochemistry: A chemical strategy for the synthesis of nanostructures, Science 254, 1312–1319.
- Whittaker, M.M. and J.W. Whittaker, 1988, The active site of galactose oxidase, J. Biol. Chem. 263, 6074–6080.
- Willner, I., V. Heleg-Shabtai, R. Blonder, E. Katz, G. Tao, A.F. Bückmann and A. Heller, 1996, Electrical wiring of glucose oxidase by reconstitution of FAD-modified monolayers assembled onto Au electrodes, J. Am. Chem. Soc. 118, 10321–10322.
- Willner, I., E. Katz and B. Willner, 1997, Electrical contact of redox enzyme layers associated with electrodes: Routes to amperometric biosensors, Electroanalysis 9, 965–977.
- Wollenberger, U., 2005, Third generation biosensors – integrating recognition and transduction in electrochemical sensors. Biosensors and Modern Biospecific Analytical Techniques, Vol. XLIV, Ed. L. Gorton, Elsevier, Amsterdam, pp. 65–130.
- Wollenberger, U., V. Bogdanovskaya, S. Bobrin, F. Scheller and M. Tarasevich, 1990, Enzyme electrodes using bioelectrocatalytic reduction of hydrogen peroxide, Anal. Lett. 23, 1795–1808.
- Wollenberger, U., J. Wang, M. Ozsoz, E. Gonzalez Romero and F. Scheller, 1991, Bulk modified enzyme electrodes for reagentless detection of peroxides, Bioelectrochem. Bioenerg. 26, 287–296.
- Wong, Y. and J. Yu, 1999, Laccase-catalyzed decolorization of synthetic dyes, Water Res. 33, 3512–3520.
- Wood, J.D. and P.M. Wood, 1992, Homology between cellobiose oxidase from *Phanerochaete chrysosporium* and other proteins, Biochem. Soc. Trans. 20, 109S.
- Wright, C. and A.G. Sykes, 2001, Interconversion of Cu(I) and Cu(II) forms of galactose oxidase: Comparison of reduction potentials, J. Inorg. Biochem. 85, 237–243.
- Wu, X.-Q., X.-Y. Meng, Z.-S. Wang and Z.-R. Zhang, 1999, Study of the direct electron transfer process of superoxide dismutase, Bioelectrochem. Bioenerg. 48, 227–231.
- Wynn, R.M., H.K. Sarkar, R.A. Holwerda and D.B. Knaff, 1983, Fluorescence associated with the type 3 copper center of laccase, FEBS Lett. 156, 23–28.
- Xiao, Y., F. Patolsky, E. Katz, J.F. Hainfeld and I. Willner, 2003, “Plugging into enzymes”: Nanowiring of redox enzymes by a gold particle, Science 299, 1877–1881.
- Xu, F., R.M. Berka, J.A. Wahleithner, B.A. Nelson, J.R. Shuster, S.H. Brown, A.E. Palmer and E.I. Solomon, 1998, Site-directed mutations in fungal laccase: Effect on redox potential, activity and pH profile, Biochem. J. 334, 63–70.
- Xu, F., J.J. Kulys, K. Duke, K. Li, K. Krikstopaitis, H.J. Deussen, E. Abbate, V. Galinyte and P. Schneider, 2000, Redox chemistry in laccase-catalyzed oxidation of N-hydroxy compounds, Appl. Environ. Microbiol. 66, 2052–2056.
- Xu, F., A.E. Palmer, D.S. Yaver, R.M. Berka, G.A. Gambetta, S.H. Brown and E.I. Solomon, 1999, Targeted mutations in a *Trametes villosa* laccase, axial perturbations of the T1 copper, J. Biol. Chem. 274, 12372–12375.
- Xu, F., W. Shin, S.H. Brown, J.A. Wahleithner, U.M. Sundaram and E.I. Solomon, 1996, A study of a series of recombinant fungal laccases and bilirubin oxidase that exhibit significant differences in redox potential, substrate specificity, and stability, Biochim. Biophys. Acta 1292, 303–311.
- Yabuki, S. and F. Mizutani, 1997, D-Fructose sensing electrode based on electron transfer of D-fructose dehydrogenase at colloidal gold-enzyme modified electrode, Electroanalysis 9, 23–25.
- Yamada, Y., K. Aida and T. Uemura, 1967, Enzymatic studies on the oxidation of sugar and sugar alcohol. I. Purification and properties of particle-bound fructose dehydrogenase, J. Biochem. 61, 636–646.
- Yamaguchi, T., Y. Murakami, K. Yokoyama, H. Komura and E. Tamiya, 1995, Electrochemical characterization of galactose oxidase coupled with ferrocene derivatives, Denki Kagaku 63, 1179–1182.

- Yamamoto, K., K. Takagi, K. Kano and T. Ikeda, 2001, Bioelectrocatalytic detection of histamine using quinohemoprotein amine dehydrogenase and the native electron acceptor cytochrome c-550, *Electroanalysis* 13, 375–379.
- Yanai, H., K. Miki, T. Ikeda and K. Matsushita, 1994, Bioelectrocatalysis by alcohol dehydrogenase from *Acetobacter aceti* adsorbed on bare and chemically modified electrodes, *Denki Kagaku* 62, 1247–1248.
- Yaropolov, A.I., A.A. Karyakin, S.D. Varfolomeev and I.V. Berezin, 1984, Mechanism of H₂-electrooxidation with immobilized hydrogenase, *Bioelectrochem. Bioenerg.* 12, 267–277.
- Yaropolov, A.I., A.N. Kharybin, J. Emnéus, G. Marko-Varga and L. Gorton, 1995, Flow injection analysis of phenols at a graphite electrode modified with co-immobilized laccase and tyrosinase, *Anal. Chim. Acta* 308, 137–144.
- Yaropolov, A.I., A.N. Kharybin, J. Emnéus, G. Marko-Varga and L. Gorton, 1996, Electrochemical properties of some copper-containing oxidases, *Bioelectrochem. Bioenerg.* 40, 49–57.
- Yaropolov, A.I., V. Malovik, S.D. Varfolomeev and I.V. Berezin, 1979, Electroreduction of hydrogen peroxide on an electrode with immobilized peroxidase, *Dokl. Akad. Nauk. SSSR* 249, 1399–1401.
- Yaropolov, A.I., A. Naki, G.S. Pepanyan, E.L. Saenko and S.D. Varfolomeev, 1986, Mechanism of laccase activation in pre-steady-state reaction stage, *Moscow University Chem. Bull.* 27, 93–96.
- Yaropolov, A.I., O.V. Skorobogat'ko, S.S. Vartanov and S.D. Varfolomeyev, 1994, Laccase. Properties, catalytic mechanism, and applicability, *Appl. Biochem. Biotechnol.* 49, 257–280.
- Ye, B. and X. Zhou, 1997, Direct electrochemical redox of tyrosinase at silver electrodes, *Talanta* 44, 831–836.
- Yeh, P. and T. Kuwana, 1977, Reversible electrode reaction of cytochrome c, *Chem. Lett.* 1145–1148.
- Yu, A. and F. Caruso, 2003, Thin films of polyelectrolyte-encapsulated catalase microcrystals for biosensing, *Anal. Chem.* 75, 3031–3037.
- Yu, X., D. Chattopadhyay, I. Galeska, F. Papadimitrakopoulos and J.F. Rusling, 2003a, Peroxidase activity of enzymes bound to the ends of single-wall carbon nanotube forest electrodes, *Electrochem. Commun.* 5, 408–411.
- Yu, X., G.A. Sotzing, F. Papadimitrakopoulos and J.F. Rusling, 2003b, Wiring of enzymes to electrodes by ultrathin conductive polyion underlayers: Enhanced catalytic response to hydrogen peroxide, *Anal. Chem.* 75, 4565–4571.
- Zaitsev, V., I. Zaitseva, G. Card, B. Bax, A. Ralph and P. Lindley, 1996, The three-dimensional structure of human ceruloplasmin at 3.0Å resolution, *Fold. Design* 1, S71.
- Zamocky, M., M. Hallberg, R. Ludwig, C. Divne and D. Haltrich, 2004, Ancestral gene fusion in cellobiose dehydrogenases reflects a specific evolution of GMC oxidoreductases in fungi, *Gene* 338, 1–14.
- Zeravik, J., T. Ruzgas and M. Franek, 2003, A highly sensitive flow-through amperometric immunosensor based on the peroxidase chip and enzyme-channeling principle, *Biosens. Bioelectron.* 18, 1321–1327.
- Zhang, J., Q. Chi, A.M. Kuznetsov, A.G. Hansen, H. Wackerbarth, H.E.M. Christensen, J.E.T. Andersen and J. Ulstrup, 2002a, Electronic properties of functional biomolecules at metal/aqueous solution interfaces, *J. Phys. Chem. B* 106, 1131–1152.
- Zhang, J.D., Q.J. Chi, T. Albrecht, A.M. Kuznetsov, M. Grubb, A.G. Hansen, H. Wackerbarth, A.C. Welinder and J. Ulstrup, 2005, Electrochemistry and bioelectrochemistry towards the single-molecule level, *Theoretical notions and systems* 50, 3143–3159.
- Zhang, Z., S. Chouchane, R.S. Magliozzo and J.F. Rusling, 2002b, Direct voltammetry and catalysis with *Mycobacterium tuberculosis* catalase–peroxidase, peroxidases, and catalase in lipid films, *Anal. Chem.* 74, 163–170.
- Zhang, W.J. and G.X. Li, 2004, Third-generation biosensors based on direct electron transfer of proteins, *Anal. Sci.* 20, 603–609.

- Zhang, Y., A. Pothukuchy, W. Shin, Y. Kim and A. Heller, 2004, Detection of $\sim 10^3$ copies of DNA by an electrochemical enzyme-amplified sandwich assay with ambient O_2 as the substrate, *Anal. Chem.* 76, 4093–4097.
- Zhang, D., G.S. Wilson and K. Niki, 1994, Electrochemistry of adsorbed cytochrome c_3 on mercury, glassy carbon, and gold electrodes, *Anal. Chem.* 66, 3873–3881.
- Zherdev, A.V., N.A. Bizova, A.I. Yaropolov, N.V. Lyubimova, O.V. Morozova and B.B. Dzantiev, 1999, Laccase from *Coriolus hirsutus* as alternative label for enzyme immunoassay: Determination of pesticide 2,4-dichlorophenoxyacetic acid, *Appl. Biochem. Biotechnol.* 76, 203–215.
- Zhou, Y., N. Hu, Y. Zeng and J.F. Rusling, 2002, Heme protein-clay films: Direct electrochemistry and electrochemical catalysis, *Langmuir* 18, 211–219.
- Zimmermann, H., A. Lindgren, W. Schuhmann and L. Gorton, 2000, Anisotropic orientation of horseradish peroxidase by reconstitution on a thiol-modified gold electrode, *Chem. Eur. J.* 6, 592–599.

Amperometric Enzyme Sensors based on Direct and Mediated Electron Transfer

Sabine Borgmann, Gerhard Hartwich, Albert Schulte and Wolfgang Schuhmann

Anal. Chem. – Elektroanalytik & Sensorik, Ruhr-Universität Bochum, Universitätsstr. 150, D-44780 Bochum, Germany

Contents

1. Electron-transfer pathways between redox proteins and electrode surfaces	599
1.1. Introduction	599
1.2. Marcus-theory of electron transfer	602
1.3. Structural and ET properties of redox proteins	604
1.3.1. Small redox proteins	605
1.3.2. Redox proteins with tightly bound cofactors inside the protein shell	606
1.3.3. Multi-cofactors redox proteins	606
1.4. Immobilisation of proteins on electrode surfaces	607
1.5. Design of ET pathways	614
1.6. Optimisation of sensor architectures	624
1.7. Enzyme microstructures	628
2. ET pathways in recognition of DNA hybridisation	629
2.1. Affinity-based recognition of dsDNA	632
2.1.1. Detection of dsDNA via intercalators	632
2.1.2. Detection of dsDNA via signalling ODNs	632
2.2. Amplified recognition of DNA hybridisation	633
2.2.1. Enzyme-amplified recognition of dsDNA	633
2.2.2. Chemical amplification for recognition of dsDNA	634
2.2.3. Bioelectronic hybrid devices for recognising DNA hybridisation	636
3. Conclusion and outlook	636
List of abbreviations	637
References	637

1. ELECTRON-TRANSFER PATHWAYS BETWEEN REDOX PROTEINS AND ELECTRODE SURFACES

1.1. Introduction

A biosensor is defined as an analytical device consisting of a biological sensing element either integrated within or in close vicinity of a transducer element which transforms the selective information of the presence of an analyte of interest into a quantifiable signal (Hall, 1992; Thevenot *et al.*, 2001). A typical

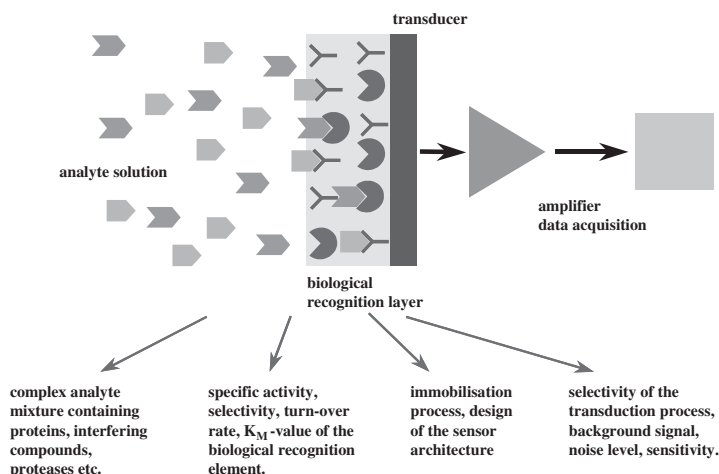


Fig. 1. Schematic representation of a biosensor and the factors defining the sensor signal.

biosensor architecture comprises three features: a biological recognition element which is usually immobilised on the surface of a suitable transducer for converting the primary signal into a proportional change of a physical or chemical property, and an amplification or processing element (Figure 1).

The design of appropriate sensor architectures for a given analyte depends on the specific demands arising from the analytical problem, which has to be solved such as selectivity, sensitivity, dynamic range, detection limit, response time, precision, reproducibility, stability, and cost of the measurement.

The high selectivity and specificity of biosensors are realised by integration of a biological recognition element within the sensing chemistry, thus providing an intrinsic advantage by making use of the existing variety of complementary biological recognition reactions. Usually, sensors based on *catalytic* biorecognition elements (enzymes, cells, microorganisms, tissues) and sensors based on *affinity-based* recognition elements (antibodies, antigens, receptor proteins such as ion channel receptors, G-protein-linked receptors, receptors with single transmembrane segments, synthetic receptors, and nucleic acids) are distinguished (Griffiths and Hall, 1993). As a matter of fact, sensors using catalytic biorecognition elements possess an in-built signal-amplification ability concomitant with a regeneration of the active site of the biorecognition element after the catalytic reaction. In contrast, affinity-based sensors are mainly restricted by the equilibrium constant of the recognition reaction and have to be coupled with suitable amplification strategies. However, since high affinity is a crucial prerequisite for a low detection limit affinity-based sensors often lack reversibility. Therefore, most applied research was done in the field of immunosensors, especially miniaturised electrochemical immunosensors (Aguilar *et al.*, 2002). The application of enzymes for biosensors (Guilbault and Schmid, 1991; Bilitewski *et al.*, 2000; Chaubey and Malhotra, 2002) and the use of affinity-based sensors (Scheller *et al.*, 2002; Umezawa *et al.*, 2002; Subrahmanyam *et al.*, 2002) has been extensively reviewed in detail over the past years. The sensitivity and the

detection limit of a biosensor is strongly dependent on the affinity or catalytic properties of the sensing elements on the one hand, and the sensitivity of the physical transducer on the other hand. In the case of an electrochemical transduction scheme different techniques can be applied for quantifying the concentration of the analyte of interest. Among these are potentiometric transducers such as pH electrodes, potentiometric gas sensors, ion-selective electrodes, ion-selective field-effect transistors (ISFET), and enzyme field-effect transistors (ENFET) in which the variation of the activity of a potential-determining species (e.g. H^+ , NH_3 , CO_2 , metal ions) caused by the biological recognition reaction is determined. Here, the focus is directed towards electron-transfer (ET) reactions subsequent to redox reactions catalysed by suitable redox enzymes. In this case, the transducer is usually a noble metal or carbon electrode and often dynamic voltammetric methods such as cyclic voltammetry (CV), differential pulse voltammetry (DPV), and differential pulse amperometry (DPA) are used to elucidate the chosen biosensor architecture and the properties of the immobilised redox proteins (Armstrong, 2002). In addition, constant-potential amperometry is frequently used to obtain correlations between substrate concentration and sensor output. Combination with spectroscopic techniques (UV-vis, NMR, EPR) allows to obtain further information.

The most simple design of an amperometric biosensor is the direct measurement of either an enzymatically generated product or of an ET mediator naturally involved in the biocatalytic process. A typical example for this design is the basic set-up of glucose sensors comprising the enzyme glucose oxidase as the biorecognition element and recording either the enzymatically produced product H_2O_2 or the decrease of the concentration of the co-substrate O_2 for collecting information about the glucose concentration in a sample (Clark and Lyons, 1962; Guilbault and Lubrano, 1973). The corresponding glucose sensors are typical examples of the so-called 'first-generation biosensors' (Updike and Hicks, 1967; Harrison *et al.*, 1988; Shimizu and Morita, 1990). However, since this detection principle may lead to a poor reproducibility of the overall sensing process due to varying O_2 concentrations in the sample under investigation, the application of artificial redox mediators was introduced in order to avoid the interference-prone oxygen dependence. Moreover, it is essential to decrease the unfavourable working electrode potential necessary for either the reduction of O_2 or the oxidation of H_2O_2 . Sensors realising a design with artificial mediators at known/constant concentration are addressed as 'second generation biosensors' (Ianniello *et al.*, 1982a; Kulys and Cenas, 1983; Cass *et al.*, 1984; Umana and Waller, 1986; Foulds and Lowe, 1988; Hill and Sanghera, 1990; Kajiya *et al.*, 1991). In second generation biosensors redox enzymes donate or accept electrons to or from electrochemically active redox mediators having a redox potential adjusted to that of the enzyme's cofactor.¹ Ideally the mediator is

¹In biology, the term 'prosthetic group' or 'coenzyme' is used for tightly bound, specific non-polypeptide units required for the biological activities of proteins. In bioelectrochemistry, the term 'cofactor' is often used synonymously with the term 'prosthetic group' or 'coenzyme'. This is even more problematic since proteins containing more than one prosthetic group are usually called multi-cofactor proteins. In this chapter, the term 'cofactor' was used exclusively for redox-active non-polypeptide substructures in an enzyme which are tightly but not necessarily covalently bound within the protein. Free-diffusing coenzymes like NAD^+/NADH are not included in this meaning of the term 'cofactor'.

otherwise inactive, i.e. highly specific only for the desired ET process between the recognition element and the transducer. As a matter of fact, free-diffusing low-molecular weight redox mediators are prone to leak from the electrode surface thus imposing an overall decreased long-term operation stability to this type of enzyme electrodes. This inherent problem, however, is not preventing the successful application of such sensors in one-shot devices, an application field which is especially important for self-monitoring of blood glucose levels (Tang *et al.*, 2001; Louie *et al.*, 2000; Kost *et al.*, 2000).

Another alternative approach is seen in immobilising the redox enzyme on a suitable electrode surface in such a way that the protein-integrated redox site can directly exchange electrons with the electrode (Armstrong *et al.*, 1988; Frew and Hill, 1988) avoiding any free-diffusing redox mediator (Kulys *et al.*, 1980; Lötzbeyer *et al.*, 1996; Contractor *et al.*, 1994; Schuhmann, 1995b; Khan, 1996; Chaubey *et al.*, 2000a). This sensor design was named 'third-generation biosensors'.

1.2. Marcus-theory of electron transfer

For a principal understanding of the ET processes underlying the functionality of all amperometric biosensors the same theoretical background can be used as it was developed for the elucidation of ET processes that play a vital role in a variety of biological reactions or for artificial 'donor-acceptor system'. These donor-acceptor reactions can be very rapid, even when the reactants are separated over longer distances, e.g. by multi-step tunnelling processes (Winkler, 2000). The underlying principal mechanism was intensively investigated and reviewed (Beratan and Skourtis, 1998). In the following, a brief summary of the Marcus-theory of ET is presented.

Electron transfer is a radiationless electronic rearrangement occurring isoenergetically: an electron moves from an initial state on an electrode or reductant to a receiving state on another solvated species or on an electrode of the same energy. A conventional theoretical description of the elementary reaction rates is given in equation (1), the so-called single mode quantum mechanical treatment of non-adiabatic ET theory according to Marcus, Levich, Jortner and Gerischer (Marcus, 1965; Gerischer, 1961; Levich and Dogonadze, 1959; Bixon and Jortner, 1968; Marcus, 1987, 1988; Marcus and Sutin, 1985; Jortner, 1980; Heitele, 1993; Bixon and Jortner, 1986).

$$k = \frac{2\pi}{\hbar^2 \omega_m} \cdot V^2 \cdot \left(\frac{v+1}{v} \right)^{p/2} \cdot \exp[-S(2v+1)] \cdot I_P[2S(v(v+1))^{1/2}]. \quad (1)$$

In this equation, $\hbar\omega_m$ is the energy of the (protein/enzyme) mode that is coupled to the ET process (the vibration that is physically transferring the electron from the initial donor state to the final acceptor state). The term $v = [\exp(\hbar\omega_m/k_B T) - 1]^{-1}$ reflects the thermal population of that mode. The expression $p = -\Delta G^0/\hbar\omega_m$ is the free energy gap of the reaction (the

driving force) reduced by $\hbar\omega_m$ (to get rid of the unity). The electron–phonon coupling parameter, S , corresponds to the reduced nuclear reorganisation energy λ ($S = \lambda/\hbar\omega_m$), which can be viewed as a parameter that accounts for the reorganisation of the donor and acceptor and their corresponding surrounding in course of the ET process (changes of the internal geometry, coordination, etc. of donor and acceptor due to the oxidation of the one and reduction of the other. V is the two centre, one electron electronic interaction term that might be interpreted as the success probability of an ET-transfer trial. I_p is the modified Bessel function of order p , k_B and \hbar are the Boltzmann and the Planck's constant (divided by 2π), respectively, and T is the temperature.

A simplified expression of the basic rate constant is given by the typical Marcus-equation (equation (2)), where non-adiabatic ET is described by the Franck–Condon weighted density of states of the (protein/enzyme) mode:

$$k = \frac{2\pi}{\hbar} \cdot V^2 \cdot \sqrt{4\pi\lambda k_B T} \cdot \exp[-(\Delta G^0 + \lambda)^2/4\lambda k_B T]. \quad (2)$$

The distance dependence of ET is reflected in the electronic interaction term V . The ET rate decreases exponentially with increasing distance according to

$$V = V^0 \cdot \exp[-\beta(r - r^0)] \quad (3)$$

In equation (3), the distance between donor and acceptor is given by r and V^0 is the electronic coupling at nearest distance r^0 between donor and acceptor and β is a 'material-constant' reflecting the ET-properties of the medium between donor and acceptor. For a given donor–acceptor distance a plot of $\ln k$ vs. ΔG^0 is parabolic with a maximum rate at $-\Delta G^0 = \lambda$ (Miller *et al.*, 1984; McCleskey *et al.*, 1992, 1994), however, since for electrochemical biosensors one of the ET partners in the overall rate is an electrode with a continuum of electronic states in the so-called inverted region ($-\Delta G^0 > \lambda$) and/or transfer of charge to the electrode may be diffusion limited, one would not expect the typical decrease of $\ln k$ vs. ΔG^0 in the inverted region for this type of heterogeneous ET reactions.

In general, a complete mechanistic explanation of the overall rate of a biosensors on the basis of the given equations is difficult due to the complexity of the kinetic system with several ET reactions, enzyme kinetics, diffusion, heterogeneous ET reactions, etc. and the imprecise knowledge of the involved parameters. There are different mechanisms for intra-molecular and inter-molecular ET: direct or superexchange-mediated ET between cofactors, a hopping mechanism from one cofactor via protein residues to another cofactor or large, redox-dependent conformational changes could enable direct ET between cofactor. In metallo-proteins, for example, ET can take place over very long distances (up to 30 Å) at a tremendous rate ($> 10\text{ s}^{-1}$). In biological systems, ET often occurs along specific protein–protein complexes, such as in the respiratory chain. These complexes need to be stable enough for a molecular recognition process, but also labile enough to allow a fast overall electron flow. The electron

exchange process is dependent on the surface structure of the proteins and the molecular dynamics of protein–protein complexes. It seems that evolutionary process of nature mainly relies on a close proximity between the involved redox relays while tuning the energetic properties by means of the surrounding (protein) medium.

Summarising, ET is – according to Marcus theory – mainly regulated by (Williams, 1989; Beratan *et al.*, 1992; Moser *et al.*, 1992; Winkler, 2000; Petrov *et al.*, 2001)

- the distance between the electron donor and acceptor,
- the driving force for the overall process,
- the reorganisation energy of the involved redox centers, and
- the intervening medium/the nature of the protein matrix.

1.3. Structural and ET properties of redox proteins

Enzymes are favoured as recognition elements in biosensors because they provide a broad range of changes of physico-chemical parameters such as electrons, protons, ions, mass, light, and heat during the enzymatic reaction (Lowe, 1989), which can be detected using suitable transducer elements. General properties of enzymes have been intensively discussed in Lippard and Berg (1994) and Williams (2003). With the focus on ET reactions as basis of sensor architectures, it is obvious in a general sense that ET reactions and pathways in biology are involving a large variety of different types and classes of proteins (Vervoort, 1991). Thus, in order to understand biological ET pathways which may eventually serve as models for the design of ET pathways in biosensors, the specific features of ET pathways have to be elucidated (Brunori, 1994).

A large number of enzymes can catalyse redox transformations and these so-called oxidoreductases are essential for fundamental biological reactions, such as respiration, photosynthesis, metabolism, and cellular defence. In general, redox proteins make use of either bioinorganic or organic prosthetic groups, which may be covalently bound or non-covalently fixed within the protein shell. Alternatively, free-diffusing coenzymes are used as electron donors or acceptors involving a simultaneous binding of substrate and coenzyme in the active site of the enzyme. Oxidoreductases cover about 30% of nature's enzymes. The redox potentials of the cofactors (iron–sulphur clusters, hemes, quinones, etc.) are confined to a relatively narrow potential window of 0 to ± 1 V vs. NHE. The formal potential of the cofactors integrated within the protein shell is dramatically modulated by the protein side chains serving as ligands for the metal complexes, by a change in the stereochemistry of the metal centre. In addition, the whole protein structure influences the redox potential in analogy to the influence of the solvent on redox potentials of redox species in solution by factors, such as local hydrophilicity or hydrophobicity, steric blocking of coordination sites, and hydrogen bridges. Metal ions located in the active centre of an enzyme can change their reactivity in the presence of an external substrate during

the catalytic process. In addition, metal ions induce the formation of a specific tertiary structure of the protein and may help in the interaction between proteins or stabilise them. The metal-binding part of redox enzymes is tailored for exhibiting minimal structural changes in the protein following a change in the redox state of the cofactor. However, some redox proteins (e.g. cytochrome *cd₁* nitrite reductase (Williams *et al.*, 1997) exhibit dramatic conformational changes induced by a change in their redox state which may be applied for an allosteric regulation of the enzyme activity or to modulate the binding constant of the product inside the active site to facilitate the completion of the catalytic cycle.

1.3.1. Small redox proteins

The so-called small redox proteins often serve as free-diffusing redox mediators in biological systems assuring the function of ET chains by coupling membrane-bound, and hence relative immobile redox proteins. Cytochromes are redox shuttles containing at least one ferro-heme as a cofactor. They perform a variety of different biological functions and are used physiologically in ET pathways, e.g. in the respiratory chain in the mitochondria. During respiration cytochrome *c* oxidase transports electrons from cytochrome *c* to water. Often multi-electron redox reactions have to be coupled with the possibility to establish ET chains using one-electron redox shuttles. For example, the reduction of one oxygen molecule to two water molecules requires four electrons, while cytochrome *c* is able to transfer only one electron at a time. The production of toxic radicals by this incomplete reduction of oxygen is, however, avoided though the mechanism is still not completely understood (Niki *et al.*, 2003; Wei *et al.*, 2004). The heme group of cytochromes consist of Fe(III) coordinated to a porphyrin group. The redox potentials of the Fe(III)/Fe(II) couples of different types of cytochromes are significantly different despite their obvious structural similarities. These differences are closely related to the nature of the active site of the cytochrome, such as hydrophobicity, solvent accessibility, and nature of the protein side chains with respect to their electrostatic and hydrogen-bonding interaction capability. Small heme-containing proteins, such as cytochrome *c*, and microperoxidase MP11 seem to be suitable redox proteins for the use in biosensors, however, their ET capabilities with electrodes was shown to be highly dependent on electrode surface modifications (see below). Myoglobin and haemoglobin, however, although they had been demonstrated to exhibit direct ET with electrode surfaces, show slow ET kinetics and were hence not applied in biosensors.

Blue copper proteins, such as azurins, plastocyanins, pseudo-azurins and amicyanins, received their classification name because of their blue colour. They have a closely fixed structure, and have similar copper coordination by two histidine, one cysteine and one methionine residue. Their catalytic reaction is pH sensitive because the acid-base properties of coordinating ligands can specifically change the redox potential of the protein (Chapman, 1991). These ET proteins do not perform a significant structural change of the protein during the ET process. Thus, they have a small reorganisation energy and consequently high ET rates. Moreover, blue copper proteins have no cofactor that is

associated with the copper centre, but residues of the protein matrix serve as ligands to the metal centre. Interestingly, two distinct proteins, plastocyanin and cytochrome c_6 , have identical purposes in the photosynthetic ET chain. Both differ in composition and structure, but they possess very similar redox potentials. Because their surface topology is similar and the involved parts of the proteins in the ET reaction have similar positions, both can perform the same biological function.

1.3.2. Redox proteins with tightly bound cofactors inside the protein shell

Redox proteins with tightly bound cofactors, such as flavins, quinones, hemes, disulfide groups, or metal centres are frequently used in amperometric biosensors. They are classified with respect to their cofactor which can be covalently or non-covalently bound. There are, for example, five classes of flavoenzymes which are defined by the mechanism of the ET with their substrate: transhydrogenases, dehydrogenase-oxidases, dehydrogenase-monooxygenases, dehydrogenase-electron transferases, and electron transferases. Often, the cofactor of these enzymes are deeply buried within the protein shell leading to a successful insulation of the cofactor from unwanted ET reactions. This is a key feature of life, since potential differences necessary to perform metabolic reactions have to be prevented to get lost in thermodynamically driven down-hill reactions under dissipation of the energy in form of heat.

1.3.3. Multi-cofactors redox proteins

Multi-cofactor redox proteins consist usually of more than one subunit with different cofactors such as pyrrolo-quinoline-quinone (PQQ), flavin-adenine-dinucleotide (FAD), nicotinamide-adenine-dinucleotide (NAD^+), flavin-mononucleotide (FMN) or heme. Following a primary redox conversion in the active site of the enzyme leading to the oxidation or reduction of the substrate, the primary cofactor is regenerated by a fast internal ET with the secondary cofactors bound in the same or other subunits of the protein (Page *et al.*, 2003). This fast regeneration of the active site allows a high turnover rate and concomitantly prevents the back-reaction of the product thus shifting the equilibrium of the reaction to the product side. Moreover, the redox equivalents are made available to specific partners in the overall ET cascade following a pre-defined pathway thus preventing unfavourable loss of energy in unwanted side reactions. Obviously, one cofactor is used for the catalytic reaction with the substrate of the enzyme, and the others serve as secondary electron acceptors or donors for channelling electrons along a pre-defined ET pathway.

Two possible mechanisms for the exchange of electrons can be assumed for these multi-cofactor enzymes. The first is involving an ET pathway from one cofactor to the next according to the differences in the formal potentials of the involved redox centres (electron-hopping mechanism), while the second is assuming a direct ET between each of the cofactors with the electrode surface (Figure 2).

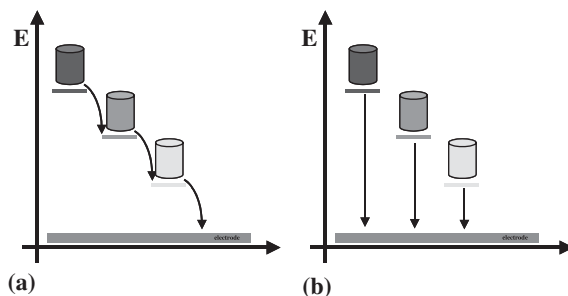


Fig. 2. ET mechanism in multi-cofactor redox proteins. (a) a hopping mechanism, (b) non-hopping mechanism.

In general, it is assumed that multi-cofactor proteins follow an intra-molecular ET pathway via the hopping mechanism schematically shown in Figure 2a. In order to prove this assumption the ET properties in two different fumarate reductases were investigated using square wave voltammetry (Jeuken *et al.*, 2002). To distinguish between the two mechanisms the ET rate was measured as a function of the driving force, assuming that in the case of a direct non-hopping ET the rate should increase with the applied potential of the working electrode. In the case of the hopping mechanism, the overall ET rate is controlled by the slowest rate in the sequence of ET reactions between the redox partners in the electron-hopping chain. Hence, the ET rate should be independent from the applied electrode potential. For fumarate reductase the ET rate was found to be independent from the applied electrode potential. A compilation of the specific characteristics of a number of multi-cofactor enzymes is given in Table 1, possible ET pathways for some selected enzymes are demonstrated in Figure 3 showing the differences of possible ET chains in dependence from the number of involved cofactors, their orientation and their location in the different subunits.

1.4. Immobilisation of proteins on electrode surfaces

Techniques for the preparation of biosensors are well established and are mainly dealing with the fixation of the biological recognition element on the transducer surface. Here, the focus is directed towards the fabrication of suitable biosensor architectures facilitating electrochemical communication between the immobilised redox proteins and the electrode surface. As a matter of fact, the chosen immobilisation technique and its impact on the biological recognition element affects significantly the overall biosensor performance and determines the selectivity, sensitivity, specificity, dynamic range, response time, and reliability of the biosensor. Several techniques for the immobilisation of redox protein on electrode surfaces are available and described in detail (Murray, 1980; Bard, 1983; White and Turner, 1997; Stoecker and Yacynych, 1990; Barendrecht, 1990; Zhang *et al.*, 2000). Possibilities to immobilise proteins on electrode surfaces are schematically summarised in Figure 4.

Table 1. Multi-cofactor redox enzymes summarising structural and ET properties

Analyte of interest	Biological recognition element	Subunits of multi-cofactor proteins	References (applications in biosensors)
<i>Quinoproteins (PQQ or derivatives; non-covalently bound)</i>			
Ethanol, higher alcohols	Quinohemoprotein alcohol dehydrogenases (QH-ADH)	Type III ADH: subunit 1: PQQ (reaction with substrate), heme <i>c</i> (electron acceptor); subunit 2: 3 heme <i>c</i> (electron acceptors); subunit 3: no redox group	Laurinavicius <i>et al.</i> (2002), Davidson (2004), Oubric (2003), Ikeda and Kano (2003), Jeuken <i>et al.</i> (2002), Davis <i>et al.</i> (1983), Niculescu <i>et al.</i> (2002), Ikeda <i>et al.</i> (1993b), Yanai <i>et al.</i> (1994), Ramanavicius <i>et al.</i> (1999), Toyama <i>et al.</i> (2004), Razumiene <i>et al.</i> (2003), Stigter <i>et al.</i> (1997)
Fructose	Quinohemoprotein fructose dehydrogenase (FDH)	Subunit 1: PQQ (reaction with substrate), heme <i>c</i> (electron acceptor)	Ikeda <i>et al.</i> (1990), Paredes <i>et al.</i> (1997)
Amines	Quinohemoprotein amine dehydrogenase	Subunit 1: CTQ (cysteine tryptophylquinone) (reaction with substrate); subunit 2: 2 hemes <i>c</i> (electron cceptors); subunit 3: no redox group	Fujieda <i>et al.</i> (2002), Yamamoto <i>et al.</i> (2001), Hyun and Davidson (1995), Bishop and Davidson (1997)
<i>Flavoproteins (FMN non-covalently bound, FAD covalently or non-covalently bound)</i>			
Succinate	Succinate dehydrogenase (SDH)	Subunit 1: covalently bound FAD, three Fe-S clusters	Hirst <i>et al.</i> (1996), Leger <i>et al.</i> (2001), Pershad <i>et al.</i> (1999)
Fumarate	Fumarate reductase (FR)	Subunit 1: FAD; subunit 2: three Fe-S clusters; subunit 3: two heme <i>b</i>	Jeuken <i>et al.</i> (2002), Leger <i>et al.</i> (2001), Heering <i>et al.</i> (1997)
Cellobiose	Cellobiose dehydrogenase (CDH)	Subunit 1: FAD (reaction with substrate); subunit 2: heme <i>b</i> (electron acceptor)	Fridman <i>et al.</i> (2000), Larsson <i>et al.</i> (1996), Lindgren <i>et al.</i> (2000a), Lindgren <i>et al.</i> (1999b), Stoica <i>et al.</i> (2004)
D-gluconate	D-gluconate dehydrogenase (GADH)	FAD, heme <i>c</i> , Fe-S clusters;	Ikeda <i>et al.</i> (1992, 1993a)
Sulfide	Flavocytochrome <i>c</i> ₅₅₂ (FCC)	Subunit 1: FAD; subunit 2: cytochrome <i>c</i>	Kinnear and Monbouquette (1993)

In general, one has to consider several factors before choosing an appropriate immobilisation technique aiming on the preservation of a maximum of enzyme activity and stability, a sufficient enzyme loading on the sensor surface, and a proper design of the sensor architecture to enable a productive communication between the biocatalytic recognition process and the transducer surface.

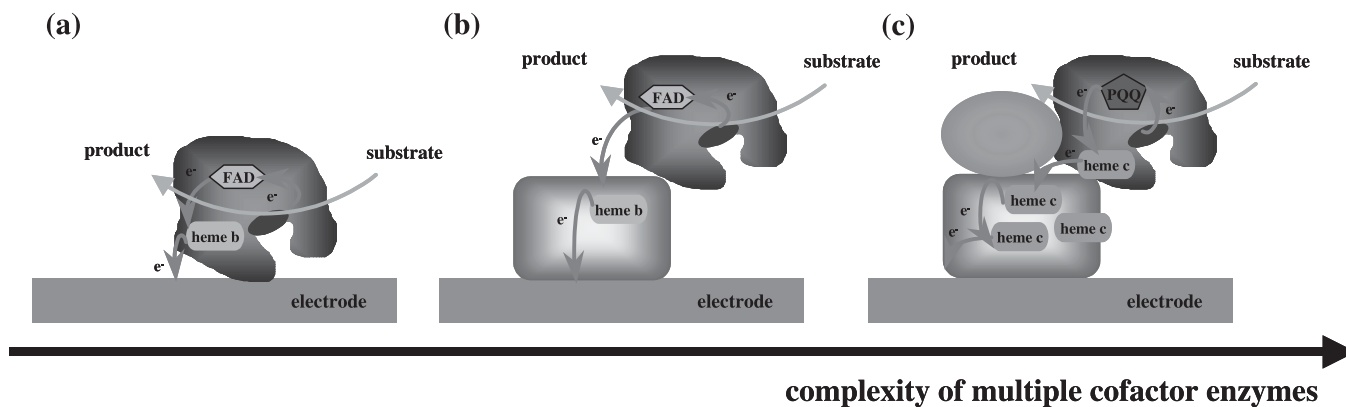


Fig. 3. Schematic representation of selected types of multi-cofactor enzymes immobilised at an electrode interphase (a) and (b) flavohemoproteins with one or two subunits, (c) quinohemoproteins.

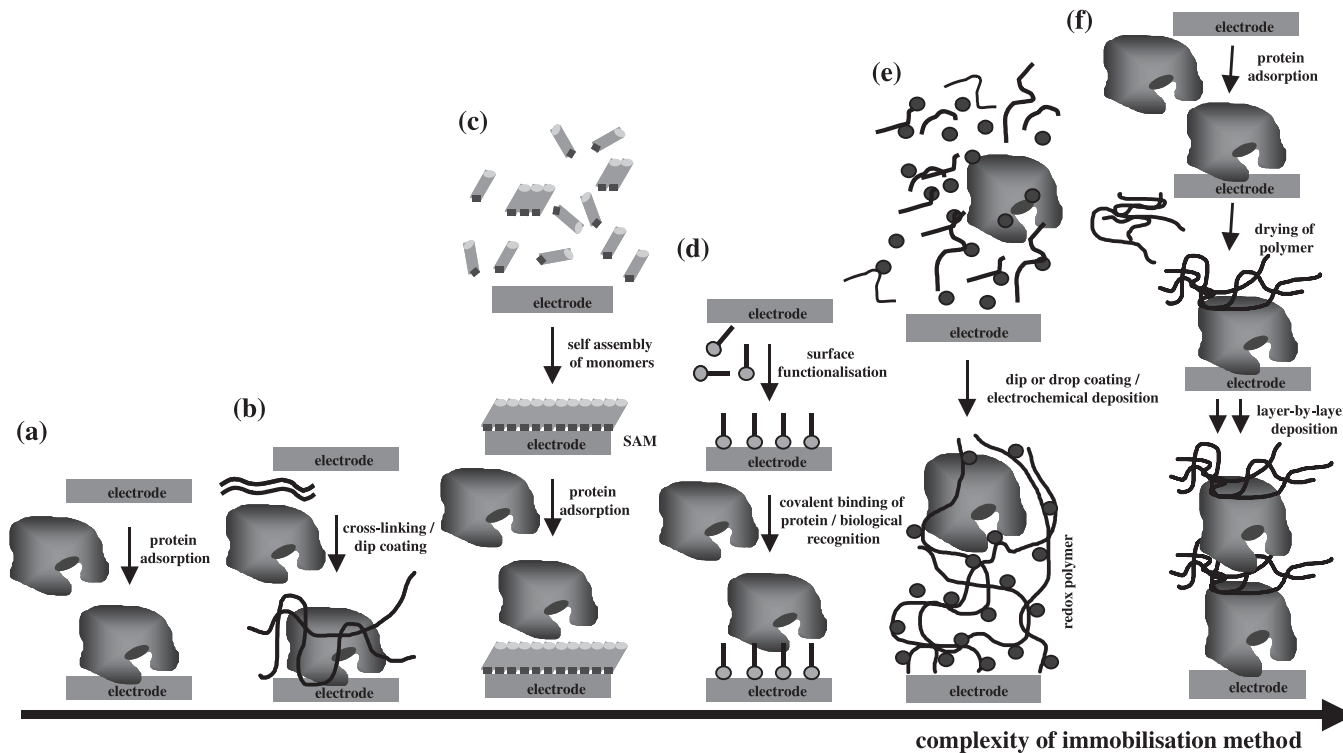


Fig. 4. Schematic representation of protein immobilisation techniques for the modification of transducer surfaces: (a) adsorption of proteins, (b) cross-linking of proteins, (c) formation of self-assembled monolayers (SAM) and protein attachment on SAM, (d) covalent attachment of proteins to the electrode surface or binding of proteins via biological recognition, (e) formation of redox polymers with entrapped proteins by means of dip or drop coating or electro-deposition, (f) layer-by-layer deposition.

Proteins adsorb spontaneously on a variety of electrode materials with the binding mainly depending on the interaction forces (Figure 4a). Adsorption is mainly due to electrostatic, dipole–dipole, or hydrophobic interactions in addition to the formation of hydrogen bonds. As a matter of fact, the stability of the obtained sensing layer is highly dependent on the ionic strength, the pH-value, temperature, etc., and hence not clearly defined especially in complex real samples. However, adsorption is a valid technique for first sensor tests, for one-shot biosensors, or for sensors which have to be regenerated, e.g. by provoking desorption of the adsorbed protein by means of pH changes or using electrolytes with high ionic strength. However, one has to take into account the fact that proteins often denature when they are in direct contact with noble metal or carbon surfaces.

To overcome problems of denaturation of proteins in direct contact with metal surfaces a variety of layers which may separate the protein from the transducer surface was developed. In this respect, self-assembled monolayers (SAMs) have found wide application as interface layers between the electrode surface and the enzyme, concomitantly allowing to covalently attach the proteins to the SAM using specifically integrated functional head groups at the monolayer (Wink *et al.*, 1997). In addition, SAMs can be tailored with respect to their surface charge to provide a surface with a certain degree of biocompatibility for *in vitro* or *in vivo* applications. Chemical self-assembly is used for surface modification and functionalisation and occurs when alkanethiols or related derivatives spontaneously chemisorb onto oxide-free metals (e.g. Au, Ag, Hg) from liquid or vapour phase (Figure 4c). The formation of SAMs on electrode surfaces proceed via a sequence of stages of different order from an unordered physisorbed assembly via a stacked lying assembly to densely packed phases with the alkane chains standing at a certain tilt angle to the surface plain (Poirier, 1999). Surface stress, kinetics, and structure of alkanethiol SAMs were monitored with *ex situ* STM imaging (Godin *et al.*, 2004). Investigations on SAMs on electrodes were reviewed in Finklea (1996). The overall formation of SAMs is fast, relatively easy, and flexible with respect to further modification reactions by means of adsorption or covalent binding of modifiers at suitable head groups. A variety of biosensor architectures based on monolayers (Willner *et al.*, 1992; Willner and Riklin, 1994) or multilayers (Willner *et al.*, 1993) entrapping redox enzyme were described.

Covalent attachment of biomolecules on the electrode surfaces provides more stable and better defined sensor architectures (Figure 4d). However, the electrode surface needs to be activated and suitable functional groups for the secure fixation of biological recognition elements have to be introduced to the surface. Pt electrodes can be modified using condensation of functionalised silane derivatives with the Pt-oxide layer at the electrode surface (Weetall, 1993) or with cyanuric chloride followed by reaction with an alcohol or amine function (Cho and Bailey, 1979; Ianniello *et al.*, 1982b). Similarly, silicon wafers, glass surfaces, and indium-tin-oxide electrodes can be functionalised. Carbon surfaces can be modified after chemical or electrochemical surface oxidation using thionyl-chloride or carbodiimide activation of the surface carboxyl groups (Bourdillon *et al.*, 1980).

Multi-layer films of organic compounds on solid surfaces allow fabrication of multi-composite molecular assemblies of tailored architecture. Both the Langmuir–Blodgett technique and chemisorption from solution were successfully used for electrode modification. Functionalisation of electrode surfaces was reviewed in Willner and Katz (2000). Multi-composites make it possible to combine two or more desirable properties, or to provide additional stability for otherwise highly labile biomolecules or biomolecular assemblies. Higher device functionality may arise from a combination of physical and chemical processes such as electron or energy transfer and photochemical energy conversion. Such devices require control of molecular orientation and organisation on the nano-scale. Therefore, the controlled assembly of multi-component nanostructures is of increasing importance, which may be achieved by sequentially depositing monomolecular layers onto planar solid supports. Within the formed multilayers, nanoscale arrangements of molecules can be controlled at least to a certain extent. A layer-by-layer assembly (Figure 4f) allows the formation of amperometric biosensors with controlled sensor architecture (Decher and Hong, 1991; Decher, 1997; Lvov *et al.*, 1993; Decher *et al.*, 1994; Panchagnula *et al.*, 2004) which offers control over amount and spatial distribution of the immobilised enzymes. Sufficiently stable films are obtained because of electrostatic attraction between the layers. In thicker films and multilayers only those molecules which are directly located in close proximity to the electrode surface may be able for direct ET. Thus, strategies have to be developed allowing for addressing also enzyme molecules which are immobilised outside the direct ET distance (Lvov and Möhwald, 1999; Panchagnula *et al.*, 2002; Lvov *et al.*, 1998; Rilling *et al.*, 1997; Wang and Hu, 2001; Loew *et al.*, 2004). For example, cytochrome *c* multilayers entrapped within polyelectrolytes showed increasing redox current with the number of layers (Beissenhirtz *et al.*, 2004). The layer-by-layer technique offers a relatively simple approach for surface modification with potentials for adapting it for miniaturised sensors and automated sensor fabrication. In addition, depending on the composition of the film interference-elimination layers can be implemented into the sensor architecture.

The biological recognition of antibodies and antigens were not only successfully applied for immunological purposes, but also as an analytical tool in biochemistry, e.g. for labelling of proteins, in enzyme immunoassays, or affinity chromatography. Based on these techniques, it is possible for immobilising enzyme molecules by using antigen–antibody recognition (Bourdillon *et al.*, 1993). Glassy-carbon electrodes, for example were modified with gelatine on which rabbit-IgG-antibodies were adsorbed. An anti-rabbit-IgG-antibody-glucose oxidase conjugate was bound to the first antibody layer resulting in a functional glucose sensor (Bourdillon *et al.*, 1994). Antigen–antibody interactions can be even used for the construction of multi-layered electrodes with up to 10 layers (Bourdillon *et al.*, 1996). In general, the affinity interactions are very strong (K_a (antibodies) = 10^{-6} to 10^{-8} M^{-1} , K_a (biotin–streptavidin) = 10^{-15} M^{-1}). Hence, due to its very strong affinity constant especially biotin–streptavidin recognition was frequently applied for the immobilisation of enzymes.

For entrapping of enzymes within a polymer film (Figure 4e) the pore size of the polymer needs to be chosen large enough to allow the free diffusion of substrates and products, but small enough to retain the enzymes within the film. In addition, structural rigidity and flexibility of the polymer film determines the properties of related biosensors. The entrapment of redox enzymes in polymers is facilitated by chemical and/or physical interactions between the protein shell and the polymer chains, however, the deposited polymer films form a diffusion barrier thus usually prolonging the response time, shifting the linear measuring range, and decreasing the sensitivity of the sensor. Dip coating followed by cross-linking of the polymer layer using bifunctional molecules were applied for incorporation of biomolecules into three-dimensional films with comparatively high activity (Figure 4b) (DeSantis and Jones, 1999; Wong and Wong, 1992). Cross-linking using, e.g. hexamethyl diisocyanate, glutaraldehyde (Chaubey *et al.*, 2000b) or poly(ethyleneglycol) diglycidylether reduces the leakage of the biorecognition elements and may even stabilise the entrapped protein. Redox polymer hydrogels (reviewed in Katakis and Heller, 1997) with entrapped redox enzymes have been frequently used for the construction of the so-called reagentless biosensors (for details see below). The hydrogel properties of the redox polymer in general ensure a fast diffusion of substrates and products within the film, and may provide an enzyme-friendly surrounding. Alternatively, electrochemically generated conducting and non-conducting polymers were used to entrap biomolecules. A suitable precursor monomer, which can be electrochemically oxidised at the electrode surface under formation of a radical cation within the diffusion zone in the front of the electrode surface, is mixed with the biorecognition element. Film deposition is invoked by means of potential cycling or the application of a sequence of potential pulses (Schuhmann *et al.*, 1997) is oxidised in the presence of a redox enzyme. First monomeric and dimeric cation radicals are obtained which form oligomers via radical recombination reactions. At a certain chain length, the oligomers become insoluble in the used solvent and precipitate on the electrode surface. For example, polypyrrole can be obtained by applying potentials greater than +0.6 V vs. SCE using cyclic voltammetry or pulse techniques. Due to the electrochemical control of the polymer formation process, a pre-defined film thickness can be obtained by adjusting the concentration ratio of the compounds, the applied potential and/or the deposition technique. The film properties are dependent on the used monomers, the polymerisation technique/rate, the electrode material, the nature of the redox enzyme, the components and pH-value of the buffer. It is important to choose a polymeric film that is compatible with the enzyme of interest. For example, it is difficult to entrap positively charged enzymes within polypyrrole films because of the electrostatic repulsion of the protein and the overall positively charged polymer film. A large number of contributions in this area was already published which had been comprehensively reviewed (Lorenzo *et al.*, 1998; Bartlett and Cooper, 1993; Schuhmann, 1995b; Trojanowicz and Krawczyk, 1995; Cosnier, 1999) (Figure 4e). Non-conducting polymers, e.g. poly(phenol), poly(phenylenediamine) (McMahon *et al.*, 2004) and poly(diamino benzene) (Geise *et al.*, 1993) can be used to form self-limiting thin hydrophobic and insulating films (Bruno *et al.*, 1977) with extraordinary

size-exclusion properties (Bartlett and Caruana, 1992). Interestingly, the size of the electrode surface seems to have an influence on the electrochemically induced film formation process thus altering the film properties (McMahon *et al.*, 2004) and the observed size-exclusion effect (Bartlett and Caruana, 1992).

1.5. Design of ET pathways

Due to its outstanding properties especially its high stability, glucose oxidase is often chosen as a biological recognition element for a primary evaluation of envisaged sensor designs. After oxidation of β -D-glucose in the active site of the dimeric enzyme the integrated cofactor flavine-adenine-dinucleotide (FAD) is reduced to FADH₂. The regeneration of the enzyme is achieved either by its natural electron acceptor O₂ (Gough *et al.*, 1985; Strike *et al.*, 1995; Wang and Lu, 1998) or artificial free-diffusing redox mediators (Schlapfer *et al.*, 1974; Kulyś and Cenas, 1983; Cass *et al.*, 1985). The limitations of using either the natural or artificial free-diffusing redox mediators are obvious since the availability of sufficient O₂ at the measuring site or the leakage of artificial mediators from the electrode surface have a severe impact on the sensor performance. Thus, possibilities for controlling ET processes between immobilised redox enzymes and the electrode surface are fundamental presuppositions for the development of biosensors with properties which can be optimised with respect to the analytical problem in question. Besides the theoretical knowledge about factors which may influence ET processes in sensor assemblies and the possibility to immobilise the sensor components on the electrode surface, ET pathways between the immobilised oxidoreductase and the electrode surface have to be designed. As a matter of fact, possible ET pathways have to be compatible with the immobilisation procedure and the specific properties of the biological recognition element. Moreover, rate-limiting steps of the overall reaction sequence have to be specified to select appropriate optimisation strategies. Because productive ET between a redox enzyme and an electrode mainly depends on the distance between the involved redox couples (for details see above; Marcus and Sutin, 1985), different sensor designs can be realised at various levels of complexity (Figure 5) (Mehrvar and Abdi, 2004; Chaubey and Malhotra, 2002).

In order to control the fabrication and later function of an amperometric biosensor to its largest extent the development of the so-called reagentless biosensors is of increasing importance (Schmidt and Schuhmann, 1996). A reagentless biosensor does not depend on any free-diffusing component with the exception of the analyte to be enzymatically converted. This implies that all sensor components are securely immobilised on the transducer surface in a carefully designed sensor architecture allowing productive interaction between all sensor components. For the development of a reagentless biosensor the most appropriate methods are the use of an enzyme with tightly bound redox centres and an ET pathway either by direct ET or via securely immobilised redox relays. As pointed out above, with respect to Marcus theory (Marcus and Sutin, 1985;

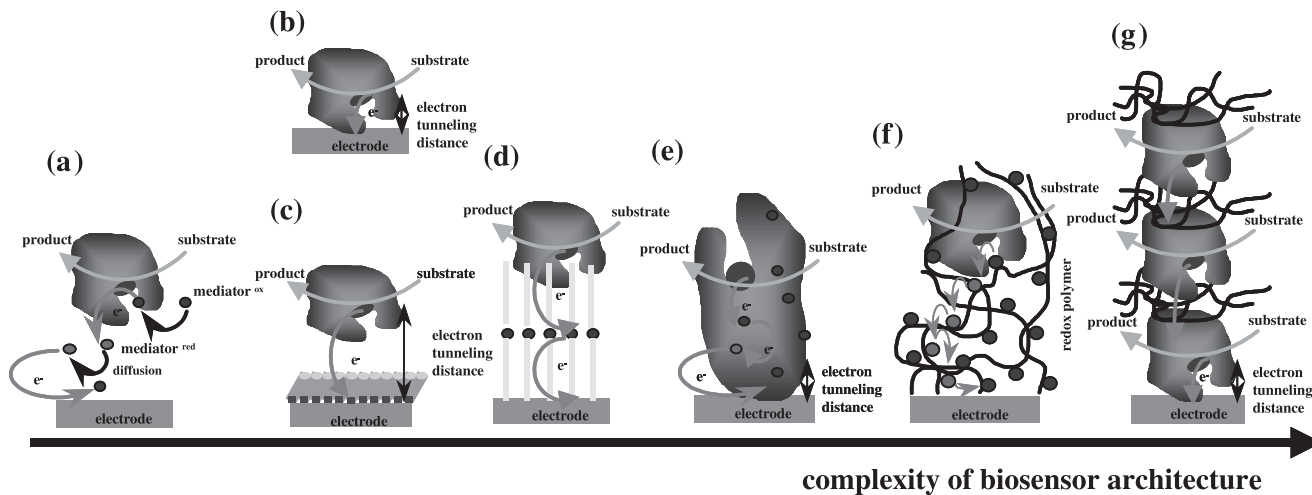


Fig. 5. Schematic representation of possible biosensor architectures allowing for productive ET between the immobilised biological recognition element and the electrode surface; (a) ET involving free-diffusing redox mediators, (b) direct ET from an oriented adsorbed redox enzyme, (c) direct ET via SAM, (d) ET cascade via SAM architectures, (e) mediated ET within a multi-cofactor or mediator-modified enzyme, (f) mediated ET via a redox polymer, (g) ET in a layer-by-layer assembly.

Marcus, 1993) three major factors concerning the direct ET between two redox sites call for careful consideration: the reorganisation energy qualitatively reflecting the structural rigidity of the redox compound in its oxidised and reduced form, the potential difference between the involved redox sites, and the distance between the redox sites (Carter *et al.*, 1995).

Direct ET between an enzyme, even immobilised in the first monolayer on the electrode surface, and the electrode is normally very slow or even precluded due to the effective kinetic barrier imposed by the deep encapsulation of the redox-active cofactor and the active substrate binding site in the enzyme structure. Thus, for an efficient ET involving most of the immobilised redox enzymes and allowing fast ET kinetics, cascades of a sequence of ET reactions have to be designed using additional, eventually tightly bound redox relays with a formal potential, which is adapted to that of the redox species involved in the overall ET process. Thus, the overall distance between the two redox sites is divided into a number of shorter distances increasing the overall ET kinetics while keeping the driving force constant.

The total efficiency of the ET cascade is dependent on the whole system architecture. One option is to shorten the distance between the active site of the redox enzyme and the electrode surface, however, the properties of the used redox mediator, the electrode material, the type of enzyme, etc. all influence the sensor properties in a complex way (Table 2).

In the case of mediated ET, redox mediators shuttle electrons between the active centre of the enzyme and the electrode (Figure 6a). Mediated biosensors are usually less susceptible to interferences because they can be operated at moderate electrode potentials. The diffusional properties and ET rate of the mediator is dependent on the size and shape of the mediator, the hydrophobic and/or hydrophilic properties and the charge interaction of the mediator with charged side chains at the protein shell of the enzyme. The use of free-diffusing redox mediators opened the route for successful applications of amperometric biosensors in single-use devices in combination with dissolved enzymes or with enzymes immobilised using all possible immobilisation strategies. As free-diffusing mediators among a large variety of other compounds ferrocene derivatives, organic dyes, ferricyanide, Ru- and Os-complexes, and other compounds have been used (Bartlett *et al.*, 1991). The application of free-diffusing redox mediators was intensively investigated in the last two decades and comprehensively reviewed (Bartlett and Cooper, 1993; Schuhmann, 1995b; Trojanowicz and Krawczyk, 1995; Cosnier, 1999).

A relatively easy method for integrating redox mediators is their mixing into a carbon paste (graphite powder/oil) (Senda *et al.*, 1986; Dicks *et al.*, 1986; Wang *et al.*, 1990; Kulys *et al.*, 1992; Kacaniklic *et al.*, 1994; Hedenmo *et al.*, 1997) eventually together with the biological recognition element. In order to optimise long-term stability and response time of the sensor, carbon pastes can be further modified with additives. It can be assumed that mediator molecules dissolve from the carbon paste into the overlying enzyme layer. If leakage from the enzyme layer into the electrolyte solution is slow enough, a reservoir with a steady-state concentration of mediator molecules is established close to the electrode surface. The ET mechanism is then comparable to that of

Table 2. Optimal properties of biosensor components and entire amperometric biosensors

Characteristics of an ideal redox enzyme	Selective reaction with the desired analyte; redox potential of the primary redox site in a suitable potential window; stable at the working conditions of the sensor; sufficient long-term stability; possibilities to introduce functionalities for chemical modifications with redox compounds, binding or cross-linking with the immobilisation matrix; tuneable enzyme properties by genetic or chemical techniques; low costs
Properties of an ideal mediator	Reversible electrochemistry; stable in oxidised and reduced form; no side reactions; redox potential adapted to the enzymatic reaction; amenable for immobilisation on the electrode; functional side chains for covalent binding to polymer backbones, the protein shell, or the electrode surface; low costs; non-toxic
Advantages of mediated ET	Independence from molecular oxygen or the presence of other natural electron acceptors or electron donors; working potential defined by the formal potential of the redox mediator; decrease of the influence of interfering compounds by proper selection of the redox mediator; controlled dependence from pH value
Properties of an ideal immobilisation matrix	Secure fixation of redox mediators and redox enzymes at the electrode surface; matching charge and hydrophobicity/hydrogen-binding sites of the redox enzyme; flexible backbone; suitable binding sites for mediators, spacers, or redox enzymes; suitable environment for proteins (amphiphilic); sufficient stability at the application site; possibilities to address exclusively the electrode surface for the deposition of the immobilisation matrix; optimisation of matrix properties possible; biocompatible; low costs
Advantages of a reagentless biosensor architecture	All compounds are securely fixed on the electrode surface; no loss of valuable coenzymes or redox mediators; no toxic effects of free-diffusing sensor compounds; ideal for applications <i>in vivo</i> or in samples as implantable sensor
Characteristics of an ideal biosensor	High selectivity; high sensitivity; low detection limit; fast response time; sufficient long-term stability with respect to the envisaged application; good bio- and/or environmental compatibility; easy to use; low costs; self-calibrating

free-diffusing redox mediators, and the contamination of the sensor environment with mediator compounds cannot be excluded. Alternatively, the redox mediators can be bound to the backbone of the immobilisation matrix by covalent or coordinative bonds, or electrostatic forces. This is a basic architecture for the development of reagentless biosensors (see below) in which all sensor components are securely fixed on the electrode surface (Schmidt and Schuhmann, 1996; Heller, 1990, 1992) shown schematically in Figure 5f (Gorton, 1995).

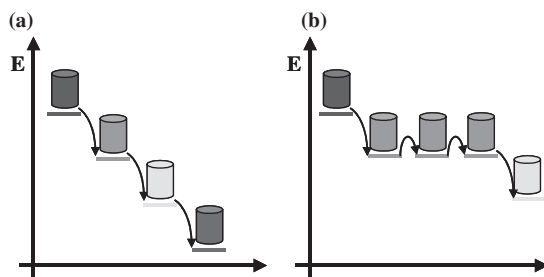


Fig. 6. Dividing the overall ET distance between an immobilised enzyme and an electrode surface by means of ET cascades; (a) ET cascade via a sequence of redox relays with decreasing redox potential, (b) ET cascade via self-exchange processes of redox relays at the same redox potential.

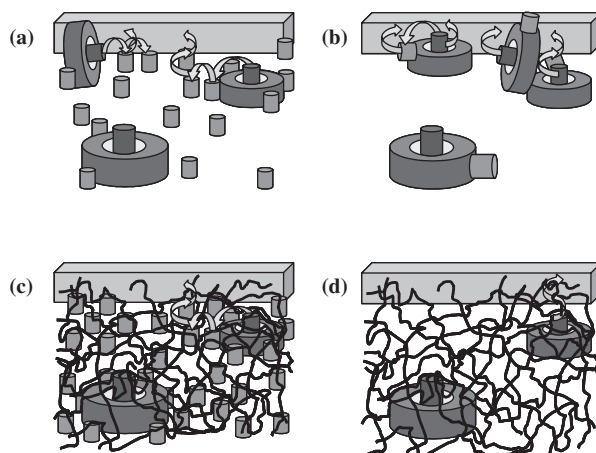


Fig. 7. Schematic representation of ET possibilities between enzymes and electrodes, (a) shuttle mechanism based on free-diffusing redox species, (b) direct ET of (redox-relay-modified) redox proteins at a bare or monolayer-modified electrode, (c) electron hopping in a redox-relay-modified polymer hydrogel, (d) ET via a conducting-polymer chain.

Due to the electrochemical insulation of enzyme-integrated cofactors imposed by the protein shell the observation of direct ET is restricted to either small redox proteins or to specific classes of redox enzymes having their cofactor located close to the protein surface (see [Figure 7b](#)). However, even then there is a need for a proper orientation of the protein with the redox site pointing towards the electrode surface ([Figure 5b, c](#)). Often, the number of proteins being in direct ET distance can be evaluated by a sequence of measurements in the absence and presence of a suitable free-diffusing redox mediator. The ratio of the current is correlated with the ratio of enzyme molecules being in direct and mediated ET communication with the electrode. Direct ET between redox proteins and electrode surfaces has been investigated and comprehensively reviewed ([Frew and Hill, 1988](#); [Gorton *et al.*, 1999](#); [Ghindilis, 2000](#); [Zhang *et al.*, 2000](#)). It was in as early as 1972 that direct ET on Hg-electrodes was observed

with cytochrome *c* (Betso *et al.*, 1972), but due to the denaturing of the adsorbed cytochrome *c* the observed electrochemistry was not reversible. A similar behaviour is observed for many other redox proteins adsorbed on bare metal electrodes. Obviously, the binding forces leads to a significant distortion of the three-dimensional structure of the protein which finally inactivate or denature the enzyme. Reversible ET of cytochrome *c* was proved on tin-doped indium oxide electrodes (Yeh and Kuwana, 1977) and using 4,4'-bipyridyl as a promoting monolayer on Au-electrodes (Eddowes and Hill, 1977). It was supposed that the electroinactive promoter was adsorbed in the form of a monolayer on the electrode surface. On the one hand, the promoter leads to an anisotropic orientation of cytochrome *c* at the electrode surface, and on the other hand serves as a protecting layer preventing denaturation of the protein. Other promoters, such as imidazole, iodide, or thiophene have been used successfully. Later, direct ET with a number of redox proteins such as among others microperoxidase (Razumas *et al.*, 1996; Lötzbeyer *et al.*, 1994; Lötzbeyer *et al.*, 1997; Kranz *et al.*, 1997; Ruzgas *et al.*, 1999), cytochrome *c* peroxidase (Armstrong and Lannon, 1987), or horseradish peroxidase (HRP) (Ruzgas *et al.*, 1995, 1996; Yao *et al.*, 1995; Lindgren *et al.*, 1999a, 2000b) was evaluated.

In order to define the distance between the electrode surface and a redox protein and, moreover, to study interfacial ET properties of redox proteins (Elatrash and O'Neill, 1995; Bain *et al.*, 1989) SAM spontaneously formed on clean gold surfaces from solutions of thiol derivatives (Bain *et al.*, 1989; Finklea, 1996) were investigated. Especially, due to the inherent possibility to modify SAMs with a variety of head groups having different surface charges and/or functionalities, covalent binding of molecules such as redox mediators or enzymes becomes possible (Richardson *et al.*, 1995; Gooding and Hibbert, 1999). The distance between the functional head groups and the Au surface, and hence the distance over which ET processes have to occur, can be tailored by variation of the chain length of the alkyl spacer (Smalley *et al.*, 1995; Feng *et al.*, 1997). Moreover, SAMs are sufficiently stable against changes in temperature or pH value as well as in a broad potential range (−1.4 to +0.8 V vs. SCE). Initially, investigations about the direct ET between adsorbed or covalently linked cytochrome *c* and electrode surfaces were performed (Armstrong, 1992). Due to the fact that cytochrome *c* shows a positive charge accumulation in the vicinity of its active heme site, negatively charged SAM head groups such as carboxylic acid residues promote anisotropic binding of cytochrome *c* and hence the direct ET between cytochrome *c* and an electrode (Tarlov and Bowden, 1991; Collinson *et al.*, 1992). Binding of small heme-containing redox proteins on cystamine-modified Au-electrodes revealed close to reversible electrochemistry for $\text{Fe}^{3+/2+}$ and high electrocatalytic activity for the reduction of H_2O_2 (Lötzbeyer *et al.*, 1997; Narvaez *et al.*, 1997; Ruzgas *et al.*, 1999). Even hemin itself could be successfully tethered to a cystamine SAM (Lötzbeyer *et al.*, 1995; Chen *et al.*, 2000).

However, due to the large size of the enzyme, direct electrochemistry between HRP and SAM-modified Au-surfaces is unlikely. The overall ET distance can only be decreased by attempting an anisotropic orientation of the protein prior to covalent immobilisation with the active site exposed towards the electrode

surface. One possible strategy is the covalent binding of the active centre of the protein preferentially via a flexible spacer to the surface of a suitable SAM. Subsequently, the reconstitution of the active holo-enzyme is achieved by immersing the modified electrode in a solution containing the apoprotein. Examples for this strategy are the reconstitution of holo-oxidases using thiol-derivatised FAD (Willner *et al.*, 1996, 1997a, b), PQQ-dependent dehydrogenases using PQQ-modified SAMs (Katz *et al.*, 1994a, b), myoglobin using monolayers of thiol-derivatised hemin, or HRP using a SAM with diluted anchor groups to which hemin was bound via flexible spacer chains (Zimmermann *et al.*, 2000).

Another strategy to enable ET between immobilised redox proteins was seen in dividing the overall ET distance by introducing an additional redox relay. This strategy was already suggested by nature through the existence of multi-subunit multi-cofactor enzymes. These enzymes possess an enzyme-integrated ET pathway from a primary redox site, where the substrate is converted, to additional redox sites located in the same or a different subunit of the protein and finally to the target molecule. Usually, multi-cofactor proteins have more than one subunit with different cofactors like PQQ and heme in e.g. D-fructose dehydrogenase (Khan *et al.*, 1991; Ikeda *et al.*, 1991) and alcohol dehydrogenase (Gulcev *et al.*, 2002; Ramanavicius *et al.*, 1999) or FAD and heme (in e.g. cellobiose dehydrogenase (Larsson *et al.*, 1996; Gorton *et al.*, 1999; Lindgren *et al.*, 2000a, 2001). The electrical 'wiring' to the electrode surface can be realised using an internal ET via the natural secondary redox sites of the protein and is shown in Figure 5e. Direct ET of quinohemoprotein alcohol dehydrogenase (QH-ADH), a multi-subunit enzyme containing a primary PQQ redox site which is connected via an internal ET pathway to four heme groups (Marcinkeviciene *et al.*, 1999), occurs via the oxidation of ethanol and an intermediate storage of electrons in the primary cofactor, PQQ. From there, a fast inner-enzymatic ET to one or more heme *c* units, which are located in close proximity to the protein surface, takes place enabling a good accessibility for direct ET processes. In addition, it could be demonstrated that attractive forces between polycationic polypyrrole chains and a negatively charged multi-cofactor enzyme like QH-ADH allows direct ET from the enzyme's active site to the conducting-polymer backbone in the absence of any free-diffusing or polymer-bound redox mediator. The observed ET process occurs at the formal potential of at least one of the heme sites (Ramanavicius *et al.*, 1999) and the extremely fast regeneration of the primary redox site was supposed to be responsible for the significant decrease of the affinity between ethanol and the enzyme and the correspondingly increased linear detection range.

Using SAMs with differently charged head groups allowed for an oriented adsorption of the enzyme prior to its covalent binding leading to a biosensor architecture combining the advantages of an ET pathway via redox relays (inner enzymatic ET of QH-ADH) with an optimised direct ET due to oriented immobilisation of the enzyme (Schuhmann *et al.*, 2000). Direct ET from multi-cofactor enzymes to SAM-modified electrode surfaces was also described for cellobiose dehydrogenase (Gorton *et al.*, 1999; Lindgren *et al.*, 1999b, 2000a) even showing the backloading of the primary redox site during slow-scan cyclic

voltammograms in accordance with the natural engineering principles of electron tunnelling (Page *et al.*, 1999). The rate-determining step in a complex ET cascade in reagentless biosensors is often the ET between the enzyme-integrated primary redox relay and the 'first' polymer-bound redox mediator (see below). Therefore, multi-cofactor enzymes should be well suited for fast ET in 'redox hydrogels'. Integration of PQQ-dependent enzymes such as PQQ glucose dehydrogenase was used successfully for fast responding glucose sensors with high current densities (Ye *et al.*, 1994; Niculescu *et al.*, 2002).

A different approach to improve ET pathways between active sites of the enzymes and the electrode surface is the chemical modification of the redox enzyme itself (Figure 7b). Redox modification enables non-diffusional ET or can be used in combination with a redox-relay modified matrix immobilised on the electrode. By covalent attachment of electron mediators to suitable binding sites at the protein periphery or the inner active site, ET distances are shortened (Figure 5e). Electron hopping or tunnelling is enhanced, but often the enzyme activity is decreased due to conformational changes after the modification. Several strategies have already been applied for the covalent attachment of redox relays for realising the so-called 'electro-enzymes' (Heller and Degani, 1988). As binding sites for the modification terminal side chains of the amino acids at the outer protein shell (Schuhmann *et al.*, 1991a; Ryabov *et al.*, 1992; Schmidt *et al.*, 1993; Tsai and Cass, 1995) the cofactor of the enzyme (Riklin *et al.*, 1995; Katz *et al.*, 1999), the active site of the protein preferentially in close proximity to the redox-active cofactor (Degani and Heller, 1987; Heller and Degani, 1988; Bartlett *et al.*, 1987; Sampath and Lev, 1996) were investigated. In addition, coordination chemistry offers a selective way for the attachment of Ru- or Os-complexes via the exchange of labile ligands against histidine side chains at the protein (Ryabova *et al.*, 1999; Durham *et al.*, 1990; Reiter *et al.*, 2001b). Besides the electrochemical investigation of free-diffusing 'electro-enzymes', ferrocene-modified glucose oxidase was entrapped within a polypyrrole film on an electrode. The successful 'electrical wiring' between the immobilised enzyme and the electrode surface could be observed (Schuhmann, 1995a), however, the current was small due to the low concentration of redox relays involved in the ET process. In order to increase the local concentration of redox mediators within the immobilisation layer, additionally redox relays were covalently linked to the polymer backbone.

Wrapping of enzyme molecules into a polymer network containing a high concentration of redox mediators (Figure 7c) covalently attached to the polymer backbone was the basis for the development of reagentless biosensors (Schmidt and Schuhmann, 1996; Heller, 1990, 1992; Andrieux and Saveant, 1992) (Figure 5f). The synthesis of the redox polymers can be done under optimised conditions utilising, e.g. organic solvents or elevated temperature. The generally used 'redox hydrogels' consist of a highly hydrophilic polymer backbone such as poly(vinyl pyridine) (Degani and Heller, 1989; Gregg and Heller, 1990; Leech *et al.*, 1991; Doherty *et al.*, 1991; Pishko *et al.*, 1991; Calvo *et al.*, 1996), poly(vinyl imidazole) (Taylor *et al.*, 1995; Larson *et al.*, 1998), poly(acrylic acid) (Kashiwagi *et al.*, 1994), or poly(allyl amine) (Danilowicz *et al.*, 1998) to which redox mediators like Os-complexes or ferrocene

derivatives are covalently bound. The ET process is dominated by an electron hopping between neighbouring redox relays attached to the polymer film, although often the rate-limiting step is the ET reaction between the cofactor inside the protein shell and the closest redox relay at the polymer chain. The preparation of this type of biosensors is usually done by dropping a mixture of redox polymer, bifunctional crosslinker, and enzyme onto an electrode surface. A well-adhering hydrophilic redox-polymer film is obtained, which swells when the sensor is immersed into the buffer. The hydrogel provides an increased flexibility of the polymer backbone which improves the ET rate, the diffusion of the enzyme's substrate and its reaction product within the polymer film, and the mobility of the counter ions leading to a fast charge-transport through the film (Aoki and Heller, 1993; Aoki *et al.*, 1995). Although miniaturised biosensors such as needle-type implantable glucose sensors (Csöregi *et al.*, 1994a, 1995; Yang *et al.*, 1997; Abel and von Woedtke, 2002; D'Orazio, 2003) were realised on the basis of redox hydrogels by manual dropping or dipping procedures, the concepts of sensor miniaturisation, preparation of multi-sensor arrays, or mass production, would benefit from a non-manual automated immobilisation technique that additionally ensures that the sensing chemistry is deposited exclusively on the electrode surface. Conducting-polymer films as immobilisation matrix for redox enzymes seem to be suitable because of their localised formation exclusively on the electrode surface due to the electrochemical initiation of the polymerisation process (Figure 7d). Monomers can either be modified with suitable redox compounds prior to the electrochemically induced formation of the conducting-polymer film (Cosnier *et al.*, 1985; Schuhmann *et al.*, 1991b) or by a heterogeneous polymer-analogue reaction (Schuhmann *et al.*, 1993, 1997; Hiller *et al.*, 1996; Schuhmann, 1998) after the polymerisation.

An optimal immobilisation matrix for the development of ET pathways in reagentless biosensors should combine advantages of conducting-polymer films with the hydrogel characteristics of non-conducting redox polymer. This would bring together a controlled and localised deposition of the polymer film with a fast substrate and counterion diffusion, high flexibility and hence fast ET rates. Following this idea, Os-complexes were covalently bound to a *N*-substituted pyrrole derivative via long spacer chains and copolymerised with pyrrole under simultaneous entrapment of a PQQ-dependent glucose dehydrogenase. The spacer chain improves the flexibility of the polymer-bound redox relay. The obtained glucose sensors showed a high sensitivity, although the limitation of substrate diffusion was still high (Habermüller *et al.*, 2000). A further improvement of the ET rates of the Os-complex modified polypyrrole films was suggested by introducing hydrophilic side chains at the polypyrrole backbone or at the Os-complexes. As expected, due to the increased hydrophilicity and thus improved swelling properties of the polymer film in aqueous solution, the glucose-dependent currents were significantly enhanced (Reiter *et al.*, 2001a; Habermüller *et al.*, 2003).

Another technique which allows to selectively address the electrode surface for polymer film deposition, however, avoiding the complexity of the electrochemically induced formation of intermediate radicals involved in the formation of conducting polymers, is the local precipitation of electrodeposition paints

(EDP) by means of an electrochemically induced modulation of the pH value in the diffusion zone in front of the electrode surface (Kurzawa *et al.*, 2002). Within this reaction zone in front of the electrode surface, which is defined by the rate of water oxidation or reduction and the buffer strength of the electrolyte, acidic or basic side chains at the EDP are protonated or deprotonated leading to a loss of the ionic character of the polymer chains. This changes the solubility of the polymer chains leading to their precipitation exclusively onto the electrode surface. If an enzyme is simultaneously present in the EDP solution, it is incorporated within the polymer film during its deposition on the electrode surface. Due to the hydrogel properties of the EDP the swollen film allows a fast diffusional mass transport of the enzyme's substrate and product, and may stabilise the enzyme. The synthesis strategy of EDP allows to functionalise the polymer backbone with redox relays.

The principal architecture of layer-by-layer assemblies is shown schematically in Figure 5g. Applying the stepwise layer-by-layer deposition of enzymes and the covalent attachment of relay units, a more controlled superstructure can be designed such as a multi-layer glucose oxidase electrode modified with (6-ferrocenemethylamino)hexanoic acid (Willner *et al.*, 1993). The number of protein layers correlate with the current response of the sensor implying that all enzyme layers are electrically 'wired' with the electrode. These assemblies may enhance the chemical stability of the redox enzymes. Layer-by-layer assemblies can also be used for interference elimination by applying additional layers for size exclusion or charge repulsion. Moreover, this technique allows to immobilise different enzymes for coupled enzymatic reactions and may be used to optimise bi-enzyme systems (Chen *et al.*, 1998).

For several applications it would be advantageous to have biosensors that can be turned on and off. In principle, two strategies are possible to change the activity of a biological recognition element in a reversible manner. First, it should be possible to prevent the cofactor of an enzyme to be regenerated, hence switching the enzyme in an off-state. Although this approach seems to be feasible, it was not demonstrated until now. Second, one may take advantage of the fact that enzymes are in general labile molecules which are sensitive to their environment. Therefore, reversible structural changes of photoisomerisable molecules after exposure of light have been used to modulate the activity of enzymes which were modified with photoisomerisable groups. In this case, the activity of the enzyme may be influenced by light invoking changes of the photolabile molecule leading concomitantly to conformational changes in the three-dimensional structure of the enzyme. Following this strategy, glucose oxidase was modified with a nitrospiropyran derivative as a photoisomerisable unit and transformed into a photoswitchable enzyme (Lion-Dagan *et al.*, 1994). A similar concept is based on the application of magnetic particles for modulating the activity of enzymes. In this approach, magnetic particles are functionalised with a redox-relay unit, which can be controlled by an external magnetic field (Figure 5d). The relay units are used to electrically 'wire' the redox enzyme with the electrode surface thus being a part in the overall ET pathway. Using the alternating position of an external magnet below and above the electrochemical cell, the magnetic particles can be moved or removed, which

enables or prevents the oxidation of the relay units and the following bioelectrocatalysed oxidation.

If there is no direct enzymatic reaction available for the detection of the desired analyte, it is possible to use consecutive enzymatic reactions in an amperometric biosensor to finally convert the information of a primary conversion of the analyte into a terminal proportional redox reaction which can be used for the detection of the analyte. The most simple approach is the coimmobilisation of two or more enzymes within the immobilisation matrix by, e.g. cross-linking procedures or coentrapment within a polymer layer. Mainly peroxidases and H_2O_2 producing oxidases were combined with the aim to decrease the working electrode potential of the amperometric biosensor (Ohara *et al.*, 1993; Vijayakumar *et al.*, 1996; Leca *et al.*, 1996). The primarily generated H_2O_2 diffuses in to the peroxidase where it is reduced at potentials of about -50 mV vs. an Ag/AgCl reference electrode either in a direct ET pathway between the carbon electrode and the adsorbed peroxidase or by using a redox polymer for electron transduction (Csöregi *et al.*, 1994b; Mikeladze *et al.*, 2002a, b). Tri-enzyme electrodes were also successfully designed using acetylcholinesterase, choline oxidase, and HRP for the detection of acetylcholine (Garguilo *et al.*, 1993).

1.6. Optimisation of sensor architectures

A specific biosensor design is largely dependent upon the operation principle of the transducer, the involved analytes and the working environment. In Figure 8,

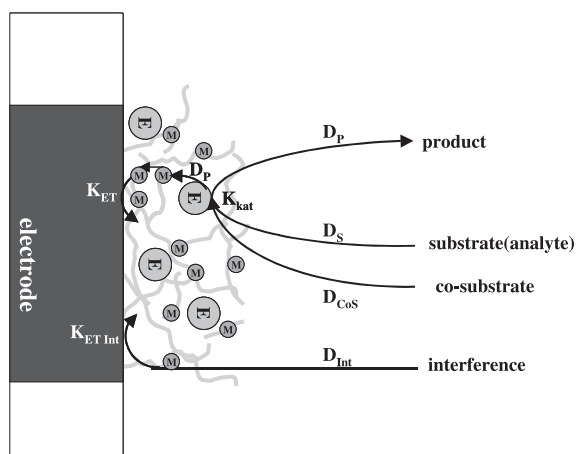


Fig. 8. Model outlining the complex diffusion processes in an enzyme biosensor focusing on the analyte and an interference compound, D_S = diffusion coefficient of substrate, D_{CoS} = diffusion coefficient of co-substrate (e.g. natural mediator), D_P = diffusion coefficient of product, K_{kat} = rate constant of enzymatic reaction, K_{ET} = rate constant of ET, $K_{ET Int}$ = rate constant of ET of interference oxidation.

a simple model for the complex diffusion processes and reactions in an enzyme biosensor is shown.

This model may help to understand the complexity of the processes involved in order to find appropriate biosensor architectures and ET pathways for the desired analyte. In the case of an enzyme biosensor, the amperometric signal is a result of the ET rates originating from the complex kinetics induced by substrate (and co-substrate) diffusion, enzymatically generated product formation, mediating ET steps and the heterogeneous ET reaction from a mediator to the electrode. Assuming diffusion-limited conditions, the current response is first-order dependent on the bulk analyte concentration and the obtained steady-state currents show a linear dependence for substrate concentrations lower than the apparent K_M -value. The rate-limiting step can also be the mass transport, analyte consumption, or the 'first' ET from the cofactor inside the three-dimensional structure of the enzyme to the nearest redox mediator of an ET hopping chain. In addition, the properties of a biosensor are determined by the characteristics of the transducer, the nature, amount and specific activity of the immobilised enzyme and the local concentration of the redox mediator within the immobilisation matrix. Moreover, ET rates and diffusion constants of all involved species including potential interferences, the ionic strength of the electrolyte solution, its pH-value and the temperature influence the sensor signal.

A theoretical analysis of a reagentless amperometric biosensor assembly was proposed (Calvo *et al.*, 1993; Bartlett and Pratt, 1995). The internal diffusion of the enzymatically produced product is bi-directional as well as the diffusion of the natural electron acceptor, assuming that no limitation of the natural electron acceptor exists. The temperature at which the sensing device is operated has an impact on all reaction rates including the enzyme kinetics, and accelerates transport processes due to its influence on the viscosity of the reaction layer. Due to the complex reaction sequence of the enzymatic process, the temperature effect on the overall biosensor current signal is different for the analyte part and the interference part. This has been shown recently by using electrically heatable glucose biosensors (Lau *et al.*, 2004). Measuring the responses of the sensor by switching between at least two different temperatures, enabled for compensating the effect on the sensor signal imposed by the presence of an interfering compound such as ascorbic acid. If a polymer film is used as an immobilisation matrix in a specific biosensor architecture, the properties of the deposited polymer film such as density, layer thickness, hydrophilic or hydrophobic characteristics, swelling ability, pore size, etc. as well as the polymer properties themselves highly influence the final sensor characteristics. Optimisation of biosensors includes the variation of several parameters of the sensor architecture. The main parameters are summarised in Figure 9.

Based on the specific application and the properties of the sample solution an appropriate biosensor architecture has to be designed focusing on each individual component of the sensor architecture. In general, for the biological recognition element its accessibility is the most important factor thus enabling a fast ET rate with the next element in the ET cascade. Thus, steric effects, orientation, and distance dependence of the ET reaction has to be considered. The chosen redox mediator should be stable under working conditions, be

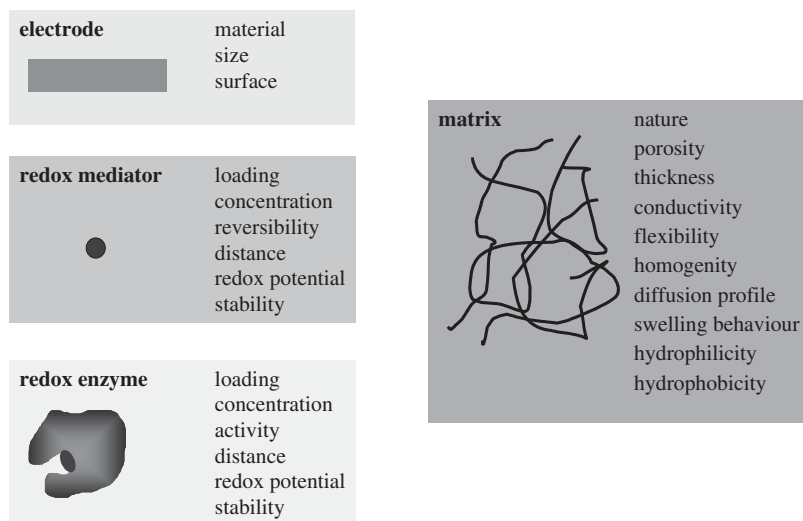


Fig. 9. Specific properties of the different components needed for the development of an optimised reagentless amperometric biosensor.

soluble in aqueous or organic solvents, and be inert to side reactions. In addition, it is important that they show a reversible electrochemical behaviour and an appropriate redox potential. A low redox potential allows to avoid interferences, however, the sensor design is a compromise between low interfering currents and high ET rates. Another important requirement for a redox mediator is to enable high ET rates with the enzyme on the one hand and with neighbouring mediators of the same (or different) type on the other hand to realise high substrate-dependent currents. Materials, size, shape, and methods of sensor constructions need to be adapted to the desired ET pathway. In addition, electrochemical pre-treatment such as repeated potential cycling may sometimes improve specific sensor properties (Jaffari and Pickup, 1996). Moreover, the sensor architecture may involve additional enzymes for interference elimination, enzyme amplifications cascades (Schubert *et al.*, 1985; Scheller *et al.*, 1988; Pfeiffer *et al.*, 1995), or enzyme-based competition reactions. Furthermore, the used electrode may be tailored to enable redox amplification using, e.g. interdigitated electrodes (Nice *et al.*, 1993; Niwa, 1995) or SECM-based amplification schemes (Zhao and Wittstock, 2004a; Niculescu *et al.*, 2004).

Classically, biosensor optimisation assumes linear independent parameters which allow for optimising one parameter assuming the others are constant. Beginning to design a new biosensor starts with the definition of the analyte of interest followed by identification of the appropriate enzyme and immobilisation method. For a rational optimisation of the desired biosensor architecture the main parameters influencing the ET pathway have to be elucidated. Variation of parameters such as enzyme and mediator concentration, nature and, deposition parameters of the immobilisation matrix leads to different substrate-dependent currents and dynamic ranges. The design of the most efficient ET is

selected for further applications of the biosensor. With this partly rational approach a great variety of biosensors were developed and adapted to the specific field of application. Physical, chemical, and mathematical analyses provide the theoretical basis for this type of biosensor optimisation. However, in general, it is not possible to reach the global minimum in the parameter space for all parameters following the classical, rational optimisation strategy. Another possibility is based on a combinatorial approach for improving the optimisation process for the design of biosensors using techniques adapted from high-throughput screening (HTS). Combinatorial methods were introduced in electrochemistry by Reddington *et al.* (1998) stimulating several other contributions to this field (Liu and Smotkin, 2002; Jiang and Chu, 2002; Kulikov and Mirsky, 2004; Mirsky *et al.*, 2004; Yudin and Siu, 2001). In the field of biosensor research a combinatorial search for catalyst alloys for glucose oxidation was performed on electrode arrays (Sun *et al.*, 2001).

A fully automated screening method for finding optimised immobilisation matrices for amperometric glucose biosensors was developed using a library of cathodic electrodeposition paints (Reiter *et al.*, 2004). This first approach towards the development of a combined sensor preparation and characterisation process in one screening procedure was made with the help of an electrochemical robotic system using conventional microtiter plates as array format. The corresponding automated system is compatible to other plate-based HTS technologies. Such a systematic screening of all involved biosensor components may be additionally useful for a more detailed understanding of the complex interaction of different biosensor parameters and their impact on the developed biosensor architecture (Figure 10).

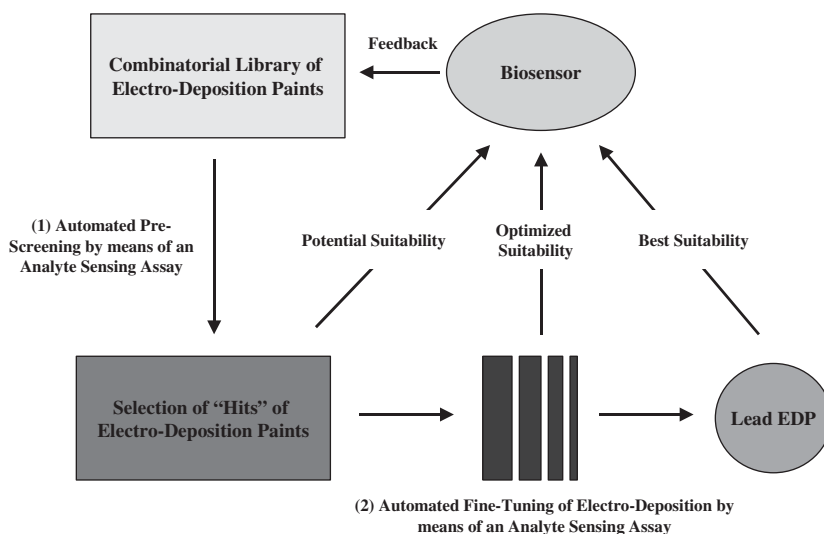


Fig. 10. Biosensor screening strategy using an automatic electrochemical robotic system for sensor fabrication and evaluation.

A combinatorial compound library can be rapidly screened for one or two selected parameters such as maximal current or apparent Michaelis–Menten constant (Ngounou *et al.*, 2004). The hits are then selected with respect to a set of chosen parameters and then collected in a sub-library, that is screened afterwards in more detail with respect to some or most remaining parameters to obtain biosensors with the desired properties. Interesting parameters may be response time, reproducibility, or long-time stability.

1.7. Enzyme microstructures

Great interest arose in recent years in biomedical, biotechnological, industrial, and environmental fields on miniaturised multi-functional biosensing devices for the rapid and simultaneous detection of several analytes in aqueous sample solutions of minimised volumes. A number of strategies was suggested to establish the desired high-throughput microbiosensors (biochips) comprising of an array of the relevant biological recognition elements, most often specific enzymes, with closely spaced and individually addressable test sites each of them targeting a different analyte. Exposing such arrayed multi-enzyme bioassays once to a sample solution offers the opportunity to quickly screen for a set of analytes.

Successful fabrication and application of enzyme-based biochips critically depends on the capability to immobilise many of the active biocomponents in a spatially accurate micropattern on suitable (disposable) surfaces as well as to precisely read out the information that is generated locally by the interaction of the immobilised enzymes with its target substrate (analyte) in the final detection step (Gaspar *et al.*, 2002). Current methodologies used for the formation of enzyme microstructures in the geometries of patterned dots, lines, or grids include for instance screen printing (Nagata *et al.*, 1995; Sapelnikova *et al.*, 2003; Dequaire and Heller, 2002; Wang *et al.*, 1996; Rohm *et al.*, 1996), lithographical photoresist/lift-off methods (Revzin *et al.*, 2002; Di Fabrizio *et al.*, 1996; Nakamoto *et al.*, 1988; Hanazato *et al.*, 1989; Gernet *et al.*, 1989), microcontact printing (Rinaldi *et al.*, 2004; Mrksich and Whitesides, 1995; Gooding *et al.*, 2003), photochemical activation of pre-immobilised coupling agents (Röhm *et al.*, 1995; Jimenez *et al.*, 1997; Strike *et al.*, 1994), microspotting through microarrays, ink-jet printing or microdispensing (Yamada and Seki, 2004; Newman and Turner, 1992; Johnson, 1991; Gaspar *et al.*, 2001), electron beam patterning (Glezos *et al.*, 2002) and last but not least the locally performed electrochemical deposition of polymers entrapping the enzyme during placement (Bourdillon *et al.*, 1993; Bartlett and Birkin, 1993; Schuhmann, 1995b; Kurzawa *et al.*, 2002).

The way of electrochemically detecting the spatially confined interaction of surface-attached enzymes on biochips and their targets can be divided into two major classes: the application of carbon or noble metal microelectrode arrays and methods involving local electrochemical measurement with a positionable microelectrode that is scanned in close proximity above the enzyme-modified surface. The latter has an advantage in that the surface to be micropatterned

with enzymes need not necessarily be conductive and thin sheets of glass or plastic can be used as carriers for the biological recognition elements. The use of microelectrode arrays, on the other hand, requires, that the chosen enzymes have to be immobilised on the electroactive surfaces of pre-fabricated arrays of disk- or line-shaped microelectrodes, which have to be independently addressable to enable the spatially resolved detection of enzymatically produced/consumed species (Sandison *et al.*, 2002; Hayashi *et al.*, 2000; Matos *et al.*, 2000; Lenigk *et al.*, 1999; Murakami *et al.*, 1998; Frebel *et al.*, 1997; Sangodkar *et al.*, 1996; Niwa, 1995; Dzyadevich *et al.*, 1994; Wollenberger *et al.*, 1994; Ross and Cammann, 1994; Wang and Chen, 1994). Scanning electrochemical microscopy (SECM), however, serves the ideal tool for the local electrochemical detection of spatially confined processes on enzyme-containing microstructures (Wipf, 2003; Horrocks, 2003; Shiku *et al.*, 2002; Wittstock, 2003; Mirkin and Horrocks, 2000; Barker *et al.*, 1999; Mandler *et al.*, 1996; Bard *et al.*, 1995a, b). In SECM, a disc-shaped microelectrode, the so-called SECM tip, is scanned at close distance over the surface of interest using a high-precision positioning device for tip movements while collecting topographic and electrochemical information at the same time through the acquisition of the amperometric or potentiometric response of the tip electrode as a function of position. It has been documented in a number of recent publications, that the feedback and generator/collector modes of SECM are well suited for studying enzymatic reactions at surfaces (Niculescu *et al.*, 2004; Kranz *et al.*, 1997, 2004; Zhao and Wittstock, 2004a; Csoka *et al.*, 2003; Oyamatsu *et al.*, 2003; Kurzawa *et al.*, 2001; Horrocks *et al.*, 1993). SECM is the ideal tool for visualising and characterising the activity of enzyme micropatterns. The SECM approach was successfully applied for high-resolution electrochemical imaging in order to characterise the shape and size of active domains of arrayed microspots of paramagnetic beads to which specific enzymes were coupled (Wittstock *et al.*, 2001; Zhao and Wittstock, 2004b; Zhao *et al.*, 2004; Wittstock, 2001). In addition, microscopic multi-enzyme grids on gold surfaces that were fabricated by means of a flow-through microdispenser and then visualised using SECM operated in the generator/collector mode demonstrated the feasibility of this approach (Gaspar *et al.*, 2001).

2. ET PATHWAYS IN RECOGNITION OF DNA HYBRIDISATION

An electrochemical DNA sensor comprises a nucleic acid recognition layer for selectively detecting a specific DNA sequence under formation of complementary double stranded (dsDNA) in the recognition layer. The recognition layer has to be immobilised at a suitable transducer surface enabling the transduction of the complementary recognition process into a measurable signal (Figure 11). Obviously, if an electrochemical transduction scheme is envisaged, some aspects related with the design of electrochemical DNA sensors are similar to considerations made above for the development and optimisation of enzyme-based reagentless amperometric biosensors. Especially, ET pathways have to be designed for coupling the information generated during the hybridisation of DNA

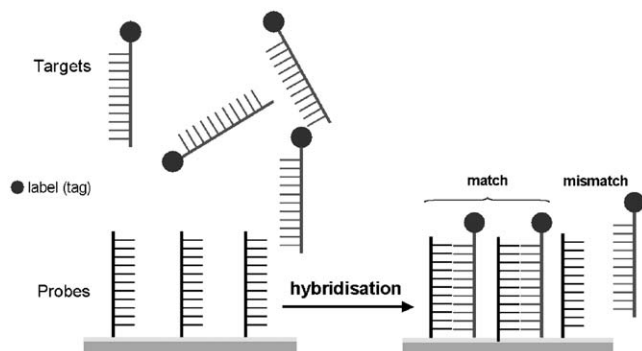


Fig. 11. Schematic representation of a complementary recognition of a (labelled) target oligonucleotide (ODN) using an immobilised capture probe ODN at the transducer surface.

to an electrode surface used as underlying transducer. Since genetic information is stored in a huge library of different DNA sequences it is important to rapidly detect various DNA sequences in a fast and reliable way, a task which is usually accomplished by means of DNA microarrays. Thus, the main challenge in the development of DNA microarrays is the fabrication of the recognition layer which allows immobilisation of a large variety of different capture probes at specific pre-defined sites at the transducer surface concomitantly enabling an (amplified) signal transduction process to take place.

In the following, some important aspects in fabricating a variety of different DNA recognition interfaces and the main approaches to the electrochemical transduction of DNA hybridisation are summarised. (For general reviews on DNA biosensors and DNA arrays also focusing on electrochemical detection of hybridisation, see Gooding, 2002; Drummond *et al.*, 2003; Kerman *et al.*, 2004; De-los-Santos-Alvarez *et al.*, 2004a, b).

Successful recognition of a specific sequence of DNA requires a highly specific recognition layer. DNA biosensors exploit the ability of a single strand of DNA (ssDNA) to recognise and hybridise with a complementary ssDNA at the recognition interface. The strand of DNA which does the detection, which is usually called 'probe' or 'capture probe', is immobilised at the transducer surface. Exposure of the recognition surface to a sample containing single strands of the complementary DNA, which is usually called 'target', will result in the formation of the double-helical dsDNA through hybridisation. Factors that influence the hybridisation efficiency were discussed in detail in Levicky *et al.* (1998). The immobilised capture probe most frequently consists of an oligonucleotide (ODN) with a length of about 15–50 bases. To a large extent the selectivity, sensitivity, and reproducibility of a DNA recognition interface depends on the strategy employed for immobilisation of the DNA probe strands. After immobilisation, the probe strand needs to have sufficient flexibility and space to enable coiling of the target around the probe. In general, terminal modification of the chosen ODN chain is used to attach the probe on the transducer surface using similar methodology as discussed for enzyme-based biosensors above. The most frequently applied immobilisation principle is based

on utilising thiol-modified ODNs to bind the probes at a gold electrode surface in a monolayer assembly. By means of a chemisorptive process, often by additional simultaneous or subsequent immobilisation of short-chain alkyl thiols as lateral spacers between the ODN probes (Takenaka *et al.*, 2000; Wang *et al.*, 1997; Mascini *et al.*, 2001), mixed SAM as recognition layer are generated achieving a typical surface coverage of probe DNA in the order of 10^{12} ODNs/cm². Other immobilisation procedures are covalent ODN binding to carbon, indium-tin oxide, gold, and mercury electrodes (Thorp, 1998; Wang, 1999) or electrical wiring of ODN probes to the transducer in a polymeric, three-dimensional recognition layer (Campbell *et al.*, 2002; Dequaire and Heller, 2002).

The principles of signal generation and transduction for electrochemically visualising hybridisation events of DNA sensors are based either on catalytic biorecognition processes (utilising enzymes or other means for intrinsic signal amplification) or on affinity-based sensor architectures with specifically designed ET pathways. An overview of different detection principles of electrochemical DNA sensors is given in Table 3. Some of these examples are described in more detail in the following sections.

Table 3. Characteristics of electrochemical DNA sensors

Assay set-up	ET-principle
<i>Affinity-based detection principles</i>	
Unmodified ODN-probe; hybridisation of unlabelled targets; addition of an intercalating label	Direct detection of the intercalator redox reaction
Unmodified ODN-probe; hybridisation of unlabelled targets; addition of redox labelled signalling ODNs to form a sandwich structure	Direct detection of the signalling-ODN redox reaction
Unmodified ODN-probe; pre-occupation of probes with redox labelled signalling-ODN; hybridisation of unlabelled targets	Direct detection of the decrease of signalling-ODN redox reaction
<i>Catalytic detection principles</i>	
Unmodified ODN-probe; hybridisation of unlabelled targets; addition of enzyme-labelled signalling ODNs to form a sandwich structure with the probe-target-complex	Electrical wiring the enzymatic process to the electrode via polymer-immobilised redox mediators
Unmodified ODN-probe; labelling of target with enzyme; hybridisation of labelled targets	(mediated) diffusion of enzyme product to electrode; detection of the product (mediator) redox reaction
Unmodified ODN-probe; hybridisation of unlabelled targets	Direct detection of target-DNA oxidation
Unmodified ODN-probe; hybridisation of unlabelled targets	Label-free SECM detection

2.1. Affinity-based recognition of dsDNA

2.1.1. Detection of dsDNA via intercalators

Early work on DNA hybridisation sensors concentrated on using redox indicators to differentiate between single and double strands of DNA on the electrode (Storhoff *et al.*, 1998; Taton *et al.*, 2000; Wang *et al.*, 1999). A molecule which predominantly associates with dsDNA but not with ssDNA is used as reporter compound. If this so-called intercalator is redox active, an increased electrochemical response is observed after hybridisation due to the favourable integration of the intercalator into the double-helix structure (Figure 12). Variants of this strategy have been demonstrated (Wang, 2002a, b; Patolsky *et al.*, 2001; Fritz *et al.*, 2000; Palecek, 1960, 1988; Singhal and Kuhr, 1997; Jelen *et al.*, 2002). Despite its simplicity, excellent specificity and detection limits could be achieved (Wang and Kawde, 2002; Gooding, 2002). A similar approach uses intercalated redox molecules for detecting perturbations in base stacking. The DNA base pair stack is assumed to mediate charge transfer between an intercalator bound at the top of the dsDNA and the electrode due to a long-range ET. If the base pair stack is intact, current can flow taking advantage of the property of dsDNA to mediate charge transport. Although mechanism and efficiency of charge transfer along dsDNA is still under debate, it has been shown that dsDNA can transfer charge over distances of up to 30 Å with sufficiently high rates. As a matter of fact, the ET rate of the long-range ET is highly sensitive to perturbations in the dsDNA structure (Boon and Barton, 2002).

2.1.2. Detection of dsDNA via signalling ODNs

Another possibility to detect hybridisation using an electrochemical transduction scheme has been proposed by Clinical Microsensors (CMS) (Figure 13). A gold electrode is functionalised with the capture of DNA sequences that are laterally separated by molecular oligophenylethynyl wires and insulating

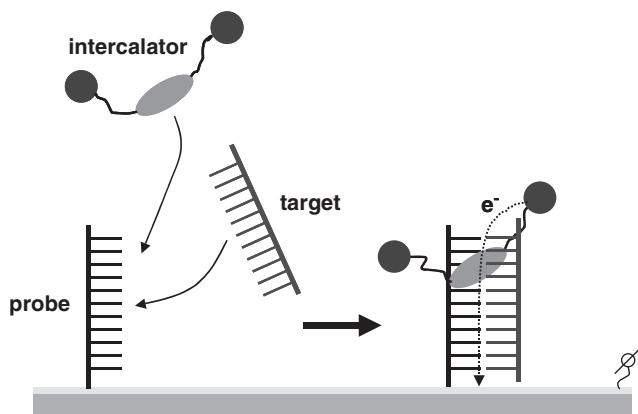


Fig. 12. Schematic representation of the detection of hybridisation of DNA using an intercalator selectively integrating into dsDNA.

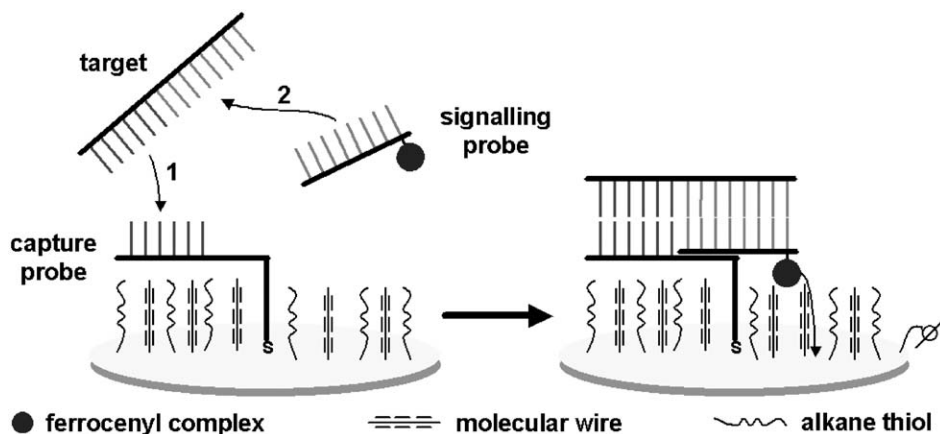


Fig. 13. Schematic representation of the detection of hybridisation of DNA using a ferrocene-modified signalling ODN and ET via molecular wires integrated into an insulating monolayer.

polyethylene glycol molecules. Once the target sequence from the sample is captured, a signalling ODN carrying redox-active ferrocenyl residues hybridises with a surmounting target sequence not involved in the association with the probe (Umek *et al.*, 2001; Yu *et al.*, 2001). The specific monolayer architecture with the capture probe embedded in an insulating monolayer containing a defined number of molecular wires allows for electrochemical interrogation of the ferrocene molecules at the signalling ODNs via the molecular wire while the insulating monolayer prevents non-specific adsorption of signalling ODN.

A similar sandwich-type DNA sensor has been described even earlier by Ihara *et al.* (1997). The main difference from the CMS approach is the use of a non-passivated electrode surface thus not requiring the molecular wires within the monolayer to enable ET reactions. Another approach using signalling ODNs as reporter molecules for hybridisation has been described in Hartwich and Wieder (2001). Unlabelled capture probes are immobilised at an electrode surface via thiol functionalities. The immobilised capture probes are pre-occupied with signalling ODNs carrying covalently attached redox moieties. In a chronoamperometric or chronocoulometric reference measurement, the signalling probes located in close proximity to the electrode surface are quantified from the current or charge transient. Complementary target sequences which may be present in the sample displace the associated signalling probes resulting in decreased or vanished electrochemical signal in a second measurement after hybridisation.

2.2. Amplified recognition of DNA hybridisation

2.2.1. Enzyme-amplified recognition of dsDNA

Low detection limits have been obtained using enzyme labels for detection of DNA hybridisation (Delumleywoodyear *et al.*, 1996; Caruana and Heller, 1999; Campbell *et al.*, 2002). A capture probe DNA sequence is immobilised within a

polyacrylamide-based electron-conducting redox hydrogel on a carbon electrode. The target DNA is labelled with peroxidase. The redox hydrogel enables molecular wiring of the DNA-bound peroxidase by a sequence of electron-hopping steps with the electrode surface as described for reagentless enzyme sensors above. After hybridisation, H_2O_2 is added which is subsequently reduced by the peroxidase, which is by itself regenerated via ET from the redox hydrogel. Using a peroxidase label it has been possible to detect as little as 20 molecules of complementary DNA strands. In a similar sandwich-type mode a 38-base DNA sequence has been immobilised within a conducting-polymer layer as capture probe. After target hybridisation a signalling ODN being labelled with peroxidase is hybridised to a surmounting target sequence not involved in the association with the probe. In this arrangement a target concentration of 20 pmol L^{-1} in 15–35 μL droplets has been detected (Zhang *et al.*, 2002). Obviously, the hybridisation of the signalling ODN in the sandwich configuration brings the peroxidase label into ET distance with a pre-electro-deposited redox polymer, thus allowing fast ET. Recently, Zhang *et al.* (2003) reported about a major improvement of the peroxidase-amplified amperometric detection of DNA hybridisation. They achieved the detection limit of DNA as low as 3000 DNA copies in a 10 μL droplet at a concentration of 0.5 fM.

Attaching an enzyme to the target strand of DNA followed by electrochemical transduction has also been demonstrated using alkaline phosphatase as the biocatalytic recognition element (Bagel *et al.*, 2000; Wang *et al.*, 2002). Enzyme labelling is combined with magnetic separation for improving selectivity. In this multi-step assay, the biotinylated capture probe is attached to a streptavidin-coated magnetic bead. Alkaline phosphatase-labelled target strands are introduced as sample, and after hybridisation a magnet is used to separate the magnetic beads with the hybridised target from the sample solution. The enzyme-labelled dsDNA is then incubated with substrate (4-amino-phenyl phosphate) for 20 min and the obtained supernatant is placed in an electrochemical cell for measurement. A different electrochemical assay for voltammetric enzyme-amplified detection of DNA hybridisation has recently been described by Nebling *et al.* (2004). The detection is based on an ultramicroelectrode array manufactured in silicon technology. The 200 μm circular array positions consist of interdigitated gold ultramicroelectrodes with a distance of 800 nm embedded in silicon oxide. Immobilisation of ODN capture probes at the interdigitated gold electrodes is accomplished via chemisorption of the thiol-modified ODN. The target strands are labelled with alkaline phosphatase. After hybridisation, the enzyme label at the formed complementary dsDNA converts the electrochemically inactive substrate 4-aminophenyl phosphate into the active 4-hydroxylaniline that is diffusionally transported to the interdigitated electrodes. Redox amplification (Figure 14) is achieved by a sequence of oxidation/reduction cycles between the differently polarised fingers of the interdigitated electrodes.

2.2.2. Chemical amplification for recognition of dsDNA

A chemical amplification scheme has been reported using methylene blue as intercalating compound (Singhal and Kuhr, 1997; Jelen *et al.*, 2002). In contrast

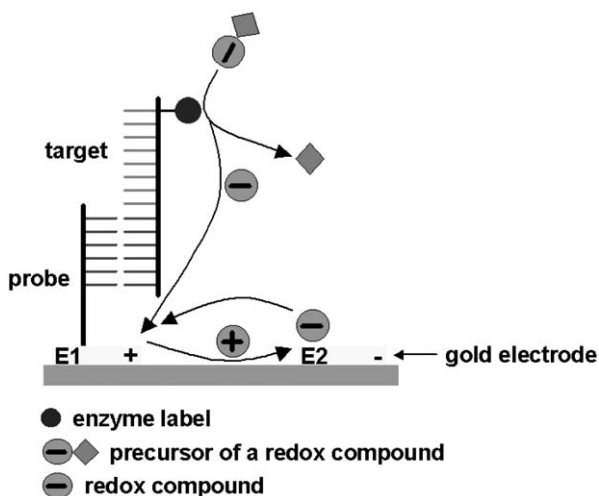


Fig. 14. Schematic representation of the detection of hybridisation of DNA using an enzyme-labelled target strand and redox amplification at interdigitated electrodes.

to previous approaches in which the intercalating compound exhibited a higher affinity towards dsDNA, methylene blue shows a specific affinity towards exposed guanine bases. Hybridisation prevents the interaction between guanine and methylene blue leading to a decrease in the electrochemical signal which is indicative of successful hybridisation. A similar loss of the accessibility of guanine bases for a redox mediator after hybridisation has been exploited using $[\text{Ru}(\text{bpy})_3]^{3+}$ as free-diffusing redox mediator to oxidise the guanine bases (Kerman *et al.*, 2003; Armistead and Thorp, 2002; Yang *et al.*, 2002; Yang and Thorp, 2001). The reduced $[\text{Ru}(\text{bpy})_3]^{2+}$ complexes are reoxidised at the electrode surface forming an electrochemically amplified catalytic cycle. As a matter of fact, hybridisation prevents the reduction of the redox mediator and hence lowers the catalytic current. The sensitivity of the method increases with the number of guanine bases in the probe strand.

One of the key drawbacks of the concepts discussed above is the requirement for an indicator or label to enable electrochemical communication with the electrode surface, thus transducing the hybridisation event. Hence, recent developments are aiming on the transduction of hybridisation events avoiding labelling of the probe strand, target strands, or the addition of labelled signalling ODN. Direct oxidation of guanine at about 1 V (vs. Ag/AgCl) has been successfully employed for detecting hybridisation (Wang *et al.*, 1998; Wang and Kawde, 2001). The probe ODN, which is adsorbed onto a carbon electrode, is modified by substituting guanine with inosine. Due to the fact that guanine exhibits a lower oxidation potential, the oxidation signal of inosine is well separated from that of guanine. Like guanine the inosine moiety binds to cytosine, however, with reduced selectivity. Hybridisation with the target strand brings guanine residues in contact with the electrode where they are detected using constant current chronopotentiometry.

A promising label-free method resides on an electrostatic approach for visualising the status of surface-bound DNA probes (Turcu *et al.*, 2004a, b). Detection of complementary DNA hybridisation is simply achieved through coulomb interactions between a negatively charged, free-diffusing redox mediator and the phosphate groups in the backbone of the immobilised DNA strands verified by SECM. An ultramicroelectrode (the SECM tip) at working distances of only a few electrode radii above the structure to be examined is kept at sufficient constant cathodic potential for reducing $[\text{Fe}(\text{CN})_6]^{3+}$ under diffusion control. Far above the sample surface, the amperometric tip current is controlled by the diffusion of $[\text{Fe}(\text{CN})_6]^{3+}$ molecules towards the tip, which leads to a steady-state current. However, after approach of the SECM tip into close proximity of propane thiol-modified gold surface, consumed mediator molecules are reconverted into their initial oxidation state leading to a distance-dependent increase in the tip current. Above a DNA spot, the anionic phosphate groups repel the tip-generated $[\text{Fe}(\text{CN})_6]^{3+}$ molecules leading to a local drop in the observed cathodic tip current. Hybridisation increases the immobilised negative charge at the surface, which leads to a further drop in tip current.

2.2.3. Bioelectronic hybrid devices for recognising DNA hybridisation

A silver deposition technique has been exploited for the construction of sensors, in which hybridisation is the first step to form a bioelectronic hybrid that is used as a switch in a miniaturised electronic circuit (Park *et al.*, 2002). A small array of microelectrodes with gaps of about 20 μm width between the electrode leads is constructed, and probe sequences are immobilised on the substrate between the gaps. Target DNA is hybridised and a reporter ODN tagged with a gold nanoparticle is hybridised to the probe-target complex to form a sandwich. The gold nanoparticles are then developed in a silver plating solution for enhancing the amount of metal deposition, leading finally to the precipitation of silver metal onto the gold nanoparticles. The deposition of silver closes the electrical connection between the two flanking microelectrodes, and target capture is signalled by a sharp drop in the resistance of the circuit.

3. CONCLUSION AND OUTLOOK

After about four decades of development of amperometric biosensors, a variety of techniques for a controlled modification of electrode surfaces with the required biological recognition elements together with all necessary compounds needed for an efficient signal transduction have been developed. This broad knowledge concerning sensor architectures, immobilisation schemes, design of ET pathways, etc. opens the route to potentially adapt similar transduction schemes to a variety of new applications in genomics and proteomics. As a matter of fact, labelling with enzymes or redox reporters is a straight forward approach, however, also label-free detection schemes involving fast and carefully designed ET pathways may find application in new assays in which an

easy to use and cheap equipment with a potential for parallelisation and miniaturisation is important. In addition, electrochemical robotics and electrochemical high-throughput screening will improve the impact, electrochemical sensors will have on emerging assay technologies in future.

LIST OF ABBREVIATIONS

CV	cyclic voltammetry
CDH	cellobiose dehydrogenase
DNA	deoxyribonucleic acid
DPA	differential pulse amperometry
DPV	differential pulse voltammetry
ds	double stranded
ET	electron transfer
FAD	flavin adenine dinucleotide
FCC	flavocytochrome c_{552}
FDH	quinohemoprotein fructose dehydrogenase
FMN	flavin-mononucleotide
FR	fumarate reductase
GADH	<i>D</i> -gluconate dehydrogenase
HTS	high-throughput screening
NAD ⁺	nicotinamide-adenine dinucleotide
NHE	normal hydrogen electrode
ODN	oligodeoxyribonucleotide
PQQ	pyrrolo-quinoline-quinone
QH-ADH	quinohemoprotein alcohol dehydrogenase
SAM	self-assembled monolayer
SCE	standard calomel electrode
SDH	succinate dehydrogenase
SECM	scanning electrochemical microscopy
ss	single stranded

REFERENCES

- Abel, P.U. and T. von Woedtke, 2002, Biosensors for *in vivo* glucose measurement: Can we cross the experimental stage, *Biosens. Bioelectron.* 17, 1059–1070.
- Aguilar, Z.P., W.R.I.V. Vandaveer and I. Fritsch, 2002, Self-contained microelectrochemical immunoassay for small volumes using mouse IgG as a model system, *Anal. Chem.* 74, 3321–3329.
- Andrieux, C.P. and J.M. Saveant, 1992, *Molecular Design of Electrode Surfaces*, Wiley, Verlag, 209.
- Aoki, A. and A. Heller, 1993, Electron diffusion coefficients in hydrogels formed of cross-linked redox polymers, *J. Phys. Chem.* 97, 11014–11019.
- Aoki, A., R. Rajagopalan and A. Heller, 1995, Effect of quaternization on electron diffusion coefficients for redox hydrogels based on poly(4-vinylpyridine), *J. Phys. Chem.* 99, 5102–5110.

- Armistead, P.M. and H.H. Thorp, 2002, Electrochemical detection of gene expression in tumor samples: Overexpression of Rak nuclear tyrosine kinase, *Bioconjug. Chem.* 13, 172–176.
- Armstrong, F.A., 1992, Dynamic electrochemistry of iron-sulfur proteins, *Adv. Inorg. Chem.* 38, 117–163.
- Armstrong, F.A., 2002, Encyclopedia of Electrochemistry, Voltammetry of Proteins, Chapter Bioelectrochemistry, Vol. 9, Wiley-VCH Verlag GmbH, Weinheim, 13–29.
- Armstrong, F.A., S.J. George, A.J. Thomson and M.G. Yates, 1988, Direct electrochemistry in the characterization of redox proteins: Novel properties of *Azotobacter* 7-iron ferredoxin, *FEBS Lett.* 234, 107–110.
- Armstrong, F.A. and A.M. Lannon, 1987, Fast interfacial electron transfer between cytochrome *c* peroxidase and graphite electrodes promoted by aminoglycosides: Novel electroenzymic catalysis of H₂O₂ reduction, *J. Am. Chem. Soc.* 109, 7211–7212.
- Bagel, O., C. Degrand, B. Limoges, M. Joannes, F. Azek and P. Brossier, 2000, Enzyme affinity assays involving a single-use electrochemical sensor. Applications to the enzyme immunoassay of human chorionic gonadotropin hormone and nucleic acid hybridization of human cytomegalovirus DNA, *Electroanalysis* 12, 1447–1452.
- Bain, C.D., E.B. Troughton, Y.T. Tao, J. Evall, G.M. Whitesides and R.G. Nuzzo, 1989, Formation of monolayer films by the spontaneous assembly of organic thiols from solution onto gold, *J. Am. Chem. Soc.* 111, 321–335.
- Bard, A.J., 1983, Chemical modification of electrodes, *J. Chem. Ed.* 60, 302–304.
- Bard, A.J., F.-R.F. Fan and M.V. Mirkin, 1995a, Scanning electrochemical microscopy, Physical electrochemistry: Principles, Methods and Applications, Ed. I. Rubinstein, Dekker, N.Y., pp. 209–242.
- Bard, A.J., Fan, F.R.F. and Mirkin, M.V., 1995b, Scanning electrochemical microscopy. Handbook of Surface Imaging and Visualization, Ed. A.T. Hubbard, CRC Press, Boca Raton, FL, Chapter 48, pp. 667–679.
- Barendrecht, E., 1990, Chemically and physically modified electrodes: Some new developments (general review), *J. Appl. Electrochem.* 20, 175–185.
- Barker, A.L., M. Gonsalves, J.V. Macpherson, C.J. Slevin and P.R. Unwin, 1999, Scanning electrochemical microscopy: Beyond the solid/liquid interface (general review), *Anal. Chim. Acta* 385, 223–240.
- Bartlett, P.N. and P.R. Birkin, 1993, The application of conducting polymers in biosensors, *Synth. Met.* 61, 15–21.
- Bartlett, P.N. and D.J. Caruana, 1992, Electrochemical immobilization of enzymes. 5. Microelectrodes for the detection of glucose based on glucose oxidase immobilized in a poly(phenol) film, *Analyst* 117, 1287–1292.
- Bartlett, P.N. and J.M. Cooper, 1993, A review of the immobilization of enzymes in electropolymerized films (general review), *J. Electroanal. Chem.* 362, 1–12.
- Bartlett, P.N. and K.F.E. Pratt, 1995, Theoretical treatment of diffusion and kinetics in amperometric immobilized enzyme electrodes. 1. Redox mediator entrapped within the film, *J. Electroanal. Chem.* 397, 61–78.
- Bartlett, P.N., P. Tebbutt and R.G. Whitaker, 1991, Kinetic aspects of the use of modified electrodes and mediators in bioelectrochemistry, *Prog. React. Kinet.* 16, 55–155.
- Bartlett, P.N., R.G. Whitaker, M.J. Green and J.E. Frew, 1987, Covalent binding of electron relays to glucose oxidase, *J. Chem. Soc. Chem. Commun.* 1603–1604.
- Beissenhirtz, M.K., F.W. Scheller, W.F.M. Stocklein, D.G. Kurth, H. Mohwald and F. Lisdat, 2004, Electroactive cytochrome *c* multilayers within a polyelectrolyte assembly, *Angew. Chem. Int. Ed.* 43, 4357–4360.
- Beratan, D.N., J.N. Onuchic, J.R. Winkler and H.B. Gray, 1992, Electron-tunneling pathways in proteins (general review), *Science* 258, 1740–1741.
- Beratan, D.N. and S.S. Skourtis, 1998, Electron transfer mechanisms, *Curr. Opin. Chem. Biol.* 2, 235–243.
- Betso, S.R., M.H. Klapper and L.B. Anderson, 1972, Electrochemical studies of heme proteins. Coulometric, polarographic, and combined spectroelectrochemical methods for reduction of the heme prosthetic group in cytochrome *c*, *J. Am. Chem. Soc.* 94, 8197–8204.

- Bilitewski, U. and A.P.F. Turner, Eds., 2000, *Biosensors for Environmental Monitoring*, Harwood Academic Publishers, Amsterdam, The Netherlands, p. 421.
- Bishop, G.R. and V.L. Davidson, 1997, Catalytic role of monovalent cations in the mechanism of proton transfer which gates an interprotein electron transfer reaction, *Biochemistry* 36, 13586–13592.
- Bixon, M. and J. Jortner, 1968, Intramolecular radiationless transitions, *J. Chem. Phys.* 48, 715–726.
- Bixon, M. and J. Jortner, 1986, Coupling of protein modes to electron transfer in bacterial photosynthesis, *J. Phys. Chem.* 90, 3795–3800.
- Boon, E.M. and J.K. Barton, 2002, Charge transport in DNA (general review), *Curr. Opin. Struct. Biol.* 12, 320–329.
- Bourdillon, C., J.B. Bourgeois and D. Thomas, 1980, Covalent linkage of glucose oxidase on modified glassy carbon electrodes. Kinetic phenomena, *J. Am. Chem. Soc.* 102, 4231–4235.
- Bourdillon, C., C. Demaille, J. Gueris, J. Moiroux and J.M. Saveant, 1993, A fully active monolayer enzyme electrode derivatized by antigen antibody attachment, *J. Am. Chem. Soc.* 115, 12264–12269.
- Bourdillon, C., C. Demaille, J. Moiroux and J.M. Saveant, 1994, Step-by-step immunological construction of a fully active multilayer enzyme electrode, *J. Am. Chem. Soc.* 116, 10328–10329.
- Bourdillon, C., C. Demaille, J. Moiroux and J.M. Saveant, 1996, From homogeneous electroenzymatic kinetics to antigen–antibody construction and characterization of spatially ordered catalytic enzyme assemblies on electrodes (review), *Acc. Chem. Res.* 29, 529–535.
- Bruno, F., M.C. Pham and J.E. Dubois, 1977, Polarographic study of polypyrrole film formation on metal electrodes by electrolysis of disubstituted phenols, *Electrochim. Acta* 22, 451–457.
- Brunori, M., 1994, Control of electron-transfer in metalloproteins, *Biosens. Bioelectron.* 9, 633–636.
- Calvo, E.J., C. Danilowicz and L. Diaz, 1993, Enzyme catalysis at hydrogel-modified electrodes with redox polymer mediator, *J. Chem. Soc. Faraday Trans.* 89, 377–384.
- Calvo, E.J., R. Etchenique, C. Danilowicz and L. Diaz, 1996, Electrical communication between electrodes and enzymes mediated by redox hydrogels, *Anal. Chem.* 68, 4186–4193.
- Campbell, C.N., D. Gal, N. Cristler, C. Banditrat and A. Heller, 2002, Enzyme-amplified amperometric sandwich test for RNA and DNA, *Anal. Chem.* 74, 158–162.
- Carter, M.T., G.K. Rowe, J.N. Richardson, L.M. Tender, R.H. Terrill and R.W. Murray, 1995, Distance dependence of the low-temperature electron transfer kinetics of ferrocenylcarboxy-terminated alkanethiol monolayers, *J. Am. Chem. Soc.* 117, 2896–2899.
- Caruana, D.J. and A. Heller, 1999, Enzyme-amplified amperometric detection of hybridization and of a single base pair mutation in an 18-base oligonucleotide on a 7-mm-diameter microelectrode, *J. Am. Chem. Soc.* 121, 769–774.
- Cass, A.E.G., G. Davis, G.D. Francis, H.A.O. Hill, W.J. Aston, I.J. Higgins, E.V. Plotkin, L.D.L. Scott and A.P.F. Turner, 1984, Ferrocene-mediated enzyme electrode for amperometric determination of glucose, *Anal. Chem.* 56, 667–671.
- Cass, A.E.G., G. Davis, M.J. Green and H.A.O. Hill, 1985, Ferricinium ion as an electron acceptor for oxido-reductases, *J. Electroanal. Chem.* 190, 117–127.
- Chapman, S.K., 1991, *Perspectives in Bioinorganic Chemistry*, Vol. 1, Blue Copper Proteins, JAI Press, London, pp. 95–140.
- Chaubey, A., M. Gerard, R. Singhal, V.S. Singh and B.D. Malhotra, 2000b, Immobilization of lactate dehydrogenase on electrochemically prepared polypyrrole-polyvinylsulphonate composite films for application to lactate biosensors, *Electrochim. Acta* 46, 723–729.
- Chaubey, A. and B.D. Malhotra, 2002, Mediated biosensors (review), *Biosens. Bioelectron.* 17, 441–456.
- Chaubey, A., K.K. Pande, V.S. Singh and B.D. Malhotra, 2000a, Co-immobilization of lactate oxidase and lactate dehydrogenase on conducting polyaniline films, *Anal. Chim. Acta* 407, 97–103.

- Chen, Q., Y. Kobayashi, H. Takeshita, T. Hoshi and J. Anzai, 1998, Avidin-biotin system-based enzyme multilayer membranes for biosensor applications: Optimization of loading of choline esterase and choline oxidase in the bienzyme membrane for acetylcholine biosensors, *Electroanalysis* 10, 94–97.
- Chen, J., U. Wollenberger, F. Lisdat, B.X. Ge and F.W. Scheller, 2000, Superoxide sensor based on hemin modified electrode, *Sens. Actuat. B* 70, 115–120.
- Cho, Y.K. and J.E. Bailey, 1979, Immobilization of enzymes on activated carbon: Selection and preparation of the carbon support, *Biotechnol. Bioeng.* 21, 461–476.
- Clark, L.C. and C. Lyons, 1962, Electrode systems for continuous monitoring in cardiovascular surgery, *Ann. NY. Acad. Sci.* 102, 29–45.
- Collinson, M., E.F. Bowden and M.J. Tarlov, 1992, Voltammetry of covalently immobilized cytochrome *c* on self-assembled monolayer electrodes, *Langmuir* 8, 1247–1250.
- Contractor, A.Q., T.N. Sureshkumar, R. Narayanan, S. Sukeerthi, R. Lal and R.S. Srinivasa, 1994, Conducting polymer-based biosensors, *Electrochim. Acta* 39, 1321–1324.
- Cosnier, S., 1999, Biomolecule immobilization on electrode surfaces by entrapment or attachment to electrochemically polymerized films. A review (review), *Biosens. Bioelectron.* 14, 443–456.
- Cosnier, S., A. Deronzier and J.-C. Moutet, 1985, Oxidative electropolymerization of polypyridinyl complexes of ruthenium(II)-containing polypyrrol groups, *J. Electroanal. Chem.* 193, 193–204.
- Csoka, B., B. Kovacs and G. Nagy, 2003, Scanning electrochemical microscopy inside the biocatalytic layer of biosensors, investigation of a double function complex multienzyme reaction layer, *Electroanalysis* 15, 1335–1342.
- Csőregi, E., L. Gorton and G. Marko-Varga, 1994b, Amperometric microbiosensors for detection of hydrogen peroxide and glucose based on peroxidase-modified carbon fibers, *Electroanalysis* 6, 925–933.
- Csőregi, E., C.P. Quinn, D.W. Schmidtke, S.E. Lindquist, M.V. Pishko, L. Ye, I. Katakis, J.A. Hubbell and A. Heller, 1994a, Design, characterization, and one-point *in vivo* calibration of a subcutaneously implanted glucose electrode, *Anal. Chem.* 66, 3131–3138.
- Csőregi, E., D.W. Schmidtke and A. Heller, 1995, Design and optimization of a selective subcutaneously implantable glucose electrode based on wired glucose oxidase, *Anal. Chem.* 67, 1240–1244.
- Danilowicz, C., E. Cortón, F. Battaglini and E.J. Calvo, 1998, An OS(byp)2 CIPyCH₂NHPoly(allylamine) hydrogel mediator for enzyme wiring at electrodes, *Electrochim. Acta* 43, 3525–3531.
- Davidson, V.L., 2004, Electron transfer in quinoproteins (review), *Arch. Biochem. Biophys.* 428, 32–40.
- Davis, G., H.A.O. Hill, W.J. Aston, I.J. Higgins and A.P.F. Turner, 1983, Bioelectrochemical fuel cell and sensor based on a quinoprotein, alcohol dehydrogenase, *Enzyme Microb. Technol.* 5, 383–388.
- De-los-Santos-Alvarez, P., M.J. Lobo-Castanon, A.J. Miranda-Ordieres and P. Tunon-Blanco, 2004a, Electrochemistry of nucleic acids at solid electrodes and its applications (review), *Electroanalysis* 16, 1193–1204.
- De-los-Santos-Alvarez, P., M.J. Lobo-Castanon, A.J. Miranda-Ordieres and P. Tunon-Blanco, 2004b, Current strategies for electrochemical detection of DNA with solid electrodes (review), *Anal. Bioanal. Chem.* 378, 104–118.
- Decher, G., 1997, Fuzzy nanoassemblies: Toward layered polymeric multicomposites (general review), *Science* 277, 1232–1237.
- Decher, G. and J.D. Hong, 1991, Buildup of ultrathin multilayer films by a self-assembly process: II. Consecutive adsorption of anionic and cationic bipolar amphiphiles and polyelectrolytes on charged surfaces, *Berich. Bunsen. Gesell.* 95, 1430–1434.
- Decher, G., B. Lehr, K. Lowack, Y. Lvov and J. Schmitt, 1994, New nanocomposite films for biosensors – layer-by-layer adsorbed films of polyelectrolytes, proteins or DNA, *Biosens. Bioelectron.* 9, 677–684.

- Degani, Y. and A. Heller, 1987, Direct electrical communication between chemically modified enzymes and metal electrodes. 1. Electron transfer from glucose oxidase to metal electrodes via electron relays, bound covalently to the enzyme, *J. Phys. Chem.* 91, 1285–1289.
- Degani, Y. and A. Heller, 1989, Electrical communication between redox centers of glucose oxidase and electrodes via electrostatically and covalently bound redox polymers, *J. Am. Chem. Soc.* 111, 2357–2358.
- Delumleywoodyear, T., C.N. Campbell and A. Heller, 1996, Direct enzyme-amplified electrical recognition of a 30-base model oligonucleotide, *J. Am. Chem. Soc.* 118, 5504–5505.
- Dequaire, M. and A. Heller, 2002, Screen printing of nucleic acid detecting carbon electrodes, *Anal. Chem.* 74, 4370–4377.
- DeSantis, G. and J.B. Jones, 1999, Chemical modification of enzymes for enhanced functionality (review), *Curr. Opin. Biotechnol.* 10, 324–330.
- Di Fabrizio, E., M. Gentili, P. Morales, R. Pilloton, J. Mela, S. Santucci and A. Sese, 1996, Microlithographic techniques for laser assisted fabrication of bioelectronic devices, *Appl. Phys. Lett.* 69, 3280–3282.
- Dicks, J.M., W.J. Aston, G. Davis and A.P.F. Turner, 1986, Mediated amperometric biosensors for D-galactose, glycolate and L-amino acids based on a ferrocene-modified carbon paste electrode, *Anal. Chim. Acta* 182, 103–112.
- Doherty, A.P., R.J. Forster, M.R. Smyth and J.G. Vos, 1991, Development of a sensor for the detection of nitrite using a glassy carbon electrode modified with the electrocatalyst $\langle \text{Os}(\text{bipy})_2(\text{PVP})_{10}\text{Cl} \rangle \text{Cl}$, *Anal. Chim. Acta* 255, 45–52.
- D’Orazio, P., 2003, Biosensors in clinical chemistry (review), *Clin. Chim. Acta* 334, 41–69.
- Drummond, T.G., M.G. Hill and J.K. Barton, 2003, Electrochemical DNA sensors (review), *Nat. Biotechnol.* 21, 1192–1199.
- Durham, B., L.P. Pan, S. Hahm, J. Long and F. Millett, 1990, ACS advances in chemistry series, 226, 180–193.
- Dzyadevich, S.V., V.K. Rossokhaty, N.F. Shram, A.A. Shul’ga, A.P. Soldatkin and V.I. Strikha, 1994, Thin-films microelectrode arrays for amperometric enzyme biosensors with electrochemically synthesized glucose oxidase-polyaniline membrane, *Proc. SPIE-The Int. Soc. Opt. Eng.* 2364, 610–615.
- Eddowes, M.J. and H.A.O. Hill, 1977, Novel method for the investigation of the electrochemistry of metalloproteins: Cytochrome *c*, *J. Chem. Soc. Chem. Commun.* 771–772.
- Elatrash, S.S. and R.D. Oneill, 1995, Characterisation *in vitro* of a naphthoquinone-mediated glucose oxidase-modified carbon paste electrode designed for neurochemical analysis *in vivo*, *Electrochim. Acta* 40, 2791–2797.
- Feng, Z.Q., S. Imabayashi, T. Kakiuchi and K. Niki, 1997, Long-range electron-transfer reaction rates to cytochrome *c* across long- and short-chain alkanethiol self-assembled monolayers: Electroreflectance studies, *J. Chem. Soc. Faraday Trans.* 93, 1367–1370.
- Finklea, H.O., 1996, *Electroanalytical chemistry A Series of Advances*, Vol. 19, *Electrochemistry of Organized Monolayers of Thiols and Related Molecules on Electrodes*, Dekker, New York, pp. 110–335.
- Foulds, N.C. and C.R. Lowe, 1988, Immobilization of glucose oxidase in ferrocene-modified pyrrole polymers, *Anal. Chem.* 60, 2473–2478.
- Frebel, H., G.C. Chemnitz, K. Cammann, R. Kakerow, M. Rospert and W. Mokwa, 1997, Multianalyte sensor for the simultaneous determination of glucose, L-lactate and uric acid based on a microelectrode array, *Sens. Actuat. B-Chem.* 43, 87–93.
- Frew, J.E. and H.A.O. Hill, 1988, Review: Direct and indirect electron transfer between electrodes and redox proteins, *Eur. J. Biochem.* 172, 261–269.
- Fridman, V., U. Wollenberger, V. Bogdanovskaya, F. Lisdat, T. Ruzgas, A. Lindgren, L. Gorton and F.W. Scheller, 2000, Electrochemical investigation of cellobiose oxidation by cellobiose dehydrogenase in the presence of cytochrome *c* as mediator, *Biochem. Soc. Trans.* 28, 63–70.
- Fritz, J., M.K. Baller, H.P. Lang, H. Rothuizen, P. Vettiger, E. Meyer, H.J. Guntherodt, C. Gerber and J.K. Gimzewski, 2000, Translating biomolecular recognition into nanomechanics, *Science* 288, 316–318.

- Fujieda, N., M. Mori, K. Kano and T. Ikeda, 2002, Spectroelectrochemical evaluation of redox potentials of cysteine tryptophylquinone and two hemes *c* in quinoxinohemoprotein amine dehydrogenase from *Paracoccus denitrificans*, *Biochemistry* 41, 13736–13743.
- Garguilo, M.G., N. Huynh, A. Proctor and A.C. Michael, 1993, Amperometric sensors for peroxide, choline, and acetylcholine based on electron-transfer between horseradish-peroxidase and a redox polymer, *Anal. Chem.* 65, 523–528.
- Gaspar, S., M. Mosbach, L. Wallman, T. Laurell, E. Csöregi and W. Schuhmann, 2001, A method for the design and study of enzyme microstructures formed by means of a flow-through microdispenser, *Anal. Chem.* 73, 4254–4261.
- Gaspar, S., W. Schuhmann, T. Laurell and E. Csöregi, 2002, Design, visualization, and utilization of enzyme microstructures built on solid surfaces, *Rev. Anal. Chem.* 21, 245–266.
- Geise, R.J., S.Y. Rao and A.M. Yacynych, 1993, Electropolymerized 1,3-diaminobenzene for the construction of a 1,1'-dimethylferrocene mediated glucose biosensor, *Anal. Chim. Acta* 281, 467–473.
- Gerischer, H., 1961, Kinetics of reduction–oxidation reaction on metals and semiconductors. III. Semiconductor electrodes, *Zeitschrift Physi. Chem. (Muenchen, Germany)* 27, 48–79.
- Gernet, S., M. Koudelka and N.F. De Rooij, 1989, A planar glucose enzyme electrode, *Sens. Actuat.* 17, 537–540.
- Ghindilis, A., 2000, Direct electron transfer catalysed by enzymes: Application for biosensor development, *Biochem. Soc. Trans.* 28, 84–89.
- Glezos, N., K. Misiakos, S. Kakabakos, P. Petrou and G. Terzoudi, 2002, Electron beam patterning of biomolecules, *Biosens. Bioelectron.* 17, 279–282.
- Godin, M., P.J. Williams, V. Tabard-cossa, O. Laroche, L.Y. Beaulieu, R.B. Lennox and P. Grutter, 2004, Surface stress, kinetics, and structure of alkanethiol self-assembled monolayers, *Langmuir* 20, 7090–7096.
- Gooding, J.J., 2002, Electrochemical DNA hybridization biosensors (review), *Electroanalysis* 14, 1149–1156.
- Gooding, J.J. and D.B. Hibbert, 1999, The application of alkanethiol self-assembled monolayers to enzyme electrodes, *TRAC – Trends Anal. Chem.* 18, 525–533.
- Gooding, J.J., F. Mearns, W.R. Yang and J.Q. Liu, 2003, Self-assembled monolayers into the 21(st) century: Recent advances and applications (review), *Electroanalysis* 15, 81–96.
- Gorton, L., 1995, Carbon paste electrodes modified with enzymes, tissues, and cells (review), *Electroanalysis* 7, 23–45.
- Gorton, L., A. Lindgren, T. Larsson, F.D. Munteanu, T. Ruzgas and I. Gazaryan, 1999, Direct electron transfer between heme-containing enzymes and electrodes as basis for third generation biosensors, *Anal. Chim. Acta* 400, 91–108.
- Gough, D.A., J.Y. Lucisano and P.H.S. Tse, 1985, Two-dimensional enzyme electrode sensor for glucose, *Anal. Chem.* 57, 2351–2357.
- Gregg, B.A. and A. Heller, 1990, Crosslinked redox gels containing glucose oxidase for amperometric biosensor applications, *Anal. Chem.* 62, 258–263.
- Griffiths, D. and G. Hall, 1993, Biosensors – what real progress is being made (general review), *Trends Biotechnol.* 11, 122–130.
- Guilbault, G.G. and G.J. Lubrano, 1973, Enzyme electrode for the amperometric determination of glucose, *Anal. Chim. Acta* 64, 439–455.
- Guilbault, G.G. and R.D. Schmid, 1991, Biosensors for the determination of drug substances (general review), *Biotechnol. Appl. Biochem.* 14, 133–145.
- Gulcev, M.D., G.L.G. Goring, M. Rakic and J.D. Brennan, 2002, Reagentless pH-based biosensing using a fluorescently-labelled dextran co-entrapped with a hydrolytic enzyme in sol-gel derived nanocomposite films, *Anal. Chim. Acta* 457, 47–59.
- Habermüller, K., A. Ramanavicius, V. Laurinavicius and W. Schuhmann, 2000, An oxygen-insensitive reagentless glucose biosensor based on osmium-complex modified polypyrrole, *Electroanalysis* 12, 1383–1389.
- Habermüller, K., S. Reiter, H. Buck, T. Meier, J. Staepels and W. Schuhmann, 2003, Conducting redoxpolymer-based reagentless biosensors using modified PQQ-dependent glucose dehydrogenase, *Mikrochim. Acta* 143, 113–121.

- Hall, E.A.H., 1992, Overview of biosensors, ACS Symp. Ser. 487, 1–14.
- Hanazato, Y., M. Nakako, S. Shiono and M. Maeda, 1989, Integrated multi-biosensor based on an ion-sensitive field-effect transistor using photolithographic techniques, IEEE Trans. Electron. Dev. 36, 1303–1310.
- Harrison, D.J., R.B.F. Turner and H.P. Baltes, 1988, Characterization of perfluorosulfonic acid polymer coated enzyme electrodes and a miniaturized integrated potentiostat for glucose analysis in whole blood, Anal. Chem. 60, 2002–2007.
- Hartwich, G. and H. Wieder, 2001, DNA chips with direct electrical detection of hybridization, GDCh-Monographien 23, 347–356.
- Hayashi, K., T. Horiuchi, R. Kurita, K. Torimitsu and O. Niwa, 2000, Real-time electrochemical imaging using an individually addressable multi-channel electrode, Biosens. Bioelectron. 15, 523–529.
- Hedenmo, M., A. Narvaez, E. Dominguez and I. Katakis, 1997, Improved mediated tyrosinase amperometric enzyme electrodes, J. Electroanal. Chem. 425, 1–11.
- Heering, H.A., J.H. Weiner and F.A. Armstrong, 1997, Direct detection and measurement of electron relays in a multicentered enzyme: Voltammetry of electrode-surface films of *E. coli* fumarate reductase, an iron-sulfur flavoprotein, J. Am. Chem. Soc. 119, 11628–11638.
- Heitele, H., 1993, Dynamic solvent effects on electron-transfer reactions (general review), Angew. Chem. 105, 378–398 (See also Angew. Chem., Int. Ed. Engl., 1993, 32(3), 359–377).
- Heller, A., 1990, Electrical wiring of redox enzymes, Acc. Chem. Res. 23, 128–133.
- Heller, A., 1992, Electrical connection of enzyme redox centers to electrodes, J. Phys. Chem. 96, 3579–3587.
- Heller, A. and Y. Degani, 1988, Redox chemistry and interfacial behaviour of biological molecules [Proc. Int. Symp. Redox Mech. Interfacial Prop. Mol. Biol. Importance, 3rd, Meeting Date 1987] Direct electrical communication between chemically modified enzymes and metal electrodes: III. Electron-transfer relay modified glucose oxidase and D-amino-acid oxidase, pp. 151–171, Plenum Press, New York.
- Hill, H.A.O. and G.S. Sanghera, 1990, Biosensors: A Practical Approach. Mediated Amperometric Enzyme Electrodes, Oxford University Press, London, GB, pp. 19–46.
- Hiller, M., C. Kranz, J. Huber, P. Bäuerle and W. Schuhmann, 1996, Amperometric biosensors produced by immobilization of redox enzymes at polythiophene-modified electrode surfaces, Adv. Mater. 8, 219.
- Hirst, J., A. Sucheta, B.A.C. Ackrell and F.A. Armstrong, 1996, Electrocatalytic voltammetry of succinate dehydrogenase: Direct quantification of the catalytic properties of a complex electron-transport enzyme, J. Am. Chem. Soc. 118, 5031–5038.
- Horrocks, B.R., 2003, Scanning electrochemical microscopy, Encyclopedia of Electrochemistry 3, 444–490.
- Horrocks, B.R., D. Schmidtke, A. Heller and A.J. Bard, 1993, Scanning electrochemical microscopy. 24. Enzyme ultramicroelectrodes for the measurement of hydrogen peroxide at surfaces, Anal. Chem. 65, 3605–3614.
- Hyun, Y.L. and V.L. Davidson, 1995, Electron-transfer reactions between aromatic amine dehydrogenase and azurin, Biochemistry 34, 12249–12254.
- Ianniello, R.M., T.J. Lindsay and A.M. Yacynych, 1982a, Immobilized xanthine oxidase chemically modified electrode as a dual analytical sensor, Anal. Chem. 54, 1980–1984.
- Ianniello, R.M., T.J. Lindsay and A.M. Yacynych, 1982b, Differential pulse voltammetric study of direct electron transfer in glucose oxidase chemically modified graphite electrodes, Anal. Chem. 54, 1098–1101.
- Ihara, T., M. Nakayama, M. Murata, K. Nakano and M. Maeda, 1997, Gene sensor using ferrocenyl oligonucleotide, J. Chem. Soc. Chem. Commun. 1609–1610.
- Ikeda, T. and K. Kano, 2003, Bioelectrocatalysis-based application of quinoproteins and quinoprotein-containing bacterial cells in biosensors and biofuel cells, BBA-Prot. Proteom. 1647, 121–126.
- Ikeda, T., D. Kobayashi, F. Matsushita, T. Sagara and K. Niki, 1993b, Bioelectrocatalysis at electrodes coated with alcohol-dehydrogenase, a quinohemoprotein with heme-c serving as a built-in mediator, J. Electroanal. Chem. 361, 221–228.

- Ikeda, T., F. Matsushita and M. Senda, 1990, D-fructose dehydrogenase-modified carbon paste electrode containing para-benzoquinone as a mediated amperometric fructose sensor, *Agri. Biol. Chem.* 54, 2919.
- Ikeda, T., F. Matsushita and M. Senda, 1991, Amperometric fructose sensor based on direct bioelectrocatalysis, *Biosens. Bioelectron.* 6, 299–304.
- Ikeda, T., S. Miyaoka, F. Matsushita, D. Kobayashi and M. Senda, 1992, Direct bioelectrocatalysis at metal and carbon electrodes modified with adsorbed D-gluconate dehydrogenase or adsorbed alcohol dehydrogenase from bacterial membranes, *Chem. Lett.* 847–850.
- Ikeda, T., S. Miyaoka and K. Miki, 1993a, Enzyme-catalysed electrochemical oxidation of D-gluconate at electrodes coated with D-gluconate dehydrogenase, a membrane-bound flavohemoprotein, *J. Electroanal. Chem.* 352, 267–278.
- Jaffari, S.A. and J.C. Pickup, 1996, Novel hexacyanoferrate(iii)-modified carbon electrodes – Application in miniaturized biosensors with potential for *in vivo* glucose sensing, *Biosens. Bioelectron.* 11, 1167–1175.
- Jelen, F., B. Yosypchuk, A. Kourilova, L. Novotny and E. Palecek, 2002, Label-free determination of picogram quantities of DNA by stripping voltammetry with solid copper amalgam or mercury electrodes in the presence of copper, *Anal. Chem.* 74, 4788–4793.
- Jeuken, L.J.C., A.K. Jones, S.K. Chapman, G. Cecchini and F.A. Armstrong, 2002, Electron-transfer mechanisms through biological redox chains in multicenter enzymes, *J. Am. Chem. Soc.* 124, 5702–5713.
- Jiang, R.Z. and D. Chu, 2002, A combinatorial approach toward electrochemical analysis, *J. Electroanal. Chem.* 527, 137–142.
- Jimenez, C., J. Bartrol, N.F. de Rooij and M. Koudelka-Hep, 1997, Use of photopolymerizable membranes based on polyacrylamide hydrogels for enzymic microsensor construction, *Anal. Chim. Acta* 351, 169–176.
- Johnson, K.W., 1991, Reproducible electrodeposition of biomolecules for the fabrication of miniature electroenzymic biosensors, *Sens. Actuat. B-Chem.* 5, 85–89.
- Jortner, J., 1980, Dynamics of electron transfer in bacterial photosynthesis, *Biochim. Biophys. Acta* 594, 193–230.
- Kacantiklic, V., K. Johansson, G. Marko-Varga, L. Gorton, G. Jönsson-Pettersson and E. Csöregi, 1994, Amperometric biosensors for detection of L-amino and D-amino acids based on coimmobilized peroxidase and L-amino and D-amino acid oxidases in carbon paste electrodes, *Electroanalysis* 6, 381–390.
- Kajiya, Y., R. Tsuda and H. Yoneyama, 1991, Conferment of cholesterol sensitivity on polypyrrole films by immobilization of cholesterol oxidase and ferrocenecarboxylate ions, *J. Electroanal. Chem.* 301, 155–164.
- Kashiwagi, Y., Q.H. Pan, Y. Yanagisawa, N. Sibayama and T. Osa, 1994, The effects of chain length of ferrocene moiety on electrical communication of mediators-modified and enzymes-modified electrodes, *Denki Kagaku* 62, 1240–1246.
- Katakis, I. and A., Heller, 1997, *Frontiers in Biosensors I – Fundamental Aspects Electron Transfer Via Redox Hydrogels between Electrodes*, Birkhäuser Verlag, Basel, pp. 229–241.
- Katz, E., T. Lötzbeyer, D.D. Schlereth, W. Schuhmann and H.-L. Schmidt, 1994b, Electrocatalytic oxidation of reduced nicotinamide coenzymes at gold and platinum-electrode surfaces modified with a monolayer of pyrroloquinoline quinone – Effect of Ca^{2+} cations, *J. Electroanal. Chem.* 373, 189–200.
- Katz, E., A. Riklin, V. Heleg-shabtai, I. Willner and A.F. Buckmann, 1999, Glucose oxidase electrodes via reconstitution of the apo-enzyme: Tailoring of novel glucose biosensors, *Anal. Chim. Acta* 385, 45–58.
- Katz, E., D.D. Schlereth, H.L. Schmidt and A.J.J. Olsthoorn, 1994a, Reconstitution of the quinoprotein glucose-dehydrogenase from its apoenzyme on a gold electrode surface-modified with a monolayer of pyrroloquinoline quinone, *J. Electroanal. Chem.* 368, 165–171.
- Kerman, K., M. Kobayashi and E. Tamiya, 2004, Recent trends in electrochemical DNA biosensor technology (review), *Meas. Sci. Technol.* 15, r1–r11.

- Kerman, K., D. Ozkan, P. Kara, A. Erdem, B. Meric, P.E. Nielsen and M. Ozsoz, 2003, Label-free bioelectronic detection of point mutation by using peptide nucleic acid probes, *Electroanalysis* 15, 667–670.
- Khan, G.F., 1996, Organic charge transfer complex based printable biosensor, *Biosens. Bioelectron.* 11, 1221–1227.
- Khan, G.F., H. Shinohara, Y. Ikariyama and M. Aizawa, 1991, Electrochemical behavior of monolayer quinoprotein adsorbed on the electrode surface, *J. Electroanal. Chem.* 315, 263–273.
- Kinney, K.T. and H.G. Monbouquette, 1993, Direct electron-transfer to *Escherichia coli* fumarate reductase in self-assembled alkanethiol monolayers on gold electrodes (letter), *Langmuir* 9, 2255–2257.
- Kost, G.J., T.H. Nguyen and Z.P. Tang, 2000, Whole-blood glucose and lactate – Trilayer biosensors, drug interference, metabolism, and practice guidelines, *Arch. Pathol. Lab. Med.* 124, 1128–1134.
- Kranz, C., A. Kueng, A. Lugstein, E. Bertagnolli and B. Mizaikoff, 2004, Mapping of enzyme activity by detection of enzymatic products during AFM imaging with integrated SECM–AFM probes, *Ultramicroscopy* 100, 127–134.
- Kranz, C., T. Lötzbeyer, H.-L. Schmidt and W. Schuhmann, 1997, Lateral visualization of direct electron transfer between microperoxidase and electrodes by means of scanning electrochemical microscopy, *Biosens. Bioelectron.* 12, 257–266.
- Kulikov, V. and V.M. Mirsky, 2004, Equipment for combinatorial electrochemical polymerization and high-throughput investigation of electrical properties of the synthesized polymers, *Meas. Sci. Technol.* 15, 49–54.
- Kulys, J., W. Schuhmann and H.-L. Schmidt, 1992, Carbon-paste electrodes with incorporated lactate oxidase and mediators, *Anal. Lett.* 25, 1011–1024.
- Kulys, J.J., A.S. Samalius and G.J.S. Svirnickas, 1980, Electron exchange between the enzyme active center and organic metal, *FEBS Lett.* 114, 7–10.
- Kulys, J.T. and N.K. Cenas, 1983, Oxidation of glucose oxidase from *Penicillium Vitale* by one- and two-electron acceptors, *Biochim. Biophys. Acta* 744, 57–63.
- Kurzawa, C., A. Hengstenberg and W. Schuhmann, 2002, Immobilization method for the preparation of biosensors based on pH shift-induced deposition of biomolecule-containing polymer films, *Anal. Chem.* 74, 355–361.
- Kurzawa, C., M. Mosbach, E. Bensen and W. Schuhmann, 2001, Visualization of microstructured enzyme patterns using scanning electrochemical microscopy (SECM), *Proc. Electrochem. Soc.* 18, 304–314.
- Larson, N., T. Ruzgas, L. Gorton, M. Kokaia, P. Kissinger and E. Csöregi, 1998, Design and development of an amperometric biosensor for acetylcholine determination in brain microdialysates, *Electrochim. Acta* 43, 3541–3554.
- Larsson, T., M. Elmgren, S.E. Lindquist, M. Tessema, L. Gorton and G. Henriksson, 1996, Electron transfer between cellobiose dehydrogenase and graphite electrodes, *Anal. Chim. Acta* 331, 207–215.
- Lau, C., S. Reiter, W. Schuhmann and P. Gründler, 2004, Application of heated electrodes operating in a non-isothermal mode for interference elimination with amperometric biosensors, *Anal. Bioanal. Chem.* 379, 255–260.
- Laurinavicius, V., J. Razumiene, B. Kurtinaitiene, I. Lapenaite, I. Bachmatova, L. Marcinkeviciene, R. Meskys and A. Ramanavicius, 2002, Bioelectrochemical application of some PQQ-dependent enzymes, *Bioelectrochemistry* 55, 29–32.
- Leca, B., R.M. Morelis and P.R. Coulet, 1996, Bienzyme electrode compatible behavior for water-soluble and -insoluble substrates, *Anal. Lett.* 29, 661–672.
- Leech, D., R.J. Forster, M.R. Smyth and J.G. Vos, 1991, Effect of composition of polymer backbone on spectroscopic and electrochemical properties of ruthenium(II) bis(2,2'-bipyridyl)-containing 4-vinylpyridine styrene copolymers, *J. Mater. Chem.* 1, 629–635.
- Leger, C., K. Heffron, H.R. Pershad, E. Maklashina, C. Luna-chavez, G. Cecchini, B.A.C. Ackrell and F.A. Armstrong, 2001, Enzyme electrokinetics: Energetics of succinate oxidation by fumarate reductase and succinate dehydrogenase, *Biochemistry* 40, 11234–11245.

- Lenigk, R., H. Zhu, T.C. Lo and R. Renneberg, 1999, Recessed microelectrode array for a micro flow-through system allowing online multianalyte determination *in vivo*, *Fresen. J. Anal. Chem.* 364, 66–71.
- Levich, V.G. and R.R. Dogonadze, 1959, Theory of nonradiation electron transitions from ion to ion solns, *Dokl. Akad. Nauk SSSR* 124, 123–126.
- Levicky, R., T.M. Herne, M.J. Tarlov and S.K. Satija, 1998, Using self-assembly to control the structure of DNA monolayers on gold: A neutron reflectivity study, *J. Am. Chem. Soc.* 120, 9787–9792.
- Lindgren, A., L. Gorton, T. Ruzgas, U. Baminger, D. Haltrich and M. Schulein, 2001, Direct electron transfer of cellobiose dehydrogenase from various biological origins at gold and graphite electrodes, *J. Electroanal. Chem.* 496, 76–81.
- Lindgren, A., T. Larsson, T. Ruzgas and L. Gorton, 2000a, Direct electron transfer between the heme of cellobiose dehydrogenase and thiol modified gold electrodes, *J. Electroanal. Chem.* 494, 105–113.
- Lindgren, A., T. Ruzgas, L. Gorton, E. Csoregi, G.B. Ardila, I.Y. Sakharov and I.G. Gazaryan, 2000b, Biosensors based on novel peroxidases with improved properties in direct and mediated electron transfer, *Biosens. Bioelectron.* 15, 491–497.
- Lindgren, A., L. Stoica, T. Ruzgas, A. Ciucu and L. Gorton, 1999b, Development of a cellobiose dehydrogenase modified electrode for amperometric detection of diphenols, *Analyst* 124, 527–532.
- Lindgren, A., M. Tanaka, T. Ruzgas, L. Gorton, I. Gazaryan, K. Ishimori and I. Morishima, 1999a, Direct electron transfer catalysed by recombinant forms of horseradish peroxidase: Insight into the mechanism, *Electrochem. Commun.* 1, 171–175.
- Lion-Dagan, M., E. Katz and I. Willner, 1994, Amperometric transduction of optical signals recorded by organized monolayers of photoisomerizable biomaterials on Au electrodes, *J. Am. Chem. Soc.* 116, 7913–7914.
- Lippard, S.J. and J.M. Berg, 1994, *Principles of Bioorganic Chemistry*, University Science Books, Mill Valley, USA.
- Liu, R.X., and E.S., Smotkin, 2002, High throughput screening device for combinatorial electrochemistry (meeting abstract), *Abstr. Pap. Am. Chem. Soc.* 223, u443–u443.
- Loew, N., F.W. Scheller and U. Wollenberger, 2004, Characterization of self-assembly of glucose dehydrogenase in mono- and multilayers on gold electrodes, *Electroanalysis* 16, 1149–1154.
- Lorenzo, E., F. Pariente, L. Hernandez, F. Tobalina, M. Darder, Q. Wu, M. Maskus and H.D. Abruna, 1998, Analytical strategies for amperometric biosensors based on chemically modified electrodes, *Biosens. Bioelectron.* 13, 319–332.
- Lötzbeyer, T., W. Schuhmann, E. Katz, J. Falter and H.-L. Schmidt, 1994, Direct electron-transfer between the covalently immobilized enzyme microperoxidase mp-11 and a cystamine-modified gold electrode (note), *J. Electroanal. Chem.* 377, 291–294.
- Lötzbeyer, T., W. Schuhmann and H.-L. Schmidt, 1995, Direct electrocatalytical H₂O₂ reduction with hemin covalently immobilized at a monolayer-modified gold electrode (note), *J. Electroanal. Chem.* 395, 341–344.
- Lötzbeyer, T., W. Schuhmann and H.-L. Schmidt, 1996, Electron transfer principles in amperometric biosensors: Direct electron transfer between enzymes and electrode surface, *Sens. Actuat. B-Chem.* 33, 50–54.
- Lötzbeyer, T., W. Schuhmann and H.-L. Schmidt, 1997, Minizymes. A new strategy for the development of reagentless amperometric biosensors based on direct electron-transfer processes, *Bioelectrochem. Bioenerg.* 42, 1–6.
- Louie, R.F., Z.P. Tang, D.V. Sutton, J.H. Lee and G.J. Kost, 2000, Point-of-care glucose testing – Effects of critical care variables, influence of reference instruments, and a modular glucose meter design, *Arch. Pathol. Lab. Med.* 124, 257–266.
- Lowe, C.R., 1989, *Biosensors*, *Phil. Trans. R. Soc. Lond. B* 324, 487–496.
- Lvov, Y., G. Decher and H. Mohwald, 1993, Assembly, structural characterization, and thermal-behavior of layer-by-layer deposited ultrathin films of poly(vinyl sulfate) and poly(allylamine), *Langmuir* 9, 481–486.

- Lvov, Y.M., Z.Q. Lu, J.B. Schenkman, X.L. Zu and J.F. Rusling, 1998, Direct electrochemistry of myoglobin and cytochrome p450(cam) in alternate layer-by-layer films with DNA and other polyions, *J. Am. Chem. Soc.* 120, 4073–4080.
- Lvov, Y. and H. Möhwald, 1999, *Protein Architecture: Interfacing Molecular Assemblies and Immobilisation Biotechnology*, Marcel Dekker, New York, USA.
- Mandler, D., S. Meltzer and I. Shohat, 1996, Microelectrochemistry on surfaces with the scanning electrochemical microscope (SECM) (general review), *Isr. J. Chem.* 36, 73–80.
- Marcinkeviciene, L., I. Bachmatova, R. Semenaite, R. Rudomanskis, G. Brazenas, R. Meskiene and R. Meskys, 1999, Purification and characterisation of PQQ-dependent glucose dehydrogenase from *Erwinia* sp. 34-1, *Biotechnol. Lett.* 21, 187–192.
- Marcus, R.A., 1965, Theory of electron-transfer reactions. VI. Unified treatment for homogeneous and electrode reactions, *J. Chem. Phys.* 43, 679–701.
- Marcus, R.A., 1987, Superexchange versus an intermediate bacteriochlorophyll ion(1–) (BChl–) mechanism in reaction centers of photosynthetic bacteria, *Chem. Phys. Lett.* 133, 471–477.
- Marcus, R.A., 1988, An internal consistency test and its implications for the initial steps in bacterial photosynthesis, *Chem. Phys. Lett.* 146, 13–22.
- Marcus, R.A., 1993, Electron transfer reactions in chemistry – Theory and experiment (Nobel lecture), *Angew. Chem. Int. Ed.* 32, 1111–1121.
- Marcus, R.A. and N. Sutin, 1985, Electron transfer in chemistry and biology, *Biochim. Biophys. Acta* 811, 265–322.
- Mascini, M., I. Palchetti and G. Marrazza, 2001, DNA electrochemical biosensors, *Fresen. J. Anal. Chem.* 369, 15–22.
- Matos, R.C., M.A. Augelli, C.L. Lago and L. Angnes, 2000, Flow injection analysis-amperometric determination of ascorbic and uric acids in urine using arrays of gold microelectrodes modified by electrodeposition of palladium, *Anal. Chim. Acta* 404, 151–157.
- McCleskey, T.M., J.R. Winkler and H.B. Gray, 1992, Driving-force effects on the rates of bimolecular electron-transfer reactions, *J. Am. Chem. Soc.* 114, 6935–6937.
- McCleskey, T.M., J.R. Winkler and H.B. Gray, 1994, Bimolecular electron transfer at high driving forces, Photoreactions of gold(I) and iridium(I) complexes with pyridinium derivatives, *Inorg. Chim. Acta* 225, 319–322.
- McMahon, C.P., S.J. Killoran, S.M. Kirwan and R.D. O’neill, 2004, The selectivity of electrosynthesised polymer membranes depends on the electrode dimensions: Implications for biosensor applications, *Chem. Commun.* 2128–2130.
- Mehrvar, M. and M. Abdi, 2004, Recent developments, characteristics, and potential applications of electrochemical biosensors (review), *Anal. Sci.* 20, 1113–1126.
- Mikeladze, E., A. Collins, M. Sukhacheva, A. Netrusov and E. Csoregi, 2002a, Characterization of a glutamate biosensor based on a novel glutamate oxidase integrated into a redox hydrogel, *Electroanalysis* 14, 1052–1059.
- Mikeladze, E., A. Schulte, M. Mosbach, A. Blöchl, E. Csöregi, R. Solomonias and W. Schumann, 2002b, Redox hydrogel-based bienzyme microelectrodes for amperometric monitoring of L-glutamate, *Electroanalysis* 14, 393–399.
- Miller, J.R., L.T. Calcaterra and G.L. Closs, 1984, Intramolecular long-distance electron transfer in radical anions. The effects of free energy and solvent on the reaction rates, *J. Am. Chem. Soc.* 106, 3047–3049.
- Mirkin, M.V. and B.R. Horrocks, 2000, Electroanalytical measurements using the scanning electrochemical microscope (general review), *Anal. Chim. Acta* 406, 119–146.
- Mirsky, V.M., V. Kulikov, Q.L. Hao and O.S. Wolfbeis, 2004, Multiparameter high throughput characterization of combinatorial chemical microarrays of chemosensitive polymers, *Macromol. Rapid Commun.* 25, 253–258.
- Moser, C.C., J.M. Keske, K. Warncke, R.S. Farid and P.L. Dutton, 1992, Nature of biological electron transfer, *Nature* 355, 796–802.
- Mrksich, M. and G.M. Whitesides, 1995, Patterning self-assembled monolayers using microcontact printing: A new technology for biosensors (general review), *Trends Biotechnol.* 13, 228–235.

- Murakami, Y., K. Yokoyama and E. Tamiya, 1998, Micromachined multifunctional biosensor array, *Ann. NY Acad. Sci.* 864, 544–547.
- Murray, R.W., 1980, Chemically modified electrodes, *Acc. Chem. Res.* 13, 135–141.
- Nagata, R., K. Yokoyama, S.A. Clark and I. Karube, 1995, A glucose sensor fabricated by the screen printing technique, *Biosens. Bioelectron.* 10, 261–267.
- Nakamoto, S., N. Ito, T. Kuriyama and J. Kimura, 1988, A lift-off method for patterning enzyme-immobilized membranes in multi-biosensors, *Sens. Actuat.* 13, 165–172.
- Narvaez, A., E. Dominguez, I. Katakis, E. Katz, K.T. Ranjit, I. Ben-Dov and I. Willner, 1997, Microperoxidase-11-mediated reduction of hemoproteins: Electrocatalyzed reduction of cytochrome *c*, myoglobin and hemoglobin and electrocatalytic reduction of nitrate in the presence of cytochrome-dependent nitrate reductase, *J. Electroanal. Chem.* 430, 227–233.
- Nebling, E., T. Grunwald, J. Albers, P. Schafer and R. Hintsche, 2004, Electrical detection of viral DNA using ultramicroelectrode arrays, *Anal. Chem.* 76, 689–696.
- Newman, J.D. and A.P.F. Turner, 1992, Ink-jet printing for the fabrication of amperometric glucose biosensors, *Anal. Chim. Acta* 262, 13–17.
- Ngounou, B., S. Neugebauer, A. Frodl, S. Reiter and W. Schuhmann, 2004, Combinatorial synthesis of a library of acrylic acid-based polymers and their evaluation as immobilisation matrix for amperometric biosensors, *Electrochim. Acta* 49, 3855–3863.
- Nice, E., J. Layton, L. Fabri, U. Hellman, A. Engstrom, B. Persson and A.W. Burgess, 1993, Mapping of the antibody-binding and receptor-binding domains of granulocyte colony-stimulating factor using an optical biosensor – Comparison with enzyme-linked immunosorbent assay competition studies, *J. Chromatogr.* 646, 159–168.
- Niculescu, M., T. Erichsen, V. Sukharev, Z. Kerenyi, E. Csöregi and W. Schuhmann, 2002, Quinohemoprotein alcohol dehydrogenase-based reagentless amperometric biosensor for ethanol monitoring during wine fermentation, *Anal. Chim. Acta* 463, 39–51.
- Niculescu, M., S. Gaspar, A. Schulte, E. Csöregi and W. Schuhmann, 2004, Visualization of micropatterned complex biosensor sensing chemistries by means of scanning electrochemical microscopy, *Biosens. Bioelectron.* 19, 1175–1184.
- Niki, K., W.R. Hardy, M.G. Hill, H. Li, J.R. Sprinkle, E. Margoliash, K. Fujita, R. Tanimura, N. Nakamura, H. Ohno, J.H. Richards and H.B. Gray, 2003, Coupling to lysine-13 promotes electron tunneling through carboxylate-terminated alkanethiol self-assembled monolayers to cytochrome *c* (letter), *J. Phys. Chem. B* 107, 9947–9949.
- Niwa, O., 1995, Electroanalysis with interdigitated array microelectrodes (general review), *Electroanalysis* 7, 606–613.
- Ohara, T.J., M.S. Vreeke, F. Battaglini and A. Heller, 1993, Bienzyme sensors based on electrically wired peroxidase, *Electroanalysis* 5, 825–831.
- Oubrie, A., 2003, Structure and mechanism of soluble glucose dehydrogenase and other PQQ-dependent enzymes, *BBA-Prot. Proteom.* 1647, 143–151.
- Oyamatsu, D., Y. Hirano, N. Kanaya, Y. Mase, M. Nishizawa and T. Matsue, 2003, Imaging of enzyme activity by scanning electrochemical microscope equipped with a feedback control for substrate-probe distance, *Bioelectrochemistry* 60, 115–121.
- Page, C.C., C.C. Moser, X.X. Chen and P.L. Dutton, 1999, Natural engineering principles of electron tunnelling in biological oxidation–reduction, *Nature* 402, 47–52.
- Page, C.C., C.C. Moser and P.L. Dutton, 2003, Mechanism for electron transfer within and between proteins (review), *Curr. Opin. Chem. Biol.* 7, 551–556.
- Palecek, E., 1960, Oscillographic polarography of highly polymerized deoxyribonucleic acid, *Nature* 188, 656–657.
- Palecek, E., 1988, Adsorptive transfer stripping voltammetry: Determination of nanogram quantities of DNA immobilized at the electrode surface, *Anal. Biochem.* 170, 421–431.
- Panchagnula, V., J. Jeon and A.V. Dobrynin, 2004, Molecular dynamics simulations of electrostatic layer-by-layer self-assembly, *Phys. Rev. Lett* 93(3), 037801.
- Panchagnula, V., C.V. Kumar and J.F. Rusling, 2002, Ultrathin layered myoglobin-polyion films functional and stable at acidic pH values, *J. Am. Chem. Soc.* 124, 12515–12521.

- Paredes, P.A., J. Parellada, V.M. Fernandez, I. Katakis and E. Dominguez, 1997, Amperometric mediated carbon paste biosensor based on D-fructose dehydrogenase for the determination of fructose in food analysis, *Biosens. Bioelectron.* 12, 1233–1243.
- Park, S.-J., T.A. Taton and C.A. Mirkin, 2002, Array-based electrical detection of DNA with nanoparticle probe, *Science* 295, 1503–1506.
- Patolsky, F., A. Lichtenstein and I. Willner, 2001, Electronic transduction of DNA sensing processes on surfaces: Amplification of DNA detection and analysis of single-base mismatches by tagged liposomes, *J. Am. Chem. Soc.* 123, 5194–5205.
- Pershad, H.R., J. Hirst, B. Cochran, B.A.C. Ackrell and F.A. Armstrong, 1999, Voltammetric studies of bidirectional catalytic electron transport in *Escherichia coli* succinate dehydrogenase: Comparison with the enzyme from beef heart mitochondria, *Biochim. Biophys. Acta-Bioenerg.* 1412, 262–272.
- Petrov, E.G., Y.V. Shevchenko, V.I. Teslenko and V. May, 2001, Nonadiabatic donor-acceptor electron transfer mediated by a molecular bridge: A unified theoretical description of the superexchange and hopping mechanism, *J. Chem. Phys.* 115, 7107–7122.
- Pfeiffer, D., F.W. Scheller, C.J. Mcneil and T. Schulmeister, 1995, Cascade-like exponential substrate amplification in enzyme sensors, *Biosens. Bioelectron.* 10, 169–180.
- Pishko, M.V., A.C. Michael and A. Heller, 1991, Amperometric glucose microelectrodes prepared through immobilization of glucose oxidase in redox hydrogels, *Anal. Chem.* 63, 2268–2272.
- Poirier, G.E., 1999, Coverage-dependent phases and phase stability of decanethiol on Au(111), *Langmuir* 15, 1167–1175.
- Ramanavicius, A., K. Habermüller, E. Csöregi, V. Laurinavicius and W. Schuhmann, 1999, Polypyrrole entrapped quinohemoprotein alcohol dehydrogenase. Evidence for direct electron transfer via conducting-polymer chains, *Anal. Chem.* 71, 3581–3586.
- Razumas, V., J. Kazlauskaitė and R. Vidziunaite, 1996, Electrocatalytic reduction of hydrogen peroxide on the microperoxidase-11 modified carbon paste and graphite electrodes, *Bioelectrochem. Bioenerg.* 39, 139–143.
- Razumiene, J., A. Vilkanauskite, V. Gureviciene, V. Laurinavicius, N.V. Roznyatovskaya, Y.V. Ageeva, M.D. Reshetova and A.D. Ryabov, 2003, New bioorganometallic ferrocene derivatives as efficient mediators for glucose and ethanol biosensors based on PQQ-dependent dehydrogenases, *J. Organomet. Chem.* 668, 83–90.
- Reddington, E., A. Sapienza, B. Gurau, R. Viswanathan, S. Sarangapani, E.S. Smotkin and T.E. Mallouk, 1998, Combinatorial electrochemistry: A highly parallel, screening method for discovery of better electrocatalysts, *Science* 280, 1735–1737.
- Reiter, S., K. Eckhard, A. Blöchl and W. Schuhmann, 2001b, Redox modification of proteins using sequential-parallel electrochemistry in microtiter plates, *Analyst* 126, 1912–1918.
- Reiter, S., K. Habermüller and W. Schuhmann, 2001a, A reagentless glucose biosensor based on glucose oxidase entrapped into osmium-complex modified polypyrrole films, *Sens. Actuat. B-Chem.* 79, 150–156.
- Reiter, S., D. Rühlig, B. Ngounou, S. Neugebauer, S. Janiak, A. Vilkanauskite, T. Erichsen and W. Schuhmann, 2004, An electrochemical robotic system for the optimization of amperometric glucose biosensors based on a library of cathodic electrodeposition paints, *Macromol. Rapid Commun.* 25, 348–354.
- Revzin, A.F., K. Sirkar, A. Simonian and M.V. Pishko, 2002, Glucose, lactate, and pyruvate biosensor arrays based on redox polymer/oxidoreductase nanocomposite thin-films deposited on photolithographically patterned gold microelectrodes, *Sens. Actuat. B-Chem.* 81, 359–368.
- Richardson, J.N., S.R. Peck, L.S. Curtin, L.M. Tender, R.H. Terrill, M.T. Carter, R.W. Murray, G.K. Rowe and S.E. Creager, 1995, Electron-transfer kinetics of self-assembled ferrocene octanethiol monolayers on gold and silver electrodes from 115 to 170 k, *J. Phys. Chem.* 99, 766–772.
- Riklin, A., E. Katz, I. Willner, A. Stocker and A.F. Bückmann, 1995, Improving enzyme-electrode contacts by redox modification of cofactors, *Nature* 376, 672–675.

- Rilling, P., T. Walter, R. Pommersheim and W. Vogt, 1997, Encapsulation of cytochrome *c* by multilayer microcapsules. A model for improved enzyme immobilization, *J. Membr. Sci.* 129, 283–287.
- Rinaldi, R., P.P. Pompa, G. Maruccio, A. Biasco, P. Visconti, D. Pisignano, L. Blasi, N. Sgarbi, B. Krebs and R. Cingolani, 2004, Self-assembling of proteins and enzymes at nanoscale for biodevice applications, *IEE Proc. Nanobiotechnol.* 151, 101–108.
- Rohm, I., M. Genrich, W. Collier and U. Bilitewski, 1996, Development of ultraviolet-polymerizable enzyme pastes: Bioprocess applications of screen-printed L-lactate sensors, *Analyst* 121, 877–881.
- Rohm, I., W. Kuennecke and U. Bilitewski, 1995, UV-polymerizable screen-printed enzyme pastes, *Anal. Chem.* 67, 2304–2307.
- Ross, B. and K. Cammann, 1994, Biosensor on the base of polypyrrole modified ultramicroelectrode arrays, *Talanta* 41, 977–983.
- Ruzgas, T., E. Csöregi, J. Emnéus, L. Gorton and G. Marko-Varga, 1996, Peroxidase-modified electrodes – Fundamentals and application (review), *Anal. Chim. Acta* 330, 123–138.
- Ruzgas, T., A. Gaigalas and L. Gorton, 1999, Diffusionless electron transfer of microperoxidase-11 on gold electrodes, *J. Electroanal. Chem.* 468, 123–131.
- Ruzgas, T., L. Gorton, J. Emnéus and G. Marko-Varga, 1995, Kinetic models of horseradish peroxidase action on a graphite electrode, *J. Electroanal. Chem.* 391, 41–49.
- Ryabov, A.D., A.M. Trushkin, L.I. Baksheeva, R.K. Gorbatova, I.V. Kubrakova, V.V. Mozhaev, B.B. Gnedenko and A.V. Levashov, 1992, Chemical attachment of organometallics to proteins in reverse micelles, *Angew. Chem. Int. Ed.* 31, 789–791.
- Ryabova, E.S., V.N. Goral, E. Csöregi, B. Mattiasson and A.D. Ryabov, 1999, Coordinative approach to mediated electron transfer: Ruthenium complexed to native glucose oxidase, *Angew. Chem.* 111, 847–850.
- Sampath, S. and O. Lev, 1996, Renewable, reagentless glucose sensor based on a redox modified enzyme and carbon-silica composite, *Electroanalysis* 8, 1112–1116.
- Sandison, M.E., N. Anicet, A. Glidle and J.M. Cooper, 2002, Optimization of the geometry and porosity of microelectrode arrays for sensor design, *Anal. Chem.* 74, 5717–5725.
- Sangodkar, H., S. Sukeerthi, R.S. Srinivasa, R. Lal and A.Q. Contractor, 1996, A biosensor array based on polyaniline, *Anal. Chem.* 68, 779–783.
- Sapelnikova, S., E. Dock, R. Solna, P. Skladal, T. Ruzgas and J. Emnéus, 2003, Screen-printed multienzyme arrays for use in amperometric batch and flow systems, *Anal. Bioanal. Chem.* 376, 1098–1103.
- Scheller, F.W., R., Renneberg, and F., Schubert, 1988, *Methods in Enzymology*, Vol. 137, *Coupled Enzyme Reactions in Enzyme Electrodes Using Sequence, Amplification, Competition, and Antiinterference Principles*, Academic Press, San Diego, 29–43.
- Scheller, F.W., U. Wollenberger, C. Lei, W. Jin, B. Ge, C. Lehmann, F. Lisdat and V. Fridman, 2002, Bioelectrocatalysis by redox enzymes at modified electrodes (general review), *Rev. Mol. Biotechnol.* 82, 411–424.
- Schlapfer, P., W. Mundt and P. Racine, 1974, Electrochemical measurement of glucose using various electron acceptors, *Clin. Chim. Acta* 57, 283.
- Schmidt, H.-L., F. Gutberlet and W. Schuhmann, 1993, New principles of amperometric enzyme electrodes and of reagentless oxidoreductase biosensors, *Sens. Actuat. B-Chem.* 13–14, 366–371.
- Schmidt, H.-L. and W. Schuhmann, 1996, Reagentless oxidoreductase sensors, *Biosens. Bioelectron.* 11, 127–135.
- Schubert, F., D. Kirstein, K.L. Schröder and F.W. Scheller, 1985, Enzyme electrodes with substrate and coenzyme amplification, *Anal. Chim. Acta* 169, 391–396.
- Schuhmann, W., 1995a, Electron-transfer pathways in amperometric biosensors – Ferrocene-modified enzymes entrapped in conducting-polymer layers, *Biosens. Bioelectron.* 10, 181–193.

- Schuhmann, W., 1995b, Conducting polymer based amperometric enzyme electrodes (review), *Mikrochim. Acta* 121, 1–29.
- Schuhmann, W., 1998, *Immobilised Biomolecules in Analysis. A Practical Approach, Immobilisation Using Electrogenerated Polymers*, Oxford University Press, Oxford, GB, 187–210.
- Schuhmann, W., C. Kranz, J. Huber and H. Wohlschläger, 1993, Conducting polymer-based amperometric enzyme electrodes – Towards the development of miniaturized reagentless biosensors, *Synth. Met.* 61, 31–35.
- Schuhmann, W., C. Kranz, H. Wohlschläger and J. Strohmeier, 1997, Pulse technique for the electrochemical deposition of polymer films on electrode surfaces, *Biosens. Bioelectron.* 12, 1157–1167.
- Schuhmann, W., R. Lammert, M. Hämmerle and H.-L. Schmidt, 1991b, Electrocatalytic properties of polypyrrole in amperometric electrodes, *Biosens. Bioelectron.* 6, 689–697.
- Schuhmann, W., T.J. Ohara, H.-L. Schmidt and A. Heller, 1991a, Electron transfer between glucose oxidase and electrodes via redox mediators bound with flexible chains to the enzyme surface, *J. Am. Chem. Soc.* 113, 1394–1397.
- Schuhmann, W., H. Zimmermann, K. Habermüller and V. Laurinavicius, 2000, Electron-transfer pathways between redox enzymes and electrode surfaces: Reagentless biosensors based on thiol-monolayer-bound and polypyrrole-entrapped enzymes, *Faraday Discuss.* 245–255.
- Senda, M., T. Ikeda, H. Hiasa and K. Miki, 1986, Amperometric biosensors based on a biocatalyst electrode with entrapped mediator, *Anal. Sci.* 2, 501–506.
- Shiku, H., H. Ohya and T. Matsue, 2002, Scanning electrochemical microscopy applied to biological systems. *Encyclopedia of Electrochemistry, Vol. 9, Bioelectrochemistry*, Eds. A.J. Bard, M. Stratmann and G.S. Wilson, Wiley-VCH Verlag GmbH, Weinheim, Chapter 8, pp. 257–275.
- Shimizu, Y. and K. Morita, 1990, Microhole array electrode as a glucose sensor, *Anal. Chem.* 62, 1498.
- Singhal, P. and W.G. Kuhr, 1997, Ultrasensitive voltammetric detection of underivatized oligonucleotides and DNA, *Anal. Chem.* 69, 4828–4832.
- Smalley, J.F., S.W. Feldberg, C.E.D. Chidsey, M.R. Linford, M.D. Newton and Y.P. Liu, 1995, The kinetics of electron-transfer through ferrocene-terminated alkanethiol monolayers on gold, *J. Phys. Chem.* 99, 13141–13149.
- Stigter, E.C.A., G.A.H. De Jong, J.A. Jongejan, H.A. Duine, J.P. Van Der Lugt and W.A.C. Somers, 1997, Electron transfer and stability of a quinohemoprotein alcohol dehydrogenase electrode, *J. Chem. Technol. Biotechnol.* 68, 110–116.
- Stoecker, P.W. and A.M. Yacynych, 1990, Chemically modified electrodes as biosensors, *Select. Electr. Rev.* 12, 137–160.
- Stoica, L., A. Lindgren-sjolander, T. Ruzgas and L. Gorton, 2004, Biosensor based on cellobiose dehydrogenase for detection of catecholamines, *Anal. Chem.* 76, 4690–4696.
- Storhoff, J.J., R. Elghanian, R.C. Mucic, C.A. Mirkin and R.L. Letsinger, 1998, One-pot colorimetric differentiation of polynucleotides with single base imperfections using gold nanoparticle probes, *J. Am. Chem. Soc.* 120, 1959–1964.
- Strike, D.J., N.F. Rooij de and M. Koudelka-Hep, 1995, Electrochemical techniques for the modification of microelectrodes, *Biosens. Bioelectron.* 10, 61–66.
- Strike, D.J., A. van den Berg, N.F. de Rooij and M. Koudelka-Hep, 1994, Spatially controlled on-wafer and on-chip enzyme immobilization using photochemical and electrochemical techniques, *ACS Sym. Ser.* 556, 298–306.
- Subrahmanyam, S., S.A. Piletsky and A.P.F. Turner, 2002, Application of natural receptors in sensors and assays (general review), *Anal. Chem.* 74, 3942–3951.
- Sun, Y.P., H. Buck and T.E. Mallouk, 2001, Combinatorial discovery of alloy electrocatalysts for amperometric glucose sensors, *Anal. Chem.* 73, 1599–1604.

- Takenaka, S., K. Yamashita, M. Takagi, Y. Uto and H. Kondo, 2000, DNA sensing on a DNA probe-modified electrode using ferrocenylnaphthalene diimide as the electrochemically active ligand, *Anal. Chem.* 72, 1334–1341.
- Tang, Z.P., R.F. Louie, J.H. Lee, D.M. Lee, E.E. Miller and G.J. Kost, 2001, Oxygen effects on glucose meter measurements with glucose dehydrogenase- and oxidase-based test strips for point-of-care testing, *Crit. Care Med.* 29, 1062–1070.
- Tarlov, M.J. and E.F. Bowden, 1991, Electron-transfer reaction of cytochrome *c* adsorbed on carboxylic acid terminated alkanethiol monolayer electrodes, *J. Am. Chem. Soc.* 113, 1847–1849.
- Taton, T.A., C.A. Mirkin and R.L. Letsinger, 2000, Scanometric DNA array detection with nanoparticle probes, *Science* 289, 1757–1760.
- Taylor, C., G. Kenausis, I. Katakis and A. Heller, 1995, Wiring of glucose oxidase within a hydrogel made with polyvinyl imidazole complexed with [(Os-4,4'-dimethoxy-2,2'-bipyridine)Cl](+/2+), *J. Electroanal. Chem.* 396, 511–515.
- Thevenot, D.R., K. Toth, R.A. Durst and G.S. Wilson, 2001, Electrochemical biosensors: Recommended definitions and classification, *Biosens. Bioelectron.* 16, 121–131.
- Thorp, H.H., 1998, Cutting out the middleman: DNA biosensors based on electrochemical oxidation, *Trends Biotechnol.* 16, 117–121.
- Toyama, H., F.S. Mathews, O. Adachi and K. Matsushita, 2004, Quinohemoprotein alcohol dehydrogenases: Structure, function, and physiology (review), *Arch. Biochem. Biophys.* 428, 10–21.
- Trojanowicz, M. and T.K.V. Krawczyk, 1995, Electrochemical biosensors based on enzymes immobilized in electropolymerized films (review), *Mikrochim. Acta* 121, 167–181.
- Tsai, W.C. and A.E.G. Cass, 1995, Ferrocene-modified horseradish peroxidase enzyme electrodes – A kinetic study on reactions with hydrogen peroxide and linoleic hydroperoxide, *Analyst* 120, 2249–2254.
- Turcu, F., A. Schulte, G. Hartwich and W. Schuhmann, 2004a, Label-free electrochemical recognition of DNA hybridization by means of modulation of the feedback current in SECM, *Angew. Chem. Int. Ed.* 43, 3482–3485.
- Turcu, F., A. Schulte, G. Hartwich and W. Schuhmann, 2004b, Imaging immobilised ssDNA and detecting DNA hybridisation by means of the repelling mode of scanning electrochemical microscopy (SECM), *Biosens. Bioelectron.* 20, 925–932.
- Umana, M. and J. Waller, 1986, Protein-modified electrodes. The glucose oxidase/polypyrrole system, *Anal. Chem.* 58, 2979–2983.
- Umek, R.M., S.W. Lin, J. Vielmetter, R.H. Terbrueggen, B. Irvine, C.J. Yu, J.F. Kayyem, H. Yowanto, G.F. Blackburn, D.H. Farkas and Y.P. Chen, 2001, Electronic detection of nucleic acids: A versatile platform for molecular diagnostics, *J. Mol. Diagn.* 3, 74–84.
- Umezawa, Y., T. Ozawa and M. Sato, 2002, Methods of analysis for chemicals that promote/disrupt cellular signaling (general review), *Anal. Sci.* 18, 503–516.
- Updike, S.J. and G.P. Hicks, 1967, The enzyme electrode, *Nature* 214, 986–988.
- Vervoort, J., 1991, Electron-transferring proteins (general review), *Curr. Opin. Struct. Biol.* 1, 889–894.
- Vijayakumar, A.R., E. Csöregi, A. Heller and L. Gorton, 1996, Alcohol biosensors based on coupled oxidase-peroxidase systems, *Anal. Chim. Acta* 327, 223–234.
- Wang, J., 1999, Towards genoelectronics: Electrochemical biosensing of DNA hybridization, *Chem. Eur. J.* 5, 1681–1685.
- Wang, J., 2002a, Portable electrochemical systems (general review), *Trends Anal. Chem.* 21, 226–232.
- Wang, J., 2002b, Electrochemical nucleic acid biosensors (review), *Anal. Chim. Acta* 469, 63–71.
- Wang, J. and Q. Chen, 1994, Enzyme microelectrode array strips for glucose and lactate, *Anal. Chem.* 66, 1007–1011.
- Wang, J., M. Jiang and E. Palecek, 1999, Real-time monitoring of enzymatic cleavage of nucleic acids using a quartz crystal microbalance, *Bioelectrochem. Bioenerg.* 48, 477–480.

- Wang, J. and A.B. Kawde, 2002, Amplified label-free electrical detection of DNA hybridization, *Analyst* 127, 383–386.
- Wang, J. and A.N. Kawde, 2001, Pencil-based renewable biosensor for label-free electrochemical detection of DNA hybridization, *Anal. Chim. Acta* 431, 219–224.
- Wang, J. and F. Lu, 1998, Oxygen-rich oxidase enzyme electrodes for operation in oxygen-free solutions, *J. Am. Chem. Soc.* 120, 1048–1050.
- Wang, J., P.V.A. Pamidi and D.S. Park, 1996, Screen-printable sol-gel enzyme-containing carbon inks, *Anal. Chem.* 68, 2705–2708.
- Wang, J., G. Rivas, X. Cai, E. Palecek, P. Nielsen, H. Shiraishi, N. Dontha, D. Luo, C. Parrado, M. Chicharro, P.A.M. Farias, F.S. Valera, D.H. Grant, M. Ozsoz and M.N. Flair, 1997, DNA electrochemical biosensors for environmental monitoring. A review (general review), *Anal. Chim. Acta* 347, 1–8.
- Wang, J., G. Rivas, J.R. Fernandes, J.L.L. Paz, M. Jiang and R. Waymire, 1998, Indicator-free electrochemical DNA hybridization biosensor, *Anal. Chim. Acta* 375, 197–203.
- Wang, J., L.H. Wu, R. Li and J. Sanchez, 1990, Mixed ferrocene-glucose oxidase-carbon-paste electrode for amperometric determination of glucose, *Anal. Chim. Acta* 228, 251–257.
- Wang, J., D.K. Xu, A. Erdem, R. Polsky and M.A. Salazar, 2002, Genomagnetic electrochemical assays of DNA hybridization, *Talanta* 56, 931–938.
- Wang, L.W. and N.F. Hu, 2001, Direct electrochemistry of hemoglobin in layer-by-layer films with poly(vinyl sulfonate) grown on pyrolytic graphite electrodes, *Bioelectrochemistry* 53, 205–212.
- Wei, J.J., H.Y. Liu, K. Niki, E. Margoliash and D.H. Waldeck, 2004, Probing electron tunneling pathways: Electrochemical study of rat heart cytochrome *c* and its mutant on pyridine-terminated SAMs, *J. Phys. Chem. B* 108, 16912–16917.
- Weetall, H.H., 1993, Preparation of immobilized proteins covalently coupled through silane coupling agents to inorganic supports, *Appl. Biochem. Biotechnol.* 41, 157–188.
- White, S.F., and A.P.F., Turner, 1997, *Handbook of Biosensors and Electronic Noses: Medicine, Food and Environment, Part I: Mediated amperometric biosensors*, pp. 227–244. CRC Press Inc., Boca Raton, USA.
- Williams, P.A., V. Fulop, E.F. Garman, N.F.W. Saunders, S.J. Ferguson and J. Hajdu, 1997, Haem-ligand switching during catalysis in crystals of a nitrogen-cycle enzyme, *Nature* 389, 406–412.
- Williams, R.J.P., 1989, Electron transfer in biology (general review), *Mol. Phys.* 68, 1–23.
- Williams, R.J.P., 2003, Metallo-enzyme catalysis, *Chem. Commun.* 1109–1113.
- Willner, I., V. Helegshabtai, R. Blonder, E. Katz, G.L. Tao, A.F. Bückmann and A. Heller, 1996, Electrical wiring of glucose oxidase by reconstitution of fad-modified monolayers assembled onto Au-electrodes, *J. Am. Chem. Soc.* 118, 10321–10322.
- Willner, I., R. Kasher, E. Zahavy and N. Lapidot, 1992, Electron-transfer communication between redox-functionalized polymers and the active center of the enzyme glutathione reductase, *J. Am. Chem. Soc.* 114, 10963–10965.
- Willner, I. and E. Katz, 2000, Redoxproteinschichtwen auf leitenden Trägern – Systeme für bioelektronische Anwendungen, *Angew. Chem.* 112, 1230–1269.
- Willner, I., E. Katz and B. Willner, 1997a, Electrical contact of redox enzyme layers associated with electrodes: Routes to amperometric biosensors (review), *Electroanalysis* 9, 965–977.
- Willner, I., E. Katz, B. Willner, R. Blonder, V. Helegshabtai and A.F. Bückmann, 1997b, Assembly of functionalized monolayers of redox proteins on electrode surfaces: Novel bioelectronic and optobioelectronic systems, *Biosens. Bioelectron.* 12, 337–356.
- Willner, I. and A. Riklin, 1994, Electrical communication between electrodes and NAD(P)(+)-dependent enzymes using pyrroloquinolinequinone-enzyme electrodes in a self-assembled monolayer configuration – Design of a new glass of amperometric biosensors, *Anal. Chem.* 66, 1535–1539.

- Willner, I., A. Riklin, B. Shoham, D. Rivenzon and E. Katz, 1993, Development of novel biosensor enzyme electrodes – Glucose oxidase multilayer arrays immobilized onto self-assembled monolayers electrodes, *Adv. Mater.* 5, 912–915.
- Wink, T., S.J. Vanzuilen, A. Bult and W.P. Vanbennekom, 1997, Self-assembled monolayers for biosensors (review), *Analyst* 122, r43–r50.
- Winkler, J.R., 2000, Electron tunneling pathways in proteins (review), *Curr. Opin. Chem. Biol.* 4, 192–198.
- Wipf, D.O., 2003, Scanning electrochemical microscopy, *Charact. Mater.* 1, 636–652.
- Wittstock, G., 2001, Modification and characterization of artificially patterned enzymatically active surfaces by scanning electrochemical microscopy (general review), *Fresen. J. Anal. Chem.* 370, 303–315.
- Wittstock, G., 2003, Imaging localized reactivities of surfaces by scanning electrochemical microscopy (general review), *Top. Appl. Phys.* 85, 335–364.
- Wittstock, G., T. Wilhelm, S. Bahrs and P. Steinrucke, 2001, SECM feedback imaging of enzymatic activity on agglomerated microbeads, *Electroanalysis* 13, 669–675.
- Wollenberger, U., M. Paeschke and R. Hintsche, 1994, Interdigitated array microelectrodes for the determination of enzyme activities, *Analyst* 119, 1245–1249.
- Wong, S.S. and L.J. Wong, 1992, Chemical crosslinking and the stabilization of proteins and enzyme, *Enzyme Microb. Technol.* 14, 866–874.
- Yamada, M. and M. Seki, 2004, Nanoliter-sized liquid dispenser array for multi-biochemical analysis in microfluidic devices, *Anal. Chem.* 76, 895–899.
- Yamamoto, K., K. Takagi, K. Kano and T. Ikeda, 2001, Bioelectrocatalytic detection of histamine using quinoxaline protein amine dehydrogenase and the native electron acceptor cytochrome *c*-550, *Electroanalysis* 13, 375–379.
- Yanai, H., K. Miki, T. Ikeda and K. Matsushita, 1994, Bioelectrocatalysis by alcohol dehydrogenase from *Acetobacter-ace*ti adsorbed on bare and chemically modified electrodes, *Denki Kagaku* 62, 1247–1248.
- Yang, I.V., P.A. Ropp and H.H. Thorp, 2002, Toward electrochemical resolution of two genes on one electrode: Using 7-deaza analogues of guanine and adenine to prepare PCR products with differential redox activity, *Anal. Chem.* 74, 347–354.
- Yang, I.V. and H.H. Thorp, 2001, Modification of indium tin oxide electrodes with repeat polynucleotides: Electrochemical detection of trinucleotide repeat expansion, *Anal. Chem.* 73, 5316–5322.
- Yang, Q.L., P. Atanasov and E. Wilkins, 1997, A novel amperometric transducer design for needle-type implantable biosensor applications, *Electroanalysis* 9, 1252–1256.
- Yao, T., I. Harada and T. Nakahara, 1995, Enzyme sensors based on a direct electron transfer between graphite electrode and adsorbed horseradish peroxidase, *Anal. Sci.* 11, 685–687.
- Ye, L., I. Katakis, W. Schuhmann, H.-L. Schmidt, J.A. Duine and A. Heller, 1994, Enhancement of the stability of wired quinoprotein glucose-dehydrogenase electrode (review), *ACS. Sym. Ser.* 556, 34–40.
- Yeh, P. and T. Kuwana, 1977, Reversible electrode reaction of cytochrome *c*, *Chem. Lett.* 1145–1148.
- Yu, C.J., Y. Wan, H. Yowanto, J. Li, C. Tao, M.D. James, C.L. Tan, G.F. Blackburn and T.J. Meade, 2001, Electronic detection of single-base mismatches in DNA with ferrocene-modified probes, *J. Am. Chem. Soc.* 123, 11155–11161.
- Yudin, A.K. and T. Sui, 2001, Combinatorial electrochemistry (review), *Curr. Opin. Chem. Biol.* 5, 269–272.
- Zhang, S., G. Wright and Y. Yang, 2000, Materials and techniques for electrochemical biosensor design and construction, *Biosens. Bioelectron.* 15, 273–282.
- Zhang, Y., H.H. Kim and A. Heller, 2003, Enzyme-amplified amperometric detection of 3000 copies of DNA in a 10- μ L droplet at 0.5 fM concentration, *Anal. Chem.* 75, 3267–3269.
- Zhang, Y., H.H. Kim, N. Mano, M. Dequaire and A. Heller, 2002, Simple enzyme-amplified amperometric detection of a 38-base oligonucleotide at 20 pmol L⁻¹ concentration in a 30- μ L droplet, *Anal. Bioanal. Chem.* 374, 1050–1055.

- Zhao, C., J.K. Sinha, C.A. Wijayawardhana and G. Wittstock, 2004, Monitoring β -galactosidase activity by means of scanning electrochemical microscopy, *J. Electroanal. Chem.* 561, 83–91.
- Zhao, C. and G. Wittstock, 2004a, An SECM detection scheme with improved sensitivity and lateral resolution: Detection of galactosidase activity with signal amplification by glucose dehydrogenase, *Angew. Chem. Int. Ed.* 43, 4170–4172.
- Zhao, C.A. and G. Wittstock, 2004b, Scanning electrochemical microscopy of quinoprotein glucose dehydrogenase, *Anal. Chem.* 76, 3145–3154.
- Zimmermann, H., A. Lindgren, W. Schuhmann and L. Gorton, 2000, Anisotropic orientation of horseradish peroxidase by reconstitution on a thiol-modified gold electrode, *Chem. Eur. J.* 6, 592–599.

This page intentionally left blank

Catalytic Hydrogen Evolution at Mercury Electrodes from Solutions of Peptides and Proteins

Michael Heyrovský

*J. Heyrovský Institute of Physical Chemistry, Academy of Sciences of the Czech Republic,
Dolejškova 3, 182 23 Prague, Czech Republic*

Dedicated to the memory of Rudolf Brdička, Miroslav Březina and Pavel Mader

Contents

1. Catalytic reactions in electrochemistry	657
2. Catalytic hydrogen evolution at electrodes	658
2.1. Definition	658
2.2. Non-catalytic hydrogen evolution at mercury electrodes	659
2.3. The catalysts	660
2.4. Mechanism of catalysis	664
2.5. Electrochemical techniques	666
3. Catalysis by peptides and proteins	668
3.1. Introduction	668
3.2. Catalytically active groups	670
3.3. Brdička reaction	670
3.4. Peptides	674
3.5. Proteins	676
3.6. Changes of proteins	679
4. Summary and conclusions	679
List of abbreviations	680
References	680

1. CATALYTIC REACTIONS IN ELECTROCHEMISTRY

Similar to homogeneous chemical electron transfer reactions, in electrode electron transfer, the product of the electrode reaction can be changed back into the primary reagent by an essentially homogeneous volume reaction with a suitable species present in solution. Such a process, the catalytic regeneration, well known and often studied in electrode kinetics, is one type of electrochemical catalytic reactions (Heyrovský and Kůta, 1965, pp. 380–393; Koryta, 1967; Mairanovskii, 1968, pp. 17–26; Guidelli, 1971, pp. 266–273; Tur'yan *et al.*, 1998; Tur'yan, 1994). However, in the heterogeneous electrochemical systems more common, and in practical applications more important, are those electrocatalytic processes, where the electrode reaction itself is accelerated by heterogeneous interaction of the reagent either with the material of the electrode itself or with a catalytically active species, which is either adsorbed at the electrode

surface, or in a mere time-limited contact with it. For specific catalytic activity the working electrodes can have their surfaces specially modified. Various types of such catalytic systems found applications in electroanalytical chemistry (Mark, 1990; Banica and Ion, 2000; Bobrowski and Zarebski, 2000). Technically utilized electrocatalytic processes, e.g., in energy storage and conversion, or in organic electrosynthesis, are hydrogen evolution, oxygen evolution, oxygen reduction, or oxidation of organic molecules (Lipkowski and Ross, 1998; Wieckowski *et al.*, 2003). The International Society of Electrochemistry (ISE) has been organizing since 1983, along with its general congresses, satellite meetings on the ever-growing subject of electrocatalysis; the papers presented at these meetings are published, as a rule, in special issues of *Electrochimica Acta* (1984). The catalytic evolution of hydrogen at electrodes, one of the widely studied electrocatalytic processes, can be catalyzed by a great variety of species, among others, by peptides and proteins; when carried out on small laboratory scale, it can become a useful way for studying physico-chemical properties of the catalysts as well as for their sensitive quantitative determination. That aspect of the general electrochemical reaction of peptides and proteins is the subject of the present chapter.

2. CATALYTIC HYDROGEN EVOLUTION AT ELECTRODES

2.1. Definition

Catalytic hydrogen evolution is an electrochemical phenomenon caused by certain species – the catalysts, in presence of which in solution gaseous hydrogen evolves at a cathode polarized to potentials less negative than in absence of the species. The evolution of hydrogen is produced by cathodic catalytic current, of intensity controlled by concentration of the catalyzing species, and at potential given by kinetic efficiency of the catalyst. The catalytic current thus carries information concerning the quality as well as the quantity of the catalyst. Catalytic hydrogen evolution occurs at cathodes made of materials characterized by definite hydrogen overpotentials – it actually consists in lowering the hydrogen overpotential of the electrode. As mercury has of all metals the highest hydrogen overpotential, the phenomenon of catalytic hydrogen evolution has been most conveniently studied with mercury electrodes (Heyrovský and Kůta, 1965; Mairanovskii, 1968). The convenience is, moreover, augmented by easily attainable high purity of mercury, by its chemical character of noble metal, by the facility of precise reproduction of any kind of mercury electrodes and by homogeneity and isotropic atomic topography of the liquid mercury surface. Various substances, among others also peptides and proteins, act as catalysts of hydrogen evolution at mercury electrodes in the pH range mostly between 6 and 11 (Figure 1) (Brdička, 1933a), and owing to that activity they can be followed and determined, even in high dilution. The advantageous properties, for study of hydrogen overpotential and for practical utilization of its catalytic lowering,

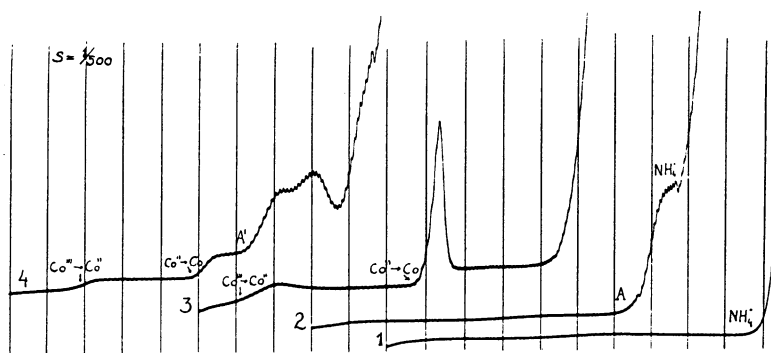


Fig. 1. Polarographic catalytic waves of human serum. Curves: 1 – pure supporting electrolyte, buffer 0.1 M ammonia/ammonium chloride; 2 – the “presodium” catalytic wave, 400 times diluted human serum (A) in buffer 0.1 M ammonia/ammonium chloride; 3 – 2-step reduction of Co(III), 1 mM $Co(NH_3)_6Cl_3$ in buffer 0.1 M ammonia/ammonium chloride; 4 – the catalytic double-wave in Brdička solution, 1 mM $Co(NH_3)_6Cl_3$ + 400 times diluted human serum (A) in buffer 0.1 M ammonia/ammonium chloride; recorded from 0 V vs mercury pool, 200 mV/abscissa. From Brdička (1933a), with permission of Coll. Czech. Chem. Commun.

have been partly ascertained also with amalgam electrodes (Yosypchuk and Novotný, 2002).

2.2. Non-catalytic hydrogen evolution at mercury electrodes

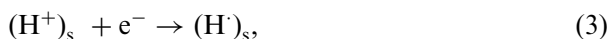
Most of the elementary steps of the electrochemical hydrogen evolution take place at the electrode surface and in interaction with it – the whole process is a typical heterogeneous reaction (Gerischer and Mehl, 1955). On the negatively charged mercury surface the protons, dissociated from the acidic component BH of the solution (BH in alkaline solutions can also be water molecule),



get dehydrated and adsorb in the inner part of the double layer (symbolized by subscript s) in close contact with the metal



When the electrode potential is being made more negative, the protons undergo gradual charge-transfer change into hydrogen atoms bound to the electrode surface by sharing with it their single electrons. At sufficiently negative potential, the charge transfer to hydrogen is accomplished



and two neighboring surface hydrogen atoms become free to combine with hydrogen molecules, which are not attached to the electrode, and as such leave

the surface



According to conditions of electrolysis, the last stage of hydrogen evolution can also occur, thus



In either way, the net reaction is



The half-wave potential of reduction of hydrated protons from aqueous solutions of strong acids is -1.60 V vs SCE, visibly starts gaseous hydrogen evolving in bubbles already at potentials more negative than -1.5 V (SCE). Electroreduction of hydrogen ions from solutions of weak acids or other proton donors occurs at more negative potentials, from aqueous alkaline solutions hydrogen ions are reduced beyond the reduction of alkali metal cations (Heyrovský and Kůta, 1965). If some catalyst of hydrogen evolution comes into contact with the negatively polarized electrode surface and initiates in some way a catalytic path of hydrogen evolution, molecular hydrogen starts evolving on the electrode catalytically at a potential less negative than normal.

2.3. The catalysts

The catalysts of hydrogen evolution are chemical entities able to transfer protons from a donor in the solution to the electrode surface (Stackelberg and Fassbender, 1958; Stackelberg *et al.*, 1958). They can either be (1) species present in solution, by themselves electroinactive in a wide potential range, which come into short or long contact with surface of negatively polarized electrode and thereby accelerate the mechanism of hydrogen evolution (cf. Figure 1, curve 2) or (2) products, stable or unstable, of electroreduction of certain ions, molecules or transition metal complexes, which act catalytically when generated at the electrode surface (cf. Figure 1, curve 4).

To the first category (1), belong, apart from some inorganic colloids, prevalently organic molecules or ions containing nitrogen atom with a free electron pair, alone or together with thiolic sulfur; high molecular ones are, in general, more active. The catalytic currents produced by these catalysts occur as a rule at fairly negative potentials; in the case of catalysis by proteins they have been called for historical reasons “presodium currents” (coined by Brdička, 1936, p. 366), as in course of continuously increasing negative electrode polarization in a physiological solution, they appeared before the currents due to electroreduction of sodium ions (Herles and Vančura, 1932; Heyrovský and Babička, 1930).

In the second category (2), three cases of catalysts are to be distinguished: (a) metals characterized by low hydrogen overpotential, such as elements of the platinum group, of limited solubility in mercury – on electrodeposition from their ions they form small islets at the electrode surface, which become centers of hydrogen evolution; (b) organic molecules or ions of the first category but not originally existing in solution and formed as intermediates or as final products at the electrode surface in course of electrode reaction (Figure 2) (Heyrovský *et al.*, 1971); (c) reduced forms, stable or not, of various transition metal complexes with particular ligands, which may be low- or high-molecular, see Figure 1, curve 4 (cf. Mader, 1971, p. 1062). The complexes may have to be synthesized separately or they are formed spontaneously on addition of the particular cations and ligands into the solution; among their reduction products can be either a low-valent catalytically active complex or a metallic deposit of hydrogen overpotential lower than mercury, which acts as catalysts sub (2a). According to conditions, the catalytic currents due to catalysts (2) can appear on the polarization curve within a wide range of potentials. The currents due to catalysts (1) and (2c) usually appear in two different potential ranges on one curve (Figure 3) (Jurka, 1939); with some catalysts of category (1) and (2c) it can happen by changing experimental conditions that the catalytic currents, originally occurring in two different potential regions, merge into one (Calusaru, 1972). Some compounds yield three separate catalytic hydrogen waves (Figure 4) (Ruttkay-Nedecký and Anderleová, 1967; Mader, 1971). Application of hanging mercury

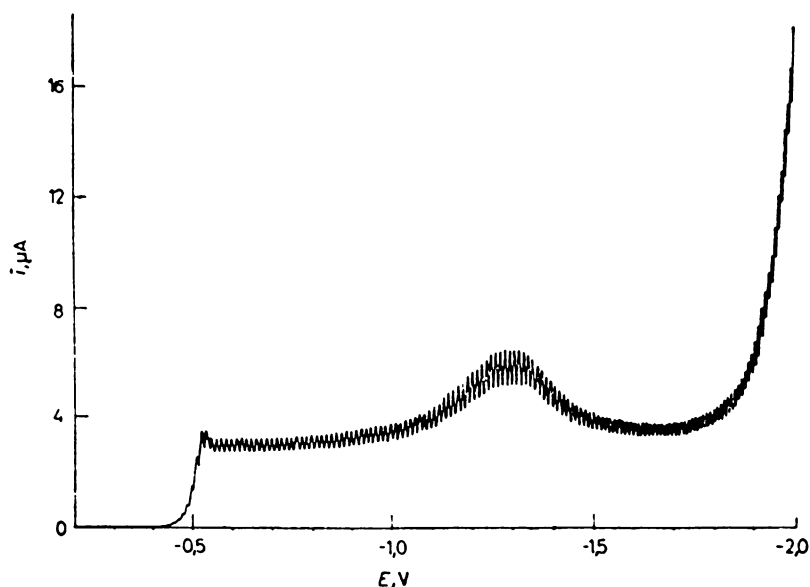


Fig. 2. Polarographic hydrogen evolution catalyzed by a reduction intermediate. Solution of 1 mM *p*-aminoazobenzene in phosphate buffer of pH 7.5, 30% ethanol, in course of its 4-electron reduction at the electrode appears *p*-aminohydrazobenzene in a limited potential range as short-lived intermediate, which catalyzes hydrogen evolution; recorded from 0 V vs SCE. From Heyrovský *et al.* (1971), with permission of Coll. Czech. Chem. Commun.

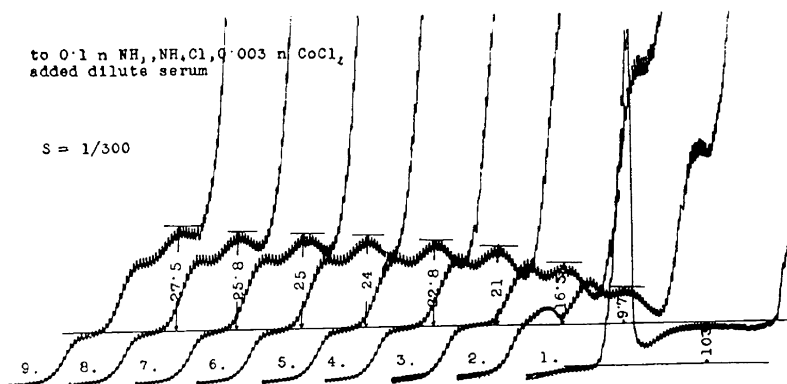


Fig. 3. Electrocatalytic hydrogen evolution in two different potential regions on one polarographic curve. Curve 1 – 1.5 mM CoCl_2 in buffer 0.1 M ammonia/ammonium chloride; curves 2–9 gradual addition of dilute blood serum. Curves 2 and 3 show both catalytic processes: the double-wave due to catalysis of cobalt–protein complex, and the more negative pre-sodium catalysis; recorded from -0.8 V vs Hg pool. From Jurka (1939), with permission of Coll. Czech. Chem. Commun.

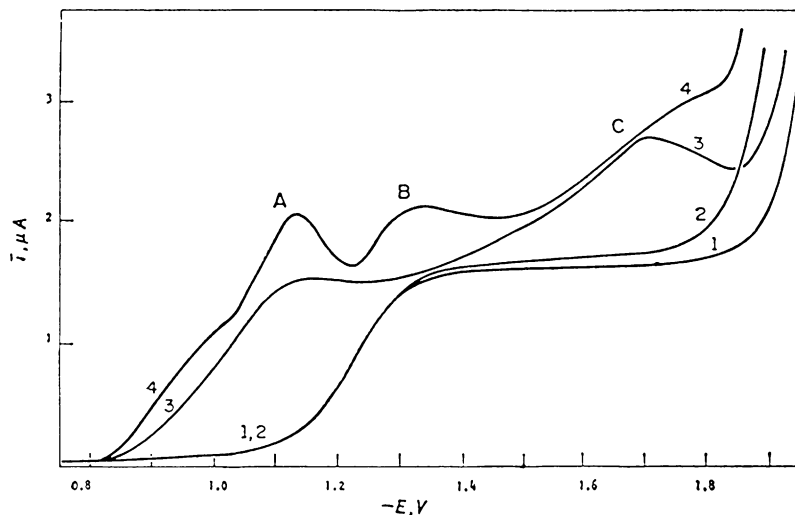


Fig. 4. Three different catalytic maxima (A, B, C) due to one compound. Polarographic curves of 0.4 mM CoCl_2 in: 1 – 0.06 M borax, pH 9.2; 2 – borate buffer, pH 7.7; 3 – 0.06 M borax + 0.01 mM thioglycolic acid; 4 – borate buffer pH 7.7 + 0.1 mM thioglycolic acid; recorded from -0.75 V vs SCE. From Mader (1971), with permission of Coll. Czech. Chem. Commun.

drop electrode to a study of catalytic system well known in polarography, introduced another hydrogen catalytic evolution reaction in “peak P”, occurring at potentials around -1.2 V (SCE); here hydrogen evolves on solid “active” cobalt, electrodeposited at about -1.0 V (SCE) (Figure 5) (Anzenbacher and

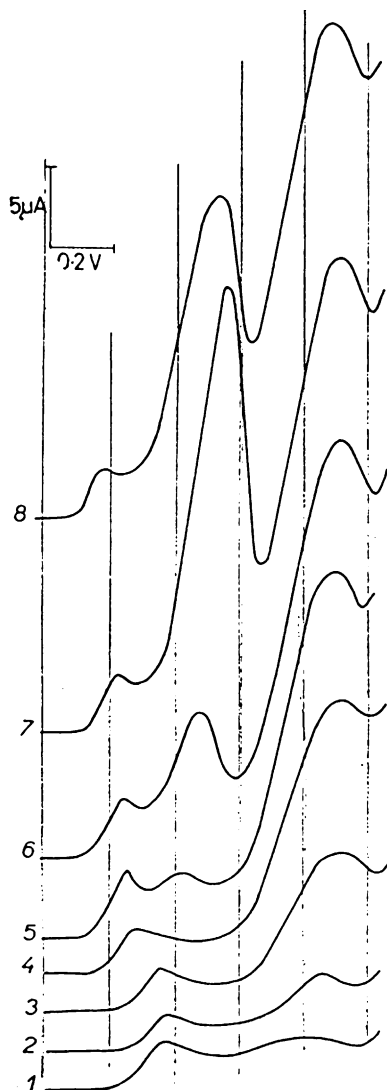


Fig. 5. Catalytic peak "P" obtained in Brdička solution with HMDE. Voltammetric curves of 1 mM CoCl_2 in buffer 0.1 M ammonia/ammonium chloride + cysteine: 1 – 0.5 μM ; 2 – 1 μM ; 3 – 5 μM ; 4 – 10 μM ; 5 – 20 μM ; 6 – 30 μM ; 7 – 50 μM ; 8 – 0.1 mM; recorded from -0.8 V vs SCE at scan rate 6.7 mV/s. The zero current for each curve shifted upwards along the ordinate. From Anzenbacher and Kalous (1972), with permission of Coll. Czech. Chem. Commun.

Kalous, 1972, 1973; Kadleček *et al.*, 1975). The different kinds of catalytic hydrogen currents can be distinguished, according to the mechanism of their origin, by their different dependence on temperature (Kolthoff and Kihara, 1980).

2.4. Mechanism of catalysis

On the microscopic solid metallic surfaces of catalysts deposited on mercury sub (**2a**) the mechanism of electrolytic hydrogen evolution differs from that schematically symbolized by equations (1)–(6), as the surface structure of each metal on molecular level is different. For mercury surface, the mechanism of catalysis by catalysts of group (**1**) and (**2b, c**) can be symbolized as follows. The catalyst R, which is a slightly weaker base than B^- , reacts invariably in its protonated form



the acid RH^+ is then slightly stronger acid than BH, and the electroreduction of proton from RH^+



occurs at a potential less negative than the proton reduction from BH.

According to conditions, the hydrogen evolution occurs either by reaction (4), or by



The deprotonated catalyst R is then reprotonated by the excess of BH



The net reaction of the catalytic process – either in the sequence $2 \times (1) + 2 \times (8) + 2 \times (9) + (4)$, or $(1) + (8) + (9) + (10) + (11) + (12)$, is again (7), the reduction of the acidic component of the solution.

As mentioned above, the catalyst has to contact the electrode surface – for the category (**1**) and (**2b, c**) it means that it has to come sufficiently close to the surface to allow reactions (9) and/or (10) to proceed. With many catalysts this condition is fulfilled when they are formed at the electrode in adsorbed state (Schmidt and Swofford, 1979; Leibson *et al.*, 1989); especially with large molecules or ions this adsorption has to take place with favorable orientation of the catalytically active site for all the elementary reaction steps to easily occur (Paleček, 1986). On the other hand, strong adsorption may lead to high coverage of the electrode surface and cause hindrance of the catalytic reaction. Some sections of biomacromolecules have prevalingly hydrophobic, others prevalingly hydrophilic characters; the hydrophobic parts, oriented toward the mercury surface, are apt to adsorption, and in that way also prone to catalytic activity. At any rate, the dependence of catalytic current on concentration of catalyst (Figure 6) (Brdička, 1936) (cf. Figure 3) follows the course of Langmuir adsorption isotherm (Brdička, 1947); of that curve only the initial part can be approximated by linear dependence. Catalyst adsorption is hence an important factor in catalysis (Kuznetsov, 1971; Kolthoff *et al.*, 1978); beside other aspects,

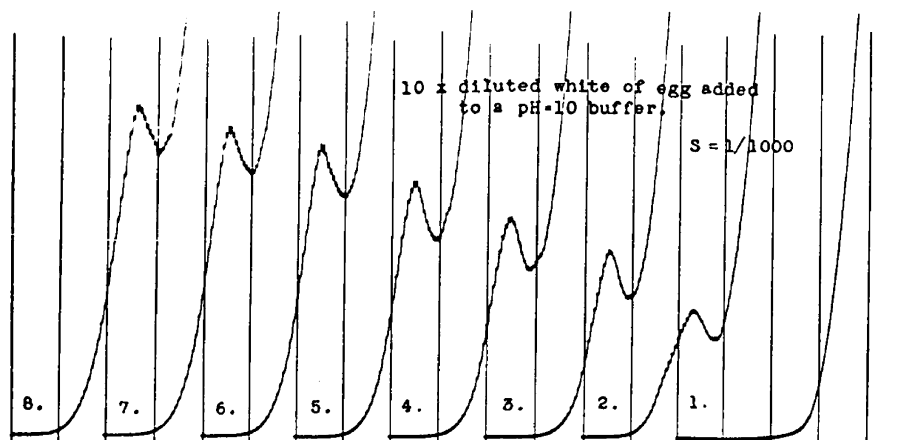


Fig. 6. Dependence of polarographic “presodium” catalytic wave on concentration of protein. The white of egg diluted 10 times by physiological solution was added by 0.1 mL to 10 mL of buffer boric acid/carbonate of pH 10; curves recorded from -1.4V vs Hg pool, 200 mV/abscissa . From Brdička (1936), with permission of Coll. Czech. Chem. Commun.

it can also be the cause of streaming of the solution in the vicinity of the electrode, that sometimes accompanies catalytic current. Sudden change of adsorption brings about sudden change of surface tension of mercury, that stirs the mercury surface together with the adjacent solution, and enhances transport of the electroactive species toward the electrode surface thereby increasing the current (Stackelberg and Fassbender, 1958; Březina and Kůtová, 1965).

Electrocatalysis of hydrogen evolution is based on proton relay by the catalyst from solution toward electrode – higher acidity of the solution leads to higher catalytic current (Figure 7) (Knobloch, 1947). The effect of catalysis is thus strongly dependent on pH of the solution, according to the pK_A value of the given catalyst (Millar, 1953b); as supporting electrolytes are therefore used various buffers. The “presodium” catalytic currents measured in buffers of one pH value are higher in ammonia buffers than in borate buffers, which in turn are higher than in tris buffers (Kolthoff *et al.*, 1975). Some buffer components have the tendency to adsorb at the electrode, which may affect the heterogeneous catalytic reaction – this should be borne in mind while selecting the buffer. Besides, with respect to the state of the electrode surface and of the electrode double layer (Mairanovskii and Frumkin, 1963), all other components of the solution and their concentrations as well as temperature, presence of oxygen, rate of potential scan, etc., play an important role in changing, in positive or negative sense, the heterogeneous reactivity of a given catalytic system. Addition of calcium chloride to the solutions of protein catalysts, e.g., markedly increases the “presodium” currents (Kolthoff *et al.*, 1975, 1978). The catalytic activity is hence an individual property of each catalyst, widely variable by experimental conditions. A common characteristic property of all currents due to catalytic evolution of hydrogen is their dependence on the buffering capacity of the supporting solution – a 10-fold increase of concentration of the

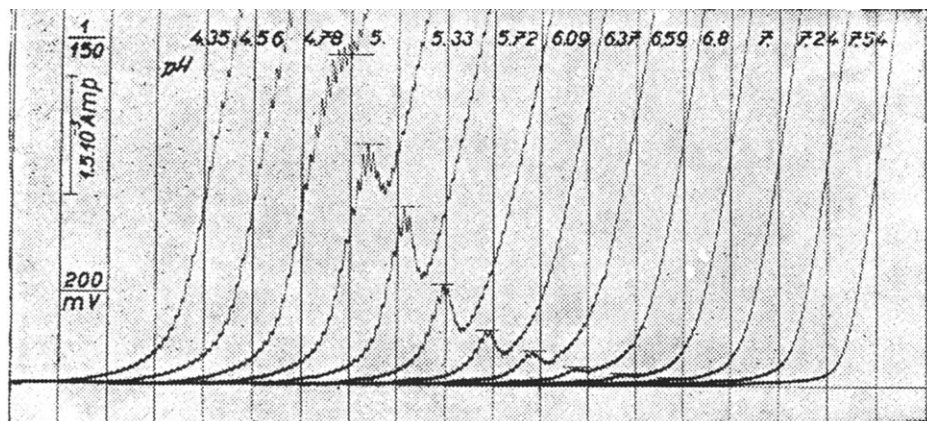


Fig. 7. Dependence of polarographic catalytic current on pH of the solution. Polarographic curves of catalytic hydrogen evolution currents of $50\ \mu\text{M}$ nicotinic acid amide in buffer solutions of pH varied from 7.54 to 4.35; recorded from $-1.0\ \text{V}$ vs SCE. From Knobloch (1947), with permission of Coll. Czech. Chem. Commun.

buffer results in about 10-fold increase of the catalytic current, and vice versa – a dilution leads to current decrease (Figure 8) (Knobloch, 1947).

2.5. Electrochemical techniques

Electrocatalytic reactions of hydrogen evolution can be followed by means of various electrochemical techniques. With dropping mercury electrode (DME) the usual polarographic methods are applied: apart from the common “mean current – potential” curves also the “instantaneous current – time” curves on single drops have been used (Kůtová and Březina, 1966; Mader, 1971). Besides d.c. polarography also a.c. polarography is often applied – preferably with distinction of phase of the measured current with respect to the polarizing voltage; when the out-of-phase current is measured (Brabec, 1985), the method, also called tensammetry, serves for the study of adsorption of the catalyst. For the same purpose the electrocapillary curves are often measured (Stackelberg and Fassbender, 1958; Kolthoff and Mader, 1969). Square-wave polarography is also used, but mainly pulse polarography – normal or differential (Paleček and Pechan, 1971). Some instruments enable the users to study the catalytic hydrogen evolution by means of static mercury drop electrode (SMDE), (Senda *et al.*, 1976; Yamaguchi *et al.*, 1986). With dropping electrodes the shape of the catalytic curves depends strongly on the drop-time (Figure 9) (Kůtová and Březina, 1966). The time factor is the main source of differences between polarographic and voltammetric curves of catalytic systems recorded with identical solutions (Kolthoff and Kihara, 1979a; Heyrovský, 2000).

With hanging mercury drop electrode (HMDE) the methods analogous to polarography are common: d.c. voltammetry (Figure 10) (Březina, 1959) and

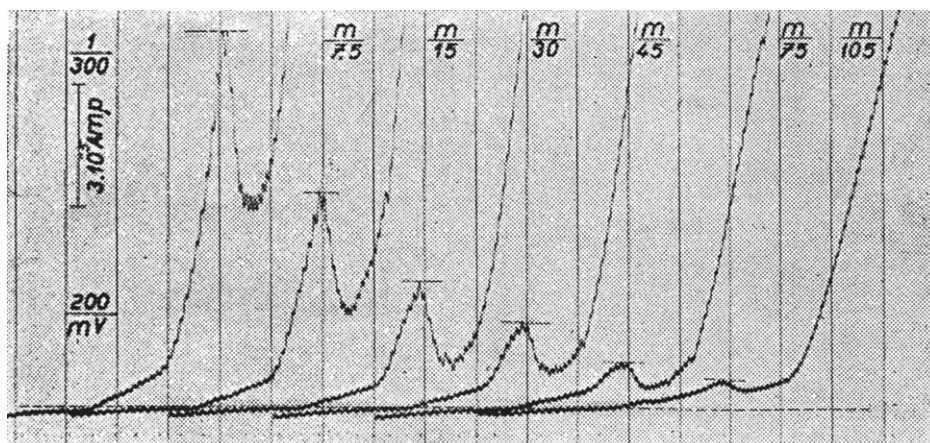


Fig. 8. Dependence of polarographic catalytic current on buffer capacity of the solution. Polarographic curves of catalytic hydrogen evolution currents of 1 mM nicotinic acid amide recorded in gradually diluted phosphate buffer of pH 7.0, dilution by 1 mM aqueous solution of nicotinic acid amide in proportions indicated on each curve, so that the concentration of catalyst remains unchanged; recorded from -1.0 V vs SCE. From Knobloch (1947), with permission of Coll. Czech. Chem. Commun.

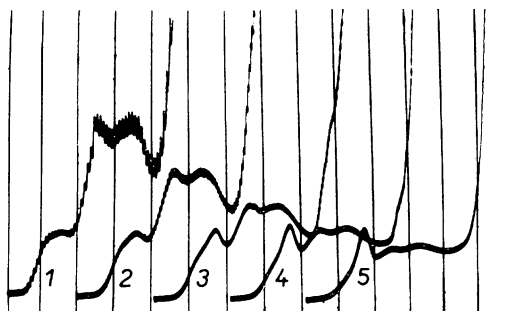


Fig. 9. Dependence of the shape of polarographic catalytic curves on drop-time. Solution of 0.008% γ -globulin + 1 mM $\text{Co}(\text{NH}_3)_6\text{Cl}_3$ in 0.1 M buffer ammonia/ammonium chloride; drop-time: 1 – 2.75 s; 2 – 1.7 s; 3 – 1.0 s; 4 – 0.55 s; 5 – 0.31 s; curves recorded from -0.8 V vs SCE, 200 mV/abscissa. From Kůtová and Březina (1966), with permission of Coll. Czech. Chem. Commun.

a.c. voltammetry (Kuznetsov *et al.*, 1988), voltammetric tensammetry, square wave-, normal- and differential-pulse voltammetry (Wang, 1994). Many of these techniques can be applied with the use of mercury film electrode (Wang, 1985) or with solid amalgam electrodes (Yosypchuk and Novotný, 2002). In voltammetry, in general, it must be borne in mind that the shape of the catalytic curve varies with the rate of potential scan: with slow scan rate the catalysts generated in a slow process can become active, with fast scan rate the catalytically active short-lived intermediates can affect the shape of the curve.

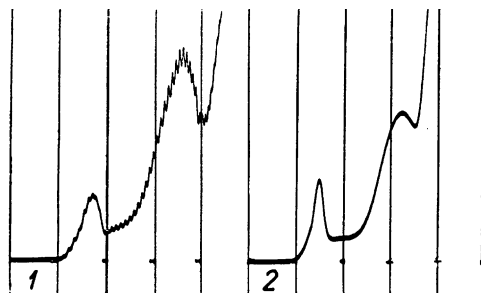


Fig. 10. Comparison of polarographic (DME) and voltammetric (HMDE) curve of catalytic current in Brdička solution. Solution of $5\ \mu\text{M}$ cystine with $1\ \text{mM}$ CoCl_2 in $0.1\ \text{M}$ buffer ammonia/ammonium chloride, recorded from $-0.6\ \text{V}$ vs SCE, $300\ \text{mV/abscissa}$, scan rate in both cases equal, $5\ \text{mV/s}$; curves: 1 – polarographic; 2 – voltammetric. From Březina (1959), with permission of Coll. Czech. Chem. Commun.

For highly sensitive analytical determinations the methods of cathodic stripping or adsorptive stripping voltammetry (Wang, 1985) are used, in which the initial phase of measurement consists in accumulation of the catalyst at the stationary electrode surface under a suitable constant potential. The method of adsorptive transfer stripping voltammetry (AdTSV) (Paleček and Postbieglová, 1986) allows transferring biomacromolecules, strongly adsorbed on the surface of a stationary electrode, from minute volume of one solution, after rinsing, to another supporting solution, for further study or determination.

The stationary mercury electrodes, in addition, offer another possibility: in the method of constant current derivative stripping chronopotentiometry (or chronopotentiometric stripping analysis, CPSA) they are polarized by current, and their potential, or, in practice, the reciprocal of derivative of their potential by time, is followed as a function of their potential.

In this method, the catalytic evolution of hydrogen, analogous to the “presodium current”, appears on the $(dE/dt)^{-1}-f(E)$ curve in the form of a sensitive, well-developed signal, the so-called “peak H” (Tomschik *et al.*, 1998).

3. CATALYSIS BY PEPTIDES AND PROTEINS

3.1. Introduction

Peptides and proteins can cause catalytic evolution of hydrogen on mercury electrodes as catalysts of both categories (1) and (2c), provided they contain catalytically active groups, or form catalytically active complexes with appropriate cations. Although the first experience with catalytic evolution of hydrogen on mercury electrodes was gained with the “presodium” current, the great majority of results in research and in practical applications of electrochemical activity of peptides and proteins have been based so far on hydrogen evolution catalyzed by their complexes with cobalt ions. Only the renewed successful

attempts to catalyze hydrogen evolution by complexes of metals other than cobalt and the recent discoveries, that CPAS method can yield the highly sensitive “peak H”, based on catalytic hydrogen evolution in absence of cobalt, and that catalytic hydrogen evolution occurs also on solid amalgam electrodes (Figure 11), have spurred new development of the specific field of peptide and protein electrochemistry. At present, the basically inexpensive electrochemical apparatus offers very sensitive methods for study and analysis of peptides and proteins, and, as the scientific knowledge in the field of electrocatalysis of hydrogen evolution has been so far more or less one-sided, the subject is now again wide open to fundamental research as well as to many-sided applications.

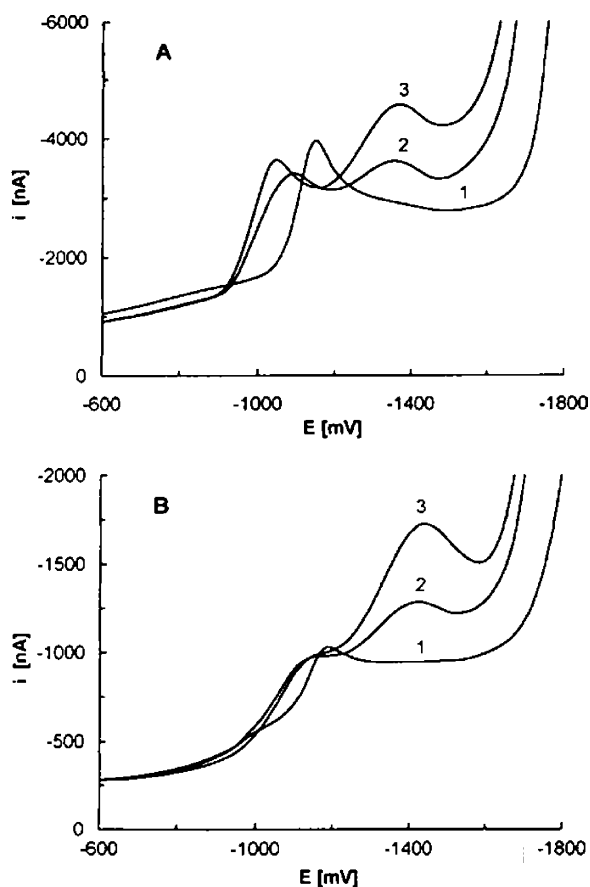


Fig. 11. Voltammetric catalytic curves on mercury and on solid amalgam electrodes. (A) Comparison of protein-catalyzed evolution of hydrogen on HMDE and (B) on mercury meniscus modified silver solid amalgam electrode. DCV, supporting electrolyte (SE) – 10 mL, 1 mM CoCl_2 in 50 mM borate buffer, pH 8.6; curves: (A) 1 – SE; 2 – SE + 0.05 mL: blood plasma (diluted 1:500); 3 – SE + 0.1 mL blood plasma; (B) 1 – SE; 2 – SE + 0.01 mL blood plasma; 3 – SE + 0.02 mL blood plasma; scan rate 10 mV/s. From B. Yosypchuk and M. Heyrovský, unpublished results.

3.2. Catalytically active groups

The active groups responsible for catalytic hydrogen evolution are the same in peptides as in proteins. The main difference between these two classes of compounds is in their size and basic conformation, for the catalytic activity it means, above all, in their adsorption properties. The proteins, due to their size and structure, tend to be adsorbable more strongly and in different ways than peptides, and hence their catalytic reactions are, on an average, more prominent. However, complete coverage of the electrode surface, bringing about the limit of concentration dependence of the catalytic current, is usually attained at lower concentrations by proteins than by peptides.

In the absence of transition metal cations in solution, the centers catalytically active in producing “presodium current” or “peak H” in weakly alkaline solutions are nitrogen atoms bearing free electron pairs (not valid for nitrogens in peptide bonds) (Millar, 1953a), whereby alkylated nitrogens tend to be more efficient, especially when they are parts of aromatic systems (Stackelberg *et al.*, 1958). The free electron pair on nitrogen atom gets protonated by the acid component of the solution, and the protonated nitrogen atom is attracted by the negatively charged electrode surface, to which the proton is ultimately transferred. Other groups, like $-SH$, $-OH$ or $-COOH$, in the molecule, may have, according to their degree of dissociation, a secondary effect on the catalytic reaction (Březina and Gultjaj, 1963), e.g., by affecting the orientation or conformation of the catalyst in contact with the electrode surface, or by assisting in the proton transfer, but normally they cannot initiate appreciable catalytic reaction in absence of the nitrogen group. Low-molecular thioacids without nitrogen, like thioglycolic, thiosalicylic or 3-mercaptopropionic acid, produce but small catalytic currents at relatively high concentrations and in solutions of increased ionic strength – catalytically active is here exceptionally the sole thiolic group, and the negative charge on the dissociated carboxyl is screened by cations of the supporting electrolyte (Mader, 1971).

3.3. Brdička reaction

Transition metal cations, which form complexes with peptides and proteins, appear as important components of efficient catalysts of hydrogen evolution at mercury electrodes (Dykhal *et al.*, 2001); catalytically active are usually short-lived reduction products of the complexes. Most thoroughly investigated in this respect are the ions of trivalent and divalent cobalt, usually in ammonia buffer solutions, in what has been known as Brdička reaction (Brdička, 1933a, b, c). Later it was ascertained, that besides ammonia any other buffer of pH around 9 can be used (Kalous, 1956; Kolthoff *et al.*, 1968); however, the catalytic currents in buffers of equal pH value show certain specific differences.

Cobalt ions readily form complexes with cysteine and with other molecules containing thiolic groups. Apart from the $-SH$ groups, also the nitrogen atoms contained in the ligands take part in formation of the catalytically active

complexes with cobalt (Zikán and Kalous, 1966). If a compound such as EDTA, which binds cobalt ions more strongly than the $-SH$ groups of the protein, is added to the solution, the hydrogen catalysis is suppressed (Figure 12) (Chmelař and Nosek, 1959). It was found that the catalytic activity increases with increasing stability constants of the cobalt complexes with the thiols (Březina and Gultjaj, 1963; Kadleček *et al.*, 1978). The catalytic current of hydrogen evolution appears in the potential region where the complexes of both, cobaltic and cobaltous, ions are completely reduced, and hence their catalytic activity is mutually comparable, with only minor differences. Similarly, the molecules containing accessible disulfidic group, get it reduced to two thiolic groups at potentials less negative than those where the catalysis of hydrogen evolution begins, and so disulfides are twice more efficient catalysts than thiols. It has been assumed, that the actual catalytically active species is the short-lived, zero-valent cobalt complex with the thiol ligands, formed as the primary product of electrode reaction (Shinagawa *et al.*, 1962; Chmelař *et al.*, 1963, Heyrovský and Kůta, 1965); however, that assumption need not be generally valid (Mairanovskii, 1987).

The cathodic current due to catalytic reaction of the reduced cystine complex with cobalt ions is about 500 times higher than the cathodic current due to diffusion-controlled two-electron reduction of the disulfidic group of cystine of the same concentration, but without cobalt (Brdička, 1933a). While cystine and cysteine yield catalytic current with one maximum in Brdička Co(II) solution, the typical shape of the protein response is catalytic “double wave”, a curve with two maxima, in Co(II) as well as in Co(III) solution; however, the exact shape of the catalytic curve of proteins varies according to experimental conditions (Kolthoff *et al.*, 1974). By decrease of temperature, by addition of

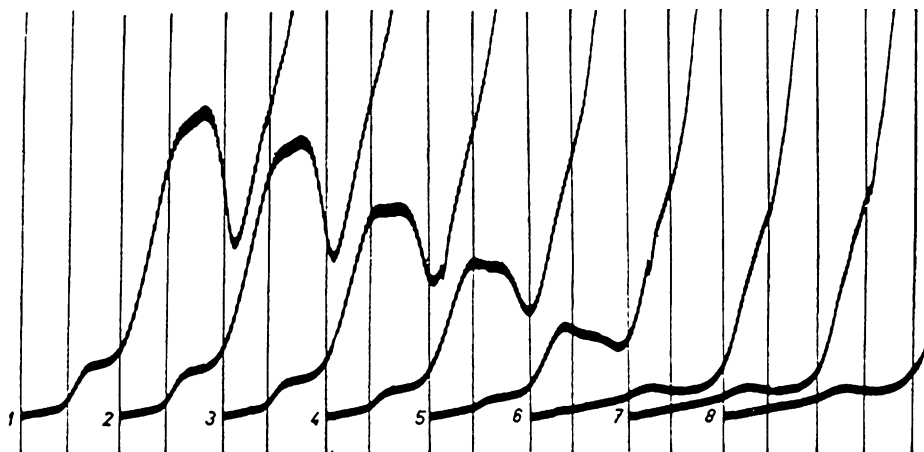


Fig. 12. Effect of strong complexing agent on Brdička polarographic reaction. To 10 mL of 1 mM $CoCl_2$ solution in buffer 1 M ammonia/0.1 M ammonium chloride containing 100 times diluted blood serum (curve 1) gradually added EDTA to concentration first 0.2 mM (curve 2) till 2 mM (curve 8); curves recorded from -1.0 V vs SCE, 200 mV/abscissa. From Chmelař and Nosek (1959), with permission of Coll. Czech. Chem. Commun.

surfactants or by increase of ammonia concentration, the double wave changes into a single maximum (Figure 13) (Marha, 1957; Lamprecht and Katzmeier, 1961; Alexandrov *et al.*, 1963). The occurrence of the two maxima in the double wave has been tentatively explained either (a) by catalytic action of different amino acids in the protein molecule (Müller, 1955), (b) by different tertiary structure of proteins (Iwanow, 1961), (c) by two different cobalt complexes of the protein (Mairanovskii and Mairanovskaia, 1961) or (d) by the protein catalyst acting first in adsorbed and then in desorbed state (Berg, 1964, 1966; cf. Mader and Veselá, 1977). In general, adsorption of the protein at the electrode plays an important role in the mechanism of Brdička catalytic reaction (Senda *et al.*, 1976; Kolthoff *et al.*, 1978). In the high-molecular proteins, the cobalt-containing catalytically active groups must be localized near the surface of the molecule, accessible to the electrode process (Kalous, 1971; Kuznetsov *et al.*, 1988). The occurrence of the double wave on the curves of the Brdička catalytic reaction of proteins poses the practical problem of how to determine the wave height (Figure 14) (Lewitová and Kalous, 1974).

Brdička reaction is hence a specific catalytic reaction of peptides and proteins, which have the $-SH$ and/or $-S-S-$ groups in their structure. The essential role of $-SH$ in the reaction is beyond doubt: carboxymethylation of the sulfhydryl group by iodoacetate leads to a complete loss of the catalytic activity of cysteine (Brdička, 1938); on the other hand, a chemical introduction of thiol groups into catalytically inactive gelatin makes this protein catalytically active (Brdička *et al.*, 1966). In a series of proteins tested by Brdička reaction the height of the catalytic double wave increases according to their cystine/cysteine content: pepsin < bovine plasma albumin < chymotrypsin < insulin < trypsin (Millar, 1953a); for establishing a strict dependence of catalytic activity on the number of $-SH/-S-S-$ groups, the accessibility to the electrode surface of the disulfidic groups "buried" in the protein structure has to be taken into account (Kalous, 1971).

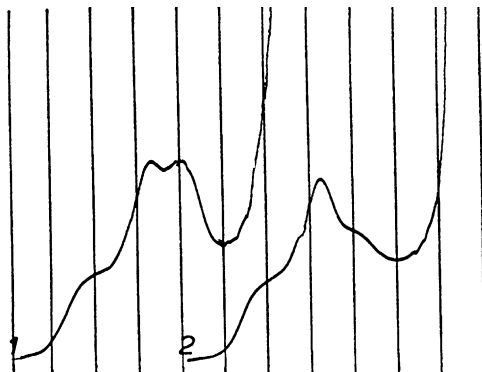


Fig. 13. Effect of surfactant on the Brdička polarographic double wave. Polarographic curves of 5 mL 1 mM $\text{Co}(\text{NH}_3)_6\text{Cl}_3$ in buffer 0.1 M ammonia/ammonium chloride + 0.75 mg serum albumin (curve 1), + 0.5 mM sodium oleate (curve 2); curves recorded from -0.95 V vs SCE, 200 mV/abscissa, Smoler capillary. From Marha (1957), with permission of Coll. Czech. Chem. Commun.

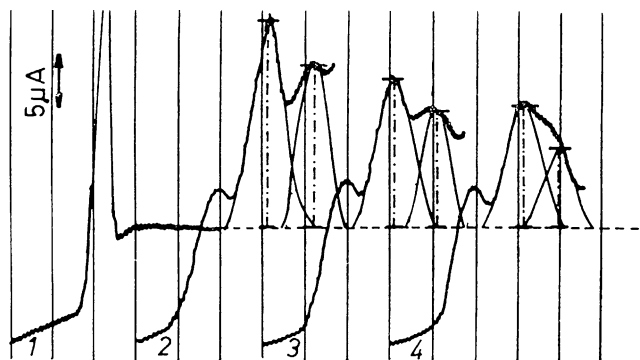


Fig. 14. Example of how to measure polarographic catalytic waves. Curves of 1 mM CoCl_2 in buffer 0.1 M ammonia/ammonium chloride (curve 1); + 60 μM lysozyme (curve 2); like curve 1 + 80 μM ribonuclease A (curve 3); like curve 1 + 80 μM α -chymotrypsin (curve 4). As in spectrophotometry, full shape of double wave supposed to be composed of two symmetrical maxima. Curves recorded from -0.8 V vs SCE, 200 mV/abscissa. From Lewitová and Kalous (1974), with permission of Coll. Czech. Chem. Commun.

On basis of rich experimental experience, a tentative complex scheme of the mechanism of Brdička reaction was suggested (Mader *et al.*, 1982). Theoretical formulation of an equation for polarographic curve of Brdička catalytic current was attempted first for low-molecular catalysts (Calusaru, 1966a, b); a theory of Brdička catalytic current considering surface concentration of adsorbed proteins was later developed for a simplified model, and verified experimentally at the potential of -1.40 V vs SCE, where hydrogen evolution is presumably catalyzed by adsorbed zero-valent protein complex of cobalt (Senda *et al.*, 1982).

The Brdička reaction between cobalt ions and $-\text{SH}$ group is not the only way how catalytic evolution of hydrogen can be generated on mercury electrodes. Some organic thiocompounds, not containing thiolic or disulfidic groups, are Brdička-active, the dithio- more so than the monothio- (Zuman and Kuik, 1958, 1959). In the high potential iron-sulfur proteins are neither free $-\text{SH}$ groups nor S-S bonds, and still in Brdička solution they provide catalytic current of hydrogen evolution (Feinberg and Lau, 1980). Imidazole and some of its derivatives are the rare cases of organic molecules not containing sulfur, which give catalytic Brdička reaction (Gudbjarnason, 1969). The presence of histidine besides the $-\text{SH}$ and $-\text{S-S}$ -groups in the protein molecule supports its catalytic activity (Lewitová and Kalous, 1974; cf. Gudbjarnason, 1969). If in the Brdička solution cobalt is used in the form of its tris-ethylenediamine complex, the catalytic wave of proteins has only one maximum, and its properties are slightly different from the common standard (Ito, 1959, 1965). In heme-containing proteins like cytochrome *c* or hemoglobin, the catalytic activity in Brdička reaction is partly carried by the heme group (Ikeda *et al.*, 1980a,b; Kinoshita *et al.*, 1980). Similar to the cobalt-induced catalytic currents, though weaker, are currents produced in solutions of sulfur-containing peptides or proteins, on addition of divalent nickel; also qualitatively the catalytic nickel effects differ to some extent from those of cobalt (Paleček, 1956; Březina, 1960; Calusaru, 1967;

Kuik, 1971). Attempts to substitute cobalt in Brdička solution by ions of divalent copper, zinc or manganese, do not lead to catalytic hydrogen evolution (Paleček, 1956; Senda *et al.*, 1976).

Catalytic electrode reactions of serum proteins, more specific and more sensitive (though more complicated) than the Brdička type, can be produced by ethylenediamine complexes of trivalent rhodium (Alexander *et al.*, 1977).

3.4. Peptides

The “presodium” catalytic effect of simplest peptides (dipeptides, tripeptides) based on cysteine, in absence of transition metal cations in the solution, consists mainly in a shift of the current due to reduction of the supporting solution, by several tens of millivolts toward positive potentials. The extent of the shift is individual for each peptide and depends on the size and concentration of the peptide, on the solution pH and on the type of the buffer. The tripeptide molecules at higher concentrations yield a separate catalytic “wave” at the foot of the shifted current – that is obviously the consequence of stronger adsorption of the larger peptides at the electrode surface (Figure 15) (Mader *et al.*, 2001). The “wave” changes more or less into the shape of a peak when recorded with the differential pulse methods (DPP or DPV), or with the chronopotentiometric method. Already with these simple catalysts the variability of their reactivity according to experimental conditions is clearly expressed (Dorčák and Šestáková, 2004). Much more pronounced difference and dependence on experimental conditions in catalytic “presodium” hydrogen evolution was dem-

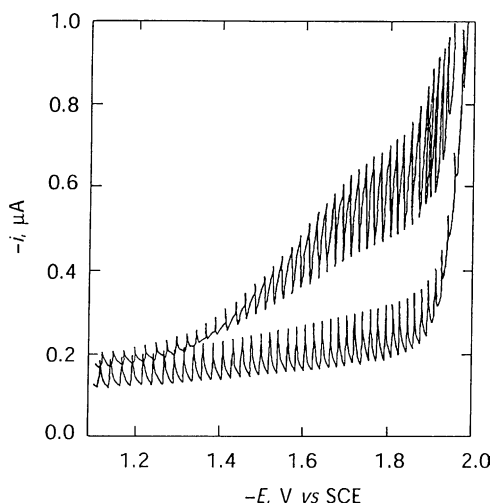


Fig. 15. Polarographic “presodium” wave of peptide, separated out at the foot of shifted catalytic current. Polarographic curves of borate buffer, pH 10.4 (lower curve), and of the same solution containing 0.8 mM reduced glutathione (upper curve). From Mader *et al.* (2001), with permission of Coll. Czech. Chem. Commun.

onstrated in a group of 10 nonapeptides, synthetic analogs of oxytocin and vasopressin (Figure 16) (Mader *et al.*, 1988). While solutions of vasopressin derivatives yielded at micromolar concentration considerable catalytic maxima, the maxima of the derivatives of oxytocin were less, and the carba-analogs of oxytocin gave practically no catalytic current. With solutions of vasopressin was observed for the first time the catalytic “peak H”, by the method of constant current chronopotentiometric stripping analysis (CPSA), allowing determination of vasopressin in nanomolar concentrations; that peak is considerably more sensitive signal than the catalytic current obtained by the voltammetric methods (Tomschik *et al.*, 1998).

As both, oxytocin and vasopressin, contain cystine, they both produce catalytic hydrogen evolution at mercury electrodes in cobalt-containing solutions, after their disulfidic group gets reduced at the electrode (Sunahara *et al.*, 1960), and this reaction has been repeatedly practically utilized (e.g., Bartík *et al.*, 1971). Similarly, the Brdička reaction was used for determining peptide-like compounds in urine of patients suffering from burns (Šafránková and Březina, 1962).

An important group of linear, cysteine-containing oligopeptides of the net formula $(\gamma\text{-Glu-Cys})_n\text{-Gly}$, where $n = 2 \rightarrow 11$, are known as phytochelatins

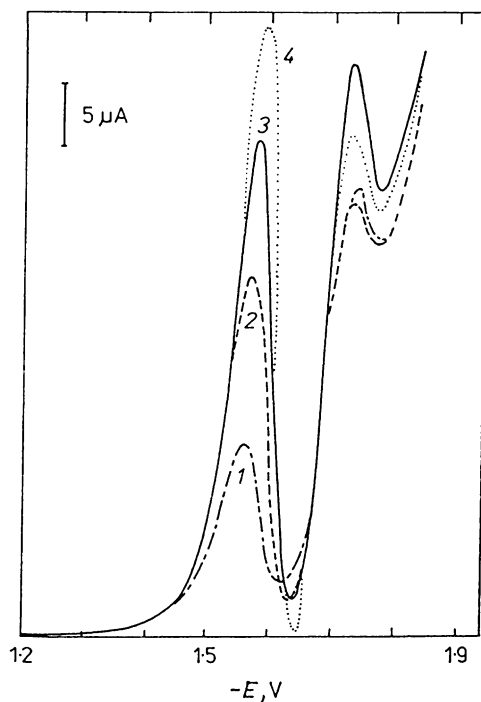


Fig. 16. Differential pulse polarographic curves of “presodium” catalytic current of oxytocin derivative. [2-*O*-methyl-tyrosine] oxytocin in 0.06 M borax, pH 9.2; concentrations of peptide in μM: 1 – 25; 2 – 50; 3 – 75; 4 – 100; E vs SCE. From Mader *et al.* (1988), with permission of Coll. Czech. Chem. Commun.

(PC); they are molecules carrying out heavy-metal detoxification in plants. The PCs represent low-molecular members of a large system of polypeptides called metallothioneins (MTs). The main family of metallothioneins consists of polypeptide chains containing 61 amino acids of which 20 are cysteines, and their function in nature is heavy-metal detoxification and metal metabolism in animals (Stillman, 1995); the smaller PCs are known as plant MTs (Kotrba *et al.*, 1999). The chemical structure of MTs (and PCs) makes them efficient catalysts of hydrogen evolution at mercury electrodes (Dorčák and Šestáková, 2004). Responding to the high number of cysteines in the molecules the Brdička reaction renders good services in analysis of MTs (Raspor and Pavicic, 1996; Raspor *et al.*, 2001). Recently, it was discovered that the CPSA “peak H” allows even more sensitive determination of metallothioneins without cobalt ions, down to femtomolar level (Tomschik *et al.*, 2000; Kizek *et al.*, 2001). A comparably high sensitivity can be reached by catalytic hydrogen evolution when complexes of MTs with cisplatin are subjected to square wave cathodic stripping voltammetry (El Hourch *et al.*, 2003).

The catalytic evolution of hydrogen by insulin, a high-molecular peptide (or a low-molecular protein, M_w 5730), containing three disulfidic groups of which two are accessible to electroreduction (Stankovich and Bard, 1977), has been often measured by Brdička reaction (Tropp, 1938; Kanner and Reed, 1939; Kalous, 1956; Lamprecht and Katzmeier, 1961; Zikán and Kalous, 1966, 1967; Kalous, 1971; Lewitová and Kalous, 1974).

3.5. Proteins

Great majority of papers (well over 500), published so far on polarographic/voltammetric reactions of proteins, deal with the catalytic evolution of hydrogen in presence of cobalt ions. That kind of analytical determinations, when based on anodic stripping voltammetry, allow reaching concentrations down to 10^{-11} M; a special procedure, utilizing the so-called “active cobalt”, electrodeposited at about -1.0 V vs SCE (Anzenbacher and Kalous, 1973), goes even to 10^{-12} M (Kolthoff and Kihara, 1977, 1979a, b). However, such determinations are limited to sulfur-containing proteins. The recently introduced even more sensitive method based on the CPSA “peak H” (Tomschik *et al.*, 1998) is not thus limited, and the topic is now open to further research. In the study of electrochemical behavior of avidin and streptavidin, e.g., it came out that while both proteins yielded the catalytic “peak H”, only avidin gave the typical catalytic Brdička double wave, a consequence that, unlike streptavidin, it contains cysteine in the molecule (Havran *et al.*, 2004).

By far, most of the papers published on Brdička reaction since its introduction in 1933 have been dealing with its application in medical diagnostics (Brdička, 1937a, b, c, 1947, 1958; Březina and Zuman, 1958; Brdička *et al.*, 1965; Homolka, 1971). It was initiated by the discovery that cancerous blood serum has a lowered ability to activate proteolytic enzymes by $-SH$ groups contained in blood (Waldschmidt-Leitz *et al.*, 1937). Brdička has shown

(Brdička, 1937c) that the difference between polarographic catalytic activity due to the -SH contents of normal and cancerous serum is increased after alkaline denaturation, and further he found (Brdička, 1939) that after deproteination by sulfosalicylic acid (and filtration), the cancerous serum yields a higher catalytic wave than the normal one. This, the so-called “filtrate reaction” (Figure 17) (Kalous and Valenta, 1957), became the most frequently used diagnostic application of polarography in the 1950–1960s (Kočent, 1958). Besides carcinomatic diseases, the filtrate test of blood serum (or of blood plasma, Müller, 1955) gave an increase of catalytic current during inflammations, tuberculosis, pneumonia, ulcers or necrotic processes; on the other hand, in case of liver trouble the Brdička double wave is decreased when compared with normal serum (Frank *et al.*, 1956; Brdička, 1958; Brdička *et al.*, 1965). Electrophoretic analysis of the substances producing the catalytic “double wave” (Kalous, 1954, 1958) indicated that the main components are at least three proteinic compounds of the character of mucoproteins or glycoproteins (Winzler, 1955); these could be separated by paper electrophoresis and further individually investigated (Kalous, 1959; Homolka, 1971). Used in tens of thousands of clinical tests in global scale, the Brdička reaction proved to be a simple and reliable, though nonspecific, indication of cancer, unable to catch the disease in its initial stage; however, it served well in following the state of patient, especially during post-operational stage (Balle-Helaers, 1956; Irmischer, 1958; Müller, 1963; Homolka,

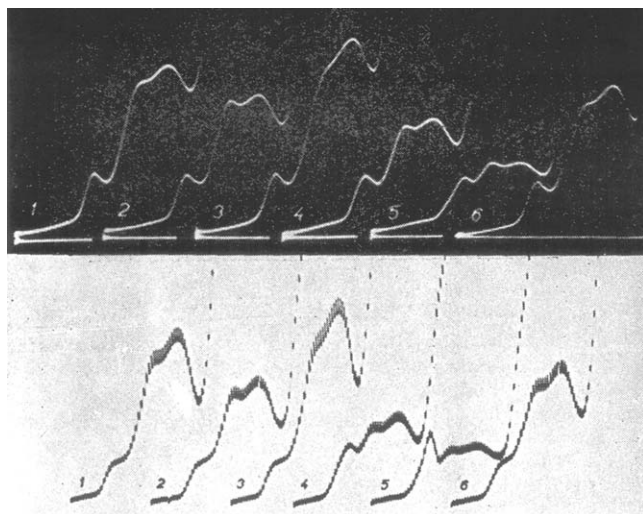


Fig. 17. Brdička “filtrate test” as diagnostic tool. Comparison of polarographic (lower curves) with voltammetric (higher curves, recorded by means of oscilloscope) records of identical solutions of the Brdička filtrate test with blood sera of six patients preliminarily diagnosed as: 1 – status febrilis; 2 – tumor hepatis susp.; 3 – ca. ventriculi susp.; 4 – normal; 5 – cirrhosis hepatis; 6 – arteriosclerosis. Preparation of filtrate: 0.4 mL serum + 1 mL, 0.1 M KOH, after 45 min + 1 mL 20% sulfosalicylic acid, after 10 min filtration. Solution for electrolysis: 0.5 mL filtrate + 5 mL, 1 mM $\text{Co}(\text{NH}_3)_6\text{Cl}_3$ in 0.1 M NH_4Cl , 1 M NH_4OH . Curves recorded from -0.8 V vs Hg pool, in voltammetry scan rate -310 mV/s. From Kalous and Valenta (1957), with permission of Coll. Czech. Chem. Commun..

1971; Puranen and Hokkanen, 1971; Siegel *et al.*, 1976). Polarographic methods were used in the study of protein content of body liquids other than blood (gastric juice – Okajima and Sasai, 1953; sperm – Buruiana and Pavlu, 1957; sweat – Jirka and Kotas, 1957; urine – Březina, 1963; saliva – Sanada and Mishiro, 1966; review – Homolka, 1971; amniotic fluid – Caselli, 1980; vaginal secretions – Velázquez *et al.*, 1988).

Apart from human medicine the Brdička reaction found many other applications, e.g., in virology for testing purity of virus- from non-virus-proteins (Figure 18) (Rutt kay-Nedecký, 1957, 1963; Rutt kay-Nedecký and Paleček, 1980), in molecular biology for determining proteins in presence of nucleic acids (Berg, 1957; Vorlíčková and Paleček, 1973), in microbiology for tracing proteinase inhibitors of microbial origin (Kano *et al.*, 1981), in general physiology for comparing animal hemoglobin with human hemoglobin (Kuik and Krasowski, 1987; Kuik, 1997), in marine zoology for research of proteins contained in aquatic animals (Kikuchi *et al.*, 1959), in research of nutrition for measuring protein content in various kinds of milk (Nakanishi and Itoh, 1965). Heights of the Brdička waves of native serum proteins were correlated with radiation sensitivity of different animal species (Csagoly, 1959). Changes of mutual proportion of the first to the second maximum in the Brdička double-wave under different conditions were used in study of tertiary structure of proteins and enzymes (Iwanow and Rachlejeva, 1964). In the Brdička reaction with nickel, an analogy was found with the hydrogenase-catalyzed hydrogen bioproduction (Banica, 1991). For applications of Brdička reaction see also Sequaris (1992) or Brabec *et al.* (1996).

A sensitive detection of –SH and –S-S-groups in various organic compounds was achieved by combining high-performance liquid chromatography with differential pulse polarographic measurement of the Brdička catalytic current in a flow-through cell (Qian *et al.*, 1990).

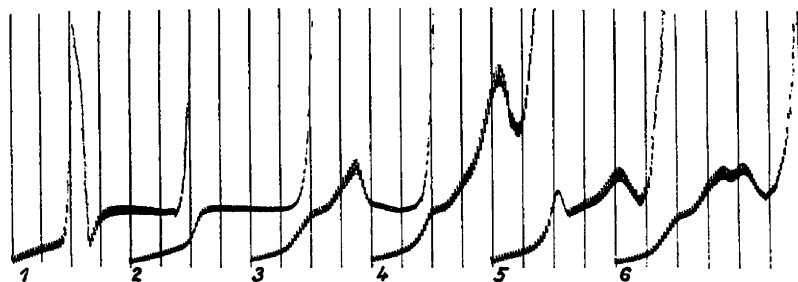


Fig. 18. Utilization of Brdička reaction in virology. Comparison of polarographic curves of Tobacco Mosaic Virus (TMV) with non-virus protein and their mixture. Solution 1 mM $\text{Co}(\text{NH}_3)_6\text{Cl}_3$ in buffer 0.1 M ammonia/ammonium chloride, pH 9.5, containing varied proportion of non-virus protein to tobacco mosaic virus (TMV) protein in percentage (P); $T = 0^\circ\text{C}$; curves recorded from -0.8 V vs Hg pool. Curves: 1 – $P = 1.00$; 2 – $P = 0.75$; 3 – $P = 0.50$; 4 – $P = 0.25$; 5 – $P = 0.10$; 6 – $P = 0.00$; concentration of TMV protein 5.2 mg/mL, initial concentration of non-virus protein 0.052 mg/mL. From Rutt kay-Nedecký (1963), with permission of Coll. Czech. Chem. Commun.

The reaction of catalytic evolution of hydrogen on mercury electrodes provides open possibilities for further development of sensitive methods of peptide and protein detection and determination. An alkaline solution of guanidine hydrochloride containing a low concentration of cobaltous chloride, e.g., allows determination of human or bovine serum albumin in the concentration range $0.005\text{--}20\text{ mg L}^{-1}$ by derivative linear scan polarography (Luo *et al.*, 2003).

3.6. Changes of proteins

Various changes occurring with proteins in solutions are indicated by simultaneous changes of catalytic currents. Denaturation and proteolytic cleavage of sulfur-containing proteins were followed by the Brdička reaction (Brdička and Klumpar, 1937). In course of the denaturation process the thiolic and disulfidic groups originally hidden inside the globular proteins come to the surface of the macromolecules and can react with cobalt ions and/or with the electrode surface, which results in an increase of catalytic current. The enzymatic cleavage of proteins leads to formation in solution of higher number of catalytically active fractions, which have higher diffusion coefficients than the original protein and hence reach the electrode faster, the result being again an increase of catalytic current. By means of Brdička reaction the process of salting-out of proteins can be conveniently followed (Kalous and Štokr, 1955). Polarographic catalytic currents were also used in a study of proteolytic action of trypsin on crystalline bovine albumin in phosphate buffer containing divalent cobalt; the resulting degradation products were studied, after separation by a sulfosalicylic filtrate, in trivalent cobalt buffer solution (Müller and Yamanouchi, 1963). The well-known reaction between avidin and biotin can be followed by a decrease of the catalytic Brdička peak of avidin on addition of biotin (Havran *et al.*, 2004). Changes of the chronopotentiometric “peak H” indicate early stage of aggregation of α -synuclein, which is an objective symptom of incipient Parkinson disease (Masařík *et al.*, 2004).

4. SUMMARY AND CONCLUSIONS

The catalytic hydrogen evolution on mercury electrodes, used from the 1930s for study and analysis of peptides and proteins, was for several decades dominated by the Brdička reaction, in solutions of cobalt ions. Although that reaction provided and still provides useful services in many directions, its complex mechanism has not been fully elucidated – further research on this problem can bring important results for up-to-date applications. Besides this old topic, the general reaction of hydrogen catalysis offers a vast field of other research possibilities: by changing the catalyzing complex, the composition of supporting solutions and of experimental conditions, specific and sensitive electrochemical reactions can be found for various kinds of peptides and proteins – some preliminary results mentioned above indicate that the way in that direction is open.

Another aspect is the search for new types and new materials for electrodes – the solid amalgam electrodes, e.g., maintaining the important advantages of mercury electrodes, can be used in special electrochemical sensors for specific needs of protein sensitive and rapid control or determination. A promising trend in electrocatalytic ways of following peptides or proteins is the introduction of CPSA method, offering the very sensitive and specific “H peak”, which is a theme for a thorough systematic research. Distinct from optical methods, e.g., the methods based on electrolytic reactions provide information on heterogeneous reactivity of the studied species, which is essential in biochemical systems. Electrochemistry, compared with other branches of physical chemistry, has further the advantage of low-priced equipment, which is another factor for the belief that the electrochemical approach will maintain its significant place in biochemical and biophysical studies in general and in studies of peptides and proteins in particular.

LIST OF ABBREVIATIONS

AdTSV	adsorptive transfer stripping voltammetry
BH	acidic component of solution
BSA	bovine serum albumin
CPSA	chronopotentiometric stripping analysis
Cys	cysteinyl
DCV	direct current voltammetry
DME	dropping mercury electrode
DPP	differential pulse polarography
DPV	differential pulse voltammetry
Glu	glutamyl
Gly	glycyl
HMDE	hanging mercury drop electrode
HSA	human serum albumin
MT	metallothionein
NPP	normal pulse polarography
NPV	normal pulse voltammetry
PC	phytochelatin
R	catalyst
SCE	saturated calomel electrode
SMDE	static mercury drop electrode

REFERENCES

- Alexander, P.W., R. Hoh and L.E. Smythe, 1977, Polarographic determination of total serum protein, *J. Electroanal. Chem.* 81, 151.
- Alexandrov, B., M. Březina and V. Kalous, 1963, Polarographische katalytische Stufe des Serumalbumins in Kobalt(II)- und Kobalt(III)-Lösungen, *Coll. Czech. Chem. Commun.* 28, 210.

- Anzenbacher, P. and V. Kalous, 1972, Catalytic polarographic double wave of cysteine on a hanging mercury drop electrode, *Coll. Czech. Chem. Commun.* 37, 3209.
- Anzenbacher, P. and V. Kalous, 1973, Polarographic investigation of the system Co(II)-thiol with respect to anodic dissolution of deposited cobalt, *Coll. Czech. Chem. Commun.* 38, 2418.
- Balle-Helaers, E., 1956, Recherches expérimentales sur la double vague de Brdicka, *Ann. Biol. Clin. (Paris)* 14, 257.
- Banica, F.G., 1991, Catalytic hydrogen evolution on the mercury electrode in the presence of nickel-aminothiols complexes. A tentative model process of hydrogenase-catalysed hydrogen bioproduction, *Bull. Soc. Chim. Fr.* 128, 697.
- Banica, F.G. and A. Ion, 2000, Electrocatalysis-based kinetic determinations. *Encyclopedia of Analytical Chemistry* Ed. R. A. Meyers, p.11115. Wiley, Chichester.
- Bartík, M., M. Teleha, V. Čunderlíková and K. Zwick, 1971, Polarographic study of the inactivation of posterior pituitary hormones by serum enzymes in pregnant and non-pregnant women, *Endocrinol. Exp.* 5, 143.
- Berg, H., 1957, Polarographische Untersuchungen an Nucleinsäuren und Nucleasen. I. Mitt. Polarographischer Nachweis von Proteinen neben Nucleinsäuren, *Biochem. Zeitschr.* 329, 274.
- Berg, H., 1964, Ueber die Ursache der polarographischen Protein-Doppelwelle nach Brdicka, *Monatsber. Deutsch. Akad. Wiss. Berlin* 6, 785.
- Berg, H., 1966, Proteindesorption als Ursache der Brdicka-Proteindoppelwelle, *Abhandl. Deutsch. Akad. Wiss. Berlin, Kl. Medizin* Nr. 4, S.479.
- Bobrowski, A. and J. Zarebski, 2000, Catalytic systems in adsorptive stripping voltammetry, *Electroanalysis* 12, 1177.
- Brabec, V., 1985, Polarography of cytochrome *c* in ammoniacal buffers containing cobalt ions, The effect of the protein conformation, *Gen. Physiol. Biophys.* 4, 609.
- Brabec, V., V. Vetterl and O. Vrana, 1996, *Electroanalysis of biomacromolecules, Experimental Techniques in Bioelectrochemistry*, Vol. 3, Eds. V. Brabec, D. Walz and G. Milazzo, Birghäuser Verlag, Basel, 287.
- Brdicka, R., 1933a, Polarographic studies with the dropping mercury kathode. Part XXXI. A new test for proteins in the presence of cobalt salts in ammoniacal solutions of ammonium chloride, *Coll. Czech. Chem. Commun.* 5, 112.
- Brdicka, R., 1933b, Polarographic studies with the dropping mercury kathode. Part XXXII. Activation of hydrogen in sulphhydryl group of some thio-acids in cobalt salt solutions, *Coll. Czech. Chem. Commun.* 5, 148.
- Brdicka, R., 1933c, Polarographic studies with the dropping mercury kathode. Part XXXIII. The microdetermination of cysteine and cystine in the hydrolysates of proteins, and the course of the protein decomposition, *Coll. Czech. Chem. Commun.* 5, 238.
- Brdicka, R., 1936, Polarographic studies with the dropping mercury kathode. Part LXI. The effect of buffer solutions on the reaction of proteins, *Coll. Czech. Chem. Commun.* 8, 366.
- Brdicka, R., 1937a, The application of the polarographic effect of proteins in cancer diagnosis, *Bull. Int. Acad. Sci. Boheme* 38, 17.
- Brdicka, R., 1937b, Application of the polarographic effect of proteins in cancer diagnosis, *Nature* 139, 330.
- Brdicka, R., 1937c, Polarographic investigations in serological cancer diagnosis, *Nature* 139, 1020.
- Brdicka, R., 1938, Recherches polarographiques sur les protéines, *J. Chim. Phys.* 35, 89.
- Brdicka, R., 1939, Zur Frage nach der Natur der polarographisch feststellbaren Serumveränderungen bei Krebs, *Klinische Wochenschrift* 18, 305.
- Brdicka, R., 1947, Polarographic cysteine and protein tests, *Research* 1, 25.
- Brdicka, R., 1958, Polarographische Eiweißreaktion und ihre Anwendungen, *Z. Phys. Chem., Sonderheft*, 165.
- Brdicka, R. and J. Klumpar, 1937, Polarographic study of denaturation and proteolytic cleavage of proteins, *Časopis Česk. Lékárnictva*, 17, 234 (in English).
- Brdicka, R., J. Homolka and J. Škáchová, 1966, Polarographic effect of thiolated gelatin, *Rev. Roum. Biochim.* 3, 35.

- Brdička, R., M. Březina and V. Kalous, 1965, Polarography of proteins and its analytical aspects, *Talanta* 12, 1149.
- Březina, M., 1959, Katalytische Ströme von Cystin und Eiweißstoffen in Kobalt(II)-Lösungen an der stationären Tropfenelektrode, *Coll. Czech. Chem. Commun.* 24, 4031.
- Březina, M., 1960, Influence of cobalt and nickel on the catalytic waves of proteins and of some amino acids, *Advances in Polarography*, Vol. 3, Ed. I.S. Longmuir, Pergamon Press, Oxford, 933.
- Březina, M., 1963, Polarographic analysis of urine, *Rev. Polar. (Jpn)* 11, 26.
- Březina, M. and M. Kůtová, 1965, Einfluß der Elektrolytströmung auf die polarographischen katalytischen Wasserstoffströme, *Coll. Czech. Chem. Commun.* 30, 4307.
- Březina, M. and P. Zuman, 1958, *Polarography in Medicine, Biochemistry and Pharmacy*, Interscience Publishers, New York.
- Březina, M. and V. Gultjaj, 1963, Ueber den Einfluß der Gruppen SH, NH₂ und COOH auf die Bildung der polarographischen katalytischen Brdička-Stufen in ammoniakalischen Kobalt- und Nickel-Lösungen, *Coll. Czech. Chem. Commun.* 28, 181.
- Buruiana, L.M. and V. Pavlu, 1957, Le comportement polarographique du sperme, *Naturwissenschaften* 44, 589.
- Calusaru, A., 1966a, Equation de la vague polarographique catalytique, *CR. Acad. Sci. Paris S.C* 262, 4.
- Calusaru, A., 1966b, Equation de la vague polarographique catalytique de substances organiques a molécules complexes, *CR, Acad. Sci. Paris S.C* 262, 676.
- Calusaru, A., 1967, Décharge catalytique de l'hydrogene en présence de cobalt et de nickel, *J. Electroanal. Chem.* 15, 269.
- Calusaru, A., 1972, Catalytic hydrogen discharge in the presence of cycloserine, *Electrochim. Acta* 17, 213.
- Caselli, M., 1980, Catalytic waves of amniotic fluid proteins, *Electrochim. Acta* 25, 1389.
- Chmelař, V. and J. Nosek, 1959, Einfluß der Aethylendiamintetraessigsäure auf die Höhe und die Gestalt der polarographischen Stufen von Eiweißstoffen, *Coll. Czech. Chem. Commun.* 24, 3084.
- Chmelař, V., M. Březina and V. Kalous, 1963, Radiopolarographie der Kobalt(II)-Testlösung in Anwesenheit von Cystin oder Eiweißstoffen, *Coll. Czech. Chem. Commun.* 28, 197.
- Csagoly, E., 1959, Polarographic studies of the -SH, -S-S- contents and the Brdička waves of native serum proteins and their dependence on radiation sensitivity, *J. Polar. Soc. (London)* 5, 30.
- Dorčák, V. and I. Šestáková, 2005, Electrochemical behavior of phytochelatins and related peptides at the hanging mercury drop electrode in the presence of cobalt(II) ions, *Bioelectrochemistry*, 68, 14.
- Dykhal, Yu.I., E.P. Medyantseva, N.R. Murtazina, G.R. Safina, G.K. Budnikov and N.V. Kalacheva, 2001, Use of metal ions for the estimation of the efficiency of antibody-antigen interactions, *J. Anal. Chem.* 56, 1118.
- Electrochimica Acta*, Special issues on Electrocatalysis: 1984, 29(11/12) 1501-1732; 1994, 39(11/12) 1467-1942; 1998, 44(8/9) 1283-1534; 2000, 45(25/26) 4075-4380; 2003, 48(25/26) 3729-3964.
- El Hourch, M., A. Dudoit and J.-C. Amiard, 2003, Optimization of new voltammetric method for the determination of metallothionein, *Electrochim. Acta* 48, 4083.
- Feinberg, B.A. and Y.-K. Lau, 1980, The electrochemistry of high potential iron-sulfur proteins and their novel Brdička waves, *J. Electroanal. Chem.* 116, 187.
- Frank, M., I. Garta and G. Lamm, 1956, Polarographic studies on blood proteins in hepatic disease, *Acta Med. Acad. Sci. Hung.* 9, 279.
- Gerischer, H. and W. Mehl, 1955, Zum Mechanismus der kathodischen Wasserstoff-abscheidung an Quecksilber, Silber und Kupfer, *Z. Elektrochem.* 59, 1049.
- Gudbjarnason, S., 1969, Molecular structures and catalytic activity. II. Proton reactivity and catalytic polarography of histidine and related imidazole derivatives, *Biochim. Biophys. Acta* 177, 303.

- Guidelli, R., 1971, Chemical reactions in polarography, *Electroanalytical Chemistry*, Vol. 5, Ed. A.J. Bard, Marcel Dekker, New York, 266.
- Havran, L., S. Billová and E. Paleček, 2004, Electroactivity of avidin and streptavidin. Avidin signals at mercury and carbon electrodes respond to biotin binding, *Electroanalysis* 16, 1139.
- Herles, F. and A. Vančura, 1932, A research on the cause of a characteristic "wave" on the polarographic curve of human serum, *Bull. Internat. Acad. Sci. Boheme.* 33, 119.
- Heyrovský, J. and J. Babička, 1930, Polarographic studies with the dropping mercury cathode. Part XIII. The effect of albumins, *Coll. Czech. Chem. Commun.* 2, 370.
- Heyrovský, J. and J. Kůta, 1965, Catalytic hydrogen currents, *Principles of Polarography*, Ch. 18, p. 407. Publishing House of the Czechoslovak Academy of Sciences, Prague, and Academic Press, New York.
- Heyrovský, M., 2000, New aspects of the Brdička reaction of low-molecular thiols: Voltammetry at low rate of potential scan, *Electroanalysis* 12, 935.
- Heyrovský, M., S. Vavříčka and L. Holleck, 1971, Auftreten des Azoxyderivates als Zwischenprodukt bei der polarographischen Reduktion von *p*-Dinitrobenzol, *Coll. Czech. Chem. Commun.* 36, 971.
- Homolka, J., 1971, Polarography of proteins, analytical principles and applications in biological and clinical chemistry, Chapter in *Methods of Biochemical Analysis*, Vol. 19, Ed. D. Glick, p. 436. Wiley, New York.
- Ikeda, T., H. Kinoshita, Y. Yamane and M. Senda, 1980a, Polarographic catalytic currents produced by cytochromes *c* in ammoniacal buffers containing cobalt ions. I. Significance of heme group, *Bull. Chem. Soc. Jpn.* 53, 112.
- Ikeda, T., Y. Yamane, H. Kinoshita and M. Senda, 1980b, Effect of pH on Brdička currents produced by cytochrome *c*, *Bull. Chem. Soc. Jpn.* 53, 686.
- Irmischer, A., 1958, Die Verwendung der polarographischen Serumreaktion in der gynäkologischen Klinik, *Z. f. Geburtsh. Gynäkol.* 150, 62.
- Ito, M., 1959, The polarographic catalytic wave of proteins in tris (ethylenediamine) cobalt (III) chloride solution, *J. Electrochem. Soc. Jpn.* (Overseas ed.) 27, E-19.
- Ito, M., 1965, Polarographic studies on proteins and enzymes. II. The polarographic catalytic wave of proteins in tris (ethylenediamine)cobalt(III) chloride solution, *Mie Med. J.* 14, 95.
- Iwanow, I.D., 1961, *Polarography of Proteins, Enzymes and Aminoacids* (in Russian), Izdat. Akad.Nauk SSSR, 156.
- Iwanow, I.D. and E.E. Rachejeva, 1964, *Die Polarographie tertiärer Strukturen von Eiweißen und Enzymen*, Abhandl. Deutsch. Akad. Wiss. Berlin, Kl. Chem., Geol., Biol., Nr.1, Ed. H. Berg, S.207, Akad.Verlag, Berlin.
- Jirka, M. and J. Kotas, 1957, The occurrence of mucoproteins in human sweat, *Clin. Chem. Acta* 2, 292.
- Jurka, E., 1939, Polarographic studies with the dropping mercury cathode. Part LXXIX. Investigation of the simultaneous occurrence of the two known protein effects produced in buffered cobalt solutions, *Coll. Czech. Chem. Commun.* 11, 243.
- Kadleček, J., P. Anzenbacher and V. Kalous, 1975, The new polarographic current of the catalytic evolution of hydrogen in a buffered system containing a thiol and cobalt(II) ions, *J. Electroanal. Chem.* 61, 141.
- Kadleček, J., P. Anzenbacher and V. Kalous, 1978, Polarographic catalytic hydrogen currents in the presence of various thiols, *J. Electroanal. Chem.* 86, 417.
- Kalous, V., 1954, Elektrophoretische Analyse der in Sulfosalicylfiltraten von Blutseren anwesenden Stoffe, *Coll. Czech. Chem. Commun.* 19, 1039.
- Kalous, V., 1956, Der polarographische katalytische Eiweisseffekt in kobalthaltigen Glycinpuffern, *Coll. Czech. Chem. Commun.* 21, 1227.
- Kalous, V., 1958, Polarographische und elektrophoretische Untersuchung der Eiweißkomponenten in Sulfosalicylsäurefiltraten von Blutseren, *Z. Physik. Chem., Sonderheft* 186.
- Kalous, V., 1959, Polarographische Bestimmung des Mucoproteins MP-1 nach der Trennung der Sera durch Papierelektrophorese, *Coll. Czech. Chem. Commun.* 25, 878.

- Kalous, V., 1971, Polarographic research of proteins and related substances, *Experientia Supplement* 18, Proc. 1. Internat. Symp. Biol. Aspects of Electrochemistry, Ed. G. Milazzo, Birkhäuser Verlag, Basel, 349.
- Kalous, V. and J. Štokr, 1955, Verfolgung der Aussalzung von Eiweißstoffen mit Hilfe der polarographischen Eiweißreaktion (full paper in Russian), *Coll. Czech. Chem. Commun.* 20, 1237.
- Kalous, V. and P. Valenta, 1957, Oszillographische Verfolgung der polarographischen Brdička Filtrat-Reaktion, *Coll. Czech. Chem. Commun.* 22, 600.
- Kanner, O. and G.J. Reed, 1939, Polarographic study of insulin, *Proc. Soc. Exptl. Biol. Med.* 42, 387.
- Kano, K., T. Ikeda and M. Senda, 1981, Polarographic catalytic current of microbial protein proteinase inhibitors and direct determination of dissociation constants of subtilisin BPN' – inhibitor complexes by polarographic method, *Agric. Biol. Chem.* 45, 223.
- Kikuchi, T., T. Hirano, A. Onuki and I. Okada, 1959, Polarographic studies on protein contained in aquatic animals, *Bull. Jpn. Soc. Sci. Fisheries* 24, 551.
- Kinoshita, H., T. Ikeda, Y. Yamane and M. Senda, 1980, Polarographic catalytic hydrogen current produced by myoglobins and hemoglobins, *Agric. Biol. Chem.* 44, 2337.
- Kizek, R., L. Trnková and E. Paleček, 2001, Determination of metallothionein at the femtomole level by constant current stripping chronopotentiometry, *Anal. Chem.* 73, 4801.
- Knobloch, E., 1947, Catalytic evolution of hydrogen at the dropping mercury cathode due to the amide of nicotinic acid and other pyridine derivatives, *Coll. Czech. Chem. Commun.* 12, 407.
- Kočent, A., 1958, Biochemistry of the blood in cancer IV. Evaluation of the polarographic activity of blood sera in the Brdička test, *Neoplasma* 4, 396.
- Kolthoff, I.M., H. Sawamoto and S. Kihara, 1978, Catalytic currents of albumin at the hanging mercury drop electrode, *J. Electroanal. Chem.* 88, 233.
- Kolthoff, I.M., K. Yamashita and T.B. Hie, 1974, Characteristics of polarographic catalytic waves observed with bovine-serum albumin: Effects of type of buffers, pH, ionic strength, calcium and tetraalkyl salts, *Proc. Natl. Acad. Sci. USA* 71, 2072.
- Kolthoff, I.M., K. Yamashita and T.B. Hie, 1975, Polarographic catalytic hydrogen currents observed with native and modified bovine serum albumin, *J. Electroanal. Chem.* 63, 393.
- Kolthoff, I.M., P. Mader and S.E. Khalafalla, 1968, Kinetic waves in systems containing cobalt(II) and cysteine-like compounds, *J. Electroanal. Chem.* 18, 315.
- Kolthoff, I.M. and P. Mader, 1969, Kinetic waves in systems containing cobalt(II) and cysteine-like compounds. Polarographic catalytic hydrogen waves in acid solutions of mercaptoanilines in presence of cobalt(II) or -(III), *Anal. Chem.* 41, 924.
- Kolthoff, I.M. and S. Kihara, 1977, Voltammetric determination of ultratraces of albumin, cysteine and cystine at the hanging mercury electrode, *Anal. Chem.* 49, 2108.
- Kolthoff, I.M. and S. Kihara, 1979a, Voltammetric and polarographic catalytic hydrogen currents of modified bovine serum albumin, *J. Electroanal. Chem.* 96, 95.
- Kolthoff, I.M. and S. Kihara, 1979b, Characteristics of a new catalytic hydrogen current observed with albumin in the presence of cobalt (III) or (II) at the hanging mercury drop electrode, *J. Electroanal. Chem.* 98, 327.
- Kolthoff, I.M. and S. Kihara, 1980, Effect of temperature on catalytic hydrogen currents on native and modified bovine serum albumin, *Coll. Czech. Chem. Commun.* 45, 669.
- Koryta, J., 1967, Electrochemical kinetics of metal complexes, *Advances in Electrochemistry and Electrochemical Engineering*, Vol. 6, Ed. P. Delahay, Interscience, New York, 289.
- Kotrba, P., T. Macek and T. Ruml, 1999, Heavy-metal binding proteins and peptides in plants. A review, *Coll. Czech. Chem. Commun.* 64, 1057.
- Kuik, M., 1971, Parameters affecting the shape of catalytic waves in the system Ni(II)-cysteine; qualitative results, *Coll. Czech. Chem. Commun.* 36, 1009.
- Kuik, M., 1997, The additivity of catalyzed hydrogen evolution currents of hemoglobins: An empirical approach, *J. Electroanal. Chem.* 423, 37.
- Kuik, M. and K. Krassowski, 1987, Brdička-type catalytic currents of hemoglobins. Part III. pH dependence of the catalytic current – an indication of quaternary structure changes?, *Bioelectrochem. Bioenerget.* 17, 71.

- Kůtová, M. and M. Březina, 1966, Studium des Charakters der polarographischen Proteindoppelwelle aus ihrer Abhängigkeit von den Konstanten der Tropfenelektrode und aus dem Verlauf der Momentanströme, *Coll. Czech. Chem. Commun.* 31, 743.
- Kuznetsov, B.A., 1971, On the nature of polarographic protein waves, *Experientia Supplement* 18, Proc. 1. Internat. Symp. Biol. Aspects of Electrochemistry, Ed. G. Milazzo, Birkhäuser Verlag, Basel, 382.
- Kuznetsov, B.A., G.P. Shumakovich and N.M. Mestechkina, 1988, Hydrophilic and hydrophobic domains in the flat protein conformer as a cause of double step polarographic waves, *J. Electroanal. Chem.* 248, 387.
- Lamprecht, W. and H. Katzlmeier, 1961, Polarographie schwefelhaltiger Proteine, *Z. Anal. Chem.* 181, 216.
- Leibson, V.N., A.P. Churillina, A.S. Mendkovich and V.P. Gulytai, 1989, New ideas of the mechanism of catalytic hydrogen evolution in the buffer solutions of organic compounds, *J. Electroanal. Chem.* 261, 165.
- Lewitová, A. and V. Kalous, 1974, Polarographic behaviour of proteins with modified histidine residues, *Coll. Czech. Chem. Commun.* 39, 369.
- Lipkowski, J. and P.N. Ross, Eds., 1998, *Electrocatalysis*, Wiley, New York.
- Luo, D., J. Lan, C. Zhou and C. Luo, 2003, Polarographic behavior of Co(II) – BSA or – HAS complex in the presence of a guanidine modifier, *Anal. Chem.* 75, 6346.
- Mader, P., 1971, Polarographic investigation of systems containing cobalt(II) and cysteine-like compounds with special reference to their ability to facilitate hydrogen evolution from buffered aqueous solutions, *Coll. Czech. Chem. Commun.* 36, 1035.
- Mader, P., I.M. Kolthoff and V. Veselá, 1982, Catalytic hydrogen activity of the low-molecular weight thiols: Kinetic control of the Brdička catalytic current, *Electrochim. Acta* 27, 1393.
- Mader, P. and V. Veselá, 1977, Effect of surfactants on the polarographic Brdička activity of cysteine, *Bioelectrochem. Bioenerget.* 4, 413.
- Mader, P., V. Veselá, M. Heyrovský, M. Lebl and M. Braunsteinová, 1988, Polarography of the oxytocin and vasopressin synthetic analogs, *Coll. Czech. Chem. Commun.* 53, 1579.
- Mader, P., V. Veselá, V. Dorčák and M. Heyrovský, 2001, The “presodium” hydrogen evolution at the dropping mercury electrode catalysed by simple cysteine peptides, *Coll. Czech. Chem. Commun.* 66, 397.
- Mairanovskii, S.G., 1968, Catalytic hydrogen evolution at the dropping mercury electrode caused by organic catalysts, Chapter IX in *Catalytic and Kinetic Waves in Polarography*, p. 241, Plenum Press, New York.
- Mairanovskii, S.G., 1987, The effect of cobalt ions on the catalytic hydrogen evolution at a mercury electrode, *J. Electroanal. Chem.* 226, 51.
- Mairanovskii, S.G. and A.N. Frumkin, 1963, Effect of the catalyst adsorption and of the double layer structure on the catalytic waves of hydrogen evolution, *Rev. Polar. (Jpn)* 11, 96.
- Mairanovskii, S.G. and E.F. Mairanovskaia, 1961, On the nature of doubling of the polarographic wave of proteins in cobalt salt solutions (in Russian), *Izv. Akad. Nauk. SSSR, Otd. Khim. Nauk.* 922.
- Marha, K., 1957, Die spezifische polarographische Reaktion des Albumins II. Der Einfluß höherer Fettsäuren und Alkohole auf die katalytische Doppelstufe des Serumweißes im Milieu von dreiwertigem Kobalt, *Coll. Czech. Chem. Commun.* 22, 153.
- Mark, H.B., Jr., 1990, Electrocatalysis and its application to analysis, *Analyst* Vol. 115, 667.
- Masařík, M., A. Stobiecka, R. Kizek, F. Jelen, Z. Pechan, W. Hoyer, T.M. Jovin, V. Subramaniam and E. Paleček, 2004, Sensitive electrochemical detection of native and aggregated α -synuclein protein involved in Parkinson disease, *Electroanalysis* 16, 1172.
- Millar, G.J., 1953a, Studies on the polarography of proteins. 1. The relation of wave heights to protein concentration and the origin of wave III, *Biochem. J.* 53, 385.
- Millar, G.J., 1953b, Studies on the polarography of proteins. 2. The influence of pH and concentration of ammonia and ammonium ion upon the polarographic waves, *Biochem. J.* 53, 393.
- Müller, O.H., 1955, Polarographic behavior of various plasma protein fractions, Chapter in *Electrochemistry in Biology and Medicine*, Ed. T. Shedlovsky, Wiley, New York, 301.

- Müller, O.H., 1963, Polarographic analysis of proteins, amino acids and other compounds by means of the Brdicka reaction, Chapter in Methods of Biochemical Analysis, Vol. 11, Ed. D. Glick, Interscience Publishers, New York, 329.
- Müller, O.H. and I. Yamanouchi, 1963, Polarographic studies of proteins and their degradation products. V. Products from tryptic digests of serum albumin and development of a sensitive polarographic trypsin assay, Rev. Polar. (Jpn) 11, 79.
- Nakanishi, T. and T. Itoh, 1965, Studies of protein in abnormal milk. Part IV. Polarographic protein wave in normal and abnormal milk, Agricult. Biol. Chem. 29, 32.
- Okajima, T. and T. Sasai, 1953, The polarogram of digested casein by pepsin, Bull. Inst. Chem. Research, Kyoto Univ. 31(6), .
- Paleček, E., 1956, Die Polarographie der Eiweißstoffe, des Cystins und Cysteins in Nickel-lösung, Die Pharm. 11, 551.
- Paleček, E., 1986, Electrochemical behaviour of biological macromolecules, Biochem. Bioenerget. 15, 275.
- Paleček, E. and I. Postbieglová, 1986, Adsorptive stripping voltammetry of biomacromolecules with transfer of the adsorbed layer, J. Electroanal. Chem. 214, 359.
- Paleček, E. and Z. Pechan, 1971, Estimation of nanogram quantities of proteins by pulse-polarographic technique, Anal. Biochem. 42, 59.
- Puranen, J. and T. Hokkanen, 1971, Modified Brdicka test as a screening method for gynecologic cancer, Obstet. Gynecol. 38, 99.
- Qian, X.-X., K. Nagashima, T. Hobo, Y.-Y. Guo and Ch. Yamaguchi, 1990, High-performance liquid chromatography of thiols with differential pulse polarographic detection of the catalytic hydrogen evolution current, J. Chromatogr. A 515, 257.
- Raspor, B. and J. Pavicic, 1996, Electrochemical methods for quantification and characterization of metallothioneins induced in *Mytilus galloprovincialis*, Fresenius J. Anal. Chem. 354, 59.
- Raspor, B., M. Paić and M. Erk, 2001, Analysis of metallothioneins by the modified Brdicka procedure, Talanta 55, 109.
- Ruttkay-Nedecký, G., 1957, A polarographic method for the detection of protein impurities in preparations of tobacco mosaic virus, Biochim. Biophys. Acta 26, 455.
- Ruttkay-Nedecký, G., 1963, Charakteristische polarographische Aktivität des Tabakmozaikvirus III. Typische Stufengestalt bei 0°C und ihre Ausnützung zur Bestimmung der Verunreinigungen im Viruspurifikat, Coll. Czech. Chem. Commun. 28, 585.
- Ruttkay-Nedecký, G. and A. Anderleová, 1967, Polarography of proteins containing cysteine, Nature 213, 564.
- Ruttkay-Nedecký, G. and E. Paleček, 1980, Differential pulse-polarographic analysis of tobacco mosaic virus, Acta Virol. 24, 175.
- Šafránková, B. and M. Březina, 1962, Peptide-like compounds in the urine of patients suffering from burns, Acta Chir. Plast. 4, 18.
- Sanada, K. and Y. Mishiro, 1966, Protein wave in the polarogram of human saliva, J. Dental Res. 45, 215.
- Schmidt, C.L. and H.S. Swofford, Jr., 1979, Electrochemical investigation of surface phenomena at a mercury electrode in vitamin B_{12a} solution, Anal. Chem. 51, 2026.
- Senda, M., T. Ikeda and H. Kinoshita, 1976, Catalytic hydrogen evolution by protein adsorbed on mercury electrode in the presence of some transition metals, Biochem. Bioenerget. 3, 253.
- Senda, M., T. Ikeda, K. Kano and I. Tokimitsu, 1982, Theory of Brdicka current and the dependence of the current on cobalt concentration, Bioelectrochem. Bioenerget. 9, 253.
- Sequaris, J.M., 1992, Analytical voltammetry of biological molecules, Analytical Voltammetry, Vol. 115, Eds. M.R. Smith and J.G. Vos, Elsevier, Amsterdam, 138.
- Shinagawa, M., H. Nezu and T. Yamada, 1962, Radiometric polarography. I. The role of cobalt on the catalytic electrode reaction of compounds containing sulfhydryl or disulfide groups, Rev. Polar. (Jpn) 10, 163.
- Siegel, G., J. Ehrig and G. Neupert, 1976, Evaluation of Brdicka's reaction in tumor diagnostics, Arch. Geschwülforsc. 46, 210.

- Stackelberg, M.v. and H. Fassbender, 1958, Untersuchungen zur Katalyse der Wasserstoffabscheidung an der Quecksilberkathode durch organische Stoffe. I. Allgemeine Untersuchungen über den Strom und die Strömungen an der Elektrode, *Z. Elektrochem.* 62, 834.
- Stackelberg, M.v., W. Hans and W. Jensch, 1958, Untersuchungen zur Katalyse der Wasserstoffabscheidung an der Quecksilberelektrode durch organische Stoffe. II. Die konstitutionellen Voraussetzungen für die katalytische Wirksamkeit, *Z. Elektrochem.* 62, 839.
- Stankovich, M. and A.J. Bard, 1977, The electrochemistry of proteins and related substances, Part II. Insulin, *J. Electroanal. Chem.* 85, 173.
- Stillman, M.J., 1995, Metallothioneins, *Coord. Chem. Rev.* 144, 461.
- Sunahara, H., D.N. Ward and A.C. Griffin, 1960, Polarographic studies on natural peptides. Polarography of oxytocin, lysine and arginine-vasopressin in cobalt (II) and (III) ammonia-ammonium chloride solution, *J. Am. Chem. Soc.* 82, 6017, 6023.
- Tomschik, M., L. Havran, E. Paleček and M. Heyrovský, 2000, The "presodium" catalysis of electroreduction of hydrogen ions on mercury electrodes by metallothionein. An investigation by constant current derivative stripping chronopotentiometry, *Electroanalysis* 12, 274.
- Tomschik, M., L. Havran, M. Fojta and E. Paleček, 1998, Constant current chronopotentiometric stripping analysis of bioactive peptides at mercury and carbon electrodes, *Electroanalysis* 10, 403.
- Tropp, C., 1938, Polarographische Untersuchungen über Insuline, *Klinische. Wochenschr.* 17, 465.
- Tur'yan, Ya.I., 1994, The parameters of polarographic catalymetry using ligand catalysis, *J. Electroanal. Chem.* 365, 185.
- Tur'yan, Ya.I., Ruvinskii, O.E., and Zaicev, P.M., 1998, Poliarograficheskaia Katalimetriia (Polarographic Catalymetry, in Russian), *Khimia, Moscow*, 272pp.
- Velázquez, A., O. Hernández-Pérez, P. Gómez, G. Gallegos and A. Rosado, 1988, Brdička reaction in vaginal secretions. A possible diagnostic tool in cervical cancer, *Arch. Invest. Med.* 19, 133.
- Vorlíčková, M. and E. Paleček, 1973, Estimation of submicrogram quantities of proteins in nucleic acid samples by pulse-polarographic technique, *Biochim. Biophys. Acta* 331, 276.
- Waldschmidt-Leitz, E., O. Conrath and J. Gloeditsch, 1937, Versuche zur Diagnose bösartiger Geschwülste, *Naturwissenschaften* 25, 60.
- Wang, J., 1985, *Stripping Analysis, Principles, Instrumentation, and Applications*, VCH Publishers, Deerfield Beach, FL.
- Wang, J., 1994, *Analytical Electrochemistry*, VCH, New York.
- Wieckowski, A., E.R. Savinova and C.G. Vayenas, (Eds.), 2003, *Catalysis and Electrocatalysis at Nanoparticle Surface*, Marcel Dekker, New York.
- Winzler, R.J., 1955, Serum glykoproteins, *Methods of Biochemical Analysis*, Vol. 2, Ed. D. Glick, Interscience, New York.
- Yamaguchi, S., T. Yamazoe, T. Tsukamoto and M. Senda, 1986, A sequence-controlled polarograph with static mercury drop electrode and trace analysis of proteins using Brdička current, *Bunseki Kagaku* 35, 858 (in English).
- Yosypchuk, B. and L. Novotný, 2002, Electrodes of nontoxic solid amalgams for electrochemical measurements, *Electroanalysis* 14, 1733.
- Zikán, J. and V. Kalous, 1966, Polarographic reaction of proteins and peptides. I. Significance of disulphides for formation of catalytic protein waves, *Coll. Czech. Chem. Commun.* 31, 4513.
- Zikán, J. and V. Kalous, 1967, Polarographic reaction of proteins and peptides. II. Catalytic and reduction waves of insulin *S*-sulphopeptides and of *S*-sulphocysteine, *Coll. Czech. Chem. Commun.* 32, 246.
- Zuman, P. and M. Kuik, 1958, Einfluß des Schwefels auf die katalytischen polarographischen Stufen in ammoniakalischen Kobalt(II)-Lösungen, *Naturwissenschaften* 45, 541.
- Zuman, P. and M. Kuik, 1959, Katalyse der Wasserstoffabscheidung in Gegenwart einiger Schwefelderivate des Hydantoin und Pyrimidins, *Coll. Czech. Chem. Commun.* 24, 3861.

This page intentionally left blank

Electroactivity of Proteins: Possibilities in Biomedicine and Proteomics

Emil Paleček

Institute of Biophysics, Academy of Sciences of the Czech Republic, 61265 Brno, Czech Republic

Contents

1. Introduction	690
1.1. History	691
1.2. Protein adsorption and immobilization	691
1.2.1. Modified electrode surfaces	692
1.2.2. Bare electrodes	693
2. Electroactivity of peptides at carbon and mercury electrodes	694
2.1. Electrooxidation at carbon electrodes	694
2.2. Electroactivity of peptides at mercury electrodes	695
2.2.1. Peak H	696
3. Electroactivity of proteins	701
3.1. Electroactivity of avidin and streptavidin	701
3.1.1. Avidin–biotin binding	704
3.1.2. Interfacial behavior of avidin and avidin–biotin	707
3.1.3. Concluding remarks	708
3.2. Native, mutant and denatured proteins	708
3.2.1. Changes in protein catalytic responses due to single amino acid exchange	709
3.2.2. Denatured proteins	712
3.3. Voltammetric and polarographic signals of some proteins in presence of guanidine	715
4. Redox states of peptides and proteins	716
4.1. Electroreduction of disulfide bonds	716
4.2. Electrochemical analysis of reduced peptides and proteins	717
5. Aggregation of proteins	718
5.1. Parkinson's disease (PD)	719
5.2. α -Synuclein (ASyn)	719
5.2.1. Electrochemical analysis of α -synuclein	720
5.2.2. Aggregation of α -synuclein	722
5.2.3. Hydrogen evolution catalyzed by α -synuclein at mercury electrodes	723
6. Signals of thiolated oligodeoxynucleotides in cobalt-containing solutions	725
6.1. Thioalkanes and thiolated ODNs at gold and mercury electrodes	725
6.2. Thiolated ODNs in cobalt-containing solutions	725
7. DNA–protein interactions	726
7.1. Electrochemical analysis of DNA–protein interactions	728
7.1.1. Single-surface techniques	729
7.1.2. Double-surface techniques	731
8. Introduction of electroactive markers to probe the protein structure	732

8.1. Concluding remarks	736
9. Summary and conclusion	736
List of abbreviations	739
Acknowledgments	740
References	740

1. INTRODUCTION

Proteins greatly differ from nucleic acids in their functions, structures and physical chemical properties. Nucleic acids store, replicate and transmit the genetic information of cells. Proteins play much greater variety of roles: Some form a large part of structural framework of tissues and cells; others carry out transport and storage of small molecules. One of the most important protein classes is the enzymes, the catalysts capable to promote enormous variety of reactions determining essential pathways of metabolism. Antibodies and a number of other important biological factors are proteins. Several thousand kinds of proteins are contained in each cell. Compared to DNA, proteins are extremely complex molecules in agreement with the multiplicity of their functions. Since the 1950s great progress in protein chemistry and biology has been done. Among the methods, which contributed to this progress are X-ray diffraction analysis, nuclear magnetic resonance, electron and scanning force microscopies, electrophoresis and isoelectric focusing, chromatography, etc. (see Appendix for details). When searching biochemistry and protein textbooks (Branden and Tooze, 1999; Campbell, 1995; Fersht, 1999; Lilley, 1995; Mathews *et al.*, 2000; Neurath, 1963; Stryer, 1988; Travers and Buckle, 2000), electrochemistry can hardly be found among these methods. Why is it so? Is electrochemistry of little use in the contemporary protein research? I do not think so. Chapters 14–18 deal with progress and potentialities of electrochemistry in the investigation of the direct electron transfer in proteins at interfaces, and in attempts to contribute to immunoassays and development of new platforms for highly parallel protein analysis. But can electrochemistry contribute to the protein research also in other directions not covered in the previous chapters of this book? I believe there are many possibilities to apply electrochemical analysis and electrochemical approaches in protein research. To realize these possibilities combination of some knowledge of the contemporary biochemistry and electrochemistry is necessary.

At present time, synthetic oligopeptides are commercially available and also larger polypeptides can be synthesized. Moreover, methods of protein engineering producing recombinant wild-type and mutant proteins and their domains are available. Particularly interesting appear mutant proteins with a single amino acid exchange. Recombinant proteins have recently been applied in the studies of the direct electron transfer of proteins, such as azurin (Fristrup *et al.*, 2001) or peroxidase (Ferapontova *et al.*, 2002). On the other hand, electrochemical studies of individual protein domains and mutants of proteins not containing any center providing fast-reversible redox reactions practically do not exist. In this chapter, I wish to deal with electrochemistry of proteins that

do not offer fast-reversible electrochemistry. Special attention will be paid to approaches, which can provide an insight into interfacial properties of specific proteins and/or provide new tools for biomedicine or biotechnologies.

1.1. History

Electrochemical analysis of proteins was successfully applied in biochemistry, pharmacy and medicine and particularly in clinical oncology research for several decades around the middle of the 20th century (Brezina and Zuman, 1958) (See Chapters 20 and 18 for details). Later, the attention of electrochemists turned to direct electrochemistry of a limited number of redox-active center-containing proteins (reviewed in Armstrong, 2002) and the potentialities of the electrochemical methods as tools for analysis of the majority of proteins important in molecular biology and biomedicine were neglected. At present, electrochemistry of proteins is mainly oriented toward direct electrochemistry of redox-active center-containing proteins offering fast reversible electrochemical processes at solid electrodes (reviewed in Armstrong, 2002). Metalloproteins represent a relatively large group of proteins but among metalloproteins only a very small fraction fulfills the requirements for fast reversible electrochemistry at solid electrodes. The problem is that the electrode should bind the protein in an orientation suitable for fast electron transfer and that protein interaction with the electrode surface should not result in denaturation of the protein molecule. Moreover the protein binding should be sufficiently selective to prevent binding of other molecules that may block the surface and interfere with the protein analysis. The renewed interest in electrochemistry of proteins in general is related to several factors, including development of new methods such as adsorptive stripping and easy preparation of protein-modified electrodes (Armstrong, 2002; Kuznetsov and Shumakovich, 1975; Kuznetsov *et al.*, 1977; Palecek and Postbieglova, 1986; Palecek *et al.*, 1993b).

1.2. Protein adsorption and immobilization

Proteins adsorb ubiquitously on surfaces, including solid and liquid (mercury) electrodes, after contacting of the protein aqueous solutions with the surface (Hlady and Buijs, 1996; Hlady *et al.*, 1999; Jackson *et al.*, 2000; Roscoe, 1996). Controlling the adsorption process to obtain well-defined and properly oriented adsorbate, which retains its conformation and biological function, is of increasing importance. Protein immobilization at surfaces and particularly at electrodes is crucial in protein sensing, including the development of sensors for DNA–protein and protein–protein interactions and in protein electrochemistry in general. Similarly to nucleic acids (Chapter 3) covalent or non-covalent binding can be used to immobilize the protein at the electrode surface. Protein immobilization based on hydrophobic or electrostatic interactions and specific ligand binding affinity has been applied. Such immobilization of proteins involved either electrodes modified by special adsorbates or direct adsorption on

bare electrodes. With commonly used bare metal electrodes such as mercury, silver, gold and platinum no generally applicable method securing proper orientation of protein molecules at the electrode surfaces is available and in some cases protein unfolding at the electrodes was reported (Roscoe, 1996; Scheller *et al.*, 1975).

1.2.1. Modified electrode surfaces

1.2.1.1. Self-assembled monolayers. Since the pioneering work of Hill (Eddowes and Hill, 1977) and Kuwana (Yeh and Kuwana, 1977) in 1977, noble metals, such as gold and silver, modified with various adsorbates, or materials such as carbon or metal oxides having natural functionalities have been increasingly applied as electrodes for protein electrochemistry. Monolayers of thiol-containing DNAs and proteins have been prepared at gold electrodes (Davis *et al.*, 1998, 2000; Friis *et al.*, 1997; Herne and Tarlov, 1997; Jones *et al.*, 1998; Lewis *et al.*, 1995; O'Brien *et al.*, 2000a,b; Peterlinz *et al.*, 1997; Prime and Whitesides, 1991; Tarlov and Bowden, 1991). Recently, alkanethiols with hydrophobic, polar or electrically charged head (terminal) groups have been increasingly applied to form self-assembled monolayers at gold electrodes to create a specific adsorbate for immobilization of a given protein in a proper orientation toward the electrode surface. In 1991, Tarlov and Bowden (1991) were the first who used the SAM of alkanethiol with negatively charged head group to immobilize cytochrome *c* at a gold electrode. Direct electronic communication between the adsorbed protein and the electrode was detected by cyclic voltammetry. The attachment of the protein was most likely due to electrostatic interaction between its positively charged lysine residues and negatively charged carboxylic group in the alkanethiol layer. This interesting system was then characterized by a number of methods, including resonance Raman spectroscopy and electroreflectance spectroscopy (Arnold *et al.*, 1997; Avila *et al.*, 2000; Clark and Bowden, 1997; Collinson *et al.*, 1992; El Kasmi *et al.*, 1998; Feng *et al.*, 1995, 1997; Nahir and Bowden, 1996).

1.2.1.2. Carbon nanotubes. In recent years, the problem of synthesis of carbon nanotubes (CNT) in large quantities has been solved (Ebbesen and Ajayan, 1992) and this materials have become commercially available. CNTs with diameters in the range of 5–50 nm and lengths up to several micrometers represent an attractive material with interesting mechanical, chemical, structural and electronic properties (reviewed in Wang, 2005). CNT can be prepared by various methods, including carbon arc methods and chemical vapor deposition. They can be divided into single- and multi-wall carbon nanotubes (SWCNT and MWCNT, respectively). It was shown that CNT can be applied as an electrode material and that proteins can be immobilized on/within opened nanotubes without losing their activity (Davis *et al.*, 1997; Wang, 2005; Kerman *et al.*, 2005). Particularly, with redox protein azurin well-behaved voltammetric responses were obtained (Davis *et al.*, 1997). CNT posses a hollow core suitable

for storing guest molecules, including nucleic acids and proteins (Wang, 2005). The above-mentioned properties make CNT highly attractive materials for electrochemical biosensors. CNT-based biocomposite electrodes (Rubianes and Rivas, 2003; Valentini *et al.*, 2003; Wang and Musameh, 2003) as well as CNT screen-printed strip electrodes (Wang and Musameh, 2004) were prepared. New bioelectronic protocols, based on the double-surface technique with magnetic beads (Section 7.1.2), were recently described. In these protocols, CNT played a role as carriers of a large number of enzyme molecules and as modifiers of the glassy carbon electrodes allowing detection of DNA and proteins at z-mole level. It can be expected that CNT will be increasingly applied in electrochemical analysis of proteins and in electrochemical biosensors.

1.2.2. Bare electrodes

1.2.2.1. Solid electrodes. Electrochemical studies of interfacial behavior of proteins not containing redox centers at bare solid electrodes were thoroughly reviewed by Roscoe (1996). At solid electrodes most of the electrochemical studies dealt with proteins adsorption, surface coverage, charge density, etc. Such investigations provided information on changes in protein conformation at surfaces and on fouling of surfaces important for various practical industrial and medical problems (Fuller and Roscoe, 1994). Under certain conditions, adsorption of carboxyl groups of some proteins at platinum electrodes was accompanied by electron transfer at anodic potentials (Roscoe and Fuller, 1992; Roscoe *et al.*, 1993). In 1980, it was shown by Brabec (1980) and Reynaud *et al.* (1980) that tyrosine (Tyr) and tryptophan (Trp) residues in proteins are electrooxidizable at carbon electrodes. The indole ring of Trp is susceptible to electrooxidation from its heteroatom (Brabec and Mornstein, 1980; Brabec and Schindlerova, 1981a,b). Electrooxidation of tyrosine residues involves one electron and single proton transfer (the electrode process is similar to the oxidation of simple p-substituted phenols) (Reynolds *et al.*, 1995). Voltammetric analysis of proteins at carbon electrodes was not very sensitive yielding at relatively high protein concentrations only poorly developed inflections and/or small peaks at the voltammetric curves (Brabec, 1980; Brabec *et al.*, 1996; Palecek *et al.*, 1993b). It was shown that the constant current chronopotentiometric stripping analysis (CPSA) with sophisticated baseline correction is capable to produce well-developed oxidation peaks of Tyr and Trp residues in peptides at nanomolar concentrations (Cai *et al.*, 1996; Tomschik *et al.*, 1998 and references therein). Similar sensitivities were obtained with square wave voltammetry in combination with baseline correction (Palecek *et al.*, 2004b; Masarik *et al.*, 2004; E. Palecek and M. Masarik, unpublished). Further increase in sensitivity of the analysis of peptides and proteins was achieved by combination of glassy carbon electrode with carbon nanotubes (Kerman *et al.*, 2005).

1.2.2.2. Mercury electrodes. Once very popular, in the last three decades mercury electrodes were little used in electrochemistry of proteins. With their extremely

high hydrogen overvoltage and very high affinity for sulfur these electrodes offer some possibilities not available with solid non-mercury electrodes. These include the so-called Brdicka reaction in cobalt containing solutions (see Chapter 18) and the polarographic pre-sodium wave of proteins (obtained with mercury dropping electrodes) reviewed in Brezina and Zuman (1958), Heyrovsky and Kuta (1965) and Palecek (1983). Both the Brdicka reaction and pre-sodium wave are due to catalytic hydrogen evolution. D.c. polarographic pre-sodium wave was little used for analytical purposes because it appeared at too negative potentials very close to the background discharge and its shape was poorly developed and difficult to measure. Recently, we have shown that using the CPSA a well-developed peak can be obtained at very low peptide or protein concentrations at a hanging mercury drop electrode (HMDE) (Masarik *et al.*, 2004; Palecek *et al.*, 2004b; Tomschik *et al.*, 1998). This peak appeared at highly negative potentials but in the CP mode it was well separated from the background discharge; it was denominated as *peak H*. Using this peak femtomoles of peptides and proteins were determined (Kizek *et al.*, 2001; Tomschik *et al.*, 1998, 1999) without any baseline correction. Taking advantage of such a high sensitivity of the electrochemical determination, we attempted to use *peak H* for the analysis of several biologically highly important proteins such as metallothionein (Kizek *et al.*, 2001 and references therein), α -synuclein (Masarik *et al.*, 2004) (important in Parkinson disease (PD)) (Dev *et al.*, 2003a,b) (Section 5.2.1), tumor suppressor protein p53 (Palecek *et al.*, 2004a; Soussi *et al.*, 1994; Vogelstein and Kinzler, 1992), MutS protein (Palecek *et al.*, 2004b) (Section 7.2.1.1) acting in DNA repair (Biswas and Hsieh, 1996; Scharer, 2003; Wu *et al.*, 2004) and other proteins and peptides (Section 3). In this chapter, we wish to show examples of utilization of electrooxidizability of oligopeptides and proteins at carbon electrodes as well as their electroactivity at liquid mercury and solid amalgam electrodes utilized in relation to important biological problems.

2. ELECTROACTIVITY OF PEPTIDES AT CARBON AND MERCURY ELECTRODES

Oligopeptides represent an important class of modulators of biological functions. A number of peptides serve the classical biological role of hormones in the endocrine system and of neurotransmitters and neuromodulators in the central nervous system. Many diverse biological functions, including learning and memory, blood pressure regulation, sexual maturation and reproduction, enzyme inhibition or thermal control, can be modulated and regulated by peptides (Cai *et al.*, 1996 and references therein). Owing to the biological importance of peptides, there is a great interest in new effective approaches for their analysis, and for probing peptide conformational properties and interactions.

2.1. Electrooxidation at carbon electrodes

About 10 years ago the electrochemical analysis of peptides was limited to cystine/cysteine-containing peptides using the mercury electrode. Electrooxidation of

Tyr and Trp residues at carbon electrodes was little used for this purpose (Palecek, 1988). With proteins, best results were obtained with differential pulse voltammetry (Brabec and Mornstein, 1980; Brabec and Schindlerova, 1981b). This method, however, was not capable (a) to determine proteins at submicromolar concentrations and (b) to produce well-resolved peaks of Tyr and Trp.

We showed that CPSA at carbon electrodes yielded well-developed peaks for very low concentrations of DNA and RNA (Wang *et al.*, 1995), under conditions where voltammetric methods produced no signals or only poorly developed inflections (Chapter 3). Having in mind this experience we used CPSA to study three biologically important peptides containing Tyr and/or Trp residues, that is bombesin, luteinizing-hormone-releasing hormone (LH-RH) and neurotensin.

The above peptides were adsorbed and accumulated at carbon paste electrode (CPE) and determined at low solution concentrations by CPSA. Well-separated oxidation peaks of tyrosine (peak Y at about 0.55 V) and/or of tryptophan residues (peak W at about 0.7 V against Ag/AgCl/3 M KCl) were obtained. Neurotensin and bombesin containing only Tyr or only Trp, respectively, produced single peaks at the corresponding potentials, while LH-RH, which contains both Tyr and Trp residues, produces two well-resolved peaks (Figure 1). Using CPSA, these peptides were determined down to nanomolar concentrations at short accumulation times. Under the same conditions no voltammetric responses were observed. After 10 min accumulation, the CPSA detection limit for bombesin was 0.2 nM. The electrode with the adsorbed peptide could be washed and transferred into the blank electrolyte to perform CPSA. In this way, interferences of a number of low-molecular-mass substances (which were not strongly attached to the electrode or removed from it by washing) were avoided. We found that instead of CPSA square-wave voltammetry with baseline correction can be used.

CPSA was also used to study [Lys⁸]-vasopressin and angiotensin II at CPE (Tomschik *et al.*, 1998). Both peptides contain a single tyrosine residue which is oxidized at CPE close to +0.6 V (against Ag/AgCl/3 M KCl electrode, in 0.2 sodium phosphate, pH 7.0) producing peak Y; in vasopressin this peak was by about 15 mV more positive than in angiotensin II. Similar results were obtained also with proteins such as insulin (Wang *et al.*, 1996) lysozyme, bovine serum albumin (L. Havran, S. Billova, E. Palecek, unpublished), avidin (Havran *et al.*, 2004), α -synuclein (Masarik *et al.*, 2004), etc. but with some proteins containing both Tyr and Trp residues it was difficult to obtain two well-separated peaks. We have found that efficient baseline correction incorporated in instruments containing CP mode represents the main factor securing the high sensitivity in protein analysis. In agreement with this finding square wave voltammetry with baseline correction provided equal sensitivity in the analysis of proteins.

2.2. Electroactivity of peptides at mercury electrodes

The same two peptides were studied by CPSA at HMDE. In 0.2 M sodium phosphate, pH 7.0, 1 μ M [Lys⁸]-vasopressin yielded peak S at -0.56 V, related to the presence of cystine in the peptide (Figure 2C). Under the same conditions, no peak S was observed with angiotensin II not containing any cystine/cysteine

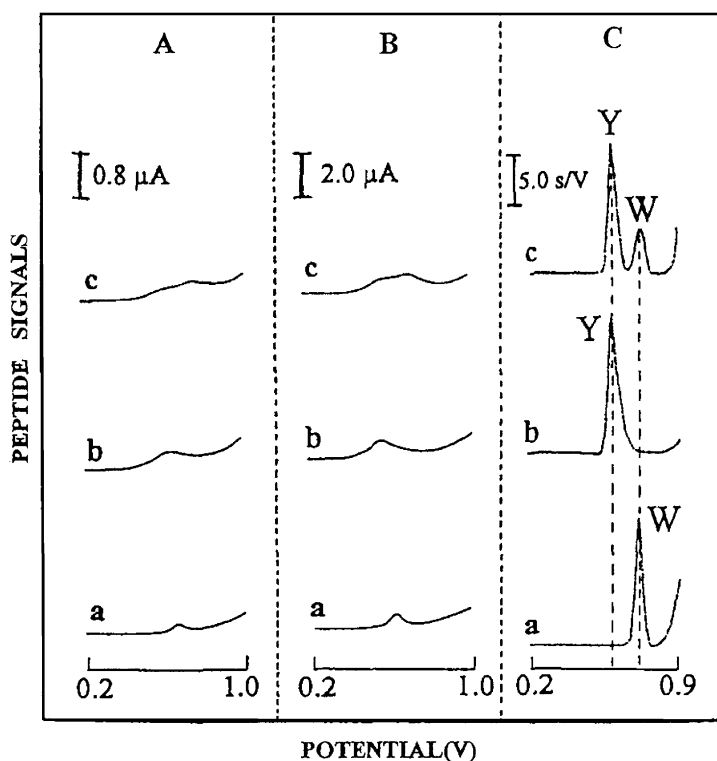


Fig. 1. (A) Linear-sweep voltammetric, (B) differential pulse voltammetric and constant current chronopotentiometric (CP) stripping responses of $3.5 \mu\text{M}$ (a) bombesin, (b) neurotensin and (c) LH-RH at the pretreated carbon paste electrodes (CPEs). Accumulation (2 min at 0.1 V) and stripping in 0.2 M phosphate buffer (pH 7.0); electrode pretreatment: 1 min at 1.5 V in 0.5 M Na_2CO_3 ; TRACELAB parameters: 20 mV s^{-1} scan rate (A); pulse height 25 mV; drop time 0.5 s; scan rate 5 mV s^{-1} (B); $5 \mu\text{A}$ stripping current (C). Y refers to tyrosine and W to tryptophan. Adapted with permission from Cai *et al.* (1996). Copyright 1996 Elsevier.

residues. Vasopressin but not angiotensin produced catalytic hydrogen reduction signals in media with cobalt ions (Figure 2A) as well as in media not containing any transition metal ions (Figure 2B, peak H).

Electroactivity of peptide nucleic acid (PNA) involving nucleic acid bases was summarized in Chapter 3. So far no reports have been published on the ability of PNA to catalyze the hydrogen evolution. Our preliminary results (L. Havran and E. Palecek, unpublished) suggest that PNA does not produce the Brdicka's signal in cobalt containing solution. On the other hand, PNA end-labeled with cysteine yields distinguished peak H as well as the Brdicka's double peak (see also Section 6.2).

2.2.1. Peak H

2.2.1.1. $[\text{Lys}^8]$ -Vasopressin and angiotensin II. Angiotensin II and $[\text{Lys}^8]$ -vasopressin were investigated by CPSA at HMDE in 0.2 M ammonium phosphate,

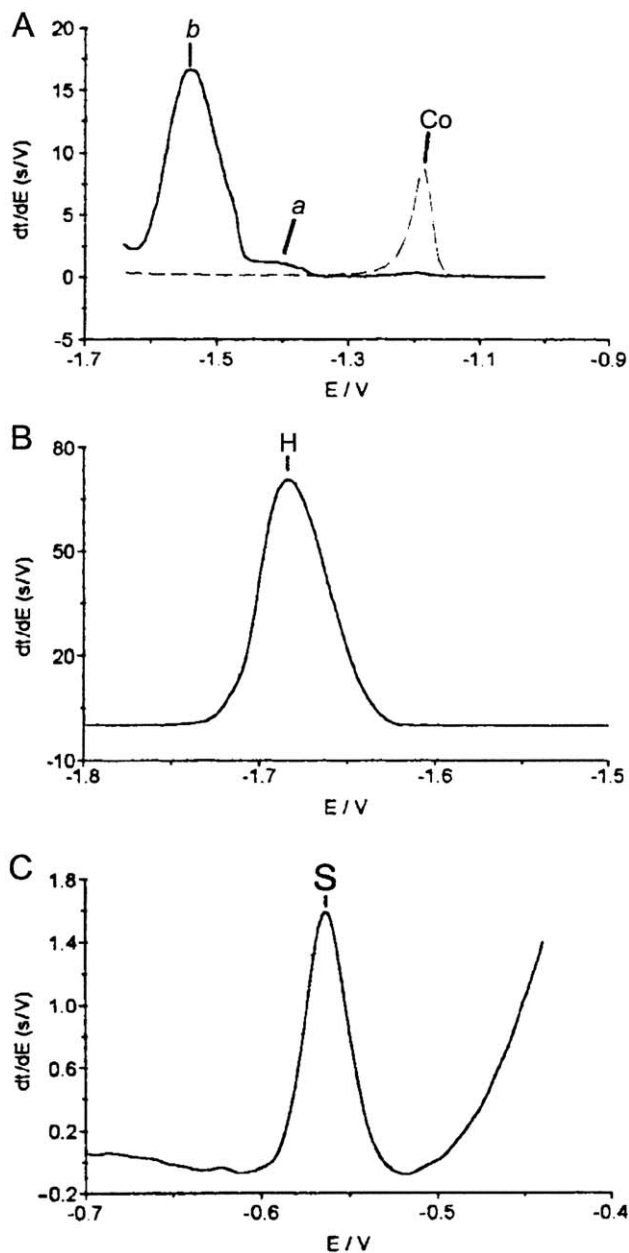


Fig. 2. CPSA signals of [Lys⁸]-vasopressin measured at HMDE: (A) peak of cobalt (Co) and catalytic peaks *a* and *b* yielded by the peptide in the presence of cobalt ions (Brdicka's solution), (B) catalytic peak H yielded in the absence of cobalt (pre-sodium wave) and (C) reduction peak S of HgS/disulfide bonds. Chronopotentiograms of 1 μ M vasopressin were measured in (A) 0.1 M NH₄Cl, 0.1 M NH₄OH, 1 mM [Co(NH₃)₆]Cl₃ ($t_A = 60$ s, $E_A = -0.6$ V, $I = -10$ μ A); (B) 0.2 M ammonium phosphate buffer, pH 7.8 ($t_A = 60$ s, $E_A = 0$ V, $I = -20$ μ A); and (C) 0.2 M sodium phosphate buffer, pH 7.0 ($t_A = 300$ s, $E_A = 0$ V, $I = -0.2$ μ A). Adapted with permission from Tomschik *et al.* (1998). Copyright 1998 Wiley-VCH.

pH 7.8 in absence of cobalt ions. [Lys⁸]-Vasopressin (1 μM) yielded a symmetrical peak close to -1.7 V , well separated from the background (Figures 2B and 3). Vasopressin (1 nM) produced at 5 min accumulation time still a well-developed peak, without any baseline correction (Figure 3). This peak, which was produced also by other peptides and proteins, was denominated as “*peak H*” because of its **H**igh sensitivity, catalytic **H**ydrogen evolution and **H**eyrovsky. In fact, it was **H**eyrovský and **B**abicka (1930) who started the history of the electrochemical analysis of proteins in 1930 when they published their paper on the so-called d.c. polarographic pre-sodium wave. CPSA *peak H* probably reflects similar electrode processes as the pre-sodium wave but this peak is better developed, allowing the determination of nanomolar and subnanomolar concentrations of peptides and proteins (Havran *et al.*, 2004; Kizek *et al.*, 2001; Masarik *et al.*, 2004; Tomschik *et al.*, 1998). Several factors contribute to the better sensitivity of the CPSA *peak H* as compared to d.c. polarography in cobalt-containing solutions (Brdicka protein waves) and in absence of cobalt (pre-sodium wave): (i) In CPSA more negative potentials can be reached (Heyrovsky and Forejt, 1953; Kalvoda, 1960) than in voltammetry and polarography. Reaching the highly negative potentials is necessary to obtain a well-developed peak H which in voltammetric and polarographic measurements is too close to the background discharge (Figure 3B); (ii) Strongly adsorbed peptides and proteins can be accumulated at HMDE (or at other stationary or solid mercury-containing electrodes, such as solid amalgam electrodes). Using the adsorptive

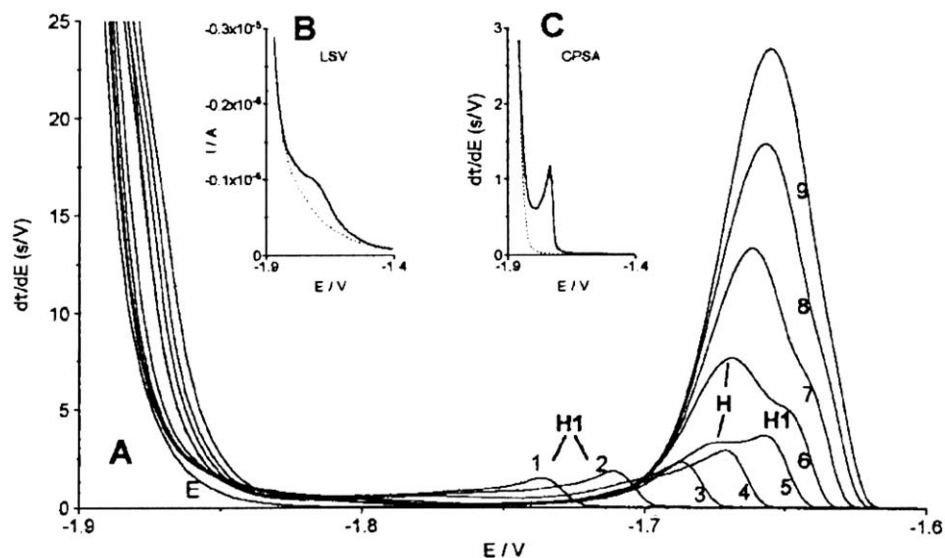


Fig. 3. (A) CPSA peaks H and H1 of vasopressin at concentrations of (1) 5 nM; (2) 10 nM; (3) 20 nM; (4) 30 nM; (5) 40 nM; (6) 50 nM, (7) 60 nM, (8) 70 nM; (9) 80 nM; E, background electrolyte; $t_A = 60\text{ s}$. Inset (B) LSV and (C) CPSA response of 1 nM vasopressin accumulated for $t_A = 300\text{ s}$; in LSV, scan rate 0.1 V s^{-1} ; in CPSA, $I = -5\text{ }\mu\text{A}$; for other details see Figures 4A, B. Adapted with permission from Tomschik *et al.* (1998). Copyright 1998 Wiley-VCH.

Table 1. Peptides **A**, containing and **B**, not containing cysteine residues

	Peptides	M.W.	Sequences
A	[Lys ⁸]-Vasopressin	1056.2	Cys-Tyr-Phe-Gln-Asn-Cys-Pro-Lys-Gly-NH ₂ [-S-S- 1-6]
	SS38	1152.2	Asn-Arg-Cys-Ser-Gln-Gly-Ser-Cys-Trp-Asn[-S-S- 3-8]
	SH38	1154.2	Asn-Arg-Cys-Ser-Gln-Gly-Ser-Cys-Trp-Asn
B	Angiotensin I	1296.5	Asp-Arg-Val-Tyr-Ile-His-Pro-Phe-His-Leu
	Angiotensin II	1046.2	Asp-Arg-Val-Tyr-Ile-His-Pro-Phe
	Bradykinin	1060.2	Arg-Pro-Pro-Gly-Phe-Ser-Pro-Phe-Arg
	[Met(O) ⁵]-Enkephalin	589.7	Tyr-Gly-Gly-Phe-Met(O)
	α ₁ -Mating Factor	1684.0	Trp-His-Trp-Leu-Gln-Leu-Lys-Pro-Gly-Gln-Pro-Met-Tyr

stripping greatly increases the sensitivity of the determination as compared to the polarographic methods; (iii) efficient baseline correction incorporated in chronopotentiometric instruments can improve the peak shape at very low protein concentrations. This is usually not necessary because the sensitivity of the CPS peak H is very good even without the baseline correction.

In addition to [Lys⁸]-vasopressin (Figures 2B and 3), we also investigated under the same conditions angiotensin II. No catalytic hydrogen reduction signal was obtained with the latter peptide suggesting that the presence of cystine/cysteine residues might be necessary for the appearance of *peak H*. We considered such a conclusion as premature (Tomschik *et al.*, 1998). We therefore tested several peptides not containing cysteine residues, including angiotensin II (Table 1) under different conditions, including different pHs and compared their behavior with that of cysteine-containing peptides, including Lys⁸-vasopressin.

2.2.1.2. Peak H is affected by peptide cysteine residues. We confirmed our previous results showing inactivity of angiotensin at pH 7.8 and we observed no *peak H* at higher pHs, where vasopressin showed *peak H* (V. Dorcak, unpublished). Slight decrease of pH from 7.8 resulted, however, in an appearance of *peak H* of angiotensin II (Figure 4). This peak was substantially smaller and appeared at more negative potentials (by about 300 mV) than that of vasopressin. These differences might be related to different adsorption of thiol-containing peptides, capable to form Hg-S bonds at the mercury surface. Generally, all tested peptides (Table 1) produced *peak H* at acid pHs but substantial differences between the groups of peptides with and without cysteine were observed in their electrochemical behavior. At alkaline pHs, all peptides not containing cysteine residues did not show any *peak H*. Under the same

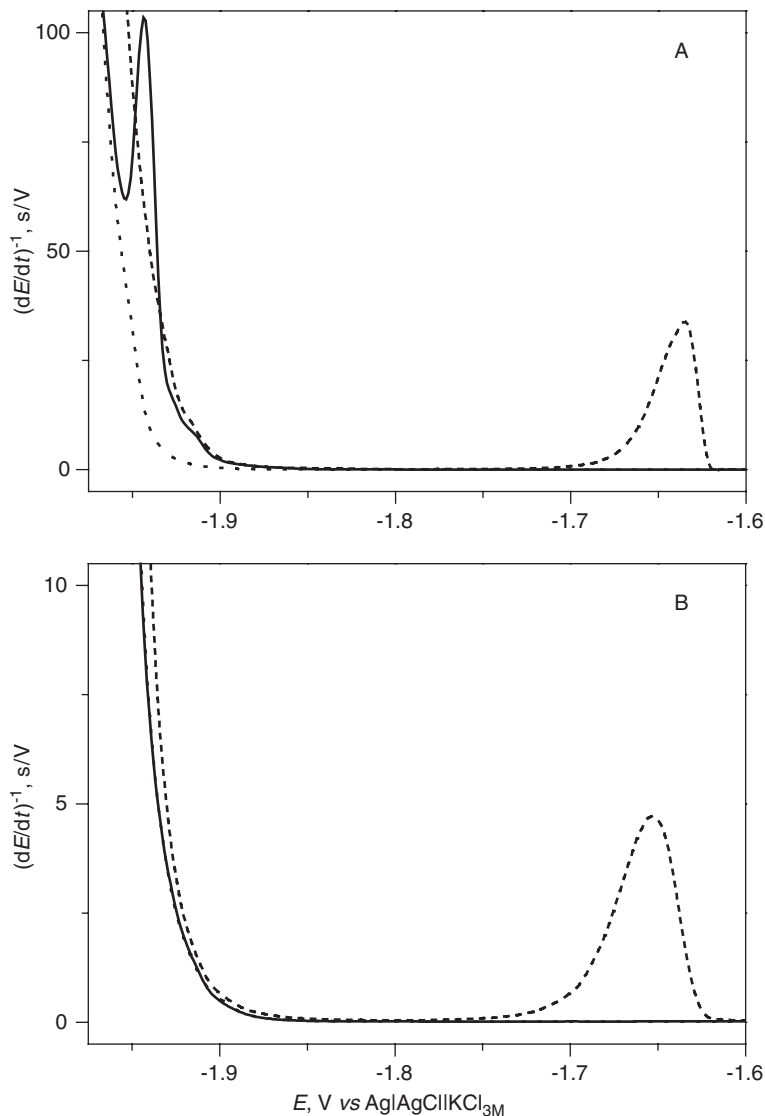


Fig. 4. CP responses of [Lys⁸]-vasopressin (-----) and Angiotensin II (—) in McIlvaine buffer (.....) at pH 7 and 8. (A) 0.1 μM [Lys⁸]-vasopressin (-----) and 0.5 μM angiotensin II (—) in 0.2 M McIlvaine buffer, pH 7.0. (B) 0.1 μM [Lys⁸]-vasopressin (-----) and 1.0 μM angiotensin II (—) in 0.2 M McIlvaine buffer, pH 8.0. Conventional AdS with HMDE, accumulation time 60 s, accumulation potential -0.1 V, stripping current -5 μA (V. Dorcak and E. Palecek, unpublished).

conditions, all cysteine-containing peptides produced well-developed peak H (Figures 2B–4, Table 1). On the other hand, at neutral and weakly acidic pHs all peptides, regardless of the presence or absence of cysteine residues in their molecules, displayed peak H (Figure 4, Table 1). We analyzed a number of peptides and proteins using peak H and found that under suitable conditions all

of them displayed peak H (V. Dorcak and E. Palecek, unpublished). Similar results were obtained with wild type (not containing cysteine) and cysteine-containing mutant of α -synuclein (Section 3.2.1). It, thus, appears that peak H might be the first electrochemical signal, which on one hand can be used for the determination of peptides and proteins regardless of their amino acid composition and on the other hand, it can be used for fast differentiation between peptides and proteins with and without cysteine residues.

Electrochemical signals of some small peptides and phytochelatin peptides (and their complexes with cobalt (II)) due to the catalytic hydrogen evolution were studied (Dorcak, 2004; Dorcak and Sestakova, 2005; Mader *et al.*, 2001). In small peptides, only a shift of the background discharge to positive potentials but no distinguished differential pulse polarography (DPV) peak was observed under the conditions where cysteine-containing peptides produced peak H (Dorcak, 2004).

3. ELECTROACTIVITY OF PROTEINS

In this chapter, electroactivity of proteins will be considered only in relation to their natural amino acid composition. Electroactivity of non-protein groups in a number of conjugated proteins, including metalloproteins will not be included as it is covered in Chapters 15–17. Below interfacial properties and electroactivity of two well-known proteins, that is avidin and streptavidin will be discussed as examples of potentialities of electrochemical analysis of proteins not undergoing reversible redox processes at bare electrodes.

3.1. Electroactivity of avidin and streptavidin

Avidin is a 66 kDa basic glycoprotein, with an isoelectric point of 9.5 (Green, 1975) and extremely high affinity for biotin (vitamin H, dissociation constant is $\sim 10^{-15}$ M) (Green, 1963, 1975). The bacterial protein streptavidin has a similar affinity for biotin (10^{-14} M) (Green, 1990). In contrast to avidin, streptavidin does not contain any cysteine residue (Buckley *et al.*, 1991) (Table 2), while avidin contains two cysteines forming a disulfide bond. Both proteins are functionally and structurally related. They consist of four identical subunits, formed by an eight-stranded, antiparallel, up-down β -barrel, bearing an active binding site for biotin (DeLange and Huang, 1971; Hendrickson *et al.*, 1989; Livnah *et al.*, 1993; Pugliese *et al.*, 1993; Weber *et al.*, 1989). Both proteins have been extensively used in biotechnologies. Biotin, coupled to a target molecule, is usually linked to (strept)avidin labeled with some reporter group. Depending on its nature, this group is subsequently detected by means of various methods, such as immunoassay (Heitzmann and Richards, 1974; Rappuoli *et al.*, 1981), immunohistochemistry (Bayer *et al.*, 1987), DNA hybridization (Diamandis and Christopoulos, 1991), flow-cytometry (Finn *et al.*, 1984), radiometry (Blanco and Dixon, 1986), electron microscopy (Spiegel *et al.*, 1982), etc.

Table 2. Comparison of avidin and streptavidin properties

Property	Avidin	Streptavidin
Subunits	4	4
Molecular weight of tetramer	66 000	60 000
Amino acid residues	128	159
Cysteine	2	0
Methionine	2	0
Tryptophan	4	6
Tyrosine	1	6
Isoelectric pH	9.5*	6.1*
Glycosylation	Yes*	No*

*From Ref.: Green, 1990

Electrochemical methods were used in studies of (strept)avidin–biotin binding using solid (mainly carbon) electrodes (Athey *et al.*, 1993; Gonzalez-Garcia *et al.*, 2000; Kuramitz *et al.*, 1999, 2000a,b; Sugawara *et al.*, 1994, 1995, 1996a,b, 1997; Tanaka *et al.*, 1999). To monitor the (strept)avidin–biotin binding, biotin derivatives with an electroactive redox markers, such as daunomycin (Sugawara *et al.*, 1995), Nile Blue A (Sugawara *et al.*, 1996b), colloidal gold (Gonzalez-Garcia *et al.*, 2000) or mediators (Kuramitz *et al.*, 1999, 2000b; Sugawara *et al.*, 1996a), e.g. dopamine (Kuramitz *et al.*, 1999) and thiourea (Kuramitz *et al.*, 2000b) were used. (Strept)Avidin–biotin binding was recently applied in DNA hybridization and protein sensors (Chapters 3–5 and 11). In the literature, both avidin and streptavidin were frequently claimed to be electroinactive species (e.g. Steiger *et al.*, 2003; Sugawara *et al.*, 1994, 1996a). Such a claim was at variance with our experience showing that proteins containing tyrosine and/or tryptophan produce oxidation signals at carbon electrodes, while proteins containing cysteine residues are electroactive at mercury electrodes. We, therefore tested electroactivity of avidin and streptavidin at carbon and mercury electrodes (Figure 5).

Electrochemical investigation of avidin and streptavidin at carbon and mercury electrodes showed (Havran *et al.*, 2004) (in contrast to the generally accepted belief about electroinactivity of these proteins, Steiger *et al.*, 2003; Sugawara *et al.*, 1994, 1996a) that both proteins produced electrochemical responses at these electrodes. Both avidin and streptavidin produced oxidation signals at carbon electrodes due to Tyr and Trp residues (Brabec and Mornstein, 1980). At HMDE these proteins yielded a CPS peak H (Kizek *et al.*, 2001; Tomschik *et al.*, 1998, 2000) at highly negative potentials. In addition avidin but not streptavidin produced at alkaline pH a peak at about -0.6 V (peak S) (Figures 2B and 5B) related to the formation of avidin compound with the electrode mercury. Characteristic (Brdicka's) catalytic signals of avidin in the cobalt-containing solutions (Ruttikay-Nedecky and Anderlova, 1967), reviewed in Brezina and Zuman (1958) and Palecek (1983), were obtained by DPV (Figure 6A). The introduction of the derivative pulse polarography in the analysis of proteins more than 30 years ago (Palecek and Pechan, 1971; Palecek *et al.*, 1977) significantly increased the sensitivity of the polarographic

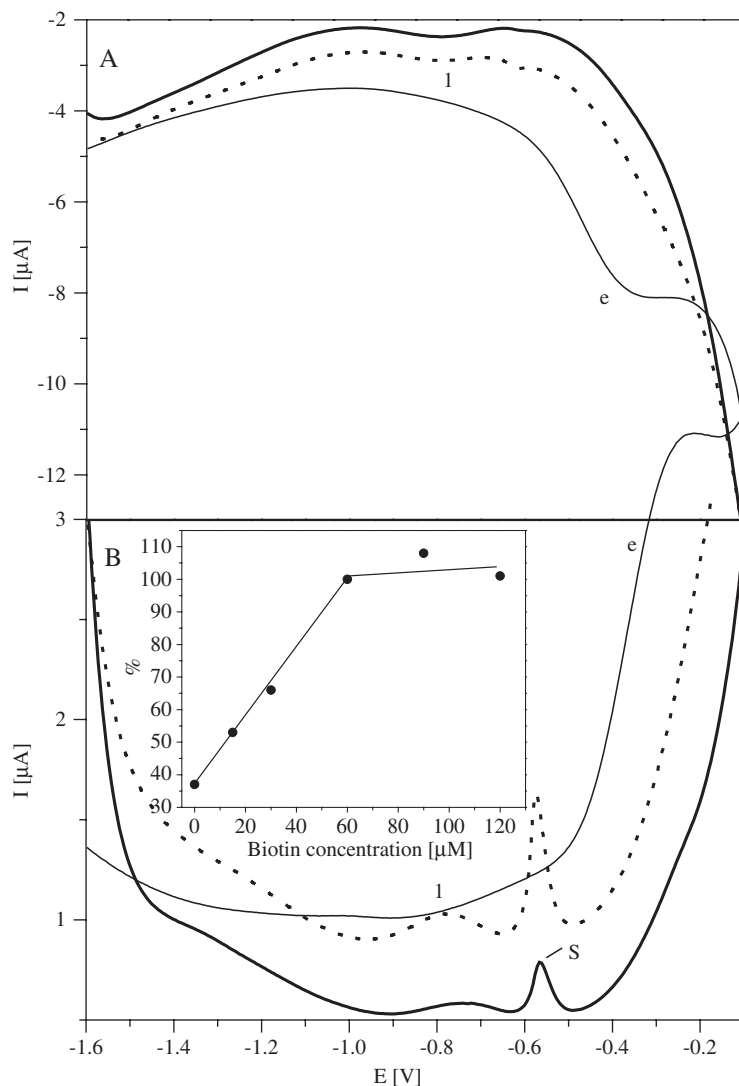


Fig. 5. Comparison of a.c. voltammetric behavior of avidin, avidin–biotin complex and biotin. (A) Out-of phase a.c. voltammograms of 15 μM avidin (solid line) and its complex with 60 μM biotin (dotted line) at HMDE. I_{av} corresponds to current of avidin and $I_{\text{av-b}}$ current of avidin–biotin complex. (B) In-phase a.c. voltammograms of (a) 15 μM avidin and its complexes with (b) 15, (c) 30 and (d) 60 μM biotin at HMDE. Inset: Dependence of peak S height on concentration of biotin in avidin–biotin complex (current value of 15 μM avidin with 60 μM biotin (1:4) was taken as 100%). Adsorptive transfer stripping a.c. voltammetry (AdTS a.c.V) in 0.1 M $\text{NH}_4\text{Cl} + \text{NH}_4\text{OH}$ (pH 9.5) (dotted line). Instrument settings: $t_{\text{A}} = 1$ min, $f = 230$ Hz, amplitude = 50 mV, phase angle: (A) 90° , (B) 0° . Other details as in Figure 1. Adapted with permission from Havran *et al.* (2004). Copyright 2004 Wiley-VCH.

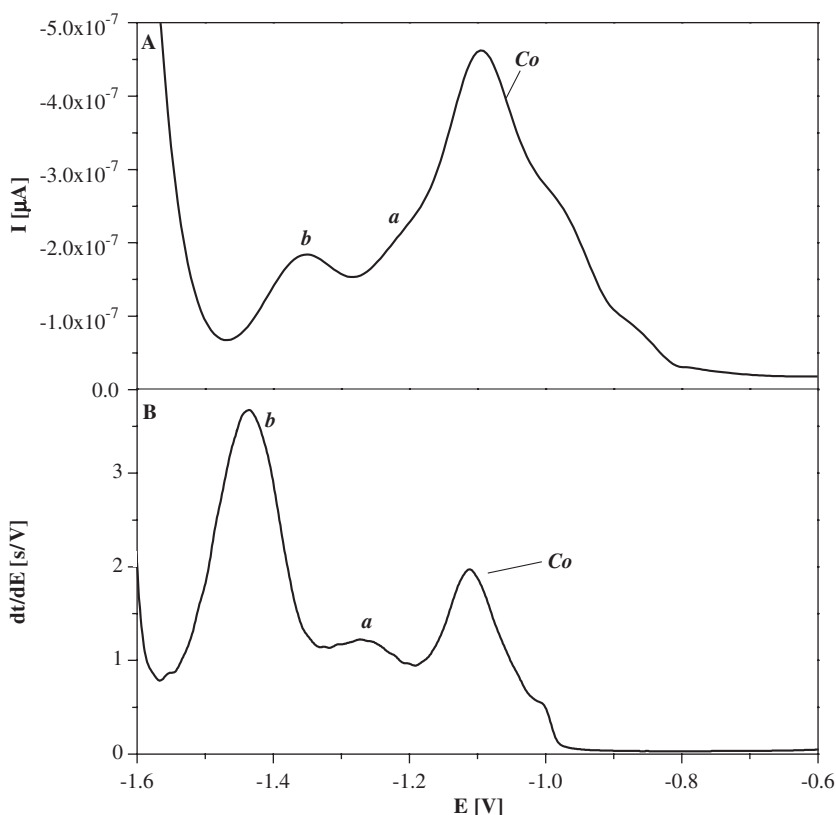


Fig. 6. Comparison of avidin BCR measured by (A) AdTS DPV and (B) AdT CPSA. Peak of cobalt(II) reduction (Co) and peaks *a*, *b* yielded by avidin in the presence of cobalt ions (Brdicka reaction) (straight line). 1 mM avidin or streptavidin (dash line) were adsorbed at HMDE and measured in Brdicka solution – 0.1 M $\text{NH}_4\text{Cl} + \text{NH}_4\text{OH}$ with 1 mM $[\text{Co}(\text{NH}_3)_6]^{3+}$ (pH 9.5). AUTOLAB settings – AdTS DPV: pulse amplitude 50 mV, scan rate 10 mV s^{-1} , initial potential 0 V, $t_A = 1 \text{ min}$; AdT CPSA: $t_A = 1 \text{ min}$, $I = -5 \mu\text{A}$. Adapted with permission from Havran *et al.* (2004). Copyright 2004 Wiley-VCH.

analysis of proteins in cobalt-containing solutions. Recently, AdTS, DPV (Figure 6A) and chronopotentiometric (CP) signals (Figure 6B) of $1 \mu\text{M}$ avidin at HMDE were compared. Both techniques produced characteristic catalytic protein signals but the peaks yielded by AdT CPSA were better separated and better developed (Figures 6A and B). In our work with other proteins, we obtained better results with CPSA as compared to DPSV; a more systematic study would be, however, necessary to find out under which conditions and for what reasons one of the techniques is superior to the other.

3.1.1. Avidin–biotin binding

As a result of biotin binding, avidin signals underwent changes related to the formation of avidin–biotin complex. The oxidation signals (obtained at

pyrolytic graphite electrode) as well as catalytic Brdicka's signals (Figure 7), and peak H decreased (Havran *et al.*, 2004), while peak S increased (Figure 5B) due to biotin binding.

3.1.1.1. Catalytic hydrogen evolution responses. Avidin (1 μM) was titrated with biotin in a test tube and the avidin catalytic responses were measured by AdT CPSA in (Brdicka) cobalt-containing solution. The titration curve showed an equivalence point corresponding to binding of a single biotin per avidin molecule (Figure 7). In this point, the height of the more negative peak *b* decreased to 16% of the original peak of avidin (with no bound biotin) while peak *a* completely disappeared. This steep decrease in both peaks was clearly related to the formation of the avidin–biotin complex. The same equivalence point was obtained when peak H was measured in sodium tetraborate (pH 9.5, in the absence of cobalt) (Havran *et al.*, 2004).

To understand the changes in the electrochemical behavior of avidin on binding a single biotin molecule, avidin structure and properties should be considered. Avidin structure is well understood and it is known that binding of a single biotin has little effect on the avidin structure. Avidin–biotin complex is more stable than avidin itself; the complex shows higher stability toward both chemical and thermal denaturation conditions. Assuming that, similarly to some other proteins (Section 3.2), avidin may undergo at the mercury surface a limited unfolding, which results in stronger adsorption of its molecule at the

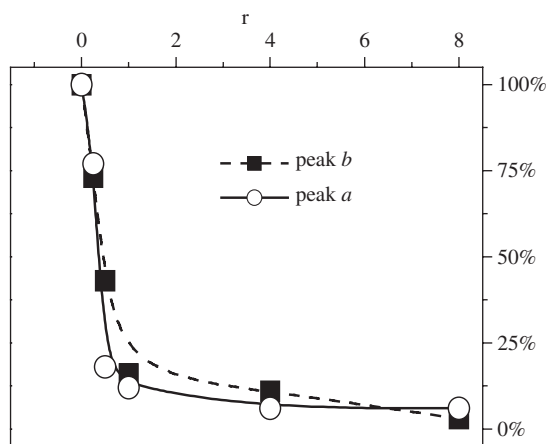


Fig. 7. Titration of avidin with biotin as measured by BCR. Dependence of avidin peaks *a* and *b* heights on concentration of biotin in avidin–biotin complex. 1 μM avidin was incubated with different concentrations of biotin – 250 nM, 1 μM , 4 μM in Eppendorf tubes, *r*, molar ratio of biotin/avidin. Avidin or avidin–biotin complexes were adsorbed at HMDE and measured by AdT CPSA in Brdicka solution. AUTOLAB settings: $t_A = 1$ min, $I = -5 \mu\text{A}$. Other details in Figure 6. Adapted with permission from Havran *et al.* (2004). Copyright 2004 Wiley-VCH.

surface, explanation of the observed changes can be sought in changes of the interfacial properties related to the solution stability of the protein (Figure 8).

3.1.1.2. Adsorption/desorption and peak S. AC voltammetric (ACV) phase-out measurements showed that the avidin–biotin complex was adsorbed in a wide potential region less firmly than avidin alone (Figure 5A). Avidin remained adsorbed at HMDE even at potentials around -1.5 V in contrast to avidin–biotin, which gave no evidence of its presence on the surface at these potentials. The surface unfolding of avidin could not be very large because unfolding of this protein by thermal denaturation induced very large changes in its electrochemical behavior (Section 3.2.2) (not observed in the adsorbed native avidin).

When phase-in mode of ACV or CV were used, avidin produced peak close to -0.6 V (peak S, Figure 5B). Under the same conditions streptavidin did not

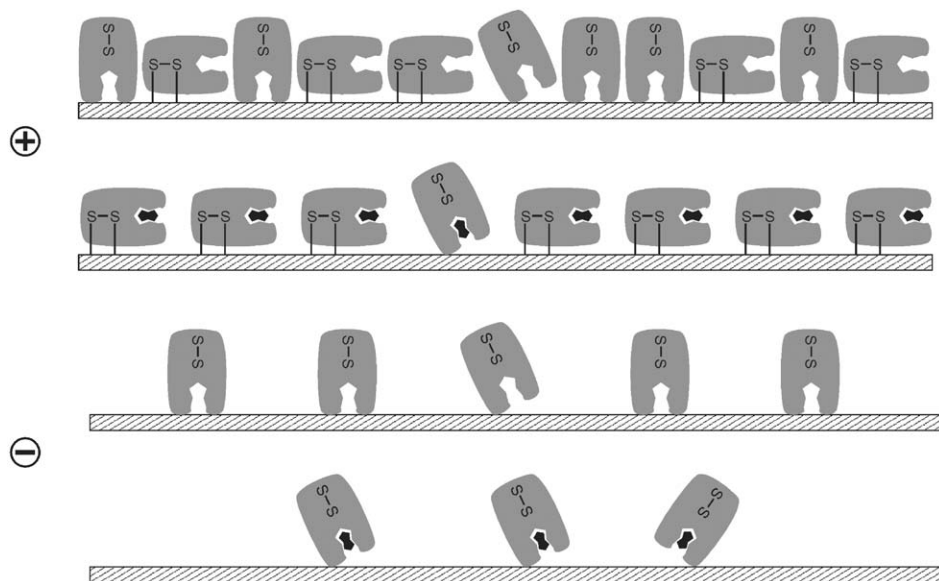
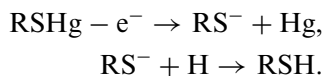


Fig. 8. Interfacial behavior of avidin and its complex with biotin at the mercury electrode. At potentials more positive than peak S, \oplus (Figure 5) avidin molecules are either chemisorbed via cystine/cysteine residues or undergo strong hydrophobic interactions with the hydrophobic mercury surface through its biotin-binding pocket. In avidin–biotin complex, the biotin-binding pocket is shielded by the bound biotin preventing the hydrophobic adsorption via this pocket and shifting the equilibrium in favor of the chemisorption (indicated by an increase of peak S, Figure 5). Around -0.6 V the Hg–S bond is reduced, followed by re-orientation of the molecules. At negative potentials of the BCR, \ominus (Figures 6 and 7) Hg–S chemisorption is absent and the adsorption of the avidin–biotin complex is much weaker than that of avidin (which still can be adsorbed via the hydrophobic pocket). Thus, the larger number of avidin molecules adsorbed at the surface at negative potentials yield higher BCR (Figures 6 and 7) than the smaller number of weakly adsorbed and probably randomly oriented avidin–biotin molecules. See the text for more details. Adapted with permission from Havran *et al.* (2004). Copyright 2004 Wiley-VCH.

yield such peak while bovine serum albumin (BSA) displayed a CV peak, which was smaller and broader than that of avidin. Avidin peak S height was strongly dependent on accumulation potential E_A showing a maximum at +0.13 V. This dependence suggested that peak S is related to formation of a compound with the electrode mercury. When the potential was scanned in the negative direction the Hg-S bond was reduced probably according to the earlier suggested mechanism for this type of protein reactions (Havran *et al.*, 2004; Heyrovsky *et al.*, 1994, 1997; Honeychurch, 1997):



The results so far obtained did not allow us to decide whether the disulfide group in avidin was reduced or remained unbroken (Havran *et al.*, 2004). The ability of avidin to form a sparingly soluble mercury compound is potentially useful for a highly sensitive determination of avidin by the cathodic stripping voltammetry.

Titration of 15 μM avidin with biotin resulted in a linear increase of this peak up to 4 equivalents of biotin (Figure 5B), showing, thus, a dependence strongly different from those of the catalytic Brdicka peaks (Figure 7) and peak H (Havran *et al.*, 2004), in which a decrease of the signals with an equivalence point corresponding to 1 biotin per avidin molecule was observed.

3.1.2. Interfacial behavior of avidin and avidin-biotin

To explain the complicated behavior of avidin and its complexes with biotin at the mercury electrode a tentative scheme was offered (Havran *et al.*, 2004). It was assumed that at potentials more positive than those of peak S, adsorption of avidin and its biotin complex involved both physical and chemical forces. In the physical adsorption of the positively charged avidin molecules, hydrophobic interactions prevailed while electrostatic interactions at the positively charged surface did not contribute to adsorption of this protein. The hydrophobic biotin-binding pocket of avidin (Livnah *et al.*, 1993), known to be partially accessible to the solvent (Pugliese *et al.*, 1993), was probably strongly attracted to the hydrophobic mercury surface. Such a strong adsorption could be facilitated by the partial unfolding of the protein at the electrode surface. It could thus be expected that hydrophobic adsorption and chemisorption (involving cystine/cysteine residues) of the avidin molecules would prevail. On the other hand, in the more stable avidin-biotin the protein unfolding at the surface would be more limited and the hydrophobic pocket would be shielded by the strongly bound biotins preventing strong hydrophobic interactions with the surface in most of the adsorbed molecules. Thus, in the population of the avidin-biotin molecules, Hg-S chemisorption would prevail. When scanning potential in the negative direction, the prevalence of the chemisorbed molecules would result in a higher peak S (Figure 5B).

After the reduction of the HgS bond reorientation of the avidin molecules (at potentials more negative than peak S) could take place as indicated by peak I (Figure 5A). Assuming that the avidin–biotin molecules had little chance to get adsorbed via the hydrophobic pocket, their adsorption at negative potentials would be much weaker than that of avidin. Actually, ACV indicated less firm adsorption of avidin–biotin complex and around -1.5 V very little adsorption of this complex took place (Figure 5A). Catalytic (Brdicka's) peak *b* appeared at these potentials (Figures 2B and 3) and its decrease on biotin binding (Figure 3) could be due (i) to smaller number of avidin–biotin molecules at the negatively charged electrode as compared to the number of avidin molecules and (ii) to a different orientation of the protein molecules (remaining at the surface) not favorable for the catalytic hydrogen evolution (Figures 6 and 8). The results suggested that binding of a single biotin to avidin was sufficient for affecting the adsorption strength and orientation of avidin at the negatively charged electrode surface.

3.1.3. Concluding remarks

Avidin and streptavidin are electroactive species producing electrochemical signals at carbon (Havran *et al.*, 2004) and mercury electrodes (Figures 5–7). Binding of biotin resulted in changes of avidin electrochemical signals. In spite of a large amount of the electrochemical literature on avidin(streptavidin)–biotin systems, such changes have not yet been reported (Steiger *et al.*, 2003; Sugawara *et al.*, 1994, 1996a). The tryptophan-containing biotin-binding pockets of avidin and streptavidin form a “hydrophobic box”. Binding of biotin to avidin or streptavidin decreased accessibility of Trp residues to the solvent and consequently also to the electrooxidation on the PGE. Thus, a decrease of the oxidation peak (Havran *et al.*, 2004) could be expected. On the other hand, the increase of peak S (Figure 5B) and the decrease of catalytic signals at more negative potentials (Figures 6 and 7) could hardly be understood without considering orientation of the protein molecule at the surface and eventually some changes in the protein folding at the interface. A decrease in peak H after biotin binding (Havran *et al.*, 2004) was in agreement with the suggested scheme (Figure 8).

The above data may be of importance in biotechnologies. For example, avidin-labeled DNAs in biosensors could be detected without using any additional label, such as enzyme–avidin conjugates. Particularly interesting appear the low detection limits obtained with peak H (Sections 2.2 and 5.2.1). Difficulties with the mercury electrodes in sensors might be overcome by using solid amalgam electrodes (Jelen *et al.*, 2002; Mikkelsen and Schroder, 2003; Yosypchuk and Novotny, 2002).

3.2. Native, mutant and denatured proteins

It is well known that protein conformation is closely related to the protein function. An exchange of a single amino acid can induce great changes in the

protein conformation and its biological activity. For example, a specific point mutation can transform the tumor suppressor function of the protein p53 into a cancer-enhancing function (Soussi *et al.*, 1994; Vogelstein and Kinzler, 1992). Therefore, fast and sensitive methods for detection of mutation and conformational changes in proteins are sought. It was perhaps Ruttkay-Nedecky *et al.* (1977, 1984), who performed first electrochemical studies of mutant proteins. They studied polarographic and voltammetric behavior of the tobacco mosaic virus (TMV) and its coat protein (Brabec, 1985; Ruttkay-Nedecky, 1964, 1971; Ruttkay-Nedecky and Anderlova, 1967; Ruttkay-Nedecky and Bezuch, 1971; Ruttkay-Nedecky and Vesela, 1977; Ruttkay-Nedecky and Palecek, 1980; Ruttkay-Nedecky and Brabec, 1985; Ruttkay-Nedecky *et al.*, 1977). They showed a good sensitivity of the d.c. polarographic Brdicka's catalytic responses (BCR) for the mutant proteins with exchanged cysteine residues and for the TMV degradation and its protein denaturation (see below for details).

Later, it was shown by means of an integrated optical technique that a neutralizing mutation (glutamic acid to glutamine) in either of two different positions (15 or 48) of the soluble fragment of cytochrome *b5* resulted in vastly different adsorption properties in the mutated proteins (Ramsden *et al.*, 1995). The protein adsorption was affected by the properties of the surface. Adsorption to a highly negatively charged surface was fully reversible and adsorption to a neutral phospholipid bilayer was very slow and practically irreversible; a highly positively charged surface acted as a sink, i.e. adsorption was limited only by transport rate. It can be expected that electrochemical methods, which are capable to provide data on electron transfer and adsorption of proteins at different surfaces charged to various potentials, might reflect changes in protein interfacial properties resulting from their mutations and from their conformational changes in solution. These methods appear potentially useful tools of protein analysis. So far, however, they have been little used in studies of mutated proteins.

Recently, surface exposed cysteines were engineered in the structure of recombinant horseradish peroxidase (HRP) (Ferapontova *et al.*, 2002). Recombinant forms of HRP with either streptavidin or histidine tags at the protein C-terminus with additional cysteine residues in positions 57, 48, 89 and 309 were prepared. The effect of the mutations on the direct electron transfer between a gold electrode and the enzyme was studied. Adsorptive immobilization of recombinant HRPs on pre-oxidized Au electrode provided a stable current response to H₂O₂, due to its biocatalytic reduction. Introduction of cysteine or the histidine tags in the C-terminal of the enzyme resulted in an increased efficiency of the electron transfer due to favorable proton and electron transfer pathways.

3.2.1. Changes in protein catalytic responses due to single amino acid exchange

3.2.1.1. Catalytic hydrogen evolution in cobalt-containing solutions. Ruttkay-Nedecky *et al.* (1984) studied BCR of the whole virus TMV-Vulgare and its protein by d.c. polarography. The coat protein (17.5 kDa) of all TMV strains and mutants contain a single cysteine residue in position 27, which is specifically

masked in the protein structure. This cysteine becomes accessible due to the protein denaturation but it does not depend on the integrity of the virus particle. It was found that BCR of isolated protein of TMV-Vulgare were identical with those of the mutant TMV-483 (histidine instead of glutamine in position 9). On the other hand, BCR of TMV-Ni-2068 mutant, containing additional cysteine residue (instead of tyrosine in position 139), were twice as much intensive as compared to TMV-Vulgare.

Wt α -synuclein does not contain any cysteine residue and accordingly this 14 kDa protein did not produce any BCR (M. Masarik, T. M. Jovin and E. Palecek, unpublished). We measured cysteine-containing mutants A18C and A140C by CPSA in 1 mM $[\text{Co}(\text{NH}_3)_6]^{3+}$, 0.1 M $\text{NH}_4\text{Cl-NH}_4\text{OH}$, pH 9.5. In this medium, A140C displayed well-developed BCR signal (Figure 9) similar to those produced by other cysteine-containing proteins (Section 3.1). In contrast, the other cysteine-containing mutant, A18C did not show any BCR under the same conditions (Figure 9). Wt α -synuclein is considered as a natively unfolded protein. Recently, the presence of some ordered structure in the wt protein was reported (Maiti *et al.*, 2004). There is, however, no information available about the ordered structure in the A18C and A140C mutants. Usually, the differences in the BCR of e.g. native and denatured proteins, were explained as being due to burying of some cysteine residues in the folded molecule. If the studied mutants

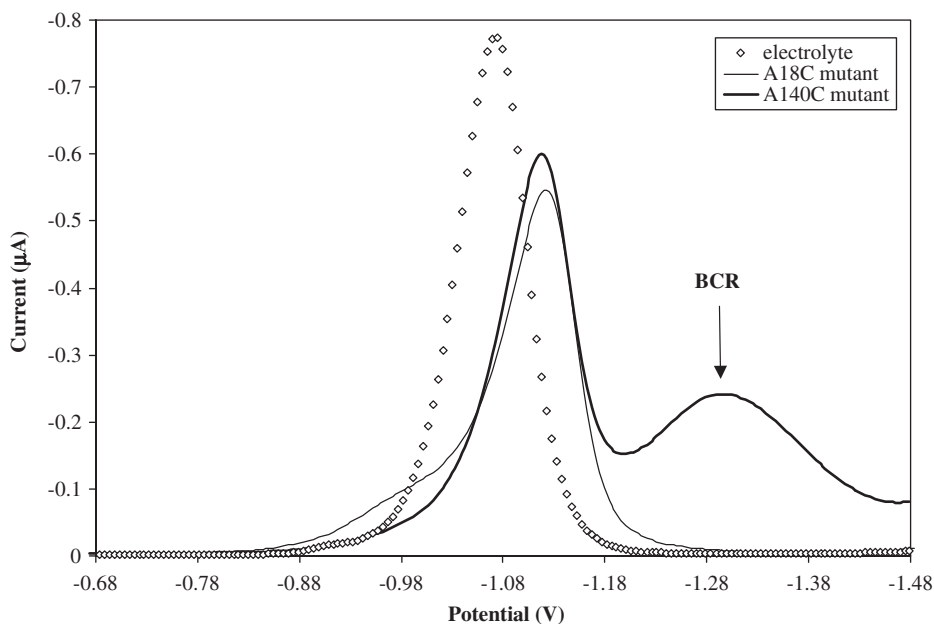


Fig. 9. Comparison of DPV BCR of two α -synuclein mutants containing cysteine residue in different positions. A140C (2.5 μM) (bold line) and A18C (thin line). Measurement was performed using adsorptive transfer technique in 0.1 M ammonium buffer + 1 mM $[\text{Co}(\text{NH}_3)_6]^{3+}$, pH 9.5 as a background electrolyte, AUTOLAB, time of accumulation was 60 s (adsorption was from 50 mM phosphate buffer pH 7.2), step potential 5 mV and modulation amplitude was 50 mV (J. Dvorak, M. Masarik and E. Palecek, unpublished).

lack any ordered structure, then the difference in their electrochemical responses can hardly be due to different accessibilities of the cysteine residues in the protein molecules. Studies of wt and mutant α -synucleins in denaturing solvents might help to find the reason for different electrochemical behavior of these proteins.

3.2.1.2. Catalytic hydrogen evolution in absence of cobalt (peak H). TMV-Vulgare and its mutant TMV-Ni-2068 were studied by d.c. polarography in 20 mM sodium carbonate, pH 10.5 (Ruttkay-Nedecky *et al.*, 1984). In this medium, TMV-Ni-2068 (containing additional cysteine) produced a pre-sodium wave, while TMV-Vulgare showed no response. It was concluded that the additional cysteine residue in the protein was responsible for the observed pre-sodium wave and generally that the d.c. pre-sodium wave is caused by cysteine residues. Considering our results obtained with peptides such as angiotensin and vasopressin (Section 2.2.1.1), we may expect that the appearance of the pre-sodium wave (and also of peak H) of TMV-Vulgare protein will depend on the ionic conditions and particularly on pH. Pre-sodium wave/peak H of TMV-Vulgare protein might appear at more acid pHs. We showed that peptides not containing cysteine produced peak H at neutral and acid pHs but not at alkaline pHs (Section 2.2). Wild-type α -synuclein, the protein, which does not contain any cysteine residue (Section 5.2), produced peak H (at neutral pH) suggesting that the presence of cysteine residue in the protein molecule is not a necessary condition for the catalytic hydrogen evolution at the mercury electrodes (Masarik *et al.*, 2004).

We used wild-type (wt) α -synuclein (Section 5.2.1) and its mutant proteins: A53 T, A18C and A140C, in which non-polar alanine (A) was replaced by polar threonine (T, in position 53) or by (polar) cysteine (C) in positions 18 or 140. Peak H was measured by CPSA of all four proteins at 150 nM concentration and peaks differing in their heights and peak potentials were obtained (Figure 10). The presence of cysteine residue in the protein molecule greatly affected the protein electrochemical behavior (J. Dvorak, T. M. Jovin and E. Palecek, unpublished). Peaks of A18C and A140C were higher and appeared at less negative potentials than the peak of the wt protein (Figure 10). Such differences in the synuclein signals were in agreement with the influence of the presence of cysteine residue in peptide molecules (Section 2.2) and could be owing to a strong effect of the $-SH$ group on the protein adsorption at the mercury surface. It is interesting that the position of the cysteine residue induced a large difference in the peak potential of cysteine-containing mutants. Surprisingly, also A53 T peak H differed from that of the wt protein, suggesting that it is not just the cysteine residue whose presence can affect the electrochemical response of the protein.

The observed differences in the electrochemical behavior of wt and mutant proteins with only single amino acid exchange per molecule are very encouraging. Studies of such protein molecules may be of great importance not only from biological point of view. Such studies may also help to understand better the interaction of proteins with surfaces and particularly with electrodes and

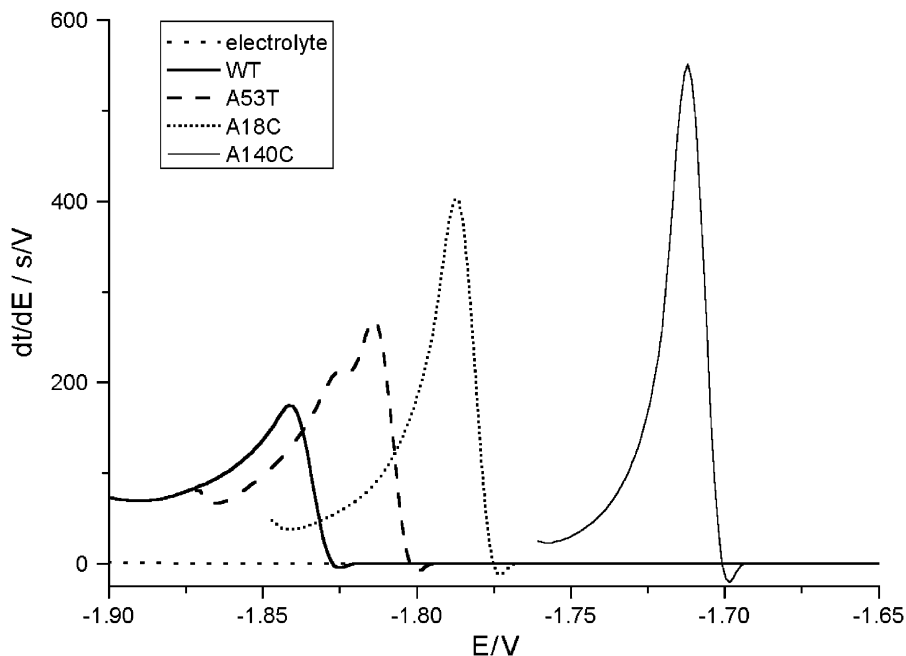


Fig. 10. CPS peaks H of 150 nM wild type (wt) and mutants of α -synuclein. Wt (—) and A53 T (-----) do not contain cysteine while A18C (.....) and A140C (——) do. Tris-(2-carboxyethyl) (1 mM) phosphine, hydrochloride was added to keep the proteins in a reduced state. AUTOLAB: Stripping current was $-3 \mu\text{A}$ and measurement was performed in electrochemical cell in 0.2 M sodium phosphate, pH 7.2. (J. Dvorak, M. Masarik and E. Palecek, unpublished).

contribute to elucidation of undergoing processes responsible for the electrochemical protein responses. While the above results have only preliminary character, we have good reasons to believe that electrochemical methods are capable to recognize mutant proteins from their wt forms. In addition to the above synuclein mutants, we are currently studying other proteins, such as wt and mutants of the tumor suppressor protein p53. Similarly to the above results, we are observing differences in the electrochemical behavior of wt and mutant p53 proteins (L. Havran, S. Billova and E. Palecek, unpublished). Our results suggest that mercury electrodes are more sensitive to tiny differences between wt and mutant proteins than carbon electrodes.

3.2.2. Denatured proteins

Proteins can be denatured by changing their chemical or physical environments. Heating, adding a chemical denaturant such as guanidium chloride or urea, changing pH or using high pressure are the most common methods (Fersht, 1999). Small protein may denature reversibly, regaining their native structure when returned to conditions favoring folding. Many larger proteins denature

irreversibly. After removing the denaturation conditions, they often aggregate and precipitate. The protein-denatured state is not a single fixed state. It is a collection of states of very similar energies that are in rapid equilibrium with one another. Optical methods give indication of residual secondary structure. Notation “D” is frequently used for the denatured state in contrast to the unfolded state in the presence of the denaturation conditions (denominated as “U”). The highly unfolded state in concentrated denaturant such as urea resembles the random coil the most.

Different responses of native and denatured proteins were observed by d.c. polarographic methods already several decades ago (Brezina and Zuman, 1958) (Chapters 1 and 18). Later, several authors showed that at least with some proteins partial or full protein unfolding might take place at the electrode surface (Scheller *et al.*, 1975; Honeychurch, 1997; Roscoe, 1996). Such “surface denaturation” can be influenced by various factors, such as the ionic conditions and particularly by specific adsorption of anions on negatively charged mercury surfaces (Razumas *et al.*, 1989), hydrophobicity and electric charge of the surface, etc. Results from a number of authors suggest that extensive surface denaturation of many proteins is improbable: (i) polarography and voltammetry was successfully applied to studies of denaturation and renaturation of some proteins (Rutt kay-Nedecky *et al.*, 1984), (ii) enzymatic activity of the protein at the mercury electrode was reversibly switched on and off depending on the electrode potential (Santhanam *et al.*, 1977) and (iii) α -helix and β -structure of polylysine were recognized by a.c. polarography and the helix-coil transition was followed by a.c. polarography (Scheller and Jehring, 1972; Scheller *et al.*, 1973).

The question of the protein surface denaturation was discussed by Honeychurch (1997). To overcome the difficulty with contradictory data, he suggested that only small protein molecules such as those studied by Scheller *et al.* (1975) (e.g. insulin, ribonuclease A and lysozyme) undergo extensive surface denaturation, while larger proteins adsorb only via a small part of the molecule and the rest of the protein is preserved. It was shown, however, that a relatively small TMV protein (17.5 kDa) produced very different electrochemical signals in its native and denatured forms (Section 3.2.1) both at the mercury (Rutt kay-Nedecky *et al.*, 1984) and carbon electrodes (Brabec, 1985). The difference between the native and denatured protein was particularly striking at the dropping mercury electrode. Native TMV-Vulgare protein yielded BCR at about -1.55 V while the denatured protein produced much higher signal at potentials by about 100 mV more negative (Rutt kay-Nedecky, 1971; Rutt kay-Nedecky and Bezuch, 1971; Rutt kay-Nedecky and Palecek, 1980). Such a striking difference suggests that conformations of native and denatured proteins differ not only in solution but also at the electrode surface. Brabec measured BCR of cytochrome *c* using derivative and normal pulse polarography (DPP and NPP, respectively) as well as phase-sensitive a.c. polarography. He found that in the characteristic double wave more negative wave B was sensitive to the denaturant-induced protein unfolding. DPP and d.c. polarographic waves B rose with increasing concentration of urea or sodium perchlorate in parallel with absorbance change of the protein solution suggesting that both polarographic

methods reflected conformational changes of cytochrome *c* induced in solution by the denaturant. On the other hand, NPP (i.e. the technique working with large voltage excursions during the drop life time) showed under the same conditions significant dependence of BCR on the initial potential (E_i). At E_i less negative than -1.0 V (against Ag/AgCl sat. KCl reference electrode) high wave B (characteristic for unfolded cytochrome *c*) was observed. It was concluded that cytochrome *c* undergoes surface denaturation in a wide range of potentials around the potential of zero charge but not at more negative potentials of the polarographic BCR. These results corresponded well with that of DPP and NPP investigations of dsDNA (Palecek, 1974), which showed dependence of the DNA NPP signals on E_i suggesting DNA surface denaturation around -1.2 V (Chapter 3). On the other hand, DPP (working with small voltage excursion during the drop life time) reflected changes in DNA structure in solution, showing no secondary changes in the DNA structure at the electrode surface.

In principle, any biomacromolecule possessing an ordered structure has to undergo at least a small structural change in the segment adhering to the surface, when it is adsorbed. The problem of the protein surface unfolding (surface denaturation) can be compared to the surface denaturation of DNA (Chapter 3). DNA can be completely unwound at the electrode surface or its denaturation can be negligible, depending on the ionic conditions, material and potential of the electrode and the mode and rate of the potential scanning. Conditions preventing or stimulating of dsDNA unwinding at mercury electrodes were already described. In contrast analogous conditions, which could be valid for all proteins can be hardly found. On the other hand, it should be not difficult to find conditions for a certain individual protein under which the surface unfolding is minimized or maximized.

Using AdT CPSA or DPSV, we have analyzed native and denatured forms of two proteins greatly differing in their structures: (i) avidin possessing a very stable conformation in its native state (Section 3.1) and (ii) natively unfolded α -synuclein (Section 5.2). Denaturation of avidin resulted in an increase in peak H height accompanied by a striking shift to negative potentials (by almost 70 mV) and change in the shape of this peak (Figure 11). Under the same conditions, also a great increase of peak S and a slight shift of its E_p to negative potentials was observed. In contrast to large differences between Brdicka DPV signals of native and denatured avidin, the signals of native α -synuclein and its cysteine-containing mutant on one hand (Figure 10) and the same proteins exposed to denaturation conditions on the other hand were almost identical (M. Masarik and E. Palecek, unpublished) in agreement with the reported lack of ordered structure in native α -synuclein (Section 5.2). The behavior of native and denatured avidin shown in Figure 11 agrees well with the electrochemical behavior of denatured ssDNA and native dsDNA at moderate ionic strengths and neutral pH. At mercury and carbon electrodes ssDNA displayed higher voltammetric or chronopotentiometric signals than dsDNA. In contrast to DNA, we cannot expect the same behavior in all proteins and perhaps not even with avidin; different experimental conditions and different electrochemical methods may affect the protein adsorption and orientation at the surface and produce different electrochemical responses. Particularly, the catalytic responses may

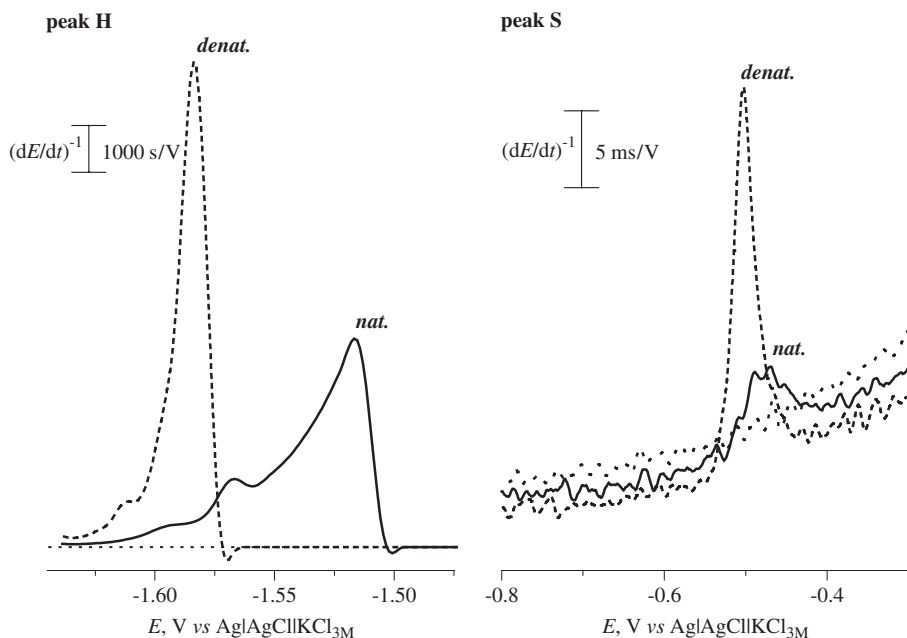


Fig. 11. AdT CPSA of native (solid line) and thermally denatured (dashed line) avidin. $2.5 \mu\text{M}$ ($40 \mu\text{g}/\text{mL}$) avidin was adsorbed on HMDE from $3 \mu\text{L}$ drop. Protein-modified HMDE was transferred in 2 mL of 0.2 M acetate buffer, $\text{pH } 5.0$ (dotted line). AUTOLAB, stripping current $-5 \mu\text{A}$, accumulation time 60 s (V. Dorcak and E. Palecek, unpublished).

depend not only on the amount of protein adsorbed at the electrode surface but also on the protein ability to catalyze the hydrogen evolution. This ability can be influenced by number of factors, including the distance of the catalytic site from the electrode surface, character of the neighboring amino acids, etc.

3.3. Voltammetric and polarographic signals of some proteins in presence of guanidine

In addition to BCR, peaks H and S yielded by some proteins at mercury electrodes, a new protein signal at negative potentials was reported (Luo *et al.*, 2003). BSA and human serum albumin (HSA) but not lysozyme produced polarographic and voltammetric signals at -1.78 V in the presence of $0.8 \mu\text{M}$ CoCl_2 and 0.2 M guanidine hydrochloride and 0.2 M NaOH at mercury electrodes. The voltammetric peak was linearly proportional to the albumin concentration in the range of $5 \mu\text{g}$ – $20 \mu\text{g}/\text{mL}^{-1}$. The nature of the observed signals was unclear. The authors claimed that these signals cannot be due to the catalytic hydrogen evolution because of lack of proton donors in 0.2 M NaOH . They did not consider, however, that under the given conditions protonated guanidine forming a complex with the protein might serve as a potential proton donor.

4. REDOX STATES OF PEPTIDES AND PROTEINS

Two cysteine (Cys) residues in various parts of the polypeptide chain can be oxidized to form a disulfide bridge, provided these residues are adjacent in the three-dimensional structure of a protein. Disulfide bridges are usually not found in intracellular proteins. The reduced state of these proteins is frequently associated with their biological activity, such as their sequence-specific DNA binding. Therefore, fast methods capable to recognize reduced and oxidized states of proteins are sought.

4.1. Electroreduction of disulfide bonds

Electrochemical methods are potentially useful for this purpose. Several reviews on adsorption and reduction of proteins as well as on their ability to catalyze hydrogen evolution at mercury electrodes were published (Banica and Ion, 2000; Dryhurst *et al.*, 1982; Honeychurch, 1997; Palecek, 1983). The reduction of disulfide bonds of proteins at mercury electrodes will be here briefly summarized; more details can be found in a review by Honeychurch (1997). Detailed studies of electrochemical reduction of cystine in aqueous solution at mercury electrodes are available (Fedurco *et al.*, 1993; Heyrovsky *et al.*, 1994, 1997; Monterroso-Marco and Lopez-Ruiz, 2003). Reduction of the disulfide bond in longer peptides and proteins is, however, more complicated and less well understood (Palecek, 1983). The possibility of the reduction of the disulfide bond was considered in early papers concerning the protein d.c. polarographic catalytic waves (Brezina and Zuman, 1958). D.c. polarographic waves due to reduction of the disulfide bond in proteins were shown by Cecil and Weitzman in 1964 (1964; Weitzman, 1965) in all studied proteins containing the disulfide groups (i.e. in serum albumin, chymotrypsin, trypsin, ribonuclease and insulin) at acid pH. Similar signals were obtained with linear sweep voltammetry (Lee *et al.*, 1970; Stankovich and Bard, 1977) and DPP (Palecek *et al.*, 1977). DPP peaks were much better developed than the d.c. polarographic waves obtained under the same conditions. Cecil and Weitzman (1964) pointed out that the accessibility of the disulfide groups to electroreduction depended on protein conformation.

Stankovich and Bard (1977) studied in detail insulin and proposed a mechanism of its electrochemical behavior at HMDE. They showed that two accessible disulfide bonds were broken, while the third one, which was folded in the hydrophobic pocket, remained intact. Reoxidation of the reduced species to parent occurred only at short times; at longer times reoxidation of only one disulfide group was possible. The reformation of the reduced disulfide groups at short times was possible presumably because the protein conformation was partially maintained at the surface by Hg-S interactions and intramolecular hydrogen bonding. To achieve the reoxidation, the suhydryl groups (formed originally due to the electroreduction) had to remain in close proximity (on the short time scale) to allow reformation of the disulfide group. This behavior of insulin consisted with that of urease, in which its enzymatic activity was

destroyed and restored upon oxidation and reduction of the enzyme (Santhanam *et al.*, 1977). Cecil and Weitzman (1964) observed an additional d.c. polarographic wave at about -1.2 V, which they explained by the reduction of the protein in a second adsorption layer. Later, cyclic voltammetric studies suggested involvement of a solution species rather than an adsorbed one. Studies of BSA showed electrochemical behavior in principle similar to that of insulin. Containing 17 disulfide bonds and one sulfhydryl group, 69 kD BSA is a more complicated protein than 5.7 kD insulin with three disulfide bonds. A model of BSA mercury electrode interaction involved adsorption of BSA with strong interaction of several of the exposed disulfide bonds with the electrode surface, while BSA structure was maintained by internal disulfide bonds and intramolecular hydrogen bonding. After the electroreduction of the exposed disulfide at least some sulfhydryl groups remained in a close proximity to reform upon electrooxidation.

4.2. Electrochemical analysis of reduced peptides and proteins

In spite of the above promising results, to our knowledge no attempt was done to develop electrochemical methods useful in determination of the peptide and protein redox states. Such methods, even if they can be applied only to a limited number of proteins, may be very useful in the analysis of many DNA-binding proteins, oncoproteins, etc., which keep their specific biological activities only in their reduced states. Electrochemical analysis of oxidized (disulfide bond containing) proteins is relatively easy. On the other hand some precaution is necessary when working with intracellular proteins in their reduced state, which easily oxidize on air. These proteins are routinely kept frozen (usually at -70°C) in the presence dithiothreitol (DTT), 2-mercaptoethanol or other sulfur-containing reducing agents interfering with the protein analysis at mercury electrodes. To develop a method for the analysis of the redox states of such proteins, it was, therefore, necessary first to find the procedures, which would prevent protein oxidation during the sample handling, without the addition of the reducing agents interfering with the electrochemical analysis.

We started our work with peptides commercially available in their reduced and oxidized states. We used peptide SS38 (Table 1) and its reduced form SH38 for a systematic study of their electrochemical behavior. From our current investigations a complex picture of the interfacial behavior of these peptides and some specific proteins emerged (V. Dorcak, L. Havran, M. Brazdova and E. Palecek, unpublished). Among the studied electrochemical signals we observed the most striking difference between the reduced and oxidized peptides in their peak H (Figure 12). A measure of $1\ \mu\text{M}$ reduced peptide yielded at relatively short waiting a very high peak H at about -1.69 V as compared to its oxidized form, which produced about 20-fold smaller peak H at slightly more negative potentials. Oxidation of SH38 resulted in an expected decrease of peak H. Few microliters of the sample corresponding to 3 pmol of the peptide sufficed for the analysis. The reasons for such a great difference in the ability of the reduced and oxidized peptide to catalyze the hydrogen evolution at the mercury

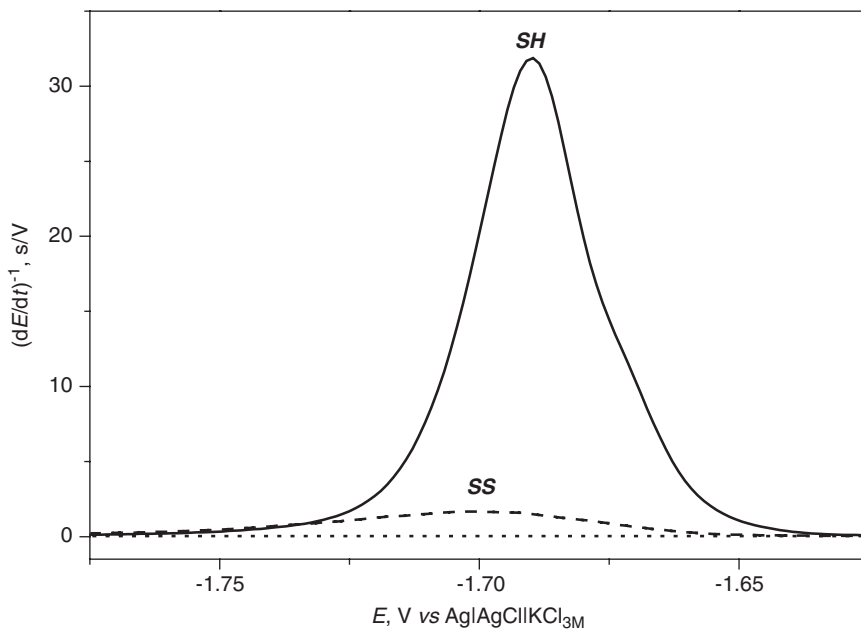


Fig. 12. AdT CPSA of reduced SH38 (solid line) and oxidized SS38 (dashed line) peptides (Table 1). Peptide (1 μM) was adsorbed on HMDE from 3 μL drop. Peptide-modified HMDE was transferred in 2 mL of 0.05 M borate buffer, pH 9.3 (dotted line). AUTOLAB, stripping current $-5 \mu\text{A}$, accumulation time 60 s (V. Dorcak and E. Palecek, unpublished).

electrode surface are not completely clear. We observed a striking dependence of these signals on the accumulation potential (V. Dorcak and E. Palecek, unpublished). It is not excluded that under the given conditions the reduced peptide is able to form an ordered, compact layer at the surface, which is a better catalyzer of the hydrogen evolution.

5. AGGREGATION OF PROTEINS

A number of human diseases is associated with protein misfolding that result in malfunctioning of the cellular machinery (Dobson, 1999; Kruger *et al.*, 2000). Recently, great attention has been focused on a group of diseases where proteins convert from their normally soluble forms into insoluble fibrils (Serpell, 2000; Serpell *et al.*, 2000; Weinreb *et al.*, 1996; Weller, 2001). The final forms of such aggregates often have a well-defined fibrillar nature known as amyloid. (This term was originally used to discuss proteinaceous aggregates because some of their properties resembled those of starch/amylose.) The group of about 20 diseases includes Alzheimer's and PDs, Creutzfeldt–Jakob's diseases, etc. Each disease is associated with a particular protein and aggregates of this protein are thought to be the indirect or direct origin of the pathological conditions. The first phase of amyloid formation seems to involve soluble oligomers resulting from relatively non-specific interactions (Bucciantini *et al.*, 2002; Dobson, 2003;

Lashuel *et al.*, 2002; Schlunegger *et al.*, 1997). The earliest species visible by atomic-force or electron microscopy resemble small bead-like structures often described as amorphous aggregates or micelles. They are thought to assemble into mature fibrils perhaps by lateral association and structural reorganization. Interestingly, the ability of polypeptide chains to form amyloid structures is not limited to the relatively small number of disease-associated proteins. Formation of fibrils was observed with many other peptides and proteins such as lysozyme, myoglobin and also with homopolymers such as polylysine and polythreonine (Dobson, 2001, 2003; Schubert *et al.*, 2000).

5.1. Parkinson's disease (PD)

Although, clinical symptoms of PD were first described about 200 years ago, reports on possible parkinsonian syndromes dates back to thousands of years (Goedert, 2001; Uversky *et al.*, 2001). PD is the second most common neurodegenerative disease, which is characterized by a loss of dopaminergic neurons in the *substantia nigra*. Some surviving nigral dopaminergic neurons contain cytosolic filamentous inclusions known as Lewy bodies (LBs) and Lewy neurites (LNs) are also involved in pathogenesis of Alzheimer's disease and multiple system atrophy (Goedert, 2001). The major fibrillar material of LBs and LNs was shown to be α -synuclein (Spillantini *et al.*, 1997, 1998). Recent studies indicate that α -synuclein is a key player in the pathogenesis of several neurodegenerative disorders (Uversky, 2003).

5.2. α -Synuclein (ASyn)

ASyn was first described in 1988 as a neuron-specific protein localized to the nucleus (Maroteaux *et al.*, 1988). Amino acid sequence of this protein possesses a high degree of conservatism. The primary sequence of the human 14 kDa ASyn is composed of 140 amino acids (aa) (Table 3). It can be subdivided into three regions: (1) Residues 1–60 form the N-terminal region. It contains four 11-aa imperfect repeats with hexamer motif (KTKEGV). (2) The central region includes the highly amyloidogenic NAC sequence (residues 61–95) containing two additional KTKEGV sequences. (3) The C-terminal region, which is constituted by residues 96–140, is enriched in acidic aa residues and prolines, suggesting disordered conformation. Three highly conserved Tyr residues are located in this region.

ASyn is highly expressed in various parts of the brain. Natively, it is unfolded but undergoes aggregation leading to fibrillar structures (Uversky, 2003). Aggregation of ASyn can be induced *in vitro* in different ways and it is promoted by a variety of conditions that generate oxidative stress and by mutations in the ASyn gene (Kruger *et al.*, 1998; Polymeropoulos *et al.*, 1997; Zarranz *et al.*, 2004). Aggregated ASyn exhibits a number of different morphologies depending on the aggregation incubation time and solution conditions, with mature amyloid fibrils constituting the main morphology in fully aggregated solutions

in physiological buffers (Conway *et al.*, 2000; Ding *et al.*, 2002; Dobson, 2003; Hoyer *et al.*, 2002, 2004; Lashuel *et al.*, 2002; Uversky, 2003). ASyn aggregation *in vitro* is commonly studied by several methods such as CD spectroscopy, fluorescence measurements (Thioflavin T binding), electron microscopy and atomic force microscopy (Harper and Lansbury, 1997). Recent reports suggest that the toxicity of amyloidogenic proteins may lie in the soluble oligomeric intermediates rather than in insoluble fibrils (Hardy and Selkoe, 2002; Kayed *et al.*, 2003). Studies of ASyn aggregation *in vitro* are associated with the hopes for better understanding, diagnosing and therapy of the PD (Caughey and Lansbury, 2003; Goedert, 2001).

5.2.1. Electrochemical analysis of α -synuclein

ASyn does not contain any redox-active center for reversible electrochemistry. Moreover, it does not contain any cystine or cysteine residues producing signals at mercury electrodes (Sections 2.2 and 3) nor tryptophan oxidizable at carbon electrodes (Section 2.1). Among 140 ASyn amino acids only 4 are tyrosines (Table 3). Possibilities of electrochemical analysis of this protein are thus rather limited. Nevertheless, we tried to investigate an ability of ASyn to catalyze hydrogen evolution at mercury electrodes and oxidizability of tyrosine residues at carbon electrodes. First we tested HMDE in connection with various methods of electrochemical stripping analysis, such as linear sweep voltammetry (LSV), square wave voltammetry (SWV) and constant current chronopotentiometry (CP) at HMDE at 60 s accumulation time (t_A) to detect 2 nM ASyn in 50 mM sodium phosphate (pH 7.0) (M. Masarik *et al.*, 2004). Best results were obtained by CPSA; no baseline correction was necessary to obtain a well-developed peak H. As expected, even at three orders of magnitude higher concentrations, native ASyn produced no BCR in a cobalt containing solution at the HMDE (no cystine/cysteine residues are contained in the protein molecule). At ASyn concentrations about 100-fold higher than those required for peak H an oxidation peak of tyrosine (Y) residues was observed at the carbon paste electrodes (CPE) at +0.8 V both by CPSA and SWV stripping analysis. In both cases baseline correction was necessary to obtain a well-developed peak.

5.2.1.1. Peak H of native α -synuclein. ASyn (150 nM) was analyzed by conventional CPSA without stirring to compare it with AdT CPSA, performed under the same conditions. The resulting peaks with identical peak potential (E_p) differed only slightly in their heights suggesting that AdT can be used in the analysis of native ASyn (M. Masarik *et al.*, 2004). The concentration dependence of the native ASyn peak H between 10 and 1000 nM at t_A 60 s produced a curve typical for adsorption processes with a linear calibration up to 175 nM ASyn. At higher concentrations the peak area did not change, indicating full coverage of the electrode. The peak potential was shifted with increasing concentration of ASyn to more positive values. ASyn (400 pM) adsorbed from a 5 μ L drop yielded a well developed peak H at t_A 10 min showing thus the ability

Table 3. Amino acid composition of α -synuclein

Amino acid residue	No. of residues	Percent content
Ala(A)	19	13.6
Arg(R)	0	0
Asn(N)	3	2.1
Asp(D)	6	4.3
Cys(C)	0	0
Gln(Q)	6	4.3
Glu(E)	18	12.9
Gly(G)	18	12.9
His(H)	1	0.7
Ile(I)	2	1.4
Leu(L)	4	2.9
Lys(K)	15	10.7
Met(M)	4	2.9
Phe(F)	2	1.4
Pro(P)	5	3.6
Ser(S)	4	2.9
Thr(T)	10	7.1
Trp(W)	0	0
Tyr(Y)	4	2.9
Val(V)	19	13.6

Number of amino acids: 140, molecular weight: 14460.1, theoretical pI: 4.67.
Tyrosines(Y) are shown in bold.

```

          10           20           30           40           50           60
          |           |           |           |           |           |
MDVFMKGLSK  AKEGVVAAAE  KTKQGVAAEA  GKTKEGVLYV  GSKTKEGVVH  GVATVAEKTK
          |           |           |           |           |           |
          70           80           90           100          110          120
EQVTNVGGAV  VTGVTAVAQK  TVEGAGSIAA  ATGFVKKDQL  GKNEEGAPQE  GILEDMFPVDP
          |           |           |           |           |           |
          130          140
DNEAYEMPSE  EGYQDYEPEA

```

From: <http://us.expasy.org/sprot/>

of AdT CPSA to detect ASyn down to 2 fmol, i.e. 30 pg. At least three factors contributed to this high sensitivity: (i) the catalytic hydrogen evolution process, (ii) adsorptive accumulation of the protein, and (iii) transfer of the adsorbed ASyn layer to a blank electrolyte which enabled the use of microliter volumes of the analyte.

5.2.1.2. Oxidation of native α -synuclein at carbon electrodes. ASyn (250 nM) in 0.2 M acetate buffer (pH 5.0) at t_A 60 s produced CPSA and SWV responses, which changed into well-developed peaks Y after baseline correction. Square

wave voltammetry of 250 nM ASyn in AdS and AdTS modes yielded almost identical ASyn oxidation signals (Figure 3B) suggesting that the transfer method (medium exchange, *ex situ* measurements) is suitable for synuclein studies at both mercury and at carbon electrodes.

5.2.2. Aggregation of α -synuclein

In vitro aggregation of ASyn was induced by stirring at 37°C employing the same solution conditions as in Antony *et al.* (2003). First, the electrochemical responses of native ASyn (Masarik *et al.*, 2004) were compared with those obtained after a time interval in which both CD spectra and Thioflavin T fluorescence showed significant changes in ASyn responses (Antony *et al.*, 2003). Peak Y of 3.5 μ M aggregated ASyn was by 9% smaller than that of the native protein and the peak potential of the aggregated protein was slightly shifted to less positive values (Masarik *et al.*, 2004). Under these conditions, the carbon electrode was close to full coverage, suggesting that the difference in the peak heights of native and aggregated ASyn was not simply due to slower transport of the aggregated molecules to the electrode surface. The observed decrease in peak Y height and E_p was small but significant and appeared potentially useful for studies of the transition between native and fully aggregated states of ASyn. However, this method did not offer any special advantage over the currently used methods used in the studies of the ASyn aggregation.

5.2.2.1. *Peak H.* Substantially greater differences between native and aggregated ASyn were observed with HMDE (Masarik *et al.*, 2004). Aggregated ASyn yielded no peak H up to about 100 nM concentration in contrast to a well-developed peak produced by 2 nM native ASyn. Peak H of 150 nM aggregated ASyn was by about 77% smaller and its E_p was slightly less negative (about 4 mV) than peak H of native ASyn. These results showed that the peak H reflected aggregation of ASyn with a substantially greater sensitivity than peak Y showing thus greater potentialities for studies of ASyn aggregation.

5.2.2.2. *Early stages of α -synuclein aggregation.* The first stage in the process of amyloid formation is particularly important because: (i) This step in the aggregation pathway determine the rate of nucleation and thus the length of the lag-time, which is regarded as a key factor for the age of onset of the related disease (Harper and Lansbury, 1997). (ii) Recent studies have indicated that small, soluble oligomers of amyloidogenic proteins and peptides may possess a higher toxicity than the mature fibrils (Bucciantini *et al.*, 2002; Kaye *et al.*, 2003). Methods commonly used to follow amyloid formation exhibit high sensitivities for the fibrillar aggregates, but not for pre-fibrillar oligomers.

We were interested in whether our electrochemical methods would be able to detect any change in interfacial properties of ASyn in the time intervals where fluorescence and CD measurement showed no changes. In our first experiments, we observed a small decrease of peak Y (exceeding only slightly the experimental error) 24 h after initiation of the aggregation (Masarik *et al.*, 2004). On the other

hand, under the same conditions peak H decreased by about 41% with a concomitant > 30 mV shift in E_p to less negative values (Figure 13). Our further work showed significant changes in the height and E_p of peak H within first hours of the ASyn incubation (M. Masarik, T. M. Jovin and E. Palecek, unpublished). These results suggest that peak H reflects processes occurring in the initial lag phase (nucleation), such as the accumulation of pre-fibrillar oligomers. This assumption is supported by our preliminary results, which show different time courses in pre-aggregation changes in peak H, induced by low molecular mass substances known to influence the time course of ASyn aggregation.

To our knowledge, our work represents the first case when aggregation of the amyloidogenic protein is traced by methods of electrochemical analysis. At partial electrode coverage, these methods can reflect large changes in molecular mass of the analyzed protein caused by the aggregation because the electrochemical signal is affected by the rate of transportation of the molecule to the electrode surface. At the end of the aggregation process, when very large aggregates are formed, the electrochemical signal may greatly decrease and even disappear. On the other hand, significant changes in E_p of peak H in the early stages of aggregation are unexpected. They might be due to changes in better ability of the oligomers to catalyze the hydrogen evolution. A detailed explanation of the interfacial behavior of the oligomers does not appear possible without a better understanding of the catalytic process responsible for peak H.

5.2.3. Hydrogen evolution catalyzed by α -synuclein at mercury electrodes

Using ASyn peak H we obtained sensitivity by several orders of magnitude higher as compared to peak Y at carbon electrodes. No baseline correction was used for peak H and the method was not optimized to obtain the highest sensitivity of the ASyn determination. High sensitivity of peak H is related to catalytic nature of the electrode processes at mercury electrodes (Tomschik *et al.*, 2000). It is well known that reduction of protons occurs at mercury electrodes with the highest overvoltage of all metal electrodes. Proteins adsorbed at the mercury surface are able to reduce this overvoltage, giving rise to electrochemical signals much higher than any signals due to usual diffusion-controlled processes (Banica and Ion, 2000; Palecek, 1996; Tomschik *et al.*, 1998). The protein binds protons, which enter the electrode reaction. Detailed schemes of the hydrogen evolution catalyzed by proteins and other compounds was proposed by several authors (Banica and Ion, 2000; Heyrovsky and Kuta, 1965; Mairanovskii, 1968). In principle, they postulated that the electron uptake by protonated catalyst BH^+ produced a radical BH^\bullet , followed by the evolution of hydrogen, and by regeneration and protonation of the catalyst through the reaction with the buffer acid component. Protonated amino groups were supposed to be involved in the protein catalytic reaction (Brezina and Zuman, 1958; Heyrovsky and Kuta, 1965; Palecek, 1983). Our preliminary results suggest that other groups might also be involved (V. Dorcak, M. Masarik and E. Palecek, unpublished).

We showed that 400 pM ASyn can be determined in 5 μ L volume at moderate accumulation times (e.g. $t_A = 600$ s) corresponding to 30 pg of the protein

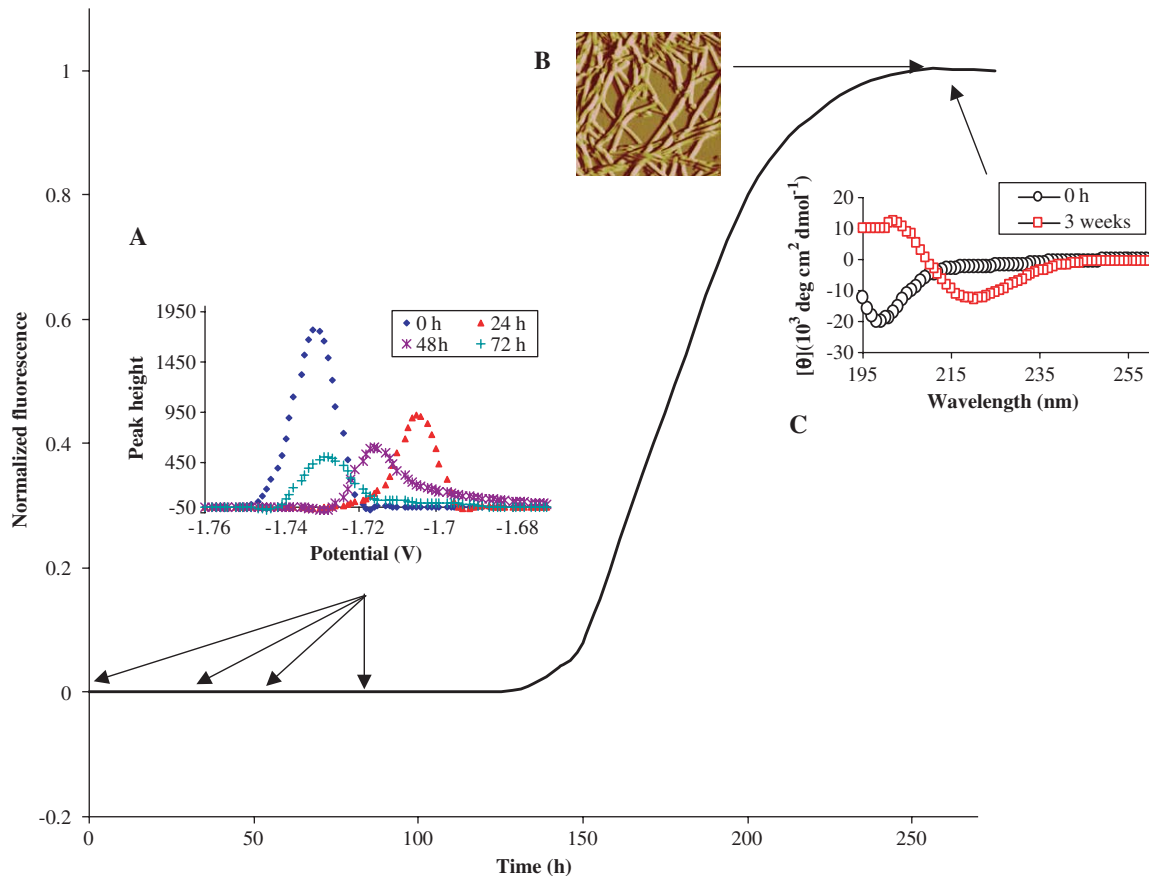


Fig. 13. Dependence on time of aggregation of wt α -synuclein *in vitro*. Aggregation was performed by stirring of 100 μ M α -synuclein solution in 25 mM Tris-HCl, pH 7.5 at 37°C for 3 weeks. Full line shows dependence of Thioflavine T normalized fluorescence on time of aggregation (the highest fluorescence value was taken as 1.0). (A) Pre-aggregation changes of α -synuclein as detected by CPS peak H; (B) atomic force microscopy amplitude image of mature amyloid fibrils, image size 1.9 \times 1.9 μ m²; (C) Far-UV CD spectra of native α -synuclein (○) before and (□) after aggregation. (B) and (C) 3 weeks of aggregation. For measurement, the sample was diluted to 10 μ M. Adapted in part from Masarík *et al.* (2004), with permission and M. Masarík, W. Hoyer, T. Jovin and E. Palecek, unpublished.

(Masariik *et al.*, 2004). This was, however, not the highest sensitivity, which can be achieved by this method. Our preliminary results suggest that optimization of the conditions, especially by decreasing the pH of the background electrolyte, will allow detection of even lower ASyn concentrations and lower ASyn amounts. Aggregation can also be traced by monitoring A_{280} of soluble material after ultracentrifugation of the ASyn sample. Using peak H very small amounts of ASyn sediments as well changes in ASyn concentration in the superantant can be analyzed to complement the data obtained by spectrophotometry. In other cases, when the high sensitivity of the determination is not necessary, other electrochemical methods besides CPSA might be used to study ASyn aggregation but the measurements will require higher ASyn concentrations.

6. SIGNALS OF THIOLATED OLIGODEOXYNUCLEOTIDES IN COBALT-CONTAINING SOLUTIONS

6.1. Thioalkanes and thiolated ODNs at gold and mercury electrodes

Self-assembled monolayers (SAMs) of thiolated ODNs (HS-ODN) were observed at gold electrodes and studied in detail by atomic force microscopy, electrochemical and other methods (Wackerbarth *et al.*, 2004a,b) (reviewed in Tarlov and Steel, 2003) (Chapters 3 and 15). In DNA sensors, they were frequently used in combination with redox indicators due to the lack of electroactivity of DNA at gold electrodes. SAMs formed by various thioalkanes were studied at mercury electrodes (Brucknerlea *et al.*, 1995; Finklea, 2000; Slowinski *et al.*, 1997; Stevenson *et al.*, 1998) offering defect-free atomically smooth mercury surface, which is ideal for SAM formation. To our knowledge, no report was published about SAMs formed by HS-ODNs at mercury electrodes. Recently, we have observed formation of HS-ODN SAMs at mercury electrodes and we found that these ODNs are electroactive, displaying different signals in various media (E. Palecek and V. Ostatna, unpublished). We have also found (Ostatna *et al.*, 2005) that these ODNs produce several specific voltammetric signals in cobalt-containing solutions not observed in absence of cobalt (Figure 14).

6.2. Thiolated ODNs in cobalt-containing solutions

We studied the voltammetric behavior of thiolated ODNs in Brdicka's cobalt-containing solutions suitable for electrochemical analysis of cysteine-containing peptides and proteins (Sections 2.2 and 3). Using DPV adsorptive transfer stripping (*ex situ*), a number of thiolated and unmodified ODNs were measured. Most measurements were performed with a 21-mer ODN, HS-(CTT)₇, which was attached to HMDE and the DNA-modified electrode was immersed in the cobalt-containing empty background electrolyte (Ostatna *et al.*, 2005). This ODN produced several DPV signals (Figure 14); two of them, that is peak 3 and

a less negative peak 2 increased with increasing buffer concentration suggesting that these peaks are due to the catalytic hydrogen evolution. These peaks have thus similar character as the polarographic and voltammetric signals of cysteine-containing peptides and proteins in the same medium. Usual background electrolyte containing 1 mM $[\text{Co}(\text{NH}_3)_6]^{3+}$, 0.1 M NH_4Cl , 0.1 M NH_4OH , pH 9.5 was used but similar results were obtained also in 1 mM $[\text{Co}(\text{NH}_3)_6]^{3+}$, 0.1 M borate buffer, pH 9.2; in the latter medium the HS-ODN signals were much smaller. Peak 3 of submicromolar HS-(CTT)₇ was much higher than the BCR of about 10-fold more concentrated cysteine-containing peptide (Ostatna *et al.*, 2005). Peak 3 appeared at less negative potentials than the peptide peaks what made thus possible to measure the HS-ODN and peptide signals separately. HS-(CTT)₇ was measured also at solid amalgam electrodes, which produced signals similar to those obtained with HMDE. The above new possibility to measure signals of thiolated DNA in the media suitable for protein analysis appears promising for the development of electrochemical sensors for DNA–protein interactions (Section 7.1.1.3), which may find use in biomedicine and proteomics.

We also measured peptide nucleic acid end-labeled with three cysteine residues (Cys-PNA) at HMDE in 1 mM $[\text{Co}(\text{NH}_3)_6]^{3+}$, 0.1 M NH_4Cl , 0.1 M NH_4OH , pH 9.5. In this medium, Cys-PNA yielded responses typical for proteins and peptides (Figure 15). The detection limit of Cys-PNA at moderate waiting times was in the range of tens of picograms per milliliter (around 10 fM). Unmodified PNA did not produce similar signals. It is interesting that the potentials of the Cys-PNA catalytic signals (Figure 15) are very similar to peptide and protein signals but differ greatly from those of HS-ODN (Figure 14). Is it because the cysteine moiety plays a critical role? Further studies of Cys-PNA, Cys-DNA and HS-ODNs may help to understand better the catalytic processes of these substances as well as peptides and proteins at mercury electrodes.

7. DNA–PROTEIN INTERACTIONS

In organisms, a large number of proteins are able to bind DNA. It was estimated that typically 6–7% of an eukaryotic genome and 2–3% a prokaryotic genome encodes DNA-binding proteins (Luscombe *et al.*, 2000). DNA-binding proteins play a central role in many aspects of genetic activity in an organism, such as transcription, replication, DNA repair, rearrangement, packaging, etc. It is, therefore, extremely important to investigate the processes of DNA–protein binding and the nature of complexes formed between DNA and proteins. In comparison to DNA and RNA, proteins are much less regular and therefore understanding them is more difficult. In the past two decades, we witnessed a great expansion in high-quality structures of DNA-binding proteins (Luscombe *et al.*, 2000). These structures and particularly those of their complexes with DNA have provided valuable insights into the principles of binding, including how specific nucleotide sequence is recognized by the protein and how DNA structure is usually modified on protein binding. On the basis of a

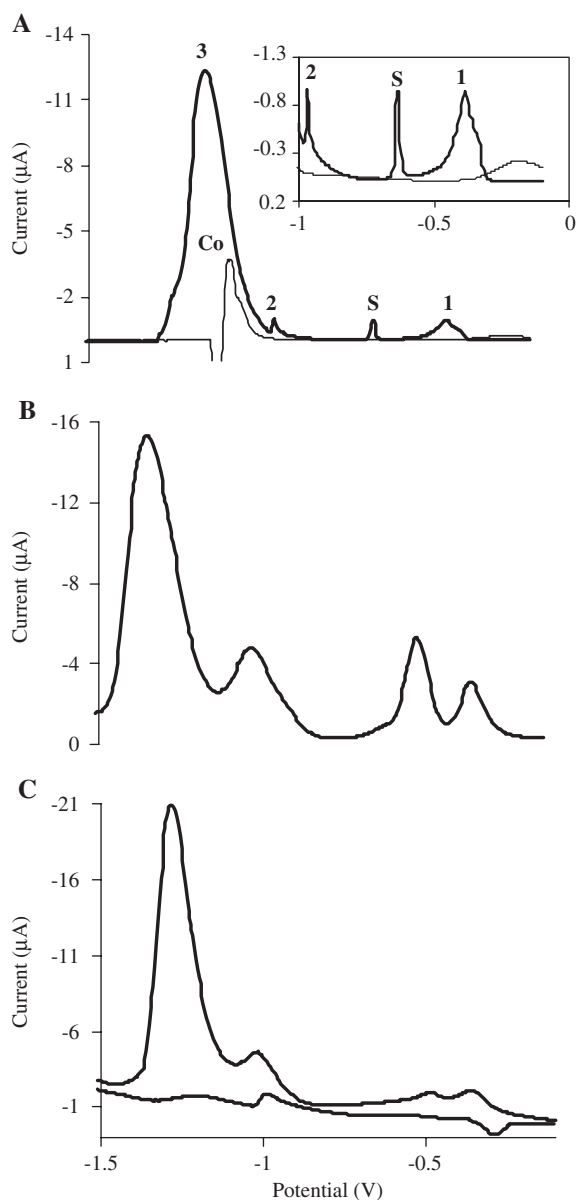


Fig. 14. Voltammetric responses of HS-(TTC)₇ in - 0.1 M NH₄Cl + NH₄OH with 1 mM [Co(NH₃)₆]³⁺ (pH 9.5). (A) AdTSDPV, 300 nM of HS-(TTC)₇ in 0.2 M NaCl, 1 mM phosphate buffer was adsorbed at the HMDE at open circuit for $t_A = 2$ min. The electrode with the adsorbed ODN layer was washed and transferred into the blank background electrolyte. AUTOLAB: Scan rate 9 mV s⁻¹, -0.1/-1.7 V, step 5 mV. (B) Square wave voltammograms of oligonucleotide 200 nM HS-(TTC)₇, $t_A = 2$ min, $f = 394$ Hz. Other details as in A. (C) Cyclic voltammogram of 200 nM HS-(TTC)₇, conventional AdS CV, $t_A = 30$ s step 5 mV, scan rate 0.5 V s⁻¹. (V. Ostatna and E. Palecek, unpublished).

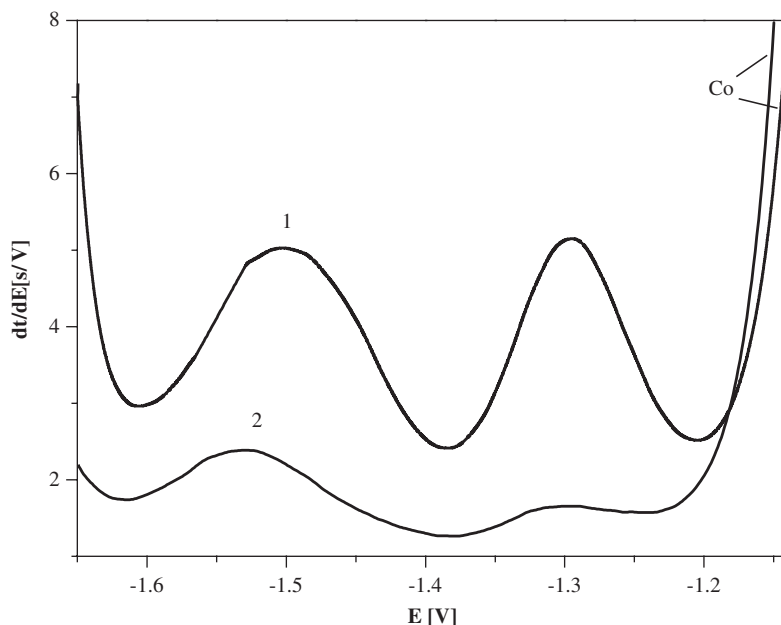


Fig. 15. AdTS CPESA of cysteine-labeled peptide nucleic acid (3Cys-PNA (H-CysGlyCysGlyCysAla-CTTCTCC-NH₂) at two concentrations: (1) 500 pg mL⁻¹, (2) 180 pg mL⁻¹ in 0.1 M ammoniacal buffer + 1 mM Co³⁺ (pH = 9.5). Adsorbed from 5 mM sodium phosphate, pH 7.0 with stirring. AUTOLAB $I_{\text{str}} = -2 \mu\text{A}$, $t_A = 7$ min (L. Havran P. Nielsen and E. Palecek, unpublished).

structural analysis of 240 DNA–protein complexes contained in the Protein Data Bank (PDB), the DNA-binding proteins were classified into eight different structural/functional groups, further sub-classified into 54 structural families. In addition to the high resolution X-ray crystal analysis, a number of methods have been used in studies of DNA–protein interactions. On the other hand, application of electrochemical analysis to studies of DNA–protein interactions was until very recently almost completely missing. Considering that both DNA and proteins are electroactive and can be analyzed with high sensitivity, application of electrochemical analysis in DNA–protein analysis appears natural and very promising.

7.1. Electrochemical analysis of DNA–protein interactions

The lack of electrochemical papers on DNA–protein interactions have been caused by several factors, such as (i) absence of sensitive determination of proteins not containing groups undergoing fast electron transfer at gold electrodes, (ii) difficulties with protein detection by the so-called single-surface techniques, mostly used in the electrochemical DNA hybridization sensors (Palecek and Fojta, 2001; Palecek *et al.*, 2002; Popovich and Thorp, 2002; Wang, 1999), (iii) lack of commercially available proteins binding specifically to

DNA and/or problems with compounds present usually in solutions in which such proteins are stored, etc. Similarly to sensors for DNA hybridization, the sensors for DNA–protein interaction can be based either on the single surface technique, in which the DNA–protein interaction and detection of this interaction is performed at the same surface, i.e. at the electrode, or on the double surface technique. In the latter technique, the DNA–protein interaction is performed at one surface while the detection is done separately on the detection electrode. Recently, first papers have appeared based on both of these approaches (Boon *et al.*, 2002a; Kerman *et al.*, 2005; Masarik *et al.*, 2004; Palecek *et al.*, 2004b). They will be briefly reviewed in the following paragraphs.

7.1.1. Single-surface techniques

7.1.1.1. Changes in DNA signals at mercury electrodes. In principle, interaction of DNA with proteins introducing changes in DNA, such as strand breaks induced by nucleases, can be easily followed by electrochemical methods. For example, cleavage of supercoiled DNA by deoxyribonuclease I in solution and at mercury surface was investigated by a.c. voltammetry (Fojta *et al.*, 1999). Introduction of a single break into the DNA molecule resulted in a specific signal (Chapter 3). This signal was used to study kinetics of the DNA cleavage. Compared to the cleavage in solution, the kinetics of cleavage of DNA adsorbed at the surface suggested restricted accessibility of the surface-confined DNA. Cleavage of immobilized DNA was affected by the electrode charge. At positively charged electrode the enzymatic reaction was inhibited in its initial stage, while moderately negative electrode charges stimulated the DNA enzymatic cleavage.

7.1.1.2. Changes in DNA and protein oxidation signals. Recently, Kerman *et al.* (2005) used single-walled carbon nanotube (SWCNT)-modified screen-printed carbon electrodes (SPCE) to monitor interaction the *Escherichia coli* single-strand binding (SSB) protein with DNA. SSB is a homotetrameric protein (4×18.8 kDa) playing an important role in DNA recombination, replication and repair (Chase and Williams, 1986). This protein binds selectively to single-stranded DNA and facilitates DNA unwinding by helicases (Meyer and Laine, 1990). Each monomer of SSB contains 4 tyrosine and 3 tryptophan residues, oxidizable at carbon electrodes (Section 2.1). DNA was bound to the SWCNT-SPCE via its end amino link and the DNA-modified electrode was immersed into the SSB solution ($10\text{--}50 \mu\text{g mL}^{-1}$). Binding of SSB to single-stranded DNA resulted in an appearance of the protein oxidation signal at about 0.55 V and in a decrease of the DNA guanine signal. No protein signal resulted from interaction of double-stranded DNA with the SSB solution.

7.1.1.3. Protein-induced changes in DNA charge transfer at gold electrodes. An interesting approach in studies of DNA–protein interactions, developed by Barton *et al.*, is based on dsDNA-mediated charge transport (Boon *et al.*,

2002b) (Chapter 3). It was shown that binding of a base flipping enzyme, MhhaI to dsDNA greatly decreased the signal of DNA-bound daunomycin suggesting that this protein binding disturbed the integrity of the base stack because of base flipping (Rajski *et al.*, 1999). Using a DNA repair enzyme (MutY, Section 7.2.1) binding to 8-oxoG:A and G:A mismatches, an attempt was made to use this approach in the detection of single base mismatches in DNA (Boon *et al.*, 2002b). However, no data consistent with the base flipping by MutY were found. On the other hand, the same group later showed (Boon *et al.*, 2003) that [4Fe4S] cluster, contained in MutY, can be utilized in the detection of MutY-DNA interactions (Boon *et al.*, 2003). Although, not detectable in the absence of DNA, the DNA-bound MutY displayed a reversible couple on cyclic voltammograms at gold electrodes. This method required enzymes with a prosthetic group capable of undergoing a redox process under certain conditions and a rather high concentration of MutY (0.8 mM) was necessary to obtain measurable signals (Boon *et al.*, 2003).

7.1.1.4. Changes in catalytic signals of thiolated DNA at mercury electrodes. The ability of peptides and proteins to produce signals due to the catalytic hydrogen evolution, such as peak H and BCR in cobalt-containing solution (Sections 2 and 3), as well as stripping currents related to the reduction of the HgS bonds offer great potentialities of the mercury electrodes in investigation of DNA-protein interactions. High sensitivity of peak H was utilized in the analysis of DNA-protein interactions by DST (Section 7.1.2).

Our preliminary results suggest that using mercury electrodes with immobilized thiolated ODNs, it might be possible to follow not only the cysteine-containing proteins (yielding the BCR) but also interactions of DNA with proteins not containing any cysteine/cystine residues, such as histones and protamines. This means that it might be possible to follow both sequence- and non-specific electrostatic DNA-protein binding. Histones mediate the folding of DNA in most of the eukaryotic cells (Wolffe, 1995; Zlatanova and Leuba, 2004). Histones can be removed from DNA by high salt concentrations, suggesting that major interactions between histones and DNA are electrostatic in nature.

We mixed 1 μ M HS-(TTC)₇ with equimolar concentration of histone H2A either at low or high NaCl concentrations and after short incubation, the HMDE was immersed in the mixture for 60 s and washed. The modified electrode was then transferred into an empty cobalt-containing background electrolyte to perform DPV measurement. The experimental arrangement was similar to that in Ostatna *et al.* (2005) (Section 6.2) but the electrolyte pH was 7.5. The catalytic signals of thiolated ODN were less intensive but qualitatively similar to those obtained at pH 9.5. Incubation of DNA with histone at low (50 mM) NaCl concentration resulted in a strong decrease of peak 3 of HS-ODN (Figure 16). No decrease of this peak was observed when this incubation was performed at 1 M NaCl, not favoring histone-DNA binding. This method appears more sensitive, than those discussed above in Sections 7.1.1.1 and 7.1.1.2.

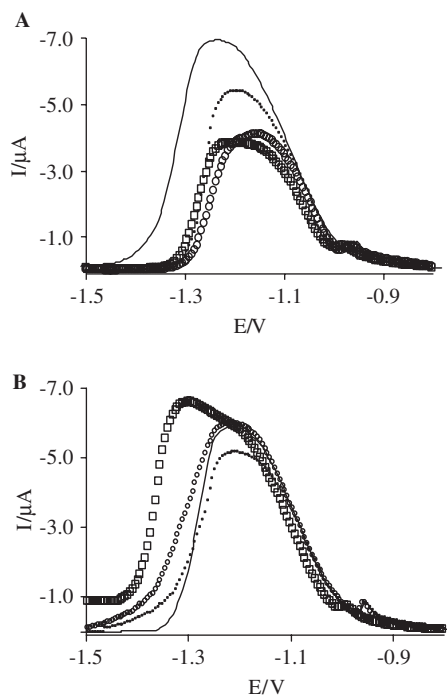


Fig. 16. AdTS DP binding histone to DNA. Voltammograms of thiolated oligodeoxynucleotide and its complexes with H2A histone in 0.1 M NH_4Cl , 0.1 M NH_4OH with 1 mM $[\text{Co}(\text{NH}_3)_6]\text{Cl}_3$, pH 7.5. Mixtures of 1 μM HS-(TTC)₇ (—) with 0.5 μM (.), 1 μM (○○○○) and 5 μM (□□□□) H2A histone A, in 50 mM (A) or B, in 1 M NaCl, 10 mM Tris, 1 mM EDTA, pH 7.5 were prepared and adsorbed at the HMDE ($t_A = 120$ s). Other details as in Figure 14A (V. Ostatna and E. Palecek, unpublished).

7.1.2. Double-surface techniques

Binding of practically any protein to DNA (or RNA) can be detected by electrochemical DST (Palecek, 2004; Palecek *et al.*, 2002). For example, DNA can be easily bound to the magnetic beads (Chapter 3) interacted with the protein followed by washing, dissociation of the bound protein and electrochemical detection (Figure 17) at mercury (e.g. using peak H) or at carbon electrodes (provided the protein contains oxidizable tyrosine or tryptophan residues). High sensitivity of peak H makes mercury electrodes particularly attractive for the protein detection but using carbon electrodes, in combination with efficient baseline correction, can be advantageous in sensors not requiring top sensitivity of the protein determination. Both types of electrodes were used in studies of MutS protein interaction with DNA aimed to detection of the DNA point mutations.

7.1.2.1. Binding of MutS proteins to DNA containing single base mismatch. MutS protein plays an important role in the DNA repair system in prokaryotic and eukaryotic cells (Jiricny, 1998, 2000; Jiricny *et al.*, 1988; Lamers *et al.*, 2000;

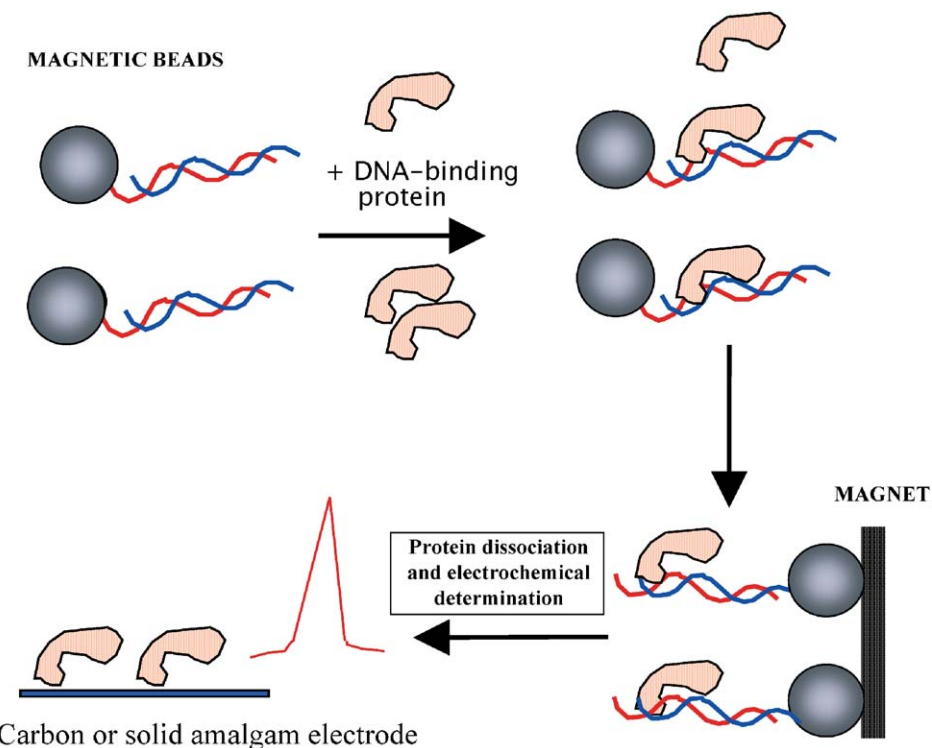


Fig. 17. Label-free assay of DNA–protein interaction using the double-surface technique. Biotinylated double-stranded DNA was immobilized on streptavidin-coated magnetic beads and interacted with the protein. After the magnetic separation, the protein was released from DNA and determined at mercury or carbon electrode. Using MutS protein, this method was used for the determination of the DNA point mutation (Palecek *et al.*, 2004b).

Obmolova *et al.*, 2000); it recognizes unpaired and mismatched bases in duplex DNA and can be used for detection of point mutations *in vitro* (Behrendorf *et al.*, 2002; Bi *et al.*, 2003; Palecek *et al.*, 2004b; Sachadyan *et al.*, 2000; Su *et al.*, 2004). Recently, we have shown that small amounts of this protein can be detected electrochemically at mercury and carbon electrodes without any labeling (Palecek *et al.*, 2004b). Using peak H, tens of attomoles of this protein were detected. The sensitivity of the determination at carbon electrodes was by more than three orders of magnitude lower. By combining high sensitivity of peak H with DST, we proposed a method for the determination of DNA point mutations (Chapter 3). We used biotinylated DNA duplexes attached to magnetic beads and interacted the immobilized DNA with MutS protein. The amount of the bound protein was detected on HMDE using peak H. DNA single base mismatches and insertion/deletions were detected in this way. Picogram amounts of MutS were determined by CPSA after MutS releasing from the beads. This highly sensitive label-free detection of MutS opened the door to development of DNA chips for a high through-put electrochemical determination of point mutation in genomic DNAs and supported the recent tendencies to

complement optical detection (Heller, 2002) in DNA hybridization sensors by simpler and less expensive electrochemical methods (Palecek and Fojta, 2001; Popovich and Thorp, 2002; Umek *et al.*, 2000; Wang, 1999). Moreover, these methods represent a new approach in the analysis of NA-protein interactions applicable to a large number of NA-binding proteins.

8. INTRODUCTION OF ELECTROACTIVE MARKERS TO PROBE THE PROTEIN STRUCTURE

When analyzing proteins by electrochemical methods the measured signals can be affected by changes in proteins conformation resulting from the interaction of the protein molecule with the electrode surface (Section 3). Moreover, studies of changes in protein conformation *in vivo* are difficult and electrochemical approaches for such studies have not been elaborated. To overcome these difficulties it would be convenient to use a chemical, reacting under mild conditions with exposed groups in a protein and introducing an electroactive marker to the protein molecule. Once the electroactive marker is covalently bound its presence in the protein molecule can be detected electrochemically (after protein isolation) and eventually also *in situ* by other methods. In fact, site-specific chemical modification has been frequently applied in characterization of proteins (Chen and Chen, 2003; Kuyama *et al.*, 2003; Kyte, 1995; Mardanyan *et al.*, 2001; Murphy *et al.*, 2002). The number of chemical probes of the protein structure, reacting with proteins in aqueous solutions under mild conditions, is however rather limited.

Earlier, we applied osmium tetroxide complexes with nitrogen ligand (Os,L) in chemical probing of the DNA structure (Chapter 3). Os,L reacted selectively with pyrimidine bases in single-stranded and distorted regions in DNA but not with intact double-stranded DNA regions (Palecek, 1992a). Os,L reaction introduced an electroactive marker in DNA producing several distinguished electrochemical signals at the mercury and carbon electrodes. Some Os,L complexes such as osmium tetroxide, 2,2'-bipyridine (Os,bipy) easily penetrated into cells recognizing local changes in the DNA structure (Palecek, 1992b, 1994). Moreover, Os,L-modified DNA was strongly immunogenic making thus possible to prepare specific antibodies for studies and localization of changes in DNA structure in cells (Palecek, 1992b, 1994; Palecek *et al.*, 1993a). We assumed that having a similar reagent for investigating the protein structure would be of tremendous significance. Earlier it was shown that complex of osmium tetroxide formed with tryptophan derivatives (Deetz and Behrman, 1980) bis(pyridine) osmate esters similar to thymine-Os,py compounds. We, therefore, attempted to use Os,L complexes and particularly Os,bipy for chemical modification of peptides and proteins.

Modification of several Trp-containing peptides with 2 mM Os,bipy resulted in characteristic electrochemical signals at mercury (Billova *et al.*, 2002) and carbon electrodes (S. Billova and E. Palecek, unpublished) (Figure 18). These signals were similar to those produced by Os,bipy-modified oligodeoxynucleotides and ssDNAs (Chapter 3). In contrast, peptides not containing Trp did not yield such

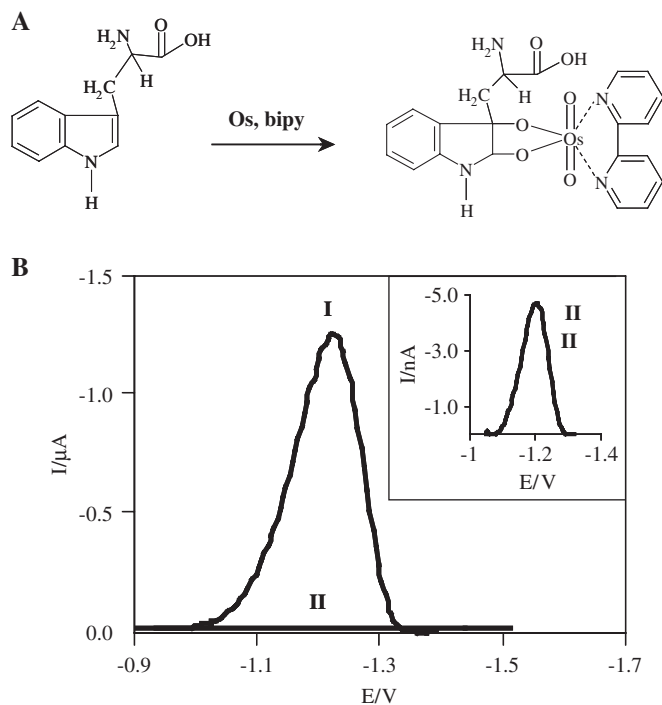


Fig. 18. (A) Formation of the ester between osmium tetroxide, 2,2'-bipyridine (Os,bipy) and tryptophan (B) Inset: differential pulse adsorptive stripping voltammograms of Os,bipy-modified Salmon Luteinizing Hormone - Releasing Hormone (SLH-RH). 200 ng mL⁻¹ of SLH in 0.1 M Britton-Robinson buffer, (I) pH 3.8, (II) pH 6.6, inset, pH 6.6 – zoom. Pulse amplitude 50 mV s⁻¹, scan rate 10 mV s⁻¹, $t_A = 120$ s, initial potential -0.10 V, stirring, moving average baseline correction. Reprinted from Billova *et al.* (2002). Copyright 2002, with permission from Elsevier.

signals. Trp-containing proteins yielded practically the same signals as Trp-containing peptides (S. Billova and E. Palecek, unpublished). In cysteine-containing peptides and proteins, Os,bipy modification resulted in a decrease or disappearance of the BCR in cobalt-containing solution, suggesting that Os,bipy modification resulted in a deep oxidation of the sulfhydryl group in the cysteine residue (S. Billova and E. Palecek, unpublished). Os,bipy-modified peptides were also investigated by capillary zone electrophoresis (CZE) and matrix-assisted laser desorption-ionization–time-of-flight mass spectrometry (MALDI–TOF MS) (Sedo *et al.*, 2004). Formation of a stable complex of Os,bipy with tryptophan residues was observed with both techniques. MALDI–TOF MS showed the formation of a product with characteristic osmium isotopic pattern (Figure 19). Oxidation of methionine and cysteine side chains to methionine sulfone and cysteic acid, respectively was detected by CZE and confirmed by MALDI–TOF and Post-Source Decay (PSD) mass spectra. Derivatization of peptides resulted in specific shifts of molecular weights of the peptides and their fragments as detected by PSD. Because not all natural amino acids were

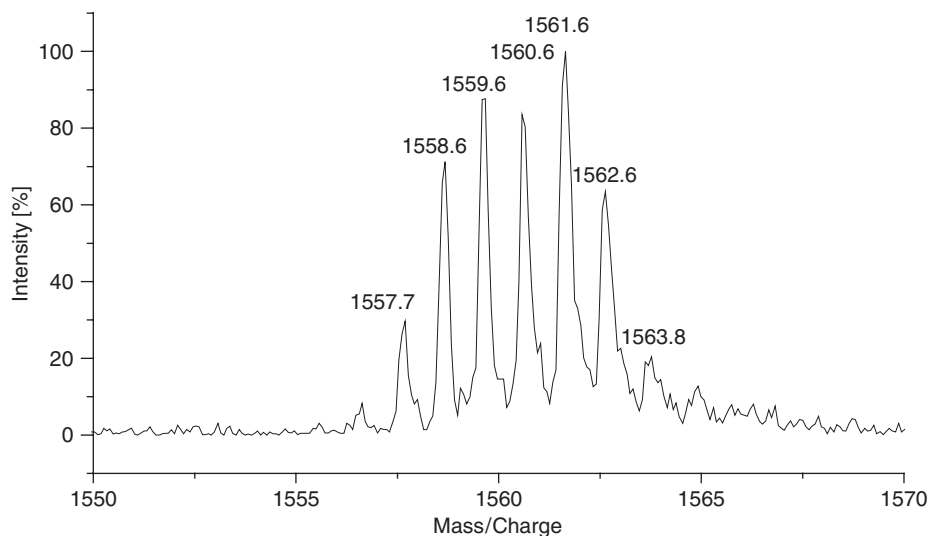
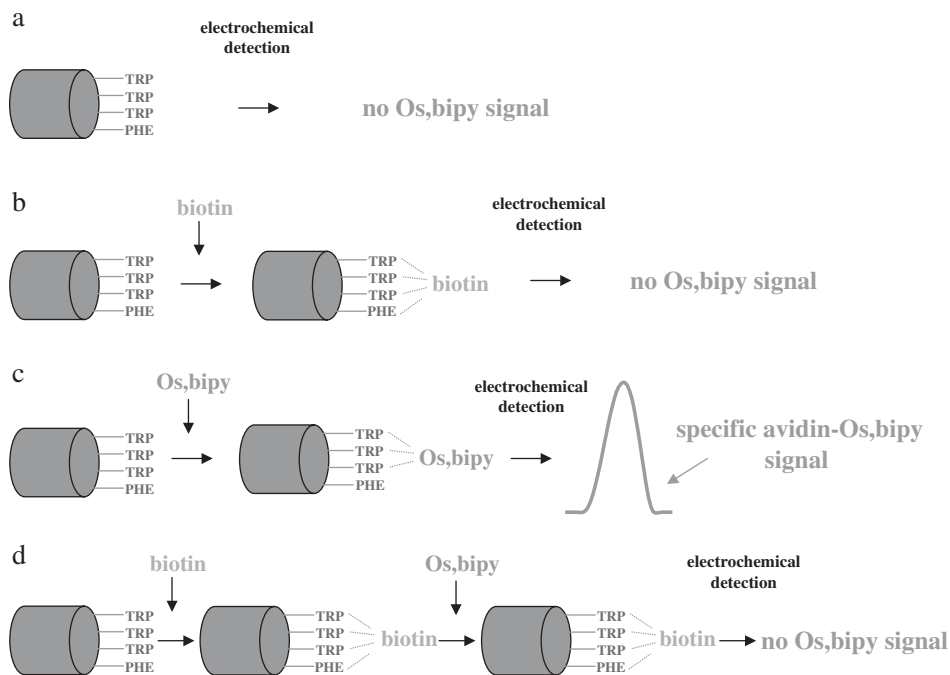


Fig. 19. Detail of the osmium isotope pattern in the selected part of the MALDI-TOF mass spectra of the Os,bipy-modified human LH-RH peptide using MHC as a matrix. This spectrum agreed well with the theoretical model. Adapted from Sedo *et al.* (2004). Copyright 2004, with permission from Elsevier.

contained in the above peptides, Os,bipy modification of avidin (i.e. of the protein in which all 20 natural amino acid residues are contained) was investigated.

Avidin is a glycoprotein displaying exceptionally strong binding properties toward biotin (Green, 1975) (Section 3.1). There are three tryptophan residues (Trp 70, Trp 97, Trp 110) in the binding site for biotin involved in biotin-binding (Lindqvist and Schneider, 1996). More than 40 years ago it was shown that modification of these Trp residues with oxidation reagent *N*-bromosuccinimide led to a loss of 90% of the initial biotin-binding activity (Green, 1963). Avidin modification with the Trp-specific reagent 2-hydroxy-5-nitrobenzyl bromide (Gitlin *et al.*, 1988) yielded similar results. To find out whether Os,bipy will show the same specificity toward accessible Trp residues, avidin was treated with the Os,bipy before and after biotin binding. Likewise the Os,bipy-modified Trp-containing peptides (Figure 18), the Os,bipy modified avidin yielded at mercury and carbon electrodes characteristic electrochemical signals (S. Billova and E. Palecek, unpublished). When avidin was pre-incubated with biotin, Os,bipy failed to modify the protein as detected by absence of the Os,bipy response at about -1.2 V at HMDE and at -0.53 V at PGE, reflecting a protection of the Trp residues by biotin and suggesting that except for Trp residues no other amino acids outside the binding site were responsible for electrochemical signals of modified avidin (Scheme 1). Neither biotin nor unmodified avidin produced any voltammetric signal characteristic of the protein-Os,L adduct at mercury or carbon electrodes (Scheme 1). Moreover, as with *N*-bromosuccinimide and 2-hydroxy-5-nitrobenzyl bromide, biotin-binding activity was lost. It may be thus concluded that in proteins containing usual amino acids, only Trp residues form a stable adduct with Os,bipy, which is responsible for the electrochemical signals



Scheme 1. Chemical modification of avidin and avidin–biotin complex with osmium tetroxide, 2,2'-bipyridine (Os,bipy). The scheme demonstrates that only tryptophan residues (located in the biotin-binding pocket) form stable osmium-containing adducts, producing specific electrochemical signals. Such modification is prevented by binding of biotin to the avidin molecule.

shown in Figures 1 and 2. Oxidation of cysteine residues to cysteic acid by Os,bipy results in a decrease or disappearance of the BCR (Sections 2.2 and 3.1.1.1) but not in production of any Os,bipy signal.

Lysozyme is a small protein (M_w 14,388 Da) with enzyme activity, splitting the peptidoglycan (the major structural element of the cell wall of Gram-positive bacteria) containing 6 Trp residues. Native and denatured lysozyme (denaturation by 6 M guanidinium chloride at 25°C) were modified by 2 mM Os,bipy and the samples were measured by AdTS SWV at PGE. Both native and denatured lysozyme produced SWV peak at about -0.55 V characteristic for Os,bipy-modified proteins. The peak of denatured lysozyme was about twice as high as that of the native protein, suggesting that protein denaturation resulted in exposition of some Trp residues for the chemical reaction (S. Billova, unpublished). Similar results were obtained also with other proteins in their native and denatured forms at carbon and mercury electrodes.

8.1. Concluding remarks

Trp containing peptides and proteins can be modified by Os,bipy under conditions close to physiological. This modification results in formation of a stable

Os,bipy adduct with Trp residues (Figure 18), which can be sensitively detected by electrochemical and mass spectrometric methods. Os,bipy treatment results also in oxidation of cysteine and methionine residues but this oxidation does not result in any stable Os-containing adduct nor in formation of any specific electrochemical signals. Cysteine oxidation can be, however, followed by a decrease or disappearance of the Brdicka's catalytic signals. The extent of modification of Trp-residues depends on the protein conformation showing greater modification of denatured proteins as compared to native ones.

9. SUMMARY AND CONCLUSION

Electrochemistry of the proteins is not limited to conjugated proteins containing redox centers, which enable fast reversible electrode processes. All proteins and peptides so far tested possessed an ability to catalyze hydrogen evolution at mercury electrode and provided analytically useful signals. Low concentrations of the proteins can be determined by constant current chronopotentiometric stripping analysis (CPSA) producing peak H at highly negative potentials. This peak sensitively reflects changes in protein conformation related to protein aggregation, denaturation and appears potentially useful in studies of mutant proteins. Cysteine-containing proteins produce in cobalt solution characteristic catalytic signals discovered 75 years ago by Brdicka and another signal (peak S) around -0.6 V (against SCE) due to reduction of the Hg-S bond (formed at less negative potentials). Both peak S and Brdicka's signals usually require higher protein concentrations than CPSA peak H. Information about the protein adsorption can be obtained by a.c. impedance measurements at atomically smooth mercury surface.

Tyrosine and tryptophan residues in peptides and proteins can be oxidized at carbon electrodes. Using CPSA or square wave stripping voltammetry in combination with efficient baseline correction well-developed peaks can be obtained. Oxidation of tyrosine or tryptophan residues at gold electrodes has not been reported.

The above methods were applied to study avidin and streptavidin, the proteins used in biotechnologies in connection with the ability of these proteins to strongly bind a low molecular mass compound biotin. In contrast to previous reports on electroinactivity of these proteins, the above-mentioned proteins produce reduction signals at mercury and oxidation signals at carbon electrodes. These signals changed stoichiometrically with the biotin binding. Studies of free and biotin-bound avidin provided a complex picture of their interfacial properties.

Peak H is produced both by cysteine-containing peptides and proteins as well as by those in which cysteine residue was absent. The presence of cysteine, however, strongly influences the height and potential of peak H and its dependence on pH. Peak H is highly sensitive to the peptide redox state. It appears potentially useful in the analysis of intracellular proteins, whose biological activity is usually connected with their redox state.

Aggregation of A β is involved in Parkinson's and Alzheimer's diseases. Such aggregation can be induced *in vitro* and followed by various methods, such

as circular dichroism, fluorescence of thioflavin T and atomic force microscopy. ASyn aggregation was studied by electrochemical methods at mercury and carbon electrodes. It was found that using CPSA peak H ASyn could be determined at subnanomolar concentrations. ASyn aggregation can be traced both at mercury and carbon electrodes. In contrast to the oxidation signals at carbon electrodes, peak H is more sensitive to ASyn aggregation. Using this peak early changes in ASyn properties, preceding its aggregation were detected. Neither CD nor fluorescence measurements uncovered such changes. Three mutant ASyn proteins produced different heights and potentials of their peaks H.

Thiolated oligodeoxynucleotides (HS-ODN) produce signals in cobalt solutions suitable for protein analysis; these signals appear at less negative potentials than those of cysteine-containing peptides and proteins and can be utilized in studies of DNA-protein interactions.

DNA-protein interactions have been studied by a number of various methods but only recently attempts have been made to apply electrochemical methods in this field. Newly designed methods can be divided (similar to the DNA hybridization sensors) in two groups: (a) one in which DNA-protein interaction and its detection is performed at one (electrode) surface (single-surface technique, SST) and (b) another one in which protein interaction with immobilized DNA is performed at one surface such as magnetic beads, and the detection of the DNA-protein interaction is detected at another surface – the detection electrode (double-surface technique, DST).

Among three SST methods, one is based on changes in charge transfer in double-stranded DNA caused by protein binding. This method is limited to proteins which flip-out a DNA base from the duplex or to conjugated proteins with electroactive groups producing reversible redox signals at gold electrodes. Another method from the SST group is based on oxidation signals of DNA (Chapter 3) and proteins (Sections 2.1 and 3) at carbon electrodes. Finally, the last method in this group is taking advantage of catalytic currents of proteins and thiolated DNAs at mercury electrodes. This method appears most sensitive among the SST methods.

In DST methods, DNA is immobilized at magnetic beads capturing the DNA-binding protein. The captured protein can be detected at carbon or mercury electrodes due to its electroactivity (Sections 2.1 and 3). Detection based on the CPSA peak H is the most sensitive one. Alternatively, the protein can be immobilized on the beads and captured DNA can be detected similarly as in the DNA hybridization sensors (Chapter 3).

Both proteins and DNA can undergo denaturation at the electrode surface. DNA-surface denaturation was observed on negatively charged electrodes; the potential range was limited to a narrow region at pHs close to neutral. In contrast to DNA, no simple rules can be expected for surface conformational changes of proteins due to their complexity and conformational variations. It is shown in this Chapter that electrochemical methods are capable to reflect conformational changes related to denaturation, aggregation, mutation, etc. in a number of proteins, suggesting that under the given conditions only limited surface denaturation could take place.

To eliminate the effect of protein adsorption and surface denaturation on the electrochemical responses of proteins chemical probes of the protein structure can be used. The chemical should react with a protein under mild conditions and introduce in solution a covalently bound electroactive label to accessible groups in the protein. Alternatively, a chemical can be used reacting specifically with some amino acid residues (such as Tyr, Trp or Cys) responsible for specific electrochemical signal. Changes in this signal can be then used to make conclusion about accessibility of the given residues in the protein. The appearance and properties of the signal of the electroactive marker in proteins modified in native and denatured states can provide information about changes in accessibility of the aa residues in the protein. It is shown that osmium complexes with nitrogen ligands (Os,L), such as 2,2'-bipyridine react covalently with tryptophan residues in peptides and proteins and produce signals at carbon and mercury electrodes. The electrochemical detection of osmium–Trp adducts can be combined also with mass spectrometry and other methods. It can be expected that modern electrochemical methods will soon gain importance in the protein research and particularly in proteomics because of their sensitivity, small requirement for the amount of the analyte and their abilities to reflect changes in protein conformations and various protein interactions. Moreover, these techniques are relatively simple and inexpensive, and can be miniaturized and adapted for parallel protein analysis.

LIST OF ABBREVIATIONS

aa	amino acid
a.c.	alternating current
ACV	a.c. voltammetry
AdS	adsorptive stripping
AdTS	adsorptive transfer stripping
Asyn	α -synuclein
BCR	Brdicka's catalytic response
CNT	carbon nanotubes
CP	constant current chronopotentiometry
CPE	carbon paste electrode
CPSA	constant current chronopotentiometric stripping analysis
CV	cyclic voltammetry
d.c.	direct current
DME	mercury dropping electrode
DPP	differential (derivative) pulse polarography
DPV	differential (derivative) pulse voltammetry
DST	double-surface technique
ds	double-stranded
HMDE	Hanging mercury drop electrode
HRP	horseradish peroxidase
HSA	human serum albumin

LSV	linear sweep voltammetry
NPP	normal pulse polarography
ODN	oligodeoxyribonucleotides
PNA	peptide nucleic acid
SAM	self-assembled monolayer
SCE	saturated calomel electrode
ss	single-stranded
SST	single-surface technique
SWV	square wave voltammetry
t_A	accumulation time
Trp	tryptophan
Tyr	Tyrosine

ACKNOWLEDGMENTS

The author is indebted to Drs. M. Fojta, M. Heyrovský, F. Jelen, M. Masařík, V. Ostatná and other colleagues for critical reading of the manuscript and to Drs. F. Jelen, M. Masařík and Z. Pechan for their help with preparation of the manuscript. This work was supported by the grant of the Grant Agency of the Czech Republic 204/03/0566.

REFERENCES

- Antony, T., W. Hoyer, D. Cherny, G. Heim, T.M. Jovin and V. Subramaniam, 2003, Cellular polyamines promote the aggregation of alpha-synuclein, *J. Biol. Chem.* 278, 3235.
- Armstrong, F.A., 2002, Voltammetry of Proteins, *Bioelectrochemistry*, Vol. 9: Encyclopedia of Electrochemistry, Ed. G.S. Wilson, Wiley-VCH, Weinheim, 11.
- Arnold, S., Z.Q. Feng, T. Kakiuchi, W. Knoll and K. Niki, 1997, Investigation of the electrode reaction of cytochrome *c* through mixed self-assembled monolayers of alkanethiols on gold(111) surfaces, *J. Electroanal. Chem.* 438, 91.
- Athey, D., M. Ball and C.J. McNeil, 1993, Avidin-biotin based electrochemical immunoassay for thyrotropin, *Ann. Clin. Biochem.* 30, 570.
- Avila, A., B.W. Gregory, K. Niki and T.M. Cotton, 2000, An electrochemical approach to investigate gated electron transfer using a physiological model system: Cytochrome *c* immobilized on carboxylic acid-terminated alkanethiol self-assembled monolayers on gold electrodes, *J. Phys. Chem. B* 104, 2759.
- Banica, F.G. and A. Ion, 2000, Electrocatalysis-based kinetic determinations, *Encyclopedia of Analytical Chemistry*, Ed. R.A. Meyers, Wiley, Chichester, 11115.
- Bayer, E.A., M. Safars and M. Wilchek, 1987, Selective labeling of sulfhydryls and disulfides on blot transfers using avidin-biotin technology: Studies on purified proteins and erythrocyte membranes, *Anal. Biochem.* 161, 262.
- Behrendorf, H.A., M. Pignot, N. Windhab and A. Kappel, 2002, Rapid parallel mutation scanning of gene fragments using a microelectronic protein-DNA chip format, *Nucleic Acids Res.* 30, e64.
- Bi, L.J., Y.F. Zhou, X.E. Zhang, J.Y. Deng, Z.P. Zhang, B. Xie and C.G. Zhang, 2003, MutS-based protein chip for detection of DNA mutations, *Anal. Chem.* 75, 4113.

- Billova, S., R. Kizek and E. Palecek, 2002, Differential pulse adsorptive stripping voltammetry of osmium-modified peptides, *Bioelectrochemistry* 56, 63.
- Biswas, I. and P. Hsieh, 1996, Identification and characterization of a thermostable MutS homolog from *Thermus aquaticus*, *J. Biol. Chem.* 271, 5040.
- Blanco, J. and G.H. Dixon, 1986, A procedure to increase the sensitivity of solid-phase immunoassays, *J. Immunol. Meth.* 89, 265.
- Boon, E.M., A.L. Livingston, N.H. Chmiel, S.S. David and J.K. Barton, 2003, DNA-mediated charge transport for DNA repair, *Proc. Natl. Acad. Sci. USA* 100, 12543.
- Boon, E.M., J.E. Salas and J.K. Barton, 2002a, An electrical probe of protein-DNA interactions on DNA-modified surfaces, *Nat. Biotechnol.* 20, 282.
- Boon, E.M., M.A. Pope, S.D. Williams, S.S. David and J.K. Barton, 2002b, DNA-mediated charge transport as a probe of MutY/DNA interaction, *Biochemistry* 41, 8464.
- Brabec, V., 1980, Electrochemical oxidation of nucleic-acids and proteins at graphite electrode – qualitative aspects, *Bioelectrochem. Bioenerg.* 7, 69.
- Brabec, V., 1985, Polarography of cytochrome-*c* in ammoniacal buffers containing cobalt ions. The effect of the protein conformation, *Gen. Physiol. Biophys.* 4, 609.
- Brabec, V. and I. Schindlerova, 1981a, Electrochemical-behavior of proteins at graphite-electrodes. 3. The effect of protein adsorption, *Bioelectrochem. Bioenerg.* 8, 451.
- Brabec, V. and I. Schindlerova, 1981b, Electrochemical-behavior of proteins at graphite-electrodes. 3. The effect of protein adsorption, *Bioelectrochem. Bioenerg.* 8, 451.
- Brabec, V. and V. Mornstein, 1980, Electrochemical-behavior of proteins at graphite-electrodes. 1. Electrooxidation of proteins as a new probe of protein-structure and reactions, *Biochim. Biophys. Acta* 625, 43.
- Brabec, V., V. Vetterl and O. Vrana, 1996, Electroanalysis of biomacromolecules, *Experimental Techniques in Bioelectrochemistry. Vol. 3: Bioelectrochemistry: Principles and Practice*, Eds. V. Brabec, D. Walz and G. Milazzo, Birkhauser Verlag, Basel, Switzerland, 287.
- Branden, C. and J. Tooze, 1999, *Introduction to Protein Structure*, Garland Publishing Inc., New York.
- Brezina, M. and P. Zuman, 1958, *Polarography in Medicine, Biochemistry and Pharmacy*, Interscience, New York.
- Brucknerlea, C., R.J. Kimmel, J. Janata, J.F.T. Conroy and K. Caldwell, 1995, Electrochemical studies of octadecanethiol and octanethiol films on variable surface-area mercury sessile drops, *Electrochim. Acta* 40, 2897.
- Bucciantini, M., E. Giannoni, F. Chiti, F. Baroni, L. Formigli, J.S. Zurdo, N. Taddei, G. Ramponi, C.M. Dobson and M. Stefani, 2002, Inherent toxicity of aggregates implies a common mechanism for protein misfolding diseases, *Nature* 416, 507.
- Buckley, E., J.M.F. Alvarez, M.R. Smyth and R. O'Kennedy, 1991, Comparison of the adsorptive voltammetric behavior of avidin and streptavidin, *Electroanalysis* 3, 43.
- Cai, X., G. Rivas, M.A.P. Farias, H. Shiraishi, J. Wang and E. Palecek, 1996, Potentiometric stripping analysis of bioactive peptides at carbon electrodes down to subnanomolar concentrations, *Anal. Chim. Acta* 332, 49.
- Campbell, M.K., 1995, *Biochemistry*, Saunders College Publishing, Philadelphia.
- Caughey, B. and P.T. Lansbury, 2003, Protofibrils, pores, fibrils, and neurodegeneration: Separating the responsible protein aggregates from the innocent bystanders, *Annu. Rev. Neurosci.* 26, 267.
- Cecil, R. and P.D.J. Weitzman, 1964, The electroreduction of the disulphide bonds of insulin and other proteins, *Biochem. J.* 93, 1.
- Chase, J.W. and K.R. Williams, 1986, Single-stranded-DNA binding-proteins required for DNA-replication, *Ann. Rev. Biochem.* 55, 103.
- Chen, G. and X. Chen, 2003, Arginine residues in the active site of human phenol sulfotransferase (SULT1A1), *J. Biol. Chem.* 278, 36358.
- Clark, R.A. and E.F. Bowden, 1997, Voltammetric peak broadening for cytochrome *c*/alkanethiolate monolayer structures: Dispersion of formal potentials, *Langmuir* 13, 559.

- Collinson, M., E.F. Bowden and M.J. Tarlov, 1992, Voltammetry of covalently immobilized cytochrome *c* on self-assembled monolayer electrodes, *Langmuir* 8, 1247.
- Conway, K.A., J.D. Harper and P.T. Lansbury, 2000, Fibrils formed *in vitro* from alpha-synuclein and two mutant forms linked to Parkinson's disease are typical amyloid, *Biochemistry* 39, 2552.
- Davis, J.J., C.M. Halliwell, H.A.O. Hill, G.W. Canters, M.C. van Amsterdam and M.P. Verbeet, 1998, Protein adsorption at a gold electrode studied by *in situ* scanning tunnelling microscopy, *New J. Chem.* 22, 1119.
- Davis, J.J., D. Djuricic, K.K.W. Lo, E.N.K. Wallace, L.L. Wong and H.A.O. Hill, 2000, A scanning tunnelling study of immobilised cytochrome P450(cam), *Faraday Discuss.* 116, 15.
- Davis, J.J., H.A.O. Hill, A. Kurz, A.D. Leighton and A.Y. Safronov, 1997, The aqueous electrochemistry of C-60 and methanofullerene films, *J. Electroanal. Chem.* 429, 7.
- Deetz, J.S. and E.J. Behrman, 1980, Kinetics of the reaction of some tryptophan derivatives with the osmium tetroxide pyridine reagent, *J. Org. Chem.* 45, 135.
- DeLange, R.J. and T.S. Huang, 1971, Egg white avidin, *J. Biol. Chem.* 246, 698.
- Dev, K.K., H. van der Putten, B. Sommer and G. Rovelli, 2003a, Part I: Parkin-associated proteins and Parkinson's disease, *Neuropharmacology* 45, 1.
- Dev, K.K., K. Hofele, S. Barbieri, V.L. Buchman and H. van der Putten, 2003b, Part II: Alpha-synuclein and its molecular pathophysiological role in neurodegenerative disease, *Neuropharmacology* 45, 14.
- Diamandis, E.P. and T.K. Christopoulos, 1991, The biotin-(strept)avidin system: Principles and applications in biotechnology, *Clin. Chem.* 37, 625.
- Ding, T.T., S.J. Lee, J.C. Rochet and P.T. Lansbury, 2002, Annular alpha-synuclein protofibrils are produced when spherical protofibrils are incubated in solution or bound to brain-derived membranes, *Biochemistry* 41, 10209.
- Dobson, C.M., 1999, Protein misfolding, evolution and disease, *Trends Biochem. Sci.* 24, 329.
- Dobson, C.M., 2001, The structural basis of protein folding and its links with human disease, *Philos. Trans. R. Soc. London* 356, 133.
- Dobson, C.M., 2003, Protein folding and misfolding, *Nature* 426, 884.
- Dorcak, V., 2004, Use of Electrochemical Methods for Studying Plant Metallothioneins and Their Complexes with Selected Heavy Metals, Czech University of Agriculture.
- Dorcak, V. and I. Sestakova, 2005, Electrochemical behavior of phytochelatin and related peptides at the hanging mercury drop electrode in the presence of cobalt(II) ions, *Bioelectrochemistry* 68, 14-21.
- Dryhurst, G., K.M. Kadish, F. Scheller and R. Renneberg, 1982, *Biological Electrochemistry*, Vol. I, Academic Press, New York.
- Ebbesen, T.W. and P.M. Ajayan, 1992, Large-scale synthesis of carbon nanotubes, *Nature* 358, 220.
- Eddowes, M.J. and H.A.O. Hill, 1977, Novel method for the investigation of the electrochemistry of metalloproteins: Cytochrome *c*, *J. Chem. Soc. Chem. Commun.* 21, 771.
- El Kasmi, A., J.M. Wallace, E.F. Bowden, S.M. Binet and R.J. Linderman, 1998, Controlling interfacial electron-transfer kinetics of cytochrome *c* with mixed self-assembled monolayers, *J. Am. Chem. Soc.* 120, 225.
- Fedurco, M., V. Vesela and M. Heyrovsky, 1993, Voltammetric reaction of the sulfide disulfide system with oxygen at mercury-electrodes, *Electroanalysis* 5, 257.
- Feng, Z.Q., S. Imabayashi, T. Kakiuchi and K. Niki, 1995, Electroreflectance spectroscopic study of the electron transfer rate of cytochrome *c* electrostatically immobilized on the -carboxyl alkanethiol monolayer modified gold electrode, *J. Electroanal. Chem.* 394, 149.
- Feng, Z.Q., S. Imabayashi, T. Kakiuchi and K. Niki, 1997, Long-range electron-transfer reaction rates to cytochrome *c* across long- and short-chain alkanethiol self-assembled monolayers: Electroreflectance studies, *J. Chem. Soc. Faraday Trans.* 93, 1367.
- Ferapontova, E., K. Schmengler, T. Borchers, T. Ruzgas and L. Gorton, 2002, Effect of cysteine mutations on direct electron transfer of horseradish peroxidase on gold, *Biosens. Bioelectron.* 17, 953.
- Fersht, A., 1999, *Structure and Mechanism in Protein Science*, W.H. Freeman and company, New York.

- Finklea, H.O., 2000, Self-assembled monolayers on electrodes, Encyclopedia of Analytical Chemistry, Vol. 11, Ed. R.A. Meyers, Wiley, New York, 10090.
- Finn, F.M., G. Titus, D. Horstman and K. Hofmann, 1984, Avidin–biotin affinity chromatography: Application to the isolation of human placental insulin receptor, Proc. Natl. Acad. Sci. USA 81, 7328.
- Friis, E.P., J.E.T. Andersen, L.L. Madsen, P. Moller and J. Ulstrup, 1997, *In situ* STM and AFM of the copper protein *Pseudomonas aeruginosa* azurin, J. Electroanal. Chem. 431, 35.
- Fristrup, P., M. Grubb, J. Zhang, H.E.M. Christensen, A.M. Hansen and J. Ulstrup, 2001, Voltammetry of native and recombinant *Pseudomonas aeruginosa* azurin on polycrystalline Au- and single-crystal Au(111)-surfaces modified by decanethiol monolayers, J. Electroanal. Chem. 211, 128.
- Fuller, K.L. and S.G. Roscoe, 1994, Surface adsorption of diarily proteins: Fouling of model surfaces, Food proteins: Structure–function relationships, Eds. R.Y. Yada, R.L. Jackman and J.A.L. Smith, Blackie Academic and Professional Publishers, London, 143.
- Gitlin, G., E.A. Bayer and M. Wilchek, 1988, Studies on the biotin-binding site of avidin–tryptophan residues involved in the active-site, Biochem. J. 250, 291.
- Goedert, M., 2001, Alpha-synuclein and neurodegenerative diseases, Nat. Rev. Neurosci. 2, 492.
- Gonzalez-Garcia, M.B., C. Fernandez-Sanchez and A. Costa-Garcia, 2000, Colloidal gold as an electrochemical label of streptavidin–biotin interaction, Biosens. Bioelectron. 15, 315.
- Green, N.M., 1963, Avidin, Biochem. J. 89, 585.
- Green, N.M., 1975, Avidin, Adv. Protein Chem. 29, 85.
- Green, N.M., 1990, Avidin and streptavidin, Methods in Enzymology, Vol. 184, Eds. M. Wilchek and E.E.A. Bayer, Academic Press, London, 51.
- Hardy, J. and D.J. Selkoe, 2002, Medicine – the amyloid hypothesis of Alzheimer’s disease: Progress and problems on the road to therapeutics, Science 297, 353.
- Harper, J.D. and P.T. Lansbury, 1997, Models of amyloid seeding in Alzheimer’s disease and scrapie: Mechanistic truths and physiological consequences of the time-dependent solubility of amyloid proteins, Annu. Rev. Biochem. 66, 385.
- Havran, L., S. Billova and E. Palecek, 2004, Electroactivity of avidin and streptavidin. Avidin signals at mercury and carbon electrodes respond to biotin binding, Electroanalysis 16, 1139.
- Heitzmann, H. and F.M. Richards, 1974, Use of the avidin–biotin complex for specific staining of biological membranes in electron microscopy, Proc. Natl. Acad. Sci. USA 71, 3537.
- Heller, M.J., 2002, DNA microarray technology: Devices, systems, and applications, Ann. Rev. Biomed. Eng. 4, 129.
- Hendrickson, W.A., A. Pahler, J.L. Smith, Y. Satow, E.A. Merritt and R.P. Phizackerley, 1989, Crystal structure of core streptavidin determined from multiwavelength anomalous diffraction of synchrotron radiation, Proc. Natl. Acad. Sci. USA 86, 2190.
- Herne, T.M. and M.J. Tarlov, 1997, Characterization of DNA probes immobilized on gold Surfaces, J. Am. Chem. Soc. 119, 8916.
- Heyrovský, J. and J. Babicka, 1930, Polarographic studies with the dropping mercury cathode. Part XIII. Effect of albumins, Coll. Czech. Chem. Commun. 2, 370.
- Heyrovsky, J. and J. Forejt, 1953, Oscillographic Polarography, SNTL, Prague.
- Heyrovsky, J. and J. Kuta, 1965, Principles of Polarography, 1st ed., Czechoslovak Academy of Science, Prague.
- Heyrovsky, M., P. Mader, S. Vavricka, V. Vesela and M. Fedurco, 1997, The anodic reactions at mercury electrodes due to cysteine, J. Electroanal. Chem. 430, 103.
- Heyrovsky, M., P. Mader, V. Vesela and M. Fedurco, 1994, The reactions of cystine at mercury-electrodes, J. Electroanal. Chem. 369, 53.
- Hlady, V. and J. Buijs, 1996, Protein adsorption on solid surfaces, Curr. Opin. Biotechnol. 7, 72.
- Hlady, V., J. Buijs and H.P. Jennissen, 1999, Methods to study protein adsorption, Methods in Enzymology: Amyloid, Prions and Other Protein Aggregates, Vol. 309, Ed. R. Wetzel, Academic Press, New York, 402.

- Honeychurch, M.J., 1997, The reduction of disulfide bonds in proteins at mercury electrodes, *Bioelectrochem. Bioenerg.* 44, 13.
- Hoyer, W., T. Antony, D. Cherny, G. Heim, T.M. Jovin and V. Subramaniam, 2002, Dependence of alpha-synuclein aggregate morphology on solution conditions, *J. Mol. Biol.* 322, 383.
- Hoyer, W.G., D. Cherny, V. Subramaniam and T.M. Jovin, 2004, Rapid self-assembly of alpha-synuclein observed by *in situ* atomic force microscopy, *J. Mol. Biol.* 340, 127.
- Jackson, D., S. Omanovic and S.G. Roscoe, 2000, Electrochemical studies of the adsorption behaviour of serum proteins on biomaterials, *Langmuir* 16, 5449.
- Jelen, F., B. Yosypchuk, A. Kourilova, L. Novotny and E. Palecek, 2002, Label-free determination of picogram quantities of DNA by stripping voltammetry with solid copper amalgam or mercury electrodes in the presence of copper, *Anal. Chem.* 74, 4788.
- Jiricny, J., 1998, Eukaryotic mismatch repair: An update, *Mutat. Res. - DNA Repair* 409, 107.
- Jiricny, J., 2000, Mismatch repair: The praying hands of fidelity, *Curr. Biol.* 10, R788.
- Jiricny, J., S.S. Su, S.G. Wood and P. Modrich, 1988, Mismatch-containing oligonucleotide duplexes bound by the *E. coli* mutS-encoded protein, *Nucleic Acids Res.* 16, 7843.
- Jones, V.W., J.R. Kenseth, M.D. Porter, C.L. Mosher and E. Henderson, 1998, Microminiaturized immunoassays using atomic force microscopy and compositionally patterned antigen arrays, *Anal. Chem.* 70, 1233.
- Kalvoda, R., 1960, Progress in alternating current oscillographic polarography, *Chem. Listy* 54, 1265.
- Kayed, R., E. Head, J.L. Thompson, T.M. McIntire, S.C. Milton, C.W. Cotman and C.G. Glabe, 2003, Common structure of soluble amyloid oligomers implies common mechanism of pathogenesis, *Science* 300, 486.
- Kerman, K., Y. Morita, Y. Takamura and E. Tamiya, 2005, *Escherichia coli* single-strand binding protein—DNA interactions on carbon nanotube-modified electrodes from a label-free electrochemical hybridization sensor, *Anal. Bioanal. Chem.* 381, 1114.
- Kizek, R., L. Trnkova and E. Palecek, 2001, Determination of metallothionein at the femtomole level by constant current stripping chronopotentiometry, *Anal. Chem.* 73, 4801.
- Kruger, R., T. Muller and O. Riess, 2000, Involvement of alpha-synuclein in Parkinson's disease and other neurodegenerative disorders, *J. Neural. Transm.* 107, 31.
- Kruger, R., W. Kuhn, T. Muller, D. Voitalla, M. Graeber, S. Kosel, H. Przuntek, J.T. Eppen, L. Schols and O. Riess, 1998, Ala30Pro mutation in the gene encoding alpha-synuclein in Parkinson's disease, *Nat. Genet.* 18, 106.
- Kuramitz, H., J. Natsui, S. Tanaka and K. Hasebe, 2000b, Electrochemical detection of the interaction between avidin and biotin based on the change of electrode response of copper enhanced by biotin labeled with thiourea, *Electroanalysis* 12, 588.
- Kuramitz, H., K. Sugawara, H. Nakamura and S. Tanaka, 1999, Control of electrocatalytic oxidation of NADH using an interaction between labeled biotin with dopamine and avidin, *J. Electroanal. Chem.* 466, 117.
- Kuramitz, H., K. Sugawara and S. Tanaka, 2000a, Electrochemical sensing of avidin–biotin interaction using redox markers, *Electroanalysis* 12, 1299.
- Kuyama, H., C. Toda, M. Watanabe, K. Tanaka and O. Nishimura, 2003, An efficient chemical method for dephosphorylation of phosphopeptides, *Rapid Commun. Mass Spectrom.* 17, 1493.
- Kuznetsov, B.A. and G.P. Shumakovich, 1975, On the mechanism of appearance of double-step polarographic protein waves, *Bioelectrochem. Bioenerg.* 2, 35.
- Kuznetsov, B.A., N.M. Mestechkina and G.P. Shumakovich, 1977, Electrochemical behaviour of proteins containing coenzyme groups and metals, *Bioelectrochem. Bioenerg.* 4, 1.
- Kyte, J., 1995, *Structure in Protein Chemistry*, Garland publishing, New York.
- Lamers, M.H., A. Perrakis, J.H. Enzlin, H.H. Winterwerp, N. de Wind and T.K. Sixma, 2000, The crystal structure of DNA mismatch repair protein MutS binding to a G × T mismatch, *Nature* 407, 711.
- Lashuel, H.A., D. Hartley, B.M. Petre, T. Walz and P.T. Lansbury, 2002, Neurodegenerative disease – Amyloid pores from pathogenic mutations, *Nature* 418, 291.

- Lee, W., T.P. Jones and B. Mooney, 1970, Cathode-ray polarography of insulin, *Biochem. J.* 119, 607.
- Lewis, M., M. Tarlov and K. Carron, 1995, Study of the photooxidation process of self-assembled alkanethiol monolayers, *J. Am. Chem. Soc.* 117, 9574.
- Lilley, D.M. Ed., 1995, *DNA-Protein: Structural Interactions*, IRL Press at Oxford University Press, Oxford.
- Lindqvist, Y. and G. Schneider, 1996, Protein-biotin interactions, *Curr. Opin. Struct. Biol.* 6, 798.
- Livnah, O., E.A. Bayer, M. Wilchek and J.L. Sussman, 1993, Three-dimensional structures of avidin and the avidin-biotin complex, *Proc. Natl. Acad. Sci. USA* 90, 5076.
- Luo, D., J. Lan, C. Zhou and C. Luo, 2003, Polarographic behavior of Co(II)-BSA or -HSA complex in the presence of a guanidine modifier, *Anal. Chem.* 75, 6346.
- Luscombe, N.M., Austin, S.E., Berman, H.M., Thornton, J.M., 2000, An overview of the structures of protein-DNA complexes. *Gen. Biol.* 1, reviews 001.1-001.37.
- Mader, P., V. Vesela, V. Dorcak and M. Heyrovsky, 2001, The "presodium" hydrogen evolution at the dropping mercury electrode catalysed by simple cysteine peptides, *Coll. Czech. Chem. Commun.* 66, 397.
- Mairanovskii, S.C., 1968, *Catalytic and Kinetics Waves in Polarography*, Plenum Press, New York.
- Maiti, N.C., M.M. Apetri, M.G. Zagorski, P.R. Carey and V.E. Anderson, 2004, Raman spectroscopic characterization of secondary structure in natively unfolded proteins: alphasynuclein, *J. Am. Chem. Soc.* 126, 2399-2408.
- Mardanyan, S., S. Sharoyan, A. Antonyan, A. Armenyan, G. Cristalli and G. Lupidi, 2001, Tryptophan environment in adenosine deaminase I. Enzyme modification with *N*-bromosuccinimide in the presence of adenosine and EHNA analogues, *Biochim. Biophys. Acta* 1546, 185.
- Maroteaux, L., J.T. Campanelli and R.H. Scheller, 1988, Synuclein: A neuron-specific protein localized to the nucleus and presynaptic nerve terminal, *J. Neurosci.* 8, 2804.
- Masarik, M., A. Stobiecka, R. Kizek, F. Jelen, Z. Pechan, W. Hoyer, T.M. Jovin, V. Subramaniam and E. Palecek, 2004, Sensitive electrochemical detection of native and aggregated alpha-synuclein protein involved in Parkinson's disease, *Electroanalysis* 16, 1172.
- Mathews, C.K., K.E. van Holde and K.G. Ahern, 2000, *Biochemistry*, Addison-Wesley Longman, San Francisco.
- Meyer, R.R. and P.S. Laine, 1990, The single-stranded DNA-binding protein of *Escherichia coli*, *Microbiol. Rev.* 54, 342.
- Mikkelsen, O. and K.H. Schroder, 2003, Amalgam electrodes for electroanalysis, *Electroanalysis* 15, 679.
- Monterroso-Marco, B. and B. Lopez-Ruiz, 2003, pH Effect on cysteine and cystine behaviour at hanging mercury drop electrode, *Talanta* 61, 733.
- Murphy, D.M., V.V. Ivanenkov and T.L. Kirley, 2002, Identification of cysteine residues responsible for oxidative crosslinking and chemical inhibition of human nucleoside-triphosphate diphosphohydrolase 3, *J. Biol. Chem.* 277, 6162.
- Nahir, T.M. and E.F. Bowden, 1996, The distribution of standard rate constants for electron transfer between thiol-modified gold electrodes and adsorbed cytochrome *c*, *J. Electroanal. Chem.* 410, 9.
- Neurath, H. Ed., 1963, *The Proteins - Composition Structure and Function*, Vols. 1-4, Academic Press, New York.
- Obmolova, G., C. Ban, P. Hsieh and W. Yang, 2000, Crystal structures of mismatch repair protein MutS and its complex with a substrate DNA, *Nature* 407, 703.
- O'Brien, J.C., J.T. Stickney and M.D. Porter, 2000a, Self-assembled double-stranded DNA (dsDNA) microarrays for protein: dsDNA Screening using atomic force microscopy, *Anal. Chem.* 122, 5004.
- O'Brien, J.C., V.W. Jones, M.D. Porter, C.L. Mosher and E. Henderson, 2000b, Immunosensing platforms using spontaneously adsorbed antibody fragments on gold, *Anal. Chem.* 72, 703.

- Ostatna, V., F. Jelen, T. Hianik and E. Palecek, 2005, Electrochemical responses of thiolated oligodeoxynucleotides in cobalt-containing solutions, *Electroanalysis* 17, 1413–1420.
- Palecek, E., 1974, Normal pulse polarography of double-helical DNA: Dependence of the wave height on starting potential, *Coll. Czech. Chem. Commun.* 39, 3449.
- Palecek, E., 1983, Modern polarographic (voltammetric) methods in biochemistry and molecular biology. Part II. Analysis of macromolecules, *Topics in Bioelectrochemistry and Bioenergetics*, Vol. 5, Ed. G. Milazzo, Wiley, London, 65.
- Palecek, E., 1988, New trends in electrochemical analysis of nucleic acids, *Bioelectrochem. Bioenerg.* 20, 171.
- Palecek, E., 1992a, Probing of DNA structure with osmium tetroxide complexes *in vitro*, *Methods in Enzymology*, Vol. 212, Eds. J.N. Abelson and M.I. Simon, Academic Press, New York, 139.
- Palecek, E., 1992b, Probing of DNA structure in cells with osmium tetroxide, 2,2'-bipyridine, *Trans. J.E. Dahlberg, Methods in Enzymology*, Vol. 212: DNA Structures. Part B, Eds. J.N. Abelson and M.I. Simon, Academic Press, New York, 305.
- Palecek, E., 1994, Probing of DNA structure with osmium tetroxide complexes *in vitro* and in cells, *Nucleic Acids and Molecular Biology*, Vol. 8, Eds. F. Eckstein and D.M.J. Lilley, Springer, Berlin, 1.
- Palecek, E., 1996, From polarography of DNA to microanalysis with nucleic acid-modified electrodes, *Electroanalysis* 8, 7.
- Palecek, E., 2004, Surface-attached molecular beacons light the way for DNA sequencing, *Trends Biotechnol.* 22, 55.
- Palecek, E., F. Jelen, C. Teijeiro, V. Fucik and T.M. Jovin, 1993b, Biopolymer-modified electrodes. Voltammetric analysis of nucleic acids and proteins at the submicrogram level, *Anal. Chim. Acta* 273, 175.
- Palecek, E. and I. Postbieglova, 1986, Adsorptive stripping voltammetry of biomacromolecules with transfer of the adsorbed layer, *J. Electroanal. Chem.* 214, 359.
- Palecek, E. and M. Fojta, 2001, Detecting DNA hybridization and damage, *Anal. Chem.* 73, 74A.
- Palecek, E., M. Fojta and F. Jelen, 2002, New approaches in the development of DNA sensors: Hybridization and electrochemical detection of DNA and RNA at two different surfaces, *Bioelectrochemistry* 56, 85.
- Palecek, E., M. Masarik, R. Kizek, D. Kuhlmeier, J. Hassman and J. Schulein, 2004b, Sensitive electrochemical determination of unlabeled MutS protein and detection of point mutation in DNA, *Anal. Chem.* 76, 5930.
- Palecek, E., M. Robert-Nicoud and T.M. Jovin, 1993a, Local opening of the DNA double helix in eucariotic cells. Detected by osmium probe and adduct-specific immunofluorescence, *J. Cell Sci.* 104, 653.
- Palecek, E., V. Brazda, E. Jagelska, P. Pecinka, L. Karlovska and M. Brazdova, 2004a, Enhancement of p53 sequence-specific binding by DNA supercoiling, *Oncogene* 23, 2119.
- Palecek, E. and Z. Pechan, 1971, Estimation of nanogram quantities of proteins by pulse-polarographic technique, *Anal. Biochem.* 42, 59.
- Palecek, E., V. Brabec, F. Jelen and Z. Pechan, 1977, Pulse-polarographic analysis of nucleic acids and proteins, *J. Electroanal. Chem.* 75, 471.
- Peterlinz, K.A., R.M. Georgiadis, T.M. Herne and M.J. Tarlov, 1997, Observation of hybridization and dehybridization of thiol-tethered DNA using two-color surface plasmon resonance spectroscopy, *J. Am. Chem. Soc.* 119, 3401.
- Polymeroopoulos, M.H., C. Lavedan, E. Leroy, S.E. Ide, A. Dehejia, A. Dutra, B. Pike, H. Root, J. Rubenstein, R. Boyer, E.S. Stenroos, S. Chandrasekharappa, A. Athanassiadou, T. Papapetropoulos, W.G. Johnson, A.M. Lazzarini, R.C. Duvoisin, G. DiIorio, L.I. Golbe and R.L. Nussbaum, 1997, Mutation in the alpha-synuclein gene identified in families with Parkinson's disease, *Science* 276, 2045.
- Popovich, N.D. and H.H. Thorp, 2002, New strategies for electrochemical nucleic acid detection, *Interface* 11, 30.
- Prime, K.L. and G.M. Whitesides, 1991, Self-assembled organic monolayers – model systems for studying adsorption of proteins at surfaces, *Science* 252, 1164.

- Pugliese, L., A. Coda, M. Malcovati and M. Bolognesi, 1993, Three-dimensional structure of the tetragonal crystal form of egg-white avidin in its functional complex with biotin at 2.7°A resolution, *J. Mol. Biol.* 231, 698.
- Rajski, S.R., S. Kumar, R.J. Roberts and J.K. Barton, 1999, Protein-modulated DNA electron transfer, *J. Am. Chem. Soc.* 121, 5615.
- Ramsden, J.J., D.J. Roush, D.S. Gill, R. Kurrat and R.C. Willson, 1995, Protein adsorption kinetics drastically altered by repositioning a single charge, *J. Am. Chem. Soc.* 117, 8511.
- Rappuoli, R., P. Leoncini, P. Tarli and P. Neri, 1981, Competitive enzyme-immunoassay for human chorionic somatomammotropin using the avidin–biotin system, *Anal. Biochem.* 118, 168.
- Razumas, V.J., G.-J.A. Vidugiris and J.J. Kulys, 1989, Reactions of proteins and polypeptides at mercury/solution and solid/solution interfaces, *Bioelectrochem. Bioenerg.* 22, 9.
- Reynaud, J.A., B. Malfoy and A. Bere, 1980, The electrochemical oxidation of three proteins: RNAase A, bovine serum albumin and concanavalin A at solid electrodes, *Bioelectrochem. Bioenerg.* 7, 595.
- Reynolds, N.C., B.M. Kissela and L.H. Fleming, 1995, The voltammetry of neuro peptides containing L-tyrosine, *Electroanalysis* 7, 1177.
- Roscoe, S.G., 1996, Electrochemical investigations of the interfacial behaviour of proteins, *Modern Aspects of Electrochemistry*, Vol. 29, Eds. J.O.M. Bockris, B.E. Conway and R.E. White, Plenum Press, New York, 319.
- Roscoe, S.G. and K.L. Fuller, 1992, Interfacial behavior of globular-proteins at a platinum-electrode, *J. Colloid Interf. Sci.* 152, 429.
- Roscoe, S.G., K.L. Fuller and G. Robitaille, 1993, An electrochemical study of the effect of temperature on the adsorption behavior of beta-lactoglobulin, *J. Colloid. Interf. Sci.* 160, 243.
- Rubianes, M.D. and G.A. Rivas, 2003, Carbon nanotubes paste electrode, *Electrochem. Commun.* 5, 689.
- Ruttkay-Nedecky, G., 1964, Charakteristische polarographische aktivitat des tabakmosai-virus IV. Ursprung der viruswelle und ursache des unterschiedlichen polarographischen effektes des virus und der nichtvirusproteine, *Coll. Czech. Chem. Commun.* 29, 1809.
- Ruttkay-Nedecky, G., 1971, Polarographic changes accompanying the re-formation of tobacco mosaic virus capsid from its disordered polypeptide chains, *Experientia Suppl.* 18, 553.
- Ruttkay-Nedecky, G. and A. Anderlova, 1967, Polarography of proteins containing cysteine, *Nature* 213, 564.
- Ruttkay-Nedecky, G. and B. Bezuch, 1971, Polarographic changes accompanying denaturation and renaturation of tobacco mosaic virus protein, *J. Mol. Biol.* 55, 101.
- Ruttkay-Nedecky, G. and E. Palecek, 1980, Differential pulse-polarographic analysis of tobacco mosaic virus, *Acta Virol* 24, 175.
- Ruttkay-Nedecky, G., G. Bezuch and V. Vesela, 1977, The state of the tobacco mosaic virus protein subunit at the dropping mercury electrode, *Bioelectrochem. Bioenerg.* 4, 399.
- Ruttkay-Nedecky, G., M. Takacova and V. Vesela, 1984, Use of amino acid replacement for study of the polarographic catalytic hydrogen currents of proteins, *Charge and Field Effects in Biosystems*, Eds. M.J. Allen and P.N.R. Usherwood, Wellingborough 377.
- Ruttkay-Nedecky, G. and V. Brabec, 1985, Voltammetry of tobacco mosaic-virus and its isolated protein at the graphite electrode, *Gen. Physiol. Biophys.* 4, 393.
- Ruttkay-Nedecky, G. and V. Vesela, 1977, Effect of amino acid replacement on the stability of the tobacco mosaic virus protein structure, *Acta Virol* 21, 365.
- Sachadyn, P., A. Stanisawska and J. Kur, 2000, One tube mutation detection using sensitive fluorescent dyeing of MutS protected DNA, *Nucleic Acids Res.* 28, E36.
- Santhanam, K.S.V., N. Jespersen and A.J. Bard, 1977, Application of a novel thermistor mercury electrode to the study of changes of activity of an adsorbed enzyme on electrochemical reduction and oxidation, *J. Am. Chem. Soc.* 99, 274.
- Scharer, O.D., 2003, Chemistry and biology of DNA repair, *Angew. Chem. Int. Edit.* 42, 2946.

- Scheller, F. and H. Jehring, 1972, Untersuchen des helix-knauel-uberganges von poly lysin mit der wechselstrompolarographie, *Studia Biophys.* 33, 211.
- Scheller, F., H. Jehring and U. Retter, 1973, Elektrosorptionsanalyse der beta-structur und der knaueform von poly-L-lysin, *Studia Biophys.* 39, 47.
- Scheller, F., M. Janchen and H.-J. Prumke, 1975, Adsorption behaviour of globular proteins at the water/mercury interface, *Biopolymers* 14, 1553.
- Schlunegger, M.P., M.J. Bennett and D. Eisenberg, 1997, Oligomer formation by 3D domain swapping: A model for protein assembly and misassembly, *Adv. Protein Chem.* 50, 61.
- Schubert, U., L.C. Anton, J. Gibbs, C.C. Norbury, J.W. Yewdell and J.R. Bennink, 2000, Rapid degradation of a large fraction of newly synthesized proteins by proteasomes, *Nature* 404, 770.
- Sedo, O., S. Billova, E.M. Pena-Mendez, E. Palecek and J. Havel, 2004, Derivatisation of peptides with osmium tetroxide, 2,2'-bipyridine: capillary electrophoretic and MALDI-TOF mass spectrometric study, *Anal. Chim. Acta* 515, 261.
- Serpell, L.C., 2000, Alzheimer's amyloid fibrils: Structure and assembly, *Biochim. Biophys. Acta* 1502, 16.
- Serpell, L.C., J. Berriman, R. Jakes, M. Goedert and R.A. Crowther, 2000, Fiber diffraction of synthetic alpha-synuclein filaments shows amyloid-like cross-beta conformation, *Proc. Natl. Acad. Sci. USA* 97, 4897.
- Slowinski, K., R.V. Chamberlain, C.J. Miller and M. Majda, 1997, Trough-bond and chain-to-chain coupling. Two pathways in electron tunneling through liquid alkanethiol monolayers on mercury electrodes, *J. Am. Chem. Soc.* 119, 11910.
- Soussi, T., Y. Legros, R. Lubin, K. Ory and B. Schlichtholz, 1994, Multifactorial analysis of p53 alteration in human cancer: A review, *Int. J. Cancer* 57, 1.
- Spiegel, S., E. Skutelsky, E.A. Bayer and M. Wilchek, 1982, A novel-approach for the topographical localization of glycolipids on the cell-surface, *Biochim. Biophys. Acta* 687, 27.
- Spillantini, M.G., M.L. Schmidt, V.M.Y. Lee, J.Q. Trojanowski, R. Jakes and M. Goedert, 1997, Alpha-synuclein in Lewy bodies, *Nature* 388, 839.
- Spillantini, M.G., R.A. Crowther, R. Jakes, M. Hasegawa and M. Goedert, 1998, Alpha-synuclein in filamentous inclusions of Lewy bodies from Parkinson's disease and dementia with Lewy bodies, *Proc. Natl. Acad. Sci. USA* 95, 6469.
- Stankovich, M.T. and A.J. Bard, 1977, The electrochemistry of proteins and related substances. Part II. Insulin, *J. Electroanal. Chem.* 85, 173.
- Steiger, B., C. Padeste, A. Grubelnik and L. Tiefenauer, 2003, Charge transport effects in ferrocene-streptavidin multilayers immobilized on electrode surfaces, *Electrochim. Acta* 48, 761.
- Stevenson, K.J., M. Mitchell and H.S. White, 1998, Oxidative adsorption of n-alkanethioates at mercury. Dependence of adsorption free energy on chain length, *J. Phys. Chem. B* 102, 1235.
- Stryer, L., 1988, *Biochemistry*, 3rd ed., W.H. Freeman and company, New York.
- Su, X.D., R. Robelek, Y.J. Wu, G.Y. Wang and W. Knoll, 2004, Detection of point mutation and insertion mutations in DNA using a quartz crystal microbalance and MutS, a mismatch binding protein, *Anal. Chem.* 76, 489.
- Sugawara, K., S. Hoshi and K. Akatsuka, 1997, Voltammetric detection of avidin and biotin by biotin labeled with cysteine, *Fresenius J. Anal. Chem.* 358, 755.
- Sugawara, K., S. Hoshi, K. Akatsuka, S. Tanaka and H. Nakamura, 1996a, Electrochemical evaluation of avidin-biotin interaction using *N*-iodoacetyl-*N*-biotinylhexylenediamine, *Bioelectrochem. Bioenerg.* 39, 309.
- Sugawara, K., S. Tanaka and H. Nakamura, 1994, Electrochemical determination of avidin-biotin binding using electroactive biotin derivate as a marker, *Bioelectrochem. Bioenerg.* 33, 205.
- Sugawara, K., S. Tanaka and H. Nakamura, 1995, Electrochemical assay of avidin and biotin using a biotin derivate labeled with an electroactive compound, *Anal. Chem.* 67, 299.

- Sugawara, K., Y. Yamauchi, S. Hoshi, K. Akatsuka, F. Yamamoto, S. Tanaka and H. Nakamura, 1996b, Accumulation voltametry of avidin and biotin using a biotin labeled with Nile Blue A, *Bioelectrochem. Bioenerg.* 41, 167.
- Tanaka, S., K. Yoshida, H. Kuramitz, K. Sugawara and H. Nakamura, 1999, Electrochemical detection of biotin using an interaction between avidin and biotin labeled with ferrocene at a perfluorosulfonated ionomer modified electrode, *Anal. Sci.* 15, 863.
- Tarlov, M.J. and A.B. Steel, 2003, DNA-based sensors, *Biomolecular Films. Design, Function, and Applications*, Ed. J.F. Rusling, Marcel Dekker, New York, 545.
- Tarlov, M.J. and E.F. Bowden, 1991, Electron-transfer reaction of cytochrome *c* adsorbed on carboxylic acid terminated alkanethiol monolayer electrodes, *J. Am. Chem. Soc.* 113, 1847.
- Tomschik, M., F. Jelen, L. Havran, L. Trnkova, P.E. Nielsen and E. Palecek, 1999, Reduction and oxidation of peptide nucleic acids and DNA at mercury and carbon electrodes, *J. Electroanal. Chem.* 476, 71.
- Tomschik, M., L. Havran, M. Fojta and E. Palecek, 1998, Constant current chronopotentiometric stripping analysis of bioactive peptides at mercury and carbon electrodes, *Electroanalysis* 10, 403.
- Tomschik, M., L. Havran, E. Palecek and M. Heyrovsky, 2000, The presodium catalysis of electroreduction of hydrogen ions on mercury electrodes by metallohionein. An investigation by constant current derivative stripping chronopotentiometry, *Electroanalysis* 12, 274.
- Travers, A. and M. Buckle, Eds., 2000, DNA-protein interactions, Oxford University Press, Oxford.
- Umek, R.M., S.S. Lin, Y.P. Chen, B. Irvine, G. Paulluconi, V. Chan, Y.C. Chong, L. Cheung, J. Vielmetter and D.H. Farkas, 2000, Bioelectronic detection of point mutations using discrimination of the H63D polymorphism of the Hfe gene as a model, *Mol. Diagn.* 5, 321.
- Uversky, V.N., 2003, A protein-chameleon: Conformational plasticity of alpha-synuclein, a disordered protein involved in neurodegenerative disorders, *J. Biomol. Struct. Dyn.* 21, 211.
- Uversky, V.N., J. Li and A.L. Fink, 2001, Evidence for a partially folded intermediate in alpha-synuclein fibril formation, *J. Biol. Chem.* 276, 10737.
- Valentini, F., A. Amine, S. Orlanducci, M.L. Terranova and G. Palleschi, 2003, Carbon nanotube purification: Preparation and characterization of carbon nanotube paste electrodes, *Anal. Chem.* 75, 5413.
- Vogelstein, B. and K.W. Kinzler, 1992, p53 Function and dysfunction, *Cell* 70, 523.
- Wackerbarth, H., M. Grubb, J. Zhang, A.G. Hansen and J. Ulstrup, 2004a, Long-range order of organized oligonucleotide on Au(111) electrodes, *Langmuir* 20, 1647.
- Wackerbarth, H., R. Marie, M. Grubb, J. Zhang, A.G. Hansen, I. Chorkendorf, C.B.V. Christensen and J. Ulstrup, 2004b, Thiol- and disulfide-modified oligonucleotide monolayer structures on polycrystalline and single-crystal Au(111) surfaces, *J. Solid State Electrochem.* 8, 474.
- Wang, J., 1999, Towards genoelectronics: Electrochemical biosensing of DNA hybridization, *J. Chem. Eur.* 5, 1681.
- Wang, J., 2005, Carbon-nanotube based electrochemical biosensors: A review, *Electroanalysis* 17, 7.
- Wang, J., G. Rivas, X.H. Cai, M. Chicharro, P.A.M. Farias and E. Palecek, 1996, Trace measurements of insulin by potentiometric stripping analysis at carbon paste electrodes, *Electroanalysis* 8, 902.
- Wang, J. and M. Musameh, 2003, Carbon nanotube/teflon composite electrochemical sensors and biosensors, *Anal. Chem.* 75, 2075.
- Wang, J. and M. Musameh, 2004, Carbon nanotube screen-printed electrochemical sensors, *Analyst* 129, 1.
- Wang, J., X. Cai, J.Y. Wang, C. Jonsson and E. Palecek, 1995, Trace measurement of RNA by potentiometric stripping analysis at carbon paste electrodes, *Anal. Chem.* 67, 4065.

- Weber, P.C., D.H. Ohlendorf, J.J. Wendoloski and F.R. Salemme, 1989, Structural origins of high-affinity biotin binding to streptavidin, *Science* 243, 85.
- Weinreb, P.H., W. Zhen, A.W. Poon, K.A. Conway and P.T. Lansbury, Jr., 1996, NACP, a protein implicated in Alzheimer's disease and learning, is natively unfolded, *Biochemistry* 35, 13709.
- Weitzman, P.D.J., 1965, The standard reduction potential and free energy change of disulphide bonds in proteins, *Biochim. Biophys. Acta* 107, 146.
- Weller, R.O., 2001, How well does the CSF inform upon pathology in the brain in Creutzfeldt–Jakob and Alzheimer's diseases?, *J. Pathol.* 194, 1.
- Wolffe, A., 1995, *Chromatin. Structure and Function*, Academic Press, New York.
- Wu, X., Z. Khalpey and M. Cascalho, 2004, Cellular physiology of mismatch repair, *Curr. Pharm. Design* 10, 4121.
- Yeh, P. and P. Kuwana, 1977, Reversible electrode reaction of cytochrome *c*, *Chem. Lett.* 10, 1145.
- Yosypchuk, B. and L. Novotny, 2002, Cathodic stripping voltammetry of cysteine using silver and copper solid amalgam electrodes, *Talanta* 56, 971.
- Zarranz, J.J., J. Alegre, J.C. Gomez-Esteban, E. Lezcano, R. Ros, I. Ampuero, L. Vidal, J. Hoenicka, O. Rodriguez, B. Atares, V. Llorens, E.G. Tortosa, T. del Ser, D.G. Munoz and J.G. de Yebenes, 2004, The new mutation, E46K, of alpha-synuclein causes Parkinson and Lewy body dementia, *Ann. Neurol.* 55, 164.
- Zlatanova, J. and S.H. Leuba, 2004, Chromatin structure and dynamics: State-of-the-art, *New Comprehensive Biochemistry*, Vol. 39, Ed. G. Bernardi, Elsevier, Amsterdam.

APPENDIX

Methods in Proteomics

Sabina Billová and Emil Paleček

The completion of the DNA sequences of more than 260 organisms including the draft sequence of the human DNA provides us an abundance of information about the structure of individual genes of an organism, about its genome. Regrettably these data are insufficient to say anything about the structure, function and regulation of gene products in a cell, tissue or organ. The reason is that a gene can undergo splicing and that assorted products of this splicing can be moreover variously post-translationally modified. This leads to the production of not a single but many proteins of assorted composition and function.

To describe the protein complement of genome Wilkins *et al.* (1996) introduced first at the Meeting on Two-Dimensional Polyacrylamide-Gel Electrophoresis organized in Sienna in 1994 the word 'proteome' (Hochstrasser, 1998). It has spread worldwide and given rise to a new discipline 'proteomics'. Proteomics can be defined as the large-scale study of protein properties (expression level, post-translational modification, interactions, etc.) that would help us to understand complex biological processes occurring at a molecular level, their heterogeneity in various cell types and their alternation in disease states (Blackstock and Weir, 1999). Just a possible application of obtained information in medicine mainly for early detection of diseases and their 'tailor-made' therapy evokes the enormous interest of scientists and pharmaceutical companies in proteomics. This can be seen from the continuously increasing number of publications related to this field (Anderson and Anderson, 1998; Blackstock and Weir, 1999; Figeys, 2003; Hochstrasser, 1998; Huber, 2003; Chambers *et al.*, 2000; Kellner, 2000; Morrison *et al.*, 2003; Pandey and Mann, 2000; Patterson and Aebersold, 2003; Resing and Ahn, 2005; Wilkins *et al.*, 1996; Zhu *et al.*, 2003).

Over the years of its existence, proteomics has achieved the extensive technology development which has contributed to its expansion and splitting into several spheres including profiling, functional and structural proteomics. Profiling proteomics includes the study of the proteome and the comparative changes in the proteome. This means the identification of proteins present in a

DOI of original article: 10.1016/S1871-0069(05)01019-0

biological sample and proteins differentially expressed between various samples. Functional proteomics deals with the discovery of protein functions at the proteome level and structural proteomics investigates the three-dimensional (3D) structure of proteins, protein complexes and small-molecule–protein complexes (Figeys, 2003).

To study a wealth of genome expressed proteins from all the above-mentioned visual angles the following techniques are used: (1) protein separation and (2) protein identification and characterization. The traditional tool capable of separating more than 1000 proteins in a single gel is two-dimensional gel electrophoresis (2-DE). With this technique, proteins are first separated in one direction by their charge in the isoelectrofocusing (IEF) step and then separated in the orthogonal direction by their molecular size using denaturing polyacrylamide gel (Chambers *et al.*, 2000). 2-DE enables to obtain information about the expression levels of a proteome under various conditions but on the other hand, it is a time-consuming and laborious approach that handicaps scarce and hydrophobic proteins and has difficulties with reproducibility. In recent years, also other protein separation methods such as liquid chromatography (LC), high-pressure LC (HPLC) and capillary electrophoresis, have been successfully used and even have started to gain ground (Hochstrasser, 1998). Multidimensional LC is more amenable to automation and allows the detection of many proteins that previously were not visible on 2-DE gels (Cottingham, 2004).

One of the most widely employed methods of identifying and characterizing proteins including their post-translational modifications is mass spectrometry (MS). In this technique, either proteins excised from the 2-DE gel and consequently digested with protease, such as trypsin, or LC fractions containing already digested proteins are converted into gas-phase ions. Created ions are then separated and detected based on their mass-to-charge ratios (m/z) (Yates, 2000). Several types of MS techniques have been developed for this purpose. However, two of them, matrix-assisted laser desorption ionization (MALDI) and electrospray ionization (ESI) are preferred. These techniques differ in the process of ion formation. While ESI achieves ionization by spraying a sample solution through a charged needle at atmospheric pressure toward the inlet of the mass spectrometer, in MALDI ions are created by emission of short laser pulses at the sample co-crystallized with a matrix and deposited on a sample plate. To separate ions of particular m/z value, these MS techniques use various mass analyzers. MALDI ion sources are most commonly coupled with time-of-flight (TOF) analyzers, whereas ESI is normally coupled with ion-trap or triple-quadrupole spectrometer (Patterson and Aebersold, 2003). Both MALDI and ESI have a great potential for proteomics. This resides in their high sensitivity and suitability for automatization. Their possible connection with chromatographic methods allows high-throughput and on-line sequential analysis of peptide or protein mixtures (Zhu *et al.*, 2003). Various combinations of the above-mentioned methods were applied for two kinds of protein profiling strategies: “top-down” and “bottom-up” proteomics. While the former analyzes intact proteins the latter analyzes peptides in proteolytic digests (Resing and Ahn, 2005).

Most of 3D protein structures are obtained by means of X-ray crystallography, nuclear magnetic resonance (NMR) and computer structure prediction based on sequence homology with proteins of known 3D fold. X-ray crystallography determines the protein structure by formation of a crystal from the protein solution and by passing X-rays through it. Produced diffraction patterns are then analyzed. In NMR, the protein sample is placed in a strong magnetic field and exposed to electromagnetic radiation of a specific frequency. Its response to radio waves is recorded. In both cases, 3D protein structures are proposed from the measured spectra. The main goal of all structural techniques is to construct 3D molecular models of proteins and protein complexes with other metabolites, which facilitate a design of pharmacological agents against precisely chosen and well-characterized protein receptors (Stolarski, 2003).

One of the key approaches of proteomics research is bioinformatics that enables experiments done in real laboratory to be projected and completed by experiments done using computer. This means bioinformatic tools aid to monitor and quantify the separation of complex protein samples, to identify and characterize the separated proteins, to compute proteins structure and to translate DNA code into probable polypeptide chains. Moreover, they allow building protein databases that are the core of proteome research. Such databases are applied for example for the comparison of mass spectra of proteins digested with virtual enzymes in the virtual laboratory with mass spectra of proteins digested in real laboratory or for the function prediction based on 3D structure modeling of proteins belonging to known families (Hochstrasser, 1998).

Despite of the ingenuity of all the above-mentioned technologies their application in proteome studies is limited. The methods are pretentious to sample purity and demand on powerful, expensive equipment and qualified staff. They are also time consuming. Present estimates of the number of genes in the human genome that are expressed in a particular cell type reach 20,000–25,000. To identify such abundance of proteins, some of them critical for disease treatment, could take a long time. Hence, methods providing only restricted information but less money- and time-consuming and applicable to sample screening might have been used for preliminary structure and function determinations. As a most perspective, it seems to be therein an electrochemical analysis exceeding the other detection methods in simplicity, high sensitivity and relatively low costs.

REFERENCES

- Anderson, N.L. and N.G. Anderson, 1998, Proteome proteomics: New technologies, new concepts, and new words, *Electrophoresis* 19, 1853.
- Blackstock, W.P. and M.P. Weir, 1999, Proteomics: Quantitative and physical mapping of cellular proteins, *Trends Biotechnol.* 17, 121.
- Chambers, G., L. Lawrie, P. Cash and G.I. Murray, 2000, Proteomics: A new approach to the study of disease, *J. Pathol.* 192, 280.
- Cottingham, K., 2004, Integrated proteomics systems bring the pieces together, *Anal. Chem.* 76, 331A.

- Figeys, D., 2003, Proteomics in 2002: A year of technical development and wide-ranging applications, *Anal. Chem.* 75, 2891.
- Hochstrasser, D.F., 1998, Proteome in perspective, *Clin. Chem. Lab. Med.* 36, 825.
- Huber, L.A., 2003, Is proteomics heading in the wrong direction?, *Nat. Rev. Mol. Cell Biol.* 4, 74.
- Kellner, R., 2000, Proteomics. Concepts and perspectives, *Fresen. J. Anal. Chem.* 366, 517.
- Morrison, R.S., Y. Kinoshita, M.D. Johnson and T.P. Conrads, 2003, Proteomics in the postgenomic age, *Adv. Protein Chem.* 65.
- Pandey, A. and M. Mann, 2000, Proteomics to study genes and genomes, *Nature* 405, 837.
- Patterson, S.D. and R.H. Aebersold, 2003, Proteomics: The first decade and beyond, *Nat. Genet.* 33, 311.
- Resing, K.A. and N.G. Ahn, 2005, Proteomics strategies for protein identification, *FEBS Lett.* 579, 885.
- Stolarski, R., 2003, Thermodynamics of specific protein–RNA interactions, *Acta Biochem. Pol.* 50, 297.
- Wilkins, M.R., J.C. Sanchez, A.A. Gooley, R.D. Appel, I. Humphery-Smith, D.F. Hochstrasser and K.L. Williams, 1996, Progress with proteome projects: Why all proteins expressed by a genome should be identified and how to do it, *Biotechnol. Genet. Eng. Rev.* 13, 19.
- Yates, J.R., 2000, Mass spectrometry – from genomics to proteomics, *Trends Genet.* 16, 5.
- Zhu, H., M. Bilgin and M. Snyder, 2003, Proteomics, *Annu. Rev. Biochem.* 72, 783.

Polarography of Proteins: A History

Petr Zuman¹ and Emil Paleček²

¹*Department of Chemistry, Clarkson University, Potsdam, NY 13699-5810, USA*

²*Institute of Biophysics, Academy of Sciences of the Czech Republic, 612 65 Brno, Czech Republic*

Contents

1. Introduction	755
2. Electrochemistry of proteins	756
2.1. Early history	756
2.2. Catalytic hydrogen evolution at mercury electrodes	759
2.2.1. Analysis of proteins	759
2.2.2. Denaturation of proteins	759
2.2.3. Cancer research	761
2.2.4. Proteolysis and immunochemistry	762
2.2.5. Adsorption of proteins	763
2.3. Voltammetry at solid electrodes	764
3. Summary and conclusions	765
Acknowledgments	765
References	765

1. INTRODUCTION

The early investigations up to the end of the 19th century established that proteins are a class of complex compounds, having both basic and acidic properties, made up of many different constituents, often associated with other compounds such as carbohydrates and nucleic acids. The quiescent period in protein research in the beginning of the 20th century was interrupted by the impetus given by electrophoretic, ultracentrifugal, X-ray and chromatographic analysis, which led to the studies of physical and chemical properties of proteins such as their quantitative amino acid composition as well as size, shape and charge distribution (Neurath and Bailey, 1953). Around 1930, the first X-ray photographs of silk fibroin and keratin fibers were published (Neurath and Bailey, 1954) but the arsenal of methods of the protein chemistry was still rather limited.

The beginning of protein electrochemical analysis dates back to the end of the 1920s that is to the time less than a decade after the invention of polarography by Jaroslav Heyrovský (1922, 1923, 1924a, b). Application of polarography as the first automatic recording instrument, in the analysis of proteins thus represented a welcome extension of this arsenal. In 1930, basic information about the biological importance of proteins was available but the biological function

of nucleic acids was not recognized. In spite of the discovery of the genetic role of DNA by Avery *et al.* in 1944 (Avery *et al.*, 1944), in 1950 it was still believed by many scientists (Haurowitz, 1950) that proteins can “self replicate” thus playing the genetic role, nowadays assigned to nucleic acids and particularly to DNA. The primary structure of nucleic acids was assumed to be a monotonously repeated “statistical tetranucleotide” composed of four different bases. Naturally, such a monotonous primary structure could not contain any complicated information. In contrast, the biological importance of proteins was greatly appreciated among the scientists at the same time. Taken together, around 1930, the chemistry and biology of proteins was more advanced than the chemistry and biology of nucleic acids, but in both cases new methods were sought at that time.

Electrochemistry of proteins was initiated in J. Heyrovský's laboratory by his co-workers, Herles, Vančura and Babička (Heyrovský, 2004). Using polarography, they discovered a new phenomenon, manifested by the ability of proteins to catalyze hydrogen evolution at the dropping mercury electrode (Heyrovský and Babička, 1930a,b; Herles and Vančura, 1932). The next important milestone was the observation of R. Brdička (1933a,b,c) who demonstrated that proteins are able to produce a characteristic catalytic double-wave in ammoniacal cobalt solutions. The ability of polarography to detect and determine cysteine-containing proteins became widely used during the next decades. Developed analytical procedures were frequently connected with the name of its inventor. Applications of Brdička's catalytic wave dominated the polarography of proteins for several decades (Březina and Zuman, 1958; Homolka, 1971; Paleček, 1983; Sequaris, 1992; Brabec *et al.*, 1996) and their impact is summarized below.

2. ELECTROCHEMISTRY OF PROTEINS

2.1. Early history

Probably the first instance, when a change in the current–voltage curves obtained by a microelectrode in the presence of proteins was reported was the observation by Herles and Vančura (1932) that addition of proteins to a solution of sodium chloride results in an increase in cathodic current at negative potentials. As the increase occurred at a potential, just before by some 0.3 V more positive than the potential at which sodium ions are reduced, the wave-shaped increase in current was denoted as a “pre-sodium wave.” Some details of the road to their discovery has recently been discussed elsewhere (Heyrovský, 2004).

Heyrovský and Babička (1930a, b) and Babička (1930) observed that with the increasing concentration of the protein, the peak current of this wave reached a limiting value. When the current–voltage curves were recorded in ammonium chloride instead of sodium chloride the waves were more pronounced, the authors concluded that the wave was due to a reduction of hydrogen ions and that the presence of proteins caused a decrease in hydrogen overvoltage.

Brdička (1936) has shown that in the electrode process preceding an electrode uptake, the ammonium ions acted as proton donors and can be replaced by other sources of hydrogen ions, such as an acid component of a buffer. Currents, which correspond to a reduction of hydrogen ions at potentials that are more positive than those of the reduction of hydrogen ions originating from the buffer used, are called “catalytic currents.” The catalytic currents observed in buffered solutions in the presence of proteins were observed at $\text{pH} > 7$. Their height was observed to decrease with increasing pH , as the concentration of the acid form acting as a proton donor decreased and at $\text{pH} > 12$ they were no more measurable. At $\text{pH} < 7$, the catalytic wave is superimposed by the current of reduction of hydrogen ions from the buffer used.

Waves of the type observed in the presence of various proteins have been subsequently described as “pre-sodium,” even when they appeared at potentials that are more positive than those of the hydrogen ion from the buffer, rather than those at which sodium ions are reduced. The height (limiting current) of “pre-sodium” waves increased with the increasing buffer capacity. Addition of some heavy metal ions, such as Co (II) resulted in an increase in the height of the “pre-sodium” wave. The occurrence of these waves in unbuffered solutions such as those of sodium or potassium chloride has been attributed to the role of protein as a buffer. The exact nature of processes involved in “pre-sodium” waves is uncertain, but a role of -SH and protonated amino groupings has been indicated. Whereas the role of the -SH groups (and possibly S-S groups after their reduction) may be predominant, the role of nitrogen-containing groups in processes involved in “pre-sodium” wave has been demonstrated by a decrease of this wave after catalytically active insulin was gradually acetylated.

Brdička (1933a) observed a much more pronounced change in current–voltage curves, if the buffer solution (usually an ammonia-ammonium chloride buffer) contained some cobalt salt, either in the oxidation state two or three. The details of the accidental discovery have recently been discussed by Heyrovský (2004).

In ammoniacal solutions of Co (II) ions the catalytic effect of proteins resulted in two increases on the current–voltage curve in the shape of a double wave. Which functional groups of proteins are responsible for each of these current increases is not known with certainty, but the role of the presence of thiol groups seems essential. Proteins, which do not contain an SH and/or an S-S grouping, like gelatin, do not yield this characteristic double wave. The catalytic current in the presence of proteins is about 500 times higher than the diffusion controlled limiting current, corresponding to the electroreduction of cobalt ions.

Simple thiols, cysteine, cystine and some thiol or S-S groups containing polypeptides also yield catalytic waves (Brdička, 1933b; Stern and Beach, 1940; Page, 1948; Page and Waller, 1949; Fraser *et al.*, 1947; Tachi and Koide, 1951a, b). 2, 3-Dimercaptopropanol shows catalytic waves also in solutions of nickel, arsenic, bismuth and iron ions (Zuman and Zumanová, 1956). Compounds in which the thiol group is alkylated do not yield the catalytic wave (Trkal, 1952). Nevertheless, catalytic waves of these low-molecular-mass thiols have a shape of a single, rounded increase in current that occurs in the potential range, where the second catalytic wave of proteins is observed. Cystine is reduced at potentials more positive than that at which the catalytic current is observed.

The cleavage of the S–S bond in cystine yields two cysteine molecules. Consequently, at equimolar concentrations cystine yields a catalytic current that is twice as big as that observed in the presence of cysteine.

For proteins, the heights of catalytic waves in the presence of Co (II) and Co (III) are comparable, but in presence of cystine the catalytic waves in Co (III) solutions are much smaller than those in the presence of Co (II), which forms weaker, labile complexes with ammonia than Co (III). Thus in mixtures of proteins and cystine, recording of current–voltage curves in solutions of Co (III) enables the determination of proteins in the presence of simpler thiol compounds (Brdička, 1933c). This approach was used in following the hydrolysis of proteins. Alternatively, comparison of catalytic waves in ammoniacal solutions containing Co (II) and Co (III) enabled determination of cysteine and cystine as products of the hydrolysis of proteins (Stern *et al.*, 1939).

At a given concentration of Co (II) or Co (III) in an ammoniacal buffer of chosen composition, the catalytic waves increase with increasing concentration of the protein and both catalytic currents reach at sufficiently high concentration of the protein a limiting value (Brdička, 1947). At low concentrations of proteins the more positive wave is higher than the second (both measured from the limiting current of the reduction of the cobalt ions), but above a certain concentration (called crossing point) the more negative catalytic current is higher (Tropp *et al.*, 1939; Tropp and Herrbach, 1944). Both catalytic currents and the crossing point depend on the nature of the protein. In general, the higher the catalytic currents, the larger is the number of sulfur-containing groups in the given protein (Millar, 1951, 1953). At a given composition of the $\text{NH}_3\text{-NH}_4^+$ buffer and at a given concentration of the protein, both catalytic waves increase with increasing concentration of cobalt ions (Brdička, 1947).

The dependence of catalytic currents of proteins on pH is complex and is not yet completely understood. At least two factors are involved: the variation in composition of the complex of Co ions with ammonia and the acid–base properties of the thiol group. When the pH-dependence was followed in buffers, where the analytical concentration $[\text{NH}_3] + [\text{NH}_4^+]$ was kept constant and the pH-varied by a variation of the ratio $[\text{NH}_3]:[\text{NH}_4^+]$, the plot of the catalytic current as a function of pH passed through a maximum. The pH, at which this maximum was observed, varied (Millar, 1951, 1953) from pH 9.3 for chymotrypsin to pH 10.25 for pepsin. It can be assumed that the decrease in the catalytic current toward lower pH-values reflects the decrease in concentration of free NH_3 . This results in a shift in composition of the ammoniacal complex of cobalt. The decrease of the catalytic current at pH higher than that at which the maximum height was observed can be attributed to increasing concentration of the thiolate form (which is assumed not to be catalytically active) as well as to a decrease in concentration of NH_4^+ ions, which are the proton donors in the catalytic process. The catalytic waves in solutions of Ni (II) ions are generally lower than those in Co (II) solutions and show similar dependences on concentration of the protein or of the metal ion. Due to their lesser sensitivity, the waves in Ni (II) solutions are less frequently used, even when the catalytic waves of low-molecular-mass thiols in the presence of Ni (II) ions have recently been extensively investigated (Banica, 1991; Ion *et al.*, 1998; Banica and Ion, 1998, 2000).

2.2. Catalytic hydrogen evolution at mercury electrodes

2.2.1. Analysis of proteins

The catalytic waves of proteins do not allow the determination of individual electroactive proteins, when present in a mixture. Hence, reported applications of catalytic waves were restricted to analyses of samples containing a single kind of protein. Since various kinds of proteins yield – at a given concentration – catalytic waves of different heights, such waves can be used for analyses of mixtures of proteins only, if the ratio of concentrations of individual components remains practically constant. Even in such a situation an electrophoretic pre-separation is advised. To eliminate contributions of effects of low-molecular-weight thiols to measured catalytic waves, the use of ammoniacal solutions containing cobalt (III) are preferred.

An example of the uses of catalytic waves for following concentration changes of a single protein is the selection of optimal conditions for the precipitation of serum globulin (Schmidt, 1940a). For serum of healthy patients, the optimum conditions for precipitation of globulin were found in the presence of 0.5% acetic acid. Under optimum conditions the double wave was lower in the serum of cancer and arthritis patients than in the serum of healthy ones. To determine globulins in intraocular fluids, they were first separated by precipitation using saturated ammonium sulfate. The resulting precipitated globulin was then dissolved in an ammoniacal solution of cobalt (II) (Franta and Gosman, 1933). Proteins in tears were determined (Balík and Hradecký, 1953) after transfer on to a chromatographic paper, elution with physiological solution and dilution of the eluate with an ammoniacal cobalt solution. Addition of thrombin to fibrinogen resulted (Jühling *et al.*, 1938, 1939; Lyons, 1945) in an increase in catalytic waves, due to an increased number of accessible thiol groups. Fibrinogen B yielded a higher catalytic current than fibrinogen A. Catalytic waves were used for determination of proteins in wool (Marron and Routh, 1944), milk (Stamberg and Bailey, 1942; Gál, 1954), beer (Sandegren *et al.*, 1949), plants (Tropp and Stoye, 1942) and in the bee-toxin (apitoxin) (Fassbender, 1944).

The pre-sodium wave was also used to estimate the content of proteins in the serum of healthy individuals (Babička, 1930; Gawalowski and Gosman, 1932) and patients suffering from syphilis (Gawalowski, 1932), in cerebrospinal liquor (Taussig *et al.*, 1937, 1938; Seuberling, 1937), saliva (Monnier and Besso, 1954), egg white (Hata and Matsushita, 1951a), beer (Salač, 1936) and plants (Babička, 1934).

2.2.2. Denaturation of proteins

Denaturation processes of proteins that result in liberation of additional thiol groups accessible to the catalytic evolution of hydrogen can be followed using polarographic catalytic waves in ammoniacal buffer solutions. When serum is added to an alkaline solution, the height of the catalytic wave increases with increasing reaction time, until it reaches a height that is about 100% higher than

the initial value. After a prolonged contact time a slow and small decrease takes place (Brdička and Klumpar, 1937). Denaturation in the presence of hydrochloric acid occurs much slower. Similar changes in the height of the catalytic current with time was observed, when the serum was treated with proteolytic enzymes, such as pepsin.

Samples taken from reaction mixtures containing various albumins isolated from plasma, kept at pH about 13, have shown an increase in catalytic currents that followed first-order kinetics (Müller *et al.*, 1952). Similar approach was used in following an alkaline denaturation of ovalbumins (Hata and Matsushita, 1951b), serum albumins and serum globulins (Elpiner, 1949; Sasai and Egawa, 1950) as well as in the investigation of protection of serum proteins against denaturation in the presence of germanin (Jirovec and Wenig, 1943). Similar protection against denaturation was observed, when a small amount of formaldehyde was added to the serum, before the alkali hydroxide was added. On the other, when formaldehyde was added after addition of the base to serum, a normal increase in the catalytic wave with time was observed (Suolahti and Laine, 1941). Addition of formaldehyde to a solution of pseudoglobulin in a borate buffer pH 7–9.5 resulted in a decrease of the catalytic wave after transfer into an ammoniacal cobalt solution. The rate of decrease in the height of the catalytic wave increased with increasing concentration of the added formaldehyde, with increasing pH and with increasing temperature (Fiala, 1943).

The addition of urea at concentrations higher than about 1.7 M resulted in a decrease in catalytic waves recorded in the presence of albumins, globulins and fibrinogens obtained from plasma and serum of horses (Tropp and Geiger, 1942). When the resulting solution was dialyzed, urea was removed and the height of the catalytic wave returned to the value before the addition of urea. When serum albumin or globulin was treated for 30 min with a solution of 1.7–8.5 M urea, the reaction mixture deproteinated with sulfosalicylic acid and in the filtrate treated with an ammoniacal cobalt solution, the catalytic wave increased with increasing concentration of urea. When the protein was first treated with sulfosalicylic acid, precipitated protein filtered off and the urea was added only to the filtrate, oppositely a decrease of the catalytic wave was reported (Elpiner, 1949).

With increasing temperature, the height of the catalytic wave of serum in ammoniacal cobalt solution gradually increased. This increase continued until a temperature was reached, at which the protein coagulated. This coagulation was accompanied by a sharp decrease in the height of the catalytic wave (Jirovec and Wenig, 1943; Sasai *et al.*, 1953). After addition of germanin, coagulation was prevented and only at a higher temperature a slight decrease was observed in the height of the catalytic wave (Jirovec and Wenig, 1943). The dependences of the heat induced denaturation on the concentration of protein and added urea were also reported (Tropp and Stoye, 1942; Jühling *et al.*, 1938, 1939).

When solutions of proteins were exposed to ultrasound, deproteinated using sulfosalicylic acid and filtrated, the height of the catalytic wave in the filtrate increased with the duration of sonication (Elpiner, 1951). Irradiation by UV-light resulted in the denaturation of studied proteins, manifested by an initial increase in the height of the catalytic wave. After a prolonged time-period of

irradiation, when coagulation of denatured proteins took place, the catalytic currents gradually decreased (Wenig and Jírovec, 1938; Schmidt, 1940b). Albumin was denatured faster than globulin (Schmidt, 1940b). On the other, irradiation of proteins by X-rays up to 100,000 R did not result in any change in the height of the catalytic current (Heeren and Seuberling, 1940).

2.2.3. Cancer research

Differences in the activity of thiol groups in enzymatic processes in normal and canceromatic sera lead Brdička (1937a, b, c, d, e, 1938a, b, c, d, e, 1947) to approach the distinguishing of these two types of sera using polarography. Initial studies based on comparison of catalytic waves in ammoniacal cobalt solutions in the presence of sera indicated insufficiently small differences between catalytic currents obtained in normal and carcinomatic sera (Brdička, 1947). Somewhat larger differences between the behavior of normal and carcinomatic sera were observed, when the rate of alkaline denaturation of sera or their proteolytic cleavage with pepsin was followed (Brdička, 1947). In the sera of patients in advanced stages of cancer, the catalytic waves of the products of denaturation or proteolysis were on an average by 10–30% lower than those obtained from sera of healthy patients. Such differences were not striking and, moreover, lower waves were observed also in the sera of patients suffering from various diseases accompanied by fever. Such observation indicated that in serum proteins of patients suffering from cancer is present a lower number of accessible cystine and cysteine residues. Such interpretation was supported by polarographic and spectrophotometric determinations of cystine in products of acid hydrolysis of sera. In these approaches it was essential to keep the dilution of sera and all components of the polarographed solution constant (Brdička, 1939).

The plot of the dependence of catalytic currents on serum concentration has namely a different shape for normal and carcinomatic sera. At a sufficiently high concentration of the serum, the catalytic wave obtained with carcinomatic serum can even become higher than in the presence of a normal one (Brdička, 1938a, b, c, d, e; Moravek *et al.*, 1938). An attempt has been made (Witwicki and Zyló, 1955) to distinguish carcinomatic from normal sera based on this difference. The above discussed total protein reaction yielded – based on analyzed sera of several hundreds of patients – positive results for 90% of sera with diagnosed cancer. Nevertheless, the test gave positive results also for numerous sera of patients, suffering from inflammatory diseases as well as patients with fever and for about 10% of healthy individuals (Brdička, 1938b, d; Abel, 1940; Albers, 1940; Felkel, 1938; Griessmann *et al.*, 1938; Chytrek, 1940; Klatt *et al.*, 1941; Meyer-Heck, 1939; Poli, 1939; Rush *et al.*, 1940; Walker and Reimann, 1939; Wedemeyer and Daur, 1939).

Limited specificity of the total protein test led Brdička (1947) to investigate the differences in the height of catalytic waves, obtained after alkaline denaturation of the protein-containing sample. After the denaturation in 0.1 M KOH was carried out at 25°C for a chosen time-interval (e.g., 45 min), the hydrolysate was treated with sulfosalicylic acid. The precipitated albumins and

globulins were removed by filtration and the clear filtrate was added to an ammoniacal solution of cobalt (III). The height of the catalytic double-wave was measured from the limiting current of cobalt (best recorded in the absence of protein). For calibration of the experimental set-up used, the height of the catalytic wave was measured using at least 30 sera of clinically healthy patients. The temperature at which the denaturation is carried out (Bartík, 1953; Bartík and Zwick, 1952) as well as the duration of denaturation (Bartík *et al.*, 1954) and amount of sulfosalicylic acid (Kalous, 1955) have to be carefully controlled.

The reliability of the filtrate test was verified based on experiments with more than 20,000 sera and was found positive in more than 90% of patients with proven cancer. It is unreliable only in cases of small, not metastasizing skin cancers. In some cases involving inflammatory and feverish conditions the test also gave positive results, but such cases can be diagnostically eliminated or ruled out by repetition of the filtrate test after some time-intervals. The test was found also useful for confirmation of the success of chemotherapy, irradiation or surgical treatments (Březina and Zuman, 1958; Müller, 1963; Homolka, 1971; Brdička *et al.*, 1965). A standardization of the test was proposed (Kalous and Pavlíček, 1963). The analysis of plasma instead of serum was also recommended (Podroužek, 1948). The increase of the catalytic active component in the sulfosalicylic acid filtrates after alkaline denaturation of the protein-containing sample was attributed to an increase in mucoproteins (Kalous, 1955, 1958, 1960, 1966; Kalous and Pavlíček, 1962). Numerous modifications of the protein filtrate test and clinical experiences with its clinical applications are discussed in some detail in the monograph by Březina and Zuman (1958) where further references are included.

2.2.4. *Proteolysis and immunochemistry*

The catalytic waves in ammoniacal cobalt solutions were used for following the reaction of proteases (Podroužek, 1943; Abderhalden *et al.*, 1945). The method was used for following the presence of cleavage products of proteins in mammal milk during menstruation (Podroužek and Jonáš, 1945). Polarographic investigation of auto proteolysis of sera of patients suffering from pernicious anemia occurs slower than the sera of healthy individuals (Janoušek *et al.*, 1955b). In cases of histamine-resistant achylia the activity of pepsin in serum is by 35–100% lower than in normal sera (Janoušek *et al.*, 1955a). The increase in the catalytic wave due to proteolysis was used for evaluation of activities of various preparations of pepsin (Brdička and Klumpar, 1937; Hrdý, 1950) and trypsin (Štokrová, 1954).

The antigen–antibody interaction was followed polarographically by measuring a decrease in the reduction wave of an azoprotein in the presence of antiserum (Breyer and Radcliff, 1951, 1953). By the investigation of interaction of low-molecular-weight antigens (haptens) with antiserum, it was possible to follow interactions of antibodies with a hapten containing 2, 4-dinitrophenol (Zikán, 1966). In the determination of equilibrium a polarographically active hapten bound to an antibody was followed, as it was displaced by an excess of an electroinactive hapten (Schneider and Schon, 1961).

2.2.5. Adsorption of proteins

Presence of adsorption of surface-active species, such as proteins, can be manifested on current–voltage curves obtained with mercury electrodes in five different ways:

- (1) As mentioned above, the current due to catalysis of the reduction of hydrogen ions in the presence of proteins – both in the “pre-sodium” wave and the catalytic waves in ammoniacal cobalt solutions – reaches with increasing concentration of the catalytically active species to a limiting value. This indicates that the process is heterogeneous, occurs at the electrode surface and depends on the surface area of the electrode. This is interpreted as due to the adsorption of the electroactive species at the electrode surface.
- (2) In some solutions, application of a voltage is accompanied by a movement of the electroactive species in the solution in the vicinity of the electrode. This results in these solutions a transport of the electroactive species to the electrode surface by convection, in addition to the transport by diffusion. This increased transport of the reducible or oxidizable species to the electrode surface results in such solutions with a steep increase in current, terminated at a certain potential. These phenomena are described as “streaming polarographic maxima.” When the goal of a given experiment is to measure exactly the limiting current – as it is in analytical applications of polarography and its congeners – such maxima are unwanted. They can be suppressed by addition of solutions of surface-active agents, very often by a dilute solution of gelatin. For the same purpose some manmade polymers can be added. Nevertheless, such polymers, like Triton-X, are adsorbed only over a certain potential range, whereas gelatin offers the advantage to be adsorbed over a wide range of potentials. Furthermore, gelatin is adsorbed at the electrode surface in such a way that it prevents the streaming phenomena, but affects very little the transport of the electroactive species by diffusion through the adsorbed layer of gelatin at the electrode surface. It may be envisaged that adsorbed gelatin forms around the electrode a kind of netting, through which transport of electroactive species by diffusion is little hindered. Alternatively, the suppression of streaming maxima by surface-active species depends on the concentration of the added soluble surface-active substance in the investigated solution. The degree of suppression of streaming maxima can be therefore used for determination of the total amount of surface-active substances in a given sample. If the only surfactant present is a protein, the suppression of the maximum current can be used for estimating the concentration of such protein.
- (3) For complex proteins containing an electroactive center, a situation can arise that in the protein molecule adsorbed at the electrode surface, the electroactive center is located in a position that is too far from the electrode surface to allow a sufficiently rapid electron transfer from or to the electrode from the electroactive center. In such cases a direct oxidation–reduction interaction between the protein and the electrode is prevented. A typical example of such behavior is that of cytochrome *c*, in which the hemin is not readily involved in an oxidation–reduction process. To obtain information

about oxidation–reduction properties of such unreactive proteins, it is necessary to use mediators. Mediators are low-molecular-weight compounds, which can undergo reversible oxidation–reduction processes within the needed potential range. Such mediators are involved in oxidation–reduction process with the investigated protein in some distance from the electrode surface. Product of the oxidation or reduction of the mediator is then transported by diffusion to the electrode surface where it is reduced or oxidized. The current flowing in such process can then be recorded as a function of the applied potential.

- (4) Another way in which an adsorption of proteins at the electrode surface is manifested, is by a change in the charging current, that is the current needed to charge the electrode at a given potential. Such adsorption phenomena can be followed by comparing the current–voltage curve in blank supporting electrolyte with that after addition of the protein (Doss and Gupta, 1952, 1954; Doss and Kalyanasundaram, 1951, 1952). More accurate and quantitative information can be obtained by measuring differential capacity or more conveniently using AC polarography (in these applications denoted as “tensammetry”) (Gupta, 1954; Berg and Gollmick, 1966; Breyer, 1958; Breyer and Radcliff, 1954; Breyer and Bauer, 1963).
- (5) Adsorption of a species that is neither reduced nor oxidized in the investigated potential range, such as a protein, can be followed by evaluating changes in current–voltage curves of some electroactive compound (Reilley and Stumm, 1962; Heyrovský and Kuta, 1965). The interpretation of changes of limiting currents of reduction of metal ions in the presence of proteins (Tanford, 1951, 1952a, b; Kačena, 1954; Zumanová *et al.*, 1957) is complicated by a possible formation of complexes of metal ions with proteins. The principles, on which the latter two approaches are based, have recently been discussed by Zuman and Rusling (2002).

2.3. Voltammetry at solid electrodes

Electrooxidation of proteins, such as lysozyme, ribonuclease, concanvalin A and bovine serum albumin was observed by Brabec (1980), Brabec and Mornstein (1980a, b) and Reynaud *et al.* (1980). The studied proteins produced oxidation signals in the vicinity of 0.7–0.8 V at neutral pH at carbon electrodes. The observed signals were assigned to irreversible oxidation of tyrosine and tryptophan residues in the proteins. In some proteins containing both amino acid residues (e.g. lysozyme) two separated signals were observed. Usually, only poorly developed peaks were obtained at micromolecular protein concentrations. An increase in these peaks was observed as a result of the treatment of the protein with various denaturation agents (Brabec, 1980; Ruttkay-Nedecký and Brabec, 1985). Voltammetry was applied to investigate accessibility of tryptophan and tyrosine residues. More details concerning protein oxidation at carbon electrodes are given in Chapter 19.

Noble metals such as gold, silver and platinum modified with various adsorbates have been increasingly applied as electrodes in protein electrochemistry

since the end of the 1970s. The interest of electrochemists turned also gradually to a relatively small group of conjugated proteins containing redox centers providing fast reversible electrode processes (Chapters 14 and 15, pp. 16–17).

3. SUMMARY AND CONCLUSIONS

Initial steps of polarography of proteins started in Heyrovský's laboratory in Prague (Czechoslovakia) on the turn of the 1920s and 1930s by the discovery of the ability of proteins to catalyze hydrogen evolution at mercury electrodes (Chapter 18). Poorly developed pre-sodium wave, attributed to this catalysis occurring at negative potentials close to the background discharge was, however, of little analytical use. In 1933, R. Brdička observed new catalytic currents in ammoniacal buffers containing cobalt ions. Brdička's characteristic protein double wave was much better developed than the pre-sodium wave; the double wave soon became a subject of numerous research papers, many of them related to medical problems particularly to cancer. At the present time, a renewed interest in the pre-sodium wave can be seen because the application of the constant current chronopotentiometry in combination with HMDE transformed the poorly developed pre-sodium wave into a well-developed peak capable to detect nanomolar and subnanomolar concentrations of peptides and proteins (Chapter 19). In 1980, it was shown by Brabec and Reynaud *et al.* that tyrosine and tryptophan residues in proteins are oxidizable at carbon electrodes. The interest of electrochemists has recently been turned (as mentioned above) to a group of conjugated proteins containing redox groupings that facilitate rapid reversible electrochemical processes, which are discussed in this Volume in Chapters 14–17. In parallel with the increased interest in solid electrodes, mercury electrodes were less applied in protein studies in spite of a number of advantages, including smooth surface, high hydrogen overpotential, excellent reproducibility, etc. At present it appears that these electrodes may find their use in proteomics and biomedicine (Chapter 19).

ACKNOWLEDGMENTS

The authors are indebted to Dr. Z. Pechan for his help in the preparation of the final version of the manuscript. This work was supported by grant COST OC D21-002 to E. P.

REFERENCES

- Abderhalden, E., R. Adberhalden and J. Klumpar, 1945, Application of polarographic method in the detection of protease activity, especially that of protective proteinase (in German), *Fermentforsch* 17, 600.
- Abel, W., 1940, Comments to polarographic carcinom reaction (in German), *Chirurg* 12, 585.

- Albers, D., 1940, Testing of the polarographic Prague cancer reaction (in German), *Biochem. Z.* 306, 236.
- Avery, O.T., C.M. Macleod and M. McCarty, 1944, Studies on the chemical transformation of pneumococcal types, *J. Exp. Med.* 19, 137.
- Babička, J., 1930, The determination of proteins by means of the analysis with the dropping mercury kathode, *Bull. Int. Acad. Sci. Boheme* 31, 177.
- Babička, J., 1934, Analyses of substances released from plants from exoosmosis (in German), *Beihefte Botan. Zbl.* 52A, 485.
- Balík, J. and F. Hradecký, 1953, Polarographic determination of unhydrated albumins (in Czech), *Českosl. Oftalmolog.* 9, 495.
- Banica, F.G., 1991, Catalytic hydrogen evolution on the mercury electrode in the presence of nickel-aminothiols complexes. A tentative model process of hydrogenase-catalysed hydrogen bioproduction, *Bull. Soc. Chim. Fr.* 697.
- Banica, F.G. and A. Ion, 1998, Electrochemical investigations of the nickel(II)-penicillamine system. 2. Direct identification of complex species involved in catalytic nickel reduction on the dropping mercury electrode, *Collect. Czech. Chem. Comm.* 63, 995.
- Banica, F.G. and A. Ion, 2000, Electrochemical investigations of the nickel(II)-penicillamine system. 3. A study of the catalytic hydrogen prewave in connection with structure of nickel(II)-penicillamine complexes, *Collect. Czech. Chem. Comm.* 65, 995.
- Bartík, M., 1953, Following of temperature dependence of the denaturation of blood proteins of domestic animals using Brdička's filtrate test (in German), *Veter. Čas. Slov. Akad. Vied* 2, 69.
- Bartík, M., A. Točík and K. Zwick, 1954, Polarography of blood sera of domestic animals. Part IV. Following the temperature dependences of denaturation of blood proteins using Brdička's filtrate reaction II, *Veter. Čas. Slov. Akad. Vied* 3, 197.
- Bartík, M. and K. Zwick, 1952, Polarography of blood sera of domestic animals on the basis of Brdička's reaction, *Veter. Sbor. Slov. Aka. Vied* 3-4, 40.
- Berg, H. and F.A. Gollmick, 1966, Photodynamic effect and polarography of nucleic acids and proteins (in German), *Abh. Deutsch. Aka. Wiss. Berlin, Kl. Med.* 1, 533.
- Brabec, V., 1980, Electrochemical oxidation of nucleic-acids and proteins at graphite electrode. Qualitative aspects, *Bioelectrochem. Bioenerg.* 7, 69.
- Brabec, V. and V. Mornstein, 1980a, Electrochemical-behavior of proteins at graphite-electrodes. 1. Electrooxidation of proteins as a new probe of protein-structure and reactions, *Biochem. Biophys. Acta* 625, 43.
- Brabec, V. and V. Mornstein, 1980b, Electrochemical-behavior of proteins at graphite-electrodes. 2. Electrooxidation of amino-acids, *Biophys. Chem.* 12, 159.
- Brabec, V., V. Vetterl and O. Vrana, 1996, Electroanalysis of biomacromolecules. Experimental Techniques in Bioelectrochemistry, Vol. 3: Bioelectrochemistry: Principles and Practice, Eds. V. Brabec, D. Walz and G. Milazzo, Birkhauser Verlag, Basel, Switzerland, 287.
- Brdička, R., 1933a, Polarographic studies with the dropping mercury kathode. Part XXXI. A new test for proteins in the presence of cobalt salts in ammoniacal solutions of ammonium chloride, *Collect. Czech. Chem. Comm.* 5, 112.
- Brdička, R., 1933b, Polarographic studies with the mercury dropping kathode. Part XXXII. Activation of hydrogen in sulphhydryl group of some thioacids in cobalt salt solutions, *Collect. Czech. Chem. Comm.* 5, 148.
- Brdička, R., 1933c, Polarographic studies with the dropping mercury kathode. Part XXXIII. The microdetermination of cysteine and cystine in the hydrolysates of proteins and the course of the protein decomposition, *Collect. Czech. Chem. Comm.* 5, 238.
- Brdička, R., 1936, Polarographic studies with the dropping mercury kathode. Part XLI. The effect of buffer solutions on the reaction of proteins, *Collect. Czech. Chem. Comm.* 8, 366.
- Brdička, R., 1937a, Application of polarographic effect of proteins in cancer diagnosis, *Nature* 139, 330.
- Brdička, R., 1937b, Polarographic investigations in serological cancer diagnosis, *Nature* 139, 1020.

- Brdička, R., 1937c, Application of the polarographic effect of proteins in cancer diagnosis, *Bull. Int. Acad. Sci. Boheme* 38, 17.
- Brdička, R., 1937d, Serological research and diagnostics of cancer by means of the polarographic method (in Czech), *Lékař. Svět* 2(2), 6.
- Brdička, R., 1937e, Microserological diagnosis of cancer using the polarographic method (in German), *Med. Klinik* 33, 1186.
- Brdička, R., 1938a, Polarographic investigations of proteins (in French), *J. Chim. Phys.* 35, 89.
- Brdička, R., 1938b, Serological investigations using the polarographic technique and its importance in the diagnosis of cancer (in German), *Acta Int. Ver. Krebsbekämpfung* 3, 13.
- Brdička, R., 1938c, The polarographic serologic reaction for cancer, *Nature* 142, 617.
- Brdička, R., 1938d, The application of Heyrovský's polarographic method in serologic diagnosis of cancer (in German), *Rev. Gesundheitsw.* 20, 74.
- Brdička, R., 1938e, Polarographic test of serum proteins and its importance in the diagnosis of cancer (in French), *Compt. Rend. Soc. Biol.* 128, 54.
- Brdička, R., 1939, Critical remarks concerning the nature of the polarographic serum reaction for cancer, *Acta Radiol. Cancerol. Bohemia et Moraviae* 2, 7.
- Brdička, R., 1947, Polarographic cystine and protein tests, *Research* 1, 23.
- Brdička, R., M. Březina and V. Kalous, 1965, Polarography of proteins and its analytical aspects, *Talanta* 12, 1149.
- Brdička, R. and J. Klumpar, 1937, A polarographic study of the denaturation and proteolytic cleavage of proteins (in Czech), *Čas. Čes. Lékárn.* 17, 234.
- Breyer, B., 1958, Tensammetry, a method for investigating surface phenomena, *Z. Physikal. Chem. (Leipzig), Sonderheft*, 28.
- Breyer, B. and H.H. Bauer, 1963, Alternating current polarography and tensammetry, *Chemical Analysis*, Vol. 13, Interscience, New York.
- Breyer, B. and F. Radcliff, 1951, Polarographic investigation of antigen-antibody reaction, *Nature* 167, 79.
- Breyer, B. and F. Radcliff, 1953, Polarographic study of the antigen-antibody complex, *Aust. J. Exp. Biol. Med. Sci.* 31, 167.
- Breyer, B. and F.J. Radcliff, 1954, Polarographic study of the adsorptive capacity of serum proteins in renal deficiency, *Aust. J. Exp. Biol. Med. Sci.* 32, 411.
- Březina, M. and P. Zuman, 1958, *Polarography in Medicine, Biochemistry and Pharmacy*, Ch. XXX, Interscience, New York.
- Chytrek, E., 1940, Is the polarographic method specific for detection of a carcinoma? (in German), *Deutsche Med. Wochschr.* 66, 1190.
- Doss, K.S.G. and S.L. Gupta, 1952, Behavior of surface active substances at the dropping mercury electrode, *Proc. Indian Acad. Sci.* 36A, 493.
- Doss, K.S.G. and S.L. Gupta, 1954, Effect of some surface active agents on the capacity of the dropping mercury electrode, *Bull. Cent. Electrochem. Res. Inst. Karaikudi* 1, 9.
- Doss, K.S.G. and A. Kalyanasundaram, 1951, Theory of capacity phenomena displayed at mercury capillary electrode, *Curr. Sci.* 20, 199.
- Doss, K.S.G. and A. Kalyanasundaram, 1952, Effect of surface active substances on the capacity of the electric double layer, *Proc. Indian Acad. Sci.* 35A, 27.
- Elpiner, I.E., 1949, The specific behavior of denaturing agents (in Russian), *Vopr. Med. Khim.* 1-2, 282.
- Elpiner, I.E., 1951, Biological and physicochemical methods in cancer diagnosis (in Russian), *Usp. Sovrem. Biol.* 31, 191.
- Fassbender, W., 1944, Investigations of the nature of the bee-toxins using a dropping mercury cathode, *Biochem. Z.* 317, 246.
- Felkel, R.K., 1938, Polarographic studies on cancerous sera (in German), *Med. Klin.* 34, 840.
- Fiala, S., 1943, About the mode of the effect of formaldehyde on proteins (in German), *Naturwissenschaften* 31, 370.
- Franta, J. and B.A. Gosman, 1933, Polarographic determination of proteins in intraocular fluids (in Czech), *Čas. Lékař. Čes.* 72, 1317.

- Fraser, J.B., L. Nowen and G. Shaw, 1947, Bal-intrav: A new nontoxic thiol for intravenous injection in arsenical poisoning. II. Chemical observations, *Biochem. J.* 41, 328.
- Gál, T., 1954, Polarographic and electrophoretic examination of milk serum proteins (in Czech), *Prumysl Potravin* 5. 152 and 206.
- Gawalowski, K., 1932, Equilibria involving proteins in the serum of patients suffering from syphilis (in French), *Bull. Soc. Fr. Dermat. Syphil.* No. 7.
- Gawalowski, K. and B. Gosman, 1932, A polarographic analysis of proteins contained in human blood serum, *Bull. Int. Acad. Sci. Boheme* 33, 94.
- Griessmann, H., K., Koehler and W. Soehnel, 1938, Blood analysis for the diagnosis and prognosis of carcinoma, as well as for the therapy of recidives (in German), *Chirurg* 10, 609.
- Gupta, S.L., 1954, Comparative study of some macromolecules and some simple molecules on dropping mercury electrode capacity, *Kolloid Z.* 137, 86.
- Hata, T. and S. Matsushita, 1951a, Sulfhydryl groups. VI. Polarographic studies on eggwhite proteins, *Bull. Res. Inst. Food Sci., Kyoto Univ.* 7, 33.
- Hata, T. and S. Matsushita, 1951b, Sulfhydryl groups. VII. Polarographic observation on the denaturation of ovalbumin, *Res. Inst. Food Sci., Kyoto Univ.* 7, 42.
- Haurowitz, F., 1950, *Chemistry and Biology of Proteins*, Academic Press, New York.
- Heeren, J.P. and O. Seuberling, 1940, A contribution to different influence of UV-light and X-rays on proteins (in German), *Strahlentherapie* 67, 130.
- Herles, F. and H. Vančura, 1932, A research on the cause of the characteristic "wave" on the polarographic curve of human serum, *Bull. Int. Acad. Sci. Boheme* 33, 119.
- Heyrovský, J., 1922, Electrolysis with the dropping mercury cathode (in Czech), *Chem. Listy* 16, 256.
- Heyrovský, J., 1923, Electrolysis with a dropping mercury cathode. I. The deposition of alkali and alkaline earth metals, *Philos. Mag.* 45, 303.
- Heyrovský, J., 1924a, The processes at the mercury dropping cathode. I. The deposition of metals, *Trans. Faraday Soc.* 19, 692.
- Heyrovský, J., 1924b, The processes at the mercury dropping cathode. II. The hydrogen overpotential, *Trans. Faraday Soc.* 19, 785.
- Heyrovský, J. and J. Babička, 1930a, Polarographic studies with the dropping mercury cathode. Part XIII. The effect of albumins, *Collect. Czech. Chem. Comm.* 2, 370.
- Heyrovský, J. and J. Babička, 1930b, Polarographic studies with the dropping mercury cathode. Part XIII. The effect of albumins, *Chem. News* 141, 369.
- Heyrovský, J. and J. Kuta, 1965, *Principles of Polarography*, Ch. XVI, Publishing House of Czech. Acad. Sci., Prague, 287.
- Heyrovský, M., 2004, Early polarographic studies on proteins, *Electroanalysis* 16, 1067.
- Homolka, J., 1971, Polarography of proteins, analytical principles and application in biological and clinical chemistry, *Methods of Biochemical Analysis*, Vol. 19, Ed. D. Glick, Wiley, New York, 435.
- Hrdý, O., 1950, Polarography determination of pepsin (in Czech), *Chem. Listy* 44, 109.
- Ion, A., F.G. Banica and C. Luca, 1998, Electrochemical investigation of the nickel(II)-pencillamine system. Inert and labile complexes detected by polarography, *Collect. Czech. Chem. Comm.* 63, 187.
- Janoušek, S., K. Herfort and J. Škachová, 1955a, The relationship between gastric pepsin and serum pepsinogen (in Czech), *Čes. Gastroenterolog. Výživa* 9, 113.
- Janoušek, S., J. Kroulíková and F. Mališ, 1955b, A polarographic study of the auto-proteolytic enzymatic activity of human serum in acidic media and its changes in serum from patients with pernicious anaemia (in Czech), *Čas. Lék. Čes.* 94, 83.
- Jírovec, O. and K. Wenig, 1943, About some interesting physico-chemical and biological properties of germanin (Bayer 205). I and II (in German), *Biochem. Z.* 314. 265 and 315, 69.
- Jühling, L., C. Tropp and E. Wöhlisch, 1938, Polarographic investigations of the processes of bleeding (in German), *Naturwissenschaften* 26, 548.
- Jühling, L., C. Tropp and E. Wöhlisch, 1939, Polarographic investigations of proteins. II. Polarographic studies of states of fibrinogens (in German), *Z. Physiol. Chem.* 226, 210.

- Kačena, V., 1954, Protein interactions III. Interaction of serum albumin with zinc ions, *Collect. Czech. Chem. Comm.* 19, 428.
- Kalous, V., 1955, Nature of the polarographically active protein components of blood serum sulfosalicylate filtrate (in Czech), *Chem. Listy* 49, 171.
- Kalous, V., 1958, Polarographic and electrophoretic investigation of the protein components in sulfosalicylic acid filtrates of blood sera (in German), *Z. Physikal. Chem. (Leipzig), Sonderheft*, 186.
- Kalous, V., 1960, Polarographic determination of mucoprotein MP-1 after separation of serums by paper electrophoresis (in German), *Collect. Czech. Chem. Comm.* 25, 878.
- Kalous, V., 1966, Investigation of chromatographically isolated orosomucoid by polarography and some other physicochemical methods (in German), *Abh. Deut. Akad. Wiss. Berlin, Kl. Med.*, 455.
- Kalous, V. and Z. Pavlíček, 1962, Polarographic characterization of proteins, *Biochim. Biophys. Acta* 57, 44.
- Kalous, V. and Z. Pavlíček, 1963, Standardization of the polarographic filtrate reaction, *Clin. Chim. Acta* 8, 170.
- Klatt, T., H.P. Rush, A. Kirksen and V.M. Meloche, 1941, Cancer diagnosis by means of the dropping mercury electrode, *Trans. Electrochem. Soc.* 79, 205.
- Lyons, R.N., 1945, Thiol-vitamin K mechanism in clotting of fibrinogen, *J. Exp. Biol. Med. Sci.* 23, 131.
- Marron, T.V. and J.I. Routh, 1944, Physicochemical studies of the water-soluble fractions of powdered wool, *Arch. Biochem.* 4, 319.
- Meyer-Heck, P., 1939, Polarographic cancer reaction and the measurement of the activity of thiol groups in sera in their reaction with methylglyoxalase, VII (in German), *Z. Krebsforschg.* 49, 560.
- Millar, G.J., 1951, Relationship between polarographic protein wave height and total potential sulfhydryl content of protein, *Fed. Proc.* 10, 92.
- Millar, G.J., 1953, Polarography of proteins. I. Relation of wave heights to protein concentration and origin of wave III, *Biochem. J.* 53, 385.
- Monnier, D. and Z. Besso, 1954, Polarographic study of saliva (in French), *Helv. Chim. Acta* 37, 455.
- Morávek, V., E. Kiliánová and O. Malý, 1938, A contribution to the serodiagnosis of malignant tumors, *Acta Radiol. Cancerol. Bohemo-Slovenica* 1, 134.
- Müller, O.H., 1963, Polarographic analysis of proteins, amino acids and other compounds by means of the Brdička reaction, *Methods of Biochemical Analysis*, Vol. 11, Ed. D. Glick, Interscience, New York, 329.
- Müller, O.H., L.H. Gerschenfeld and M.J. Elwood, 1952, Polarographic differentiation of various plasma albumins, *Fed. Proc.* 13, 340.
- Neurath, H. and K. Bailey, 1953, Preface. *The Proteins*. 1st ed., Vol. 1, Part A, Eds. H. Neurath and K. Bailey, Academic Press Inc., New York, vii.
- Neurath, H. and K. Bailey, Eds., 1954, *The Proteins – Chemistry, Biological Activity, and Methods*, Vol. II, Part B, Academic Press Inc., New York.
- Page, J.E., 1948, The polarography of penicillin, *Analyst* 73, 214.
- Page, J.E. and J.G. Waller, 1949, Polarographic determination of thiomersalate, *Analyst* 74, 292.
- Paleček, E., 1983, Modern polarographic (voltammetric) methods in biochemistry and molecular biology. Part II. Analysis of macromolecules. *Topics in Bioelectrochemistry and Bioenergetics*, Vol. 5, Ed. G. Milazzo, Wiley, London, 65.
- Podroužek, V., 1943, Polarographic following of the protective reaction of proteins (in German), *Fermentforschg* 17, 53.
- Podroužek, V., 1948, A contribution to Brdička's polarographic test in blood deproteinated with sulfosalicylic acid (in Czech), *Čas. Lekař. Čes.* 87, 1006.
- Podroužek, V. and O. Jonás, 1945, The behavior of the milk gland during the menstruation circle in the Abderhalden reaction (in Czech), *Čas. Lekar. Čes.* 84, 235.
- Poli, E., 1939, Polarographic method for diagnosis of malignant tumors (in Italian), *Diagnost. Tecn. Lab.* 10, 565.

- Reilley, Ch.N. and W. Stumm, 1962, Adsorption in polarography, *Progress in Polarography*, Vol. 1, Eds. P. Zuman and I.M. Kolthoff, Interscience, New York, 81.
- Reynaud, J.A., B. Malfoy and A. Bere, 1980, The electrochemical oxidation of 3 proteins – RNAase-A, bovine serum-albumin and concanavalin-A at solid electrodes, *Bioelectrochem. Bioenerg.* 7, 595.
- Rush, H.P., T. Klatt, V.W. Meloche and A.J. Dirkens, 1940, Effect of serum proteins on the polarographic curve, *Proc. Soc. Exp. Biol. Med.* 41, 362.
- Ruttkay-Nedecký, G. and V. Brabec, 1985, Voltammetry of tobacco mosaic virus and its isolated protein at the graphite electrode, *Gen. Physiol. Biophys.* 4, 393.
- Salač, W., 1936, Polarographic analyses in the brewery (in German), *Böhm. Bierbrauer* 63, 373.
- Sandegren, E., H.S. Suominen and D. Ekstrom, 1949, Polarographic estimation of proteins in the brewing process, *Acta Chem. Scand.* 3, 1027.
- Sasai, T. and M. Egawa, 1950, Polarographic studies of serum protein. I. On the Brdička denaturation test, *Bull. Inst. Chem. Res. Kyoto* 21, 26.
- Sasai, T., M. Egawa and M. Oka, 1953, Polarographic studies on the essential factor of blood-liability tests, especially of the heat-coagulation tests (The cobalt, cadmium and Weltmann tests), *Bull. Inst. Chem. Res., Kyoto Univ.* 31, 1.
- Schmidt, H.W., 1940a, Polarographic establishment of optimal conditions for precipitation of serum globulin (in German), *Biochem. Z.* 305, 422.
- Schmidt, H.W., 1940b, Polarographic studies of the relationship between irradiation by UV and concentration of proteins (in German), *Biochem. Z.* 306, 167.
- Schneider, H. and A.H. Schon, 1961, Determination of the lower limits for the rate constants of a hapten-antibody reaction by polarography, *Trans. NY Acad. Sci.* 24, 15.
- Sequaris, J.M., 1992, Analytical voltammetry of biological molecules. *Comprehensive Analytical Chemistry*. Vol. 27, Analytical voltammetry, Ed. J. Svehla, Elsevier, Amsterdam, 115.
- Seuberling, O., 1937, Polarographic investigation of the liquid cerebrospinalis (in German), *Klin. Wochschr.* 16, 644.
- Stamberg, O.E. and C.H. Bailey, 1942, The effect of heat-treatment of milk in relation to baking quality as shown by polarograph and farinograph studies, *Cereal Chem.* 19, 507.
- Stern, A. and E.F. Beach, 1940, Microdetermination of homocystine in pure solution with the dropping mercury electrode, *Proc. Soc. Exp. Biol. Med.* 43, 104.
- Stern, A., E.F. Beach and I.G. Macy, 1939, Polarographic microdetermination of cystine in protein hydrolysates, *J. Biol. Chem.* 130, 733.
- Štokrová, S., 1954, Polarographic determination of chymotrypsin activity (in Czech), *Chem. Listy* 48, 1082.
- Suolahti, O. and T. Laine, 1941, About the influence of formaldehyde on the alkaline denaturation of the serum (in German), *Biochem. Z.* 308, 316.
- Tachi, I. and S. Koide, 1951a, Polarographic studies of organic compounds. XVI. Polarography of vitamin B₁. 5. Catalytic waves of vitamin B₁ and related compounds in cobalt salt solution, *J. Agr. Chem. Soc. Jpn.* 26, 249.
- Tachi, I. and S. Koide, 1951b, Polarographic studies of organic compounds. XVII. Polarography of vitamin B₁. 6. Thiolthiazolone derivative of vitamin B₁, *J. Agr. Chem. Soc. Jpn.* 26, 255.
- Tanford, C., 1951, The effect of serum albumin on the polarographic diffusion current of cadmium, *J. Am. Chem. Soc.* 73, 2066.
- Tanford, C., 1952a, The effect of pH on the combination of serum albumin with metals, *J. Am. Chem. Soc.* 74, 211.
- Tanford, C., 1952b, Irreversible polarographic reduction of simple metal ions in the presence of acid serum albumin, *J. Am. Chem. Soc.* 74, 6036.
- Taussig, L., J. Prokup, O. Skaličková and R. Štrubl, 1937, Polarography of liquor cerebrospinalis (in Czech), *Sborník Lékařský* 39, 113.
- Taussig, L., J. Prokup, O. Skaličková and R. Štrubl, 1938, The estimation of proteins in the liquor cerebrospinalis (in Czech), *Čas. Čes. Lékarn.* 77, 1314.
- Trkal, V., 1952, Thesis, Charles University, Prague.

- Tropp, C. and F. Geiger, 1942, Polarographic investigations of proteins. IV. The effect of urea on solutions of proteins (in German), *Z. Physiol. Chem.* 272, 121.
- Tropp, C. and W. Herrbach, 1944, Polarographic studies of proteins. VIII. Fermentative cleavage of insulin (in German), *Z. Physiol. Chem.* 281, 50.
- Tropp, C., L. Jühling and F. Geiger, 1939, Polarographic studies of proteins. III. Albumin, globulin, fibrinogen, plasma and serum (in German), *Z. Physiol. Chem.* 225.
- Tropp, C. and W. Stoye, 1942, Polarographic investigation of proteins. VI. Proteins from plants (gliadin) and extracts from shredded wheat (in German), *Z. Physiol. Chem.* 275, 80.
- Walker, A.C. and S.P. Reimann, 1939, Polarographic studies on human blood sera, *Am. J. Cancer* 37, 585.
- Wedemeyer, H.E. and T.H. Daur, 1939, A contribution to the problem of diagnosis of cancer using polarographic investigation of sera (in German), *Z. Krebsforschg.* 49, 10.
- Wenig, K. and O. Jirovec, 1938, About the polarographic reaction of proteins, irradiated with UV-light (in German), *Biochem. Z.* 295, 405.
- Witwicki, J. and J. Zylo, 1955, Polarographic investigation of blood using the dropping mercury electrode. IV. The most important problems encountered during the determination of proteins in blood serum, *Postepy Bioch.* 1, 113.
- Zikán, J., 1966, Polarographic determination of the extent of association of antibodies against the 2,4-dinitrophenyl group with hapten, *Collect. Czech. Chem. Comm.* 31, 4260.
- Zuman, P. and J. Rusling, 2002, Polarographic studies of adsorption at mercury electrode surfaces, *Encycl. Surf. Colloid Sci.* 4143.
- Zuman, P. and R. Zumanová, 1956, Polarography of sulfur compounds. V. Heavy metal complexes with 2,3-dimercaptopropanol, *Collect. Czech. Chem. Comm.* 21, 123.
- Zumanová, R., J. Teisinger and P. Zuman, 1957, Influence of proteins on the polarographic behavior of metals and their compounds with 2,3-dimercaptopropanol (in Czech), *Chem. Zvesti* 9, 517.

This page intentionally left blank

Subject Index

- a.c. 77, 103, 105, 112
- a.c. impedance 79, 84, 100, 103, 116
- a.c. polarograms 82, 103
- a.c. polarography 77, 81, 84
- a.c. voltammetry 83, 104, 115
- a.c. voltammograms 82, 109
- abasic 405
- abasic sites 390
- AC polarographic 391
- AC voltammetric 393
- acid–base behavior 106
- acridines 401, 410, 414, 415
- actinomycin D 414
- active chips 256
- ACV 398, 405, 406, 410
- adamantynaphthalene diimide 361
- adduct with Os,bipy 735
- adducts 386, 390, 401, 403, 404, 416
- adenine 3, 6, 10–12, 74, 75, 87, 88, 90, 91, 93, 96, 97, 106, 114, 127, 130, 138, 141, 150, 287, 289, 292, 389, 404, 493
- adenosine 21, 24, 26, 28, 30, 33, 34, 36, 48, 49, 55, 56
- adlayer 493, 495–496, 506
- adrenaline 559
- adriamycin 403, 406, 410
- adsorption 78, 80–86, 88, 90, 92, 93, 98, 101, 108, 109, 114, 115, 120, 121, 123–125, 128, 392, 495, 498, 500, 706, 708, 709, 763, 764
- adsorption at fixed potential 280
- adsorption from non-aqueous solvents 51
- adsorption modes 127
- adsorption of DNA 81
- adsorption of nucleic acid components 48, 58, 67, 68
- adsorption/desorption 78, 81–85, 92, 150, 391, 410
- adsorption/desorption processes 389
- adsorptive accumulation 280
- adsorptive stripping 84, 135, 393, 691
- adsorptive stripping admittance 82
- adsorptive transfer 85
- adsorptive transfer stripping (AdTS) 90, 136, 394
- adsorptive transfer stripping cyclic voltammetry 97
- AdT CPSA 715
- AdTS 396, 410
- affinity binding 250
- affinity-binding molecules 249
- aflatoxins 401, 414, 415
- AFM 120, 147
- Ag clusters 216
- Ag-labeled nucleic acid 214
- Ag-nanowires 216
- agarose gel electrophoresis 388
- aggregation 718, 722, 725
- agricultural 252
- AgSAE 394, 396, 398, 405, 416
- alanine 504
- albumins 760, 761
- alcohol dehydrogenase 522, 548
- aldehyde oxidoreductase 522, 541
- aldriethiol 549, 556, 557
- aldriethiol modified 544
- alkaline elution assays 388
- alkaline phosphatase 205, 209, 250, 253, 271, 292, 293, 456
- alkanethiol 178, 252
- alkanethiol linker 126
- alkanethiol self-assembly 178
- alkylating agents 393
- alkylation 401
- allele 286
- allele specific hybridization (ASH) 355
- alternating current voltammetric 397
- Alzheimer's disease 718, 737
- amalgam electrodes 33, 53, 64, 66, 71, 79, 90, 127, 129, 659, 669, 680
- amine oxidases 553
- amine dehydrogenase 522
- amines 415
- amino acids 486, 498, 507, 510
- amino-phenols 566
- amperometric immunoassays 454
- amperometry 291
- amplicon 253, 289
- amplification 253, 369–372, 375–377, 379–382, 600, 626, 631, 634, 635

- amplified amperometric detection of DNA 203
 amplified analysis of DNA 205
 amplified detection of DNA 212
 amplified electrochemical analysis 151, 212
 amplified electrochemical analysis of DNA 214
 amplified electrochemical detection of DNA 195, 219
 amplified flow immunoassay 457
 amyloid 718
 amyloid structures 719
 amyloidogenic 719
 amyloidogenic protein 723
 analog-to-digital 261
 analog-to-digital conversion 257
 angiotensin II 695, 696, 699, 700
 anti-PenG antibody 271
 antibiotics 268, 269, 271
 antibodies 452, 690
 antibody immobilisation 267
 anticancer agents 413
 anticancer drugs 388, 393, 401, 407
 antigen-antibody 762
 antioxidant capacity 414
 antioxidants 414
 antioxidative 400
 antitumor agent MC 404
 AO 552, 553, 562, 563, 566
 apitoxin 759
 apolipoprotein E (apoE) 285
 apoptosis 387
 application-specific integrated circuit (ASIC) 248
 Applications 413
 aptamers 473
 apurinic acid 4
 apurinic sites 386
 area per adsorbed nucleotide 81
 aromatic amines 386, 409
 array positions 249
 arsenic oxide 402
 arsenite oxidase 523
 artificial 507
 ascorbate oxidase 519, 551-553, 562
 assays
 biomagnetic 292
 enzyme-linked 280, 292
 immuno- 292
 association rate constant 349
 association/dissociation constants 407
 ASyn 719, 722
 at the electrode 104
 atenolol 414
 Au (110)-surface 498
 Au(111)-surface 490-493, 495-501, 503-509
 avidin 177, 280, 395, 412, 701, 702, 704, 706, 708, 714, 715, 735, 737
 avidin-alkaline phosphatase conjugate 206
 avidin-biotin binding 702, 704
 avidin-biotin complex 703, 705, 706, 708, 736
 avidin-biotin system 280
 Avrami equation 20
 azepine 414
 aziridine 407
 azurins 503, 504, 551, 554, 561, 690, 692

 barriers 340, 489
 base stacking 143, 151, 390
 base flipping enzyme 730
 base mismatches 141, 144, 385, 390, 411
 base-mismatched 119
 baseline correction 78, 87, 88, 698
 BCR 709, 713, 730
 beacons 145
 bee-toxin 759
 bending 404
 benzimidazole 414
 Bewick-Fleischman-Thirsk model 26
 bias voltage 259, 487-490, 492, 509
 bilirubin oxidase 184, 519, 553, 564
 binding of Mg^{2+} 332
 binding of MutS proteins 731
 biocatalytic amplification of DNA sensing 202
 biocatalytic label 206
 biochip technology 247
 biochips 247, 264
 biocomposite electrodes 693
 bioelectrocatalytic label 203
 bioelectrocatalyzed oxidation of glucose 204
 bioelectronic detection of DNA 196
 biointerfaces 252, 264
 biological agents 252
 biological interface 271
 biological toxins 268
 biological warfare detection 264
 biologically active compounds 413
 biomarkers 388

- biosensing systems 252
biosensors 175, 252, 265, 280, 392, 394, 398,
401, 413, 415, 599–607, 611–617, 620,
622–630, 636
biotin 76, 132, 137, 280 395, 412, 701, 703,
706, 735, 737
biotin binding 124
biotin labels 232, 253
biotin-bound avidin 737
biotin-liposome tags 224
biotinylated ODNs 117, 131, 133
biotinylated probe DNA 124, 129
bioweapon toxin analyser 266
2,2'-bipyridine (Os,bipy) 412, 736
4,4'-bipyridyl 529
bis(2-aminoethyl) disulphide 562
bis(4-pyridyl) disulphide 562
bis-intercalators 122, 410
Bismuth electrodes 45
blood sample 253
blue copper proteins 503, 510
BOD 552, 565
bombesin 696
bonding 716
boron doped diamond 56, 58
botulinus toxin 266
bovine lactoperoxidase 520
bovine serum albumin (BSA) 695, 707
Brdička reaction 670, 672, 673, 675–679,
694
Brdička 696
Brdička DPV signals 714,
Brdička's catalytic responses (BCR) 709
Brdička's catalytic signals 737
Brdička's signals 696, 705
Brdička's solution 697
BSA 715

cadmium sulfide 376
calf thymus DNA 2
cancer 411, 759, 761, 762
cancer cells 230
cancer suppressor gene p53 357
cantilevers 197
CAP 271
capacitance 102, 189, 261, 264
capillary electrophoretic 390
capture antibody 266
capture oligonucleotides 253
capture solution 249
carbodiimide 281
carbon 150, 401, 708
electrodes 280
fibre 280
glassy 280
nanotubes (CNT) 292
paste 280
carbon electrodes (CE) 6, 12, 78, 80, 81,
87–89, 93, 95, 97, 114, 124, 129, 132, 133,
141, 150, 279, 393, 693, 702, 712, 713, 721,
729, 737
carbon fibre 279, 282–283
carbon nanotubes 87, 131, 184, 222, 225,
294, 692
carbon paste 282
carbon paste electrodes 395
carboproteins 507
carcinogenic 405
carcinogens 387, 393, 407, 413, 415
carcinomatic 761
catalase 520
catalysis by peptides 674
catalysis by proteins 676
catalysts 658, 660, 664, 665, 667, 668, 670,
671, 673, 674, 676
catalytic 658, 755–761
catalytic current 202
catalytic deposition of metals 227
catalytic DNA oxidation 439
catalytic double wave 670–673, 677
catalytic enlargement 212
catalytic hydrogen evolution 79, 694, 698,
715
catalytic, mechanism 664
catalytic hydrogen reduction 696, 699
catalytic oxidation 439, 442, 444, 446
catalytic reactions 657, 670
catalytically active groups 657, 668, 670,
672
catechol oxidase 554
catecholamines 559
catechols 534–536, 554, 560, 566
cathodic stripping 187
cccDNA 397
CD spectroscopy 720
CDH 544
CE 396, 399, 401, 403, 414
cellobiose 543
cellobiose dehydrogenase 521, 540, 543
cerebrospinal liquor 759
ceruloplasmin 517, 553, 566

- changes in DNA conformation 94, 104–106, 109, 115, 117, 390
changes in DNA conformation at the electrode surface 117
changes in DNA conformation in solution 117
changes in DNA structure 74, 95, 108, 114, 145, 150
channeling EIAs 467
charge density 693
charge injection 264
charge transfer 142–144, 148, 389, 412
charge transport 187
charge transport properties 199
charge transport through DNA 238
charged liposomes 222
chemically modified bases 390
chemiluminescence 230, 233
chemotherapeutics 388, 413
chloramphenicol (CAP) 269
chloroperoxidase 520
chromate 406
chromatographic 388, 390
chromosomal DNAs 77, 81, 86, 95, 97, 101, 108, 117, 137, 139, 150
chronopotentiometric stripping 215
chronopotentiometry 181, 183
chymotrypsin 716, 758
circular DNAs 96, 100, 102, 103, 116
cisplatin 414
 Cl^- exchange 340
cleavage 729
closed duplex (cd) DNA 116
CMOS 257–259
CMOS-based sensor array chips 257
coat protein 709
cobalt 1,10-phenanthroline ($\text{Co}(\text{phe})_3^{3+}$) 285
cobalt 2'-bipyridine ($\text{Co}(\text{bpy})_3^{3+}$) 282, 285
cobalt solutions 738
cobalt-containing solutions 127, 698, 725
coding 369–371, 376, 377, 379, 381
coherent electron transfer 490
colorimetric 247
colorimetric assays 227
comet 388
competitive assay 271
competitive ELISAs 269
complementary metal oxide semiconductor (CMOS) 248, 256
complexes 558
complexes of osmium tetroxide 404
concanavalin A 764
conductance 261
conductive array 229
conductive polymers 122, 124, 151, 395
conductivity 123, 127, 144, 187, 227, 373, 486, 510
 electronic 486, 487
 molecular 486
conformation changes 385, 404
conformational changes in proteins 709
constant a.c. chronopotentiometry 9
constant current chronopotentiometric stripping analysis (CPSA) 87, 393, 398, 693, 737
constant current chronopotentiometry 77, 93, 393
 $[\text{Co}(\text{phen})_3]^{2+}$ 139
copper 78, 79, 130, 403, 405, 407
copper complexes 406
copper electrodes 44, 79, 88
copper solid amalgam electrodes 130
copper, 1,10-phenanthroline complex 400
cost-effective 252
covalent immobilisation by carbodiimide 281
covalently bound electrochemical markers 6
covalently closed circular DNA 391
coverage 280
Cp 552, 567, 568
CPE 401, 409, 414
creatinine 458
creatinine sensor 464
cresol 535
cresolmethylhydrolase 521
Creutzfeldt–Jakob disease 718
cross-links 397, 404
Cu/Au core-shell NPs 214
current mirrors 259
currents, catalytic 756–765
cyclic voltammetry (CV) 8, 77, 84, 360, 396, 404, 407, 409, 414
cyclic voltammograms (CV) 336, 350
cyclodextrin 414
cystamine 526–528, 544
cysteamine 549–550
cysteine 498–505, 529, 574, 711, 716, 757, 758
 adlayer 496
 monolayer 498, 501

- cysteine oxidation 737
cysteine residues 700, 706, 709, 711
cysteine side chains 734
cysteine-containing peptides and proteins 738
cysteine-containing mutant 714
cysteine-containing peptides 699, 701
cysteine-containing peptides and proteins 725
cystine 503, 757, 758, 761
cyt *b*₅ 546
cytidine 31–33, 36–38
cytochrome *b*₂ 521
cytochrome *b*₅ 546, 709
cytochrome *c* 503, 529, 546, 549–551, 554, 574, 575, 692, 713
cytochrome *c* oxidase 551, 574
cytochrome *c* peroxidase 520
cytochrome P450 520
cytomegalovirus (CMV) 253
cytosine 3, 6, 10, 20, 21, 36, 37, 43–48, 51–53, 55–56, 58, 74, 75, 87, 90, 91, 93, 97, 99, 106, 114, 127, 141, 143, 150, 287, 389, 498
cytostatics 407
- D-fructose dehydrogenase 521
d.c. 95
d.c. polarographic methods 713
d.c. polarographic wave 91, 92
d.c. polarography 2, 93
D/A-converters 260
damage to DNA bases 400
daunomycin 137, 281, 285–287, 410, 413, 702
daunomycin, DM 144
de novo 507
deamination 386
deconformation 11
dehydrogenase 540, 543, 548
denaturation 714, 738, 759–762
denatured (ss) DNAs 5, 11, 391
denatured chromosomal DNA 10
denatured DNAs 1, 2, 4, 6, 9, 399
denatured lysozyme 736
denatured proteins 708, 712, 713, 715
deoxyguanosine 282
deoxyribonuclease I 391, 729
derivative 10, 713
derivative pulse polarography (DPP) 5, 11, 91
derivative/differential pulse polarography 74
desorption 83, 94, 95, 101, 109
desorption peak 5
detection antibodies 267
detection electrode 122, 128
detection limit 255
detection limits 253
detector 267
determination 717
determination of peptides 701
diagnostics, pharmacogenomics 252
diaphorase 521
2,4-dichlorophenoxyacetic acid (2,4D) 469
difference CV 341
differential (derivative) pulse polarography (DPP) 77, 93, 391
differential capacitance 5, 18, 19, 48, 58, 81, 104
differential pulse voltammetry (DPV) 284, 414, 695
differential pulse voltammograms (DPVs) 353
diffractive optical element 23
diffusion coefficients 407
diluent thiol 125
2, 3-Dimercaptopropanol 757
dimers 506
dimethyl sulfate 401
dimethyl sulphoxide reductase 522, 541
direct current (d.c.) polarography 77
direct electron transfer 601, 603, 605, 606, 612, 614–616, 618–620
dismutase 519, 574
disposable, sensors 279
dissociation rate constant 347
distortions 391, 401
disulfide 717
disulfide group 716
3,3'-dithiodipropionic 562
DM intercalation 144
DM-labeled ODN 144
DME 79, 81–83, 86, 91, 93, 96, 97, 102–107, 111–117, 397, 404
DME double layer 5
DMS 405
DNA 9, 10, 74, 80, 89, 137, 139, 151, 369–384, 391, 433–448, 729, 731
DNA adducts 388
DNA adsorption 81, 82, 92, 101, 121
DNA aggregation 9

- DNA analysis 3, 195
DNA biochips 304
DNA biosensors 279
DNA chip 345, 364
DNA conductivity 10, 141
DNA damage 6, 75, 76, 96, 141, 142, 145, 149–151, 386, 391, 400, 407, 415, 433, 434, 438–440, 442–444, 448
DNA damage at electrodes 406
DNA degradation 399, 414
DNA denaturation 74, 97, 107, 109, 117, 118, 120, 132, 150
DNA denaturation and renaturation/hybridization 11
DNA desorption 92, 107
DNA double helix 96, 107, 108, 110, 120, 138, 141, 145
DNA duplexes 97, 100, 108, 110, 116, 119, 120, 122, 123, 126, 128, 141, 142, 145, 147, 148, 151
DNA groove binder 346
DNA hybridization 86, 409, 411, 486, 492, 729
DNA hybridization sensors 5, 7, 75, 79, 80, 121, 123, 129, 135–136, 138, 145, 150
DNA immobilisation 106, 122, 124, 125, 150, 298, 299, 301, 311
DNA immobilization at gold electrodes 124
DNA interactions 6
DNA microarrays 264, 411
DNA modified 409
DNA opening at the electrode surface 109
DNA oxidation 88
DNA polymerase 253
DNA premelting 11, 74, 98, 150
DNA probe 279–282, 346, 364
DNA probe-immobilized electrode 346
DNA probing 404
DNA recognition layer 7
DNA reduction 5, 92
DNA renaturation 7
DNA repair 390
DNA repair endonucleases 389, 416
DNA repair enzyme (MutY) 730
DNA repair enzymes 405
DNA repetitive sequences 129, 131
DNA sensors 75, 85, 88, 122, 124, 131, 141, 142, 150, 151, 434, 441–444
DNA structure 7
DNA surface denaturation 6–7, 11, 714
DNA templates 216
DNA topology 116
DNA unwinding 5, 150, 729
DNA–drug interactions 413
DNA–protein 691
DNA–protein binding 730
DNA–protein interactions 76, 127, 142, 143, 729, 738
DNA-based molecules 492, 510
DNA-binding metal complexes 346
DNA-binding proteins 726
DNA-mediated charge transport 142, 143, 145
DNA-microarrays 252
DNA-modified CE's 414
DNA-modified electrodes 6, 102, 106, 114, 115, 144, 150, 394, 396, 409
DNA-modified HMDE 394
DNA-Os, bipy 132, 135, 136
DNA-protein interactions 726
DNAzymes 239
DOPA 559
dopamine 559
doping 333
double helix opening 396
double surface technique 88, 149
double-step sweep technique 10
double-strand 493, 496, 498
double-strand breaks 386
double-stranded DNA (dsDNA) 346
double-surface techniques (DST) 122, 129, 151, 731, 738
doxorubicin 410, 413
DP voltammetry 112
DPP 6, 9, 94, 95, 97, 98, 100, 103–105, 150
DPP peak III 75, 397
DPV 93, 104, 355, 363
DPV BCR 710
dropping mercury electrode 150, 391
drug–DNA interaction 413
drugs 413, 415
ds nucleic acids 94, 95
dsb 388, 397, 399
dsDNA 82, 83, 89, 91, 94, 96, 97, 99, 103, 106–109, 111–115, 120–122, 126, 141, 142, 144, 150, 151
dsDNA conductivity 149
dsDNA conformation 120
dsDNA unwinding 714
dsRNA 96, 98
DST 123, 131, 133

- Durand, R. 490
Dynabeads 129, 130
dye units 212
- early stages of α -synuclein aggregation 722
echinomycin 410, 413
effect of the electric field 83, 104, 111, 113
effective vibrational frequency 490
efficiency hybridisation 280
egg white 759
electric transduction 248
electrical biochip 247
electrical biochip technology 248
electrical field 264
electrical microarrays 248, 254, 264, 266, 267
electrical protein microarrays 266
electrical readout 250, 253
electrical responses 248
electrically heated CPE 400
electrically wired immunosensors 468
electroactive beads 189, 380
electroactive intercalative compounds/
 groove binders 284
electroactive markers 689, 733
electroactive sites 390
electroactivity 694, 695, 701, 725
electroactivity of nucleic acids 3
electroactivity of peptide nucleic acid (PNA)
 696
electroactivity of proteins 701
electrocatalysis 138
electrocatalytic and biocatalytic reactions
 151
electrocatalytic cycle 139, 143
electrochemical 252, 657–659, 668, 669, 676,
 679, 680
electrochemical analysis 1, 691, 720
electrochemical array (ECA) chip 362
electrochemical biosensor 252
electrochemical, catalytic 658
electrochemical detection 252, 254, 256
electrochemical detection of DNA 213
electrochemical DNA 200
electrochemical DNA chip 345
electrochemical DNA ligand 346
electrochemical DNA sensor 345
electrochemical hybridization indicator 346,
 352
electrochemical immunoassays 454
electrochemical impedance spectroscopy 55,
 59
electrochemical, noncatalytic 659
electrochemical protein detection 265
electrochemical techniques 666
electrochemical transduction 197
electrochemistry 690
electrochemical impedance spectroscopy
 23
electrode double layer 19, 58
electrode surface 738
electrode–electrode coupling 459
electrode–enzyme coupling 461
electrodeposition paints 622, 627
electrodes 80, 124, 279, 280, 389, 692, 759,
 763, 764
electrodes, dropping mercury 756–765
electrodes, solid 765
electrogenerated chemiluminescence 232
electrolysis of DNA 10
electron hopping 618, 621, 622
electron transfer 114, 138–140, 147, 511, 599,
 602, 691
electron transfer resistances 205, 207
electronic 486–491, 495, 510
electronic CMOS-microarrays 250
electronic energy density 490
 transmission coefficient 490
electronically conducting polymers (ECPs)
 297, 298
electrooxidation 764
electrooxidation at diamond electrode
 56
electrooxidation of tyrosine 693
electrooxidizability of oligopeptides 694
electrophoretic 388
electrophoretic accumulation 473
electrophoretic techniques 396, 405
electropolymerization 178, 332
electroreduction 716, 717
electroreflectance spectroscopy 692
electrostatic attraction 395
electrostatic barrier 332
elimination voltammetry 77, 84, 93
ELISAs 251, 264, 265, 267, 416
ellipsometry 81, 147
endonucleases 396, 405
enlargement of Au NPs 227
Enterobacteriaceae 254
Enterococcus faecalis 254
Environmental analysis 415

- environmental control 247
environmental monitoring 252, 416
enzymatic amplification 202
enzymatic labelling 261
enzyme 293
enzyme conjugates 253
enzyme electrode 212
enzyme immunosensors 464
enzyme, label(s) 183, 202, 289–291
enzyme labels for hybridisation detection 289
enzyme–enzyme coupling 461
enzyme-linked 132
enzyme-linked immunosorbent assay (ELISA) 183, 251, 412, 455
enzyme multiplied immunoassays 455
epirubicin 414
epoxide 407
Epstein–Barr virus (EBV) 253
Escherichia coli 254
1,*N*⁶-ethenoadenine 404
ethidium bromide 347, 410
1-ethyl-3-(3-dimethyl aminopropyl) carbodiimide (EDC) 282, 293
ex situ 487
exchange of chloride ion 333
exonuclease III 405
explosives 268
- faradaic impedance spectroscopy 183, 206, 209, 222
faradaic responses 6
Fenton type reactions 405
Fermi level 487, 489, 490
ferredoxin 503, 504
 dimers 506, 507
ferro/ferricyanide 394, 414
ferrocene 76, 136, 137, 146, 148, 189, 558
ferrocene tags 181
ferrocene-labeled 147
ferrocene-labeled ODNs 136
ferrocene-tethered deoxyuridine triphosphate 204
ferrocenyl- β -cyclodextrin 361
ferrocenylnaphthalene diimide 349, 350, 363
fibrinogens 760
filtrate test 677
flavin 518, 539
flavocytochrome *c*₃ 541
flavocytochrome *c*₅₅₂ 521
flavonoid quercetin 403
flavonoids 414
flow-through device 405
fluorescence 247
force interactions 197
formaldehyde, effect of 760
formamide 283
fouling, surface 279
FRET 233
FRET process from the semiconductor NPs 212
Friedreich ataxia (FRDA) 131, 412
fructose dehydrogenase 548
fully electronic biochip 248
fumarate reductase 522, 541
functionalized alkaline phosphatase 207
functionalized magnetic particles 216
fungal peroxidase 520
- galactose oxidase 519, 553, 556
GalOD 557, 561
gaps 497
GCE 399, 401, 403, 406, 414, 415
gene expression 252
gene sensors 252
genetic analysis 252
genetic material 386, 407, 413, 415
genomic DNA 254
genosensors 279, 280
genotoxic agents 401, 415
genotoxic substances 387, 389, 393
genotoxicity 433, 440, 443
genotype 285, 286
germanin, effect of 760
glassy carbon 279
glassy carbon electrode with carbon nanotubes 693
glassy carbon electrodes (GCE) 131, 395
globulins 759, 760
gluconate dehydrogenase 540
glucose oxidase 360
gold 78, 80, 85, 86, 119, 124–127, 144, 150, 185, 370–376, 378–381, 403, 692
gold electrodes 21, 36, 40, 78, 80, 86, 117, 124, 126, 128, 142, 144–146, 148, 151, 257, 394, 412, 414, 692, 709
gold nanoparticles 414
gold surfaces 79, 85, 120, 124–126, 142, 144, 146, 148

- groove binders 122, 284
groove binding 407
growth 18, 20, 26, 28, 31, 34, 37, 39, 40, 42, 51, 57
guanidine 689, 715
guanidine-HCl 283
guanidium chloride 712
guanine 3, 6, 9, 12, 74, 75, 79, 84, 87–89, 96, 100, 106, 114, 117, 123, 130, 137–141, 150, 186, 287, 288, 389, 393, 399–401, 403, 406, 411, 412, 415, 416, 497, 498
 hole injection 497
guanine oxidation 139, 141
guanine reduction 74
guanine residues 4
- hairpin 84, 120, 147, 199
hairpin-loop DNA 145
hanging mercury drop electrode (HMDE)
 78, 79, 392, 694
 α -helix 713
hapten microarrays 271
haptens 248, 267
health care 252
heavy metals 413
helicases 729
helix-coil transition 713
heme proteins 415, 510
hemocyanins 554
hemoproteins 395
herbicides 415
herpes simplex virus (HSV) 253
heterozygous SNP 358
Heyrovský, 2–4, 8
Hg–S bond 86, 127, 699, 707, 716
Hg–S chemisorption 707
HgS/disulfide bonds 697
high-density arrays 252
high-density microarrays 252
histidine tags 709
histones 84, 85, 121, 730
HMDE 79, 80, 83–85, 90, 91, 93, 99–107, 110–112, 114, 116, 117, 127, 130, 150, 393, 396–398, 401, 404–407, 409, 410, 414, 703, 704, 715
hole injection 497
homeland security 252
HOMO 487, 511
hopping 489
horseradish peroxidase (HRP) 183, 291, 294, 518–519, 709
HPLC 406
HRP 524, 526, 530–533, 535–538
HS-ODNs 127, 725
human 719
human DNA 149
Human Genome Project 3
human genomes 3
human lipoprotein lipase (LPL) gene 358
human serum 659, 662
human serum albumin (HSA) 715
hybridisation 251, 629–636
hybridisation reaction 283, 284
hybridisation transduction 298, 310
hybridization 7, 336, 395, 486, 510
hybridization efficiency 125
hybridization of the analyte DNA
 196, 198
hydrazine 393, 401, 415
hydrogel, surface 279, 283
hydrogels 613, 618, 622, 623, 634
hydrogen bonding 96, 134, 145, 716
hydrogen evolution 658–671, 673–677, 679
hydrogen overvoltage 79, 398
hydrogen peroxide 406
hydrogenase 521
hydrolysis 250
hydrophobic pocket 706
hydrophobicity 713
5-hydroxyindoles 566
hydroxyl radicals 405
hydroxymethyl-ferrocene 558
hypochromic effect 348
hysteresis 19
- immobilisation 253, 599, 607, 608, 610, 612, 614, 616, 617, 619, 622, 624, 627, 630, 631, 634, 636
immobilization, DNA probe 280–283
immobilization 177
immobilize 394
immobilized DNA 6, 114, 120, 126, 129, 130, 151
immunoassays 452, 690, 701
immunochemical methods 389
immunochemistry 762
immunosensors 453, 455, 457, 459, 461, 463, 465, 467, 469, 471, 473, 475
impedance 18, 22–23, 45, 55, 83, 123, 147, 262, 264

- impedance spectroscopy 205, 225, 248, 252, 393
- impedimetric biosensing 262
- in situ* 487, 489, 490, 493–495, 497, 502, 505, 510
- in situ* electrochemical detection 406
- inaccessibility of the reduction sites 96
- indicator, redox 281, 284–288
- indicator-free approach 287
- indicators 79, 181
- indium tin oxide (ITO) 78, 395
- inherited diseases 412
- inosine 287
- insertions/deletions 390, 411
- insoluble product 205
- insulin 695, 713, 716, 717
- integrated circuits 257
- integrity of base-pair stacking 144
- interactions 691, 716
- intercalated DM 144
- intercalation 410
- intercalative binding 409
- intercalators 6, 115, 122, 143, 238, 239, 252, 284, 285, 287, 409, 410, 412, 632
- Interdigitated electrode arrays (IDAs) 262
- interdigitated electrodes 248
- interdigitated fingers 250
- interdigitated gold array 472
- interfacial behavior 693, 706
- interfacial capacitance 493, 495, 498, 507, 508
- interfacial electron transfer resistance 209, 222
- interfacial properties of the electrode 205
- internal standards 253
- ion-channel 189
- ion-gating effect 264
- ionizing radiation 9, 391
- iron 405, 406
- iron-sulfur protein 503
- irreversible 78, 80, 109, 132
- irreversible opening of dsDNA 109
- irreversible reduction 91
- isoproterenol, 559
- isotopic pattern 734
- ITO 80, 86, 124, 130, 140, 141, 403, 414
- ITO electrodes 88, 124, 138, 150
- kinetics of phase transitions 17, 26, 28, 31, 33, 58
- label 293
- label enzymes 250
- label-free 185, 248, 333
- label-free detection 261, 262
- label-free DNA probe 334
- label-free immunosensors 469
- label-free impedance 264
- labelling and electrochemical detection 284
- laccases 466, 519, 568, 571
- lactate dehydrogenase 521
- Langmuire type adosorption 28, 31, 34, 37, 42
- layer-by-layer 395, 415
- Lc (laccase) 524, 552, 559, 566, 569, 572
- lead sulfide 216
- levofloxacin 414
- Lewy bodies 719
- Lewy neurites 719
- LH-RH 696
- lift-off process 257
- lignin peroxidase 520
- linear (lin) DNA 396, 397, 399
- linear sweep 393
- linear sweep voltammetry (LSV) 107
- linker 144, 148
- lipid bilayer membranes 414
- lipid membranes 189
- liposome tags 222
- liposomes 184, 189
- long-range electron transfer 199
- low-density arrays 252
- low-density electrical microarrays 248, 253
- low-density microarray 254
- LPL gene 363
- LSV 75, 78, 105, 112, 113
- lumazine 414
- LUMO 487, 509
- luteinizing-hormone-releasing hormone (LH-RH) 695
- lycorine 414
- lysozyme 695, 713, 719, 736, 764
- [Lys8]-vasopressin 695, 697, 700
- magnesium 333
- magnetic beads 292, 372, 373, 375, 376, 412
- magnetic particles 212, 220, 230, 233
- magnetic particles, with nucleic acid-functionalized 197

- magneto-mechanical deflection 197
major and minor grooves 346, 399
malignant transformations 387
manganese peroxidase 520
Marcus theory 602, 604, 614
mass spectrometric 390
mass spectrometry 398, 416
mass-spectrometric techniques 388
matrix-assisted laser desorption-
ionization–time-of-flight mass
spectrometry (MALDI–TOF MS) 734
maximum residue limit (MRL) 269, 271
MC 401, 407
ME 396, 405, 415, 416
mechanism 664
mechanism of DNA surface deconformation
113
mediated electrical contacting of a redox
enzyme 204
mediatorless 465
medical diagnosis 247
medium exchange 394
medium-density microarray 248
melting temperature 121, 126, 145, 283
mercaptoethanol 526, 546, 549
2-mercaptoethanol/cysteamine 550
mercaptopropionic acid 503, 529, 544, 574
mercaptosuccinic 556
mercaptoundecanoic 529
6-mercapto-1-hexanol/6-amino-1-
hexanethiol 550
11-mercapto-1-undecanamine 547
11-mercapto-1-undecanol 546
mercaptoundecanol- 545
11-mercapto-1-undecanol/11-mercapto-1-
undecanamine 547
mercury 78–80, 389, 396, 409, 692, 713, 737
mercury and carbon electrodes 738
mercury dropping electrodes 78
mercury electrodes 7, 18, 21, 23, 51, 58, 74,
79–84, 86, 87, 89–92, 97, 99, 101, 103, 104,
108, 109, 112, 114–117, 120, 124, 127, 128,
131, 132, 150, 401, 693, 708, 712, 725
mercury film 398
mercury film electrodes (MFE) 23, 396
mercury surface 705
metabolic activation 406
metabolic carcinogen activation 395, 415
metabolically activated carcinogens 386
metabolites 433, 434, 438, 441, 443, 448
metal chelates 409
metal ion/DNA interaction 332
metal microrods 215
metal sulfide 218
metallization 373
metallointercalator 394, 399
metalloporphyrins 409
metalloproteins 691
metallothioneins 676
methionine 734
methylamine dehydrogenase 521
methylene blue (MB) 126, 142, 285
 α -methyl-DOPA 559
metronidazole 414
MFE 398, 410
Mg²⁺ complex 334
microarray-based methods 129
microarrays 248–251
microelectrodes 416
microfluidics 264
microorganisms 252
microperoxidase 520
microprocessor-controlled 250
microrods 215
microstructures 628, 629
mifepristone 414
milk 759
minor groove 409
mismatch 393
mismatched DNA duplexes 411
mispaird bases 732
mitomycin C (MC) 393
mitoxantrone 414
Mo-pterin 518
MoCo, 539, 546
modified DNA 403
modified screen-printed carbon electrodes
729
molecular wire 389
molecular-beacon 182
monolayers 487, 488, 495, 498, 500, 503,
692
mononucleotides 492, 493, 495, 497
monothioglycerol 545
multi-cofactor enzymes 606–609, 615, 620,
621
multi-copper oxidases 562
multichannel electrochemical readout
250
multiplexed 16 channel potentiostat 271
multiplexing 264
multiplied immunoassay 455

- mutagens 387, 415
 mutant proteins 690, 711
 mutants 710
 mutants of α -synuclein 712
 mutated proteins 709
 mutations 386, 411, 415
 MutS protein 694
 myoglobin 3, 719
- N-glycosylases 386
 N-hydroxysulfosuccinimide (NHS)
 NA oxidation 79
 NA-protein interactions 733
 nagalamycin 346
 nanoparticles 85, 122, 131, 151, 184,
 369–377, 379
 nanotechnology 369
 nanowires 369, 371, 373, 381
 naphthalene diimide 346
 1-naphthol 131
 native 6, 9–10, 391
 native DNA 4, 6
 native dsDNA 5, 11
 negative control 253
 negative differential resistance 489
 negatively charged surface 709
 neurodegenerative diseases 131, 132
 neurodegenerative disorders 719
 neurotensin 695, 696
 nitrate reductase 523, 541, 553
 nitrocellulose (NC) 88, 129, 130
 nitrogen ligands (Os,L) 739
 nitrous oxide reductase 551
 nogalamycin 347
 non-catalytic 659
 non-covalent DNA interactions 389, 390,
 407
 non-specific adsorption 179
 non-specific DNA 128
 noradrenaline 559
 normal pulse polarography (NPP) 7, 10, 95,
 713
 NP labels 218
 NPP 104–105, 107, 713
 nuclease P1, 388
 nucleases 386
 nucleation 20, 26, 28, 31, 33, 34, 37, 39, 40,
 42, 51, 57
 nucleic acid samples 75
 nucleic acids 18, 19, 21, 23, 36, 51, 52, 57, 58,
 79, 86, 91, 196, 207
- nucleic acids hybridization 197
 nucleic acids, proteins 248
 nucleobase adducts 433, 441, 448
 nucleotide sequence determination
 122
 nucleotide sequencing of genomes 150
 Nyquist plots 206
- o-diphenols 558
 8-OG 389–390, 393, 401, 403, 406, 411
 o-quinones 558
 ODN-DM 144
 ODNs 84, 85, 99, 117, 119–123, 125, 127,
 128, 136, 137, 140–142, 144, 145, 147, 148,
 399, 412, 414
 oligodeoxynucleotides 76, 88, 93, 128
 oligodeoxyribonucleotides (ODN) 75, 395
 oligonucleotide 630
 oligonucleotide microarrays 251
 oligonucleotides 10, 40, 48, 53, 55, 56, 281,
 486, 492–498, 510, 630
 oncology 691
 open circular (oc) 396–397, 399
 open circular (oc) DNA 103
 opening of the dsDNA 103, 107
 optical detection of DNA 196, 227
 optical roughness 23, 24, 34
 optimum hybridization (H) surface
 128
- ORIGIN 251
 Os(III/II) couple 139
 Os,bipy 132, 133, 135, 136
 Os,bipy modification 735
 Os,bipy-modified pyrimidines 132
 oscillographic polarography at controlled
 a.c. 74, 105
 oscillographic polarography 6, 8–11, 75, 77,
 391
 oscillopolarograms 4
 oscillopolarographic indentation 94
 osmium 124, 133–135, 150, 393, 404
 osmium complexes 558, 739
 osmium isotopic pattern 734
 osmium tetroxide 132, 134, 135, 137, 391,
 412, 736
 osmium tetroxide complexes 393, 733
 osmium tetroxide, 2,2'-bipyridine (Os,bipy)
 292, 733
 osmium-modified DNA 80, 131
 overpotential 488, 489
 oxidase 519, 546, 548, 553, 554, 574

- oxidation 75, 79, 80, 84, 86–89, 96, 114, 123, 127, 130, 132, 137, 139, 141, 150, 721, 734
- oxidation of guanine 87
- oxidation peaks 695
- oxidation signals 74, 86, 87, 89, 96, 737
- oxidative damage 403
- oxidative DNA damage 386, 388, 410
- oxidized peptides 717
- oxidoreductases 604, 614
- 8-oxoguanine (8-OG) 386
- oxygen 406
- oxygen electroreduction 466
- oxygen reduction at platinum electrode 18, 56
- p*-aminophenol 250, 456
- p*-aminophenyl phosphate 250, 266, 456
- p*-APP 271
- p*-cresol 535
- p*-cresolmethylhydroxylase 541
- p*-phenylenediamines 566
- Parallel Affinity Sensor Array system (PASA) 269
- Parallax- β -lactam 260
- Parkinson's disease (PD) 694, 719, 737
- particle tolerant 252
- partly covered surfaces 81
- pathogens 253
- PCR 132, 133, 139, 149, 362
- PCR primer 363
- peak 1 397
- peak 2 391, 397, 410
- peak 3 392, 396, 397, 410
- peak CA 398
- peak H 668, 675, 676, 679, 680, 694, 696, 697, 699, 705, 708, 711, 714, 720, 722, 723, 730, 737
- peak II 94–97, 107, 391
- peak P 662, 663
- peak III 93, 95–97, 103, 107, 391, 396
- peak S 708, 737
- peanut peroxidase 520
- pencil lead 279
- penicillin G (PenG) 269, 271
- pepsin 758, 760–762
- peptide conformational properties 694
- peptide nucleic acid (PNA) 80, 180, 280, 726
- peptide-modified HMDE 718
- peptides 694
- peroxidase 559, 690
- pesticides 413
- phase transitions 20, 21, 26, 28, 31, 33, 34, 36, 57, 493
- phenothiazine 414
- photochemical 401
- photocurrents 234, 236
- photoelectrochemical effect 235
- phytochelatin 701
- piezo-electric crystal 249
- piezodispensing 249
- piezoelectric spotting 266
- plants 759
- plasmid DNAs 100, 101, 116, 117
- platinum 391, 403, 692
- platinum complexes 397, 401
- platinum electrodes 78, 79, 693
- PNA 76, 84, 85
- point mutations 131, 137, 142, 151, 411, 732
- point of care diagnosis 247, 252
- polarographic 385, 391, 396
- polarographic reducibility 11
- polarography, normal pulse (NPP) 1, 2, 7, 77, 95, 103, 105, 755, 756, 761, 763–765
- polished electrode 399
- pollutants 387, 393, 407, 409, 415
- poly(A) 10
- poly(C) 9
- polychlorinated biphenyls 401, 414, 415
- polycyclic aromatic hydrocarbons 386, 415
- polylysine 713, 719
- polymerase 204, 232
- polymerase chain reaction (PCR) 76, 253, 285, 364
- polymeric films 393
- polymorphisms 286
- polynucleation 26, 28
- polynucleotide molecules 111
- polynucleotides 75, 87, 91, 94, 95, 97, 109, 110, 399
- polypyrrole 187, 299–301, 303, 305, 307–315, 319–324, 332
- polypyrrole-modified electrodes 404
- polythreonine 719
- portable devices 252
- position-specific current responses 251
- position-specific electric responses 250
- positive control 253
- postlabeling 388, 398
- potential-dependent unwinding 390
- potential-induced unwinding 397

- potentiometric readout 249
potentiometric stripping analysis (PSA) 284
PQQ 518, 539, 548
pre-aggregation 723
presodium catalysis 660, 665, 670, 674, 687
pre-sodium wave 694, 697, 698, 711, 756, 757, 759, 763, 765
pre-treatment, surface 282
premelting 115, 391
primer extension 385, 412
primer pair 253
probe DNA 121–123, 334–336
propionic acid 504
prosthetic group 601
protamines 730
protein adsorption 691
protein biosensors 264
protein chips 471
protein conformation 716
Protein Data Bank 728
protein engineering 690
protein immobilization 691
protein microarrays 265, 473
protein p53 694, 709, 712
protein redox states 717
protein structure 733
protein surface unfolding 714
protein unfolding 713
protein-modified electrodes 691
proteins 3, 486, 503, 510, 693, 695, 697, 699, 701, 703, 705, 707, 709, 718, 721, 723, 725, 727, 729, 731, 733, 735, 737, 739, 755, 765
 adsorption 498
 artificial 507
 De novo 507
proteins, analysis of 759–761
proteins, denaturation of 760, 761
proteins adsorption 693
proteolysis 761, 762
proteolytic cleavage 679
Proteomic Chips 451
pulse polarography 77
purine bases 399
pyrimidine dimers 386, 389, 404
pyrolytic graphite 401
pyrolytic graphite electrodes 24, 31, 55
pyrroloquinoline 539
pyrroloquinoline quinone (PQQ) 518, 539
QCM 356, 436–437
quantum dots 370, 376
quartz crystal microbalance measurements 206
quartz crystal microbalance, QCM 212, 352
quinacrine 348, 414
quinone 539
 γ -rays 396
re-annealing 253
reactive oxygen species (ROS) (8-OG) 388
reagentless biosensors 613, 614, 617, 621, 622
recognition 389, 390
recombinant HRP (rHRP) 535
recombinant proteins 690
rectifier, molecular 490
redox 79, 398
redox enzymes 519, 601, 605, 613, 614, 616, 618, 622, 623
redox indicators 79, 122, 123, 151, 394, 399, 409, 410, 414
redox labels 197, 199
redox marker 391
redox mediators 264, 393, 403, 411, 601, 602, 605, 614–621, 625, 626, 635, 636
redox molecules 250
redox polymers 395, 610, 613, 615, 621, 622, 624, 634
redox recycling 250, 266, 459
redox signals 389, 401
redox-active center-containing proteins 691
redox-active intercalator methylene blue 199
redox-active intercalators 198
redox-labeled immunoassays 458
redox-labeled immunosensors 467
redox-recycling 253, 271
reduction 5, 10, 75, 79, 80, 84, 86, 89–97, 99, 106, 119, 127, 132, 143, 145, 150
reduction of cystine 716
reduction of disulfide bonds 716
reduction of proteins 716, 717
reduction of the enzyme 717
reduction of the Hg–S bond 708, 730, 737
reduction signals 74, 78, 79, 91, 93, 737
reductive desorption 493, 494, 497, 499, 507–509
region T 105, 107–109, 111, 112, 114, 115, 117
region U 105, 107–112, 114–117, 397

- region W 109, 116
regions U and T 112
relaxation 264
renaturation 98, 115, 121, 150
reorganisation energy 603, 605, 616
reorganization free energy 489, 490
repair 386
reporter probe 412
repulsion 262
residues 10, 12, 716
resistance 261
resonance Raman spectroscopy 692
revealed E° values 345, 356, 369, 562
reverse transcriptase 209
reversibility 89
reversible 89, 100, 115, 119, 124, 132
reversible reduction 144
rHRP 535, 537
ribonuclease 716, 764
ribonuclease A 713
Ribosomal RNA 254
Ricinus communis 266
RNA 3, 74, 75, 77, 80, 81, 87, 93–95, 97,
98, 106, 107, 125, 130–132, 135, 136,
143, 149
RNA adsorption 129
RNA reduction 5
ROS 398, 406, 407
rotation of the magnetic particles 230
[Ru(bipy)₃]²⁺ 139, 141
ruthenium 393, 404, 415
- SAE 131, 134
saliva 759
Salmon Luteinizing Hormone - Releasing
Hormone (SLH-RH) 734
SAMs 126–128, 148, 151, 725
sandwich hybridisation 255
sb 405, 411, 415, 416
sc 399
sc plasmid DNA 396
scanning electrochemical microscopy
(SECM) 362, 629
scanning tunneling microscopy 36, 487
scDNA 102, 116, 117, 392, 398, 410, 415
scDNA-modified electrode 398
screen-printed electrodes 180, 280, 401
screen-printed strip electrodes 693
SEB 267
Self-assembled monolayers (SAMs) 79, 125,
126, 252, 692, 725
semiconductor electrodes 46
semiconductor nanoparticles 211
semiconductor NPs 211
semiconductor quantum dots 233
semiconductor technology 247
sensitivity of the DNA analysis 151
sensor current range 260
sensors 433–435, 437–448, 691, 729
sequence 719
sequencing 251
sequential electron transfer 488
sera, carcinomatic 761
sera, normal 761
serum albumin 716
SH groups 670–673, 676–678
signal-off 403, 416
signal-on 416
signaling probes 136
signals 84, 87, 127, 696
silicon manufacturing 248
silicon substrate 256
silicon technology 248
silver 78, 88, 185, 369, 370, 372–375, 692
silver electrodes 41, 42, 62
silver solid amalgam 389
simultaneous multiple mutation detection
(SMMD) method 362
single nucleotide polymorphism 228, 252,
354
single strand breaks (ssb) 97, 107, 108, 110,
388
single-base mismatches 118, 144, 149, 151,
209, 232
single-base mismatches in DNA 203
single-base mutation 225
single-base pair mismatches 118
single-base polymorphism 218
single-crystal electrodes 33, 36, 37, 57, 58,
486, 490, 503, 504, 507
single-crystal n-CdSe 46
single-strand binding 729
single-strand interruption 116
single-stranded (ss) 253, 389, 493, 496
single-surface technique (SST) 123
single-walled carbon nanotube 729
size exclusion redox-labeled immunoassay
(SERI) 458
small molecules 267
SNP 357, 359, 362
solid amalgam 393

- solid amalgam electrodes (SAE) 79, 396, 398, 694, 698
solid electrodes 87, 104, 106, 392, 403, 409
soybean peroxidase (SBP) 291, 520
spacer (linker) 125
spacer length 126
sparingly soluble compounds 74, 75, 130
SPR gold sensor 119
square wave stripping 87
square wave voltammetry (SWV) 10, 93, 99, 284
square wave voltammograms 99
ss 399
ssb 396, 397, 399, 405, 406
ssDNA 6, 81, 83, 88, 89, 91–97, 103, 105, 107, 108, 112, 113, 115–117, 119–121, 123–125, 134–136, 141, 147, 150
ssRNA 81, 95, 98
SST 131
stable complex of Os,bipy 734
stacking 407
Staphylococcal enterotoxin B (SEB) 266
Staphylococcus aureus 254, 266
Staphylococcus epidermidis 254
stationary electrodes 105, 106
stationary mercury electrodes 78
stearic acid 282
steric hindrance 284, 289
STM 486–488, 490, 491, 496, 498, 503, 507
 ex situ 487
 in situ 486–510
strand breaks (sb) 386, 395
streptavidin 289, 291, 292, 701, 702, 708, 737
streptavidin-coated magnetic beads 732
stringency 283
stripping 87, 90, 98
stripping analysis 185
stripping voltammetric 399
stripping voltammetry 212, 372, 376, 377
 α -structure 713
structural probing 391
styrene 415
styrene oxide 405
substrate cycling 456
succinate dehydrogenase 522, 541
sugar oxidation 79
sulfhydryl groups 717, 734
sulfosalicylic acid, use of 760
sulphite dehydrogenase 522, 540
sulphite oxidase 522, 546
supercoiled (sc) DNA 100
supercoiled (sc) plasmid DNA 388
superexchange 488, 489, 497
superhelix density 102
superoxide dismutase 519, 553, 574
supramolecular complex 362
surface chemistry 177
surface concentrations 114, 127, 128, 147
surface coverage 280, 292, 693
surface denaturation 397, 399, 411, 713
surface enhanced Raman spectroscopy 59, 63
surface H 128, 130, 132
surface morphology 23, 33, 34, 57
surface packing density 125
surface plasmon resonance (SPR) 119, 125
sweet potato peroxidase 520
synthetic homopolyribonucleotides 9
 α -synuclein (ASyn) 694, 695, 701, 710, 711, 714, 719–721
 α -synuclein mutants 710
syphilis 759

T1 (type1 redox protein) 551, 554, 561, 562, 564, 566, 569, 570, 572
T2 551, 554, 556, 561, 562, 564
T2/T3 569, 570, 573
T3 551, 553, 558, 561, 562, 564
T4 endonuclease V 405
target DNA (tDNA) 122–124, 130–133, 145, 146, 333, 335, 336
Tay-Sachs genetic disorder 207, 211
tDNA 122, 129, 131, 132, 146
tears 759
telomerase 232
telomerase activity 230
telomers 232
temperature-controlled hybridization 204
tensammetric 391
tensammetric signals 398
tetracyanoquinodimethane 558
theophylline oxidase 522, 540, 548, 549
thick DNA layers 395, 406
thiol groups 252
thiol-gold interaction 125
thiol-containing 692
thiol-derivatized 125
thiolated 85, 119, 122
thiolated DNA 730
thiolated ODNs 80, 86, 125, 127, 725, 730
thiolated oligodeoxynucleotides 725, 731
thiols 757–759

- thiophene-S-oxide 406
thiotepa 401, 414
threading indicator 181
threading intercalators 122, 345, 346, 350
threonine 711
thymines 87, 106, 134, 139, 141, 404, 493
TMV protein 713
TMV strains 709
TMV-Vulgare peroxidase 709, 711
tobacco 520
tobacco mosaic virus (TMV) 709
Toxalert[®] 100 414
toxic heavy metals 407
toxicity 405, 414, 416
toxins 266
transducers 247, 599–602, 604, 607, 608, 610, 611, 614, 624, 625, 629–631
transfer 98, 115, 136
transition metal ions 405
transistor, molecular 490, 510
transmission coefficient 490
triangular sweep voltammetry 10
tributylmethyl phosphonium chloride 563
trinucleotide repeat expansions 412
triplet length expansion 131
triplet repeats 412
Trp residues 702, 708, 735
Trp-containing peptides 733
trypsin 716, 762
tryptophan (Trp) residues 693, 695, 729, 734, 737, 739
TUNEL test 389, 396
tunneling 487, 489, 497, 508
 barrier 489
 gap 497
 spectroscopy 489
two-dimensional condensation 18
Tyr 560, 562, 702
Tyr and Trp residues 695
tyrosinase 554, 558
tyrosine (Tyr) 559, 693, 695, 729, 737
tyrosine residues 720
ultramicroelectrodes 249, 252
ultrasound 391
ultrathin DNA films 395
ultrathin films 433, 434, 436, 442, 446
undoping 333
unfolded protein 710
unfolding 705
unpaired 732
unpaired bases 392
unraveling 401
untwisting 404, 410
unwinding of double-stranded DNA 104
uracil 3
urea 712
urea, effect of 760
urease 716
urinal tract infections 255
UV irradiation 386
UV light 391, 393, 402, 404, 405
van der Waals interaction 253
vasopressin 696, 698, 699
viral DNA 253
viral RNA 209
virus protein 678
voltammetric detection of DNA damage 11
voltammetric techniques 3, 391
voltammetry 97, 393, 434, 436, 438, 439, 764
wave, catalytic 90, 756–763
wHRP 535
wool 759
X-ray photoelectron spectroscopy 493

This page intentionally left blank